Volume 4

Xavier Fischer
Alain Daidie
Benoit Eynard
Manuel Paredes
Editors

Research in Interactive Design

Mechanics, Design Engineering and Advanced Manufacturing

Springer

Research in Interactive Design (Vol. 4)

Xavier Fischer · Alain Daidie
Benoit Eynard · Manuel Paredes
Editors

Research in Interactive Design (Vol. 4)

Mechanics, Design Engineering and Advanced Manufacturing

Springer

Editors
Xavier Fischer
Bidart
France

Alain Daidie
Mechanical Engineering Department
INSA
Toulouse Cedex 4
France

Benoit Eynard
Département GSM
UTC
Compiegne
France

Manuel Paredes
INSA Toulouse
Toulouse
France

ISBN 978-3-319-26119-5 ISBN 978-3-319-26121-8 (eBook)
DOI 10.1007/978-3-319-26121-8

Library of Congress Control Number: 2015959574

Printed on acid-free paper

This Springer imprint is published by SpringerNature
The registered company is Springer International Publishing AG Switzerland

Instructions

Research in interactive Design – Vol. 4 presents the last successful developments in Interactive and Integrated Product Design and Manufacturing. *Research in interactive Design – Vol. 4* is a publication addressed to all researchers, industrial experts and teachers interested in the implementation of efficient solutions to support decision making in product engineering and to improve industrial innovation.

The book includes 10 main chapters. They are referencing exhaustive works being displayed in the second part of the book. 81 full papers foster the main argumentation. These articles written by high experts of product design and manufacturing were presented during the 2014 Joint Conference on Mechanical Design Engineering and Advanced Manufacturing.

All full papers are referenced and identified in the main argumentation according to the following presentation:

Title: Article Title

Authors: list of authors.

Key Words: key words.

Details on the results, process and solutions related to a specific topic of Interactive Design and Manufacturing.

Paper Number: ID, Page: pp.

Acknowledgement

We wish to start this section by sincerely thanking all the authors for their high-quality contributions integrated within the present manuscript *Research in Interactive Design – Vol 4*.

The high quality of different technical and scientific argumentations is ensured thanks to the realization of manuscript reviews realized by an international committee of experts. These prestigious researchers are sincerly gratefully for their involvement.

This book was not able to exist without the implication of the Chapter Editors. They were also the Track Chairs of the 2014 Joint Conference on Mechanical Design Engineering and Advanced Manufacturing.

Each of these persons are named at the beginning of each book chapter.

We benefit this short section to highlight the great involvement of representative of three organizations: Pierre Castagna, University of Nantes from AIP-PRIMECA (Ateliers Inter-établissements de Productique - Pôles de Ressources Informatiques pour la MECAnique) network from France, Gianmaria Concheri, University of Padua, Antonio Lanzotti, University of Naples, Vincenzo Nigrelli, University of Palermo, Stefano Tornincasa, Polytechnic University of Turin from the italian association ADM (Associazione Nazionale Disegno di Macchine) and Guillermo Peris-Fajarnés, Polytechnic University of Valencia, David Corbella, Polytechnic University of Madrid, Felix Sanz, University of Rioja from INGEGRAF (Asociación Española de Ingeniería Gráfica) from Spain.

Preamble

From the year 2006, the book series *Research in Interactive Design* highlights original studies leading to solutions being able to foster industrial innovation.

These solutions are providing answers to all researchers, engineers or students looking for basic information on:

- original engineering processes and industrial organizations,
- new tools and softwares allowing experts to implement product engineering process in a virtual way,
- numerical methods leading to the interactive exploration of engineering spaces,
- new methodologies to model of knowledge and behaviours,
- new approaches for collaborative design and the systemic engineering.

The fourth volume of the book series *Research in Interactive Design* is addressing solutions either for product manufacturing or product designing. A new dimension related to the teaching of product design is also introduced.

The authors of *Research in Interactive Design Vol. 4* have gathered together the most significant articles on the original topic of interactive and integrated product engineering.

The reader will find enclosed the authors coming from the whole

world who have left their mark with their new proposals, often by demonstrating the impact of their own solutions by solving real industrial problems.

Research in Interactive Design Vol. 4 is presenting the latest efficient approaches allowing innovation to be reinforced.

Pr. Xavier Fischer
Editor-in-Chief of the book series
Research in Interactive Design

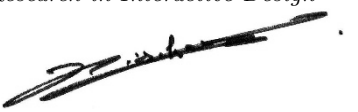

Contents

Part I

Recent Studies on Interactive Design and Manufacturing

1

Integrated and Interactive Practices in Product Engineering

Authors:
Alain Daidié
INSA, Toulouse - France

Manuel Paredes
INSA, Toulouse - France

Benoit Eynard
UT Compiègne - France

Research in interactive Design – Vol. 4 presents the most recent successful developments in mechanics, design engineering and advanced manufacturing for innovation in product, process and production engineering. The readers are invited to discover new techniques, methods, models and tools based on integrated and interactive design approaches. In a context of worldwide competition, there is an unquestionable need for such approaches to improve the reactivity, flexibility and capacity for innovation of engineers faced with particular challenges in enhancing the development of transport systems, the production of energy, the manufacture of consumer goods, the building engineering or the product design. But these approaches are also of great interest to academics, to improve the content of their curriculum and education programmes and to define novel research roadmaps in the

X. Fischer et al. (eds.), *Research in Interactive Design (Vol. 4)*
DOI 10.1007/978-3-319-26121-8_1

field of mechanics, design engineering and advanced manufacturing.

Interactive and integrated design can be of great help to designers by supplying efficient solutions from an analysis of cognitive or physical interactions. *Research in interactive Design – Vol. 4* addresses a wide range of issues related to design. Design methods such as evolutionary approaches, design of experiments, robustness and optimization are improved to help designers. Virtual prototyping and virtual reality simulations are also of key interest. In addition, the latest developments in product design and simulation, computer-aided design, computer-aided engineering and reverse engineering are presented.

The need for industrial agility also implies a need for innovations in manufacturing. *Research in interactive Design – Vol. 4* presents papers related to information technology for manufacturing, production engineering, process planning, automated processes, inspection engineering (metrology, 3D scanning, tolerancing), robotics and the continuing improvements of recent manufacturing processes and technology, such as water jet milling, additive manufacturing or orbital drilling.

Simultaneously, the worldwide increase in industrial production has to be controlled by managing the associated environmental impacts. Thus sustainability has become a major area of interest for mechanical, design, manufacture and construction engineers. Consequently, *Research in interactive Design – Vol. 4* includes papers dealing with eco-design, lifecycle assessment, recycling management, end-of-life of products and sustainability of manufacturing processes.

All the innovations and research issues presented are aimed at helping designers and engineers face the new challenges of society. We also know that the forthcoming challenges are not yet identified; there is thus a real need for innovative young engineers. It is clear that the characteristics of students are evolving greatly: today's students are known as digital natives (the millennials) and our education strategies have to be remodelled to be efficient. For that reason *Research in interactive Design – Vol. 4* includes not only "learning by doing" issues but also pilot projects, collaborative work and knowledge management experience. Of course, the management of innovation itself can be improved. Knowledge transfer, collaborative design, patent modelling, and product lifecycle management appear to be key issues for disruptive

innovation.

Research in interactive Design – Vol. 4 contains the right arguments for all researchers, industrial experts and teachers aiming to implement efficient solutions to support decision making for improving creativity and innovation. Through the various chapters, readers are invited to take a look at some papers written by top experts in mechanical engineering, product design and manufacturing process.

The papers are organized in nine chapters, successively focusing on:

- latest advances in design methods,
- innovations in behavioural modelling and simulation for design,
- new trends in decision support systems for product engineering,
- current approaches in geometric modelling and CAD,
- innovation and collaboration in product engineering,
- new methods for sustainability engineering,
- latest trends in manufacturing processes,
- current advances in robotics,
- mechatronics and product engineering, novel practices in education for product engineering.

The editors of *Research in interactive Design – Vol. 4* are convinced of the interest that discovering the deep content of the proposed research works hold for readers.

Chapter 2 presents the latest advances in design methods. The section on design from objectives includes the merging of technical drawings and graphic engineering technology for industrial design and creativity. It proposes modular structuring of products for the redesign process with an application in eco-design. A design improvement strategy for increasing the comfort of products is also developed with a case study on seats. With the section on the design process, we focus on traceability and modelling of the design process so as to capture the design rationale. A design synthesis method is proposed to enable dimensional management of the assembly process. A spline coupling test rig capable of performing wear tests on components working in

misaligned conditions is also presented. In the section on embodiment and conceptual design, the development of tools for multi-material design is discussed. A comparison of different multiple-criteria decision analysis methods in conceptual design is presented. Evolutionary optimization approaches for embodiment design of mechatronic systems is also detailed. Lastly, a section on integrated design proposes a structured method for the integration of product design and process planning.

Chapter 3 focuses on innovations for behavioural modelling and simulation for design. In the section on multi-body system modelling, a method for parametric virtual design of heavy machinery is proposed. A mechanical model is also presented for the behavioural simulation of human movements in skiing practice. With the section on experimentation and behavioural modelling and simulation, the research work discusses the influence of the cold expansion process on the fatigue performance of hard alloy holes. The design of an experimental device to characterize the behaviour of total hip implants is detailed and a study of serial manufacturing of lightened ceramic floorings is also presented. The influence of pretension on metallic shear joints is analysed. The section on modelling from finite element simulations proposes the quality evaluation of bolted assemblies through tightening monitoring and, in computational mechanics and design, an FEA approach is presented for the coupling of non-intrusive models. The application of numerical methods in the design process of a sailing yacht is also detailed. Lastly, with the section on modelling for virtual reality simulation in design, a multi-layer approach is proposed for path planning control in virtual reality simulations.

Chapter 4 deals with new trends in decision support systems in product engineering. With the section on modelling for optimization, the optimal design of sandwich plates with honeycomb core is discussed. An example of genetic algorithm optimization and robustness analysis for the design of fixture systems in automotive manufacturing is also presented. The use of optimization methods is detailed for the reduction of machining time on free-form surfaces in 3-axis milling. The optimization of how the locations are selected for storage assignment problems in logistics warehouses is proposed. In the section on modelling of experiments for decision making, the influence of minimum quantity of lubrication parameters is discussed for finishing processes in milling. A

statistical model to predict tool wear and cutting force is also presented. With the section on knowledge based engineering and knowledge re-use, a way to improve the GUI of a knowledge based system for gearbox design is proposed. A closed loop approach for information management from CNC machines to CAD/CAM systems is also detailed. In the section on knowledge processing, a constraint-based decision support system is put forward for architecture engineering and construction. Lastly, with the section on knowledge in the digital factory, a knowledge management approach is discussed to support the design and simulation of production processes.

Chapter 5 presents the current approaches in geometric modelling and CAD. In the section on advances in geometric representation, the identification of tree species from airborne LIDAR point clouds is discussed. With the section on CAD and engineering, a preliminary study on cleft lip pathology based on 3D geometric analysis is proposed. A mesh processing for the computation of morphological and clinical parameters is also detailed. The section on reverse engineering and CAD representation deals with the characterization of ultra-precise aspherical surfaces using Forbes' equation. The influence of scanning parameters on 3D inspection processes is also discussed. The section on integration of tools presents a prediction of the impact of CAD model defeaturing on heat transfer FEA results using machine learning techniques. The combination of a NURBS patch with the Nitsche method for isogeometric analysis is also introduced. With the section exploring the ways of using CAD, reverse engineering for the manufacture of parts in a routine context is proposed. A new dimensioning standard adapted to CAD systems is also presented. Lastly, a section dealing with CAD for manufacturing evaluates the performance of current CAD systems in design for additive manufacturing. The influence of the tool-material combination on dental CAD/CAM is also discussed.

Chapter 6 focuses on innovation in product engineering. The section on collaborative and cooperative design presents an approach for defining a collaborative platform to support the development of corporate engineering standards. Processes Alignment in Collaborative Engineering for project success is discussed. A comparison of computer-based and paper-based collective and co-located tasks in preliminary design is also detailed. With the section on

interoperability in design, managing the consistency of information in PLM interoperability and collaborative design is studied. A section on knowledge management and innovative engineering proposes the integration of design and manufacturing to support an improvement in quality standards and innovation in the automotive industry. A descriptive model of knowledge transfer within organizations is also discussed. The exploration of an innovative field and the associated patent portfolio is presented. Lastly, preliminary contributions of industrial management methods for microfactories are analysed.

Chapter 7 tackles new methods for sustainability engineering. The section on lifecycle integration and eco-design presents an application of lifecycle analysis in preliminary design. The integration of end-of-life options as a design criterion in eco-design is detailed. The increasing sustainability of a decentralized electricity supply thanks to remotely monitored product-service systems is discussed. With the section on design, recycling and decycling, the disassembly performance of products is assessed and the design of disassembly sequences for the end-of-life of products is also presented. In the section on sustainable manufacturing, an evaluation of the economic and ecological impacts of production processes is proposed. An IT framework for sustainable manufacturing is also introduced. Lastly, a section on design for energy efficiency presents a design methodology for optimizing energy efficiency in production systems.

Chapter 8 focuses on current trends in manufacturing processes. In the section on advanced solutions in product manufacturing, profile incision modelling in abrasive waterjet milling of titanium alloys is presented and the evolution of chip morphology during the turning of high strength stainless steel is analysed. The high speed interaction between an abradable coating and a labyrinth seal in turbo-engine application is studied. The conversion of G code programs for milling into STEP NC is presented. The section on models for product manufacturing proposes the modelling of chip geometry in orbital drilling. A thrust force and torque model applied to a vibratory drilling process is presented and an analysis of a turning process strongly coupled to a vibro-impact nonlinear energy sink is detailed. The section on manufacturing composite materials introduces an analytical model of pre-drilled thick composite plates. A burr height study in the

drilling of carbon epoxy composite-titanium-aluminium stacks is also proposed. In the section on flexible manufacturing, an emulator for the bench4star initiative is detailed. The section on reverse engineering in manufacturing discusses the influence of geometric tolerancing on reverse engineering for manufacturing. Lastly, a section on quality and manufacturing presents a multi-sensor approach for multi-scale machining defect detection.

Chapter 9 looks into research work in robotics, mechatronics and product engineering. In the section on robots and product manufacturing, the definition of a robotized polishing process for aeronautical parts is introduced. The distribution of material removal in robotized random orbital sanding is also studied. With the section on design for robotics, the harmonic functions-based type-2 fuzzy logic controller for autonomous navigation of mobile robots is presented. A hybrid force-position control for a 6 DOF parallel testing machine is detailed. The identification of material and joint properties based on the 3D mapping of Quattro static stiffness is proposed. Lastly, the section on design in mechatronics presents a method for sizing procedures and the definition of optimization problems in mechatronic systems.

Chapter 10 reveals some novel practices in education for product engineering. The section on learning collaborative design studies knowledge discovery from the traceability of design projects. A multidisciplinary approach in teaching interface design is also proposed. In the section on learning CAD and geometric modelling, a multidisciplinary PBL-based learning environment for training non-technical skills is detailed. An approach for descriptive geometry 2.0 is also presented. The section on learning innovation introduces a learning by doing experiment with a cooperative project between an University and an Ideas Hub. Implementations of 3D immersive environments in higher education are also presented. Finally, with the section on interactive learning, an experiment for learning dimensional metrology by practice describes the students' work on the control of a coordinate measuring machine.

2

Design Methods

Chapter Editors:
Xavier Espinach
University of Girona
Ingegraf Society, Spain

Antonio Mancuso
Universitá di Palermo
ADM Society, Italy

Benoit Eynard
UT Compiègne
AIP PRIMECA Society, France

2.1 Designing from Objectives

Contribution 1

Title:	New Designs of the Ceramic Bricks of Horizontal Hexagonal Hollow.
Authors:	David Corbella, Francisco Fernandez, Francisco Hernández-Olivares, Pedro Armisen, Cristina Corbella.
Key Words:	product design, industrial design and creativity, industrial innovation, product manufacturing, graphical analysis.

X. Fischer et al. (eds.), *Research in Interactive Design (Vol. 4)*
DOI 10.1007/978-3-319-26121-8_2

Technical Drawing is a multiple tool of expression and communication essential to develop inquiry processes, the scientifically basis and comprehension of drawings and technological designs beiing able to be manufactured. It is demonstrated graphically and analytically that spatial vision and graphic thinking allow the user to identify graphically real life problems, develop proposals of solutions to be analysed from different points of view, plan and develop the project, provide information needed to make decisions on objects and technological processes. From the knowledge of Technical Drawing and CAD tools graphic analyses have developed in order to improve and optimize the geometry of the rectangular cells of conventional bricks by hexagonal cells, which is protected by a Spanish patent owned by the Polytechnic University of Madrid. This new internal geometry of the bricks will improve the efficiency and the acoustic damping of walls built with the ceramic bricks of horizontal hollow, maintaining the same size of the conventional bricks, without increasing costs either in the manufacture and the sale. A single brick will achieve the width equivalent to more than four conventional bricks.

Full Article: 05-dm-98 Page: 84

Contribution 2

Title: Improving the Modular Structure of a Product to Facilitate The Redesign Process: an Example for Eco-Design.

Authors: Marco Malatesta, Michele Germani, Fabio Gregori, Roberto Raffaeli.

Key Words: modular design, product lifecycle design, eco-design , LCA.

Products are continuously redesigned to offer new variants and penetrate new market niches. Changes are often dictated by improvements which are necessary in specific Design Contexts (DC), such as performance, eco-sustainability, assembling, cost, usability. Modularity is a well consolidated approach toward the rapid product reconfiguration and is beneficial to limit the scope of changes to product subsets. However, this consideration needs to be included in the design of the modular structure of a product. The concept of Design Context Module (DCM)is introduced as a module implemented in components that will strongly affect a certain DC, letting the designer to restrict

the number of the parts to be modified. The approach moves from the traditional modularization based on the functional decomposition and introduces an iterative procedure to refine the DCMs structure. The optimization is driven by the maximization of similarities and dependencies among components of the same module and by indexes expressing the impact of the components on specific DCs. The approach has been tested in the field of the household appliances. The modular structure of a freestanding cooker has been redefined in consideration of redesign activities aiming to improve the eco-sustainability of the product. The application of the approach has led to the identification of few modules characterized by high impacts on the environment.

Full Article: 02-dm-68 Page: 91

Contribution 3

Title: Seat Design Improvement Via Comfort Indexes Based on Interface Pressure Data.

Authors: A. Lanzotti, A. Vanacore, D. M. Del Giudice.

Key Words: office chair, sitting comfort/discomfort assessment, interface pressure distribution.

Literature on seat comfort recognizes that seat interface pressures are the objective comfort measures that most clearly relate to users comfort perceptions about sitting experience. The above relationship is quantitatively investigated by performing simple but effective explorative analyses on seat comfort data collected during experimental sessions involving 22 volunteers who tested 4 office chairs (differing in terms of cushion softness). Statistical data analyses show that subjective sitting comfort/discomfort ratings are significantly related to several combinations of pressure variables. The joint analysis of synthetic indexes based on seat interface pressures reveals to be a useful tool for comparative seat comfort assessment. Besides valuable suggestions for the definition of an effective strategy for seat comfort assessment, the results of data analyses provide useful information to support the product design phase. In fact, the sitting experience results to be significantly improved by: (1) a balancing of pressures between the bilateral buttocks, and (2) a balancing of contact areas between buttocks and thighs.

Full Article: 03-dm-72 Page: 98

2.2 The Design Process

Contribution 1

Title: Design Process and Trace Modelling for Design Rationale Capture.

Authors: Emna Moones, Esma Yahia, Lionel Roucoules.

Key Words: design process, design rationale, design trace, decision making, product design.

To face the high industrial concurrence and to remain competitive, companies are asked to work in a context of collaborative engineering environment where design rationale is a prerogative to reduce their product development time. Design rationale aims to capture the knowledge from the product design at a very early stage as those decisions have higher impacts in terms of time, cost and quality in the later product lifecycle stages. We propose, in this paper, a three-layer framework to answer to the need to capture the process design knowledge and to use the construct captured to visualize the process performances and to derive rules in order to help and assist the designers.

Full Article: 04-dm-76 Page: 105

Contribution 2

Title: Design Synthesis Methodology for Dimensional Management of Assembly Process with Compliant Non-Ideal Parts.

Authors: Pasquale Franciosa, Abhishek Das, Darek Ceglarek, Luca Bolognese, Charles Marine, Anil Mistry.

Key Words: design synthesis, product and process simulation, design task integration, non-ideal compliant parts, dimensional management.

A design synthesis methodology is proposed: it is dedicated to dimensional management of assembly processes with compliant non-ideal parts which allows to integrate the critical and heterogeneous

design tasks with conflicting or coupled objectives and design constraints such as: (1) tolerancing and variation simulation analysis (VSA); (2) fixture layout design optimization; (3) part-to-part joining process parameters selection and laser beam visibility analysis; or/and; (4) in-process measurement gauge visibility and accessibility analysis. The proposed methodology is based on the Adaptive Task Graph (ATG) that has capability to model design tasks by integrating Key Product Characteristics (KPCs) and Key Control Characteristics (KCCs) with their impact on the Key Performance Indicators (KPIs); this allows to dynamically capture interactions between design tasks as well as to generate tasks sequence. The design synthesis methodology is based on the development of: (i) assembly surrogate model linking KPCs to KCCs; (ii) sensitivity analysis with capability to model and analyse the interdependencies among design tasks and KPCs, KCCs and KPIs; and, (iii) ATG model which represents the hierarchy of design tasks and is used to generate the sequence of design tasks to minimize their interdependencies during design synthesis. The proposed methodology is illustrated and validated in the process of designing configurations for automotive door assembly with remote fiber laser welding joining process. The methodology shows potential to reduce engineering changes necessary during door assembly process build and testing by 25%.

Full Article: 09-dm-107 Page: 112

Contribution 3

Title:	About Wear Damage in Straight and Crowned Misaligned Splined Couplings.
Authors:	Cuffaro Vincenzo, Curá Francesca, Mura Andrea.
Key Words:	spline couplings, fretting wear, misalignment, test rig.

The spline coupling tooth geometry may influence the surface fear pattern. In particular the difference between straight teeth and crowned teeth spline coupling is considered. The different tooth profile brings to different contact pressure distributions that, associated to the relative motion between engaging teeth may create different wear patterns on the contact surfaces. Also the effect of the lubrication conditions has been considered. The investigation has been carried on by means of

a dedicated spline coupling test rig capable to perform wear tests on components working in misaligned conditions.

Full Article: 07-dm-113 Page: 119

2.3 Embodiment and Conceptual Design

Contribution 1

Title: Development of Tools For Multi-Material Design.

Authors: F.X. Kromm, H. Wargnier, M. Danis.

Key Words: multi-material, design, architectured materials, material selection, optimization.

Multi-material design implies the selection of various parameters such as the nature of the components, their morphology (or architecture), their volume fractions, etc. Although selection methods have been developed for monolithic materials, a single method dealing with all these parameters has not been created yet. Several tools that can guide the designer in this task are described. The firstone consists in a statistical analysis of the material properties to see whether some requirements are incompatible. In this case, the result allows the separation of these requirements and helps the components selection. Another study deals with the selection of the components when the architecture of the multi-materials is known. The important benefit of the method is a filtration of the candidates that decreases drastically the number of solutions that have to be evaluated. Finally, an architecture can be selected and optimized.

Full Article: 01-dm-33 Page: 125

Contribution 2

Title: Comparison of Different Multiple-Criteria Decision Analysis Methods in the Context of Conceptual Design: Application to the Development of a Solar Collector Structure.

Authors: Mehdi El Amine, Jérôme Pailhes, Nicolas Perry.

Key Words: multi-criteria decision aid methods, selection methods, aggregative methods, conceptual design, consistency.

At each stage of the product development process, the designers are facing an important task which consists of decision making. Two cases are observed: the problem of concept selection in conceptual design phases and, the problem of pre-dimensioning once concept choices are made. Making decisions in conceptual design phases on a sound basis is one of the most difficult challenges in engineering design, especially when innovative concepts are introduced. On the one hand, designers deal with imprecise data about design alternatives. On the other hand, design objectives and requirements are usually not clear in these phases. The greatest opportunities to reduce product life cycle costs usually occur during the first conceptual design phases. The need for reliable multi-criteria decision aid (MCDA) methods is thus greatest at early conceptual design phases. Various MCDA methods are proposed in the literature. The main criticism of these methods is that they usually yield different results for the same problem. An analysis of six MCDA methods was conducted. Our analysis was performed via an industrial case of solar collector structure development. The objective is to define the most appropriate MCDA methods in term of three criteria: (1) the consistency of the results, (2) the ease of understanding and, (3) the adaptation of the decision type. The results show that TOPSIS is the most consistent MCDA method in our case.

Full Article: 06-dm-104 Page: 131

Contribution 3

Title: Contribution to the Embodiment Design of Mechatronic System by Evolutionary Optimization Approaches.

Authors: Didier Casner, Rémy Houssin, Jean Renaud, Dominque Knittel.

Key Words: mechatronic systems, design, optimization, optimization-integrated design.

Mechatronic systems are multidisciplinary devices and therefore require specific approaches to design and optimize them, unlike most approaches that consider the optimization as a manner to identify

the optimal process through a redesign strategy and at the last phase of design. Therefore optimization has limited efficiency. This paper contributes to the integration of the optimization in the embodiment design process, as part of a routine or innovative approach. The optimization will now be considered as a manner to design and optimize innovative mechatronic systems. This approach considers an evolutionary case-based reasoning process to design a technical solution from a concept by reusing, adapting and optimizing solutions or cases that have previously been used to solve similar problems. The main approach has been applied to the design of an XY table for laser cutting applications.

Full Article: 08-dm-102 Page: 137

2.4 Integrated Design

Title: Product Design-Process Selection Planning Integration Based on Modelling and Simulation.

Authors: Von Dim Nguyen, Patrick Martin, Laurent Langlois.

Key Words: modeling, simulation, product design, process selection, process planning.

As a solution for traditional design process having many drawbacks in the manufacturing process, the integration of Product design-Process selection-Process planning is carried out in the early design phase. The technological, economic and logistic parameters are taken into account simultaneously as well as manufacturing constraints being integrated into the product design. As a consequence, the most feasible alternative with regard to the products detailed design is extracted satisfying the products functional requirements. Subsequently, a couple of conceptual process plans are proposed relied on manufacturing processes being preliminary selected in the conceptual design phase. Virtual manufacturing is employed under CAM software to simulate fabrication process of the potential process plans. Ultimately, the most suitable process plan for fabricating the part is recommended based upon a multi-criteria analysis as a resolution for decision making.

Full Article: 030-itm-25 Page: 144

3

Behavioural Modelling and Simulation for Design

Chapter Editors:
César Otero
University of Cantabria
Ingegraf Society, Spain

Pierpaolo Valentini
Universitá di Roma Tor Vergata
ADM Society, Italy

Xavier Fischer
ESTIA
AIP PRIMECA Society, France

3.1 Multi-Body System Modelling

Contribution 1

Title:	Parametric Virtual Concept Design of Heavy Machinery: a case study application.
Authors:	Alberto Vergnano, Marcello Pellicciari, Giovanni Berselli.
Key Words:	virtual prototype, virtual concept, design process, CAD based simulation, vibrating screen.

X. Fischer et al. (eds.), *Research in Interactive Design (Vol. 4)*
DOI 10.1007/978-3-319-26121-8_3

Virtual prototyping enables the validation and optimization of machinery equivalent to physical testing, saving time and costs in the product development, especially in case of heavy machines with complex motions. However, virtual prototyping is usually deployed only at the end of the design process, when product architecture is already developed. Virtual prototypes are handled at conceptual design stage as Virtual Concepts in which coarse models of machinery design variants are simulated: useful information can support the choice of best design parameters. Virtual Concept modelling and preliminary validation and its later integration to a Virtual Prototype are expressly investigated using Multi Body Dynamics software. A verification case study on a large vibrating screen demonstrates that dynamic Virtual Concepts enable easier and effective evaluations on the design variants and increase the design process predictability.

Full Article: 010-vp-7 Page: 152

Contribution 2

Title: The Mechanical Link between Foot and Ski and the Ski Behavior in a model of Skating.

Authors: F. Rey, A. Ferrand.

Key Words: modelling, skating, edging, ski behavior.

Skating technique arose from both the association of a motion and development of the equipment. The specific technique studied is related to the offset. To give an account about the complexity of this motion and to be able to analyse it in a mechanical way, our aim was to build a three-dimensional dynamic model. We used the software LifeModeler, to calculate kinematic and dynamic parameters from a human body model like an anthropomorphic robot. In the aim to validate the model in its environment, we analysed kinematics by comparing it with other scientific data. We worked on the contact parameters so as to simulate the snow effect. The study enables us to show the method for building a 3D model applied to the skier gliding. It's an approach to modelling the links between the foot, the binding, the ski and the snow in the aim to understand the skis behaviour and particularly to evaluate the edging angles that are significant parameters of this gesture.

Full Article: 081-cadcae-28 Page: 159

3.2 From Experimentation to Behavioural Modelling and Simulation

Contribution 1

Title: Influence of the Cold Expansion Process on Fatigue Performance of Hard Alloys Holes.

Authors: Victor Achard, Alain Daidié, Manuel Paredes, Clément Chirol.

Key Words: Cold expansion process, hard alloys, fatigue performance, expansion ratios, Ti-6Al-4V.

The problematic of evaluation of the influence of the cold expansion process on fatigue performance of holes in hard alloys is regarded. Such materials are involved in an increasing number of aeronautic applications. Although the cold expansion of aluminium holes has been studied widely, there have been few reports concerning this issue in hard alloys. Some studies do, however, show that fatigue gains can be observed by using an extension of the processes employed on aluminium. Currently, there is no research concerning dedicated techniques to expand hard metals, despite their highly specific behaviour. The response of Ti-6Al-4V expanded holes is studied, considering various experimental parameters such as the hole thickness and diameter. Its influence on the fatigue strength of tensile specimens is also presented for various expansion rates. A new approach is presented: it allows an expert to understand which processes and methodologies are suitable for obtaining efficient expansion of hard metals.

Full Article: 071-pds-31 Page: 166

Contribution 2

Title: Design of an Experimental Device to Characterize the Behaviour of Total Hip Implants.

Authors: Camille Regnery, Julien Grandjean, Yann Ledoux, Serge Samper, Laure Devun, Thomas Gradel.

Key Words: total hip implant, squeaking, in-vitro experimental device, analytical modeling, local pressure, joint gap.

The majority of Ceramic Total Hip Implant (THI) validation tests and wear studies are done on specific devices able to require a kinematic outcome that conforms with the ISO- 14242-1 standard. The main point of interest in using Ceramic THI is their property of resistance to wear. However in some cases an unwanted noise called squeaking appears when implanted. The aim of this work is to develop an in vitro study to characterise this phenomenon from a mechanical point of view. Associated results show the limits of standard tests mainly because of the control system that disturbs the applied loads on the prosthesis. To overcome these problems the development of an experimental device based on a free kinematic is developed. Analytical models based on geometrical characteristics of THIs and the properties of the prosthesis materials are developed and used to characterise the behaviour of THI with or without squeaking. Based on the results, a change in frictional behaviour can be identified as an indicator of the squeaking phenomenon as evidenced by a dramatic increase in the deceleration for those tests where squeaking occurred.

Full Article: 072-pds-64 Page: 173

Contribution 3

Title: Serial Manufacturing of Lightened Ceramic Floorings and Indirect Calculation of Energy Saving.

Authors: B. Defez, G. Peris-Fajarnés, R. Martínez-Díaz, L. Monreal Mengual, F. Brusola Simón.

Key Words: ceramic tile, back structure, energy savings.

The optimization of the tile structure through different kinds of back reliefs is a new approach for the improvement of the tile industry, since these floorings could be manufactured with less support material and so they require less process energy. We have tested the viability of the serial production of lightened tiles, whose design is based in conclusions of previous theoretical works. Here we report genuine manufacturing handicaps and measure real energy savings. After our

study, we conclude that these tiles could be produced with current technologies. A cut within 14% and 25% while firing is estimated.

Full Article: 075-pds-78 Page: 182

Contribution 4

Title: Influence of Pretension on Metallic Shear Joints.

Authors: Taha Benhaddou, Alain Daidié, Pierre Stephan, Clement Chirol, Jean-Baptiste Tuery.

Key Words: Preload, bolted joints, fatigue testing, finite elements method, virtual testing.

Bolted joints are one of the most common elements in aerostructures. Currently, the preload applied to join the parts together is achieved by applying torque to the bolt head or to the nut. In the case of shear joints, an opportunity is emerging to optimise structural joints by applying the preload more accurately. Up to now, the preload effect has most often been neglected because of the large scatter on its value due to torque tightening. The aim of this article is to describe the effect of preload on shear joints and a numerical and experimental approach is adopted to demonstrate its influence. In the experimental approach, iterative tightening is used to reduce the scatter on preload. The benefits of preload on high load transfer double lap shear joints is discussed. In the numerical section, an approach for predicting the fatigue life of shear joints is presented. The effect of preload/coefficient of friction is also studied. Finally, practical aspects such as alternative tightening techniques are considered and an industrial application case is presented.

Full Article: 078-cadcae-65 Page: 187

3.3 Modelling from Finite Element Simulation

Title: Quality Evaluation of Bolted Assemblies through Tightening Monitoring and Simulation.

Authors: Simon Dols, Manuel Paredes, Patricia Morgue.

Key Words: bolt, quality, monitoring, stiffness, defects.

A method for the quality control of a bolted assembly by monitoring its tightening is presented. Both torque and angle are already used in the production lines as target values, but the proposed method also uses them as a means of verification. In fact, the variations of the stiffness of the bolt through the torque-angle relationship is a good indicator of the bolt's interface quality and thus of the performance of the overall assembly. The impact of gaps and friction on this relationship are investigated using a full 3D finite element model.

Full Article: 073-pds-29 Page: 194

3.4 Computational Mechanics and Design

Contribution 1

Title: Non-intrusive Model Coupling: a Flexible Way to Handle Local Geometric and Mechanical Details in FEA.

Authors: M. Duval, J.-C. Passieux, M. Salaün, S. Guinard.

Key Words: model coupling, multiscale, FEA, parallel computing, crack growth simulation.

Computer Aided Engineering (CAE) often involves structural mechanics analysis (most of the time using the finite element method). When dealing with nonlinear complex models on large 3D structures, the computational cost becomes prohibitive. We present the recent developments linked to an innovative computing method: non-intrusive way: the previously computed analysis is left unchanged. Large scale linear models can thus be easily computed, then localised nonlinear complex models can be used to pinpoint the analysis where required on the structure. After a presentation of the scientific context and a description of non-intrusive coupling methods, we will present its application to crack growth simulation and parallel structure analysis.

Full Article: 074-pds-52 Page: 201

Contribution 2

Title: Numerical Methods in the Design Process of a Sailing Yacht.

Authors: Tommaso Ingrassia, Antonio Mancuso, Davide Tumino.

Key Words: computational fluid dynamics, conceptual design, numerical methods, optimization, sailing yacht.

Most significant steps involved during the whole process of designing a sailing yacht are outlined. At first, a preliminary conceptual design process was implemented in order to fix some boundaries to the problem, then the best solution was found by using numerical simulations. As a general rule, once the target point has been decided, task of the designer is the definition of those systems of aerodynamic and hydrodynamic forces that are in equilibrium when the boat sails at its target. Unfortunately, a multi-purpose yacht does not exist. If the target point is in upwind sailing, then performances will be better for such a condition and worse for others. In the last years, thanks to hardware and software capabilities, Computational Fluid Dynamics (CFD) has become a powerful instrument to numerically compare several solutions instead of much more time-consuming experimental tests. The case study here presented is the design of hull, appendages and sails of a 15 inches skiff subject to box-rules, designed and manufactured at the University of Palermo. The entire design process has been numerically developed integrating a classical design approach with CFD simulations leading to an efficient solution.

3.5 Modelling for Virtual Reality Simulation in Design

Title: A Multi-layer Approach for Path Planning Control in Virtual Reality Simulation.

Authors: Simon Cailhol, Philippe Fillatreau, Jean-Yves Fourquet, Yingshen Zhao.

Key Words: path planning, Virtual Reality, interactive simulation, multi-layer architecture.

Path-planning processes is considered for leading manipulation tasks such as assembly, maintenance or disassembly in a virtual reality (VR) context. The approach consists in providing a collaborative system associating a user immersed in VR and an automatic path planning process. It is based on semantic, topological and geometric representations of the environment and the planning process is split in two phases: coarse and fine planning. The automatic planner suggests a path to the user and guides him through a haptic device. The user can escape from the proposed solution if he wants to explore a possible better way. In this case, the interactive system detects the user's intention and computes in real-time a new path starting from the user's guess. Experiments illustrate the different aspects of the approach: multi-representation of the environment, path planning process, user's intent prediction and control sharing.

4

Decision Support System in Product Engineering

Chapter Editors:
César Otero
University of Cantabria
Ingegraf Society, Spain

Pierpaolo Valentini
Universitá di Roma Tor Vergata
ADM Society, Italy

4.1 Modelling for Optimization

Contribution 1

Title:	Optimal Design of Sandwich Plates with Honeycomb Core.
Authors:	A. Catapano, M. Montemurro.
Key Words:	honeycomb, homogenisation, optimization, sandwich panels, genetic algorithm.

The problem of the optimum design of a sandwich structure composed of two laminatedskins and a honeycomb core is analyzed. The goal is to propose a numerical optimisation procedure that does not make any simplifying hypothesis in order to obtain a true global

X. Fischer et al. (eds.), *Research in Interactive Design (Vol. 4)*
DOI 10.1007/978-3-319-26121-8_4

optimal solution for the considered problem. In order to face the design of the sandwich structure at both meso and macro scales, weuse a two-level optimisation strategy. At the first level, we determine the optimum geometry of the unit cell together with the material and geometric parameters of the laminated skins, while at the second level we determine the optimal skins lay-up giving the geometrical and material parameters issued from the first level. We illustrate the application of our strategy to the least-weight design of a sandwich plate submitted to several constraints: on the first buckling load, on the positive-definiteness of the stiffness tensor of the core, on the ratio between skins and core thickness and on the admissible moduli for the laminated skins.

Full Article: 070-pds-22 Page: 222

Contribution 2

Title: Genetic Algorithm Optimization and Robustness Analysis for the Computer Aided Design of Fixture Systems in Automotive Manufacturing.

Authors: Matteo Ansaloni, Enrico Bonazzi, Francesco Gherardini, Francesco Leali.

Key Words: automotive manufacturing, computer aided fixture design, multi-objective optimization, robust analysis.

Fixture Systems (FS) have great importance in machining, welding, assembly, measuring, testing and other manufacturing processes. One of the most critical issue in FS design is the choice of both the type of fixing devices such as clamps, locators, and support points, (configuration), and their arrangement with respect to workpieces (layout). Several authors deal with the problem of determine the most suitable solution for FSs, often investigating their layout without considering the change of the type of locators. A computer aided design method is proposed to compare and evaluate different configurations for a FS, optimizing the locator type and analysing the roboustness of the solution. A multi-objective optimization based on a genetic algorithm is presented and the selection of the most suitable configuration is performed trough the definition of robustness indexes. The effectiveness of the design method is demonstrated for an automotive case study.

Full Article: 062-cad-74 Page: 229

Contribution 3

Title: Using the Optimisation Methods to Minimize the Machining Time on the Free-Form Surfaces in 3-axis Milling.

Authors: S. Djebali, S. Segonds, J.M. Redonnet, W. Rubio.

Key Words: machining zones, 3-axis milling, free-form surfaces, path length tool, optimization methods.

The object of the study is to minimize the machining time on the free-form surfaces while respecting a scallop height criteria. The analytical expression of the machining time is not known. By hypothesis, it is assumed proportional to the path length crossed by the cutting tool on the surface. This length depends on the feed direction and it is influenced by the topology of the surface. To have an optimal feed direction at any point, the surface is divided into zones with low variation of the normal. Each zone has an optimal feed direction and minimum path length. Furthermore, a penalty reflecting the time of movement of the tool from a zone to another one is taken into account. Several algorithms are used to resolve this problem: Clarke and Wright, Greedy Randomized Adaptive Search Procedure, Tabu search and Nearest neighbor search. A concrete example is illustrated.

Full Article: 045-pp-27 Page: 236

Contribution 4

Title: Storage Assignment Problem in logistics Warehouses: Optimization of Picking Locations by Cross-Entropy Method.

Authors: Olivier Devise, Jean-Luc Paris, Séverine Durieux, Pierre-Guillaume Fradet.

Key Words: supply chain, warehousing, storage assignment problem, combinatorial optimization, crossentropy method.

The study covers a combinatorial optimization method called

cross-entropy method. We used this method to solve an optimization problem: implementations of products in order to minimize the total distance traveled by workers during the picking order. After developing a state of the art regarding issues that a-ect the design of logistics warehouses, we will develop an overview of methods used to solve and/or optimize this type of problem. Cross-entropy method applied to shortest path problem will be developed and we will show this method can be used easily to solve an optimization problem in logistics area.

Full Article: 066-ap-84 Page: 243

4.2 Modelling of Experiment for Decision Making

Contribution 1

Title:	Influence of Minimum Quantity Lubrication Design Parameters on Milling Finishing Process.
Authors:	Arnaud Duchosal, Roger Serra, René Leroy.
Key Words:	computational Fluid Dynamics, Minimum Quantity Lubrication, Milling, Finishing Process, Taguchi method.

A numerical study of the Minimum Quantity Lubrication (MQL) design parameters effects outside a rotating tool is presented. Parameters as particle sizes for different oil mist input device parameters (inlet pressures) as function of different canalization geometries have been determinate on a previous experimental part, which are not presented here. The parameters thus identified were integrated as boundary conditions for the numerical simulation of a rotating tool during a milling surfacing process with different canalization orientations. The chip removal is not considered here. Only the numerical effectiveness of the minimum quantity lubrication is taken into account. The main goal of the oil mist is to spray the cutting edge to ensure a good lubrication on the tool-chip contact area. The simulations highlighted the impingement of the different oil particle sizes on the tool carbide inserts. A volume per unit area and a mean distance of the oil scatter from droplet impingements relative to a global virtual area from

tool/chip interface were considered. The global virtual area was taken as function of the feed rate. The Taguchi method is applied in order to optimize numerical design parameters in finishing conditions as function of different parameters. The minimum quantity lubrication design parameters evaluated are canalization orientations, inlet pressure, feed rate and particle sizes. The analysis shows that Taguchi method is suitable to solve this numerical problem. The results shows that the optimal combination for a high lubrication performance at high cutting speed is based on high feed rate, with high canalization orientations and mean particle sizes.

Full Article: 061-cad-112 Page: 250

Contribution 2

Title:	A Statistical Model for Prediction of Tool Wear and Cutting Force During High Speed Trimming of Carbon Fibre Reinforced Polymers.
Authors:	Mohamed Slamani, Jean-François Chatelain, Hossein Hamedanianpour.
Key Words:	composite, CFRP, Trimming, Tool Wear, Cutting Force.

The combination of low thermal conductivity and highly abrasive nature of Carbon Fibre Reinforced Polymers (CFRPs) leads to rapid tool wear and numerous machining problems. The development of tool wear and cutting force prediction models in the high speed trimming of CFRPs is presented. A 3/8 inch diameter CVD diamond-coated carbide tool with six straight flutes was used to trim 24-ply carbon fibre laminates. Cutting speeds ranging from 200 m/min to 400 m/min and feed rates ranging from 1524 mm per minute to 4064 mm per minute were used in the experiments. Exponential models were adjusted to predict tool wear and cutting force for different values of cutting speed, feed and cutting length. The ANOVA approach was used to test the overall significance of the models by applying F-tests. The results obtained show that the exponential model is capable of accurately predicting the cutting force and tool wear under the conditions studied.

Full Article: 043-pp-3 Page: 257

4.3 From Knowledge Based Engineering to Knowledge Re-use

Contribution 1

Title: GUI Usability Improvement for a New Digital Pattern Tool to Assist Gearbox Design.

Authors: S. Patalano, D. M. Del Giudice, S. Gerbino, A. Lanzotti, F. Vitolo.

Key Words: usability assessment, Graphical User Interface, gearbox design, participatory design.

Design team can speed up the process of managing information related to gearbox design process by adopting digital pattern tools. These tools, as KBE systems, can assist engineers in re-using previous knowledge in order to improve time-consuming task as retrieval and selection of previous architectures and to modify and virtually test a new gearbox design. A critical point in the development of a KBE system is the interface usability to demonstrate effective reduction of development time and satisfaction in its use. In this paper, the authors face the problem of usability improvement of the Graphical User Interface (GUI) of the KBE system previously proposed. An approach based on Analytic Hierarchy Process (AHP) and Multiple-Criteria Decision Analysis (MCDA) has been used. A participatory test has been performed for evaluating the Usability Index (UI) of the GUI. Taking into account the data analysis some changes have been carried out and a new GUI release has been validated with new experimentations.

Full Article: 059-cad-71 Page: 263

Contribution 2

Title:	Information Feedback from CNC to CAM through OntoSTEP-NC.
Authors:	Christophe Danjou, Julien Le Duigou, Benoit Eynard.
Key Words:	STEP-NC, OntoSTEP-NC, closed-loop manufacturing, Manufacturing Process Management.

A proposition to ensure closed-loops manufacturing from CNC machines to CAD/CAM systems is exposed. As STEP-NC allows bi-directional exchanges but does not allow incrementing traceability of machining program, the proposition set up loops using PLM systems. This proposition is based on the new OntoSTEP-NC ontology which provides trades between PDM (Product Data Management), MPM (Manufacturing Process Management) and ERP (Enterprise Resource Planning). As a solution OntoSTEP-NC is the basis to data extraction from CNC machines, and relevant information reinjection to CAM systems. To have the most relevant information reinjection a feature recognition stage has been introduced. Moreover, coupled to Case Base Reasoning, this recognition loop will allow incrementing the MPM database. This proposition will help program planner making choices based on company good practices.

Full Article: 029-itm-111 Page: 270

4.4 Knowledge Processing

Title:	Constraint-Based Decision Support System: Designing and Manufacturing Building Facades.
Authors:	A. F. Barco, E. Vareilles, M. Aldanondo, P. Gaborit, M. Falcon.
Key Words:	computer aided design, layout synthesis, building renovation, constraint satisfaction problems, constraint-based algorithms.

Layout synthesis algorithms in civil engineering have two major strategies called constructive and interactive improvement. Both strategies have been successfully applied within different facility scenarios such as room configurations and apartment layouts. The study contributes with layout synthesis field by developing a constraint-based algorithm for the layout design of building facades. The French project CRIBA is introduced: it aims to industrialize the thermal renovation of apartment buildings. Conception of the renovation, generation of bill of materials and generation of the working site assembly process are then supported by our system. Details of the layout design algorithm and its underlying model are detailed.

Full Article: 064-cad-83 Page: 276

4.5 Knowledge in the Digital Factory

Title: Towards Management of Knowledge and Lesson Learned in Digital Factory.

Authors: Marwa Bouzid, Mohamed Ayadi, Vincent Cheutet, Mohamed Haddar.

Key Words: digital factory, lesson learned, knowledge management, simulation, information system.

In a world characterized by increasing competitiveness, delivering a good product as soon as possible and increasing complexity of the product, the old method did not satisfy the needs of companies. In this context the Digital Factory is a solution that is based on the simulation and analysis of all the process of product production to reduce the cost of prototyping and physical testing. But, despite his performance there is a lack of deployment related to the lack of integration of information, knowledge and feedback. We proposed a model that includes the integration of all the information, knowledge and Lesson Learned.

Full Article: 028-itm-106 Page: 283

5

Geometric Modelling and CAD

Chapter Editors:
César Otero
University of Cantabria
Ingegraf Society, Spain

Pierpaolo Valentini
Universitá di Roma Tor Vergata
ADM Society, Italy

5.1 Advances in Geometric Representation

Title: Identification of Tree Species from Airborne LIDAR Point Clouds; early Approaches.

Authors: J. Santamaría, M.A. Valbuena, F. Sanz, D. Arancón, A. Martínez.

Key Words: lidar, convex hull, tree identification.

LIDAR flights with multi-objective are every day more widespread. Governments are aware of the high potential that can be derived from point clouds obtained from these flights. One of the major fields in which applications are developed is the agroforestry field, especially related to forest management of large numbers of trees. Quickly parameters

X. Fischer et al. (eds.), *Research in Interactive Design (Vol. 4)*
DOI 10.1007/978-3-319-26121-8_5

forests and even individual trees are achieved. We intend to initiate a new guidance on the use of LIDAR data in order to identify tree species through the envelope profile of the cloud of points composing each individual tree. The projection of the point cloud of individual trees and the study of their convex hull, will characterize a given forest stand and assign a particular species. The method used is primarily on the analysis of two-dimensional projection of the point cloud of an individual tree and obtaining their convex hull. The study of the geometrical characteristics of said envelope to a representative number of trees and their association with forest parameters such as the maximum width or height glass plant mass , will assign the woodland studied a typology of particular species.

Full Article: 063-cad-26 Page: 292

5.2 From CAD to Engineering

Contribution 1

Title:	A Preliminary Study on Cleft Lip Pathology Trough 3D Geometrical Analysis.
Authors:	Sandro Moos, Federica Marcolin, Stefano Tornincasa, Enrico Vezzetti, Maria Grazia Violante, Domenico Speranza.
Key Words:	3D ultrasound, 3D echography, syndrome diagnosis, dysmorphisms, 3D face.

A new solution leads to automatically diagnose and formalize prenatal cleft lip with representative key points and identify the type of defect (unilateral, bilateral, right, or left) in three-dimensional ultrasonography (3D US). Differential Geometry has been used as a framework for describing facial shapes and curvatures. The descriptive accurateness of these descriptors has allowed us to automatically extract reference points, quantitative distances, labial profiles, and to provide information about facial asymmetry.

Full Article: 05-cad-63 Page: 297

Contribution 2

Title:	Mesh Processing for Morphological and Clinical Parameters Computation in Dog Femur.
Authors:	G. Savio, T. Baroni, G. Concheri, M. Isola, E. Baroni, R. Meneghello, M. Turchetto, S. Filippi.
Key Words:	mesh, dog, femur, mesh processing, mesh segmentation, varus, torsion.

Currently available methods for evaluating dog femur deformities are principally based on 2D image analysis of radiographies. By CT or MRI, 3D information can be derived from points clouds or meshes. An original approach for morphological and clinical parameters assessment on meshes is presented. The method is validated on dog femur meshes measured by two 3D scanners with different resolutions. The results show that the 3D proposed approach overcomes several limits of the methods based on 2D image analysis.

Full Article: 077-cadcae-61 Page: 302

5.3 Reverse Engineering

Contribution 1

Title:	Characterization of Ultra-Precise Aspherical Surfaces Using Forbes Equation.
Authors:	N. El-Hayek, N. Anwer, H. Nouira, M. Damak, O.Gibaru.
Key Words:	asphere, form characterization, hight precision metrology, non linear least-squares method.

The field of application and use of aspherical lenses is a growing market. Although many researches have been conducted to address their manufacturing and measurement, there are still challenges in form characterization of aspherical surfaces considering a large number of data points. The study presents the measurement and form characterization of an asphere using a high precision profilometer,

traceable to the SI meter definition. The measured surface is constituted of a large number of data points. The form characterization of the aspheres surface is based on the comparison of the measured surface with the design surface, expressed as a Forbes strong asphere. The Levenberg-Marquardt algorithm is used and tested on simulated surface fitting. Experimental results are then analysed and discussed on real data and show the effectiveness of the proposed approach.

Full Article: 067-m-43 Page: 308

Contribution 2

Title:	Testing the Influence of Scanning Parameters On 3D Inspection Process with a Laser Scanner.
Authors:	Salvatore Gerbino, Gabriele Staiano, Antonio Lanzotti, Massimo Martorelli.
Key Words:	3d laser scanner, scanning parameters, 3d inspection, reverse engineering.

The quality of 3D scanned data is influenced by many factors both related to internal elements to the acquisition device, such as scanner resolution and accuracy, and external to it, such as proper selection of scanning parameters, ambient illumination and characteristics of the object surface being scanned (e.g. surface colour, glossiness, roughness, shape). Due to the recent developments in terms of accuracy, in particular for 3D laser scanners, today it is of great industrial interest to study and correctly setting the scanning parameters that allow to improve the quality of the 3D acquisitions so to increase the massive usage of these systems in the product inspection activities. In this paper the effects of some scanning parameters that may affect the measurement process, were analysed by using a commercial triangulation 3D laser scanner. The test geometry chosen for this study was a commercial sheet metal part more complex than the ones commonly used in laboratory and documented in the literature. Relative orientation, ambient illumination and scanner parameters were tested. The outcomes of the tests confirmed some results and suggestions documented in literature but also pointed out that over different conditions the most influencing factor are the relative orientation of the object with respect to the scanner, as well as its position within the field of view of the measurement device.

Full Article: 069-m-95 Page: 314

5.4 Integration of Tools

Contribution 1

Title: Prediction of CAD Model Defeaturing Impact on Heat Transfer FEA Results Using Machine Learning Techniques.

Authors: Florence Danglade, Philippe Veron, Jean-Philippe Pernot, Lionel Fine.

Key Words: defeaturing, CAD model, finite element analysis, machine learning, a priori estimation.

Essential when adapting CAD model for finite element analysis, the defeaturing ensures the feasibility of the simulation and reduces the computation time. Processes for CAD model preparation and defeaturing tools exist but are not always clearly formalized. We propose an approach that uses machine learning techniques to design an indicator that predicts the defeaturing impact on the quality of analysis results for heat transfer simulation. The expertise knowledge is embedded in examples of defeaturing process and analysis, which is used to find an algorithm able to predict a performance indicator. This indicator provides help in decision making to identify features candidates to defeaturing.

Full Article: 080-cadcae-11 Page: 321

Contribution 2

Title: NURBS Patch Coupling with Nitsche Method for Isogeometric Analysis.

Authors: Stefano Tornincasa, Elvio Bonisoli, Marco Brino.

Key Words: NURBS, isogeometric analysis, multi-patch, Nitsche method, weak coupling.

To model geometrical entities with a certain complexity to be verified with isogeometric analysis (IGA) it is often necessary to use multi-patch. Nitsche method allows the possibility of coupling the different patches even though the mesh at the interface is not conforming. Examples of three dimensional models are analysed for linear static and modal analysis to validate the method.

Full Article: 079-cadcae-77 Page: 327

5.5 Exploring Ways of CAD Using

Contribution 1

Title: Reverse Engineering for Manufacturing REFM of Parts in a Routine Context: Use of Graph Description and Matching Algorithm.

Authors: Salam Ali, Pierre Antoine Adragna, Alexandre Durupt.

Key Words: reverse engineering, process planning, matching, manufacturing, adjacency graph.

Industrial companies need new ways for defining directly a CAPP (Computer Aided Process Planning) model of an existing part from 3D information. They are confronted to avoid the passage by the CAD model; since existing solutions in the literature are based on CAD models reconstructed from 3D information to define the process planning. A new solution is detailed: it leads to the reusing of a generated CAPP model stored in a RE database in order to reengineer a new part. To apply this concept, a matching method between two adjacency graphs is used to associate the surface precedence graph of a part in the RE database to the query part. The use of the adjacency graph of a part and the matching algorithm is proposed: they lead to the association of existing CAPP model to a new part being remanufactured.

Full Article: 057-cad-55 Page: 333

Contribution 2

Title: New Standard of Dimensioning Adapted to the Programs CAD. Creation and Unification of Symbols Dimensioning.

Authors: David Arancon, Felix Sanz-Adan, Jacinto Santamaria, Alberto Martínez-Rubio.

Key Words: geometric modelling, standard dimension, CAD, technical drawing.

Vector design of objects (CAD3D) indicates its dimensions according to standards previous to existence of the CAD3D systems. In many cases, it does not meet the needs of new Information and Communication Technologies (ICT), causing the repetition of dimensioning tasks in the successive stages of product development. The dimensional standards currently used, take a long product launch time. The research states a methodology for dimensioning which allows the designer to provide the graphical representation of the product with geometric and dimensional information, complete, accurate and universal; design time is shortened and productivity is increased. As result of this methodology a new international standard of dimensioning is proposed, which unifies the utilization of signs adapted to 3D design as alternative to those currently in use and allows obtaining clearer technical drawings and with less dimensions. This proposal for a new standard has been validated by a comparative review of the most widespread dimensioning standards.

Full Article: 060-cad-91 Page: 340

5.6 CAD for Manufacturing

Contribution 1

Title: Evaluating Current CAD Tools Performances in the Context of Design for Additive Manufacturing.

Authors: A.H Azman, F.Vignat, F. Villeneuve.

Key Words: designing process, computer-aided-design, designing methodology, additive manufacturing.

Metallic Additive Manufacturing is a technology which opens a new world of opportunities in design and manufacturing. It is mainly based on melting metallic powder layer by layer and turning it into direct end user parts. The creation of complex part forms and lightweight structures have become easier with Additive Manufacturing through large usage of lattice structures. However, current design methods and Computer-Aided-Design (CAD) tools are not tailored for this type of shapes and are not yet optimized to achieve the great potential offered by this new technology. The breakthrough in manufacturing technology is not yet followed by a breakthrough in design and CAD tools. The current study aims at evaluating current CAD softwares performances and proposes requirements for CAD tools to be efficient in design for additive manufacturing. The results show that current CAD tools and CAD file formats have insufficient performance in the context of design for Additive Manufacturing and a new file format together with new CAD human interaction needs to be created to overcome these problems.

Full Article: 040-pp-44 Page: 347

Contribution 2

Title: Influence of the Tool-Material Couple on the Dental CAD CAM Prosthetic Roughness.

Authors: N. Lebon, L. Tapie, E. Vennat, B. Mawussi, JP. Attal.

Key Words: roughness, dental materials, surface integrity, tool-material couple, milling.

The study aims at investigating the tool-material couple in CAD/CAM dental machining. The tool-material couple is studied through the observation of milled surface roughness and tool geometrical properties. The influence of two tool-material couple parameters is also studied: the feedrate and the milling mode (flank, top). Three diamond burs and three dental biomaterials (ceramic, polymer, hybrid) were tested. The surface roughness was observed for nine tool-material couples in flank and top milling. Ra, Rt, Rz, Sa, Sq, Sz roughness criteria were measured. It has been concluded that in flank milling the measured surface roughness is in direct proportion to the diamond tool grain size. In top milling, the roughness is mainly due to the diamond

grain size, and the radial depth is not a predominant parameter. The surface roughness was influenced by material hardness in flank milling mode. Moreover, the surface roughness was not affected by the feedrate.

6

Innovation in Product Engineering

Chapter Editors:
María Luisa Martinez
Polytechnic university of Madrid
Ingegraf Society, Spain

Maurizio Muzzupappa
Universitá della Calabria
ADM Society, Italy

Jean-François Boujut
INP Grenoble
AIP PRIMECA Society, France

6.1 Collaborative and Cooperative Design

Contribution 1

Title:	An Approach for Defining a Collaborative Platform to Support the Development of Corporate Engineering Standards.
Authors:	Rachad El-Badawi-El-Najjar, Guy Prudhomme, Nicolas Maussang-Detaille, Eric Blanco.

X. Fischer et al. (eds.), *Research in Interactive Design (Vol. 4)*
DOI 10.1007/978-3-319-26121-8_6

Key Words: standards, standardization, collaborative platform, collaborative platform specification process.

In a global economy, the conquest of new markets has led many companies to expand their business around the globe. However, new challenges have aroused from this expension. Our study field context is Alstom Hydro that designs and manufactures hydraulic turbines. The research aims at studying and supporting the involvement of experts and future users in the co-creation of corporate engineering standards. A collaborative platform specification method and a collaborative standardization process are presented. Formalizing the standardization process stands as a key element of the approach, and we will explain, based on field studies and focus groups, how this was done within the company. Then, we will detail how this standardization process was used to define the collaborative platform, its main features, roles and privileges.

Full Article: 034-i-53 Page: 362

Contribution 2

Title: Towards the Success of Design Projects by the Alignment of Processes in Collaborative Engineering.

Authors: Rui Xue, Claude Baron, Philippe Esteban, Daniel Esteve, Michel Malbert.

Key Words: system design, engineering processes, project management, systems engineering standards, decision support.

With increasingly complex systems, relying on systems engineering (SE) as an interdisciplinary method to manage engineering processes is becoming essential for companies. However, too many projects still fail and industrial groups have argued that these failures may be related to the managerial techniques used. Indeed organizational processes are more or less specifically mentioned in SE standards but in practice project managers tend to rely more on their own standards which sometime set forth practices not in line with those of the SE domain, hence the reported discrepancies which very often lead to project failure. Thus to improve the companies competitiveness when developing new

products, cooperation between processes related to system development and project management (PM) is key to getting performance and success. New arguments are detailed: they tend to support this theory and introduces an ongoing project with a method and tool aiming to integrate both domains.

Full Article: 035-i-86 Page: 369

Contribution 3

Title: UP: A Unified Paradigm to Compare Computer-Based and Paper Based Supporting Tools for Collective Co-Located Preliminary Engineering Design Activities.

Authors: Thierry Gidel, Andrea Luigi Guerra, Enrico Vezzetti.

Key Words: disruptive innovation, design methods and tools, design observations paradigm, computer supported cooperative Work in design, design research.

Are Computer Supported Cooperative Work in Design (CSCWD) media worth to be used or do we need to maintain the traditional paper-based ones? Several studies exist, but address heterogeneous functions and criteria, and are not comparable. This contribution introduces an exploratory study toward a Unified Paradigm of evaluation (UP). UP aims to ease the set-up of comparable design studies to evaluate if CSCWD are worth to be used in respect of actual supports. The most adapted paradigm to provide a valuable answer prescribes ethnographic qualitative descriptive studies between a traditional paper-based and a CSCWD media. A scenario centered on a common function is presented (isofunctional comparison). The criterion assessed is effectiveness, expressed as the combination of efficacy and usefulness. Efficacy is measurable through objective factors. Usefulness is measurable through subjective factors. In order to confront studies involving different people, we suggest that individual characteristics should be properly considered.

Full Article: 038-i-100 Page: 375

6.2 Interoperability in Design

Title: Consistency Management and PLM Interoperability to Support Collaboration in Preliminary Design.

Authors: Diana Penciuc, Alexandre Durupt, Matthieu Bricogne, Benoit Eynard.

Key Words: collaborative engineering, preliminary design, product lifecycle management, PLM interoperability, PLM connector.

During design, several actors contribute with their expertise in specific design tasks and need to collaborate several times in order to validate the decisions taken in order to converge to a common-agreed solution. Although a lot of tools exist to support collaborative activities during design, there still is a lack of tools enabling the integration of all the engineering results and consistency check. To overcome this drawback, a new approach of Product Lifecycle Management (PLM) interoperability is proposed in this paper, taking in account the coherence and collaboration needs specific to early design activities. The proposal is explained trough a case study and PLM connector prototype.

Full Article: 037-i-48 Page: 382

6.3 Knowledge Management and Innovative Engineering

Contribution 1

Title: Facilitating Integration to Face Modern Quality Challenges in Automotive.

Authors: A. Riel, S. Tichkiewitch, C. Kreiner, R. Messnarz, D. Theisens.

Key Words: integration, quality, knowledge management, integrated manufacturing, sector skill alliance.

Assuring quality in automotive has grown to a huge challenge and

competition factor driven mainly by the permanent cost pressure in a mass market that is increasingly confronted with the safety criticality of various mechatronic systems and subsystems. The most successful companies have realized the necessity of integrating the development and manufacturing processes significantly more than this is done today even in the most innovative industrial organizations. This article introduces a novel vehicular qualification concept facilitating this integration process for quality and risk management in automotive industry. In particular, this concept integrates the various dimensions of the quality, safety and reliability of automotive products and systems as well as their associated processes in a way that allows quality, reliability, and safety experts from development and manufacturing to collaborate in an integrated manner.

Full Article: 037-i-57 Page: 389

Contribution 2

Title: Toward a Descriptive Model of Knowledge Transfer within Organisations.

Authors: J. Mougin, J-F Boujut, F. Pourroy, G. Poussier.

Key Words: knowledge transformation, descriptive model, participant observation, knowledge management.

Design activities are becoming more and more complex. This leads designers to work in highly collaborative and distributed teams. The Purpose of this study is to investigate on improving the use of KMS by defining a descriptive model of the knowledge transfer within engineering teams. We started by a literature review and we adopted a participant observation methodology in order to propose this model. Then we tested our model through case studies. This investigation enables us to observe, define and model more finely the dynamics of the exchanges between knowledge workers.

Full Article: 033-i-23 Page: 395

Contribution 3

Title: Innovative Field Exploration and Associated Patent Portfolio Design Models.

Authors: Olga Kokshagina, Pascal Le Masson, Benoit Weil, Yacine Felk.

Key Words: industrial property, innovation, patent design, C-K Theory, patentability criteria.

Patents play an ever-increasing role in the modern economies and are often used as a measure of technology innovativeness. The purpose of this studyn is the innovative field exploration where companies are constantly under pressure to generate high quality patents that will ensure future firms growth, their survival and protect their inventions at the early stages of technological exploration. The work builds on the methods of patent modeling that appear to be adapted for disruptive innovation. By drawing on the patentability criteria, their interpretation in the patent model driven by the design theory frameworks like Concept-Knowledge theory, the paper examines the means of applicability of these methods within the high-velocity industries like semiconductors or nanotechnologies. As a result, two processes of patent design are proposed: 1) technology design that brings to define patent proposals or 2) patent proposals design that add new innovative attributes prior to technology creation. The insights are given on which approach companies have to pursue regarding their problematic.

Full Article: 036-i-99 Page: 402

Contribution 4

Title: Preliminary Contributions of Industrial Management Methods to Microfactory Context: Case of Micro-Conveyors Integration.

Authors: Magali Bosch-Mauchand, Christine Prelle, Joanna Daaboul, The Anh Tuan Dang, Sandy Bradbury Lobato.

Key Words: microfactory, micro-conveyor, control, information system.

The increased interest in manufacturing smaller products leads to develop automatic, flexible, reconfigurable and upgradable microfactory systems. To achieve this, a specific information system is required

to have access to the small scale of the micro-world and to control it. The conveying systems used to transport the micro-components within the microfactory have specific characteristics adapted to the small scale requirements. The proposed approach consists in defining the technical information system needed to control and manage specific micro-conveyors using the Unified Modeling Language (UML). At the Université de Technologie de Compiègne, some researchers of the Roberval Laboratory have been working on the mechatronic devices used in the micro scale. These include actuators, sensors, three-dimensional optical inspection and conveyance systems. An initial database for managing the technical information of these systems is created. Conventional industrial management methods are analysed for their adaptation and application on microfactories.

Full Article: 031-itm-42 Page: 409

7

Sustainability

Chapter Editors:
Xavier Espinach
University of Girona
Ingegraf Society, Spain

Antonio Mancuso
Universitá di Palermo
ADM Society, Italy

Benoit Eynard
UT Compiègne
AIP PRIMECA Society, France

7.1 From Product Life Cycle Integration to Ecodesign

Contribution 1

Title:	Life Cycle Analysis in Preliminary Design Stages.
Authors:	Lina-María Agudelo, Ricardo Mejía-Gutiérrez, Jean-Pierre Nadeau, Jérôme Pailhes.
Key Words:	life cycle analysis, eco-design, design process.

In a design process the product is decomposed into systems along

X. Fischer et al. (eds.), *Research in Interactive Design (Vol. 4)*
DOI 10.1007/978-3-319-26121-8_7

the disciplinary lines. Each stage has its own goals and constraints that must be satisfied and has control over a subset of design variables that describe the overall system. When using different tools to initiate a product life cycle, including the environment and impacts, its noticeable that there is a gap in tools that linked the stages of preliminary design and the stages of materialization. Different eco-design methodologies under the common denominator of the use of a life cycle analysis have been compared in time efficiency of use and in which stages of the life cycle they can be used. A case study was developed by the application of these methodologies to obtain first-hand information and interpretable results to define advantages and disadvantages of the selected methodologies.

Full Article: 019-sd-18 Page: 418

Contribution 2

Title:	Integration of End-of-life Options as a Design Criterion in Methods and Tools for Ecodesign.
Authors:	Yoann Le Diagon, Nicolas Perry, Stéphane Pompidou, Reidson Pereira Gouvinhas.
Key Words:	ecodesign, design for X, life cycle assessment, end-of-life, wind turbine.

Ecodesigning a product consists (amongst other things) in assessing what its environmental impacts will be throughout its life (that is to say from its design phase to its end of life), in order to limit them. Some tools and methods exist to (eco)design a product, just like methods that assess its environmental impacts (more often, a posteriori). But it is now well accepted that these are the early design decision that will initiate the greatest consequences on the products end-of-life options and their impacts. Thus, the present work aims at analysing traditional design tools, so as to integrate end-of-life possibilities in the form of recommendations for the design step. This proposal will be illustrated by means of a wind turbine design.

Full Article: 020-sd-20 Page: 425

Contribution 3

Title: Increase Sustainability of Decentralized Electricity with Remotely Monitored Product-Service Systems.

Authors: Kevin Wrasse, Haygazun Hayka, Anne Pförtner, Rainer Stark.

Key Words: product service system, solar home system, decentralized electricity, lifecycle-engineering, remote monitoring.

Solar home systems (SHS) are a potential sustainable solution for rural areas of developing countries in order to supply human beings with electricity. However those SHS face many challenges in those particular areas e.g. minimal traffic infrastructure, inadequate education or declining confidence in handling this technology. Therefore, SHS give much of its potential away to improve all dimensions of sustainability. A new approach is described which is applied within the MESUS (micro-energy supply system) project where SHS as a single product are shifted to a product-service system in combination with an information system based on remote monitoring. Sustainability can be increased by focusing on customer needs with respect to the whole product lifecycle. Efficiency of service processes is increased by gathering and analysing operational data. In conclusion, the new approach is capable of granting incentives for providers of SHS and their end-users to create long-term satisfactory relationships and to support the socio-economic development.

Full Article: 022-sd-82 Page: 432

7.2 Design, Recycling and Decycling

Contribution 1

Title: DFD Evaluation for not Automated Products.

Authors: Daniela Francia, Gianni Caligiana, Alfredo Liverani.

Key Words: design for disassembly, handcrafted product, assembly time, disassembly time, reusing of parts.

The design process is subjected to economical and environmental restrictions since the early phases of preliminary design. Recycling or reusing of parts have to be optimized in order to enhance the ecological impact of a product. This impact can be evaluated through the disassembly capability of joints assembling the product, even when the production process is subject to an important contribute of workmanship. In this paper a useful method is proposed to analyze the disassembly capability of products, also of handcrafted products, in order to optimize the design process in the early preliminary phase. The aim is to define some parameters that describes the attitude of a product to be disassembled by means of the evaluation of an index. The Disassembly Index is influenced by three parameters: the number of different materials of each joint, the time necessary to disassemble each joint, the recoverability of parts after the disassembly is completed.

Full Article: 021-sd-46 Page: 439

Contribution 2

Title: Disassembly Sequencing for End-of-life Products.

Authors: H. Said, P. Mitrouchev, M. Tollenaere.

Key Words: disassembly, disassembly sequences, modules, products, hierarchical analysis.

When a product reaches its end of lifecycle, its components can be reused, recycled or disposed depending on their conditions and recovery value. All these strategies involve the disassembly of products. A method for generation of disassembly sequences is proposed. It is based on hierarchical analysis of the modules constituting the product. The method uses information such as: list of subsets (modules), liaison-component graph, part geometry, functional contacts between components and modules, component properties (density, surface treatment,) all contained in a database. It has been tested on several products disassembly. The application of the method is explained with an example.

Full Article: 023-sd-109 Page: 446

7.3 Sustainable Manufacturing

Contribution 1

Title:	Toward Sustainable Manufacturing: Evaluation of the Economic and Ecological Impacts of Production Lines.
Authors:	Michele Germani, Marco Mandolini, Marco Marconi, Eugenia Marilungo.
Key Words:	environmental and economic sustainability, sustainable manufacturing, energy consumption.

The sustainable manufacturing is becoming an ever more important research topic since the industry is the main responsible of the environmental problem. A method leads from the estimation of the economic and ecological impact of production lines to the aim of favouring the adoption of sustainable processes within a manufacturing company. It considers the whole lifecycle, from manufacturing to use and maintenance, till dismantling at the end-of-life. The method considers costs and environmental impacts of the initial deployment (i.e. initial investment and set-up), use (i.e. workload or maintenance required by each machine) and end of life (i.e. retirement) of the analysed system. The method has been validated by a company producing extruded plastic pipes, during the re-design of one of its production lines.

Full Article: 024-sd-17 Page: 452

Contribution 2

Title:	IT Framework for Sustainable Manufacturing.
Authors:	Kiyan Vadoudi, Nadege Troussier, Toney Wh Zhu.
Key Words:	sustainability manufacturing, eco design, product lifecycle management, geographical information system, lifecycle assessment.

With today's global awareness of environmental issue as well as social and economic aspects, manufacturing industry is seeking a comprehensive strategic approach to be more sustainable. By continuous sharing of information among the different product lifecycle phases

product lifecycle management acts as an information strategy, which builds a coherent data structure by consolidating systems. Moreover, when the manufacturing is happening, there is location base information available within manufacturing process, which can be used into tools to assess manufacturing process in context of sustainability. A new information strategy framework is presented: the green manufacturing paradigm based on integration between current PLM structure and geographical information systems is the core of the study. The proposed IT framework is a comprehensive qualitative answer to the question of how to design and/or improve green manufacturing systems as well as a roadmap for future quantitative research to better evaluate this new paradigm.

Full Article: 026-sd-108 Page: 459

7.4 Design for Energy Efficiency

Title: Design Methodology for Energy Efficiency of Production System.

Authors: T.A.L. Nguyen, M. Museau, H. Paris.

Key Words: energy efficiency, production system, energy consumption, design for energy efficiency, methodology.

Nowadays, it is important to reduce the energy consumption of production system because of the deficit of energy resource, the growing concern of the carbon emission and environment impact in industrial production. Therefore, to achieve the long term goal sustainable manufacturing, energy efficiency has to be considered as the central priority in the design process of the production system. In this paper, the principal objective is to present the issues of the integration of energy efficiency in the design process and then to propose a design methodology to redesign the production system with a high energy efficiency, while maintaining the initial manufacturing process. First of all, an analysis of existing production system is realized in order to identify the opportunities of saving energy in production system. From that, the strategies to reduce energy consumption of production system will be identified and proposed. Then, these scenarios of redesign will be tested to obtain the information of the best scenario of redesign.

Full Article: 025-sd-47 Page: 466

8

Manufacturing Process

Chapter Editors:
Antonio Bello
University of Oviedo
Ingegraf Society, Spain

Salvatore Gerbino
Universitá del Molise
ADM Society, Italy

Yann Landon
Manufacturing 21
AIP PRIMECA Society, France

8.1 Advanced Solutions in Product Manufacturing

Contribution 1

Title:	Profile Incision Modeling in Abrasive Waterjet Milling of Titanium Alloys Ti6Al4V.
Authors:	Tarek Sultan, Patrick Gilles, Guillaume Cohen, François Cenac, Walter Rubio.

X. Fischer et al. (eds.), *Research in Interactive Design (Vol. 4)*
DOI 10.1007/978-3-319-26121-8_8

Key Words: abrasive waterjet milling, incision, titanium alloy, process parameters, gaussian model.

Abrasive water jet milling (AWJM) is a new way to perform controlled depth milling especially for hard materials, but it is not yet enough reliable because of large variety of process parameters and complex footprint geometries that are not well mastered. In order to master the milling device in AWJM, a deep study on the footprint of a single path of the cutting head should first be considered. The flow of the AWJ and the distribution of abrasive particles coming out of the jet are related to the profile measured on the footprint. In this study, experiments were made on titanium alloys specimen to compare several theoretical models to the measured profile of the footprint. The study establishes new models to fit the incision profile taking in consideration the behavior of the abrasive particles impacting the workpiece.

Full Article: 039-pp-9 Page: 474

Contribution 2

Title: Evolution of Chip Morphology during High Strength Stainless Steel Turning.

Authors: V. Wagner, G. Dessein, J.Y. Gendron.

Key Words: chip formation, stainless steel, cutting process, chip morphology.

During machining operation, the control of the chip morphology is essential in order to ensure the surface quality and to improve the chip convoying. However, the development of new materials with low thermal properties and high mechanical properties limits the chip fragmentation. In order to improve the knowledge of chip formation during turning of high strength stainless steel an experimental campaign has been done. The chip morphology and the cutting process have also been analysed. Concerning the cutting process, based on cutting power, the tests show a high influence of cutting speed and a poor influence of feed. The chip morphology and the chip formation show the difficult to get some fragmented and small chips. The chip fragmentation occurs generally with the chip curling which increases the strength inside the workpiece material.

Full Article: 041-pp-60 Page: 481

Contribution 3

Title: High Speed Interaction Between an Abradable Coating and a Labyrinth Seal in Turbo-Engine Application.

Authors: C. Delebarre, V. Wagner, J.Y. Paris, G. Dessein, J. Denape, J. Gurt-Santanach.

Key Words: labyrinth seal, abradable material, high speed interaction.

The design of gas turbine aims to enhance the engine efficiency by developing new materials able to work at higher temperatures, or to promote new technologies, fuel management and airflow direction. One solution is the reduction of clearance between rotary parts in turbomachinery air systems. This clearance reduction causes direct interactions in the secondary air system of a turbo-engine when a rotary seal, called labyrinth seal, rubs on the turbo-engine as a result of successive starts and stops, thermal expansions and vibrations. The purpose of the study is to analyze interaction phenomena between an abradable material (Al-Si 6%) and a nickel alloy (718 alloy) during high speed contacts. A high speed test rig has been designed to simulate interactions between labyrinth seals and abradable coatings in similar operating conditions of turbo-engine in terms of geometries, rotational and linear velocities. A series of experiments has been carried out in order to get a first assessment under different turbo-engine operating conditions. Experimental results are presented using visual observations of test samples, quantitative approaches of interacting forces and micrographic observations. This work provides new basic data for a preliminary study of the interaction between a labyrinth seal teeth tips and its casing for turbo-engine applications.

Full Article: 049-pp-38 Page: 488

Contribution 4

Title: Conversion of G code Programs for Milling into STEP NC.

Authors: Shixin Xú1, Nabil Anwer, Sylvain Lavernhe.

Key Words: G code, STEP NC, manufacturing features, canonical machining functions, process plan.

STEP NC (ISO 14649) is becoming a promising standard to replace or supplement the conventional G code programs based on ISO 6983 due to its feature based machine independent characteristics and its centric role to enable efficient CAD/CAM/CNC interoperability. The reuse of G code programs is important for both manufacturing and capitalization of machining knowledge, nevertheless the conversion is a tedious task when carried out manually and machining knowledge is almost hidden in the low level G code. Mapping G code into STEP NC should benefit from more expressiveness of the manufacturing feature-based characteristics of this new standard. The study proposes an overall method for G code to STEP NC conversion. First, G-code is converted into canonical machining functions, this can make the method more applicable and make subsequent processes easier to implement; then these functions are parsed to generate the neutral format of STEP NC Part21 toolpath file, this turns G code into object instances, and can facilitate companies usage of legacy programs; and finally, also optionally, machining features are extracted to generate Part21 CC2 (conformance class) file. The proposed extraction method employs geometric information of cutting area inferred from toolpaths and machining strategies, in addition to cutting tools data and workpiece dimension data. This comprehensive use of available data makes the extraction more accurate and reliable. The conversion method is holistic, and can be extended to process a wide range of G-code programs (e.g. turning or mill-turn codes) with as few user interventions as possible.

Full Article: 027-itm-89 Page: 495

8.2 Models for Product Manufacturing

Contribution 1

Title: Modeling of the Chip Geometry in Orbital Drilling.

Authors: P.A. Rey, K. Moussaoui, J. Senatore, Y. Landon

Key Words: orbital drilling, TiAl6V4, tool geometry, cutting forces.

The orbital drilling is a complex operation. Due to the tool trajectory, which is helical, chip thickness is highly variable. This is why the cutting forces are very difficult to estimate. The aim of this study is to develop a model to predict cutting forces depending on the tool geometry and cutting conditions in order to control the final quality of the machined hole. At first, the geometry of the chip is modeled taking into account the parameters defining the trajectory and the tool. A cutting force model based on the instantaneous chip thickness is then set up. An experimental part validates the cutting force model through measures of cutting force made during orbital drilling tests.

Full Article: 042-pp-67 Page: 502

Contribution 2

Title:	Thrust Force and Torque Model Applied to the Vibratory Drilling Process.
Authors:	John Le Dref, Yann Landon, Gilles Dessein, Florent Blanchet.
Key Words:	vibratory drilling, thrust force, torque, indentation.

Drilling process is highly complex however necessary to assemble parts. It gets even more complex with the assembly of metallic parts with carbon-based composites in the aircraft industry. Vibratory drilling has been developed to meet industrial needs in terms of productivity and quality. This process is quite young and optimal cutting conditions with vibrations have yet to be determined. To assess the quality, and to understand the cutting mechanisms, vibratory drilling has been studied and a thrust force model and a torque model have been carried out. These models present the interaction of several zones of the tool with the material and explain the particular shape of the thrust force observed. The work presented is a part of a complete study of the impact of vibratory drilling on hole quality. The models are identified and validated through an application on aluminium 7010.

Full Article: 048-pp-32 Page: 508

Contribution 3

Title: Analysis of a Turning Process Strongly Coupled to a Vibro-Impact Nonlinear Energy Sink.

Authors: Tao Li, Etienne Gourc, Sébastien Seguy, Alain Berlioz.

Key Words: dynamics, turning, chatter, nonlinear energy sink, vibro-impact.

Recently, it has been demonstrated that a vibro-impact nonlinear energy sink (VI-NES) can be used to efficiently mitigate vibration of a Linear Oscillator (LO) under transient loading by irreversible energy transfer from LO to VI-NES. The possibility of application of VI-NES to control the instability of chatter in turning as a passive control method is studied as a typical delay system. The dynamic responses of machine tool strongly coupled to VI-NES in turning are investigated theoretically by supposing that the tool just vibrates in the predominant direction and numerically with the help of Matlab dde23 algorithm. Three typical response regimes are obtained through numerical simulation under different parameters, that is, stable oscillation and complete suppression of regeneration chatter, relaxation oscillation and partial suppression, and unstable oscillation. Finally, a developed experimental setup is presented and the first test to acquire the stability lobe without VI-NES is accomplished.

Full Article: 050-pp-41 Page: 514

8.3 Manufacturing of Composite Materials

Contribution 1

Title: Analytical Model for Pre-Drilled Thick Composite Plates.

Authors: Pierre Rahme, Yann Landon, Robert Piquet, Frederic Lachaud, Pierre Lagarrigue

Key Words: drilling, reaming, composite materials, analytical models, twist drill, delamination.

In aeronautical, the machining of composite materials is more and more used. Drilling is in particular the most used process in the assembly of aeronautical structures. When drilling composite materials, delamination occurs at the exit of the hole. These defects diminish the strength of the structure to failure. To minimize delamination, drilling process with pilot hole is used. Analytical model for drilling thick composite structures with pilot hole using a twist drill is proposed. This model predicts the critical thrust force at delamination. Different hypothesis of boundary conditions and external loading are proposed. Punching tests with twist drill are realized in order to select the corresponding hypothesis of boundary conditions and external loading. These results may be used to optimize the cutting conditions when drilling thick composite plates with pilot hole.

Full Article: 044-pp-19 Page: 519

Contribution 2

Title:	Burr Height Study for Drilling Carbon Epoxy Composite/Titanium/Aluminum Stacks.
Authors:	Xavier Rimpault, Jean-François Chatelain, Jolanta E. Klemberg-Sapieha, Marek Balazinski
Key Words:	drilling, burr heights, titanium alloy, aluminium alloy, carbon fibre reinforced polymer.

A stack of carbon fibre reinforced polymer (CFRP), titanium and aluminium alloys was drilled using a different set of cutting parameters for each layer. The analysis of the burr heights at the outlet of the titanium and aluminium alloys is exposed. The burr heights are observed in terms of the thrust force, the torque, the hole diameter and circularity, and the clearance tool wear. The selected input parameters were the feeds and speeds of each layer of the studied stack, with three feeds and three speeds for each material of the stack selected. The impact of these parameters on the burr heights of aluminium and titanium parts is presented, as well as correlations between the burr heights with the thrust force, the torque and the clearance tool wear. Three twist drills, with a common geometry and coating, were used.

Full Article: 052-pp-105 Page: 524

8.4 Flexible Manufacturing

Title: Arezzo: an Emulator for the Bench4star Initiative.

Authors: Thierry Berger, Dominique Deneux, Thérèse Bonte, Etienne Cocquebert, Damien Trentesaux.

Key Words: benchmarking, flexible manufacturing systems, manufacturing control, component-based, emulation.

In the manufacturing and production shop floor control context, benchmarking is a popular means to test and compare several strategies, so as to make high level design decisions, to fix the main control choices and to adjust the control parameters. A benchmarking process involves experimentation. Several kinds of experiments can be performed, either in simulation or based on the real manufacturing system. An advantageous intermediary approach can be adopted, based on emulation. For this purpose, an emulator of the shop floor of the targeted manufacturing system is required. After defining the general benchmark context, the Bench4star initiative is introduced in this paper. Thereafter, the Arezzo emulator we have developed in Bench4star is described. Arezzo emulates the shop floor of the real AIP-Primeca Flexible Assembly Cell, located in the University of Valenciennes. It is implemented in NetLogo.

Full Article: 065-ap-49 Page: 530

8.5 Reverse Engineering in Manufacturing

Title: Influence of Part Geometrical Tolerancing in the REFM Methodology.

Authors: Pierre-Antoine Adragna, Salam Ali, Alexandre Durupt, Von Dim Nguyen, Pascal Lafon.

Key Words: reverse engineering, CAPP, set-ups, directed graph, tolerancing.

The study deals with the remanufacturing of existing part in a context of Reverse Engineering (RE). The proposed methodology called

Reverse Engineering for Manufacturing (REFM) consists in generating a Computer Aided Process Planning (CAPP) of a part from 3D information, point cloud, and user knowledge. The idea of this methodology is to avoid the passage by the CAD model. Steps of this methodology are based on a Surface Precedence Graph (SPG) build on a suggested geometrical tolerancing of the part. This graph leads to machining operation precedence graph (MOPG) that leads to the CAPP model. A problem of this approach is that different tolerancing of the same part lead to different process planning. To solve this problem, rules are presented to facilitate the user work. This paper presents the REFM methodology illustrated on a study case.

Full Article: 068-m-94 Page: 537

8.6 Quality and Manufacturing

Title: Multi-Sensor Approach for Multi-Scale Machining Defect Detection.

Authors: Lorène Dubreuil, Yann Quinsat, Claire Lartigue.

Key Words: multi-sensor, digitalization, stereoscopic system, machining defect, sculptured surface.

Several measuring systems used in industries are most often used in a separated way and not efficiently. Multi-scale multi-sensor measurements are nowadays challenging to improve quality and decrease measuring time. However, this requires that each class of defects can be link with the appropriate measuring system. This paper deals with a comparative study of several measuring techniques for the measurement of multi-scale machining defects. In particular, an attention is paid to a new measuring method based on stereo-correlation along with classical measuring technique such as laser scanner, touch probe and confocal interferometry. Considering some well-known defects, the comparative study assesses the ability of each system to measure a class of defects. This study constitutes the first stage towards the definition of a multi-sensor multi-scale measuring system.

Full Article: 032-itm-58 Page: 544

9

Robotics, Mechatronics and Product Engineering

Chapter Editors:
Francesco Leali
Universitá di Modena e Reggio Emilia
ADM Society, Italy

Michel Taix
LAAS Toulouse
AIP PRIMECA Society, France

9.1 Robots and Product Manufacturing

Contribution 1

Title:	Definition of a Robotic Polishing Process for Aeronautics Parts in High Strength Steel.
Authors:	Bastien Guichard, Hélène Chanal, Laurent Sabourin.
Key Words:	polishing, robot, force control, aeronautic.

The first step of the robotic polishing process for aircraft large parts

X. Fischer et al. (eds.), *Research in Interactive Design (Vol. 4)*
DOI 10.1007/978-3-319-26121-8_9

is related to the choice of tools and adjustment of process parameters. The parts have a finish state obtained by 5 axis machining with ball end tool. The objective of the polishing operation is to erase the tool marks, ensuring the imposed profile surface defect and surface state. This requires the choice of polishing tools and the setting of strategy parameters, particularly the polishing force. It must be controlled according to the contact surface between the tool and the part and the attempted polishing pressure. This polishing pressure is defined from a desired removal rate and surface quality. Then, polishing condition parameters are studied in order to propose a first setting for flat parts and cylinders polishing.

Full Article: 046-pp-39 Page: 552

Contribution 2

Title:	Material Removal Distribution in Robotized Random Orbital Sanding.
Authors:	Raphael Poirée, Sébastien Garnier, Benoit Furet.
Key Words:	random orbital sanding, material removal, Preston law, free-form surface.

In random orbital sanding, in order to automate the process, the Material Removal (MR) has to be controlled at each point of the sanded part. Being a two body abrasive process, the pressure and the velocity are two mains parameters which have to be controlled. The pressure depends on the normal force, the lead angle and the curvature of the surface. It is shown that a particularity of random orbital sanding is that the velocity depends on the motor speed but also of the normal force, the lead angle and the curvature. In this study, the MR on a random orbital sander is simulated and validated on a point trajectory. The validation is used to simulate and validate the MR on a whole fractal trajectory on a flat surface. The influence of pressure distribution is shown by the sanding of a free-form surface with the same fractal trajectory. A comparison of the MR on the flat and on the free-form surface with the same trajectory permits to discuss about the influence of the curvature of the surface.

Full Article: 051-pp-103 Page: 558

9.2 Design for Robotics

Contribution 1

Title: Harmonic Functions-Based Type-2 Fuzzy Logic Controller for Autonomous Navigation of Mobile Robots.

Authors: Achille Melingui, Rochdi Merzouki, Jean Bosco Mbede.

Key Words: type-2 fuzzy logic control, artificial potential field, autonomous navigation, hybrid control, intelligent control.

One of the requirements for navigation algorithms is to cope with the large amount of uncertainties that are inherent in real environments. Traditional type-1 Fuzzy Logic Systems (FLSs) using precise type-1 fuzzy sets cannot fully handle such uncertainties. Higher order FLSs, such as an interval type-2 FLSs have been proven to be able to model and handle such uncertainties. The performances of the latter are strongly related to the fuzzy rule base, usually given by experts. However, the linguistic rules obtained from experts are usually not enough for designing a successful control system, because some information is lost when the experts express their experience by linguistic rules. Thus, the sampled imput-output data pairs obtained from a navigation system based on harmonic potential functions are combined with the linguistic rules to build the Interval Type-2 Fuzzy Logic (IT2FL) Controller rule base. One of the most important properties of harmonic functions is that they are free from local minima; they completely eliminate the local minima even in cluttered environments. The proposed controller is implemented in real-time on an omnidirectional mobile robot navigating in unstructured dynamic environments. Through comprehensive experiments, the effectiveness of the proposed IT2FL controller is demonstrated.

Contribution 2

Title: A Hybrid Force-Position Control for a 6 DOF Parallel Testing Machine.

Authors: Julien Le Flohic, Flavien Paccot, Nicolas Bouton, Hélène Chanal.

Key Words: parallel machine, hybrid control, testing machine, multiaxial test, model.

For the first time, a Nooru-Mohammed test was realized using a new kind of loading machine based on Gough-Stewart platform. However, it has been shown that boundary conditions on the concrete specimen are not respected. As a consequence, a new control strategy needs to be developed. The study aims at applying a well-known control loop based on hybrid force/position law to a loading application. This new control algorithm has been developed according to the task and the structure specificities. Indeed, it permits to realize multi-axial test where the boundary conditions are controlled and respected by using the extra degrees of freedom of the platform.

Full Article: 055-r-50 Page: 572

Contribution 3

Title: Identification of Material and Joint Properties Based on the 3D Mapping of the Quattro Static Stiffness.

Authors: Adel Mekaouche, Frédéric Chapelle, Xavier Balandraud.

Key Words: identification, robotic structure, static stiffness, mapping, adept quattro.

We present an identification procedure of mechanical parameters of a parallel robotic structure, the Adept Quattro robot. Two parameters are identified: the torsional stiffness of the actuated revolute joints, and the Young's modulus of the composite material used for the arms of the robot. The experimental static stiffness map is obtained using static loads and a tracker laser. A wire-frame finite element model is

used to simulate static stiffness maps. The identification is based on the comparison between the numerical and the experimental 3D maps. The Quattro robot is mainly studied in the literature for its dynamic performances. The present analysis of its static stiffness is however interesting for the determination of its polyvalence in operational tasks.

Full Article: 056-r-56 Page: 579

9.3 Design in Mechatronics

Title: Design Graphs for Sizing Procedures and Optimization Problems Definition of Mechatronic Systems.

Authors: Marc Budinger, Aurélien Reysset, Jean-Charles Maré.

Key Words: mechatronics, sizing procedure, graph theory, matching.

The study is dedicated to the generation of sizing procedures used during the preliminary optimal sizing of physical parts of mechatronic systems. The inputs are the objectives and design constraints coming from the specifications document or the chosen architecture. As output, components (rod end, roller or ball screw, gear reducer, brushless motor, etc.) specifications are generated in order to obtain an assembled actuation system which fully meets upper requirements. Graphs are used to represent the constraints and links between models. This graphical representation, here called Design Graph, can be used with advantage as a teaching tool with students or as an analysis tool for an engineer in the case of new design scenarios or new technology.

Full Article: 054-r-36 Page: 585

10

Education in Product Engineering

Chapter Editors:
Fernando J. Aguilar
University of Almería
Ingegraf Society, Spain

Maria Grazia Violante
Politecnico di Torino
ADM Society, Italy

Patrick Martin
ENSAM Metz
AIP PRIMECA Society, France

10.1 Learning Collaborative Design

Contribution 1

Title:	Knowledge Discovery from Traceability of Design Projects.
Authors:	Xinghang Dai, Nada Matta, Guillaume Ducellier.

X. Fischer et al. (eds.), *Research in Interactive Design (Vol. 4)*
DOI 10.1007/978-3-319-26121-8_10

Key Words: knowledge representation, engineering design, project management, classification, project memory.

Nowadays, design projects tend to be undertaken concurrently by a project team with a diversity of competences and backgrounds (culture, organization etc.). Knowledge management is supposed to enhance experience reuse by transforming tacit knowledge that is produced in projects into reusable explicit one. However, due to the characteristics of modern design projects, knowledge management has to pay attention not only to decision-making activities, but also the influence of project context.

Full Article: 014-e-97 Page: 594

Contribution 2

Title: Multidisciplinar Approach in Teaching Interfaces Design: a Pilot Project.

Authors: Aranzazu Fernández Vázquez, Anna Maria Biedermann.

Key Words: multidisciplinary work, interfaces design, graphic design and informatics teaching.

The study presents the multidisciplinary approach in interface design performed as a pilot project on the University of Zaragoza in collaboration between the Industrial Design and Product Development Engineering Degree and the Informatics Engineering Degree. It presents the complementary development of the interfaces' aspects of usability, the differences along its evaluation, the conclusions from the pilot project seen from the perspective of graphic design and improvement proposals for implementing future experiences. The aim of the project is to prepare students for fulfilling their future professional works in the complex field of interfaces design, enabling them to work in collaborative environments.

Full Article: 015-e-14 Page: 600

10.2 Learning CAD and Geometric Modelling

Contribution 1

Title: A Multidisciplinary PBL-Based Learning Environment for Training Non-Technical Skills in the CAD Subject.

Authors: Nerea Toledo, Jaime Lopez, Pello Jimbert, Isabel Herrero.

Key Words: PBL, CAD, multidisciplinary projects, teaching innovation, skills.

Future engineers need to foster technical and nontechnical skills to confront global societies competitiveness in terms of innovative products and solutions. To this end, a multidisciplinary learning environment provides a perfect framework to train the required transversal competences as well as gain expertise in their knowledge area. Following our previous work in teaching innovation for the Graphic Expression subject and more precisely for the CAD part, we have opened the scope of the assemblies students have to address by defining a multidisciplinary project where students from different knowledge areas solve corresponding issues using PBL methodology while they work on a collaborative environment. With this initiative we expect that students train non-technical skills and get acquainted with coordination, teamwork and meeting methodologies, and therefore, get accustomed to labour reality dynamics.

Full Article: 016-e-80 Page: 607

Contribution 2

Title: Descriptive Geometry 2.0.

Authors: Javier García Mateo, Fernando Lara Ortega, Lara García Calvo.

Key Words: descriptive geometry, spatial visualization, education.

Both plane and spatial graphic geometry are allotted fewer teaching hours in Spanish study plans. This reduction in hours applies equally

to traditional methods and to the incorporation of technology, in the form of CAD programmes, which facilitate operations and precision in the study of this discipline. We shall present the example of the Civil Engineering qualification at Burgos University and will moreover show the way we have adapted to these changes, trying not to weaken the capabilities of our future professionals. We shall demonstrate how spatial vision capabilities are developed in similar ways using classic procedures from descriptive geometry and the spatial constructions that 3D CAD offers us.

Full Article: 017-e-92 Page: 613

10.3 Learning Innovation

Contribution 1

Title: Learning By Doing; A Cooperative Project Between the University of Zaragoza and the Ideas Hub.

Authors: Anna Maria Biedermann, Aránzazu Fernández Vázquez.

Key Words: graphic design teaching, corporate design, knowledge transfer, entrepreneurship, University and Business collaboration.

The study describes a pilot project developed between the subject of Graphic Design and Communication (DGyC) of the second year of Industrial Design and Product Development Engineering Degree at the University of Zaragoza and the program named Semillero de Ideas: a first stage business incubator. It presents the objectives and the project development by which the students create a graphic image for the business projects raised by the entrepreneurs while they learn to use graphic creation tools and the principles of corporate design. The results reached and the satisfaction level of the students as well as the entrepreneurs ones, together with the subject academic goals fulfillment

allow to positively evaluate this experience, where the learning process is done by doing and not only simulating a real work.

Full Article: 012-e-13 Page: 618

Contribution 2

Title: 3D Immersive Environments in Higher Education B-Learning Implementations; Preliminary Results.

Authors: Fernando J. Aguilar, Manuel Lucas, Manuel A. Aguilar, Juan Reca, Antonio Luque, Antonio Cardona, María S. Cruz, José J. Carrión.

Key Words: b-learning, e-learning, 3d immersive environment, second life, higher education.

The emergence of a fourth dimension (time) and the development of photorealism, by including materials, textures, lights and special effects, allow the configuration of more and more realistic 3D virtual worlds. These are true 3D immersive spaces where the user can interact with virtual objects and other users. These emergent technologies are being applied, we believe in a definitive way, for improving the teaching-learning process in b-Learning environments. The preliminary results of our teaching innovation group are presented in this paper, briefly consisting of creating a WWW 3D virtual meeting point between students and teachers by using the semi open source WWW platform called Second Life. The first stage of experimentation has proved the potential of 3D immersive environments to develop a formative offer wherein the universities can provide an alternative to the traditional face-to-face learning regarding the presential component. In this sense it is boosted a distance learning approach but mainly using almost a presential method where the meeting point turns out to be a virtual classroom rather than a physical one.

Full Article: 018-e-96 Page: 624

10.4 Interactive Learning

Title: Learning Dimensional Metrology in Practice: Students Controlling a Coordinate Measuring Machine (CMM) from their Computers.

Authors: César García-Hernández, José-Luis Huertas-Talón, Rafael-María Gella-Marín, José-María Falcó-Boudet, Panagiotis Kyratsis, Jean-Noel Felices.

Key Words: interactive learning, collaborative learning, metrology, remote control, educational resources optimization.

A pilot study in presented: a coordinate measuring machine (CMM) is handled by students, using remote control software. This is part of a metrology practical session, during a professional training course. They, instead of just paying attention to what their teacher is doing and his explanations, have to practice with a real machine, giving instructions, from their laptops, to the computer that is controlling that CMM. We describe the preparation process, the experience, how it was assessed and, finally, results are assessed. These results confirm an improvement, both in students skills and in other important aspects, like participation, interest and friendliness. Although further studies are needed, this teaching methodology can be applied to remote and in-person classes, especially in professional training, where different educational centres and even industries can share their different machines, helping to optimize resources.

Part II

Full Argumentations on Interactive Design and Manufacturing

1

Design Methods

Major topics of the full argumentations are the following:

X. Fischer et al. (eds.), *Research in Interactive Design (Vol. 4)*
DOI 10.1007/978-3-319-26121-8_11

Article 05-dm-98

New designs of the ceramic bricks of horizontal hexagonal hollow

David Corbella [1], Francisco Fernandez [2], Francisco Hernández-Olivares [3], Pedro Armisen [4]

(1) : Department of Engineering of Desing & Product
Polytechnic University of Madrid
Phone/Fax 0034913367694 / 0034913367677
E-mail : david.corbella@upm.es

(2) : Department of Industrial Chemistry and Polymers
Polytechnic University of Madrid
Phone/Fax 0034913367682 / 0034915309244
E-mail : francisco.fernandezm@upm.es

(3) : Department of Architectural Technology
and Construction
Polytechnic University of Madrid
Phone/Fax 0034913364245 / 0034913366560
E-mail : fhernandez@upm.es

(4) : Department of Mechanical Engineering
Polytechnic University of Madrid
Phone/Fax 0034913367693 / 0034913367710
E-mail : pedro.armisen@upm.es

Abstract:

This article is intended to state that Technical Drawing is a multiple tool of expression and communication essential to develop inquiry processes, the scientifically basis and comprehension of drawings and technological designs that can be manufactured.

We demonstrate graphically and analytically that spatial vision and graphic thinking allow us to identify graphically real life problems, develop proposals of solutions to be analysed from different points of view, plan and develop the project, provide information needed to make decisions on objects and technological processes.

From the knowledge of Technical Drawing and CAD tools we have developed graphic analyses to improve and optimize our proposed modification of the geometry of the rectangular cells of conventional bricks by hexagonal cells, which is protected by a Spanish patent owned by the Polytechnic University of Madrid.

This new internal geometry of the bricks will improve the efficiency and the acoustic damping of walls built with the ceramic bricks of horizontal hollow, maintaining the same size of the conventional bricks, without increasing costs either in the manufacture and the sale. A single brick will achieve the width equivalent to more than FOUR conventional bricks.

Key words: Product Design, Industrial Design and Creativity, Industrial Innovation, Product Manufacturing, Graphical Analysis.

1 - Introduction.

Ceramics is composed by four simple elements: *earth*, *water, air and fire*. Today it is as modern as it was in antiquity. This material has always been submitted to continuous improvements. To produce it, the *earth* must be ground and mixed with other natural elements in order to give them certain properties. Once mixed with *water*, it must be moulded to yield different products, which can be grouped into: refractory ceramics, decorative ceramics, technical ceramics and structural ceramics. Then the ceramic material is introduced into an *air* dryer, and finally placed in an oven where with *fire* it acquires the desired physical properties.

Ceramics is a versatile material that has been used in many different ways. It can be seen as decorative elements or may be present as various passing us unnoticed building elements. A clear example is the ceramic bricks after being covered with plaster or any other coating material: we cannot see them, but we know that they are on the walls surrounding us.

Ceramic bricks can withstand temperature changes of the environment. For example, when cold passes through the brick, it loses intensity. The same goes for heat.

The secret is in the inner cells or chambers and in the tiny pores of the ceramic material (Fig.-1), which alters temperature transmission (hot / cold) that decreases as it moves through the brick until it dissipates.

A width greater brick there will be a greater damping. As a consequence of this, the conventional bricks with rectangular cells have given rise to large blocks, which acquire the name block ceramic brick.

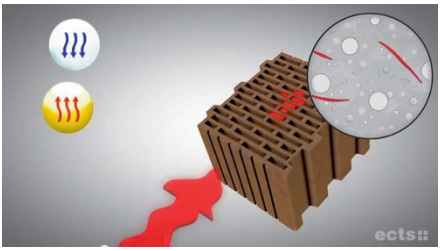

Figure 1: Image from European Ceramic Technology Supliers

Architects, construction engineers and brick manufacturers say: "*Ceramics is the building material with better thermal insulation properties. Proper insulation is the best solution to minimize power consumption in both heating and cooling. The use of ceramic materials therefore involves saving money by reducing energy consumption*". [E1]

For the same reason we can ask: Can bricks have acoustic insulation properties? Similarly wider dimensions of ceramic brick dissipate temperature transmission; they will also dissipate sound transmission.

In all materials that offer thin slits or porous appearance, when a sound wave enters, it will attempt to penetrate the material between its interstices. Thus the molecular movement is the incident sound energy will move the fibres and / or the pore walls, spending part of the sound energy into kinetic energy. At the same time the air within the pores or between the fibres will also be forced to move, generating other costs of sound energy that will be transformed into heat energy.

The thickness of the material is important to determine the maximum sound absorption. The sound energy penetrates the material only to a certain width, beyond the absorption or dissipation of sound does not increase. Isover Manual [C2].

The walls of the rectangular cells perpendicular to the faces of the ceramic brick transmit cold, heat and airborne noise, perpendicular and directly to outer faces of the brick. The thermo-acoustic damping and absorption capacity shall be limited by the width of the ceramic brick, among other factors.

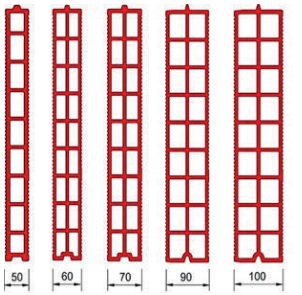

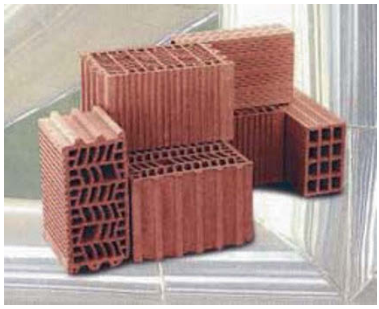

Figure 2

Such is the reason whereby other bricks of greater dimensions and ceramic blocks can replace the conventional ceramic bricks of horizontal cells in parallel to the bearing surface. That is the best solution to the problem of damping lack thermo-acoustic (Fig.-2).

Nevertheless, an alternative ingenious solution that satisfies the requirements of thermo-acoustic insulation of walls can be achieved with a new design of the brick internal geometry maintaining the outside dimensions of conventional brick.

A Spanish Patent [1], offers an innovative geometric modification of cells of the ceramic fired clay destined to the manufacture of bricks, according to an hexagonal cells geometry [P1].

[1] *The owner is the Polytechnic University of Madrid and the inventors are three full professors: Corbella Ribes, David; Fernández Martínez, Francisco and Hernandez Olivares,*

Article 05-dm-98

2 - Principles of the Research and Innovation

A heavy concrete wall is a good airborne noise insulator that does not allow passes much noise through the wall from one side to another (Fig.- 3) -the following diagram shows the behaviour of sound when there is a concrete wall, from which we deduce the model to study the sound insulation, the walls in this investigation-. This example makes us think about the hypothesis that acoustic insulation depends on the width of the wall or mass quantity that has to go through it [L1].

While the concrete wall reflects almost all noises that come from inside the same room, because it is an insulator but it is not an absorbent, noise that penetrates is weakened according progresses through the wall.

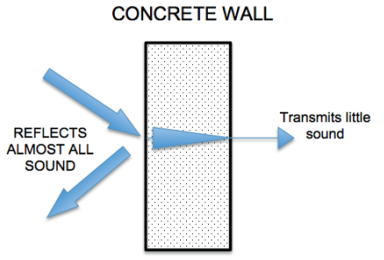

Insulator but is not absorptive

Figure 3

This explains the above mentioned increase in the size of bricks and gave us the idea of replacing conventional rectangular holes by hexagonal holes, in order to increase the distance between the outer faces of the brick, just changing the shape of the cells and maintaining the external dimensions of the conventional bricks.

We are aware that the sound insulation depends not only on the mass but also on the geometry of the piece, the percentage of voids or holes, on the "loss" (loss of internal factor), and on the velocity of propagation of longitudinal waves (CL), which is related to Young's E modulus (depending on the clay type, additives, drying and baking). However, without going into complex studies, it is enough to note that the intensity of the sound signal decreases exponentially with the same path according to the following expression:

$$I = I_0 \exp(-\beta x)$$

I_0 is the intensity of the emitting source, β is the absorption coefficient and x is the path of the wave. From this expression, we can easily deduce the following result: for the same material and the same wall thickness, the observed intensity, I, decreases when the path is increased performed by the sound [CF1].

Subsequently we show both analytical and graphically that those new designs of the ceramic bricks of horizontal hexagonal hollow, as the exposed hypothesis that a longer path increases thermal or acoustic dampening, compared with traditional brick rectangular holes, assume that these new bricks will buffer better the airborne sounds.

Under this approach, our investigations [C1] enable us to document the morphological characteristics of the cells of the new designs of ceramic bricks and to make other recommendations to manufacturers.

3 - Graphical investigation

The first graphical analysis of hexagonal brick geometry has detected that the line defined by two opposite corners of the hexagonal cell polygon (diagonal of hexagon), if placed parallel to the outer face of the brick used in the manufacturing of the early prototypes, only increases the travel 15.49%. (Fig.-4). The path from one to another side of the wall of 70 mm wide with hexagonal cells would be 80.84 mm. With the same analysis applied to another brick 100 mm wide, the path would be 115.49 mm. In this case, the percentage value is obtained directly discounting 100. We will see it in the following figures.

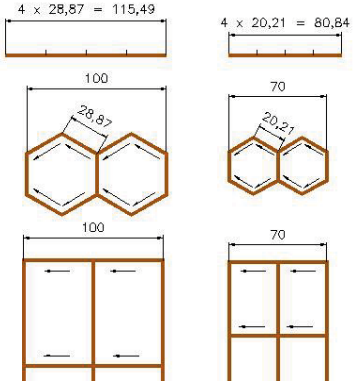

Figure 4

This diagram shows graphical analysis for bricks 70 and 100 mm wide between faces, so that in the hexagonal cell the path increases 15.49% compared with the rectangular cell.

On the other hand, one rotation of 90º sexagesimal degrees in the placement of the hexagonal cells, provides that the diagonal of the hexagonal cell is positioned perpendicular to the outer faces of the brick. In this way the path increases (Figure-5).

Article 05-dm-98

As told before, that the path from one to another side of the wall of 100 mm wide, would be 142.86 mm. The increase is 42.86%. If the path between the faces of the wall is 70 mm in width, it would be 100 mm.

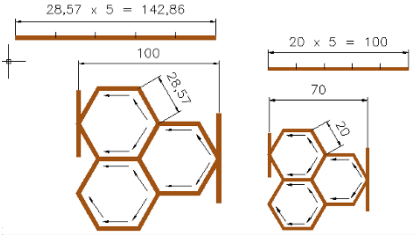

Figure 5

These schemes representing the graphic analysis come to justify that when the orientation of a diagonal of the hexagon is rotated and placed perpendicular to the faces of the brick, the path is increased with respect to the initial case (Fig. 4), in which the diagonal of the hexagonal cells remains parallel to the brick faces.

It is noteworthy that increasing the number of hexagonal cells, keeping the distance between the faces, it doesn't provides any gain in the path (Fig. - 6). If the number of hexagonal cells between the faces of the brick is the lowest possible the path will be the longest and therefore there will be a higher thermo-acoustic absorption. For example, keeping a distance of 70 mm between the faces of the brick, two lines of "complete hexagons" juxtaposed represent a path of 100 (20x5 = 100). When one row is increased from two to three lines of juxtaposition of "complete hexagons" it means a lower path (7x14 = 98) with respect to the initial case. In that case the path between the faces of the ceramic brick is lower (- 2,86 %).

(5x20=100) > (7x14=98)

42,86% > 40%

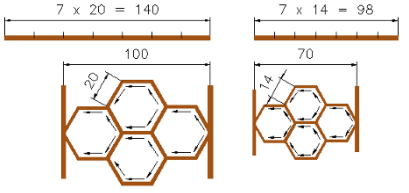

Figure 6

These schemes of graphical analysis show that increasing the number of cells and keeping the distance between the faces of the ceramic brick, no gain is provided.

Subsequent investigations, other graphic analyses (fig. 7) in which a rotation of 90° was applied with additional deformation of the hexagonal cells that maintain their angles of 120°, show that the path increases progressively - hex orientation as in Fig. 4- from 15.49% to 29,9% and - hex orientation as in Fig. 5- from 33.33% to 66.66% maximum, as illustrated in the following study:

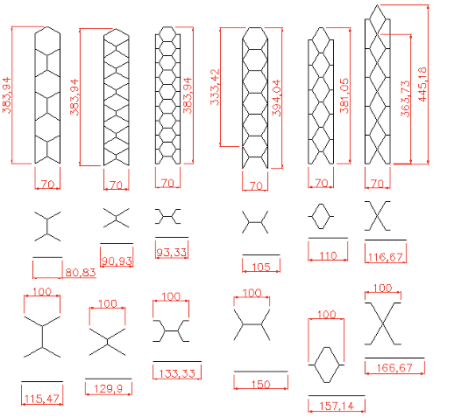

Figure 7

From left to right, there is an illustration of graphic analysis in which the deformation of the hexagonal cells provides greater lengths and increases the insulation.

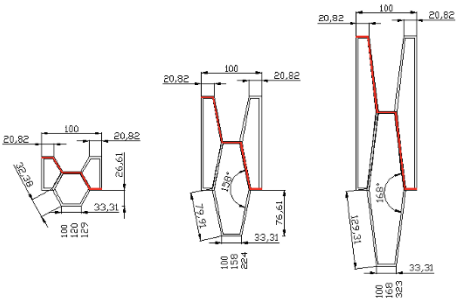

Figure 8

Further investigation about the hexagonal deformation at the extreme case, modifying the angles of the hexagonal cells leads to higher path over than 300% with respect to the distance between the opposite faces of the brick. Such as seen (Fig.- 8) the deformation it posed from the angular variation of the adjacent sides of the cell, for example: from

Article 05-dm-98

120° to 158° and 168°, without modifying the distance between the faces of conventional ceramic brick. It increases considerably the length of bridges of transmission between the two opposite faces of the brick with the increase of one pair of opposite angles of the hexagonal cells.

4. Research Results.

The exploitation of the mentioned invention, patented by Polytechnic University of Madrid, is open to all manufactures. It has been materialized as shown in Figure-9, under the name CERAGRAN-H ®, manufactured by RosoSL company, located in Illescas-Toledo (Spain), with the following nominal dimensions:

LENGTH	HEIGHT	WIDTH
710	500	50
710	250	50
710	500	60

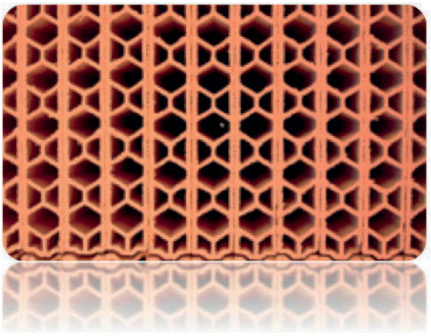

Figure 9: Matchboard ceramic bricks CERAGRAN H®
Made in Spain

This new ceramic product replaces the conventional ceramic rectangular hollow brick used for making walls, as they are sold in Europe and worldwide with square or rectangular cells.

Revised this new design of ceramic brick called CERAGRAN H®, made by that company of Toledo, the results of acoustic damping has been very low, because of the hexagonal cell orientation, defined by position of the hexagon, as in Fig. 4.

They applied a deformation of the hexagonal cell that still maintains all angles of 120° (second case of Figure 7). In this case the path only increases 15.49%. The trajectory between the faces of a brick of 60mm wide increases only 9.28 mm, and obtains the equivalent width to 69.28 mm, that is very low (first case of Figure 10).

Therefore, the acoustic attenuation of CERAGRAN-H ® is the lowest studied in this article and it does not achieve the highest levels of isolation obtained with the new geometries and new designs.

This design of the brick manufacturer could be improved if a diagonal is placed perpendicular to the outer surfaces and it amends the orientation of the cells of the brick. In this way the path increases around 52.91%. That is, the path between the faces of one ceramic brick of 60 mm wide would reach a width equivalent to 91.75 mm.

However, results must increase significantly if the same orientation of the hexagonal cell is maintained (a diagonal remains perpendicular to the outer surfaces of the brick) and if it also applies a deformation to hexagonal cells that modifies the angle of their faces.

Changing the angle of 120 ° to, for example, an angle of 168°, the path would be 442.37%. In this case, the path between the faces of one ceramic brick of 60 mm wide would reach a width equivalent to 265.42 mm. This is approx. equal to a path of 4,5 conventional bricks.

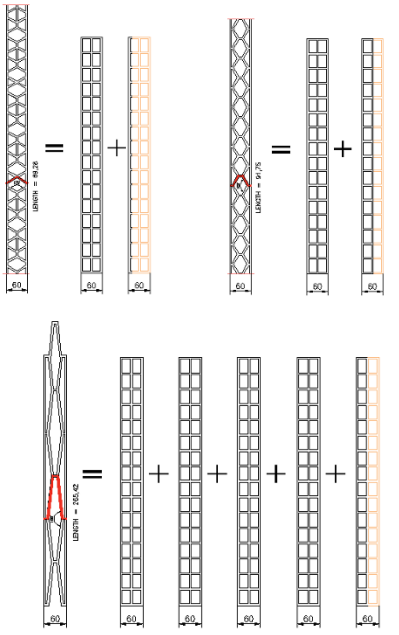

Figure 10: Comparative analysis of the new geometries.

This comparison (fig. 10) proves that the companies that manufacture bricks still have much to improve about the design of their bricks to increase the insulation.

Finally taking as a reference the study of orientation and deformation of hexagonal cells and the ceramic bricks matchboards, we can define a full range of new designs: single hollow brick, triple hollow brick, large format brick, blocks of brick, single hollow brick board, triple hollow brick board ... (Fig. 11). This proposal for new designs of ceramic bricks could be inside the HORIZON 2020 program in order to contribute to improve the thermo-acoustic absorption in better performing buildings.

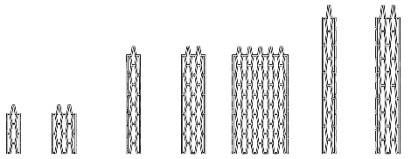

These new designs of the ceramic bricks matchboards have the innovation that the horizontal locking tongue and groove take the form of the cell to avoid paths perpendicular to the faces of the wall in horizontal joints. Nevertheless these joints should necessarily be filled with a thin layer of adhesive or gripping paste. Thus the transmission bridges between the two faces of the walls by the joints of bricks are avoided.

Foreseeably these new large formats brick with horizontal hollow are those that have a better performance in the thermo-acoustic absorption, keeping the conventional width of the walls. Therefore, we are talking of the most competitive design for building walls with ceramic bricks.

The advantages of these designs in large format bricks compared to traditional solutions, taken directly from the Spanish Manufacturers of Fired Clay for Roof Tiles and Bricks, Hispalyt Association, [H1] are as follows:

1. Ruggedness and lower cost of execution on site.
2. Quick and easy installation on site execution.
3. Spotless in execution on site.
4. High performance execution on site.
5. Best finish and planarity of the completed wall.
6. Ability to tilling directly on the brick.
7. Grooves easier to implement and less costly in time.
8. Since it is a ceramic element it has good thermo-acoustic properties, fire resistance, and resistance to suspended loads and impacts.
9. Large format LGF-LD, uncoated commercial bricks are obtaining an attenuation of 33 dBA (CTE DB-HR) and the LGF-LD “ladriyesos” ceramic bricks coated with plaster with a thickness between 5 and 10 mm are obtaining an attenuation over 50 dBA.

5. Conclusions

We have to point out that if the manufacturers decide to use the new designs of ceramic bricks developed by our investigation, **it would be necessary to revise upward the acoustic damping values indicated on this last point**, No.9, both for uncoated and coated bricks, multiplied by more than FOUR times.

We show graphical and analytically that spatial vision and graphic thinking get the graphic research on new alveolar geometries. This research has led to concept of new designs of ceramic bricks that will improve the walls construction system.

This first step in graphic research needs to contact institutions and brick manufacturers interested in financing and participating in this research project, in order to determine the real coefficients of both thermal and acoustic absorption, and mechanical resistance (vertical load, horizontal load) in laboratory and work placement of these new designs.

We would offer this research to suppliers of machinery and technology for the ceramic industry, to manufacturers and users of bricks. We would offer them the use of these designs and the patent for their participation with us in this project R+ D + I, with the sale of operating licenses and / or our expertise advise. For more information, stakeholders may contact Professor Corbella by e-mail using the references cited at the heading of this article.

6. References

[CF1] CORBELLA D., FERNÁNDEZ F., HERNÁNDEZ F., DEL RÍO M., Ladrillo Hueco Hexagonal, I Jornada Nacional de Investigación en Edificación I+D+I, Escuela Universitaria de Arquitectura Técnica -Universidad Politécnica de Madrid. Proceedings of the conference, Madrid. May 10 th -11 th. 2007.

[C1] CORBELLA D., Ladrillo Fonoresistente, II Jornada Nacional de Investigación en Edificación I+D+I, Escuela Universitaria de Arquitectura Técnica-Universidad Politécnica de Madrid. Proceedings of the conference. Madrid, July 3er, 2008.

[C2] CRISTALERÍA ESPAÑOLA, ISOVER Isolation Manual, Madrid: Author. Vol 1-182, 1987.

[E1] EUROPEAN CERAMIC TECHNOLOGY SUPLIERS (ECTS), Video-report Modern Life – Modern Buildings, Available at the URL: http://www.youtube.com/watch?v=2y0aMe007L0. Consulted January 7 th, 2014.

[H1] HISPALYT. Spanish Manufacturers of Fired Clay for Roof Tiles and Bricks, Hispalyt Association. (2014) · C/ Orense, 10 - 2ª Planta, Ofic. 13-14 28020 MADRID · Tel: 917 709 480 ·E-mail: hispalyt@hispalyt.es. Available at the URL: http://www.hispalyt.es/default.asp?id_cat=2 and consulted January 8th, 2014.

[L1] LABEIN - Technology Centre Conference Acoustic Criteria in Designing Educational Centres organized by STEE-EILAS, Vitoria. May 12 (2001).

[P1] POLYTECHNIC UNIVERSITY OF MADRID. Spanish Patent ES2265234. Ladrillo Hueco Hexagonal.

Spanish regulation applicable to the design of ceramic bricks:

CTE-DB-HR Technical Building Code Basic Document. Protection against noise, 2009.

UNE-EN ISO 717-1: Acoustic. Evaluation of Acoustic Insulation in Buildings and of Building Elements. Part 1: Noise Insulation Aerial, 2013.

UNE-EN 771-1: Specification for masonry units. Part 1: Pieces of Fired Clay, 2011.

UNE-EN 772-3: Methods of assay for masonry pieces. Part 3: Determination of net volume and percentage void by hydrostatic weighing of pieces of fired clay for masonry, 1999.

UNE-EN 772-9 / UNE-EN 772-9 A1: Methods of assay for masonry pieces. Part 9: Determination of the volume percentage void and net volume of clay and sand-lime pieces for masonry units by sand filling, 1999 &2008.

UNE-EN 772-13: Methods of assay for masonry pieces. Determination of the dry density and the apparent dry density of masonry pieces (except natural stone), 2001.

UNE-EN 772-16: 2011 Methods of assay for masonry pieces. Part 16: Determination of dimensions.

UNE-EN 1745: Masonry and factory components. Methods for determining thermal design values, 2013.

UNE 67030 / UNE 67030: ERRATUM Fired clay bricks. Measurement of dimensions and shape verification, 1985 & 1986.

UNE 67042: Ceramic pieces of fired clay, large format. Determination of the resistance to flexion, 1988.

UNE 67043: Ceramic pieces of fired clay, large format. Measurement of dimensions and shape verification, 1988.

Article 02-dm-68

Improving the modular structure of a product to facilitate the redesign process: an example for eco-design

Marco Malatesta[1], Michele Germani[1], Fabio Gregori[1], Roberto Raffaeli[2]

(1) : Università Politecnica delle Marche
Ancona, 60131, Italy / +390712204797
{m.malatesta,m.germani,f.gregori}@univpm.it

(2) : Università Telematica eCampus
Novedrate, 22060, Italy / +390317942500
roberto.raffaeli@uniecampus.it

Abstract: Products are continuously redesigned to offer new variants and penetrate new market niches. Changes are often dictated by improvements which are necessary in specific Design Contexts (DC), such as performance, eco-sustainability, assembling, cost, usability. Modularity is a well consolidated approach toward the rapid product reconfiguration and is beneficial to limit the scope of changes to product subsets. However, this consideration needs to be included in the design of the modular structure of a product.
The paper introduces the concept of Design Context Module (DCM), as a module implemented in components that will strongly affect a certain DC, letting the designer to restrict the number of the parts to be modified. The approach moves from the traditional modularization based on the functional decomposition and introduces an iterative procedure to refine the DCMs structure. The optimization is driven by the maximization of similarities and dependencies among components of the same module and by indexes expressing the impact of the components on specific DCs.
The approach has been tested in the field of the household appliances. The modular structure of a freestanding cooker has been redefined in consideration of redesign activities aiming to improve the eco-sustainability of the product. The application of the approach has led to the identification of few modules characterized by high impacts on the environment.

Key words: modular design, product lifecycle design, eco-design, LCA

1- Introduction

The design plays an important role in the production process and has a direct effect on the quality and cost of a product [LK1]. Products offered on the market are continuously updated to meet new requirements and satisfy new needs of the customers. The modification of the features of an existing product often spread in its structure and in the whole lifecycle, such as the production facilities or the end of life management.
According to Smith et al. [SS2], current redesign techniques can limit product innovation. Besides, the impact of introducing new features should be limited and controllable, in order to speed the redesign phase and bound the uncertainty connected with the management of a new product. New product variants in product families are generally derived by adapting existing products to new requirements, scaling or changing their modules and components. Then, it is strategic to support the redesign phase conceiving product structures which are suitable to be reconfigured in short time and limited efforts.
Modularity is one of the most powerful approaches to this aim [FM1]. In fact, a modular product consists of several basic modules which are combined in different arrangements and at different assembly stages. The flexibility of a modular structure is guaranteed by limited dependencies and standardized interfaces between the modules. So, changes can be obtained by substituting modules or concentrating the design activity on selected subsystems.
Given a product, its module structure can be defined on the basis of various criteria. In general, it is not possible to have an optimal structure; rather it is derived according to specific goals [MJ1], [L1]. The assembly process is one of the most common drivers to guide the module identification in the industry. A module typically collects components and assemblies on the basis of the mounting sequence and tends to group parts which are handled homogeneously in the assembly line. However, such approach does not guarantee the minimization of the module dependencies.
On the other hand, several modularization approaches have been developed in the literature [OH1]. The majority relies on an abstract representation of the product that is its functional decomposition. Heuristics as well as matrix based approaches have been proposed. Even though such methods have proved to be general, the module definition process should also consider specific design goals to reach high effectiveness in specific goals of the redesign process.
In this paper, the perspective under a certain product change is seen and evaluated is referred as *Design Context* (DC). DC acts as a driver or area of interest that pushes the designer choices toward some specific direction. Performance, assembling, cost and usability are examples of DC. Eco-sustainability is for sure one of the most interesting and challenging for the industry and the research community.
The proposed approach aims to rearrange the product as a set of DCMs. The scope is the redesign phase of a product to

Article 02-dm-68

meet new requirements. The final goal is to restrict the impact and limit the efforts required to accomplish the modifications.
An initial structure of modules is derived from the functional decomposition. Physical components and assemblies are located in the modules on the basis of the implemented functions. Then, modularity indices are computed to numerically express the internal and external dependencies as well as the suitability of the identified modules to be redesigned under a certain DC viewpoint. The modules composition is then reorganised to maximise such indices.
After a review of the state of the art, the approach is reported in section 3. Then an application is described, i.e. the redefinition of the modules of a freestanding cooker supplied by Electrolux company. The test case has focused on the eco-sustainability context because, nowadays, this issue is a crux for the companies. A method to measure the eco-sustainability of the product is the Life Cycle Assessment (LCA) that, in this paper, will help the designer to identify the values of the features that represent the product from a point of view of the CO_2 emissions. The results show that the new module structure allows the environmental impact to be improved acting on a smaller number of modules. However the integrity of the modules in terms of geometry and physical interfaces is still valid.

2- State of the art

Many methods are reported in the literature to identify modules and product architectures. A module is defined as an independent building block of a larger system, having specific functions and well-defined interfaces [OH1], [H1]. Modules can be interchanged within a product architecture producing a variety of similar products [SS1]. Dahmus et al. [DG1] have affirmed that if a module is successfully designed it could be easily updated on regular time cycles or easily swapped to gain added functionality. Moreover, a modular architecture allows a design change to be limited to few modules [E1].
The two main characteristics of a modular product are: similarity between the functional and physical architecture, minimization of the interactions among physical components belonging to different modules [UE1].
The functional model of the product can be defined following the well-known guidelines of Pahl et al. [PB1]. A functional analysis represents, at different levels of granularity, what the product and its parts do. Functions are expressed by pairs of noun-verb, connected by flows of energy, material and signal. The main characteristic of a functional analysis is the abstraction of the description, which should not include any perspective on technical solutions. In order to form modules out the functional decomposition, Stone et al. [SW1] described three heuristics. Other approaches make use of matrix-based representations and clustering approaches to minimise the flows among the modules [YB1].
The main limitation of the function-based approaches regards the absence of a connection with the physical implementation of a product. The geometrical and structural dependencies among the components are neglected in the formation of the modules. Other approaches overcome such limitations. For instance, Gershenson [GP1] [GP2] investigates the potentialities of the concept of modularity that is not only based on functional considerations. He highlights the importance of considering life-cycle aspects such as manufacturing, assembling and recycling. In his works, indexes are proposed for measuring the degree of the modularity of a product, they have inspired the development of the procedure shown in this paper. In Sosa et al. [SE1] a more extended comparison of several modularity indices can be found.
Another method for structuring the product is the Modular Function Deployment (MFD) developed by Erixon [E2] that uses the concept of “module drivers” to create a modular representation. His approach comprises five main steps, ranging from costumer requirements to modules definition according to physical aspects of the product implementation.
Yang et al. [YY1] investigate the environmental performances and the end-of-life of product families in the context of the modular design area. In this work the eco-design considerations are incorporated into the product family design, by using genetic algorithms to group components. The approach is applied for redesigning a “green” refrigerator family. The paper highlights the importance of considering lifecycle aspects, mainly environmental aspects, in the redesign phase. However, the approach lacks in the definition of a product structure optimised for being modified in the perspective of a specific design contexts as prerequisite for effective redesign activities and increased product standardization.
Other attempts in the literature can be found concerning the optimization of the modular structure for specific design goals. For instance, consumer satisfaction [HC1] or quality issues [BL1] can be incorporated into modular design. These papers highlight the lack of a unique reference modular structure and the necessity of the incorporation of DCs in its definition. The approach presented in this paper aims to a formalization of a modularization procedure based on the identification of indices from specific features of the considered DC.

3- Method

This section describes the approach to define a structure in terms of modules, i.e. DCMs, oriented to a particular DC. The Design Context Module (DCM) is a cluster composed by product components that match similar product functionalities and similar features for a specific DC. Those modules will identify, for the chosen DC, the grouped components that have similar impacts on the product and, hence, where the designer should focus his action to achieve the wanted improvement. The approach applies on existing products, aiming to a redefinition of the product implementation to foster modifications in the area of the selected DC.
Every DC can be further described by some *Design Context Feature* (DCF). DCF are specific product performances and requirements that are the scope of the modifications. They are identified by the marketing experts and reviewed by experienced designers for what concerns technical and economic feasibility.
The main steps of the approach are depicted in the Figure 1. They are described in detail in the following paragraphs.

1. *Definition of the functional decomposition of the product*

The first step regards the analysis of the product and the

Article 02-dm-68

abstraction of its functional structure. The traditional approach described in the section 2 is employed to identify elementary functions and flows of material, energy and signal. A suitable level of granularity is required for the next step.

2. *Modularization on the basis of the lowest level of the functional analysis*

The sub-functions from the lowest level of the functional decomposition are grouped in pure functional modules. Heuristics or matrix-based approaches could be used as reviewed in the previous section. Each function belongs to one and only one module. Such modular structure acts as the initial state of the following optimization steps.

3. *Components mapping to the functional analysis*

The aim of this step is to recognize the sub-functions implemented by each component of the product. Each component may carry out more sub-functions. For instance, an electronic card may acquire and transmit data from a sensor and power a motor. Since modules gather sub-functions, components can be located in one or more functional modules, depending on the sub-functions being implemented.

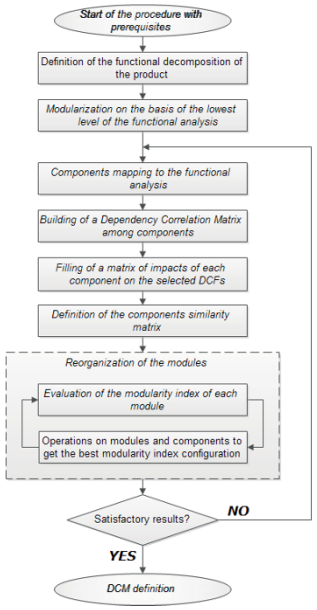

Figure 1: flow chart of the DCM definition procedure

4. *Building of a Dependency Correlation Matrix among components*

The Dependency Correlation Matrix (DCMx) is a symmetric matrix containing the information on the structural connection between components. The components of the product represent the rows and columns of the matrix in the same order. The values d_{ij} in the cells are indices representing the intensity of the physical connections between the parts. Values are dimensionless, normalised and vary between 0 and 1, where 0 means that two components are not connected in any way, while 1 means that there is a strong physical correlation between the two. The matrix can be filled from the analysis of the product as it is realized. CAD models can be helpful to this aim. Sometimes the expertise of senior designer can be required for certain constraints. For instance, two components should be positioned close each other for safety or accessibility reasons. This may be not so evident to a novice designer.

5. *Filling of a matrix of impacts of each component on the selected DCFs*

In this step a table, namely the Impacts Matrix, is filled (Table 1). It put in relation the components with the DCFs of the DC of interest. The generic score *Iif* in a cell of the table express the impact of a component *i* on a certain DCF *f*. If a DCF has a very low impact on a part the value is 0 while 1 means just the opposite. The determination of these values requires more expertise than the previous matrix. Depending on the type of DC, specific approaches and tools may be advisable to determine the values. For instance, in case of eco-sustainability aspects, LCA tools may be used to obtain the impact indices, as shown in the test case section.

Module	Product Components	DCF1	DCF2	DCF3
Module1	*Component a*	0,3	0,5	1
Module1	*Component b*	0,8	0	0,3
Module2	*Component c*	0,1	1	0

Table 1: Exemple of Impact Matrix

6. *Definition of the Components Similarity Matrix*

The Components Similarity Matrix (CSM) is built from the Impact Table. As the DCMx, this matrix is symmetric and correlates pairs of components. Give a pair of components *i* and *j* the value s_{ij} appearing in the cell is computed as:

$$s_{ij} = 1 - \sqrt{\frac{\sum_f (Iif - Ijf)^2}{N}} \qquad (1)$$

where *N* is the cardinality of the DCF set, *Iif* and *Ijf* are respectively the impacts on a DFC *f* as resulting from the Impact Matrix. The formula (1) express the similarity of two components. It is evaluated as the 1's complement of the normalised Euclidian distance between the arrays of the DCF impacts of the two components.

7. *Evaluation of the modularity index of each module*

For a given module *m* under optimization, a set of components has been initially identified from the step 2. Dependencies and similarities, included respectively into the DCMx and the CSM are used to determine a modularity index MI_m as follows:

$$MI_m = k \frac{S_{m,in}}{S_{m,in}+S_{m,out}} + (1-k)\frac{D_{m,in}}{D_{m,in}+D_{m,out}} \qquad (2)$$

where $S_{m,in}$ and $S_{m,out}$ represent respectively the internal and the external similarities of the module *m*, while $D_{m,in}$ and $D_{m,out}$ represent respectively the internal and the external dependencies. Internal refers to the relations among the components belonging to the module m, while external are those relations from components of the module towards components of other modules.

For instance, $S_{m,in}$ is defined as:

$$S_{m.in} = \sum_{i=1}^{c}\left(\sum_{j=i+1}^{c} s_{ij}\right) \qquad (3)$$

The other values are defined in a similar manner. *k* is a factor

Article 02-dm-68

varying from 0 to 1 which weights the relative influences of the DC similarities of the components of a module towards the geometric and structural dependencies.

8. Evaluation of the Global Modularity Index

A global indicator of the current module set is required to assess the necessity of improvements to the product structure. A Global Modularity Index is defined as:

$$\mathrm{GMI} = \frac{\sum_m MI_m}{M} \quad (4)$$

It is used to compare different module combinations and to assess if the current module set has reached an optimal configuration.

9. Reorganization of the modules

Three operators on the modules structure have been defined to change the definition of the modules and to maximise the *GMI*:

- *Module splitting*: separate a module in two.
- *Modules merging*: combine two or more modules together.
- *Components moving*: shift one or more components from one module to another.

The designer will use these operators to improve the *MIm* values and consequently the *GMI*. At the moment, the operators are applied on the basis of the designer experience and considerations.

Splitting a module is suggested when two groups of components are weakly linked each other, by their similarities or dependencies. On the contrary, in other cases it is beneficial to merge some modules. This second option is advisable weather two modules exhibits connections and similar impacts on the selected DC.

The last operator is used in case a component is strongly dependent with other modules. Alternatively, a component could be removed form a module if its influence on the DC contrasts with the rest of the components. For instance, the impact of the component is negligible in a module which strongly determines the behaviour of the product. Changing the module definitions by adding or removing components requires to assess the compatibility of the modification and to redesign the physical structure of the modules being involved.

10. Iteration from point 3 to 8 until the result is satisfactory

As the definition of the modules is updated, steps from 3 to 8 are repeated. In fact, the redefinition of the modules structure may imply some components to be redesign to adapt to the new modules. So, step 3, 4 and 5 could require slight revisions. Then, the MI_m indexes can be recomputed. The process is iterated until improvements of the GMI are possible.

4- Test case

In this section, a case study, based on the redesign process of a freestanding cooker, is shown. Electrolux, a global leader in home and professional appliances, provided the household appliance and its bill of material (BOM). This test case tends to demonstrate how the modular representation can be improved for a specific DC into the redesign phase. The steps of the method will be followed.

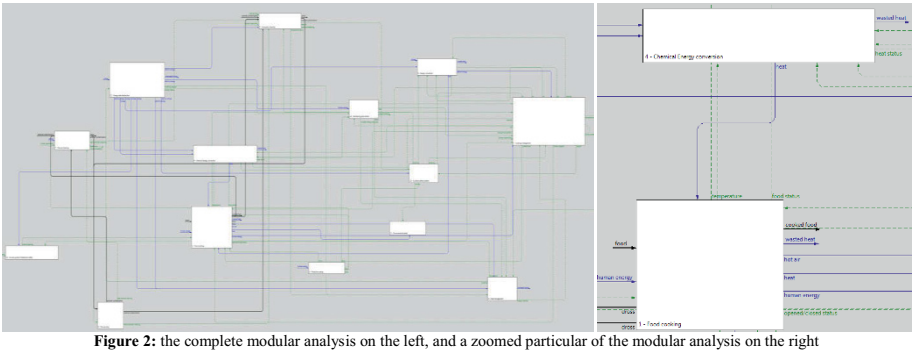

Figure 2: the complete modular analysis on the left, and a zoomed particular of the modular analysis on the right

First of all the DC for the redesign is identified. The approach for the eco-sustainability context is proposed: this means that the modular structure will concern also sustainability features.

The first phase of the proposed modular procedure, the modular analysis, is a standard task and is independent from the chosen DC. The functional analysis is developed in order to obtain the modular analysis. The main function of the product is defined as “To Cook food”. This function needs flows of material, energy and signals in input to operate. Once these flows are defined, also the output ones are determined. The functional analysis continues splitting the black box into sublevels and maintaining coherence of input and output flows. The result of the analysis are the following. In the first level of detail 3 functions are defined: provide food, ensure safety, allow cleaning. In the second level 11 functions are found and in the last level, the third, 44. With the third level, the functional analysis is considered completed.

The functions defined in the previous step are now re-arranged into modules following the three kinds of flows (dominant, branching and conversion/transmission). For this product 14 modules are identified: *Food cooking - Automatic cleaning, Protective casing - Chemical energy conversion - Cooking management - Energy conversion - Manual cleaning - Prevent dirty - Heat management - Auxiliary safety systems - Environmental safety - Energy safe distribution - Human-product interaction safety - Monitoring*

Article 02-dm-68

and control. Figure 2 shows the identified modules with their flows of material, energy and signal. The software tool called MODULOR helped to perform the multilevel analysis and to group the modules.
Now, following the proposed procedure, is necessary to link the components to the modular analysis. Every component of the product is developed to perform at least a function, its main function has to fit with one of the functions that have been defined into the functional analysis. As shown in Table 2 every component is associated to one of the functions found previously. For example, considering the resistance of the oven, the "base element", the function that performs is "convert energy to heat". This task is then repeated for every component. Since any function belongs to a module, every component is now associated automatically to a module too. For example, the "base element" is associated to module 6, "energy conversion". In order to evaluate the physical dependencies that exist between components, depending on their interfaces, a dependency correlation matrix is provided. The 71 components of the freestanding are placed in rows and columns.

Article name	*Theoretical function associated*	*Associated module*
SIDE PANEL SO RIGHT WH CE	1.4.1 -Provide smooth surfaces	***8 - Prevent dirty***
PILLAR SO CE	2.1.5 - provide support plane	***1 - Food cooking***
DRAWER ROOF 60	1.4.1 -Provide smooth surfaces	***8 - Prevent dirty***
HINGE BRACKET 55/60	3.2.2 - avoid food container sudden opening	***13 - Human - product interaction safety***
REARPANEL SO 60 CE GAS	1.4.1 -Provide smooth surfaces	***8 - Prevent dirty***
MAINTERMINAL COVER SO	2.2.9 - provide energy connection	***6 - Energy conversion***
BRACKET HING. RIGHT CE	2.1.5 - provide support plane	***1 - Food cooking***
FEET	2.1.5 - provide support plane	***1 - Food cooking***
FRONT FR.60 SO RAW FLAT	2.1.5 - provide support plane	***1 - Food cooking***
AIR GUIDING 60	3.4.4 - permit product cooling	***9 - Heat management***
COOLING FAN MOTOR 230V	3.2.4 - convey energy safely	***12 - Energy safe distribution***
COOL FAN MOTOR PLATE	3.4.4 - permit product cooling	***9 - Heat management***
CAVITY WRAPPER	2.1.6 - allow variable food positioning	***1 - Food cooking***
CAVITY ROOF	2.1.3 - permit hot place	***1 - Food cooking***
LAMP BJB 25W/FAST	2.1.4 - allow food cooking status check	***5 - Cooking Management***
GASKET OVEN SO/MO (387_4985)	2.1.3 - permit hot place	***1 - Food cooking***
HEAT.ELEM.TOP/GRILL 230V	2.2.10 - convert energy to heat	***6 - Energy conversion***
BASE ELEMENT 230V/1000W	2.2.10 - convert energy to heat	***6 - Energy conversion***

Table 2: component - function association

The score is evaluated depending on the physical connections that are present into the assembly. If there is a threaded connection, as in the case of side panel and rear panel of the structure, the score of the dependency between these two components will be 1. Otherwise, if there are none connections, as between the knobs, the score will be 0. Some values d_{ij} of the product parts are depicted on the Table 5.
The chosen DC, for evaluating the redesign of the freestanding, is the eco-sustainability. Three DCFs will describe the DC: the impacts of the raw materials collection, the manufacturing and the use phase. The Life Cycle Assessment (LCA), described by the UNI EN ISO 14040, involves the evaluation of some environmental aspects of a product through all stages of its life cycle, including those relating to the 3 DCFs. In order to fill the Impact Matrix, a LCA tool is used to evaluate the features.
All the 71 components of the product are classified by their weights and materials to perform the LCA analysis. CAD model of the product is visible in Figure 3. For evaluating the use phase, an energetic consumption of 2,1 kWh is considered. This concerns the energy requested from the oven resistances, the 25W lamp and the 20W ventilation system. It has been estimated an average life of the product of 10 years, considering an use of 90 minutes per day on 180 days per year. Also the hob requires energy to operate: it needs gas that is estimated to be 1500 Kg, considering 1Kg of usage every 2 day for 300 days per year, for 10 years.
The End of Life scenario proposed is, according to Ecodom data: the 75% of the product recycled and the last 25% processed for landfill.

Figure 3: free standing CAD model

Trough the calculation with ICPP GWP (100a) method, this model produces the results reporting on Figure 4.
The use phase (GAS + electricity) has the biggest impact on the whole product CO2 footprint.

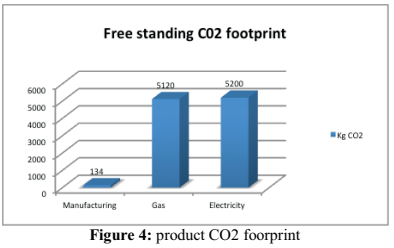

Figure 4: product CO2 foorprint

Those results are necessary to estimate the DCFs. Filling the LCA data into a matrix, the impact matrix is created for this product. A matrix to identify the single score for every one of the chosen three DCFs is calculated. The matrix is composed by 71 rows, corresponding to the 71 components, and 3 columns, reporting the DCFs score for each component. Scores of every single component depends on the results obtained from LCA.

Module	Product Components	DCF1 (Raw materials)	DCF2 (Manufacturing)	DCF3 (Use phase)
Module6	HEAT.ELEM.TOP/GRILL 230V	0,314	0,118	0,500
Module6	BASE ELEMENT 230V/1000W	0,328	0,123	1,000

Table 3: Impact Matrix for two components

The scores are assigned on the basis of how many Kg of CO2 are issued in atmosphere. 1 implies a higher impact. For the "use phase impact" a feature score is assigned only to that

components that are involved into this phase (ex: burners and resistances). To define the matrix data from LCA are used: in the use phase case, 5120 Kg of eq. CO2 derives from gas consumption and 5200 Kg of eq. CO2 derives from electric energy use. The cooker has in fact two different kind of alimentation: electric energy and gas furniture.

Components / Components	Smart aub. wh gas knob	Smart aub. wh gas knob	Smart aub. wh gas knob	Smart aub. wh gas knob	Front glass so 60 wh flat	Lamp bjb 25w/fast	Heat.elem.to p/grill 230v	Base element 230v/1000w	Mainterminal cover so	Cont. panel 60 fls wh gas	Drawer roof 60	Bracket front wh	Bracket rear	Rearpanel so 60 ce gas	Side panel so left wh ce	Side panel so right wh ce
Smart aub. wh gas knob		1,000	1,000	1,000	0,845	0,982	0,373	0,180	0,983	0,916	0,827	0,797	0,846	0,695	0,711	0,711
Smart aub. wh gas knob	1,000		1,000	1,000	0,845	0,982	0,373	0,180	0,983	0,916	0,827	0,797	0,846	0,695	0,711	0,711
Smart aub. wh gas knob	1,000	1,000		1,000	0,845	0,982	0,373	0,180	0,983	0,916	0,827	0,797	0,846	0,695	0,711	0,711
Smart aub. wh gas knob	1,000	1,000	1,000		0,845	0,982	0,373	0,180	0,983	0,916	0,827	0,797	0,846	0,695	0,711	0,711
Front glass so 60 wh flat	0,845	0,845	0,845	0,845		0,833	0,504	0,281	0,829	0,837	0,804	0,786	0,814	0,708	0,721	0,721
Lamp bjb 25w/fast	0,982	0,982	0,982	0,982	0,833		0,369	0,182	0,981	0,910	0,821	0,791	0,840	0,689	0,705	0,705
Heat.elem.top/grill 230v	0,373	0,373	0,373	0,373	0,504	0,369		0,710	0,361	0,391	0,415	0,420	0,411	0,425	0,425	0,425
Base element 230v/1000w	0,180	0,180	0,180	0,180	0,281	0,182	0,710		0,170	0,194	0,214	0,218	0,210	0,224	0,224	0,224
Mainterminal cover so	0,983	0,983	0,983	0,983	0,829	0,981	0,361	0,170		0,920	0,830	0,800	0,850	0,698	0,714	0,714
Cont. panel 60 fls wh gas	0,916	0,916	0,916	0,916	0,837	0,910	0,391	0,194	0,920		0,910	0,880	0,929	0,778	0,794	0,794
Drawer roof 60	0,827	0,827	0,827	0,827	0,804	0,821	0,415	0,214	0,830	0,910		0,970	0,980	0,868	0,884	0,884
Bracket front wh	0,797	0,797	0,797	0,797	0,786	0,791	0,420	0,218	0,800	0,880	0,970		0,951	0,898	0,914	0,914
Bracket rear	0,846	0,846	0,846	0,846	0,814	0,840	0,411	0,210	0,850	0,929	0,980	0,951		0,848	0,864	0,864
Rearpanel so 60 ce gas	0,695	0,695	0,695	0,695	0,708	0,689	0,425	0,224	0,698	0,778	0,868	0,898	0,848		0,984	0,984
Side panel so left wh ce	0,711	0,711	0,711	0,711	0,721	0,705	0,425	0,224	0,714	0,794	0,884	0,914	0,864	0,984		1,000
Side panel so right wh ce	0,711	0,711	0,711	0,711	0,721	0,705	0,425	0,224	0,714	0,794	0,884	0,914	0,864	0,984	1,000	

Table 4: Similarity matrix.

Components / Components	Smart aub. wh gas knob	Smart aub. wh gas knob	Smart aub. wh gas knob	Smart aub. wh gas knob	Front glass so 60 wh flat	Lamp bjb 25w/fast	Heat. elem.top/ orill 230v	Base element 230v/1000w	Mainterminal cover so	Cont. panel 60 fls wh gas	Drawer roof 60	Bracket front wh	Bracket rear	Rearpanel so 60 ce gas	Side panel so left wh ce	Side panel so right wh ce
Smart aub. wh gas knob		0	0	0	0	0	0	0	0	1	0	0	0	0	0	0
Smart aub. wh gas knob	0		0	0	0	0	0	0	0	1	0	0	0	0	0	0
Smart aub. wh gas knob	0	0		0	0	0	0	0	0	1	0	0	0	0	0	0
Smart aub. wh gas knob	0	0	0		0	0	0	0	0	1	0	0	0	0	0	0
Front glass so 60 wh flat	0	0	0	0		0	0	0	0	0	0	0	0	0	0	0
Lamp bjb 25w/fast	0	0	0	0	0		0,1	0	0	0	0	0	0	0	0	0
Heat. elem.top/grill 230v	0	0	0	0	0	0,1		0	0	0	0	0	0	0	0	0
Base element 230v/1000w	0	0	0	0	0	0	0		0	0,6	0	0	0	0	0	0
Mainterminal cover so	0	0	0	0	0	0	0	0		0	0	0	0	1	0	0
Cont. panel 60 fls wh gas	1	1	1	1	0	0	0	0	0		0	0	0	0	0,85	0,85
Drawer roof 60	0	0	0	0	0	0	0	0,6	0	0		0	0	0,9	0,9	0,9
Bracket front wh	0	0	0	0	0	0	0	0	0	0	0		0	0	0,9	0,9
Bracket rear	0	0	0	0	0	0	0	0	0	0	0	0		0	1	1
Rearpanel so 60 ce gas	0	0	0	0	0	0	0	0	1	0	0,9	0	0		1	1
Side panel so left wh ce	0	0	0	0	0	0	0	0	0	0,85	0,9	0,9	1	1		0
Side panel so right wh ce	0	0	0	0	0	0	0	0	0	0,85	0,9	0,9	1	1	0	

Table 5: Dependencies matrix.

Taking the "base element" as an example, it will be identified into the matrix by three feature scores: 0,328 for raw material collection, 0,123 for the process and 1 for the use phase. The scores derive from the CO2 consumption.

The score 1 in the use phase of the "base element" (Table 3) is justified because, among the other components, has the maximum impact. Completing the calculation for all components means completing the impact matrix.

The similarity matrix is then performed, according to the formula (1). Then, the similarity is calculated for each component. For example the similarity among the two components, base element and heating element, is here calculated according to the Table 3:

$$s_{\text{heat elem-base elem}} = 1 - \sqrt{\frac{(0{,}314-0{,}328)^2 + (0{,}118-0{,}123)^2 + (0{,}5-1)^2}{3}}$$

Defining the similarities between all pairs of components, the whole Similarity matrix for the product is filled, a 71x71 symmetrical matrix.

Data on similarities and dependencies are necessary to estimate the modularity index of each module. As example, the calculation of the $S_{5.in}$ is reported according to the Table 4 and the Table 5.

$S_{5.in=}1*6+0{,}845*4+0{,}982*4+0{,}833=14{,}141$. Since the matrix is symmetric, only the superior part of the matrix is considered. $D_{in=}$ 0. Also S_{out} e D_{out} are computed.

For this test case was chosen a k factor of 0,5. Once the $S_{m.in}$, $S_{m.out}$, $D_{m.in}$, $D_{m.out}$ are calculated for every module, also the MI is defined.

	Module5	Module6	Module7
S_{in}	14,14	1,24	18,89
S_{out}	42,16	19,23	42,82
D_{in}	0,00	0,000	10,20
D_{out}	4,10	1,700	5,60
MI	0,13	0,03	0,48

Table 6: MI calculated

Table 6 shows the MI values calculated on three modules. For the previous three modules, the GMI is so calculated:

$$\text{GMI} = \frac{MI_5 + MI_6 + MI_7}{3} = 0{,}42$$

According to the method, an iteration of the reorganization of the modules step is performed to improve the GMI and hence

Article 02-dm-68

the product modularity based on eco-sustainability.

- The Main terminal cover component has been MOVED to the module 7 thanks to its similarities with the components of that module.
- Control panel has been MOVED to module 5.
- Module 5 has been SPLITTED into two modules, the mini submodule containing the Lamp and the Front glass has been MERGED to module 6.

These considerations has conducted to a MI of 0,48, 0,11 and 0,56 respectively for the modules 5, 6 and 7. The enhancement of all the modularity indexes is verified, and hence the modularity for eco-sustainability. For this case of study the iteration is stopped, considering positive this modularization result.

4- Conclusions

This paper has discussed a method to optimize the modularization of a product in the context of redesign activities. The approach moves from a functional based definition of the modules that is refined in consideration of implementation constraints and specific design targets.

The method is based on a procedure to be performed iteratively. The performances of the product are described through specific features that represent tangible measures of the performances of the product, while the introduced improvements are measured through indexes. The presented test case has demonstrated the method in the context of the eco-sustainability of a freestanding cooker.

The approach has been applied manually but is suitable to be partially automated. It could be implemented in a supporting tool in order to be applied faster and with better results. Once a software system has been conceived and implemented, the application to a wider set of products would lead to a deeper validation of the method.

Therefore, the aims for future studies is the measurement of the benefits introduced by a context depended modularization for the redesign of household appliances and also of products of other sectors. To evaluate the procedure could be useful comparing the re-design time spent to improve the product with or without the method. Not only could the time be analysed, but, for a chosen DC, also the efficacy of the change made on the product, that is the better-adopted solution in terms of cost-saving or other evaluation areas.

7- References

[BL1] Bimal N., Leslie M. and Nanua S. A Methodology for Integrating Design for Quality in Modular Product Design. In Journal of Engineering Design, 17(5): 387-409, 2006.

[DG1] Dahmus J.B., Gonzalez-Zugasti J.P. and Otto K.N. Modular product architecture. In Design Studies, 22: 409-424, 2001.

[E1] Eggen O. Modular product development. A review of modularization objectives as well as techniques for identifying modular product architectures, presented in a unified model. 2003.

[E2] Erixon G. Modular Function Deployment (MFD), Support for Good Product Structure Creation. In Proceedings of the 2nd WDK Workshop on Product Structuring. Delft, University of Technology. Netherlands. 1-16, 1996.

[FM1] Frenken K. and Mendritzki S. Optimal modularity: a demonstration of the evolutionary advantage of modular architectures. In Journal of Evolutionary Economics, 22(5): 935-956, 2012.

[GP1] Gershenson J.K., Prasad G.J. and Allamneni S. Modular Product Design: A Life-cycle View. In Journal of Integrated Design and Process Science, 3(4): 1-9, 1999.

[GP2] Gershenson J.K. and Prasad G.J. Modularity in product design for manufacturability. In International Journal of Agile Manufacturing, 1(1), 1997.

[H1] Hölttä K.M.M. Incorporating design effort complexity measures in product architectural design and assessment. In Design Studies, 26: 463-485, 2005.

[HC1] Hwang S-C. and Choi Y. Modular Design of a Product to Maximize Customer Satisfaction with Respect to Body Size: A Case Study for Designing Office Chair. In International journal of precision engineering and manufacturing, 12: 791-796, 2011.

[L1] Lau A.K.W. Managing Modular Product Design: Critical Factors and a Managerial Guide. In PICMET 2009. Proceedings of the conference, Portland, Oregon, USA, 2009.

[LK1] Li Z.S., Kou F.H., Cheng X.C. and Wang T. Model-based product redesign. In International Journal of Computer Science and Network Security, 6(1): 99-102, 2006.

[MJ1] Meng X., Jiang Z. and Huang G.Q. On the module identification for product family development. In International Journal of Advanced Manufacturing Technology, 35: 26–40, 2007.

[OH1] Otto K.N., Hölttä-Otto K. and Simpson T.W. Linking 10 years of modular design research: alternative methods and tool chain sequences to support product platform design. In Proceedings of the ASME 2013, Portland, Oregon, USA, 2013.

[PB1] Pahl G., Beitz W., Feldhusen J and Grote K.H. Engineering Design: A Systematic Approach. 3rd ed. London: Springer, 2007.

[SE1] Sosa M.E., Eppinger S.D. and Rowles C.M. A Network Approach to Define Modularity of Components in Complex Products. In Journal of Mechanical Design, 129(11): 1118-1129, 2007.

[SS1] Simpson T.W., Siddique Z. and Jiao R.J. Product platform and product family design: methods and applications. New York: Springer, 2006.

[SS2] Smith S., Smith G. and Shen Y.T. Redesign for product innovation. In Design Studies, 33: 160-184, 2012.

[SW1] Stone R.B., Wood K.L. and Crawford R.H. A heuristic method for identifying modules for product architectures. In Design Studies, 21: 5-31, 2000.

[UE1] Ulrich K.T. and Eppinger S.D. Product Design and Development. 3rd Edition, McGraw-Hill, New York, 2004.

[YB1] Yassine A.A. and D. Braha D. Complex Concurrent Engineering and the Design Structure Matrix Method. In Concurrent Engineering, 11(3): 165-176, 2003.

[YY1] Yang Q., Yu S. and Jiang D. A modular method of developing an eco-product family considering the reusability and recyclability of customer products. In Journal of Cleaner Production. 64: 254–265, 2014.

Article 03-dm-72

SEAT DESIGN IMPROVEMENT VIA COMFORT INDEXES BASED ON INTERFACE PRESSURE DATA

A. Lanzotti[1], A. Vanacore[1], D. M. Del Giudice[1]

(1) : University of Naples Federico II, Department of Industrial Engineering
P.le Tecchio, 80, 80125, Naples (NA), Italy
Phone +39-0817682506 – Fax +39-0817682187
E-mail : {antonio.lanzotti, amalia.vanacore, domenicomaria.delgiudice}@unina.it

Abstract: Literature on seat comfort recognizes that seat interface pressures are the objective comfort measures that most clearly relate to users' comfort perceptions about sitting experience. In this paper, the above relationship is quantitatively investigated by performing simple but effective explorative analyses on seat comfort data collected during experimental sessions involving 22 volunteers who tested 4 office chairs (differing in terms of cushion softness). Statistical data analyses show that subjective sitting comfort/discomfort ratings are significantly related to several combinations of pressure variables. The joint analysis of synthetic indexes based on seat interface pressures reveals to be a useful tool for comparative seat comfort assessment. Besides valuable suggestions for the definition of an effective strategy for seat comfort assessment, the results of data analyses provide useful information to support the product design phase. In fact, the sitting experience results to be significantly improved by: (1) a balancing of pressures between the bilateral buttocks; and (2) a balancing of contact areas between buttocks and thighs.

Key words: office chair; sitting comfort/discomfort assessment; interface pressure distribution.

1- Introduction

Research in the field of medicine and epidemiology has shown that, over the past decades, the incidence of backache has considerably increased (Harkness *et al*. 2005; Rubin 2007) due to sedentary lifestyle, closely related to prolonged period of sitting (Ehrlich 2003; Dul *et al*. 1987). More than 60% of people experience have at least one episode of lower back pain at work, in almost 45% of cases the first attack of lower back pain happens while working (Rezaee *et al*. 2011), with an incidence in the office workers of at least one episode backache every 3 years (Lengsfeld *et al*. 2000). The remedy that is most useful to prevent backache is the adoption of ergonomic chairs (Nelson *et al*. 1998, Herbert 2001, Loisel *et al*. 2001). Given the importance of ergonomic seat and prevention, this study aims to investigate the biomechanical aspects and the comfort evaluation of ergonomic office chairs, which are necessary steps to identify guidelines for designers to improve human wellness.

Specialized literature does not provide a universally recognized definition of comfort, but in recent years the assumption that comfort and discomfort are two distinct entities is winning broad respect (Vink 2012). Typically comfort assessment is realized on the basis of subjective evaluations and/or postural analysis.

Subjective evaluations are collected by surveying potential seat users who are asked to express their feelings of comfort/discomfort with the seat and/or compare, in terms of perceived comfort/discomfort, similar seats.

Postural analysis is realized by measuring one or more objective parameters, such as:

- the pattern of muscle activation measured through electromyography (EMG);
- the stress acting on the spine measured through pressure transducer and radio waves;
- the postural angles obtained using contact or non contact (like photogrammetric) techniques in real experiments or using virtual manikins in virtual experiments;
- the body–seat interface pressure measured through capacitative or resistive mats.

Anyway, subjective and objective methods are not alternative since they complement each other.

One of the main factors that affect seat comfort is seat-interface pressure distribution (Stinson *et al*. 2009). Moreover, pressure distribution is the objective measure with the clearest correlation with the subjective evaluation methods (De Looze *et al*. 2003, Kyung *et al*. 2008, Noro *et al*. 2012). In particular, in office chair design (Reed *et al*. 1993) pressure maps have been used to qualitatively verify the effectiveness on seat comfort of product features like, *e.g*., cushion shape and materials (Kamijo *et al*. 1982, Park *et al*. 2000, Fujimaki *et al*. 2002) through correlation studies with the subjective user perceptions. Nevertheless the widespread use of pressure maps, just few authors have proposed synthetic indexes for the related multidimensional data, collected by performing real or virtual experiments involving a selected sample of potential users (Lanzotti *et al*.

Article 03-dm-72

2011). Furthermore, little effort has been made to highlight the usefulness of these pressure measures for specific purposes defined by designers, (*e.g.* design for a specific user or design for a generic user).

In this paper the main results of an extensive explorative analysis on seat interface pressure data are described. The explorative data analysis was aimed at investigating three critical aspects of seat comfort assessment: a) gender-based differences in seat interface pressure distribution; b) the relationship between subjective and objective measures of seat comfort; c) discriminant effectiveness of indexes based on seat interface pressure.

2- Methods

2.1 - Overview of experiment

The data analysed in this paper were obtained from a study aimed to validate a seat comfort index proposed by the authors. All details on the criteria for selection of participants and office chairs, the subjective rating scales and the experimental design have been provided in a previous paper (Lanzotti *et al*. 2011) only a synthetic description is given here.

Each of 22 volunteers [age 20-31, 14 males and 8 females, mean (SD) mass = 75.0 (12.2) kg, mean (SD) stature = 175.3 (11.6) cm] participated in short-term experimental sessions for the comfort evaluation of 4 office chairs.

Total duration of an experimental session (with 1 volunteer testing 1 seat) was 10-15 minutes including few minutes (≤5) for initial seat and posture adjustments and 10 minutes performing the task of reading a test on VDU. The choice of short-term experimental session is recommended when using pressure data for assessment of sitting comfort/discomfort (Helander *et al*. 1997; Kyung *et al*. 2008). In contrast, more extended durations are generally used when investigating sitting discomfort largely due to fatigue in seated postures not depending on chair design.

The 4 office chairs had a typical architecture of product (*i.e*., a five-pointed base, a backrest and two armrests) but differed in shapes and materials of the cushion.

In particular, different Seat Conditions were represented by the characteristic softness of the seat cushion (S) considered as a qualitative ordinal variable with four levels (0, soft; 1, medium; 2, compact; 3, semi-rigid). Each seat was representative of a specific Seat Condition level.

During each experimental session subjective measures of comfort perception as well as seat interface pressures were collected.

The comfort/discomfort ratings were based on a verbal numeric scale, with the comfort and discomfort at the extremes, thereby measuring a mixture of comfort and discomfort. In particular, for this assessment the scale Borg CR10 modified by Kyung *et al*. (2008) was used. This scale includes scores from 0 (no comfort, and maximum discomfort) to 10 (maximum comfort and minimum discomfort). Besides, in order to assess comfort and discomfort separately, another set of subjective measures was collect using two different scales. A verbal rating scale with four levels was used to collect data about perceived comfort, whereas to assess discomfort participants were asked to rank the chairs based on perceived discomfort.

Objective measures were obtained from pressure measured at the seat interface; these measures consisted of both overall and local pressures (Table 1).

Type	Name	Area to measure
Objective	PCP, Peak Contact Pressure (N/cm^2)	• Left/right thighs (TL/TR)
	CP, Contact Pressure (N/cm^2)	• Left/right buttocks (BL/BR)
	CA, Contact Area (cm^2)	
	UW, Unloaded Weight (kg)	
	PCL, Press. Comfort Loss Index	• Sum of 4 local body part press.
Subjective	RT, Comfort/Discomfort Rating	• Whole body
	CR, Chairs Ranking	• Whole body
	CD, Comfort Degree	• Whole body

Table 1: Comfort Variables

2.2 - Experimental protocol

The experiments were performed at the Department of Industrial Engineering, University of Naples Federico II, in a suitable room cleared of furnishings.

For each session, a pressure mat was placed on the seat cushion and secured with masking tape to facilitate seat adjustments. The participants were instructed to sit carefully to minimize wrinkles on the pressure mat. In order to avoid the noise due to the sequence of the tested seats, participants tested the office chairs following a randomized experimental plan. Besides, in order to avoid that visual impact with the tested chair could affect comfort/discomfort assessments, each participant was introduced into the room blindfolded and made to sit. Subsequently, she/he was asked to take off the blindfold and adjust the chair in such a way that the legs were in rest conditions and the feet were comfortably on the floor so as to form an angle between the thigh and the leg equal to 90°. Thus, after an initial seat and posture adjustments, the participant had to read a text on a VDU for 10 minutes, after which it was blindfolded again and taken back out of the room.

2.3 - Data collection and processing

Subjective ratings were collected in a consistent order to minimize confusion: the *"Comfort/discomfort Rating (RT)"* and the *"Comfort Degree (CD)"* were obtained using a questionnaire immediately after each session; instead, the "*Chairs Ranking (CR)*" was obtained from a questionnaire submitted only after the participant had tested all four office chairs.

Pressure data were collected continuously during the reading text on VDU, using a Novel Gmbh (Munich, Germany) pressure mat (S2027 Pliance™). The pressure mat comprised 256 (16x16) thin (<1.2 mm) capacitive sensors that could easily conform to the contour of the seat, and measure pressures typically in a range from 0.2 N/cm^2 up to 6 N/cm^2. Thanks to its flexible structure the mat is a minimally invasive instrument, which does not interfere with user

Article 03-dm-72

Variable	Description	Measurement Unit
caTL (caTR)	Average contact area Thigh Left (Right)	cm^2
caBL (caBR)	Average contact area Buttock Left (Right)	cm^2
caSUM (caTL + caTR + caBL + caBR)	Sum of average contact areas	cm^2
caTL/caSUM, caTR/caSUM, caBL/caSUM, caBR/caSUM	Relative Average contact areas	
cpTL (cpTR)	Average contact pressure Thigh Left (Right)	N/cm^2
cpBL (cpBR)	Average contact pressure Buttock Left (Right)	N/cm^2
cpSUM (cpTL + cpTR + cpBL + cpBR)	Sum of average contact pressures	N/cm^2
cpTL/cpSUM, cpTR/cpSUM, cpBL/cpSUM, cpBR/cpSUM	Relative average contact pressures	
pcpTL (pcpTR)	Average peak contact pressure Thigh Left (Right)	N/cm^2
pcpBL (pcpBR)	Average peak contact pressure Buttock Left (Right)	N/cm^2
pcpSUM (pcpTL+pcpTR+pcpBL+pcpBR)	Sum of peak contact pressures	N/cm^2
pcpTL/pcpSUM, pcpTR/pcpSUM, pcpBL/pcpSUM, pcpBR/pcpSUM	Relative peak contact pressures	

Table 2: Contact area and pressure variables

perception of seat comfort. The mat had an active area of 392 mm x 392 mm, and sensor pitch was 24.5 mm (0.167 sensore/cm^2). Pressures were recorded at 50Hz. This sampling rate was considered sufficient to monitor the frequency of postural changes.

Contact area and contact pressure were calculated by including only data from sensors that were pressed (i.e. a positive value) at least once, and average (arithmetic mean) values were determined for the last 4 minutes of each session. Earlier data were excluded since they were transient due to settling into the chair (Reed et al., 1999).

2.4 – Data analysis

Data analysis aimed at deepening the following three aspects:

- effects of anthropometric variability and of differences in seat conditions on contact pressures;
- relationship between subjective evaluations and objective measurements of seat comfort/discomfort;
- discriminant effectiveness of indexes based on seat interface pressure in predicting comfort/discomfort.

The first aspect was investigated by building new pressure maps of the maximum Peak Contact Pressure (PCP) and analyzing the sampling distributions of the unloaded weight for male and female users.

The dependency of subjective ratings from contact area and pressure variables was investigated via Principal Component Regression (PCR) which develops into two steps: (1) a Principal Component Analysis (PCA, based on the correlation matrix) to reduce the number of explanatory variables (*i.e.* contact area and pressure variables) and (2) a multiple regression of each subjective rating on the factors from the PCA (obtained at step 1), which are in turn combinations of the contact area and pressure variables.

Following the data analysis strategy proposed by Kyung et al. (2008), all the collected contact area and pressure data were divided into four groups corresponding to four local body parts (*i.e.* right/left buttock and right /left thigh see Figure 1) and a total of 27 explanatory variables were derived (Table 2) to be used at step 1 of PCR. The first 9 variables were related to average contact areas and ratios; the second 9 variables described average contact pressures and ratios; and the last 9 variables indicated average peak contact pressures and ratios. Three overall pressure variables (caSUM, cpSUM, and pcpSUM) were only used to derive 12 ratio variables but they were not further analyzed.

The number of Principal Components (or Factors) was determined by two criteria, the size of the eigenvalue (>1) and the cumulative percentage (≈90%) of variance accounted for by the selected components. The selected factors were rotated by the varimax method. Statistical results were considered 'significant' or 'marginal' when $p \leq 0.05$ and $0.05 < p \leq 0.1$, respectively.

In order to select a robust response (*i.e.* a good proxy of perceived comfort/discomfort) to be used in step 2 of PCR and verify the consistency of the subjective data, the association among the three evaluation scales adopted was evaluated.

Finally, the discriminant effectiveness in predicting seat comfort/discomfort was evaluated for two indexes based on seat interface pressure: Peak of Contact Pressure (PCP) and Pressure Comfort Loss (PCL). The latter (Lanzotti et al., 2011) is based on a "Nominal is the Best" (NB) comfort loss function, standardized with respect to the nominal pressure. The formulation of this index takes into account the need to design for a specific target population through the introduction of a parameter θ related to the composition of the sample in terms of gender (eq. 1):

$$WPCL(\theta) = \theta \cdot WPCL_f + (1-\theta) \cdot WPCL_m \qquad (1)$$

with:

- $WPCL_f$, is comfort loss function (PCL) for the female population;
- $WPCL_m$, is comfort loss function (PCL) for the male population.

As regard the PCP index was considered the maximum PCP registered among the four groups of pressure

Article 03-dm-72

corresponding to four local body parts (*i.e.* right/left buttock and right /left thigh in Figure 1).

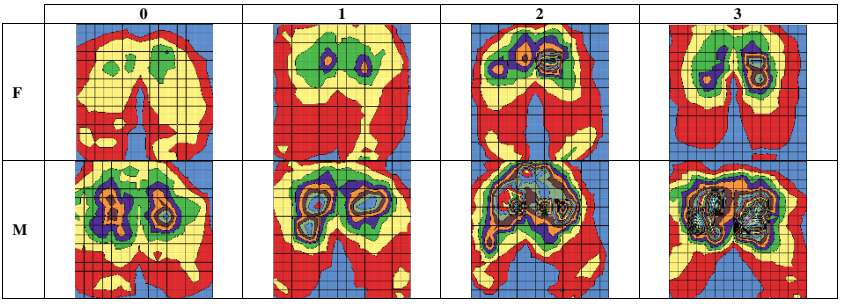

Table 3: Maps of the maximum PCP for the different sub-samples stratified by gender and softness of the cushion

3- Results

3.1 – Effects of anthropometric variability and seat conditions on interface pressures

In order to analyse the effects of anthropometric variability and of seat conditions on the contact pressures, the average peak contact pressure detected by each sensor mat was analysed. Specifically, new pressure maps stratified by gender and seat condition were developed, in which each map cell represents the PCP greater among all PCP sampled from a particular sensor (16 x 16), for a given seat condition (0, 1, 2, 3) and for a given gender (M, F). Thus the new maps were obtained (Table 3). The female maps (first row of the table) show PCP values lower than the corresponding male maps (second row of the Table 3). Similarly, the table was also examined by columns, in other words from the first column (soft cushion level) to the fourth (semi-rigid cushion level), PCP values shown gradually increase. It can be said that the Seat Condition 0 and 1, show pressure levels lower than the Seat Condition 2 and 3, for both males and females. One can assume that, independently of the anthropometric variability, the ideal contact pressure distribution of males differs from that of females. Hence, the seat designers could take this result into account when designing for a Target. Indeed, pressure levels and contact areas change significantly between males and females. It would seem that the males are more sensitive to changes in the seat condition and this could mean an amplification of discomfort effects in the long period.

In addition Figure 1 shows that, independently of the seat condition, the female users significantly differ from male users in terms of unloaded weight.

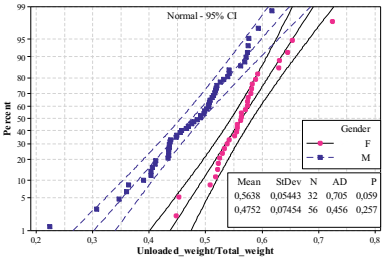

Figure 1: Probability Plots for the r.v. unloaded weight

3.2 – Relationship between subjective evaluations and objective measurements of seat comfort/ discomfort

The relationship between comfort degree and contact pressures was analysed from the statistical standpoint via PCR analysis. At step 1, a PCA was performed on the set of 27 variables listed and described in Table 2. Five principal components with an eigenvalue >1 accounted for 86.9% of the total variance (Table 4). After varimax rotation, each component appeared to have a more general interpretation (as indicated in Table 10). Indeed, a subset of (2 to 4) pressure variables was found in each principal component that predominantly determined the respective component level, as evidenced by high coefficients (>0.4). Further, these subsets of variables were mutually exclusive and distinguishable in terms of relevant body part, or type of pressure, and the principal components were termed accordingly to this (Table 4). Firstly, it's worthwhile to observe that for Factor 4, relating to contact area ratios, coefficients with opposite signs were found between the thigh and buttock average contact area ratios (i.e., caTL/caSUM vs. caBL/caSUM). In other words, there were negative associations between the thigh and buttock in terms of contact area ratio. Secondly for

Article 03-dm-72

Variable	Factor 1	Factor 2	Factor 3	Factor 4	Factor 5
	Left buttock (pressure)	Buttock (area)	Right buttock (pressure)	Left buttock vs thigh (area)	Right thigh (pressure)
caTL	0.024	-0.104	0.025	-0.422	0.028
caTR	-0.003	-0.247	-0.011	-0.501	0.014
caBL	0.101	-0.477	-0.007	0.025	0.021
caBR	-0.052	-0.568	0.050	-0.111	0.043
caTL/caSUM	0.035	0.257	0.029	-0.288	-0.014
caTR/caSUM	-0.020	0.070	-0.040	-0.445	-0.024
caBL/caSUM	0.057	-0.082	-0.030	0.443	0.019
caBR/caSUM	-0.092	-0.286	0.044	0.271	0.018
cpTL	0.001	0.092	0.067	0.042	0.380
cpTR	-0.004	-0.108	-0.031	-0.007	0.497
cpBL	-0.440	0.070	-0.151	-0.036	0.106
cpBR	-0.094	0.024	-0.453	-0.022	0.166
cpTL/cpSUM	0.161	0.113	0.260	0.014	0.108
cpTR/cpSUM	0.157	-0.128	0.151	-0.032	0.261
cpBL/cpSUM	-0.381	0.058	0.121	-0.007	-0.241
cpBR/cpSUM	0.084	-0.032	-0.413	0.020	-0.078
pcpTL	-0.126	0.253	0.037	0.010	0.280
pcpTR	-0.109	0.022	-0.121	0.005	0.499
pcpBL	-0.478	-0.019	-0.057	0.001	0.095
pcpBR	-0.025	0.087	-0.419	-0.003	0.033
pcpTL/pcpSUM	0.115	0.256	0.246	-0.024	0.042
pcpTR/pcpSUM	0.178	-0.052	0.121	-0.020	0.249
pcpBL/pcpSUM	-0.459	-0.135	0.184	0.025	-0.076
pcpBR/pcpSUM	0.235	-0.021	-0.423	0.006	-0.118
Eigenvalue	11.036	4.027	2.574	1.887	1.330
Cum percent	46.0	62.8	73.5	81.3	86.9

Table 4: Five principal components after varimax rotation (underlined values are >0.4 and maximal across factors in absolute value)

Factor 2, relating to contact areas of the bilateral buttocks, high coefficients were all negative.

The consistency of the subjective data was analysed via the Goodman and Kruskall's index, being all three adopted scales ordinal and polytomous. The Goodman and Kruskall's index was calculated for all possible combinations of binary association. Results (Table 5) show a substantial consistency of the scales.

The minimum value for Goodman and Kruskall's index in Table 5 is 0.653 which reveals a medium-high level of association between the scales ranking and rating. It is evident that the responses given on the scale "comfort degree" were highly associated with the other ones (0.984 e 0.860). So this scale was selected as a good proxy of perceived comfort/discomfort and set as a robust response function for step 2 of PCR analysis.

Rating (RT)	0.984	0.653
	Degree (CD)	0.860
		Ranking (CR)

Table 5: Results for association analysis on the evaluation scales

All three fitted regression models for comfort degree were significant ($p \leq 0.01$). As coefficients in table 6 show, increasing Factor 2 (significant for the mixed sample of users and male sub-sample) and decreasing Factor 1 (significant for the mixed sample of users and female sub-sample) and Factor 5 (marginal for the mixed sample of users and significant for the female sub-sample) would be effective at improving comfort degree. In particular, the coefficients for Factor 2 (-0.348 and -0.360, respectively for mixed sample and male sub-sample) indicated that increasing contact areas at the buttocks (specifically, caBL and caBR) would be the most effective method for improving comfort degree. Similarly, the coefficients for Factor 1 (0.174 and 0.350, respectively for the mixed sample and female sub-sample) suggest that decreasing average (peak) contact pressures and ratios relevant to the left buttock (specifically, cpBL, pcpBL e pcpBL/pcpSUM) would be the second most effective way of improving the subjective ratings. Finally, the coefficients of Factor 5 (-0206 and -0901, respectively for the mixed sample and female sub-sample) suggest a third strategy, the decrease of the contact pressure and peak at the right thigh (specifically, cpTR e pcpTR).

Term	Mixed		Males		Females	
	Coef	p	Coef	p	Coef	p
Intercept	2.602	0.000	2.648	0.000	2.449	0.000
Factor 1	0.174	0.024	0.132	0.209	0.350	0.004
Factor 2	-0.348	0.001	-0.360	0.003	-0.276	0.166
Factor 3	0.013	0.836	0.018	0.810	0.157	0.247
Factor 4	-0.037	0.575	-0.076	0.333	-0.054	0.784
Factor 5	-0.206	0.064	-0.139	0.273	-0.901	0.024

Table 6: Standard coefficients for regression models relating PCA factors to comfort degree expressed by mixed sample of users, male sub-sample and female sub-sample

3.3 – Discriminant effectiveness of indexes based on seat interface pressure in predicting comfort/discomfort

Mean values of PCP and WPCL for the four tested chairs were compared to verify the consistency of discriminant information provided by these indexes.

Article 03-dm-72

The results, assuming WPCL as a response function, are shown in Figure 2 on the next page, for the sub-sample of female users, the mixed sample of users and for the sub-sample of male users. Level 0, corresponding to the level Soft, was the best one in terms of WPCL, whereas levels 2 and 3 got the worst results. Level 3 seems to be the most robust one against changes in the composition of the reference (sub-)sample. In fact, all other levels showed higher slopes for the mean effect plots. Assuming that the population were composed exclusively of males, level 3 would be better than level 2.

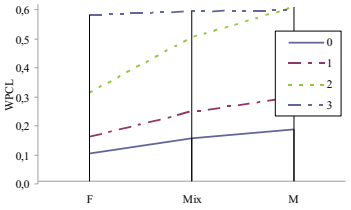

Figure 2: Mean effects assuming WPCL as response for the sample of MIXed users, the sub-sample of Male users, and the sub-sample of Female users

The same analysis was carried out, assuming the peak contact pressure, PCP, as a response function (Figure 3). The lowest values were recorded for level 0, which is the best one independently of the gender of users. Level 1 got comparable performance, whereas level 2 and 3 once again resulted to be the worst ones. Assuming that the (sub-)sample were composed exclusively of male users, level 3 would be better than level 2. Moreover, it's worthwhile to highlight that in the WPCL diagram the differences between the level 0 and 1 are clearer than in the PCP diagram. In order to verify if the two indexes significantly differ for capacity to discriminate among the four seat conditions, the Wilcoxon-Mann-Whitney test was performed. So for both indexes, three binary comparisons of seat condition (0 vs. 1, 1 vs. 2 and 2 vs. 3) were carried out for each composition of (sub-)sample (Mixed, Males and Females). Results (Table 7) show that, independently from the composition of the reference (sub-)sample, the WPCL is able to discriminate between the seat conditions 0 and 1, and between 1 and 2; whereas, the PCP only distinguishes between the seat conditions 1 and 2.

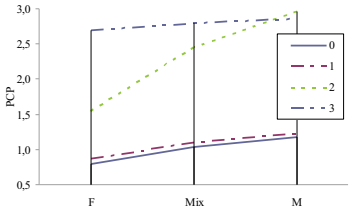

Figure 3: Mean effects assuming PCP as response function for the sample of MIXed users, the sub-sample of Male users, and the sub-sample of Female users.

The ranking of the four tested chairs shows substantial coherence of the results provided by PCP and WPCL, although WPCL seems to be more sensitive to the contact pressure distribution than PCP. This coherency in results does not mean that PCP and WPCL provide the same information. Indeed, for the sub-sample of male users, the maximum values of these indexes refer to different pressure maps and so identify different users (Figure 4).

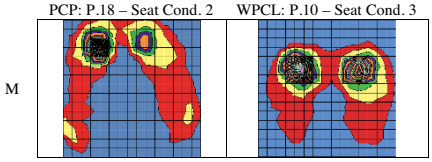

Figure 4: Pressure maps related to maximum values of WPCL and PCP for all seats

4- Discussion and conclusions

The purpose of this paper was to investigate some critical aspects of seat comfort/discomfort assessment. The illustrated experiment refers specifically to office chairs for use at VDT workstation, however the strategy of analysis can be easily adapted to assess seat comfort/discomfort in different context of use.

The results of data analysis provided satisfactory answers to the research questions.

Subjective evaluations resulted significantly correlated to several combinations of pressure variables. Consequently, these pressure variables, derived in terms of average contact area and average (peak) contact pressure, could be used

Variable	Mixed			Males			Females		
	0 vs 1	1 vs 2	2 vs 3	0 vs 1	1 vs 2	2 vs 3	0 vs 1	1 vs 2	2 vs 3
PCP		able to discr.			able to discr.			able to discr.	
WPCL	able to discr.	able to discr.		able to discr.	able to discr.		able to discr.	able to discr.	

Table 7: Results of non-parametric Wilcoxon-Mann-Whitney test

across anthropometric variability for the assessment of sitting comfort/discomfort.

An improved sitting experience is argued as requiring a balancing of pressures between the bilateral buttocks and a balancing of contact areas between buttocks and thighs. Indeed, asymmetrics of contact areas and pressure distributions can be considered undesirable as they appear to lead to lower subjective ratings.

However, use of pressure data is suggested as more appropriate for assessing short-term comfort/discomfort, reflecting seat support and the distribution of body load on it.

Interface pressures resulted significantly affected by anthropometric variability and gender, in particular. As shown in section 3.1, in fact, the pelvis of women is developed more in width, while in men the sacral and iliac bone is thicker and heavier, generating localized peaks of greater magnitude. Consequently, the analysis of pressure maps stratified by gender helps to take into account anthropometric variability and provides valuable suggestions to design the seat shape and choose materials. Moreover, the joint analysis of synthetic indexes (WPCL, PCP) could be a useful tool to discriminate among different seats conditions.

5- References

[DK1] De Looze, M., Kuijt Evers, L., Van Dieen, J., 2003. Sitting comfort and discomfort and the relationships with objective measures. Ergonomics, 46, (10), 985-997.

[DH1] Dul, J., Hilderbrandt, V. H., 1987. Ergonomic guidelines for the prevention of low back pain at the workplace. Ergonomics, 30, (2), 419-429.

[E1] Ehrlich, G. E., 2003. Low Back Pain. Bulletin of the World Health Organization, 81, (9), 671-676.

[FM1] Fujimaki, G., Mitsuya, R., 2002. Study of the seated posture for VDT work. Displays, 23, (1-2), 17-24.

[HM1] Harkness, E. F., Macfarlane, G. J., Silman, A. J., McBeth J., 2005. Is musculoskeletal pain more common now than 40 years ago?: Two population-based cross-sectional studies. Rheumatology, 44, (7), 890–895.

[HZ1] Helander, M., Zhang, L., 1997. Field studies of comfort and discomfortin sitting. Ergonomics, 40, (9), 895-915.

[HD1] Herbert, R., Dropkin, J., Warren, N., Sivin, D., Doucette, J., Kellogg, L., Bardin, J., Kass, D., Zoloth, S., 2001. Impact of a joint labor-management ergonomics program on upper extremity musculoskeletal symptoms among garment workers. Applied Ergonomics, 32, (5), 453-60.

[KT1] Kamijo, K., Tsujimara, H., Obara, H., Katsumatu, M., 1982. Evaluation of seating comfort. SAE Technical Paper Series 820761. Society of Automotive Engineers, Troy, MI.

[KN1] Kyung, G., Nussbaum, M. A., 2008. Driver sitting comfort and discomfort (part II): Relationships with an prediction from interface pressure. International Journal of Industrial Ergonomics 38, (5-6), 526-538.

[LV1] Lanzotti, A., Vanacore, A., Trotta, M., 2011. Validation of a new index for seat comfort assessment based on objective and subjective measurements. Proceedings of the IMProVe International conference on Innovative Methods in Product Design – ADM-INGEGRAF, June 15th – 17th, Venice, Italy.

[LF1] Lengsfeld, M., Frank, A., van Deursen, D.L., Griss, P., 2000. Lumbar spine curvature during office chair sitting. Medical Engineering and Physics, 22, (9), 665-669.

[LG1] Loisel, P., Gosselin, L., Durand, P., Lemaire, J., Poitras, S., Abenhaim, L., 2001. Implementation of a participatory ergonomics program in the rehabilitation of workers suffering from subacute back pain. Applied Ergonomics, 32, (1), 53-60.

[NS1] Nelson, N. A., Silverstein, B. A., 1998. Workplace changes associated with a reduction in musculoskeletal symptoms in office workers. Human Factors, 40, (2), 337-50.

[NN1] Noro, K., Naruse, T., Lueder, R., Nao-i N., Kozawa, M., 2012. Application of Zen sitting principles to microscopic surgery seating. Applied Ergonomics, 43, (2), 308-319.

[PK1] Park, M. Y., Kim, J. Y., Shin, J. H., 2000. Ergonomic design and evaluation of a new VDT workstation chair with keyboard-mouse support. International Journal of Industria.l Ergonomics, 26, (5), 537-548

[RG1] Reed, M., Grant, C., 1993. Development of a measurement protocol and analysis techniques for assessment of body pressure distributions on office chairs. TR. Ann Arbor, MI: Univ. of Michigan, Center for Ergonomics.

[RJ1] Rezaee, M., Jafari, N. J., Ghasemi, M., 2011. Low Back Pain and Related Factors among Iranian Office Workers. International Journal of Occupational Hygiene, 3, (1), 23-28.

[R1] Rubin, D., 2007. Epidemiology and risk factors for spine pain. Neurological Clinics, 25, (2), 353-371.

[SC1] Stinson, M., Crawford, S., 2009. Optimal Positioning: Wheelchair Seating Comfort and Pressure Mapping. In International Handbook of Occupational Therapy Interventions, Springer, 83-90.

[V1] Vink, P., 2012. Editorial: Comfort and discomfort studies demonstrate the need for a new model. Applied Ergonomics, 43, (2), 271-276.

Acknowledgements

The present work was developed with the contribution of the Italian Ministry of University and Research (MIUR) performing the activities of the PON01_01268 DIGIPAT Project, Digital Pattern Product Development: A Pattern Driven approach for industrial product design, simulation and manufacturing.

Article 04-dm-76

Design process and trace modelling for design rationale capture

Emna Moones[1], **Esma Yahia**[1], **Lionel Roucoules**[1]

(1) : Arts et Metiers ParisTech, CNRS, LSIS, 2 cours des Arts et Metiers, 13617 Aix-en-Provence, France
+33 (0)4 42 93 81 40

E-mail : esma.yahia@ensam.eu

Abstract: To face the high industrial concurrence and to remain competitive, companies are asked to work in a context of collaborative engineering environment where design rationale is a prerogative to reduce their product development time. Design rationale aims to capture the knowledge from the product design at a very early stage as those decisions have higher impacts in terms of time, cost and quality in the later product lifecycle stages. We propose, in this paper, a three-layer framework to answer to the need to capture the process design knowledge and to use the construct captured to visualize the process performances and to derive rules in order to help and assist the designers.

Key words: Design process, design rationale, design trace, decision making, product design.

1- Introduction

Nowadays in a highly competitive industrial environment, companies must respond to new market demands in terms of improving quality, reducing costs, shortening time and increasing changes reactivity. Therefore enterprises must develop a comprehensive approach to master their products design phase in order to get more competitive and reactive and to save more time for innovation.

In order to meet these requirements, researchers and manufacturers, for approximately twenty years, offer to work in a collaborative engineering environment to bring together a large number of professional skills within a project and to cooperate all together using these various expertise.

The paper is organized in four sections. In section 2, the research context related to the mastering of the decision making during virtual product development is presented. A bibliographic background, based on rationale modelling and tracing issues, is presented in section 3, it contributes to the definition of traceability, its objectives and its main approaches in the domain of product engineering. In the light of this state of art, a framework based on three-layer traceability approach is presented in section 4. Finally, in section 5, conclusion and further work are discussed.

2- Research context and orientation of the proposal

2.1 - Potential industrial improvement, issues and objective: design rationale modelling

Currently, different industries run their product development process in a collaborative way using well-known commercial solutions for PLM, CAD and CAX modelling. In this context, many researches ([G1], [KK1] and [T1]) have also been proposed to enrich this collaboration by identifying the relations between product concepts related to function, structure or multiple views description.

The main industrial focus concerns the product design assessment and improvement. Nevertheless, many industrial experiences highlight the difficulty to retrieve information (i.e. decision) related to previous design solutions and therefore to adapt their solutions when the industrial environment is changing. For example, it's difficult to identify how and where do industrialists have to adapt the design when dealing with improvement and innovation? And to know if a new industrialization solution is better than the previous one?

When dealing with the companies competitiveness decrease especially at the design phase, the following observations could be listed:

- Issue n°1: Time loss when engineers are seeking for the necessary information needed to finalize their design activities

In fact, various studies [FG1] and [U1] have shown that a considerable amount of time, spent by engineers during the design phase, is dedicated to research information. Thus, it is interesting to facilitate information search, in order to save this time and to exploit into innovation.

- Issue n°2: Time loss when engineers are managing different changes

To ensure their place in the market, companies must also demonstrate capacities in identifying industrial context variations and abilities to manage changes as soon as possible in the product lifecycle and especially during the design phase. In fact, during this creative phase, it is important to master the impact of several changes that could be extremely costly if they are not properly propagated. Besides, [BB1] argues that 85 % of the decisions made during the design phase, impact more than 80 % of the product final cost.

- Issue n°3: Time loss when engineers are exchanging data

In fact, in the context of collaborative design, different employees with different background and skills are required to exchange data. Then, it is important to facilitate data exchange and to ensure coherence between all the exchanged data.

In consequence, the main research objectives consist in mastering choices (i.e. decisions), taking by different stakeholders during the design and manufacturing phases and adapting them when the industrial context is changing.

2.2 - Orientation of the proposal and questions of research: decision making in product design process

Modelling the design rationale could answer to the above research objectives. In fact, the authors assumed that it is important firstly, to trace how designer made choices during the design process and secondly, to reuse some pattern of the choice process in their future design processes. Besides, the authors assume that tracing and capitalizing the decision making will reduce the time loss for information retrieval and information exchange. Thus, the designers will have more time for innovation.

The scientific community has already dealt with Design rationale and so far, many representations have been proposed by [HP1]. This paper aims at identifying the main design rationale concepts and implementing them based on the Six W's (who, what, why, where, when and how) conceptual model [Z1]. By capturing those concepts during the collaborative design phase, the authors assume that information retrieval and change management will be faster. Therefore, in order to achieve the research objectives, the authors propose to answer to the following four functions (i.e. questions of research):

- F1. How to model collaborative design information based on Six W's: who takes a decision, what is the decided information, when and where the decision has been taken, how and why the decision has been taken? The capitalizing of those concepts reduces the time of information retrieval (Issue n° 1).
- F2. How to manage changes through the identification and simulation of the changes propagation? The use of dedicated algorithms to mastering changes and tools to simulate them will act on design agility and then reduce the time to change management. (Issue n° 2).
- F3. How to trace design rationale and capitalize learning processes. Those learnt situation will be used on future situations.
- F4. How to ameliorate design process by studying the change impact on the process?

Those two last functions assume to faster assess new design solutions and then to better go toward innovation.

Figures 1 describes the global view of each function (i.e. questions of research) in order to support decision making in engineering design. The authors assume that when the design is complex, several decisions have to be taken since all the solutions cannot be assessed and considered:

- Initial design space which is mastered using knowledge modelling that constrains the admissible solutions. Those constraints are related to the design context.
- Assessment of each admissible solution in the performance space.
- Final decision making using multi-criteria analysis.
- One decision, with respect to specific parameters, can be propagated to another decision making activity, etc.

This paper deals, only, with functions 1, 2 and 3. Hence, the state of the art, presented in section 3, is structured according to those functions.

3- Background Literature

Within the collaborative engineering product development cycle, the design process is considered as a creative process [GP1]. It is a high added value process regarding its complexity and the various business expertise which is involved under a collaborative context with different specificities, actors and organizations. This creative process is also a dynamic process as it is adjusted and adapted frequently during its execution when answering to the recurrent modification demands. In order to master this creative and dynamic process, it is primordial to emphasize on a non-functional feature [GP1] which is the traceability.

In this article section, we aim, at first, to define traceability and its objectives in the context of product design process and then to make a state of the art of the different traceability approaches.

3.1 - Process modelling

A multitude of process meta-models have been proposed during those last decades. Based on [W1], the authors argue that those models are providing adequate concepts to tackle the issues introduced above:

- IDEF meta-model is based on ICOM concepts: Input, Control, Output and Mechanisms [RD1]. They are close to Six W's concepts. The "what" can be supported by I/O, "Who, How, Why" can be seen as Resources or Mechanism of IDEF. Finally the "When" is implicit to the meta-model as it provides sequential links among the process activities.
- UML activity diagram [F1] also provides concepts related to the design process (activity, data flows, synchronisation bar ...). However, its applications are more dedicated to business process used, for example, in manufacturing system control.
- BPMN provide also different concepts to answer to the Six W's one [B1]. It will not be more detailed since the activity diagram is very similar to the UML one (data flows and control flows).

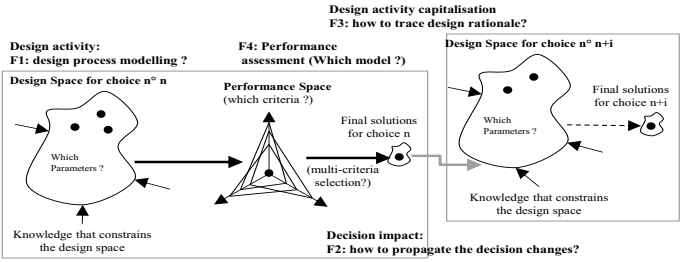

Figure 1: overview of decision making and main functions of the proposal.

As presented by [GP1], a process can be classified in three categories: creative, interactive and automatic. Those three categories rank the level of autonomy in running a process. Therefore, the authors argue that the design process is a creative process since the design process of a complex system is not known when the design starts. The process is, then, created dynamically.

3.2 - Change management

Change management represents a recurrent activity in collaborative design process that occupy between 20% to 30% of the project global time [K1] and [BS1]. To reduce this time loss, it is important to master the impact of the different modifications that concerns the input, control, and the process mechanisms. One major issue concerns the identification of the impacted modifications area in order to localise the specific activity to be executed without acting the modifications on all the process activities. The other issue concerns the simulation and the propagation of these modifications through the identified activities.

Different approaches, methods and tools were developed to master the change management. The following state of art (table 1) allows the comparison of these approaches based on their capability to identify, simulate and propagate the change.

Methods and tools	Change identification	Change simulation	Change propagation
CREOPS2 (Multi-agent distributed system) [C1]	Yes		
Architecture based agent to support the collaborative design process [CM1]	Yes	Yes	Yes
SHARED-Design Recommendation and Intel Management System (SHARED –DRIMS) [PSL1]	Yes	Yes	Yes
Protocol for change simulation [LN1]	Yes	Yes	
COllaborative COnflict Management in Engineering Design (CO2MED) [R1]	Yes	Yes	
What if design approaches [HL1]	Yes	Yes	Yes
Impact analyses method : CSP solver [OG1]	Yes		Yes
Monte Carlo method [JE1]	Yes	Yes	Yes
Algorithm to validate the parameters modification [RC1]	Yes		Yes
Dependences Graph describing the existing relations between the entities and impact and Analysis based on probability estimation [OS1]	Yes		
Probability of modification matrix, impact matrix, risk matrix [CS1]	Yes		Yes
DEPNET(product Data dEPendencies NETwork identification and qualification [OB1]	Yes	Yes	Yes
Propagation algorithm, identification and change impact algorithm [B1]	Yes	Yes	Yes

Table 1: Change management state of the art synthesis

3.3 - Traces for Product Design Process

The concept of traceability evolved in different engineering context among computer science and product development. It refers to the action to follow or mark something (oxford dictionary). In the context of Product development process, traceability is the action to collect the diverse events occurring during the execution of a given process [M1]. It aims to record the process lifecycle history by capturing:

- The design routes and the evolution of design items [S1].
- The information relative to the product and the process as well as their relations in the various product lifecycle phases [OB1]
- The important decisions and justification during the process lifecycle [OB1]
- The diverse modifications that took place during the conception process lifecycle

According to [A1], traces are then used to (a) understand lessons from previous experiences and to (b) reuse the '*captured design knowledge to adapt past solution and apply them to current and future problems'*. This design knowledge is captured with respect to different design decision-making frameworks proposed by [HA1], [OB1] which are adapted from the Zachman framework [Z1]. The latter, structures the holistic enterprise mechanisms representation by answering to the basic communication interrogatives: Six W's.

The meta-model for achieving traceability proposed by [HA1] describes different constructs:

- 'What' represents the design objects that correspond to I/O of the design process, it could correspond to requirements, technologies, functions, parts…
- 'Who' corresponds to the actors with different competencies that are creating and using the design object.
- 'How and where' represent the 'sources' that documents the design objects between numerical documents, procedures and with different format types and formalization levels.
- 'When' represents two 'time dimensions' related to the design object: the relative time that corresponds to the order of execution and the absolute time that corresponds to the version, state and the stage of the design object.
- 'Why' represents the design rationale behind the creation, evolution and changing of the design. It corresponds to the decisions, made and justified by the actors, which affect the selection and the evaluation of the design objects.

The traceability constructs proposed by [OB1] rely on the design product knowledge.

- 'What' refers to the product knowledge such as the design elements, constraints...
- 'Who' represents the actors creating, using and modifying the product knowledge.
- 'Where' identifies the activity that handles the product knowledge.
- 'When' informs about the time and date of creation or modification of the product knowledge.
- 'Why'corresponds to the objectives of the activity creation or modification.
- 'How' represents the justification or the design rationale behind the decision of the product Knowledge creation or modification.

3.4 - A comparison of different traceability approaches

Several researchers have proposed different approaches to capture and trace the design experience knowledge and to exploit, dynamically, those traceability constructs to infer some knowledge rules. The traces are supposed to facilitate the understanding of the design activities and their analyses by visualizing the 'captured knowledge' [RL1] in order to evaluate the process performance and to detect the frequent sequences, delays and the eventual conflicts …

The MUSETTE approach developed by [CP1], in the context of computer system use, exploit the interaction traces between the systems and its users in order to assist the Agent-Task Management. The approach, developed by [BV1], aims to retrieve necessary and useful activities supervision information for the users involved in a context of Computer Learning Environments with heterogeneous tools. Besides, [PS1] exploit the traces, in the context of collaborative process, to improve the communication between users and to contribute to the establishing of a common knowledge. Moreover, [KC1] approach aims to specify and elaborate a knowledge oriented maintenance platform by exploiting the traceability constructs under the SBT (System Based on Traces) proposed by [SP1].

4- Discussion of the state of the art and proposal overview

Despite their different contexts of use, the studied traceability approaches are mainly articulated around three major connected phases: (a) traceability constructs collection based on the design process observation, (b) traces generation with respect to the objective of use and (c) traces visualization and exploitation.

In order to trace the process rationale in the context of collaborative design, the authors propose a framework based on the three-layer traceability approach (figure 2).

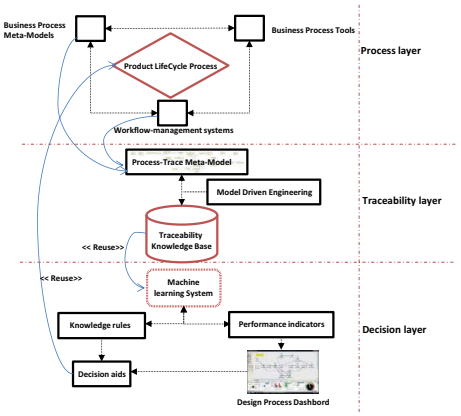

Figure 2: Overview of the proposal.

4.1 – Framework Process Layer

The first layer depicts the observation phase of process design which is characterized by different process models and tools and workflow execution tools.

IDEF0 is selected by the authors to model design process. Figure 3 shows how each of the IDEF concept answer modelling the Six W's concepts expected in a design process. As presented on figure 3, IDEF0 process model will be also used to identify relation among decision making activity and to propagate some change from one decision to another.

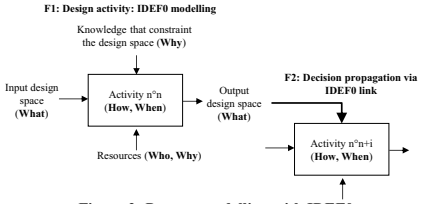

Figure 3: Process modelling with IDEF0

Figure 4 shows in UML formalism the design rationale model describing all the constructs that contribute to the creation of product knowledge during the design phase.

Figure 5 presents an illustration of the design process modelling on a simple example that aims at selecting four parameters in the design space. It has proven that changes can be propagated via concepts and relations identified in the process model. As far as IDEF0 constraints, resources or outputs are changing; only impacted activities can be re-computed.

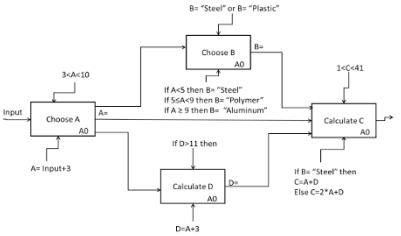

Figure 5: Change management based on process modelling.

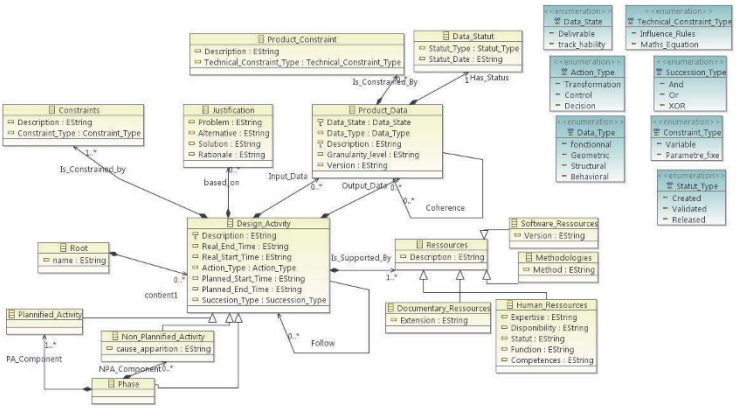

Figure 4: Proposed UML formalism to identify knowledge construct for design rationale

4.2 – Framework traceability Layer

The challenge of this layer is to identify the process trace constructs in order to build the traceability knowledge base. The authors assume that the trace process model corresponds to all the knowledge constructs identified under the process design model and to all the constructs related to the workflow execution such as the real time process start and end.

This traceability model was implemented under the Eclipse environment in order to derive automatically an Excel table that could be exploited in the framework decision layer to establish the performance keys.

4.3 – Framework decision Layer

This layer corresponds to the exploitation and reuse of the collected traces. It consists of two parts:

- Performance key generation and process design dashboard.
- Design rules deduction using machine learning. Those rules could be used automatically by the software resources in the design process or by the actors themselves and this according to their experiences feedbacks

5- Conclusion and recommendation for further work

This paper proposes a process model based design rationale capture. This allows modeling the Six W's concepts, supporting the design change identification and tracing the decision making. The three-layer traceability approach is currently partly implemented (process modelling, trace modelling).

Future works will consist in deploying design example and to couple the two first layers with learning approach in order to support decision making based on capitalized design situation. Those examples will also be benchmarked with current approach in order to validate all the assumptions of this work:

- Accelerate information retrieval
- Accelerate change propagation
- Support decision making and alternatives performances assessment

6- References

[A1] Ahmed, S., 2005. Encouraging reuse of design knowledge: a method to index knowledge. Design Studies, 26(6), pp. 565--592.

[B1] Bennama, Y., 2012. Modélisation du couplage processus-produit pour la gestion des modifications en conception, Aix en Povence.

[BB1] Berliner, C. & J.A.Brimson. Cost management for today's advanced manufacturing. The CAM-I. conceptual Design, Harvard Business School Press, 1988

[BP1] BPMN, Business Process Modelling Notation, http://www.omg.org/spec/BPMN/index.htm (visited April 2014)

[BS1] Badke-Schaub, P. & Stempfle, J., 2000. Analysis of solution finding processes in teams. Human Behaviour in Design: Individuals, Teams, Tools., pp. pp. 121-130..

[BV1] Broisin, J. & Vidal, P., 2007. Une approche conduite par les modèles pour le traçage des activités des utilisateurs dans des EIAH hétérogènes. Revue des Sciences et Technologies de l'Information et de la Communication pour l'Education et la Formation (STICEF), Volume 14.

[CM1] Cutkosky, M. & Mori, T., 1998. Agent-base Collaborative Design of Parts in Assembly. Atlanta, Georgia, USA.

[CMR1] Cointe, C., Matta, N. & Ribière, N., 1997. Design Proposition Evaluation: using Viewpoints to Manage Conflicts in CREoPS2.

[CP1] Champin, P., Prié.Y & Mille, A., 2003. Musette: Modelling uses and tasks for tracing experience. ICCBR, Volume 3, pp. 279--286.

[CS1] Clarkson, P. J., Simons, C. & Eckert, C., 2004. Predicting Change Propagation in Complex Design. Journal of Mechanical Design , Volume 126, pp. 788-797.

[F1] Fawler M., UML distilled. A brief guide to the standard object modelling language, Addison-Wesley, 2005.

[FG1] FREY ,E., GOMES, S.& SAGOT,J ;C,. Application de la méthode QFD comme outil d'extraction des connaissances métier en conception intégrée, 2007.

[G1] Gero, J. S., 1990. , Design prototypes: a knowledge representation schema for design. AI Magazine, 11(4), pp. 26--3.

[GP1] Godard C. & Perrin O., Les processus métiers : concepts, modèles et systèmes. Lavoisier, ISBN 978-2-7462-2300-4, 2009.

[HA1] Hansen, C. & Andreasen, 2000. Basic thinkings patterns of decision-making in engineering design. Neukirchen, s.n., pp. 1-8.

[HL1] van Houten, F. & Lutters, E., 2006. What-if' Design as an Integrative Method in Product design. Advances in Design, pp. 37--47.

[HP1] Hu, X., Pang, J., Pang, Y., Atwood, M., Sun, W., Science, C., & Regli, W. C. A survey on design rationale: representation, capture and retrieval. In ASME Design Engineering Technical Conferences, 2000.

[**JE1**]Jarratt, T., Eckert, C., Caldwell, N. & Clarkson, P., 2011. Engineering change: an overview and perspective on the literature. Research in engineering design, 22(2), pp. 103--124.

[K1] Klein, M., 2000. Toward a systematic repository of knowledge about managing collaborative design conflicts. Worcester MA, pp. 129-146.

[KC1] Karray, M.-H., Chebel-Morello, B. & Zerhouni, N., 2013. A Trace based system for decision activities in CBM Process. Gaithersburg, MD, pp. 1--6.

[KK1] Krause, F., Kimura, F., T., K. & Lu S.C, P., 1993. Product Modelling. Journals of the CIRP, 42(2).

[LN1] Lara, M. A. & Nof., S.Y. 2003. Computer-supported conflict resolution for collaborative facility de signers. International Journal of Production Research, 41(2), pp. 207-234.

[M1] Moones, E., 2013. Analyse de performance d'un processus créatif pour une activité d'ingénierie de produit, Aix en provence.

[OB1] Ouertani, M., Baina, S., Gzara, L. & Morel, G., 2011. Traceability and management of dispersed product knowledge during design and manufacturing. Computer-Aided Design, May, 43(5), pp. 546–562.

[OG1] Ouertani, M. Z., Gzara, L. & Lossent, L., 2004. Engineering change process: state of the art, a case study and proposition of an impact analysis method. Bath , UK.

[OS1] Ollinger, G. A.& Stahovich, S. F., 2004. Redesign IT-a Model-Based Tool for Mana ging Design Changes. Journa of Mechanical Design, Volume 126, pp. 208-213.

[PS1] Pavkovic, N., Storga, M., Bojcetic, N. & Marjanovic, D., 2013. Facilitating design communication through engineering information traceability. Artificial Intelligence for Engineering Design, Analysis and Manufacturing, 27(2), pp. 105--119.

[PSL1] Pena-Mora, F., Sriram, D. & Logcher, R., 1993. SHARED-DRIMS: SHARED design recommendation-intent management system, pp. 213 - 221.

[R1] Rose, B., 2004. Proposition d'un référentiel support à la conception collaborative : CO²MED (COllaborative COnflict Managament in Engineering Design), Prototype logiciel dans le cadre du projet IPPOP, Nancy.

[RC1] Rouibah, K. & Caskey, K. R., 2003. Change management in concurrent engineering from a parameter perspective. Computers in Industry, Volume 50, pp. 15-34.

[RD1] Ross Douglas T., Structured Analysis (SA): A Language for communicating ideas, Transactions on software engineering, Vol. SE-3, pp. 19-34, 1997.

[RL1] Rossi, F., Lechevallier, Y. & El Golli, A., 2005. Visualisation de la perception d'un site web par ses utilisateurs. Paris, Cépaduès-Edition, pp. 563--574.

[S1] Storga, M., 2004. Traceability in product developement. Dubrovnik.

[SP1] Settouti, L., Prié, Y., Marty, J. & Mille, A., 2007. Vers des Systèmes à Base de Traces modélisées pour les EIAH. Analyses des traces d'utilsation dans les EIAH, STICEF.

[T1] Tichkiewitch, S., 1996. Specification on integrated design methodology using a multi - view product model. Proceedings of ASME System Design and Analysis Conference.

[U1] Ullman, D., 2003. The mechanical design process. 3 rd éd. McGraw-Hill.

[W1] WFMC, Terminology and glossary. Technical Report WFMS-TC-1011, Technical report, Workflow Management Coalition Brussels – Belgium, 1996.

[Z1] Zachman, J. A., "A Framework for Information Systems Architecture". IBM Systems Journal. 26(3). 276-292, 1987.

Article 09-dm-107

Design Synthesis Methodology for Dimensional Management of Assembly Process with Compliant non-Ideal Parts

Pasquale Franciosa[1], Abhishek Das[1], Darek Ceglarek[1], Luca Bolognese[2], Charles Marine[3], Anil Mistry[4]

(1) : The University of Warwick, UK, CV4 7AL
E-mail: {p.franciosa, abhishek.das, d.j.ceglarek}@warwick.ac.uk
(3) : Stadco Limited, UK, TF1 7LL
E-mail: c.marine@stadco.co.uk

(2) : COMAU, IT, Grugliasco (TO), 10095
E-mail: luca.bolognese@comau.com
(4) : Jaguar Land Rover Limited, UK, CV3 4LF
E-mail: amistry@jaguarlandrover.com

Abstract: This paper proposes a design synthesis methodology for dimensional management of assembly processes with compliant non-ideal parts which allows to integrate the critical and heterogeneous design tasks with conflicting or coupled objectives and design constraints such as: (1) tolerancing and variation simulation analysis (VSA); (2) fixture layout design optimization; (3) part-to-part joining process parameters selection and laser beam visibility analysis; or/and; (4) in-process measurement gauge visibility and accessibility analysis. The proposed methodology is based on the *Adaptive Task Graph* (*ATG*) that has capability to model design tasks by integrating Key Product Characteristics (KPCs) and Key Control Characteristics (KCCs) with their impact on the Key Performance Indicators (KPIs); this allows to dynamically capture interactions between design tasks as well as to generate tasks sequence. The design synthesis methodology is based on the development of: (i) assembly surrogate model linking KPCs to KCCs; (ii) sensitivity analysis with capability to model and analyse the interdependencies among design tasks and KPCs, KCCs and KPIs; and, (iii) ATG model which represents the hierarchy of design tasks and is used to generate the sequence of design tasks to minimize their interdependencies during design synthesis. The proposed methodology is illustrated and validated in the process of designing configurations for automotive door assembly with remote fiber laser welding joining process. The methodology shows potential to reduce engineering changes necessary during door assembly process build and testing by 25%.

Key words: Design Synthesis, Product & Process Simulation, Design Task Integration, non-ideal Compliant Parts, Dimensional Management.

1 - Introduction

Current competitive market requirements demand significantly shorter new product realization cycles. Indeed, in automotive industry it is forecasted that the life-cycle of the vehicle will be shortened by up to 1-2 years in the next few years implying that the product and process development cycle needs to comply with the market demand.
Usually, when new models are introduced, very little of the old assembly system can be retained for a new product. To satisfy market demands, in terms of time-to-launch, cost and product quality, the product development process needs to be improved significantly. A new product development process consists of five main steps: (i) determination of product requirements; (ii) conceptual and detailed product/process design; (iii) prototyping; (iv) testing and ramp-up; and, (v) production launch. Prototyping and testing are necessary steps to refine product and process design and eliminate unforeseen failures during the design stage. It was reported that only 60-70% of *First-Time-Right* (FTR) is reached during the design stage. Failures not predicted during the design phase, can appear during ramp-up, which in turn, require engineering changes thus leading to not only significant cost increase ('Rule of 10') but also cause delay in the launch of a new product. Results from a survey carried in [**CH2**, **CO1**] examining automotive assembly process found that thousands of engineering changes are made after the design has been released. For example, during design of a single closure panel fixture around a hundred of engineering changes are made after design release. These changes can include adding new design features, move/change fixture locators, or modify part flanges, etc. For each of the change the fixture design has to be revised, verified and validated (V&V) and finally design need to be updated.
Moreover, in aerospace and automotive industries, around 65-70% of all design changes are related to product-dimensional variation [**CO1**]. It is widely recognized that geometric and dimensional variation are among the most important quality and productivity factors in many assembly processes used not only in automotive and aerospace but also in appliance, shipbuilding and other industries. This becoming even more critical with introduction of new materials and multi-material assemblies and new or hybrid joining processes such as Remote Laser Welding (RLW) for steel/galvanized steel or aluminium sheet metal parts. For emerging processes, such as RLW, product variation is recognised as one of the most crucial barrier to deliver high quality product [**C1**]: indeed, the joint quality is directly related to the part-to-part gap which is imputed to dimensional and geometric variation of stamped sheet-metal parts. A number of studies have investigated dimensional management of compliant parts. For example, Liu and Hu [**LH1**] proposed a model to analyse the effect of deformation

and spring-back on assembly variation by using sensitivity matrix for compliant parts. Camelio et al. [**CC1**] demonstrated that part error, tooling error and assembly spring-back have significant impact on dimensional quality of assembly. These studies underscore a need to consider non-ideal compliant part model for accurate assembly process simulations [**DF2**]. To date, existing approaches have mainly focused on modelling product variation without integrating non-ideal-parts with assembly process models [**CC1**, **FG1**, **GP1**, **WC1**]. However, the design of a complex sheet metal product, such as an automotive body, requires integrating heterogeneous product and process models. For example, some of the design tasks necessary for RLW joining process development are: (i) fixture & clamp layout design optimization; (ii) laser joining process parameters selection and laser beam visibility analysis; and (iii) in-process measurement gauge visibility and accessibility analysis.

To weld galvanized steel satisfactorily using RLW process, the part-to-part gap requirement of 0.05-0.3 mm needs to be satisfied. The part-to-part gap during the process is affected by the Key Product Characteristics (KPCs) such as part variation (non-ideal part model) and process parameters (Key Control Characteristics (KCCs)) such as fixture location and tooling variations [**CH1**]. Further, the joining process is affected by the laser beam visibility of all stitches and the weld quality is affected by the process parameters such as laser power, welding speed, and material stack-up. Moreover, the non-contact optical scanners used for part measurements are affected by part visibility which might be limited due to given clamps layout and fixture design. Thus, the sequence of design tasks needs to be established to facilitate the interactions among multiple aforementioned heterogeneous models/tasks.

Often, design tasks have conflicting or coupled objectives and design constraints. The traditional way to solve this challenge is through the use of a sequential computer simulations and physical experimentations methods [**MB1**]. However, while this approach can provide fast simulation results, the obtained solutions are not optimum, have low accuracy and reliability as they do not take into consideration hidden interactions among tasks defined by heterogonous models consisting KPCs, KCC and Key Performance Indicators (KPIs)). Therefore, going towards an FTR paradigm requires comprehensive and systematic approaches to model the interactions between KPCs and KCCs by integrating variation simulation models that can predict the sensitivity of product/process variations on final KPIs (i.e., time-to-launch, cost and product quality).

This paper addresses these challenges by proposing a design synthesis methodology, named *Adaptive Task Graph* (*ATG*), for dimensional variation management of compliant non-ideal parts.

The proposed design synthesis methodology is based on the development of: (i) assembly surrogate model linking KPCs to KCCs; (ii) sensitivity analysis with capability to model and analyse the interdependencies among design tasks and KPCs, KCCs and KPIs; and, (iii) ATG model which represents the hierarchy of design tasks and is used to generate the sequence of design tasks to minimize their interdependencies during design synthesis.

The rest of the paper is arranged as follows: the state of art in design synthesis is reviewed in Section 2; Sections 3 and 4 present the problem formulation and the proposed methodology, respectively; lastly, an industrial case study is reported in Section 4 to demonstrate the effectiveness of the proposed methodology, whereas conclusions and final remarks are reported in Section 5.

2 - Related works

A significant milestone in design synthesis was the concept of axiomatic design introduced by Suh [**S3**]. Axiomatic design is based on top-down design process wherein design solutions are generated by mapping the relationships between four design domains: (i) customer attributes; (ii) functional requirements; (iii) design parameters; and, (iv) process variables. The design solutions are then evaluated and selected based on two criteria defined as independence axiom and minimum information axiom. Still, while axiomatic design is a systematic method to handle multiple design tasks, it does not detail how to model product and process variations. Further, for some assembly processes, the independence axiom cannot be satisfied due to the intrinsic coupling of individual design tasks.

The Design Structure Matrix (DSM) was originally proposed by Steward [**S2**] as a Boolean matrix, consisting of the binary {0, 1} elements which determine task precedence relations. An element (i, j) of the matrix is equal to "1" if task i-th requires information from task j-th and "0" otherwise. In a design structure matrix the diagonal elements can be considered to be tasks that are in a particular sequence on the diagonal. If a task passes information to another task later in the sequence, the coupling is termed as feed-forward. If a task requires information from a task later in the sequence, the coupling is seen to be feed-back. To some extent, the DSM approach is adopted and implemented in most advanced design tools (CAD), such as CATIA by Dassault Systemes or Pro/Engineer by PTC, in the form of Knowledge Based Engineering (KBE) toolkit. However, the design matrix generated by DSM is obtained based on the historical data or past experience. Therefore, it cannot be applied for new product development, which requires definitions of related KPCs and corresponding KCCs.

A more comprehensive framework is provided by Multidisciplinary Design Optimization (MDO) which is a set of engineering systems design methods which handle optimization of a several tasks. The MDO methods aim to take advantage of the couplings and synergies between different disciplines in order to reach the global optimal design [**S1**]. The main objectives of the MDO process are accuracy of the found solution, computation time and robustness of the optimization process (i.e., the ability to converge to an optimum from large initialization domain).

MDO has been successfully applied to a wide range of applications. Recently, Balesdent et al. [**BB1**] applied MDO to vehicle launch design specifically examining product architecture/thickness optimization and product size/shape optimization. However, optimal product design does not completely satisfy the FTR paradigm. In fact, product-to-process interactions need to be addressed and coupled with product and process variation models. Current MDO approaches are limited only to product-driven analysis and optimisation. Further, some of the MDO approaches are mainly limited to task sequencing problem, under the assumption that the task-to-task relation is given by the

designer's expertise. Statistical-based approaches (such as Design of Experiment - DoE) have also been introduced to analyse the sensitivity of KCCs having the most significant effect on product characteristics. However, those approaches cannot be applied directly in design stage due to un-modelled interactions between KPCs and KCCs. In fact, since most current CAD and Variation Simulation Analysis (VSA) systems are based on ideally sized, ideally located rigid geometry, they are unable to accurately model or predict the effects of variations in product and process, considering simultaneously product compliancy.

Axiomatic Design - AD
• Literature: [**S3**, **SC1**]
• Model type: **Qualitative**
• Product- vs. Process-oriented: **Product/process oriented**
Design Structure Matrix - DSM
• Literature: [**S2, PC1**]
• Model type: **Qualitative**
• Product- vs. Process-oriented: **Product/process oriented**
Multidisciplinary Design Optimization - MDO
• Literature: [**S1**, **BB1**]
• Model type: **Quantitative**
• Product- vs. Process-oriented: **Product oriented**
Design of Experiments - DoE
• Literature: [**V1**]
• Model type: **Quantitative**
• Product- vs. Process-oriented: **Product oriented**

Table 1: State-of-the-art of design synthesis methods.

Table 1 summarises the main design synthesis methods. Methods are usually limited to product or process oriented applications, without a comprehensive mapping of KPCs, KCCs and KPIs on the design tasks. This paper goes beyond the state-of-art by proposing a detailed quantitative relationship between product and process parameters on design task sequence. Task-to-task interaction and task priority are calculated by evaluating the sensitivity of a given design task on the input KPCs and KCCs. The sensitivity of a design task defines the strength of that task. Tasks with the smallest strength are evaluated first as they do not necessarily depend on the estimation of parameters from other tasks.

3 - Problem formulation

The dimensional quality of a product is evaluated by its KPCs defined by GD&T-ISO such as part features (holes, slots) and edge features, etc. The KPCs must be controlled within design specifications in order to ensure that product functions meet design requirements. KCCs are then designed to satisfy KPCs.

$$KPC=\{KPC_1,...,KPC_{N_{KPC}}\} \quad (1a)$$

$$KCC=\{KCC_1,...,KCC_{N_{KCC}}\} \quad (1b)$$

Let us assume that the set of KPCs and KCCs in an assembly process are grouped as in equation (1) where N_{KPC} and N_{KCC} are the number of KPCs and KCCs, respectively.
Moreover, let us assume that a subset of KPCs or KCCs corresponds to final KPCs (that is, KPC_f) or KCCs (that is, KCC_f) being delivered during the design stage (refer to equation (2)). Finally, KPC_f or KCC_f corresponds to the final set of parameters delivered by the whole design process. For example, in RLW joining process part-to-part gap (i.e., KPCs) is understood as an intermediate parameter, but the final critical KPCs is the joint penetration, which is coupled to the gap itself.

$$KPC_f=\left\{KPC_{f,1},...,KPC_{f,N_{KPC_f}}\right\}\subseteq KPC \quad (2a)$$

$$KCC_f=\left\{KCC_{f,1},...,KCC_{f,N_{KCC_f}}\right\}\subseteq KCC \quad (2b)$$

Moreover, let DC be the set of design constraints (such as, model accuracy, computational time), acting on a specific design task. It has:

$$DC=\{DC_1,DC_2,...,DC_{N_{DC}}\} \quad (3)$$

where N_{DC} is the number of design constraints.
For a given assembly process, let DT be the list of design tasks, as represented in equation (4), where N_{DT} is the number of design tasks. Each design task links generic KPCs to generic KCCs taking into consideration design constraints, DCs, and it delivers refined KPCs or KCCs depending on the specific analysis and/or optimisation.

$$DT=\{DT_1,DT_2,...,DT_{N_{DT}}\} \quad (4)$$

Three type of design tasks have been identified (see Figure 1): (i) Type-I; (ii) Type-II; and (iii) Type-III. Subscript "r" relates to the subset of KPCs or KCCs refined by the design task, whereas subscript "T,k" indicates the subset of KPCs pr KCCs related to given k-th task.

Type	Design task representation
Type-I	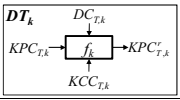
Type-II	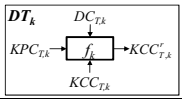
Type-III	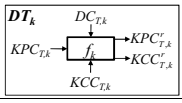

Figure 1: Representation and classification of design tasks.

The mathematical representation is shown in equation (5), where f_k is the k-th design task function. The f_k function can be evaluated by computer simulation or physical experimentation as explained in Section 4.

***Type-I** design task*

This type of design task generates a refined subset of KPCs. For example, RLW joining processes aim to design and/or optimise the joint layout ($KPC^r_{T,k}$) for a given clamp layout ($KCC_{T,k}$) and initial joint layout as per designer experience ($KPC_{T,k}$).

***Type-II** design task*

This design task generates a refined subset of KCCs. For example, in RLW joining process, one is aimed to design and optimise the clamp layout ($KCC^{*}_{T,k}$) for a given joint layout ($KPC_{T,k}$) and an initial clamp strategy ($KCC_{T,k}$).

***Type-III** design task*

This type of design task refers to scenarios when both subsets of KPCs and KCCs are refined through design analysis and/or optimisation. For example, clamp layout and joint quality are expected to be optimised simultaneously in RLW assembly process.

$$\begin{aligned}
&\textbf{Type I} \rightarrow KPC^{*}_{T,k} = f_k\left(KPC_{T,k}, KCC_{T,k}\right)\\
&\textbf{Type II} \rightarrow KCC^{*}_{T,k} = f_k\left(KPC_{T,k}, KCC_{T,k}\right)\\
&\textbf{Type III} \rightarrow \left.\begin{matrix} KPC^{*}_{T,k} \\ KCC^{*}_{T,k} \end{matrix}\right\} = f_k\left(KPC_{T,k}, KCC_{T,k}\right)
\end{aligned}$$

$$\begin{aligned}
KPC_{T,k} &= \left\{KPC_{T,k,1},\ldots,KPC_{T,k,N_{KPC_{T,k}}}\right\} \subseteq KPC\\
KCC_{T,k} &= \left\{KCC_{T,k,1},\ldots,KCC_{T,k,N_{KCC_{T,k}}}\right\} \subseteq KCC
\end{aligned} \qquad (5)$$

$$subject\ to\ DC_{T,k} = \left\{DC_{T,k,1},\ldots,DC_{T,k,N_{DC_{T,k}}}\right\} \subseteq DC$$

In automotive or aerospace assembly, the relationships among DTs are such that they might be mutually interdependent. For example, in RLW assembly process the joint layout task is coupled to the clamp layout task. The part-to-part gap (the target specification is 0.05-0.3 mm for galvanised steel) can be controlled both by moving/relocating the joint layout and/or moving/orienting the clamps and locators. Moreover, the clamp orientation can affect the laser visibility check (clamps or supports can shade the line of sight of the laser). (Type-III design task).
One leading challenge is how to determine the task-to-task interactions so that the final KPC_f or KCC_f are correctly delivered. Moreover, task priority needs to be addressed to minimise feedback loops, so as to reduce the computational time when solving the whole set of tasks.

Task-to-task interaction

Figure 3 depicts a general configuration of task-to-task interaction, which depends on the mutual interaction between the i-th task, DT_i, and the j-th task, DT_j.
The *Task Graph*, as proposed in this paper, is a graph representation of the potential interactions among design tasks. Usually, graph models are used in engineering and computer science applications to model coupling effects. In this paper the *Task Graph* is understood as a directed graph, where each node represents a design task, whereas links between nodes are interactions between tasks.

$$L_{TG}(i,j) = \begin{cases} S_{ij} \rightarrow DT_i\ affecting\ DT_j \\ -S_{ij} \rightarrow DT_j\ affecting\ DT_i \\ S_i \rightarrow i=j \\ 0 \rightarrow otherwise \end{cases} \qquad (6)$$

The graph may be described by means of a square asymmetric matrix (the number of rows/columns equals N_{DT}), L_{TG}, (also called Laplacian or Kirchoff matrix), as defined in equation (6), where S_i defines the strength of the i-th design task, whereas S_{ij} represents the coupled strength between tasks i-th and j-th. The coupled strength provides a quantitative measure of the task-to-task interaction. Section 4 will describe how to evaluate S_i and S_{ij} strengths.

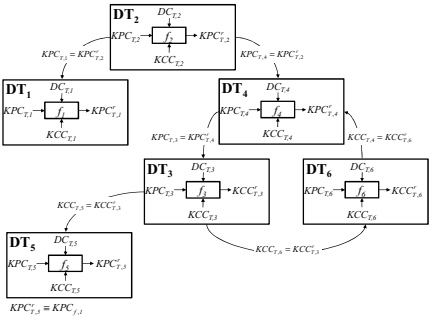

Figure 3: Design tasks interaction.

For example, the *Task Graph* matrix related to the design process of Figure 3 is:

$$L_{TG} = \begin{bmatrix} S_1 & -S_{12} & 0 & 0 & 0 & 0 \\ S_{12} & S_2 & 0 & S_{24} & 0 & 0 \\ 0 & 0 & S_3 & -S_{34} & S_{35} & S_{36} \\ 0 & -S_{24} & S_{34} & S_4 & 0 & S_{46} \\ 0 & 0 & -S_{35} & 0 & S_5 & 0 \\ 0 & 0 & -S_{36} & -S_{46} & 0 & S_6 \end{bmatrix} \qquad (7)$$

Task priority

Looking at Figure 3, if we assume that the DT_5 delivers the final KPCs (i.e., $KPC_{f,1}$), than a suitable task sequence is $\{DT_2, DT_4, DT_3, DT_5\}$. However, the task DT_4 requires information from DT_6, which is coupled to DT_3. This generates a closed loop among tasks $\{DT_4, DT_3, DT_6\}$.
The task strength can be utilised to prioritise tasks. Intuitively, if the strength of the i-th design task, S_i, is significantly small compared to others, then the related design task can be evaluated first since the initial evaluation of input KPCs and KCCs has a small effect on the design task itself.

This paper proposes a methodology to analytically determine the task-to-task interactions and the task priority.

4 - Proposed methodology

The main steps of the methodology are detailed in the following sub-Sections.

***Step I:** development of surrogate model*

Each design task links product and process key characteristics. For example, in case of fixture analysis for RLW joining process it is expected to relate part variation (i.e., KPCs) and clamp location (i.e., KCCs) to part-to-part gap (i.e., KPCs).

Article 09-dm-107

The flowchart to obtain a general surrogate model (also called response surface model [**GC1**]) is reported in Figure 4. Input parameters ($KPC_{T,k}$, $KCC_{T,k}$) are initially sampled (**step 1**) using, for example, uniform or random sampling. Then, a physics-based modeller (**step 2**) calculates the corresponding output refined values ($KPC^r_{T,k}$, $KCC^r_{T,k}$). A regression analytical model (**step 3**) is built using the generated dataset: polynomial, Spline, MARS or Kriging fitting can be utilised for this purpose. Lastly, an adaptive technique (**step 4**) is employed to refine the prediction of the regression model (i.e, f_k): i.e., Lipschitz adaptive sampling is a well-known technique to add sample points where the derivatives exhibit the highest variations.

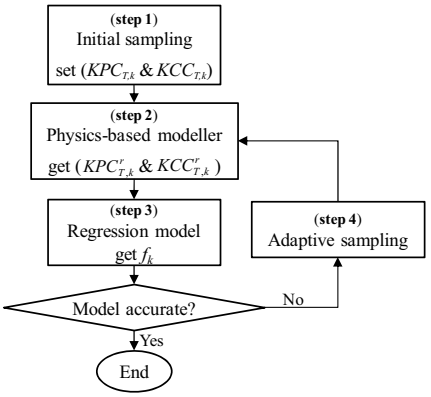

Figure 4: Flowchart for developing the surrogate model.

The key role is played by the physics-based modeller. It can either be computer simulation tool or physical experimentation. For example, with respect to the fixture analysis task, commercial software packages such as 3DCS Compliant Modeller, Elastic Assembly Variation Simulation (EAVS), Robust Design and Tolerance (RT&D) [**WW1**], and Tolerance Analysis of Deformable Assembly (TADA) can be used to model the compliant parts and fixture tools.
This paper uses Variation Response Method (VRM) [**FD1**] with capability to determine critical KPCs (such as part-to-part gap) for given set of input KCCs (such as fixture location or number of locators), considering: (i) non-ideal part modelling; (ii) assembly constraints; (iii) assembly sequence; (iv) compliancy of parts being assembled; (v) variability of fixture and tooling systems; and, (vi) part-to-part interaction.

Step II: *calculating strength and coupled strength*

The strength of the k-th design task, S_k, is defined as the sensitivity of the design task function f_k with respect to the input KPCs and KCCs. S_k can be formulated as in equation (8a) which corresponds to the second derivative (curvature) of the function f_k. Then, assuming that design tasks DT_i and DT_j interact each-other by sharing $KPC^r_{T,i}$=$KPC^r_{T,j}$ and $KCC^r_{T,i}$=$KCC^r_{T,j}$, the coupled strength, S_{ij}, is defined as in equation (8b). It should notice that both the design task strength, S_k, and the coupled strength, S_{ij}, are analytical functions.

$$S_k\left(KPC_{T,k},KCC_{T,k}\right)=\left|\sum_{z=1}^{N_{KPC_{Tk}}}\frac{\partial^2 f_k}{\partial KPC_{T,k,z}^{\ 2}}+\ldots+\sum_{z=1}^{N_{KCC_{Tk}}}\frac{\partial^2 f_k}{\partial KPC_{T,k,z}^{\ 2}}\right| \tag{8a}$$

$$S_{ij}\left(KPC_{T,i=j},KCC_{T,i=j}\right)=\left|\frac{\partial^2 f_i}{\partial KPC^r_{T,i}{}^2}+\frac{\partial^2 f_i}{\partial KCC^r_{T,i}{}^2}+\ldots+\frac{\partial^2 f_j}{\partial KPC^r_{T,j}{}^2}+\frac{\partial^2 f_j}{\partial KCC^r_{T,j}{}^2}\right| \tag{8b}$$

Step III: *building the Adaptive Task Graph*

Adaptive Task Graph allows to generate a particular instance of the *Task Graph* for a given configuration of KPCs and KCCs.

1. assign set of KPCs and KCCs
   $KPC^*_{T,k}\subseteq KPC\ ;\ KCC^*_{T,k}\subseteq KCC$
   $\forall\ k=1,\ldots,N_{DT}$
2. evaluate design strength, S^*_k, and coupled strength, S^*_{ij}, as per equation (8)
   $S^*_i=S_i\left(KPC^*_{T,k},KCC^*_{T,k}\right)$
   $S^*_{ij}=S_{ij}\left(KPC^*_{T,i=j},KCC^*_{T,i=j}\right)$
   $\forall\ i,j=1,\ldots,N_{DT}$
3. calculate the Laplacian *Task Graph* matrix, L^*_{TG}, as per equation (6)
   $L^*_{TG}(i,j)\ \propto\left(S^*_i,S^*_{ij}\right)$
4. perform design synthesis
   - **task priority**
   - **task-to-task interaction**

Table 2: Procedure for evaluating the *Adaptive Task Graph*.

The procedure is detailed in Table 2. The superscript "*" denotes a particular instance of KPCs or KCCs, which might be assigned by the designer (design analysis process) or passed in input by any optimiser (design optimisation process). Steps 1-4 can be repeated for any new instance of KPCs and KCCs and then the *Task Graph* is updated accordingly.

5 - Case study

The proposed methodology has been applied with respect to RLW assembly joining process. Automotive door inner panel and hinge reinforcement have been selected (refer to Figure 5).
Hinge reinforcement is remote laser welded with door inner panel: the gap between the hinge reinforcement (1.8 mm thick) and door inner panel (0.75 mm thick) should be within 0.05-0.3 mm to ensure the joining quality. Maximum gap (0.3 mm) is directly controlled by properly locating the clamps (DT_2) close enough to the laser stitches to compensate part errors. Minimum gap (0.05 mm) is controlled by dimpling operation (DT_1).
Then, the performance of stitches, in terms of joint penetration, is affected by part-to-part gap and combination of laser power and laser speed (DT_3).

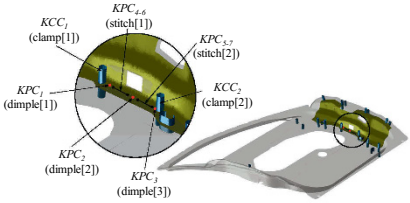

Key Product Characteristics - KPCs
$KPC_{1\text{-}2\text{-}3}$: dimple height (dimple [1], dimple [2], dimple [3])
$KPC_{4\text{-}5}$: part-to-part gap (stitch [1] and stitch [2])
$KPC_{6\text{-}7}$: joint penetration (stitch [1] and stitch [2])
KPC_8: part variation model (based on [**DF1**])
Key Control Characteristics - KCCs
$KCC_{1\text{-}2}$: clamp location (clamp [1] and clamp [2])
KCC_3: laser power
KCC_4: laser speed
KCC_5: focal position
Design Tasks - DTs
DT_1: laser parameters selection for dimpling
DT_2: fixture layout analysis
DT_3: laser parameters selection for welding

Figure 5: Door inner and hinge reinf. industrial case study.

The related functions of the three design tasks are:

$$\begin{aligned} KPC_{1\text{-}2\text{-}3} &= f_1(KPC_3, KCC_4, KCC_5) \\ KPC_{4\text{-}5} &= f_2(KPC_8, KCC_{1\text{-}2}) \\ KPC_{6\text{-}7} &= f_3(KPC_{4\text{-}5}, KCC_3, KCC_4) \end{aligned} \quad (9)$$

The steps of the ATG methodology are described as follows:

Step I: *development of surrogate model*

Figure 6 shows the surrogate models generated for the three design tasks. A third order polynomial regression model has been used.

Step II: *calculating strength and coupled strength*

The task's strengths and the coupled strengths were calculated as per equation (8). To prove the methodology, five sets of KPCs and KCCs were randomly generated (uniform random sampling). Table 3 shows the calculated strength's values.

Step III: *building the Adaptive Task Graph*

Following the procedure in Table 2, Figure 7 shows the generated ATG models. It is interesting to point out that the combination of KPCs/KCCs related to "Set 1" is such that both design task DT_3 and all the three links between tasks are suppressed, since the related strengths are not significant.

	Set 1	Set 2	Set 3	Set 4	Set 5
S_1	0.473	0.473	0.473	0.286	0.473
S_2	0.532	0.532	0.532	0.532	0.499
S_3	0.000	16.923	6.909	14.397	14.397
S_{12}	0.000	0.000	0.000	0.000	0.000
S_{13}	0.000	0.000	9.126	0.000	0.000
S_{23}	0.000	16.888	6.937	14.371	14.371

Table 3: Calculation of strength's values.

ATG methodology has been applied to optimise the fixture design (see Figure 8). In current Industry practice around a hundred of engineering changes are made after design release. The proposed ATG allows to predict about 25% of the potential failures, so to achieve almost 100% of satisfactory quality requirements.

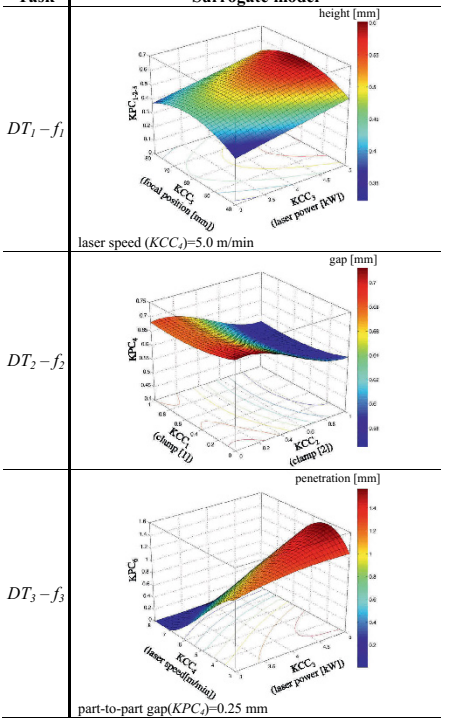

Figure 6: Surrogate models development.

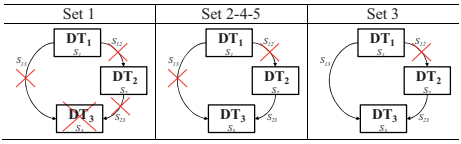

Figure 7: ATF generation
(red cross indicates that the task and/or the link is suppressed).

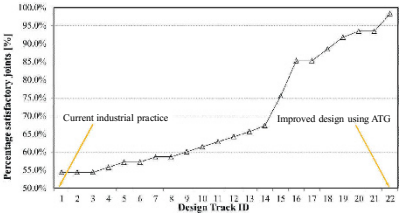

Figure 8: Engineering changes for fixture design using ATG.

6 - Conclusion and final remarks

The proposed methodology provides a systematic design synthesis approach to identify task-to-task interaction and task priority, considering KPCs and their impact on process variables in the form of KCCs. The proposed *Adaptive Task Graph* (ATG) allows to prioritise design tasks so as to improve the efficiency of the whole design process. The developed approach can be utilised in the following ways:

- Reduce trial-and-error approaches, which are usually time-consuming;
- Identify significant KPCs and KCCs relations. The task strength index gives a quantitative measure of the sensitivity of a given set of KPCs or KCCs;
- Shorten design phase by improving the efficiency of the design process. This leads to a shorter product development cycle; and,
- As an interactive tool for visualising the task sequence/priority.

The proposed framework has been demonstrated with three design tasks: (i) dimpling task; (ii) fixturing task; and, (iii) welding task. This approach can be further extended in more complex scenarios by considering additional design tasks such as laser visibility check, optical 3D non-contact measurement device visibility check, and joining layout design. The methodology shows potential to reduce engineering changes necessary during door assembly process build and testing by 25%. Future investigations will explore the interaction of KPCs and KCCs on production systems performances in terms of time and cost.

7 - Acknowledgments

This study was supported by the European research project "EU-FP7 FoF-ICT-2011.7.4: Remote Laser Welding System Navigator for Eco and Resilient Automotive Factories (Collaborative STREP project)".

8 - References

[BB1] Balesdent M., Bérend N., Dépincé P. and Chriette A. A survey of multidisciplinary design optimization methods in launch vehicle design. Structural and Multidisciplinary Optimization, 45(5): 619-642, 2011

[CC1] Camelio J., Ceglarek D., Hu S. J. Modeling variation propagation of multi-Station assembly systems with compliant parts. J. of Mech. Design, 125(4): 673-681, 2003

[C1] D. Ceglarek. RLW System Navigator for Eco and Resilient Automotive Factories. Digital Factories Theme. WMG, University of Warwick, 2011

[CH1] Camelio J. A., Hu S. J. and Ceglarek D. Impact of fixture design on sheet metal assembly variation. Journal of Manufacturing Systems, 23(3): 182-193, 2004

[CH2] Ceglarek D., Huang W., Zhou S., Ding Y., Kumar R. and Zhou Y. Time-based competition in multistage manufacturing: Stream-of-Variation Analysis (SOVA) Methodology—Review. International Journal of Flexible Manufacturing Systems, 16(1): 11-44, 2004

[CO1] CONSAD Research Corporation. Estimating economic impacts of new dimensional control technology applied to automobile body manufacturing. The Journal of Technology Transfer, 23(2): 53-60, 1998

[DF1] Das A., Franciosa P., Selim Y. and Ceglarek D. Modelling Geometric Variation of compliant sheet-metal parts using geometric modal analysis. Uni. of Warwick, 2014.

[DF2] Das, A., Franciosa, P., Prakash, P.K.S., Ceglarek, D., Transfer function of assembly process with compliant non-ideal parts, 24th CIRP Design Conference, April 14-16, Milano, Italy, 2014.

[FD1] Franciosa P., Das A., Yilmazer S., Gerbino S. and Ceglarek D. Variation Response Method (VRM): a Kernel for dimensional management simulation of non-ideal compliant parts. Uni. of Warwick, 2014.

[FG1] Franciosa P., Gerbino S. and Patalano S. Simulation of variational compliant assemblies with shape errors based on morphing mesh approach. The International Journal of Advanced Manufacturing Technology, 53(1-4): 47-61, 2011

[GP1] Gerbino S., Patalano S. and Franciosa P. Statistical variation analysis of multi-station compliant assemblies based on sensitivity matrix. International Journal of Computer Applications in Technology, 33(1): 12-23, 2008

[GC1] Gorissen D., Couckuyt I., Demeester P., Dhaene T. and Crombecq K. A surrogate modeling and adaptive sampling toolbox for computer based design. J. Mach. Learn. Res., 11: 2051-2055, 2010

[LH1] Liu S. C. and Hu S. J. Variation simulation for deformable sheet metal assemblies using Finite Element Methods. Journal of Manufacturing Science and Engineering, 119(3): 368-374, 1997

[MB1] McCulley C. and Bloebaum C. L. A genetic tool for optimal design sequencing in complex engineering systems. Structural optimization, 12(2-3): 186-201, 1996

[PC1] Phoomboplab T. and Ceglarek D. Design Synthesis framework for dimensional management in multistage assembly system. CIRP Annals - Manufacturing Technology, 56(1): 153-158, 2007

[S1] J. Sobieszczanski-Sobieski. Multidisciplinary Design optimization: an emerging new engineering discipline. In Advances in Structural Optimization, 25: 483-496, 1995

[S2] D. V. Steward. The design structure system: A method for managing the design of complex systems. Engineering Management, IEEE Transactions on, EM-28(3): 71-74, 1981

[S3] N. P. Suh. Axiomatic design of mechanical systems. Journal of Mechanical Design, 117(B): 2-10, 1995

[SC1] Suh N. P., Cochran D. S. and Lima P. C. manufacturing system design. CIRP Annals - Manufacturing Technology, 47(2): 627-639, 1998

[V1] G. N. Vanderplaats. Numerical optimization techniques for engineering design: with applications. McGraw-Hill Ryerson, 1984 Journal of Engineering Design, 1-24, 2014

[WC1] Wang, H., Ceglarek, D. Variation propagation modeling and analysis at preliminary design phase of multi-station assembly systems, Assembly Automation, Vol. 29, pp. 154-166, 2009

[WW1] Wickman C., Wagersten O., Forslund K. and Söderberg R. Influence of rigid and non-rigid variation simulations when assessing perceived quality of split-lines.

Article 07-dm-113

ABOUT WEAR DAMAGE IN STRAIGHT AND CROWNED MISALIGNED SPLINED COUPLINGS

Cuffaro Vincenzo [1], Curà Francesca [2], Mura Andrea [3]

(1) : Politecnico di Torino – Corso Duca degli Abruzzi 24 – 10129 Torino -Italy
Phone: ++390110905907
E-mail : vincenzo.cuffaro@polito.it

(2) : Politecnico di Torino – Corso Duca degli Abruzzi 24 – 10129 Torino -Italy
Phone: ++390110906930
E-mail : francesca.cura@polito.it

(3) : Politecnico di Torino – Corso Duca degli Abruzzi 24 – 10129 Torino -Italy
Phone: ++390110905907
E-mail : andrea.mura@polito.it

Abstract: Aim of this work is to present how the spline coupling tooth geometry may influence the surface fear pattern. In particular the difference between straight teeth and crowned teeth spline coupling is considered. The different tooth profile brings to different contact pressure distributions that, associated to the relative motion between engaging teeth may create different wear patterns on the contact surfaces. Also the effect of the lubrication conditions has been considered. The investigation has been carried on by means of a dedicated spline coupling test rig capable to perform wear tests on components working in misaligned conditions.

Key words: spline couplings, fretting wear, misalignment, test rig.

1- Introduction

Spline couplings are mechanical components widely used to connect and transmit torque between two rotating shafts by means of a certain number of teeth. These components are composed of two parts: a shaft with external teeth and an hub with internal teeth.
Spline couplings find application in many industrial sectors, from aerospace, to automotive, power generation, and so on. They are classified according to the tooth geometry and the fitting mode.
Since these components are usually over dimensioned concerning both static and fatigue behaviour (or at least doesn't presents particular problems), their weak point is the wear phenomena that may affect the teeth surfaces [CC1], [CM1].
Currently robust design criteria to predict fretting damage on components are still not available.
Nevertheless, design criteria are needed in order to check components about this phenomenon, avoiding the formation of this type of damage or at least to keep it under control.
For these reasons, in recent years an increasing interest is growing for the study of the fretting, both with regard the scientific community, both in the industrial world.
In particular wear phenomena (such as fretting wear) appear on teeth surface when a relative motion between engaging teeth is generated.
The relative displacement between teeth may be caused by vibrations, cyclical tooth deflection or misalignment between hub and shaft.
Angular misalignments in spline couplings may also effect both tooth stiffness [CM2] and reaction moments such as tilting moment [CM3].
Misalignments between hub and shaft may be due to manufacturing and assembly tolerances. Angular misalignments are present, in particular, in aerospace applications considered in this work [MO1].
Anyway the literature is lacking about the investigation about fretting damage on spline coupling; only few works are available in literature, as some examples: Limmer et al [LN1] and Wavish et al. [WH1] created a simplified workbench to reproduce fretting wear on spline coupling teeth without considering angular misalignment; Leen et al. [LH1, LM1, LH2] developed a spline coupling test rig to investigate fretting wear in helical [LH1] and barrelled [LM1] spline couplings, capable to apply multiaxial loads [LH2]: also this test rig doesn't allow the application of angular misalignments to the spline coupling.
Wear damage pattern in spline coupling teeth contact surfaces may wary according to the tooth geometry.
Aim of this work is to show the main results obtained from an experimental research activity about wear damage on misaligned spline couplings, performed by means of a dedicated test rig.
In particular, the effect of tooth geometry and lubrication conditions on wear pattern have been investigated. Experimental tests have been performed considering two king of tooth geometries: straight and crowned teeth spline couplings.
Results presented in this work refer to the wear damage identification; these results will be useful, in addition with

more deep investigation, to develop new spline coupling design criteria allowing to take into account wear damage.

2- Straight and crowned teeth spline couplings

As mentioned before, spline couplings may transmit torque between two shafts by means of teeth engaging each other. As shown in Figure 1, when a torque T is transmitted, each shaft tooth is pushed against the corresponding hub tooth with a certain force F (if the spline coupling is ideal, without any manufacturing error, each tooth pair is subjected to the same contact force). This contact force generate a contact pressure distribution. The contact pressure distribution is not uniform [BP1] and influenced by many parameters such as tooth stiffness, load direction, [BP2, CC2, BP3, BS1] and it may vary its behaviour according to the tooth geometry.

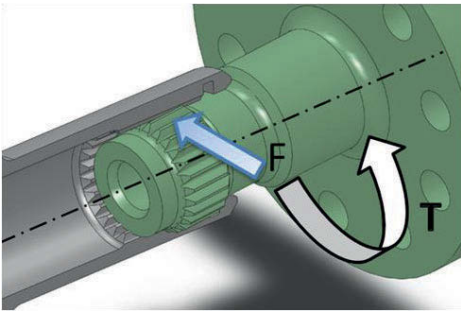

Figure 1: crowned tooth (A) and straight tooth (B).

Spline couplings are classified according to the tooth profile along the radial direction (involute profile ,straight parallel profile,…), the engaging conditions (side fit, diameter fit) and the tooth profile along the axial direction (straight teeth and crowned teeth) [CC3].
Figure 2 shows the difference between two involute spline couplings teeth: the one on the left (Figure 1A) presents a crowing radius while the other on the right (Figure 1B) has straight teeth. Usually crowned spline couplings are used to allow relevant misalignment angles between hub and shaft.

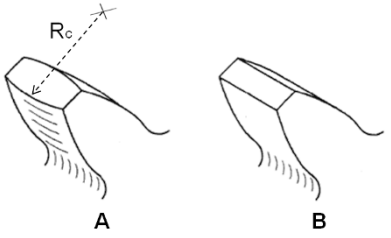

Figure 2: crowned tooth (A) and straight tooth (B).

This last classification is very important for what concerns both contact pressure trend and the wear damage when an angular misalignment is present between hub and shaft.
In particular, considering crowned teeth spline coupling, the contact pressure regime may be represented by the Hertz theory, in which the maximum pressure is located in the centre of the contact area (Figure 3 left), while in straight teeth spline couplings the contact pressure distribution may be considered as a punch on flat where two pressure peaches are identified at the two extremities of the contact area (Figure 3 right).

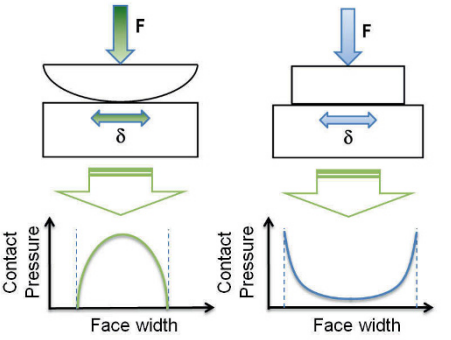

Figure 3: crowned tooth (left) and straight tooth (right) contact pressure distribution.

The pressure trend in crowned and straight teeth spline coupling has been confirmed by experimental tests performed by means of pressure sensitive films [CC2].

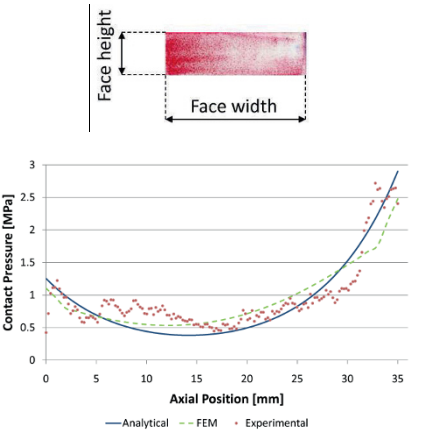

Figure 4: pressure sensitive film and comparison between experimental, numerical and theoretical pressure trends for straight teeth spline coupling [CC2].

As an example, Figure 4 shows the experimental pressure trend obtained for a straight teeth spline coupling compared with both theoretical and numerical one [CC2].
Figure 5 shows the experimental pressure trend obtained for a crowned teeth spline coupling compared with the theoretical one.

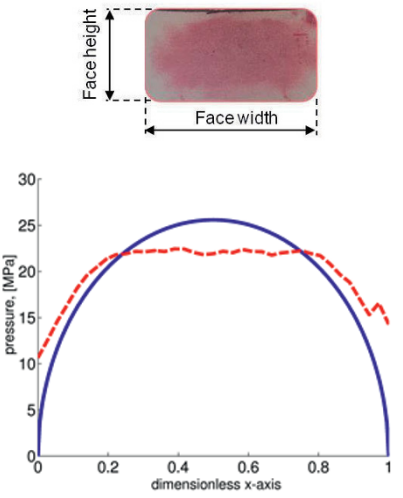

Figure 5: pressure sensitive film and comparison between experimental, and theoretical pressure trends for crowned teeth spline coupling.

If a relative displacement δ between the engaging teeth is generated, wear phenomena may appear on the teeth contact surfaces and, as better explained in the next section, the contact pressure regime may affect the surface wear pattern; this is why it is very important to well understand how is the contact pressure trend on engaging teeth surfaces.

3- Wear damage in spline couplings

If spline couplings work with an angular misalignment, a relative displacement between engaging teeth is generated due to kinematical conditions, and fretting wear damage may appear on teeth contact surfaces. Moreover the contact regime between engaging teeth totally changes when a spline coupling is misaligned (in particular if straight teeth are considered) and this brings to different wear pattern on the teeth surface [CC4].
In the case of straight teeth spline coupling, if the tooth is considered as a rigid body, only one point at one edge of the tooth will be in contact (in the real case, because of the tooth deformability, the contact region is a kind of rectangular area, see Figure 6); this brings to the generation of wear phenomena placed at the extremities of the tooth width.

On the other hand, if a crowned tooth is considered, the contact area comes from an Hertian contact and the wear phenomena will be located near the centre of the tooth width (Figure 7).

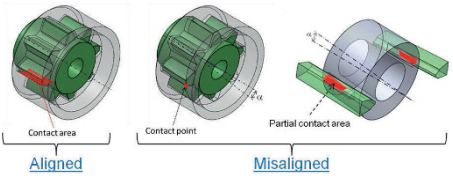

Figure 6: straight tooth in aligned and misaligned conditions

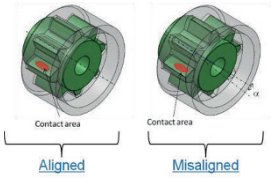

Figure 7: crowned tooth in aligned and misaligned conditions.

3.1 – Experimental set up

Results presented in this work have been obtained by means of a dedicated spline couplings test rig (Figure 8). This test rig has been designed to reproduce the real working conditions that spline couplings find in aerospace applications. In particular the test rig allows to perform test with angular misalignments between hub and shaft [CC5].

Figure 8: spline couplings test rig.

Main performance of the test rig are: 5000Nm maximum torque applicable to the test article, 2000 rpm maximum rotating speed and 10’ maximum misalignment angle (this angle may be varied during the test).

Dimensions of the test rig are 2.5m in length, 1.2m in width, and about 3500 kg in weight.
This test rig has a power recirculation scheme (Figure 9 [CC5]) allowing compact design and low energy consumption: a 6.3kW electric motor has been installed instead of a 1000kW motor needed if the test rig had been designed with a power dissipation scheme.
The temperature of all roller bearings is monitored by temperature sensors.

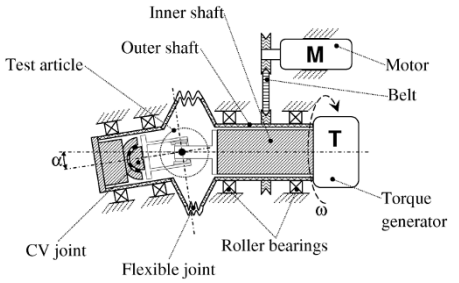

Figure 9: spline couplings test rig power recirculation scheme [CC5].

This spline couplings test rig allows different tests such as wear tests of aligned spline couplings, wear tests of misaligned spline couplings with constant angle, wear tests of misaligned spline couplings with continuous, varying angle during the test, real time wear monitoring by means of the oil debris system investigation about reaction moments due to the misalignments, investigation about teeth stiffness.
Test rig control and the data acquisition are managed by a dedicated software written in LABView environment.

3.2 – Results

Experimental tests have been performed on two kind of steel made splined couplings specimens, both with the same main characteristics (27 teeth, 1.27mm modulus, 30° pressure angle), but one kind with straight teeth and the other with 200mm crowing radius. Tests have been performed by varying the misalignment angle (from zero to 10') with the same torque (700Nm). All tests, except two, have been preformed with lubrication active [CC4].
Table 1 resumes the tests parameters, each test lasts in 10M cycles and has been performed on both straight teeth and crowned teeth specimens. Totally 8 tests have been done.

Test number	Torque [Nm]	Speed [rpm]	Misalignment [']	Lubrication
1	700	1500	0	YES
2	700	1500	5	YES
3	700	1500	10	YES
4	700	1500	10	NO

Table 1: tests parameters.

As an example, Figures 10 and 11 shows two spline coupling specimens after a wear test performed with the same working conditions (transmitted torque, misalignment angle, lubrication). The two specimens presented in Figures 10 and 11 have the same characteristics (modulus, teeth number, pressure angle, material), but the one in Figure 10 has crowned teeth and the one in Figure 11 has straight teeth; it is possible to observe how the different tooth profile have influenced the wear pattern [CC4].

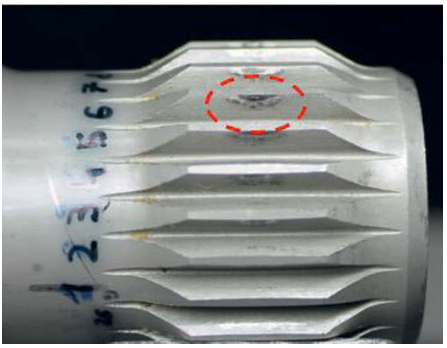

Figure 10: wear damage in crowned teeth spline couplings.

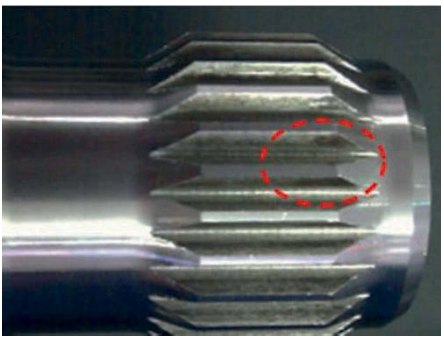

Figure 11: wear damage in straight teeth spline couplings.

In particular the crowned spline coupling specimen (Figure 10) presents wear damage concentred on the middle of the contact area, this is due because of the Hertian behaviour of the pressure distribution (Figure 3), while the straight teeth spline coupling specimen (Figure 11) shows wear damage on the extremity of the contact area according to the bunch pressure distribution (Figure 3) associated to the partial contact area due to the angular misalignment (Figure 4).
Figures 12 and 13 shows respectively the teeth surface of straight and crowned teeth spline coupling after two tests performed without lubrication. It is possible to observe that the wear damage is more deep respect to the tests performed

with lubrication active (Figures 10 and 11) and, in particular considering the straight teeth spline coupling specimen (Figure 13), the wear zone is extended to the whole tooth contact surface and big traces of oxidation may be observed.

Figure 12: wear damage in crowned teeth spline couplings after test performed without lubrication.

Figure 13: wear damage in straight teeth spline couplings after test performed without lubrication.

By considering the angular rotation clearance as wear entity parameters [CC5], it is possible to compare how the wear affects the two kind of spline coupling considered in this work.

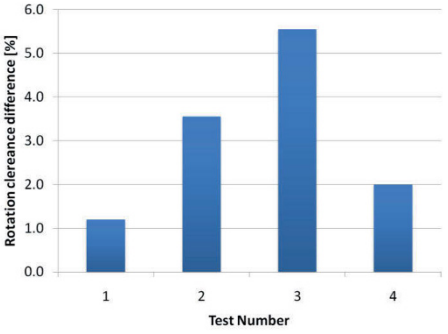

Figure 14: difference in rotation clearance variation between straight and crowned teeth spline couplings.

Figure 14 shows the difference of rotation clearance variation between straight and crowned teeth spline couplings (% rotation measured in crowned teeth spline coupling minus % rotation measured in straight teeth spline coupling). The rotation clearance has been measured before and after each test by means of a dedicated device [CC4]. In particular Figure 9 represents the results of four tests performed at 700Mm torque, 1500rpm rotating speed and angular misalignment of respectively 0' for test 1, 5' for test 2 10' for test 3 and 10' for test 4. The difference between test 3 and test 4 is that the second one has been performed without lubrication. It is possible to point out that crowned teeth spline couplings show higher wear damage level respect to straight teeth spline couplings and the difference increase by increasing the misalignment angle (Tests 1 to 3); the difference decreases if the test is performed without lubrication (Test 4).

4- Conclusions

In this work an experimental study about fretting wear damage on misaligned splined coupling has been described. Experimental tests have been performed by means of a dedicated test rig on specimens working in misaligned conditions and the effect of tooth geometry, angular misalignment value and lubrication condition has been analyzed. In particular two kind of specimens have been used: straight teeth and crowned teeth spline coupling.

Results show that wear patterns on teeth contact surfaces vary according to the tooth geometry. In particular in crowned teeth spline couplings the wear damage is present in the middle of the face width while in straight teeth spline couplings the wear damage is located at the extremity of the tooth width.

These two different wear patterns may be due to the different contact regimes and the relative different contact pressure distribution (Hertzian pressure distribution for crowned teeth and punch distribution for straight teeth).

Also the effect of lubrication condition has been considered showing that, as expected, the absence of lubrication bring to more deep material removal. Considering the wear pattern, in the case of crowned teeth the wear zone shape remains elliptic as in the tests with lubrication active, while in straight teeth the wear zone seems to involve the whole tooth width; moreover in this last case also big traces of oxidation have been found.

As future work it will be interesting to investigate different load level in order to investigate how the transmitted torque may influence the wear pattern in the two tooth geometries considered in this work.

The results from this research activity give better understanding about wear phenomena affecting spline couplings and it represents a step forward to develop new design criteria for spline couplings taking properly into account wear phenomena.

7- References

[BP1] A. Barrot, M. Paredes, M. Sartor, An Assistance Tool

for Spline Coupling Design, Advances in Integrated Design and Manufacturing in Mechanical Engineering, 329-342, Springer, 2005.

[BP2] A. Barrot, M. Paredes, M. Sartor, Determining both radial pressure distribution and torsional stiffness of involute spline couplings, Proceedings of the Institution of Mechanical Engineers, Vol. 220, Part C: Journal of Mechanical Engineering Science, IMechE 2006, 1727-1738.

[BP3] A. Barrot, M. Paredes, M. Sartor - "Extended equations of load distribution in the axial direction in a spline coupling" - Engineering Failure Analysis, Volume 16, Issue 1, January 2009, Pages 200–211.

[BS1] A. Barrot, M. Sartor, M. Paredes - "Investigation of torsional teeth stiffness and second moment of area calculations for an analytical model of spline coupling behaviour" - Proceedings of the Institution of Mechanical Engineers, Vol. 222, Part C: Journal of Mechanical Engineering Science, IMechE 2008, 891-902.

[CC1] G. Curti, F. Curà, V. Cuffaro, A. Mura, Calcolo degli accoppiamenti scanalati: i metodi tradizionali, Organi di trasmissione Maggio 2010 pp. 64-73 ISSN: 0030-4905.

[CC2] V. Cuffaro, F. Curà, A. Mura, Analysis of the pressure distribution in spline couplings, Proc IMechE Part C: J Mechanical Engineering Science (2012) 226(12) 2852–2859, DOI: 10.1177/0954406212440670.

[CC3] V. Cuffaro, F. Curà, A. Mura, Accoppiamenti scanalati: classificazione e danneggiamento, Organi di trasmissione - Aprile 2013 pp. 22-25.

[CC4] V. Cuffaro, F. Curà, A. Mura, Experimental investigation about surface damage in straight and crowned misaligned splined couplings, Key Engineering Materials Vols. 577-578 (2014) pp 353-356, doi:10.4028/www.scientific.net/KEM.577-578.353.

[CC5] V. Cuffaro, F. Curà, A. Mura, Test Rig for Spline Couplings Working in Misaligned Conditions, Journal of Tribology 136(1), January 2014, doi:10.1115/1.4025656.

[CM1] F. Curà, A. Mura, M. Gravina, Load distribution in spline coupling teeth with parallel offset misalignment, ProcIMechE Part C: J Mechanical Engineering Science Vol. 227 Issue 10 October 2013 pp. 2193 – 2203 DOI:10.1177/0954406212471916.

[CM2] F. Curà, A. Mura, Experimental and theoretical investigation about reaction moments in misaligned splined couplings, Mechanical Systems and Signal Processing 45 (2014), pp. 504–512, DOI: http://dx.doi.org/10.1016/j.ymssp.2013.12.005.

[CM3] F. Curà, A. Mura, Experimental procedure for the evaluation of tooth stiffness in spline coupling including angular misalignment, Mechanical Systems and Signal Processing 40 (2013) 545–555, DOI: 10.1016/j.ymssp.2013.06.033.

[LH1] S. B. Leen, T. R. Hyde, E. J. Williams, A. A. Becker, I. R. McColl, T. H. Hyde, J. W. Taylor, Development of a representative test specimen for frictional contact in spline joint couplings, Journal of Strain Analysis Vol 36 (65): 521-544, 2000.

[LH2] S. B. Leen, T. R. Hyde, C. H. H. Ratsimba, E. J. Williams, I. R. McColl, An investigation of the fatigue and fretting performance of a representative aero-engine spline coupling, Journal of Strain Analysis for Engineering Design, Volume 37 (6) 2002.

[LM1] S. B. Leen, I. R. McColl, C. H. H. Ratsimba, E. J. Williams. Fatigue life prediction for a barrelled spline coupling under torque overload, Proc. Instn Mech. Engrs Part G: J. Aerospace Engineering IMechE Vol. 217: 123-142 , 2003.

[LN1] L. Limmer, D.Nowell, D.A.Hills. A combined testing and modelling approach to the prediction of the fretting fatigue performance of splined shafts, Proc. IMechE Part G, vol. 215: 105-112, 2001.

[MO1] S. Medina, A.V Olver: Regimes of Contact in Spline Couplings, Journal of Tribology, Vol. 124, 2002, 351-357.

[WH1] P. M. Wavish, D. Houghton, J. Ding, S. B. Leen, E. J Williams, and I. R. McColl. A multiaxial fretting fatigue test for spline coupling contact, Journal compilation Blackwell Publishing Ltd. Fatigue Fract Engng Mater Struct 32: 325-345, 2009.

Article 01-dm-33

DEVELOPMENT OF TOOLS FOR MULTI-MATERIAL DESIGN

F.X. Kromm [1], H. Wargnier [1], M. Danis [1]
(1) : Université Bordeaux, I2M, UMR5295,
F-33400 Talence, France
+33 5 56 84 58 55/+33 5 56 84 58 43
E-mail : {herve.wargnier, francois-xavier.kromm, michel.danis}@u-bordeaux.fr

Abstract: Multi-material design implies the selection of various parameters such as the nature of the components, their morphology (or architecture), their volume fractions... Although selection methods have been developed for monolithic materials, a single method dealing with all these parameters hasn't been created yet. This paper describes several tools that can guide the designer in this task. The first one consists in a statistical analysis of the material properties to see whether some requirements are incompatible. In this case, the result allows the separation of these requirements and helps the components selection. Then, another study deals with the selection of the components when the architecture of the multi-materials is known. The important benefit of this method is a filtration of the candidates that decreases drastically the number of solutions that have to be evaluated. Finally, a last paragraph shows how an architecture can be selected and optimised.

Key words: Multi-material - Design – Architectured materials – Materials selection - Optimisation

1- Introduction

In order to get simpler mechanical or functional systems, designers try to integrate more and more functions in a single part. As a result, some functions have to be fulfilled thanks to the material properties, so that the material set of requirements becomes more and more complex.
When the functional requirements and the geometry of the part are defined, several methods allow a single material selection to be made, either using a performance index or an expert questionnaire[LS1][LS2]. If no solution can be found, the designer has to define a suitable combination of materials, in other words design a multi-material.
In accordance with the definitions proposed by Ashby, Bréchet, or Kromm [AB1][BE1][KQ1] a multi-material or an architectured material is considered to be composed of one or several materials placed according to a predefined architecture such that a representative elementary volume has at least one dimension that is very small compared with the dimensions of the part.
The parameters that the designer must define in the design of a multi-material are:
– components, which are usually materials, but they may also be semi-products, this is the case, for example, for multilayer structures or stratified composites;
– volume fractions of the components;
– architecture and morphology of the components, i.e. their spatial disposition;
– coupling modes between the components, especially the nature of the interfaces and their behaviour.

The aim of this contribution is to present several tools for multi-material design that have been developed to solve specific problems at different steps of the general design procedure. It is worthy of note that all these studies are based on industrial applications. The complementarity of these methodological studies is explained, showing that their addition allows to deal with lots of different cases.

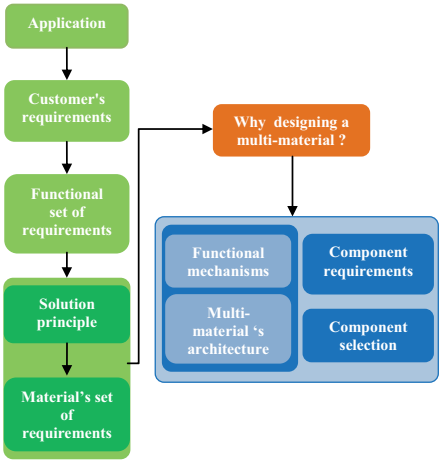

Figure 1: General design method

The method (illustrated in figure 1) shows that before selecting a material for an application, a principle of solution

has to be determined, which means that some design parameters of the product are chosen (for example the general shape of the part, or the functional mechanisms…).

Then, in the case where no monolithic material can be found to satisfy the constraints, a multi-material must be designed. The first tool that is described here consists in an analysis of the set of requirements that gives an answer to the question "why should a multi-material be designed?". The result of this analysis can then be used to define sets of requirements for the components of a multi-material.
As it has been noted previously, the number and variety of design parameters for a multi-material is great, so they can't all be taken into account simultaneously. As a consequence, the studies presented in the following parts concern cases where some of these parameters are fixed. Thus, the developed tools correspond to different configurations defined by free or fixed parameters.

2- Analysis of the set of requirements

3.1 – Holes in material space

One of the reasons for the designer to develop a multi-material for an application is the incompatibility of the requirements. Indeed, as the functions and constraints of the material become complex and numerous, it happens that the required properties fall in a hole of the material space [A1]. The explanation of the presence of holes in material property space lies in the correlation that is observed between some properties, generally coming from fundamental reasons. In order to detect the couples of requirements that may be problematic, an analysis can be made on the values of the different properties for the materials available in the database and shows which properties are strongly correlated [WC1]. The analysis of the repartition of these values is made using principal component analysis (PCA).

3.2 – PCA for material properties

Before beginning the PCA, the variables (here, the material properties) have to be centred on the average value, and normalised so that the variance is one. Then, for two properties x and y, the correlation coefficient can be evaluated by calculating the covariance c(x,y):

$$c(x,y) = \frac{1}{n}\sum_i x_i y_i \qquad (1)$$

where x_i, y_i are the x and y properties normalised values for the i^{th}material, and n the total number of materials in the database.

When two properties or constraints are strongly correlated, i.e. when $|c(x,y)|$ is great (i.e. higher or equal to 0.8), it is necessary to examine the compatibility of the requirements using the factorial axes.
Considering the materials placed in the property space, a set of specific directions called factorial axes can be defined as follows:

- the first factorial axis minimises the inertia of the series of point;
- the second factorial axis is perpendicular to the first and chosen so that the plane it defines with the first one minimises the inertia of the series of point;
- the same method is applied to determine the other factorial axes.

If the designer has to focus on two correlated properties concerned by the requirements, the study can be represented in a single plane defined by these properties. Each material of the database can be represented by a point, and can be located thanks to his position on the first factorial axis F_1 (figure 2).

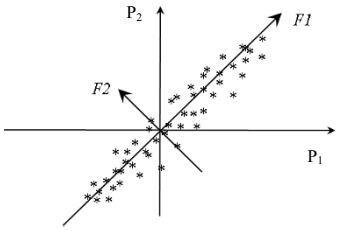

Figure 2: Representation of the factorial axes

The constraints, previously expressed as limits on material properties, are then be traduced in intervals of validity on the F1 factorial axis. This method allows one axis to evaluate two criteria concerning different properties, and can be applied as well to combinations of properties (like performance indices for example).

3.3 – Exploitation of the results

After having expressed the location of the materials on the factorial axis, the compatibility of the examined constraints can be evaluated, as illustrated in figure 3. This diagram represents the materials placed on the factorial axis F_1 in a plane defined by the properties P_1 and P_2. The intervals I_1 and I_2 correspond to the materials satisfying the constraints $P_1<P_{1max}$ and $P_2>P_{2min}$.

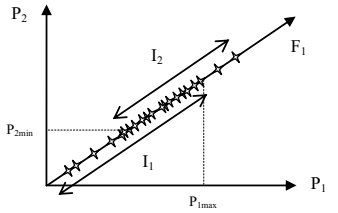

Figure 3: Estimation of compatibility on factorial axis

In the case where the intersection of the two available intervals is not void, the solution can be given as an interval of solutions. On the contrary, in the case where the intersection is void, the analysis gives an evaluation of the distance on the axis between the groups of solution for each constraint. This distance gives an idea of the magnitude of

the incompatibility of the requirements, and indicates whether a small modification of one requirement can give solutions or not.

3.4 – Application to a machine tool frame

This analysis method has been applied to an industrial application concerning the replacement of a cast iron for a machine tool frame.
The requirements and the related performance indices for this application are summarised in table 1.

Objective (with given static stiffness)	Performance index
Minimise cost	$I_1 = \frac{E^{1/3}}{\rho C_m}$
Maximise vibration frequency	$I_2 = \frac{E^{1/3}}{\rho}$
Minimize transversal dynamic excitation	$I_3 = \eta \frac{E^{1/3}}{\rho}$
Minimize thermal distortion	$I_4 = \frac{\lambda}{\alpha}$

Table 1: Material set of requirements

Calculating the covariance on the material database for each pair of performance indices, the correlation matrix can be built (table 2).

	I_1	I_2	I_3	I_4
I_1	1			
I_2	0.156	1		
I_3	0.139	0.41	1	
I_4	-0.138	-0.233	**-0.794**	1

Table 2: Correlation matrix

As it can be seen in table 2, the unique couple of correlated requirements are those concerning vibration damping and thermal stability (I_3 and I_4). These two performance indices are studied with PCA, and the solutions are searched on the factorial axis F_1, where the available materials lay on a range from -3 to 3.8. As the objective is to propose new materials for this application, an interval can be given for each criterion to show the materials with higher performance than the cast iron (resp. S_3 for performance index I_3 and S_4 for I_4) as illustrated in figure 4.

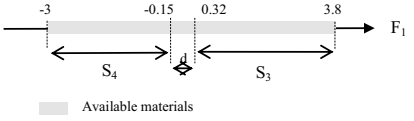

Figure 4: Application of PCA on I_3 and I_4

The intersection of the allowable intervals is empty, and the distance of incompatibility is evaluated at 0.47, which corresponds to about 8% of the total range of value of F_1 on the database. This value seems too high to consider that solutions can be found near the requirements, so the incompatible functions have been studied specifically, and a multi-material solution has to be searched..
As some studies showed the interest of civil engineering materials for this kind of applications [SN1] [RM1], the usual hydraulic concrete properties are evaluated regarding the I_3 and I_4 performance indices. It appears that this material increases the performance on both dynamic and thermal criteria. However, problems due to residual stresses, interaction with hydrocarbons or the very long time to obtain de final properties make this solution irrelevant for this application. As these drawbacks only come from the cement properties, the general architecture of the material has been conserved, and the use of coarse granulate material (like sand, gravel or crushed stone) is validated. The last step of the design which consists in the selection of the new matrix results in the choice of an epoxy resin to make a polymer concrete.

3.5 – Conclusions

The PCA provides the designer with an analysis tool that can show incompatible requirements early in the design process. The exploitation of the results indicates then if a small change in one constraint can allow solutions to be found or if they should be considered separately.
The next step in the procedure is to choose all the characteristics that define a multi-material. The studies presented forward aim at limiting the number of potential solutions or guide the designer in the architecture selection.

3- Database filtration

The number of parameters in multi-material design increases greatly in comparison with a single material selection. Indeed, it has been noted previously that it implies the determination of:

- the components,
- the volume fractions of the component,
- the architecture, or morphology of the multi-material,
- the coupling mode, the nature of the interface.

In order to reduce the study domain and the number of candidates, a concept of solution (i.e. the functional mechanism) and some parameters have to be predetermined. For example, we firstly consider that the architecture of the multi-material and the nature of the interface are fixed. In this case, the only parameters remaining free are the constitutive materials and their volume fraction. It appears that the number of possible combination is still very important, even if the material database is reduced, so it seems necessary to operate a filtration on the database to determine the materials that can be a component of the multi-material before ranking the solutions.

3.1 – Filtration steps and criteria

The filtration is divided in several steps [GK1], using the requirements to eliminate some materials from the candidates (figure 5).

Two kinds of constraints can be found in the set of requirements: those that depend on the free geometrical parameter, and those that don't. The second group of constraint can be taken into account easily, and allow the elimination of some materials directly.
The constraints depending on the free design variable have to be considered by pairs. Indeed, some of them impose a minimum value to the free variable, whereas the others force it not to be superior to a specified value of the free variable. These two values define for each material an allowable interval for the free design parameter. If this interval is void, the pair of constraints can't be met by the considered material. As a result, it appears that couples of constraints can define filters for component selection.

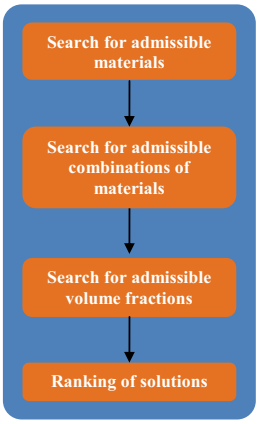

Figure 5: Filtration steps

The rules for searching a suitable combination of materials in the database are:

(1) to be a component, a material must fulfil at least one filter
(2) each filter must be fulfilled by at least one of the components

The properties of a multi-material depend on the volume fraction of each component. On a chart representing the property P_1 on x-axis and P_2 on y-axis, the properties of a multi-material composed of materials 1 and 2 for all the volume fractions are schematised by a continuous line linking the two components. The shape of this curve depends on the architecture, and its equation is defined by the corresponding homogenisation model.
As shown in figure 6, with a suitable architecture, the multi-material enables new combinations of properties to be reached and incompatible requirements to be met. Indeed, even if no monolithic material can fulfil both $P_1<P_{1max}$ and $P_2<P_{2max}$, some values of the volume fractions of material 1 and 2 make it possible.
The next step of filtration consists in determining the interval of volume fractions that satisfy the requirements, and eliminating the pairs of materials for which it is void. This calculation has to be made with a constraint optimisation software because the number of materials and parameters is still high. This method has been generalised to any constraints and free variable numbers.

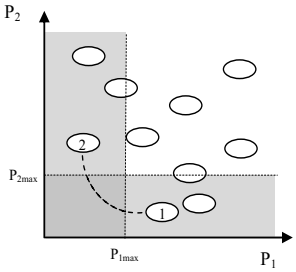

Figure 6: Property chart with multi-material

3.2 – Application to an offshore oil extraction pipe

In order to illustrate the interest of a filtration before ranking the solutions in multi-material design, the example of an offshore oil extraction pipe is presented. The set of requirements for this application concerns the installation and service phases. The architecture is supposed to be axisymmetric, composed of two layers and the free variables are the layers' thicknesses. The database used for this example contains 62 materials, which leads to a maximum of 3782 possible combinations.
The requirements have been divided in three types: group 1 for the inner layer with requirements that don't depend on the free variable, equivalent group 2 for the outer layer, and group 3 concerning both layers and depending on the thickness (table 4).
The first step of the filtration consists in the elimination of the materials that do not fill the constraints of the first or the second group because they cannot be used as an inner or outer layer of the multi-materials. After the filtration, there are only 18 materials left for the internal layer and 14 for the external one.

The second step consists in applying the criteria fixed by the third group of constraints. There are four constraints imposing a minimum thickness and two imposing a maximum thickness, so eight filters can be defined. After this step, there are only 8 couples of materials left.
Finally, for each couple of materials, the interval of acceptable volume fractions to satisfy the requirements has been calculated, leading to a set of only five possible bi-materials for this application.
However, the relevance of the results is questionable because polymer foams are always proposed as a component. If the constraint of the foam / fluid contact is taken into account, all these solutions should be invalidated, so a three layer material has to be searched.

Group	Implied layer	Relation with the free variable	Description of the functions
1	Inner	No	- Resistance to service temperature - Resistance to corrosion due to the effluent (hydrocarbon)
2	Outer	No	- Resistance to service temperature - Resistance to corrosion due to sea water - Wear resistance
3	Inner / Outer	Minimum thickness Maximum thickness Minimum thickness Minimum thickness Minimum thickness Maximum thickness	- Resistance to mechanical loads during installation - Maximum force on the installation ship - Resistance to local buckling due to external pressure during exploitation - Limited thermal losses to ensure the effluent flow - Buoyancy: the pipe mustn't float - External diameter must be adapted to installation system

Table 4: Set of requirements by layer and type of constraints

In this case, the set of requirements is completed with a third group of constraints concerning the medium layer. The same filtration steps are then applied, leading to the results detailed in table 5.

Type of combination (inner layer/medium layer/outer layer)	Number of solutions
Metal/polymer foam/metal	4
Metal/polymer foam/composite	2
Composite/polymer foam/metal	8
Metal/polymer foam/polymer	10
Polymer/polymer foam/metal	24

Table 5: Results for three layer material

It is important to note that currently used structures of materials can be found with these combinations (metal/polymer foam/ metal), and new combinations including composite materials as a component are proposed but would require further developments, because several parameters (number of plies, orientations, volume fractions, etc.) have to be determined.
This example shows that the number of solutions that will have to be evaluated and ranked has been reduced drastically from 3782 to 48 for three component materials, only by the application of the filtration method. Then, the evaluation can be processed with more precise numerical simulation of the behaviour of the multi-material, and taking into account their manufacturability. As a conclusion, this method seems to be efficient to narrow the solution space for selecting the components of a multi-material. However, it lies on an architecture selection which is still arbitrary.

4- Conclusions, perspectives

This paper presents several tools dedicated to specific cases in multi-material design. Indeed, the number of parameters controlling the multi-material behaviour is too important to take all of them into account at the same time. As a result, the specificity of each situation concerns the determination of the free variables and the fixed parameters that allow the reduction of the solution set.
A study, currently under development, concerns the case where the constitutive materials and the nature of the interface between them are known, whereas the architecture, that is to say their morphology, and their volume fractions are free.

The approach for this selection is a screening method, so this implies that an architecture database has to be built. This database is organised hierarchically as a function of the scale of the considered morphology. Indeed, some architecture will be placed at macroscopic scale (plane or axisymmetric, multi-layer…) but other will be put at mesoscopic scale, as constitutive parts of the macroscopic ones (particles, fibres…). More, in order to calculate the properties of the multi-material, the architecture database must include homogenisation models, and must be linked to a materials database for the components properties (figure 7).
The selection of an architecture implies to deal with very different parameters: continuous or not, qualitative or quantitative… Genetic algorithms have been chosen for this operation for their ability in the manipulation of such variables and their capacity to generate solutions without screening the whole candidate set.

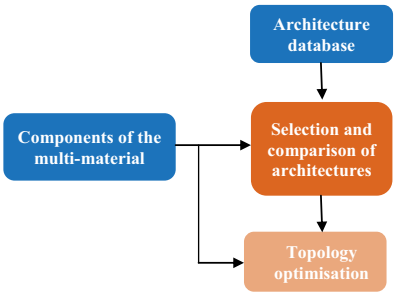

Figure 7: Method for the selection of the architecture

After having selected an architecture, a shape optimisation method (like level set [L1] for example) can be used in a final step to determine precisely the most suitable value of all the parameters of the multi-material.
This method will be applied to the case of an electronic packaging for aerospace. On this example, the design aims at reducing the mass of this product while satisfying various functions dealing with thermal conduction (to evacuate the heat produced by the electronic components), resistance to vibrations or electro-magnetic protection.

The addition of specific studies allows a step by step approach of the complex problem of the multi-material

design. Some other situations are still to develop, like for example searching answers in a database of pre-established solutions, or operate a selection on the interface properties in the multi-material. The next step will be to integrate them in a single structured method

6- References

[A1] Ashby MF, Designing architectured materials, Scripta Materialia, 68: 4–7, 2013

[AB1] Ashby MF, Brechet Y. Designing hybrid materials. Acta Materialia,;51:5801–21 2003

[BE1] Brechet Y, Embury JD. Architectured materials: expanding materials space. Scripta Materialia; 68:1–3, 2013

[GK1] Giaccobi S, Kromm FX, Wargnier H, Danis M. Filtration in materials selection and multi-materials design, Materials and Design,;31(4):1842–7, 2010

[KQ1] Kromm FX, Quenisset JM, Lorriot T, Harry R, Wargnier H. Definition of a multimaterials design method. Materials and Design,;28:2641–6, 2007

[L1] Laszczyk L. Homogenization and topological optimization of architecture panels, Thèse de doctorat: Université de Grenoble; 2011

[LS1] Lovatt AM, Shercliff HR. Manufacturing process selection in engineering design. Part1: the role of process selection, Materials and Design, 19:205–15, 1998

[LS2] Lovatt AM, Shercliff HR. Manufacturing process selection in engineering design. Part 2: a methodology for creating task-based process selection procedures, Materials and Design, 19:217–30, 1998

[RM1] Rahman M., Mansur M.A., Feng Zhou, Design, fabrication and evaluation of a steel fibre reinforced concrete column for grinding machines, Materials and Design 16(4):205-9 , 1995

[SN1] Sugishita H., Nishiyama H., Nagayasu O., Shin-nou T., Sato H., O-hori M., Development of Concrete Machining Center and Identification of the Dynamic and the Thermal Structural Behavior,CIRP Annals - Manufacturing Technology, 37(1):377-80, 1988

[WC1] Wargnier H, Castillo G, Danis M, Brechet Y. Study of the compatibility between criteria in a set of materials requirements. Application to a machine tool frame, Materials and Design,;31:732–40, 2010

Article 06-dm-104

Comparison of different Multiple-criteria decision analysis methods in the context of conceptual design: application to the development of a solar collector structure

Mehdi El Amine [1], Jérôme Pailhes [2], Nicolas Perry [3]

(1) : Arts et Métiers ParisTech, I2M - UMR 5295, F-33400 Talence, France
+33 6 19 82 85 42
E-mail : mehdi.el-amine@ensam.eu

(2) : Arts et Métiers ParisTech, I2M - UMR 5295, F-33400 Talence, France
+33 5 56 84 54 22
E-mail : j.pailhes@i2m.u-bordeaux1.fr

(3) : Arts et Métiers ParisTech, I2M - UMR 5295, F-33400 Talence, France
+33 5 56 84 79 83
E-mail : n.perry@i2m.u-bordeaux1.fr

Abstract: At each stage of the product development process, the designers are facing an important task which consists of decision making. Two cases are observed: the problem of concept selection in conceptual design phases and, the problem of pre-dimensioning once concept choices are made. Making decisions in conceptual design phases on a sound basis is one of the most difficult challenges in engineering design, especially when innovative concepts are introduced. On the one hand, designers deal with imprecise data about design alternatives. On the other hand, design objectives and requirements are usually not clear in these phases. The greatest opportunities to reduce product life cycle costs usually occur during the first conceptual design phases. The need for reliable multi-criteria decision aid (MCDA) methods is thus greatest at early conceptual design phases. Various MCDA methods are proposed in the literature. The main criticism of these methods is that they usually yield different results for the same problem [MG, ZSWD, GM, TL]. In this work, an analysis of six MCDA methods (weighed sum, weighted product, Kim & Lin, compromise programming, TOPSIS, and ELECTRE I) was conducted. Our analysis was performed via an industrial case of solar collector structure development. The objective is to define the most appropriate MCDA methods in term of three criteria: (i) the consistency of the results, (ii) the ease of understanding and, (iii) the adaptation of the decision type. The results show that TOPSIS is the most consistent MCDA method in our case.

Key words: Multi-criteria decision aid methods; Selection methods; Aggregative methods; Conceptual design; Consistency.

1- Introduction

Decision making is an inherent task in the product development process. It can be broken into (i) conceptual design decisions, when decision makers have to choose between several design concepts, and (ii) embodiment design decisions, when designers have to optimize design variables for the selected concepts. In this paper, we treat only the problem of conceptual design decisions.

Decision support was first proposed by Nobel Prize winner Herbert Simon in the nineteen sixties [S1]. In a broad sense, decision making is conducted in four steps: (i) identifying the problem (ii) generating design alternatives, (iii) evaluating design alternatives via evaluation schemes, and (iv) selecting the best alternative. The research community in decision support methods usually recognize that the most critical step in decision making process is how to choose among a given number of design alternatives (step (iv)). The ability of decision makers to make the best choice is strongly conditioned by two factors: (i) having a clear definition of design objectives and requirements, and (ii) being able to evaluate or predict the performance of the proposed alternatives. However, uncertainties and vagueness are inherent in engineering design and they characterize both design objectives and alternatives evaluation schemes. This is particularly true in the first steps of conceptual design. The decisions taken at this design phase have the greatest influence on overall product life cycle cost. In order to minimize risk and reduce the cost of regret in later processes, companies often opt for a least commitment and late design decisions during product development process. This usually implies the development of several design concepts in parallel to finally settle down the optimal solution. Indeed this strategy is effective to minimize risk. It is very important to adopt appropriate methodologies and theories to structure and ease decision making process. This can significantly reduce product development lead-time as well as the amount of human and material resources involved in the development process.

As shown in Figure 1, multi-criteria decision making process can be decomposed into three principal steps: (i) an observation step, when data are collected about each

alternative, (ii) an interpretation step, when decision makers express their preferences for each design criterion on the basis on data collected in the observation step, and (iii) a results analysis step, when decision makers combine interpretation step outcomes for different design criteria in order to determine the best alternative(s).

Because of the great difficulty for decision makers to intuitively follow this process, especially to combine information in appropriate ways (step 3 of decision making process), MCDA methods can be used to aid in multi-criteria decision making.

The preference expression mode used in step (ii) can have an important influence on decision making results [GM]. The different expression modes used by the MCDA methods are: direct rating, pairwise comparisons, and lotteries. Each mode has its advantages and disadvantages. There are three factors to consider when choosing the preference expression mode: (i) it must be adapted to the type of information available on the design alternatives (step 1 in decision making process), (ii) decision makers must feel comfortable when using it, and (iii) the type of yielded information must be adapted to the decision situation.

Various MCDA methods are proposed and adopted by researchers and engineers to support design decision-making in engineering design. Choosing the most suitable MCDA method to compare multiple alternatives is a critical issue because these methods may yield different results for the same problem [MG,ZSWD,GM,TL]. There are two families of MCDA methods: (i) multi-criteria selection methods, where interpretation step results are taken into account simultaneously to compare alternatives, and (ii) aggregative methods, where interpretation step results are aggregated into a single variable called performance index (PI) that reflect the performance of the design alternatives.

In the next section, the MCDA methods analysed in our study are presented. After that, the industrial case study is presented and examined. Then, in Section 4, the objectives of the study and the proposed approach are presented. Finally, the results and the interpretations are presented and recommendations are given at the conclusion.

2- Presentation of MCDA methods

In this work, five aggregative methods (weighed sum, weighted product, Kim & Lin, compromise programming, and TOPSIS) and one selection method (ELECTRE I) were considered.

The weighted sum is the most widely used aggregation method. The weights assignment reflects the proportional importance of the different aggregated variables. However, the major disadvantage of this method is that it doesn't satisfy the principle of annihilation, which is generally not acceptable in design decision problems. The performance index is expressed by:

$$PI = \sum_i (w_i . x_i) \quad (1)$$
$$\text{With} \quad \sum_i w_i = 1 \text{ et } w_i \geq 0$$

The weighted product (WP) provides a conservative aggregative method that satisfies the principle of annihilation. However, the meaning of weights is less intuitive than weighted sum. They reflect the exponential relative importance, and not proportional between variables. The performance index is expressed by:

$$PI = \prod_i ((x_i)^{w_i}) \quad (2)$$
$$\text{With} \quad \sum_i w_i = 1 \text{ et } w_i \geq 0$$

Kim & Lin [KL] is the most conservative aggregative method. It also satisfies the principle of annihilation. However, the biggest disadvantage is that it does not allow any kind of compensation. Its use is thus very limited in engineering design. The performance index is expressed by:

$$f_{agg}(x_1, x_2, \dots, x_i, \dots) = \min (x_i) \quad (3)$$

TOPSIS (Technique for Order Preference by Similarity to Ideal Solution) is a compensatory method that was developed by Hwang (Hwang and Yoon [CH]) and widely applied by other researchers (Deng et al. [DYW]; Tsaur et al. [TCY]; Opricovic and Tzeng [OT]; Cheng et al. [CCH]; Montanari [M]; Tong et al. [TWCC]; Tzeng et al. [TLO], etc.). In conceptual design, TOPSIS has been used in a very limited way [LWCC]. The basic principle of TOPSIS is that the best alternative should have the shortest distance from the ideal solution and the farthest distance from the negative-ideal solution. The TOPSIS procedure consists of the following steps: (i) calculate the normalized decision matrix, (ii) calculate the weighted normalized decision matrix, (iii) determine the ideal and negative-ideal solution, (iv) calculate the separation measures from the ideal and negative-ideal solution (respectively A^- and A^+) by using the n-dimensional Euclidean distance, (v) calculate the relative closeness to the ideal solution, and (iii) calculate the performance index of each solution by the following formula:

$$PI = \frac{A^-}{A^- + A^+} \quad (4)$$

The separation measures from the ideal and negative-ideal solution for the solution *i* are calculated by the following formula:

$$A_i^+ = \sqrt{\sum_{j=1}^{n} \left(x_{ij} - x_j^+\right)^2} \quad (5)$$

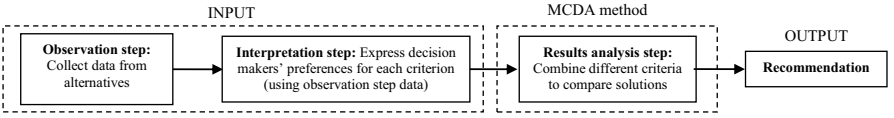

Figure 1: Schematization of the decision making process.

$$A_i^- = \sqrt{\sum_{j=1}^{n} \left(x_{ij} - x_j^-\right)^2} \quad (6)$$

With x_j^-: The minimum interpretation value for criterion j

x_j^+: The maximum interpretation value for criterion j

Compromise Programming (CP) was developed by Yu [Y] and Zeleny [ZC]. The basic principle of CP is that the best alternative should have the shortest distance from the ideal solution. The performance index is expressed by:

$$PI = 1 - \left(\sum_{j=1}^{n} \left(w_j \frac{|x_j^+ - x_j|}{|x_j^+ - x_j^-|}\right)^p\right)^{1/p} \quad (7)$$

$$\text{With } \sum_i w_i = 1 \text{ et } w_i \geq 0$$

Where x_i^+ and x_i^- have the same meaning as in TOPSIS. The parameter p defines the desired type of distance. In this study, the CP method has been applied twice by using the parameter p equal to 1 and 2.

The ELECTRE I is an outranking method that is widely used by decision makers in many fields. It was first developed by Roy [R]. The ELECTRE I procedure consists of the following steps: (i) define a concordance index for each pair of alternatives, it represents the sum of weights of attributes for which alternative A is better than B, (ii) define a discordance index for each pair of alternatives. It denotes the absolute difference of this pair of attributes divided by the maximum difference over all pairs, (iii) establish threshold values for the two indices, (iv) generate the set of alternatives that is not outranked by any other alternative. In order to obtain an overall ranking of the alternatives, many threshold values are used in our study and each alternative is ranked according to how many times it belong to the set of non-outranked alternatives.

3- Presentation of industrial case

A previous work has been performed within a design department developing a collector for a solar thermal power plant with Fresnel mirrors. The main function of the solar collector is to concentrate and redirect solar radiation into the absorber tubes to heat up the transfer medium in absorber tubes. The recovered heat is then used to generate high pressure steam which drives a turbine to produce electricity. The solar collector is composed of a reflecting glass and a metal structure, whose function is to give and maintain reflecting glass shape (Figure 2). A support solution is performed between the reflecting surface and the metal structure to ensure the connection between the two. Solar collector is driven by a rotation movement in order to pursue the movement of the sun.

In order to maintain a good thermal efficiency of the plant, a high reflection performance is required from the collector. This implies that the elastic deformation of the structure must remain as low as possible. A high level of precision must also be considered when manufacturing the collector.

The technology of solar thermal power plant with Fresnel mirrors is relatively recent and thus the historical background is limited. This induces a real difficulty when evaluating design alternatives. In addition, in order to reduce logistics cost, the concept of a movable factory has been adopted by the company. This choice induces directly and indirectly a set of particular constraints on the solar collector design. The interaction product/manufacturing process in this context is not well understood by development engineers. The implementation site also has a strong influence on collector design: climatic data, market data, etc. The difficulty is that the choice of implementation sites is not made and there is a variety of possible implementation sites where the conditions may vary significantly.

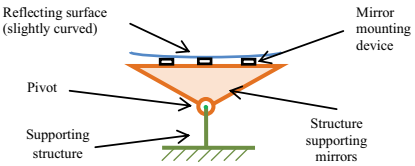

Figure 2: Schematization of solar collector structure.

In this study, we treat only the preliminary design of the metal structure (see Figure 2). Three main solutions have been proposed for the metal structure: truss structure (S1), sandwich structure (S2) and tube structure (S3). Compared to the tube and truss structure, the sandwich structure is the most mature solution. Its behavior is well characterized by the company due to the many prototypes that have been made. By contrast, truss and tube structures are new solutions for the company and there are much less mature than the sandwich solution. As the product development progresses, the behavior models used become more and more accurate especially due to prototypes testing. Rectifications are introduced to the three solutions throughout the development process.

The criteria taken into account in this study are: elastic deflection (C1), angular elastic deformation (C2), raw material cost (C3), durability (C4), development time (C5), ease of industrialization (C6), adaptation to the mirror mounting solution (C7), adaptation to the guidance solution (C8).

The development process is composed of three major milestones. At each milestone, a set of tasks is planned in order to investigate the performance of each concept. These actions generally consist in: numerical analysis and prototyping/tests. At the end of each milestone, an assessment grid is established to synthesize investigation works of designers. The results are discussed by different actors participating in the development process. The development team decides then what concepts should be eliminated and what actions must be done for the next milestone. In this study, we treat the decision making problem at the first milestone.

Article 06-dm-104

4- Objectives and approach

In the present study, various MCDA methods were tested and analysed based on the conceptual design phase of a solar collector of a thermodynamic solar power plant. The objective is to evaluate the appropriateness of MCDA methods in our context.

The first step of our study is to evaluate weights for the different criteria. It is difficult and risky to directly assign weights to criteria because they are from different natures. In our study, pairwise comparison was used because it is more appropriate to this case. Using the semantic scale in Table.1, the judgment matrix was constructed. The results are given in Table. 2. The matrix normalization method [L] was then used to calculate criteria weights from the judgment matrix. In order to limit the inconsistencies that occur when performing pairwise comparisons, the Consistency Ratio (CR) proposed by Saaty [S2] was used as a guidance to check for consistency. As recommended by Saaty [S2], a value of 0,1 was used as threshold for CR.

After the evaluation of criteria weights, the next step is the evaluation of alternatives against each criterion (the interpretation step). A direct rating was used to evaluate each alternative against each criterion. This preference expression mode was used because it is simple and it yields a cardinal rating. Pairwise comparison is more suitable to deal with qualitative criteria and uncertainty in data. However, it yields ordinal evaluation of alternatives which is not suitable to use with aggregative methods. In order to help decision makers to assign interpretation values, the semantic scale in Table. 1 was used. The results of the interpretation step are presented in Figure 3.

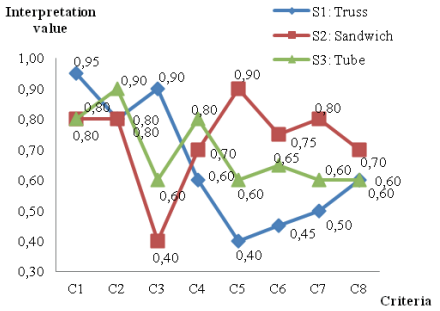

Figure 3: interpretation results

Based on the interpretation results (Figure 3) and criteria weights obtained by pairwise comparisons, different MCDA methods were used to rank alternatives. From this survey, MCDA methods were evaluated in terms of three criteria: (i) the consistency of results, (ii) the ease of understanding and, (iii) the adaptation the decision type.

1.1. The consistency of results

The consistency of results is a very important criterion of MCDA methods. It measures the closeness of the result given by the MCDA method to what really corresponds to decision makers' preferences. In our study, this criterion was evaluated by comparing the ranking results given by MCDA methods to the intuitive ranking addressed by decision makers

Table. 1 Semantic scales used (a) for direct rating; (b) for pairwise comparison.

(a)

Satisfaction degree	Interpretation value
Extremely high	1
Very high	0,9
High	0,8
Fairly high	0,7
Moderately high	0,6
Moderate	0,5
Moderately low	0,4
Fairly low	0,3
Low	0,2
Very low	0,1
Null	0

(b)

Relative priority degree	Judgement value assigned
Capital	9
Extreme	8
Very strong	7
Strong	6
Fairly strong	5
Moderate	4
Fairly moderate	3
low	2
Equal	1

1.2. The ease of understanding

This aspect measures the effort and the time required for the decision makers to understand the MCDA method (assumptions, trade-offs, and procedures of method). The less time and effort required to understanding the method, the better decision makers will use the method and the more effective the method will be [MG]. Experienced decision makers generally prefer simple, more transparent methods [HCHS]. The MCDA methods were tested by three persons participating in the development project. The methods were then ranked on a scale of 1 to 5 (1 if the method is very difficult to understand and 5 if the method is very easy to understand).

Table 2. Evaluation of criteria weights by pairwise comparisons.

	C1	C2	C3	C4	C5	C6	C7	C8
C1		0,14	0,13	0,20	0,20	0,13	0,17	0,50
C2			0,20	0,50	3,00	0,20	0,33	5,00
C3				3,00	7,00	4,00	5,00	8,00
C4					2,00	0,25	3,00	5,00
C5						0,17	0,50	4,00
C6							5,00	7,00
C7								5,00
C8								
Final criteria weight	**0,02**	**0,08**	**0,38**	**0,12**	**0,05**	**0,25**	**0,09**	**0,02**

1.3. Adaptation to the decision type

It is important that the type of decision given by the MCDA method corresponds to the type of decision expected by decision makers. For example, if the decision makers want to get a cardinal ranking of alternatives, then an outranking method is not appropriate.

5- Results and interpretation

As shown in Figure 4, clear discrepancies are observed in the ranking of alternatives between compensatory and non-compensatory aggregation methods. All the compensatory aggregation methods (weighted sum, TOPSIS, compromise programming with p=1, 2) yield the following ranking: A1→A3→A4. On the other hand, the two non-compensatory strategies (Kim & Lin and weighed product) yield the following ranking: A3→A1→A4. ELECTRE I yields the same ranking as compensatory aggregative methods.

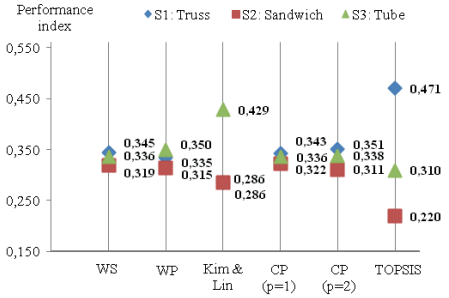

Figure 4: ranking of alternatives by each aggregative method.

Apart from TOPSIS and Kim & Lin aggregation methods, the performance indexes obtained by the other aggregation methods are very close together. It is thus difficult and risky to draw a conclusion based on these results since a small error in interpretation values could reverse the ranking. Kim & Lin aggregation is not suitable for our case because it does not provide any kind of compensation.

According to the interpretation results (Figure 3), the truss alternative highly satisfies the criterion of raw material cost which is the most important criterion. In contrast, because of its low maturity, it collects low interpretation values (Figure 3) for other criteria, in particular for the criterion 'ease of industrialization' which also has a very strong importance in our case. Therefore truss alternative obtains a low performance index by conservative aggregative methods. But the important fact that should be considered here is that the truss structure is a novel and immature alternative compared with the others. The potential of improvement is thus high. That is why this alternative was particularly attractive for decision makers. This statement was intuitively felt by decision makers and it was highlighted strongly by TOPSIS and little by the other compensatory aggregative methods. For the other two solutions, the ranking yielded by compensatory aggregative methods is also coherent with the preferences of decision makers. From this observation we can estimate the consistency of evaluated MCDA methods in our case.

It can be remarked that TOPSIS intensifies the relative importance between alternatives compared to other compensatory aggregative methods. This intensification effect can be attributed to two factors: (i) the two reference points (ideal and negative-ideal solutions) are obtained according to the alternatives tested (relation (5) and (6)), and (ii) this method uses an Euclidian distance to calculate the closeness of alternatives to the reference points.

For the criterion of 'ease of understanding', WS and Kim & Lin were the easiest methods to understand, followed by WP, CP, TOPSIS and finally ELECTRE I which was particularly difficult to understand by decision makers who participate in the survey. Table 3 gives more details about the evaluation of MCDA methods against this criterion.

For the criterion of 'adaptation of the decision type', the most adapted decision type in our case is the cardinal ranking. Ordinal ranking (yielded by ELECTRE I) is not suitable because decision makers need to know how much better an alternative is over the others in order to be able to make a decision. Aside from ELECTRE I, all the other methods respect this criterion since they yield a cardinal ranking.

Another disadvantage of the ELECTRE I method is that it evaluates a criterion even if it has a weight equal to zero. This can mislead the decision maker, since the discordance calculation does not consider the value of the weights. The use of ELECTRE I is clearly not suitable in our case.

Table 3. Evaluation of MCDA methods against the three criteria.

	Consistency	Ease of understand	Adaptation of the decision type
WS	Average	5	Good
WP	Poor	4	Good
Kim & Lin	Poor	5	Good
CP (p=1)	Average	3	Good
CP (p=2)	Average	3	Good
TOPSIS	Good	2	Good
ELECTRE I	Poor	1	Poor

6- Conclusion

A comparative study of different MCDA methods was performed in this paper based on an industrial case study of a solar structure development. The study focused on the two main steps of decision making: the interpretation step and result analysis step (Figure 1). Even if pairwise comparison seems to be more suitable to deal with qualitative criteria, the direct rating was privileged in the interpretation step because it allows having cardinal interpretation values which are much more suitable to use with aggregative methods. Many MCDA methods were then used to rank alternatives. It was found that the ranking differs between conservative and non-conservative methods.

Generally it was found that the results yielded by compensatory aggregative methods are more consistent. TOPSIS was the most consistent with decision makers' preferences because the results yielded by this method respect very well the decision makers' preferences. However, in the final design phases, it could be more appropriate to use non compensatory aggregation methods because the potential of improvement is low and decision makers cannot afford to take risks.

A further investigation should be done in a future works in order to evaluate more efficiently the performance of the MCDA methods. For example, a sensitivity analysis could be performed in order to evaluate the robustness of these

methods with respect to uncertainties in interpretation values or criteria weights. Further industrial cases of product development could also be considered.

7- References

[S1] Simon HA. The new science of management decision. New York: Harper & Row; 1960.

[S2] Saaty TL. A scaling method for priorities in hierarchical structures. J Math Psychol 1977;15:234-281.

[KL] Kim K, Lin D. Simultaneous optimization of mechanical properties of steel by maximizing exponential desirability functions. J R Stat Soc Ser C Appl Stat 2000;49:311-325.

[CH] Chen SJ, Hwang CL. Fuzzy multiple attribute decision making: methods and applications. Berlin: Springer-Verlag; 1992.

[DYW] Deng H, Yeh CH, Willis RJ. Inter-company comparison using modified TOPSIS with objective weights. Comput Oper Res 2000;27:963-973.

[TCY] Tsaur SH, Chang TY, Yen CH. The evaluation of airline service quality by fuzzy MCDM. Tourism Manag 2002;23:107-115.

[OT] Opricovic S, Tzeng GH. Multicriteria planning of post-earthquake sustainable reconstruction. Comput Aided Civ Infrastruct Eng 2002;17:211-220.

[CCH] Cheng S, Chan CW, Huang GH. An integrated multi-criteria decision analysis and inexact mixed integer linear programming approach for solid waste management. Eng Appl Artif Intell 2003;16:543-554.

[M] Montanari R. Environmental efficiency analysis for fresnel thermo-power plants. J Cleaner Prod 2004;12:403-414.

[TWCC] Tong LI, Wang CH, Chen CC, Chen CT. Dynamic multiple responses by ideal solution analysis. Eur J Oper Res 2004;156:433-444.

[TLO] Tzeng GH, Lin CW, Opricovic S. Multi-criteria analysis of alternative fuel buses for public transportation. Energy Policy 2005;33:1373-1383.

[ZC] Zeleney M, Cochrane JL. Compromise programming. In: Multicreteria decision making. Columbia: University of South Carolina Press; 1973. p. 262-301.

[Y] Yu PL, Multiple criteria decision-making: concepts, techniques and extensions. New York: Plenum Press; 1985.

[HCHS] Hobbs BJ, Chankong V, Hamadeh W, Stakhiv E. Does choice of multicriteria method matter? An experiment in water resource planning. Water Resour Res 1992;28:1767-1779.

[MG] Mahmoud MR, Garcia LA. Comparison of different multicriteria evaluation methods for the Red Bluff diversion dam. Environ Modell Softw 2000;15:471-478.

[ZSWD] Zanakis SH, Solomon A, Wishart N, Dublish S. Multi-attribute decision making: A simulation comparison of select methods. Eur J Oper Res 1998;107:507-529.

[GM] Guitouni A, Martel JM. Tentative guidelines to help choosing an appropriate MCDA method, Eur J Oper Res 1998;109:501-521.

[TL] Triantaphyllou E, Lin CT. Development and evaluation of five fuzzy multiattribute decision-making methods, Int J Approximative Reasoning 1996;14:281-310.

[L] LeBel L. Prise de décision multi critères. Prise de décision Multi critères. Université Laval; 2009.

[LWCC] Lin MC, Wang CC, Chen MS, Chang CA. Using AHP and TOPSIS approaches in customer-driven product design process. Comput Ind 2008;59:17-31.

[R] Roy B. Classement et choix en présence de points de vue multiples. Revue française d'automatique, d'informatique et de recherche opérationnelle 1968 ; Volume: 2, Issue: V1, page 57-75

Article 08-dm-102

CONTRIBUTION TO THE EMBODIMENT DESIGN OF MECHATRONIC SYSTEM BY EVOLUTIONARY OPTIMIZATION APPROACHES

Didier Casner [1], Rémy Houssin [1,2], Jean Renaud [1], Dominque Knittel [1,2]

(1): INSA de Strasbourg, Laboratoire du Génie de la Conception, 24 Boulevard de la Victoire, 67084 Strasbourg Cedex
+33 3 88 14 47 00
E-mail: {didier.casner,jean.renaud}@insa-strasbourg.fr

(2): Université de Strasbourg, UFR de Physique et d'Ingénierie, 17 rue du Maréchal Lefebvre, 67100 Strasbourg
+33 3 68 85 46 61
E-mail: {remy.houssin,dominique.knittel}@insa-strasbourg.fr

Abstract: Mechatronic systems are multidisciplinary devices and therefore require specific approaches to design and optimize them, unlike most approaches that consider the optimization as a manner to identify the optimal process through a redesign strategy and at the last phase of design. Therefore optimization has limited efficiency. This paper contributes to the integration of the optimization in the embodiment design process, as part of a routine or innovative approach. The optimization will now be considered as a manner to design and optimize innovative mechatronic systems. This approach considers an evolutionary case-based reasoning process to design a technical solution from a concept by reusing, adapting and optimizing solutions or cases that have previously been used to solve similar problems. The main approach has been applied to the design of an XY table for laser cutting applications.

Keywords: mechatronic systems, design, optimization, optimization-integrated design

1 - Introduction

Constant evolving needs and markets implies that new products are always more efficient, less expensive, and the design time always lower. This also implies to combine technologies from several disciplines, such as mechatronic products that synergistically integrate solutions from mechanics, electronics, control and computer engineering [1], that are the heart of our work. Mechatronic system [2] design is therefore very difficult because such devices tend to be even more complex and because most current modeling tools operate over only a single domain [3]. This then requires new approaches to design and optimize mechatronic devices.

This paper deals with the use of optimization as a method to improve mechatronic designs from the embodiment stage. To design a mechatronic system, it is required to develop four different subsystems [4]:

- A "base structure", which often consist of a mechanical structure or a material,
- One or more actuators that can act on a machine or a process to change its behavior or states,
- One or more sensors to provide information on the current state of the machine that can be analyzed and processed by an information processing device,
- One or more information processing device, often a computer or an embedded system, analyze and process the information given by the sensors and control the actuator to obtain the desired behavior. The control law synthesis consists of the main part of these processing devices.

The optimization process of mechatronic devices often occurs during the detailed design process [5] and is restricted to a sizing problem solving: optimization methods are used to identify the best parameters that solve the problem without affecting the architecture of the system. Such optimization is therefore used to improve performances of an already designed device and is then constrained by choices made during early design steps [6]. The design phase of a product is responsible for only 5% of the cost of the product but can determine 75% of the manufacturing costs and 80% of the product quality [7]. So, the optimization of an already designed product has a limited efficiency. That is why, it is important to improve the effectiveness of the optimization by doing it earlier in the design phase [8].

Following [9] optimization is mostly used as a redesign process to enhance the performance of a system during the detailed design phase of the product, once it has been developed during the conceptual and embodiment phases [10] using other advanced tools, such as TRIZ [11], Case-Based Reasoning [12], etc. This development is often done using design models that had been created for

Article 08-dm-102

monodisciplinary system design [6], such as the systematic approach proposed by Pahl and Beitz [5]. In 1994, Cooper [13] proposed a "third generation new product process", the stage-gate process, which has widely been adopted by R&D departments and gain legitimacy each year. It is moreover based on the three development, evaluation and selection steps that are fairly closed from those used in optimization. In 2004, the mechatronic community, as a guideline to develop multidisciplinary devices, adopted a design model for mechatronic system, known as the V-*cycle [4]*.

The work presented in this paper deals with the innovative design process [14] of mechatronic systems. Starting from a principle solution or concept of a technical concept, our research work aim to propose a design approach to develop and optimize the mechatronic design layout. To perform this, our contribution should solve the following problems:

- The multidisciplinary aspect of the mechatronic device and the integration of different technologies from mechanical, electronic, control and computer engineering should been considered;
- The architecture, the structure of the system should also been modified during the process;
- The parameters of a candidate structure should be optimized along criteria that can also be used to evaluate the solution among the design problem;
- The best mechatronic solution(s) that solves the given design problem according to the previously defined concept of solution should be selected.

The paper is subdivided into four parts. The state of the art concerning our problem is firstly introduced. Then the approach we developed to design and optimize the mechatronic layout that shapes the design problem and concepts. This approach is then applied to a case study that aims to design and optimize an XY table for laser cutting. And, further developments regarding the automated design and the characterization of the proposed approach are finally introduced.

2 - Literature review

In this section, we present the state of the art regarding our problem in which first of all we present the different design approaches and then we present the problem concerning the design and the optimization of mechatronic systems. In this part, we want to position our problem regarding the existing design models and approaches. We considered three of the most used design models in engineering: the systematic design model by Pahl and Beitz, Cooper's stage-gate process and the V-model.

2.1 - The systematic design approach

In 1977, G. Pahl and W. Beitz [15], first modeled the process used to design new products. This representation is a sequential process, which means that tasks only begin if the previous one is already completed and does not include verification steps.

2.2 - The "Stage-gate" process

In 1994, Cooper [13] proposed an approach which is rather considering an idea as the input data and then works whatever the method used to generate this idea. Instead of validating the design at the end of the development stage, this approach uses a linear progression through a series of stages and adds "gates" between stages. These gates offer the possibility to control and evaluate the design through the whole process after one stage is realized.

This approach alternates stages with gates that can be summed in three steps [13]:

- Development: candidate solutions are designed considering the design problem and choices eventually made in previous stages.
- Evaluation: candidate solutions are evaluate among criteria.
- Selection: the best solutions are retained for the next steps.

This approach, as well as the previously presented Pahl's model, still is sequential however it is possible to evaluate the design through its process. Today's design approach tends to be less sequential and aims to realize some design steps in parallel, known as the concurrent engineering [6], such as the V-cycle presented below.

2.3 - From sequential to concurrent design

In 2004, the German engineering society (VDI) published a practical guide that advocates the use of the V-cycle shown in Figure 1 to replace the systematic development model while developing mechatronic systems [4]. This model subdivides the design process as a two steps approach: the first one consists of the specification and design step and the second one consists of the integration and validation phases; and realizes the design following four levels: functional, system, subsystem and component levels.

Compared with the model presented in section 2.1, this design model adds the verification and validation aspects that are required in a number of safety-critical industry [16] sectors.

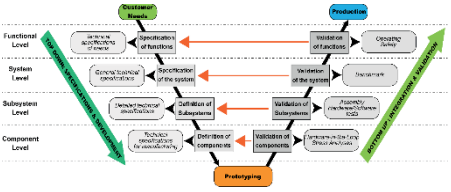

Figure 1. V-cycle for mechatronic systems design [4]

2.4 - Optimization and research problem

From one hand, based on the different design models presented above, we find that optimization is done at the

Article 08-dm-102

final phase of sequential model. It occurs during the fourth and last stage in the stage-gate model and in the "bottom up" phase of V-Model. These design models however concur on the manner how the optimization is currently used. The optimization is indeed often limited to a redesign process to improve the characteristics of an already designed system and can then be positioned in the 4th stage (Cooper's model), integration and validation (V-cycle) or detailed design phases (in the systematic design model).

In the classical approach presented in figure 4the optimization is mainly realized once the mechatronic product has been designed and limited to an identification of the best parameters to improve the performances of system without affecting the topology of the system. That means that the optimization process is constrained by the selection done during the design process as the structure is fixed. In the classical design approach, the optimization is therefore actually realized during the detailed design phase. That is why, it is important to perform optimization in earlier stages, such as the embodiment design, which is the heart of the approach proposed in this paper.

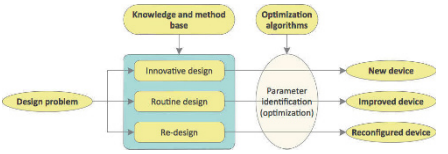

Figure 2. The classical design and optimization approach

On the other hand, based on the defined design concept, which may be built using inventive or routine design tools, a technical solution is built using design tools. But, the internal organization of the research and development teams in companies globally remained at the stage where each engineering office is specialized in only one domain without real communication between them [17]. However an engineer will not think in the same manner [18]:

- Mechanical engineers think in term of physical shapes and motion,
- Electronic engineers think in term of signals and circuits,
- Computer engineers think in term of logical and syntax.

This organization also involves the development of mechatronic products that are more assemblies of technologies from different disciplines than a real synergy. The overall design approach usually adopted then was to decompose the system into several subsystems (each on a specific discipline) and to study and optimize these subsystems separately. In the classical approach, although each specialists work in the most efficient manner, its isolation implies that he only has a partial view of the overall system and thus potentially creates interfacing problems with the other subsystems. But, it is known that the combination of local optimum almost never lead to a global optimum for the overall system.

In recent years, to solve this problem, methods, known as the multidisciplinary design optimization, have been developed to optimize systems with interactions between more than one discipline. However they permit a consideration of several disciplines during the optimization process, they are still only optimizing parameters from a parametric model that has previously been developed.

To improve the effectiveness of the optimization, it is needed to do it earlier in the design phase and to allow it to act on the structure or the architecture of the mechatronic system too. Our contribution therefore deals with the integration of both topology and parametric optimization from the mechatronic development stage.

3 - Proposed method

Figure 3 presents the global design and optimization approach we developed to integrate the optimization during the design stage of mechatronic systems.

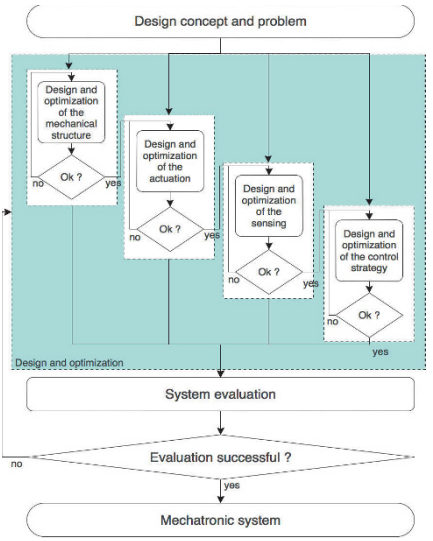

Figure 3. Proposed approach for mechatronic system design and optimization

To develop this approach that can be used to integrate optimization during the embodiment development stage of mechatronic systems, the following problems had to be solved:

- In which order should the different subsystems of a mechatronic system be designed?
- How to use optimization as a method for the embodiment design?
- How optimization can act on the topology of a mechatronic device?

Article 08-dm-102

4 - Mechatronic subsystems Design

Based on the definitions of the several subsystems introduced in section 1, we may define the requirements imposed by a given subsystem:

- The definition of the actuation and sensing subsystems requires information about the base structure they should act on, for example concerning the type of joints from the kinematic structure.
- The definition of sensors moreover often require characteristics of the actuators if these sensors should measure the state of the actuator (in the joint space of a robot for example);
- The control synthesis requires a model of the system it should control, regarding its performances, its stability, its robustness, and its damping ratio…

These requirements imply to design these subsystems using a hierarchical design approach that is presented in Figure 4.

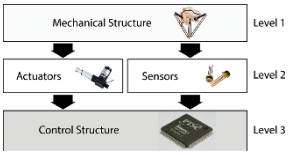

Figure 4. Hierarchical design approach of mechatronic systems in the early design phase

The design approach considers the three following design levels:

- In the first level, the skeleton of the mechatronic system consisting of the mechanical structure is designed.
- Based on the choices made for the mechanical structure, actuation and sensing subsystems are defined. This selection should be made from the skeleton, as it will constrain the amount of possible solutions: for example, the type of motion an actuator should apply depends on the type of joint from the kinematic structure.
- Finally, once the mechanical structure, the actuators and sensors have been selected, we get all required information to synthetize the control strategy. The control structure will indeed strongly depend on the nature of the mechatronic system to be designed.
- In the different stages and levels, optimization is integrated in the embodiment design phase to optimize both the structure and the parameters from the subsystem. The strategy used is presented in the next subsection.

4.1 - Evolutionary case-based design

The proposed approach to use optimization from the embodiment design starts from the definition of the main design problem. This design problem is better defined as a number of objectives to minimize or maximize and a couple of design constraints. This form helps defining the design problem that can easily be translated to a design optimization problem. During this step, the design problem is usually defined under an abstract and/or textual form.

To perform the development process of mechatronic systems, some advanced design strategies such as the Case-Based Reasoning (CBR) [19] were considered. However the classical Case-Based Reasoning approach allows to propose a solution that solves a given design method by using adaptation and reusing possibilities, which can therefore be used as both routine and innovative design tools, it does not evaluates the optimality of the given solution. To improve the effectiveness of both the optimization and the CBR approaches by:

- Allowing the optimization to act on both the topology and the parameters of the mechatronic system
- Optimizing the solution obtained using the classical CBR approach.

A basic comparison of the CBR and optimization principles can moreover highlight many similarities between the manner how the CBR solves a design problem and the manner how an evolutionary algorithm solves a combinatorial optimization problem. These similarities may also be seen as complementary elements: the CBR may be completed with genetic operators to improve the efficiency of the process and to increase the performance of the given solution. This improvement leads to the development of the evolutionary case-based design (ECBD) method, presented in Figure 5, which is used to design each subsystem layout based on the defined solution concept.

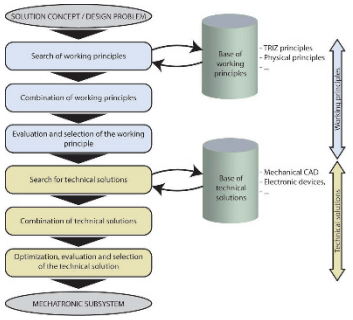

Figure 5. Evolutionary Case-Based Design

- Based on the concept of solution and the design problem, compatible working principles are defined. This base is made of principles such as TRIZ, physical principles and is populated by known working principles or may be completed using new knowledge obtained from creative design stages.

	1	2	3	…	n
Function 1	WP11	WP12	WP13		
Function 2	WP21	WP22			
…					
Function k	WPk1	WPk2	WPk3	…	WPkn

Table 1. Example of a morphological matrix

Article 08-dm-102

The given set of solution is then filtrated to reduce the number of working principles. The results of the selection stage can be represented using the morphological matrix presented in Table 1.

Once the working principles have been selected, combinatorial optimization method such as genetic algorithms [20] is used to build combinations of working principles that can solve the design problem or embody the concept of solution that has been defined at the inventive design stage. To perform this step, compatibility matrices as presented in Table 2 may be considered to identify the compatibility level between working principles.

	WP11	*WP12*	*WP13*	*WP21*	WP22	. . .	*WPk1*
WP1		$\alpha_{11,12}$	$\alpha_{11,13}$	$\alpha_{11,21}$	$\alpha_{11,22}$	. . .	$\alpha_{11,k1}$
WP1	$\alpha_{12,11}$		$\alpha_{12,13}$	$\alpha_{12,21}$	$\alpha_{12,22}$	. . .	$\alpha_{12,k1}$
WP1	$\alpha_{13,11}$	$\alpha_{13,12}$		$\alpha_{13,21}$	$\alpha_{13,22}$	. . .	$\alpha_{13,k1}$
WP2	$\alpha_{21,11}$	$\alpha_{21,12}$	$\alpha_{21,13}$		$\alpha_{21,22}$	. . .	$\alpha_{21,k1}$
WP2	$\alpha_{22,11}$	$\alpha_{22,12}$	$\alpha_{22,13}$	$\alpha_{22,21}$		. . .	$\alpha_{22,k1}$
. . .	. . .	. . .	. . .	. . .	. . .		. . .
WPk	$\alpha_{k1,11}$	$\alpha_{k1,12}$	$\alpha_{k1,13}$	$\alpha_{k1,21}$	$\alpha_{k1,22}$	. . .	

Table 2. Compatibility matrix

In this matrix, we evaluate the compatibility noted $\alpha_{i,j}$ for each couple of solutions (WP_i, WP_j) $\forall i \neq j$. This matrix may be filled using a binary or a decimal code. In most cases, a decimal code will be preferred, because it also allows us to set preferences or degrees of compatibility. For example, a bottle cap, it is possible to define degree of compatibility in terms of the porosity, the chemical compatibility of the liquid contained in the bottle and the cap (etching, oxidation…). Based on this matrix, we can eliminate operating principles that are incompatible with the others.

To combine the working principles, usual method consists of evaluating all possible combinations. But, in most cases the number of solutions to investigate becomes overwhelming, which implies that this method cannot be used anymore. If considering large scale or problems, the required computation time increases exponentially. That is why; we proposed to use optimization heuristics to solve this problem. By considering genetic methods [21], we can use selection, crossing, and mutation operators to search for an optimal combination. Even if heuristics does not ensure optimality, those methods can afford to approach it in a reduced calculation time. The combination of solution is then done using genetic heuristics.

The proposed combinations of working principles are then evaluated and the best combinations are selected. The selection may be performed using decision-making tools to automate the operation and is done by considering selection criteria, for example selecting the solutions that solves the problem using the fewest number of principles, the solutions that requires less manufacturing operations, or the solutions that are cheaper. Some working principles can indeed be used to solve more than one objective and may therefore be privileged.

For each selected combination of working principle, optimization or decision-making tools are used to select technical solutions from the database that can be integrated into the system to embody the given working principle. This selection can also be represented as the morphological matrix to identify, for each working principle, the technical solution that can be used to embody the working principle.

Based on the morphological matrix, we may also build a compatibility matrix to identify the compatibilities between the different technical solutions. Combinatorial optimization tools to propose candidate subsystems by combining the given technical solution use this analysis.

The parameters of the proposed subsystem designs are finally optimized. The optimization results help improving the efficiency of the subsystem and these results are also considered to evaluate each proposed subsystem for each combination of working principles. The evaluation that is processed using decision-making tools is finally used to select the mechatronic subsystem that better solves the design problem.

5 - Application on a X-Y table for laser cutting

To illustrate the presented design and optimization approach, we decided to apply it on the development of a XY table for laser cutting. XY tables are devices that operates in two axes of motion along X and Y-axis. The design problem has been defined using Functional analysis. It aims to propose a device to rapidly and precisely cut metal part.

5.1 - Design and Optimization of the x-y table

The definition of the concept of solution, which may be defined using tools as TRIZ or FAST, is not the subject of this paper. This concept is considered as the following:

- The laser source will be fixed and the beam is moved over the metal part using optical mirrors.
- Each X and Y-axes are decoupled: the structure is built so that the beam can be moved along one axis without interfering along the other axis.
- The laser beam is moving, not the cutting support. That implies that no fixation means are required: the atmospheric pressure is enough to keep the metal part on place.
- The material of the cutting support is chosen so that the melting point is never attained when the laser is operating at its maximal power.

Based on this concept, we may define the morphological matrix containing technical solutions. Table 4 presents an example of morphological matrix defined for the mechanical structure.

Working principles	TS1	TS2	TS3	TS4
Translational guidance	Screw-ball	Pulley-Belt	…	…
Avoid axial and motion play	Guide rail			
Move the laser mirrors	Platform	Rods		
Avoid friction	Polishing	Lubrication		

Table 4. Morphological matrix for the mechanical structure

Article 08-dm-102

To build the mechanical structure, we also built the compatibility matrix using a binary code. This compatibility matrix has then been used to identify which solutions are compatible together. The coefficients presented in the matrix can be used as preferences weights to favor one solution over another. Starting from the morphological and compatibility matrices, which can be defined in the same manner for the other subsystems we want to design, we may then try to combine one solution for each working principle.

To do this, if the number of combination is relatively low (2 x 1 x 2 x 2 = 8 in our case), we may evaluate all the possible combination, but in most cases, the number of combination is relatively high and stochastic optimization tools should therefore be used. In addition with the compatibility criterion or constraint, which may be easily evaluated (by considering the product of all coefficients from the compatibility matrix for each couple of solution taken two by two), additional criterion may also be defined, such as economic ones. The selection may likewise be done using fitness functions, like those used in evolutionary algorithms. For example, if we consider the compatibility matrix presented in Table 5, we can determine that polishing should be avoided, as it is not compatible with any solution for the translational guidance principle.

Once we obtained a set of possible solutions for each subsystem, morphological and compatibility matrices can equally be considered to look for the best combinations of subsystems by building the matrices for the whole system and considering subsystem technical solutions instead of working principles. To finally perform the design of the mechatronic system, combinatorial optimization can be used to find the best combination.

		Translational guidance		Motion play	Move the mirrors		Avoid friction	
		Screw-ball	Pulley-Belt	Guide rail	Platform	Rods	Polishing	Lubrication
Translational guidance	Screw-ball		0	1	1	1	0	1
	Pulley-belt	0		1	1	1	0	1
Motion play	Guide rail	1	1		1	0	1	1
Move mirrors	Platform	1	1	1		0	1	1
	Rods	1	1	0	0		1	1
Avoid friction	Polishing	0	0	1	1	1		1
	Lubrication	1	1	1	1	1	1	

Table 5. Compatibility matrix for the mechanical structure

5.2 - Results

The model of the system has been implemented using Matlab/Simulink and optimized using ModeFrontier to identify the optimal system based on the two objectives:

- Minimize the precision of the system which is calculated as the integrated square error between the desired and obtained position
- Maximize the displacement velocity of the system.

The parameters to identify are:

- Mechanical structure: radius of the pulley
- Actuators: Motor characteristics (inertia, resistance, inductance, speed/torque constant)
- Control: Proportional, integration, derivative, filter constants.

The optimization leads to the results presented in Figure 6. A scatter of possible solutions has been obtained and it is now needed to analyze these results. The Pareto frontier containing the non-dominated solutions, represented as the bold line on the plot, has been determined from the scatter.

We may see that there is a contradiction between the minimization of the ISE (Integrated Square Error) and the maximal velocity. Two solutions to solve this contradiction may be applied:

- Choose the best compromise between those criterion;
- If the previous option does not lead to a satisfactory solution, the structure of the mechatronic system or even the concept of solution should be revised. For example, considering TRIZ principles, one option to solve the contradiction between the velocity and the accuracy may be to use non-mechanical interactions, by replacing some mechanical interactions with electrical, magnetic or electromechanical fields.

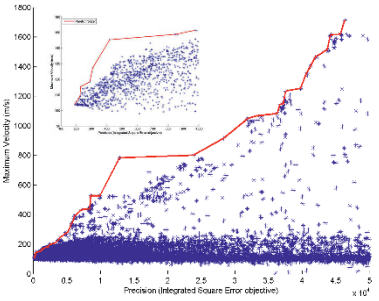

Figure 6. Optimization results

These results allow us to select the solution presented in Figure 7 as the optimal structure. Based on the proposed design approach for the different subsystems and considering the morphological and compatibility matrices, we obtained the mechatronic structure presented in Figure 7 made of the following subsystems:

- Mechanical structure: the structure is composed with two rods that are translating using a belt and rails for translational guidance. The rails ensure one rod can only move in one single direction.
- Actuation: Two DC motors are considered to deliver a rotational motion to the pulley that will convert it to a translational motion using the belt.
- Sensing: Linear encoders to measure the position of the

rods along each axis. As a first approach, the other states will be considered as measurable, to limit the number of parameters of the system, but will be implemented using state observers.

- Control: PID controllers are implemented.

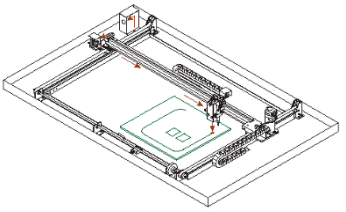

Figure 7. Concept of the XY table for laser cutting

The final step of the design process consists of the evaluation and the selection of one solution from the given mechatronic system. In the case the evaluation does not lead to a valid solution that solves the problem, we may start the approach again with one another structure. This part will be developed in further work. Due to the lack of existing software tool to perform automatically the modification of the structure during the optimization process, this step has been done manually, however a software tool to do it is currently in development and will be present in a future publication.

6 - Conclusion

This paper presented an approach to integrate optimization in early design process of mechatronic systems. This approach aimed to perform optimization from the preliminary design stage of multidisciplinary devices. To optimize both structure and parameters of a mechatronic device, a strategy based on the evolutionary case-based design approach has been developed. In this approach, we integrated computational and parametric optimization in the embodiment process of multidisciplinary devices. The design approach has then been applied to a practical study-case which shown how it works and how the optimization can be used as a design method. The application to an industrial case to validate the approach and the development of a software platform to realize the topology optimization of the mechatronic system are currently in development and will be the subject of further papers.

- References

[1] AFNOR, "NF E01-010," ed, 2008.

[2] N. Kyura and H. Oho, "Mechatronics-an industrial perspective," *Mechatronics, IEEE/ASME Transactions on,* vol. 1, pp. 10-15, 1996.

[3] J. Dupuis, F. Zhun, and E. D. Goodman, "Evolutionary Design of Both Topologies and Parameters of a Hybrid Dynamical System," *Evolutionary Computation, IEEE Transactions on,* vol. 16, pp. 391-405, 2012.

[4] Verein Deutscher Ingenieure, "VDI 2206 - Entwicklungsmethodik für mechatronische Systeme (design methodology for mechatronic systems)," ed. Berlin: Verein Deutscher Ingenieure, 2004.

[5] G. Pahl, W. Beitz, J. Feldhusen, and K.-H. Grote, *Engineering Design : A systematic approach*, 3rd edition ed.: Springer, 2007.

[6] D. Bradley, "Mechatronics – More questions than answers," *Mechatronics,* vol. 20, pp. 827-841, 2010.

[7] S. Dowlatshahi, "Product design in a concurrent engineering environment: an optimization approach," *International Journal of Production Research,* vol. 30, pp. 1803-1818, 1992/08/01 1992.

[8] R. Guserle and M. F. Zaeh, "Application of multidisciplinary simulation and optimization of mechatronic systems in the design process," *Proceedings, 2005 IEEE/ASME International Conference on Advanced Intelligent Mechatronics.,* pp. 922-927, 2005.

[9] Y. Collette and P. Siarry, *Multiobjective optimization principles and case studies*, Corr. 2nd print. ed. Berlin: Springer, 2004.

[10] A. Cardillo, G. Cascini, F. Frillici, and F. Rotini, "Computer-aided embodiment design through the hybridization of mono objective optimizations for efficient innovation process," *Computers in Industry,* vol. 62, pp. 384-397, 5// 2011.

[11] D. Cavallucci, F. Rousselot, and C. Zanni, "Linking Contradictions and Laws of Engineering System Evolution within the TRIZ Framework," *Creativity and Innovation Management,* vol. 18, pp. 71-80, 2009.

[12] A. Aamodt and E. Plaza, "Case-based reasoning: foundational issues, methodological variations, and system approaches," *AI Commun.,* vol. 7, pp. 39-59, 1994.

[13] R. G. Cooper, "Perspective third-generation new product processes," *Journal of Product Innovation Management,* vol. 11, pp. 3-14, 1// 1994.

[14] N. Leon, "The future of computer-aided innovation," *Computers in Industry,* vol. 60, pp. 539-550, 10// 2009.

[15] G. Pahl and W. Beitz, *Konstruktionslehre: Handbuch für Studium und Praxis*: Springer, 1977.

[16] R. Houssin and A. Coulibaly, "An approach to solve contradiction problems for the safety integration in innovative design process," *Computers in Industry,* vol. 62, pp. 398-406, 5// 2011.

[17] A. Jardin, "Contribution à une méthodologie de dimensionnement des systèmes mécatroniques : analyse structurelle et couplage à l'optimisation dynamique," PhD thesis, Institut National des Sciences Appliquées de Lyon, Villeurbanne, 2010.

[18] C. Badufle, "Conceptual aircraft design: towards multiobjective, robust and uncertain optimisation," PhD thesis, UFR Mathématiques, Informatique et Gestion, Université Paul Sabatier - Toulouse III, Toulouse, 2007.

[19] J. L. Kolodner, *Case-based reasoning*: Morgan Kaufmann Publishers, 1993.

[20] E. Zitzler, M. Laumanns, and S. Bleuler, *A tutorial on evolutionary multiobjective optimisation*, 2004.

[21] D. Motte and R. Bjärnemo, "Dealing With The Combinatorial Explosion Of The Morphological Matrix In A “Manual Engineering Design” Context," presented at the ASME IDETC/CIE 2013, Portland, Oregon, USA, 2013.

Article 030-itm-25

Product design-Process selection-Process planning Integration based on Modelling and Simulation

Von Dim Nguyen [1], Patrick Martin [2], Laurent Langlois [2]

(1) : LASMIS Laboratory, University of Technology of Troyes, 12 rue Marie Curie – CS 42060 – 10004 Troyes Cedex, France
Phone:+33325715702
E-mail : von_dim.nguyen1@utt.fr

(2) : LCFC Laboratory, Arts et Métiers ParisTech, 4 rue Augustin Fresnel, Metz Technopole, 57078 Metz Cedex 3, France
Phone:+33387375465
E-mail : {patrick.martin, laurent.langlois}@ensam.eu

Abstract: As a solution for traditional design process having many drawbacks in the manufacturing process, the integration of Product design-Process selection-Process planning is carried out in the early design phase. The technological, economic, and logistic parameters are taken into account simultaneously as well as manufacturing constraints being integrated into the product design. As a consequence, the most feasible alternative with regard to the product's detailed design is extracted satisfying the product's functional requirements. Subsequently, a couple of conceptual process plans are proposed relied on manufacturing processes being preliminarily selected in the conceptual design phase. Virtual manufacturing is employed under CAM software to simulate fabrication process of the potential process plans. Ultimately, the most suitable process plan for fabricating the part is recommended based upon a multi-criteria analysis as a resolution for decision making.

Key words: Modeling, Simulation, Product design, Process selection, Process planning.

1- Introduction

1.1 – Context

In a context where it is necessary to respond industrial challenges towards shorter lead times, lower cost and better customer satisfaction. Concurrent Engineering (CE) was born as a solution to these issues. The solution of the CE is carried out in a manner that the different tasks in the product design and manufacturing process are integrated and performed at the same time rather than in sequence [S1].
In order to do this, it is essential to take into consideration the product's specifications and the constraints of manufacturing process in the design phase. Presently, the design process concentrates on the geometric model built from the choice of architecture to respond to the functional requirements of the product. Traditionally, manufacturing process is determined from the choices which were assigned in the product definition without taking into consideration of manufacturing constraints. So the manufacturing time and cost can be higher than the optimal process plan taking into account of manufacturing process and equipment performances. The CAD models merely represent the information in respect to the product's nominal geometry after that they might not relate to fabrication process or will cause the difficulties in process planning. For resolving these problems, Design for Manufacture (DFM) which allows doing simultaneously (Figure 1) the design and manufacturing process choice activities, was proposed by combining the manufacturing information into the product in the product definition stage [BD1]. In order to implement the integrated engineering of DFM approach (or minimum engagement principle or best least commitment), it is fundamental to formalize and structure the knowledge of manufacturing process capabilities with rules and parameters which allow to select fabrication process and define the intermediary states of the product, and conceptual process planning has to be developed as soon as possible in parallel with the design process. Different process plans can be created. Moreover, concurrent engineering design method starts with a target cost for the product which is compared with the estimated cost of the product.

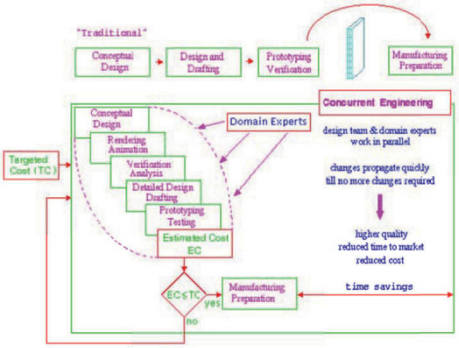

Figure 1: Concurrent Engineering as expressed by Prime European Region [S1].

In the framework of concurrent engineering and DFM, this paper proposes an approach contributing to integrated design and manufacturing process for a typical part including disk

and tube component. This contributes to the development of integrated design tools such as CAD/CAM and CAPP where following constraints are taken into account concurrently:

- Functional constraints: accuracy requirements (perpendicularity and cylindricity…), mechanical behavior, lower weight.
- Geometry: the part can be made with only one manufacturing process or by assembling one disk and one tube.
- Technical constraints: machining, casting, forging, assembly process process capabilities.
- Production constraints: single or a couple of parts.

So several parts design and process plans can be obtain and the choice between them is finally calculated.

1.2 – Issue and objective

Currently, there are several approaches as well as dedicated softwares for selecting manufacturing processes in order to meet the product's technical and geometrical characteristics which have been proposed by scientific community as shown in Table 1.

Approach	Choice of manufacturing processes	Choice of materials	Associated tool	Economical evaluation
Ishii	Yes	No	HyperQ/Process	Yes
Ashby	Yes	Yes	CES	n.a.
Gupta	Yes	Yes	Seer-DFM	Yes
Boothroyd	Yes	Yes	DFMA	Yes
Lovatt	Yes	n.a.	n.a.	Yes

Table1: Comparison of the approaches "manufacturing processes selection" [TS1].

However, these approaches and applications only take into account specifications for finishing the product. In other words, they just support for selection of manufacturing process corresponding to each features' specifications belonging to a product, as well as mechanical products being fabricated by a manufacturing process. On the other hand, in practice, process planning with the sequence of manufacturing processes is necessary to carry out for yielding complex parts. In particular, complicated parts, for instance, the forward steering part of the Shell Eco-marathon (MASH) vehicle presented in Figure 2 owning basic shapes such as disk and tube are considered in this approach.

The main objective of our work is to propose an approach of to the development of CAPP systems in which conceptual process plans are generated relied on conditions of elimination of incompatible manufacturing processes with the product design.

Figure 2: Various proposed design for forward steering part with combination of disk and tube shape [LC1].

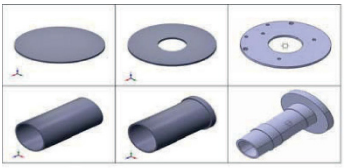

Figure 3: Basic shapes built up the forward steering part

2- Methodology and tool used

2.1 – Methodology

At first from the product's requirements and functional constraints, product's functional models are obtained. Secondly selection of manufacturing processes being compatible with the part's characteristics and requirements is get by using dedicated softwares which formalize manufacturing knowledge .

The major activities of the integrated design process expressed as above are rendered with the IDEF-0 diagram in the Figure 4 [FS1]. Where, the main activities are decomposed four activities (A1-A4).

- A1: Analyze product's functional requirements. DFM actor must take into consideration the product's demands and identify functional surfaces satisfying product's design requirements.
- A2: Model and characterize product's functional surfaces. Modeling functional surfaces under the form of usage skin and usage skeleton is realized by CAD tools. Features' attributes are represented by UML classes. Product's alternatives solutions are created as the output of this activity.
- A3: Define manufacturing constraints. This activity proposes manufacturing constraints such as tolerance interval (IT), surface roughness (Ra) being oriented according to fabrication method. As a result, these manufacturing constraints will be as the constraints to select manufacturing process.
- A4: Select processes and identify manufacturing plans and their constraints. This activity figures out selected manufacturing processes based on the identified constraints. Corresponding to each constraint, processes which are not eligible are eliminated by applying specialized software. As a consequence, a list of fabrication processes is proposed as well as attribute values of manufacturing interface model are integrated to product design.

Obviously, the integrated design is no longer sequential method; instead of that it is iterative method as synthesis loop. In other words, the information exchanges in relation to the product's properties and manufacturing knowledge are realized between designers, process planners and manufacturing engineers as well.

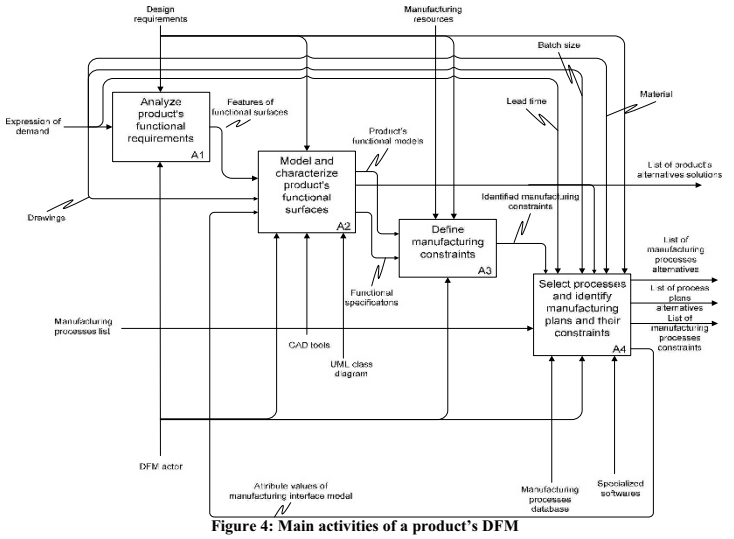

Figure 4: Main activities of a product's DFM

With the recommended fabrication processes, conceptual process planning is used in order to propose the alternatives of the part process plans. Subsequently, the proposed process plans are deducted from the production demands including lead-time, batch-size, economic criteria and so forth.
As a result, the potential process plans after deduction are simulated by using the CATIA and DELMIA software so as to identify manufacturing time as well as foresee problems being able to occur in manufacturing process. From the simulated results, manufacturing cost estimation is considered applied the ABC (Activity Based Costing) and CE (Cost Entity) methods. Finally, in order to support for decision making of the potential process plans in selection of the most suitable plan for fabricating the part, the AHP (Analytic Hierarchy Process) method is used.

2.1 – Tool used

In order to carry out the proposed methodology, several tools are essential to use as follows:

- Modeling languages are used including IDEF0 functional modeling for modeling the product design activities and UML language for modeling the product's features in which its attributes are presented. Flowchart diagram provided by MS Visio is also used to create conceptual process plans. CES EduPack 2010 and Custompartnet.com software are used for selecting manufacturing processes [AM1].
- Finite Element Method (FEM) is served for analyzing the behavior of the part.
- Online integrated cutting data module of Sandvik firm is used in choosing cutting conditions corresponding types of cutting tools.
- CATIA and DELMIA softwares are applied for modeling the product's models as well as simulating manufacturing process. The DPM module of DELMIA is used for defining digital processes and manufacturing resources.
- The ABC (Activity Based Costing) and Cost Entity methods are applied for manufacturing cost estimation [PD1]. Calculations are executed by MS Excel.
- Analytic Hierarchy Process (AHP) method is used for making a decision of multiple criteria.

3- Case study

The case study is a forward steering part, one of the components of the forward direction system of the Shell Eco-marathon (MASH) vehicle as presented in Figure 5. The part must satisfy constraints related to two cylindrical surfaces for wearing the bearings, three holes for fixing the part on the insert and four holes for fixing the stops on the pivot de direction.

It is necessary to take into consideration the weight constraint of the part. Indeed, the principal challenge which needs to be satisfied is that the vehicle travels the furthest on the least amount of energy.

ure 5: Forward steering part [LC1].

3.1 – Analysis and part modelling

A featured-based model is applied in this case study for process planning where operations of various types are directly assigned to specific features without considering their interaction. Starting from the part's functional requirements, each design feature is assigned a potential manufacturing process. The specifications of the part are built on the basis of constraints, resources and manufacturing process capabilities.

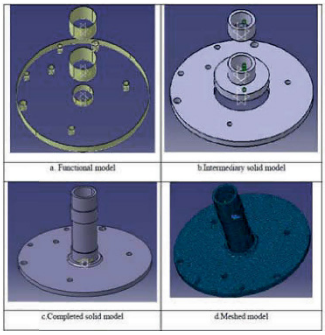

Figure 6: The forward steering part's design models

Based on the part's functional and technical requirements, as well as its constraints with the other components in the system, modeling the part from initial entities relied on its functions to solid models is carried out under CATIA V5 software. More specifically, the functional model on Figure 6.a is generated under the inital entities in which surfaces are modeled from functional analysis including the surfaces for mounting bearings and hole surfaces for fitting bolts. From this functional model, several manufacturing processes are selected preliminarily envisaged for fabricating the part. In order to describe the topological entities, solids are added to show clearly the part's geometrical shapes as shown on Figure 6.b. These components are solely restricted the functional constraints, but they are not mounted together. The part's completely geometric model created by connecting the functional solids is rendered as on Figure 6.c. This model expresses fully functional requirements of the part and serves as a starting point for process planning.

3.2 – Process selection

As mentioned in previous section, process selection is realized as soon as the part's functional surfaces are built under the initial entities. In order to support for preliminary selection of manufacturing processes, CES EduPack 2010 software and Custompartnet.com website are applied in which manufacturing knowledge is formalized. Exploitation of the two informatics applications is employed based upon the part's specifications in which specific values of tolerance, roughness, shape and type of material are entered as the input parameters. As a result, a couple of manufacturing processes are recommended as processes for finishing the part's functional surfaces satisfying the technical requirements.

In particular, the specifications of the functional surfaces are used as the input parameters for selecting manufacturing processes via dedicated software. For CES EduPack 2010 software, tolerance range fitting, roughness and part shape are directly entered as input data to get recommended processes. The input data and results are as shown respectively in Table 2.

Function	Input parameters	Output parameters
Surfaces for mounting bearings	**Shape:** Circular prismatic **Tolerance:** 0.013 mm **Roughness:** 3.2	Electric Discharge Wire Cutting Planning/Shaping/Slotting
Surfaces for mounting bolts	**Shape:** Circular prismatic **Tolerance:** 0.058 mm **Roughness:** 6.3	Drilling Milling Planning/Shaping/Slotting Pressing and Sintering Turning/Boring/Parting

Table 2: The input data and results from dedicated software

It can be seen that , few eligible manufacturing processes are proposed for manufacture each functional surfaces of the part. Consequently, a couple of part designs are generated. Particularly, one of the detailed designs is recommended with the input parameters for process planning being shown in Table 3.

The part's information	
Shape group	Disk shape with unilateral element - No.213 (ASM Handbook Classification)
Material	Alloy Steel: 4140 (AISI/SAE)
Roughness	Ra 3.2, Ra 6.3
Tolerance	IT10, IT6 (ISO)
Max wall thickness	7 mm
Batch-size	20,000 parts per year

Table 3: The information of the part

3.3 – Process planning

Generation of process plan is mainly based upon expert system as well as process planner's knowledge and exper actice, it also depends on resource of a

workshop where is intended to manufacture the part. The conceptual process planning would be done with DELMIA; as a result, virtual manufacturing process would be simulated with the purposes of defining manufacturing time and foreseeing unpredictably issues being able to arise during manufacturing process.
In order to facilitate for generating conceptual process plans, it is necessary to give types of conditions in which manufacturing processes are incompatible with the product's technical and production requirements. Four types of the conditions have been defined as follows [TS1]:

- Conditions of elimination relative to the limits of the manufacturing processes,
- Conditions of elimination linked to the uselessness of the manufacturing processes,
- Conditions of elimination according to the knowledge of an expert,
- Conditions of recommandation.

As can be seen from the output's software in manufacturing process selection, the part's functional surfaces are finished by machining processes in which turning and drilling processes are compatible with the part's specifications.

From the product's demands, the authors proposed three potential process plans which are eligible to manufacture the part. Furthermore, these process plans are successful candidates after applying the conditions to eliminate incompatible process plans as well as relying on the expert knowledge. They are visualized on the DELMIA's PPR (Product-Process-Resource) screen.
Subsequently, machining simulation is operated with resources existing in the DELMIA's library such as machines and tools in which cutting conditions are recommended from the online integrated cutting data module of Sandvik firm.

The process plan 2 (Figure 7) is built from band sawing and forging processes for workpiece preparation, and drilling and turning for finishing the part. Where, circular sawing is eliminated due to not satisfying lead-time and workpiece requirements. Moreover, both hot extrusion and cold heading processes are eliminated because of conditions of elimination of lead-time and batch-size. Again, both ECM and wire EDM processes are eliminated due to lead-time requirement. Milling, planning, shaping and slotting are removed due to the condition related to the uselessness of the processes.
Similarly, surface finishing in the process plan 4 is machined with turning and drilling processes. However, the part is separated into two components accounting for cylindrical component and disk component in this case.

Subsequently, the two components are welded together to complete the part. Likewise, conditions of elimination are applied for the p shown on the Figure 8.

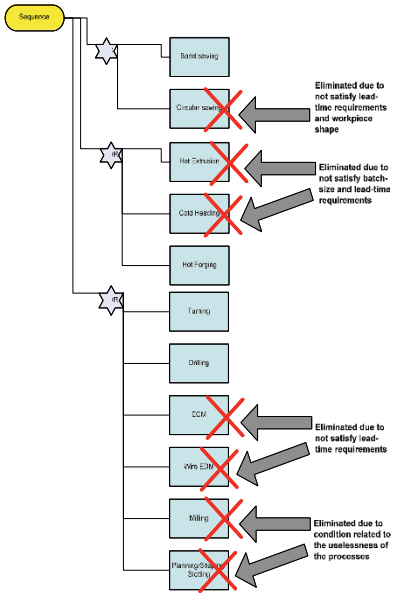

Figure 7: Generating conceptual process plan 2

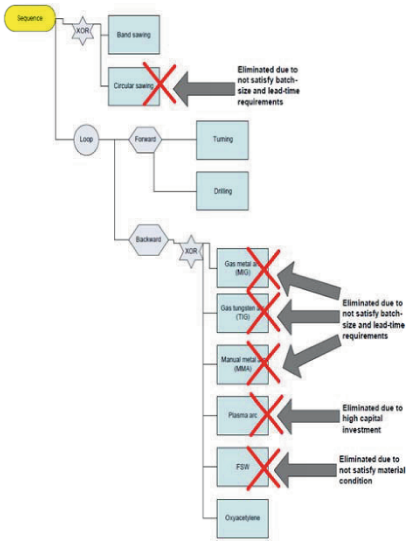

Figure 8: Generating conceptual process plan 4

For process plan 5 (Figure 9), band sawing is applied for cutting the workpiece from stock. Circular sawing is eliminated because of not satisfying lead-time and higher capital investment requirements. Afterwards, the part would be finished by machining process in once fixture.

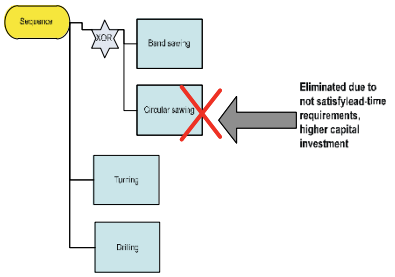

Figure 9: Generating conceptual process plan 5

Conceptual process plan 5 is created with PPR tree under DELMIA served for simulation of virtual manufacturing process.

After simulating manufacturing process according to the three process plans for the forward steering part, manufacturing time is synthesized from the GANTT diagram with the result as shown Table 4.

3.4 – Manufacturing cost estimation

Manufacturing cost is estimated by using ABC method [MD1]. Where, each manufacturing process plan comprises several processes considered as activities. Thereby, the total manufacturing cost of a process plan is calculated in the following formula equation:

$$C_{ma} = \sum_{i=1}^{N} C^{i}_{activity} \qquad (1)$$

In addition to that, each activity is estimated based on the cost entity approach was proposed by H'Mida [HM1].

Particularly, each cost entity is calculated in the following formula [[HM1]: Cost CE = D x $\sum(\alpha_R$ x IR$_r$) (2)

Where,

D: Unique driver chosen for the Cost Entity

α_R : Resource R consumption coefficient

IR$_r$: Resource R imputation rate

As consequences of the calculations of each process plan, the total manufacturing and operations costs are synthesized as in Table 5.

Process	Processing time (min)
Process plan 2	
Sawing process	18.5
Closed die forging process	5.6
Machining process	19.106
Total operation time	43.206
Process plan 4	
Sawing process	23.73
Machining process	39.01
Welding process	8.14
Total operation time	70.88
Process plan 5	
Sawing process	18.5
Machining process	78.18
Total operation time	96.68

Table 4: Synthesis of manufacturing process plans

	Sawing process	Machining process	Forging process	Welding process	Totals
Process plan 2	9.92€	32.07€	178.02€	n/a	220.01€
Process plan 4	15.66€	43.16€	n/a	2.73€	61.54€
Process plan 5	40.87€	53.08€	n/a	n/a	93.94€

Table 5: Estimated manufacturing cost

4- Process plan selection

In order to make a decision regarding the selection of the most suitable process plan, AHP (Analytic Hierarchy Process) method is used with the goal, criteria and alternatives shown in Figure 10 as below.

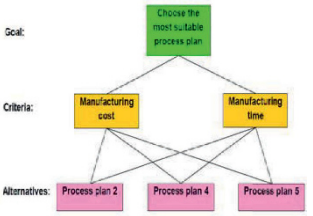

Figure 10: The AHP decision hierarchy for the decision

To support for decision makers, the judgment matrices consisting of weights in respect to manufacturing cost and manufacturing time between process plans as well as priorities of them are given in Table 6.

The judgement matrix with respect to manufacturing time				
Manufacturing time	Process plan 2	Process plan 4	Process plan 5	Priority
Process plan 2	1	1.70	2.30	0.49
Process plan 4	0.60	1.00	1.4	0.30
Process plan 5	0.43	0.71	1	0.21

Table 6: Judgement matrices with respect to the criteria

Note that pairwise comparisons are assigned the weights relied on the calculated results from the estimation of manufacturing time and manufacturing cost corresponding to the proposed process plans.
It is crucial for decision makers to evaluate the criteria with respect to their importance in reaching the goal through the matrix of comparison in Table 7 as below.

Criteria	Manufacturing time	Manufacturing cost	Priority
Manufacturing time	1	0.33	0.25
Manufacturing cost	3.00	1.00	0.75

Table 7: Evaluation of the criteria in reaching the goal

After evaluation and analysis of the priorities between the alternatives, the criteria and the goal, the final score of process alternative groups deduces the synthesized results in Table 8 as follows.

Alternative	Manufacturing cost	Manufacturing time	Goal
Process plan 2	0.11	0.12	0.23
Process plan 4	0.39	0.07	0.46
Process plan 5	0.25	0.05	0.31
Totals	0.75	0.25	1.00

Table 8: The final score of alternatives

Based on the analyzed choice of decision criteria, it can be seen from Figure 11 that the process plan 4 is the most suitable process plan for fabricating the Pivot de Direction with the priority of 0.46, is higher than the others.

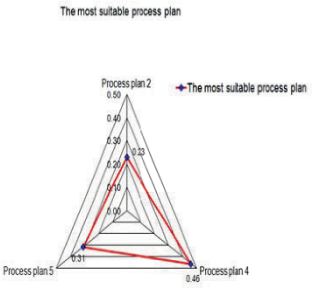

Figure 11: The best choice for manufacturing the part

5- Conclusion

The works of this paper carried out are to tackle the issue in terms of the integration of the product detailed design and the conceptual process plan in the early design stage by using numerical modeling and simulation. As a result, the most feasible process plan is extracted for the case study of the forward steering part. The advantages which get from this approach consisting of that we can foresee the problems arising in manufacturing early and correct the design as soon as possible. Consequently, lead-time as well as the product's cost is decreased significantly. Furthermore, this approach contributes to collaborative design in which product design and its manufacturing process information supporting for integrated design tools such as CAD/CAM and CAPP.

Nevertheless, a couple of issues are necessary to be taken account in the future works. In the framework of this project, the QFD (Quality Function Deployment) technique has not used to assess the process quality as well as FMEA analysis has not carried out to assess failure modes and estimate failure cost [HS1]. Due to the fact that the defect rate is considered as zero percent and the project has only considered the manufacturing time and cost of the conceptual process plans. Moreover, it will be interesting to simulate several assembly processes by taking into account of the thermo- mechanical behavior which introduces geometrical constraints for designing the part.

6- References

[AM1] M.F. Ashby, F. Michael Materials selection in mechanical design, Butterworth-Heinemann publishers, Oxford ISBN: 9780750643573 (0750643579), 2004

[BD1] G. Boothroyd, P. Dewhurst, W. Knight, "Product Design for Manufacture and Assembly", Marcel Dekker, ISBN 0-8247-9176-2, 1994

[FS1] S., C. Feng, E. Y. Song, "A Manufacturing Process Information Model for Design and Process Planning Integration", Journal of Manufacturing Systems, Vol. 22/No. 1, 2003

[HS1] A. Hassan, A. Siadat, J.-Y. Dantan, P. Martin, "Conceptual process planning – an improvement approach using QFD, FMEA, and ABC methods", Robotics and Computer-Integrated Manufacturing, N°26: 392-401, 2010

[HM1] F. H'mida, P. Martin, F. Vernadat, "Cost estimation in mechanical production: The Cost Entity approach applied to integrated product engineering", International Journal Production Economics 103: 17-35, 2006

[LC1] L. Langlois; J.B. Croué,; A. Delamezière,; P. Martin; S. Zimmer. Reconception de produit en intégrant les contraintes et les potentialités d'un procédé innovant : le FSW, 13e colloque national AIP PRIMECA, 28-30 March, Le Mont-Dore, France,2012

[MD1] P. Martin, J.-Y. Dantan, A. Siadat, Cost estimation and Conceptual Process Planning, Digital Enterprise Technology, Springer Information Systems, ISBN 978-0-387-49863-8, , 243-250, 2007

[S1] Sohlenius G. Concurrent Engineering .Annals of the CIRP 1992; 41:645-655.

[SR1] A. Skander, L. Roucoules, J.-S. Klein Meyer, Design and Manufacturing interface modeling for manufacturing process selection and knowledge synthesis in design, International Journal Advanced Manufacturing Technology 37:443-454, Springer-Verlag,2008

[TS1] A. Thibault, A. Siadat, M. Sadeghi, R.Bigot, P. Martin,"Knowledge formalization for product-process integration applied to forging domain". International Journal Advanced Manufacturing Technology, 44:1116-1132, Sprin

2

Behavioural Modelling for Design

Major topics of the full argumentations are the following:

X. Fischer et al. (eds.), *Research in Interactive Design (Vol. 4)*
DOI 10.1007/978-3-319-26121-8_12

Article 010-vp-7

Parametric virtual concept design of heavy machinery: a case study application

Alberto Vergnano, Marcello Pellicciari, Giovanni Berselli

University of Modena and Reggio Emilia – Engineering Department "Enzo Ferrari"
Via Vignolese 905/B – 41125 Modena – Italy
Phone: +39 0592056278 / Fax: +39 0592056126
E-mail: {alberto.vergnano, marcello.pellicciari, giovanni.berselli}@unimore.it

Abstract: Virtual prototyping enables the validation and optimization of machinery equivalent to physical testing, saving time and costs in the product development, especially in case of heavy machines with complex motions. However, virtual prototyping is usually deployed only at the end of the design process, when product architecture is already developed. The present paper discusses the introduction of virtual prototypes since conceptual design stage as Virtual Concepts in which coarse models of machinery design variants are simulated obtaining useful information, sometimes fundamental to support best design choices. Virtual Concept modeling and preliminary validation and its later integration to a Virtual Prototype are expressly investigated using Multi Body Dynamics software. A verification case study on a large vibrating screen demonstrates that dynamic Virtual Concepts enable easier and effective evaluations on the design variants and increase the design process predictability.

Key words: Virtual Prototype, Virtual Concept, design process, CAD based simulation, vibrating screen.

1- Introduction

A design process must develop technically successful and profitable products, identifying since early stages the best product architecture. The design solutions must be defined, that is forecasting the actual performances before manufacturing any single part. Then, sooner or later, the parameters tuning and the performances verification require one or more prototypes.
Important research efforts are focused to develop methods and technologies for setting up Virtual Prototypes (VPs), to identify and solve design flaws before physical testing. First a 3D CAD model is generated, enabling then to simulate the prototype behaviors with Computer Aided Engineering (CAE) software, **[AL1]**. As for mechanical engineering, Multi Body Dynamics (MBD) enables very effective evaluations of the machine evolutions in time. Since VPs must enable testing and data gathering similarly to physical prototypes, a deeper modeling of the machine behaviors requires the integration of different modeling techniques and simulation tools. Multiphysics combines the VP with other numerical models, as e.g. heat transport and thermal stresses, electromechanical or fluid structure interaction, chemical reactions, and process physics, **[AG]**, **[BS]**, **[D]**. Finally, different simulation models can be synchronized to run in parallel including also the control system, **[AL2]**, **[PB2]**.
Literature reports many applications where virtual prototyping enables a very deep analysis of the design performances, **[HL]**, **[GR]**, however the main drawback is still the modeling long time effort. Besides, modeling can start only after the machine layout is defined, especially in case the accurate CAD models are required, severely delaying the investigation on different design alternatives, which is assumed as based on the designer experience in the conceptual design stage and barely aided by numerical models. This method can be quite questionable since conceptual design has a decisive influence on the overall system. Many behaviors result from multiple interactions between the machine elements, difficult or impossible to evaluate by simple formulas, and better and maybe more economic but unconventional solutions are limited by the conventions stored in the design office. Possible design contradictions would be noticed much later during development, when adjustments are difficult to handle. So an engineering method to link design specifications and solutions in the early development stages would drastically improve the overall efficiency of the development process, **[RB]**.
Since virtual prototyping and simulations allow saving times and costs by early errors identification on a digital model of the future product, we propose the integrated adoption of VPs as Virtual Concepts (VCs) in the conceptual design stage, to identify the best product architecture. Assuming a Top-Down design methodology, **[PB1]**, the feasibility of many different design alternatives is quickly evaluated on VCs, before key decisions are made. Since many working principles of heavy machinery are achieved through mechanisms with complex motions, in the present work the VCs are set up as MBD models. The other problems, such as fluid dynamics, heat transfer and interaction with electric motors actuation, are considered important but side

phenomena, thus studied in depth in the next embodiment phase which follows the conceptual one. However, the VCs methodology will be still valid even if it can be extended for specific application with other physics models. The VCs are here coarse models fast set up with just the necessary basic features. Very important is the integration of MBD modeling within the CAD software, to evaluate dynamic geometries and not just mockups, to reuse the parameters automatically created with the CAD models and to keep a system perspective accounting for trajectories, envelopes and collisions. The evaluations extensively look for innovations and reject the unsuitable concepts. Furthermore, the main design parameters are automatically tuned, reducing the risk of not recognizing bad design flaws.
The paper is organized as follows: Section 2 argues the main parameters collection for the VCs set up, then the reuse and refinement of the models from the selected VC to prototype is described in Section 3, a case study on a vibrating screen for inert materials is reported and discussed in Section 4, followed by the conclusions of the paper.

2- Virtual Concept modeling

The Top-Down design approach breaks down the design specifications into essential problems through abstraction. The problems must then be solved by working principles, combined into a working structure. The synthesis of the working principles behaviors delivers the system performances. Since the effects of the behaviors integration cannot be trivially assessed, each integration structure is roughly analyzed by a VC. In order to time effectively assess the different design variants, the modeling must be simplified, including all but only the basic features necessary for its quick set up, and possibly exploiting the tools yet available into the design office. The use of a CAD software can then be advanced in the conceptual design stage to reuse its modeling capabilities for part geometry and assembly kinematics, while a MBD add-in is the necessary extension for evaluating dynamics. Preliminary virtual experiments assess then the advantages and limitations of the concept variants, passing to the sequent virtual prototyping the best candidate(s) only.

Mating interfaces: in [W1] the motions in an assembly are limited by mates and contacts. A mate surface generates a condition of geometric compatibility, eliminating one or more Degrees-Of-Freedom (DOF). Contact surfaces are more hyperstatic connections with stresses and strains which make stable a positioning. VC foundation should rely on mates, which determine the degrees of freedom of the assembly, thus the allowed motions, delivering the key characteristics. On the contrary, the contacts mean static indeterminacy, too complex to model at VC stage. A schematic modeling of the mates is sufficient to numerically fast define how the parts kinematically interact together.

3D dynamic parameters: 3D CAD software automatically computes the mass properties of a part or assembly, as volume, mass, center of gravity, principal axes of inertia and inertia matrices, which are difficult to calculate otherwise. A MBD tool embedded in a CAD software then natively reuses such parameters, that, even if coarse, are useful to identify the strengths and weaknesses of the design solution. First attempt primitive geometries are very often sufficient to represent the dynamic parameters. The material density information is essential for the VC, since it determines some design main parameters, and the material class must be here advanced. The exact chemical composition can wait for sequent design stages.

Working principle(s): a VC should describe the basic working principle. Gravity, functional contacts and lumped features, as actuators, ideal springs, forces and dampers may complete the model. Of course only simplified parameters are necessary and sufficient to represent a behavior. The top problem should be broken down to individual elements to be separately analyzed. In this stage, already known design solutions can be grouped in big chunks and modeled as black boxes, just to pass variables to the other elements. Other phenomena can be introduced as logical or numerical functions, or as splines interpolating external data stored in lookup tables.

Subsystem critical resource budget: the different working principles, synthesized to deliver the system performances, may have to share one or more critical resources with limited availability in the system. It can be the case of mass, stiffness, allowable error or other important side effects and costs-determining parameters. Following the same Top-Down design approach, the goal is to simplify the main design problem by allocating the system resources onto the subsystems. Specific information must complement the model, thus creating rules on the aforementioned 3D CAD parameters or including annotations or even external documents into the CAD feature tree. Not only the parameters values are important but also their distribution, because they are nonlinearly combined into the overall model. The critical resource budget is to be updated during the conceptual design stage and the budget shares have to be satisfied by the subsystems, but the sharing can be reconsidered in case of criticalities. That way, the design more safely achieves the overall performances while, at the same time, saves time and cost for not trying to uselessly save resource usage.

Simplified CAD envelope: a CAD envelope identifies collisions and arranges the subsystems in layout. The allowable envelope for a subsystem can be viewed as another subsystem critical resource share. However, it is separately discussed because it is an important resource and always necessary and it is an obvious visualization of the VC into a CAD based tool.

3- From Virtual Concept to Virtual Prototype

The VP of a machine should reuse the VCs features. The subsystems comply with the main parameters from the previous conceptual design stage even during embodiment and detail design stages. The given critical resource share and the allowable CAD envelope are restrictions for the design and must never be exceeded. Just little refinements are allowed and the conceptual stage can be gone over again with bigger modifications only if an important review

demand arises.
The VP include then the necessary features for a deeper evaluation, as contacts, detailed CAD geometries, more refined working principles, now also with secondary effects and errors models.

Mates and contacts: the mates are now designed as durable and practically manufacturable ones for strength and geometric compatibility. The assembly process must be advanced and eventually reviewed to result in subsystems with robust behaviors. Mates are then fixed by the contacts. Exact contact forces and deformation have also to be included in the model.

Detailed CAD model: the CAD model is now refined with detailed geometries, toward the definitive ones for the definition of the technical drawings. The conceptual design stage followed a Top-Down method but virtual prototyping must now receive Bottom-Up solutions to the problems also. In fact economic feasibility requires reusing commercial or existing solutions. These solutions usually allow only minor modifications and their CAD models are already available, so they act as new constraints for the custom solutions.

Finely dimensioned working principle(s): the working principle must now include the parameters as detailed as possible, compatibly with the time schedule and with the necessary accuracy of the virtual model with the physical. The lumped parameters can be distributed, and the rigid bodies are integrated with compliances and stiffness. Other than the main effects, also the secondary are here included in the model.

Errors models: errors are a special class of behavioral models which address particular scenarios. In fact position actuators can introduce errors to account for non-nominal scenarios and transitions between them. It is the case of thermal effects or other operation induced deformations.

4- Case study on a vibrating screen for inert materials

This section reports about the setting up of the VCs and the sequent virtual prototyping of a heavy machine which undergoes to very rough working conditions. A vibrating screen is a mechanical sieve used in the selection of quarry and mining inert materials and crushed aggregates by their mean dimensions. The virtual models were defined within SolidWorks CAD and the integrated Motion tools.

4.1 – Virtual Concepts for the vibrating screen

The analysis on the existing solutions reveals that the screen has to vibrate along two directions. The vertical movements separate the materials from the screen, loosing contact and enabling front discharge or downfall. The horizontal movements in the flow direction are necessary to advance and discharge the materials. The third direction is to be avoided for simplicity sake, other than for it is useless. Two different working structures are then evaluated as best candidates. They adopt similar working principles, as shown in Fig.1a and Fig.1b. The whole screen structure is moved by synchronous centrifugal forces originated from the eccentric

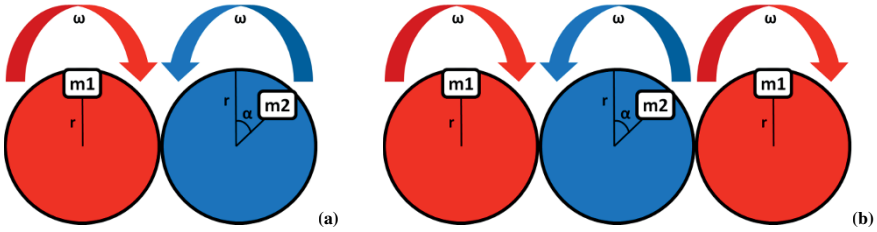

Figure 1: Schematic of two working principles with two (a) or three (b) counter-rotating flywheels.

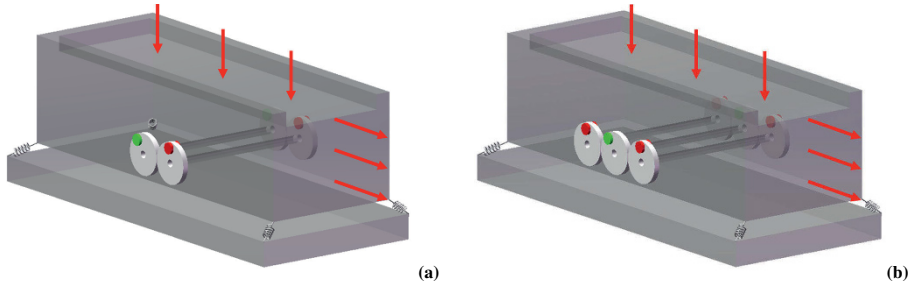

Figure 2: VCs of the two working structures with the principles with two (a) or three (b) counter-rotating flywheels.

masses of two or three counter-rotating flywheels. The basic parameters are the eccentric masses m1 and m2, the radius r, the angular velocity ω and the phase angle α, but the ways how they combine each other and with the other working principles in the working structures in the two cases are not easy to evaluate. Then, Fig.2a and Fig.2b show the respective VCs. The arrows just clarify the material charging and discharging directions. Screen dimensions and suspension springs are other working principles, interacting with the vibration sources principles.

The simulations of the VCs reveal that in both cases the magnitude of the vertical (z) and horizontal (x) displacements can be adjusted as required just by changing m1 and m2, with constant α, as in Fig.3a and Fig.3b. Of course, similar effects result from changing the radial positioning of the eccentric masses. Then, fixed the masses, the axes of the elliptic trajectory, then its inclination, can be set at any value, as in Fig.4a and Fig.4b, by increasing the phase α between m1 and m2 angular positions. This would be a not critical assembly specification, and the machine can be easily adjusted for different material physics. Finally, the concept with two flywheels was rejected because its centrifugal forces generate a resultant moment by the center of gravity, as shown in Fig.5 for the cases of changing the masses aa) or the phase ab). The screen pitching is undesirable, because it adds behavior complications hard to correct in the sequent design stages. The moment for the other concept is not shown because it is always, theoretically, null.

4.2 – Virtual Prototype of the vibrating screen

In the next design stages the best candidate VC is detailed with more refined suspension models. Yet existing commercial suspensions are reused, but here analyzed and

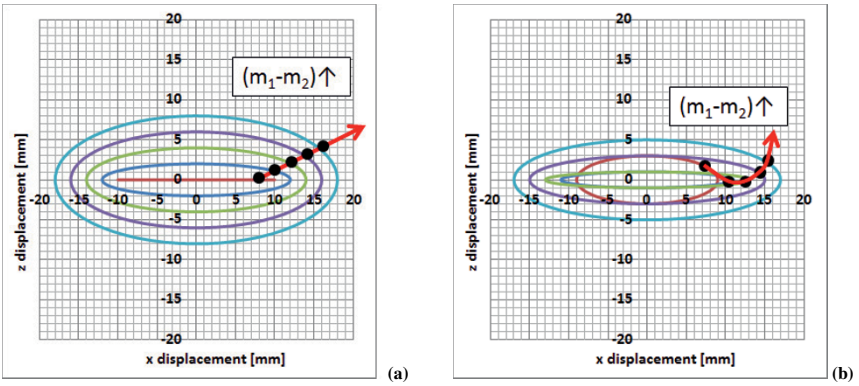

Figure 3: x and z displacements for the two (a) or three (b) flywheels VCs when changing the masses.

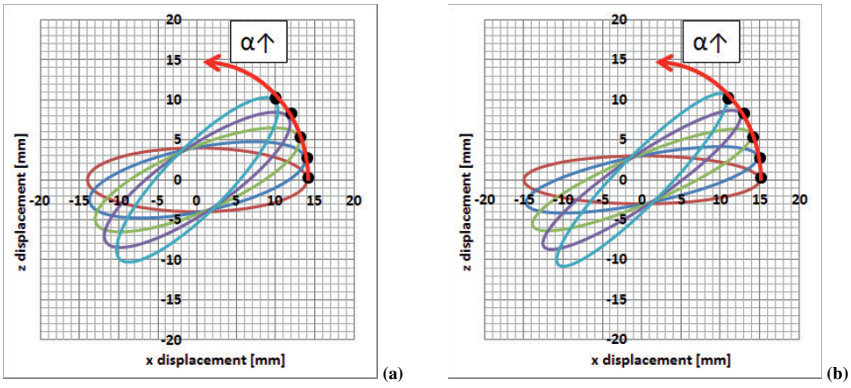

Figure 4: x and z displacements for the two (a) or three (b) flywheels VCs when changing the angle phase

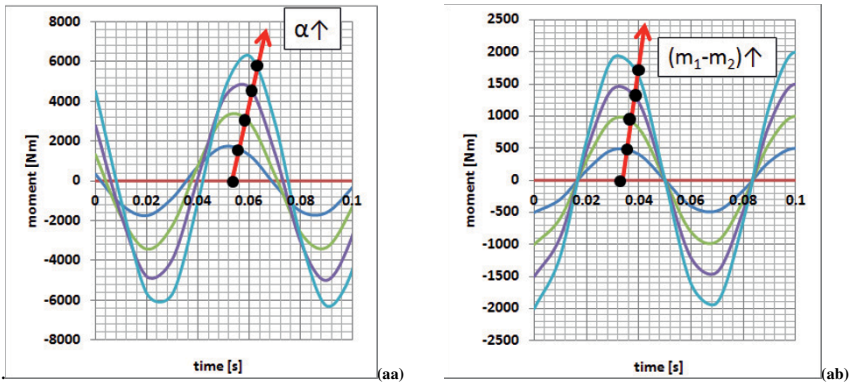

(aa) (ab)

Figure 5: Resultant moment by the center of gravity for the two flywheels VC when changing the masses aa) or the angle phase ab).

simulated one by one by lumped mass, 3D stiffness, damping and initial forces. The transmission shafts are refined with 3D rotational springs to account for the overall deformation for torsional and bending moments.

Translational actuators simulate then the deformations due to differential temperatures by commanding the resulting displacements. These errors are serious for gear teeth engagement, so two refined prototypes are set up. The first prototype uses one gearing and three long shafts to synchronize the wheels, as shown in Fig.6a, while the second has two different gearings synchronized by just one shaft, as in Fig.6b. The second is a little bit more costly, but was finally selected because it results in a much more robust and reliable behavior.

The final evaluations include also the material sieving to adjust the aforementioned masses and phase and to validate the overall behavior. The final resulting trajectories are reported in Fig.7a in case of dry run, easily comparable with the displacements of Fig.7b for the case of material flow. The trajectories of the VP show the same order of magnitude and direction previously obtained by tuning the masses and the phases in the VC, as from Fig.3 and Fig.4. The differences come up from the effects not accounted for in the VC but only in the VP, such as the just mentioned machine interaction with the material flow and the part deformation for torsional and bending moments, forces and differential temperatures effects.

The benefits in introducing the VCs in Sec.4.1 are not easily numerically analyzable. However, the apparently chaotic last charts of Fig.7 give a clear idea of how it would be complicated to absolutely compare the performances of VPs with different architectures, as in the previous Fig.4, without recurring to their simplified VCs. Following the Top-Down design approach, the virtual prototyping analyses are then used to detail the final CAD models, shown in Fig.8.

5- Conclusions

The present paper discusses about the VC modeling for the design of heavy machinery. The VCs should include the main working parameters and boundary conditions in coarse models, saving time and efforts by avoiding detailing the side effects, working errors and noises. The overall performances integration is then evaluated to define one (or few) layout(s) to be passed to the sequent virtual prototyping stage. Here more refined models are included for a much deeper

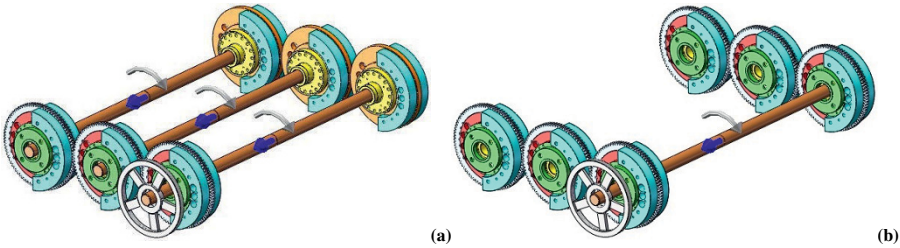

(a) (b)

Figure 6: VPs of the vibrating system with the flywheels synchronized by three a) or one b) shafts.

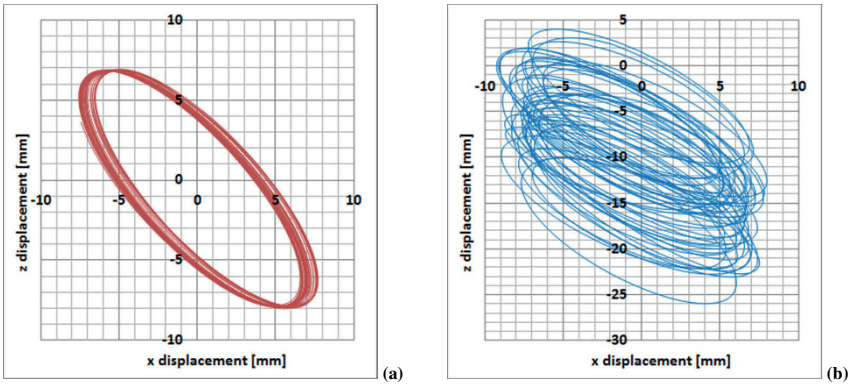

Figure 7: Refined trajectories of the VPs for a dry run a) or in case of material flow b).

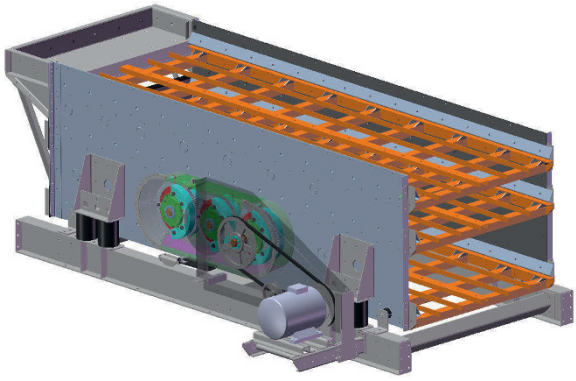

Figure 8: Final model of the vibrating screen.

evaluation. The goal of the VC is to quickly evaluate the different design alternatives to identify the best machine architecture, while the VPs are used to reproduce the actual behavior as deeply as possible. Since many working principles of heavy machinery are achieved with mechanisms motions the integration of the MBD tool within the CAD modeling software is very important to step by step add details to the dynamics model of the VCs, while preserving the possibility to simulate and analyze the results in the whole system.

The first evaluation by simulation opens the way for innovation possibilities by analyzing many different working structure alternatives, without taking it just upon the designer expertise. The VCs simulation is a design method and not just a verification test bench. The main parameters can be optimized with adjustments resulting from the simulation results, and not from trial and error loop steps. Then the virtual prototyping is conveyed and restricted by the passed set of main parameters to reduce the complexity of the great number of variables. The VP also advances some design verifications that were traditionally carried out on real prototypes.

The case study on a vibrating screen for inert materials verified the VC ideas in really designing a machine which undergoes to complex working conditions. The simulations of the VCs showed that the parameters interactions can be noticeably evaluated and tuned, quickly rejecting possible design weaknesses. Then the dynamic VP is less biases prone and can focus on the loads on every part for the dimensioning, fine tuning and verification.

Future works may include more detailed models for the load distribution on the parts, for their deformations and for the material flow for a refined dimensioning and simplification of the machine elements focusing on their durability.

6- References

[AG] Andrisano A.O., Gherardini F., Leali F., Pellicciari M., Vergnano A. Design Of Simulation Experiments method for Injection Molding process optimization. In International conference on Innovative Methods in Product Design IMProVe, Venice - Italy, 2011.

[AL1] Andrisano A.O., Leali F., Pellicciari M., Pini F., Vergnano A. Hybrid Reconfigurable System design and optimization through virtual prototyping and digital manufacturing tools. In. Journal on Interactive Design and Manufacturing, 6(1): 17-27, 2012.

[AL2] Andrisano A.O., Leali F., Pellicciari M., Vergnano A. Engineering Method for Adaptive Manufacturing System Design. International Journal on Interactive Design and Manufacturing, 3(2): 81-91, 2009.

[BS] Ben Haj Ali A., Soulaimani, A. Combined Functional and Geometrical Decompositions for Multiphysics Problems with Application to Fluid-Structure Interaction. In 22nd International Symposium on High Performance Computing Systems and Applications, HPCS 2008, Quebec City - Canada.

[D] Dede, E.M. Multiphysics optimization, synthesis, and application of jet impingement target surfaces. 12th IEEE Intersociety Conference on Thermal and Thermomechanical Phenomena in Electronic Systems (ITherm). Las Vegas – NV - USA.

[GR] Goldstein Y., Robinet P., Kartsounis G.A., Kartsouni F.F., Lentziou Z., Georgiou H., Rupp M. Virtual Prototyping: From Concept to 3D Design and Prototyping in Hours. In Transforming Clothing Production into a Demand-driven, Knowledge-based, High-tech Industry: 95-139, 2009.

[HL] Hervé Y., Legendre A. Functional Virtual Prototyping for Heterogeneous Systems. Design Technology for Heterogeneous Embedded Systems: 223-253, 2012.

[PB1] Pahl G., Beitz W., Feldhusen J., Grote K.H. Engineering Design: A Systematic Approach. Springer-Verlag, 3rd ed., 2007.

[PB2] Pellicciari M., Berselli G., Ori M., Leali F. The role of co-simulation in the integrated design of high-dynamics servomechanisms: an experimental evaluation. Applied Mechanics and Materials, Vol. 278-280, pp.1758-1764, 2012.

[RB] Rudtsch V., Bauer F., Gausemeier J. Approach for the Conceptual Design Validation of Production Systems using Automated Simulation-Model Generation. Conference on Systems Engineering Research (CSER -13), Atlanta, GA, USA, Procedia Computer Science, 16, pp.69-78, 2013.

[W1] Whitney D.E. Mechanical Assemblies: Their Design, Manufacture, and Role in Product Development. Oxford Univ Pr (Sd), 2004.

Article 081-cadcae-28

The mechanical link between foot and ski and the skis behavior in a model of skating

Rey F. [1], Ferrand A. [2]

INSA, UPS, Mines Albi, ISAE, ICA (Institut Clément Ader), Université de Toulouse, 135 Avenue de Rangueil, 31077 Toulouse, France
(1) : phone 33561559388/ Fax 33561559700 rey@insa-toulouse.fr
(2) : phone 33561559698/Fax 33561559700 ferrand@insa-toulouse.fr

Abstract: Skating technique arose from both the association of a motion and development of the equipment. The specific technique studied in this paper is the "offset". To give an account about the complexity of this motion and to be able to analyse it in a mechanical way, our aim was to build a three-dimensional dynamic model. We used the software LifeModeler, to calculate kinematic and dynamic parameters from a human body model like an anthropomorphic robot.
In the aim to validate the model in its environment, we analysed kinematics by comparing it with other scientific data. We worked on the contact parameters so as to simulate the snow effect. This study enables us to show the method for building a 3D model applied to the skier gliding. It's an approach to modelling the links between the foot, the binding, the ski and the snow in the aim to understand the skis behavior and particularly to evaluate the edging angles that are significant parameters of this gesture.

Key words: Modelling; skating; edging; skis behavior.

1- Introduction

In skating techniques, skis orientation changes throughout the cycle, so it is difficult to obtain the force components which act on them. The forces' measurements in cross-country skiing are more intricate because of skis behavior and of the consistency of the snow surface. Our approach is to realize a dynamic analysis of the motion by inverse and forward dynamic simulation with the aim to understand the skis behavior on the snow. We present the modelling method used to create the skating contact area the most realistic possible. The skis' orientations during a complete cycle are calculated.
We use the commercial software LifeModeler, a plug-in of Adams software, to investigate the interactions of a human body with equipment and environment. In this study, the skier uses skating offset technique, also called V1 skating. This technique is used on an uphill terrain when there is a great difference in performance between skiers during races. It makes possible to maintain velocity and even to accelerate. Offset technique is a non-symmetrical stride with asynchronous ski pole plant: Figure 1. This figure shows an offset technique cycle on an uphill terrain (6°). The body is simulated with bones, joints and muscles.

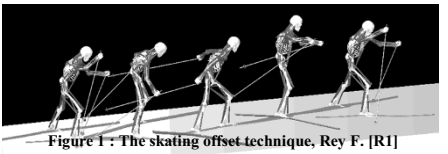

Figure 1 : The skating offset technique, Rey F. [R1]

In a recent past, we have made a human body model with correct motion and we have obtained some convincing results [RC1]. We thus have continued in this way, by creating an equipped model (Rey 2008 [R1]). This approach allowed us to insert the equipment, ski poles and skis into the model. Our work was focused on 3D dynamic simulation and its validation. We have studied a one-cycle skier's movement. We explained the steps of the modelling and we analysed the offset technique from the mechanical and biomechanical point of view thanks to a human model simulation which integrated the behavioral typology of skier, environment, equipment and snow. The trajectories of some particular points, duration of cycle phases and contact forces may be measured directly. This model and the contact forces results, give cause for Scientific's articles [**RF2**],[**RF3**].
The other studies that we can find are a combination of video analysis and simulation. They start with the film of a moving competitor and make several representations of the skier: a stick representation (Ruby [**R1**]) and a 3D graphical mannequin (Verriest[**V1**]; Tavernier and Coll[**TB1**]). After mechanics calculi with or without computers, dynamic analyses can exist (Ruby[**R1**], Coulmy [**C1**]). The software does not process the kinematic data into mechanics data; at the present time some laboratories could make that but no study of this gesture was undertaken. The studies of this pattern arise from video analyses in two or three dimensions: Smith [**SM1**], [**SN1**], [**SH1**], Street[**SG1**], Gregory [**GH1**], Ruby [**R1**], Coulmy[**C1**].
Some authors have also made dynamic analysis with equipment carried by a competitor: Smith [**SN1**], or by sensor platform under snow, Komi [K**1**].

Article 081-cadcae-28

However, these models include rarely the skier's inertial properties and do not calculate contact forces, muscular efforts or energy expenditure of the body parts. In this paper, our work is focused on the mechanical link between foot and ski and skis' orientations about a skier model. The aim is to achieve a tool that would permit to do performance tests. This tool will include a parameterization of skis orientation and of the link between the ski and shoe. In offset technique, it is possible that the outside edging be more effective than the inside edging during the beginning of contact phase; edging consist in tilting ski to grip snow with ski edge: figure 3. Such a tool would solve this type of questioning about gesture technique.

2- The musculo-skeletal model

2.1 – Introduction

This simulation is done under LifeModeler, plug-in of engineering software Adams. This software can create a human body 3D model like an anthropomorphic robot by an inverse and forward dynamic simulation. Adams, is for mechanical system simulation, we have used it to create equipment and to run its postprocessor tools.
We create a file with anthropometrical data (age, height, weight, gender) and motion. This study is based on Ruby's data [R1], which describes skating techniques. The skier is a 24 years old woman, 166 cm tall and 60 kg weight. LifeModeler's anthropomorphic database automatically creates bones, joints and muscles. For this analysis we use also Ruby's data which were got during a world level competition. By a geodetic method and with three cameras, some measurements give the Cartesian coordinates in 3D of 26 precise points located on the skier and her equipment. This motion data are assigned to the model. [**R1**]. Some "motion agents" are created at locations of motion targets (markers), specified when the body was created (Figure 2). In this software the model is positioned in the initial position of the motion data and a static analysis is carried out (equilibrium analysis: Figure 4). It is performed to minimize distance between marker locations from data source and marker locations on the human model. During inverse dynamic simulation, motion agents are associated with the human model markers in the aim to move according to the prescribed data trajectories and to influence the model through some springs elements. During forward dynamic simulation, with joint motion history and soft tissue elongation, both recorded from the inverse dynamic simulation, it may be used a proportional-derivative controller to produce a torque in the joints and a force in the contractile tissues. Thus, the internal forces like joint torques, muscle forces, but also the external forces like gravity, contacts, etc, drive musculo-skeletal model.

2.2 – Import the environment

The physical environment is defined by any external object which interacts with human model. Adams software is used to build ski poles, "snow block", skis and contacts of skis with snow (Figure 4)

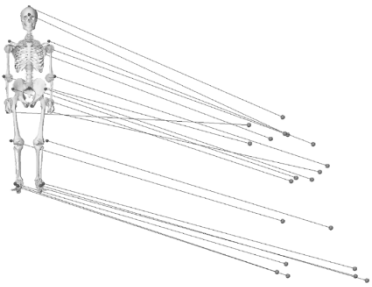

Figure 2 : Location of the motion agents

Figure 3 : Edging for left ski with interior edge; beginning of contact phase for right ski

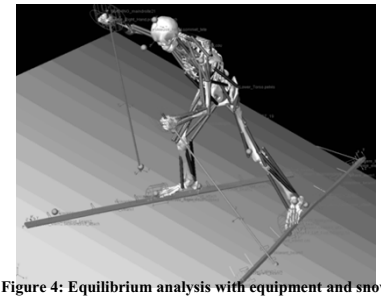

Figure 4: Equilibrium analysis with equipment and snow

Ski pole is imported in LifeModeler, it is placed in the hand. We combine grip marker and hand marker. Integration with the movement requires the use of Ruby's data [R1]. About motion agents which will control ski poles, markers corresponding respectively to left and right baskets were added. The initial orientation of ski poles was obtained while baskets were placed to correspond with motion agents already positioned in space.

Article 081-cadcae-28

Integration of skis is more complex than that of ski poles. Indeed, we can consider that in fact, hands and contact with snow determine ski pole orientation, but ski has a degree of freedom around the rotation axis of binding which is not directly controlled by the foot. The efforts developed in this link are the result of a complex dynamic balance with the effects of the ski inertia and inner technology of the binding (spring, joint stop...).

For modelling the skis, we used the same method as for the ski poles, but this did not give convincing results. Moreover we didn't want to control the skis with trajectory markers given by Ruby [R1] because we wish that the model glides on its skis. The ski must be responsive to the particular characteristics of a skating ski, i.e. be flexible and light. The adopted solution for the modelling is the association of rigid parts and flexible parts. In order to model as accurately as possible the flexibility and damping characteristics of the ski, we use the possibility of Adams software which consists in integrating flexible parts in a structure. Thus, the ski is built with rigid and flexible parts. The spatula, the binding part and the tail are modelled with rigid parts. They are connected each other by flexible links, two intermediate links in the front and two intermediate links in the rear. (Figure 5).

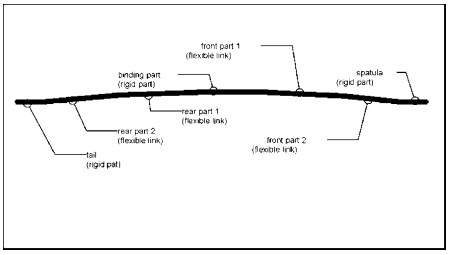

Figure 5 : Ski model

2.3 – Connectors and contact

We created the contacts on the seven portions of the ski sole. A "Solid-Solid" contact is chosen with the "impact" option. The contact force uses the following equation (1):

$$F = k\ x^n + c_t\, dx/dt \qquad (1)$$

Where:
k: stiffness
x: penetration depth
n: penalty coefficient which has been experimentally chosen
C_t: damping coefficient

Thus, before implementation, the skis with their contacts on the ground are already placed; we use Shimbo's data [**S1**] for the parameters.

We tried two mechanical connectors, a pivot and a pivot with a recall spring for modelling the binding in the aim to obtain the more possible realistic behavior, but the results were not satisfactory [**RF3**].

Thus we use a bushing element (figure 6). We can restrict or release the link in some directions, like ankle for example. We place it on the ski.

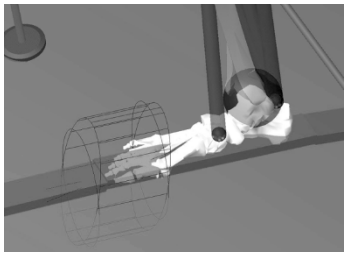

Figure 6 : The right foot bushing

The bushing is a link with six degrees-of-freedom. The displacement along a degree-of-freedom is constrained by using a spring and a dashpot, configured by stiffness and a damping coefficient. Six springs, 3 translational and 3 rotational and six dashpots, were tuned. The values of stiffness and damping coefficients are collected in a 6x6 matrix (Table 1). A force is applied between two markers, which are respectively in front of the binding and in the big toe. This force depends on their relative displacement and velocity.

$1E^4$	0	0	0	0	0
0	$1E^4$	0	0	0	0
0	0	$1E^4$	0	0	0
0	0	0	$1E^3$	0	0
0	0	0	0	$1E^3$	0
0	0	0	0	0	$1E^3$

Translational stiffness | Rotational stiffness

$1E^6$	0	0	0	0	0
0	$1E^6$	0	0	0	0
0	0	$1E^6$	0	0	0
0	0	0	$1E^5$	0	0
0	0	0	0	$1E^5$	0
0	0	0	0	0	$1E^5$

Translational damping coef. | Rotational damping coef.

Table 1: Matrix of bushing

Initially, the bushing coefficient values were chosen in order to respect the motion kinematics. In a second time, we have tuned these values in order to obtain realistic contact forces from the skis in regard to the values reported in Smith [**S1**]. When the bushing's coefficients increase the skis remain close to the snow part. When the values decrease the skis leave the snow part. The model is a bit late in relation to the motion.

In reality, the shoe front axis intrudes into the clamping ring of the front binding (Figure 7). The heel is free to move during the gesture in air phase. In the contact phase (gliding and propulsive phase) (Bilodeau [**BB1**]) longer is the gliding phase, better will be the performance. But the edging is

Article 081-cadcae-28

necessary during the propulsive phase and it's here where the technical difficulty is special for the offset technique. When we observe skiers during contact phase, some of them use the outside edge and others use the inside edge, in order to do not slip on the side. The skating boots are also designed to support the lateral push-off of the stride.

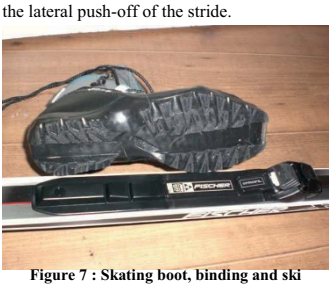

Figure 7 : Skating boot, binding and ski

3- Results

3.1 – Foot busching

After several tests aiming to validate the dynamic model and to stabilize it, we found fitted values for the bushing parameters. The stiffness and damping values are transcribed in table 2, they are the same for the two feet. We can simulate the various ski binding types thanks to the bushing specificity; it restricts sagittal, transverse and frontal orientations.

TRANSLATIONAL MOVEMENT	VALUES		
	X	Y	Z
Stiffness N/mm	10	100	150
Damping N/mm.s	10	15	15

ROTATIONAL MOVEMENT	VALUES		
	X	Y	Z
Stiffness N.mm/rd	1000	1000	100
Damping N.mm/rd/s	100	1000	10

Table 2: Translational and rotational values for the foot bushing

3.2 – Orientations angles of the skis

With ADAMS software we can measure the skis orientation angles.
We create a marker whose the origin is the centre of mass of the ski binding (figure 8) this marker define the reference axes: horizontal axis is Z, side axis is X and the vertical axis is Y. The angles are calculated around these axes. **The edging angle is measured around the Z axis**, the one on X is the antero-posterior orientation.
Figure 9 shows the exact location of the marker at the center of mass of the ski binding with the reference axes. The musculo-skeletal model of the left foot with its connector to the ski is also illustrated.
Thanks to a kinematic and dynamic analysis [RF1], [RC1], [R1], we identify the contact phase, the air phase and the double contact phase of the model in time.
We report them in figure 10, 11 in which there are the 3 angles graphs of the right foot (figure 10) and the left foot (figure 11). The kinematics of the ski can be analyzed.

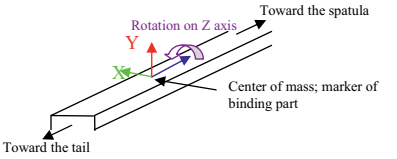

Figure 8: Reference axes for the measure of the ski angles (right ski)

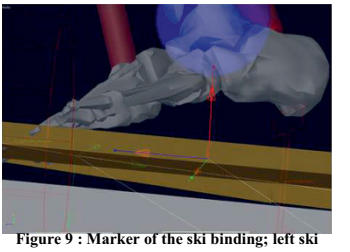

Figure 9 : Marker of the ski binding; left ski

4- Discussion

4.1 – Discussion about skis orientation

The comparison of all curves, shows that the greater angular variation for both skis is around the vertical axis (Y) in the transverse plane, particularly for the left ski where the deflection is about 90° (75° for the right ski). The angles around X, frontal plane, and Z, sagittal plane, for the right ski are about 10°, more than those of the left ski. For the right ski the angle variation around X is about 40° and around Z is about 50°. For the left ski the angle variation around X is about 30° and around Z about 40°.
These differences allow us to identify the weak side and the strong side: Smith [S1]. Coulmy[C1] distinguishes also "a contralateral side" (left side of musculo-skeletal model) and "a side of attack", the right side of this competitor. The left leg motion is characterized by the gliding phase; the ski is as flat as possible on the snow. During the gliding phase the angular variations around Z are minimal for the left ski, there are many small oscillations. Many curves show oscillations due to instabilities.
While, the right leg motion performs edging to grip snow which results in an important pressure transfer on the weak side due to the displacement of the skier's center of gravity.

Article 081-cadcae-28

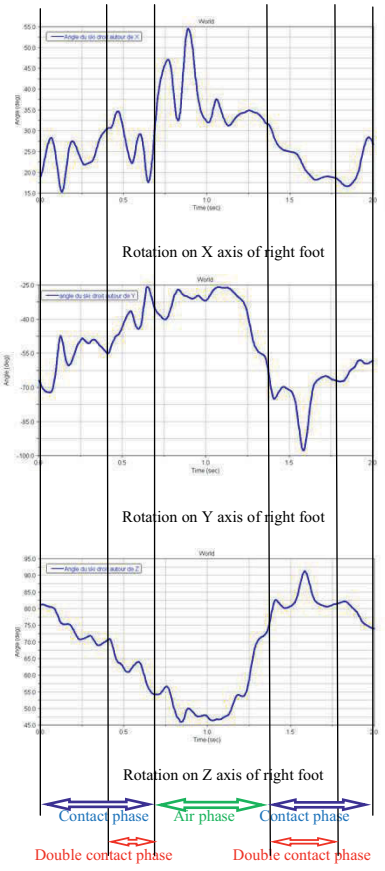

Figure 10: Rotations on X, Y, Z of right foot

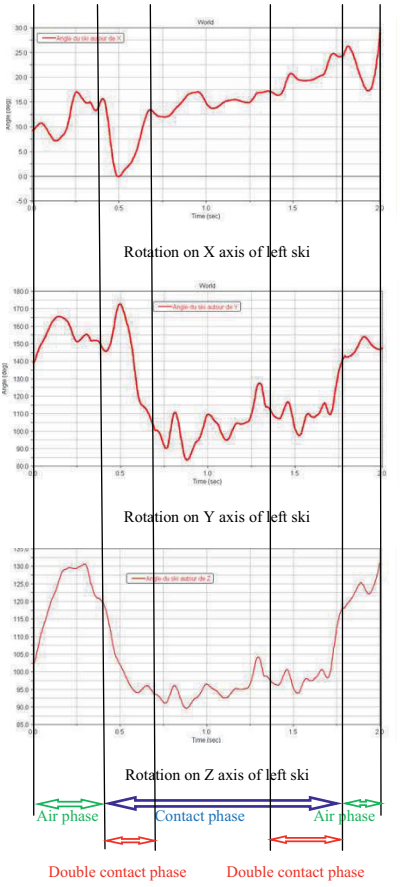

Figure 11: Rotations on X, Y, Z of left foot

Right ski angle variations around Z are faster with a marked peak in the graph of contact phase. For Z angle, the shape of curves appears cyclical, meaning that edging angle variations are very accurate. Orientation shift of ski takes place in the middle of air phase. Skier seems to stabilize rotations on X, Y and Z during the gliding phase of weak side. This would determine the edging phase quality.

4.2 – Double contact phase comparisons

Double contact phases show significant angular variations both for the strong side and the weak side. They are different according to the axes and according to if it's the beginning or the end of double contact phase.

- For left ski, around the Z axis, angular variations are not different, however they are significant around X and Y axes in the beginning of contact and not at the end of it. This reflects the left foot hold, the soft edging in the beginning and the sliding at the end of contact phase.
- For the right ski, around Z and Y axes, curve makes a peak without oscillation around X axis during double contact in the beginning. Double contact phase of the end of contact doesn't reveal important variations. This translates right foot hold, which makes a hard ski edging in the beginning and decreases it until the end. We observe again the offset characteristic with stability and sliding on the left ski at the end of the gliding phase in transversal plane and in the frontal plane and like an impulse on right ski.

	contact phase	air phase	contact phase	air phase
Rotations on X axis	20°	23°	25°	23°
Rotations on Y axis	75°	35°	90°	27°
Rotations on Zaxis	35°	30°	30°	30°

Table 3: maximal variation of angles around X, Y, Z axes for right and left ski during contact and air phases

- Around X axis, angles have smaller values, around 20°. The antero-posterior stability of skis for uphill terrain is related to the overall balance of skier and corresponds to a static posturing.
- Around Y axis, largest values appear during the contact phase. The graph curves of show a peak in the beginning of contact phase and continuity at the end. Left ski has a clearance bigger than right ski, skis are widely spaced.
However authors, Smith[**SN1**], [**SH1**], Bilodeau [**BB1**], Gregory [**GH1**], Street [**SG1**] agree that the skier from flat to uphill terrain, can be generated more forces by increasing the ski orientation angle or by increasing the ski edging angle on the snow. The gravity is an additional force which compels skier to open the skis.
- Around Z axis, there are identical rotations of about 30°. Only in contact phase, right ski takes an edging of about 35°, this confirms the strong side. Smith [S1], has found in his study an ski edging of only 10° during fast skating on flat terrain during the men's 50 km race of the 1992 Olympics. In our study model skates on a slope of 6°, she is a woman during an international race and the nature of the snow layer can cause some differences, the value of edging angle looks correct. However, the curves profiles of graphs for two skis are different during the contact phase.
- The curve of left ski is symmetrical and makes a large U almost flat in the center with the same angular variation of about 25° during double contact phase. During the gliding phase, there are many small variations with a maximum at about 13° and with an average position of 95° (90° being the snow level). This means that ski is still on its edge and is not completely flat on the snow.
- The curve of right ski shows a sharp peak at the beginning of contact phase, during double contact phase with a quick variation of 15°. It decreases gradually of 13° during gliding phase and it continues to decrease of 15° during the second double contact phase.
Edging in skating doesn't seem as critical as in Alpine skiing; that is the combination of skis' rotations which reflects position-holding effective on snow without side slip.

5- Conclusion

In this paper, we first explain the method we have used for modeling a skier with his equipment in the practice of offset technique. Our work was focused on connector chosen to link foot and ski. Next we have analyzed orientation angles of skis during a part of a race.
The results of this study suggest that edging and flat position of ski, are for the offset technique, characteristics for performance but others skis angles of can be important too.
We have shown.

-The two legs synchronization

- The synchronization of the three angles on both skis

This analysis should highlight the technical complexity of the movement and to bring motor responses against stresses due to climb uphill and against the speed loss. In this technique, it is no longer uncommon in high level that skiers take an impulse from strong to weak leg.

6- References

[**BB1**] BILODEAU B., BOULAY M.R, ROY B. (1992). Propulsive and gliding phases in four cross-country skiing techniques. Medicine and science in sports exercise, vol.24, n° 8, p. 917-925.

[**C1**] COULMY N. (2000). Contribution à l'analyse cinématique et énergétique du pas de patineur en ski de fond, 196 p. Thèse : Sciences et Techniques des Activités Physiques et Sportives : Université Joseph Fourier Grenoble I.

[**GH1**] GREGORY R.W., HUMPHREYS S.E., STREET G.M. (1994).Kinematic analysis of skating technique of Olympic skiers in the women's 30-km race.Journal of applied biomechanics, n° 10, p. 382-392.

[**K1**] KOMI P.V. (1987). Ground reaction forces in cross-country skiing. International journal of sport biomechanics, n° 3, p. 370-381.

[**RF1**] F. REY, A. FERRAND, J. CORBEAU. Etude d'un geste sportif en biomécanique : le pas de patineur. In : *actes de* : IDMME 2002, *4ème conférence internationale sur la conception et la fabrication intégrées en mécanique*, (Cédérom), Clermont-Ferrand, France, 2002, 10 p.

[**RC1**] REY F., CORBEAU J., FERRAND A. (2005). Construction d'un modèle dynamique d'un geste sportif, le pas de patineur. In : 9ème Colloque National AIP PRIMECA, Méthode et Modèles Innovants pour la conception de Systèmes Industriel, La Plagne, France, 11p.

[**R1**] REY F. (2008). Contribution à la modélisation cinématique et dynamique d'un geste sportif : le pas de patineur, 231 p. Thèse : Génie Mécanique : Université de Toulouse.

[**RF2**] F. REY, A. FERRAND. Contribution à la modélisation d'une skieuse de ski de fond dans son environnement. In : 12*ème Colloque National AIP PRIMECA, Produits, procédés et systèmes industriels : intégration Réel-Virtuel*, Le Mont Dore, France, 29 mars - 1 avril 2011, 14 p.

[**RF3**] REY F., FERRAND A., MAKHLOUFI H. (2012) Contribution to the modelling of a cross-country skier skiing in its environment. Mechanics&Industry, n° 13, p. 127-136.

[**R1**] RUBY A. (1997). Contribution à la méthodologie de l'analyse de la performance sportive. Non paginée. Thèse : Sciences et Techniques des Activités Physiques et Sportives : Université Claude Bernard Lyon I.; N° d'ordre 184-95.

[**S1**] SHIMBO M. (1971). Friction on snow of ski soles, unwaked and waxed.In : Science Study of Skiing in Japan. Tokyo : The Society of Ski Science, p. 101-112.

[**SM1**] SMITH G.A., MCNITT-GRAY J., NELSON R.C. (1988).Kinematic analysis of alternate stride skating in cross-country skiing.International journal of sport biomechanics, n° 4, p. 49-58.

[**SN1**] SMITH G.A., NELSON R.C., FELDMANET A., RANKINEN J.L. (1989). Analysis of VI skating technique of olympic cross-country skiers. International journal of sport biomechanics, n° 15, p. 185-207.

[**S1**] SMITH G.A. (1992).Biomechanical analysis of cross-country skiing techniques. Med. Sci. Sports Exerc., vol.24, n° 9, p. 1015-1022.

[**SH1**] SMITH G.A., HEAGY B.S. (1994). Kinematic analysis of skating technique of olympic skiers in the men's 50 km race. Journal of applied biomechanics, n° 10, p. 89-90.

[**SG1**] STREET G.M., GREGORY R.W. (1994).Relationship between glide speed and Olympic cross-country ski performance.Journal of applied biomechanics, n° 10, p. 393-399.

[**TB1**] TAVERNIER M., BORSONI G., VERIEST J.P., BRUNEL N. (1993). Méthode de la détermination du centre de masse d'un sportif pour l'analyse du mouvement par images numérisées. Application au ski alpin et au ski de fond. Modèle CGS13. Rapport interne FFS/INREST.

[**V1**] VERRIEST J.P. (1990). Une méthode simplifiée de simulation du geste du membre supérieur pour mannequin graphique 3D. In : actes du 15ème congrès de la société de biomécanique, Cluny, p. 123-124.
Biomechanics Research Group, Inc. LIFEMODELER. Version BRG.LifeMOD 2005.2.0 Biomechanics Modeler

Article 071-pds-31

Influence of the cold expansion process on fatigue performance of hard alloys holes

Victor ACHARD [1,2], Alain DAIDIE [1], Manuel PAREDES [1], Clément CHIROL [2]

(1) : Université de Toulouse, INSA/ICA (Institut Clément Ader), 135 avenue de Rangueil, 31077 Toulouse Cedex 04, France.
+33561559702
E-mail : {victor.achard, alain.daidie, manuel.paredes}@insa-toulouse.fr

(2) : Airbus Operations S.A.S.
316 route de Bayonne
31060 Toulouse Cedex 09
+33582054700
E-mail : {victor.achard, clement.chirol}@airbus.com

Abstract: This paper presents an evaluation of the influence of the cold expansion process on fatigue performance of holes in hard alloys, as such materials are involved in an increasing number of aeronautic applications. Although the cold expansion of aluminium holes has been studied widely, there have been few reports concerning this issue in hard alloys. Some studies do, however, show that fatigue gains can be observed by using an extension of the processes employed on aluminium. Currently, there is no research concerning dedicated techniques to expand hard metals, despite their highly specific behaviour. In this article, the response of Ti-6Al-4V expanded holes is studied, considering various experimental parameters such as the stack thickness and hole diameter. The influence on the fatigue strength of tensile specimens is also presented for various expansion rates. Thus, this work aims to define an approach to understand which processes and methodologies are suitable for obtaining effective expansion of hard metals.

Key words: Cold expansion process, hard alloys, fatigue performance, expansion ratios, Ti-6Al-4V.

1- Introduction

1.1 – Context of the study

In the aeronautic field, further understanding and improving the behaviour of materials under complex combinations of stresses has become a serious challenge. It can lead to the optimization of fatigue performance of parts and assemblies which, in turn, can work towards a highly desirable weight reduction of the structure and thus increase the efficiency of aircraft. This search for optimization is currently expressed in the increasing use of high-performance materials, particularly within the primary structure. These new materials include, in particular, the family of hard alloys, whose physical properties often allow the best compromise to be found between density and the characteristics needed for the application. Regarding the different justifications for the use of hard metals and superalloys in the design of an aircraft structure, optimization of the various components is a major requirement. On the other hand, in modern aircraft, they enable the integration of a large proportion of composite materials (CFRPs) as structural material. They ensure good galvanic and thermal dilation compatibility in multi-material hybrid connections together with good shock response of the overall structure. Finally, new engines, running at ever-higher speeds and temperatures, open up many possibilities for applications where hard metal fatigue becomes a significant problem. Ezugwu et al. [E1] recall that each kilogram removed from the total mass of a jet engine saves 150 000 USD of fuel over the engine's working life. Despite all the advantages offered by this family of metals, the costs they generate make it necessary to optimize their use, by adapting their morphologies and therefore their characteristics according to their loading environment, especially to resist against fatigue.

This study focuses on optimizing the fatigue performance of bolted joints using hole cold expansion. Aeronautic structures consist of a large quantity of riveted or bolted sub-assemblies that require the presence of fastening holes. These sections are often critical in the design and act as major sources of stress concentrations where fatigue damage initiates [P1]. Thus, it has been observed that, statistically, fatigue of bolted joints accounts for 50-90% of all of the cracks sustained by an aircraft in operation [LY1]. Hole cold expansion involves the generation of compressive residual stress fields induced by hardening and modifies the kinetics and onset areas of the initial cracks, which will then spread later, to a less critical region beneath the surface of the material [T1]. The material is thus submitted to compressive and tensile residual stresses that allow its overall equilibrium, the compressive stresses being generally balanced by a tensile field away from the hole [PC1]. In order to be optimal, radial expansion of the hole should induce circumferential stresses that are close to the compressive limit at which the material yields. They thus compensate the mean value of future tensile fatigue loading (Fig.1). This

Article 071-pds-31

process reduces the criticality of these joints as methods involving the control of the fastener preloads [BS1] or interference fit [PN1].

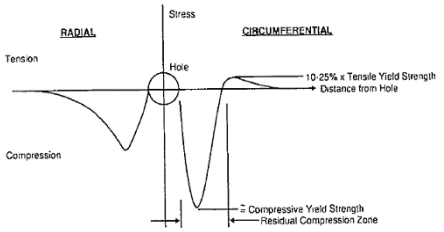

Figure 1 : Biaxial stress field in the hole edge after expansion [R2].

Among the existing processes designed to generate extensive and controllable residual stress fields at the edge of the hole while minimizing damage of the hole surface, split sleeve cold expansion remains the most widely used in industry [R1], [R2] (Fig.2).

On a technological point of view, a split sleeve is inserted in an initial hole in order to protect it and the cold working is performed by pulling an oversized tapered mandrel through the whole. Then, the cold expanded hole is reamed to its functional diameter. This process greatly improves the fatigue performance of the hole. For example, it is commonly noted that the lifespan of a hole that has been cold expanded using the split sleeve process is three to ten times that of an "as drilled" hole in aluminium alloys such as 2024 T351. On the other hand, gains on the fatigue quality index can reach +30% [ZW1], [OH1]. Because of the simplicity of the operations involved and the gains observed, this process appears very interesting to improve the quality, reliability and performance of bolted joints during their design, repair or post-production phases. Thus, it appears interesting to evaluate the cold expansion process on hard metals, by observing their responses and the potential fatigue gains that could be generated. In the literature, few studies describe the application of the cold expansion processes to hard metal and, because of the very specific mechanical and metallurgical characteristics of these materials, it seems impossible to make a direct analogy with other materials.

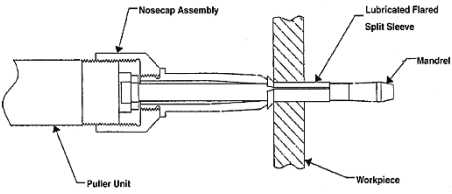

Figure 2 : Split sleeve cold expansion process, from [KB1].

1.2 – Hole cold-expansion process in hard alloys

The first studies, dating from the 1970s, by Philips [P2], Rich and Impellizzeri [RI1] and Sha et al [SC1] show that the cold expansion process was applied on hard alloys, but concerned almost exclusively titanium alloys. Some interesting results can be found in the literature, obtained on tensile specimens in "open-hole" or "filled-hole" configurations having width to diameter ratios between 4 and 5. Philips [P2] performed tests on hard metals such as Ti-6Al-4V, Ti-6Al-6V-2Sn, or AISI4340 steel. He obtained gains in fatigue performance on numerous configurations, despite a small number of specimens tested. More precisely, gains in lifespan of the specimens in the ratio 4:1 (+23% on the IQF) were observed on Ti-6Al-4V specimens with a split sleeve expansion of 5% on a 9.52 mm hole. In the same way, Rich & Impellizzeri [RI1] observed increases in the ratio 4:1 on the lifespan of 6.35 mm "filled-hole" Ti-6Al-4V specimens (i.e. that contains a pin with clearance fit) which were expanded (4%) with the split sleeve process. During the same period, a publication by Rufin [R2] reported interesting results obtained after expansion of isolated hard metal applications, almost exclusively titanium alloys, with or without bush installation. Mainly all these studies were performed on behalf of industry or organizations such as the USAF. Testing concerned very specific areas such as engine parts, clevis or other specimens and sections involving high load transfer. The test cases selected were representative of applications where the expansion appeared as a solution for repair or improving fatigue performance of the structural detail. However, over this period, no precise analysis was made of the response of hard metals subjected to expansion and only studies of specific cases can be found, where generic processes designed for the expansion of aluminium alloys hole were considered. In addition, it is difficult to quantify the fatigue gains obtained in these studies as the various configurations tested involved many parameters influencing fatigue behaviour. Furthermore, scatter on the results is large and reduces the validity of the assumptions made. More recently, two general studies have been conducted by Yan et al. [YW1] and Liu et al. [LW1] regarding Ti-6Al-4V hole expansion. In particular, they observe its influence on fatigue performance and crack propagation. Again, the split sleeve process is considered and threefold increases are observed in the lifespan of cold expanded (4%) 6.35 mm "open-hole" Ti-6Al-4V specimens [YW1]. Finally, a process where residual stresses are set up by indentation of surfaces has also been tested ([FW1] and [S1]) on tensile specimens and medical implants made of Ti-6Al-4V. The authors observed that the lifespan of the tensile specimens was multiplied by 4.7.

So studies concerning the expansion of hard metals mainly converge to extensions and implementations of processes and methodologies that remain identical to those used on aluminium alloys. In addition, the influence of the thickness and the diameter of the hole is not considered, neither is the influence of the expansion rate. Thus, there are few quantitative results available on the response of expanded hard metal holes and there has been no research concerning dedicated processes for expanding hard metal holes and improving their fatigue performance. Their highly specific

Article 071-pds-31

behaviours, concerning both thermal and metallurgical issues or regarding the integrity of the surfaces generated, are not taken into account for the installation of residual stresses at the hole edge. Finally, these studies concern almost exclusively Ti-6Al-4V applications. Thus, it appears interesting to generalize hole cold expansion to the hard alloys that are the most used within aircraft structures nowadays, such as precipitation hardening stainless steels and nickel-based alloys.

The main difficulties in studying the expansion process in hard metals arise first from the behaviours of these materials when subjected to expansion. Their static and fatigue response appears very different from that observed on an aluminium alloy. Also, this family of materials exhibits significant disparities concerning specific strength (stress-strain up to the failure) and monotonic behaviours. For example, the mechanical properties of titanium alloys are highly dependent on their thermo-mechanical loading history and initial composition and microstructure. Thus, alloys such as Ti-6Al-4V in annealed condition predominantly contain α phase (HCP) at ambient temperature and exhibit typical anisotropic mechanical properties, particularly tension-compression asymmetry (Fig.3). Moreover, this behaviour is highly dependent on strain rate and temperature [OO1], [MM1], [MS1] and [KY1]. Therefore, this material is commonly observed to present compressive failure stresses and strains that are much greater than their tensile counterparts. On the other hand, the materials may exhibit significant kinematic behaviour, which appears particularly important in titanium alloys, for example. This behaviour is attributed to the limited number of slip systems in hexagonal close-packed (α-phase) material at ambient temperature [C2]. Thus precise characterization of the materials considered is important in order to understand the various phenomena observed and to be able to simulate them.

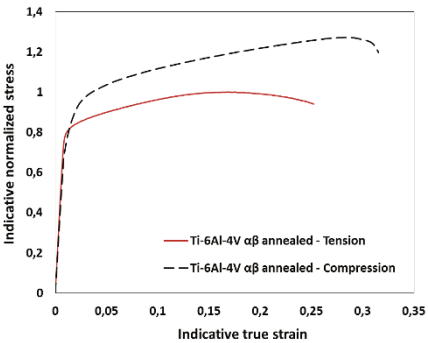

Figure 3. Typical monotonic behaviour of titanium alloys at 20°C

To understand the source of the fatigue gains that have been observed, numerical methods such as finite element modelling appear to be good tools for predicting the response of the material and particularly the residual fields generated, on condition that the modelling strategies are sound. There are numerous studies concerning the split sleeve expansion process in the literature [CV2], [NP1]. However, in the case of hard alloys, we found only two [YW1], [R2]. The modelling choices must be clearly selected in order to simulate highly non-linear behaviours, justified by the localized phenomenon caused by the split of the sleeve, the complexity of the intrinsic behaviours of hard metals, the various contacts affecting the material and the nature of the tools used for the expansion. For these reasons, it is well known that residual fields in the depth of the hole are highly non-uniform. In order to overcome this problem, various experimental methods have been developed, from SWCW patented by the StressWave Company [EL1] to the process designed by Chakherlou et al. [CV1], which generates nearly uniform residual fields.

In the present work, the response of Ti-6Al-4V holes subjected to split sleeve expansion is evaluated experimentally. First of all, feasibility tests are performed in order to highlight the specificities of expansion in titanium hole, testing various configurations of "5 holes" specimens. Afterwards, the influence of expansion on the fatigue strength of tensile specimens is observed, considering various expansion rates. Thus, these first results will provide information regarding the application of the expansion process to hard alloys and will define an approach for understanding which processes and methodologies are suitable for the efficient expansion of hard metals. Specifically, the initial aim is to assess whether the processes designed for the expansion of aluminium alloys are suitable in terms of rate of expansion, and to determine the physical limits of the process that ensure the operating characteristics of the hole are maintained.

2- Experimental procedure

2.1 - Split sleeve expansion of Ti-6Al-4V holes

The objective of this experimental study was to evaluate the behaviour of titanium specimens when they were subjected to expansion, to observe whether a plastic strain field might be generated in the hole edge and if fatigue gains were indeed observed. The aim was thus to see if expansion was achieved easily in hard metals and to evaluate potential associated risks, such as the generation of cracks at the hole edge. From the technological point of view, the split sleeve expansion process was chosen.

This process can basically be divided into six key steps. First of all, after dimensional control of the original hole, a pre-lubricated split sleeve is placed on the mandrel, which is connected to the hydraulic actuator. The sleeve is positioned on the minimum diameter of the mandrel so that the tooling can be inserted from one side of the hole. The angular position of the split is then carefully adjusted to ensure that the affected zone (extensive distortion) will not correspond to the main directions of loads operating on the treated part (Fig.4). The actuator is subsequently triggered and the mandrel is pulled through the sleeve and the hole, performing the expansion. In the split sleeve process, the sleeve is then removed from its housing, which leaves the hole ready to receive a fastener for example. Here, the pre-lubricated sleeve is useful to reduce the axial effort involved in pulling

Article 071-pds-31

the mandrel and protect the contact surface. Finally, the hole is reamed to its functional diameter and checked. The theoretical expansion rate applied is defined by relation (1).

$$Ie = \frac{\phi tooling - \phi initial}{\phi initial} \quad (1)$$

Where the tooling diameter corresponds to the maximum diameter of both the mandrel and sleeve as an assembly and the initial diameter is the one measured after drilling of the specimens.

Parameter tested for each configuration
➢ 2 Orientations of the split sleeve ➢ 3 Thicknesses (5, 10 & 20 mm)
Diameters / expansion levels tested
➢ 6.35 mm final hole, 8 expansion levels 2% to 5.5% ➢ 9.52 mm final hole, 7 expansion levels 2% to 5% ➢ 15.88 mm final hole, 5 expansion levels 2% to 4%

Table 1 : Split sleeve expansion configurations chosen for feasibility tests in Ti-6Al-4V specimens.

The material considered in this study was Ti-6Al-4V αβ annealed, the chemical composition of which is given in the aeronautic standard. Here, holes were machined with orbital drilling in order to reduce residual stresses generated on the surface of the hole and reduce the scatter of results during the tests. Similarly, specimens were treated to relieve stress after milling of the external faces, and maximal tolerance on the hole diameter was ± 0.02 mm, which ensured good accuracy of the expansion rate actually applied. Expansion was first performed on "5 holes" feasibility specimens, according to the configurations shown in Table 1. Various expansion rates were tested on three main diameters and for three thicknesses. Moreover, two orientations of the sleeve relative to the main direction of grain flow were considered (0° or 90°), the fracture toughness of the material being particularly different in these two directions.

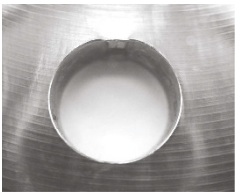

Figure 4 : Zone affected by the split in cold expanded Ti-6Al-4V 6.35 mm hole.

During these tests, no cracking of the material was observed in the microscopic inspection. The residual expansion rate versus theoretical applied rate was analysed. Residual expansion rate is obtained by measurement of the cold worked hole (residual hole) using an internal micrometer (out of the affected zone). The residual expansion rate is calculated for each specimen and defined by relation (2).

$$Ie = \frac{\phi residual - \phi initial}{\phi initial} \quad (2)$$

Figure 5 shows the expansion ratio obtained from 5 to 8 different expansion levels, where each point corresponds to the mean value obtained on 5 holes. These curves are plotted only for 5 mm thick specimens. The expansion ratio was defined as the residual expansion rate divided by the theoretical rate applied. It was observed that expansion ratios did not exceed 60% for 6.35 mm holes and 50% for 15.88 mm. Thus, it was noted that expanding Ti-6Al-4V holes having high yield strength and significant springback presented some difficulty. Similarly, the expansion ratio did not grow linearly with the expansion rate. These results appear quite remarkable, especially when they are compared with those observed during the expansion of aluminium alloys, where the ratio measured is between 68% and 72% for 2024 T3 holes for an expansion rate range of 2% to 6%. On the other hand, no conclusions can be drawn on the influence of the thickness of the plate or about the influence of the orientation of the sleeve.

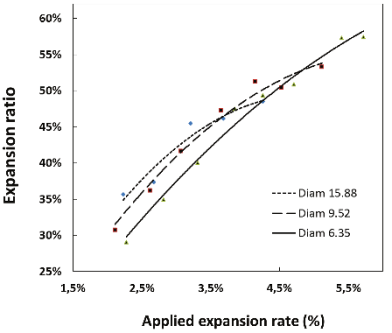

Figure 5 : Evolution of the expansion ratio for Ti-6Al-4V specimens

Evolution of the hardness from the edge of the hole to the free edges of the specimens was measured on 9.52 mm diameter specimens. After preparation and polishing of the specimens, the hardness profiles were recovered using HV1 Vickers measurement method, over nearly 35 hardness values distributed over the width of the specimen. Figure 6 shows measurement extracted from the "exit surface", which is identified as the exit side of the expansion mandrel during the process. The normalized hardness values measured are plotted for specimens that were cold expanded at 2, 4 and 5.5%. Values are normalized over the diffused hardness of each specimen considered (surface away from the hole), separating the results between specimens and allowing trends to be easily distinguished and ease the figures' readability. We can see clearly that the expansion process implies an

Article 071-pds-31

important increase of the hardness at the hole edge (up to 15%). Furthermore, the trend between these values highlights a dependence on the hardness and the distance to the hole edge. More precisely, results show that, statistically, hardness increases as we move from the free edge to the edge of the cold expanded hole. Moreover, the hardness's slope increases proportionally with the expansion ratio. The analysis of this distribution should be subjected to further evaluation in order to determine the shape of these hardness curves accurately, control dispersion and compare it to a theoretical expression of the profile. Thus, it would be possible to determine the hardened area's geometry during the expansion process, depending on the configuration of the considered hole and the applied rate.

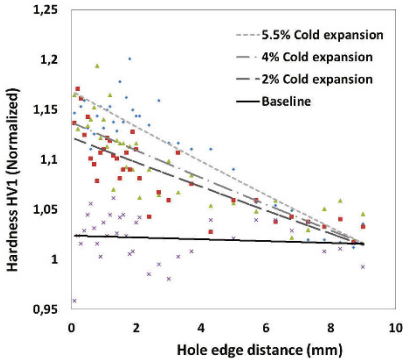

Figure 6 : Evolution of the hardness along the width of cold expanded Ti-6Al-4V specimens

2.2 – Fatigue performance of Ti-6Al-4V specimens

After noting that cold expansion using the split sleeve process allowed residual fields to be generated at the hole edge, we sought to observe the fatigue behaviour of these expanded Ti-6Al-4V specimens. "Open-hole" fatigue specimens were manufactured and expanded at theoretical ratios ranging from 3% to 4.5%. The specimens tested in fatigue were 5 mm thick and drilled to a diameter of 9.52 mm. They exhibited a stress intensity factor of 2.3, ensuring that the hole edge would be the place of onset of cracking and so the weak point of the specimens. The overall roughness of the specimen (hole and outer surfaces) was less than 1.6 µm to avoid potential locations of crack onset in other places.

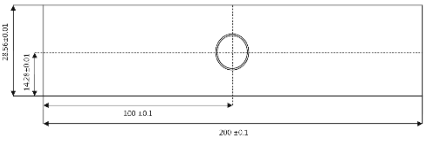

Figure 7 : Geometry of fatigue specimens geometry. All dimensions in mm

In order to decrease the scatter on test results, holes were machined by orbital drilling and specimens were treated for stress relieving. The geometry of the fatigue specimens is presented in Figure 7. Specimens were first expanded to the theoretical ratio, then reamed (orbital) and chamfered to their nominal diameters. Again, maximum tolerance on hole diameters was ±0.02 mm. Fatigue tests were performed by using a sinusoidal wave of a tensile-tensile load spectrum (R=0,1), with a frequency of 20 Hz and for various stress levels to obtain Wohler curves. These stress levels correspond to the average theoretical longitudinal stress in the net section of the specimen (without hole), that is reached for the maximum load applied during a fatigue cycle. The curves (Fig.8) show a logarithmic interpolation of Wohler curves plotted for baseline specimens "as drilled" and for 3 different expansion ratios, each curve being obtained through the tests results of 10 specimens. These curves are plotted with 50% reliability over the number of cycles sustained until failure of the specimens (as many specimens on the left as on the right of the curve).

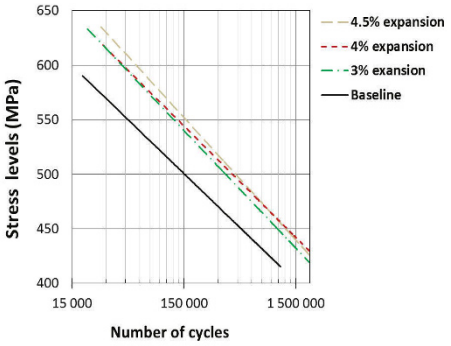

Figure 8 : Fatigue tests of Ti-6Al-4V expanded "open-hole" specimens

Improvements in fatigue performance of the specimens were observed after expansion. More precisely, for an expansion rate of 4.5%, the lifespan increased by ratios that reached 3:1 and these gains became greater as the applied expansion ratio increased. Failure patterns exhibited typical crack propagation plus ductile failure occurring when the net section was too severely reduced by fatigue damage. Observation of the fracture surfaces after fatigue failure (Fig.9), revealed that onset occurred at the base of the chamfer nearly every time for expanded holes, whereas it occurred randomly in the hole surface for "as drilled" specimens. These differences probably stand for the influence of the entry side of the mandrel. These results show that a fatigue gain can be observed in titanium holes subjected to the classical expansion process usually intended for aluminium alloys. These results are promising for the continuation of the study, in which new configurations dedicated to hard metals will be tested.

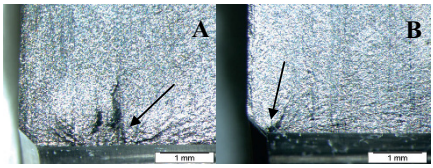

Figure 9 : Typical failure patterns of "as drilled" specimens (A) and 4.5% expanded specimens (B)

3- Discussion and perspectives

The present study focused on the evaluation of the cold expansion process for holes in hard alloys. First of all, a review of the literature revealed only a few experimental studies concerning cold expansion of hard metal holes. However, fatigue gains have been observed by applying the methodologies, processes and ranges of expansion rates typically used for aluminium alloys. Furthermore, these studies concern almost exclusively titanium alloys and therefore cover a very limited number of test cases, providing little quantitative information on the response of these expanded holes. The objective of our study was therefore to generalize the hole cold expansion process to "hard metal" applications.

This study also presents the first experimental results obtained on Ti-6Al-4V "open-hole" specimens, in terms of feasibility and response to cold expansion. It was observed that the use of the split sleeve process was compatible with this alloy, considering several diameters and thicknesses of holes. Although no cracking was observed for the expansion rates considered, the difficulty of expanding hard metals to the desired rate was noted. The observed residual expansion rate was much lower than those observed for aluminium alloys. Subsequently, fatigue tests on expanded Ti-6Al-4V specimens checked the efficiency of the process in increasing the fatigue performance of the holes. These results provide first information regarding the application of the expansion process to hard alloys, and should help to define an approach for understanding which processes and methodologies are suitable for the efficient expansion of hard metals.

Ongoing work therefore concerns the fine modelling of the expansion process in hard alloy holes using finite elements method, in terms of geometry, loading environment and boundary conditions. Efforts are also being made to provide reproducible responses for the specific behaviour of the various alloys considered. The results thus obtained will be compared with experimental tests in order to validate or invalidate the assumptions made.

4- References

[BS1] Benhaddou T., Stephan P., Daidié A., Chirol C. and Tuery J-B. "Effect of Axial Preload on Double-Lap Bolted Joints: Numerical Study." Nantes: Proceedings of ASME 2012 11th Biennial Conference On Engineering Systems Design And Analysis, 2012.

[CV1] Charkherlou T. N. and Vogwell J. "A novel method of cold expansion which creates near-uniform compressive tangential residual stress around a fastener hole." Fatigue fracture engineering material and structures 27: 343-351, 2004.

[CV2] Charkherlou T.N. and Vogwell J. "The effect of cold expansion on improving the fatigue life fasteners holes." Journal of engineering failure analysis 10: 13-24, 2003.

[C2] Collings E.W. Applied superconductivity, metallurgy, and physics of titanium alloys. New York : Plenum Press, 1986.

[EL1] Easterbrook E.T. and Landy M.A. Evaluation of the StressWave cold working (SWCW) process on high strength aluminum alloys for aerospace. AIR FORCE RESEARCH LABORATORY AFRL-RX-WP-TR-2009-4027, 2009.

[E1] Ezugwu E.O. "Key improvements in the machining of difficult-to-cut aerospace superalloys." International Journal of Machine Tools and Manufacture 45: 1353–1367, 2005.

[FW1] Flinn B.D., Wiegman M.E., Sigelmann M., Eaterbrook E. and Mines A. "StressWave fatigue life improvement of 6Al-4V titanium for medical implants." Proceedings of the materials & processes for medical devices conference, 2003.

[KB1] Karabin M.E., Barlat F. and Schultz R.W. "Numerical and experimental study of the cold expansion process in 7085 plate using a modified split sleeve." Journal of Materials Processing Technology 189: 45–57, 2007.

[KY1] Khan Akhtar S. and Shaojuan Yu. "Deformation induced anisotropic responses of Ti–6Al–4V alloy Part I: Experiments." International Journal of Plasticity, 2012.

[LW1] Liu J., Wu H., Yang J. and Yue Z. "Effect of edge distance ratio on residual stresses induced by cold expansion and fatigue life of TC4 plates." Engineering Fracture Mechanics, 2013.

[LY1] Liu J., Yue Z.F. and Liu Y.S. "Surface finish of open holes on fatigue life." Theoretical and Applied Fracture Mechanics 47: 35-45, 2007.

[MM1] Mayeur J.R. and McDowell D.L. "A three-dimensional crystal plasticity model for duplex Ti–6Al–4V." International Journal of Plasticity 23: 1457–1485, 2007.

[MS1] Medina Perilla J.A. and Sevillano J.Gil. "Two-dimensional sections of the yield locus of a Ti-6%Al-4%V alloy with a strong transverse-type crystallographic a -texture." Materials Science and Engineering, 1995.

[NP1] Nigrelli V. and Pasta S. "Finite-element simulation of residual stress induced by split-sleeve cold-expansion process of holes." journal of materials processing technology, 2005.

[OO1] Odenbergera E.-L., Oldenburgb M., Thilderkvista P., Stoehrc T., Lechlerc J. and Merklein M. "Tool development based on modelling and simulation of hot sheet metal forming of Ti–6Al–4V titanium alloy." Journal of Materials Processing Technology 211: 1324–1335, 2011.

[OH1] Ozdemir A. T. and Hermann R. "Effect of expansion technique and plate thickness on near-hole residual stresses and fatigue life of cold expanded holes." Journal of material and sciences 34: 1243-1252, 1999.

[PC1] Paredes, M., Canivenc R. and Sartor M. “Tolerance optimization by modification of Taguchi's robust design approach and considering performance levels: Application to the design of a cold-expanded bushing” Proceedings of the Institution of Mechanical Engineers, Part G: Journal of Aerospace Engineering 2013.

[PN1] Paredes, M., Naoufel N. and Sartor M. "Study of an interference fit fastener assembly by finite element modelling, analysis and experiment." International Journal on Interactive Design and Manufacturing Volume 6, Issue 3 171-177, 2012.

[P1] Peterson R.E. Stress concentration design factors. New York: Wiley, 1953.

[P2] Phillips Joseph L. "Technical Sleeve coldworking of fastener holes." Air Force Materials Laboratory (SAE Paper no. 73095): AFML-TR-74-10, 1974.

[R1] Reid L.F. "Advanced structural fastening and jointing methods utilizing synergistic cold expansion and high interference fit methodology." EUROPEAN CONFERENCE FOR AEROSPACE SCIENCES (EUCASS).

[RI1] Rich D.L. and Impellizzeri L.F. "Fatigue Analysis of Cold-worked and Interference Fit Fastener Holes / Cyclic Stress-Strain and Plastic Deformation Aspects of Fatigue Crack Growth." ASTM STP (ASTM STP) 637: 153-175, 1977.

[R2] Rufin A.C. "Extending the fatigue life of aircraft engine components by hole cold expansion technology." J. Eng. Gas Turbines Power 115, 1993.

[SC1] Sha G. T., Cowles B. A. and Fowler R. L. "Fatigue Life of a Coldworked hole." In Emerging technologies in aerospace structures, design structural dynamics and materials, by Jack R. Vinson, 125-140. American Society of Mechanical Engineers. Aerospace Division, 1980.

[S1] StressWave. "Fatigue testing of 6Al-4V titanium." 2001.

[T1] Taylor G. I. "The Mechanism of Plastic Deformation of Crystals. Part I." Proceedings of the Royal Society of London. Series A, Containing Papers of a Mathematical and Physical Character, no. 362: 145 (855), 1934.

[YW1] Yan W.Z., Wang X.S., Gao H.S. and Yue Z.F. "Effect of split sleeve cold expansion on cracking behaviors of titanium alloy TC4 holes." Engineering Fracture Mechanics 88: 79-89, 2012.

[ZW1] Zhang X. and Wang Z. "Fatigue life improvement in fatigue aged fastener holes using the cold expansion technique." International Journal of Fatigue: Vol 25 ISS 9-11 p.1249-1257, 2003

Article 072-pds-64

Design of an experimental device to characterise the behaviour of Total Hip Implants

Camille Regnery [1], Julien Grandjean [2], Yann Ledoux [3], Serge Samper [1], Laure Devun [2], Thomas Gradel [2]

(1) : SYMME, Polytech'Savoie, BP 80439, 74944 ANNECY LE VIEUX Cedex
E-mail : {camille.regnery,serge.samper}@univ-savoie.fr

(2) : Laboratoire TURAL, Recherche et Essais, Marignier, France
E-mail : {grandjean,devun,gradel}@tural.fr

(3) : Université de Bordeaux, I2M UMR 5295, Esplanade des Arts et Métier, 33400 TALENCE
E-mail : yann.ledoux@u-bordeaux1.fr

Abstract:

The majority of Ceramic Total Hip Implant (THI) validation tests and wear studies are done on specific devices able to require a kinematic outcome that conforms with the ISO-14242-1 standard [I1]. The main point of interest in using Ceramic THI is their property of resistance to wear. However in some cases an unwanted noise called squeaking appears when implanted. The aim of this work is to develop an in vitro study to characterise this phenomenon from a mechanical point of view. Associated results show the limits of standard tests mainly because of the control system that disturbs the applied loads on the prosthesis. To overcome these problems the development of an experimental device based on a free kinematic is developed. Analytical models based on geometrical characteristics of THIs and the properties of the prosthesis materials are developed and used to characterise the behaviour of THI with or without squeaking. Based on the results, a change in frictional behaviour can be identified as an indicator of the squeaking phenomenon as evidenced by a dramatic increase in the deceleration for those tests where squeaking occurred.

Key words: Total hip implant, squeaking, in-vitro experimental device, analytical modeling, local pressure, joint gap

1- Introduction

The deterioration of the hip generally manifests itself as pain and a reduction of the patient's motor function. When medical treatment can no longer ease the patient, the surgeon resorts to surgery that will replace the natural joint with a Total Hip Implant (THI).
THI is currently one of the most frequently performed procedures in orthopaedic surgery. In 2004, according to the Avicenne Institute, 730,000 were implanted in Europe, including 160,000 in France [**A2**]. This number is constantly increasing due to the aging of the population but also because of the growing number of overweight individuals.
Different pairs of materials performing the rubbing part of the joint are used by THI manufacturers. Several can be named such as pairs of metal-metal, metal- UHMWPE and ceramic-ceramic. The major convenience of the ceramic-ceramic pair its wear resistance and it is often implanted on young patients.
In the latest generation of ceramics the use of alumina (Al_2O_3) or zirconia (ZrO_2) has overcome the brittleness of the ceramic and allowed limiting the breakage of implants. However a sound phenomenon has occurred during normal use of the THI by the patient. This phenomenon called squeaking affects approximately 0.3% of implanted THIs according to Walter and Ecker **[WO1, ER1]**, and has been classified according to the seriousness of the phenomenon by Swanson **[SP1]**.
Understanding and explaining the causes of appearance of the phenomenon is not an easy thing. These problems arise from the difficulty of taking measurements directly on patients presenting some squeaking and related to the different communities studying this problem (surgeons, tribologists, mechanicians etc...). Thus according to the literature, the conclusions about the explanation of this phenomenon are often contradictory involving patients related parameters (weight, sex, morphology ...), the design of the THI (head diameter, size the implants ...) or surgery (poor orientation of THI ...).
Several studies have also been made *in vitro* whereby metallic (**[CT2]**) or ceramic (**[BW1]**) fragments have been added to a hip implant in order to determine the result on squeaking or frictional behaviour. Results from these studies indicated - for the metallic fragments an immediate and constant squeaking - and for the ceramic fragments a significant increase in friction factor. Whether this represents a realistic *in vivo* phenomenon is yet to be determined. It is commonly found that metallic particles have been present in

Article 072-pds-64

THIs explants, however the effect of biological fluids and particles is as yet unknown.
To clearly identify behaviour modifications between a prosthesis squeaking or not, it is proposed to perform in vitro tests, applying loading and kinematic conditions defined by the ISO- 14242-1standard **[I1]** which are conventionally used for THI certifications. In a first step, tests are performed on a specific device developed by Instron (MTS 858 Mini Bionix II) on which is adapted a support to maintain the THI. A force sensor has been added to the device to measure, during testing, the mechanical loads that the THI undergoes. These initial tests clearly show the limits of such experimental devices as the coupling between kinematics and loading are evolving over time, and this resulted in a strong variation of the load, making it difficult to take any measurements. We then developed an experimental system based on a free swinging pendulum-like motion, where the ball-joint connection between the frame and the oscillating part of the pendulum is formed by the THI. It is then possible to track the evolution of the applied load on the THI as a function of the angular position of the pendulum. In addition to these tests, analytical models taking into account the values of the gap between the parts of the THI, and the values of local stresses are developed and compared. The validation is based on a quantification of the frictional forces working in the THI and an estimation of the friction coefficient.
This new device allows, through a simple experimental device, characterisation of the behaviour changes in the normal and degraded modes of operation (with or without squeaking phenomenon).

2- THI and squeaking

2.1- Presentation of the THI

Total hip implant (THI) is a mechanical ball joint that has the same function as the natural joint of a normal hip. It is implanted in cases where the normal hip joint has failed – the causes of the failing can be femoral neck rupture, osteoarthritis among others. It consists of a cup shaped structure and a femoral stem put together. Each of these subsets can be either integral or modular. The prostheses investigated in this study are the most commonly used. Their cup shaped structure is made of a metal-back and an insert. Their femoral set is made of a prosthetic femoral head and a shank (Figure 1). The metal-back is a metal hemisphere embedded in the acetabulum of the pelvis. A ceramic insert is fitted inside the metal back and this set metal-back insert is also called acetabulum. The femoral stem is the metal part inserted in the upper end of the femur to which the surgeon will have cut off the head. The rod carries at its end the prosthetic head (ceramic, stainless steel or cobalt-chromium) accommodated in the insert. The different THI items are represented in Figure 1.

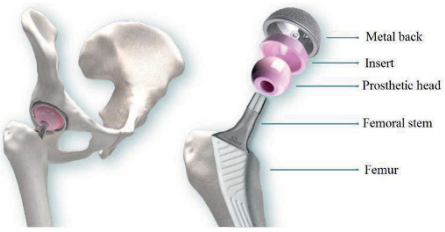

Figure 1: Total hip Implant (THI)

2.2- The squeaking phenomenon

A THI might emit noises during a patient's day-to-day movement – such as walking, climbing stairs, rising from a sitting position or leaning forward. This characteristic sound is called squeaking and is often described as a creaking door. Squeaking is completely painless for the patient and was already known for pairs of materials such as metal-metal, however it was known to disappear with time [**C1**, **HB1**, **EW1**, **HW1**, **BD1**]. In some rare cases it is produced daily for each patient's movement. The prosthesis becomes very difficult to bear for the patient and requires a surgery called revision to replace the implant.
Eickman et al [**EM1**] is one of the first articles in the literature about this phenomenon on a pair of ceramic-ceramic material. In 2007, one sees numerous studies in scientific journals or in the press (New York Times) [**F1**]. These studies highlight the importance of investigating this phenomenon. According to the literature, it is necessary to develop typical experimental devices and methodologies to clearly identify the phenomena and associated parameters responsible for the occurrence of squeaking.

3- THI behaviour: standards and trials

3.1- Specific trials

In the literature different authors have developed specific mechanisms to identify phenomena that may occur during the use of THI. Their main goal was to confirm or reject hypotheses that could explain the occurrence of squeaking. Curriers work can be quoted as an example wherein the author provides a mechanical system to study two explants where the measurement is performed by an accelerometer bonded to the insert **[CA2]**. Brockett and Chevillotte have also designed test benches to simulate and identify potential causes that could create the squeaking phenomenon of the prosthesis **[CT1, BW1]**. Sariali has developed a gait simulator replicating the micro-separation phenomenon during oscillation phases **[SS1]**. Although these works are relevant and provide some conclusions on the squeaking, it could be underlined that the experimental devices and associated protocol differ greatly from the tests used for the THI certifications.

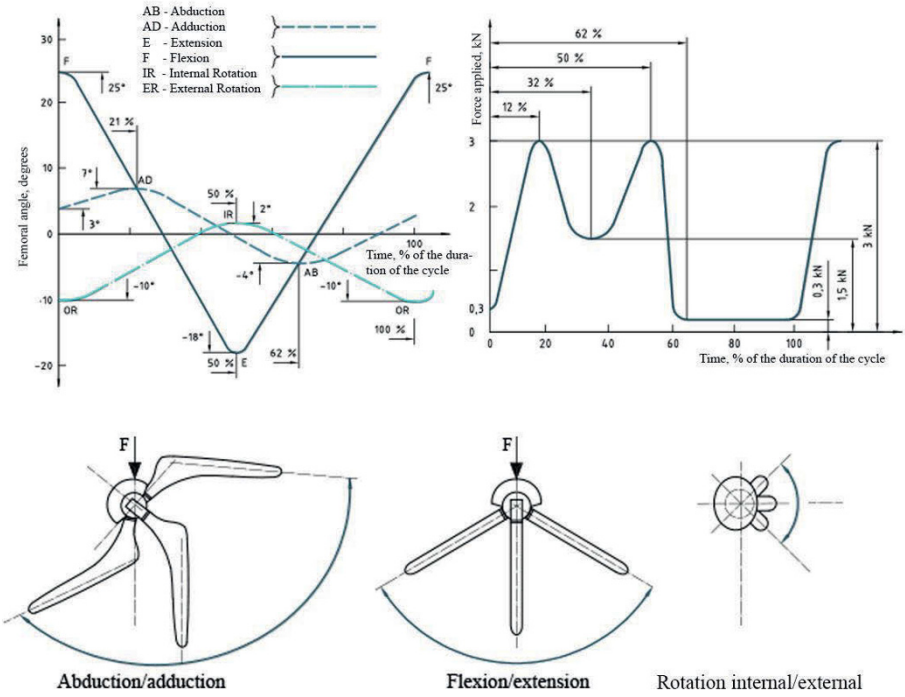

Figure 2: Angular variation and load applied to the femoral component [I1]

3.1- Standard tests

Standard tests correspond to a model of a specific step of an average individual (ISO 14242-1), derived from measurements of the hip joint made in 1969 by Smith and Johnson **[H1]**. The norm is therefore defined as a specific walking cycle. Three angle values are defined that are time-dependent between the prosthetic head and the cup of the THI and the vertical loading values. The speed and duration of the test are also specified. These data are defined to check the wear resistance of the prosthesis **[I1]**. The characteristic curves are shown in Figure 2. The magnitude and changes in the force to be applied according to ISO- 14242-1 are also visible in Figure 2. The maximum value of the force is set to 3000N to reproduce the conditions of maximum stress during the operation of a 75kg person. The cycle is applied at a frequency of 1 Hz.

3.2- Testing device associated to standard trials

In order to control both the loading and the angular position, it is necessary to use a specific test device. The MTS 858 Mini Bionix II has been specially developed by Instron to realise wear tests. This device is a tensile-testing machine equipped with special hydraulic equipment (cylinders). The device has two degrees of freedom through the central actuator that can perform translations and rotations along the z axis. The module attached to the end of the rod adds two degrees of rotational freedom about the x and y axes (Figure 3a). A steel bowl is attached to the base of the machine to fix the THI . In each of these parts can be cemented the stem and metal back. The cement used is a product used by orthopaedic surgeons and recommended by the ISO-14242-1 standard for implant fixation on a simulator **[I1]**. The lower part of the simulator which supports the bowl can translate freely on the x and y axes for lining up the metal-back during installation. During testing this part remains stationary while the upper portion, which maintains the metal-back, performs the rotation and applies the vertical force. This configuration allows the rod to be taken as a reference and to keep the direction of the force fixed when a kinematic walk is applied. Thus the x-axis reproduces the movements of flexion / extension, the y axis abduction / adduction and z axis internal /external rotation (defined on Figure 2).

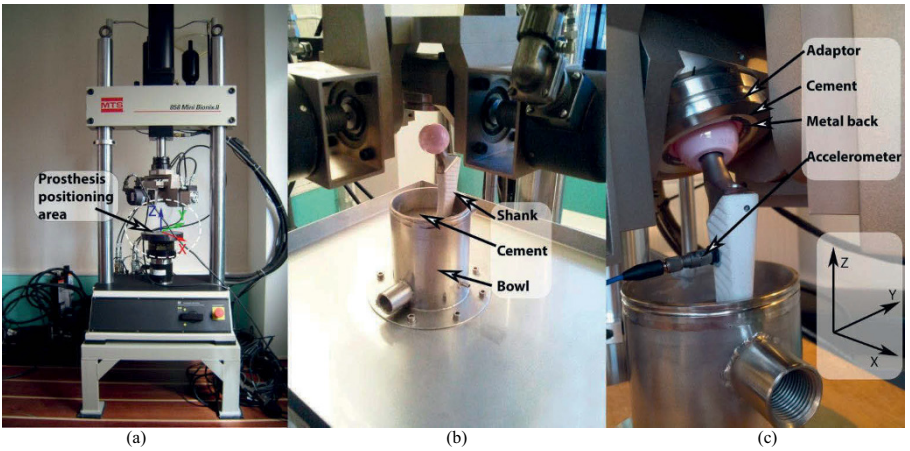

(a) (b) (c)

Figure 3: MTS 858 Mini Bionix II gait simulator

3.3- Trials and first results

Standardized tests were performed on the MTS device. The angle and frequency of 1Hz are consistent with those defined by the ISO-14242-1 standards. To validate the device control, a sensor for measuring the mechanical loads (i.e. the vectors corresponding to the force and the moment) has been added under the steel bowl supporting the cemented stem. This particular experimental sensor was developed by [**C3**]. Due to technical limitations of the sensor, it was decided to proportionally reduce the loading curve (Figure 2, b) from 3000 to 1500N. A THI used for the experiments corresponds to the *Exclusif* model commercialised by *ATF* company. The prosthetic head and the insert have a diameter of 32mm and are made of zirconium oxide ceramic (ZrO_2). The parts undergo cleaning with ethanol once mounted to remove any particles that could pollute the interface.

The aim is to measure the mechanical action wrench over time and observe its evolution. Furthermore the number of cycles at which the THI starts squeaking is wanted.

The squeaking phenomenon appeared after 1180 cycles on the tested implant which is about 20 minutes. The test was immediately stopped in order to assess the implant.

The first force and moment measurements tracked by the device (MTS 858 Mini Bionix II) and the additional load sensor do not allow conclusions to be drawn on evolution of the THI behaviour during the trials. Various reasons explain these difficulties. First, the measured moment values are less than 1Nm while the load values are around 1.5kN. This significant difference in sensitivity between the force and moment values requires the development of a more specific sensor. On the other hand it was found a large disturbance on the load related to the hydraulic actuators that generates vibrations and unwanted movements. These movements related to the rigid mounting generate significant force variations. The control system tends to regulate the load imposed during the cycles and generates significant instabilities. These points make difficult to obtain any operating results.

It was then decided to create a new testing device to compensate these problems.

4- Development of a new device

4.1- Device presentation

An in vitro approach has been decided upon to study the squeaking phenomenon, through a system which is free to move in order to minimise any external disturbances during the measurements. A mechanism of a free swinging pendulum-like motion has therefore been developed, consisting of a metal frame and a swing. The swing is attached to the frame with a total hip prosthesis that acts as a ball joint (Figure 4).

The prosthetic head is fitted onto a cemented femoral stem. This assembly is screwed onto a movable support. The implant metal-back is embedded in a synthetic cortical bone plate. This assembly is attached to the metal frame by two screws. The upside down position of the prosthesis (acetabulum below) simulates more closely the in vivo kinematics of the prosthesis where the femoral part (stem + head) is moving.

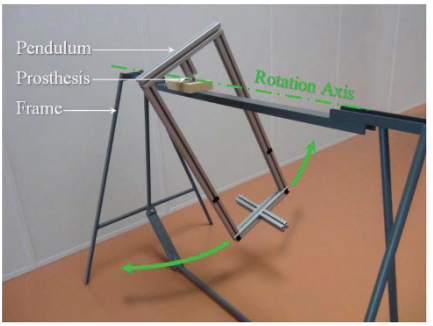

Figure 4: Presentation of the device: the pendulum

4.2- Associated means of measurements

To measure the oscillation angle of the pendulum a method of video tracking was chosen. Sights were glued onto the pendulum and a video camera carrier has been designed to allow filming the tests. Data post-processing was performed on the Matlab ® software.
In parallel, a sound recording is made during the test. The advantage of this measure is that it make possible a analysis of the sound signature of the squeaking phenomenon. If this phenomenon appears during the trails, it is then possible to compare the obtained frequences and typical frequencies identified in the literature both during in-vitro and in-vivo tests. This will confirm that the identified phenomenon corresponds to the squeaking. Typical identified frequencies in the literature are between 1500 and 7500Hz, from measurements of Sariali and Currier (respectively **[SS1]** and **[CA2]**).

5- Tests and associated results

5.1- Description of the tests

The Total hip prosthesis used in these studies is identical to the one previously tested, described in section 3.1. It corresponds to the model *Exclusif* sold by *ATF*. The prosthetic head and the insert still have a diameter of 32mm and are composed of ceramic alumina Al_2O_3.
A typical test is to manually move the arm of the pendulum (lying at rest in the vertical position). The user then releases the pendulum which starts to oscillate. The user allows the pendulum to oscillate until it stops. The measurement of the variation of the amplitude of an oscillation, from one oscillation to another allows quantification of the energy dissipation linked to the frictional force work.

5.2- Results

Table 1 shows different tests. We find in the columns the values of head diameters (diam. in mm), the applied load to the pendulum (Weight in kg), the initial angle of the pendulum (init. angle in mrad) and finally the end time of oscillation (T in s).

Ceramic type	Diam. (mm)	Weight (kg)	Init. angle (mrad)	T (s)	Ang. dec. ($mrad.s^{-1}$)
Al_2O_3	28	6	291	28	11.4
Al_2O_3	28	26	213	45	4.8
Al_2O_3	28	56	270	38	6.9
Al_2O_3	**28**	**6**	**226**	**7**	**36.7**

Table 1: list of results from the trials on the pendulum

The three first rows of Table 1 correspond to three tests in which the load on the pendulum has increased from 6, to 26, to 56kg. The last line corresponds to a test with a load of 6kg with squeaking.
Figure 5 shows the results of two tests obtained with a load of 6kg with and without squeaking (respectively Figure 5a, and Figure 5b). In both cases the displacement follows a sinusoidal curve which reflects the behaviour of a rigid pendulum with damping.

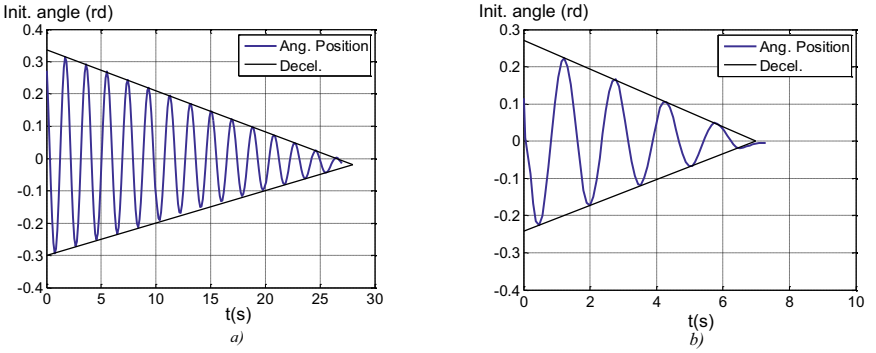

Figure 5: Evolution of the pendulum amplitudes versus time for a 6kg load. a) without squeaking; b) with squeaking.

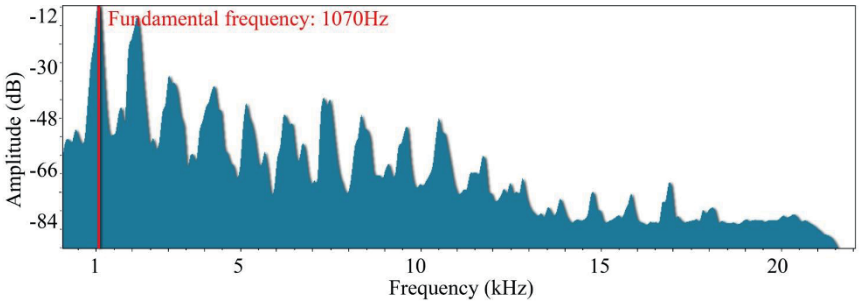

Figure 6: Spectral decomposition of the squeaking sound produced by the pendulum

From the measurements, one can observe that the loss of amplitude from one oscillation to another decreases linearly. This reflects the behaviour associated with dry friction dissipation in the ball joint. It is then possible to calculate for each test an average angular deceleration versus time (Ang. dec. in mrad.s^{-1}). The values obtained are given in the last column of Table 1. These decelerations are drawn in black colour on Figure 5. In addition, it shows that the viscous friction of the air on the pendulum during the test is negligible.
The last line of Table 1 represents a test with squeaking, it may be noted that the oscillations of the pendulum are similar to those obtained in the case without squeaking. However the calculated deceleration value is higher passing from 11.4mrad.s to 36.7mrad.s for the same test without squeaking. This dramatic increase is due to the change in behaviour (regular friction at the hinge) to a jerky motion generating vibrations. When the sound from this test is analysed the decomposition of the signal reveals a fundamental frequency located at 1070Hz (Figure 6). This value is close to what is found in the literature (presented in section 4.2).

This unusual prosthesis behaviour leads to greater energy dissipation since it results from friction effects and generation of vibrations.

5.3- Overview

With the set up based on a free movement, it is possible to test the prosthesis in speed conditions close to a normal human step by varying the loading. It is possible to obtain tests with or without squeaking - the device does not clearly define the conditions that lead to having the squeaking phenomenon. It is important to note that no specific intervention was made and that there was no particle deposition made to force the appearance of the phenomenon. We have found that cleaning the prosthesis with a soaked ethylene cloth is enough to remove the squeaking in the following test.
In the following section, it is proposed to establish an analytical model of the pendulum to compare the experimental results and those obtained analytically.

6- Establishment of the analytical model

6.1- Development of an analytical modal for a hinge with no gap

Modelling associated to a weighted pendulum's behaviour is relatively classical in mechanics. To simplify the study it is necessary to develop specific hypotheses. It is therefore assumed: i) a punctual contact is maintained during movement of the hinge and that the connection is free of gap; ii) the defects of the friction part surfaces are neglected; iii) that the frictional behaviour is characterised by Coulomb model; iv) the movement is assumed to be planar; v) Damping effects are considered negligible due to the shape of the obtained experimental curves (the deceleration being linear).
In the literature the values of the friction coefficient of the Al_2O_3 ceramic used for the THI are between 0.04 and 0.15 **[WZ1, MH1, M1]**.
The aim is to write a model allowing linking of the experimental conditions for each test (loads, angular values etc...) and to deduce the value of the friction coefficient. If this value is close to that given by the literature, it will validate the formulated hypotheses.

6.2- Analytical model

Applying Newton's second law to the system and assuming small oscillations, the following equation is obtained:

$$I_{(O,x)}.\ddot{\theta} + m.g.L.\theta = C_f.signum(\dot{\theta}) \qquad (1)$$

with m the pendulum mass, g the acceleration L the length of the swing and $C_f = f.F.r$ where F is the force applied on the pendulum at the contact point, r the sphere radius and f the friction coefficient.
We can deduce from this equation the pendulum's oscillation period:

$$T_0 = 2\pi\sqrt{\frac{I_{(O,x)}}{m.g.L}} \qquad (2)$$

The general solution of a weighted oscillating pendulum is given depending of each half-period i by the following equation:

$$\theta_i(t) = \left(\theta_0 - c.(2i-1)\right).\cos(\omega_0.t) - c \qquad (3)$$

With the assumption of small disturbances the value of F can be approximated by the weight value (small angles).
Then $C_f = m.g.f.r$, and

$$c_{Theor} = \frac{C_f}{m.g.L} = \frac{f.r}{L} \qquad (4)$$

In addition, one can calculate the experimental torque on the hinge:

$$c_{Exp} = \frac{T_0.\theta_0}{4.t_{end}} \qquad (5)$$

The theoretical friction coefficient on this punctual contact model is calculated using the above equations with experimental results for each test:

$$f = \frac{L.T_0.\theta_0}{4.t_{end}.r} \qquad (6)$$

Where L is pendulum arm [centre of rotation - centre of gravity], r the prosthetic head radius, T_0 the period, θ_0 the initial angle and t_{end} the motion duration.

6.3- Friction coefficient calculation

Using equation (6) obtained in the preceding paragraph and the test conditions it is possible to calculate the friction coefficient f. For these tests the period is measured from each test result, the radius of the prosthesis (r) equals 14mm and the value L is calculated based on the weight of the swing and additional masses. The results are given in Table 2.

Ceramic type	Diam. (mm)	Weight (kg)	Init. angle (mrad)	t_{end} (s)	f
Al_2O_3	28	6	291	28	0.13
Al_2O_3	28	26	213	45	0.12
Al_2O_3	28	56	270	38	0.14
Al_2O_3	**28**	**6**	**226**	**7**	**0.31**

Table 2: Friction coefficient calculation regarding testing conditions.

Regarding the three first lines of Table 2, which correspond to oscillations without any squeaking, we can note that the values obtained for f are between 0.12 and 0.14. These values fall within the range given in the literature [0.04, 0.15]. Applying this same relationship to the test with squeaking the calculated friction coefficient is around 0.3. This coefficient is higher and reflects the two phenomena noted during the squeaking (friction effect and vibrations). We then speak of apparent friction coefficient since it combines two dissipative phenomena that are not of the same nature.

6.4- Overview

These initial results are interesting since it allows testing of the behaviour of THIs through a simple device based on free oscillations. Moreover the associated model is relatively simple and can be validated by comparison of the friction coefficient reported in the literature.

We can note that the obtained coefficient values appear to be high. It would be advantageous to enrich the behaviour models taking into account the phenomena of local deformations of the contact surfaces and the value of the radial clearance between the two rubbing part surfaces. Although the composite materials used are very rigid, small local deformations generate greater frictional torque and are likely to result in a lower friction coefficient.
Finally it has been shown that there is a significant change in behaviour of the hinge between a movement with or without squeaking. During the test the frequency of the emitted sound was constant while the angular velocity was varying. This observation allows determination of some information concerning the causes of squeaking occurrences.
From a mechanical point of view the instability of the movement of one surface on another can be caused by various phenomena which are related to the contact pressure between solids, the surface state (roughness) and the relative velocity of one solid over another.
If a roughness noise (developed for instance by (**[A1]**)) is assumed it means that the frequency of the sound should vary depending on the relative speed of the rubbing surfaces. Other instability hypotheses have been made in other studies, for example movements like stick-slip or sprag-slip in [**C2**]. From the results obtained it is possible to conclude that the resulting sound correspond to a vibration of the structure parts. The unstable movement (stick or sprag-slip) would lead to an excitation of the structure and some eigenmodes of the structure would be audible.
These preliminary findings should be confirmed by further testing including putting greater loads on the hinge and also testing other types of composite ceramics such as Al_2O_3/ZrO_2.

7- Conclusions

The aim of the work presented in this paper is to establish an in-vitro test device of THI. Initially tests were made on a walking simulator conventionally used for THI wear testing. The first tests have shown the limits of this particular device linked to the control system and movement imposed by the device. A new testing device based on a pendulum -type mounting was then proposed. The hinge between the fixed part and the movable part of the pendulum is then achieved by a THI. It is easy to apply different loads on this assembly. The measurements associated with the trials are based on a video camera tracking the swing movements to measure the angular change with time. Various tests were carried out with or without squeaking. It is possible to see that the movement corresponds to an oscillation of a pendulum with dissipation. Such dissipations are related to friction between the ceramic surfaces of the prosthesis. It was proposed to establish an analytical model of the pendulum behaviour which is validated by calculating the friction coefficient.
A trial has highlighted the influence of squeaking during movement. Energy dissipation is then much larger and the apparent friction coefficient has tripled compared to the coefficient calculated without any squeaking. Before each experiment, the prosthesis is wiped with a dry tissue in order to remove any potential third body parts. However, the

conditions creating the squeaking phenomenon have not yet been clearly identified.
In the literature several hypotheses have been proposed to explain the phenomenon of squeaking and a model of behaviour associated. Based on the measurements it appears that only models related to contact instabilities such as stick or sprag slip may be responsible for the phenomenon . The recorded sound during the test corresponds to the resonance parts of the pendulum and the THI.
Different perspectives are considered for this work. First it is necessary to continue the trial campaign with other types of ceramics used by prosthesis manufacturers, but also other models of THI where the head radius and the clearance between parts can change. Tests will also be performed with higher loads nearer to the real applied mechanical stresses on an implanted prosthesis.
A following work concerning analytical models is considered regarding the inclusion of the gap in the hinge, the local deformations and the calculation of pressure fields depending on the position of the prosthesis. This will be achieved through the use of Hertzian contact mechanics.
Finally we noticed that if THI was squeaking while moving during testing, cleaning the rubbing surfaces is enough to eradicate the phenomenon. On the contrary when there is presence of squeaking during the movement, the squeaking reappears systematically as soon as the pendulum begins to swing. This phenomenon may be caused by the presence of particles which are removed during cleaning. To conclude on the presence of particles some investigations using a microscope device will be established to look for the presence of these particles and identify their nature.

8- Acknowledgements

This work is part of a collaboration between three laboratories: SYMME in Annecy, I2M-IMC of Bordeaux and Tural company located in Marignier (74 - France), an industrial research laboratory working on medical implants.

9- References

[A1] Abdelounis H. B., Le Bot A., Perret-Liaudet J., Zahouani H., An experimental study on roughness noise of dry rough flat surfaces, Wear, Volume 268, pp 335-345, 2010

[A2] Avicenne (2005). Avicenne développement - european orthopaedics market.

[BD1] Back, D. L., Dalziel, R., Young, D., and Shimmin, A. (2005). Early results of primary birmingham hip resurfacings. an independent prospective study of the first 230 hips. *The Journal of bone and joint surgery. British volume*, 87(3) :324–329. PMID : 15773639.

[BW1] Brockett, C. L., Williams, S., Jin, Z., Isaac, G. H., and Fisher, J. (2012). Squeaking hip arthroplasties. *The Journal of Arthroplasty*.

[C1] Charnley, J. (1979). Low friction arthroplasty of the hip: theory and practice; Springer.

[CT1] Chevillotte, C., Trousdale, R. T., Chen, Q., Guyen, O., and An, K. A. (2009). The 2009 frank stinchfield award hip squeaking : A biomechanical study of ceramicon- ceramic bearing surfaces. *Clinical Orthopaedics and Related Research*, 468(2) :345–350.

[CT2] Chevillotte, C., Trousdale, R. T., Guyen, O., Chen, Q., Berry, D. J. and An K. A. (2008). Etude expérimentale des phénomènes de grincement ou "squeaking" avec les couples de frottement céramique/céramique dans les prothèse totales de hanche. *Journées Lyonnaises de chirurgie de la Hanche.*

[C2] Coudeyras, N. (2009). Analyse non-linéaire des instabilités multiples aux interfaces frottantes : application au crissement de frein. PhD thesis, Ecole Centrale de Lyon.

[C3] Couétard, Y. (2000). Caracterisation et etalonnage des dynamometres a six composantes pour torseur associe a un systeme de forces. PhD thesis, Université Sciences et Technologies-Bordeaux I.

[CA2] Currier, J. H., Anderson, D. E., and Citters, D. W. V. (2010). A proposed mechanism for squeaking of ceramic-on-ceramic hips. *Wear*, In Press, Corrected Proof.

[ER1] Ecker, T., Robbins, C., Flandem, G. V., et al. (2008). Squeaking in total hip replacement : No cause for concern. *Orthopedics*, 31(9) :875.

[EM1] Eickmann, T., Manaka, M., Clarke, I. C., and Gustafson, A. (2003). Squeaking and neck-socket impingement in a ceramic total hip arthroplasty. *Key Engineering Materials*, 240 :849–852.

[EW1] Esposito, C., Walter, W. L., Campbell, P., and Roques, A. (2010). Squeaking in metal-on-metal hip resurfacing arthroplasties. *Clinical Orthopaedics and Related Research*, 468(9): 2333–2339. PMID : 20383616 PMCID: PMC2919861.

[F1] Feder, B. J. (2008). That must be bob. i hear his new hip squeaking. *The New York Times*.

[H1] Hausselle, J. (2007). Etude de la dégradation par chocs de têtes et cupules de prothèses de hanche en biocéramique. PhD thesis, Ecole Nationale Supérieure des Mines de Saint-Etienne.

[HB1] Hing, C. B., Back, D. L., Bailey, M., Young, D. A., Dalziel, R. E., and Shimmin, A. J. (2007). The results of primary birmingham hip resurfacings at a mean of five years. an independent prospective review of the first 230 hips. *The Journal of bone and joint surgery. British volume*, 89(11) :1431–1438. PMID : 17998177.

[HW1] Holloway, I., Walter, W. L., Zicat, B., and Walter, W. K. (2009). Osteolysis with a cementless second generation metal-on-metal cup in total hip replacement. *International Orthopaedics*, 33(6) :1537–1542. PMID : 18985349 PMCID : PMC2899158.

[I1] ISO-14242-1 (2012). Implants chirurgicaux – Usure des prothèses totales de l'articulation de la hanche – Partie 1 : Paramètres de charge et de déplacement pour machines d'essai d'usure et conditions environnementales correspondantes d'essai.

[MH1] Mann, D. J. and Hase, W. L. (1999). Computer simulation of sliding hydroxylated alumina surfaces. *Tribology Letters*, 7(2-3) :153–159.

[M1] Mann, D. J., Zhong, L., and Hase, W. L. (2001). Effect of surface stiffness on the friction of sliding model

hydroxylated α-alumina surfaces. *The Journal of Physical Chemistry B*, 105(48) :12032–12045.

[SS1] Sariali, E., Stewart, T., Jin, Z., and Fisher, J. (2010c). Three-dimensional modeling of in vitro hip kinematics under micro-separation regime for ceramic on ceramic total hip prosthesis : An analysis of vibration and noise. *Journal of Biomechanics*, 43(2) :326–333.

[SP1] Swanson, T. V., Peterson, D. J., Seethala, R., Bliss, R. L., and Spellmon, C. A. (2010). Influence of Prosthetic Design on Squeaking After Ceramic-on-Ceramic Total Hip Arthroplasty. *Journal of Arthroplasty*, 25(S) :36–42.

[WO1] Walter, W. L., O'Toole, G. C.,Walter, W. K., Ellis, A., and Zicat, B. A. (2007). Squeaking in ceramic-on-ceramic hips : The importance of acetabular component orientation. *The Journal of Arthroplasty*, 22(4) :496–503.

[WZ1] Wei, D. and Zhang, Y. (2009). Friction between α-Al_2O_3(0001) surfaces and the effects of surface hydroxylation. *Surface Science*, 603(16) :L95–L98.

Article 075-pds-78

SERIAL MANUFACTURING OF LIGHTENED CERAMIC FLOORINGS AND INDIRECT CALCULATION OF ENERGY SAVING

B. Defez [1], G. Peris-Fajarnés [1], R. Martínez-Díaz [2], L. Monreal Mengual[1], F. Brusola Simón [1]

(1) : Centro de Investigación en Tecnologías Gráficas, Universitat Politècnica de València
+34963879518
{bdefez,gperis,lmonreal,fbrusola}@upv.es

(2) : Universitat Politècnica de València
+34963877920
rmartin@cc.upv.es

Abstract: The optimization of the tile structure through different kinds of back reliefs is a new approach for the improvement of the tile industry, since these floorings could be manufactured with less support material and so they require less process energy. We have tested the viability of the serial production of lightened tiles, whose design is based in conclusions of previous theoretical works. Here we report genuine manufacturing handicaps and measure real energy savings. After our study, we conclude that these tiles could be produced with current technologies. A cut within 14 and 25% while firing is estimated.

Key words: ceramic tile, back structure, energy savings.

1. Introduction

Ceramic tiles lightened by the execution of a deep back relief could be manufactured with substantially less raw material than the traditional ones, which has an effect not only in the saving of bulk material (mass), but also in the saving of production and transport energy. Additionally, a lighter product could be attractive to producers and builders, since it improves the working conditions on the shopfloor and at the building site due to the handling of lighter bodies. Nevertheless, lightened tiles are structurally different from the conventional one, and so should be their mechanical and thermal behaviour. Because it is a constructive element it is necessary to know its response under typical loads to assure that it accomplishes with the valid standards.

Previous researches show that deep back relief tiles could simultaneously improve mechanical and thermal features. Main conclusions of these works are that deep reliefs could save from 2 up to a 31% of mass, and could equal and even improve the structural capabilities of ordinary ceramic tiles **[DP1] [DP2].**

2. Objective of the research

Our research aims at testing the viability of the serial production of lightened tiles and investigating their bending response, based in conclusions of previous theoretical works. We report genuine manufacturing handicaps and measure real flexural strength of the products **[AE1].**

We have considered the influence of the different decoration technologies as much as firing cycles to evaluate the goodness of lightened floorings. These variables have been considered in order to establish in which conditions lightened models provide a more satisfactory performance. The influence of the different firing cycles on the mechanical performance of a ceramic tile has been widely studied **[MR1] [MD1] [MR2] [OE1]**. However, it has never before been correlated with geometric changes of the back surface. On the other hand, the repercussion of the different decoration technologies in the behavior of the products is a new field of research.

3. Experimental procedure and results

In order to achieve the objectives of our research, we designed a set of standard and lightened tiles and make them underwent several production phases and quality controls through a real manufacturing line.

Besides, we developed an indirect method to estimate the real energy saving obtained in the kiln, based in the employment of the two indicators: percentage of water absorption (%W.A.) and percentage of linear contraction (%L.C).

In the following paragraphs, this methodology is explained.

3.1. Representative models

A common paste was prepared for all models. This was a typical mixture for stoneware floorings: feldspathoids 29%, semiplastic clays 20%, kaolinitic clays 16%, plastic clays 12%, quarz 12%, feldspars 8% and talc 2%.

All flooring models were pressed with a force of 355 Kg/cm^2 with hydraulic press of two exits. They had a format of 50*50 cm^2, and a thickness of 10 mm. Apparent density was to be 2.04 g/cm3, whereas average water absorption (%W.A.) and linear contraction (%L.C.) were 0.01% and

Article 075-pds-78

7.02% respectively. Parts were dried for 15 minutes at 300ºC in a vertical drying shed. Afterwards, they underwent the decoration and firing phases, as it will be explained later on.

In terms of geometry, 2 different models were considered: one with a conventional relief (parallel strips of less than 1mm depth) and another one with a deep relief. The chosen geometry for the deep relief was the honeycomb tessellation (hexagonal net). Nominal parameters of this particular structure were relief depth 6mm and wall angle 70º. With such geometry, carved tiles were about a 20% lighter than conventional ones.

This choice was based in the results obtained in previous researches. In these works, the honeycomb structure offered the best ratio "mass saving/mechanical performance". Therefore it was designated as the most convenient structure in comparison with other proposed geometries. A view of the relief is given by Figure 1.

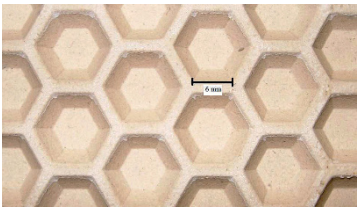

Figure 1: Honeycomb structure

For the serial production and quality tests designed in this experiment, 16 samples were prepared, 8 standard and 8 lightened. For the estimation of the energy consumption inside the kiln, 28 samples more were conformed, 14 standard and 14 lightened. Manufacturing lightened and commercial models together would bring us to obtain conclusions by comparison.

The amount of samples may seem low for a scientific work. However, it is important to bear in mind that trials were performed using real production means, in the facilities of the collaborating enterprise Keros Ceramica S.A., of the Spanish ceramic cluster of Castellón (Spain). Therefore, time and resources for the execution of the tests were very limited.

3.2. Serial production and quality tests

We designed several suitability tests in order to check the real problematic of the serial manufacturing of lightened models.

In particular, we pay attention to the decoration and firing phases, which are the ones which require the most demanding mechanical and thermic features in the manufacturing process. We also calculated the quality parameter "Flexural strength" to determine the appropriateness of these new products with regard to the international standardization.

1.1.1. Glazing and decoration test

We established 4 groups of 4 parts (2 conventional and 2 carved). Each one of them underwent a different decoration technique, namely: non-decoration, serigraphy, rotocolor and milling machine, which are the most common decoration mechanism on the sector.

After decoration, a visual check was carried out. We decided to opt for this kind of test instead of micrography or non-invasive internal recognition through ultrasound of thermography, in order to represent real in-line quality controls. None of the parts presented cracks or fractures.

1.1.2. Firing test

In order to evaluate the response of the parts inside the kiln, a typical firing cycle was programmed for the 16 parts. Table 1 shows the details of this cycle:

FIRING CYCLE		
Maximal temperature (ºC)		1190
Cycle time (min)	Preheating	26
	Baking	5
	Cooling	24
	TOTAL	55

Table 1: Firing cycle details

After firing, a visual check was carried out on each part. Two kinds of defects were found out. First, we detected peripheral cracks in both decorated and back surfaces. Mainly, these cracks were about 1-2cm long and crossed the whole thickness of the tile. It was easily observed that back cracking started in the lateral edges of the part, and then expanded towards the internal edges of the relief. The recurrence of these defects was about a 2%. Figure 2 and 3 exposed an example of these fractures.

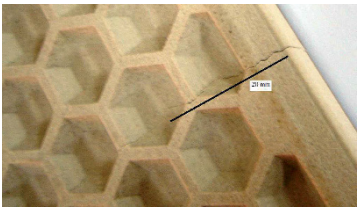

Figure 2: Peripheral crack at back structure

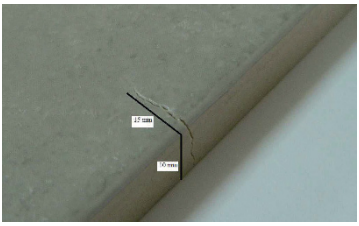

Figure 3: Peripheral crack at decorated surface

Secondly, the external surface of the back relief was damaged by the action of the rollers of the kiln. According

Article 075-pds-78

our calculation, about a 3% of the parts presented this problem, with a percentage of damaged surface on each of them of near a 5%. Figure 4 shows one of the damaged parts.

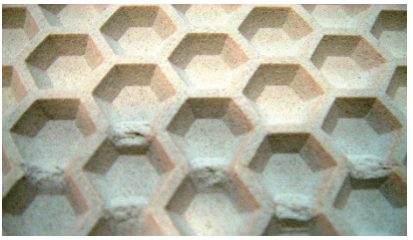

Figure 4: Damage of the external surface of the structure

We compared these percentages with those obtained by the analysis of the historical quality control data of the collaborating enterprise Keros S.A. After this study we could state that the typology and recurrence of the defects were completely usual.

1.1.3. Flexural strength test

For the evaluation of the flexural strength (R) of ceramic floorings, the international standard ISO 10545-4 establishes a mechanic test. In this test tiles are placed upon two metallic cylinders covered by hard rubber (50±5 IRHD, ISO 48), located at a distance that depends on the width of the product. Then, a vertical load is applied on the upper surface, along the middle section, through another cylinder of the same characteristics. The charge should be augmented 1±0.2 N/mm^2 per second up to the fracture of the tile. Once the part has collapsed, R can be calculated as follows:

$$R = \frac{3FL}{2bh^2}$$

Where "F" is the force applied at the fracture point, "L" is the length of the support span, "b" is the width of the tile and "h" is its thickness at the fracture section. As h is considered as constant, the formula can only be directly used considering either the minimal or the maximal thickness of the relief. In fact, the standard itself pointed out that in the case of irregular reliefs, the minimal thickness at the fracture section could be used, as an approximation to the problem.

The calculation of the flexural strength was performed just for the lightened models. Numeric values of R should meet the international standard. Therefore, for green tiles, R should be within the interval [1, 6] N/mm2, while for fired tiles, the interval would be [18, 50] N/mm2.

We verified that lightened models meet these requirements before baking. Nevertheless, fired tiles presented a slightly lower R when considering the maximal thickness. On the other hand, the consideration of the minimal thickness conducted to extremely high values of R, also difficult to justify under real performance conditions.

Since either of the extreme values of the thickness (maximal or minimal) seemed to provide satisfactory and realistic results, we propose the employment of the average thickness, which could be calculated as:

$$h_{average} = \frac{h_{Maximal} + h_{Minimal}}{2}$$

A detailed summary of all the commented results is given by Table 2.

FLEXURAL STRENGTH R (N/mm2)					
MANUFACTURING PHASE	THICKNES	DECORATION TECHNOLOGY			
		Non decorated	Serigraphy	Rotocolor	Milling machine
GREEN TILE	maximal: 10.00 mm	1.85	1.96	1.94	1.93
	minimal: 6.15 mm	4.90	5.18	5.12	5.11
FIRED TILE	maximal: 9.30 mm	16.66	17.76	16.59	17.34
	minimal: 5.70 mm	44.34	47.27	44.15	46.15
	average: 7.50 mm	25.62	27.31	25.51	26.66

Table 2: Average flexural strength for green and fired lightened tiles

The employment of the average thickness for the calculation of the flexural strength is not taken into account by the ISO so far. This is due to the lack of deep back relief tiles until now. Our research group is currently working in the recompilation of evidences in order to propose this change in the standard ISO 10545-4.

3.3. Energy consumption estimation

As previously said, carved models considered in our research were about a 20% lighter than conventional ones. A similar percentage of energetic saving during the firing phase was expected and needed to be confirmed experimentally.

However, this experimental confirmation was not easy to carry out. Continuous kilns have a very high thermic inertia and work 24/7 for years, until repair or substitution is mandatory. So, the volume of natural gas employed in the baking of a particular model is virtually impossible to determine with accuracy, especially when there is not a separate counter for the kiln, which was our case. Moreover, the size of the furnace (97m long) and the speed of baking (1.845m/min), involved an important source of inaccuracy.

Due to the difficulties of a direct measuring just reported, we employed the indirect readings of %W.A. and %L.C. for estimation, with the aim of checking the level of stoneware-vitreous growth.

We designed 7 different firing cycles, equal to the cycle

Article 075-pds-78

programmed for the firing test, but with different peak temperatures. These cycles were thought to assure uniform firing and controlled shrinkage for any type of tile, since the times considered for preheating, baking and cooling were long enough according to our experience.

A set of 28 tiles was conformed, 14 standard and 14 lightened. All parts had the same characteristics of those used in the rest of the trials (pressing force 355 Kg/cm^2 format 50*50 cm^2, thickness 10 mm, and apparent density 2.04 g/cm3). In order to simplify the experiment, none of these tiles were decorated.

2 standard tiles and 2 carved models were baked for each cycle. The calculations of both parameters were made as described by the international standard ISO 10545-3 and ISO 10545-8. Table 3 shows the average results obtained by this procedure:

CICLE		STANDARD		LIGHTENED		INCREASE %L.C. LIGHTENED to STANDARD	DECREASE %W.A. LIGHTENED to STANDARD
NUMBER	T(ºC)	%L.C.	%W.A.	%L.C.	%W.A.		
1	1120	1.76	8.71	2.74	8.18	36%	6%
2	1140	3.14	5.50	4.04	6.29	22%	-14%
3	1160	3.91	4.01	4.58	4.36	15%	-9%
4	1180	6.77	1.91	7.00	1.81	3%	5%
5	1200	6.80	0.94	7.31	0.77	7%	18%
6	1220	6.84	0.47	7.39	0.06	7%	88%
7	1240	6.88	0.18	7.38	0.03	7%	81%
GLOBAL AVERAGE						14%	25%

Table 3: Average %LC and %W.A. for standard and lightened tiles at 7 different kiln cycles used to estimated firing energy consumption

Globally, the increase of %L.C. of lightened models with regard to the conventional one is around a 14%. As per %W.A., the decrease is about a 25%. Considering these two factors, we can set up that the vitreous phase grows within a 14-25% faster in carved models. Therefore, an energy saving in this range is realistic. The hypothesis of an energy cut equal to the mass descent has been proved to be adequate, since our first calculation placed this value at around a 20%.

4. Conclusions

After the research here presented, we are able to set out several remarkable conclusions.

On one hand, we have proved that lightened models could be manufactured with current technology. Decoration and firing phases, which were said to be the most conflictive for the response of the new structure, have been successfully overcome. Quality defects found in both decorated and back surfaces were typical defects of ceramic tiles, so they were not related to the structure.

With regard to the flexural strength, which is a basic quality parameter in the tile industry, lightened models meet the standard ISO 10545-4 in green state. In the case of baked floorings, R is totally dependent on the value considered for the thickness. For a more fair calculation, here we propose the employment of the average thickness. Under this hypothesis, fired models also meet the international rule. The employment of the average thickness for the calculation of the flexural strength is not taken into account by the ISO so far. This is due to the lack of deep back relief tiles until now. Our research group is currently working in the recompilation of evidences in order to propose this change in the standard ISO 10545-4.

Finally, we have introduced an indirect method to control the firing energy consumption of a new ceramic model. This method could be used as a design parameter in the development of any kind of ceramic product. By means of this method, we have checked that lightened models actually save an interesting amount of energy while firing. Bearing in mind the price of natural gas and the need for meeting the Kyoto protocol, an average energy cut within 14-25% is more than encouraging. This value is in accordance with the 20% initially estimated, which was proportional to the mass reduction in the lightened models.

Just to sum up, it is to be stressed that enterprises could invest in the definition of new back structures for their products. With these structures, they could assure optimal mechanical and thermic features, and a considerable saving of raw materials and energy consumption, without modifying their production lines and means.

5. Discussion and further research

Although our research has proved that lightened models vitrified faster than conventional tiles, it would be interesting to evaluate the correlation between mass and energy savings. The increase of contact surface between part and furnace atmosphere due to the back structure should in theory facilitate sintering, diffusion and degasification processes. Therefore, an energy saving higher than the one strictly proportional to the mass descend is expected. Hence, it might be possible to find a rule to establish the most convenient structure and mass to reduce the energy consumption to a minimum.

Also necessary would be to compare these results to those provided by standard tiles of equivalent mass, that is to say, thinner standard floorings (thickness from 10 to 6 mm). Comparing energy consumption and mechanic response of both kinds of products would enhance the real advantages of carved floorings.

Currently under research is the possibility of injecting low density materials in the empty spaces generated by the structure, once the tile has been fired. First, these materials could come from the waste of other industries, such as the tire manufacturing sector. Then, lightened coverings could help to an environmentally friendly management of non-dangerous residual matter. Secondly, injected tiles are expected to present new and allegedly better attributes than conventional and lightened tiles. Serial injection would be a

j

process to solve in advance. Laboratory prototypes, where different kinds of foams have been manually injected and cured, have shown interesting properties such as high thermal and acoustic insulation and very low density. Nowadays, a new project is been defined to explore the possibilities of these tiles.

6. References

[DP1] B. Defez, G. Peris-Fajarnés, I. Tortajada, L. Dunai, F. Brusola, "Optimal design of deep back relief in ceramic floorings by means of the finite element method", J. Ceram. Soc. Jpn., (2008); 116(1357):941-9

[DP2] B. Defez, G. Peris-Fajarnés, I. Tortajada, F. Brusola and S. Morillas, "Flexural strength of non-constant thickness ceramic floorings by means of the finite element method", Int. J. Appl. Ceram. Technol., (2009); in press.

[AE1] International and Spanish Standard UNE-EN ISO 10545, Spanish Association for Standardization and Certification (AENOR), 1997.

[MR1] Martín-Márquez J., Rincón J.M., Romero M., Effect of firing temperature on sintering of porcelain stoneware tiles, Cer. Int., 34(8):1867-1873, 2008.

[MD1] Martín-Márquez J., De la Torre A.G., Aranda M.A.G., Rincón J.M., Romero M., Evolution with Temperature of Crystalline and Amorphous Phases in Porcelain Stoneware, J. Am. Ceram. Soc., 92 [1] 229–234 (2009)

[MR2] Martín-Márquez J., Rincón J., Romero M., Mullite development on firing in porcelain stoneware bodies, Journal of the European Ceramic Society, 30(7):1599-1607, 2010

[OE1] Orts M.J., Escardino A., Amorós J.L., Negre F., Microstructural changes during the firing of stoneware floor tiles, Appl. Clay Sci. **8** (1993), pp. 193–205

[AE2] International and Spanish Standard UNE-EN ISO 10545-4 Determination of modulus of rupture and breaking strength, Spanish Association for Standardization and Certification (AENOR), 2012.

[AE3] International and Spanish Standard UNE-EN ISO 10545-3 Determination of water absorption, apparent porosity, apparent relative density and bulk density, Spanish Association for Standardization and Certification (AENOR), 1997.

[AE4] International and Spanish Standard UNE-EN ISO 10545-8 Determination of linear thermal expansion, Spanish Association for Standardization and Certification (AENOR), 1997.

Article 078-cadcae-65

Pretension influence on metallic shear joints

Taha BENHADDOU [1], Alain DAIDIE [2], Pierre STEPHAN [3], Jean GUILLOT[4], Clement CHIROL[5], Jean-Baptiste TUERY [6]

(1)(2)(3)(4): Institut Clément Ader - Insa de Toulouse
135 avenue de Rangueil - 31077 Toulouse Cedex 4
05.61.55.99.68
E-mail : {taha.benhaddou, alain.daidie@insa-toulouse.fr}
pierre.stephan@univ-tlse2.fr

(1)(5)(6): Airbus Operations SAS
316 Route de Bayonne. 31060. Toulouse Cedex 9
E-mail :{Taha.benhaddou, Clement.chirol , Jean-baptiste.tuery}@airbus.com

Abstract: Bolted joints are one of the most common elements in aerostructures. Currently, the preload applied to join the parts together is achieved by applying torque to the bolt head or to the nut. In the case of shear joints, an emerging opportunity to optimise structural joints is to apply the preload more accurately. Up to now, the preload effect is most often neglected due to the large scatter on its value due to torque tightening. The aim of this article is to describe the effect of preload on shear joints, for this reason, a numerical and experimental approach has been adopted to demonstrate its influence.

In the experimental approach, iterative tightening was used to reduce the scatter on preload. The benefits of preload on high load transfer double lap shear joints will be discussed. In the numerical section, an approach of predicting fatigue life of shear joints is presented. The effect of preload is also studied. Finally, practical aspects like alternative tightening techniques are also presented.

Key words: Preload, bolted joints, fatigue testing, finite elements method, virtual testing.

1- Introduction

Mechanical fastening is the most used technique to assemble aerostructural elements due to several advantages: it is a relatively low cost process that allows the joining (and the unjoining) of multimaterial parts, it permits material physical discontinuity so that fatigue cracks propagation may be arrested throughout the joint. In the opposite side, one major drawback is the stress concentration areas created during the holes drilling which may lead to structural fatigue issues.

Currently, the clamping force (or preload) applied to join the parts together is achieved by applying torque to the bolt head or to the nut. In fact, torque specifications can be considered as unreliable because it can often lead to high uncertainties of the amount of preload that has been really achieved whilst preload is the only parameter that can define the joint behaviour under thermo-mechanical loads.

One way of improving structural efficiency is to ensure an accurate preload during fasteners installation. In the case of shear joints for example, mastering the load transfer mechanisms and ensuring their efficiency is the best way to optimize existing components and obtain the most of their function.

In the practical side, accurate pretension is more difficult to achieve than accurate torque: it generally requires an extra step or an extra component to master the pretension but the beneficial effect that can be expected is very significant for some bolted configurations. In addition, breakthrough technologies such as iterative tightening, ultrasonic control or alternative tensioning techniques are mature enough and has proven their applicability via industrial qualification and testing programs.

We will explain in this article why bolt tension really matters in optimized shear joints: the first section presents states of art of preload in bolted joints; in the second section we will present the theoretical background and explanation of involved phenomena. The final part will rely on fatigue and virtual testing of preloaded joints.

2- State of art and preload technology overview

One might observe that the main advances over the last years in civil aircraft sector have been focused into reduction of the aircraft weights and the global costs, increasing simultaneously efficiency, reliability and performance. Optimisation of structural fastener joining processes is one viable way to do it as structures' manufacturing cost represents a large part of the production costs of an aircraft [MW1].

Conventionally, the design of bolted joints is based to a large extent on preload as the main factor that defines the mechanical behaviour of bolted joints. Engineering fundamentals of threaded fasteners analysis such as design guideline VDI 2230 or MSFC-STD-486B design code[T1] determines joint stress thresholds based on preload value and its scatter caused by the tightening technique via the tightening factor. Therefore, in the case of torque tightening, installation and maintenance of fasteners are purely guesswork based on torque measurement and uncertainties that are generated on preload: a variation in installed fastener preload of 30 percent is typical with tightening control methods based on the measurement of applied torque [B1].

In fact, several direct or indirect factors affect the pretension when tightening torque is applied [P1]. In particular, the friction in both the underhead and threaded zones plays a

crucial role in defining the relationship between the pretension and torque and explain to some extent the scatter that can be found in this relationship.

Besides the main benefit linked to the improvement of quality, safety, reliability and performance principally by the decrease of structural weight, some key benefits can be allocated to preload technology and need to be considered in order to evaluate the global added engineering value to preload technology. First of all, it represents an alternative repair solution like other design and manufacturing proposals used to improve fatigue resistance: interference fit, cold expansion, shot peening. In addition, preload process and classical processes like interference or cold expansion are not mutually exclusive and can be added for a maximal fatigue benefit (benefits are non-accumulative[CA1][CA2]). Finally, numerous additional advantages can be addressed: increase fluid tightness (water and dust ingestion), enhance joint integrity (minimize the risk of misalignment, cramping, leaks… [B1]), avoid penetration of corrosion beside the joints, decrease the detrimental effect of secondary bending on joints durability.

In the literature, some experimental works has been dedicated to evaluate the effect of torque tightening on static and fatigue life of shear joints. The beneficial effect of high pretension (via torque application) on fatigue life of shear joints has been physically demonstrated by several authors [CO1] [MV1] [SD1] on specimens subjected to constant amplitude fatigue testing with a load ratio $R=\sigma_{min}/\sigma_{max}=0$. This effect reaches an asymptote after which the fatigue life remains stable and the preload is then limited by the resistance of the association bolt-nut and the admissible bearing pressures underhead.

Conversely, Wagle and Al [WK1] have demonstrated through ultrasonic measures of fretting phenomenon that occurs under high torque levels that fatigue life of specimens appears to decrease if the applied torque is too high. An optimal value of preload for a maximal durability can then be identified [S1]. This example of study shows that the preload must be *precisely* installed in order to optimise the fatigue life and that torque application is not necessary the best method to do so because of its inaccuracy. Moreover, several studies have shown that the friction coefficient between shear plates plays a key role in observed tendencies. Starikov [S2] and De Crovoisier and Al [CS1] indicates a net increase of global friction coefficient in metallic and hybrid joints due to wear mechanisms. Finally, Boni and Al [32] have shown that the sealant application has a detrimental effect on fatigue life of joints due to the decrease of friction coefficient.

Related studies has also been conducted to investigate the preload variation during a static loading or temperature variation, Oskouei et al [BL1] indicates that under a static tensile loading of a double lap shear joint, the preload decreases first due to the Poisson's effect then increases due to the consequent bending of the fastener. In effect, the proportions of these evolutions might be different (or inexistent) depending on the geometrical and materials configurations. The preload loss due to the temperature gradient has also been studied by several authors, including Jaglinski and al. [JN1] who shows that the typical preload evolution under temperature variation conditions is more complex than typical creep or relaxation curves.

Analytical models have also been developed to study the evolution of fasteners flexibility during cyclic loading, one can mention the most used one in bolted joints design proposed by Huth [H1]. In the case of pretensioned shear joints, the calculation proposed by Alkatan et Al [AA1] allow the determination of assemblies flexibilities on the basis of two simulations (or measures) of the assembly in the bearing mode and in the friction mode. This model has been generalized by Andriamampianina et al. [AA2] for multi-bolted joints while considering the non-bearing (by-pass) load transfer mechanism.

Due to rapid increases in computing power and parallelization possibilities in the last years, sophisticated and realistic simulations can be performed and an important number of investigations were conducted with the aid of finite elements method. Pratt and al [PP1] have drawn up a list of fundamental parameters to identify in order to numerically characterize bolted joints via extensive numerical tests. Geoffrey et al [GT1] analysed the influence of bolt-hole clearance while taking into account the friction coefficient effect on bearing interfaces. Paredes and al. [PN1] studied the effect of interference on the preload loss in aeronautical shear joints.

It is important to note that in the case of aeronautical shear joint analysis, the effect of preload is not accounted for due to the fact that preload remains small and that the presence of interface sealant in the interfaces decreases the friction coefficient.

Further numerical studies has been made by Chakherlou and Al on the conjoint influence of interference and torque [CA1]or cold expansion and torque [CA2]and showed an additional enhancement of fatigue life when multiple processes are used. Numerical predictions have also been performed via the application of AFGROW programs or multiaxial fatigue criterion on a basic preloaded specimen (a filled single plate) and shows good agreement between simulations and experiments [CA3]. However, it should be noted that the specimens that has been chosen for fatigue life determination in the studies proposed by Chakherlou do not present enough features to be classified as shear joints because the fastener is not directly involved in the load transmission.

One can also cite a compilation of numerical parametrical studies made to understand the effect of technological processes like interference or pretension on structural shear joints [HR1].To sum up the essential information from this review, the stress distribution is modified around the fastened hole and depending on the preload value, a high portion if not the entire portion is transferred via friction mechanism [PR1]. The initiation point position is also modified: for low preload values, the initiation point is localised in the stress concentration area as the bearing shear joints, when increasing the preload, this position migrates to the exterior of compressed area[S1][KF1]. A similar pattern is found for assemblies with a high level of interference or expansion [HR1].

In the case of composite or hybrid joints, Ekh and al [ES1] modelled the composite bolted joints by approximating bolts to springs or rigid bodies and plates to shell elements which

provided rapid but less efficient numerical models. A few years ago, McCarthy and al [MC1] [MC2] developed 3D numerical models that studied the influence of bolt-hole clearance on the stress distributions in single and double lap composite joints and performed extensive experimental investigation. Stocchi and Al [SR1] developed a detailed numerical model of single lap shear joints made of composite joints in order to characterise the effect of bolt-hole clearance, torque and coefficient of friction on the static behaviour of the joints. Most recently, the same authors [SR2] proposed an experimental method to monitor the loss of preload during the fatigue testing of composite bolted joints, he observed that the clamping force remains constant for most of the joint fatigue life and drops rapidly as the bolt failure progresses.

A last word on the static behaviour of preloaded shear joints which has been considered by some works [BS1] [SR1] and has been showed to be independent of the preload magnitude. A slight improvement of yield load has been noticed but the ultimate strength load is not modified.

Despite these improvements, the effects of several key parameters, such as accurate preload effect, coefficient of friction between plates and its evolution during fatigue testing, effect of bolt-hole clearance and geometrical details on the metallic bolted joint behaviour still need further investigation. The separation of pretension and torque which is also a focal (and original) point of our study is generally not accounted for in most cited works. Hereafter in this work, experimental means that have been used, either for installing or for monitoring, are preload- aimed ones. This means that the scatter on preload value is reduced from about 30% (typical torque tightening scatter) to about 10%.

3- The role of preload in shear joints

3.1 – General considerations

The role of preload may be represented schematically as follows: in the elastic range, the different parts that compose the assembly represented in figure 1 can be assimilated to springs with respective stiffness's: K_B is the stiffness of the bolt (in brown) and K_P is the stiffness of the plates (in blue and green). Before tightening, the equilibrium state is represented in the left of the figure and after tightening, the bolt stretches (extra elongation ΔL_B) and in counterpart the plates compresses with respect to the different stiffnesses. A certain amount of preload F_0 is then established on a constrained length L_C (roughly from under the head to the first thread engaged) and this new state of equilibrium leads to the creation of axial tensile stresses in the bolt shank versus axial compressive stresses in the plates. The distribution of compressive stresses usually forms what is called a compressive cone [B1].

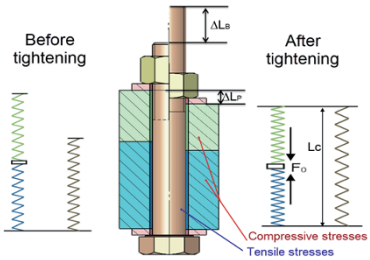

Figure 1: The effect of preload in the general case

As briefly discussed earlier, the correct preload avoids the separation of parts, support a percentage of applied cyclic loads in the fastener for tension joints but most importantly in our case, it introduces compressive stresses through the thickness of metallic joints. The next paragraph will explain why the amplitude of those stresses is determinant for the stress distribution when the joint is externally loaded.

3.2 – Involved mechanisms

Hereafter in this article, the range of joint design that will be covered to illustrate the role of preload in shear joints are mainly high load transfer joints constituted by one or two fasteners that are solicited in double shear and that are mounted with bolt-hole clearance (no interference) in metallic plates. One can see that for the same external load, the proportion of load that is transferred via bearing and friction is different: the load transfer is made by hybrid mechanisms: at a first level the stress carrying capacity of friction is the predominant mode, when the applied stress exceeds the value of friction capacity (monitored only by preload), the plates are expected to slide ending the slip resistant phase.

Analytical formulations that resolves the distribution over bearing and friction exists in the literature, the work carried out by [PR1] is an example that permits to know the predominant load transfer mechanism for different configurations of joint design (i.e. preload, friction, contact surfaces…).. Validated numerical models based on finite elements method can also be used to study this distribution based on the friction coefficients in interfaces and contact surfaces, the preload and the areas in contact…Specifically, current finite elements software (Abaqus® for example which has been used for this study) allows the development of accurate numerical models with several optimized features like modelling of friction, preload (bolt-load function) or several mesh elements types in order to correctly model coupled or uncoupled physical phenomenon.

To illustrate this numerical distribution, let's consider the double lap shear joints composed of one fastener. Bearing load can be obtained by multiplying the contact pressure by the contact elements surface between the bolt and holes. The same can be made for tangential frictional force: the multiplication of frictional shear stress by the contact

element surface between the slip interfaces. A typical distribution of these two mechanisms is given in figure 2: we can observe for slightly loaded joints, the entire load can be transferred by friction: interfacial tractions are created along the clamped interfaces and the applied load is transmitted from plate-to-plate and fastener head-to-plate by friction. The major part is obviously the interface between the different plates because of the largest area of contact.

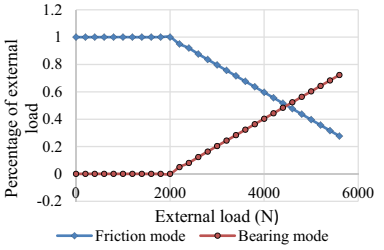

Figure 2: Contribution of bearing and friction modes to the external load transfer

Beyond the load carrying capacity of the friction mode (which is **preload dependent**); the load transfer is accomplished by the combination of a decreasing friction component and a growing bearing component. However, even after the bearing component becomes the major load transfer mechanism, the preload still introduces a beneficial effect by reducing the peak stresses at the stress concentration areas. In fact, the introduction of compressive stresses creates a residual compressive stress field that interacts with the stresses introduced when the joint is loaded all along the external loading. This residual stress distribution is axisymmetric and creates a circular area of normal compression (the cone of compression [B1] under the fastener head as well as circumferential and radial in-plane compression at the outer edge of the hole, and an annular ring of circumferential and radial tension stresses. One viable way to demonstrate this effect experimentally is to look at contact pressures at the interface of different levels clamp to in aluminium plates. Figure 3 shows the effect of preload on the distribution of contact pressures in the plate's interfaces.

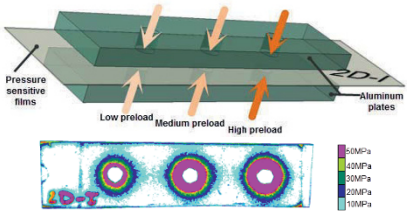

Figure 3: Effect of preload on contact pressure between aluminium plates (6kN-11kN-17.5kN)

In order to highlight the reducing peak stresses effect, we can look at the longitudinal tensile stresses before and after applying the external load. The figure 4-a defines the path where longitudinal stresses have been numerically calculated for 2 preload levels. The model has been then submitted to two different preload magnitudes then to the same tensile load applied to the middle plate then the stresses has been re-calculated and figure 4-b presents the plot of the different stress levels during those measurements. It shows that the higher the preload, the more compressive circumferential (and radial) in-plane compression at the outer edge of the hole. When the external load was applied, the model that was highly preloaded sees less magnitude of stresses in general, and in particular the peak stresses at point A are reduced.

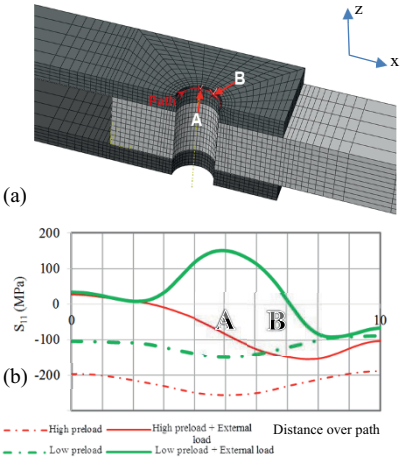

Figure 4: (a) Definition of critical path - (b) Effect of preload on longitudinal tensile stresses at the critical path before and after application of external load

The combination of those phenomena leads to enhanced durability of highly preloaded joints. This fatigue life enhancement cannot be achievable in the case of torque tightened joints due to the unreliability of preload.

3.3 – Multiaxial state of stresses

The introduction of compressive stresses via the preload application and longitudinal tensile stresses via external loading application implicate a tri-axial state of loadings. In order to perform consistent fatigue life estimation, the classical calculation methods based on the estimation of concentration stress factor K_T that multiplies the average stress on net section cannot be applicable as for uniaxial problems.

During the past years, several multiaxial fatigue criteria have been developed and listed in reference books [WC1]. In the present study, we develop an approach based on a critical plan criterion which was chosen because it is easier to

implement and to apply to a complex joint in an industrial context. The formula proposed is a linear combination of the maximum amplitude of the equivalent shear stress variation and the maximum hydrostatic pressure value within a loading cycle. The reader may refer to the work under review [BS1] for more details concerning the implemented multiaxial model. For sake of simplifying, the equation (1) that defines the fatigue life is given below:

$$N = 10^5 \left(\frac{A_N}{T_{eq,a,max} + B_N \cdot P_{max}}\right)^p \quad (1)$$

Where:
N is the fatigue life that is calculated at each point of the structure.
$T_{eq,a,max}$ Is the maximum variation of the octahedral stress amplitude.
P_{max} Is the maximal hydrostatic pressure.
B_N, A_N and p are given by two fatigue tests (at R=0.1 and R=-1) of the considered material and considering that for different loading ratios R on a logarithmic diagram (Log (Stress), Log (Fatigue life)) forms a network of parallel straight lines of slope –p.

4- Fatigue life enhancement via preload

4.1 – Experimental study

To illustrate the effect of preload on fatigue life of shear joints, we consider the two assemblies presented in figure 5 that has been numerically and physically tested. The first one on the left is composed of three 2024T3 aluminium plates (marked as 3-4), a Ta6V titanium fastener (1) and a steel nut (2). The nominal diameter is 6.35mm and the assembly was realised with a bolt-hole clearance of 10µm. The assembly on the right presents the same architecture, the only difference being that 2 fasteners have been used. The total thickness of plates to bolt diameter ratio is equal to 2 and 4 respectively. An aluminium doubler has also been used as a grip span between the external plates. Test specimens were then tested at constant amplitude loading with a load ratio R=0.1.

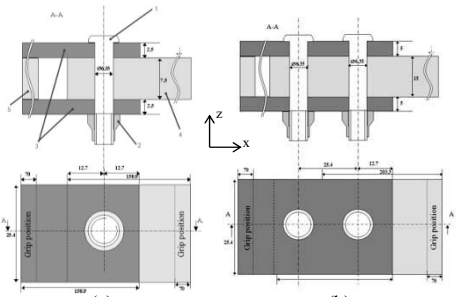

(a) (b)

Figure 5: fatigue specimens: (a) double lap bolted joint with one fastener (b) double lap bolted joint with two fasteners

It should be noted that introducing preload was done with the aid of iterative tightening process so that the scatter on final preload is less than 10% of the desired preload. The relaxation of preload has also been verified to be less than 5% after tightening tooling release.

4.2 – Numerical study

3D modelling was performed using the finite elements of the Abaqus® software. Only a half of the model was considered in order to reduce the time needed for numerical calculations and Y-direction symmetry conditions were applied. Tensile stresses were applied on the free end of the median plate following the X direction to simulate the external loading and Z direction displacement was locked on fatigue machine grip position to correspond with fatigue tests and to prevent rigid body motion.

Elastic isotropic materials were used to simulate the mechanical behaviour of the bolted connection. The plate's material (2024T351) is described with an elasto-plastic model.

A normal "hard" contact was defined to transmit contact pressures between the different surfaces, and a tangential contact based on the Coulomb model was defined between the plates with a friction coefficient of 0.4 when the sealant was not modelled and 0.2 when the sealant was modelled. Finally the degrees of freedom of nodes in contact between the shank of the bolt and the nut were coupled in order to model the tie contact between them. The mesh used was composed of 3D hexahedral elements with linear integration and reduced integration. The mesh was partitioned in order to be refined near to the zones where results had to be accurate. 13 steps of loading were applied to model the entire cycle: the first two steps of the FE calculation represented the preload installation using a bolt-load function, then this preload was maintained during an intermediate step and the eleven following steps of loading/unloading.

Figures 6 and 7 presents the Wohler curves of numerical and experimental fatigue test specimens for single and double fastener specimens tightened to 5.9kN and 17.6kN.

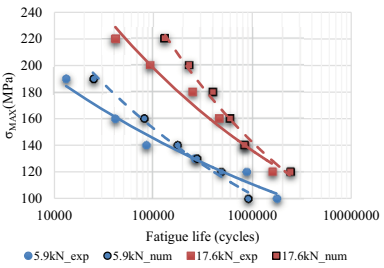

Figure 6: experimental and numerical Wohler curves for double lap bolted joints with one fastener at two preload levels

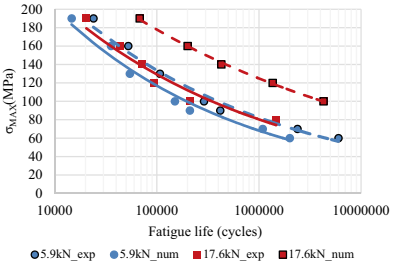

Figure 7: experimental and numerical Wohler curves for double lap bolted joints with two fasteners at two preload levels

4.3 – Results and discussion

We observe that a positive correlation was established either between predicted and experimental fatigue lives and in term of fatigue initiation locations at load ratios R=0.1 for the assembly composed of one fastener with a slight non conservatism. They also indicate the high impact of preload on such joints. However, In the case of the assembly composed of 2 fasteners, the correlation was successful for low preload but unsuccessful for high preload. The non-conservatism of the prediction method is still present and several hypothesis can be made to explain the observed differences:

- Modelling of interfay sealant: a more appropriate modelling technique may be used instead of penalty contact: the sealant can be modelled as a hyperelastic material or the contact between plates can be modelled as a cohesive contact. This feature may enhance the quality of predicted fatigue lives, especially in the case of double lap bolted joints composed of two fasteners.
- Low preloaded joints: figure 8 shows the numerical prediction versus the experimental results of single fastener specimens. Aside from the non-conservatism, the first portion of the curve is not well predicted. One solution is to reduce the mesh size near to the stress concentration point in order to better predict this transition. The benefit of preload is clearly highlighted and the maximum benefit is obtained only with an accurate preload.

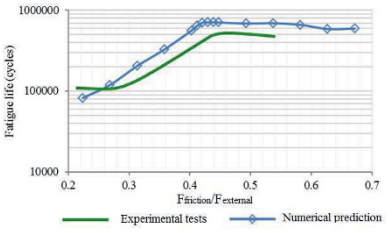

Figure 8: Evolution of preload in relation to the portion of load transferred by friction

- The effect of uncertainties: fatigue is known to be a dispersive phenomenon, numerical Wohler curves can be enlarged while taking into account the different uncertainties. The chosen multiaxial model should also be compared to other classical models. A parametric study on friction coefficient, fatigue parameters cited in equation (1) should allow the calibration of the numerical methodology.

4.4 – Fatigue initiation area modification:

As described in chapter 2, some authors show that the initiation point position is also modified: for low preload values, the initiation point is localised in the stress concentration area as the bearing shear joints, when increasing the preload, this position migrates to the exterior of compressed area[S1][KF1]. The numerical model predicts successfully this phenomenon as described in figure 9.

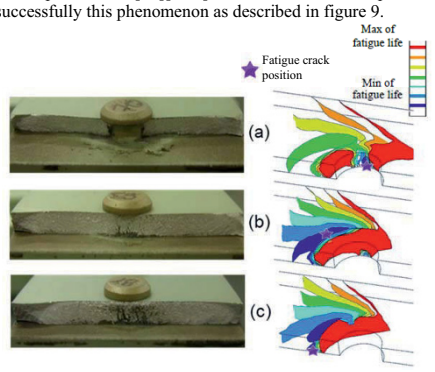

Figure 9: (a) Net section failure - (b) modified net section failure - (c) gross section failure

Three positions were detected as the minimum fatigue life dependent on the preload: (a) Net Section Failure. For joints dominated by the bearing mode with low preload, the crack initiation and stress concentration sites are found near the net section locations at the contact surface. (b) Modified Net Section Failure. High stresses are generated away from the hole edge at angular locations. (c) Gross Section Failure. The dominant stress concentration in lap joints is the friction mode. This mode of failure is also present for joints with a high interference degree or expansion rate. The mode of failure shows the dominant mode of load transfer (bearing vs friction) or fretting fatigue.

For preloaded joints it is difficult to detect fretting fatigue from pure mechanical fatigue because both mechanisms favor the gross section failure mode. In fact, fatigue joints also experience fretting, the cyclic microslip state of contacting plates and plate-fastener interfaces. Fretting can produce changes in the surface quality or paint chipping; it can initiate wear and fatigue failure, affecting the fatigue life of joints.

5- Conclusion:

In this article, the influence of preload on fatigue life of metallic shear joints has been demonstrated throughout the use of experimental and numerical methods. The theoretical analysis shows that the preload influence can be analysed by finite elements method. In addition, an approach based on a critical plan criterion has been developed because it is easier to implement and to apply to a complex joint in an industrial context. It shows that good correlations can be obtained. It is proposed that further studies will be dedicated to enhance the accuracy of the developed model.

6- References

[AA1] Alkatan F., Andriamampianina J., Stéphan P., Guillot J. (2013). Flexibility of hybrid load transfer assemblies: influence of tightening pre-stress. Aerospace Science and Technology, 25(1), 84-92.

[AA2] Andriamampianina J., Alkatan F., Stéphan P., Guillot J. (2012). Determining load distribution between the different rows of fasteners of a hybrid load transfer bolted joint assembly. Aerospace Science and Technology, 23(1), 312-320.

[B1] Bickford, J. H. (1997). An Introduction to the Design and Analysis of Bolted Joints, 3rd ed., Marcel Dekker.

[BL1] Boni, L. and Lanciotti, A. (2011), Fatigue behaviour of double lap riveted joints assembled with and without interfay sealant. Fatigue & Fracture of Engineering Materials & Structures, 34: 60–71.

[BS1] Benhaddou, T., Stephan, P., Daidie, A., Chirol, C., Tuery, J.B., Effect of axial preload on double lap bolted joints – numerical study. Proceedings of the ASME 2012 11th Biennial Conference on Engineering Systems Design and Analysis, 2012.

[BS2] Benhaddou, T., Stephan, P., Daidie, A., Chirol, C., Tuery, J.B., Guillot,J. (2014), Pre-tensioning effect on fatigue life of bolted shear joints. Aerospace Science and Technology, In press, 1-17.

[CA1] Chakherlou, T. N., & Abazadeh, B. (2012). Experimental and numerical investigations about the combined effect of interference fit and bolt clamping on the fatigue behavior of Al 2024-T3 double shear lap joints. Materials & Design, 33, 425–435.

[CA2] Chakherlou, T. N., Shakouri, M., Akbari, a., & Aghdam, a. B. (2012). Effect of cold expansion and bolt clamping on fretting fatigue behavior of Al 2024-T3 in double shear lap joints. Engineering Failure Analysis, 25, 29–41.

[CA3] Chakherlou, T. N., & Abazadeh, B. (2011). Estimation of fatigue life for plates including pre-treated fastener holes using different multiaxial fatigue criteria. International Journal of Fatigue, 33(3), 343-353.

[CS1] De-Crevoisier J., Swiergiel N., Champaney L., Hild F. (2012). Identification of In Situ Frictional Properties of Bolted Assemblies with Digital Image Correlation. Experimental Mechanics, 52(6), 561-572.

[CO1] Chakherlou, T. N., Oskouei, & R. H., Vogwell, J. (2008). Experimental and numerical investigation of the effect of clamping force on the fatigue behaviour of bolted plates. Engineering Failure Analysis, 15(5), 563-574.

[ES1] Ekh, J., & Schön, J. (2008). Finite element modeling and optimization of load transfer in multi-fastener joints using structural elements. Composite Structures, 82(2), 245–256.

[GT1] Geoffrey J., Turvey A., Pu Wang B. (2008). An FE analysis of the stresses in pultruded GRP single-bolt tension joints and their implications for joint design. Computers and structures, 86(9), 1014-1021.

[H1] Huth H. (1986). Influence of fastener flexibility on the prediction of load transfer and fatigue life for multiple row joints. Fatigue in mechanically fastened composite and metallic joints: a symposium, page 221.

[HR1] Hahn, G. T., & Rubin, C. A. (2005). Structural shear joints: analyses, properties and design for repeated loadings. ASME Press.

[JN1] Jaglinski, T., Nimityongskul, a., Schmitz, R., & Lakes, R. S. (2007). Study of Bolt Load Loss in Bolted Aluminum Joints. Journal of Engineering Materials and Technology, 129(1), 48.

[KF1] Kulak, G. L., Fisher, J. W., & Struik, J. H. A. (2001). Guide to Design Criteria for Bolted and Riveted Joints Second Edition. 2nd edition, American institute of steel construction.

[MC1] Mccarthy, M., Mccarthy, C., Lawlor, V., & Stanley, W. (2005). Three-dimensional finite element analysis of single-bolt, single-lap composite bolted joints: part I—model development and validation. Composite Structures, 71(2), 140–158.

[MC2] Mccarthy, C., & Mccarthy, M. (2005). Three-dimensional finite element analysis of single-bolt, single-lap composite bolted joints: Part II—effects of bolt-hole clearance. Composite Structures, 71(2), 159–175.

[MV1] Minguez, J., & Vogwell, J. (2006). Effect of torque tightening on the fatigue strength of bolted joints. Engineering Failure Analysis, 13(8), 1410–1421.

[MW1]. Munroe, J., Wilkins, K., Gruber, M.: Integral Airframe Structures (IAS)—Validated Feasibility Study of Integrally Stiffened Metallic Fuselage Panels for Reducing Manufacturing Costs. Technical Report: NASA/CR-2000-209337, Prepared by Boeing for Langley Research Center under Contracts NAS1-20014 and NAS1-20267 (2000).

[P1] Engineering Fundamentals of Threaded Fastener Design and Analysis, PCB Load and Torque, White paper 2005.

[PN1] Paredes, M., Nefissi, N., & Sartor, M. (2012). Study of an interference fit fastener assembly by finite element modelling, analysis and experiment. IJIDEM, 6(3), 171–177.

[PP1] Pratt, J. D., & Pardoen, G. (2002). Numerical Modeling of Bolted Lap Joint Behavior. Journal of aerospace engineering, 15(1), 20–31.

[PR1] Paletti, L., Rans, C., & Benedictus, R. (2009). An analytical model for load transfer in a mechanically fastened, double-lap joint. 25th ICAF Symposium, 987–1004.

[S1] Schijve, J. (2009). Fatigue of structures and materials. 2nd edition, Springer.

[S2] Starikov, R. (2004). Fatigue behaviour of mechanically fastened aluminium joints tested in spectrum loading. International Journal of Fatigue, 26(10), 1115–1127.

[SD1] Shankar, K., & Dhamari, R. (2002). Fatigue behaviour of aluminium alloy 7075 bolted joints treated with oily film corrosion compounds. Materials & Design, 23(2), 209–216.

[SR1] Stocchi, C., Robinson, P., Pinho, S.T. A detailed finite element investigation of composite bolted joints with countersunk fasteners. Proceedings of the 18TH international conference of composite materials, 2011.

[SR2] Stocchi, C., Robinson, P., Pinho, S.T. Using strain gauges to monitor bolt clamping force and fracture in composite joints during fatigue tests. Proceedings of the 15TH European conference of composite materials, 2011.

[T1] Torque limits for standard, Threaded Fasteners. MSFC-STD-486B, November 1992.

[WK1] Wagle, S., & Kato, H. (2009). Ultrasonic detection of fretting fatigue damage at bolt joints of aluminum alloy plates. International Journal of Fatigue, 31(8-9), 1378–1385.

[WC1] Weber, B., Carmet A., Robert, J.L. (2011). Les critères de fatigue multiaxiaux : Application au dimensionnement en fatigue de structures métalliques. Editions universitaires européennes.

Article 073-pds-29

Quality evaluation of bolted assemblies through tightening monitoring and simulation

Simon DOLS [1,2], Manuel PAREDES [1], Patricia MORGUE [2]

(1) : Université de Toulouse, INSA/ICA (Institut Clément Ader), 135 avenue de Rangueil, 31077 Toulouse Cedex 04, France.
+33561559702
E-mail : {simon.dols, manuel.paredes}@insa-toulouse.fr

(2) : Airbus Operations S.A.S.
316 route de Bayonne
31060 Toulouse Cedex 09
+33582054700
E-mail : { simon.dols, patricia.morgue}@airbus.com

Abstract This paper presents a method for the quality control of a bolted assembly by monitoring its tightening. Both torque and angle are already used in the production lines as target values, but the proposed method also uses them as a means of verification. In fact, the variations of the stiffness of the bolt through the torque-angle relationship is a good indicator of the bolt's interface quality and thus of the performance of the overall assembly. The impact of gaps and friction on this relationship are investigated using a full 3D finite element model.

Key words: bolt, quality, monitoring, stiffness, defects

p : thread pitch (mm)
θ : rotation angle (°)
θ_t : amount of angle lost in torsion (°)
d : nominal diameter (mm)
C_b : compliance of the bolt (mm/N)
C_p : compliance of the parts (mm/N)
C_{cyl} : compliance of the cylinder (mm/N)
C_t : shear compliance of the bolt (mm/N)
T : applied torque (N.mm)
T_t : torsional torque (N.mm)
μ_t : friction coefficient in the thread
μ_h : friction coefficient under the nut
r_m : mean radius of contact under the nut (mm)
P_r : preload (N)
E_P : Young modulus of the parts (Mpa)
E_b : Young modulus of the bolt (Mpa)
G : shear modulus of the screw (Mpa)
l_0 : length of the unthreaded part of the screw (mm)
l_1 : length of the threaded part of the screw (mm)
A_0 : cross section of the unthreaded part of the screw (mm²)
A_s : cross section of the threaded part of the screw (mm²)
l_{bi} : length of an i part of the bolt (mm)
d_{bi} : diameter of an i part of the bolt (mm)
d_2 : diameter on the flank (mm)
d_3 : internal diameter of the screw (mm)
D_a : outer diameter of the bolt's head (mm)

1- Introduction

The rate at which aircraft are produced has to increase if the growth of the global civil aviation market is to be sustained. But in aircraft manufacturing, one of the main drivers remains passenger safety, so shorter production time must not lead to a reduction in the high quality standards needed to ensure the reliability of the aircraft. An example of such standards can be found at a very basic level: the bolted joint. The interface between the components of a bolted assembly has to be free from burrs, chips and geometrical defects in order to ensure the transmission of loads through the assembly. So, after drilling, the parts are separated, cleaned and prepared for bolting, with an interlayer of mastic for sealing purposes. However, the disassembly of large aircraft components is time consuming, complex and costly. So the question that arises is the following: How can the contact between the parts in a bolted assembly be ensured without checking the interface by disassembly? So far, the literature can be divided into two categories: articles concerning the actual tightening of joints without any defects and those concerning the behaviour of faulty bolted joints during their service life but not during tightening. Thus, the literature regarding defects in bolted assemblies during the tightening phase is scarce.
However, the essence of our problem is to evaluate the quality of the contact between two solids and some methods developed for other subjects might be of use.

For example, several attempts have been made to check the pressure at an interface and its effect on the conductance of bolted joints [YW1] (Fig 1). This pressure at the interface can be used as one of the indicators of the contact between the plates, as the pressure between the plates increases with the torque. The micro gaps and rough patches are progressively reduced leading to an increase in the contact conductance.

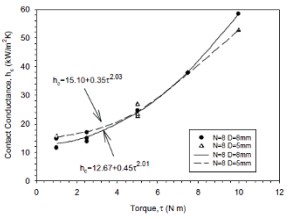

Figure 1 An experimental investigation of thermal contact conductance across bolted joints [YW1]

The same approach is used for health monitoring through electrical conductivity [AS2]. A more direct method is to check the interface directly using ultra sound techniques [PB1] (Fig 2). Pau M et al, compare the results given by the ultrasound with those provided by a pressure sensitive film inserted between the plates. Unfortunately, this method cannot be used in our case because of the mastic at the interface. A pressure film could also be useful, but its presence would affect the stiffness of the joint during tightening. Simulations have been performed to take this into account, and an attempt will be made to verify them during the coming experimental campaign.

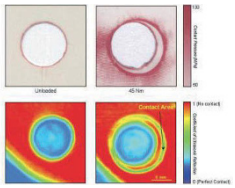

Figure 2 Comparison of contact surface measurements made by ultrasound and pressure sensitive film

Finally, X-ray tomography has already been used by Lalechos et al. [LS1] and will be the means of validation for the method. These authors use a code based on the pixel density to create a map of the pressure distribution. Then they compare this distribution for different amounts of torque within their assembly.

Once the contact between the plates is ensured, tightening starts. The models usually used to design, calculate or control bolted assemblies assume that the interface between the plates is perfect. So these models can be used as a baseline to evaluate the impact of defects on the tightening phase. The general idea as presented in VDI 2230 [V1] is to idealise the joint as springs, one for the bolt and one for the parts. The stiffness of these springs can be calculated so as to predict the amount of elongation the bolt will sustain for a given preload and the amount of compression the plates will endure accordingly. To calculate its stiffness, the bolt is divided into several cylinders according to the cross sectional area, the total stiffness being the sum of the cylinder stiffnesses. For the head and the threaded parts, the height of the cylinder is artificially increased, the amount depending on the type of bolt. The method is detailed in VDI 2230.

The compliance (or the stiffness) of the clamped parts is determined by the basis of Rotscher's pressure cone, the effective area A_e at the interface (Fig 3). But several models exist to calculate the compliance of parts starting from this basis. Some of them are presented by Nassar and al. [NA1], as an introduction for their new model.

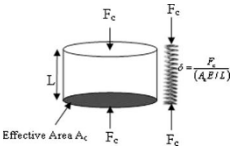

Figure 3 Equivalent elastic model of a joint [NA1]

Another way to calculate the stiffness of the parts is to use a finite element model. If the investigators are only concerned by the effect of preload for in-life service or joint stiffness, a common method is to simulate this preload by a force within the bolt, without detailing the bolt's geometry. This approach was used in [NS1] to evaluate the axial and bending stiffness of clamped parts. Nevertheless, the geometry not being detailed, the effect of the elliptical shape of the threads is totally left aside. More precise models have been proposed with the increase of power of modern finite element solvers. These models allow the simulation of contacts between the nut and the screw, taking into account the geometry of the threads. Several ways of creating threads are presented by Fukuoka et al. [FN1], who describe a very detailed model to calculate the stress concentration at thread roots. In this model, the screw and the thread are created at the same time with the rotation of the cross section of the external thread (Fig 4). Another way to construct the model is to create the threads and the screw body separately and to tie them. The work needed to create and mesh the parts is reduced but the computation time is increased [ZJ1].

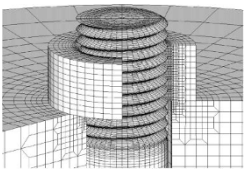

Figure 4 Detailed modelling of the threads [FN1]

In all these models, because the preload is created by an axial force within the bolt, the torsion caused by the tightening is not taken into account. However, in our case, this torsion has an impact on the tightening behaviour.

The means available in the literature for detecting the contact between two plates near the bolt are not compatible with industrial production rates and a new tightening method has therefore been developed. In this paper, after a brief presentation of a typical study case, this new method is exposed. Then the modifications made to existing analytical models so that they correspond to our case are explained, followed by a presentation of the full 3D finite element model and a comparison of the results. The finite element model is then used to investigate the influence of several parameters on tightening, such as thickness, friction and gaps between the plates.

2- Presentation of the proposed method

2.1 – Case study

Some preliminary tests were performed prior to this study. The idea was to create an artificial gap between the plates by means of two rigid shims (Fig 5). The test set-up consisted of two plates (28.8*28.8 mm) bolted together by a titanium screw/nut. The thickness of the plates and the length of the screw could vary to cover different cases encountered on the assembly lines. Different gap sizes were tested for each thickness of plates in order to measure the response of the assembly in terms of a torque/angle relationship. For example, the curve below (Fig 6) shows the result for a 0.5 mm gap and a total thickness of 4.8 mm.

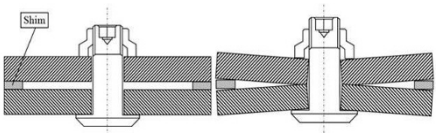

Figure 5 Type of sample used for the trials, before and after tightening

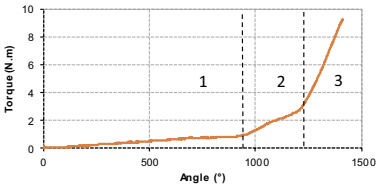

Figure 6 Experimental torque/angle response for a 0.5 mm gap

The different slopes of the curve mark the occurrence of three events. The first corresponds to the locking phase of the screw, a standard in the aeronautical industry.
Then the gap is reduced with the bending of the plates (event 2). The contact between the plates at the beginning of event 3 is illustrated by a sudden increase of the stiffness. This linear behaviour corresponds to the effective tightening of the assembly.
The idea of the proposed method is to detect this change of stiffness and then to control the slope of the third part. If chips, burrs or geometrical defects have an influence on the tightening curve, it will be possible to detect them without disassembly.
However, the final stiffness on the curve is inevitably influenced by the specificities of the test bench used for the experiments. Instead of calculating all the different stiffnesses and modelling the entire bench, another test campaign will be carried out to validate the method.

2.2 – Analytical model

Concerning the tightening phase, as mentioned above, some models exist for flawless cases. Here, the expression giving the torque as a function of the angle through which the nut turns was slightly modified so as to correspond to our case. This relationship will be used to check the validity of our finite element model, and later on, compare the results with the experiments.
This model is an extension of Alkatan's work [AS1] on the stiffness of prismatic parts in bolted joints.
During the tightening, the bolt will sustain an elongation while the parts are compressed. This is represented by:

$$\Delta L_b = \frac{p\theta}{360} - \Delta L_p \qquad (1)$$

Staying in the elastic domain, the compliances of the different elements are used to link these deformations with the preload introduced by the tightening:

$$P_r C_b = \left(\frac{p\theta}{360} - P_r C_p\right) \qquad (2)$$

$$P_r = \left(\frac{p\theta}{360} - P_r C_p\right)\frac{1}{C_b} \qquad (3)$$

In our case, this model needs to be modified a little to take the cylindrical part at the base of the nut into account (Fig 7). The compliance of the cylinder C_{Cyl} is added.

$$P_r = \frac{p\theta}{360(C_p + C_b + C_{Cyl})} \qquad (4)$$

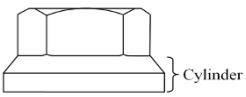

Figure 7 Cylinder at the base of the nut

A part of the rotation angle is lost due to torsion inside the

bolt:

$$P_r = \frac{p(\theta - \theta_t)}{360(C_p + C_b + C_{Cyl})} \quad (5)$$

The amount of angle lost depends on the shear compliance of the bolt and torsional torque.

$$\theta_t = C_t T_t \quad (6)$$

This torque is created at the bearing surface between the nut and the part:

$$T_t = \mu_h r_m P_r \quad (7)$$

The preload become:

$$P_r = \frac{p(\theta - \mu_h r_m P_r C_t)}{360(C_p + C_b + C_{Cyl})} \quad (8)$$

$$P_r = \frac{p\theta}{360(C_B + C_P + C_{Cyl}) + \mu_h r_m C_t p} \quad (9)$$

The relation linking the torque to preload is the following:

$$P_r = \frac{C}{(0.16p + 0.58\mu_t d_2 + \mu_h r_m)} \quad (10)$$

So finally we can write:

$$\boxed{C = \frac{p(0.16p + 0.58\mu_t d_2 + \mu_h r_m)}{360(C_B + C_{Cyl} + C_P) + \mu_h r_m C_t p}\theta} \quad (11)$$

The compliances of the different elements need to be calculated. For the plates, Alkatan uses the same approach as described in the first part, where the compliance of the plates is equivalent to the compliance of a cylinder, calculated using the compression cone (Rotscher's pressure cone). He generalizes the method for prismatic parts with offset holes. The size and shape of the cone depend on the thickness of the plates and diameter of the bolt's head. This diameter is used by Alkatan to set a number of dimensionless variables marked with a small star:

$L_p^* = L_p / D_a$	dimensionless thickness of the prismatic part
$X^* = X / D_a$	dimensionless abscise of part's hole
$Y^* = Y / D_a$	dimensionless ordinate of part's hole
$D_t^* = d / D_a$	dimensionless diameter
$A_{eq}^* = A_{eq} / D_a^2$	dimensionless equivalent cross section

Using these variables we can compute the diameter of the equivalent cylinder D_{eq}^*:

$$D_{eq}^* = \frac{9.Min(X^*, Y^*) + 2.Min\left\lfloor Max(X^*, Y^*); 1\right\rfloor}{4} \quad (12)$$

An then A_{eq}^*,the equivalent reduced cross section of the cylinder:

$$A_{eq}^* = \frac{\pi}{4}\left(1 - D_t^{*2}\right) + \frac{1}{2}\left(D_{eq}^{*2} - 1\right)\tan^{-1}\left\lfloor \frac{0.8.(L_p^* - 0{,}2)}{(D_{eq}^{*2} - D_t^{*2})} \right\rfloor \quad (13)$$

Finally, the part compliance is:

$$C_P = \frac{L_P}{E_P A_{eq}} \quad (14)$$

For the bolt, Guillot's [G1] simplified model is used, where the bolt is divided into two basic parts: the working part (under the threads) and the non-working part, following the philosophy of VDI (Fig 8):

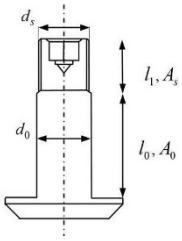

Figure 8 Division of the screw

$$C_B = \frac{1}{E_B}\left\lfloor \frac{l_0 + 0.4d}{A_0} + \frac{l_1 + 0.4d}{A_s} \right\rfloor \quad (15)$$

This model has already been improved but this simple formulation has been sufficient so far.
The torsional compliance of the screw is also calculated following Guillot's model.

$$c_t = \frac{180}{\pi}\left(\frac{32.l_1}{\pi G d_s^4} + \frac{32.l_0}{\pi G d_0^4}\right) \quad (16)$$

Article 073-pds-29

2.3 – Finite element model

A finite element model has been created in order to investigate the effect of different types of defects and their geometry (chips, burrs, etc.) on the slope of the curve. Because of the unsymmetrical aspect of the problem, the model is a 3D one (Figs 9 and 10). The software used in this study is the commercial FE software Abaqus V6.12.

The rotation is transferred to the nut via cinematic coupling and the same coupling is used to maintain the bolt. The plates are prevented from turning under the action of the tangential forces due to friction (Fig 11).
The threads are modelled separately from the screw/nut and tied on the corresponding surface, thus making it easier to mesh each component precisely. In addition, thread imperfections are not modelled here, again to simplify the meshing. The locking phase (Part 1 on Fig 4) is not investigated here; additional work will be needed to simulate this complex process.
All the parts are meshed using hexahedral (C3D20R) and wedges (C3D15R) elements when the geometries are not suited for hexahedral only. These elements are quadratic with reduced integration. The sizes of the mesh are 0.4 mm for the screw, nut and bearing area of the plates, 0.15 mm for the treads and 1.5 mm for the plates. Denser meshing only increases the computation time with no effect on what this study is focused on.

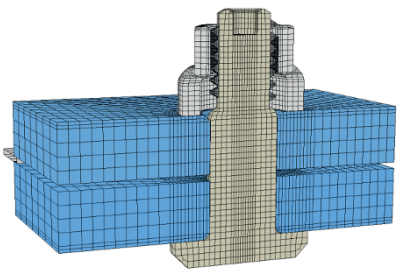

Figure 9 Finite element model

Figure 10 View of the screw and nut

The bolt is made of titanium and the plates of aluminium. All the materials in the model follow elastic-plastic laws. For the elastic part, Abaqus uses the young modulus and Poisson's coefficient of the materials. The plastic part of the elasto-plastic curve is discretized in a series of true strain/true stress couples. These couples are used by the software to compute the plastic behaviour of the elements. All these data come from internal tests and database.
The shims are rigid surfaces.
The contacts between the various parts are modelled using surface to surface contact. The normal behaviour of these contacts is called hard contact, meaning that no penetration is allowed between the slave nodes and the master surface. The tangential behaviour is a classical isotropic coulomb friction model with constant friction coefficients corresponding to a lubricated case. The friction coefficients used here were determined in a previous study [PN1] performed in the lab. The only difference between the contact surfaces is the sliding formulation: small or finite. Abaqus allows the user to select small sliding formulation in order to simplify the calculation for contact where the slave nodes will interact with the same area of the master surface. The repartition of the contact surfaces is shown in the figure below along with the boundary conditions (Fig11).

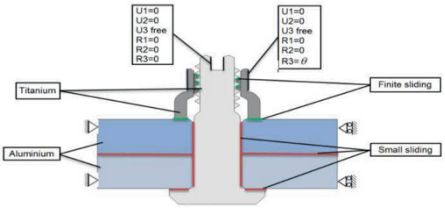

Figure 11 Materials and contact formulations

First, the results from the simulation are compared with the analytical model. The behaviour of the reference case (when there is no gap at the interface) and the calculation are very close (Fig 12). Now that the finite element model has been checked for a pristine case, it can be used for more complex situations with defects at the interface. The reference model will serve as a baseline for all the study to come.

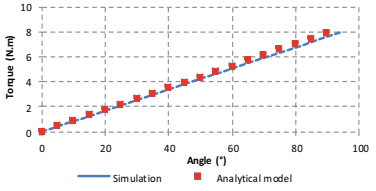

Figure 12 Comparison between analytical model and simulation

2.4 – Additional observation: pressure in the threads

Another use of the simulation was to check the pressure distribution within the assembly. Especially in the case of a simulated gap, the contact surface between the plates will be useful to update the analytical model and understand how the gaps affect the stiffness of the joint.
But here, the pressure on the screw threads is plotted (Fig 13). The measurement was taken every 45°, starting where the contact between the threads began.
The pressure is plotted along the cross section of the screw thread, from the root to the summit.

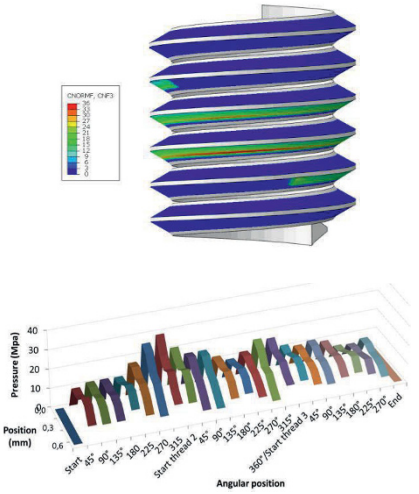

Figure 13 Pressure distributions on the screw threads

In accordance with the literature, the first thread sustains much of the load. But the load is not evenly distributed on this thread, one side being more loaded than the other. In addition, there is a delay at the beginning, with a sudden increase of pressure due to the non-realistic geometry. This will be improved in the future with the model of imperfect threads on the nut and screw.

3- Early results

3.1 – Thickness of the plates

Depending on the thickness of the plates, the precision of the model varies. The slope given by the analytical model and the one coming from the finite element simulation have been compared for various thickness. The diameter, nut and "working part" of the screw remain the same; only the length of the smooth part of the screw and the thickness of the plates change.

Total thickness of the plates	2 mm	4 mm	6 mm	9 mm
Slope from simulation	0.11	0.103	0.094	0.08
Slope calculated	0.12	0.11	0.10	0.09
Difference	9%	5%	6%	4%

Table 1 Influence of thickness

The difference varies between 4 and 9 %, which is partly due to the fact that the model is based on the compression cone. But the shape of the cone changes depending on the thickness and, for the 1st case, the cone is not complete, which explains the larger difference. Although a more detailed model exists, the aim here is to verify the validity of our simulation and the result is satisfactory.

3.2 – Influence of gap

Now the effects of gaps and friction can be simulated. Here, the comparison is made between the slopes of the reference curve (without gap) and the slope of the curve in the third part i.e. when the plates are in contact and the tightening is effective.
The graph below represents several trials with increasing gaps, with a total thickness of 6 mm (Fig 14). Apart from the gaps, the geometry is identical in each case, which is why all the samples behave in the same way until the plates touch each other.

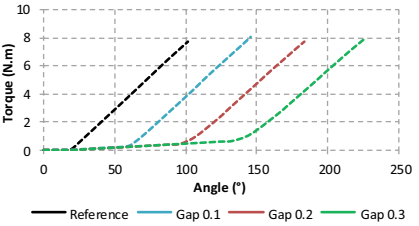

Figure 14 Influence of initial gap on torque/angle response

On the table below, the slopes of the curves are compared to the reference case. The slope is determined once the tightening is effective.

	Reference case	Gap 0.1	Gap 0.2	Gap 0.3
Slope from simulation	0.094	0.093	0.09	0.087
Difference		1%	4%	6%

Table 2 Influence of gaps

The stiffness after contact decreases when the initial gap increases. If these results are confirmed by experiments, the initial gap in a bolted joint will become an interesting point of the study regarding joint stiffness.

3.3 – Influence of friction

To evaluate the impact of friction on the stiffness of the joint during tightening, the overall friction coefficient was increased.

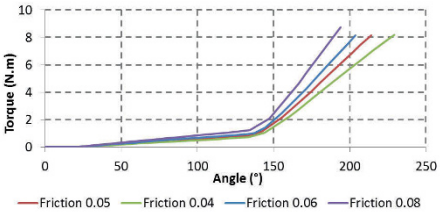

Figure 15 Effect of friction

	Slope	Difference with 0,04
Friction 0.04	0.087	
Friction 0.05	0.103	15%
Friction 0.06	0.118	26%
Friction 0.08	0.145	40%

Table 3 Influence of friction

As expected, the slope increases with the friction (Fig 15). In reality, since even a small increase of friction leads to an increase of slope, a target torque can be reached even if the preload remains low. Thus monitoring one parameter is not sufficient to ensure correct tightening.

4- Conclusion

With a new method responding to industrial needs for quality control, comes a new approach regarding bolted joints. The proposed method uses the change of stiffness of an assembly to verify that an initial gap between the plates has been reduced during tightening.

Other studies deal with perfect assembly, whereas the fact that the proposed method focuses on the stiffness of real assemblies will lead to a study of the defects at the interface and their effects. So far, a finite element model and an analytical formulation corresponding to our problem have been tested. These models have been used to verify the influence of two common variables in bolted assemblies: friction and gaps.

Although the influence of friction has already been investigated experimentally and described in many publications, new light has been shed here on the effect of gaps on the stiffness. These early results will be validated through an experimental campaign. Following the same approach, more complex aspects of bolted joints, such as burrs, chips, surface ridges, and elastic interactions, will be tested in order to fully describe the behaviour of real tightening.

5- References

[AS1] Alkatan F, Stephan P, Daidie A, Guillot J, Equivalent axial stiffness of various components in bolted joints subjected to axial loading. In Finite Elements in Analysis and Design, Vol 43 -8, 589-598, 2007.

[AS2] Argatov I, Sevostianov I, Health monitoring of bolted joints via electrical conductivity measurements. In International Journal of Engineering Science 48: 874-887, 2010

[FN1] Fukuoka T and Nomura M, Proposition of helical thread modeling with Accurate Geometry and Finite Element Analysis. In Journal of Pressure Vessel Technology vol 130, 2008.

[G1] Guillot J, Assemblages par éléments filetés; Modélisation et calculs. In Techniques de l'ingénieur, Tome 1 B5560 - B5562. 1987

[LS1] Lalechos A.V, Swingler J and Crane J, Visualisation of the contact area for different contact forces using X-ray computer tomography. Proceedings of the 54th IEEE Holm conference on electrical contacts, 2008

[NA1] Nassar S.A and Abboud A, An improved stiffness model for bolted joints. In Journal of Mechanical Design vol 131, 2009

[NS1] Naruse T and Shibutani Y, Equivalent stiffness evaluations of clamped plates in bolted joints under loading. In Journal of Solid Mechanics and Materials Engineering, Vol 4 No 12, 2010.

[PN1] M. Paredes, N. Nefissi and M. Sartor, Study of an interference fit fastener assembly by finite element modelling, analysis and experiment. International Journal on Interactive Design and Manufacturing. 6, 171-177, 2012.

[PB1] Pau M, Baldi A and Leban B Visualization of contact areas in bolted joints using ultrasonic waves. In Experimental Techniques, July/August 2008

[V1] Verein Deutscher Ingenieure (VDI), Sytematic calculation of high duty bolted joints. Joints with one cylindrical bolt, 2003

[YW1] Yeh C.L, Wen C.Y, Chen Y.F, Yeh S.H, Wu C.H An experimental investigation of thermal contact conductance across bolted joints. In Experimental Thermal and Fluid Science 25, 2001

[ZJ1] Zhang M, Jiang Y and Lee C.H, Finite element modelling of self-loosening of bolted joints. In Journal of Mechanical Design, Vol 129 2007.

Article 074-pds-52

NON-INTRUSIVE MODEL COUPLING: A FLEXIBLE WAY TO HANDLE LOCAL GEOMETRIC AND MECHANICAL DETAILS IN FEA

M. Duval [1], J.-C. Passieux [1], M. Salaün [1], S. Guinard [2]

(1) : Université de Toulouse, Institut Clément Ader, INSA/UPS/Mines Albi/ISAE – 1, rue Caroline Aigle, 31400 Toulouse, France
{mduval, passieux}@insa-toulouse.fr, michel.salaun@isae.fr
(2) : Airbus Group Innovations – BP 90112, 31703 Blagnac Cedex, France
stephane.guinard@eads.net

Abstract: Computer Aided Engineering (CAE) often involves structural mechanics analysis (most of the time using the finite element method). When dealing with nonlinear complex models on large 3D structures, the computational cost becomes prohibitive. In this paper, we present the recent developments linked to an innovative computing method: non-intrusive coupling. Such a method allows to efficiently taking into account local modifications on an initial existing model in a non-intrusive way: the previously computed analysis is left unchanged. Large scale linear models can thus be easily computed, then localised nonlinear complex models can be used to pinpoint the analysis where required on the structure. After a presentation of the scientific context and a description of non-intrusive coupling methods, we will present its application to crack growth simulation and parallel structure analysis.

Key words: model coupling, multiscale, FEA, parallel computing, crack growth simulation

1- Context and industrial issues

Every time one wants to create a new mechanical object, a design cycle has to be respected, involving Computer Aided Design (CAD) and Finite Element Analysis (FEA).
When dealing with a critical part of a mechanical product, a particular attention should be paid to the FEA – and most of the time, it involves complex simulations.
This is the point we will focus on in this paper. Indeed, in order to perform a mechanical simulation, one needs both a geometrical and a mechanical model. Some cases require a complex mechanical model, and some other a detailed geometry.

The works which will be presented in this paper try to bring a solution to a recurrent FEA problem: how to compute a complex mechanical problem in a way requiring the least effort? There are two main problems which need to be addressed: geometric complexity and mechanical behavior complexity.

1.1 – Geometric modifications in FEA

The most direct way to perform a structural analysis *via* numerical simulation is to use the CAD model as the geometric model for the simulation. Indeed, the creation of a structure geometric model can be very time consuming. Moreover, for some critical parts, the mesh has to be certified before being used (aeronautical parts for instance).
All in all, the fact is that we cannot afford to create a new geometric model or a new mesh each time we need to perform a simulation.
Moreover, it appears that in the life cycle of a product, its geometric specifications can change (a crack can appear, some holes can be drilled). One objective of the computing method presented here is to bring a way to reuse an initial geometric model and its finite element mesh to compute structural analysis involving local details.

1.2 – Localised complex mechanical behaviour

Another class of complex problems involves mechanical behaviour of the structure we need to analyse. Indeed, in the field of structural analysis, two types of models have to be considered: linear and nonlinear ones. Of course, the time required to complete the analysis will depend on the type of model. The use of certain complex nonlinear models on very large structures fatally leads to considerable cost in terms of computer resources, often beyond what is currently available. The fact is that most of time, a nonlinear model is useful only on a small part of the structure (*e.g.* localised plasticity), which can be represented elsewhere with a linear model.

Again it is possible to save a lot of computation time by reusing an existing linear model (and the corresponding solution) on a full structure: a nonlinear model will thus be considered only on localised areas (see [AG1]). The objective of non-intrusive coupling is here to make us able to merge several local complex nonlinear models with a global linear one, without actually modifying this last one.
In other words, if we need to perform several analysis of a

large scale structure, the linear model will be assembled on the full structure only once, whereas the localised analysis will be performed as many times as necessary.

2- Model coupling method and algorithm

As said previously, the non-intrusive coupling algorithm (see [GA1]) aims to perform a structural analysis using two separate models:

- a pre-existing simple model involving the full structure, which will represent the global mechanical behaviour (linear elasticity),
- an ad-hoc complex model involving only a small part of the structure, representing the local mechanical behaviour (plasticity for example).

2.1 – Coupling algorithm

In this paper, a two scale finite element method is considered.
We will denote with the letter Ω the geometric domains and with the letter M the mechanical behaviour models.
Two coupled overlapping models are considered (see Fig. 1): a global one $M = M_1 \cup M_2$ (involving the full structure $\Omega = \Omega_1 \cup \Omega_2$, *i.e.* including a large number of nodes) and a local one $\widetilde{M}_2$ (involving only $\widetilde{\Omega}_2$). Thus the global model will be treated as a coarse linear one, whereas the local one will take into account the localised (potentially nonlinear) behaviour.

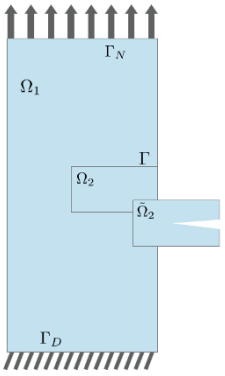

Figure 1: Non-intrusive coupling – Situation overview.

Basically, the idea is to reach the equilibrium between the global M_1 and the local $\widetilde{M}_2$ models at the interface by the mean of an iterative algorithm, similar to those used in domain decomposition methods, i.e. solving alternately the Dirichlet (resp. Neumann) problem on the local (resp. global) model until convergence (see Fig. 2). Actually, we seek to replace the global solution from M_2 (for example a non-cracked domain) on Ω_2 by the one we would get with $\widetilde{M}_2$ (for example a cracked domain).

Let us consider a domain decomposition in the linear case involving M_1 and $\widetilde{M}_2$: we then get a monolithic coupling system (see Eq. 1).

$$\begin{bmatrix} K_1 & 0 & C_1^T \\ 0 & \tilde{K}_2 & -\tilde{C}_2^T \\ C_1 & -\tilde{C}_2 & 0 \end{bmatrix} \begin{bmatrix} U_1 \\ \tilde{U}_2 \\ \Lambda \end{bmatrix} = \begin{bmatrix} F \\ 0 \\ 0 \end{bmatrix} \tag{1}$$

Here K_1 and $\tilde{K}_2$ stands for the stiffness matrices, F for the load vector, U_1 and $\tilde{U}_2$ for the displacement fields, C_1 and $\tilde{C}_2$ for the interface coupling matrices and Λ for the Lagrange multipliers vector.
An iterative algorithm is then set up in order to dissociate the two models when solving the linear system (see Eq. 2).

$$\begin{aligned} & K_1 U_1^{k+1} = F - C_1^T \Lambda^k \\ & \begin{bmatrix} \tilde{K}_2 & -\tilde{C}_2^T \\ -\tilde{C}_2 & 0 \end{bmatrix} \begin{bmatrix} \tilde{U}_2^{k+1} \\ \Lambda^{k+1} \end{bmatrix} = \begin{bmatrix} 0 \\ -C_1 U_1^{k+1} \end{bmatrix} \end{aligned} \tag{2}$$

Here, the non-intrusiveness of the method comes from a fictitious prolongation of the solution from Ω_1 to the full global domain Ω (see Eq. 3 and Eq. 4). We then define U so that $U|_{\Omega_1} = U_1$ and $U|_{\Omega_2} = U_2$.

$$\begin{aligned} & K U^{k+1} = F - C_1^T \Lambda^k + K_2 U_2^k \\ & \begin{bmatrix} \tilde{K}_2 & -\tilde{C}_2^T \\ -\tilde{C}_2 & 0 \end{bmatrix} \begin{bmatrix} \tilde{U}_2^{k+1} \\ \Lambda^{k+1} \end{bmatrix} = \begin{bmatrix} 0 \\ -C_1 U_1^{k+1} \end{bmatrix} \end{aligned} \tag{3}$$

Actually, the iterative algorithm tends to replace the global stiffness on Ω_2 by the local one, through an additional right hand side load vector.

$$\begin{aligned} & K_2 U_2 = \mathcal{F}_{\Omega_2/\Omega_1} \\ & C_1^T \Lambda = \left(C_1^T \tilde{C}_2^{-T}\right) \tilde{K}_2 \tilde{U}_2 = \mathcal{F}_{\tilde{\Omega}_2/\Omega_1} \end{aligned} \tag{4}$$

In a few words, the global and the local models are coupled *via* displacement and effort swap at the interface. The computational cost involved by the algorithm can be significantly smaller than the one involved by a full scale nonlinear complex computation.

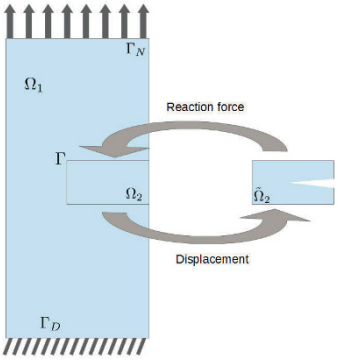

Figure 2: Iterative algorithm – Interface data exchange.

Still, it may be noted that, as such, the performance of the method is dependent on the stiffness gap between the two models M_2 and $\tilde{M}_2$. Indeed, the more the stiffness gap is important, the more the algorithm will require a large number of iterations to converge. This is very inconvenient for crack propagation simulation: the stiffness gap increases as the crack growths. Fortunately, a Quasi-Newton correction (see [GA1]) allows to get rid of that problem: thanks to the Sherman-Morrison-Woodbury formula, it is possible to modify the tangent stiffness of the global model in a non-intrusive way (see [AG1]).

2.2 – Connections with standard methods

For several years, model coupling is used in nearly all the engineering departments. One can cite two main classes of method:

- First, when dealing with large mechanical structures, one often needs a very precise analysis on localised small parts. As said before, we cannot afford to use a fine mesh and a precise model on the whole structure. Instead, structural zooming is often a solution (see [DD1]).
  It consists in computing a precise solution on a small area of a structure, using the pre-computed coarse solution on the full structure as boundary conditions. No iteration is applied in such methods.
- Then, one can cite domain decomposition method. These methods allow to efficiently couple models and meshes; nevertheless it requires significant efforts in order to make interconnections between the models (see *e.g.* [BR1], [BM1] and [FR1]). Moreover, no pre-computed solution can be reused, resulting on very large computing resource needs.

In fact, the non-intrusive coupling algorithm provides a generic method which allows coupling several models with the least effort, while preserving the inherent advantages of the methods presented above:

- The global pre-existing model is unmodified.
- Incompatible meshes can be interconnected *via* a mortar-like method, for example.
- Parallel resolution can reduce the computation time in case of multiple local models.

3- Application to crack growth simulation

The main application we focus on in this paper is crack growth simulation. For a lot of engineers, sustainability in construction (aeronautical, naval) is a priority. Indeed, during the life cycle of a mechanical structure (steel, concrete), cracks can appear, endangering the integrity of the structure. Thus, forecasting the propagation path of such cracks is a major issue for engineers. Nevertheless cracks locations cannot be known *a priori* when designing a structure or setting up a finite element mesh for initial structural analysis.

Using the common FEA tools, if one needs to simulate crack propagation, two main solutions are available:

- Set up a crack conforming mesh (see [BW1], [CR1]) at each step of the propagation. When combined to an adapted mesh refinement at crack tip, it leads to accurate results. The main drawback of conforming meshing is the substantial computational resulting cost. For that reason, direct crack meshing is rarely used as such, unless a very fast and efficient remeshing algorithm is set up.
- Use X-FEM method (see [MD1]) on an existing mesh. Theoretically, such a method allows the mesh to be not conforming to the crack faces. Nevertheless, most of time, remeshing is necessary at crack tip if one wants to get an accurate enough solution.

All in all, common methods do not allow reuse of existing meshes without (at least local) modifications, resulting in an extra computational cost. Here, the idea is to consider two different models, standing for different scales: a global linear elastic model, representing the full structure (healthy structure) and a local (potentially nonlinear and/or XFEM) model for the cracked domain (see Fig. 3).

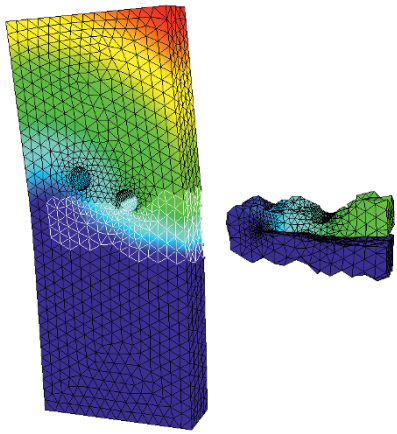

Figure 3: Non-intrusive FEM/XFEM coupling.

Using the non-intrusive algorithm for crack propagation simulation (see [GP1], [PR1]) will provide the following advantages:

- Remeshing will be necessary only on the local model.
- Nonlinear behaviour will be used only on the local model.
- The global linear model will be assembled once and the stiffness matrix will be factorised only once too.

Altogether, the non-intrusive coupling algorithm allows reusing a pre-existing mesh and linear elastic model (*i.e.* stiffness matrix) in order to perform computationally cheap crack growth simulation.

The results presented in this paper have been computed using Code_Aster, a structural engineering software developed by Électricité de France (see [CA1]). Both global and local models have been computed as a black box using this software, whereas the coupling (*i.e.* interface data exchange) has been done using a Python code developed for that purpose.

4- Parallel computing, distributed micro models

The two main features of the non-intrusive coupling algorithm are: “non-intrusive” which is the possibility to locally modify an initial model, and “coupling” which is the possibility to use different models to compute a single structure. This last feature will be developed now more in details.

Indeed, it is possible to consider several non-overlapping local models (for example if we want to represent several cracks on the same structure). Each local model will be completely independent from the others, allowing for an efficient parallel solver to be set up, using for instance MPI communications (see Fig. 4).

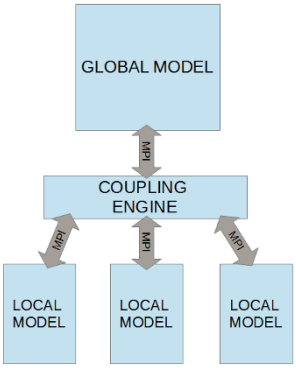

Figure 4: Non-intrusive parallel solver.

When dealing with nonlinear local models, parallelism is often the only possibility making FEA possible.
We want to draw the reader’s attention here on an important detail: unlike domain decomposition methods (*e.g.* FETI method, see [FR1]), each local analysis can be carried out independently from the others.
An application of this property is assemblies analysis. Indeed, for very large structures, simulation of assemblies is computationally very expensive. Moreover, if the model contains too much contact areas, it becomes difficult to make the analysis possible because of the high complexity of the nonlinear behaviour. Thanks to non-intrusive coupling, it is possible to compute each junction assembly separately: common contact algorithms will be able to perform the computation easily.

We present here another application of parallel computing applied to non-intrusive coupling: a multi-cracked plate (see Fig. 5). We consider here, as an academic test case, three disjoint cracks. From a global coarse mesh, we generate three local refined patches on which an X-FEM model is applied. For a given iteration of the coupling algorithm, the three local models are computed in parallel. The important point here is that there is no direct communication between the local patches. Every interface data exchange (displacement and effort) takes place between the global and one local model, through a coupling engine.

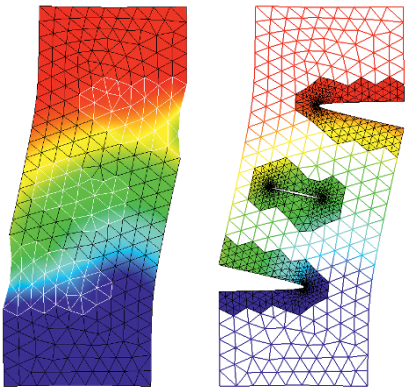

Figure 5: Multi-crack distributed patches.

It may also be noted that, in that example, no load is applied to the global model; we constrained only three degrees of freedom in order to disable rigid body motion. The only load applied is a hydrostatic pressure on the crack lips. Then, the local loading spreads to the global model only through the additional global right hand side load vector.

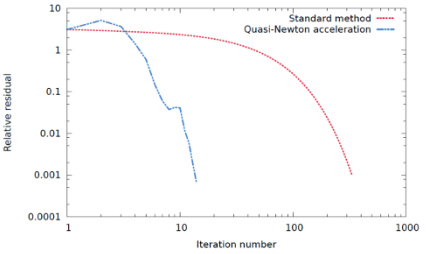

Figure 6: Convergence of the algorithm.

Moreover, the stiffness gap between the global and the local models is very important here, as we considered three cracks (two of which being emerging). Still, the Quasi-Newton method allows for an important speed-up (see Fig.6), the number of iteration dropping from about three hundreds to twelve.

5- Integration of research codes into commercial softwares

Finally, the last interest of non-intrusive coupling we will develop is the possibility to easily merge research codes and commercial softwares. Indeed, as presented previously, the only data exchange occurring between the global and the local models is interface displacements and forces. Thus it is

possible to compute the global solution from a commercial software using the existing models and solvers, and compute the local solution using an ad-hoc model developed with any code. Using a MPI communication between the two codes (*i.e.* between the two models, global and local) makes the communication straightforward: we only have to focus about the data we need to exchange, as MPI will provide his own standard for language compatibility (see Fig. 7).

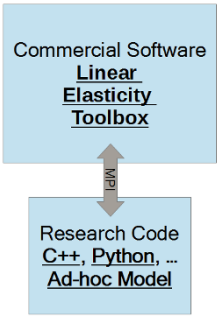

Figure 7: Commercial software - Research code integration

For instance we can cite [GA1] who compute an aeronautical structure analysis with localised plasticity within a linear model from Abaqus/Standard. If we direct our interest on crack growth simulation, we can cite [CL1] and [PR1] who propose a special treatment for crack tip displacement singular field (analytical solution, adapted radiating mesh) within an elastic linear model.

6- Patch definition and extend: caution

At this point, one could legitimately ask oneself on the manner the patches are defined. In fact, there is no constrain nor generic rule about the way to define the patch extend. In the crack propagation example, we simply select a given number of stitch layers from the global mesh around the crack location. Then those stitches are duplicated and saved as local mesh (see Fig. 3). Any refinement of the freshly generated local mesh is possible, particularly at crack tip.

For instance, let us consider a cracked bending plate. From a practical point of view, one can extend the patch as far as desired (see Fig. 8). Nevertheless, the patch extend is not without consequence on the algorithm convergence properties. Indeed, as said previously, the convergence speed depends on the stiffness gap between the local and the global model. In the treated example, the global model stands for a non-cracked plate whereas the local model stands for the cracked one. According to the Saint-Venant principle, the crack influence will decrease when getting far from the perturbation (the crack). Thus, the more the patch extends far from the crack, the less the stiffness gap between the global and the local model will be important, allowing for faster convergence.

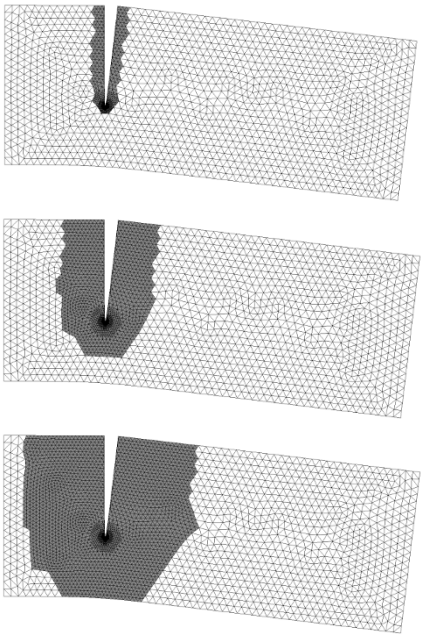

Figure 8: Cracked bending plate - Patch extend (1, 5 and 10 layers)

We plotted on Fig. 9 the number of iteration required to reach the fixed tolerance ($\epsilon = 10^{-3}$) as a function of the patch thickness (*i.e.* the number of global stitches from which the patch has been generated). As predicted, the more the patch extends, the faster the algorithm converges. Without any acceleration, one can nearly divide the required number of iteration by ten, thanks to the patch extend. When using the Quasi-Newton acceleration, the same result stands for true (the number of iterations is divided only by two extending the patch from one to ten layers).

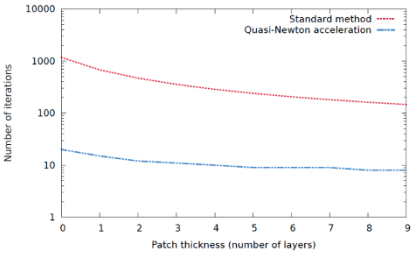

Figure 9: Patch extend – Convergence properties

Still, the more the patch extends, the more it will be computationally expensive to work out, as it will involve a larger number of degrees of freedom. Then engineers' skills must prevail in order to determine the best choice of parameters in such situations.

7- Conclusion and perspectives

In this paper, a non-intrusive coupling approach has been presented. This method allows to take into account local features in existing FEA models without actually modifying it.
The main purpose of the method is to make FEA easier, as finite element models preparation can sometimes be more time consuming than the computation itself.

Thanks to this algorithm, we have been able to set up a two and three dimensional crack growth simulation, using Code_Aster for the mechanical computations and MPI based communications for the interface coupling. All of the process is wrapped into a Python API. The distributed implementation of the algorithm we proposed here allows for high performance multi-patch parallel computations.
In a near future, we seek to make the method even more flexible by extending it to non-coincident patches (see [LP1]).

It may be noted that the algorithm can also be used to couple different mechanical representations (*e.g.* 2D/3D coupling, see [GA3]) or to couple different analysis methods (deterministic/stochastic models, see [CN1]) in a non-intrusive way.

This work is supported by the French National Research Agency (Grant ANR-12-MONU-0002 ICARE).

8- References

[AG1] M. A. Akgün, J. H. Garcelon, R. T. Haftka. Fast exact linear and non-linear structural reanalysis and the Sherman-Morrison-Woodbury formulas. International Journal for Numerical Methods in Engineering, 50:1587-1606, 2001.

[BR1] H. Ben Dhia, G. Rateau. The Arlequin method as a flexible engineering design tool. International Journal for Numerical Methods in Engineering, 62(11):1442–1462, 2005.

[BW1] T.N. Bittencourt, P.A. Wawrzynek, A.R. Ingraffea, J.L. Sousa. Quasi-automatic simulation of crack propagation for 2D LEFM problems. Engineering Fracture Mechanics, 55(2):321-334, 1996.

[BM1] F. Brezzi, L.D. Marini. The three-field formulation for elasticity problems. *GAMM Mitteilungen,* 28:124-153, 2005.

[CA1] Code_Aster. Électricité de France. *http://www.code-aster.org/*

[CL1] E. Chahine, P. Laborde, Y. Renard. Spider-xfem, an extended finite element variant for partially unknown crack-tip displacement. European Journal of Computational Mechanics 17(5-7):625-636, 2008.

[CN1] M. Chevreuil, A. Nouy, and E. Safatly. A multiscale method with patch for the solution of stochastic partial differential equations with localized uncertainties. Computer Methods in Applied Mechanics and Engineering, 255:255-274, 2013.

[CR1] V. Chiaruttini, V. Riolo, F. Feyel. Advanced remeshing techniques for complex 3D crack propagation. 13th International Conference on Fracture, Beijing, China, 2013.

[DD1] L. Daridon, D. Dureisseix, S. Garcia, S. Pagano. Changement d'échelles et zoom structural. CSMA, 2011.

[FR1] C. Farhat, F. X. Roux. A method of finite element tearing and interconnecting and its parallel solution algorithm, International Journal for Numerical Methods in Engineering, 32:1205-1227, 1991.

[GA1] L. Gendre, O. Allix, P. Gosselet, and F. Comte. Non-intrusive and exact global/local techniques for structural problems with local plasticity. Computational Mechanics, 44(2):233-245, 2009.

[GA2] P.-A. Guidalt, O. Allix, L. Champaney, J.-P. Navarro. A micro-macro approach for crack propagation with local enrichment. Proceedings of the Seventh International Conference on Computational Structures Technology, Lisbon, Portugal, 2004.

[GA3] G. Guguin, G. Allix, P. Gosselet. Techniques de raccord 2D-3D pour l'analyse non-intrusive de structures composites stratifiées. CSMA 2013, 2013.

[GP1] P. Gupta, J. Pereira, D.-J. Kim, C. Duarte, and T. Eason. Analysis of three dimensional fracture mechanics problems: A non-intrusive approach using a generalized finite element method. Engineering Fracture Mechanics, 90:41-64, 2012.

[LP1] A. Lozinski, O. Pironneau. Numerical Zoom for localized multiscales. Numerical Methods for Partial Differential Equations, 27:197-207, 2011.

[MD1] N. Moës, J. Dolbow, T. Belytschko. A finite element method for crack growth without remeshing. International Journal for Numerical Methods in Engineering, 46(1):131–150, 1999.

[PR1] J.-C. Passieux, J. Réthoré, A. Gravouil, and M.-C. Baietto. Local/global non-intrusive crack propagation simulation using a multigrid X-FEM solver. Computational Mechanics, 52(6):1381-1393, 2013.

Article 076-pds-81

Numerical methods in the design process of a sailing yacht

Tommaso Ingrassia [1], Antonio Mancuso [1], Davide Tumino [2]

(1): Università degli Studi di Palermo – Dipartimento di Ingegneria Chimica, Gestionale, Informatica, Meccanica – Viale delle Scienze ed.8 – Palermo, Italy
Phone: +39 091 23897263
E-mail : {tommaso.ingrassia,antonio.mancuso} @unipa.it

(2): Università degli Studi di Enna Kore, Facoltà di Ingegneria e Architettura, Cittadella Universitaria, Enna, Italy
Phone: +39 0935 536491
E-mail : {davide.tumino}@unikore.it

Abstract: In this paper most significant steps involved during the whole process of designing a sailing yacht are outlined. At first, a preliminary conceptual design process was implemented in order to fix some boundaries to the problem, then the best solution was found by using numerical simulations. As a general rule, once the target point has been decided, task of the designer is the definition of those systems of aerodynamic and hydrodynamic forces that are in equilibrium when the boat sails at its target. Unfortunately, a multi-purpose yacht does not exist. If the target point is in upwind sailing, then performances will be better for such a condition and worse for others. In the last years, thanks to hardware and software capabilities, Computational Fluid Dynamics (CFD) has become a powerful instrument to numerically compare several solutions instead of much more time-consuming experimental tests. The case study here presented is the design of hull, appendages and sails of a 15" skiff subject to box-rules, designed and manufactured at the University of Palermo. The entire design process has been numerically developed integrating a classical design approach with CFD simulations leading to an efficient solution.

Key words: Computational fluid dynamics, conceptual design, numerical methods, optimization, sailing yacht.

1- Introduction

The design of a sailing yacht, as well known, is a very challenging task. The main reason relays on the need to find the equilibrium between hydrodynamic and aerodynamic forces [LE1]. Differently from an airplane or a submarine, the yacht moves into water and air at the same time. Moreover, while keel and rudder are generally completely under water, as well as the sails are inside the air, the hull moves contemporarily between water and air giving rise to a free surface whose effect must be properly evaluated and taken into account in the yacht equilibrium. This is the reason why a simultaneous and integrated design [HE1] of hull, appendages and sail has not been solved yet, being a very complex problem whose variables are often correlated. Usually, the design of a yacht starts from the hull fairing. Once the hull has been optimized, the sail plan (usually giving the higher thrust with the lower side force) is designed according to the main sailing conditions. Keel and rudder are then chosen in order to balance forces and moments, minimizing the drag. Of course the designer needs to recursively adjust design parameters in order to match the desired requirements.

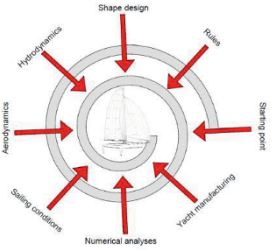

Figure 1 – The spiral design process

This is the most time consuming step which leads, at the end of the spiral process depicted in figure 1, to the target design point. However, making use of Computer Aided Engineering (CAE) tools [IM1] [IN1] [OW1] and optimization methods [IN2] [CM1] the target point can be reached earlier. A strong push in this direction has been given by numerical simulations. In the last years, in fact, thanks to hardware and software capabilities, CFD has become a powerful instrument for the designers. Many authors have addressed their works firstly concerning the design of International America's Cup Class yacht (IACC). Harries [HA1] elegantly solved the design of the hull by means of CFD simulations while Nicolopoulos [NB1] set up a mixed method (experimental/numerical) to optimize the bulb. Richards [R1], and more recently Viola [V1], modeled the sail plan of IACC yachts and compared numerical and experimental results in downwind sailing conditions. More recently, the field of interest moved to less blazoned (but not less important than IACC) competitions like the International Measurement System (IMS) Class. Masuyama [MT1] has developed a comparison between experimental and numerical data for a new designed boat moving in upwind condition, while Viola [VF1] has investigated both upwind and downwind sailing on a *Sparkman & Stephens* 24-foot yacht. Kim [KY1] has used the hydro – and aerodynamic

Article 076-pds-81

results to confirm the design of a 30-foot sloop. Although several papers have been found in literature concerning the design of medium and large yachts, to the authors knowledge, no researches have been yet performed on small boats like dinghies [IH1].
This is why in this work, the design of a little sailing yacht (i.e. a skiff) will be considered as far as concerns hull, sail rigging and appendages. First of all, following the typical guidelines of the conceptual design processes [IA1], some possible solutions (related to the hull, sails and appendages) have been proposed. After, the proposed solutions have been deeply investigated by means of numerical simulations in order to choose the best one. The result of the design process leads to the manufacturing of the first boat in the world entirely manufactured with unidirectional flax fibres as a structural material. This choice follows by results given in [BB1][WI1], where flax fibres appear, among commercial natural fibres, the best compromise in terms of performances, market availability and costs. The yacht, called LED (acronym of Linen Epoxy Dinghy), has been made with a sandwich structure of flax fibre and cork by means of a moulded vacuum bag process, the deck, instead, has been made with marine plywood.

2- Yacht conceptual design process

In the following, the developed conceptual design process is described. The most significant steps concern hull, sails and appendages design. The case study is the design and manufacturing of a sailing yacht that the Faculty of Engineering of Palermo presented at the *1001VelaCup*® regattas [www.1001velacup.eu]. The participation to this event is subject to technical rules briefly summarized as follows:
Hull: (Length x Beam x Height)$_{max}$ = (4.6 X 2.1 X 1.1) m;
Sails: Main, Jib, Gennaker: upwind$_{max}$ =16 m^2; downwind$_{max}$ =33 m^2;
Materials: hull, wings and appendages: 70%$_{min}$ natural fibres (e.g. wood, flax, bamboo); rig: fractional with 1 spreader and mast in extruded aluminum alloy.
The skiff analysed in the present paper has been designed considering the imposed regattas rules but also following considerations given in some papers in literature [CM1][AM1]. In particular, the main objective was to obtain high values of structural stiffness together with a consistent weight saving.

2.1 Hull

According to previous works in literature [LE1] [M1], the above mentioned spiral process (fig. 1) starts with the definition of the target point. Once it is defined, the most relevant dimensionless coefficients can be chosen and refined until satisfactory results are achieved. These parameters (mainly related to the length of water line, L_{WL}) are quite different depending on the hull to design, i.e. for sailing windward or downward; for ocean yachts (which are usual to sail in hard environment) or match race ones (whose regattas are sometimes held in closed seas and in breeze conditions). In this study, it has been fixed as target point the designing of a yacht to sail close-hauled in a breeze condition. This choice is justified even by the statistical analysis of the wind which gives an average wind of 7 knots for the regatta period.
A lot of time has been spent in the hull design by finding the best values of coefficients and parameters. Starting point of the procedure is the shape of Zyz [MM1], a classical dinghy similar to a Flying Junior, designed and manufactured in 2009 at the University of Palermo, in order to improve its performances. More than 15 different solutions have been studied before the approval of the final version. For each shape, the hull fairing has been obtained with the aid of the commercial software Rhinoceros while the resistance of the bare hull has been calculated according to the formula proposed by Keuning [KO1].

		Zyz	#1	#2	#3	#4	#5	#6	#7	#8	#9	LED1	LED2	LED3
L_{WL}	[m]	4,38	4,57	4,39	4,57	4,60	4,57	4,56	4,53	4,51	4,48	4,41	4,38	4,41
A_{wet}	[m^2]	3,27	3,62	3,57	3,32	4,06	3,47	3,37	3,66	3,65	3,49	3,35	3,33	3,38
A_{WL}	[m^2]	3,04	3,43	3,39	3,10	3,93	3,28	3,15	3,45	3,49	3,30	3,11	3,09	3,14
A_s	[m^2]	0,10	0,10	0,11	0,10	0,10	0,09	0,11	0,11	0,10	0,10	0,10	0,10	0,10
C_p	[-]	0,57	0,55	0,52	0,55	0,51	0,57	0,52	0,51	0,51	0,54	0,52	0,52	0,53
C_b	[-]	7,01	7,31	7,01	7,29	7,36	7,32	7,24	7,19	7,52	7,15	7,11	7,05	7,12
C_1	[-]	0,71	0,66	0,70	0,67	0,67	0,67	0,66	0,63	0,65	0,67	0,67	0,67	0,68
C_2	[-]	0,81	0,69	0,65	0,80	0,53	0,84	0,77	0,62	0,64	0,75	0,64	0,64	0,61
T_C	[m]	0,14	0,12	0,13	0,15	0,10	0,14	0,16	0,13	0,13	0,14	0,14	0,14	0,14
LCF	[m]	2,63	2,73	2,57	2,68	2,73	2,69	2,68	2,76	2,77	2,66	2,63	2,63	2,65
0	[deg]	9,32	7,47	6,37	6,87	7,77	8,11	6,76	12,04	3,87	6,93	7,36	9,70	7,23
V_c	[m^3]	0,24	0,25	0,25	0,25	0,24	0,24	0,25	0,25	0,25	0,25	0,24	0,24	0,24
B_{WL}	[m]	0,98	1,14	1,11	1,02	1,29	1,06	1,04	1,20	1,14	1,10	1,05	1,05	1,05

Table 1 - Coefficients and parameters of the analysed hulls

Table 1 shows these parameters (defined in [LE1]) for the most interesting analysed configurations, while figure 2 shows the plot of the total resistance (expressed in Newton) versus the hull velocity (expressed in knots) for the more promising hulls.

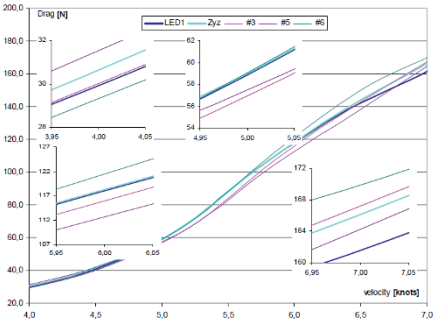

Figure 2 – Drag (in Newton) vs. velocity (in knots) of the most promising hulls.

It can be observed from the close up that at low velocity the best hull is the #6; for medium values the best one is the #3 and at high velocity the best hull is the #5. These considerations have led to a new hull LED1, (thick blue line in fig 2), which represents a trade-off hull able to maintain good performances in all the range of examined velocities. In order to better explore the domain close to the selected hull, two different version have been designed by slightly modifying parameters and coefficients to move a little bit volumes ahead (LED2) and astern (LED3) (see table 1). These three shapes will be deeply investigated with CFD analyses.

Article 076-pds-81

2.2 Sail plan

Basically, there are several sails configuration that can be designed and adapted to a yacht [G1]. However these can be divided into two main categories: with or without overlap.
This means that in the first case the jib partially overlaps the mainsail while in the second case the jib is self-tacking (fig.3). As a general rule, with a self-tacking jib it is common practice to have a square-top mainsail.

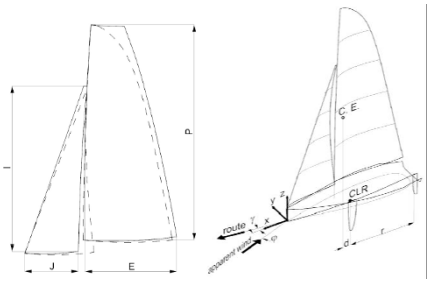

Figure 3 – On the left main and jib with overlap (dashed line) and without overlap (solid line); on the right reference frame attached to the hull.

Independently of the plan layout the sail maker job consists in designing a few sections (typically 4-5) and assigning to that an appropriate twist angle. Once these parameters have been defined and optimized, a smoothed surface can be drawn out. The goal is to obtain the higher thrust with the lower side force. However, concerning a skiff, the vertical location of the center of effort (CE in the following) plays an important role. In fact, the moment generated along the x-axis (in figure 3) by the side force –the heeling moment– must be balanced by the crew over the wings (righting moment) since there is not ballast on the keel. So, the higher is located CE, the greater is the moment, with the possibility of capsizing. Furthermore, the flow around sails significantly influences the yacht performances. Generally speaking, sailing close-hauled the overlap between mainsail and jib permits to go upwind better than without overlap. However, a square top mainsail gives a better response in terms of flow stabilization during tacking (or jibing). Thus the designer has to carefully evaluate many factors before choosing the plan layout. The sail plan for LED has been designed in collaboration with Doyle Sails Italy, according to the regattas rules and considering a light crew sailing close-hauled in a breeze. After several attempt, two different configurations have been considered for a deep investigation. One set is with a mainsail with roach and jib with 110% overlap and another with square top main and self-tacking jib. Table 2 gives the most significant dimensional parameters for each of the configurations.

	I *[m]*	**J** *[m]*	**P** *[m]*	**E** *[m]*
SET #1	4.89	2.02	6.2	2.5
SET #2	5.09	1.57	6.2	2.6

Table 2 – dimensions of main and jib

2.3 Appendages

Keel and rudder are generally designed with different plan forms and sections [CM2]. Lift and drag produced by the appendages play an important role in the equilibrium and should be carefully evaluated also according to other forces (due to sails and crew) applied to the yacht. Also for this reason, the keel and rudder design process should be strongly related to the sail designing and to other variables concerning the crew and the considered sailing conditions. Concerning the sections, except particular cases of optimized shapes [LV1], usually NACA sections, for which the literature gives both theoretical and experimental details [AV1], are chosen. Being the leeway angle very small for modern yacht, it is common practice to choose a laminar section (e.g. NACA six-digit) for the keel and a four-digit for the rudder.
According to regatta rules, no systems able to reduce the induced drag like winglets or foils can be used. Moreover, the use of high strength materials like carbon fibres or Kevlar is forbidden, then, to ensure the needed flexural rigidity and strength, root chords for keel and rudder have been dimensioned safety. A not too thin chord at the tip was also chosen in order to avoid problems during the vacuum bag manufacturing. For these reasons a classical design approach has been applied. Particularly, the keel plan has been designed to have an elliptical lift distribution with a focus line as straight as possible with NACA 65-010 sections. While the rudder has been drawn with a straight trailing edge with NACA 0010 sections.

3.0 Numerical simulations

In what follows a summary of the numerical simulations will be shown. The software Ansys has been adopted both for pre-processing (ICEM-CFD) and solution (Fluent). Table 3 shows details of domain extensions (with respect to a characteristic length), mesh type and number of cells, viscous models and wall y^+ range.
In order to evaluate the free surface effect, the Volume Of Fluid (VOF) model has been applied with a high quality hexahedral mesh which better fits with the VOF model. All the simulations have been carried out until convergence of the residuals (fixed at $1x10^{-5}$). This value ensures convergence of both drag and lift.

	Reference length	Domain extension x	y	z	Mesh type	Numbers of cells	Turbulence model	y^+ range	Free surface
Hull	L_{wl}	10 L_{wl}	4 L_{wl}	2 L_{wl}	hexa	$2.7x10^6$	k-ε RNG	[30, 120]	VOF
Sail	E	13 E	10 E	6 E	tetra	$1.8x10^6$	k-ω SST	[30, 50]	-
Appendages	c_{Ri}	20 c_{Ri}	16 c_{Ri}	6 c_{Ri}	tetra	$0.7x10^6$	k-ε RNG	[20, 50]	-

Table 3 – Details of the computational domains.

Note that experimental data are not available so that yacht velocity, leeway angle, wind velocity and apparent wind angle must be heuristically chosen. Even if it could appear a rough approximation, it will be shown how reasonable values of these variables give very good agreement. Figure 3 shows the yacht sailing close hauled with a leeway angle γ and an apparent wind angle φ with respect to the reference frame x,y,z.

Article 076-pds-81

3.1 Hulls

Three hulls (as well as Zyz) have been selected for a deep investigation via CFD analyses; for each of them an hexahedral mesh has been generated with the same topology and blocking strategy. Figure 4 shows the mesh around the hull at the water line elevation and at the maximum beam. In order to evaluate the real draft of the hull, the approach described by Yang [YL1] has been followed.

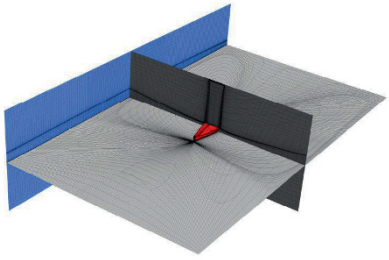

Figure 4 – Domain mesh of the hull with cutting planes (gray coloured) at the water line elevation and at the maximum beam.

Effectively, only the sinkage correction has been considered. In fact, for these light skiffs, the crew weight (close to 140 kg) is approximately one and half the boat weight (90 kg including rigging and sail). Thus, even little movements of the crew can change the trim. Moreover it is well known that skiffs should run flat at medium speed and trimmed backward at high speed. For this reason it has been considered more interesting the evaluation of the hull response to a small trim variation of half a degree. Particularly, three velocities for each of the hulls (5, 6 and 7 knots) have been simulated at a constant leeway angle of 3 degrees. Figure 5 shows the plot of the resistance, along the x-axis, for the analysed hulls. One can find good agreement with respect to the plot of figure 2, even if the empirical formula usually underestimates the total resistance.

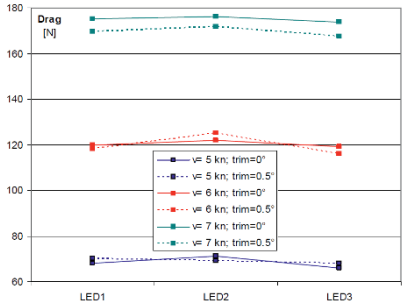

Figure 5 – Drag along x-axis for the hulls at 5, 6 and 7 knots with trim (dashed lines) and without trim (solid lines)

In order to better compare the obtained results, in figure 6 the percentage reduction of resistance with respect to Zyz has been shown.

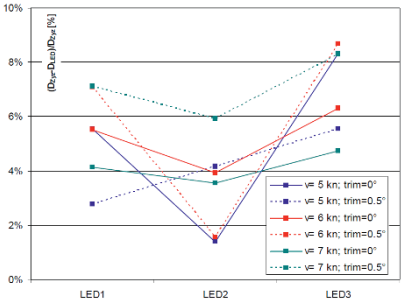

Figure 6 – Comparison of the drag variation in percentage with respect to the corresponding value of Zyz

Note that this variation is positive for each of the hulls; this event confirms a good design approach. It has been decided to select LED3 since, according to figure 6, it has the best performances. In fact, the range variation of the resistance for LED1, LED2 and LED3 are [3%-7%], [2%-6%] and [5%-9%] respectively. Finally, figure 7 shows the lines plan of LED3 (LED in the following).

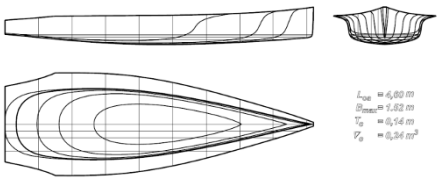

Figure 7 – Lines plan of LED

3.2 Sails

In order to select an appropriate sail plane, several configurations have been simulated at different apparent wind velocity (10, 12, 15 and 18 knots) always at 20 degrees of incidence. Moreover, three different settings in terms of jib angle φ_0 (6.5, 9, 13 degrees) have been considered. The minimum and maximum values of φ_0 are mainly related to the deck layout of the skiff. Regarding details of the surface mesh used for the sails (both set#1 and set#2), the maximum element size is about 64 mm. To capture boundary effects, prismatic layers have been included with the first cell height chosen in order to obtain the range of wall y^+.

Figure 8 and figure 9 show the pressure coefficient for both the sail set. From these plots it is evident the benefit given by the overlap between main and jib in terms of pressure distribution. Figure 10 and figure 11 show the thrust and the side force, respectively, for all the analysed configurations. In all the cases, there are small differences in terms of performance between the sail set #1 and #2. However, according to figure 10, one can note that at low wind velocities the best jib angle is 9° for both the sail set. While

Article 076-pds-81

at higher velocities better thrust can be obtained with a jib angle of 6.5° for set #1 and always 9° for set #2.

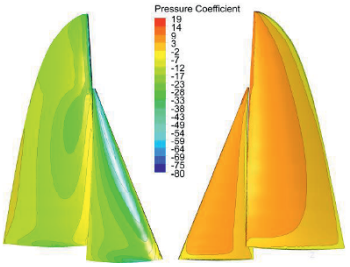

Figure 8 – Pressure coefficient distribution on leeward side (left) and windward side (right) for sail set #1

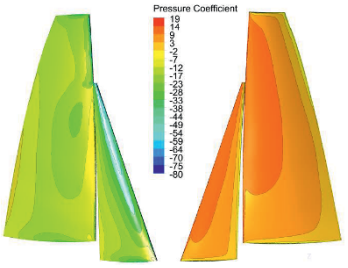

Figure 9 – Pressure coefficient distribution on leeward side (left) and windward side (right) for sail set #2

For this reason, a fine angle regulation of the overlapped jib (i.e. set #1) could favour a thrust increase. On the other hand, according to figure 11, the lower the jib angle, the greater is the side force that, as previously said, must be balanced by the crew on the wings.

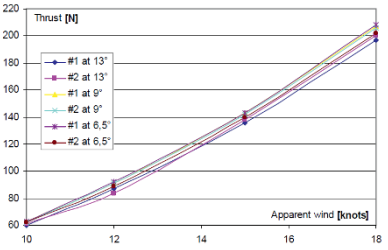

Figure 10 – Thrust developed by sail set #1 and #2 at different jib angles and apparent wind velocity.

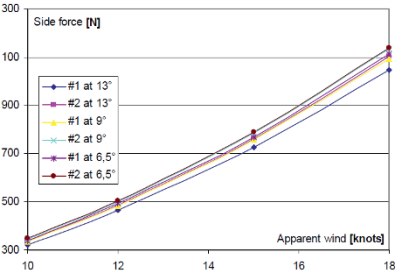

Figure 11 – Side force developed by sail set #1 and #2 at different jib angles and apparent wind velocity.

Furthermore, the vertical location of the centre of effort C.E. (see figure 3) depends mainly on the plan form and only marginally on the apparent wind velocity and the jib angle. Particularly, for set #1 the vertical C.E. moves around 2.8 metres; while for set #2 moves around 3.2 metres. In order to establish which set gives better performances, a common practice can be here applied, dealing with skiffs, by calculating the so called "sail carrying power" which is a dimensionless parameter given by the following equation:

$$S_{cp} = \frac{R_m / CE}{W} \qquad (1)$$

being R_m the righting moment and W the weight (approximately 230 kg including the crew). Since the crew weight is about 140 kg and the crew arm (from the center of buoyancy) can be estimated as 2.1 m, the above equation gives a "sail carrying power" of 0.46 and 0.4 for set #1 and #2 respectively. As a matter of course the same calculation for the 49er class gives a values of 0.43. In other words, the designed skiff sails almost as fast as the 49er.

3.3 Appendages

Appendages, as previously said, have been designed following a classical approach. Numerical simulations have been executed in the hypothesis of sailing close hauled with a leeway angle of 3° and velocities of 5, 6 and 7 knots.

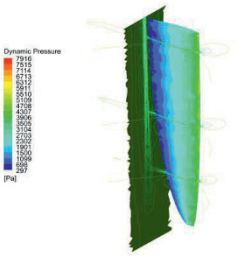

Figure 12 – Dynamic pressure contours of the centreboard at 3° of leeway and 5 knots of velocity

Article 076-pds-81

Figure 12 shows the dynamic pressure contours on the centreboard. Even in this case, prismatic layers have been included in order to obtain the range of wall y^+ as reported in table 3. Finally, figure 13 gives the side force for both centerboard and rudder.

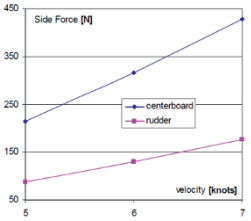

Figure 13 – Side force developed by centreboard and rudder at different velocities.

4.0 Concluding remarks

The knowledge based design approach followed in this work, has given interesting results not only from the qualitative standpoint. In fact, considering the contribution of each single component of the yacht, i.e.: hull, sails and appendages, the vectorial equilibrium equations lead to:

$$\begin{cases} \sum F = F_H + F_K + F_R + F_S = 0 \\ \sum M = M_H + M_K + M_R + M_S = 0 \end{cases} \quad (2)$$

where H, K, R, S stand for hull, keel, rudder and sail respectively. By substituting in the first row eq. (2) the corresponding values obtained from the above CFD simulations (related to the sail set #1) one can write:

$$\begin{cases} \sum F_x = -66 + 4 + 2 + 63 = +3 & v = 5 \text{ knots} \\ \sum F_y = -31 - 215 - 88 + 335 = +1 & \varphi = 20° \\ \sum F_z = 2314 + 0 + 0 + 16 = +2330 & \varphi_0 = 9° \end{cases} \quad (3)$$

The right side of eq. (3) gives the associated input data. Note the remarkable consistency of this result in terms of absolute values. Moreover, the total force along the z-axis, (neglecting the small contribution of the appendages) gives a value of 238 Kg (2330/g) which exactly matches the skiff displacement. The moment equilibrium (second row in eq. (2)), is always satisfied. In fact, the component along x (heeling moment) is balanced by the crew over the wings; the component along y (pitch moment) is balanced by the longitudinal position of the crew which moves along the x-axis; while the moment along the z-axis (yaw moment) is balanced by the helmsman which continuously act on the rudder. Similar considerations can be done for other input data combinations as depicted in figures 14-15 which permits to compare the hull resistance along x and y axes with thrust and side force. For instance, the hull runs at 6 knots if the apparent wind is close to 14 knots. Note that at 18 knots of apparent wind, the skiff reaches its maximum allowable heeling moment given by the side force 1.094 N (see figure 15) multiplied by the CE (2.8 m) which gives a moment of 3063 N m. In fact, the crew (140 Kg) over the wings (with an approximate arm of 2.2 m) generates a maximum righting moment close to 2884 N m. This means that at higher wind velocities, in order to avoid capsizing, the crew needs to depower the sail.

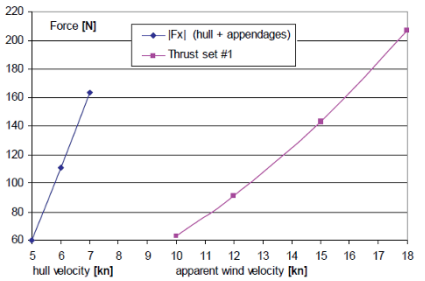

Figure 14 – Thrust force at different hull speed (5-7 knots) and different apparent wind velocity (10-18 knots)

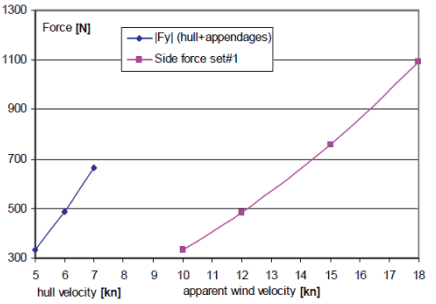

Figure 15 – Side force at different hull speed (5-7 knots) and different apparent wind velocity (10-18 knots)

5.0 Conclusions

In this paper, the complete design of a little sailing yacht – a so called skiff – has been developed. Starting from the target point a classical spiral process has been followed until satisfactory hull shapes have been drawn out. Working in collaboration with specialized sail makers, suitable sail plans have been modelled. Finally, the appendages have been designed with the aim to guarantee the appropriate lift with the minimum drag. In order to choose the best of the configurations in terms of hulls, sails and appendages, a deep CFD investigation has been carried out. Since no experimental data were available, a heuristic approach has been applied. The assumptions made in terms of hull velocity, leeway angle and apparent wind give rise to reasonable results. Original aspects of the present work can be associated to the full integration of all numerical simulation methods in spiral design process applied to the

definition of all components of a light yacht. Future works will concern the set up of an experimental equipment based on GPS technology (to be installed on board) with the aim to record data for experimental/numerical comparison

7- References

[AM1] Alaimo A., Milazzo A., Tumino D., 2012. Modal and structural FEM analysis of a 50 ft pleasure yacht. Applied Mechanics and Materials Vols. 215-216 pp 692-697.

[AV1] Abbott I.H.,Von Doenhoff A.,1959.Theory of Wing Sections. Dover Publications Inc., NewYork, USA.

[BB1] Bodros, E., Baley, C. 2008. Study of the tensile properties of stinging nettle fibres (Urtica dioica), Materials Letters, 62 (14), pp. 2147-2149.

[CM1] Cappello, F., Mancuso, A., 2001. Lay-up optimisation for the hull of a racing sailing yacht. ADES, International Journal Advances in Engineering Software 32 (1), 133–139.

[CM2] Cirello A., Mancuso A., 2008. A Numerical Approach to the Keel Design of a Sailing Yacht. Ocean Engineering 35 1439-1447, doi:10.1016/j.oceaneng.2008.07.002.

[G1] Garrett R.,1987.The Symmetry of Sailing. Adlard Coles Ltd., London, UK.

[GA1] Harries S., Abt C., Hochkirch K., 2001. Hydrodynamic Modeling of Sailing Yachts. The 15th Chesapeake Sailing Yacht Symposium; Annapolis.

[HE1] Hubka V., Eder W. E., 1992. Design Science. Springer.

[IA1] Ingrassia, T., Alaimo, G., Cappello, F., Mancuso, A., Nigrelli, V. A new design approach to the use of composite materials for heavy transport vehicles. (2007) International Journal of Vehicle Design, 44 (3-4), pp. 311-325.

[**IH1]** Inukai Y., Horiuchi K., Kinoshita T., Kanou H., 2001. Development of a single-handed hydrofoil sailing catamaran. Journal of Marine Science and Technology 6 (1), pp. 31-41.

[IM1] Ingrassia, T., Mancuso, A., Nigrelli, V., Tumino D., Numerical study of the components positioning influence on the stability of a reverse shoulder prosthesis, International Journal on Interactive Design and Manufacturing, 2014, DOI : 10.1007/s12008-014-0215-6

[IN1] Ingrassia T., Nalbone L., Nigrelli V., Tumino D., Ricotta V., Finite element analysis of two total knee joint prostheses, International Journal on Interactive Design and Manufacturing, 7(2), pp 91-101, 2013.

[IN2] Ingrassia T., Nigrelli V., Buttitta R., "A comparison of simplex and simulated annealing for optimization of a new rear underrun protective device", 2012, Engineering with Computers, DOI: 10.1007/s00366-012-0270-1

[KO1] Keuning J. A., Onnink R., Versluis A., van Gulik A. A. M., 1996. The Bare Hull Resistance of the Delft Systematic Yacht Hull Series. HISWA Symposium on Yacht Design and Construction, Amsterdam RAI.

[KY1] Kim W.-J., Yoo J., Chen Z., Rhee S.H., Chi H.-R., Ahn H., 2010. Hydro- and aerodynamic analysis for the design of a sailing yacht. Journal of Marine Science and Technology 15 (3), pp. 230-241.

[LE1] Larsson L., Eliasson R.E., 1996. Principles of yacht design. Adlard Coles Nautical, London.

[LV1] Lombardi G., Vannucci S., Ciampa A., Davini M., 2007. The aerodynamics of the keel of America's Cup yacht: an optimization procedure. Proceedings of the International Aerospace Computing Conference, Paris, 18 – 19 June.

[M1] Mancuso A., 2006. Parametric Design of Sailing Hull Shape. Ocean Engineering (33) 234–246. **[MM1]** Mancuso A., Milone S., Tumino D., A Simultaneous Engineering Approach to the Yacht Design. NAV 09 – 16th International Conference of Ship and Shipping Research, MESSINA, Italy 25 - 27 November 2009.

[MT1] Masuyama Y., Tahara Y., Fukasawa T. Maeda N., 2009. Database of sail shapes versus sail performance and validation of numerical calculations for the upwind condition. J. of Marine Science Technology 14:137-160.

[NB1] Nicolopoulos D., Berton E., Gouvernet G., Jaques A., 2009. A hybrid numerical method to develop America's Cup yacht appendages. Sports Eng 11:177-185.

[OW1] Otto K., Wood K., 2001. Product Design. Prentice Hall, New Jersey (USA).

[R1] Richards P.J., 1997. The effect of wind profile and twist on downwind sail performance. Journal of Wind Engineering and Industrial Aerodynamics 67&68, 313-321.

[VA1] Van Nierop E. A., Alben S., Brenner M. P., 2008. How Bumps on Whale Flippers Delay Stall: An Aerodynamic Model. Physical Review Letters, doi: 10.1103/PhysRevLett. 100.054502.

[V1] Viola I. M., 2009. Downwind sail aerodynamics A CFD investigation with high grid resolution. Ocean Engineering 36, 974-984. doi:10.1016/j.oceaneng.2009.05.011.

[VF1] Viola I. M., Flay Richard G. J., 2011. Sail pressures from full-scale wind-tunnel and numerical investigations. Ocean Engineering 38, 1733-1743.

[WI1] Wambua, P., Ivens, J., Verpoest, I. 2003, Natural fibres: Can they replace glass in fibre reinforced plastics? Composites Science and Technology, 63 (9), pp. 1259-1264.

[YL1] Yang C., Löhner R., Noblesse F., Huang T. T., 2000. Calculation of Ship Sinkage and Trim Using Unstructured Grids. European Congress on Computational Methods in Applied Sciences and Engineering, Barcelona (Spain), 11 – 14 September.

Article 011-vp-70

A multi-layer approach for path planning control in Virtual Reality simulation

Simon Cailhol[1], Philippe Fillatreau[1], Jean-Yves Fourquet[1] , Yingshen Zhao[1]

(1) : ENIT-LGP, 47, avenue d'AzereixBP 1629 - 65016 Tarbes CEDEX, FRANCE
Tél: +33 5 62 44 27 00 - Fax: +33 5 62 44 27 27
E-mail : {simon.cailhol, philippe.fillatreau, jean-yves.fourquet, yingshen.zhao} @enit.fr

Abstract: This work considers path-planning processes for manipulation tasks such as assembly, maintenance or disassembly in a virtual reality (VR) context. The approach consists in providing a collaborative system associating a user immersed in VR and an automatic path planning process. It is based on semantic, topological and geometric representations of the environment and the planning process is split in two phases: coarse and fine planning. The automatic planner suggests a path to the user and guides him trough a haptic device. The user can escape from the proposed solution if he wants to explore a possible better way. In this case, the interactive system detects the user's intention and computes in real-time a new path starting from the user's guess. Experiments illustrate the different aspects of the approach: multi-representation of the environment, path planning process, user's intent prediction and control sharing.

Key words: Path planning, Virtual Reality, Interactive simulation, multi-layer architecture.

1- Introduction

The industrial product development process is going faster and faster with more and more complex products. This leads to a need of tools allowing to rapidly test a product at all the PLM stages during the design phase. There is a particular need for the tasks that involve human operator manipulation. Here comes the interest of Virtual Reality (VR) to run these tests with virtual prototypes instead of expensive and time consuming real ones [FF1].

The main issue of tasks such as the ones involved in assembly, dismantling and maintenance is to find paths for the systems components and parts.

In this context, we propose a collaborative path-finding system based on the interaction of a user immersed in a VR simulation and an automatic path planning process inspired from robotics.

Collaboration is defined as follows. The system provides a initial planned path and the user is guided along a computed trajectory through an haptic device. However, the user can disagree the proposed path and try to go in another direction. The system must compute a new path every time the user tries to test another solution. Thus, it must be able to take into account the user's interactions in real time to update the suggested path and it requires control sharing between the user and the planner while performing the task.

Robotics path planners mainly deal with geometric aspects of the environment. The VR context of our planner involves a human in the loop with a different environment representation. Thus, we chose to split the planning process in two phases: a coarse planning dealing with topological and semantic models of the environment (the places, their semantics and their connectivity) and a fine planning dealing with geometry and semantics (geometry of obstacles and places and their complexity). This planning process partitioning provides a framework compatible with the human path planning process described in [AT1].

Thus, the proposed interactive path planner is based on a multi-layer environment representation (semantic, topological and geometric). All these environment models are used by distinct planner layers to perform the coarse (semantic and topological aspects) and fine (semantic and geometric aspects) planning and to assist VR user.

2- State of the art

2.1- Automatic path planning

The automatic path planning issue has been deeply studied in robotics. These works are strongly based on the Configuration Space (CS) model proposed by [L1]. This model aims at describing the environment from a robot's Degrees of Freedom (DoF) point of view. The robot is described using a vector where each dimension represents one of his DoF. A value of this vector is called a configuration. So, all the possible values of this vector form the CS. This CS can be split into free space and colliding space (where the robot collides with obstacles of the environment). With this model, the path planning from a start point to a goal point consists in finding a trajectory in the free space between these two points in the CS.

The main strategies for path planning are given in the Table I where we distinguished the deterministic from the

Article 011-vp-70

probabilistic ones, but also, the ones involving global approach from the ones involving local one. More details on path planning algorithms and techniques are available in [L2].

Table 1: The main path planning approaches

	Global approaches	Local approaches
Deterministic strategies	Cells decomposition Roadmaps	Potential fields
Deterministic strategies	PRM	RRT and RDT

2.2- Control sharing

There already exist some applications involving path planners with human interactions (robot tele-operation, semi-autonomous vehicles, virtual environment exploration,...). These applications allow us to identify two aspects in control sharing:

• Authority sharing: it aims at defining how the authority on the system is shared between automatic planner and human. To deal with this issue, different strategies can be found in the literature. The use of virtual fixtures [ML1], authority switched to robot for fine motion operations [AM1], authority progressively transferred to robot while reaching the goal [WN1], for an anthropomorphic robot, Cartesian (position and orientation of end effector) control by user and joint control by planner [YH1]. The authority sharing through haptic devices were studied for semi-autonomous vehicles driving. In this case, from the horse riding experience, [FH1] suggests to use an haptic interface with a *H-mode* to perceive user's involvement and allocate the authority according to it (the more the user is involved, the more authority he has).

• Intent prediction: it aims at predicting the intent of the human to define the goal of an automatic controller and so to assist the human performing the task. These techniques are strongly based on behavior or trajectory recognition [AE1], [FR1], [LO1], [YA1], on minimum jerk criterion [WN1], on model predictive control [LK1], [AP1]. Dragan also recently proposed to find the targeted goal among a set of potential ones from the current movement direction [DS1].

We summarize these two control sharing aspects in Fig. 1 where the yellow boxes illustrate the control sharing.

These techniques allow involving human and automatic planning system to perform a task. However, the user's actions do not affect the automatic planner strategy to compute the path.

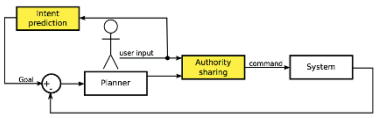

Figure 1: Sharing control model in semi-automated planning.

2.3- Interactive path planning

Some works propose collaboration between a human operator and an automatic planner in the path planning process. The simpler one [LF1] uses a potential field strategy. An attractive field to the goal is computed and used to guide the user thanks to a haptic device. Another interactive planner from [LF1] guides the user along a computed trajectory. To compute this trajectory in real time, a cell decomposition of the free space is used to define a 3D tunnel. Then a RDT algorithm computes a path within this 3D tunnel. The whole trajectory computation process is restarted if user goes away the proposed trajectory. Finally, an interactive planner build from a probabilistic strategy [TF1] uses the user's action to constraint the random sampling of the configuration space in the RRT growing.

These three planners do not involve the human user in the same way. The first one gives a strong responsibility to the user (it's up to him to deal with the obstacles and to avoid collisions). The second one suggests a whole trajectory the user can go away from to restart the whole planning process. The last one allows the user to point a direction that gives to the planner a preferred direction to explore. These differences of roles induce different computational load for the planner and cognitive load for the user as illustrated in Fig. 2.

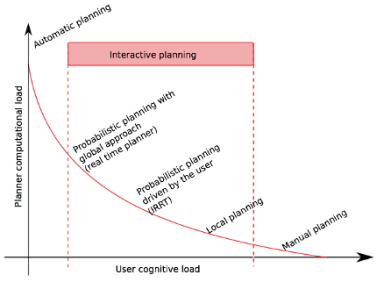

Figure 2: Computational vs cognitive load for interactive planning.

3- Proposed interactive planner

This section presents the concepts of the strategy used in the interactive planner shown in the Fig. 3 where colors are linked to the environment and planning layers: yellow for geometry, orange for topology and red for semantics. The concepts used are illustrated here with 2D illustrations for clarity, but the model stands identical for 3D simulations.

We argue that involving semantic and topological aspects in path planning in addition to the common geometric ones allows adapting the planning strategy to the local complexity of the environment. To deal with it, a coarse planning is performed first using semantic and topological information. Then, heavy geometric path planning strategies are used merely locally, (according to the place complexity). This allows us to plan path in real time (without disturbing user's immersion in the VR simulation), and to take into account users action while performing the task to interactively update the planned path.

Article 011-vp-70

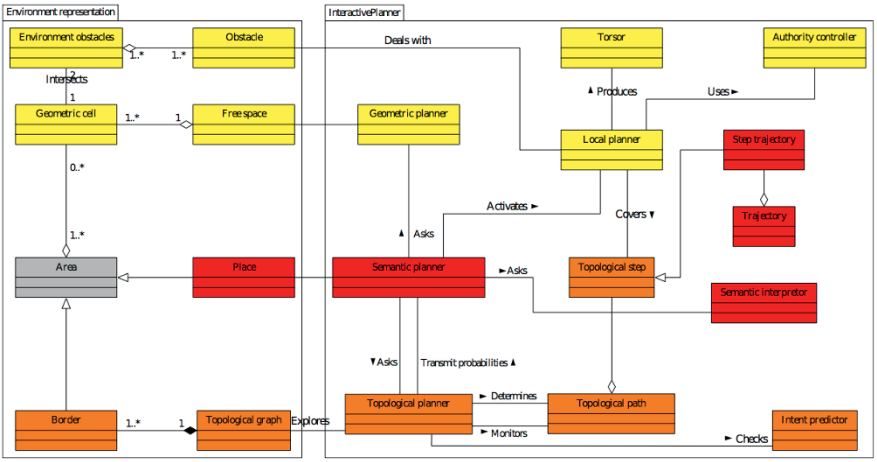

Figure 3: UML domain model of environment representation and interactive planner.

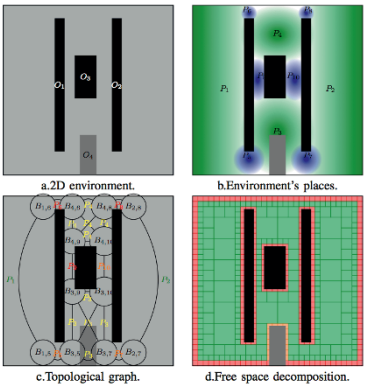

Figure 4: Different models of environment.

3.1- Environment representation

The environment example given in Fig. 4.a to illustrate the concepts is made of a square workspace cluttered by 3 fixed obstacles (O_1 to O_3) and 1 moving obstacle (O_4).

The semantic layer of environment representation given in Fig. 3 is made of places. A *Place* [1]is identified (Fig. 4.b) taking into account only the static obstacles to build a static representation of the environment. Semantic attributes are assigned to the places to describe their complexity (size, shape, cluttering,...) for path planning.

The topological layer connects the places thanks to Borders. A *Border* $B_{i,j}$ represents the overlapping area of places P_i and P_j. These borders are then used to build the *Topological graph* of the environment shown in Fig. 4.c. In this *Topological graph*, the nodes correspond to the borders, and the edges to places (and so to their semantics). The Fig. 5.a shows the distance between the borders' centers in place P_4. These distances are set to the edges of topological graph as attributes (Fig. 5.b for place P_4). In Fig. 4.c, the place attribute corresponding to the edges are given in a color linked to their complexity (from (green) low to very high (red)).

The geometric environment representation consists in a geometric description of the obstacles surfaces thanks to meshes (*Obstacle* and *Environment obstacle*). Then, a cell decomposition of the environment (*Free space* and *Geometric Cell*) is made with a quadtree (an octree in 3D) to describe the 2D (3D) free space (Fig. 4.d).

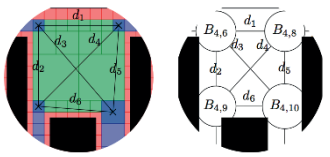

Figure 5: Topological graph building for place P_4.

3.2- Planning aspects

According to these environment models, the planning process is split in two stages: the coarse planning involving semantic and topological layers and the fine planning involving semantic and geometric layers

[1] Terms in italic refer to cncepts in UML domain model of Fig. 3

3.2.1- Coarse planning

To adapt the geometric planning strategy to local complexity, the whole path is split in steps. A step refers to a place of environment representation. A step also refers to a border to reach to fulfill the step. The geometric planning strategy is thus chosen according to the semantic of step's place.
To run this planning stage, two nodes corresponding to start and goal configurations are added to the topological graph. To direct the graph exploration the *Semantic planner*, thanks to the *Semantic interpreter*, assigns costs (C) to graph's nodes ($n_{i,j}$) and edges (e_k) accordingly to the semantic information of involved places (see equation 1).

$$\begin{aligned} C_{n_{i,j}} &= f(sem(P_i), sem(P_j)) \\ C_{e_k} &= f(d_k, sem(P(e_k))) \end{aligned} \quad (1)$$

Where *sem(P)* is the semantic information of place *P*, e_k is a graph's edge, d_k its distance attribute and *P(ek)* its place attribute; $n_{i,j}$ is the node linked to the border $B_{i,j}$ between P_i and P_j.
These costs make the cost of a path (C_{path}) computation possible (see equation2).

$$C_{path} = \sum_{n_{i,j} \in} pathC_{n_{i,j}} + \sum_{e_k \in path} C_{e_k} \quad (2)$$

Then the graph is explored by the *Topological planner* thanks to a Dijkstra algorithm [D1] to find the less expensive *Topological path* between start and goal nodes. This *Topological path* is used to split the trajectory in *Topological steps*, each step corresponding to a place to cross (a edge of *Topological path*) and a *Border* to reach (a node of topological path).

3.2.2- Fine planning

This planning stage consists in finding the concrete geometrical path. To do so, each *Topological step* is used to define a milestone configuration within the border to reach. Then, accordingly to the semantic information of the place to cross, we adapt the geometric path planning strategy. Depending on the cluttering semantic attribute, an A* algorithm can be ran on the place to set intermediate milestones within the step. When all the milestones have been defined, the *Local planner* guides the user toward the next milestone. This one compute a torsor applied on a haptic device from a linear interpolation.

3.2.3- Coarse and fine planning organization

The coarse and fine planning are used to manage the whole planning. The *Topological path* and its steps are concepts allowing the different planning layers to share the information. Once the *Topological path* found and the *Topological step*s defined, the steps information is used by the *Semantic planner* to accurately set the geometric layer.

3.3- *Process monitoring*

While the user is performing the task, he is guided toward the next milestone configuration thanks to the haptic device. This next milestone must be updated while the user is progressing along the path. On the geometric layer, the next milestone is set to the *Local planner* for the guidance computation when the current one is considered as reached. The goal is considered as reached when the distance between the goal and the current position is smaller than θ_d. On the topological layer, the milestone is a *Border*, so even if the user is guided toward a geometric configuration set within the *Border*, the milestone is considered as reached as soon as the user enters the *Border*. When the target *Border* is reached, the next *Topological step* is used to set the *Local planner* and to monitor the process.

3.4- Control sharing aspects

The planner provides user with a guidance torsor through the haptic device used for object manipulation. The Local planner computes this guidance torsor. For each layer of such planner architecture, specific ways to share control can be envisaged as shown in Table II.
In Table II it appears that the intent prediction for the geometric layer is directly linked to the authority sharing of topological layer. Indeed, within a *Place*, the set of potential goals to get out of this *Place* is made of the corresponding Border s. The intent prediction is made with geometric movement and geometric information on Borders. The re-planning is made by the *Topological planner* for a new *Topological path* definition.
The same applies for the intent prediction of the topological layer and the authority sharing of the semantic layer. Cost functions of equation 1 may be learned from the places the user prefers to cross. These preferred places' attributes can be identified from all the re-planning done due to user's action. The new cost value defined with these functions will thus change all the incoming topological re-planning.
The control sharing of the proposed planning architecture is focused on the geometric and topological layers. A H-mode from [FH1] had been implemented for geometric authority control. An intent prediction inspired from [DS1] had also been set to make the topological path re-planning available.

	Authority sharing	Intent prediction
Semantic layer	Learn from users action new semantics informa- tion or means to deal with them to accurately set the topological and geometric planners	Interpret planning query expressed in natural lan- guage (*assemble this part on this one*, *bring this ob- ject on this one*,...)
Topological layer	Check if user agrees the proposed topological path. Trying to predict his in- tents on the topological layer (which place he is targeting)	Learn the kind of paces the user prefers to cross to advantage them during the topological path planning process
Geometric layer	Dynamically balance the authority on the object manipulation (between hu- man and automatic plan- ner) by modulating the au- tomatic planner guidance force.	Find the targeted next place to redefine the geo- metric planner goal

Table 2: Interaction means on the different layers.

Article 011-vp-70

4- Implementation

4.1- VR platform

We implemented this architecture in Virtools™ 4.1 software through libraries developed in C++ language. We developed 3 distinct libraries: 2 autonomous libraries corresponding to *environment model* and *path planner* and an interface library. The VR devices used are a large 3D display to immerse interactive user in the environment, a motion capture system to allow him to turn around and a haptic arm to manipulate the objects. The Fig. 6 shows the corresponding VR platform. The devices used in these simulations are:

- A large passive stereo-visualization screen
- A ART motion capture system ARTTRACK2
- A Haption virtuose 6D 35-45 haptic arm

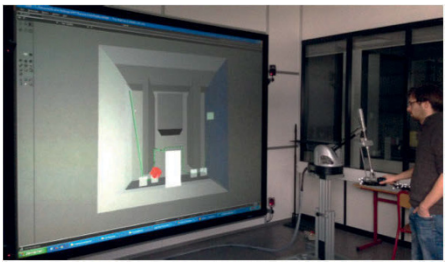

Figure 6: Simulation on VR platform.

4.2- Environment representation built

The environment model is implemented in a dedicated library interfaced to Virtools™ with a specific library.
The environment representation we use is made of 4 models:

- The objects of the environment represented through meshes and positioning frames. We distinguish among them the fixed ones and the moving ones thanks to a flag parameter to be able to exclude the moving ones while identifying the places (static mapping of the environment). All the objects of the environment can have semantic attributes assigned. This part is strongly based on the CGAL project [C1].
- The free space description through an octree decomposition of the 3D scene (in this case also, the nodes colliding with fixed object are distinguished from those colliding with only moving objects)
- The topological graph to model the places connectivity (the graph's nodes are the borders, and the edges the places)
- The set of places and their borders. We defined some procedure to automatically identify the places from the octree structure and the semantic information attachment is manually made, choosing for each place the right attributes among a set of available ones. One attribute is automatically set: *cluttered* if the place contain moving obstacles

The attributes available in our simulations allow describing the level of complexity of a place: low, average, high, and very high.

4.3- Planner implementation

The planner is also implemented in a dedicated library and interfaced to Virtools™ using the same interface library used to interface the environment.

4.3.1- Planning classes

Four classes had been defined corresponding to the four planners. Each of these planner classes deals with an environment model. The *Local Planner* provides the user with the guidance. The geometric planner finds, if necessary, a path on the octree. The *Topological Planner* explores the *Topological Graph* to build the path and the steps managed by the local and the geometric planners. The *Semantic Planner* coordinates the whole planning process, asking the *Topological Planner* for the *Topological Path* and planning which strategy will be used on the geometric layer.
For the weights computation, we defined the function of equation 1 assigning the weights as given in equation 3.

$$\begin{aligned} C_{n_{i,j}} &= \frac{C_{complexity}}{2} \\ C_{e_k} &= d_k.C_{complexity} \end{aligned} \tag{3}$$

Where $C_{complexity}$ is set according to the involved places complexity to 0, 0.5, 1 and 5 for low, average, high and very high complexity.

4.3.2- Control sharing classes

Two main classes improve the planner for the control sharing. The first one is correspond to the *Authority Controller*. It aims at modulate the guidance norm corresponding to user involvement. It allows user to feel free when he is exploring for others ways. The second one is the *Intent Predictor*. It detects the user intents to compute a new *Topological Path* when the user goes away the proposed one. These two classes and there computation are strongly based on the instantaneous movement computation made thanks to the *Trajectory Step Trajectory*.

5- Simulations and results

5.1- Environment used

To test the multi-layer structure on the laboratory's VR platform, the environment used is a 3D instance of the environment described in section 3. This environment is a cubic workspace with four obstacles cluttering the scene (3 fixed and 1 moving). Different environment configurations have been tested moving the fixed obstacles to change the complex passages location (O_1 and O_2 are moved vertically and O_3 horizontally). The corresponding topological graphs are given in Fig. 7. This figure also illustrates the planning query in these environments. It aims at bringing a piece from a start point S in place P_1 to a goal point G in place P_2. The topological paths found by the topological planner are also displayed in bold blue lines in the topological graphs.

Article 011-vp-70

5.2- Path planning

The Fig. 8 shows the real path computed in the environment illustrated in Fig. 7. The object to move is the red cube and the targeted goal is the green one. The path is displayed in green. The paths on place P_3 avoid mobile obstacle O_4 thanks to the A* algorithm performed on this cluttered place. To find such paths, the computational time for the Dijkstra algorithm in the topological graph was about 1ms, and the A* algorithm when necessary to cross the cluttered place took from 50ms to 750ms depending on the path to find. Thus, the whole path is find in less than 1s where using the A* algorithm alone without any semantics or topology planning process take about 3.5s without avoiding complex passages (in this case the past computed is the shortest but not the easiest to perform).

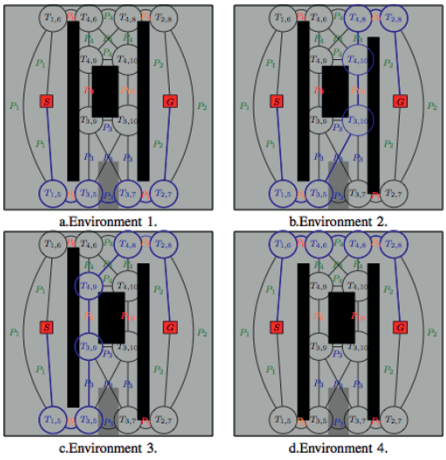

Figure 7: Experimental environments.

5.3- Path re-planning

Fig. 9 illustrates the topological re-planning in real time. In Fig. 9.a, in the first step, the user seems to prefer the narrow passage. Detecting it, the topological path is recomputed taking into account this intent. In Fig. 10.b, the user does not follow the guidance along the A* path in the third step. Thus, the topological planner computes a new topological path. The path re-planning including A* process is done in less than 150*ms* in this case.

5.4- Results evaluation

Computation times given above allow interaction in real time. However, some code parallelization is on progress to optimize it. Although, the running planner had been tested by its developer team. It still need to be evaluated by a panel of users non involved in this study. Indeed, for this interactive planning architecture, we need an objective feedback on the planner about its behavior. The main issue of such feedback is to evaluate the ergonomics of our interaction paradigms. We already know from [LF1] that the haptic device is particularly suited for such virtual manipulation tasks; we need, now, to validate our authority control and intent prediction strategies.

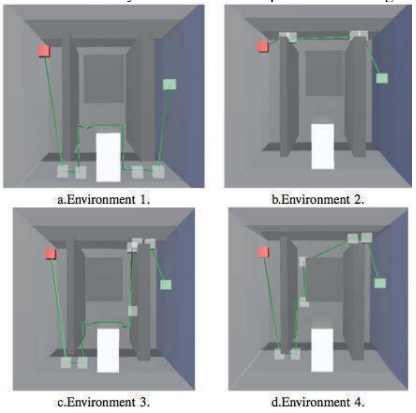

Figure 8: Planning results.

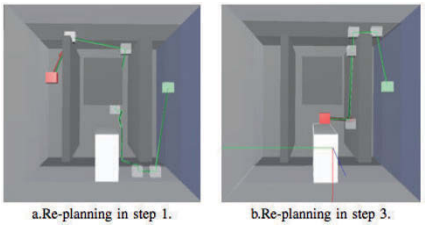

Figure 9: Topological re-planning in environment 1.

6- Conclusion

This paper presents a multi-layer architecture for interactive path planning in VR simulations. This architecture is based on a multi-layer environment model and a multi-layer planner. Each layer deals with specific information (semantic, topological and geometric).
The contribution of such architecture is two-fold.
First, it provides the user with real-time path planning thanks to the semantic and topological layers by splitting the path in steps and then by adapting the geometric planning strategy to the local complexity of each step.
Second, it integrates efficiently a human in the loop: real-time re-planning is computed based on user's intent and the user and the planner share motion control.

The interest of such a planner architecture had been demonstrated here with semantic information of the environment based on "complexity" and "cluttering". However, real manipulation task for industrial processes involve more complex semantic information (functional surface, multi-physics interactions, surfaces or material properties). Future work will be to define both the meaningful

information of such tasks and the way to use it. The proposed architecture meets the requirements for such semantic information. The next step in this direction will be to directly include semantic information related to common geometric figures such as plan, cylinder, cube, etc. and to adapt the planning strategy in a context similar to the one given in Fig. 10 where the goal is to find a path for the red objects.

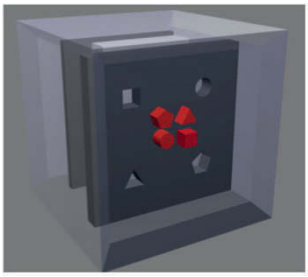

Figure 10: Next environment for interactive path planning simulations.

Moreover, with an accurate semantic description, such a planner structure seems also well suited for off-line path planning allowing to rapidly find hard passages using the topological planning and to rapidly adapt the geometric planning strategy according to the local planning context.

7- References

[AM1] D. A. Abbink and M. Mulder, "Neuromuscular analysis as a guideline in designing shared control," *Advances in haptics*, vol. 109, pp. 499– 516, 2010.

[AP1] S. Anderson, S. Peters, K. Iagnemma, and J. Overholt, "Semi- autonomous stability control and hazard avoidance for manned and unmanned ground vehicles," DTIC Document, Tech. Rep., 2010.

[AT1] M.A.Ahmadi-Pajouh, F.Towhidkhah, S.Gharibzadeh, and M.Mash-hadimalek, "Path planning in the hippocampo-prefrontal cortex path- way: An adaptive model based receding horizon planner," *Medical hypotheses*, vol. 68, no. 6, pp. 1411–1415, 2007.

[AE1] D. Aarno, S. Ekvall, and D. Kragic, "Adaptive virtual fixtures for machine-assisted teleoperation tasks," in *International Conference on Robotics and Automation, ICRA. Proceedings*. IEEE,2005,pp.1139– 1144.

[C1] "CGAL, Computational Geometry Algorithms Library," http://www.cgal.org.

[D1] E. W. Dijkstra, "A note on two problems in connexion with graphs," *Numerische mathematik*, vol. 1, no. 1, pp. 269–271, 1959.

[DS1] A. D. Dragan and S. S. Srinivasa, "A policy blending formalism for shared control," *International Journal of Robotics Research*, 2013.

[FF1] P. Fillatreau, J.-Y. Fourquet, R. Le Bolloch, S. Cailhol, A. Datas, and B. Puel, "Using virtual reality and 3d industrial numerical models for immersive interactive checklists," *Computers in Industry*, 2013.

[FH1] F. Flemisch, M. Heesen, T. Hesse, J. Kelsch, A. Schieben, and J. Beller, "Towards a dynamic balance between humans and au- tomation: authority, ability, responsibility and control in shared and cooperative control situations," *Cognition, Technology & Work*, vol. 14, no. 1, pp. 3–18, 2012.

[FR1] A. H. Fagg, M. Rosenstein, R. Platt, and R. A. Grupen, "Extracting user intent in mixed initiative teleoperator control," in *Proc. American Institute of Aeronautics and Astronautics Intelligent Systems Technical Conference*, 2004.

[L1] T. Lozano-Perez, "Spatial planning: A configuration space approach," *IEEE Transactions on Computers*, vol. 100, no. 2, pp. 108–120, 1980.

[L2] S. LaValle, *Planning algorithms*, Cambridge, Ed. Cambridge Uni- versity Press, 2006.

[LF1] N. Ladeveze, J.-Y. Fourquet, and B. Puel, "Interactive path planning for haptic assistance in assembly tasks," *Computers & Graphics*, vol. 34, no. 1, pp. 17–25, 2010.

[LK1] S. G. Loizou and V. Kumar, "Mixed initiative control of autonomous vehicles," in *International Conference on Robotics and Automation*. IEEE, 2007, pp. 1431–1436.

[LO1] M. Li and A. M. Okamura, "Recognition of operator motions for real-time assistance using virtual fixtures," in *11th Symposium on Haptic Interfaces for Virtual Environment and Teleoperator Systems. HAPTICS. Proceedings*. IEEE, 2003, pp. 125–131.

[ML1] P. Marayong, M. Li, A. M. Okamura, and G. D. Hager, "Spatial motion constraints: Theory and demonstrations for robot guidance using virtual fixtures," in *International Conference on Robotics and Automation, Proceedings. ICRA*, vol. 2. IEEE, 2003, pp. 1954–1959.

[TF1] M. Taïx, D. Flavigne´, and E. Ferre´, "Human interaction with motion planning algorithm," *Journal of Intelligent & Robotic Systems*, vol. 67, no. 3-4, pp. 285–306, 2012.

[WN1] C. Weber, V. Nitsch, U. Unterhinninghofen, B. Farber, and M. Buss, "Position and force augmentation in a telepresence system and their effects on perceived realism," in *EuroHaptics conference, 2009 and Symposium on Haptic Interfaces for Virtual Environment and Teleop- erator Systems. World Haptics 2009. Third Joint*. IEEE, 2009, pp. 226–231.

[YA1] W. Yu, R. Alqasemi, R. Dubey, and N. Pernalete, "Telemanipulation assistance based on motion intention recognition," in *International Conference on Robotics and Automation, ICRA Proceedings*. IEEE, 2005, pp. 1121–1126.

[YH1] E. You and K. Hauser, "Assisted teleoperation strategies for aggres- sively controlling a robot arm with 2d input," *Robotics: Science and Systems VII*, p. 354, 2012.

3

Decision Support System in Product Engineering

Major topics of the full argumentations are the following:

X. Fischer et al. (eds.), *Research in Interactive Design (Vol. 4)*
DOI 10.1007/978-3-319-26121-8_13

Article 070-pds-22

OPTIMAL DESIGN OF SANDWICH PLATES WITH HONEYCOMB CORE

A. Catapano [1], M. Montemurro [2]

(1) : Université de Bordeaux, I2M CNRS UMR 5295, F-33400 Talence, France
+33 (0) 5 56 84 54 22 / +33 (0) 5 40 00 69 64
E-mail : anita.catapano@ipb.fr

(2) : Arts et Métiers ParisTech, I2M CNRS UMR 5295, F-33400 Talence, France
+33 (0) 5 56 84 54 22 / +33 (0) 5 40 00 69 64
E-mail : marco.montemurro@ensam.eu

Abstract: This work deals with the problem of the optimum design of a sandwich structure composed of two laminated skins and a honeycomb core. The goal is to propose a numerical optimisation procedure that does not make any simplifying hypothesis in order to obtain a true global optimal solution for the considered problem. In order to face the design of the sandwich structure at both meso and macro scales, we use a two-level optimisation strategy. At the first level, we determine the optimum geometry of the unit cell together with the material and geometric parameters of the laminated skins, while at the second level we determine the optimal skins lay-up giving the geometrical and material parameters issued from the first level. We will illustrate the application of our strategy to the least-weight design of a sandwich plate submitted to several constraints: on the first buckling load, on the positive-definiteness of the stiffness tensor of the core, on the ratio between skins and core thickness and on the admissible moduli for the laminated skins.

Key words: Honeycomb, homogenisation, optimisation, sandwich panels, genetic algorithm.

1- Introduction

One of the most important challenges for automotive, naval and aerospace industries is the reduction of the weight of structures. Due to their high stiffness-to-weight ratio, sandwich structures are widely used in several fields: aviation, automotive, naval, construction, industry, and so on. Their application, in fact, ranges from the most performing structures such as aircraft wings, helicopters rotor blades, racing yachts keels to home furnishings.

The main characteristic of a sandwich structure concerns the presence of a low-density cellular solid, i.e. the core, between two stiffer thin plates, that increases the geometric moment of inertia of the plate with a few increment of weight. We can identify, in addition, several types of sandwich structures according to the geometry and shape of the core: honeycomb, solid, foam, corrugated, truss, web cores, and so on. The most important feature of the core is the relative density (ratio between the density of the cellular material and that of the material from which the cells walls are made) that can generally vary from 0.001 to 0.4, see [GA1]. Almost any material can be used to build a cellular solid: polymers, metals, ceramics, composites and so on. Sandwich panels, in aircraft applications, are composed by glass or carbon-fibre composite skins separated by aluminium or resin honeycombs, or by polymer foams. In particular, the honeycomb cell size can be chosen to provide cores with different stiffness and density properties. The result is a panel with very high bending stiffness-to-weight and strength-to-weight ratios. A review on sandwich structures and their applications can be found in [GA1, V3, V5].

The optimal design of sandwich structures is much more cumbersome than that of a classical monolithic structure. The difficulties increase when the sandwich structure is made of composite skins and a honeycomb core. In this case, we have to face, into the same design process, both the difficulty of designing a laminated plate (concerning the skins) and the difficulty of designing a complex 3D cellular continuum such as the honeycomb core. Therefore, the engineers always use some simplifying assumptions or rules to obtain, in an easier and faster way, a solution. For example, in [A1, HA1] the optimal design of a sandwich plate is addressed determining exclusively the optimum thickness of both the core and the skins, keeping constant the rest of geometric and material parameters describing their behaviour.

The problem of designing a sandwich panel can be formulated as an optimisation problem. However, unlike what is usually done in literature, our objective is twofold: on one hand, we want to formulate and solve such a problem on different scales and on the other hand, we want to include within the design process all the possible parameters defining the structure (at each scale) as optimisation variables. Therefore, in the framework of the design of a sandwich

panel with honeycomb core and composite skins, we will consider, as optimisation variables, both their geometric and material constitutive parameters at each scale.

To this purpose, we propose a very general design strategy that consists in a numerical optimisation procedure that we set free from any simplifying hypothesis to obtain a true optimal configuration of the system. The design process that we propose is not submitted to restrictions: any parameter characterising our structure is an optimisation variable (thickness of the core, number of plies of skins, plies orientations, geometry of the unit cell).

In order to deal with the design problem of the sandwich plate at both meso and macro scales, we used a two-level optimisation strategy. At the first level we determine the optimum geometry of the unit cell (core meso-scale) together with the material and geometric parameters of the laminated skins (at this level the laminate representing each skin is modelled as an equivalent homogeneous anisotropic plate whose behaviour at the macro-scale is described in terms of the laminate polar parameters, see [V4]). At the second level of the strategy, we determine the optimal skins lay-up (the skin meso-scale) that satisfies the optimal combination of material and geometrical parameters issued from the first level of the strategy. The whole strategy is based on the use of the polar formalism [V1, V2, V4] and on the Genetic Algorithm (GA) BIANCA [M1, MV1, MV2] and it can be easily generalised to other problems.

The paper is organised as follows: the mechanical problem considered in the study as well as the two-level strategy are introduced in Section 2. The mathematical formulation of the first-level problem is detailed in Section 3 and the problem of determining a suitable laminate is formulated in Section 4. A concise description of the Finite Element (FE) model of the sandwich structure at both meso and macro scales is given in Section 5, while in Section 6 we show some numerical results to prove the effectiveness of the optimisation strategy. Finally, Section 7 ends the paper with some concluding remarks and perspectives.

2- Optimum design of sandwich panels with honeycomb core

2.1 – Problem description

The optimisation procedure presented in this work is applied to a sandwich plate composed by two laminated skins and a honeycomb core with hexagonal cells, see Fig. 1.

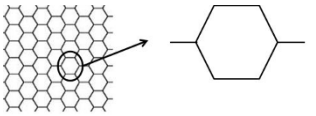

Figure 1. Honeycomb core and the repetitive unit cell.

The skins are made of carbon-epoxy unidirectional orthotropic plies, while the honeycomb core is obtained from aluminium alloy foils whose material properties are listed in Table 1.

Concerning the honeycomb core, the basic classical assumptions used to evaluate its elastic response and, hence, to determine its effective material properties (at the macro-scale) are:

- linear, elastic behaviour for the material of the cell walls;
- perfect bonding for the wall-to-wall contact;
- buckling of the cell walls disregarded.

Concerning the mechanical behaviour (at the macro-scale) of the two laminated skins they are modelled as quasi-homogeneous, fully orthotropic laminates, see Section 3.

Material properties of the aluminium		
E [MPa]	ν	ρ [Kg/mm^3]
70 000	0.33	2.7 x 10^{-6}
Material properties of the carbon-epoxy		
E_1 [MPa]	E_2 [MPa]	E_3 [MPa]
181 000	10 300	10 300
G_{12} [MPa]	G_{23} [MPa]	G_{13} [MPa]
7 170	3 843	7 170
ν_{12}	ν_{23}	ν_{13}
0.28	0.34	0.28
ρ_s [Kg/mm^3]	1.58 x 10^{-6}	

Table 1. Material properties of the aluminium foils and of the carbon-epoxy plies.

In addition, no simplifying hypotheses are made on the geometric and mechanical parameters of both the skins and the core, i.e. any parameter characterising our structure is an optimisation variable: geometry of the unit cell as well as number and orientation of the plies for the skins. Only avoiding the use of *a priori* assumptions one can hope to obtain the true global optimum for a given problem: this is a key-point in our approach.

2.2 – Description of the two-level strategy

The goal of our problem is the minimisation of the weight of the sandwich plate subject to mechanical constraints on the first buckling load, on the positive-definiteness of the stiffness tensor of the core and on the admissible moduli for the laminated skins together with geometrical constraints on the ratio between skins and core thickness. The optimisation strategy is articulated into two distinct problems as described here below.

First-level problem. The aim of this phase is the determination of the optimal geometry of the unit cell together with the material and geometric parameters of the

laminated skins in order to minimise the weight of the entire structure. At this level the laminate representing each skin is modelled as an equivalent homogeneous anisotropic plate whose behaviour at the macro-scale is described in terms of the laminate polar parameters, see [V1, M1, MV1], by means of the classical stiffness tensors **A**, **B** and **D**. It is worth noting that, concerning the model of the core, the first level of the strategy involves two different scales:

- the meso-scale wherein the core is modelled via the single unit cell characterised by its geometric variables;
- the macro-scale where the core is modelled as an homogeneous orthotropic solid whose mechanical response is described through the full set of elastic moduli that depend on the geometric parameters of the unit cell.

Therefore, the link between these two scales is represented by the homogenisation phase of the honeycomb core that leads us to represent the core, at the macro-scale level, as a homogeneous continuum characterised by its equivalent material properties, namely $E_1^c, E_2^c, E_3^c, G_{12}^c, G_{13}^c, G_{23}^c, \nu_{12}^c, \nu_{13}^c, \nu_{23}^c$. This last aspect has led us to search an accurate method to determine the material properties of the orthotropic core that will be assigned to the equivalent solid at the macro-scale.

Second-level problem. At the second level of the strategy, we have to determine the optimal skins lay-up (the skin meso-scale) that satisfies the optimal combination of their material and geometrical parameters issued from the first level of the strategy. The goal of this phase is, hence, to find at least one stacking sequence, for each skin, which has to be quasi-homogeneous, fully orthotropic and has to meet the optimal polar parameters issued from the first step. At this level of the strategy, the design variables are the layers orientations.

3- Formulation of the first level problem

3.1 – Optimisation variables

In this phase, we have to determine the optimal values of the following parameters:

- the thickness of both top and bottom skins, h_t and h_b respectively;
- the mechanical properties of each skin, namely the anisotropic polar parameters of the plate ($\left(R_{0K}^{A^*}\right)_t$, $\left(R_1^{A^*}\right)_t$ and $\left(\Phi_1^{A^*}\right)_t$ for the top skin and $\left(R_{0K}^{A^*}\right)_b$, $\left(R_1^{A^*}\right)_b$ and $\left(\Phi_1^{A^*}\right)_b$ for the bottom skin);
- the thickness of the core h_c;
- the geometrical properties of the unit cell of the honeycomb core (l_1, l_2, t_c and ϑ), see Fig. 2;

We also remark that at this level of the optimisation procedure, the thickness h_t and h_b of the laminated skins are considered as discrete optimisation variables, the discretisation step being equal to the thickness of the elementary ply employed for the fabrication of the laminate, i.e. $\Delta h_t = \Delta h_b = 0.125$mm. This assumption responds to a technological constraint and, in addition, the optimal value of these parameters will give us the optimal number of layers n to be used during the second-level problem.

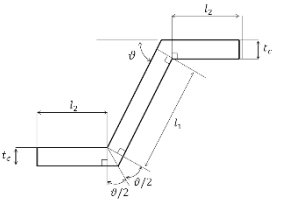

Figure 2. Geometrical parameters of the unit cell.

Concerning the mechanical variables, we use the polar formalism, which gives a representation of any planar tensor by means of a complete set of tensor invariants. A great advantage in the design of anisotropic structures is that the polar parameters are directly linked to the different symmetries of the tensor, see [V1, V2, V4]. Using the polar formalism, the representation of the reduced stiffness tensor $\boldsymbol{Q}$ of the orthotropic lamina is:

$$\begin{aligned}
Q_{xxxx} &= T_0 + 2T_1 + (-1)^K R_0 \cos 4\Phi_1 + 4R_1 \cos 2\Phi_1 \\
Q_{xxyy} &= -T_0 + 2T_1 - (-1)^K R_0 \cos 4\Phi_1 \\
Q_{xxxy} &= (-1)^K R_0 \sin 4\Phi_1 + 2R_1 \sin 2\Phi_1 \\
Q_{yyyy} &= T_0 + 2T_1 + (-1)^K R_0 \cos 4\Phi_1 - 4R_1 \cos 2\Phi_1 \\
Q_{yyxy} &= -(-1)^K R_0 \sin 4\Phi_1 + 2R_1 \sin 2\Phi_1 \\
Q_{xyxy} &= T_0 - (-1)^K R_0 \cos 4\Phi_1
\end{aligned} \quad \textbf{(1)}$$

where T_0, T_1, R_0, R_1 and K are the polar tensor invariants. T_0 and T_1 represent the isotropic moduli, R_0 and R_1 are the anisotropic ones, K is the shape orthotropy parameter (that can get the values 0 or 1), whilst Φ_1 is the polar angle that gives the othotropy orientation with respect to the global frame $\{0; x,y,z\}$.

The constitutive law of a laminate in the framework of the Classical Laminate Plate Theory (CLPT) is:

$$\begin{Bmatrix} \mathbf{N} \\ \mathbf{M} \end{Bmatrix} = \begin{bmatrix} \mathbf{A} & \mathbf{B} \\ \mathbf{B} & \mathbf{D} \end{bmatrix} \begin{Bmatrix} \boldsymbol{\varepsilon} \\ \boldsymbol{\chi} \end{Bmatrix} \quad \textbf{(2)}$$

where **N** and **M** are the tensors representing the membrane forces and the bending moments , respectively. $\boldsymbol{\varepsilon}$ and $\boldsymbol{\chi}$ are the second-order tensors of in-plane strains and curvature of the laminate middle plane, whilst **A**, **D** and **B** are the fourth-order tensors of membrane, bending and coupling stiffness, respectively.

In addition, even the laminate stiffness tensors can be expressed through the polar formalism, see [V1]. Here we want to highlight that, for a laminate with identical plies, thanks to quasi-homogeneity assumption and to the polar formalism, we are able to reduce the number of polar

parameters describing the mechanical response of the laminate, see [MV1]. In fact, they reduce from 18 to only three for each skin: the anisotropic polar moduli, i.e. $R_{0K}^{A^*}$ and $R_1^{A^*}$, and the polar angle $\Phi_1^{A^*}$. Moreover, in the formulation of the optimisation problem for the first level of the strategy, we have also to consider the geometric and feasibility constraints on the polar parameters ensuring, in this way, that the polar parameters issued from the optimisation correspond to a feasible laminate that will be designed during the second step of the strategy. For more details about these aspects, the reader is addressed to [V2].

3.2 – Mathematical statement of the optimisation problem

As previously said, the aim of the first level optimisation is the weight minimisation of the sandwich panel satisfying, simultaneously, constraints of different nature.
The design variables of the problem can be grouped into the following vector:

$$\mathbf{x} = \left\{\vartheta, t_c, l_2, l_1, h_c, \left(R_{0K}^{A^*}\right)_t, \left(R_1^{A^*}\right)_t, \left(\Phi_1^{A^*}\right)_t, h_t, \ldots \right. \\ \left. \ldots \left(R_{0K}^{A^*}\right)_b, \left(R_1^{A^*}\right)_b, \left(\Phi_1^{A^*}\right)_b, h_b \right\} \tag{3}$$

The optimisation problem can now be formulated as follows:

$$\begin{aligned} &\min_{\mathbf{x}} \; W(\mathbf{x}) \\ &\text{subject to:} \\ &\lambda_{\text{ref}} - \lambda(\mathbf{x}) \le 0 \\ &\frac{x_9}{x_5} - \alpha \le 0 \\ &\frac{x_{13}}{x_5} - \alpha \le 0 \\ &2\left(\frac{x_7}{R_1}\right)^2 - 1 - \frac{x_6}{R_0} \le 0 \\ &2\left(\frac{x_{11}}{R_1}\right)^2 - 1 - \frac{x_{10}}{R_0} \le 0 \\ &-E_1^c < 0 \\ &-E_2^c < 0 \\ &-E_3^c < 0 \\ &-G_{12}^c < 0 \\ &-G_{13}^c < 0 \\ &-G_{23}^c < 0 \\ &\left|\nu_{12}^c\right| - \sqrt{\frac{E_1^c}{E_2^c}} < 0 \\ &\left|\nu_{13}^c\right| - \sqrt{\frac{E_1^c}{E_3^c}} < 0 \\ &\left|\nu_{23}^c\right| - \sqrt{\frac{E_2^c}{E_3^c}} < 0 \\ &2\nu_{12}^c\nu_{13}^c\nu_{23}^c \frac{E_3^c}{E_1^c} + \left(\nu_{12}^c\right)^2 \frac{E_2^c}{E_1^c} + \left(\nu_{23}^c\right)^2 \frac{E_3^c}{E_2^c} + \left(\nu_{13}^c\right)^2 \frac{E_3^c}{E_1^c} < 0 \end{aligned} \tag{4}$$

where W is the weight of the sandwich plate, while λ is the first buckling load. λ_{ref} is the buckling load determined on a reference structure having the same in-plane dimensions and boundary conditions than those of the sandwich plate that will be optimised, while α is the maximum admissible aspect-ratio between the thickness of the core and each skin. Constraints 4 and 5 are geometrical and feasibility constraints imposed on the polar parameters of top and bottom skins. Finally, constraints from 6 to 15 are imposed in order to ensure the positive definiteness of the stiffness tensor of the core.

3.3 – Numerical procedure

Problem **(4)** is a non-linear, non-convex problem in terms of both geometrical and mechanical variables. The total number of design variables is 13, see Eq. **(3)**, while the total number of optimisation constraints is 15.

For the resolution of problem **(4)** we used a numerical strategy, that makes use of the GA BIANCA [M1] coupled with a meso-scale FE model for the numerical homogenisation of the honeycomb core and a macro-scale FE model for the buckling analysis of the whole panel, see Fig 3.

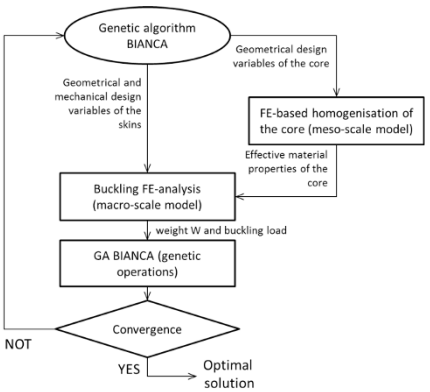

Figure 3. Numerical procedure scheme for the first-level problem.

As shown in Fig. 3, for each individual at each generation, we perform a numerical simulation for the evaluation of the effective material properties of the core and a subsequent numerical simulation for the evaluation of the first buckling load of the sandwich structure along with its weight. The meso-scale FE model uses the geometrical parameters of the unit cell, given by the GA BIANCA, in order to homogenise the honeycomb core and to determine its effective material properties. Afterwards, the macro-scale FE model uses the geometrical and mechanical design variables of the skins given by the GA BIANCA along with the effective material properties of the core to evaluate the first buckling load of the structure and its weight. Therefore, for these purposes the

genetic algorithm BIANCA has been interfaced with the commercial FE code ANSYS®.
The GA BIANCA elaborates the results of the two FE analyses in order to execute the genetic operations. These operations are repeated until the GA BIANCA meets the user-defined convergence criterion.

The generic individual of the GA BIANCA represents a solution. The genotype of the generic individual, for the optimisation problem of the first level of the strategy, is characterised by only one chromosome composed of 13 genes representing, each one, a component of the vector of the design variables, see Eq. **(3)**.

4- Formulation of the second level problem

The second-level problem concerns the lay-up design of top and bottom skins. Such a problem consists in determining a laminate stack satisfying the optimum values of both geometric and polar parameters issued from the first level of the strategy. The problem of finding a laminate stacking sequence having a given elastic behaviour is rather cumbersome and difficult because the laminate properties depend upon a combination of powers of circular functions of the layers orientations, see [MV2].
In the framework of the polar formalism, such a problem can be stated in the form of an unconstrained minimisation problem:

$$\min_{\boldsymbol{\delta}} I(f_i(\boldsymbol{\delta})) = \sum_{i=1}^{r} f_i^2(\boldsymbol{\delta}) \qquad \textbf{(5)}$$

where $\boldsymbol{\delta}$ is the vector of the layer orientations, i.e. the design variables of this phase, while $f_i^2(\boldsymbol{\delta})$ are quadratic functions in the space of polar parameters, each one representing a requirement to be satisfied, such as orthotropy, uncoupling and so on.
It is worth noting that the function $I(f_i(\boldsymbol{\delta}))$ of Eq. **(5)** is convex in the space of the laminate polar parameters, though it is highly non-convex in the space of the plies orientations (the true design variables) whose minima are known *a priori*, i.e. they are zeroes of this function. For more details about the nature of the second-level problem, see [C1, MV2].

We used the GA BIANCA to find a solution also for the second-level problem. In this case, each individual has a genotype composed of *n* chromosomes, one for each ply, characterised by a single gene coding the layer orientation.

5- Finite element models

The FE models used at the first-level of the strategy are built using the FE commercial code ANSYS®. The need to analyse, within the same generation, different geometrical configurations (plates with different geometrical and material properties), each one corresponding to an individual, requires the creation of an ad-hoc input file for the FE code that has to be interfaced with BIANCA. The FE model must be conceived to take into account a variable geometry, material and mesh. Indeed, for each individual at the current generation the FE code has to be able to vary in the correct way the number of elements wherein the structure is discretised, thus a correct parameterisation of the model has to be achieved.

5.1 – FE model of the unit cell

In order to determine the effective properties of the core, a homogenisation technique reveals to be necessary. In this way, the periodic honeycomb structure can be replaced by an equivalent orthotropic homogeneous solid whose material properties depend on the geometric parameters of the repetitive unit of the honeycomb. In particular, these properties are determined using the strain energy-based homogenisation technique of periodic media. This technique makes use of the repetitive unit of the periodic structure to approximate its effective properties at the macro-scale level. The basic feature of the strain energy-based homogenisation technique consists in the assumption that the repetitive unit of the periodic structure and the corresponding volume of the homogeneous solid undergo the same deformation having, hence, the same strain energy, see [B1]. In this case, the periodic structure is the honeycomb core whose repetitive unit cell has three planes of symmetry, thus we decided to exploit these symmetries using, in the homogenisation process, only an eighth of the repetitive unit cell. As illustrated in Fig. 4 the model is built using the 20-node ANSYS solid element SOLID186.

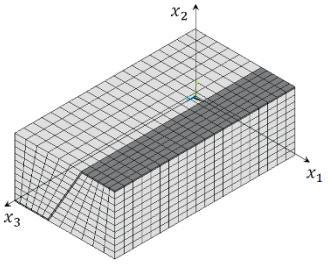

Figure 4. FE model of the repetitive unit cell.

In Fig. 4, the dark-grey elements represent the aluminium foils of the honeycomb core, while the light-grey ones are the fictitious elements used to model the "second phase" which has the properties of the so-called "elastic air", see [A2].

5.2 – FE model of the sandwich panel

At the macro-scale the structure is modelled with a combination of shell and solid elements. In particular, the laminated skins are modelled using ANSYS SHELL281 elements with eight nodes and six degrees of freedom (DOFs) per node, and their mechanical behaviour is described by defining directly the normalised stiffness tensors $\mathbf{A}^*$, $\mathbf{B}^*$ and $\mathbf{D}^*$. The equivalent solid representing the core is modelled using ANSYS SOLID186 elements with 20 nodes and 3 DOFs per node having the material properties

calculated using the FE model of the unit cell. Concerning the Boundary Conditions (BCs) of the FE model at the macro-scale, they are depicted in Fig. 5 and listed in Table 2. In particular, such BCs are applied only on the edges of top and bottom skins. The compatibility between the displacement field of the skins (modelled with shell elements) and that of the core (modelled with solid elements) is obtained by means of constraint equations on each node belonging to contiguous solid and shell elements, see Fig. 5. In particular, we imposed rigid constraints between the nodes of the middle plane of the top (bottom) skin and the corresponding ones of the top (bottom) surface of the solid core. Through such constraints, the displacements of the nodes belonging to the top and bottom surfaces of the solid core are equal to those of the bottom and top faces of the top and bottom skins, respectively.

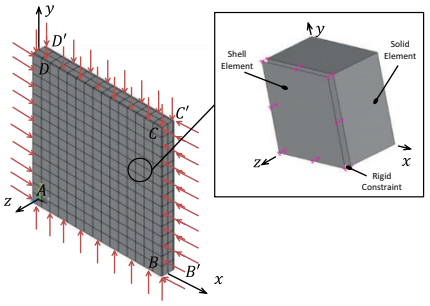

Figure 5. FE model at the macro-scale.

Sides	Constraint
AB, A´B´, CD, C´D´	$U_x = 0$ $U_z = 0$
BC, B´C´, DA, D´A´	$U_y = 0$ $U_z = 0$

Table 2. BCs of the FE model of the sandwich panel.

6- Numerical results

In order to show the effectiveness of the proposed approach we studied several cases. However, for the sake of brevity, here we show only the results concerning one of these cases: a sandwich panel with different skins and with a core having a fixed thickness. In this case the core thickness does not belong to the vector of design variables, see Eq. **(3)**, being equal to that of the reference structure. The reference structure is a square plate of side $a = 1500$ mm characterised by the material properties listed in Table 1 and the geometrical properties listed in Table 3.

Concerning the genetic parameters of the GA BIANCA used to solve the problem for this particular case, we consider one population of 140 individuals evolving along 300 generations with crossover and mutation probabilities of 0.85 and 0.017 respectively. The roulette-wheel operator performs selection, the elitism is active whilst the ADP method is used for handling constraints, see [MV3].

Core				
ϑ [deg]	l_1 [mm]	l_2 [mm]	h_c [mm]	t_c [mm]
60	3.666	1.833	80	0.0635
Skins				
h_t [mm]		h_b [mm]		
4 (32 plies)		4 (32 plies)		
Top skin sequence [deg]				
$[45/0/45/45/-45/45/-45/0/0/45/-45/45/-45/-45/0/45]_s$				
Bottom skin sequence [deg]				
$[45/0/45/45/-45/45/-45/0/0/45/-45/45/-45/-45/0/45]_s$				
Weight [Kg]		**1st buckling load** [N/mm]		
41.02		5691.88		

Table 3. Geometrical properties of the reference structure.

The optimal values of the geometric as well as mechanical design variables issued from the first-level are listed in Table 4. As it can be easily seen, the optimum configuration has a weight of 36.88 Kg (about 10 % less than that of the reference structure) with a first buckling load of 5704.33 N/mm (about 0.2 % greater than the reference one).

Core					
ϑ [deg]	l_1 [mm]	l_2 [mm]	h_c [mm]	t_c [mm]	
47	4.90	0.30	80	0.065	
Skins					
h_t [mm]			h_b [mm]		
3.5 (28 plies)			3.5 (28 plies)		
$\left(R_{0K}^{A*}\right)_t$ [MPa]	$\left(R_1^{A*}\right)_t$ [MPa]	$\left(\Phi_1^{A*}\right)_t$ [deg]	$\left(R_{0K}^{A*}\right)_b$ [MPa]	$\left(R_1^{A*}\right)_b$ [MPa]	$\left(\Phi_1^{A*}\right)_b$ [deg]
19594	356	-45	19324	168	45
Top skin sequence [deg]					
[-44/46/-44/46/41/-44/-44/46/46/46/-49/-44/51/-44/46 -49/41/-44/-39/41/46/-44/46/-44/-44/46/-49/46]					
Bottom skin sequence [deg]					
[43/43/-45/-45/-45/49/49/-41/-53/47/-44/43/-45/ -45/39/43/-46/40/48/-44/48/48/-41/-50/-45/44/44/-45]					
Weight [Kg]			**1st buckling load** [N/mm]		
36.88			5704.33		

Table 4. Geometrical and mechanical properties of the optimum configuration.

The optimal laminate stacks, satisfying the values of the geometric and polar parameters issued from the first-level problem, for both top and bottom skins are also listed in Table 4. It is worth noting that these stacking sequences represent true general solutions: no hypotheses are imposed on the stack in order to meet the elastic requirements, unlike what is often done in the literature (for example symmetric

stacks in order to obtain the elastic uncoupling, balanced stacks to obtain the membrane orthotropy, and so on).

7- Conclusions

The main aim of the present work is to deal with the problem of the optimum design of a sandwich panel composed of two laminated skins and a honeycomb core. The design strategy that we propose is a numerical optimisation procedure that does not make use of any simplifying assumption. The design process that we propose is not submitted to restrictions: any parameter characterising our structure is an optimisation variable (geometry of the unit cell of the honeycomb core, as well as the orientations and the number of plies for the skins). In order to face the design of the sandwich structure in a very general way a two-level multi-scale strategy has been considered. The first level of the procedure involves two scales:

- the macro-scale wherein the sandwich panel is composed by two homogeneous anisotropic plates (the skins) whose behaviour is described in terms of the laminate polar parameters along with an homogeneous anisotropic core whose mechanical response is defined in terms of its effective elastic properties;

- the meso-scale of the honeycomb core where we need to model the related representative volume element in order to determine the effective material properties of the core used at the macro-scale.

Many types of design variables are included at this first level: the geometrical parameters of the honeycomb unit cell (meso-scale) together with the total thickness and the laminate polar parameters of each skin (macro-scale). The second level of the procedure concerns the meso-scale of the laminated skins: in this phase, we look for the optimal stacking sequences giving the optimum value of the thickness and of the laminate polar parameters issued from the first step.

Several features that make it an innovative, effective and general method for the design of complex multi-scale structures characterise the optimisation strategy presented in this work. The example presented in this paper shows that when standard rules for the laminate stacks are abandoned and when all the parameters characterising the structure, at each scale, are included among the design process a significant weight saving can be obtained: up to 10 % when compared to that of the reference structure with almost the same buckling load (0.2 % greater).

As a concluding remark, it can be noticed that the proposed strategy is really effective and robust and can be easily applied to other different problems.

7- References

[A1] H. G. Allen, Analysis and design of structural sandwich panels, Pergamon Press, 1969.

[A2] ANSYS, Inc., 275 Technology Drive, Canonsburg, PA 15317, ANSYS Mechanical APDL Modeling and Meshing Guide, 2012.

[B1] E. J. Barbero, Finite element analysis of composite materials, Taylor and Francis Group, 2008.

[C1] A. Catapano, Stiffness and strength optimisation of the anisotropy distribution for laminated structures, PhD thesis, Université U.P.M.C. Paris VI, 2013. http://tel.archives-ouvertes.fr/tel-00952372

[GA1] L. J. Gibson, M. F. Ashby, Cellular solids - Structure and properties, Cambridge, University Press, 1997.

[HA1] Huang, S. N. and Alspaught, D. W., Minimum weight sandwich beam design, AIAA Journal, 12: 1617-1618, 1974.

[M1] M. Montemurro. Optimal Design of Advanced Engineering Modular Systems through a New Genetic Approach. PhD thesis, Université U.P.M.C. Paris VI, 2012. http://tel.archives-ouvertes.fr/tel-00955533/

[MV1] M. Montemurro, A. Vincenti, P. Vannucci, A two-level procedure for the global optimum design of composite modular structures - application to the design of an aircraft wing. Part 1: theoretical formulation, Journal of Optimization Theory and Applications, 155(1): 1-23, 2012.

[MV2] M. Montemurro, A. Vincenti, P. Vannucci, A two-level procedure for the global optimum design of composite modular structures - application to the design of an aircraft wing. Part 2: numerical aspects and examples, Journal of Optimization Theory and Applications 155 (1): 24-53, 2012.

[MV3] M. Montemurro, A. Vincenti, P. Vannucci, The Automatic Dynamic Penalisation method (ADP) for handling constraints with genetic algorithms, Computer Methods in Applied Mechanics and Engineering 256: 70–87, 2013.

[V1] P. Vannucci, Plane anisotropy by the polar method, Meccanica 40: 437-454, 2005.

[V2] P. Vannucci, A note on the elastic and geometric bounds for composite laminates. Journal of Elasticity 112(2): 199–215, 2013.

[V3] A. Vautrin, Mechanics of sandwich structures, Springer, 2010.

[V4] G. Verchery, Les invariants des tenseurs d'ordre 4 du type de l'élasticité, Proc. Of Colloque Euromech 115, VIllard-de-Lans, (France), 1979.

[V5] J. R. Vinson, The behavior of sandwich srtuctures of isotropic and composite materials, Technomic Publishing Company, 1999.

Article 062-cad-74

Genetic algorithm optimization and robustness analysis for the computer aided design of fixture systems in automotive manufacturing

Matteo Ansaloni [1], Enrico Bonazzi [1], Francesco Gherardini [2], Francesco Leali [1]

(1) : Department of Engineering "Enzo Ferrari", University of Modena and Reggio Emilia, via Vignolese 905, 41125 Modena, Italia
Phone/Fax: 059/2056278
E-mail : {matteo.ansaloni,enrico.bonazzi,francesco.leali}@unimore.it

(2) : InterMech-MO.RE - Interdepartmental Research Centre for Applied Research and Services in the Advanced Mechanics and Motor Sector, University of Modena and Reggio Emilia, via Vignolese 905, 41125 Modena, Italia
Phone/Fax: 059/2056278
E-mail : francesco.gherardini@unimore.it

Abstract: Fixture Systems (FSs) have great importance in machining, welding, assembly, measuring, testing and other manufacturing processes. One of the most critical issue in FS design is the choice of both the type of fixing devices such as clamps, locators, and support points, (configuration), and their arrangement with respect to workpieces (layout). Several authors deal with the problem of determine the most suitable solution for FSs, often investigating their layout without considering the change of the type of locators. A computer aided design method is proposed to compare and evaluate different configurations for a FS, optimizing the locator type and analysing the roboustness of the solution. A multi-objective optimization based on a genetic algorithm is presented and the selection of the most suitable configuration is performed through the definition of robustness indexes. The effectiveness of the design method is demonstrated for an automotive case study.

Key words: Automotive manufacturing, computer aided fixture design, multi-objective optimization, robust analysis

1- Introduction

1.1- Operating scenario

A Fixture System (FS) is a device composed by clamps, locators and support points to rapidly, accurately and securely position workpieces during the different phases of their manufacturing process. FSs are widely used in various fields of manufacturing (e.g. machining, welding, assembly, inspection and testing) and requirements on FSs are different for each process. For example, in machining, due to the high process forces, compliance of FS has to be accounted for because it is a non-negligible source of error which impacts the workpiece final quality. On the contrary, during an assembly process FS deformation may generally be neglected and FS can be treated as a rigid structure.

FS design is a significant topic for industry since the cost associated with FS can account for 10–20% of the total cost of a manufacturing system [WR1].

Effectiveness of FS design depends both on type and position of locators. Different disposition of the same group of locators and different types of locators placed in the same position lead to very different performances.

In the following, we distinguish between two properties of FS: layout and configuration.

The layout is the result of the application of the principles used to pose the part in the space. It also takes into account position and orientation of locators.

The configuration refers to the set of locator types used to realize the layout. The configuration is the actual implementation of the layout, since a layout is obtainable through the combination of different types of locators.

Table 1 shows the degrees of freedom constrained by locators for some main types of locators used in automotive manufacturing. The Z direction represents the normal to the contact surface or the axial direction of the cylindrical feature.

Degree of Constraint	Locators	Direction of Constraint
1 DoC	Pad Pin/Pocket	Z X or Y
2 DoC	Pin/Hole Pin/Pocket + Pad V-Block	X or Y X or Y, Z X, Y
3 DoC	Pin/Hole + Pad	X, Y, Z

Table 1: Classification of locators

According to the literature, the FS design process can be divided in four steps: setup planning, fixture planning, unit design, and verification [BR, WR2, HV].
During the setup planning, workpiece and technological information are analysed to determine the number of setups required to perform all the manufacturing operations and to define appropriate locating datum for each setup.
Fixture planning defines the datum and the disposition of locators based on the fixing requirements. The number and position of the locating points have to assure that all the degrees of freedom of the workpieces are adequately constrained.
During the unit design, suitable units for locating and clamping the workpieces are designed and produced.
The FS is finally tested during the verification phase, to ensure that it satisfies all the fixturing requirements which drive the design process.
FS design represents a critical task especially in those processes that are characterized by high modularity [AL].
One important example is represented by automotive industry, where accuracy and roboustness of manufacturing processes play a fundamental role, especially in the top class car sector, where very high overall quality is mandatory [SK].
Chassis design, for example, asks for balancing very different design requirements, e.g. static and dynamic performance, safety, lightness, cost. Moreover, a chassis is a complex modular system which can be decomposed in subgroups, differing in materials (e.g. aluminium and cast iron), manufacturing processes (e.g. casting and extrusion) and assembly technologies (e.g. welding, riveting, gluing). Even small misalignments between parts of the frame can lead to reject the total chassis, so that, actually, just a detail optimization of every module permits to achieve the desired targets [CB].
Product design and process design have to be closely integrated, tolerances on parts (functional goals) and assemblies (technological goals) have to be accurately chosen and managed, and FSs have to be specifically tailored and designed.

1.2- Scientific background in Computer Aided Fixture System Design

Since the FS design process is affected by an inherent complexity, Computer Aided Fixture Design (CAFD) tools have been developed in order to support it. Moreover, computer aided techniques could lead to find design issue in the early phase, avoiding expensive late testing and corrections during the development and industrialization phases. This could lead to an improvement in the geometric product tolerance fulfilling functional demands [LL].
The current scientific research on CAFD is focused on two main issues: how to represent and collect the design knowledge about FSs within a computer aided environment; how to implement an engineering procedure for designing FSs in industry.
Many authors have investigated the codification of the design knowledge in a CAE environment and have proposed different integrated approaches to solve such criticism, with a particular focus on fixture design for machining.
Wang et al. [WR1] describe different research aspects that are promising in CAFD: knowledge-related techniques, knowledge modelling, data mining and machine learning. Moreover, they underline the absolute importance of FS design within product/process development and suggest to consider it as a mandatory task for engineers.
Boyle et al. [BR] present a review of over seventy-five CAFD tools focused on the FS design phases they support and on the underlying technology upon which they are based. They conclude that more attention has to be paid on the cohesive integration between the segmented CAFD approaches within a unique framework, in order to enhance the comprehensive understanding of all the basic requirements needed by FSs and to use this understanding to drive the FS design process.
Wang et al. [WR2] propose a method called Case-Based Reasoning aimed at investigating and systemizing the most important achievements in FS design over the past years. Such method draws a procedure to quickly derive conceptual FSs from the representation and systemization of many fixture design solutions and related devices, e.g. depository units.
Hunter et al. [HV] further develop some models for collecting and organizing the FS design knowledge and extending it to many field of application. In particular they present a knowledge template based on the distinction between analytic and synthetic tasks. The knowledge template represents a pattern which defines the most common entities used in FS design for machining.
According to their approach, such knowledge is easily reused in an automatic process [HR] to design fixtures for inspection, assembly or welding.
The implementation of engineering procedures for designing FSs in industry is often treated as a problem of FS layout definition and optimization.
Roy et al. [RS] propose a heuristic algorithm for the automatic selection of the position of locators and clamps for a given workpiece geometry. They also propose the integration of the algorithm within a knowledge-based framework.
Ngoi at al. [NT] state some FS design principles and subdivide a FS in locating, supporting and clamping elements, according to their functions.
Qin et al. [QZ] present a method to design the FS scheme trough the calculation of the influence on the final accuracy given by the fixture elements and the workpiece itself.
Yu et al. [YW] describe an approach for quickly and automatically determining the main clamping points in a FS, starting from the geometry of a workpiece. The procedure consist of the initial projection and extraction of the workpiece boundaries, their simplification, the determination of feasible clamping plans on the workpiece and the selection of the optimal plans.
Wu et al. [WR3] present a geometric analysis for the automated design of the FS layout considering different positions of the locators.
Pelinescu et al. [PW] adopt multiple quality criteria in order to define the best layout for FSs. The final choice depends on a trade-off among multiple performance requirements.

Kaya [K] applies genetic algorithms to draw the best FS layout, considered as supports, locators and clamps, in order to minimize the errors induced by elastic deformation of the workpiece.
Liu et al. [LZ] propose a method to optimize the FS layout in the peripheral milling of a workpiece characterized by low-rigidity.

1.3- Open issues in Computer Aided Fixture System Design

After the setup planning phase there are two common FS design scenarios: in the first, geometric and technological requirements on the part determine both the layout and the configuration. Existing Computer Aided Fixture System design can be very useful here.
In the second case, requirements do not completely determine neither layout nor configuration, so designers rely just on their knowledge and experience to select the best one among alternative solutions. In several situations, however, the layout is imposed by reachability limits of the manufacturing system and the choice of the configuration becomes the discriminating factor for FS design. In such cases, despite the significant number of existing methods and tools cited, FS design is still not fully codified in CAE environments but, especially in small-medium enterprises, deeply based on designers' experience and trial and error approaches.
One notable reason for such lack is that the FS engineering design approaches are very often limited to the investigation of the layout while the configuration is rarely taken into account. The problem of the analysis of different configurations in FS design seems not to be fully addressed even in the scientific literature, due to the inherent difficulties in comparing different locators types. In fact, locators fulfil different functions (e.g. a hole constrains different direction from a pad) and are affected by different tolerances (e.g. a pad and a hole have different dimensional tolerances). As a consequence, computer aided methods tools frequently consider a given configuration and optimize the layout of the locators without considering their functions.
In the present work a computer based design method is proposed to enhance the FS design process and reduce the heavy participation of very skilled and experienced designers.
The method describes how to select the most suitable and robust FS configuration through a multi-objective optimization approach based on an evolutionary algorithm and robustness indexes. A computer aided environment has been also developed for the implementation of the method and validated on an automotive case study.
The paper is organised as follows: Section 2 describes the proposed computer aided design method; Section 3 presents the case study and the results of the robust analysis; Conclusions are finally presented in Section 4.

2- Computer aided fixture system design method

The proposed method integrates numerical and statistical tools and techniques; it consists of four steps, as outlined in Figure 1.

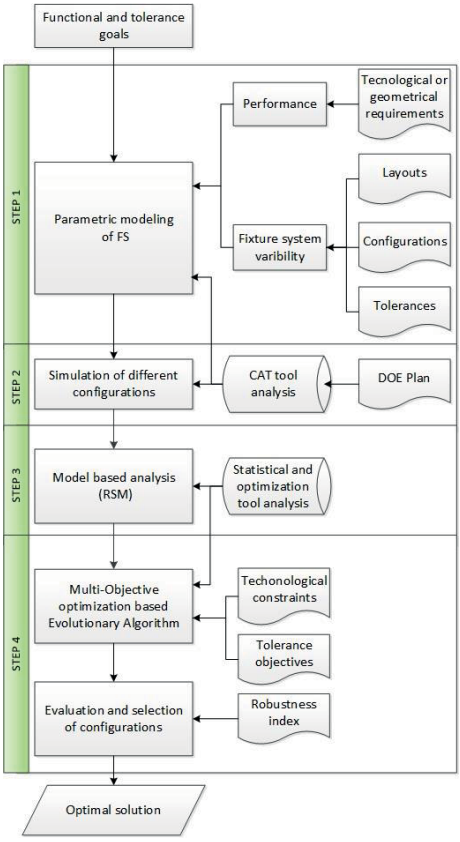

Figure 1: Computer aided design method workflow

FS parametric modelling
The first step deals with the definition of a parametric model, which addresses the functional goals of the FS (e.g. a gap position and orientation measured between two subgroups in a manufacturing process) and the related tolerance fields (i.e. tolerance goals). FS performance is stated through the technological or geometrical requirements. FS variability depends on its layout, configuration while tolerances on locators. Using such information, a Computer Aided Tolerance (CAT) tool allows to define a FS parametric model that represents the output of this step.
CAT numerical simulations
In the second step, the parametric model is used to simulate the different configurations through the statistical variation of the tolerances. This variation can be efficiently organised by means of a Design Of Experiments (DOE) plan, that combines tolerances on every locator through a set of

sampling points in the design space defined by the tolerances of locators. In addition, the DOE plan allows to investigate the different interactions between the factors.
In order to accomplish this step a CAT tool is employed. This step outputs a set of numerical simulations of the different FS configurations.
Model-based analysis
After the CAT simulations, a model that correlates the tolerances on the locators with the design objectives is determined. The third step is the development of a FS model-based analysis. The model is obtained fitting a suitable Response Surface (RS) to FS performance. This model is the input for the following optimization step.
Evaluation and selection of the configurations
The last step performs a multi-objective optimization analysis of the model for every FS configuration, in order to identify the most suitable and robust FS design to achieve the functional and tolerance goals.
Starting from the RS and DOE sampling points, an evolutionary algorithm is used to further investigate the design space in order to solve a multi-objective problem: the main goals are to check regions where tolerances can be maximized and, at the same time, they can generate the most suitable gaps between parts. The optimization analysis is subjected to design constraints, due to technological and functional requirements on parts and their manufacturing process (e.g. interference between parts, gap dimensional and geometrical conditions, etc.). As a result, this constrained optimization underlines a feasibility region of the design space, that contains all the tolerance values able to achieve the performance goals and to satisfy the design constraints. Moreover, for each configuration, a Pareto frontier is obtained.
A robust analysis of each Pareto frontier is finally performed, in order to identify the maximum allowable values for each tolerance. The tolerance values t_i of each Pareto point are used to calculate the robustness index *TB*, as expressed in equation (1):

$$TB = \prod_{i=1}^{n} \frac{t_i}{\Delta TL_i} \qquad (1)$$

where n corresponds to the number of tolerance types and ΔTL_i is the difference between upper and lower levels in the design space for the i-th tolerance. *TB* represents a partition of the feasibility region, in the following called "Tolerance Box". In particular, for each configuration, the maximum value of *TB* corresponds to the most suitable set of tolerance for the locators. As a consequence, TB_{max} can be used as a robustness index to overcome the difficulties in comparing different locators types.

3- Fixture system design for an automotive chassis manufacturing

FS parametric modelling
The subgroup shown in Figure 2 (on the left) for a top class car chassis is investigated to validate the method proposed. The subgroup is composed of three extruded parts (A, B and C) welded using the MIG technology.

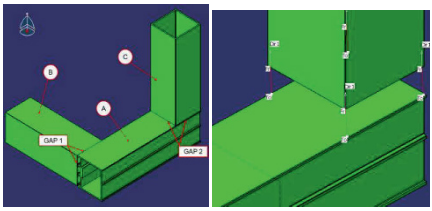

Figure 2: The chassis subgroup investigated (left) and the detail of a measure gap (right)

This welding technology imposes constraints on the relative distances between the functional surfaces of the extruded parts that have to be joined: measure gaps Gap1 and Gap2 shown in Figure 2 on the left. A detail view of Gap 2 measure gap is shown in Figure 2 on the right.
Simulation of different configurations
3DCS CAT software provided by the US Company Dimensional Control Systems (DCS) is used to simulate the dimensional and geometrical variations.
The variation of tolerances on parts and locators are considered along the three directions Y (primary), Z (secondary) and X. Since the subgroup is built of rigid parts, the layout fully comply the 3-2-1 locating principle for every configuration. The software allows the simulation of the fixture system without the need to have the mathematical CAD model, through the representation of the locators, as shown in Figure 3.

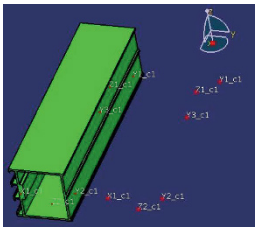

Figure 3: Simulation of the FS by 3DCS software

According to the previous assumptions, the following three system configurations are proposed as a combination of pads and pins, as reported in Table 2.
In particular:
• C1: 6 pads, one for each degree of freedom (3 in Y direction, 2 in Z and 1 in X);
• C2: 4 pads (2 in Y and 2 in Z) and 1 pin/hole mate which restrains two degrees of freedom (X-Y);
• C3: 3 pads (1 in Y and 2 in Z), 1 pin/hole mate which restrains two degrees of freedom (X-Y) and 1 pin/slot mate which suppresses the last degree of freedom (Y).

Configuration	Locators type	Number of locators
C1	Pad	6
C2	Pad	4
	Pin/Hole	1
C3	Pad	3
	Pin/Hole	1
	Pin/Slot	1

Table 2: System configurations

In the following simulations, locators are modelled as contact points allowed to move along the prescribed directions. In particular the pads are subjected to a position tolerance along the related direction (e.g. t_X, t_Y, t_Z). Pins are modelled as contact points which can vary the position within a circular area with the centre on the pin axis (e.g. t_{XY}). This is equivalent to simulate the variation between the coupling pin/hole.
In the proposed CAT model each tolerance range on locators varies from 0 to 2mm, in order to define the maximum admissible values to satisfy the technological and functional requirements.
Two measures are created between the reference part (A in Figure 2 on the left) and the other two parts (B and C in Figure 2 on the left) for the definition of the gaps: the first measure A-B is in Y-direction and the second measure A-C in Y-direction. These two measures are implemented with four couples of point to point measures between the parts, as exampled in Figure 2 on the right. Due to the technological requirements, a nominal value of 0,5mm is set for each gap.
Then, a DOE plan of 200 runs defines a sampling set of tolerances values used as input for the 3DCS simulation.
For every point, the software computes the statistical distribution of the gaps measure on the basis a Monte Carlo algorithm. The output, shown in Figure 4, returns statistical values for every gap measure: minimum and maximum gap values (Gmin and Gmax), mean (μ), standard deviation (STD), Cp, Cpk, etc.

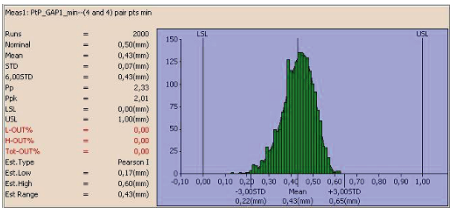

Figure 4: 3DCS statistical output

Model-based analysis
Multiple runs of the simulation generate a metamodel, which describes the relationship between the variability of the gaps values and the tolerances on the fixture locators. In order to obtain the metamodel, Neural Networks (NN) interpolation was used. NN used method is based on classical feedforward Neural Networks, with one hidden layer, and with an efficient Levenberg-Marquardt back propagation training algorithm and the initialization of the NN parameters is based on the proper initialization approach.
Evaluation and selection of the configurations
The goal of the problem is now to maximize the values of the tolerances of the locators for every configuration; this goal is subject to dimensional and geometrical constraints about the two gaps in order to avoid interference between parts and to obtain the most uniform gaps within a desired range (from 0 to 1mm). This problem is approached as a constrained multi-objective optimization.
Equation (2) expresses the formulation of objectives and constraints for each configuration:

$$\max \bar{f}(t_i) = [t_1, t_2, \ldots, t_n]^T \qquad (2)$$
$$t_i \in TL$$

Subject to

$$\mu G_{\min} - 3\sigma G_{\min} \geq 0$$
$$\mu G_{\max} + 3\sigma G_{\max} \leq GapLim$$
$$\Delta Gap = \mu G_{\max} - \mu G_{\min} \leq \Delta GapLim$$

These constraints formulize the following condition for every statistical distribution of simulated gaps:
- absence of interference between parts;
- maximum gap value respecting the design specification: in this case, *GapLim* is set at a value of 1mm;
- condition of gap uniformity, corresponding to the maximum distance between each measure point of the gap: in this case, *ΔGapLim* is set at a value of 0,3mm.

Figure 5 shows the graphical representation of the constraints and the statistical distribution of each gap measure.

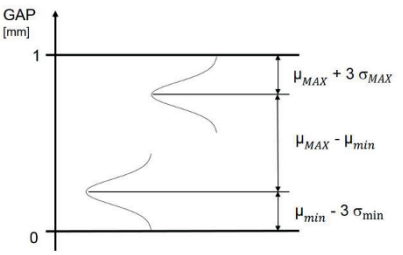

Figure 5: Graphical representation of the constraints

A multi-objective Genetic Algorithm (MOGA) approach is then used to investigate the tolerances design space in order to define a Pareto frontier of the most suitable solutions for each configuration [C, YG]. Every point of the frontier represents Pareto-optimal point, in term of tolerances, which is able to satisfy the functional constraints on the gaps. Figure 6, Figure 7 and Figure 8 illustrate the Pareto front for the three configurations investigated.

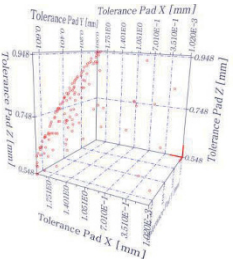

Figure 6: Pareto front for configuration C1

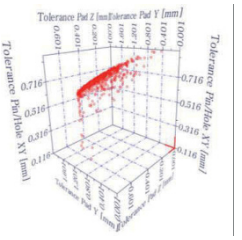

Figure 7: Pareto front for configuration C2

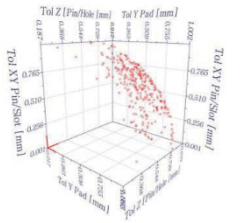

Figure 8: Pareto front for configuration C3

Table 3 presents the values of *TBmax* for every configuration. Moreover, each triad of values of locators tolerances that originates the maximum *TB* can be used to define the maximum tolerance range on locators.

Configuration	*TBmax*	t_i [mm]
C1	0,099	$t_X = 2$ $t_Y = 0,64$ $t_Z = 0,61$
C2	0,068	$t_{XY} = 1,58$ $t_Y = 0,54$ $t_Z = 0,63$
C3	0,046	$t_{XY} = 0,75$ $t_Y = 0,71$ $t_Z = 0,69$

Table 3: Comparison index TBmax for the three configurations

The output of the multi objective simulation is a frontier of optimal solutions, where at each points corresponds a set of tolerance values. All these results represent suitable solutions in relation to the desired goals and to the constraints. However they cannot lead to an univocal solution and, at the same time, they cannot lead to a comparison between configurations. The difficulties in such a comparison is overcame by mean of a robustness index *TB*, as expressed in Equation 1. In the analysed case, Equation 1 can be simplified as in Equation 3, due to the same width of ΔTL_i for each tolerance, equal to (2-0)mm:

$$TB = \prod_{i=1}^{n} \frac{t_i}{\Delta TL_i} = \frac{1}{\Delta TL^n} \prod_{i=1}^{n} t_i \qquad (3)$$

This index leads to reach two important objectives:
- the *TBmax* underlines a configuration able to maximize the tolerance space for each configuration. In this way, as shown in Table 3, a set of tolerance for t_X, t_Y, t_Z for C1 can be obtained. *tx* can reach the maximum allowable value, equal to 2 mm; *ty* is fixed to 0,64 mm and *tz* to 0,61mm. This means that every combination of tolerances values sets respectively under these limits leads to achieve the uniformity of gaps and their dimensional requirements.
The same for the other two configurations: for C2, t_{XY} is fixed to 1,58mm, t_Y to 0,54mm and t_Z to 0,63mm. For C3, t_{XY} 0,75mm, t_Y 0,71mm, t_Z 0,69mm.
In this way, the *TB* index can be used to set the tolerance range on the locators, in order to maximize them but obtaining uniform gaps values.
- the *TBmax* index represents an objective tool to define the most robust configuration and can be used for its evaluation and selection.
According to such considerations, the tolerance box volume results maximum for C1. It means that, in order to maximized the tolerance on the FS, i.e. its robustness, the configuration C1 leads to respect all the technological and functional requirements with the maximum tolerance range on its locators. The result of this analysis determines the choice of the configuration that better provides the desired performance.

4- Conclusions

The common approach to computer aided FS design is principally based on the evaluation of the layout influence on the overall robustness. Such approach does not consider the effect due to different configurations i.e. the sets of locators adopted to reference parts during their manufacturing or assembly process.
In the present paper the authors consider the problem of extending and deepening the study of the FS design process and propose a computer aided design method aimed at evaluating the effect of FS configuration on its roboustness.
The method integrates numerical and statistical tools and techniques: a dedicated CAT tool has been configured and used to run numerical simulations for evaluating the influence of every tolerance contribution on the final target

tolerance for many system configurations, varied according to a DOE plan. Using a CAT tool it has been possible to consider a model-based approach to perform an optimisation analysis.
Since a FS can be considered as a multi-performance system, every FS configuration has been investigated and optimized with a multi-objective genetic algorithm in order to reach the tolerance and functional requirements.
As a result, for each configuration many optimal values for locators tolerances have been obtained in correspondence to a Pareto frontier.
The difficulties in directly comparing different types of locators have been overcame by introducing a robustness index, called "tolerance box" by the authors, that correspond to the volume of a partition of the feasibility region described by every optimal point.
The outputs of this analysis have allowed to define the tolerances values to attribute to the locators aiming to reach the most robust configuration, i.e. to maximize the tolerances values.
The proposed method has been implemented within a computer aided design environment and applied to an automotive case study.
The analysis of different configuration showed that the effects of the tolerances on the locators are highly dependent on the configurations themselves.
Since the investigation of locators type is not addressed during the traditional approach to FS design, a direct comparison with the traditional techniques is not feasible due to different investigation objectives.
Nevertheless, future developments are foreseen: experimental testing will be performed on similar industrial cases to further examine the accuracy of the proposed method.

5- Acknowledgements

The authors want to acknowledge Ing. Patrizio Moruzzi and Ferrari SpA for their support to the present research.

6- References

[AL] Andrisano A.O., Leali F., Pellicciari M., Pini F. and Vergnano A. Hybrid Reconfigurable System design and optimization through virtual prototyping and digital manufacturing tools. In International Journal on Interactive Design and Manufacturing (IJIDeM), 6:17-27, 2012.

[BR] Boyle I., Rong Y. and Brown D.C. A review and analysis of current computer-aided fixture design approaches. In Robotics and Computer-Integrated Manufacturing 27: 1–12, 2011.

[C] Cavazzuti M. Optimization Methods, from Theory to Design Scientific and Technological Aspects in Mechanics. Springer, Berlin Heidelberg, 2013.

[CB] Cavazzuti M., Baldini A., Bertocchi E, Costi D., Torricelli E. and Moruzzi P. High performance automotive chassis design: a topology optimization based approach. In Structural and Multidisciplinary Optimization, 44(1), 2011.

[HR] Hunter R., Rios J., Perez J.M. and Vizan A. A functional approach for the formalization of the fixture design process. In International Journal of Machine Tools & Manufacture, 46: 683–697, 2006.

[HV] Hunter R., Vizan A., Perez J.M. and Rıos J. Knowledge model as an integral way to reuse the knowledge for fixture design process. In Journal of Materials Processing Technology, 164–165: 1510–1518, 2005.

[K] Kaya N. Machining fixture locating and clamping position optimization using genetic algorithms. In Computers in Industry, 57: 112–120, 2006.

[LL] Lindaua B., Lindkvistb L., Anderssonc A. and Sderbergb R. Statistical shape modeling in virtual assembly using PCA-technique, Journal of Manufacturing Systems, 32(3): 456–463, 2013.

[LZ] Liu S.G., Zheng L., Zhang Z.H., Li Z.Z., Liu D.C. Optimization of the number and positions of fixture locators in the peripheral milling of a low-rigidity workpiece. In International Journal of Advanced Manufacturing Technology, 33: 668–676, 2007.

[NT] Ngoi B., Tay M. and Wong C. Development of an Automated Fixture Set-up System for Inspection. In International Journal of Advanced Manufacturing Technology, 13: 342-349, 1997.

[PW] Pelinescu D. and Wang M.Y. Multi-objective optimal fixture layout design. In Robotics and Computer Integrated Manufacturing, 18: 365–372, 2002.

[QZ] Qin G.H., Zhang W.H. and Wan M. A mathematical approach to analysis and optimal design of a fixture locating scheme. In International Journal of Advance Manufacturing Technologies, 29: 349–359, 2006.

[RS] Roy U.R. and Sun P.L. Selection of preliminary locating and clamping positions on a workpiece for an automatic fixture design system. In Computer Integrated Manufacturing Systems, 7(3): 161-172, 1994.

[SK] Schubert E., Klassen M., Zerner I., Walz C. and Sepold G. Light-weight structures produced by laser beam joining for future applications in automobile and aerospace industry. In Journal of Materials Processing Technology Volume, 115(1): 2-8, 2001.

[WR1] Wang H., Rong Y., Li H. and Shaun P. Computer aided fixture design: Recent research and trends. In Computer-Aided Design 42: 1085–1094, 2010.

[WR2] Wang H. and Rong Y. Case based reasoning method for computer aided welding fixture design, In Computer-Aided Design, 40: 1121-1132, 2008.

[WR3] Wu Y., Rong Y., Ma W. and LeClair S. Automated modular Fixture planning: Geometric analysis. In Robotics and Computer-Integrated Manufacturing, 14: 1- 15, 1998.

[YG] Yu X. and Gen M. Introduction to Evolutionary Algorithms. Springer, London, 2010.

[YW] Yu J., Wen T., Hu Q. Research on Automatic Planning of Main Clamping Points in Rapid Fixture Design System. FSDK 2010 - Seventh International Conference on Fuzzy Systems and Knowledge Discovery, 2010.

Article 045-pp-27

Using the optimisation methods to minimize the machining time on the free-form surfaces in 3-axis milling

Djebali.S [1], Segonds.S [1],Redonnet.JM[1], Rubio.W [1]

(1) : Institut Clément Ader, Université Paul Sabatier ,*135 avenue de Rangueil F-31077 Toulouse, France*.
Phone: (33) 5.61.55.84.26
E-mail : {djebali, redonnet }@lgmt.ups-tlse.fr
E-mail : {walter.rubio, stephane.segonds }@univ-tlse3.fr

Abstract: The object of this study is to minimize the machining time on the free-form surfaces while respecting a scallop height criteria. The analytical expression of the machining time is not known. By hypothesis, it is assumed proportional to the path length crossed by the cutting tool on the surface. This length depends on the feed direction and it is influenced by the topology of the surface. To have an optimal feed direction at any point, the surface is divided into zones with low variation of the normal. Each zone has an optimal feed direction and minimum path length. Furthermore, a penalty reflecting the time of movement of the tool from a zone to another one is taken into account. Several algorithms are used to resolve this problem: Clarke and Wright's, Greedy Randomized Adaptive Search Procedure, Tabu search and Nearest neighbor search. A concrete example is illustrated.

Key words: Machining zones, 3-axis milling, free-form surfaces, path length tool, optimization methods.

1- Introduction

The free-form surfaces are used in various fields of activity, such as aeronautic, automotive industry or capital goods. The competition leads to the elaboration of products having a design more and more complex and increasing quality. These surfaces require a high quality level and reduced shape defects. The machining of the free-form surfaces, manufacturing moulds or matrix used to make the models is time consuming, not optimized and costly. The main factor influencing the global cost of the free-form surfaces production is the machining time. It is the optimization parameter taking into account.
The free-form surfaces are modeled using computer-assisted design software. The associated mathematical models are parametric surfaces with poles, as NURBS, B-Spline, Bezier curves... **[FI1]**.
Their machining is done by removal of material using Numerically Controlled Machine Tools, with movements of one or several hemispherical or toric end mills **[MK1]**. It has been demonstrated **[SS1]** that: if the cutting feed direction is well chosen, the toric end mill cutter allows to decrease the machining time. It is the type of tool that will be used in the present study.
There are several machining strategies: parallel planes milling **[HO1]** guide surfaces **[KC1]** and iso-parametric milling **[LG1]** these strategies are obtained directly from 3-axis machining researches. The one that's used in this study is the parallel planes milling, it's the most used and mastered in the industry. It consists in determining the tool paths using the intersection between the work piece and the parallel planes oriented along one machining direction. Advantages of parallel planes milling strategy are:

- Do not generate an overlapping tool path, allowing a considerable time saving.
- To avoid the appearance of non-machined areas.

The parallel planes milling strategy is not optimal. Indeed, during the machining of the surfaces with large variation of the normal direction, the successive paths become nearer to respect scallop height criteria, thus increasing manufacturing time. When a tool moves on the surface, it sweeps a volume by leaving an imprint on this surface, it's a swept surface **[PP1]**. Between two adjacent paths, the intersection of the swept surface produces a scallop. Usually, a maximum given scallop height criteria must be respected.
The main object of this study is to minimize the machining time of free-form surfaces while respecting the quality imposed by the engineering consulting firm, by 3-axis machining with toric end mill cutter. A considerable number of works have been devoted to reduce machining time **[CV1]**, **[ML1]**. Indeed, the first path is calculated according to the optimal feed direction. Then secondary paths are calculated, respecting a fixed step-over distance that guaranties a maximal scallop height, inferior to the imposed scallop height

Article 045-pp-27

criteria. The problem is that secondary path deviates rapidly and may not be in optimal direction engendering time loss.
To minimize the machining time, the free form surfaces are zoning. Each zone will be machined according to specific feed direction. Furthermore, a penalty reflecting the displacement of the tool from one zone to another one is taken into account. The problem appearing during the machining of the zones is the determination of the number and geometry of zones. Indeed:

- The number of zones should not be too high to a void spending too much time going from a zone to another one.
- The number of zones should not be too small to keep the feed direction not so far from optimal value in every point of the zone.

To minimize the global machining time of a given surface, this study concerns the optimization of the number and geometry of the zones.

This paper is organized as follows: the section 2 presents the context of our study and the optimization parameters. The section 3 is dedicated to the approach of the resolution of our problem with optimization methods. In the section 4, an example of application of our methods on a free-form surface is presented. The last section is devoted to a conclusion and perspectives.

2- Reminder of machining

2.1– Machining direction

The free-form surfaces present a set of curved zones. The geometry is obtained by successive passes of a tool. For this study the toric end mill with cutter radius R and torus radius r is used (fig.1), and the adopted machining strategy is the parallel planes of type one-way.
During the machining, the tool moves tangentially to the workpiece at the contact point C_c. At this point the tool can move in any direction. This parameter is called feed motion direction, it is directly influenced by the topology of the surface. The optimal direction at a given point of the surface is the steepest slope direction **[RD1].**
For example, let be an inclined plan (S=30°) and a toric end mill cutter (R=5mm, r=2mm) presented partially by a quarter of torus. The (fig.1), illustrates two cases of this tool movement. The thick-lined curve presents the trace left by the tool on the workpiece at C_c.

1. During the movement of the tool following a direction perpendicular to the greatest slope direction (α=90°), the trace radius of curvature left by the tool is equal to R
2. During the movement of the tool along the horizontal direction (α=0°), the trace left by the tool at contact point C_c is a curve with a curvature radius greater than r.

For the same path length, the quantity of material removed in the case (1) is much more important than in the case (2), then the number of paths required to machine the whole surface in the case (1) is inferior than in the case (2). So, the time required to machine the surface in case (1) is less than the machining time for the same surface in case (2).

The previous example illustrates that, the choice of the feed direction has an important role on the radius of the trace left by the tool on the surface. The more the radius of this trace is important and the more the machining time decreases. The radius of curvature of this trace at C_c is called effective radius R_{eff}. The toric end mill enables to keep a large effective radius while avoiding unsightly marks.

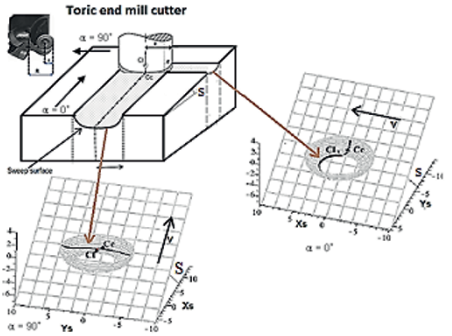

Figure 1: The trace left by the tool on the workpiece along the feed direction

2.2- The step-over distance

Step-over distance P_t corresponds to the distance between two successive and parallel tool paths, while not overpassing the imposed scallop height criteria h_c, (fig2). Generally, h_c is in the order of 0.01mm, then the following hypothesis are made:

- The tool makes a circular trace with radius equal to R_{eff} in the neighborhood of C_c.
- The radius of curvature ρ of the surface is assumed locally constant in a plan perpendicular to the feed rate direction.
- h_c is smaller than R_{eff} and ρ .

The calculation of the step-over distance P_t is made in the perpendicular plan to the feed rate direction.

Article 045-pp-27

$$P_t = \vec{P_t} * \vec{u} = \sqrt{\frac{8*h_c*R_{eff}*(R_{eff}+\rho)}{\rho}}, \quad \|\vec{u}\| = 1. \qquad (1)$$

At the contact point C_c, the scallop height and the curvature of the surface are fixed. R_{eff} has a direct influence on the machining time. Indeed, when R_{eff} increases the step-over distance increases too. The number of paths required to machine the surface decreases significantly and reduces the machining time.

Using a toric tool is relevant only when allowing machining time reduction compared too spherical tool use. Also, this condition is satisfied when the effective radius of the toric tool is greater than R. When the slope angle is low, the toric end mill cutter is recommended because the effective radius is important in a large feed direction interval.

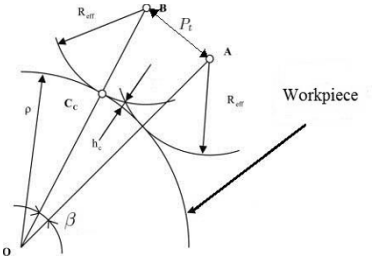

Figure 2: The step-over distance.

3- Optimization problem

3.1 – Problem formulation

Let S(u, v) be a parametric free-form surface, at any point of this surface the optimal feed direction corresponds to the steepest slope direction. Machining the surface with a single feed direction cannot ensure the maximum R_{eff} at any point, because of the variation of the normal direction on the surface. Indeed, an optimal feed direction at one point of a path can be very far from the optimal feed direction at another point of the same path. This induces decreasing of the average value of the effective radius, contracting the distance between the parallel planes and increasing machining distance.

In order to allow a machining with a near optimal feed direction at any point, the surface S(u, v) is mapped with a parametric meshing following (u, v). Each mesh $m_i \in M$ presents an elementary surface, with a low variation of the normal direction and then an optimal feed direction. Each mesh has a fixed size, determined during the meshing, a slope angle S_{mi} and an optimal machining direction associated to the minimum length path $Lg_{mi}(\alpha_{mi}^{opt})$.

If the crossing time of the tool from one mesh to another one is neglected, the optimal solution is to machine each mesh independently following its optimal direction. But, in practice this approximation is not acceptable. For this, the meshes will be combined into zones, reducing then the unproductive time of the tool.

A zone is a composition of a set of associated meshes. Two meshes can be associated if they are contiguous, meaning that they have at least one border in common.

Two adjacent meshes m_i, m_j are combined to zone z_{ij} if the length path trajectory $Lg_{zij}(\alpha_{zij}^{opt})$. of the z_{ij} following optimal direction α_{zij}^{opt} is lower than the sum of the lengths path, $Lg_{mi}(\alpha_{mi}^{opt})$.and $Lg_{mj}(\alpha_{mj}^{opt})$.of the meshes m_i, m_j following the respective direction, α_{mi}^{opt}, α_{mj}^{opt} plus a penalty P reflecting the time of movement of the tool from one mesh to another one.

The optimization problem studied in this paper relates to the minimization of the total distance crossed by the tool, respecting the constraint of an imposed maximum scallop height. The optimization parameters are the geometry of the zones and the feed direction used in each one.

More formally, the problem of minimization of the machining time is formulated as follows:

$$Min\left(\left(\sum_{i=1}^{|Z|} Lg_{z_i}(\alpha_{z_i}^{opt})\right) + (|Z| - 1) * P\right) \qquad (2)$$

With:

- $Z_i \in Z$ corresponds to one zone of the global surface zoning..
- $|Z|$ number of zones covered the whole surface.
- $Lg_{z_j}(\alpha_{z_j}^{opt})$ the path length crossed by the tool to machine the zone following the optimal direction $\alpha_{z_j}^{opt}$.
- P penalty due to the withdrawal of the tool outside the surface (material).

The calculation of the path length crossed by the tool to machine one zone zi following the optimal direction is very costly. Indeed, it requires:

- The use of the simplex algorithm to calculate $\alpha_{z_j}^{opt}$.
- To calculate the length path crossed by the tool on the surface it must to add all elementary segments defining the trajectory, this segments it is calculated by the SSI method (Surface/Surface intersection)

Article 045-pp-27

[BK1].

The saving $G(m_i, m_j)$ for this combination is:

$$(mi, mj) = \left(Lg_{m_i}\left(\alpha_{m_i}^{opt}\right) + Lg_{m_j}\left(\alpha_{m_j}^{opt}\right) + P\right) - Lg_{z_{ij}}(\alpha_{z_{ij}}^{opt})) > 0 \quad (3)$$

To summarize:

1. Let $M = \{m_1, m_2, \dots, m_n\}$ be a set of meshes covering the whole surface.
2. Let $\mathcal{Z} = \{z_1, z_2, \dots, z_n\}$ be a set of zone covering a set of contiguous meshes, with $z_i = \{m_1, m_2, \dots, m_p\} \subset \mathcal{Z}$, such as the machining time of is lower than the sum of machining time of all meshes $\{m_1, m_2, \dots, m_p\}$ plus the penalty P.
3. The set $\mathcal{Z}$ must cover all meshes of the set: $\sum_{i=1}^{l} |(zi)| = |(M)|$.

3.2- Optimization methods

To solve the minimization of the length path tool problem, the global optimization methods are adapted. In this section Clarke and Wright's algorithm, Greedy randomized adaptive search procedure algorithm, Tabu search algorithm and Nearest neighbour search algorithm are presented. The initial solution of each algorithm is to machine each mesh individually following this optimal direction:

$$Sol_{init} = \left(\sum_{i=0}^{card(M)} Lg_{m_i}(\alpha_{m_i}^{opt})\right) + (card(M) - 1) * P$$

Sol_{inter}: is the intermediate solution.

3.2.1- Clarke and Wright' s algorithm

Clarke and Wright algorithm (C&W) is the most widely known heuristic for solving constraints vehicle routing problem **[PR1]**. The main is to minimize the total distance travelled by the vehicles in each routing. The algorithm is based on the saving notion. To applicant this algorithm to the machining problem, the number of the vehicles to define is assimilated to the number of zones and the routings are assimilated to meshes affected to each zone. The object of the algorithm is to combine the meshes following a decreasing list of saving.

Pseudo code

1.Calculate the initial solution Sol_{init}

2.do

. For each pair of adjacent meshes (or zones)

.mi, mj, calculate the saving, $G(m_i, m_j)$.

. Store the saving in decreasing order

. Starting from the top of the savings list and combine all meshes with $G(m_i, m_j)$>0 to zones.

3. Repeat process and stop when $G(m_i, m_j)$<0.

3.2.2– Tabu search algorithm

The main idea of the Tabu search algorithm is to introduce the notion of history and the politic of exploration of the solution. In each step of the algorithm, each mesh examines the possible combinations with the adjacent meshes offered the minimum length path trajectory (maximum saving) and then selects it. This proceeding can repeat infinitely the same movements, then the t last movements are considered as forbid ("Tabu"). In each step, the best movement not Tabu is chosen **[GL1]**. One movement allows moving from one solution to another.

Pseudo code

1.Calculate the initial solution Sol_{init} , $Sol_{inter} = Sol_{init}$, Tabu list =φ

2.The best solution $S^* = Sol_{init}$.

3.Calculate the total length path of the configuration Sol_{init},

f(Sol_{init}) =$\sum_{i=0}^{l}(Lg_{m_j}(\alpha_{m_j}^{opt}))$ + $(P * (l-1))$,

4.Repeat

. $N(m_i)$.the best movement among the not Tabu movements

.If $f(Sol_{inter})$< f(S^*) then $S^* = Sol_{inter}$, include the move in the Tabu list.

5.Until <any movements is possible>

6.Return S^*

3.2.3 – Nearest neighbor search algorithm

The Nearest neighbor algorithm (NNS) is one of the first algorithms used to resolve the travelling salesman problem **[LK1]**. In this algorithm, one mesh mi is chosen randomly and it combined with another mesh mj offered a minimum path length (maximum saving). Then the two meshes, mi, mj will be marked as visited meshes. The mesh mj choses to combine with not marked mesh mk offered a minimum length path, then marked the mesh mk. When one marked mesh not found another not marked mesh offered a maximum saving, all marked meshes are combined to zone. To create another zone, one not marked mesh is chosen and the process is repeated until all meshes of the surface are marked.

Article 045-pp-27

Pseudo code

1.Repeat
.Choose one not marked mesh mi∈ M
.Choose an adjacent mesh mj not marked with a maximum saving
.Marked the meshes mi, mj,

2.Until <all marked meshes not found an adjacent meshes with maximum saving>

3.Combine all marked meshes to zone z

4. Go to step1.

5.Stop when all meshes are marked

3.2.4 – Greedy Randomized Adaptive Search Procedure algorithm

Greedy Randomized Adaptive Search Procedure algorithm (GRASP) is based on two knows optimization technic **[FT1]**.

- Greedy algorithm: step of construction of the solution, set of zones.
- Local research: improvement of the solution.

The algorithm maintains a list of possible combination of adjacent meshes (RCL: restricted candidate list). The solution is constructed step by step in selecting randomly the meshes in the RCL list.

Pseudo code

1.Calculate the initial solution Sol_{init}=φ,
Sol_{inter}=Sol_{init},

2.The best solution S^{*}=Sol_{inter}

3.Repeat
.Chose randomly one mesh mi ∈ M
. $Sol_{inter} = Sol_{inter} \cup \{mi\}$
. Calculate f(Sol_{inter})= f(Sol_{init})

$=\sum_{i=0}^{l}(Lg_{m_j}(\alpha_{m_j}^{opt})) + (P * (l-1))$,
. If f(Sol_{inter}) < f(S^{*}) then S^{*}= Sol_{inter}
. Update the list RCL

4. Until RCL = φ.
5. Return Sol_{inter}.

4- Application to an example

Let be a parametric free-form surface S(u, v) defined by (fig. 3), this surface is symmetrical in relation to the plane X=20.In this example the torus end milling cutter (R=5 and r=2) is used.

$$S(u,v) = \begin{pmatrix} 40u \\ 80v \\ 20u + 10uv^2 - 20u^2 - 10u^2v^2 + 10v + 10v^2 \end{pmatrix}$$

The scallop height to respect is equal 0.01mm.
For this simulation a personnel computer with the following specifications is used:

- Intel Core i7 2630QM / 2 GHz (2.9 GHz).
- RAM: 4 Go (DDR3 SDRAM - 1333 MHz - PC3-10600).
- The programming language used is Java.

This surface is mapped (fig4) following a parameter (u, v) 10*10, each mesh presents a simple surface with low variation of the normal. The optimal direction is calculated and the length path is evaluated for each mesh.
The initial solution $\boldsymbol{Sol_{init}}$ is to machine each mesh individually with length path trajectory $\boldsymbol{Lg_{m_j}}\left(\boldsymbol{\alpha_{m_j}^{opt}}\right)$.
The penalty P is equal to 40mm.

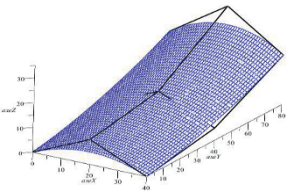

Figure 3: S(u,v) free-form surface.

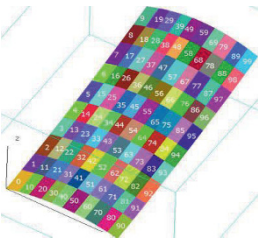

Figure 4: mapped S(u,v).

Article 045-pp-27

$Sol_{init} = \sum_{i=0}^{99}(Lg_{m_i}(\alpha_{m_i}^{opt})) + (40 * (99 - 1)) =$ 8532.57 mm

The savings of all adjacent meshes are calculated. The table of result is not presented, but an example to calculate the saving between two meshes is illustrated.

Example: Let be m_0 mesh of the surface S(u, v), (fig.4), its adjacent meshes are m_1 and m_{10}. According to the equation 3:

- $G(m_0, m_1)$ = 39.95 mm, optimal direction of the combination is 88.29°
- $G(m_0, m_{10})$ = 38.29mm optimal direction of the combination is 85.51° .

To have a maximum saving the mesh m_0 will combine with the mesh m_1 offering a maximum saving (39.95>38.29).

All savings are stored in list. This list will be decreasing for the requirement of: the C&W algorithm and Tabu search algorithm. For Greedy Randomized Adaptive Search Procedure algorithm and Nearest neighbor search algorithm the list must not be ordered.

The results of the simulation of the four algorithms are presented in this table 1. The last column is dedicated to the machining with single zone, as it done currently to machine the surface.

Methods	C&W	Tabu	NNS	GRASP	Single zone
Length path(mm)	**5039.47**	**5039.47**	5935.88	5381.388	6557.94
Running time (s)	60.53	80.61	70.941	61.740	6.27
Number of zones	7	7	4	2	1
Saving (%)	**23.15**	**23.15**	9.58	18.98	

Table1: Saving comparison methods.

Analyze:

- **Run time**

The algorithms C&W, Tabu search and GRASP are executed in parallel, i.e., the zones are created simultaneously and then aggregated with their adjacent meshes offered the maximum saving. Then these zones are combined with each other' s with respecting the maximum saving criteria.

The sequential algorithms like Nearest neighbor search create one zone by combining two adjacent meshes and in each step one mesh is add to the zone until saturation. Then a new zone is created. In this type of algorithm the meshes are crossed sequentially.

The running time on the sequential algorithms is slower than the parallel algorithms.

The Tabu search is the parallel algorithm but its running time is slower than C&W and GRASP, because of the calculation of the length paths crossed on the surface in each step of the algorithm.

- **Saving machining time**

The machining time savings presented in these algorithms are variable. The Nearest neighbor search algorithm have a smaller saving, because the combinations between meshes are done without taken in account the objective function. For example, one combination can be locally very advantageous, but the moving away the optimal direction of each zone engenders not negligible perturbation of the machining time. The result of the two algorithms GRASP and Nearest neighbor search depending of the initial configuration, and the results present in this example are the average of 80 simulations.

- **Discussion**

The two algorithms with maximum saving, 23.15%, are the Tabu search algorithm and Clark and Wright algorithm.

The running time of the Clark and Wright algorithm is lower than the Tabu search algorithm, because of the calculation of the paths length crossed on the surface in each step.

Machine the free-form surfaces with zones with different feed rate direction allows to take into account the variation of the normal direction at every points of the surface. The optimal direction of one zone offers the important step over distances and then minimum distance between two passes, then minimizes the number of passes to machining the surface.

We have supposed that the machining time varied linearly according to the length path crossed by the tool. This hypothesis is true only in 3-axis machine **[PL1]**.

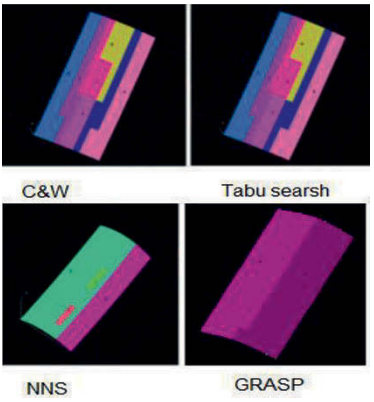

Figure 5: Results of algorithms.

Article 045-pp-27

5- Conclusion

In this article, we have interested to the optimization of the partitioning of the free form surfaces to minimize the path length crossed by the tool. By hypothesis the path length is supposed proportional to the machining time. The free-form surfaces are characterized by the complex topology then the large variation of the normal. Currently, in the various strategies, the initial set-up, first tool paths, cutters and the feed motion direction are often imposed from the start. This direction is not optimal in all points of the surface, this induces, in the parallel strategy, to the contraction of parallel planes distance, reduce the step-over distances and then long machining time.

To have an optimal direction at any point of the surface, this last is devised on zones. Each zone is machined following the optimal direction. To have an optimal division of zones, the optimization methods are used. After have mapped the surface with parametric meshing, the meshes are combined on zones to radius the loss time due to the movement of tool from a mesh to another.

The optimization methods used to solve this problem are: Clarke and Wright's, Greedy randomized adaptive search procedure, Tabu search and Nearest neighbor search. These methods are the aggregation and no backtracking algorithm. It is penalizing, indeed, in step of the algorithm, if one mesh is combined on zone , it cannot be detached of this zone , even if the mesh penalize the zone in the step

The results obtained by the C&W and Tabu search algorithms on the presented workpiece show a significant reduction of machining time (23 %).

Our future work will consisted to study minimization of the machining time of the free-form surfaces by zones using other optimization methods with backtracking and taking into account kinematic and dynamic behavior of the machine.

6-Acknowledgment

This work has been partially supported by French National Research Agency (ANR) through the COSINUS program under the grant ANR-09-COSI-005.

7-References

[BK1] Barnhill R.E and Kersey S.N. "A marching method for parametric surface/surface intersection". Computer-Aided Geometric Design 7. Page 257-280. (1990).

[CV1] Chen, Z., Vickers, G., Dong, Z.:" Integrated steepest-directed and iso-cusped tool path generation for three-axis CNC machining of sculptured parts". Journal of manufacturing systems 22(3), 190-201 (2003).

[FI1] Faux, I.D., Pratt, M.J.: "Computational geometry for design and manufacture". Halsted Press (1985).

[FT1] Feo, T. A., & Resende, M. G. "Greedy randomized adaptive search procedures". Journal of global optimization, 6(2), 109-133. (1995).

[GL1] Glover, F., & Laguna, M. Tabu search (Vol. 22). Boston: Kluwer academic publishers. (1997).

[HO1] Huang, Y., Oliver, J.H.: "Non-constant parameter NC tool path generation on sculptured surfaces". The International Journal of Advanced Manufacturing Technology 9 (5), 281-290 (1994).

[KC1] Kim, B., Choi, B.: "Guide surface based tool path generation in 3-axis milling": an extension of the guide plane method. Computer-Aided Design 32(3), 191-199 (2000).

[LK1] Lenstra, J. K., Kan, A. R., & Shmoys, D. B. The traveling salesman problem: a guided tour of combinatorial optimization (Vol. 3). Chichester: Wiley.(1985).

[LG1] Loney, G.C., Ozsoy, T.M.: Nc machining of free form surfaces. Computer-Aided Design 19(2), 85-90 (1987)

[ML1] Maeng, H.Y., Ly, M.H., Vickers, G.W.: Feature-based machining of curved surfaces using the steepest directed tree approach. Journal of Manufacturing Systems 15(6), 379-391, (1996).

[MK1] Marciniak, K.: "Geometric modelling for numerically controlled machining author". Krzysztof marciniak, publisher: Oxford university press (1992).

[PL1] Pessoles, X., Landon, Y., Segonds, S., & Rubio, W. Optimisation of workpiece setup for continuous five-axis milling: application to a five-axis BC type machining centre. The International Journal of Advanced Manufacturing Technology, 1-13. (2013).

[PP1] Peternell M. Pottman H., S.T., H, Z.: "swept volumes".Computer aided design 2(5), 599-608 (2005).

[PR1] T. Pichpibul and R. Kawtummachai, "New enhancement for ClarkeWright savings algorithm to optimize the capacitated vehicle routing problem," European Journal of Scientific Research, vol. 78, no. 1, pp. 119–134, (2012).

[RD1] Redonnet, J. M., Djebali, S., Segonds, S., Senatore, J., & Rubio, W. (2013). "Study of the effective cutter radius for end milling of free-form surfaces using a torus milling cutter". *Computer-Aided Design,* vol 45, Issue 6, pp 951-962, June (2013).

[SS1] Senatore, J., Segonds, S., Rubio, W., Dessein, G.: Correlation between machining direction, cutter geometry and step-over distance in 3-axis milling: Application to milling by zones. Computer-Aided Design, vol 44, Issue 12. Pages 1151–1160. (2013).

Article 066-ap-84

Storage Assignment Problem in logistics Warehouses: Optimization of Picking Locations by Cross-Entropy Method

Olivier Devise, Jean-Luc Paris, Séverine Durieux, Pierre-Guillaume Fradet

Clermont Université – IFMA, Institut Pascal, CNRS, CS 20265, F-63175 Aubière
Phone: +33 (0)4.73.28.81.01 / Fax: +33 (0)4.73.28.81.00
E-mail : {devise, paris, durieux, pfradet}@ifma.fr

Abstract: This paper covers a combinatorial optimization method called cross-entropy method. We used this method to solve an optimization problem: implementations of products in order to minimize the total distance traveled by workers during the picking order. After developing a state of the art regarding issues that affect the design of logistics warehouses, we will develop an overview of methods used to solve and/or optimize this type of problem. Cross-entropy method applied to shortest path problem will be developed and we will show this method can be used easily to solve an optimization problem in logistics area.

Key words: supply chain, warehousing, storage assignment problem, combinatorial optimization, cross-entropy method.

1 - Introduction

The primary purpose of managing logistics warehouses is to find the most effective way to ensure the functionality of the warehouse in the supply chain, which may be the distribution operation based way to other innovative value-added activities. Driven by customer demand for service in minimal time, efficiency, quality, but inexpensive as possible, the performance of logistics operations has become critical in today's competitive market. The order picking -removing the product storage areas in response to a specific request from a customer- is considered the most expensive in labor and the most critical process in terms of time spent [F, THS, TWB$^+$]. It is responsible for nearly 60% of all work activities of a warehouse according [MMB].

The ordering process by picking therefore have a strong impact on the reactivity of warehouses, and control systems in picking poorly managed can easily jeopardize the performance of the warehouse and interrupt the supply chain. It is therefore a major challenge for distribution centers. Recent innovations in the field such as dynamic storage and picking system, RFID and voice picking [KLDR, LÖ, P] and challenges such as e-fulfillment have proven their ability to improve the supply chain. Accordingly, the order by picking is considered the best way to which managers of storage facilities should lead to improve the performance and efficiency of their distribution [KLDR, P].

In practice, the policies used by manufacturers to control the process of picking include policies specific storage, batch control groups, and path optimization preparer control [KLDR, DKVDP, DKVdPW]. This last point is crucial for the optimization and it gives birth to numerous studies and research about it. It is a complex combinatorial optimization problem closely linked to other issues such as the implementation of references picking. These two key concepts of warehouse management are the factors that promote productivity and order preparation.

This section has the primary purpose of drawing up a short state of the art on these issues. In a second step, we will examine the methodologies to optimize the layout of picking areas: dimension number of locations, choose the best way of picking and choosing a particular implementation of these multiple references given in a warehouse in order optimizing the movement of the worker. The ultimate goal is to achieve an optimal implementation that promotes the smallest possible total length traveled. Then offer numerous strategies to manage ordering and picking product to meet this problem. Multiple parameters must be taken into account to successfully optimize the picking as the amount, layout and type of lanes, the assignment policy products in storage, the path picking, picking the density to interior walkways, the combination of control, etc.. [HT]. These areas are the subject of research, but there are only a few methods applied to these problems in the literature for both attempt to link the different parameters between them [CGDKVN] but also for more

Article 066-ap-84

locally optimize the components of the performance and efficiency of a warehouse as the minimization of the total distance traveled.

However, in all situations, these problems are of combinatorial optimization problems, which are envisaged by means of heuristics providing results more or less optimal. These problems are solved by well-known algorithms such as Tabu Search, the problem of the shortest path or the TSP (Traveling Salesman Problem). Among these algorithms exists a more recent optimization method called cross-entropy. Attributed to [R], cross-entropy, a versatile algorithm for the Monte Carlo algorithm, is an efficient and generic method for estimating probabilities of rare events, and quickly proved to be a technical powerful and versatile for both the rare event simulation and combinatorial optimization. The method originates from the field of rare event simulation, where very low probabilities to be estimated accurately [DBKMR]. It is based on a probabilistic algorithm wherein the probability densities are evolving to converge to a density providing an optimal solution. This method therefore uses a population of solutions at each iteration, the population generated according to probability densities [R].

2 - Problematic

When designing a logistics warehouse, we can count seven influential factors in [BKY]: batching, the sequence of collection, storage policy, zoning, the management of the warehouse picking equipment and design information picking. More generally, we reference in the literature four major cornerstones in the design and modeling of a warehouse [HT] that we adopt to define our research framework: (1) the layout of the warehouse and planning; (2) strategy assignment storage; (3) policy path followed by the preparer of the order; (4) the combination and order scheduling. In this issue, the question is more complex since it is optimizing the implementation reference product picking in order to minimize the total distance traveled. Finally, the major difficulty we face is that we do not have precursors on the technique we propose : using the cross-entropy method to build and optimize the storage location assignment problem.

Our problem refers to a problem of "storage assignment problem" (SAP) found quite frequently discussed in the literature, sometimes under the name of "local optimization problem," or of storage allocation strategy. Many researchers have worked on this subject because it provides many improvements and gains, both in terms of space occupation rate, cost of stockpiling and unloading, etc. Solving this problem is to provide an effective way to locate the products in the order in a warehouse in order to reduce the necessary preparations for the control efforts. This affects almost all performance indicators such as a warehouse order picking and associated costs [MA2].

We simply take an example here of [EO] that combine the study of optimization implementations products in the automotive industry to optimize the collection by picking product orders. To do this, they proceed in two stages: the first, the problem of assigning the storage location is solved with a policy based storage product classes in order to minimize the flow of information sent to in the warehouse and in the second, the problems subdivision of products and routing are considered simultaneously to reduce costs of transport operations in the warehouse in question. They manage, using genetic algorithms to apply it to any type of warehouse available in the automotive industry. Finally, the problems of SAP types are part of the class of NP-hard problems [FS]. Therefore, a large number of heuristics have been proposed. On the other hand, routing or path picker control in a warehouse has also received considerable attention in the literature relating to operational research. It has been widely demonstrated and is now recognized that the determination of the path of the order picker under the constraint of minimizing the distance in a warehouse is a variant of the well known Traveller Salesman Problem (TSP) problem, which is NP-hard [L, LLRKS]. TSP asks the following question: Given a list of locations and the distances between each pair of location, what is the shortest possible route that visits each location exactly once and returns to the origin point? In the case of the path of the order picker, each product or article to be picked corresponds to a peak, and the distance between two vertices of them must be as short as possible between the corresponding locations in the warehouse. Usually, since the distances are symmetric, the fact of finding the shortest route to do the picking is a symmetric TSP. However, in some warehouse aisles are unidirectional, the distance matrix is asymmetric, and in fact the corresponding TSP too. Many efficient algorithms exist and TSP can be used to optimize routes picker control. So, we want to solve a problem very closed of the shortest-path problem (SPP). This problem finds many applications in operations research, but we could not find any work relating to issues of settlements in order to find the shortest path. However, and we will develop in the third part, the SPP can be solved and applicable to our case under certain assumptions.

Unfortunatly the location strategies of products (that is to say, the allocation of products in locations to facilitate the preparation of orders) have received less attention. The theoretical contributions are rare, because the location of the product strongly depends on the configuration of the warehouse, the strategy of picking and technology in place. Thus, most research in the literature dealing with specific case studies.

3 - Short literature review

3.1 - Similar problems concerning the workers way

Although the general problem of picking path has been shown as an NP-hard problem, some particular configurations of storage can be used to help to solve the problem. For example, [RR1] showed that if the picking is done in a rectangular warehouse with intersections only

at the ends of aisles. The routing problem is transformed into a particular TSP solvable in polynomial time. [GR] studied the case in which preparers must complete their tour down along each aisle collecting the elements of the order, without being able to reach both sides simultaneously unless you change position. They then showed that the most optimal solution can be found by solving a SPP.

3.2 - Similar problems concerning the implementation of products

The literature presents numerous articles about specific locations of products in storage locations. In [DC], authors have solve a SAP in a semi-automated picking-orders system by simulated annealing method. They apply this algorithm in order to minimize the waiting time in stations, one of the main performance indicators in picking-orders system. They then fail to provide improvements in terms of number of stops in stations (and thus time-out). Their results show an improvement of makespan about 15%.

In [JM] authors have developed a model of localization of products in a warehouse so that the average preparation time control is minimized. [VF] have examined the problem of optimal location of products in a bidirectional carousel storage with a collection system with the objective of minimizing the average distance between two successive collections picking in the long term. [PS] have studied, with a storage strategy based on the volume of the element, the effect of placing the products high near the starting point and from the warehouse volume, to minimize sampling distances. [LA] meanwhile, analyzed the time required to collect multiple items through a carousel system used to store and retrieve properties of small and medium size.

3.3 - Similar problems concerning the minimization of the total time

[FS] have succeeded in developing a procedure for assignment heuristic to minimize the total time items whose demand is dependent, that is to say, a product that requires another to fill a certain demand. [BJ] have developed a strategy for allocating storage locations extracted from the structure of the product applied to reduce the sampling time using different properties such information picking in the construction of a coherent policy of assignment. [JL] proposed a clustering algorithm for assigning elements balancing the workload among all processors of the order so that the use of the control system is improved. Their work has shown interest in the time saved in an area of synchronized control "mother", where each sub-area of the warehouse processes the same command simultaneously.

3.4 - Problem of optimal location to minimize the distance

A study in [RR2] seeks to find the optimal location of products in order to minimize the total distance traveled. Their work is very interesting about the approach, which is aimed at reducing this distance using a local search procedure based on the exchange of two products by neighbourhood. Starting from an initial solution and of a number of lists of goods to be taken by picking heuristics evaluates, for each possible pair of products, decreasing the distance if their storage locations had been exchanged. Once all possible exchanges were evaluated, the one offering the most improvement in terms of distance is selected and implemented. This process continues until no better improvement can be obtained.

On the other hand, the work done by [PW] on the allocation of items to storage locations problem, show that we can handle this problem by Markov chains applied to a line storage within which runs on a conveyor which order pickers affiliated with small zones fulfill the command in turn. To find the expected distance of a preparer for the realization of an order, this study aims to describe the removal operation as a Markov chain and simulation results validate the accuracy of the analytical model. They then determine the properties and algorithms that provide the optimal positions of the items in the locations with the objective of minimizing the total travel time.

3.5 - Algorithms

The literature is very rich of algorithms applied to various problems about logistics warehouses: the optimization of their performances is an important source of gain. We present different work on our problems and demonstrate their interest in the desire to optimize the picking locations to reduce the total distance traveled during the preparation of the order. We focus here on particularly algorithms deployed in order to solve the problem of shortest path to echo our general problem.

Tabu search is an optimization method where the neighbors are evaluated: if a better solution is found, it is selected, and then we explore again neighbors. This method has been tested on the problem of cell formation in [SLB] with the objective to minimize the flow inter cells . The disadvantage of this method is of course the high sensitivity to local optima. To do this, [WYC] developed an algorithm combining Tabu search with genetic algorithms. Combining these two methods can greatly reduce the risk of being confined to a local optimum. We have seen that the power of the cross-entropy is to converge to an optimal solution without being sensitive to local optima. In the Tabu search method , another risk exists when strong constraints are taken into account. In fact , it becomes more difficult to find a better neighbor and viable solution , while the simulated annealing method can tolerate poorer solutions. Evolutionary methods are not aware of this possibility because they work on a population.

Genetic algorithms are, in turn , widely used for solving

Article 066-ap-84

assignment problems. In [HCC], authors developed an approach batch control based on genetic algorithms to directly reduce the total distance covered to prepare the order. In [WZ], authors continued in this direction by using the same algorithm, while focusing on the sources commands in batch control. As he defines himself, bulk orders represent an aggregation of a set of commands in a number of subsets, each of which can then be taken from a single individual in order picking tour. This technique takes to be a very powerful approach in a storage system because it can achieve greater productivity, particularly due to the acceleration of the movement of goods in the warehouse. Other well-known algorithms were used as the algorithm Branch-and-Bound found in [MA1].

3.6 - Method of realization

We focus here on the way to treat a shortest path problem. Some simple classical algorithms to address these problems, use the label setting and correction algorithms label. The simplest problem of the shortest path, where the weights of the network are static case can be solved in time $O(n^2)$ using Dijkstra's algorithm. There are several methods for finding the shortest path between the source node to the end node through dynamic programming, zero-one programming but also thanks to the theory of flow. In [OG], authors discussed the problem of finding the shortest path from an origin to a specified fixed in a network with arcs represented as intervals on the real line node. [GCW] studied the possibility of using genetic algorithms to solve shortest path problems. [GP] presented an algorithm for the problem of the shortest path that connects the arcs connected to a transmission system in which they are represented in the form of interval numbers.

4 - Cross-entropy applied to the shortest path problem

The cross-entropy method has been invented by Rubinstein [R] to enable the estimation of the probabilities of rare events. This is a general method for optimizing Monte Carlo combinatorial or continuous type, and preferential sampling. The cross-entropy quickly proved to be a powerful and versatile technique for many cases of applications : it allows the simulation of rare events and treatment of combinatorial optimization problems. The method was originally developed for the simulation of rare events, where very low probability densities must be estimated properly, for example, in the analysis of network security models queue, or performance analysis of telecommunication systems. It takes its name from the "distance cross-entropy " (otherwise known as " Kullback-Leibler") which is a well-known information in the network systems measure. In information theory, cross-entropy between two probability distributions measuring the average number of bits needed to identify an event from a probability space.

CE method can be applied to any combinatorial optimization problem or deterministic problems where observations are noisy: the traveling salesman problem (TSP), the optimization problem of quadratic assignment, the alignment problem DNA sequences, the maximum cut problem (max-and-cut problem), the memory allocation problems, as well as continuous optimization problems with many local extrema. This method has been used to treat problems with the configuration of logistics warehouses: different types of scheduling problems, and the buffer allocation problem (buffer allocation problem, BAP) for production lines and the problem multidimensional assignment (multidimensional assignment Problem, MAP) studied in [LTNPD].

According [AM], the method of cross-entropy can be easily applied to combinatorial optimization problems of various kinds, including the shortest-path problem. It is proposed here to examine their work on the use of the method in order to obtain a partial response to this problem. Their work set in a static network, where costs are constant and are based on the method of cross-entropy of Rubinstein to solve complex combinatorial problem.

4.1 - Definitions

We are given a network $G = (N, A)$ where N is a set of nodes $N = \{1, 2, \ldots, N\}$ and a set of arcs A such that $A \subseteq N \times N$.
Let m be the number of arcs in G network, that is to say, $m = |A|$. To simplify the notation, we assume that each pair of nodes is connected by at most one edge. Each arc $(i, j) \in A$ has a transition cost from i to j, denoted c_{ij}.
Then, we assume that the length of a path is equal to its cost and we will use the terms cost and length of equivalently as terminology. Assume that the graph is complete. A path P is said to be the shortest path from node i to node j if the cost $[P] \leqslant [Q]$ for all Q path node i to node j.

4.2 - Proposed algorithm

Let X be the set of possible paths, $S(x)$ the sum of the lengths of the paths $x \in X$ and $f(x)$ the aggregate capacity of these paths X. Each path can be represented by means of a permutation of $(1, 2, \ldots, N)$. For example, for $N = 4$, the permutation $(1, 2, 3, 4)$ represents the path $1 \to 2 \to 3 \to 4$. In fact, we might as well be a way via a permutation $x = (x_1, x_2, \ldots, x_n)$. We can then formulate the problem as follows:

$$\min_{x \in X} [S(x)] = \min_{x \in X} \left\{ \sum_{i=1}^{N} C_{x_i, x_{i+1}} \right\} \tag{1}$$

To apply the CE algorithm, we need to precise how to generate random paths and how to update the parameters in each iteration. Let us define the equivalent problem of minimization:

Article 066-ap-84

$$\bar{X} = \{(x_1, x_2, \ldots, x_n) : x_1 = 1\ , \quad x_i \in \{1, \ldots, n\}, i = 2, \ldots n\} \quad (2)$$

The set of arcs that correspond to those starting at 1 and ending in N. Again, we define the function $\bar{S}$ on $\bar{X}$ by $tildes(x) = S(x)$ if $x \in X$, $\tilde{s}(x) \in \infty$ otherwise. It becomes obvious that the equation 1 is equivalent to the following minimization problem:

$$\min_{x \in \bar{X}} \tilde{s}(x) \quad (3)$$

A simple method to generate a random trajectory $X = (x_1, x_2, \ldots, x_n)$ is to use a Markov chain of the graph G from a node (source node) and stopping after n steps. Let $P = (p_{ij})$ denotes the transition matrix in a single step of the Markov chain. We assume that the diagonal elements of P are zero, and all other elements of P are strictly positive. On the other hand, P is a general stochastic matrix $n \times n$. The probability density function $f(.; P)$ of X is to then set by the matrix P and its logarithm is given by:

$$\ln f(x; P) = \sum_{r=1}^{n} \sum_{i,j} \mathbb{I}_{\{x \in \tilde{X}_{ij(r)}\}} \ln p_{ij} \quad (4)$$

Where $\tilde{X}_{ij(r)}\}$ represents the set of paths in $\bar{X}$ for which the transition occurs at node i to j. The update rules of this optimization problem modified drift $\{S(X_i) \leqslant \gamma\}$, provided that the rows of P are equal to 1. Using Lagrange multipliers $u_1, u_2, \ldots, u_n$, we obtain the following maximization problem:

$$\max_{p} \min_{u} \left[\mathbb{E}_P \mathbb{I}_{\{S(X_i) \leqslant \gamma\}} \ln f(X; P) + + \sum_{i=1}^{n} u_i \left(\sum_{j=1}^{n} p_{ij} \right) \right] \quad (5)$$

Differentiating the expression within brackets above and within all p_{ij} for all $j = 1, 2, \ldots, n$:

$$\frac{\mathbb{E}_P \mathbb{I}_{\{S(X_i) \leqslant \gamma\}} \sum_{r=1}^{n} \mathbb{I}_{\{x \in \tilde{X}_{ij(r)}\}}}{p_{ij}} + u_{ij} = 0 \quad (6)$$

Summing over $j = 1, 2, \ldots, n$, we obtain $\mathbb{E}_P \mathbb{I}_{\{S(X_i) \leqslant \gamma\}} \sum_{r=1}^{n} \mathbb{I}_{\{x \in \tilde{X}_{i(r)}\}} = -u_{ij}$ where $\tilde{X}_{i(r)}$ is the set of paths for which the transition begins at node i. It follows that the optimal p_{ij} is given by:

$$p_{ij} = \frac{\mathbb{E}_P \mathbb{I}_{\{S(X_i) \leqslant \gamma\}} \sum_{r=1}^{n} \mathbb{I}_{\{x \in \tilde{X}_{ij(r)}\}}}{\mathbb{E}_P \mathbb{I}_{\{S(X_i) \leqslant \gamma\}} \sum_{r=1}^{n} \mathbb{I}_{\{x \in \tilde{X}_{i(r)}\}}} \quad (7)$$

The estimator corresponding to this equation will be:

$$\hat{p}_{ij} = \frac{\sum_{k=1}^{N} \mathbb{I}_{\{\tilde{S}(x_k) \leqslant \gamma\}} \sum_{r=1}^{n} \mathbb{I}_{\{x_k \in \tilde{X}_{ij(r)}\}}}{\sum_{k=1}^{N} \mathbb{I}_{\{\tilde{S}(x_k) \leqslant \gamma\}} \sum_{r=1}^{n} \mathbb{I}_{\{x_k \in \tilde{X}_{i(r)}\}}} \quad (8)$$

To update p_{ij}, we take the fraction of time of transitions from i to j have, but taking into account only the routes with a total length less than or equal to γ. Now since we only generate paths, the updated value for p_{ij} can be estimated by:

$$\hat{p}_{ij} = \frac{\sum_{k=1}^{N} \mathbb{I}_{\{\tilde{S}(x_k) \leqslant \gamma\}} \mathbb{I}_{\{x_k, k \in X_{ij}\}}}{\sum_{k=1}^{N} \mathbb{I}_{\{S(x_k) \leqslant \gamma\}}} \quad (9)$$

Where X_{ij} is the set of paths for which the transition of i to j is performed. To complete this algorithm, we need to specify the stopping criterion. For the initial matrix $\hat{P}_0$, we just take all the elements outside the diagonal equal to:

$$\frac{1}{\text{non-zero elements in each row}} \quad (10)$$

For the stopping criterion, we use:

$$\hat{\gamma}_t = \hat{\gamma}_{t-1} = \ldots = \hat{\gamma}_{t-d} \quad (11)$$

where t is the final iteration.

The algorithm for generating a path is given by:

1. Let define $P^1 = P$ et $X_1 = 1$. Then $k = 1$.
2. Get P^{k+1} from P^k by first fixing the X_k-th column of P^k to 0, then normalize the lines so that their sum is equal to 1. Then generate X_{k+1} from the distribution formed by the X_k-th row of P^k.
3. If $k = n$, then stop, otherwise $k = k + 1$ and repeat step 2.

5 - Industrial application

The industrial case of this article is a real warehouse of one of leaders in the logistics dedicated to the mass-market retailing in France. This warehouse consists of 1071 locations. There are three types of locations: picking, half-picking and dynamic picking. We have to place 474 products, one product by location and one location by product. These products are grouped in five families. The sizes of these families are respectively 127, 102, 67, 130 and 48 products. The size of the search space is then (127! x 102!

Article 066-ap-84

x 67! x 130! x 48!), which is about $8.35\,10^{750}$ solutions. The enterprise has first itself decided of the grouping of products in family, regarding weight constraint and stackable capacity. It has decided, as well, of order of families: the first family must have the first locations, the second family's locations must follow the first family locations, and so on. The order of the products in each family is then what we have to decide in this article.

The evaluation function is the total distance to satisfy a real set of customer's commands (10851 commands). Satisfying a command means to build all the pallets, on which will be piled the commanded products. The distance to build a pallet is the distance between the entry of the warehouse added of the sum of the distances to pick the necessary products one by one following a given circuit added to the distance between the last product and the exit of the warehouse.

To solve this problem, we have realized a C++ program based on the cross-entropy approach. After a large campaign of tests to set cross-entropy parameters, the best solution is reached with a population of 1500 potential solutions, a size of 300 best solutions kept from an iteration to the following one, during 1000 iterations. The computation time of one replication of this configuration takes about three hours on a standard PC. The following figure shows the convergence of the proposed algorithm. It has to be noted that solution we computed is about 25% better than the empirical solution built by the enterprise.

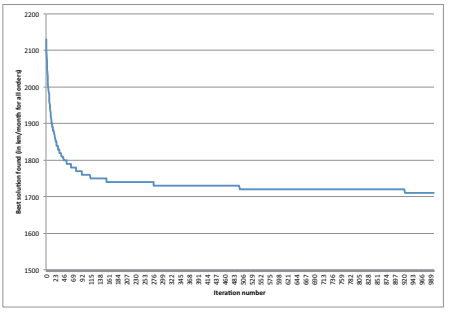

Figure 1: Evolution of the best solution found at each iteration

6 - Conclusion

In this article, we presented the global problem of logistic warehouse design and we focused on the storage assignment problem. We presented a literature review of this problem and we noticed that nobody, to our knowledge, has to try to solve it via cross-entropy. However, it is a new optimization method considered very effective in other optimization domains, where probabilities are low. To test the relevance of this approach, we applied it to a real large warehouse of one of French leaders in the logistics dedicated to the mass-market retailing.

The success which we have met consolidated us in our first impression: cross-entropy is an effective method, simple to implement and very relevant to attack a large range of optimization problem. Now, we should improve the cross-entropy method studying the set-up. cross-entropy method has two main parameters: the quantile selected to compute the next probability density function $(1 - \rho)$ and the size of generated sample N at each step. We did not find study about how to set-up this method in the case of very large optimization problem.

References

[AM] S. Abbasi and F. Moosavi. Finding shortest path in static networks: using a modified algorithm. *International Journal of Finance & Banking Studies*, 1(1):29–33, 2012.

[BJ] H. Brynzér and M.I. Johansson. Storage location assignment: Using the product structure to reduce order picking times. *International Journal of Production Economics*, 46–47:595 – 603, 1996.

[BKY] Yossi Bukchin, Eugene Khmelnitsky, and Pini Yakuel. Optimizing a dynamic order-picking process. *European Journal of Operational Research*, 219(2):335 – 346, 2012.

[CGDKVN] Chien-Ming Chen, Yeming Gong, René B.M. De Koster, and Jo A.E.E. Van Nunen. A flexible evaluative framework for order picking systems. *Production and Operations Management*, 19(1):70–82, 2010.

[DBKMR] Pieter-Tierk De Boer, Dirk P. Kroese, Shie Mannor, and Reuven Y. Rubinstein. A tutorial on the cross-entropy method. *Annals of Operations Research*, 134(1):19–67, 2005.

[DC] Olivier Devise and Christophe Caux. Modeling for design and optimization of product-mapping by simulated annealing in an automated distribution system. *Journal Européen des Système Automatisé*, 44(2):209–228, 2010.

[DKVDP] René De Koster and Edo Van Der Poort. Routing orderpickers in a warehouse: a comparison between optimal and heuristic solutions. *IIE Transactions*, 30(5):469–480, 1998.

[DKVdPW] M. B. M. De Koster, Edo S. Van der Poort, and M. Wolters. Efficient orderbatching methods in warehouses. *International Journal of Production Research*, 37(7):1479–1504, 1999.

[EO] Seval Ene and Nursel Oztürk. Storage location assignment and order picking optimization in the automotive industry. *International Journal of Advanced Manufacturing Technology*, 60(5-8):787–797, 2012.

[F] E. H. Frazelle. *World-Class Warehousing and Material Handling*. McGraw-Hill, New-York, 2002.

[FS] E. H. Frazelle and G. P. Sharp. Correlated assignment strategy can improve any order-picking operation. *Industrial Engineering*, 21:33–37, 1989.

[GCW] M. Gent, R. Cheng, and D. Wang. Genetic algorithms for solving shortest path problems. In *IEEE International Conference on Evolutionary Computation*, pages 401–406, 1997.

[GP] A. S. Gupta and T. K. Pal. Solving the shortest path problem with interval arcs. *Fuzzy Optimization and Decision Making*, 5:71–89, 2006.

[GR] M. Goetschalckx and H. D. Ratliff. Order picking in an aisle. *IIE Transactions*, 20:53–62, 1988.

[HCC] Chih-Ming Hsu, Kai-Ying Chen, and Mu-Chen Chen. Batching orders in warehouses by minimizing travel distance with genetic algorithms. *Computers in Industry*, 56(2):169 – 178, 2005. <ce:title>Applications of Genetic Algorithms in Industry</ce:title>.

[HT] L.F. Hsieh and L. Tsai. The optimum design of a warehouse system on order picking efficiency. *International Journal of Advanced Manufacturing Technology*, 28(5-6):626–637, 2005.

[JL] Chin-Chia Jane and Yih-Wenn Laih. A clustering algorithm for item assignment in a synchronized zone order picking system. *European Journal of Operational Research*, 166(2):489 – 496, 2005.

[JM] J. M. Jarvis and E. D. McDowell. Optimal product layout in an order picking warehouse. *IIE Transactions*, 23(1):93–102, 1991.

[KLDR] René De Koster, Tho Le-Duc, and Kees Jan Roodbergen. Design and control of warehouse order picking: A literature review. *European Journal of Operational Research*, 182(2):481 – 501, 2007.

[L] Gilbert Laporte. The traveling salesman problem: An overview of exact and approximate algorithms. *European Journal of Operational Research*, 59:231–247, 1992.

[LA] N. Litvak and I. Adan. On a class of order pick strategies in paternosters. *Operations Research Letters*, 30:377–386, 2002.

[LLRKS] E. L. Lawler, J. K. Lenstra, A. H. G. Rinnooy Kan, and D. B. Shmoys. *The traveling salesman problem. A guided tour of combinatorial optimisation*. John Wiley & Sons, Chichester, 1985.

[LÖ] Hau Lee and Özalp Özer. Unlocking the value of rfid. *Production and Operations Management*, 16(1):40–64, January-February 2007.

[LTNPD] HoaiAn Le Thi, DucManh Nguyen, and Tao Pham Dinh. Globally solving a nonlinear uav task assignment problem by stochastic and deterministic optimization approaches. *Optimization Letters*, 6(2):315–329, 2012.

[MA1] V.R. Muppani and G.K. Adil. A branch and bound algorithm for class-based storage-location assignment. *European Journal of Operational Research*, 189:492–507, 2008.

[MA2] V.R. Muppani and G.K. Adil. Efficient formation of storage classes for warehouse storage location assignment: A simulated annealing approach. *International Journal Management Science*, 36:609–618, 2008.

[MMB] Yuri Merkuryev, Galina Merkuryeva, and Aurelija Burinskiene. *Warehouse Order Picking Process*, chapter Simulation-Based studies in Logistics: Education and Applied Research, pages 147–165. Springer-Verlag, London, 2009.

[OG] Shinkoh Okada and Mitsuo Gen. Fuzzy shortest path problem. *Computers & Industrial Engineering*, 27(1–4):465 – 468, 1994.

[P] Charles G. Petersen. An evaluation of order picking policies for mail order companies. *Production and Operations Management*, 9(4):319–335, 2000.

[PS] C.G. Petersen and R.W. Schmenner. An evaluation of routing and volume-based storage policies in an order picking operation. *Decision Sciences*, 30(2):481–501, 1999.

[PW] J.C.H. Pan and M.H. Wu. A study of storage assignment problem for an order picking line in a pick-and-pass warehousing system. *Computers & Industrial Engineering*, 57:261–268, 2009.

[R] R. Y. Rubinstein. Optimization of computer simulation models with rare events. *European Journal of Operational Research*, 99:89–112, 1997.

[RR1] H.D. Ratliff and A.S. Rosenthal. Order-picking in a rectangular warehouse: a solvable travelling salesman problem. *Operations Research*, 31(3):507–521, 1983.

[RR2] J. Renaud and A. Ruiz. Improving product location and order picking activities in a distribution center. *Journal of the Operational Research Society*, 59:1603–1613, 2008.

[SLB] Dake Sun, Li Lin, and Rajan Batta. Cell formation using tabu search. *Computers & Industrial Engineering*, 28(3):485 – 494, 1995.

[THS] M. Ten Hompel and T. Schmidt. *Warehouse Management: Automation and Organisation of Warehouse and Order Picking Systems*. Springer, Berlin, Germany, 2007.

[TWB+] J.A. Tompkins, J.A. White, Y.A. Bozer, E.H. Frazelle, and J.M.A. Tanchoco. *Facilities Planning*. John Wiley & Sons, New-Jersey, 2003.

[VF] R. G. Vickson and A. Fujimoto. Optimal storage locations in a carousel storage and retrieval system. *Location Science*, 4(4):237–245, 1996.

[WYC] T.H. Wu, J.Y. Yeh, and C.C. Chang. A hybrid tabu search algorithm to cell formation problem and its variants. *World Academy of Science, Engineering and Technology*, pages 1090–1095, 2009.

[WZ] Jie Wan and Shaoqing Zhang. The research on distance optimization of batch-order picking based on genetic algorithm. In *Management and Service Science, 2009. MASS '09. International Conference on*, pages 1–4, 2009.

Article 061-cad-112

Influence of Minimum Quantity Lubrication design parameters on milling finishing process

Arnaud DUCHOSAL[1], Roger SERRA [2], René LEROY [3]

(1) : ENISE - LTDS 58, rue Jean Parrot, 42000 Saint Etienne
0477437596
E-mail : arnaud.duchosal@enise.fr

(2) : INSA Centre Val de Loire – LMR-CEROC
3, rue de la chocolaterie, 41000 Blois
0254558422
E-mail : roger.serra@insa-cvl.fr

(3) : Polytech' Tours, LMR-CEROC, 7 avenue Marcel Dassault, 37200 Tours
0247361307
E-mail : rene.leroy@univ-tours.fr

Abstract: This paper proposed a numerical study of the Minimum Quantity Lubrication (MQL) design parameters effects outside a rotating tool. Parameters as particle sizes for different oil mist input device parameters (inlet pressures) as function of different canalization geometries have been determinate on a previous experimental part, which are not presented here. The parameters thus identified were integrated as boundary conditions for the numerical simulation of a rotating tool during a milling surfacing process with different canalization orientations. The chip removal is not considered here. Only the numerical effectiveness of the minimum quantity lubrication is taken into account. The main goal of the oil mist is to spray the cutting edge to ensure a good lubrication on the tool-chip contact area. The simulations highlighted the impingement of the different oil particle sizes on the tool carbide inserts. A volume per unit area and a mean distance of the oil scatter from droplet impingements relative to a global virtual area from tool/chip interface were considered. The global virtual area was taken as function of the feed rate. The Taguchi method is applied in order to optimize numerical design parameters in finishing conditions as function of different parameters. The minimum quantity lubrication design parameters evaluated are canalization orientations, inlet pressure, feed rate and particle sizes. The analysis shows that Taguchi method is suitable to solve this numerical problem. The results shows that the optimal combination for a high lubrication performance at high cutting speed is based on high feed rate, with high canalization orientations and mean particle sizes.

Key words: Computational Fluid Dynamics, Minimum Quantity Lubrication, Milling, Finishing Process, Taguchi method.

1 Introduction

Finishing process in milling is the most important operation to ensure steady state quality, especially on surface roughness. At High Speed Machining (HSM), the chip was subjected to strong elastoplastic strains. The local stresses obtained on the cutting edge, increased the temperature and enable the sticking phenomena. [IM1]. Some experimental studies have advocated the use of the minimal fluid process and have underlined its benefits. Lubrication has a significant effect on these machined surface characteristics. The two-phase "air + oil" mixture has significant influence on the work piece versus carbide tool thermo mechanical behaviour. The pressurized oil mist sprayed on the cutting edge avoids the sticking phenomena highlighted by [BB1]. Temperature decreasing during machining, really good finishing surface and exceptional tool life time were largely obtained with minimal fluid coolant compared with dry or flood lubrication process [DI1, LA1, KM1]. All these parameters ensured with the minimal fluid process lead to high production rate.

All studies to date have focused on external minimal fluid coolant process. Some authors showed the influence of the minimum quantity lubrication cooling with external nozzles in milling [RS1], in drilling [KW1] or in turning process [KO1]. Tool elaboration with inner canalizations answered to large-scale industries production request. The geometry of the inner canalizations depends on different parameters (inlet pressures, cutting speed) and is not easy to determinate as the external spray nozzles. Several phenomena appear during the tool rotation and the small particle size of the oil mist has to be preserved [DR1, A1]. Moreover, the lubrication is only efficient for oil included on the tool/chip interface calls "cutting area". The objective is to optimize parameters to have the maximum of oil quantity in the defined-cutting area and this volume has to be the closest to the cutting edge. To the complexity to reach the right conditions of micro spray efficiency because of the large amount of parameters, Taguchi method is used in this study. This method is largely used for reducing time for experimental investigation and investigating the effects of multiple factors on performance [GC1]. But this method is exceptionally used here in this numerical study.

This paper describes a case study in a numerical surfacing

milling machining simulation. A first step of numerical simulation at high cutting speed with a specific surfacing tool is presented. Different inner canalization orientations, inlet pressures and contact area depending on feed rates which have significant effects on micro spray efficiency on the cutting edge have been considered. Moreover, different particle sizes found in previous studies, which have significant effects, are considered [DR1]. All these parameters are taken into consideration to find a combination of milling parameters to achieve high micro spray performance based on oil mist quantity and the mean distance of the micro spray to the cutting edge. The chip removal is not considered because of its complex physic. Only the contact area is considered to simulate the chip removal. Taguchi method is used, in a second step, in order to optimize the cutting design parameters. The main objective is to find combination of cutting design parameters to reach a large volume per unit area of oil and small mean distance of the mist impingement to the cutting edge.

2 Simulation techniques

All the simulations were in steady state conditions. The flow motion is ensured by the continuity and momentum equations with the standard *k-ε* turbulent transport equation, for the two-phase flow. The Lagrangian multiphase flow is used to simulate the particle tracks of the oil mist [DS1]. Finally, a Motion Reference Frame is used in the steady state condition to ensure the rotation of the milling tool and the diphasic mixture. An in-place interface is defined to separate the motion area (milling tool) and the outlet area. The motion modeling affects the continuum transport equations as a body force due to the system rotation in the momentum equations, depending on the rotational velocity. Boundary conditions are taken from experimental part: i.e. inlet pressures oil mist characteristics, particle sizes and oil flow rates. Initial conditions are a relative external atmospheric outlet pressure (P_o *= 0.1 MPa*) and the study cutting velocity (*Vc = 5026 m/min*). The wall boundary interaction mode for the Lagrangian Phase is set to Rebound. The surface roughness for the wall region is taken as smooth. The main goal of this section is to define parameters, such as: inlet pressures, canalization orientations, and cutting area from the feed rates, with the effect of the particle size. This section gives the parameter values and the tool-chip contact areas to collect data which are analyzed for the Taguchi optimization process.

2.1 Numerical milling prototype

Figure 1 showed the studied tool. It is consisted of seven carbide inserts with a diameter *D= 80 mm*.

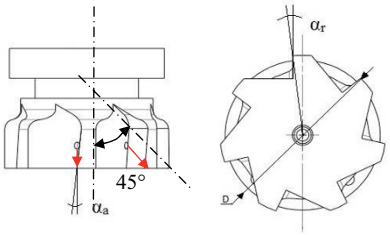

Figure 1: Illustration of the milling prototype and its geometric parameters.

The main goal of this prototype is to be used in a minimum quantity lubrication production line. A main canalization was drilled in the center of the tool as well as small canalizations (ramifications) in the sides to ensure the oil mist spray on each insert cutting edge (red arrows on figure 1 show the direction of the spray). The secondary canalizations (ramifications) were oriented at *45°* relative to the vertical axis (Figure 1). As the canalization orientation is a significant parameter, *45°*, *60°* and *75°* oriented canalizations are considered, for further calculations.

2.2 Surface areas

The tool chip contact area is determined by the cutting depth (*Ap*) and contact length (l_c) as the chip slide on the carbide tool. [IM1] summarized the different contact length models as function of work piece material and the cutting speed.
Thus, the studies of [BN1] allowed calculating the contact length with the following equation (Eq 1):

$$a = t_1\left[t_2\left(\frac{1-\tan\alpha_a}{t_1}\right)+\frac{1}{\cos\alpha_a}\right] \quad (1)$$

where t_1 is the undeformed chip thickness, $a = t_2$, t_2 is the chip thickness and α_a the rake angle. For tungsten carbide tools, Stephenson [S1] proposed the following relation (Eq 2)

$$l_c = 1.75\, t_2 \quad (2)$$

The chip formation is created by successive tooth passes, in milling process. The chip size is evaluated as function of the tooth position, but whatever the rotation compared to the work piece, a maximal chip is created. Thus, the remove material configuration is considered as continue (as in turning process). Equations *1* and *2* can be used to have the contact length. The rake angle α_a is usually used for turning configuration, but the radial rake angle α_r has to be considered here, in milling process (see on figure 1).

2.3 Cutting parameters

Feed rate f_z (*mm/rev*) and thus cutting areas S_i (*mm²*) are variables for a specific cutting speed of *Vc = 5026 m/min*. For this kind of surfacing tool, and the finishing configuration the cutting depth (A_p) is set to *0.5mm*. Inlet pressures and particle sizes were taken from previous experimental study, which

consisted on characterizing the oil mist [DL1].

The following table 1 summarises data of the different variables used in this study:

Vc (m/min)	*Fz (mm/rev)*	*P_{inlet} (MPa)*	*Contact area (mm^2)*	*Canalization orientations (deg°)*	*Particle diameters (µm)*
5026	*0.05*	*0.03*	*S_1=0.739*	*45°*	*1*
	0.01	*0.077*	*S_2=1.479*	*60°*	*10*
	0.015	*0.1*	*S_3=2.217*	*75°*	*100*

Table 1 : Variable data used for the analysis of the optimization.

However in this study a full factorial design is used to study the influence of minimum quantity lubrication coolant design parameters (Canalization orientations, Particle diameters and Inlet pressure) on milling finishing process like an average length and an oil quantity volume per unite area.

2.4 Numerical results

Numerical simulations were carried out for each feed rate, inlet pressures and canalization orientations, which represent, respectively, *3x3x3x3 = 81* simulation runs, for the highest cutting speed

Figure 2 shows an example of the particle impingements on the insert for *Vc = 5026 m/min*, *0.03 MPa* inlet pressure and *45°* oriented canalization. The "x" axis represents the total insert width. The insert height is represented by the *"y"* axis. Linear regression is done from the scatter plot to have the trend of the main flux for each particle size impingements (straight lines on figure 2).

Figure 2 shows also details about the contact areas *S1*, *S2* and *S3* considered for this study. They depend of the cutting depth *Ap* and the calculated contact length *lc* from each feed rate (section 2.2). The two evaluated parameters taken into consideration are: (i) an average length and (ii) an oil amount volume per unite area.

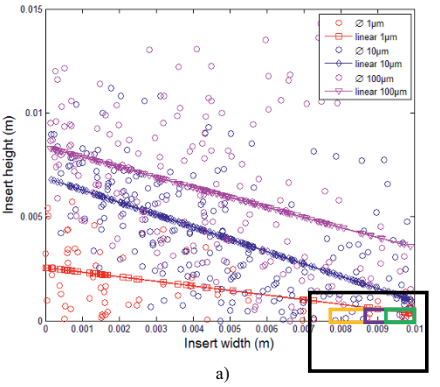

a)

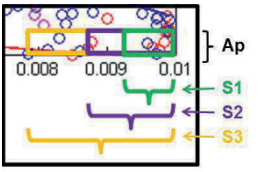

b)

Figure 2 : Example of the results showing the particle impingement a) on the insert and b) on the different tool-chip contact areas (S_1, S_2, S_3), for *Vc = 5026 m/min* and P_{inlet} *= 0.1 MPa* inlet pressure, for 45° canalization orientation.

For the first one, it is important to know where the particle impingement is and then an average particle is calculated in each area. The distance from this average particle and the cutting edge (insert width=*0.01m* and insert height = *0m*) is measured. More the distance closes to zero, better the results.

For the second one, oil amount is recommended for good lubrication efficiency. Then, the number of particle is counted in each contact area. More the volume of oil per unite surface is important, better the results.

3 Linear regression and ANOVA analysis

In many experimental conditions, it is possible to represent independent factors in quantitative form as given by Eq. (3). Then these factors can be represented of as having a functional relationship or response as follows:

$$Y = \Phi(x_1, x_2, \ldots, x) \pm e_r \qquad (3)$$

Between the response Y and $x_1, x_2, \ldots, x_k$ of k quantitative factors, the function "Φ" is called response function. The residual *"e_r"* measures the experimental errors. For a given set of independent variables, a characteristic function is responded. When the mathematical form of "Φ" is unknown, it can be approximated satisfactorily within the experimental region by a polynomial function. In the present investigation, a linear regression has been applied for developing the mathematical model in the form of multiple regression equations for chosen parameters. In applying the regression the independent variable was viewed as a function to which a mathematical model is fitted. The Multiple Linear Regression method is the most informative method of analysis of the result of a factorial experiment. The second order polynomial (regression) equation with interaction used to represent the response surface Y is given by [CC1]:

$$Y = b_0 + \sum b_i x_i + \sum b_{ij} x_i x_j + e_r \qquad (4)$$

where b_0, b_1, b_2, etc., are the linear term coefficient and b_{ij} the interaction term coefficient to be estimated by the method of least squares. The resolution of this full factorial design allows us to estimate all the main effects and interactions. Note that run orders are used randomly during the experiments.

In order to ensure the goodness of fit of the models obtained in this study, the adequacy of the model was tested using the analysis of variance (ANOVA) technique. The test for significance on individual model coefficients was performed, the calculated F-ratio of the model does not exceed the standard value and the calculated R-ratio of the model is above the standard value for a desired *95%* level of confidence.

Parameters	*Unit*	*Levels*		
Canalization orientations (Co)	*degree*	*45*	*60*	*75*
Inlet pressure (Ip)	*MPa*	*0,03*	*0,077*	*0.1*
Particle diameters (dp)	*µm*	*1*	*10*	*100*
Feed rate (fz)	*mm/rev*	*0.05*	*0.01*	*0.015*

Table 2 : Parameters and levels used in the study.

4 Results and analysis

The objective of the ANOVA technique is to find parameters which have significant effects on design geometry for optimizing micro spray effects. In this perspective, the average length and the oil amount volume per unit area are analyzed. Table 3 shows the actual data for the average length and the volume per unite area for the all *81* simulations.

Numerical run	*Input parameters*				*Output parameters*	
	fz	*Co*	*Ip*	*dp*	$L_{average}$	$\mu m^3/mm^2$
1	*0.05*	*45*	*0.03*	*1*	*7.39E-01*	*0.00E+00*
2	*0.05*	*45*	*0.03*	*10*	*3.14E-01*	*2.83E-06*
3	*0.05*	*45*	*0.03*	*100*	*4.52E-01*	*5.67E-03*
4	*0.05*	*45*	*0.077*	*1*	*7.39E-01*	*0.00E+00*
5	*0.05*	*45*	*0.077*	*10*	*7.39E-01*	*0.00E+00*
6	*0.05*	*45*	*0.077*	*100*	*3.88E-01*	*1.42E-03*
7	*0.05*	*45*	*0.1*	*1*	*3.33E-01*	*4.25E-09*
8	*0.05*	*45*	*0.1*	*10*	*3.87E-01*	*2.83E-06*
9	*0.05*	*45*	*0.1*	*100*	*7.39E-01*	*0.00E+00*
10	*0.05*	*60*	*0.03*	*1*	*3.67E-01*	*4.25E-09*
11	*0.05*	*60*	*0.03*	*10*	*5.01E-01*	*1.13E-05*
12	*0.05*	*60*	*0.03*	*100*	*1.44E-02*	*1.42E-03*
13	*0.05*	*60*	*0.077*	*1*	*3.80E-01*	*4.25E-09*
14	*0.05*	*60*	*0.077*	*10*	*3.15E-01*	*4.25E-06*
15	*0.05*	*60*	*0.077*	*100*	*3.55E-01*	*5.67E-03*
16	*0.05*	*60*	*0.1*	*1*	*2.64E-01*	*8.50E-09*
17	*0.05*	*60*	*0.1*	*10*	*4.75E-01*	*8.50E-06*
18	*0.05*	*60*	*0.1*	*100*	*3.23E-01*	*1.42E-03*
19	*0.05*	*75*	*0.03*	*1*	*7.39E-01*	*0.00E+00*
20	*0.05*	*75*	*0.03*	*10*	*4.43E-01*	*1.13E-05*
21	*0.05*	*75*	*0.03*	*100*	*5.09E-01*	*5.67E-03*
22	*0.05*	*75*	*0.077*	*1*	*3.04E-01*	*1.13E-08*
23	*0.05*	*75*	*0.077*	*10*	*3.69E-01*	*4.25E-06*
24	*0.05*	*75*	*0.077*	*100*	*1.50E-01*	*1.42E-03*
25	*0.05*	*75*	*0.1*	*1*	*3.95E-01*	*1.13E-08*
26	*0.05*	*75*	*0.1*	*10*	*5.47E-01*	*2.83E-06*
27	*0.05*	*75*	*0.1*	*100*	*7.39E-01*	*0.00E+00*
28	*0.1*	*45*	*0.03*	*1*	*1.48E+00*	*0.00E+00*
29	*0.1*	*45*	*0.03*	*10*	*6.97E-01*	*2.83E-06*
30	*0.1*	*45*	*0.03*	*100*	*5.67E-01*	*2.13E-03*
31	*0.1*	*45*	*0.077*	*1*	*1.48E+00*	*0.00E+00*
32	*0.1*	*45*	*0.077*	*10*	*1.43E+00*	*7.09E-07*
33	*0.1*	*45*	*0.077*	*100*	*3.88E-01*	*7.09E-04*
34	*0.1*	*45*	*0.1*	*1*	*7.07E-01*	*3.54E-09*
35	*0.1*	*45*	*0.1*	*10*	*7.20E-01*	*2.13E-06*
36	*0.1*	*45*	*0.1*	*100*	*1.48E+00*	*0.00E+00*
37	*0.1*	*60*	*0.03*	*1*	*3.67E-01*	*2.13E-09*
38	*0.1*	*60*	*0.03*	*10*	*7.50E-01*	*9.21E-06*
39	*0.1*	*60*	*0.03*	*100*	*7.04E-01*	*1.42E-03*
40	*0.1*	*60*	*0.077*	*1*	*3.80E-01*	*2.13E-09*
41	*0.1*	*60*	*0.077*	*10*	*8.19E-01*	*4.96E-06*
42	*0.1*	*60*	*0.077*	*100*	*3.55E-01*	*1.42E-03*
43	*0.1*	*60*	*0.1*	*1*	*6.00E-01*	*7.09E-09*
44	*0.1*	*60*	*0.1*	*10*	*7.61E-01*	*7.09E-06*
45	*0.1*	*60*	*0.1*	*100*	*7.42E-01*	*1.42E-03*
46	*0.1*	*75*	*0.03*	*1*	*1.48E+00*	*0.00E+00*
47	*0.1*	*75*	*0.03*	*10*	*7.07E-01*	*9.92E-06*
48	*0.1*	*75*	*0.03*	*100*	*5.09E-01*	*1.42E-03*
49	*0.1*	*75*	*0.077*	*1*	*4.93E-01*	*7.79E-09*
50	*0.1*	*75*	*0.077*	*10*	*3.69E-01*	*2.13E-06*
51	*0.1*	*75*	*0.077*	*100*	*6.23E-01*	*1.42E-03*
52	*0.1*	*75*	*0.1*	*1*	*3.95E-01*	*5.67E-09*
53	*0.1*	*75*	*0.1*	*10*	*5.09E-01*	*2.13E-06*
54	*0.1*	*75*	*0.1*	*100*	*1.48E+00*	*0.00E+00*
55	*0.15*	*45*	*0.03*	*1*	*2.21E+00*	*0.00E+00*
56	*0.15*	*45*	*0.03*	*10*	*1.49E+00*	*4.72E-06*
57	*0.15*	*45*	*0.03*	*100*	*5.67E-01*	*1.42E-03*
58	*0.15*	*45*	*0.077*	*1*	*2.21E+00*	*0.00E+00*
59	*0.15*	*45*	*0.077*	*10*	*1.78E+00*	*1.42E-06*
60	*0.15*	*45*	*0.077*	*100*	*3.88E-01*	*4.72E-04*
61	*0.15*	*45*	*0.1*	*1*	*7.07E-01*	*2.36E-09*
62	*0.15*	*45*	*0.1*	*10*	*1.32E+00*	*2.83E-06*
63	*0.15*	*45*	*0.1*	*100*	*2.21E+00*	*0.00E+00*
64	*0.15*	*60*	*0.03*	*1*	*7.36E-01*	*1.89E-09*
65	*0.15*	*60*	*0.03*	*10*	*1.18E+00*	*9.45E-06*
66	*0.15*	*60*	*0.03*	*100*	*9.77E-01*	*1.42E-03*
67	*0.15*	*60*	*0.077*	*1*	*3.80E-01*	*1.42E-09*
68	*0.15*	*60*	*0.077*	*10*	*8.19E-01*	*3.31E-06*
69	*0.15*	*60*	*0.077*	*100*	*1.23E+00*	*2.36E-03*
70	*0.15*	*60*	*0.1*	*1*	*8.54E-01*	*5.67E-09*
71	*0.15*	*60*	*0.1*	*10*	*7.61E-01*	*4.72E-06*
72	*0.15*	*60*	*0.1*	*100*	*1.35E+00*	*2.36E-03*
73	*0.15*	*75*	*0.03*	*1*	*2.21E+00*	*0.00E+00*
74	*0.15*	*75*	*0.03*	*10*	*9.42E-01*	*8.50E-06*
75	*0.15*	*75*	*0.03*	*100*	*1.05E+00*	*1.42E-03*
76	*0.15*	*75*	*0.077*	*1*	*7.67E-01*	*6.61E-09*
77	*0.15*	*75*	*0.077*	*10*	*3.69E-01*	*1.42E-06*
78	*0.15*	*75*	*0.077*	*100*	*6.23E-01*	*9.45E-04*
79	*0.15*	*75*	*0.1*	*1*	*5.21E-01*	*4.25E-09*
80	*0.15*	*75*	*0.1*	*10*	*1.29E+00*	*3.31E-06*
81	*0.15*	*75*	*0.1*	*100*	*2.01E+08*	*4.72E-04*

Table 3 : Numerical results for average length and oil amount volume per area

4.1 Influence on average length ($L_{average}$)

The second-order empirical model of selected minimum quantity lubrication design parameters on average length was calculated. The second order model can be expressed as a function of design parameters (*Co, Ip, dp* and *fz*) with their regression coefficients presented in table 4.

The direct and the interaction effects were analyzed and by selecting the backward elimination procedure to automatically reduce the terms that are not significant, the resulting ANOVA analysis for the reduced second-order model for

response ($L_{average}$) is given in Fig. 3 as histogram representation.

Variables	Coefficients
Constante	-8061044.611
F	74316043.31
Co#	247720.01134
Ip#	14309299.02
dp#	52546.6896
f*Co	7431603.538
f*Ip	271460775.2
f*dp	2343298.449
Co*Ip	904869.2457
Co*dp	7810.995
Ip*dp	285319.1479
f*Co*Ip	27146077.57
f*Co*dp	234329.8468
f*Ip*dp	8559574.203
Co*Ip*dp	28531.9135
f*Co*Ip*dp	855957.4019
f^2	1486320736
Co^2	16514.6759
Ip^2	46159030.017
dp^2	834.0746

Table 4 : Variable interactions with their regression coefficients, for the length average.

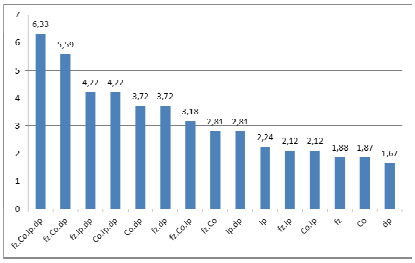

Figure 3 : Histogram of the contribution of the effects for the average length.

The analysis of the contribution of the effects of the minimum quantity lubrication design parameters shows that the average length is more important with all parameters together.
The contribution of the effects on average length must be taken carefully. Since the average length must be as small as possible, the study of Figure 3 shows the contributions of some parameter effects which have minor impact on the average length. Thus, particle sizes (*dp*), canalization orientations (*Co*) and the feed rate (*fz*) from the contact area have an inverse significant effects on the average length. Indeed, large particles are heavier and are sprayed far away from the secondary canalizations. The large canalization orientations (*Co*) make easier the oil mist spray away from the canalizations. Another important point is the feed rate or the contact area. The analysis seems to show that particles impinge mostly in large feed rate (*fz*) (large contact area).

4.2 Influence on oil amount volume per unite area (*Vs*)

The second-order empirical model of selected minimum quantity lubrication design parameters on oil amount volume per unite area was calculated. The second order model can be expressed as a function of design parameters (*Co, Ip, dp* and *fz*) with their regression coefficients presented in table 5.

Variables	Coefficients
Constante	0.0003
F	-0.0044
Co	0
Ip	-0.001
dp	0
f*Co	0
f*Ip	0.0147
f*dp	-0.0001
Co*Ip	0
Co*dp	0
Ip*dp	0
f*Co*Ip	0.0001
f*Co*dp	0
f*Ip*dp	0.0005
Co*Ip*dp	0
f*Co*Ip*dp	0
f^2	0.01015
Co^2	0
Ip^2	-0.0016
dp^2	0

Table 5 : Variable interactions with their regression coefficients, for the oil amount volume per unite area.

The direct and the interaction effects were analyzed and by selecting the backward elimination procedure to automatically reduce the terms that are not significant, the resulting ANOVA analysis for the reduced second-order model for response (V_s) is represented on figure 4.

The analysis of the contribution of the effects of the minimum quantity lubrication design parameters shows that the oil amount volume per unite area is more important with large particles (*dp*).
Contrary to the average length, the contribution of the effects has to been taken in the right sense Indeed, the maximum radius is $50\mu m$ and the calculated volume is raised with exponential three (cubic meter). The analysis of the effects suggests that the inlet pressure (*Ip*) and more particularly the couple particle diameter/inlet pressure have significant effects on the oil amount volume.

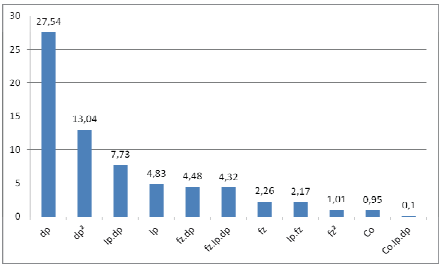

Figure 4 : Histogram of the contribution of the effects for the oil amount volume per unite area.

Inlet pressure increases the particle spray on the carbide

insert. Most of the particles impinge more precisely on the direction of the main flux on the insert. Whereas the feed rate or the contact area or the feed rate/particle diameter has no significant contribution of the effect on the oil amount volume per unite area.

In the above case studies, two contributions of the effects of the minimum quantity lubrication design parameters have been analyzed for the average length and the oil amount volume per unite area.
The effects of the average length are taken as inverse function to have the minimum contributions of the parameters for the average length. The effect consists in having the smaller average length. This seems to be consistent since the largest particles (*dp*) are sprayed closer to the cutting edge as greater than *Ø10µm* particles have an inertial effect [DS1]. In the same way the particles are sprayed far away from the output canalizations as the secondary canalizations orientation (*Co*) is more horizontal (about *75°*). This contribution is coupled with the increased inlet pressure (*Ip*) which decreased the average length by spraying the particles closer to the cutting edge. The feed rate (*fz*) contribution consists in having larger contact area. Small particles are more likely to be in the highest contact area. Indeed, this contribution is coupled with the inlet pressure (*Ip*) which helped particles to reach the cutting edge.
Whereas, the contribution of the effects for the oil amount volume per unite area is taken as the right interpretation. Particle diameter seems to be the most important parameter for the both effects. The increased inlet pressure (*Ip*) coupled with the particle size (*dp*) increased the oil amount. This contribution goes in the same way than the effects of the average length.

Parameters	*Calculated values*
fz	*0.01645*
Co	*59.7499*
Ip	*0.10006*
dp	*43.9099*

Table 6 : Predicted values for the study parameters from the ANOVA analysis.

The analysis based on empirical functions allowed also getting optimal parameters. Thus, optimal predicted values are obtained, as showed in table 4. Expectation values are given from the analysis. The inlet pressure (*Ip*) and the feed rate (*fz*) have to be larger, respectively *0.016 mm/rev* and *0.1 MPa*.
Whereas, the analysis of the oriented canalization (Co) and the particle diameter (*dp*) parameters gave averaged values as *60°* and *Ø44µm* respectively.

5 Conclusion and future works

This paper has presented a numerical influence analysis of the minimum quantity lubrication design parameters in milling finishing process, with a Tagushi method.
A numerical rotating of a milling prototype has been considered in finishing configuration with minimum quantity lubrication process by inner canalizations. The numerical simulation produced a scatter plot from the impingement of the different particle size on the carbide inserts. The average length (*mm*) and the oil amount per unit area ($\mu m^3/mm^2$) effects have been realized.
The study of the minimum quantity lubrication process optimization has been done as functions of different parameters:

- ✓ the canalization orientations (*Co*)
- ✓ the particle diameters (*dp*)
- ✓ the inlet pressure (*Ip*)
- ✓ the feed rate (*fz*) or the tool/chip contact area.

The main conditions for the analysis are the following:

- ✓ the particle impingement has to be close to the cutting edge (small average length)
- ✓ the oil amount has to be necessary in the tool/chip contact area (important oil amount volume per unite area).

The Tagushi analysis allowed determining the most influence parameters, the maximized parameters and the following conclusions are:

- ✓ the feed rate has to be high enough, which is hope in high speed machining.
- ✓ the canalization orientation has to be high enough. This high orientation is wanted to improve the spray direction.
- ✓ the inlet pressure has to be high enough to make easy the oil mist spray on the cutting edge, because of cutting speed and the aerodynamic effect of the rotating tool.
- ✓ an average particle size gave by the analysis

Parameters as cutting speeds and cutting depth have to be considered, on future works. These machining configurations have significant effects on the oil mist spray on the cutting edge.

6 References

[A1] T. Aoyama, Development of a mixture supply system for machining with minimal quantity lubrication, CIRP Annals - Manufacturing Technology, 51: 289-292, 2002.

[BB1] W. Bouzid Saï, N. Ben Salah, J.L. Lebrun, Influence of machining by finishing milling on surface characteristics, Internal journal of machine tools and manufacture, 41: 443-450, 2001.

[BN1] S. Bahi, M. Nouari, A. Moufki, M. El Monsori, A. Molinari, A new friction law for sticking and sliding contacts in machining, Tribology International, 44: 764-771, 2011.

[CC1] W. G. Cochran, G. M Cox “Experimental design”,

Asia Publishing House, 1962.

[DI1] N. R. Dhar, M. W. Islam, M. A. H. Mithu, The influence of minimum quantity of lubrication (MQL) on cutting temperature, chip and dimensional accuracy in turning AISI 1040 steel, Journal of Material Processing Technology, 171: 93-99, 2006.

[DL1] A. Duchosal, R. Leroy, L. Vecellio C. Louste, N. Ranganathan, An experimental investigation on oil mist

characterization used in MQL milling process, International Journal of Advanced Manufacturing Technology, 66: 1003–1014, 2013.

[DS1] A. Duchosal, R. Serra, R. Leroy, Static numerical simulation of oil mist particle size effects on a range of internal channel geometries of a cutting tool used in MQL strategy, International Journal of Engineering Science and Innovative Technology, 1 (2): 43-59, 2012.

[GC1] J. A. Ghani, I. A. Choudhury, H H. Hassan, Application of Taguchi method in the optimization of end milling parameters, Journal of Matéerials Processing Technology, 145: 84-92, 2004.

[IM1] S. A. Iqbal, P. T. Mativenga, M. A. Sheikh, A comparative study of the tool-chip contact length in turning of two engineering alloys for a wide range of cutting speeds, International Journal of Advance Manufacturing Technology, 42: 30-40, 2009.

[KM1] P. Kalita, A. P. Malshe, S. A. Kumar, V. G. Yognath, T. Gurumurthy, Study os specific energy and friction coefficient in minimum quantity lubirication ginding using oil-based nanolubricants, Journal of Manufacturing Processes, 14: 160-166, 2012.

[KO1] Y. Kamata, T. Obikawa High speed MQL finish turning of Inconel 718 with different coated tools. Journal of Material Processing Technology, 192: 281–286, 2007.

[LA1] L. N. Lopez de Lacalle, C. Angulo, A. Lamikiz, J. A. Sanchez, Experimental and numerical investigation on the effect of spray cutting fluids in high speed milling, Journal of Material Processing Technology, 172: 11-15, 2006.

[S1] D. A. Stephenson, Assessement of steady-state metal cutting temperature models based on simultaneous infrared and thermocouple data, Journal of Engineering for Industry: 113: 121-128, 1991.

Article 043-pp-3

A Statistical model for prediction of tool wear and cutting force during high speed trimming of Carbon fibre reinforced polymers

Mohamed Slamani [1], Jean-François Chatelain [2], Hossein Hamedanianpour [3]

(1,2,3) : École de technologie supérieure (ÉTS),
Mechanical Engineering Department.
1100 Notre-Dame Street West, Montréal (Qc), H3C 1K3, Canada
Phone/Fax: (514) 396-8512/ (514) 396-8530
(1) : *E-mail* : *mohamed.slamani.2@ens.etsmtl.ca*
(2) : *E-mail* : jean-francois.chatelain@etsmtl.ca
(3) : *E-mail* : hhamedanian@gmail.com

Abstract: The combination of low thermal conductivity and highly abrasive nature of Carbon Fibre Reinforced Polymers (CFRPs) leads to rapid tool wear and numerous machining problems. This paper presents the development of tool wear and cutting force prediction models in the high speed trimming of CFRPs. A 3/8 inch diameter CVD diamond-coated carbide tool with six straight flutes was used to trim 24-ply carbon fibre laminates. Cutting speeds ranging from 200 m/min to 400 m/min and feed rates ranging from 1524 mm/min to 4064 mm/min were used in the experiments. Exponential models were adjusted to predict tool wear and cutting force for different values of cutting speed, feed and cutting length. The ANOVA approach was used to test the overall significance of the models by applying F-tests. The results obtained show that the exponential model is capable of accurately predicting the cutting force and tool wear under the conditions studied.

Key words: Composite, CFRP, Trimming, Tool Wear, Cutting Force.

1- Introduction

The advent of Carbon Fibre Reinforced Polymers (CFRPs) has led to significant breakthroughs in the manufacturing industry, thanks to their desirable mechanical and physical properties, including high strength, high stiffness, low weight, durability, and extreme corrosion resistance. CFRP parts are usually produced by moulding or near net shape; moreover, in some applications, trimming, milling, drilling, turning and grinding are still required in order to bring CFRP parts to their final shapes and sizes. However, CFRPs are naturally inhomogeneous, and are anisotropic in every layer. As a result of their anisotropic and highly abrasive nature, numerous machining problems, such as rapid tool wear, matrix cracking or thermal damage, fibre pull-out, fibre fracture, and delamination are encountered **[D1]**. Koplev **[K1, KL1]** was one of the first researchers who studied CFRP orthogonal cutting. He found that chip formation was strongly affected by fibre orientation, and occurred during a series of successive ruptures. He also concluded that surface quality and the delamination factor were strongly influenced by cutting forces and tool geometry. The development of process control schemes for avoiding delamination by controlling and regulating the cutting process parameters require an accurate prediction of the cutting forces **[KS1]**. Cutting forces represent an important factor of machinability evaluation, and their size will directly influence the quality of machined parts. They are related to many factors, such as cutting parameters, workpiece materials and tools. Haiyan et al. **[HX1]** used an analytical cutting force model based on mechanistic modeling techniques to simulate cutting forces in the helical milling of CFRP. In addition, the cutting force coefficients were corrected according to the experimental data, and the established model was tested through cutting experiments. They found that the resultant radial and axial cutting forces decrease with an increase in the cutting speed and increase with an increase in the feed rate per tooth and axial feed rate. Kalla et al. **[KS1]** developed a methodology that combines the mechanistic modeling techniques from metal machining and neural network approximation in order to obtain a predictive cutting force model for helical end milling of carbon fibre reinforced polymers (CFRP). They concluded that the mechanistic modeling approaches from metal cutting are valid for machining FRPs. Furthermore, model predictions were compared with experimental data and were found to be in good agreement in cutting unidirectional laminate, but in lesser agreement in the case of a multidirectional laminate. More recently, Karpat and Polat **[KP1]** proposed a mechanistic model for the milling of multidirectional CFRP laminates using double helix milling tools. In the model, cutting and edge coefficients are calculated based on the laminate fibre direction. Issues related to surface quality and tool wear were also investigated. Zaghbani et al. **[ZC1]** presented a comprehensive analysis of the instantaneous cutting forces at

play during the trimming process of unidirectional laminates. They developed an empirical model for cutting forces, using a high mechanistic order model. They found that for machined laminates, the fibre orientation does not significantly influence the profile of the tangential and radial forces; however, it influences their amplitude. An experimental investigation was conducted by Surinder et al **[SM1]** to determine the effects of cutting conditions and tool geometry on the cutting forces in the turning of the unidirectional glass fiber reinforced plastics (UD-GFRP) composites. They found that the depth of cut is the cutting parameter, which has greater influence on cutting forces. The effect of the tool nose radius and tool rake angles on the cutting forces are also considerably significant. Furthermore, a multiple regression model for cutting forces is derived with satisfactory coefficient R^2.

In addition to delamination, machining precision and surface quality are directly related to tool wear **[SY1, IG1, DR1]**. The high mechanical resistance of carbon fibres is most responsible for excessive tool wear. Furthermore, the cutting tools are loaded with heavy forces and friction resulting from the interactions between the tool and workpiece, which cause the increased milling temperature. Because the thermal conductivity of the CFRP is very low, most of the heat produced during the milling process can only transfer to the cutting tool. Consequently, the temperature at the tool-chip interface rises, causing tool wear, and then lower tool life, as well as quality issues such as delamination, matrix degradation and lower dimensional or geometrical accuracies. Haiyan et al. **[HX1]** analyzed the effects of the cutting parameters and tool wear on the cutting forces during helical milling of carbon fibre reinforced plastic, and found a direct proportional relationship between tool wear and cutting forces. They report that in all, the wear is smooth, and is uniformly distributed along the entire cutting edge. Unfortunately, no model was developed to predict the tool wear. Wang et al. **[WW1]** studied the effect of low temperature on the performance of drilling Carbon Fibre Reinforced Polymer and Ti Stack Materials. They showed that low temperature air can reduce tool wear and thrust force effectively. A similar approach was used by Khairusshima et al. **[KH1]** to study the effect of tool wear and surface roughness on the milling of carbon fibre-reinforced plastic using chilled air. They showed experimentally that there is demonstrably less tool wear at lower feed rates and higher cutting speeds. They observed that the wear is shiny and polished at the cutting edge because of excessive wear during machining; they also showed that the life of the carbide tool shortens as the feed rate and the cutting speed increase. They state that the suitable temperature for machining CFRP in their study is approximately 91.5 °C.

Based on the literature reviews above, machining precision, surface quality, cost price, and productivity are directly related to the cutting force and tool wear. Therefore, it is very important that priority be given to the modelling and prediction of cutting forces and tool wear during high speed machining of Carbon fibre reinforced polymers. This paper presents the development of statistical predictive models for cutting forces and tool wear during high speed trimming of Carbon fibre reinforced polymers, using machining variables such as cutting speed, feed rate and length of cut. Furthermore, ANOVA is used to test the significance of the fit by applying F-tests on the ratio of variances.

2- Methodology

The workpiece material used in our experiments was an autoclave-cured 24-ply CFRP laminate produced using pre-impregnated technology, with a fibre volume fraction of 64% and a stacking sequence [(90˚,-45˚,45˚,0˚,45˚,-45˚,45˚,-45˚,0˚,-45˚,45˚,90˚)]s. This resulted in a laminate thickness of 4.44 mm. The end mill router was a CVD diamond coated carbide tool with six straight flutes. The specifications of the cutting tool are shown in Table 1.

No. of teeth	Rake	Relief	Helix	LOC	Tool type	Diameter
6	8°	10°	10°	1"	Coated Carbide	3/8 "

Table 1: Cutting tool specifications.

The experiments were carried out with the cutting parameters, as specified in Table 2.

Test No.	Feed(mm/min)	Speed(m/min)
1	1524	400
2	2794	300
3	4064	200

Table 2: Cutting parameters.

The parameters were selected according to Berube **[B1]**, who proposed the best operational conditions for similar tool and composite materials. Three feed rates and three cutting speeds including minimum, intermediate and maximum values of feed rate and cutting speed were chosen from those ranges. Then nine preliminary tests were carried out according to Table 3.

Test No.	Cutting Speed (m/min)	Feed Rate (mm/min)
1	200	1524
2	200	2794
3	200	4064
4	300	1524
5	300	2794
6	300	4064
7	400	1524
8	400	2794
9	400	4064

Table 3. Cutting conditions of preliminary tests

In each preliminary test, cutting forces in x, y and z directions were recorded. All recorded signals were verified for the absence of distortion using Fast Fourier Transform (FFT) program. In all preliminary tests, the harmonics of the spindle speeds and the tooth passing frequency were not superposed and the recorded signals were harmonic in all directions; meaning that the cutting force FFT analysis didn't

show the presence of amplification at measuring system resonance. Based on the results of these preliminary tests, three tests were selected in order to carry out the tool life tests. The first test had the highest cutting speed and the lowest feed rate, the second test had the intermediate cutting speed and feed rate and finally the third test had the lowest cutting speed and highest feed rate for our feed rate and cutting speed ranges. Table 2 shows the parameters of tool life experiments.

To properly relate the quality of the trimmed laminates as a function of the length of cut expressed in linear meters, two set-ups were used, one to generate tool wear of several meters and transform the laminate into "chips and dust", and the other, to trim test coupons dedicated to full inspection and related to the length of wear cut achieved at each step of an iterative process. Thus, in each tool life experiment, the cutting tool machined 100 mm using short cut set-up and then 900 mm using long cut set-up. On the other hand, at first, each tool life experiment started by machining of short panel and then long panel was trimmed alternately. This process was repeated until the tool wear reached the flank wear criterion. This tool life limit indicates that a cutting tool, reaches the end of its useful life. In this work, the tool life criterion was considered an average maximum flank wear of 0.3 mm according to ISO 8688-2 standard **[I1].** Before each short cut, the cutting tool was removed in order to measure its wear with an optical type Keyence VHC-600+500F microscope. At the beginning of each tool life test, the teeth of cutting tool were marked in order to identify them during tool wear measurement. Before each short cut, the tool holder including cutting tool was removed from CNC tool magazine, and then the tool holder including cutting tool was mounted and fixed on magnetic clamp. For each tooth, the maximum flank wear (VBmax) was measured using this optical microscope. VBmax is the maximum tool wear on the flank face of the cutting tool. The cutting tool had six teeth, so tool wear of all six teeth were measured. Finally, tool wear was calculated according to ISO 8688-2 standard. Finally, based on the results of tool wear measurement in each tool life experiment, average tool wear was obtained as a function of cutting length for Test 1-3.

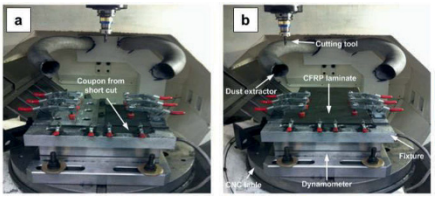

Figure 1: Experimental set-up: short cut (a), long cut (b).

The CNC machine used for the experiments was a 3-axis high speed center HURON K2X10, with a maximum spindle speed of 28000 RPM at 30 kW. The machine was equipped with a dust extraction system. A total of ten clamps were used to secure the panels for long cuts and seven clamps for short cuts. The fixtures were attached to a 3-axis dynamometer table (type Kistler 9255B), as shown in Fig. 1.

3- Results and discussion

To obtain cutting force and tool wear models, specimens were trimmed under different cutting conditions, and the cutting forces were measured in the x, y, and z directions with a 3-axis dynamometer table. The cutting force data were then recorded for further analysis and evaluation. After completing one meter trimming, the tool was removed from the chuck for observation of the cutter flutes under the optical microscope and to measure the amount of tool wear; the latter was measured on all six flutes and the average value was calculated. When tool wear evaluation was completed, other 100 mm long specimens were machined after the tool being worn, with long cuts 900 mm in length. Again, the cutting force and the average tool wear value were calculated for each specimen. This iterative process lasted until the tool-life criterion was met.

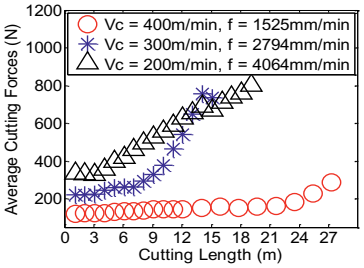

Figure 2: Average cutting force as a function of cutting length.

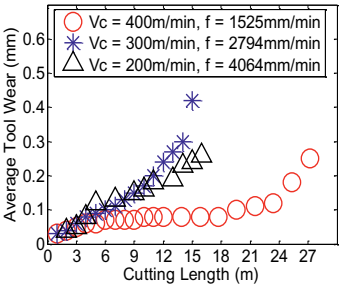

Figure 3: Average tool wear as a function of cutting length.

Results show that in all three cutting conditions, the cutting forces and tool wear both increased with an increase in the cutting length. Figure 2 indicates a strong correlation between cutting force and the ratio of cutting speed to federate *Vc/f*. The lower the ratio *Vc /f* the higher the cutting force. Furthermore, as shown in Figure 3, a longer tool life was observed at lower feed rates and higher cutting speeds, while a shorter tool life was obtained with intermediate feed rate and cutting speed values.

The results obtained using a scanning electron microscope (SEM) showed increasing defect rates with increased tool wear. The worst surface integrity, including matrix cracking,

fiber pull-out and empty holes, was also observed for plies oriented at -45 degrees. For more detail about the impact of tool wear on quality obtained for these tests see **[HC1]**.

3.1 –Tool wear model

By introducing interaction between independent variables, the exponential model can be represented by the following equation:

$$T_w = e^{b_0+b_1V_C+b_2f+b_3L+b_4V_C\times f+b_5V_C\times L+b_6f\times l}\varepsilon \quad (1)$$

The exponential model can be transformed to one of linear form by tacking logarithms of both sides of the equation as follows

$$y = \beta_0 + \beta_1x_1 + \beta_2x_2+\beta_3x_3 + \beta_4x_4 + \beta_5x_5 + \beta_6x_6 + \varepsilon^l \quad (2)$$

where, $y = \log(T_w)$, equation (2) in matrix form becomes

$$Y = X\beta+\varepsilon \quad (3)$$

In least-squares estimation, the sum of the squares of the residual vector elements is minimized. The minimization is equivalent to:

$$\hat{\beta} = (X'X)^{-1}X'Y = X^+Y \quad (4)$$

provided the inverse of $(X'X)^{-1}$ exists. The matrix $X^+ = (X'X)^{-1}X'$ is the Moore-Penrose pseudoinverse of X (sometimes just called the pseudoinverse).

Redundancies exist amongst the coefficients of the model (2), and as a result, the X matrix is ill-conditioned (very high condition number). It was therefore necessary to remove redundant coefficients from the analysis in order to lower the condition number and obtain more reliable estimates of the unknowns. Using an analysis of singular values, the columns of weakly contributing coefficients or redundant ones were removed.

Coefficients $\beta_0$and β_5 of Eq. (2) were found to be redundant and then removed from the model. The size and the rank of the X matrix became 5.

In order to improve the conditioning of matrix X, it was preferable to normalize the variables x_i by subtracting from these values their average $\overline{x_i}$ and dividing the result by its standard deviation s.

$$x_{nr,i} = \frac{(x_i - \bar{x})}{s} \quad (5)$$

After normalization, the condition number was reduced to 64. The obtained statistical model was

$$T_w = e^{-0.0079V_C-0.00089f+0.282L+0.000002V_C\times f-0.00057f\times l} \quad (6)$$

The ANOVA analysis in Table 4 shows that the model is adequate since $F = \frac{3.5044}{0.032} = 109.51$ is bigger than $F_{0.05,5,41} = 2.45$ at a significance level of 5%.

The total and error sum of squares presented in the ANOVA table can be expressed as **[MG1]**

$$TSS = \sum_{i=1}^{n}(y_i - \bar{y})^2 \quad (7)$$

$$SSE = \sum_{i=1}^{n}(y_i - \hat{y}_i)^2 \quad (8)$$

The regression sum of squares is

$$SSR = \sum_{i=1}^{n}(\hat{y}_i - \bar{y})^2 \quad (9)$$

Effect	Sum of squares	D.F	Mean squares	F-level
Regression (SSR)	17.5222	5	3.5044	109.51
Residual (SSE)	1.3425	41	0.032	
Total (TSS)	18.8647	46		

Table 4: ANOVA table for the exponential model for tool wear

The test used to measure the model adequacy consists in calculating the variance ratio or F-ratio between the mean square due to regression (MSR) and the mean square error (MSE). The usual procedure is then to compare the ratio $F = \frac{MSR}{MSE}$ with the $F_{\propto,p,n-p-1}$, where $F_{\propto,p,n-p-1}$ is the critical value of Fisher given by the Fisher table at threshold $\propto$=0.05.

$$MSR = \frac{SSR}{p} \quad (10)$$

$$MSE = \frac{SSE}{n-p-1} \quad (11)$$

One useful measure of the adequacy of the fitted model is the coefficient of determination R^2. A preferred choice for calculating R^2 is as follows:

$$R^2 = 1 - \frac{SSE}{TSS} \quad (12)$$

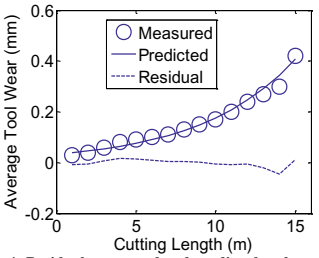

Figure 4: Residual, measured and predicted tool wear as a function of cutting speed, feed rate and cutting length at feed of 200 m/min

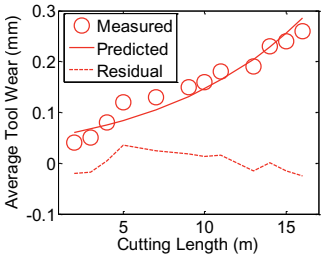

Figure 5: Residual, measured and predicted tool wear as a function of cutting speed, feed rate and cutting length at feed of 300 m/min

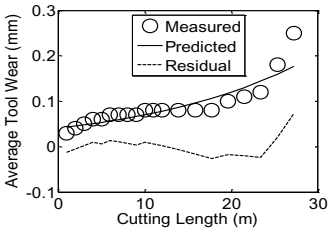

Figure 6: Residual, measured and predicted tool wear as a function of cutting speed, feed rate and cutting length for feed of 400 m/min

For least-squares estimates of the model parameters, the value of R^2 lies between 0 and 1; the closer it is to 1, the closer the predicted responses are to the observed responses. Results show that the exponential model has a high coefficient of determination $R^2 = 0.93$. That means that the exponential model is capable of accurately predicting of tool wear under the conditions studied (Figures 4 to 6).

3.2 – Cutting force model

After parameter estimation, the cutting force exponential model obtained was

$$\hat{F} = e^{0.0031V_c - 0.00008f + 0.160781L + 0.0000059V_c \times f - 0.000345f \times L} \quad (13)$$

Table 5 shows that the model is adequate since $F = 435.8421$ is bigger than $F_{0.05,5,48} = 2.41$ at a significance level of 5%.

Effect	Sum of squares	D.F	Mean squares	F-level
Regression	20.7024	5	4.1405	435.8421
Residual	0.4639	48	0.0095	
Total	21.1663	53		

Table 5: ANOVA table for the exponential model for cutting force

As shown in Figures 7, 8 and 10, a comparison between the measured and predicted cutting force show very good agreement. The coefficient of determination was $R^2 = 0.98$.

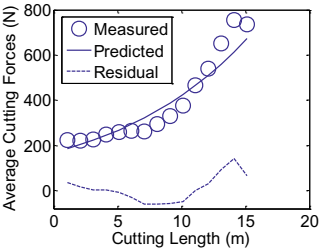

Figure 7: Residual, measured and predicted cutting force as a function of cutting speed, feed rate and cutting length at feed of 200 m/min

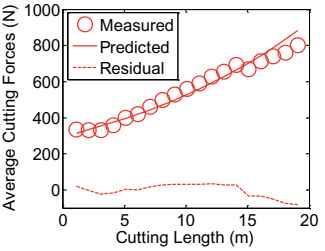

Figure 8: Residual, measured and predicted cutting force as a function of cutting speed, feed rate and cutting length at feed of 300 m/min

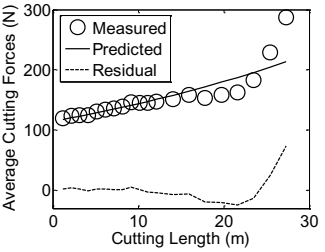

Figure 9: Residual, measured and predicted cutting force as a function of cutting speed, feed rate and cutting length at feed of 400 m/min

4- Conclusion

During the trimming of Carbon Fibre Reinforced Polymers, the quality of the machined part, cost price, and productivity are directly related to cutting tool conditions. Regarding the effect of cutting parameters on tool wear, it was found that a lower tool wear was measured at lower feed rates and higher cutting speeds, while a higher tool wear was measured at intermediate feed rates and cutting speed values. This paper also presented models developed to predict tool wear and cutting forces in high speed trimming. By taking cutting speed, feed and cutting length as independent variables in the model, results show that exponential models demonstrate a high capacity to accurately predict tool wear and cutting force under the conditions studied. Furthermore, the coefficients of determination reached 98% and 93% for the cutting force and tool wear models, respectively.

5- References

[B1] Berube S. Évaluation de la performance d'outils de coupe dédiés au détourage de structures composites carbone/époxy. Master dissertation, École de technologie supérieure, 2012.

[D1] Davim J.P. Machining Composite Materials, John Wiley & Sons Inc., London, England

[DR1] Davim J.P and Reis P. Drilling carbon fiber reinforced plastics manufactured by autoclave—experimental and statistical study, Materials & Design, 24, 315–324, 2003.

[HC1] Hamedanianpour H and Chatelain J-F. Effect of Tool Wear on Quality of Carbon Fiber Reinforced Polymer Laminate during Edge Trimming, Applied Mechanics and Materials Vols. 325-326 (2013) pp 34-39 (2013) Trans Tech Publications, Switzerland

[HX1] Haiyan W, Xuda Q, Hao L and Chengzu R. Analysis of cutting forces in helical milling of carbon fiber-reinforced plastics, Proceedings of the Institution of Mechanical Engineers, Part B: Journal of Engineering Manufacture, doi: 10.1177/ 0954405412464328, 2012.

[I1] ISO Standard 8688-2. International Standard For Tool Life Testing in End Milling, Part 2, First Edition, 05-01-1989

[IG1] Iliescu. D , Gehin. D , Gutierrez. M.E, Girot. F, Modeling and tool wear in drilling of CFRP, International Journal of Machine Tools & Manufacture, 50, 204–213, 2010

[KS1] Kalla D, Sheikh-Ahmad J, Twomey J. Prediction of Cutting Forces in Helical End Milling Fiber Reinforced Polymers. International Journal of Machine Tools and Manufacture. 50:882–891, 2010.

[KP1] Karpat Y, Polat N. Mechanistic force modeling for milling of carbon fiber reinforced polymers with double helix tools CIRP Annals - Manufacturing Technology, 62: 95–98, 2013.

[KH1] Khairusshima N, Hassan Ch, Jaharah A and Nurul A. Tool wear and surface roughness on milling carbon fiber-reinforced plastic using chilled air, Journal of Asian Scientific Research 2(11):593-598, 2011.

[K1] Koplev A. Cutting of CFRP with single edge tools. Proceedings of the third international conference on composite materials, Paris 2: 1597-1605, 1980.

[KL1] Koplev A, Lystrup A and Vorm T. The cutting process, chips and cutting forces in machining CFRP, Composites, 14 (4): 371-376, 1983.

[MG1] Mason R-L, Gunst R-F and Hess J-L. Statistical design and analysis of experiments, with applications to engineering and science, John Wiley & Sons, Inc, 2003.

[SM1] Surinder K.G, Meenu G, Satsangi P.S. Prediction of cutting forces in machining of unidirectional glass fiber reinforced plastics composite, Frontiers of Mechanical Engineering, 8(2): 187–200, 2013.

[SY1] Shengchao H, Yana CH, Jiuhua X, Jingwen. Z. Experimental Study of Tool Wear in Milling Multidirectional CFRP Laminates, Materials Science Forum, 770 : 276-280, 2014.

[WW1] Wang X, Wang Ch, Shi R, Song Y and Hu Y. Research on the effect of low temperature on the performance of drilling Carbon Fibre Reinforced Polymer and Ti Stack Materials, Materials Science Forum 723:30-34, 2012.

[ZC1] Zaghbani I, Chatelain J-F, Berube S, Songmene V, and Lance J. Analysis and modelling of cutting forces during the trimming of unidirectional CFRP composite laminates, International Journal of Machining and Machinability of Materials (IJMMM), 12(4): 337 – 357, 2012.

Article 059-cad-71

GUI USABILITY IMPROVEMENT FOR A NEW DIGITAL PATTERN TOOL TO ASSIST GEARBOX DESIGN

S. Patalano[1], D. M. Del Giudice[1], S. Gerbino[2], A. Lanzotti[1], F. Vitolo[1]

(1) : Department of Industrial Engineering, University of Naples Federico II
P.le Tecchio, 80, 80125, Naples (NA), Italy
Phone +39 0817682506 – Fax +39 0817682187
E-mail : { stanislao.patalano, domenicomaria.delgiudice, antonio.lanzotti}@unina.it; ferdy.vitolo@tiscali.it
(2) : DiBT Dept., University of Molise, Via Duca degli Abruzzi, Termoli (CB), Italy
Phone +39 0874 404593 - Fax +39 0874 404652
E-mail: salvatore.gerbino@unimol.it

Abstract: Design team can speed up the process of managing information related to gearbox design process by adopting digital pattern tools. These tools, as KBE systems, can assist engineers in re-using previous knowledge in order to improve time-consuming task as retrieval and selection of previous architectures and to modify and virtually test a new gearbox design. A critical point in the development of a KBE system is the interface usability to demonstrate effective reduction of development time and satisfaction in its use. In this paper, the authors face the problem of usability improvement of the Graphical User Interface (GUI) of the KBE system previously proposed. An approach based on Analytic Hierarchy Process (AHP) and Multiple-Criteria Decision Analysis (MCDA) has been used. A participatory test has been performed for evaluating the Usability Index (UI) of the GUI. Taking into account the data analysis some changes have been carried out and a new GUI release has been validated with new experimentations.

Key words: Usability assessment; *Graphical User Interface*; gearbox design; participatory design.

1- Introduction

Large and small companies adopt structured work teams to develop products [SB1]. These groups need a software toolset to help them to keep their design systems more and more effective. In such context, a "Digital Pattern" (DP) platform is recommended. A DP platform is a set of geometric and numeric data structures as well as models preconfigured and parametric which can be adapted to specific contexts. Therefore, a DP acts as a KBE system aimed to improve quality and reduce times and costs for product development through a massive use of knowledge and tools integration inside company. Such aims are accomplished through the fast and the best re-use of company knowledge, i.e. through technical and technological predefined solutions that quickly marry new projects, allowing fast performance evaluations and immediate checks. Such solutions should also be able to give feedback on designing and production costs. In [LP1] and [PV1] a Digital Pattern system, developed to assist gearbox design, was described.

In KBE system development the evaluation of interface usability, to demonstrate the effective reduction of development time and satisfaction in use, is a critical point. Indeed, usability can be defined as *the extent to which specific users, in a specific context of utilisation, can use a product to their satisfaction, in order to effectively and efficiently achieve specific goals* [MA1]. Sohaib and Khan [SK1] claim that agile projects needs to adopt aspects of *usability engineering* by incorporating user scenarios and including usability specialists in the team. During the designing of mechanical parts, designers need to verify the correctness of the hypotheses in use, especially in relation with multi-objective tasks [PV1]. Furthermore, the use of a KBE system is strategic for designers if we consider that they spend up to 30% of their time searching data [S2] and this percentage rises to 50 when we take into account the time spent validating the data [B1].

Following the approach in [DM1] this paper proposes the usability assessment of the gearbox software tool through a participatory testing, in order to evaluate the Usability Index (UI). The evaluation of the UI has been carried out with Saaty's *Analytic Hierarchy Process* (AHP), which implies the decomposition of the problem into several levels [S1]. In this case study, three dimensions of UI have been considered: effectiveness, efficiency and satisfaction. Taking into account the experimental data analysis, some changes have been carried out and a new release of the GUI has been validated with new experimentations.

The paper is arranged as follows. Section 2 summarizes the approach. Section 3 provides the experimental phases. Section 4 deals with results of experimentations. Finally,

Article 059-cad-71

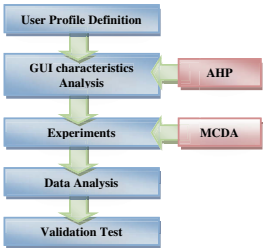

Figure 1: The logic flow chart of methodological approach

Section 5 draws conclusions.

2- The methodological approach

Usability evaluation is based on both objective aspects and subjective ones. Starting from [DM1], the adopted approach is participative, requiring the involvement of potential users during all phases of the usability evaluation process. In Figure 1 the logical flow chart of methodological approach is shown.

2.1 - User Profile Definition and GUI characteristics

A Graphical User Interface (GUI), developed in MatLAB® environment, was released in order to support the design of automotive manual transverse gearboxes (Figure 2). This tool has two main tasks: 1) - design gearboxes rapidly, reducing the risks of using incomplete information when making product development decisions; 2) - assist the designer in redesigning the gearboxes previously developed (for more details see [PV1][LP1]). It was developed for a user not very experienced in design, such as a junior designer.

The main window is divided in three fields (Figure 2): the upper field where the gearbox is pre-configured; the middle field where the gearbox is configured and the gears are characterised; the lower field where are located the post-processing and evaluating commands.

The designer can set: type of gearbox (among preconfigured types); number of gears (up to six); parameters layout controller (axle bases and angle between them); characteristic parameters for each gear (gear ratio, pressure angle, helical angle)(in viable range); gear teeth number (among those automatically generated). Specific panels to set reverse and differential gear were developed. By changing these parameters a new gearbox could be defined; otherwise a previous design could be edited.

As regards the post-processing, by clicking on "Plot" command, the surface models of toothing, i.e. head, sides and foot of helical-toothed gears, could be automatically generated and displayed on screen as mesh models; furthermore, it is possible to change the mesh degree in order to edit both representation and file export definition, ensuring the generation of the 3D solid model in any CAD environment. The designer could also evaluate the bounding volumes of CAD models. In a separate window, in fact, it is possible to evaluate the distance between two points and its components along assigned directions and, then, to easily assign different input values to gearbox parameters to fit, after the automatic re-generation of geometries, the desired bounding volume.

2.2 - The AHP model

The usability evaluation of the graphical user interface has been carried out by using Saaty's AHP [S1], essentially based on two steps: the first is to model the problem as a hierarchy to explore the factors of the problem at levels from general to detailed, then the scoring of the factors related to each level, by comparing them in pairs. In our case, the top level of the hierarchy is the usability of the GUI.

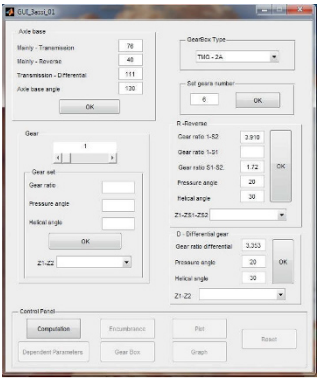

Figure 2: GUI for the gearbox CAD modeling software tool

The first decomposition can be made according to ISO 9241-11:1998 and, in *"Usability Dimensions"*, namely:

- *Effectiveness*: the measurement of the effectiveness related to the targets with the accuracy and completeness of the results achieved. The effectiveness value can be assigned in terms of accuracy related to the main task of the GUI (to assist the gearbox design);
- *Efficiency*: ratio between the effectiveness level and the use of resources, meant as time and computational operations;
- *Satisfaction*: user-perceived benefit and level of comfort felt during the use of the GUI. This dimension is strongly related to the subjective perception of user performance.

Starting from such considerations, the decomposition of the usability is shown in Figure 3. At the first level, there is the GUI's Usability (U) that is decomposed in Usability Dimensions (UDs) at second level. In turn, these dimensions are broken down at the next level in Usability Functions (UFs). Therefore, the last step in the model definition has been the definition of each *UF* that is strictly related to the design of the experimental task. The aim at this stage was to consider critical aspects in the usability assessment of the GUI. According to the hierarchical decomposition above

Article 059-cad-71

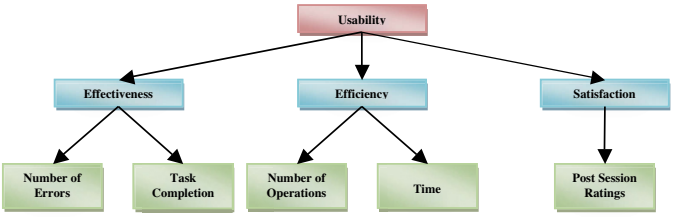

Figure 3: Usability hierarchical decomposition

described, the analysis of the characteristics provides the following *UFs*:

- *Number of Errors* (*E*), measure of effectiveness, is the number of error messages reported by the GUI during the task execution.
- *Task Completion (TC)*, measure of effectiveness, is the level of completion and accuracy in achieving the goals of the task.
- *Number of Operations* (*NO*), measure of efficiency, is defined as the number of operations used to complete a task in terms of mouse clicks and keystrokes.
- *Time* (*T*), measure of efficiency, is the effective time to perform a task or sub-activities.
- *Post Session Ratings* (*PSR*), measure of satisfaction, is a score, which expresses the feeling of users about the GUI use.

The *UFs* define the lowest level of the hierarchical model.

2.3 - The Usability Index definition

Starting from the assumption the factors of the hierarchy, for each level, are preferentially independent to each other, a simple linear additive evaluation model could be applied. By means of Multi-Criteria Decision Analysis (MCDA) all the measures corresponding to the factors could be combined into one overall value. In particular, the measure of each factor is multiplied by a weight based on a specific criterion, and then the weighted scores are summed up. The calculation of the index starts from the *UFs*, by using data collected during experiments. Being data of different nature and magnitude, a preliminary normalisation is required, in order to ensure the comparison between them.

The normalisation techniques, adopted for the specific UFs, are briefly described in the following:

- *0-Max* normalisation performs a linear transformation of the original data. The considered value e_{ij} is transformed in a new value e'_{ij} ranged in the interval [0, 1] using the equation (1):

$$e'_{ij} = \frac{e_{ij}}{\max_i} \quad (1)$$

- *Min*/e_{ij} normalisation performs a linear transformation of the original data that reverses the direction of preferences. The considered value e_{ij} is transformed in a new value e'_{ij} ranged in the interval [0, 1] using the equation (2):

$$e'_{ij} = \frac{\min_i}{e_{ij}} \quad (2)$$

- e_{target}/e_{ij} normalisation performs a linear transformation of the original data that reverses the direction of preferences and requires a target value. The considered value e_{ij} is transformed in a new value e'_{ij} ranged in the interval [0, 1] using the formula (3):

$$e'_{ij} = \frac{e_{t\arg et}}{e_{ij}} \quad (3)$$

The above techniques adopted for each UF are reported in Table 1.

Normalisation technique	Usability Functions
0-Max	*PSR*
Min/e_{ij}	*NE*, *TC*
e_{target}/e_{ij}	*NO*, *T*

Table 1: Normalisation techniques adopted for each UF

The outcomes of the normalisation procedure are the usability measures (um_i) that range from 0 to 1. Then, for each subgroup of usability measures, the usability dimension index (*UDI*) is defined (4):

$$UDI_i = \sum_{i=1}^{n} w_i \cdot um_i \quad (4)$$

where w_i is the weight of each usability measure, that could be different, based on the level of priority of usability measures in the specific application. The three usability dimension indexes are: 1- the effectiveness index; 2- the efficiency index; 3- the satisfaction index .

The weighted sum of these three indexes provides the overall results for the UI (5):

$$UI = \sum_{i=1}^{n} w_i \cdot UDI_i \quad (5)$$

In details, the AHP is applied in order to evaluate the relevance of the factors in the hierarchy, taking into account the analysis of GUI interaction. Starting from the hierarchy structure of the model, the matrix of weights has been defined. This matrix is accomplished for each level of the

Article 059-cad-71

hierarchy and for each group (elements in the lower level hinge on the same element in the upper level), by placing the elements of the group both on matrix rows and columns. Hence, all the elements of the same group are compared in pairs. The generic matrix element a_{ij} is the result of the pairwise comparison between the attribute of the row *i-th* and the column *j-th*, with respect to a certain task, using the Saaty scale that is a 9-points scale anchored at the end with the terms *"Equivalent alternatives"* and *"The chosen alternative is absolutely better than the other one"*. Thus, the main diagonal of the matrix consists of unit elements only, while the values of the other cells are always positive, according to the reciprocity property (6):

$$a_{ij} = \frac{1}{a_{ij}} \tag{6}$$

Once the pairs comparison matrix has been defined, the weight of each element is assumed as (7):

$$w_i = \frac{\left(\prod_{j=1}^{n} a_{ij}\right)^{\frac{1}{n}}}{\sum_{i=1}^{n}\left(\prod_{j=1}^{n} a_{ij}\right)^{\frac{1}{n}}}; \quad i, j = [1, n] \tag{7}$$

where n is the dimension of the metrics related to the element at issue. In particular, the allocation of weights is done with a bottom-up logic, from the lowest level of the hierarchy (*UFs*) to the highest (Usability).

3- Experimental phase

3.1 – Overview of experiment

Preliminarily, a GUI *Tutorial* was defined to present the graphical interface, to explain the procedures for data entry and to discuss about the features of the interface. An example was also illustrated.

The first phase of testing involved the selection of a representative sample of the GUI user profiles. The minimum skills of the users were identified: 1) a good knowledge (at least theoretical) of a gearbox, 2) a good expertise with the use of graphical user interfaces, and more generally, with the use of specialized software. On this basis, participants were 12 newly graduated engineers (i.e. mechanical, electrical and management) selected, under the R&D project *Digital Pattern Development*, for highly specialized training in Computer-Aided Design.

To collect data an experimental session was prepared. In such session, each user had to complete two tasks: the first related to a new design activity, the second related to the modification of an existing gearbox model. As regards the first task, users were asked to design a new gearbox according to the specifications assigned, to assess the overall dimensions and, subsequently, to save the model. Then, for the second task, users were asked to modify the gearbox, designed in the previous task, according to new instructions, and, then, they were asked to carry out a new evaluation of the overall dimensions and to save again. At the end of the two previous tasks, the users were asked to fill a questionnaire; in particular, they were asked to express their agreement related to ten statements, all set in a positive sense, by using a seven-point scale, whose ends were the positions: *"strongly agree"* and *"strongly disagree"*.

3.2 - Experimental protocol

Several days before the test session, a preparatory meeting with the participation of users involved in the tests was accomplished. The purpose of the incoming experimentation and the functionality of GUI were presented. A detailed description of the *Tutorial* was given.

Then, on the day fixed for the tests and before starting the tests, users were informed, once again, that the aim of the experiment was to evaluate the GUI usability, and not the user's ability to quickly perform a set of assigned tasks. In this way, we tried to minimize the "stress" that, generally, may affect the outcome of a proof. Furthermore, the inspectors of test session have shown the procedures of the experimental session, with particular attention to the rules of test performing. Then, they provided further details about the *Tutorial* and a short questionnaire for the personal details and for the informed agreement. The questionnaire was filled and returned before the start of the test. Finally, an ID code to each user was assigned.

Users tested the GUI individually and in random order to avoid noise factors. During the test, the inspectors recorded many details: the start and the ending time of the tasks, any notes on the bringing of the test, the number and kind of assistance provided. Specifically, if the user explicitly required the assistance of the inspector, then the inspector invited him to consult the *Tutorial* (classifying this as a *level 1* assistance). Otherwise, if the user was not able to continue the test, the inspector removed all doubts (classifying this as a *level 2* assistance).

3.3 - Data collection and processing

The experiments were performed at the Department of Industrial Engineering in a suitable room cleared furnishings and with a Visual Display Unit (VDU). The time limit for each test was set at 30 minutes after which the user was asked to suspend the operations. Furthermore, for each test was used a software that recorded all the user's activities carried out on the monitor. Table 2 summarises the sources related to *UFs*.

As regards *UFs*, all the measures were collected. In the calculation phase, the total value of each *UF* was obtained as the sum of the measures/ratings respectively noted to perform both the Task 1 and Task 2 for the same user. This operation was repeated for all participant users.

Usability Dimensions	Usability Functions	Source
Effectiveness	Number of errors (NE) Task Completion (TC)	Video test Panel of experts
Efficiency	Number of operations (NO) Time (T)	Video test

Article 059-cad-71

Satisfaction	Post-session ratings (PSR)	Questionnaire

Table 2: The sources of *UFs*

Effectiveness: the *Number of Errors (*NE*)* was derived from the video by counting each time the GUI reported an error message; the *Task Completion (*TC*)* was measured using a rating given by a panel of experts who were asked to assess the completeness of the goals reached for all the activities performed in the test by using the following six-point scale: (1) Complete success without assistance, (2) Complete success with assistance, (3) Partial success without assistance, (4) Partial success with assistance, (5) Failure: the user didn't understand that the task is not complete, (6) Failure: the user does not completed the task despite the assistance. The references to determine the level of completion in task execution were decided beforehand.

Efficiency: the *Number of Operations (*NO*)* was derived from video by counting, from time to time, the operations that were performed to complete the task; the *Time* (T*)* was measured by the inspector as the difference between the ending and the beginning time of the session. This measure was subsequently validated by a comparison with the clock of VDU shown in video recordings.

Satisfaction: the *Post-Session Ratings (*PSR*)* were got from the post-session questionnaire that users filled out at the end of the test.

For the calculation of the UI the average values arithmetic mean) of all the aforementioned *UFs* were used.

4- Results

The following data were obtained. Table 3 shows the normalized measures of UFs split among users and subgroups.

	Effectiveness		Efficiency		Satisfaction
ID user	Number Errors (NE)	Task Completion (TC)	Number of Operations (NO)	Time (T)	PostSession Ratings (PSR)
1	0.50	0.25	0.84	0.43	0.56
2	0.20	0.33	0.80	0.57	0.95
3	0.10	0.33	0.47	0.36	1.00
4	0.17	0.33	0.75	0.37	0.87
5	0.25	0.40	0.77	0.49	0.82
6	0.25	0.40	0.70	0.46	0.93
7	0.11	0.40	0.53	0.45	0.46
8	0.08	0.33	0.49	0.24	0.46
9	0.20	0.40	0.63	0.32	0.90
10	0.10	0.50	0.78	0.43	0.72
11	0.33	1.00	0.85	0.58	0.92
12	1.00	0.40	0.64	0.32	0.84

Table 3: Normalized measures of *UFs*

According to the above UI definition (par. 2.3), the average values of UFs were obtained using the collected measurements. The weights of UFs were obtained submitting Saaty's questionnaire to a panel of experts and using the Equation 7, as summarised in Table 4.

UFs	NE	TC	NO	T	PSR
w_i	0.74	0.26	0.25	0.75	1
um_i	0.27	0.42	0.69	0.42	0.79

Table 4: Weights and values of *UFs*

Likewise, the weights and values of UDs were obtained (Table 5). Therefore the index of usability integrated obtained is equal to 0.42 (UI). This is a low value.

UD	$UDI_{effectiveness}$	$UDI_{efficiency}$	$UDI_{satisfaction}$
w_i	0.59	0.31	0.10
UDI_i	0.31	0.49	0.79

Table 5: Weights and values of *UDs*

The table 5 shows that the satisfaction index ($UDI_{satisfaction}$) is the highest (79%). However, this value could be smaller as the degree of satisfaction of the users could be influenced by the achievement of the goal (i.e., the effective gearbox modeling) rather than the difficulties they overcome in using interface. In any case, the satisfaction is the usability dimension that has a limited effect on the calculation of the global index. So, the results in Table 5 suggest that to improve the usability of the GUI it is necessary to increase the values of effectiveness and efficiency, improving the functions *Time* and the *Number of Errors*, respectively (Table 4). For a more detailed analysis, both Task 1 and Task 2 were divided into the following critical sub-activities: the choice of the gearbox architecture, the choice of the gears number, the setting of the dependent parameters, the setting of the wheel parameters, the setting of the reverse gear, the setting of the differential parameters, the overall dimensions, the procedure for file exporting. In this perspective, the measurement of efficiency was analysed.

Figure 4 shows the radar chart that highlights how the normalized average value, related to the number of operations due for each sub-task, is different from the normalized optimal value, equal to 1. For example, the value equal to 3, related to one of the axes, means that, on average, the number of operations necessary to accomplish that subtask, in order to obtain the required result, were equal to 3. Figure 4 shows that the more critical sub-tasks, involved in the first task, are (in descending order): the setting of the parameters of the differential (6.10), the setting of the reverse gear (5.29), the file exporting (4.42), the setting of the gear parameters (2.43). Further results for Task 2 are: the setting of the reverse gear (4.17) and setting of the differential parameters (2.35).

Also the Time was a critical UF. In fact, if we consider only the users who accomplished the Tasks, in a complete and without assistance way, the average Time was found to be almost double than the predetermined optimum value. More generally, the Time to complete the Task 1 was greater than the one related to the Task 2 (Fig. 5).

Article 059-cad-71

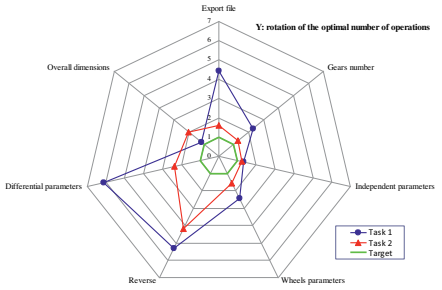

Figure 4: Rotation of the Number of Operations by sub-activity

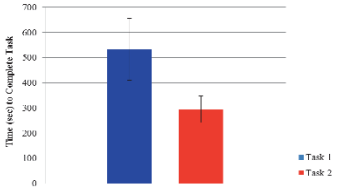

Figure 5: Average *Time* to complete Task 1 and Task 2

Tackling the measures of effectiveness, it is possible to highlight that there were no significant differences between the number of errors related to the Task 1 and Task 2, but the average values are not negligible (Fig. 6).

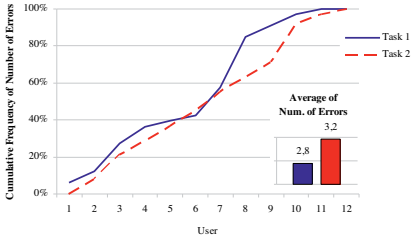

Figure 6: Cumulative frequency of number of errors related to each task and average values

The determinations of *Task Completion*, grouped using the level of success, are depicted in Figure 7. It should be noted that most users carried out the Task 1 in a complete success. Otherwise, in the accomplishment of Task 2, only 1 user had completely achieved the goals (complete success), while 10 users have had a partial success. There was also 1 user who had failed.

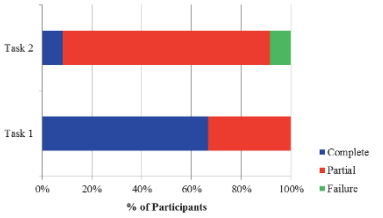

Figure 7: Stacked bar chart showing different levels of success based on task completion

The measures of satisfaction were analysed. Figure 8 shows that the lowest value of the satisfaction is related to the clarity and effectiveness of the GUI (D8), while the highest value is related to the actual benefit perceived in the use of the GUI, to improve the gearbox design (D5).

Based on what has been analysed, after careful viewing of the videos of the tests, the following critical issues were identified: 1) the default fields are not empty; 2) the interface does not allow users to overwrite the selected values in the fields, so the users are forced to cancel the existing; 3) the user does not have a feedback on the correct setting of the parameters; 4) the provision of the sections in the main window is not consistent; 5) the function for file exporting is poorly visible; 6) the reset command has an insufficient functionality.

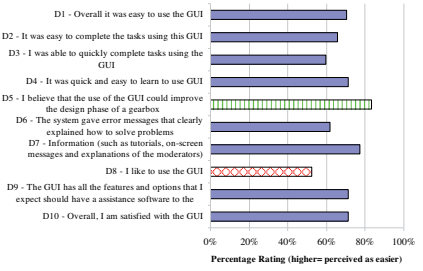

Figure 8: Average subjective ratings split by statement

These problems involve a difficulty in achieving the Tasks and, they generally cause an increase of the operating time also due to a more than proportional increasing number of operations to be performed. In some cases, the user is confused and, then, he is led to the error or makes continuous action controls.

Once these critical issues have been identified, it has been decided to design the GearBox 2.0 that was developed keeping unchanged the dimensions of initial GUI, avoiding radical changes and aiming to improve efficiency, and effectiveness. A series of new features were introduced (Figure 9). A new provision of sections, with different

Article 059-cad-71

background colours, that promotes the logical procedure for the input of project data was introduced. A new visibility to the button aimed to file exporting was given. The buttons on the control panel were divided, and a section with the new *"TEST"* function, the upgraded *"RESET"* function and a new confirmation "SET" function were inserted. The latter turns on only when the input parameters are correct. In this way it provides an immediate feedback to the user. To assess the validity of the new features a pairwise comparison between the Gearbox 2.0 GUI and the initial version was performed. For each change users were asked if they preferred the original version or the GearBox 2.0. They expressed their degree of preference on a scale of six points. The survey results demonstrated a preference of the users for the new GUI far higher than the initial one. Therefore, all the features of Gearbox 2.0 GUI were definitively implemented and new tests were started for evaluating the UI, according a continuous improvement loop.

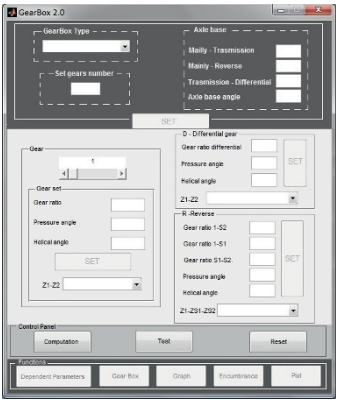

Figure 9: The Gearbox 2.0 GUI

5- Conclusions

In this paper the characteristics of the GUI belonging to a software tool for gearbox design were analysed. Then, an AHP model was proposed and an experimentation to calculate the integrated UI was performed. In particular, the experimental data, which have led to a lower UI, were collected and analysed. Therefore, a new release of the GUI was proposed. Further experimentations were carried out in order to validate the new release of the GUI and a positive evaluation of the new features was accomplished. This improvement induces to state that the use of the new release of the GUI could contribute to reduce the development time in gearbox design and, therefore, the overall *time to market* for new gearboxes. Further steps deal both with a further feature evaluation and improvement of the new GUI. In fact, by using the present approach, new characteristics of GUI could be introduced and evaluated.

6- Acknowledgements

The present work was developed with the contribution of the Italian Ministry of University and Research (MIUR) performing the activities of the PON01_01268 DIGIPAT Project, *Digital Pattern Product Development: A Pattern Driven approach for industrial product design, simulation and manufacturing*.

The authors also thank prof. Giuseppe Di Gironimo (Department of Industrial Engineering, University of Naples Federico II), coordinator of DIGIPAT Formation Project for selecting the GUI users, and the engineers who took part to the experiments. Finally, the authors thank eng. Alfonso Vitolo for his technical support.

7- References

[B1] Bourke D. Software gives engineers quick access to product info from layers of company files. Mechanical Engineering: 44-47, 2013.

[DM1] Di Gironimo G., Matrone G., Tarallo A, Trotta M, Lanzotti A. A virtual reality approach for usability assessment: case study on a wheelchair-mounted robot manipulator. Engineering with Computers 29 (3): 359-373, 2013.

[LP1] Lanzotti A., Patalano S., and Vitolo F. A graph-based approach to CAD modeling: a digital pattern application to the sizing and modeling of manual transverse gearboxes. In International Conference on Graphic Engineering, Madrid, 2013.

[MA1] Madhavan R., Alagarsamy K. Usability issues in software development lifecycle. International Journal of Advanced Research in Computer Science and Software Engineering, 3 (8): 1331-1335, 2013.

[PV1] Patalano S., Vitolo F., and Lanzotti A. A graph-based software tool for the CAD modelling of mechanical assemblies. In Proceedings of the International Conference on Computer Graphics Theory and Applications and International Conference on Information Visualization: 60-69, Barcelona, DOI: 10.5220/0004299000600069, 2013.

[S1] Saaty L. Decision making with the analytic hierarchy process. International Journal of Services Sciences 1 (1): 83-98, 2008.

[S2] Sandeberg M. Knowledge based engineering – in product development. ISSN: 1402-1536, 2003.

[SB1] Sharmin M., Bailey B. P., Coats C., Hamilton K. Understanding knowledge management practices for early design activity and its implications for reuse. In Proceedings of the 27th International Conference on Human Factors in Computing Systems: 2367-2376, 2009.

[SK1] Sohaib O., Khan K. Integrating usability engineering and agile software development. In Proceedings of the International Conference on Computer Design and Application, volume 2: 32-38, 2010.

Article 029-itm-111

Information feedback from CNC to CAM through OntoSTEP-NC

Christophe Danjou[1], Julien Le Duigou[1], Benoît Eynard[1]

(1) : Mechanical Engineering Systems Department, Université de Technologie de Compiègne, Mechanical laboratory Roberval UMR UTC/CNRS 7337, Rue du Docteur Schweitzer, BP 60319, 60203 Compiègne cedex, France.
E-mail : {christophe.danjou, julien.le-duigou, benoit.eynard}@utc.fr

Abstract: This paper exposes a proposition to ensure closed-loops manufacturing from CNC machines to CAD/CAM systems. As STEP-NC allows bi-directional exchanges but does not allow incrementing traceability of machining program, the proposition set up loops using PLM systems. This proposition is based on the new OntoSTEP-NC ontology which provides trades between PDM (Product Data Management), MPM (Manufacturing Process Management) and ERP (Enterprise Resource Planning). As a solution OntoSTEP-NC is the basis to data extraction from CNC machines, and relevant information reinjection to CAM systems. To have the most relevant information reinjection a feature recognition stage has been introduced. Moreover, coupled to Case Base Reasoning, this recognition loop will allow incrementing the MPM database. This proposition will help program planner making choices based on company good practices.

Key words: STEP-NC; OntoSTEP-NC; closed-loop manufacturing, Manufacturing Process Management.

1- Introduction

In a "rapid-development" context, manufacturers must well-industrialize products improving the triptych: Cost, Time, and Quality.

French FUI project called ANGEL (Atelier Numérique coGnitif intEropérable et agiLe) focuses on the capitalization of cuts know-how in order to improve the competitiveness of companies developing tools and methods to retrieve information from the CNC machine. To achieve the information flow bi-directionality from CNC machines to CAD, the systems must be able to exchange information and to use this information.

According to Wegner [W1], the previous needs are defined by the term interoperability: "The ability of two systems (or more) to communicate, cooperate and exchange services and data, thus despite the differences in languages, implementations, executive environments and abstraction models". Defined by 3 level – Semantical, Technical and organizational [E1] – interoperability can be achieved using various solutions. One concerns the use of standard format which allows having a unified approach. To achieve the interoperability between the manufacturing technologies (CAX software) the STEP-NC standard seems to be one of the most promising [X1].

Beyond interoperability aspect this paper focuses on the feedback from the machining to the design and industrialization phases. The main question the paper would answer is: "How to integrate manufacturing expertise from manufacturing in the design / industrialization process for mechanical parts?". Indeed incrementing the cutting knowledge would help to manufacture the right part-the first time thus despite the formats differences.

To answer this question, the next section presents a state of the art on STEP-NC standard as a basis for CAX software trades. The third section will explain the proposal to achieve the integration of manufacturing expertise and knowledge extracted from the CNC machining. Section 4 concludes this paper presenting future works.

2- State of the art

2.1 – STEP-NC a solution for data exchange

Designing and manufacturing systems trades (CAD, CAM, Post-Processor, CNC machine, etc.) are led by specific file. Indeed, software has its own language and disable to have the best trades between the systems. For example, CATPart and CATProcess will be used respectively for Dassault Systems CAD and CAM systems, Top'CAM for TopSolid CAM system, G-Code and M-Code will be used as specific inputs according the CNC controller, etc.

Therefore to ensure trades between software, one solution consists in using standard format. Indeed this unifying approach allows having the same language for all

the manufacturing technologies. To first achieve the data exchange between CAD and simulation, STEP standard has been developed [LJ1]. The STEP standard is an open and normalized standard that aims to promote the data exchange in a format which is understandable and shared by all. According to Rachuri [RS1], the STEP standard provides a neutral, sustainable and scalable data exchange format.

In the last years, STEP-NC, a new standard format with enriched data has been developed in order to improve the systems interoperability [LR1] by integrating processing data. Indeed, the STEP-NC standard encompasses machining process, cutting tools description, and CAD features and requirements. This enriched standard format allows having in the same file all the information required for the whole development stage from the early design to the machining.

STEP-NC is led by two norms which are interested in two different levels – AIM and ARM:

- ISO 10303 AP238 which concerns the AIM (Application Interpreted Model) level. This level is based on the ISO 10303 norm which defines the STEP standard. The Application Protocol (AP) 238 untitled "Computer numerical Controllers" mainly allows adding information for CNC machining. In this way, the STEP standard is enriched with the manufacturing feature.
- ISO 10649 deals with the ARM (Application Reference Model) level. This level is higher than the previous one and it also defines the machining strategy.

The STEP-NC standard structures a large number of information. Therefore, the same file can be used for all the CAX systems and then all the modifications are propagated from one to another. The use of STEP-NC also helps to archive the modifications. Indeed there is no more coherence problem from CAM and CNC program. All the modifications and optimization made by the operators in the CNC machine are translated in the STEP-NC file. This program can be then archived and re-use if necessary. The use of STEP-NC can help to save time because the post-processor can be overpass. Indeed, the machining intelligence is moved from CAM systems to CNC machines thus the translation from computer language to machine understandable language (Post-Processors and G-Code) is no more necessary. Therefore, the following works will be based on STEP-NC standard and not on G-code. Nassehi [NN1] has defined in figure 1 the information flow through the CAX systems from CAD to CNC.

2.2 – STEP-NC enabling feedback and optimization

As seen in the previous section, the use of STEP-NC standard file makes possible the propagation of modification to all the other manufacturing systems. Therefore changes made directly in the CNC machine will be propagated back to CAM system.

In addition to the flow bi-directionality, STEP-NC standard will simplify the industrialization phase. As a result of optimization, according to the NIST, the STEP standard can potentially save up to a billion dollars a year by reducing the costs of interoperability in sectors such as automotive, aerospace and shipbuilding. The following list summarizes the major works using STEP-NC for feedback and optimization:

- Campos [CM1] achieve vertical integration with STEP-NC in order to have a standard process monitoring and traceability programming. The traceability is ensured at three different levels: Business level, Manufacturing Level, and shop floor level. This allows monitoring the capitalization.
- Xu [XW1] uses STEP-NC as a universal programming for CNC machines. Indeed the same CAM program can be spread to many CNC machines. Thus it has been made possible with the intelligence transfer from CAM system to CNC machines to use the same CAM program into many different CNC machines.
- Through the use of STEP-NC Ridwan [RX1] defines an automatic correction of cutting parameters based on the Machine Condition Monitoring. He has developed optiSTEP-NC system which helps to perform cutting parameters optimization.
- In the same way, Zhao [ZX1] has defined closed-loop machining thanks to STEP-NC to achieve on-line inspection. To succeed this inspection he has developed a closed-loop between CAPP and CNC machine.
- Borgia [BM1] based on STEP-NC allows having automatic recognition of feature and generating toolpath based on machining working step. Then a mathematical optimization is conducted.

According to this short review on STEP-NC works it appears that the standard is a promising solution for bi-directional trades and for optimization (Cutting parameters, toolpath optimization, feature recognition, etc.).

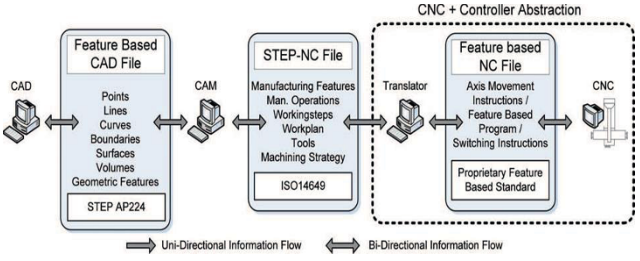

Figure 1: Information flow in an ISO14649 chain [NN1]

2.3 – Lacks in STEP-NC

The previous study has highlighted that automatic correction/optimization and feature recognition are made reality thanks to STEP-NC use. But there is no feedback from the CNC machine to the CAD or CAM systems. This kind of feedback would help people in design or program choices. Indeed Newman [NN2] formulated the following assertion: "Interoperability will enable manufacturing businesses to produce legacy components, based on the original process planning knowledge, on modern and future machine tools without the overhead of re-planning the fixturing, tooling and tool paths. This will enable future parts to be manufactured with confidence, as and when required without having to rely on the original equipment, past tooling and part programs which would be typically obsolete." Based on this assertion, it clearly appears STEP-NC is the basis for future data exchanges and to interoperability.

Although STEP-NC allows sharing and propagating data in both ways – CAD to CNC and CNC to CAD – STEP-NC is not yet a solution for archiving CNC machining information in order to be injected at the right time. This is why the next section will propose a solution to insure interoperability and a way to succeed in feedback from CNC machine to CAM systems. This feedback will create closed-loop manufacturing.

3- Solution for data feedback

3.1 – Information feedback trades

As highlighted in the previous sections, STEP-NC standard file encompasses lot of information and permits the data propagation to the whole lifecycle. But STEP-NC does not allow incrementing manufacturing loops. Those loops include all the phases between CAM systems and CNC machines. Indeed, STEP-NC file in its own format cannot support the incrementing evolution of good practices. STEP-NC requires to be connected to information systems (PDM-MPM-ERP) to ensure traceability to improve the industrialization phase for the future manufactured products.

This is why figure 2 exposes a proposition to achieve incrementing manufacturing loops. This implementation is being made possible thanks to the interaction between information systems and the CAX systems. In this proposition 3 loops can be clearly identified:

- PDM-MPM-ERP trades allow extracting manufacturing information from the CNC machine based on STEP-NC and to inject this information in the CAM (1). The extracted information concerns the machine behavior and the machining parameter as feedrate, spindle, lubrication, etc. The injected information help program planners to make choices giving them values range according the machining parameters.
- Until the reinjection of the relevant CAM information in the manufacturing technologies chain, a stage of process validation should be passed to ensure the good practices (2). Indeed to ensure the program planners to have good range of values, a systematic validation of data extraction has to be made. This validation will be part of the good practices to be exploited for future products.
- A third loop can be identified with the geometrical feature recognition from CAD and CAM systems (3). This loop prepares the feedback from MPM to CAM systems: The goal is to recognize the geometrical feature in order to have relevant CAM information feedback.

To summarize the proposition, 3 loops can be identified: The first one concerns the feedback from CNC machine to CAM system, the second is about the validation process of good practices and third one deals with the geometrical recognition. Thanks to CBR methodology, this third loop will contribute to the database update

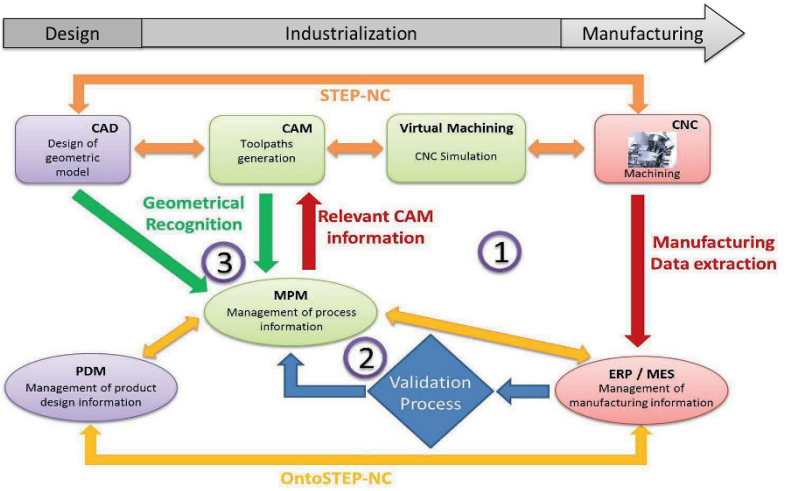

Figure 2 : Information feedback trades

3.2 – OntoSTEP-NC for PDM-MPM-ERP trades

To achieve interoperability between information systems it has been chosen to use an ontology. Indeed it has been chosen to use an ontology called OntoSTEP-NC based on the STEP-NC standard as support PDM-MPM-ERP trades [DL1]. The ISO 14649 standard has been chosen as a basis for OntoSTEP-NC model. The standard format is a meta-level model for CNC information so on OntoSTEP-NC describes a meta-level data. This model has been built using the Protégé software (edited by Stanford University) [NK1] defining entities as classes.

First based on ARM level the OntoSTEP-NC can be then modified to AIM model. Indeed the ontology lets a large range of possibilities to modify the model structure and to add new entities and features. Therefore the interoperability of the information systems is achieved thanks to the adaptability of the ontology model to perfectly feet with the data exchange between PDM, MPM and ERP. Moreover, the use of the recent developed OntoSTEP-NC will allow interoperability with CAX systems as explained by Newman [NN2]: "Though STEP-NC has given the opportunity for machining process information to be standardized, the lack of a semantic and ontology representation makes it almost impossible to inter-relate the existing systems and languages."

3.3 – Extraction of manufacturing information

To achieve manufacturing loops it is bounded to have data extraction from manufacturing and more precisely from the CNC machining. Through the STEP-NC exploration, machining working step can be identified and related information can be archived into the ERP systems. This would help to have a traceability of the real machining program and to extract specific data as spindle, cutting tools, feedrate, feed per tooth, approach and retract macro, radial and axial depth of cut, overhang ratio, center path overlap, toolpath strategy.

The same work must also be done using G-code due to the CNC controller inability to understand STEP-NC in today companies. Indeed, one partner of the ANGEL project consortium is currently working on data extraction from CNC machine using G-code.

This extraction has to be then treated to link the correspondence between, the materials, the tools, the specific machining operations and all the machining parameters (spindle, feedrates, etc.). Once this data treatment achieved, the information have to be transferred to the MPM systems through the validation process to be then re-used.

3.4 – Use of extracted information

Before using this extracted information the correspondences have to be validated. Indeed the aim of this validation process is to identify the good practices and to eliminate practices which are not totally satisfactory. The validation process is led by the CAM programmer. If the process realized in the CNC is the same the programmer made, then it is automatically set in the database as references and if the process has been modified after the first programming, the CAM programmer must validate all the process. This allows the programmer learning about errors for the next time.

This information is then stocked in the MPM system as feature. Indeed contrary to the classification which is yet set in MPM system using products or items, the proposition sets a classification using manufacturing features. To each manufacturing feature is associated a material, a cutting-tool and machining parameters. As databases, the MPM systems can classify information according the feature to be then used according the needs and the requirements.

To close the manufacturing loop the data reinjection must be relevant at the right time for CAM systems. Indeed, this reinjection has to help the technician to make choices by proposing him past validated solutions. These solutions based on information contained in the MPM system must be presented as a list of value range in which the technician can choose the machining parameters.

This list of approaching solutions is proposed according the following criteria:

- Manufacturing feature,
- Material,
- Cutting tool.

To generate this list of approaching solutions yet treated in the past it is necessary to identify the manufacturing feature and then to compare it with the database.

3.5 – Geometrical recognition with CBR

To have the best answers it is essential to well identify the geometrical tips and then to find the closer solutions that have been yet registered in the database.

The geometrical recognition can be based on the design feature and on the manufacturing feature engaged by the technician. This information is carried by the STEP-NC file and by analyzing the STEP-NC entities the geometrical recognition can be achieved [TK1].

Once this recognition achieved the major works consist in identifying in the MPM system the relevant solutions. Using the Case Base Reasoning methodology allows finding the best solutions in database. According to De Mantaras [D1], "Case-based reasoning (CBR) is a major paradigm in automated reasoning and machine learning. In case-based reasoning, a reasoner solves a new problem by noticing its similarity with one or several previously solved problems and by adapting their known solutions instead of working out a solution from scratch". In many aspects, case-based reasoning is a problem solving method different from other AI approaches. In particular, instead of using only general domain dependent heuristic knowledge like in the case of expert systems, it is able to use the specific knowledge of concrete, previously experienced, problem situations. Another important characteristic is that CBR implies incremental learning since a new experience is memorized and available for future problem solving each time a problem is solved. Case-based reasoning is a powerful and frequently used way of human problem solving. Aamodt [AP1] defines the CBR cycle with 4 steps as show in figure 3:

- Retrieve the most similar case or cases
- Reuse the information and knowledge in that case to solve the problem
- Revise the proposed solution
- Retain the parts of this experience likely to be useful for future problem solving

The CBR will not only help the geometrical recognition it will also help to improve the database with new information.

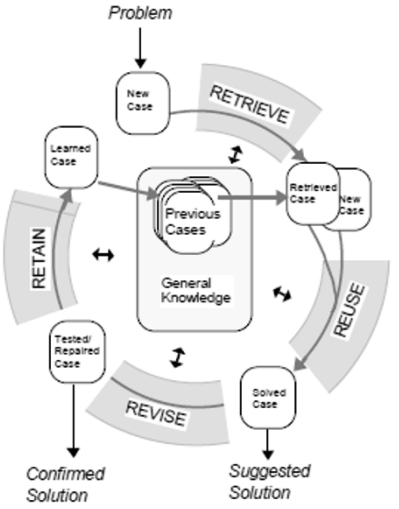

Figure 3: The CBR cycle [AP1]

3.6 – Future works

This proposition must be implemented using OntoSTEP-NC and the main work will concern the connection between information system and the ontology. Once OntoSTEP-NC implemented, information exchange and storage will be set through the information system ensuring the first loop. Then the geometrical recognition will be developed by using the CBR methodology as the main part of the closed-loop manufacturing.

As a validation of the proposition, three tests with three different parts will be realized. Those tests will be extracted from aeronautical parts. The first part is an aluminum one which presents a large number of manufacturing features (drilling, pocket, surfacing…). This first part will test the recognition of geometrical design and the ability to compare to the manufacturing features in the database. The second part which is an aeronautical turning-milling part also in aluminum will test the data extraction due to the numerous complex form of this part. The third part equal to the second one will be in titanium. This one will allow testing the increment of the database and also to test the answers from MPM concerning the relevant CAM information trades. The extrapolation of this proposition will concern complex forms for aeronautical parts with raw material as titanium and Inconel.

4- Conclusion

As seen in section 2 STEP-NC can support through its rich data format, much information that can be integrated in the bi-directional flow CAD-CAM-CNC. Although STEP-NC allows feedback from the CNC machine to CAD and CAM systems, STEP-NC standard file does not allow archiving and capitalizing information. Indeed, there is no incrementing process in order to capitalize good practices yet existing.
This is why the proposition of this paper uses information systems (PDM-MPM-ERP) to ensure this capitalization setting the MPM as a pivot for trades between information systems and CAX technologies. Those trades are led using OntoSTEP-NC and allow having three loops This proposition will be tested in our future works on three industrial use cases.

Acknowledgements: This work is done in the French FUI project ANGEL. We also thank all consortium partners for their contribution during the development of ideas and concepts proposed in this paper.

6- References

[AP1] Aamodt, A., & Plaza, E. (1994). Case-Based Reasoning : Foundational Issues, Methodological Variations, and System Approaches. AI Communications, 7(1), 39–59.

[BM1] Borgia, S., Matta, A., & Tolio, T. (2013). STEP-NC compliant approach for setup planning problem on multiple fixture pallets. Journal of Manufacturing Systems, 32(4), 781–791.

[CM1] Campos, J. G., Miguez, L. R. (2011). Standard process monitoring and traceability programming in collaborative CAD/CAM/CNC manufacturing scenarios. Computers in Industry, 62(3), 311–322.

[DL1] Danjou, C., Le Duigou, J., & Eynard, B. (2013). Integrated Platform from CAD to CNC : State of the Art. In Proceedings of International Conference on Product Lifecycle Management (pp. 130–139). Nantes, France.

[D1] De Mantaras, R. L. (2001). Case-Based Reasoning. In In Machine Learning and Its Applications (Springer B., pp. 127–145).

[E1] EIF. (2004). European Interoperability Framework. White Pages.

[GO1] Gallaher, M. P., O'Connor, A., & Phelps, T. (2002). Economic Impact Assessment of the International Standard for the Exchange of Product Model Data (STEP) in Transportation Equipment Industries (p. 193). NIST Report.

[LR1] Laguionie, R., Rauch, M., & Hascoet, J. (2008). Toolpaths programming in an intelligent STEP-NC manufacturing context. Journal of Machine Engineering, 8(1), 33–43.

[LJ1] Lee, S.-H., Jeong, Y.-S. (2006). A system integration framework through development of ISO 10303-based product model for steel bridges. Automation in Construction, 15(2), 212–228. doi:10.1016/j.autcon.2005.05.004

[NN1] Nassehi, A., Newman, S. T., Xu, X. W., & Rosso, R. S. U. (2008). Toward interoperable CNC manufacturing. International Journal of Computer Integrated Manufacturing, 21(2), 222–230.

[NN2] Newman, S. T., Nassehi, A., Xu, X. W., Rosso, R. S. U., Wang, L., Yusof, Y., Dhokia, V. (2008). Strategic advantages of interoperability for global manufacturing using

CNC technology. Robotics and Computer-Integrated Manufacturing, 24(6), 699–708.

[NK1] Noy, N., Klein, M. (2004). Ontology Evolution: Not the Same as Schema Evolution. Knowledge and Information Systems, 6(4), 428–440.

[RS1] Rachuri, S., Subrahmanian, E., Bouras, A., Fenves, S. J., Foufou, S., & Sriram, R. D. (2008). Information sharing and exchange in the context of product lifecycle management: Role of standards. Computer-Aided Design, 40(7), 789–800.

[RX1] Ridwan, F., Xu, X. (2013). Advanced CNC system with in-process feed-rate optimisation. Robotics and Computer-Integrated Manufacturing, 29(3), 12–20.

[TK1] Tan, C. F., Kher, V. K., & Ismail, N. (2013). Design of a Feature Recognition System for CAD / CAM Integration. World Applied Sciences Journal, 21(8), 1162–1166.

[W1] Wegner, P. (1996). Interoperability. ACM Computing Surveys (CSUR), 28(1), 285–287.

[X1] Xu, X. W. (2006). Realization of STEP-NC enabled machining. Robotics and Computer-Integrated Manufacturing, 22(2), 144–153.

[XW1] Xu, X. W., Wang, L., & Rong, Y. (2006). STEP-NC and function blocks for interoperable manufacturing. IEEE Transactions on Automation Science and Engineering, 3(3), 297–308.

[ZX1] Zhao, F., Xu, X., & Xie, S. (2008). STEP-NC enabled on-line inspection in support of closed-loop machining. Robotics and Computer-Integrated Manufacturing, 24(2), 200–216.

Article 064-cad-83

Constraint-based Decision Support System: Designing and Manufacturing Building Facades[1]

A. F. Barco[1] , E. Vareilles[1] , M. Aldanondo[1] , P. Gaborit[1], M. Falcon[2]

(1): Université de Toulouse, Mines d'Albi
Route de Teillet Campus Jarlard, 81013 Albi Cedex 09, France
Tel. +33 563 493 185 / Fax. +33 563 493 138
E-mail : {abarcosa,elise.vareilles,aldanondo,paul.gaborit}@mines-albi.fr
(2): TBC Générateur d'Innovation
25 Bvd Victor Hugo, 31770 Colomiers, France
E-mail : mfalcon@tbcinnovation.fr

Abstract: Layout synthesis algorithms in civil engineering have two major strategies called constructive and iterative improvement. Both strategies have been successfully applied within different facility scenarios such as room configurations and apartment layouts. The present paper contributes with layout synthesis field by developing a constraint-based algorithm for the layout design of building facades. This work is part of a French project called CRIBA whose goal is to industrialize the thermal renovation of apartment buildings. Conception of the renovation, generation of bill of materials and generation of the working site assembly process are then supported by our system. Details of the layout design algorithm and its underlying model are the core of this paper.

Key words: Computer aided design, layout synthesis, building renovation, constraint satisfaction problems, constraint-based algorithms

1- Introduction

As pointed out by Liggett in [L1], a layout configuration, commonly referred to as space planning or layout synthesis, "...is concerned with the allocation of activities to space such that a set of criteria (for example, area requirements) are met and/or some objective optimized...". Layout configuration algorithms have two major and often mixed strategies. The first strategy is called constructive and the seconde one iterative [L1]. The former follows an incremental approach, i.e., each activity (e.g. room, office, panel) is put in the space following a given criteria and, if all conditions are satisfied, the algorithm proceeds by placing the next activity until the construction of the entire layout has been done. The iterative improvement strategy, on the other hand, is based on the improvement of an already configured space that, although fulfill some requirements, does not satisfy all criteria.

Both strategies have been applied, for instance, in room configurations [ZT1], apartment layouts [LK1], activities within a business office [HH1] and finding an optimal configuration for hospital departments [E1]. Underlying models used in these approaches include but are not limited to evolutionary computation (genetic algorithms [TS1]), graph theoretic models (adjacency graphs [G1]) and constraint satisfaction problems (filtering algorithms [BF1,FB1]) .

Yet, regardless the considerable body of literature, most of the work share two commonalities. On the first hand, they attack problems in which the reference plane is parallel to the Earth, meaning that they do not deal with gravity or other natural forces that will, potentially, affect the layout design. On the other hand, in most cases the number of activities are known in advance, given the possibility to use existing algorithms to tackle the problem [E1,L1,LK1,TS1,ZT1]. Our problem, by constrast, deals with weights and geometric properties where the number of activities (panels) is unknown.

The present paper contributes with the layout synthesis field by developing a constraint-based algorithm for the layout design of building facades. This work is part of a French project called CRIBA whose goals is to industrialize the thermal renovation of apartment buildings. Conception of the renovation, generation of bill of materials and generation of the working site assembly process are then supported by a decision support system. The decision support system, and hence

1 The authors wish to acknowledge the Millet and SyBois companies, and all partners in the CRIBA project, for their involvement in the construction of the CSP model.

the algorithm, use the notion of Constraint Satisfaction Problems (CSPs) to describe relations among components [BF1,ZT1]. The presented algorithm deals with the geometry of facades and the weight of panels by using the knowledge of constraints inherent to any building facade and those improves performance at the implementation of the renovation.

The paper is divided in six sections. We present the context of the CRIBA project and the environment setup in Section 2. In Section 3, the constraint model describing the problem is introduced. Afterwards, we present the first version of the constraint-based layout generation algorithm in Section 4. An example illustrating the algorithm is drawn in Section 5. Finally, some conclusions are discussed in Section 6.

2- Context

The project CRIBA aims to industrialize high performance thermal renovation of apartment buildings [FF1,VB1]. This industrialization is based on an external new thermal envelope which wraps the whole building. The envelope is composed of prefabricated rectangular panels comprising insulation and cladding, and sometimes including in addition, doors, windows and solar modules. As a requirement for the renovation, facades have to be strong enough to support the weight added by the envelope. Elements taking part in the renovation are:

- Working site: Is the bigger spatial division in the renovation. It is commonly referred by a name and brings attached crucial aspects for the renovation process, e.g., accessibility constraints and weather. Such entity is divided into blocks.
- Block: Is a set of buildings attached by a common wall. A block has also accessibility constraints which has an impact on the configurable components.
- Building: This is the actual place where apartment are arranged. It is the host of several facades and have attached dimensions (height and width) which have an impact on the configurable components.
- Facade: A facade is a composition of apartments along with its doors, windows and so on. At the model level, a facade will be represented by a 2D coordinate plane which includes a set of rectangles defining frames, a set of lines defining supporting areas and rectangles defining zones out of configuration. For convenience, the origin of coordinates (0,0) is the bottom-left corner of the facade.
- Configurable components: At the current stage of the project, we only consider rectangular panels (Figure 1) that are attached to the facade by means of fasteners. In addition, the panels may come with rectangular frames (windows, doors or solar modules). Panels are prefabricated in the factory when the user inputs the renovation profile.

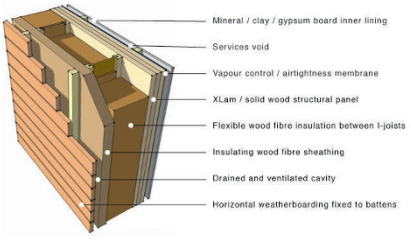

Figure 1 : Prefabricated panels.

Following the constructive approach, we establish what we consider a well-configured facade. A panel is well configured if it satisfies all its facade related constraints (presented in Section 3.2), i.e., has the right dimensions, can be hang on the facade, is consistent with the facade frames, does not overlap with other panels and if it does not interfere with other panels placement. A facade is said to be well configured if all its composing panels are well-configured and if they cover all facade area.

Consider the facade (a) in Figure 1 which represents a facade to be renovated. Horizontal and vertical lines represent the supporting areas in the facade. These are places in which we are allowed to attach weight-fasteners to supports panels. These fasteners will be put at the center of each supporting area because at these centers the weight supported by the fastener will be evenly distributed.

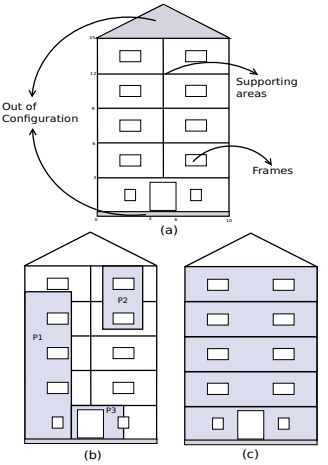

Figure 2 : Facade to renovate along with well and ill-configured panels.

Article 064-cad-83

As a constraint, distance between two fasteners is two meters minimum. Small rectangles in the facade are frames (e.g. windows and doors). Two zones are out the configuration: The gable and the bottom part before the first horizontal supporting area: Those parts need specific panels design.

Facade (b) in Figure 1 presents three ill-configured panels. This is due to the impossibility to place another panel north to the already placed panel *P1*, because there is not supporting areas at the corners of panel *P2* and, in the case of panel *P3*, because it partially overlaps a frame. Finally, the facade (c) in Figure 1 is well configured because it satisfy all criteria.

3- Model

Recall that a CSP problem is described in terms of a tuple $\langle V, D, C \rangle$, where *V* is a set of variables, *D* is a collection of potential values associated for each variable, also known as domains, and *C* is a set of relations over those variables, referred to as constraints. See [B1,M1] for further references.

3.1 – Variables

Following the CSP model, we have identified 16 variables that allow us to represent the core of the layout configuration for a given facade: The spatial positioning of panels. The list of constraint variables and their domains is presented in Table 1.

Variable	***Description***	***Domain***
w_{fac}	Facade width	[2,18] meters
h_{fac}	Facade height	[3,21] meters
e_{fac}	Environmental property	[easy, hard]
(p_{x0}, p_{y0})	Panel origin	$x0 \in [0, w_{fac}], y0 \in [0, h_{fac}]$
(p_{x1}, p_{y1})	Panel end	$x1 \in [0, w_{fac}], y1 \in [0, h_{fac}]$
w_p	Panel width	[0.9,13.5]
h_p	Panel height	[0.9,13.5]
(f_{x0}, f_{y0})	Frame origin	$x0 \in [0, w_{fac}], y0 \in [0, h_{fac}]$
(f_{x1}, f_{y1})	Frame end	$x1 \in [0, w_{fac}], y1 \in [0, h_{fac}]$
fai_{load}	Maximum weight load	[0,500]
X_{sa}	Vertical supporting areas	$\forall x \in X_{sa} \rightarrow x \in [0, w_{fac}]$
Y_{sa}	Horizontal supporing areas	$\forall y \in Y_{sa} \rightarrow y \in [0, h_{fac}]$

Table 1 : Model constraint variables.

From the above description we can deduce the constraints $p_{x0} < p_{x1}$ and $p_{y0} < p_{y1}$.

3.2 – Relations

First, in order to configure the layout of a given facade we use constraints to ensure relations over the variables representing components. In this section, we present the set of relevant constraints over panels and components w.r.t. the facade. The underlying CSP model we use is that of Disjunctive CSP [BF1]. Disjunctive CSP are boolean combination of atomic constraints (e.g. <,<=, >, >=). The canonical form of a disjunctive constraint is expressed as $C_i = (d_{i1} \vee d_{i2} \vee \ldots \vee d_{ik})$ where each d_i are atomic constraints connected by the $\wedge$ operator, $d_j = (c_{j1} \wedge c_{j2} \wedge \ldots \wedge c_{jk})$. Some of the constraints in our model follow this approach.

Environmental: Impact on domains from environmental properties are expressed as inequalities. The width w_p and height h_p of panels may be constrained because accessibility, transportation or wind difficulties (e.g. trees, water sources, only small trucks available or wind speed more than a given threshold). The following formula express these constraints:

$$(w_p \leqslant \Gamma) \wedge (h_p \leqslant \Theta) \wedge (e_{fac} = Hard) \qquad (1)$$

where Γ and Θ represents the upper bound for panel dimensions, width and height respectively.

Dimensions: The width w_p and height h_p of each panel is in the range [0.9,13.5] meters. However, this is actually a combination of values. For instance, it is possible to have a panel with dimensions 0.9x13.5, 3x8.4 or 13x2.6, but it is not possible to have one with dimensions 13.5x13.5, this is due to fabrication and transportation constraints. In consequence, we constraint the combination of values for the width and height of panels using

$$(w_p \in [0.9,3.5] \wedge h_p \in [0.9,13.5]) \vee (w_p \in [0.9,13.5] \wedge h_p \in [0.9,3.5]) \qquad (2)$$

Area: As a requirement, we have that the entire area of the facade must be renovated, provided it has the corresponding supporting areas. In consequence, a constraint

$$(w_{fac} \times h_{fac}) = \sum_{i=1}^{N} (w_{pi} \times h_{pi}) \qquad (3)$$

forcing the sum of panel areas to be equal to the facade area, is posted. The variable *N* is the number of panels covering

the facade.

Non-Overlap: In addition, we must ensure that panels do not overlap so we can have a valid solution. Thus, for each pair of panels p and q we define the non-overlap constraint using the formula

$$(p_{x1} < q_{x0}) \vee (q_{x1} < p_{x0}) \vee (p_{y1} < q_{y0}) \vee (q_{y1} < p_{y0}) \quad (4)$$

Weight: A given fastener in a supporting area is defined by its coordinates and its maximum weight load. Let ATP_i be the panels attached to the fastener fa_i and let *computerWeight(p)* be a function that returns the weight of panel p. This function uses the next values to calculate the weight of a panel: Dimensions of the panel, insulation type of the panel, weight of the frames within the panel (if any) and weight of any other component (e.g. solar modules). Constraint over panels weight is defined by

$$\sum_{j=1}^{|ATP_i|} computeWeight(ATP_i[j]) \leq fai_{load} \quad (5)$$

Borders: We shorten the width or height of a given panel if there exists a frame near to it. Either the panel overlaps the frame or the panel is right, left, up or down to the frame. This is a typical case addressed by disjunctive CSP. In any case, due to the internal structure of the panel, borders of frames and borders of panels must be separated by a minimum distance that we denote by Δ. These disjunctive constraints are model as

$$\begin{array}{l} (p_{x1} + \Delta \leq f_{x0}) \vee (p_{x0} - \Delta > f_{x1}) \vee \\ (p_{y1} + \Delta \leq f_{y0}) \vee (p_{y0} - \Delta > f_{y1}) \text{ and} \\ (p_{y0} + \Delta \leq f_{y0}) \wedge (f_{y1} \leq p_{y1} - \Delta) \wedge (p_{x0} + \Delta \leq f_{x0}) \wedge \\ (f_{x1} \leq p_{x1} - \Delta) \end{array} \quad (6)$$

4- Constraint-based Algorithms

Keep in mind that our problem, unlike other works, does not count with the number of activities (panels) in advance. Now, suppose that we want all possible panels configuration for a given facade. We could use an algorithm following a naive approach to solve the problem. In other words, an algorithm that, given either an arbitrary number of panels or testing all possible number of panels, does an extensive and complete search over the search space using constraint propagation and backtracking search.

Recall that the minimum width or height for a panel is 0.9 meters and its maximum is 13.5 meters. Then, the maximum number of panels that can be placed in a given axis is length/0.9. On the other hand, the minimum number of panels that can be fixed in a given axis is length/13.5 if length module 13.5 is equal 0 and length/13.5+1 otherwise. Let $[min_v, max_v]$ and $[min_h, max_h]$ be the minimum and maximum number of panels that may be fixed in the vertical and horizontal axis, respectively. A naive algorithm could use each possible combination of values starting from the minimum until either find a solution or reach the maximum allowed. This algorithm would work as follow.

Panels are created with valid domains both in coordinates and dimensions. Then, all panels are constrained with the *Non-Overlap* constraint (4). Afterwards, a constraint stating that all facades area is equal to the summation of all panels areas is posted, i.e., *Area* constraint (3). Using the *Non-Overlap* constraint (4) and the *Area* constraint (3) the algorithm ensures that all the facade is covered and configured. Indeed, up to now this CSP, although does not have a trivial complexity due the *Non-Overlap* constraint (4), could be efficiently solved by backtracking search. Notice, however, that we are not taking into account frames nor supporting areas which are, in fact, the most complex relations in our model.

Suppose now that we have found several solutions to the previous CSP. If we want to get the solutions that respect the positions of frames, we have to add to our constraint model the disjunctive constraint between frames and panels (see *Borders* constraint (6) in Section 3.2). Suppose there exists 8 frames in the facade. Also, suppose that we can cover the facade with 15 panels, lets say a 5x3 configuration. Lets consider the constraints over one frame with one panel. Valid positions for the panel can be at the right, left, up or down side of the frame; no overlapping in at least one axis. In addition, the panel can surround the frame; completely overlapping the frame. Thus, we have 5 possibilities. Now, all 15 panels have to be constrained against the same frame which will result in $5^{15} = 30517578125$ possible configurations. Of course, with 8 different frames this value becomes even bigger.

Nevertheless, it turns out that this number can be significantly reduced by reducing the number of relations frame-panel. Given that frames are fixed holes in the facade, we can choose 8 panels to satisfy the disjunctive constraint (6) *Borders* w.r.t. the 8 frames. Furthermore, we know that any panel is as good as any other to cover the frame, thus, we can remove symmetries by applying each atomic constraint to one and only one panel: Force a panel to take a given position.

Given the complexity added when configuring a panel w.r.t. frames, we develop an algorithm that does not deal with such complexity. This algorithm combines the constructive and iterative improvement approaches and makes use of the constraints of our model. It is worth noting that this

algorithm will not generate only one configuration but many different configurations satisfying the criteria. The main characteristic of the algorithm is the use of global constraints to narrow possibilities and the use of loops to incrementally add panels if a given number of them is not enough to cover all the facade area.

Step 1. Create a number of panels, n_p , equal to the number of frames and constraint their placement to surround each frame, i.e., for each pair frame *i* and panel *j* post the right part of *Borders* constraint (6).

Step 2. Constraint the coordinate y_0 for all panels to be aligned with a horizontal supporting area using the collection Y_{sa} , i.e., $p_{y0} = Y_{sa}$ for each panel *p*.

Step 3. Post the *Non-overlap* constraint (4) over all panels.

Step 4. Impose that the summation of all panels areas is equal to the facade area (see *Area* constraint (3) in Section 3.2). If this constraint is inconsistent, then current panels are not enough to cover all the facade area. In this case go to Step-5. In the other case go to Step-6.

Step 5. Calculate an optimal number of panels to add to the configuration, lets call it *extra*, using the area still not covered as criterion. Start again the process from Step 1 with $n_p + extra$ panels, i.e., backtrack.

Step 6. At this stage there exist many solutions satisfying all constraints but that regarding the *Weight* constraint (5). Take one of these solutions.

Step 7. Inject *Weight* constraint (5) (Section 3.2) in the selected solution. If the constraint is satisfied then return the valid solution and go to Step-6. Otherwise go back to Step-6 until a solution is found or until exhaustion.

5- Illustrations

An illustration of the algorithm is presented in Figure 2. Literal (a) of the figure presents the facade, its frames and supporting areas. Afterwards, in literal (b), it shows many, but not all, possibilities of panel positions when the algorithm forces each panel to cover each frame. Following, the algorithm constraints the base of the panel to be aligned to an horizontal supporting area, literal (c). Next, the non-overlap constraint is posted, as presented in literal (d). Finally, after adding extra panels, all the facade area is covered using the *Area* constraint, literals (e) and (f).

Unlike the naive algorithm, the algorithm using global constraints avoids the problem of placing panels w.r.t. frames by constructing a valid partial solution and using the constraint non-overlap. Global constraints make possible to find many different and valid configurations of panels.

In addition, the parametrization of this algorithm makes it possible to generate different layout configurations. For instance, if a constraint such as $h_{pi} = w_{pi}$ is added, the configuration will be drawn with square panels only. Another parameter could be the minimum number of frames covered by a given panel, in this scenario a reduced number of panels will be generated.

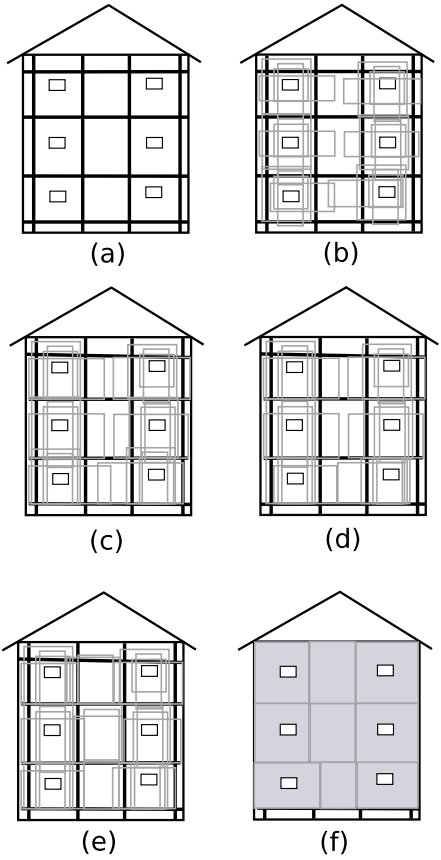

Figure 3 : Configuration example.

Now let us present results of the algorithm in real-world scenarios. Figure 3 and Figure 4 present two facades in the commune Saint-Paul-lès-Dax in the department of Landes, France. These facades are part of a 5-block working site called La Pince. Each figure presents in its literal (a) the structure of the facade. In literal (b) the figures present the facade configured with vertical panels and in literal (c) the facade configured with horizontal panels. In both cases, the panels try to overlap up-to four frames in order to use as few as possible panels (how many frames are covered by a panel and its orientation are optional soft constraints).

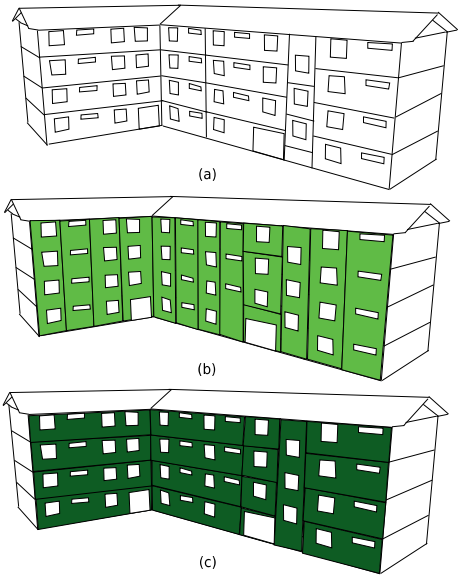

Figure 4 : La Pince: Facade 1.

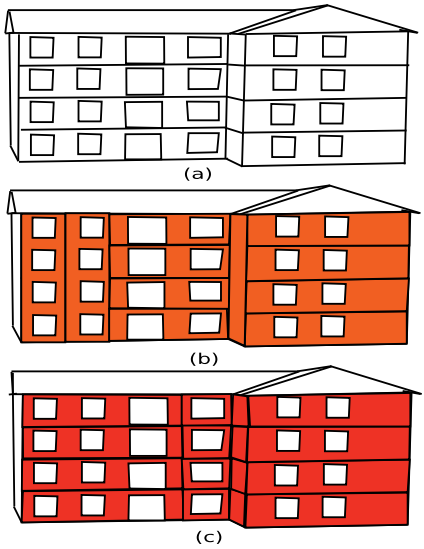

Figure 5 : La Pince: Facade 2.

6- Remarks

In the present document we have shown a constraint-based algorithm for the layout synthesis of building facades. This work is part of a French project called CRIBA: A joint effort between academics at Ecole des Mines d'Albi - Carmaux and several French companies. Essentially, it investigates the possibility of automated building renovation based on prefabricated rectangular panels and supported by a decision support system. Conception and implementation for the renovation of building facades in smart cities are then improved. In addition, the algorithm presented in the paper contributes with the field of layout synthesis and civil engineering discipline.

Previous works on industrial scenarios have prove benefits of CSP modelling. In particular, the constrained nature of configuration processes makes clear that techniques on CSP field are mature enough to be used in big scale problems. For instance, in [BF1] authors use Disjunctive CSP to the assignment of house activities (e.g. kitchen, bathroom, etc) to a given space. Among the same lines is a work presented in [ZT1] which does not only address the layout of a given apartment floor but the entire configuration of an apartment with several floors. Another example of CSP in configuration

processes is shown in [VA1], a CSP approach is combined with a case-based reasoning approach in order to configure the maintenance process of helicopters.

Nonetheless, although several layout configuration models have been proposed in previous works, we consider that literature needs more effort in this field in order to widespread the use of optimization techniques, such as constraint programming, in the industry world. This work is part of these efforts.

Future work: For the layout configuration algorithm, we propose several improvements to facilitate the generation of several layout configurations.

- Minimize the number of panels used. This implies that the number of frames covered by panels may vary among panels.
- Take into account holes that are not going to be renovated (e.g. balconies).
- Consider small distances introduced by the glue used to joint two consecutive panels.

7- References

[B1] Bartak R.. Constraint Programming: In Pursuit of the Holy Grail. In: Proceedings of the Week of Doctoral Students (WDS) (Jun 1999)

[BF1] Baykan C.A. and Fox. M.S. Spatial synthesis by disjunctive constraint satisfaction. Artificial Intelligence for Engineering, Design, Analysis and Manufacturing 11, pp. 245–262 (9 1997)

[BP1] Brailsford, S.C., Potts, C.N. and Smith, B.M. Constraint satisfaction problems: Algorithms and applications. European Journal of Operational Research 119(3), pp. 557 – 581 (1999)

[C1] Charman, P. Solving space planning problems using constraint technology (1993)

[E1] Elshafei, A.N. Hospital layout as a quadratic assignment problem. Operational Research Quarterly 28(1), pp. 167–179 (1977)

[FF1] Falcon, M. and Fontanili, F. Process modelling of industrialized thermal renovation of apartment buildings. eWork and eBusiness in Architecture, Engineering and Construction, European Conference on Product and Process Modelling (ECPPM 2010) pp. 363–368 (2010)

[FB1] Flemming, U., Baykan, C., Coyne, R. and Fox, M. Hierarchical generate-and-test vs constraint-directed search. In: Gero, J., Sudweeks, F. (eds.) Artificial Intelligence in Design '92, pp. 817–838. Springer Netherlands (1992)

[G1] Goetschalckx, M. An interactive layout heuristic based on hexagonal adjacency graphs. European Journal of Operational Research 63(2), pp. 304 – 321 (1992)

[HH1] Hassan, M.M.D., Hogg, G.L. and Smith, D.R. Shape: A construction algorithm for area placement evaluation. International Journal of Production Research 24(5), pp. 1283–1295 (1986)

[LK1] Lee, K.J., Kim, H.W., Lee, J.K. and Kim, T.H.: Case- and constraint-based project planning for apartment construction. AI Magazine 19(1), pp. 13–24 (1998)

[L1] Liggett, R.S. Automated facilities layout: past, present and future. Automation in Construction 9(2), pp. 197 – 215 (2000)

[M1] Montanari, U. Networks of constraints: Fundamental properties and applications to picture processing. Information Sciences 7(0), pp. 95 – 132 (1974)

[TS1] Tate, D.M. and Smith, A.E. A genetic approach to the quadratic assignment problem. Computers and Operations Research 22(1), pp. 73 – 83 (1995)

[VA1] Vareilles E., Aldanondo M., Codet de Boisse A., Coudert T., Gaborit P. and Laurent Geneste. How to take into account general and contextual knowledge for interactive aiding design: Towards the coupling of CSP and CBR approaches 25(1), pp. 31–47 (2012)

[VB1] Vareilles, E., Barco, A.F., Falcon, M., Aldanondo, M. and Gaborit, P.: Configuration of high performance apartment buildings renovation: a constraint based approach. In: Conference of Industrial Engineering and Engineering Management (IEEM). IEEE. (2013)

[ZT1] Zawidzki, M., Tateyama, K. and Nishikawa, I. The constraints satisfaction problem approach in the design of an architectural functional layout. Engineering Optimization 43(9), pp. 943–966 (2011)

Article 028-itm-106

Towards Management of Knowledge and Lesson Learned In Digital Factory

Marwa BOUZID[1,2], Mohamed AYADI[1], Vincent CHEUTET[2], Mohamed HADDAR[1]

(1) : LA2MP/ENIS
B.P 1173
w.3038 Sfax – Tunisie
+216 74 666 535
E-mail : ayadi1med@yahoo.com,
mohamed.haddar@enis.rnu.tn

(2) : LISMMA / SUPMECA
3 rue Fernand Hainaut
93400 Saint-Ouen – France
+33 1 49 45 29 38
E-mail :
{marwa.bouzid,vincent.cheutet}@supmeca.fr

Abstract: In a world characterized by increasing competitiveness, delivering a good product as soon as possible and increasing complexity of the product, the old method did not satisfy the needs of companies. In this context the Digital Factory is a solution that is based on the simulation and analysis of all the process of product production to reduce the cost of prototyping and physical testing. But, despite his performance there is a lack of deployment related to the lack of integration of information, knowledge and feedback.

So in this article we proposed a model that includes the integration of all the information, knowledge and Lesson Learned.

Key words: Digital Factory, Lesson Learned, Knowledge Management, Simulation, Information System.

1- Introduction

To evolve in the current economic environment, companies must achieve increasingly higher performance levels. To achieve this aim, they are showing adaptability and responsiveness, while continually seeking quality improvement. In order to survive, organizations are challenged to faster design, develop and produce cheaper products that meet user's requirements. But it is not enough to make the right product or good service, it must be better than the competition provides.

In this context of collaborative engineering, the digital prototyping (based on the concepts of digital models representing the product, its physical behaviour, and its manufacturing process) is a solution to test and validate a product earlier in its lifecycle [H1]. The simulation, associated to these digital prototypes, becomes an essential tool to avoid unexpected problems occurring during upstream phases of the product lifecycle, and so it allows reducing time spent in the product design project by helping the decision making process.

In particular, **Digital Factory** (DF) was born to design and simulate production systems throughout the product design process. It can be defined as a set of software tools and methodologies allowing the design, simulation, initiation and optimization of production systems [BM1], [CM1], [K1]. This approach, originating from concurrent engineering and from Computer Integrated Manufacturing (CIM), aims to reduce validation loops by ensuring, as early as possible in the product lifecycle, integration of the product manufacturability and productibility with business constraints.

Despite the high performance of simulation tools in digital manufacturing [CK1], there is a lack of deployment related to [AC1], [NL1]:

- The intrinsic complexity of DF, due to the different levels of detail co-existing (from the operation on a specific station to the global supply chain) [WE1] and to the variety of simulation type (prescriptive vs. based on events) [AC1],
- The absence of integration of information and knowledge from previous projects simulation of production systems,
- A lack of exchanged information with other enterprise services and their information systems, especially ERP and PDM.

The management of information and knowledge between the product and its production process, including data related to resources, is essential. Indeed, the solution adopted for product development is to integrate different types of information and knowledge (product, process and resources) as soon as possible to make the right decisions at the right time.

As a consequence, the main objective of our research work is to model and implement a framework for the management and the control of data, information and knowledge for digital design and production, allowing to manage and

improve the possible simulations of DF, and also focusing on knowledge capitalization and experience feedback towards the new Digital Factory projects.

The article is structured as follows. Section 2 presents a study of art state: first, we define digital manufacturing and information systems then knowledge management. Section 3 describes the proposals. Finally, Section 4 presents the conclusions.

2- State of the art

2.1 – Digital Factory

By definition, Digital Factory is attached to the simulation of the production system according to a product development process. Even if, according to the Moore's law, the computational power is currently growing roughly at an exponential rate, the simulation complexity is approximately growing with the same rate [HH1].

As a consequence, the notion of **granularity** is important in order to define a simulation easy to develop and likely to obtain concrete results, according to the amount of information and its maturity known at a given time of the PDP. For instance, the authors of [BF1] propose a three-stage approach to equilibrate the simulation effort with expected precision of simulation results:

- Calculation: approximate calculation of the system capacity
- coarse simulation with a custom standard modules based on standardized modules approach
- Detailed simulation, specific aspects of the production system are examined by exact models

Generally a detailed simulation requires a significant development time, or a coarser simulation does not take into account the important details. It may prove necessary to eventually leave the choice of simulation detail level based on actual needs of product's development process actors [AC1].

In this context, the projects Digital Factory and Digital Factory 2 [B1], from the SYSTEM@TIC Paris-Region cluster, have proposed a structured representation of the Digital Factory on six levels of details, corresponding to an aeronautic vision of the extended enterprise (figure 1).

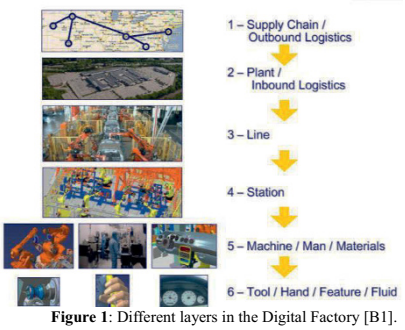

Figure 1: Different layers in the Digital Factory [B1].

These layers correspond to specific needs for the design and simulation of the production system behaviour, and so to specific actors of the production system development process, with their own tools and methodologies. For example, at level 1 or 2, the objective can be to determine the physical supply flows inside the extended enterprise. At level 3, the objective can be to validate a physical layout inside the plant and a line rate. At level 5 or 6, the objective can be to validate the settings of a manufacturing program in the production environment (robots, CNC machining, etc.).

Digital Factory is based on a large number of heterogeneous simulation tools based on different levels representation of the production system. It is therefore possible to perform a simulation of flow line production to determine inventory levels necessary to satisfy the needs of customers, or the simulation of a machining operation on a workstation, for conceive and validate the offline programming of the digital control.

For each level of detail, there are specific simulation tools corresponding to specific actors. In figure 2, two principal families of simulation tools which can be used in the Digital Factory [CL1]:

- Based simulation of events: it is constituted by elements that react to certain events
- Prescriptive simulation: it describes the behaviour of the production system over time

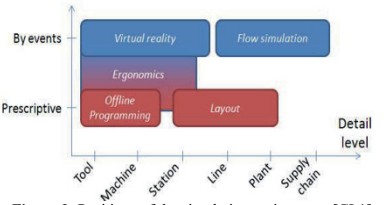

Figure 2: Positions of the simulation major types [CL1].

2.2 – Information System for Digital Factory

Based on this diversity of software tools and simulation objectives, information management between the product and its production process including data related to resources is so essential and requires a specific **Information System**.

An information system can be defined as a set of individual or collective instruments participating in the process of information management in the organization [R1]. Another definition has been proposed by [C1]: "an information system is a set of resources organized for the collection, storage, treatment, maintenance, use, sharing and dissemination, making available, display or transmission of information". Resources are defined as personnel, equipment, budgets and information technology. Thus, the main goal of the information system is to provide every actor in the organization with all the information about its current or previous situation.

In this context, the "perfect" information system should be

dedicated to the integration and the management of information related to the product/process simulation throughout the first phases of product lifecycle. Such information system must be able to integrate different **views** (design, production and simulation) [GY1], [KV1], from different information systems used in design and production phases.

The main existing IS are actor-oriented, i.e. defined for a particular point of view. In the context of our study, we classified them into three families:

- IS dedicated to the product design process and especially the **Product Data Management** (PDM) [EG1], [DC1],
- IS dedicated to the production process and especially the **Enterprise Resource Planning** (ERP) [KA1], [BM2],
- IS dedicated to the simulation management and especially the **Simulation Lifecycle Management** (SLM) [PR1], [L1].

Moreover, few approaches [FH1] and some software (for instance DELMIA Process Engineer from Dassault Systèmes or Windchill MPMLink from PTC) have been proposed in the context of DF, namely the Manufacturing Data Management (MDM) systems.

Despite the development of such IS, these systems are focusing on specific areas of the company. Until now, there is not an IS covering all information necessary for overall product's decision making, in addition there is a lack of interoperability between these different tools.

InfoSim is a IS dedicated to manage information on simulations in digital factory [AC1]. Its objective is the integration of product's information, production processes and simulation.

Thus, InfoSim enables to integrate product's information, production process and simulation. Through this integration, the actors who can be part of different departments of a company have a better visibility of the project evolution of product development, and access to different information, which will help them make better decisions in soon as possible.

Nevertheless, InfoSim only allows the integration of data and information related to the product, process and simulation but not the integration of knowledge and experience from previous projects. So there is a lack of exchange and transfer of knowledge between all actors PDP.

2.3 – Knowledge Management for Digital Factory

A lot of companies sought to valorise intangible investment (research and development, training, advertising, organizational methods, etc...). And, in particular, their knowledge capital. Knowledge has become a major concern for companies and organisations; knowledge mastery replaces, at least in part, to industrial mastery [BT1], [L2], [U1].

The **information** is considered as treated **data**, it is an aggregation of data that have meaning, which implies that the facts were placed in a context which was organized for a goal [E1], [T1]. **Knowledge** is based on contextual, relevant and exploitable information. Knowledge is information with additional details regarding how it should be used or applied.

Knowledge is unavailable directly: it is obtained by the interpretation of the information deduced from the analysis of data. Data are available to an organization in the form of observations, calculation results, etc. The interpretation, abstraction or combination of these data leads to the production of information. Finally, knowledge is obtained through experience and learning of this information [CR1].

In this context, literature expresses two different types of knowledge: explicit one and tacit one.

Explicit knowledge refers to knowledge transmitted through a "formal and systematic" language [L3]. It is the result of an extraction of a knowledge part of enterprise memory (rules, stored experiences and feedback from experience) [FB1].

Tacit knowledge refers to know-how that is difficult to formalize and communicate and can not be transferred that by the willingness of people to share their experiences, it is usually acquired over a long period of learning and experience [CR1], [L3]. It is owned by actor useful in completing the task and not in shared memory. This part of the knowledge comes from learning, intuition and experience. Unfortunately, this knowledge is also lost with the loss of the person or team of the organization.

Experience is defined as "an event experienced by a person that may bring a teaching" [R1]. This experience of an individual or group of individuals, resulting in one or information related to a given context. This information therefore includes:

- The situation in which the event appeared
- The description of the event
- The lessons learned by the individual or group who experienced it

Experience is the result of the implementation of know-how in previous projects. It specifies the use of knowledge well as the result of use in qualitative term. We thus find sometimes the terms of positive experience (or best practice) and negative experiences (mistakes to avoid) [FB1].

The Lesson Learned is the result of an analysis of the experience and aimed at to discover the cause of the judgment on the activity and designed to lead to a change in the behaviour of individuals [FB1].

Today companies of all kinds and all sizes are interested in the preservation of knowledge and methods of **Knowledge Management** (KM). Grundstein in [G1] defines KM as the management of activities and process supposed to amplify the use and creation of knowledge inside an organization according two complementary purposes, strongly connected: a legacy purpose and a purpose of sustainable innovation. These methods so aim to capitalize knowledge and experience available within a company and ensure their transmission. We can summarize clearly the aim of the KM operation with: "Getting the right knowledge to the right people at the right time in the right size without being asked"

Article 028-itm-106

[L3].

So, KM leads to the usage of a set of tools and methods to better use the knowledge and knowledge potentially available to an organization with the aim to improve storage capacities, learning, collaboration and innovation through better management of its intellectual and informational assets.

According to [ML1], two main approaches exist in KM: **codification** approaches, which focus on the reification of knowledge, and **personalisation** approaches, which focus on individuals as holders of knowledge.

Personalisation approaches cover the various knowledge transformation mechanisms as applied within an individual or between individuals (Figure 3) when they are freely expressed and lead to solutions oriented towards practices communities [AR1] as well as CSCW-type (Computer-Supported Collaborative Work) tools [K2]. Codification approaches cover the elicitation of knowledge in a controllable form beyond the actual individual and are, for the most part, based on information and communication technology [CH1].

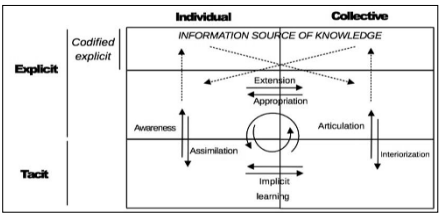

Figure 3: Extension of knowledge transformation mechanisms in an encoded environment [B2].

In this context and according to the type of KM approaches chosen, several types of tools have been developed for various applications [CR1], [L2], [VB1]. These tools allow you to manage all the knowledge of the organization actors, in order to have a better exploitation. One can cite as KM tools:

- General Tools and methods for the formal and informal exchange of knowledge
- KM Tools for knowledge capitalization
- KM tools for knowledge sharing
- KM tools for retrieving knowledge
- KM tools for query

In the literature, we find that knowledge management and simulation are separate, but in reality they are inseparable in practice. The data obtained from the simulation model after testing and analysis can generate new knowledge.

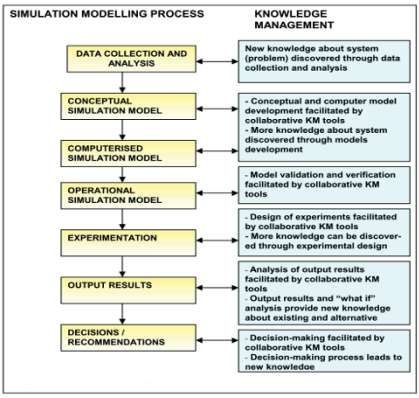

Figure 4: Interdependencies between simulation modelling process and KM [HV1].

Figure 4 shows how knowledge management is linked to the simulation process.

During these processes, new knowledge can be discovered and can be used for problem solving and decision making. Simulation models can be used to study the processes of knowledge management, knowledge flows and processing activities of knowledge, to simulate missing data necessary for the management of knowledge, or to evaluate alternative models of strategies knowledge management [HV1] and the effect of new knowledge management practices on business processes [LH1]. Figure 5 shows them.

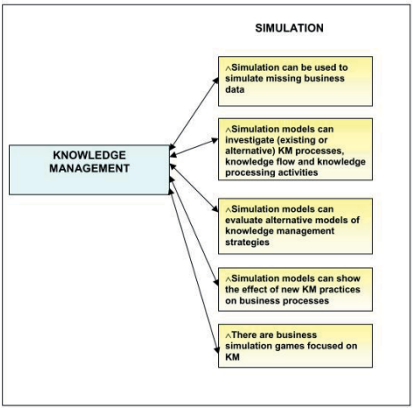

Figure 5: Simulation models in the context of knowledge management [HV1].

The use of knowledge management with simulation has several advantages, which is why the researchers are interested in combining these two approaches.

Edwards and Alifantis are presented a simulation model as part of the knowledge elicitation process in a project simulating maintenance operations in an automotive engine production facility [EA1].

Canals, Boisot and MacMillan develop an evolutionary agent-based simulation model derived from a knowledge-based theoretical framework, and use it to explore the effect of knowledge management strategies on the evolution of a group of knowledge-intensive organizations located in a given geographical area [CB1].

Srinivasan and Horowitz propose the use of simulation as a tool for assessing the quality of an analytical knowledge management model constructed using a technique called Root Causes Analysis (RCA) Modelling, generically known as Structural Equation Modelling [SH1].

Thus, the digital factory needs a model that uses the applications of knowledge management tools in the study of process simulation.

3- Propositions

All companies are based on the learning capacity of its staff. The lessons learned and the transfer of knowledge is the keys to this success.

Proposition 1: An information model that can capitalize on and manage knowledge of design, production and simulation. The model is based on the collection and storage of information, after we will interpret this information to create knowledge of the company.

Our model will contain transformation knowledge, specific knowledge and lesson learned.

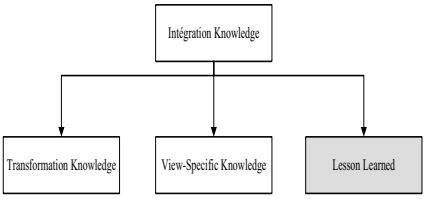

Figure 6: Some top-level classes of Integration knowledge.

Transformation knowledge is knowledge that allows the navigation information from a phase to another: requirement to concept, concept to function, function to process and process to simulation, it allows the transformation of information between views such as the functional view information transformed to assembly view information from explicit knowledge.

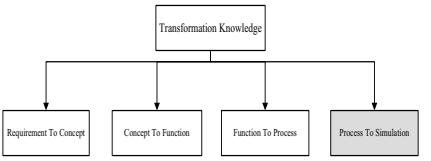

Figure 7: Some top-level classes of transformation knowledge.

Specific knowledge is the specific knowledge resources (machines, tools, etc.) that will transform product view information to manufacturing view information and validate the operation, such as specific knowledge of machine will transform information of the sub-functional and assembly views of to the machining view and validated against machining view-point considerations.

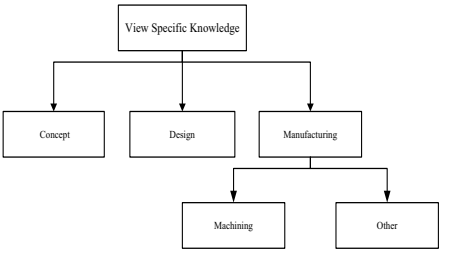

Figure 8: Some top-level classes of View Specific knowledge.

Lesson Learned is the knowledge created through the collection and interpretation of information which can be validate with simulation [AC1], the results of interpretation of this information either by validation or not, will create new knowledge which is crucial in new projects.

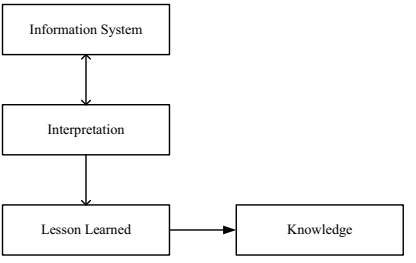

Figure 9: knowledge creation from Lesson Learned.

Class Lesson Learned is divided into two sub-classes: sub-class reserved for results and sub-class reserved for errors.

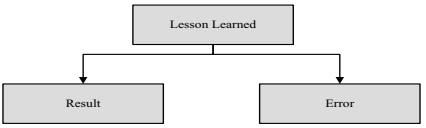

Figure 10: Some top-level classes of Lesson Learned.

4- Conclusion

The old methods for product development didn't satisfy the needs of companies that are summarized in the implementation of an innovative and fast development cycle. So in this paper we showed the use to other method which is the management of knowledge and feedback. After recalling the meaning of certain central terms of this method we proposed a model that allows the integration of all information, explicit and tacit knowledge and feedback to facilitate the transformation of information between all actors of PDP and the validation of process.

5- References

[AC1] Ayadi M., Costa Affonso R., Cheutet V., Masmoudi F., Riviere A., Haddar M. Conceptual Model for Management of Digital Factory Simulation Information. International Journal of Simulation Modelling, 12(2):107-119, 2013.

[AR1] Amin A., Roberts J. Knowing in action: Beyond communities of practice. Research Policy, 37(2):353-369, 2008.

[B1] Boime B. Le projet Usine numérique : Un projet du pôle de compétitivité SYSTEM@TIC Paris Région. Revue internationale d'ingénierie numérique, 1(4):393-402, 2005.

[B2] Baumard P. Tacit knowledge in organizations. Sage publication Ltd, 1999.

[BF1] Bley H., Franke C. Integration of Product Design and Assembly Planning in the Digital Factory. CIRP Annals - Manufacturing Technology, 53(1):25-30, 2004.

[BM1] Bracht U., Masurat T. The Digital Factory between vision and reality. Computers in Industry, 56(4):325–333, 2005.

[BM2] Botta-Genoulaz V., Millet P., Grabot B. A survey on the recent research literature on ERP systems. Computers in Industry, 56(6):510-522, 2005.

[BT1] Bernard A., Tichkiewitch S. Methods and tools for effective knowledge life-cycle management. Springer, 2008.

[C1] Committee on National Security Systems. National Information Assurance (IA) Glossary, 2006.

[CB1] Canals A., Boisot M., MacMillan I. Evolution of knowledge management strategies in organizational populations: a simulation model. Working paper series: WP04-007, 2004.

[CH1] Chen Y.Y., Huang H.L. Knowledge management fit and its implications for business performance: A profile deviation analysis. Knowledge-Based Systems, 27:262-270, 2012.

[CK1] Coze Y., Kawski N., Kulka T., Sire P., Sottocasa P., Bloem J. Virtual concept real profit with digital manufacturing and simulation. Dassault Systèmes and Sogeti, ISBN 9789075414257, 2009.

[CL1] Cheutet V., Lamouri S., Paviot T., Derroisne R. Consistency management of simulation information in Digital Factory. Proceedings of 8th International Conference of Modeling and Simulation (MOSIM'10), Hammamet (Tunisia), 2010.

[CM1] Chryssolouris G., Mavrikios D., Papakostas N., Mourtzis D., Michalos G., Georgoulias K. Digital manufacturing: history, perspectives, and outlook. Proceedings of the I MECH E Part B Journal of Engineering Manufacture, 223:451-462, 2009.

[CR1] Chandrasegaran S.K., Ramani K., Sriram R.D., Horváth I., Bernard A., Harik R.F., Gao W. The evolution, challenges, and future of knowledge representation in product design systems. Computer-Aided Design, 45:204–228, 2013

[DC1] Do N., Chae G. A product data management architecture for integrating hardware and software development. Computers in Industry, 62(8-9):854-863, 2011.

[E1] Elgh F. Supporting Management and Maintenance of Manufacturing Knowledge in Design Automation Systems. Advanced Engineering Informatics, 22:445–456, 2008.

[EA1] Edwards J.S., Alifantis T., Hurrion R.D., Ladbrook J., Robinson S., Waller A. Using simulation model for knowledge elicitation and knowledge management. Simulation Modelling Practice and Theory 12, 527 – 540, 2004.

[EG1] Eynard B., Gallet T., Roucoules L., Ducellier G. PDM system implementation based on UML. Mathematics and Computers in Simulation, 70(5-6):330-342, 2006.

[FB1] Faure A., Bisson G. Gérer les retours d'expérience pour maintenir une mémoire métier, étude chez PSA Peugeot Citroën.

[FH1] Fortin C., Huet G. Manufacturing Process Management: iterative synchronisation of engineering data with manufacturing realities. International Journal of Product Development, 4(3/4):280-295, 2007.

[G1] Grundstein M. De la capitalisation des connaissances au management des connaissances dans l'entreprise. Chapitre 1 dans Management des connaissances en entreprise, Edition Hermès Science, Pages 25-54, 2004.

[GY1] Gunendran A.G., Young R.I.M. An information and knowledge framework for multiperspective design and manufacturing. International Journal of Computer Integrated Manufacturing, 19(4):326-338, 2006.

[H1] Hoppmann J. The Lean Innovation Roadmap - A Systematic Approach to Introducing Lean in Product Development Processes and Establishing a Learning Organization. PhD University of Braunschweig, 2009.

[HH1] Hägele J., Hänle U., Kropp A., Streit M. The CAE-Bench project – A web-based system for data, documentation and information to improve simulation processes. Available

from:
http://www.mscsoftware.com/support/library/conf/auto00/p03300.pdf, 2010.

[HV1] Hlupic V., Verbraeck A., Vreede G.J. Simulation and knowledge management: separated but inseparable? In Verbraeck, A. and Krug, W. (eds.), Proceedings 14 th European Simulation Symposium, 2002.

[K1] Kühn W. Digital Factory – Integration of simulation enhancing the product and production process towards operative control and optimisation. International Journal of Simulation Systems, Science & Technology, 7(7):27–39, 2006.

[K2] Karacapilidis N. Modeling discourse in collaborative work support systems: A knowledge representation and configuration perspective. Knowledge-Based Systems, 15(7):413-422, 2002.

[KA1] Kelle P., Akbulut A. The role of ERP tools in the supply chain information sharing, cooperation, and cost optimization. International Journal of Production Economics, 93(94):41-52, 2005.

[KV1] Koning H., van Vliet H. A method for defining IEEE Sdt 1471 viewpoints. Journal of Systems and Software, 79(1):120-131, 2006.

[L1] Lalor P. Simulation life-cycle management: Opens a New Window on the Future of Product Design and Manufacturing. Bench mark, october, 2007.

[L2] Louis-Sidney L. Modèles et outils de capitalisation des connaissances en conception - Contribution au management et à l'ingénierie des connaissances chez Renault – DCT. PhD Ecole Centrale Paris, 2011.

[L3] Lalouette C. Gestion des connaissances et fiabilité organisationnelle : état de l'art et illustration dans l'aéronautique. Les Cahiers De La Sécurité Industrielle, 2013.

[LH1] Luban F., Hîncu D. Interdependency between Simulation Model Development and Knowledge Management. Theoretical and Empirical Researches in Urban Management, Number 1(10)/2009.

[ML1] McMahon C., Lowe A., Culley S. Knowledge management in engineering design: personalization and codification. Journal of Engineering Design, 15(4):307-325, 2004.

[NL1] Nagalingam S.V., Lin G.C.I. CIM—still the solution for manufacturing industry. Robotics and Computer-Integrated Manufacturing, 24(4):332–344, 2008.

[PR1] Popielas F., Ramkumar R., Tyrus J., Kennedy B. Simulation Life Cycle Management as Tool to Enhance Product Development and its Decision-Making Process for Powertrain Applications. USA, 2010.

[R1] Rakoto H. Intégration du Retour d'Expérience dans les processus industriels. PhD ENI Tarbes, 2004.

[SH1] Srinivasan A., Horowitz B.M. Use of simulation experiments to evaluate knowledge management modeling quality. Journal of Knowledge Management Practice, Volume 5, (2004).

[T1] Tsuchiya S. Improving Knowledge Creation Ability through Organizational Learning. International Symposium on the Management of Industrial and Corporate Knowledge (ISMICK), Compiègne, 1993.

[U1] United Nations Educational, Scientific and Cultural Organization (UNESCO). 2005. Towards Knowledge Societies.
http://www.unesco.org/new/en/unesco/resources/online-materials/publications/unesdoc-database/ (Lien validé en décembre 2012).

[VB1] Verhagen W.J.C., Bermell-Garcia P., van Dijk R.E.C., Curran R. A critical review of Knowledge-Based Engineering: An identification of research challenges. Advanced Engineering Informatics, 26:5–15, 2012.

[WE1] Wiendahl H.P., Elmaraghy H.A., Nyhuis P., Zäh M.F., Wiendahl H.H., Duffie E.N., Brieke M. Changeable Manufacturing - Classification, Design and Operation. CIRP Annals - Manufacturing Technology, 56(2):783–809, 2007.

4

Geometric Modelling and CAD

Major topics of the full argumentations are the following:

X. Fischer et al. (eds.), *Research in Interactive Design (Vol. 4)*
DOI 10.1007/978-3-319-26121-8_14

Article 063-cad-26

IDENTIFICATION OF TREE SPECIES FROM AIRBORNE LIDAR POINT CLOUDS. EARLY APPROACHES.

Santamaría, J. [1], Valbuena, M.A. [2], Sanz, F. [3], Arancón, D. [4], Martínez, A.[5] ,

(1) : University of La Rioja (Spain)
Phone/Fax: +34 941 299 530
E-mail : jacinto.santamaria@unirioja.es

(2) : Department of Education. Basque Government (Spain)
E-mail : mavalbuena66@gmail.com

(3) : University of La Rioja (Spain)
Phone/Fax: +34 941 299 533
E-mail : felix.sanz@unirioja.es

(4) : University of La Rioja (Spain)
Phone/Fax: +34 941 299 535
E-mail : david.arancon@unirioja.es

(5) : University of La Rioja (Spain)
Phone/Fax: +34 941 299 533
E-mail : albertoclarinet@hotmail.com

Abstract: LIDAR flights with multi-objective are every day more widespread. Governments are aware of the high potential that can be derived from point clouds obtained from these flights.
One of the major fields in which applications are developed is the agroforestry field, especially related to forest management of large numbers of trees. Quickly parameters forests and even individual trees are achieved. **[DW1] [ME1]**
In this paper, we intend to initiate a new guidance on the use of LIDAR data in order to identify tree species through the envelope profile of the cloud of points composing each individual tree. The projection of the point cloud of individual trees and the study of their convex hull, will characterize a given forest stand and assign a particular species.
The method used is based primarily on the analysis of two-dimensional projection of the point cloud of an individual tree and obtaining their convex hull. The study of the geometrical characteristics of said envelope to a representative number of trees and their association with forest parameters such as the maximum width or height glass plant mass , will assign the woodland studied a typology of particular species. **[MA1]**

Key words: LIDAR, CONVEX HULL, TREE IDENTIFICATION.

1- Introduction

The identification of tree species from LIDAR points obtained by airborne scanners is theoretically feasible, thanks to the possibilities of individualization of the points that define the individual trees or also from the analysis of profiles properly oriented regular plantations or forests spontaneous . The major constraints are given by a low density of LIDAR points and excessive heterogeneity of stands. **[HM1] [HK1]**

Fig. 1 : Outline tree crowns.

The characterization of trees from terrestrial LIDAR points (fixed or mobile), initially emerged as the most reliable and simple to perform, since the point density is much higher.

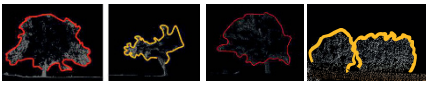

Fig. 2 : Terrestrial LIDAR points.

This paper aims to be a first approach to the problem of identification of tree species from the contours of sections of trees or stands, obtained from airborne LIDAR point clouds, ie obtained from a platform flying at a certain height.

2- Material and Methods

The study was conducted on the point cloud of a LIDAR flight over Ortigosa de Cameros (La Rioja, Spain), on a wooded area of about 20 sq km and an average density of points 5 points per sq m.

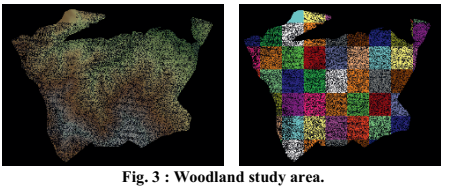

Fig. 3 : Woodland study area.

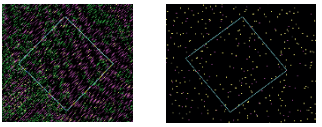

Fig. 4 : Points inside 4x4 square.

The dominant tree species in the municipality are**:** Pino silvestre (Pinus sylvestris L.), Rebollo (Quercus pyrenaica Willd.) and Haya (Fagus sylvatica L.).

Pinus sylvestris L.: the port is conical-pyramidal, but when it gets older, goes deform ostensibly and can be very asymmetric. The shape of the crown is very variable.

Quercus pyrenaica Willd. : crown of tree is usually wide and stem often twisted. Usually presented as a tortuous and messy small tree up to about 12 or 15 m high.

Fagus sylvatica L.: if it is isolated, branches out to the middle of the stem and are horizontal rather forming a rounded crown, but if it is in a more or less dense forest stands, the branches are up and appear above half stem.

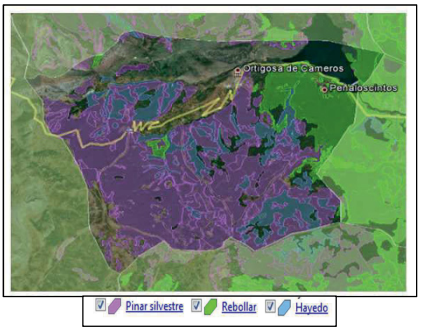

Fig. 5: Distribution area of the studied species.

For viewing, managing and editing of LIDAR points, FUSION / LDV (U.S. Forest Service - Department of Agriculture) software, FUGROVIEWER (Fugro Geospatial Services) and AUTOCAD (Autodesk) have been used. To obtain minimum convex hull of point clouds on individual tree was used CONVEX-HULL algorithm gvSIG (GIS software government of Valencia-Spain) or minimum envelope tool of SEXTANTE.

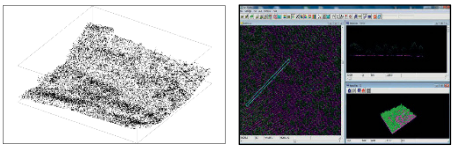

Fig. 6: Software AUTODESK (Point Clouds) and FUGROVIEWER.

The methodology has basically consisted of generating sections of the tree stands in specific directions and with varying thicknesses (boxes) to check the geometric definition of the profile generated by LIDAR points content in these boxes. The thickness ranges considered have been from 1 m to 6 m.

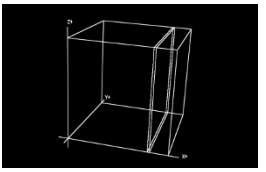

Fig. 7: Sections in boxes.

The analysis of generated profiles was performed from two different perspectives:

a) Observation of the top profile line generated by the crown of stand included in the section.

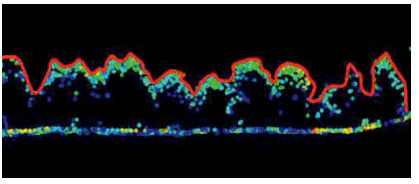

Fig. 8 : Top profile line.

b) Observation profile or envelope of the detected individual trees.

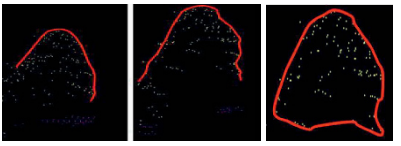

Fig. 9: Envelope of the individual trees.

2.1 Parameters to be considered.

We must clearly differentiate the parameters to be considered according to the methodology. The study and observation of individual trees or whole stands for species identification, requires first determining the rating morphogeometrical aspects. **[MM1] [RK1]**

Analyzing individual trees, the most significant parameters that define the profile and should be considered, could be:

- Total height of the crown.
- Maximum width of the crown.
- Relative positioning within the total height of the maximum width.
- Existence of a secondary width and relative positioning.
- Height of the crown starting.
- Crown shaped sections at different heights.

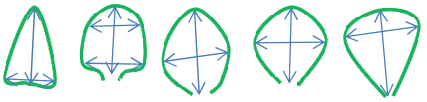

Fig.10: Measures to make.

Whereas complete stands, to establish a system of automatic or semi-automatic identification of the species from LIDAR point clouds, one should focus especially on the profile defined by the top of the tree crowns. It will be easier to set parameters in regular plantations and uniforms and much more complex, in heterogeneous forests stands. **[HP1]** For the latter, there is no other solution to individualize the point clouds of individual trees and analyze its envelope to relate it to a particular species. Other parameters such as density or crown-closure of stand, facilitate or hinder this work of identification.**[LT1][B1]** Observing the profile of the top of the crowns, we can analyze:
- Spacing between tops.
- Symmetry of forms.
- Angle in the apical vertex.
- Straightness of lines or rounded profile.

Studying the complete point cloud and using mathematical algorithms to detect individual trees, enables the generation of sections at different heights. Analyzing these shapes, we can associate to certain species of trees **[V1]**.

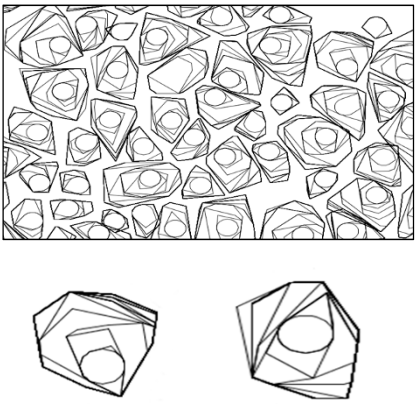

Fig. 11: Tree shapes detected at different heights.

3- Results

One of the main drawbacks of LIDAR point clouds obtained from flights on forest stands is precisely the low dot density, generating profiles of individual trees with poor definition. General flights with close to 5 points per square meter densities are still very scarce and returns only the first few laser pulses are usually better define the shape of the tree.

In this situation, and to study the set of LIDAR points of an individual tree, it is more often found with maximum 50-100 points, of which as much as 30% of them can be said to define the profile.

Analysis of the three dominant species in the study area, we deduce:

3.1. – Pinus sylvestris L.

The studied stands were compact, disordered and tree heights between 15 m and 25 m.

Study of crown profile in stand: a clear definition of the apexes of crown is observed, with the apical vertex angles between 60° and 80°. With increasing the thickness of the box in study, the contours and shape of the typical profile of conifers become blurred.

For thicknesses greater than 4 m box, trees profile are rounded and individuals are worst identified.

For these conditions of trees and density of points per square meter, are considered optimal profiles at 2 m thick, which sufficiently define the shape of the tree and its outline is not affected by too many no contour points.

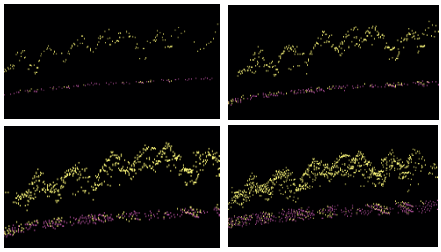

Fig. 12: Profile of crowns in Pinus sylvestris L. stands (x1, x2, x4, x6 m width box)

Typical profile:

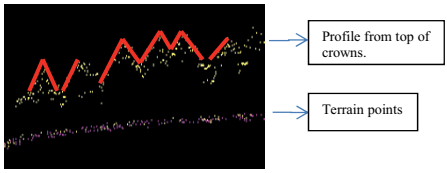

Fig. 13: Typical profile in Pinus sylvestris L. stands

The study of individual tree profile: the tree-crowns are defined by about 80 points LIDAR, preferably located on the periphery area, which facilitates geometric definition. Most of the cases studied are tall trees, with a single dominant apex and principal width at half-height.

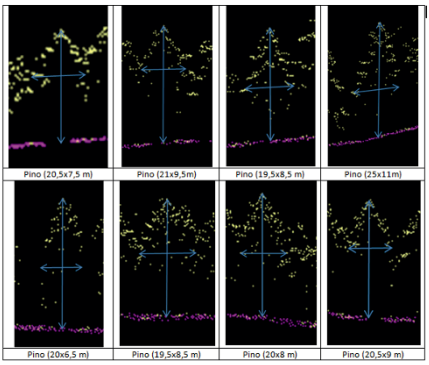

Fig. 14: Geometric measurements in Pinus sylvestris L.

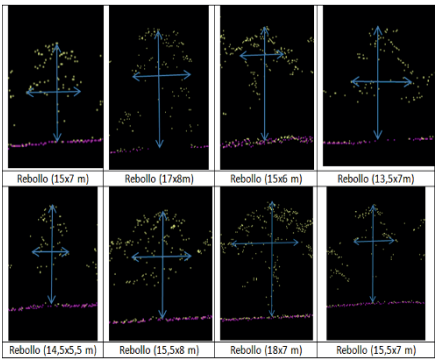

Fig. 17: Geometric measurements in Quercus pyrenaica Willd.

3.2. – Quercus pyrenaica Willd.

Trees of stand have a uniform sized between 14 m and 18 m, with a disordered and dense distribution.

Study of crown profile in stand : over 2m profile box thickness, trees become tooo much blurred and lose their individualization. The distribution of LIDAR points in the crown is fairly homogeneous. The profile of the top of the crown, unclear identifies each tree, appearing rounded shapes that intersect each other.

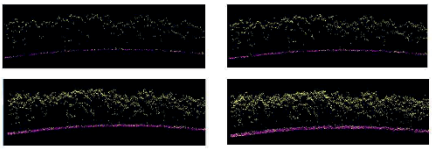

Fig. 15: Profile of crowns in Quercus pyrenaica Willd stands. (x1, x2, x4, x6 m width box)

Typical profile:

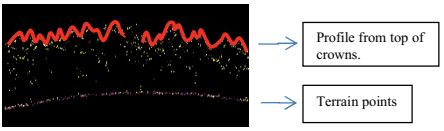

Fig. 16: Typical profile in Quercus pyrenaica Willd stands.

The study of individual tree profile: the profile is more irregular and unclearly LIDAR points define the shape and form of the tree. Appear between 40 and 80 points LIDAR within the crown, but there is no clearly dominant width.

3.3. – Fagus sylvatica L.

Beech forests studied show a medium-high size, between 16 m and 21 m. The densities are rather high and the disorderly distribution.

Study of crown profile in stand : the profile of the top of the crowns, is sufficiently defined with a thickness of up to 2 m box. Over this thickness, the crowns are filled with points, but the profile does not improve. The tree identification is complicated due to the stand density.

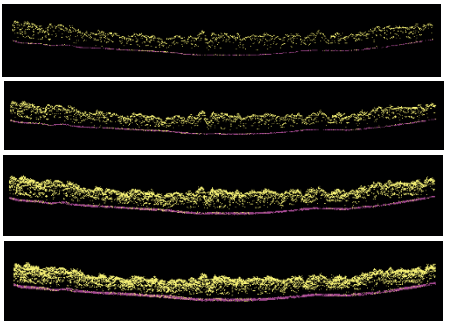

Fig. 18: Profile of crowns of Fagus sylvatica L.stands. (x1, x2, x4, x6 m width box)

Typical profile:

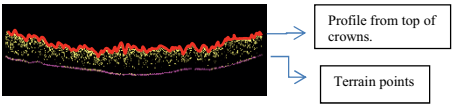

Fig. 19: Typical profile in Fagus sylvatica L.stands

The study of individual tree profile: the profile is typical of a large broad-leaved, with rounded shapes and LIDAR points rather accumulated on the outside of the crowns. Predominant width appears at an intermediate height of the tree.

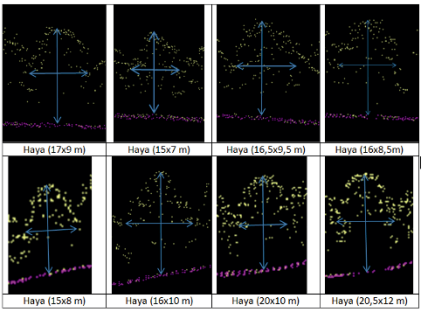

Fig. 20: Geometric measurements in Fagus sylvatica L.

4- Conclusions.

After this initial approach to the possibilities offered by the LIDAR point clouds in the forest environment, we can say that the identification of species through the profile is extremely complex. To this very decisively influences, the great heterogeneity of the plantations and the low density of points in profile defining the tops and trees.

Establish a one-one correlation between the detected profile through LIDAR point cloud and a particular species is extremely difficult, as the same species has different developments depending on growing conditions. And, although these conditions were very similar, the final size of each tree depends on both their genetic and other difficult control aspects of their immediate environment characteristics.

As there is no single pattern for each species, identification from LIDAR point clouds will require more or less human intervention to carry out this assignment. Automating the process minimally require , in all probability , the use of other LIDAR data , such as the RGB color values of each point and the type and intensity of returns. **[HP2] [ON1]**

The study of sections at different heights and the crown profile shapes seems to be the only system to address the identification of species from airborne LIDAR point clouds.

Acknowledgement

The Government of La Rioja (Spain), as owner of the flight data LIDAR in Ortigosa de Cameros, for facilitating its use in this research.

References

[B1] Brandtberg T. Classifying individual tree species under leaf-off and leaf-on conditions using airborne lidar. ISPRS Journal of Photogrammetry and Remote Sensing. Volume 61, Issue 5, January 2007, Pages 325–340

[DW1] Donoghue D., Watt P., Cox N. and Wilson J. Remote sensing of species mixtures in conifer plantations using LiDAR height and intensity data. Remote Sensing of Environment Volume 110, Issue 4, 30 October 2007, Pages 509–522

[HK1] Heinzel J., Koch B. Exploring full-waveform LiDAR parameters for tree species classification. International Journal of Applied Earth Observation and Geoinformation. Volume 13, Issue 1, February 2011, Pages 152–160

[HM1] Hollaus M., Mücke W., Höfle B., Dorigo W., Pfeifer N., Wagner W., Bauerhansl C. and Regner B. Tree species classification based on full-waveform airborne laser scanning data. Silvilaser 2009, 14–16 October 2009, College Station, USA (2009), pp. 54–62

[HP1] Holmgren J. and Persson A. Identifying species of individual trees using airborne laser scanning. Remote Sensing of Environment, 90 (2003), pp. 415–423

[HP2] Holmgren J., Persson A. and Söderman U. Species identification of individual trees by combining high resolution LiDAR data with multispectral images. International Journal of Remote Sensing Volume 29, Issue 5, 2008 pages 1537-1552

[LT1] Lim K.S., Treitz P.M., Wulder M., St-Onge B. and Flood M. LiDAR remote sensing of forest structure. Progress in Physical Geography, 27 (2003), pp. 88–106

[MA1] Means J.E., Acker S.A., Brandon J.F., Renslow M., Emerson L. and Hendrix C.J. Predicting forest stand characteristics with airborne scanning lidar. Photogrammetric Engineering and Remote Sensing, 66 (2000), pp. 1367–1371

[ME1] Moskal L.M., Erdody T., Kato A., Richardson J., Zheng G. and Briggs D. Lidar applications in precision forestry. Proceedings of Silvilaser 2009, 14–16 October 2009, College Station, USA (2009), pp. 154–163

[MM1] Moffiet T., Mengersen K., Witte C., King R. and Denham R. Airborne laser scanning: Exploratory data analysis indicates potential variables for classification of individual trees or forest stands according to species. ISPRS Journal of Photogrammetry and Remote Sensing, 59 (2005), pp. 289–309

[ON1] Orka H.O., Naesset E. and Bollandsas O.M. Classifying species of individual trees by intensity and structure features derived from airborne laser scanner data. Remote Sensing of Environment, 113 (2009), pp. 1163–1174

[RK1] Reitberger J., Krzystek P. and Stilla U. Analysis of full waveform LiDAR data for tree species classification. International Archives of Photogrammetry, Remote Sensing and Spatial Information, Vol. 36 Bonn, Germany (2006), pp. 228–233

[V1] Valbuena M.A. Determinación de variables forestales de masa y de árboles individuales mediante delineación de copas a partir de datos LIDAR aerotransportado. Tesis Doctoral. Universidad de La Rioja, 2014.

Article 05-cad-63

A preliminary study on Cleft Lip Pathology trough 3D Geometrical Analysis

Sandro Moos [1], Federica Marcolin [1], Stefano Tornincasa [1] Enrico Vezzetti [1] Maria Grazia Violante [1] Domenico Speranza [2]

(1) : DIGEP – Politecnico di Torino, Corso Duca degli Abruzzi 24 10129 Torino
Phone: +39 011 090 7294
E-mail : enrico.vezzetti@polito.it

(2) : DiCEM – Università di Cassino e del Lazio Meridionale, via G. Di Biasio 43 - 03043 Cassino (FR)
Phone: +39 0776 299 3988
E-mail : d.speranza@unicas.it

Abstract: The aim of this work is to automatically diagnose and formalize prenatal cleft lip with representative key points and identify the type of defect (unilateral, bilateral, right, or left) in three-dimensional ultrasonography (3D US). Differential Geometry has been used as a framework for describing facial shapes and curvatures. The descriptive accurateness of these descriptors has allowed us to automatically extract reference points, quantitative distances, labial profiles, and to provide information about facial asymmetry.

Key words: 3D ultrasound; 3D echography; Syndrome Diagnosis; Dysmorphisms; 3D face.

1- Introduction

Three-dimensional ultrasound (US) has been introduced more than twenty years ago into clinical practice [RP1]. Its applications on diagnosis of anomalies and diseases were a direct consequence of its use. In particular, cleft lip and palate (CLP) detection, whose incidence is 1/700 in United States [TL1], was widely addressed, as they could be difficult to be diagnosed with bi-dimensional US especially in earlier gestational ages [HY1]. In the effort to evaluate the performance of routine ultrasonographic screening on an unselected population, the Eurofetus study [GL1] shows that CLP has the lowest rates of detection (18%) and it is diagnosed usually later in pregnancy (only 31.6% before 24 weeks). Furthermore CLP is diagnosed less frequently by antenatal ultrasound if the anomaly is isolated than if the foetus has multiple anomalies, as often seen at autopsy following termination of pregnancy when multiple anomalies are detected [L1].

Complementarily, 3D, despite some criticisms [MB1], has been considered superior to 2D in identifying normal lips at less than 24 weeks [PH1]. In this work we will focus on cleft lip (CL) alone. CL, both unilateral and bilateral, includes clefts involving the alveolus and hard palate anterior to the incisive foramen, i.e. the embryological primary palate [DK1]. The reported rates of prenatal recognition of cleft lip range between 21% and 30% [RL1].

Cleft lip has been associated with more than 100 different chromosomal abnormalities and genetic syndromes [J1], and sometimes may be the only sign of a chromosomal anomaly, as trisomy 18 [C1], trisomy 13, or syndromes as Cornelia de Lange or Smith-Lemli–Opitz [RH1]. Thus an accurate scan searching for other foetal anomalies and a genetic counselling are paramount when a cleft lip is diagnosed. CL is not accompanied by any palatal anomaly in 15-25% of cases [BF1, OJ1]. More generally, if we consider CLP as a whole, the incidence of structural abnormalities and syndromes associated with cleft lip and palate ranges between 21% and 38% [CL1]. But it is important to note that, although they often occur with each other, cleft lip and palate anomalies are developmentally distinct processes [LK1]. In particular, the embryological origins of clefts of the lip and alveolus appear to be distinct from those of clefts of the secondary palate [CL1].

Lee [LK1] used three-dimensional ultrasonography to support cleft lip and palate detection. Cleft lip was identified by an examiner as a loss of continuity of the orbicularis oris muscle from a coronal or axial view of the lips, so the diagnosis was not automatic. Campbell [CL1] assessed the clinical value of a 3D US technique, the 'reverse face' view, in the prenatal categorization of facial clefting including CL. Then, Platt [OJ1] proposed the 'flipped face' view to diagnose lip and palate cleftings, relying on 3D US. When a static volume is acquired, the volume is rotated 90° so that the cut plane is directed in a plane from the chin to the nose and scrolled to examine in sequential order different zones, including lips. Mailáth-Pokornyet [MW1] investigated the role of foetal MRI in the prenatal diagnosis of facial clefts, including cleft lip, although no particular detection technique has been employed. Martinez-Ten [MA1] determined whether systematic examination of primary and secondary palates aided in the identification of orofacial clefts in the first trimester. Gindeset [GW1] evaluated the ability of three-dimensional ultrasound for demonstrating the

palate of foetuses at high risk for cleft lip and palate. A detailed assessment of palate was made using both two-dimensional and 3D ultrasounds on the axial plane. Then, antenatal diagnoses were compared with postnatal findings.

Some authors used landmarks as reference points. Johnson [JP1] assessed the advantages of 3D US in diagnosing cleft lip. The volume data were displayed in two formats: three orthogonal planar images and a 3D rendered image of the surface of the foetal face. The planar images were rotated with the interactive display into a standard anatomic orientation, so that the three planar images corresponded to the frontal, sagittal, and transverse facial planes. The rendered image provided landmarks for the planar images. Roelfsema [RH1] used 3D US to employ craniofacial pattern profile analysis in foetal facial clefts and evaluate the craniofacial variability index (CVI) in distinguishing between isolated cleft lip/palate and cleft lip/palate in chromosomal anomalies or syndromes. Facial landmarks such as tragus, nasion, gnathion, glabella, subnasion, and others were employed to extract sixteen craniofacial measurements for the assessment of postnatal (ab)normal craniofacial development. Although none of the foetuses evaluated in their study was affected by cleft lip, Sepulveda [SW1] proposed a new first-trimester sonographic landmark, the 'retronasal triangle', useful in the early screening for cleft palate. This landmark has been termed this way because coronal plane displays three easily recognizable echogenic lines corresponding to the two frontal processes of the maxilla and the primary palate. Manganaro [MT1] evaluated cleft lip and palate through MRI and US, although not 3D. The main facial landmarks were measured and analyzed for each foetus (forehead, occiput, orbits, nose, lips, chin, mandible). Tonni and Lituania [TL1] proposed a new three-dimensional sonographic software, the OmiView algorithm, and applied it to unilateral CL, bilateral CLP, and isolated CP. They showed that 3D imaging of the foetal hard and soft palates by OmniView was technically easier than with previously reported 3D techniques. OmniView allowed visualization of all of the anatomic landmarks of the specific targeted area (labia, primary palate, alveolar ridge, posterior palate, uvula, velum, and tongue).

In this work we present an algorithm that automatically detects the presence of cleft lip and that provides to the practitioners with some useful information about the cleft, such as the transverse and the cranio-caudal length, the upper lip outline and the asymmetry of the face. The paper is divided in three sections: section 2 explains the used method; section 3 describes used data; section 4 shows the results obtained.

2- The proposed Methodology

The proposed methodology studies the geometrical features of baby's face in order to detect the deformation. Moreover, the algorithm identifies if the cleft lip is unilateral or bilateral, it localizes some key points of the deformation and performs some measurements in order to assess the dimensions of the cleft. We also automatically extract the outline of the upper lip, in order to better describe its shape and the size of the deformation.

The first step of the strategy involves the Deformity Detection. Cleft lip is a gap or an indentation in the upper lip. This deformity is easily recognizable using geometrical descriptors. This indentation is characterized by very high values of coefficient e (of the second fundamental form) and of Curvedness Index C. Moreover, the two parts of the lip that are situated beside the gap or indentation are characterized by two maximums of the principal curvature k_2.

The elaborated algorithm uses the previous geometrical features in order to detect whether the cleft lip is present or not in a foetus. Moreover, this algorithm is able to distinguish between unilateral and bilateral cleft lip

The steps of the process are explained in the scheme of Figure 1.

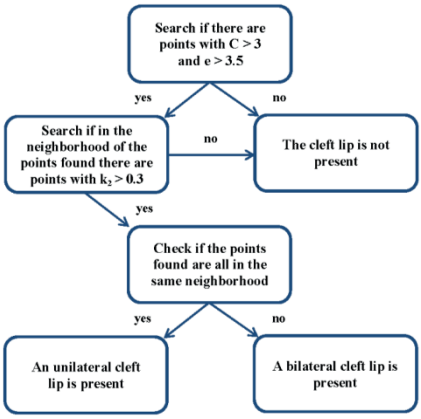

Figure 1: Scheme of the process for the cleft lip diagnosis.

In order to better describe the deformation, we decided to localize four key points: the two points of the lip that are beside the cleft and the ending points of the cleft. As already said above, the principal curvature k_2 has two maximums in the first two points. The other two points are situated in the gap of the lip. This area is characterized by high values of the Curvedness Index C and of the coefficient e. To extract these points, firstly the algorithm localizes the centre of the cleft maximizing the coefficient e. Then, it analyzes the neighbourhood of this point, moving upwards from the centre for the high ending point and downwards for the low ending point. The algorithm, for each y value, maximizes the coefficient e in a neighbourhood of the cleft lip. The ending points are the first two maximums that are lower than a proper threshold value.

In order to have more information about the deformation, we measured the transverse diameter of the cleft computing the Euclidean distance between the first two points extracted and its cranio-caudal length computing the Euclidean distance between the last two points extracted. We have chosen to compute these two distances because they are the most used in the estimation of cleft size.

We decided to extract also the outline of the upper lip, in order to provide more information about its shape. For the extraction of this outline we used the Curvedness Index, because it is one of the geometrical descriptors that better

describe the upper lip. The Curvedness Index has a maximum behaviour in correspondence to the upper lip. To extract the outline, for each x value in the upper lip area we maximize the Curvedness Index. In this way, we obtain a sequence of points, namely a line, in the 3D-space that describes the upper lip outline, giving us important information about the cleft lip shape.

We decided to evaluate also the asymmetry of the face due to the unilateral cleft lip. To do this evaluation, we have computed the mean of the absolute value of the coefficient e in the left part of the mouth and in the right part of the mouth. By comparing these two mean values, we obtain an useful information about the asymmetry of the face. We chose the coefficient e, because is one of the descriptors that better describe the cleft lip. We decided to take its absolute value because in correspondence of the cleft lip two minimum and a maximum are present, so taking the absolute value will avoid that the minimum and maximum behaviour will annul each other when we compute the mean value on the area.

3- Experimental Validation

Three-dimensional volumes of 18 foetuses at 22-32 weeks' gestation were acquired, keeping eight faces with cleft lip.

The ultrasound equipment was a Voluson system (GE Healthcare, Wauwatosa, WI, USA), with a RAB 4-8 (real time 4D convex transducer probe). The GE RAB 4-8 has a frequency range of 4 to 8 MHz and is used for OB applications (Footprint 63.6 x 37.8 mm, FOV 70°, V 85°x70°).

Using 4D VIEW software, it is possible to see the images acquired with the Voluson System on three orthogonal planes, i.e. axial, sagittal, and coronal.

The distance between two successive slices is 0.4 mm. For each slice composing the whole volume, the relative DICOM format file is created and stored. The final store is exported into Simpleware ScanIP software for the 3D model reconstruction. Face data were collected in points clouds (shells), then these shells were imported in Matlab®, triangulated, and then converted into a square grid.

The algorithm we developed for foetal diagnosis of cleft lip was elaborated, implemented, and run on these shells.

4- Results and Discussion

The algorithm for the diagnosis of cleft lip was tested on the eighteen ultrasounds (eight with cleft lip and ten without). In all these cases, the algorithm detected correctly the presence or not of the cleft lip and, in the two shells with bilateral cleft lip, the algorithm detected both the clefts.

In the five ultrasounds with cleft lip, the four key points were localized. In Figure 2 the resulting key points are shown for each shell.

After having localized the key points, we have computed the transverse and the cranio-caudal length of the cleft. In Table 1, the values of these distances for each shell are shown, the unit of measurement is the millimetre.

As can be seen in Table 1, the shells that present the lowest cranio-caudal length are the ones with an incomplete cleft. For each shell with cleft lip, we have also extracted the upper lip outline. In Figure 2 the resulting outline is shown for each shell.

Shell	Transverse diameter	Cranio-caudal length
A	7.19	6.78
B	8.31	9.59
C (left cleft)	15.08	7.00
C (right cleft)	12.04	7.06
D (left cleft)	12.65	6.09
D (right cleft)	10.01	12.34
E	6.69	1.81
F	6.67	1.64
G	6.19	4.34
H	3.17	0.62

Table 1: Computed distances for each shell.

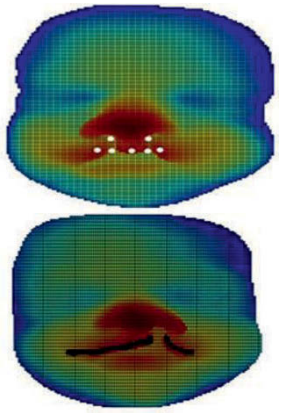

Figure 2: The resulting four key points and upper lip outline for a shell with cleft lip

We computed the asymmetry of the face in the six shells with unilateral cleft lip and on the ten shells without cleft lip, the evaluation was not performed on the two shells with bilateral cleft lip. The results are shown in Table 2 (shells with unilateral cleft lip) and 3 (shells without cleft lip).

Shell	Side with cleft lip	Side without cleft lip	Difference
A	1.08	0.41	0.68
B	1.34	0.4	0.94
E	1.10	0.36	0.74
F	0.82	0.60	0.22
G	1.09	0.33	0.76
H	0.44	0.28	0.16

Table 2: Results of asymmetry evaluation for shells with unilateral cleft lip.

Shell	Left side	Right side	Difference
Anto	0.28	0.33	0.05
Bart	0.30	0.48	0.18
Elena	0.16	0.27	0.11
Fede	0.33	0.30	0.03
Gian	0.22	0.33	0.11
Gio	0.16	0.24	0.08
Lisa	0.36	0.21	0.14
Paul	0.17	0.22	0.05
Pie	0.15	0.20	0.05
Simon	0.18	0.25	0.07

Table 3: Results of asymmetry evaluation for shells without cleft lip.

As can be seen in Tables 2 and 3, the difference between the two sides of the face is usually higher in the shells with cleft lip. The mean difference value is 0.58 in shells with cleft lip instead it is 0.09 in shells without cleft lip, i.e. about six times smaller. The shell with cleft lip with the lowest difference value is H, where an incomplete cleft lip is present. Probably in this case the asymmetry was not high because the cleft lip was not accentuated, as it is also shown in Table 1 where the shell H has the lowest cranio-caudal length. Also the other shell with a low difference value, namely the shell E, presents an incomplete cleft lip. Instead, in the shells without cleft lip the difference between the two face sides is usually low, with values in the range between 0.05 and 0.18. The highest values (Bart and Lisa) are probably due to the quality of the ultrasound.

3- Conclusions

This work presents a new algorithm for diagnosing cleft lip on 3D ultrasound. The algorithm says whether the defect is present or not, classifies it (unilateral, bilateral, right, left), extracts four key points, transverse and cranio-caudal length of the cleft, and outline of the upper lip, and provides information on the facial asymmetry. The defect has been correctly diagnosed and classified for all the foetuses.

Differential Geometry provided us with a set of descriptors leading this research activity. The result is that these descriptors are suitable to describe face shape and curvedness, allowing an accurate extraction of the interested facial features.

7- References

[BF1] Bäumler, M., Faure, J.M., Bigorre, M., Bäumler-Patris, C., Boulot, P., Demattei, C., Captier, G., 2011. Accuracy of prenatal three-dimensional ultrasound in the diagnosis of cleft hard palate when cleft lip is present. Ultrasound ObstetGynecol38, 440–444.

[CL1] Campbell, S., Lees, C., Moscoso, G., and Hall, P., 2005. Ultrasound antenatal diagnosis of cleft palate by a new technique: the 3D 'reverse face' view. Ultrasound ObstetGynecol 25, 12-18.

[C1] Carlson, D.E., 2000. Opinion — The ultrasound evaluation of cleft lip and palate—a clear winner for 3D. Ultrasound ObstetGynecol 16, 299-301.

[DK1] Demircioglu, M., Kangesu, L., Ismail, A., Lake, E., Hughes, J., Wright, S., and Sommerlad, B.C., 2008. Increasing accuracy of antenatal ultrasound diagnosis of cleft lip with or without cleft palate, in cases referred to the North Thames London Region. Ultrasound ObstetGynecol31, 647–651.

[GW1] Gindes, l., Weissmann-Brenner, A., Zajicek, M., Weisz, B., Shrim, A., Geffen, K.T., Mendes, D., Kuint, J., Berkenstadt, M., and Achiron, R., 2013. Three-dimensional ultrasound demonstration of the fetal palate in high-risk patients: the accuracy of prenatal visualization. Prenatal Diagnosis 33, 436–441.

[GL1] Grandjean H, Larroque D, Levi S. The performance of routine ultrasonographic screening of pregnancies in the Eurofetus Study. Am J Obstet Gynecol. 1999 Aug;181(2):446-54.

[HY1] Hata, T., Yonehara, T., Aoki, S., Manabe, A., Hata, K., and Miyazaki, K., 1998. Three-Dimensional Sonographic Visualization of the Fetal Face. American Journal of Roentgenology 170 (February), 481-483.

[L1] Luck CA. Value of routine ultrasound scanning at 19 weeks: a four year study of 8849 deliveries. BMJ. 1992 Jun 6;304(6840):1474-8.

[JP1] Johnson, D.D., Pretorius, D.H., Budorick, N.E., Jones, M.C., Lou, K.V., James, G.M., and Nelson, T.R., 2000. Fetal Lip and Primary Palate: Three-dimensional versus Two-dimensional US. Radiology 217(1), 236–239.

[J1] Jones MC. Facial clefting. Etiology and developmental pathogenesis. ClinPlast Surg. 1993 Oct;20(4):599-606.

[LK1] Lee, W., Kirk, J.S., Shaheen, K.W., Romero, R., Hodges, A.N., and Comstock, C.H., 2000. Fetal cleft lip and palate detection by three-dimensional ultrasonography. Ultrasound ObstetGynecol 16, 314-320.

[MB1] Maarse, W., Bergé, S.J., Pistorius, L., Van Barneveld, T., Kon, M., Breugem, C., Mink van der Molen, A.B., 2010. Diagnostic accuracy of transabdominal ultrasound in detecting prenatal cleft lip and palate: a systematic review. Ultrasound ObstetGynecol35, 495–502.

[MW1] Mailáth-Pokorny, M., Worda, C., Krampl-Bettelheim, E., Watzinger, F., Brugger, P.C., and Prayers, D., 2010. What does magnetic resonance imaging add to the prenatal ultrasound diagnosis of facial clefts?. UltrasoundObstetGynecol 36, 445–451.

[MT1] Manganaro, L., Tomei, A., Fierro, F., Di Maurizio, M., Sollazzo, P., Sergi, M.E., Vinci, V., Bernardo, S., Irimia, D., Cascone, P., and Marini, M., 2011. Fetal MRI as a complement to US in the evaluation of cleft lip and palate. Radiol med 116, 1134–1148.

[MA1] Martinez-Ten, P., Adiego, B., Illescas, T., Bermejo, C., Wong, A.E., and Sepulveda W. 2012. First-trimester diagnosis of cleft lip and palate using three-dimensional ultrasound. Ultrasound ObstetGynecol 40, 40–46.

[ML1] Mittermayer, C. and Lee, A., 2003. Picture of the Month — Three-dimensional ultrasonographic imaging of cleft lip: the winners are the parents. Ultrasound in Obstetrics and Gynecology 21, 628-629.

[OJ1] Offerdal K, Jebens N, Syvertsen T, Blaas HG, Johansen OJ, Eik-Nes SH.Prenatal ultrasound detection of facial clefts: a prospective study of 49,314 deliveries in a non-selected population in Norway. Ultrasound Obstet Gynecol. 2008 Jun;31(6):639-46. doi: 10.1002/uog.5280.

Platt, L.D.,

[PD1] Pretorius, D.H. and DeVore, G.R., 2006. Improving Cleft Palate/Cleft Lip Antenatal Diagnosis by 3-Dimensional Sonography — The "Flipped Face" View. J Ultrasound Med 25, 1423–1430.

[**PH1**] Pretorius, D.H., House, M., Nelson, T.R., and Hollenbach, K.A., 1995. Evaluation of Normal and Abnormal Lips in Fetuses: Comparison Between Three- and Two-Dimensional Sonography. American Journal of Roentgenology 165(5), 1233-1237.

[RP1] Riccabona, M., Pretorius, D.H., Nelson, T.R., Johnson, D., and Budorick, N.E., 1997. Three-Dimensional Ultrasound: Display Modalities in Obstetrics. J Clin Ultrasound 25(4), 157–167.

[RH1] Roelfsema, N.M., Hop, W.C.J., Van Adrichem, L.N.A., and Wladimiroff, J.W., 2207. Craniofacial variability index determined by three-dimensional ultrasound in isolated vs. syndromalfetal cleft lip/palate. Ultrasound ObstetGynecol29, 265–270.

[RL1] Rotten, D. and Levaillant, J.M., 2004. Two- and three-dimensional sonographic assessment of the fetal face. 1. A systematic analysis of the normal face. Ultrasound ObstetGynecol 23, 224-231.

[SW1] Sepulveda, W., Wong, A.E., Martinez-Ten, P., and Perez- Pedregosa, J., 2010. Retronasal triangle: a sonographic landmark for the screening of cleft palate in the first trimester. Ultrasound ObstetGynecol35, 7–13.

[TL1] Tonni, G. and Lituania, M., 2012. OmniView Algorithm — A Novel 3-Dimensional Sonographic Technique in the Study of the Fetal Hard and Soft Palates. J Ultrasound Med 31, 313–318.

[TL2] Tonni, G. and Lituania, M., 2013. Arthrogryposis multiplex congenita-like syndrome associated with median cleft lip and palates: First prenatally detected case. Congenital Anomalies 53, 137–140.

Article 077-cadcae-61

Mesh processing for morphological and clinical parameters computation in dog femur

G. Savio [1], T. Baroni [2], G. Concheri [1], M. Isola [3], E. Baroni [2], R. Meneghello [1], M. Turchetto [1], S. Filippi [4]

(1) : Università di Padova - Dept. ICEA - Lin.
Via Venezia 1, 35131, Padova, Italy.
Phone: +39 049 8276735 - 6739 - 6736 - 6734
E-mail: {gianpaolo.savio, gianmaria.concheri, roberto.meneghello, matteo.turchetto}@unipd.it

(2) : Clinica veterinaria Baroni
Via Martiri Belfiore 69/D, 45100, Rovigo, Italy.
Phone: +39 0425 404918
E-mail: {teresa.baroni, gildo.baroni}@clinicaveterinariabaroni.com

(3) : Università di Padova - Dept. Maps
Viale Dell'Universita' 16, 35020, Legnaro (PD), Italy.
Phone: +39 049 8272951
E-mail: maurizio.isola@unipd.it

(4) : Università di Udine - Dept. DIEG
Via Delle Scienze, 206 - 33100 Udine
Phone: +39 *0432 558289*
E-mail: stefano.filippi@uniud.it

Abstract: Currently available methods for evaluating dog femur deformities are principally based on 2D image analysis of radiographies. By CT or MRI, 3D information can be derived from points clouds or meshes. This work proposes an original approach for morphological and clinical parameters assessment on meshes. The method is validated on dog femur meshes measured by two 3D scanners with different resolutions. The results show that the 3D proposed approach overcomes several limits of the methods based on 2D image analysis.

Key words: Mesh, dog, femur, mesh processing, mesh segmentation, varus, torsion.

1- Introduction

Angular deformities of canine pelvic limbs are relatively common and related to the main pathologies that affect pets. Medial patellar luxation (MPL), hip dysplasia and cranial cruciate ligament rupture are some leading and increasingly frequent causes of pelvic limb lameness in many dog breeds. Many skeletal abnormalities, including excessive femoral varus or torsion, for example, have been associated with those pathologies.
Corrective osteotomies are generally performed to treat limb misalignment and preoperative evaluation is fundamental to achieve a good result. This evaluation is usually accomplished by radiographic projections of both limbs, where there are some limits related to:

- the actual orientation of the dog limbs during the radiographic examination,
- the ability of the operator to select the points for the parameters computation,
- different definitions for the same geometric element (e.g. anatomical axis [P1]),
- only parameters projected in the radiographic plane are measured,
- axes are derived from single points without taking into account the surrounding portion,
- no dimensional information are available.

In human medicine the determination of limb deformities has been studied using 3D models (usually triangular meshes) derived from computed tomography (CT) and magnetic resonance imaging (MRI) [CM1]. In veterinary medicine, 3D models have been recently introduced, in order to define a better orientation of the limbs, while the parameters are still estimated like in radiographic projections [DK1]. An attempt of deriving axes in 3D has been previously performed, but the results show high dispersion in the same mesh due to different operators [M1].
Taking into account several methods proposed in human medicine [CM1, V1], an automatic approach for the estimation of dog femur morphological and clinical parameters is proposed. The procedure is based on mesh processing which can be derived from CT or MRI measurements.
The method is tested in a femur of a dog cadaver measured with two different 3D scanners and adopting three mesh resolutions.
A detailed discussion of the parameters investigated will be the subject of future works.
The tools, available at [R1,S1], are developed in Rhinoceros® Version 5 environment using IronPython and Meta.Numerics [MN1], a library for advanced scientific computation.

2- 2D Radiographic approach

A critical step in the radiographic measurement of a femur is the accurate orientation of the limbs. A wrong disposition of the dog can induce errors in the estimation of the

morphological and clinical parameters.

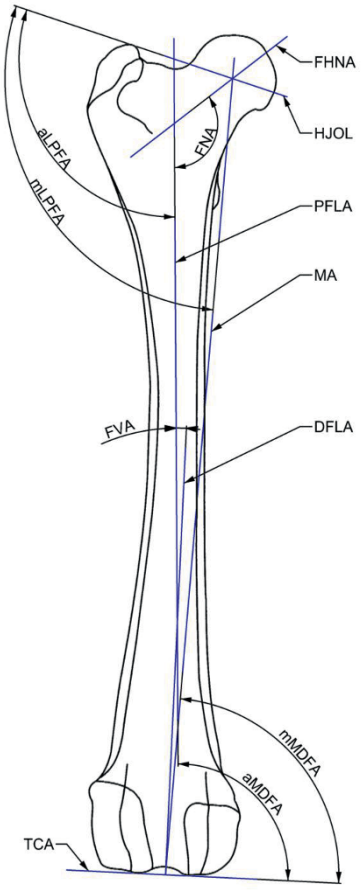

Figure 1: Morphological and clinical parameters in the craniocaudal radiograph.

Several axes are derived by two orthogonal radiographies. In the craniocaudal radiograph (fig. 1) it is possible to draw the:

- hip joint orientation line (HJOL), line from the tip of the greater trochanter to the center of the femoral head,
- mechanical axis (MA), line connecting the centre points of the proximal and distal joints,
- femoral head and neck axis (FHNA), line connecting the head centre with the mid point of the neck,
- transcondylar axis (TCA), line drawn tangential to the distal articular surface of the femoral condyles,
- proximal femoral long axis (PFLA) line connecting the centres of the proximal femoral diaphysis,
- distal femoral long axis (DFLA) line bisecting the intercondylar notch, perpendicular to the transcondylar axis [DK1].

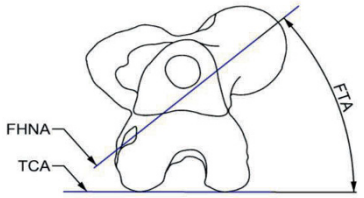

Figure 2: Morphological and clinical parameters in the distal-proximal axial femoral radiograph.

In the distal-proximal axial femoral radiograph (fig. 2) it is possible to identify the:

- transcondylar axis (TCA),
- femoral head and neck axis (FHNA).

As described in literature [P1,M1], there are different or non rigorous definitions to compute these axes, and consequently significantly different results can be found in the study of the same case. Moreover the same axis in different radiograph planes, takes different positions (e.g. TCA).

The evaluation of the normality of a femur is established analyzing the angles between the previous mentioned axes. In the craniocaudal radiograph (fig. 1) it is possible to compute:

- anatomic lateral proximal femoral angle (aLPFA), between HJOL and PFLA axes,
- mechanical proximal femoral angle (mLPFA), between HJOL and MA,
- anatomic medial distal femoral angle (aMDFA), between TCA and PFLA,
- mechanical medial distal femoral angle (mMDFA), between TCA and MA,
- femoral Neck Angle (FNA), between FHNA and PFLA,
- femoral varus angle (FVA), between DFLA and PFLA.

In the distal-proximal axial femoral radiograph (fig. 2) only the femoral torsion angle (FTA), between TCA and FHNA axes, is defined.

Uncertainty due to the orientation of the dog limbs during the radiography, different definition of the same axes, uncertainty due to the operator during the drawing of the axes induce high chance of error in the computation of the normality of the femur and consequently in the decision of surgery. These issues can be overcome adopting the proposed automatic approach.

3- The proposed 3D approach

The proposed approach improves and integrates some recent studies [CM1,V1] developed for the femur analysis in human medicine, customized for the veterinary. Polygon meshes

representing dog femurs shape are studied. These meshes are available in different imaging modalities, like CT, MRI (in vivo) or 3D scanner (cadaver).
The method follows the following computational steps:

1- femur orientation and PFLA,
2- femur head and centre,
3- tip of the greater trochanter and HJOL,
4- neck analysis and FHNA,
5- DFLA axis and symmetry plane of the distal portion (SPD),
6- condyles, TCA and MA.

In the following paragraphs a detailed description of the method is outlined, while the discussion of the choices is available in section 5.1.

3.1 – Femur orientation and PFLA

The femur orientation phase consists of 3 steps (fig. 3). Firstly the area principal moments of inertia about centroid and principal axes are computed and then the mesh is aligned in the reference frame positioning the origin in the centroid, orienting the z-axis with the principal axis with minimum moments, and ensuring that the z-coordinate of the head is positive. Then the PFLA is preliminarily assessed:

- ten sections, perpendicular to the z-axis, are calculated in the upper range 1/2 ÷ 1/3 of the femur length (FL),
- the centroid of each section is calculated,
- the fitting line through the centroids is computed: this is the tentative PFLA,
- the femur is re-oriented aligning the fitting line on the z-axis.

Finally the actual PFLA is re-computed repeating the above procedure.

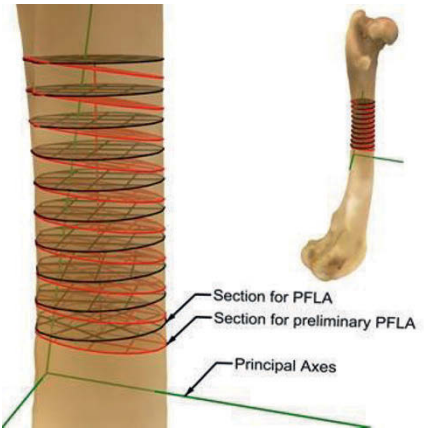

Figure 3: Femur orientation and PFLA computation.

3.2 – Femur head analysis and centre

To reduce the computational cost, the mesh can be split in portions: a proximal portion, above 1/6 of FL for head, neck and greater trochanter analysis, and a distal portion below 2/3 for the condyles analysis.
The head of the femur is approximated with a sphere obtained fitting a specific set of mesh vertices (red vertices in fig.4). These vertices are obtained:

- selecting all the vertices V1 inside a neighbourhood with radius R=FL/50, centred in the upper vertex of the head (head tip),
- computing the mean curvature k in each vertex of V1,
- calculating the mean value kmm and the standard deviation SD of k,
- selecting all the vertex topologically connected to each others (starting from the head tip), having a maximum and minimum curvature in the range kmm±2*SD.

The curvature in each mesh vertex is computed by a local quadratic fitting with 4 coefficients, following the method proposed in [SM1]. The local quadratic fitting is computed adopting all the vertices inside a neighbourhood with radius R=FL/50.

3.3 – Tip of the greater trochanter and HJOL

Firstly, the highest vertex of the trochanter is identified, then the vertices inside a neighbourhood with radius R=FL/200 are selected. Finally a quadratic fitting with 6 coefficients is computed on the selected vertices. The axis connecting the maximum of the quadratic fitting with the centre of the head is assumed as the HJOL.

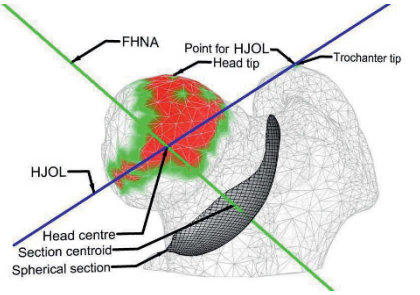

Figure 4: Proximal femur analysis.

3.4 – Neck analysis and FHNA

Due to the very short distance between the points defining FHNA, the "centre of the neck" selection plays a significant role in the computation of this axis.
The proposed approach is based on sectioning the neck by a sphere concentric with the head centre. The centre of the neck is assumed as the centroid of the portion of the spherical surface inside the femur.
To establish the radius of this sphere, 3 methods have been investigated:

a) the radius which ensure the minimum area of the spherical portion (AN),
b) the radius which ensure the minimum ratio between

area of the spherical portion the radius itself,

c) a radius proportional to the head radius HR.

3.5 – DFLA axis, SPD and FVA

The literature definition of the DFLA [DK1] can be computed only in 2D images. To overcome this limit, the DFLA computation follows the same strategies adopted for the PFLA. In this case, 10 sections perpendicular to the z-axis in the range 2/3 ÷ 5/6 of the femur length (FL) are taken into account for the axis calculation. No further orientation of the femur is done.

With respect to the literature, adopting this axis for FVA computation, large difference is found due to the inclination in the lateral view between PFLA and DFLA, which is not taken into account in the 2D radiographies. To overcome this inconsistency, the FVA is assumed as the angle between the symmetry plane of the distal portion (SPD) an PFLA.

The SPD is computed following this procedure:

- a starting mirror plane is define passing through DFLA and the centroid of the distal portion,
- the distal portion is mirrored with respect to the starting mirror plane,
- the starting mirror plane is copied,
- registration (ICP) of the mirror portion with the distal portion is carried out, moving together the copy of the mirror plane,
- the mirror plane is calculated as the mid plane between the starting plane and its copy.

3.6 – Condyles, TCA and MA

Analyzing the condyles, the TCA can be derived, which is the line tangential to the distal articular surface of the femoral condyles [DK1]. The condyles in the dog are in contact with the tibial plateau which can be approximated by a plane. Locally the condyles (articular surface) could be approximated by fitting a sphere [VV1]. Consequently the TCA can be represented by a line connecting the contact points between two spheres (condyles) and a plane (tibial plateau). This line can assume different positions depending on the rotation between femur and tibia.

To compute the TCA the following steps are proposed (fig. 5):

- a line (LCS) in the SPD is drawn, which is rotated with respect to DFLA of an angle RTF,
- a plane (PN) normal to LCS is constructed in front of the condyles,
- the vertex (VC) of each condyle closest to PN are identified,
- for each VC, the vertices (VCS) inside a neighbourhood with radius FL/50 are selected,
- the VCS are fitted with spheres (SC),
- the SC are sectioned with a plane PFTA, obtaining two circles (CC),
- the TCA is assumed as the line tangent CC.

The PFTA is a plane through the femoral transverse axis (FT) (connecting the SC centres) which gives an established rotation (RTF-90°) around FT from a reference plane. The plane through FT and point of minimum distance (PMD) between PFLA and FT is selected as reference.

Finally, the MA is obtained connecting the centre of the head with the intersection between TCA and SPD.

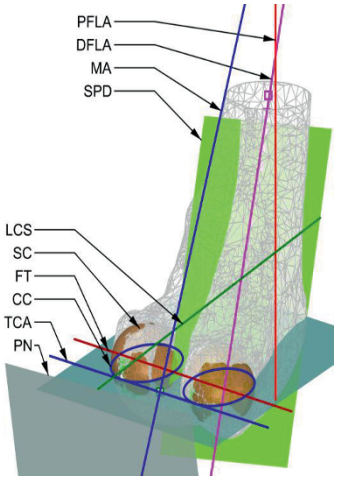

Figure 5: Distal femur analysis.

4- Results

The method has been preliminarily assessed on a dog cadaver femur, measured by two 3D scanners (S1.S2) with different mesh resolution as in tab. 1. The scanner S1 is more accurate than S2.

Mesh	3D Scanner	Vertices	Faces
1	S1	10082	19882
2	S1	100184	200022
3	S1	918506	1837008
4	S2	105715	209300

Table 1: Meshes analyzed.

To compare the test cases, the angles described in the section 2, evaluated in the 3D model, are adopted, with exception of FVA and FTA. FVA is calculated as in sec. 3.5, while FTA is computed in a plane perpendicular to the PFLA.

Due to the critical estimation of the centre of the neck, a preliminary investigation on the proposed method is needed.

	FNA [°]				FTA [°]				R/R			
	1	2	3	4	1	2	3	4	1	2	3	4
a	124.5	123.6	123.7	123.0	19.9	19.6	19.7	20.7	1.399	1.389	1.395	1.334
b	127.3	126.8	126.9	125.9	17.7	17.6	17.6	19.3	1.676	1.660	1.675	1.536
c1	126.0	125.4	125.4	125.7	19.0	18.7	18.8	19.5	1.5			
c2	126.9	126.4	126.5	126.2	18.2	18.0	18.1	19.1	1.6			
c3	127.4	127.0	127.0	126.5	17.5	17.3	17.4	18.8	1.7			

Table 2: FNA and FTA adopting different method for the neck mid point computation.

Tab. 2 shows the FNA and FTA angles computed adopting the approach described in sec. 3.4 for the 4 test meshes, where c1, c2, c3 indicates the different ratio (R/R) between the radius of the spherical section and the head radius.

In tab. 3 the other angles computed adopting the c1 criteria are summarized, together with femur length, head radius and area of the neck spherical section.

Mesh	aLPFA	mLPFA	aMDFA	mMDFA	FVA	FL	HR	AN
1	118.6	108.9	90.2	86.7	3.2	209.1	11.4	265.7
2	118.7	109.0	90.3	86.6	3.6	209.1	11.5	266.8
3	118.6	109.0	90.2	86.5	3.3	209.1	11.4	266.1
4	118.8	109.5	90.4	87.1	3.6	209.5	11.8	285.7

Table 3: Computed angles [°], femur length (FL) [mm], head radius (HR) [mm] and area of neck spherical section (AN) [mm^2].

5- Discussion and conclusion

5.1 – Proposed method discussion

Similarly to Tomlison [T1], PFLA computation is parameterized on the femur length; 10 sections allow reducing the effects due to local defects or noise of the mesh, where highest values do not show significant difference in the results.
In literature several approaches are proposed for analyzing the head (e.g. [CM1]), but the selection of the points for the sphere fitting is crucial because fovea is often considered in the fitting or the vertices selected for the head computation are not clearly delimited. The proposed approach overcame the mentioned limits.
Several studies propose to compute the neck centre by sectioning the neck with a plane [KE1, CM1]; the results obtained with these approaches are based on the minimization of a function with 3 parameters and consequently is highly dependent on the mesh accuracy. The proposed method reduces the minimization to a unique parameter: the radius of the spherical section. Consequently it is less sensitive to the mesh characteristics. The first proposed approach is conceptually similar to the literature: minimize the area of a section. The second approach would simulate the mechanical resistance: increasing the distance from the load (center of the head), the moment increases proportionally, so it is possible to suppose that the more critical section have the minimum ratio between area and distance (radius of the section). The third approach is proposed to avoid local minimum and trouble related to undercuts of the mesh due to 3D scanners acquisition limits.
The trochanter tip estimation includes a local surface; in this way errors depending on local spikes, noise or similar mesh imprecision are avoided.
Varus estimation [DK1] as proposed in literature could be only computed in a projection plane; moreover, the torsion could induce an error in the estimation of the varus. Both these are overcome adopting the symmetry plane of the distal portion.
The symmetry plane could be computed in 2 ways [DD1]. The proposed approach, based on mirroring and registration, proposes an original approach for the ICP algorithm which will be discussed in a future work.
The condyles are studied taking into account the knee kinematics, fitting the distal articular surface of the femur with two spheres [V1,VV1] as in literature. The angle RTF for the computation of TCA is 90°, which is conceptually similar to the TCA computed in the distal-proximal axial femoral radiograph. Other values of RTF could be adopted, with no significant difference in the results.

5.2 – Results discussion

To compare the different approaches for the centre of the neck computation, the ranges of FNA and FTA are computed. FNA angles have a range up to 3.5° adopting different criteria, while FTA have a range up to 2.4°. The range computed adopting the same criteria on different mesh are in tab. 4.

	Mesh 1-3		All meshes	
	Δ FNA [°]	Δ FTA [°]	Δ FNA [°]	Δ FTA [°]
a	0.89	0.27	1.47	1.10
b	0.56	0.11	1.47	1.69
c1	0.62	0.29	0.62	0.79
c2	0.48	0.23	0.67	1.08
c3	0.47	0.15	0.96	1.45

Table 4: Maximum range of FNA and FTA.

Adopting the same scanner with different resolution the b criteria has the minimum range for FTA, while the c3 criteria has the minimum range for the FNA. Considering only the meshes with highest resolution (mesh 2 and 3), all the criteria show highly close results.
Considering all the meshes, the minimum range for both FNA and FTA is the c1 criteria. This is probably related to the inaccuracy of the measure performed by the scanner S2 in the neck where undercuts exist; near to the head this effect is smaller and consequently the results are more reliable. By the data available it is possible to conclude that all the criteria gives good results for high quality mesh, while for not very accurate or low resolution data the c1 criteria is the best option.
In tab 5the range of other parameters are shown.

	aLPFA	mLPFA	aMDFA	mMDFA	FVA	FL	HR	AN
Δ 1-3	0.15	0.05	0.16	0.20	0.40	0.01	0.06	1.2
Δ all	0.28	0.54	0.27	0.62	0.46	0.42	0.38	20.0

Table 5: Range of the computed parameters for the meshes 1-3 and for all the meshes.

The meshes generated by the same scanner with different resolutions show a maximum variation for all angles of ±0.20° (FVA), while considering all the meshes a maximum variation for all angles of ±0.31° (mMDFA). The mesh measured with scanner S2 is larger: this is confirmed both from the femur length and head radius. Finally the mentioned question related to the neck centre is mirrored by the area of the spherical section which take a larger value in the mesh of the scanner S2.

5.3 – Conclusions

In this paper a robust and original method for the computation of morphological and clinical parameters of dog femur is proposed.
This approach leverages the capabilities of the 3D models, which can be obtained by CT, MTI or 3D scanner. The availability of these models allows to overcame the main troubles related to the radiographic approach such as the orientation, the dependency of the operator and the 2D limits.

Moreover any other dimensions should be taken into account as the distance between the head centre and the anatomical axis or the distance between the transcondylar axis and the anatomical axis. Finally a review of the clinical and morphological parameters is needed in order to reduce the number of angles and to establish a clinical-physical meaning in 3D.

6- References

[CM1] Cerveri P., Marchente M., Bartels W., Corten K., Simon J.P. and Manzotti A. Automated Method for Computing the Morphological and Clinical Parameters of the Proximal Femur Using Heuristic Modeling Techniques. In Annals of Biomedical Engineering, 38(5): 1752-1766, 2010.

[DD1] Di Angelo L. and Di Stefano P. Bilateral symmetry estimation of human face. In International Journal on Interactive Design and Manufacturing, 7(4): 217-225, 2013.

[DK1] Dudley R. M., Kowaleski M. P., Drost W. T. and Dyce J. Radiographic and computed tomographic determination of femoral varus and torsion in the dog. In Veterinary Radiology and Ultrasound, 47:546–552, 2006.

[KE1] Kang Y., Engelke K., Fuchs C. and Kalender W. A. An anatomic coordinate system of the femoral neck for highly reproducible BMD measurements using 3D QCT. In Computerized Medical Imaging and Graphics, 29(7): 533-541, 2005.

[MN1] http://www.meta-numerics.net/

[M1] Meggiolaro S. Comparison of a 3-dimensional model and standard radiographic evaluation of femoral and tibial angles in the dog. PhD thesis, Università degli Studi di Padova, 2009.

[P1] Petazzoni M. Atlante di goniometria clinica e misurazioni radiografiche dell'arto pelvico. Ed. Merial, 2008.

[R1] http://www.food4rhino.com/project/rp

[S1] https://sites.google.com/site/gianpaolosavio/rhino-open-projects/dogfemursegmentation

[SM1] Savio G., Meneghello R., Concheri G. Optical Properties of Spectacle Lenses Computed by Surfaces Differential Quantities. In Advanced Science Letters 19(2): 595-600, 2013.

[TF1] Tomlinson J., Fox D., Cook J. L. and Keller G. G. Measurement of femoral angles in four dog breeds. In Veterinary Surgery, 36(6): 593-598, 2007.

[V1] Victor J. Rotational alignment of the distal femur: a literature review. In Orthopaedics & Traumatology: Surgery & Research, 95(5): 365-372, 2009.

[VV1] Victor J., Van Doninck D., Labey L., Van Glabbeek F., Parizel P. and Bellemans J. A common reference frame for describing rotation of the distal femur. A CT-BASED kinematic study using cadavers. In The Bone & Joint Journal, 91-B(5): 683-690, 2009.

Article 067-m-43

Characterization of Ultra-precise aspherical surfaces using Forbes equation

N. El-Hayek [1,2,*], N. Anwer [3], H. Nouira [2], M. Damak [1,4], O.Gibaru [1]

(1) : LSIS, Arts et Métiers ParisTech, 8 blvd. Louis XIV, 59046 Lille, France
+33(0)320622210
E-mail : {nadim.el-hayek, olivier.gibaru}@ensam.eu

(2) : Laboratoire Commun de Métrologie (LCM), 1 rue Gaston Boissier, 75015 Paris, France
+33(0)140433763
E-mail : hichem.nouira@lne.fr

(3) : LURPA, ENS de Cachan, 61 av. du Président Wilson, 94235 Cachan, France
+33(0)149406164
E-mail : anwer@lurpa.ens-cachan.fr

(4) : GEOMNIA SAS, 165 av. de Bretagne, EuraTechnologies - 59000 Lille, France
+33(0)359059123
E-mail : m.damak@geomnia.eu

Abstract: The fields of application and use of aspherical lenses is a growing market. Although many researches have been conducted to address their manufacturing and measurement, there are still challenges in form characterization of aspherical surfaces considering a large number of data points. This paper presents the measurement and form characterization of an asphere using a high precision profilometer, traceable to the SI meter definition. The measured surface is constituted of a large number of data points. The form characterization of the asphere's surface is based on the comparison of the measured surface with the design surface, expressed as a Forbes strong asphere. The Levenberg-Marquardt algorithm is used and tested on simulated data in order to assess its behaviour regarding aspherical surface fitting. Experimental results are then analyzed and discussed on real data and show the effectiveness of the proposed approach.

Key words: Asphere; form characterization; high precision metrology; non linear least-squares method.

Nomenclature

LM: Levenberg-Marquardt
MS: Measured Surface
DS: Design Surface
NIST: National Institute of Standards and Technology
PV: Peak-to-Valley
RMS: Root Mean Square
ICP: Iterative Closest Point
L-BFGS: Limited memory-Broyden-Fletcher-Goldfarb-Shanno
NMI: National Metrology Institute
EMRP: European Metrology Research Program
IPi: i^{th} Initial Position

1- Introduction

Aspheric surfaces have become widely used in various applications such as optics, photonics and biomedicine. The manufacturing and measurement of such elements is still a common challenge in industry as the form characterization of aspheric surfaces is not yet normalized. This process becomes even harder when considering a large number of measurement points. This paper presents an adaptation of the very-well known Levenberg-Marquardt (LM) algorithm for the fitting of Forbes strong aspheres. The algorithm is first tested on simulated data containing random and systematic errors. The random errors are represented by Gaussian noise with a magnitude that reflects probing errors that can manifest in real measurements. Optical and tactile single point scanning probe systems are commonly used in dimensional metrology applications. However, in order to reach a nanometric level of accuracy in the measurement of aspheric lenses, ultra-high precision machines should be employed. Therefore, the design of the LNE's high precision profilometer, traceable to the SI meter definition is presented. Its architecture complies with the Abbe principle and its metrology loop is optimized. The performance and capability of the machine in the scope of aspheric lenses metrology are discussed. The measured surfaces (MS) obtained from the aforementioned system are characterized by a large number of data points (> 100,000 points). The Design Surface (DS) of the aspheric lens can be described using different models. A conic-polynomial model which serves as a basis for aspheric lens specification, a discretized form of the polynomial into a set of reference points to create a nominal CAD form, or a mapping of that polynomial into a linear combination of orthogonal basis functions. The form characterization of aspheric lenses is based on Orthogonal Least-Squares fitting techniques by comparing the measured

surface with the design surface using the LM algorithm recommended by the NIST [S1]. The fitting algorithm is adapted to fit aspherical surfaces using the newly developed Forbes definition [F1]. The algorithm is first tested on simulated data of an asphere with added noise and form errors and then applied to a real measured dataset. The characterization proposed in this article which is based on the Forbes equation is compared with the characterization based on the classical model.

2- Form characterization of aspheres

2.1 – Mathematical representation

The classical way of describing aspheres is defined as the composition of a quadric and a polynomial (set of monomials) as shown in (Eq. 1). This definition is derived from the normalized form found in ISO 10110-Part 12 [I1] and in which the a_2 coefficient of x^2 is already integrated within c of the quadric part of the equation.

$$z(x) = \frac{cx^2}{1+\sqrt{1-\kappa c^2 x^2}} + \sum_{i=1}^{M} a_{2i} x^{2i} \qquad (1)$$

where x is the radial coordinate, z is the sag (sagittal representation), c is the curvature at the apex, and κ is the conic constant. The $a_{2i}r^{2i}$ terms are the higher order aspheric terms that represent the additive departure from the quadric. M denotes the number of components constituting the polynomial.

The new paradigm in representing asphere surfaces is leaning towards a representation derived by Forbes [F1] (Eq. 2). He demonstrates that with his formulation, the model parameters are independent parameters making each one of them unique and meaningful. The reason for this is that the right-hand-side of the equation contains a set of orthogonal polynomials. There exists a conversion software (QED surface conversion tool retrieved from [Q1]) developed by Forbes in order to convert classical models into Forbes models and conversely (Fig. 1).

$$z(x) = \frac{cx^2}{1+\sqrt{1-\kappa c^2 x^2}} + \upsilon^4 \sum_{i=0}^{P} a_i Q_i^{con}(\upsilon^2) \qquad (2)$$

where c and κ and the a_i's have different values than in the classical model. $a_i Q_i^{con}$ are the terms of a set of orthogonal polynomials that represent the departure from the conical shape and $\upsilon = x / R_{max}$ with R_{max} being the aperture of the asphere. The first few polynomials are a set of Jacobi polynomials.

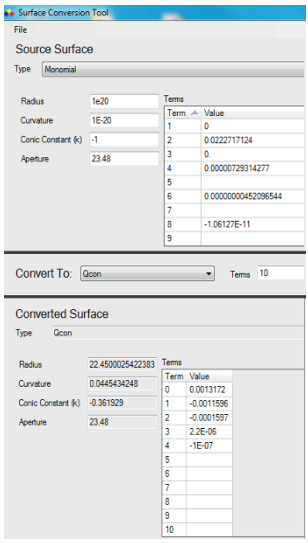

Figure 1: Screenshot of the surface conversion tool free software.

2.2 – Asphere surface fitting

The form evaluation of aspheres can be done through the association of the aspherical model to the measured data according to a criterion such as least-squares or minimum zone. Residuals are then evaluated: the Peak-to-Valley (PV) and the Root Mean Square (RMS) are the most widely adopted parameters for the assessment of form deviations of aspheres.

Many fitting techniques are reported in the literature, but only few discuss the fitting of aspheres. Chen *et al* [CG1] propose an aspheric lens characterization by fitting 2D aspherical profiles using the LM algorithm [M1] for its quick convergence and precision. Similar works have been published and also deal with aspheric profile identification and conic sections fitting [A1]. Sun *et al* [SM1] use the Gauss-Newton algorithm for the fitting of aspherical curves and surfaces on simulated data with vertical distance minimization, assuming that the model and the data are both defined in the same reference frame. In a parallel work to this paper, El-Hayek *et al* [EG1] show that orthogonal distance minimization is more accurate than vertical distance minimization for the fitting of aspheres by testing both approaches on simulated data and measurement data. The problem of fitting the data to the aspherical surface model is set as a nonlinear least-squares problem which is defined as follows (Eq. 3).

$$\min_{\lambda} \sum_{i=1}^{N} \left\| \mathrm{R}p_i + \mathrm{T} - q_i \right\|^2 \qquad (3)$$

where λ is the set of shape, position and orientation variables,

R, T are the transformation parameters, p_i is a data point, and q_i is the orthogonal projection of the data point p_i onto the reference model (footpoint). In the fitting process all the λ parameters are estimated so the objective function to minimize is written as follows (Eq. 4):

$$f = \min_{c,\kappa,\alpha;\theta,\gamma,t_x,t_y,t_z} \sum_{i=1}^{N} \left\| \mathrm{R}_{\theta,\gamma} p_i + \mathrm{T} - q_i \right\|^2 \qquad (4)$$

The classical algorithm for registration of point clouds and fitting of shapes is the Iterative Closest Point (ICP) algorithm and its variants [RL1, P1]. The ICP finds a spatial transformation to align two point-sets, making it a relatively fast algorithm with negligible storage. It can be used for fitting applications when one of the point-sets is a theoretical point model or mesh model. ICP is based on two main operations, point identification and point matching and these operations are usually computationally expensive. An iterative loop identifies pairs of points and matches them across both entities. The matching phase results in a transformation matrix that brings one point-set to the other with residual errors. If the errors are larger than the threshold value, point identification and matching restarts until the two point-sets are closely aligned. In order to have fine precision on the results, it is preferable that the size of both sets be equal and this is not always met in practice.

Other algorithms are also abundantly used and found in literature. The Gauss-Newton type [BM1] and the LM type [M1, JZ1] have been recommended by NMIs [S1]. Quasi-Newton approaches also exist and perform very well in practice [EG1]. For example the Limited memory-Broyden-Fletcher-Goldfarb-Shanno (L-BFGS) algorithm shows equal accuracy to the LM algorithm and has been observed to have slightly better performance for large data and number of variables. Quasi-Newton methods seek to approximate the inverse Hessian matrix of the objective function directly without having to go through matrix inversion like it is the case with Gauss-Newton approaches.

In this paper, we use the LM algorithm for the minimization of orthogonal distances and a simple Newton-Raphson routine for the footpoint approximations. The Newton-Raphson method [SM2] is used in optimization problems that are not highly non-linear. The goodness of the approximation depends on the stop criterion and on the quality of the initial guess (relative position of the point data and the model should be close to the optimal solution). For this part, the vertical projection point is taken as an initial guess and is actually close to the orthogonal projection point on aspherical surfaces, since aspheres are almost planar surfaces. The Newton-Raphson method iterates until the orthogonal projection point is accurately approximated.

The LM is based on a blend between a Gauss-Newton approach and the gradient descent. It has been approved by the NIST for metrology applications that require fitting simple curves and surfaces in 3D [S1]. Generally, this algorithm converges reasonably quickly and accurately for a wide range of initial guesses that are relatively close to the optimal solution. The fitting of parametric curves and surfaces using the LM algorithm also requires the calculation of a large Jacobian matrix and the storage of a considerable system of linear equations, as stated by Speer *et al* [SK1]. The update rule for the LM optimization method follows Eq. 5.

$$x_{j+1} = x_j - (H(x_j) + \lambda_j . diag[H(x_j)])^{-1} . \nabla f(x_j) \qquad (5)$$

Where x_j is the solution vector at iteration j, H_j is the Hessian matrix at iteration j. λ is the parameter that can be assimilated to the coefficient of the gradient. λ changes at each iteration such as when it is large, the gradient descent predominates the optimization process and when it is small, Gauss-Newton predominates. A suggested starting value of 0.0001 is reasonable according to the certification given by the NIST [S1].

3- Measurement apparatus

Measuring aspheric surfaces to an accuracy of few tens of nanometres remains an important challenge in manufacturing and metrology of freeform optics [1]. To achieve the best possible accuracies, specific ultra-high precision machines have been developed by the National Metrology Institutes (NMIs) that ensure the traceability chain. In this regard, a three-year project has been launched by the European Metrology Research Program (EMRP) [2] and encompasses a multitude of European National Metrology Institutes (LNE, PTB, VSL, METAS, SMD and CMI), industry and academia aiming at improving apparatus and methods for high-precision measurement of aspheric and freeform optics and characterizing their form. The apparatus are generally related to small-volume coordinate measuring machines that feature measuring ranges of hundreds of millimetres. These machines respect the Abbe principle, apply the dissociated metrological structure and incorporate high-precision mechanical guiding elements.

3.1 – Description and evaluation of the apparatus

LNE's high precision profilometer is a measurement machine (Fig. 2) capable of performing independent motions in all x, y and z directions using three independent high-precision mechanical guiding systems equipped with encoders. Three sub-nanometric interferometers control the displacements in x, y and z directions respectively. The working range in the xy-plane is 50×50 mm². The probe and its supporting structure are mounted on the vertical guiding system in the z-direction along which the measurement is done. The working range of the mechanical guiding system in z-direction is about 100 mm. The metrology frame is made of Invar for minimal sensitivity to environmental influence. The machine can be equipped with either confocal probes or a tactile probes. It allows the in-situ calibration of the probes by means of a differential laser interferometer considered as a reference.

3.2 – Tactile probing of aspheres

The measurements and take place in the LNE's cleanroom in which environmental conditions are optimal. Temperature is controlled to 20±0.3 °C and humidity to 50±5 %RH. The asphere is posed on the Zerodur table (Fig. 2) and is

measured by a tactile probe which has been previously calibrated in-situ. On the LNE's profilometer, it is not possible to exactly align the asphere's axis with the z axis of the measurement, however, an approximation of the apex position can be done by estimating the cusp of the surface. For this matter, the surface is once scanned in the x- direction and once in the y- direction and a peak is computed. This peak represents an approximation of the cusp around which a symmetrical measurement is performed. A large number of data points (>> 100,000 points) are recorded in the form of XY-grids over a squared area of 6×6 mm².

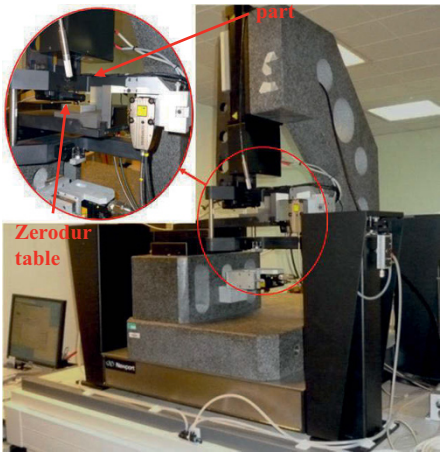

Figure 2: The LNE apparatus.

4- Results and analysis

The fitting algorithm used is tested on both the classical and the Forbes conic models of aspherical surfaces. The algorithm is first validated on simulated data with added random and systematic errors, and then applied on measured data. The analysis is based on whether the residuals returned by the optimization process are conform to the simulated ones. The application to real data allows for a form characterization of the measured asphere. The effectiveness of LM is tested through different initial positions of the MS with respect to the DS.

4.1 – Simulated datasets

The Forbes asphere model is simulated based on Eq. 2 as shown in Fig. 3 by generating symmetrically distributed points around the asphere's axis. The design parameters of the asphere have the following values (c=0.0445434248, κ=-0.361929, a_0=0.0013172, a_1=-0.0011596, a_2=-0.0001597, a_3=2.2E^{-6}, a_4=-1.0E^{-7}). The classical asphere model used for comparison is based on Eq. 1. It has the exact same form as the surface defined by Forbes with a few hundredths of nanometres difference. The design parameters of the classical asphere have the following parameter values (c=1E^{-20}, κ=-1, a_2=0.0222717, a_4=7.29314E-06, a_6=-0.0001597, a_8=2.2E^{-6}, a_{10}=-1.0E^{-7}). For readability in the tables later we will number the a parameters with the same index numbering as Forbes.

Simulations are performed in order to study the effect of data subject to errors both from measured object (form deviations) and measurement (Gauss noise) [12]. Measurement errors simulation involves generating Gaussian noise with controlled mean and standard deviation, $N(0,8.33)$. This value is coherent with probing errors of the used tactile instrument. A MATLAB random function generates the noise data which are added to the theoretical data in the orthogonal direction at each data point. Form errors are also superimposed on the theoretical data in order to simulate form deviations. The systematic errors are described by Fourier harmonics such as stated in the ISO standard [12] and shown in Eq. 6. The number of harmonics n for an asphere is taken as a compromise between the number of harmonics needed for a plane and the number needed for a sphere (n=6). The combined errors are illustrated in Fig. 4.

$$F(X)=\sum_{k=1}^{n} A_k \sin(2\pi k w_0 X)+B_k \cos(2\pi k w_0 X) \qquad (6)$$

where A_k and B_k are the amplitudes of the k-th harmonic and w_0=2 mm^{-1} is the fundamental spatial frequency. A_k has values of 100, 70 and 75 nm and B_k has values of 100, 90 and 55 nm, respectively.

The LM algorithm is used to fit the data to the model and the residuals as well as the estimated parameters are analyzed. The RMS and PV values of the residual errors are reported in table 1. The model and transformation parameters are reported in table 2. The RMS and PV values are identical. For a theoretical dataset simulated without any added noise, fitting returns parameters that are identical to the design parameters; whereas in the case of added noise, these parameters present a slight variation.

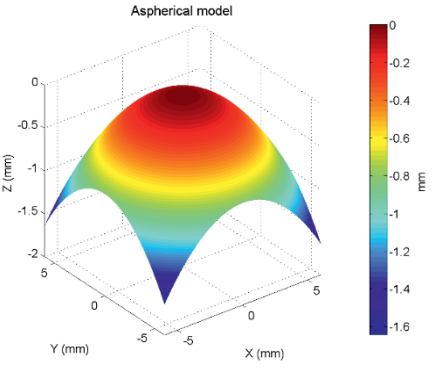

Figure 3: The asphere model without any added errors.

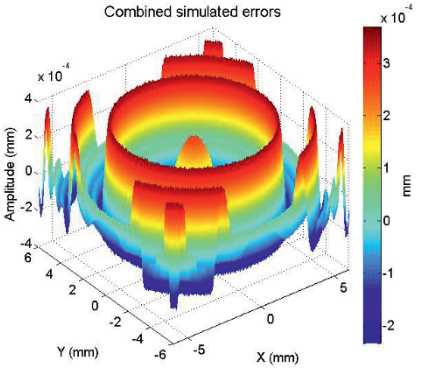

Figure 4: The combined systematic and random errors.

Forbes parameters	Fitted values
c	0.044647122
κ	-0.3720941
a_0	0.0012998
a_1	-0.0011417
a_2	-0.0001583
a_3	2.231108E^{-6}
a_4	-1.03298E^{-7}
RMS (nm)	129.735
PV (nm)	594.829

Table 1: Fitting using LM algorithm for the combined systematic and random errors.

4.2 – Experimental datasets

The surface is scanned using a tactile probe over an area of 6×6 mm², giving a grid of about 1,500,000 points. The fitting results are detailed and compared for the experimental datasets for three different relative initial positions with respect to the reference model (table 2). The first initial position (IP_1) is manually positioned to be very close to the model, IP_2 is shifted by few millimeters (+10 mm) in x and y directions, and IP_3 is the same as IP_1 but rotated with an angle of almost 90° about x. The algorithm converges for all three positions of the real data. The residual errors return a RMS value of 134 nm and a PV of 1461 nm.

The experimental data have been tested also with other fitting algorithms but this is beyond the scope of this article. Nonetheless, results from a comparative study show an equivalent accuracy among L-BFGS, LM and ICP [EG1]. The residual errors are illustrated in Fig. 5.
LM performs relatively fast within the order of a few minutes for 1.5×10^6 points and 12 variables (5 transformation parameters and 7 model parameters) in the case of the classical model fit. In the case of Forbes model fitting, the computational time is a bit more expensive. However, in both cases memory storage is very low and datasets of several millions of points can be processed. It is to be observed that a selection of a subset of points in the minimization process returns the same residual errors as the entire dataset. The most important thing to note here is that the results in table 3 show that the fit parameters are a bit far from the design parameters. This can be interpreted by the fact that the measured area covers only about 25% of the surface around its axis. Plotting the model with the fitted parameters shows a remarkable deviation towards the tip of the asphere (Fig. 6).

	Forbes model		Classical model	
N	RMS (nm)	PV (nm)	RMS (nm)	PV (nm)
IP_1				
75, 000	133.426	1450.418	133.997	1455.023
200, 000	133.426	1456.122	133.998	1458.396
500, 000	133.425	1456.345	133.999	1459.105
1, 500, 000	133.425	1456.193	133.999	1459.025
IP_2				
75, 000	133.426	1450.424	133.997	1455.031
200, 000	133.426	1456.130	133.998	1458.406
500, 000	133.425	1456.378	133.999	1459.095
1, 500, 000	133.425	1456.201	133.999	1459.028
IP_3				
75, 000	133.426	1450.427	133.997	1455.039
200, 000	133.426	1456.122	133.998	1458.412
500, 000	133.425	1456.362	133.999	1459.108
1, 500, 000	133.425	1456.209	133.999	1459.019

Table 2: Fitting results of the measurement. N is the number of points considered in the fitting.

Parameters		Forbes model	Classical model
t_p	θ (°)	0.1331636	0.13313546
	γ (°)	0.0953888	0.10341516
	t_x (mm)	0.036369196	0.03950963
	t_y (mm)	-0.052374529	-0.0523625
	t_z (mm)	-0.000321956	-0.00031206
m_p	c	0.044831432	1.000E-020
	κ	-0.35719573	-1.00
	a_0	0.0013003	0.022384659
	a_1	-0.0011932	-6.8163913E-7
	a_2	-0.0001628	5.06997814E-7
	a_3	2.319736E^{-6}	-2.5792152E-8
	a_4	-1.19264E^{-7}	4.6201995E-10

Table 3: The estimated model parameters of the asphere and transformation parameters after fitting.

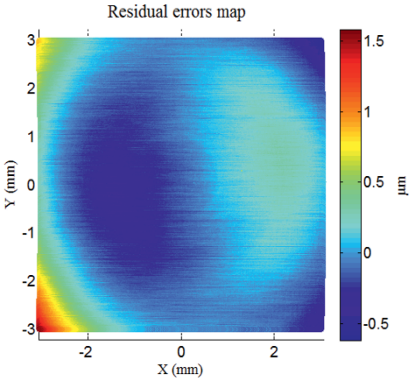

Figure 5: Residual errors map after fitting of the measurement data.

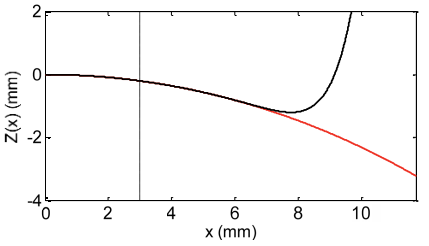

Figure 6: Forbes aspherical model half-profile: fitted Forbes model with estimated parameters (black curve); original Forbes model (red curve); Limit of the measured area (vertical cashed line).

5- Conclusion

The form characterization of aspheres is done based on the orthogonal fitting of the measured data to the Forbes model using the LM algorithm. The algorithm has been applied with the classical model as well for comparison. Tests reveal that on simulated datasets they return similar results for the fitting on a given aspherical surface model. The algorithms are also tested on an experimental dataset and the RMS and PV values are very comparable to the theoretical ones. Future works will include implementing an algorithm based on MinMax norm.

6- Acknowledgements

This work is part of EMRP Joint Research Project-IND10 "Optical and tactile metrology for absolute form characterization" project. The EMRP is jointly funded by the EMRP participating countries within EURAMET and the European Union.

7- References

[A1] H. Aceves-Campos. Profile identification of aspheric lenses. Appl. Opt. 37(34): 8149-8150, 1998.

[BM1] Besl P. and McKay N. Method for registration of 3-D shapes. Pattern Anal. and Mach. Intel. IEEE Transactions 14(2): 239-256, 1992.

[CG1] Chen Z., Guo Z., Mi Q., Yang Z. and Bai R. Research of fitting algorithm for coefficients of rotational symmetry aspheric lens. Proc. SPIE 7283, 4th Intl. Symp. on Adv. Opt. Manuf. and Tes. Tech.: Opt. Test and Meas., 2009.

[EG1] El-Hayek N., Gibaru O., Nouira H., Anwer N. and Damak M. Large-volume datasets fitting of aspherical surfaces. Submitted to Precision Engineering, 2014.

[F1] G.W. Forbes. Shape specification for axially symmetric optical surfaces. Optical Express 15(8): 5218-26, 2007.

[I1] ISO 10110-12, Optics and photonics - Preparation of drawings for optical elements and systems - Part 12: Aspheric surfaces, 2007.

[I2] ISO 10360-6. Geometrical Product Specifications (GPS)-Acceptance and re-verification tests for coordinate measuring machines (CMM) - Part 6: Estimation of errors in computing Gaussian associated features, 2002.

[JZ1] Jiang X., Zhang X. and Scott P. Template matching of freeform surfaces based on orthogonal distance fitting for precision metrology, Meas. Sci. and Tech. 21 (2010) 045101.

[M1] J. Moré. The Levenberg-Marquardt algorithm: implementation and theory. In Numerical analysis, Springer, 1978, 105-116.

[PC1] Pomerleau F., Colas F., Siegwart R. and Magnenat S. Comparing ICP variants on real-world data sets. Auton. Rob. 34(3): 133-148, 2013.

[Q1] QED Technologies: http://www.qedmrf.com

[RL1] Rusinkiewicz S. and Levoy M. Efficient variants of the ICP algorithm. 3D Dig. Im. & Mod. 145-152, 2001.

[S1] C. Shakarji. Least-squares fitting algorithms of the NIST algorithm testing system. J. of res. of the Nat. Inst. of Stan. and Tech. 103: 633-641, 1998.

[SK1] Speer T., Kuppe M. and Hoschek J. Global reparametrization for curve approximation. Comp. Aid. Geom. Des. 15(9): 869-877, 1998.

[SM1] Sun W., McBride J.W. and Hill, M. A new approach to characterizing aspheric surfaces. In Precision Engineering 34(1): 171-179, 2010.

[SM2] Süli E. and Mayers D. An introduction to numerical analysis, Cambridge University Press, 2003.

Article 069-m-95

TESTING THE INFLUENCE OF SCANNING PARAMETERS ON 3D INSPECTION PROCESS WITH A LASER SCANNER

Salvatore Gerbino [1], Gabriele Staiano [2], Antonio Lanzotti [2], Massimo Martorelli [2]

(1) : University of Molise - DiBT Department
Via Duca degli Abruzzi - 86039 Termoli (CB) - Italy
Phone +390874404593
E-mail: {salvatore.gerbino}@unimol.it

(2) : University of Naples Federico II - Department of Industrial Engineering – P.le V. Tecchio 80 Naples - Italy
Phone/Fax +390817682470
E-mail: {*name.surname*}@unina.it

Abstract: The quality of 3D scanned data is influenced by many factors both related to internal elements to the acquisition device, such as scanner resolution and accuracy, and external to it, such as proper selection of scanning parameters, ambient illumination and characteristics of the object surface being scanned (e.g. surface colour, glossiness, roughness, shape). Due to the recent developments in terms of accuracy, in particular for 3D laser scanners, today it is of great industrial interest to study and correctly setting the scanning parameters that allow to improve the quality of the 3D acquisitions so to increase the massive usage of these systems in the product inspection activities. In this paper the effects of some scanning parameters that may affect the measurement process, were analysed by using a commercial triangulation 3D laser scanner. The test geometry chosen for this study was a commercial sheet metal part more complex than the ones commonly used in laboratory and documented in the literature. Relative orientation, ambient illumination and scanner parameters were tested. The outcomes of the tests confirmed some results and suggestions documented in literature but also pointed out that over different conditions the most influencing factor are the relative orientation of the object with respect to the scanner, as well as its position within the field of view of the measurement device.

Key words: 3D laser scanner, scanning parameters, 3D inspection, Reverse Engineering.

1- Introduction

3D scanners are devices mainly addressed to the task of 3D digital reconstruction of real-world objects, even of complex shape, through principles codified in complete sets of procedures, specific to various applications. Non-contact active and passive 3D scanners are today widely used in numerous industrial applications, also for getting measurements for quality inspection. They mainly include systems based on the following optical technologies: laser triangulation, structured light, time-of-flight and photogrammetry. All these technologies have reached a good level of confidence and accuracy for Reverse Engineering applications and some of them (mainly those based on laser triangulation) are currently employed in a number of factories as quality inspection device [MC1]. They allow, in fact, to get a high speed in the acquisition of a large set of points over each surface, and the consequent time/cost reduction.
Coordinate Measuring Machine (CMM) systems based on touch probe still offer a higher accuracy in the inspection process for verifying dimensional and geometrical tolerance specifications of mechanical parts. The main drawback of such a technology is the long operational time to acquire also few points, that becomes prohibitive when a complex shape needs to be accurately measured in many points [MC1].
The ability of 3D optical scanners to capture thousands of points in few seconds, together with the increased accuracy they recently offer, make possible to extend the quality control to the whole part's shape. In [HL1 and LL1] authors documented researches aimed to check and model the statistical variational behaviour of automotive sheet metal components for virtual simulation of compliant assemblies by acquiring the whole geometry of each flexible component. This need will become more and more common also in other industrial fields, so it is important to understand well the several conditions and parameters the user can chose to get the best from the 3D scanners, in particular the ones based on laser triangulation which are more common.
In the present paper the commercial 3D laser scanning system, VI 9i by Konica Minolta, was used for this purpose on a sheet metal car component, taking into account different scanning parameters, such as the relative position laser-to-object, the ambient illumination and other internal settings of the laser scanner device.

2 – Main parameters in 3D data acquisition with a triangulation laser stripe system

The most common laser systems used in metrological applications are those based on principle of triangulation through a laser stripe. The reasons are the high precision, the relative lower cost with respect to other systems, and the possibility they offer to acquire objects on site.
In these non-contact active systems an incident laser beam,

with known width, is projected onto a part to be scanned and the stripe generated on the surface is detected by a CCD sensor; then through the triangulation principle, 3D coordinates of the surface points are acquired.
The main parameters of these systems are depicted in Figure 1. We may distinguish parameters imposed by the system manufacturer and parameters depending on the user choices.

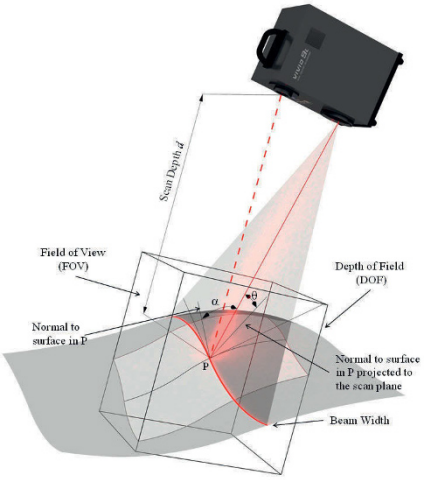

Figure 1: Main parameters of a laser stripe 3D scanner.

The main parameters imposed by the system manufacturer are:
- Field of view (FOV): 3D region within which the CCD sensor can acquire points on the scanned surface. It is defined by the depth of field and the scan width.
- Depth of Field (DOF): range of distance from the laser source within which the CCD sensor can acquire points on the scanned surface.
- Scan width: width of the laser beam measured in the half position of the depth of field.
- Stand-off distance: distance from the laser source to the reference surface located in the half zone of the field of view.

The main parameters not depending by the manufacturer, and that the user can (partially) control, are:
- Incident angle (θ): angle between the incident laser beam and the projected surface normal of the scanned point in the scanning plane [PL1].
- Projected angle (α): angle between the scanning plane and the normal (minimum) at the surface in the scanned point [PL1].
- Laser light intensity.
- Ambient light.

More factors influencing the accuracy of a measurement with a laser scanner must be added:
- Topology of the object to be acquired.
- Characteristics of the material object (e.g. surface colour, glossiness, roughness).
- Processing software.

The related orientations of the scanned surface with respect to the incident laser beams, represented by the incident angle θ (in the laser plane) and the projected angle α (measured out of the laser plane) in Figure 1, are the main scanning process parameters mostly influencing the measurement accuracy [FL1]. In fact, the intensity of the reflected laser beam and its impression on the optical CCD sensor is strictly related to the incident/projected angles. This dependency was empirically measured in [MJ1].
In [PL1] the following ranges were suggested for the angles θ and α: $-35° \le \theta \le +35°$ and $-15° \le \alpha \le +15°$, from which an algorithm was proposed for the optimal choice of the relative orientation laser-to-object_surface, starting from a planning based on the object's CAD model. This positioning error has a systematic nature and it can be partially controlled by the user thanks to the right positioning of the scanner with respect to the object, being usually the normal position laser-surface the best one for getting higher accuracy.
The ambient light plays a very important role in the optical measurements. In the recent version of laser devices, released by different manufacturers, it is pointed out their ability to work in a large range of ambient light conditions, as well as with different colours of the object's surface, but in practice many users still report a sensitivity to this effect. A technical solution more adopted in these cases is the use of specific light filters on CCD sensor [FS1]. Practical solutions are the use of coating spray to cover the object with a matte white layer, as discussed later.
In [BF1] the authors reported the results of a specific study on the influence of ambient light on the quality of laser scanner-based measurements on different typology of materials with the same surface treatment. Best results, in terms of less variability and more available data, were generated by using mercury vapour lamps instead of halogen illumination.
In [CR1] the influence of the ambient light to the quality of captured signal by CCD sensor is confirmed and the dependency of the measurement from surface roughness of the component was pointed out. They suggested making measurements in absence of or limiting the ambient illumination. This condition is often difficult to apply in many real cases.
The intensity of laser source is strictly dependent from the surface's roughness. For surface with ISO roughness grade N1 (Ra=0.025μm) to N11 (Ra=25μm) the maximum laser intensity (whose correspond the highest amount of acquired data) is strongly related to the machining process generating that surface. The authors proposed a table with suggested ranges of laser intensity for getting the maximum results from the measurements for different roughness rate and machining processes. For sheet metal deep drawing components the recommended value for optimal laser intensity is about 20% of full power of laser source.
In [FL1] the authors studied the random error which is strictly related to the surface's roughness causing the speckle effect: surface roughness during the scanning process produces a slight variation on the reflected light signal, and on CCD sensor the wave amplitude of the captured light can be cancelled or reinforced. This local interference between captured lights makes difficult to get the right centre point on

CCD which is used to make the 3D measurement of the digitised point. This phenomenon is more evident when the laser wave length is close to the one of the scanned surface's roughness (around 1/10 µm).
Martínez *et al*. [MC1] pointed out how difficult is the acquisition of dark, glossy and translucent surfaces. With very shiny surfaces a significant noise is added to the measurements, and points not belonging to the real surface can be generated.
Glossy surfaces affect the saturation of light captured by CCD sensor, whereas dark surfaces absorb too much light intensity. In these cases the CCD sensor is unable to acquire data locally (missing data) or the measurement is highly affected. In such conditions it is suggested using coating sprays to cover objects with a thin white matte layer, which is specifically helpful for scanning dark, glossy or translucent surfaces. In [MJ1] it was evaluated in 5-15 µm the added thickness and the additional variation of about 45 µm by using very thin coating sprays.
Black coloured surfaces are harder to scan (they usually require the coating spray) but the new released devices provided by some scanner producers offer a limited solution to reduce measurement uncertainties by automatically tuning on the laser power and adopting specific filters for CCD on the captured signal.

3- Materials and Methods

The test geometry chosen for this study (Fig. 2) is a commercial sheet metal part used in automotive field with a general shape complexity that allows to test some aspects previously described.
A commercial laser scanner – VI 9i by Konica Minolta, whose measurement ranges for different interchangeable lenses (tele, middle and wide) are summarised in Table 1 – was used for the measurements.
The black original colour of the component resulted hard to acquire, so it was necessary to use a coating spray, as shown in Figure 2. Tests made with different operators demonstrated that the measurement result (also related to reference spheres located onto the part) was strongly dependent on the operator spraying the component, so we decided to paint the whole part with a matte light grey colour, very similar to the colour of the original calibration device of VI 9i scanner.

Figure 2: Tested sheet metal part partially sprayed with a white matte layer to allow acquisition with a laser scanner very sensitive to the original black colour of the part.

The part was firstly acquired with a CMM laser scanner to generate the whole reference model for the test as the original CAD model of the part was missing. This is acceptable for the higher accuracy of the used CMM laser scanner (Metris LC15 mounted on DEA Global Image Clima), equal to 8µm, than the one of the VI 9i scanner, equal to 50µm. Figure 3 depicts an intermediate step of the acquisition phase with the CMM laser scanner.

Measurement ranges (X direction × Y direction × Z direction)

	TELE	MIDDLE	WIDE
Distance: 600mm	111×83×40mm	198×148×64mm	359×269×108mm
Distance: 1000mm	185×139×110mm	329×247×176mm	598×449×284mm

Table 1: Measurement ranges for different interchangeable lens for the VI 9i laser scanner.

All scan data were post-processed in Geomagic 2012 software to generate the final polygonal model (made by about 970k triangles, referred to the only component) shown in Figure 4.
The model in Figure 3 also shows the use of reference spheres to make easier and repeatable the alignment process of point data sets to the reference model (RPS method). We used spheres of diameter 1" and 1/2".

Figure 3: Acquisition phase with CMM laser scanner to generate the reference 3D model.

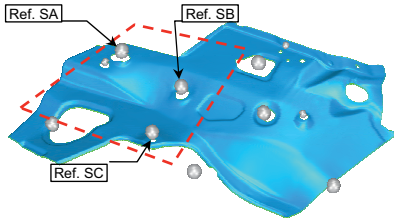

Figure 4: Full reference model for the case study. Reference spheres used to align point data sets are also shown.

In the context of the present work for the experimental tests the attention was focused on the acquisition of a limited portion of the component with more evident shape variation (highlighted in the left area in Fig. 4). This allowed to work always with a single shot of the VI 9i scanner, having the possibility to capture a significant portion of the component by using the Middle lens whose measurement range is

Article 069-m-95

329x247x176 mm at about 880 mm far away from the part (see Table 1), and the accuracy and precision of less than 0.20 mm and 0.048 mm, respectively. In this way each acquired portion of scan data was aligned and compared with the reference model by using three sphere features always captured in the three different rotation of the part: -30°, 0° and +30° (by using a rotating table mounted on a tripod). Figure 5 shows how the part appears on the scanner's camera at different orientations, whereas Figure 6 shows the set up of the experimental tests. Working only with a single shot for each combination of parameters eliminated the additional error occurring during the registrations phase of more scan data sets.

To test the effect of the ambient illumination the acquisitions were made in two very different environmental constant conditions: *light* with a white halogen lamp of 1000W not directly oriented to the object (so generating diffuse illumination), and *dark* condition with just a dim light.

Figure 5: Scanner's camera snapshots for the three orientations.

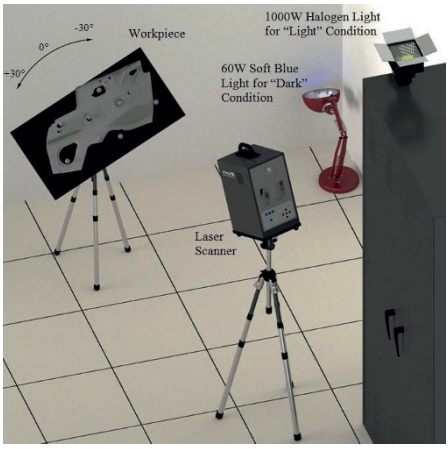

Figure 6: Set up of the experimental test.

Figure 7: How the model appears on an external camera in *dark* (left) and *light* (right) illumination conditions.

The illumination condition with a complete absence of external light source was not applicable to out test (as suggested in [CR1] where a CMM laser scanner was used) as the laser scanner was unable to properly set up the camera lens focus in that condition. So a dim light with a blue filament lamp of 60W located far away from the laser/object position was used. Figure 7 shows two pictures captured in both illumination conditions.

All parameters and conditions set for the experimental tests are listed in Table 2 and described below. Usually, in the industrial applications the light condition is a noise factor as it is hard (sometimes impossible) to properly set it up for accurate measurements. In our lab tests, instead, light condition was controlled and kept constant in two different conditions to evaluate its specific influence on the accuracy of the measurements.

Parameters	**Levels**		
Part rotation	-30°	0°	+30°
Ambient light	"Light"	"Dark"	
High Quality (HQ) filter*[2]	ON	OFF	
White Balance (WB)	Default	User	
Laser Intensity (LD)	vary		
Stand-off distance*[1]	vary		

*[1] It refers to the focus distance parameter of the camera.
*[2] It refers to the inner scanner filter.

Table 2: List of conditions and laser parameters set for the experimental tests.

Factors		**Levels**		
		1	**2**	**3**
Rotation	**A**	-30°	0°	+30°
Illumination	**B**	Light	Dark	
HQ	**C**	OFF	ON	

Table 3: List of factors and levels analysed with the DoE.

VI 9i Minolta laser scanner offers an automatic setting both for the camera focus, AutoFocus (AF), and the balance of Laser Intensity (LD). These parameters may change a little when running consecutively more times the automatic setting in the same conditions, so an average value over five runs were set and kept constant for each repetition referred to a part rotation. In particular, the autofocus distance (taken in *light* condition) was used as reference stand-off distance and assigned to all scans related to both *light* and *dark* conditions for each part rotation. Laser Intensity, instead, was set differently for *light* and *dark* conditions, as previous tests have pointed out the influence of this parameter on the scan quality.

Both laser intensity and stand-off distance can be classified as noise factors in the experimental tests.

High Quality (HQ) filter is an option of the laser scan tool that, if ON, discards unreliable scan data, usually located close to the FOV boundary.

The white balance (WB) option is suggested to set the internal level of ambient illumination and it can be carried out with a special matt white lens before starting the

measurements. It was set once for all acquisitions in *light* condition, whereas for *dark* illumination the default inner value of the scanner was used for the difficulty of setting this parameter in absence of enough ambient light.

SCAN	ANGLE [°]	LIGHTING	FILTER [HQ]	INTENSITY [LD]	DISTANCE (AF) [mm]	WHITE BALANCE
1	-30	LIGHT	OF	57	866	USER
2	-30	LIGHT	ON	57	866	USER
3	-30	DARK	OF	56	866	DEFAULT
4	-30	DARK	ON	56	866	DEFAULT
5	0	LIGHT	OF	49	884	USER
6	0	LIGHT	ON	49	884	USER
7	0	DARK	OF	53	884	DEFAULT
8	0	DARK	ON	53	884	DEFAULT
9	30	LIGHT	OF	50	882	USER
10	30	LIGHT	ON	50	882	USER
11	30	DARK	OF	50	882	DEFAULT
12	30	DARK	ON	50	882	DEFAULT

Table 4: Experimental plan (DoE) of the scan tests.

Focusing the attention on the factors "rotation" (A), "illumination" (B) and "high quality filter" (C), at the levels listed in Table 3, a DoE study with the full factorial experimental plan of 12 scans was carried out in the lab test (Table 4). Notice that the laser intensity automatically set by the scanner is about 20% of full power of laser source (250) according to [CR1] for sheet metal deep drawing components.
No smoothing was applied on the acquired data. Only outliers were detected and deleted when occurred (near edges). Data processing was conducted in Geomagic 2012.

4- Results and discussion

Tests were firstly limited on spheres SA, SB and SC of Ø1" (see Figure 4) used as targets. Best fit spherical features were extracted from point data and the fitting error (deviation) was recorded. Figure 8 shows the deviations for each sphere in any angular position and in different conditions: L-nHQ = Light and HQ Off; L-HQ = Light and HQ On; D-nHQ = Dark and HQ Off; D-HQ = Dark and HQ On. Sphere SA in -30° reported the highest deviation as it was farer from the camera with respect to the FOV (see Figure 5). Lower deviations corresponded to sphere SC in "dark" illumination.
These variations will have an effect of the alignment process of all data sets as shown later on.
Spherical features were used to look for the best sequence combination of reference features during the registration phase. Over the 12 acquisitions the analysis pointed out that the mating sequence SA-SC-SB was the one to which a general lower mating error occurred, so this combination was used for the subsequent steps of the analysis. On the other hand, the sequence SC-SB-SA for the position -30° and +30° resulted the worst one in terms of deviations, and the sequence SB-SC-SA the worst one for the position 0°. Then all sequences with SA as last sphere in the mating sequence caused worst results. This finding is consistent with the results listed in Figure 8. A slightly better result (than the one with SA-SC-SB) for the only angular position -30° came out for the sequence SB-SA-SC.
Based on the RPS alignment method with those three spherical features (in SA-SC-SB sequence) the root mean square (RMS) error was used as estimation parameter of the deviations of each scan data to the reference model. To make comparable the results in terms of RMS, a common subset of scan data (of about 970k polygons) for the three angular positions was extracted and used in the next steps.
Taking as reference the labels listed in Table 3 and the ANOVA test reported in Table 5, we may note that the factor A, related to the angular position of the part, played the most influent role on the accuracy of the measurements, as it resulted P=0.039 less than alpha=0.05; whereas ambient illumination (B) and quality filter (C) had marginal effects (Figures 9). Also the interaction effects between parameters were not significant (Figure 10). In particular, lowest deviations were related to the 0° position (Figure 9). This seems to be in relation with the best "central" position (in terms of average distance) of all three spheres with respect to the FOV of the scanner, also valid for the +30° position.

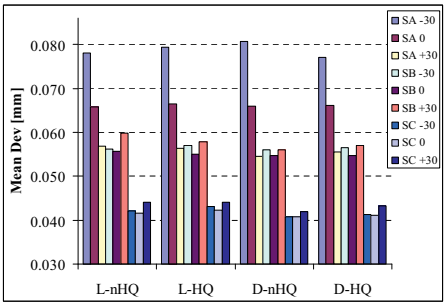

Figure 8: Deviations in the generation of spherical features.

Source	DF	Adj SS	F	P
A	2	0.0023915	24.930	0.039
B	1	0.0000095	0.200	0.699
C	1	0.0000006	0.010	0.921
A*B	2	0.0002679	2.790	0.264
A*C	2	0.0000462	0.480	0.675
B*C	1	0.0000025	0.050	0.840
Error	2	0.0000959		
Total	11	0.0028142		

Table 5: ANOVA test table.

On the other side, a lower accuracy corresponded to A1 (rotation at -30°) where sphere SA was farer away from the FOV of the scanner. This result is in accordance with the deviations plot of the reference spheres in Figure 8.
From all the experimental campaign we may conclude that

the best results correspond to 0° angular position, good diffuse light illumination and quality filter ON, having the angular position the most influent effect on the accuracy of the measurements.

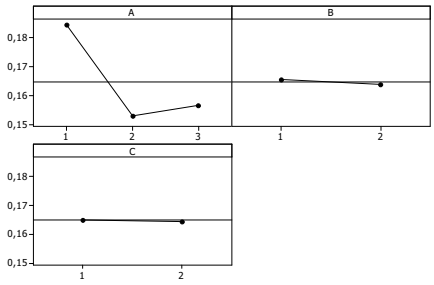

Figure 9: Mean effect plot on RMS [mm].

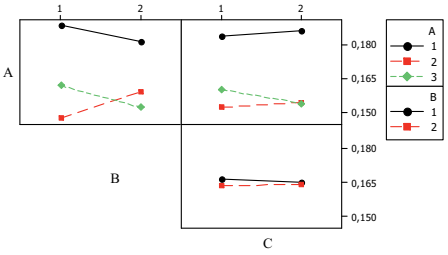

Figure 10: Interaction effect plot on RMS [mm].

6- Conclusions

The technical literature is worth of studies on measurement tests made with optical scanners (mainly based on laser triangulation) on simple workpieces and assisted by CMM device, aimed to highlight the factors most influencing the accuracy of the measurements.

We presented a study related to a quite complex commercial part acquired by a mobile 3D laser scanner, VI 9i by Konica Minolta, with the aim to point out the influence of some external factors such as the relative position part-scanner and the ambient illumination, and an internal factor such as the quality filter of that specific scanner. Considering the working ranges of the scanner, a middle distance part-to-laser was adopted with the intent to capture a significant portion of the part without limiting so much the overall accuracy of the acquisitions. Reference spheres were included and used for the RPS alignment with a reference model. The study pointed out that part-scanner angular position has a great effect on the measurement accuracy, while the illumination conditions (if diffuse and not oriented to the part) only have a marginal positive effect for the VI 9i scanner we used.

In particular, the accuracy of the acquired reference spheres plays an important role: they should be in a central position with respect to the FOV of the scanner to get the best result. The sphere SA, in a far away position with respect to FOV in -30° orientation, presented a relative higher deviation and this affected the alignment of the data sets.

Closer acquisitions are required to improve accuracy even though this means that, when acquiring a large object, more scans have to be done, so introducing errors during the registration phase of such data patches. To make highly repeatable the measurements over a large batch of components, the use of well defined features as references (see also fixtures) is highly recommended. Separated tests highlighted that a direct illumination of the object may alter the ability of the scanner to locally detect points as the ambient light interferes with the reflected laser signal on the camera's CCD. In the presented test we used a part with a grey colour very close the one of the calibration device for that scanner. More investigation is needed to well understand the behaviour of the laser scanner with different colour objects under multi-level ambient illumination.

7- Acknowledgment

This work has been supported by National Project PON01_01268 entitled 'Digital pattern product development: a pattern driven approach for industrial product design'. The authors wish to thank dr. M. Antoniello for his support in the measurement set up at the CREAMI lab of the University of Naples Federico II, Italy.

8- References

[**BF1**] Blanco D., Fenandez P., Cuesta E., Mateos S. and Beltran N. Influence of surface material on the quality of laser triangulation digitized point cloud for reverse engineering tasks. In ETFA2009, Palma de Mallorca (S), 2009.

[**CR1**] Cuesta E., Rico J.C., Fernández P., Blanco D. and Valino G. Influence of roughness on surface scanning by means of a laser stripe system. In Int J Adv Manuf Technol. Int J Adv Manuf Technol, 43: 1157–1166, 2009.

[**FL1**] Feng H.Y., Liu Y. and Xi F. Analysis of digitizing errors of a laser scanning system". Precision Engineering, 25: 185–191, 2001.

[**FS1**] Forest J. and Salvi J. Laser stripe peak detector for 3D scanners. A FIR filter approach. In 17th Int. Conf. on Pattern Recognition (ICPR'04), Cambridge (UK), 3: 646-649, 2004.

[**HL1**] Huang W., Liu, J., Chalivendra, V., Ceglarek, D., Kong, Z. and Zhou, Y. Statistical Modal Analysis (SMA) for Variation Characterization and Application in Manufacturing Quality Control. In IIE Transactions, Vol. 45, 2013.

[**LH1**] Liu C. S. and Hu J. S. Variation Simulation for Deformable Sheet Metal Assemblies Using Finite Element Methods. In ASME Journal of Manufacturing Science and Engineering, 119: 368-374, 1997.

[**LL1**] Lindau B., Lindkvist L., Andersson A. and Soderberg R., Statistical shape modeling in virtual assembly using PCA-technique. In Journal of Manufacturing Systems, 32: 456-463, 2013.

[**MJ1**] Mahmuda M., Joannic D., Royb M., Isheil A. and Fontaine J.F. 3D part inspection path planning of a laser scanner with control on the uncertainty. In Computer-Aided Design, 43: 345–355, 2011.

[**MC1**] Martínez S., Cuesta E., Barreiro J. and Álvarez B. Analysis of laser scanning and strategies for dimensional and geometrical control. In Int J Adv Manuf Technol, 46: 621–629, 2010.

[PL1] Prieto F., Lepage R., Boulanger P. and Redarce T. A CAD-based 3D data acquisition strategy for inspection. In Machine Vision and Applications, 15: 76–91, 2003.

Article 080-cadcae-11

Prediction of CAD model defeaturing impact on heat transfer FEA results using machine learning techniques

Florence DANGLADE [1], Philippe VERON [1], Jean-Philippe PERNOT [1], Lionel FINE [2]

(1) : LSIS - UMR CNRS 7296
Arts et Métiers ParisTech
Aix-en-Provence, France
{Florence.Danglade, Philippe.Veron, Jean-Philippe.Pernot}@ensam.eu

(2) : EADS France IW
Suresnes, France
Lionel.Fine@eads.net

Abstract: Essential when adapting CAD model for finite element analysis, the defeaturing ensures the feasibility of the simulation and reduces the computation time. Processes for CAD model preparation and defeaturing tools exist but are not always clearly formalized. In this paper, we propose an approach that uses machine learning techniques to design an indicator that predicts the defeaturing impact on the quality of analysis results for heat transfer simulation. The expertise knowledge is embedded in examples of defeaturing process and analysis, which will be used to find an algorithm able to predict a performance indicator. This indicator provides help in decision making to identify features candidates to defeaturing.

Key words: Defeaturing, CAD model, Finite Element Analysis, Machine Learning, a priori estimation.

1.- Introduction

In the field of transfer from Computer Aided Design (CAD) to Finite Element Analysis (FEA), CAD model adaptation ensures the quality and the reliability of analysis results. Among all techniques [TB1] (deleting parts, defeaturing, simplification, merging, idealization) defeaturing is essential for CAD model adaptation. Defeaturing consists in removing irrelevant features (protrusion, pockets, holes, fillets/rounds, chamfers).
The choice of candidates for defeaturing and tools used depend on the target of the simulation (structural, dynamic/fluid/heat transfer analysis, assembly/disassembly procedure evaluations) as well as on the type of method adopted for solving it (Finite Differences, Finite Element Analysis and so on) and the type of the CAD model (B-REP, STEP, Mesh, ...). Today, the choice of candidates for defeaturing is often empirical and leads, by precaution, to have model for analysis more precise than necessary. This significantly increases the cost of meshing and solving. It is important to know the thresholds that drive engineers during their decision to propose rules.
Machine learning [M1] tools, like neural networks, support vector machine or decision tree, are able to imitate and accurately predict behaviour from carefully selected examples. Moreover, these techniques can take into account equations or known relations. Therefore, they can capitalize the knowledge from a set of process examples for CAD model adaptation and predict impact of defeaturing process for a new case.
We propose in this paper to validate one of the process steps of the preparation of CAD models for heat transfer analysis. It will be shown that the machine learning techniques can be used to estimate the defeaturing impact on analysis results by predicting a performance indicator of defeaturing. Section 2 presents a state of art related to impact of defeaturing and the use of machine learning tools on CAD. Then, in section 3 an algorithm for estimating the impact of defeaturing on FEA results is proposed. Some results are discussed in section 4.

2.- Related works

For convective heat transfer analysis, the numerical analysis is applied to a mesh of a fluid volume. Without simplification, a huge number of elements to mesh local detail is necessary. The volume meshed can be difficult to obtain (often the meshing is impossible), and the computing time is very high. Thus, defeaturing significantly reduces processing time.
The experts select the candidates for defeaturing based on the solving feasibility and on the result accuracy target of analysis. For that, experts take into account boundary conditions (adiabatic, constant temperature, heat flux surfaces). Then, they estimate if the impact on the results is low and the computation time faster.
In the field of finite element static analysis Tang [TG1] studied the defeaturing impact on analysis by using the change of a model's strain energy. In recent years, *a posteriori* evaluation of defeaturing impact has aroused great interest [FC1]. However, only few attentions have been paid so far to the need for an *a priori* evaluation.
In the field of heat transfer analysis, Gopalakrishnan [GS1] propose a theory for estimating analysis errors in case of heat

transfer with a high accuracy of the error estimated. This method can be used for local applications or simple cases (with a reduced number of parts and features). In the case of a complex product, a very large number of details are deleted; the characteristics of the CAD model are strongly impacted, so it is difficult in these conditions to implement such a theoretical method.

Most of approaches about decision making for defeaturing propose [DP1] a feature by feature analysis. It is also difficult to take a global decision on the overall product when we have a large number of features.

Therefore, we propose to predict impact of defeaturing on heat transfer analysis from global examples of defeaturing processes.

Machine Learning tools are widely used in design to address optimization problems [SL1], decision-making problems [L1], shapes recognition [JK1], item recognition or extraction for reuse, recognition from point cloud scans [GM1], feature recognition [SA1] and transfer CAD/CAM [DM2]. In this present paper, we propose a use of machine learning techniques for the prediction of the performance indicator of process defeaturing. A process defeaturing is defined by a list of features to delete, techniques used for features removal (feature removal for native CAD model, deleting and reconstruction of faces, deleting and reconstruction of meshes …) and the sequencing of operations. The main objective of this paper is to evaluate defeaturing process in order to identify an optimal list of features to remove and to estimate the impact of defeaturing on Finite Element Analysis. Defeaturing impact evaluation is performed by estimating the quality of the analysis results and the costs of defeaturing, meshing and analysis operations.

3.- Algorithms for prediction of FEA result quality

Figure 1 represents the general algorithm of the proposed approach. The first step “pre-processing” consists in building a database of defeaturing process examples. For this, we extracted all data from initial CAD model and from prepared CAD model and simulation. Data are information like the format (e.g. CATIA native, STEP, IGES, tessellated model), the material, the dimensional quantities (e.g. size, surface area, volume, number of meshes elements, number of faces) and relations between features and boundary condition. Data about simulation are information on boundary conditions and analysis results. CAD preparation process should be described by a list and sequencing of simplification operations. Proposed by several experts, the initial CAD model data must be as exhaustive as possible (the database contains more than 250 attributes). Useful prepared CAD model data are selected in next step “learning”.

In the second step, machine learning techniques are used for carrying out learning models for the prediction of process performance indicators. For each learning model, determinant attributes are selected from the extracted examples.

The final step consisted in selecting candidates for defeaturing by estimating the quality of analysis results and costs (duration of defeaturing, meshing and analysis). It was performed in 4 sub-steps, namely features classification, prediction of quality of analysis results, prediction of cost and decision making.

Details of various models are described in the following sections.

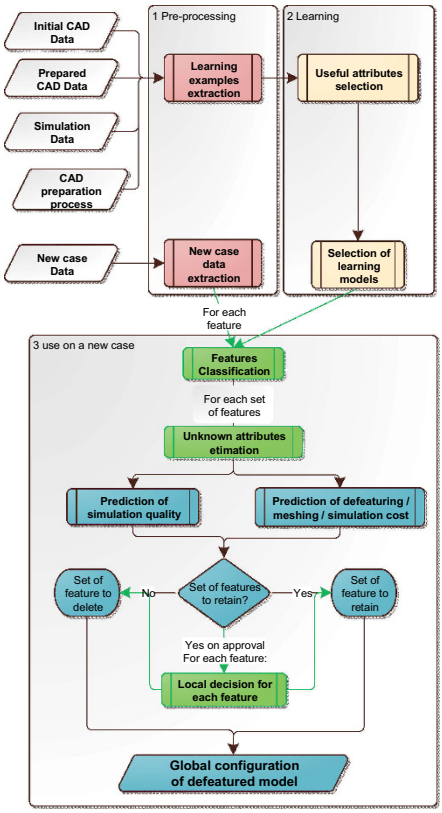

Figure 1: algorithm for evaluation of defeaturing process

3.1- Pre-processing

The database used for learning must be as exhaustive as possible. It contains a set of collected information:

- a global description of the initial CAD model (type of CAD model, boundary conditions, geometry, materials) ;
- a description of each feature (type of feature, relationship between features and with boundary conditions, geometry) ;

	x1 protusion	*x2 pocket*	*x3 hole*	*x4 round*	*x5 chamfer*	*x6 size*	*x7 BC distance*	*Configuration*
k1	0	0	0	0	0	0	0	Initial CAD model before defeaturing
k2	0	0	1	0	0	0	0	all holes are deleted, other features are retained
k3	0	0	1	0	0	1	0	Small holes are deleted, other features are retained
k4	0	0	0	1	0	0	0	Small rounds are deleted, other features are retained
k5	0	0	1	1	1	1	0	Small holes, rounds and chamfer are deleted, other features are retained
k6	1	1	1	1	1	0	1	All features far from boundary conditions are deleted

Table 1. Examples of CAD model configurations and associated attribute values

- a description of the prepared CAD model (type of CAD model, gains on volume/surface/mesh elements, geometry, mesh characteristics, list of deleted features) ;
- information about simulation (simulation goal, accuracy of results, targets of analysis) and industrial constraints.
- information about the process of preparation (list of deleted features, tools used for defeaturing/meshing, cost of meshing, cost of defeaturing).

This database must include a significant number of already known examples.
Then, for a new case, only initial CAD data (geometrical characteristics, material, type of data,..), objectives (physical quantity to calculate, position of boundary conditions, values on boundary condition) and constraints are indicated.

3.2- Learning

We use Machine Learning tools for prediction of analysis results quality and for prediction of defeaturing / meshing / analysis costs. In this paper, we describe the prediction of the analysis result quality (ARQ).
In this section, an algorithm to predict a performance indicator, illustrated in figure 2, is proposed.

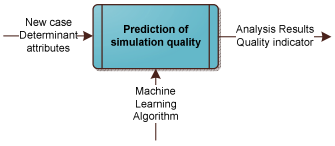

Figure 2 : ARQ prediction

The quality of analysis results is evaluated by predicting an indicator *ARQ* (analysis result quality). For learning, *ARQ* (1) is calculated from the value of analysis result for the initial cad data (*I_AR*) and for the defeatured CAD data (*D_AR*). For a new case, ARQ indicator will be predicted from determinant attributes (described in section 3.2.1) by machine learning techniques.

$$ARQ = 1 - 6{,}67\frac{\sum_{1}^{R}\left(\frac{(D\_AR - I\_AR)}{I\_RA}\right)}{R} \qquad (1)$$

Where R is the number of results observed. ARQ=0 if analysis is impossible, ARQ=0,2 if the error is greater than 15%, ARQ=1 if the error is negligible.

A significant number of examples are extracted, whose results of heat transfer analysis from initial CAD model and from defeatured CAD model are both known.

3.2.1- useful attributes selection

The major stage in using Machine Learning tools like Neural Network is to define input data. These data are represented by a vector of attributes which is defined by specific attributes for each learning goal. Attributes are selected from the database by means of classification methods of input variables according to the impact of each attribute on the output.
Regarding the prediction of the quality indicator, 12 relevant attributes has been identified. Selected attributes are described below:

Table 1 gives some examples of CAD model configurations (CAD models with different level of simplification) with their associated attribute values for each configuration.
Attributes x1 to x7 describe set of features deleted

- **attribute x1 to x5** specifies the state of each type of feature (0= set of feature retained, 1= set of feature deleted) ;
- **attribute x6** gives a deleting condition according to the size of the feature (0= 0= small and large features are deleted; 1= large features are retained) ;
- **attribute x7** gives a deleting condition according to the distance between the feature and the nearest boundary condition (0= none feature is retained ; 1= features near boundary condition are retained) ;

Attributes x6 and x7 are applied to all features from x1 to x5.

f is a factor equal to 0 if the feature is retained or *k*=1 is the feature is deleted.
Attributes x8 and x9 give indications on the weight of features deleted relative to initial CAD model.

- **attribute x8** is the volume ratio (2) between the set of feature deleted and the product, where $VolF_i$ is the volume of each feature F_i (for i=1 to i_{max}=number of features of the product), *I_VolP* is the volume of the initial product;

$$VolRatio = \frac{\sum_{i=1}^{i\max}(VolF_i \times f)}{I\_VolP} \quad (2)$$

- **attribute x9** is a ratio (3) between the number of mesh element in the set of feature deleted and in the product (*I_MeshP)*, where *MeshFi* is the number of mesh element for each feature F_i;

$$MeshRatio = \frac{\sum_{i=1}^{i\max}(MeshF_i \times f)}{I\_MeshP} \quad (3)$$

- **attribute x10** is the minimal Euclidian distance (4) between the feature deleted and the nearest boundary conditions;

$$D\_F\_BC = MIN(D\_F_i\_BC \times f) \quad (4)$$

Attributes x11 and x12 give gains obtained by defeaturing.

- **attribute x11** is the gain (5) of volume between initial (*I_VolP*) and defeatured product (D_*VolP*) ;

$$VolGain = \frac{D\_VolP - I\_VolP}{I\_VolP} \quad (5)$$

- **attribute x12** is the gain (6) of number of mesh element between initial (*I_MeshP*) and defeatured product (D_*MeshP*) ;

$$MeshGain = \frac{D\_MeshP - I\_MeshP}{I\_MeshP} \quad (6)$$

3.2.2- learning model selection

In this section, we identify the best Machine Learning tools for predicting the Analysis Result Quality (ARQ) from the 12 selected attributes described in section 3.2.1. Machine Learning tools are selected [DM1] for each learning model on the overall examples by cross-validation methods. The evaluation criteria of learning model are the percentage of correctly classified instances and the average quadratic error *AQE (7):*

$$AQE = \sqrt{\frac{1}{N}\sum_{k=1}^{N}\left(y(x^k) - p(x^k)\right)^2} \quad (7)$$

Where x^k is the vector of attributes for the example *k*, $y(x^k)$ is the known output value, $p(x^k,w)$ is the output value predicted by learning model tool, w is the vector of weight between nodes.

In the context of our database and for our study (preparation with CATIA V5, heat transfert analysis with *ANSYS [A1]*, and learning with *Weka* [W1]), the learning model whose quadratic error is the smallest for a high percentage of correctly classified instances is a neural network (Multi Perceptron) as shown table 2.
Figure 3 illustrates the selected neural network with 3 layers using back-propagation method:

- input layer contains 12 nodes matched to the 12 selected attributes;
- output layer is the discrete value of the ARQ indicator ($0 \leq ARQ \leq 1$);
- hidden layer: contains m nodes whose weight and number depend on learning examples.

Weights w are found by means of Tan Sigmoid methods.

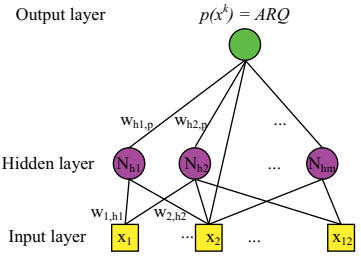

Figure 3: Neural Network

Learning model	AQE	% correctly classified instances
Naive Bayes	0,06	75
Multilayer Perceptron	0,03	78
RBF Network	0,05	63
Super Vector Machine	0,05	78
Decision tree	0,05	69

Table 2: Evaluation of learning models

Table 3 gives some examples of Analysis Result Quality predicted with the selected learning model.

3.3- Use on a new unknown case

Each feature Fi belonging to the global product according to :

- its type (5 classes = protrusion, pocket, hole, fillet/round and chamfer) ;
- its size (2 classes = small and large) ;
- its Euclidian distance between boundary conditions (2 classes = near from boundary conditions and far from boundary conditions).

A new unknown case is a CAD model configuration whose one or several type of features is deleted. For a new case, several configurations should be studied. A first approach consists in evaluating a defeaturing process proposed by an expert. Indication thus obtained does not identify an optimal process. Another approach consists in studying different typical configurations with some features deleted. Table 1 shows examples of CAD models configurations. A great number of random configurations should be used.
The 12 determinant attributes are extracted from the data of new case. For a new case, we know *a posteriori* only initial CAD model characteristics and simulation goal. Some selected attributed described in section 3.2 are unknown (volume and number of mesh elements). These values can be estimated from known rules or by using machine learning techniques (this step is not described in this paper).
The next stage consists in predict the indicator of quality *ARQ* described in section 3.2.2.
Then, costs of defeaturing, meshing and analysis are estimated by predicting the duration of these operations.

A crossed analysis of the defeaturing impact on simulation for all configurations makes it possible to take a decision for each set of feature. These set of features should be classified in 3 groups "the set of feature must be retained", "the set of feature should be deleted" and "the set of feature should be deleted on approval". If the decision is conditional, an individual analyze on each feature *Fi* is necessary. From first hypotheses and criteria proposed by experts, which will be completed as and when the study, we propose to retain feature if:

- the feature is parent of another feature to retain ;
- the size of the feature is larger than a limit size;
- the distance between the feature and the boundary condition is smaller than a limit distance.

From results on all cases, a best global configuration should be compiled.

4.- Results

This paper focuses on convective heat transfer analysis with ANSYS CFD. Examples for learning were single parts and products whose defeaturing process was proposed by experts. Defeaturing examples were distributed in 2 sets: a training set (66%) and a test set (33%) statically equivalent.

Meshing was carried out by *ICEM [I1]*. Meshes characteristics were the same for all configurations on a new case (triangular volume mesh, medium size, without adaptation).
Table 3 shows volume gain, mesh element gain, defeaturing cost and quality of analysis results for the new case illustrated in figure 3. Impact of defeaturing was done for 20 configurations. Examples of configurations k_1 to k_6 are described in table 1. Configuration k_7 is the configuration proposed by an expert.

	Volume gain	**Mesh element gain**	**Quality of analysis results (predicted)**	***Quality of analysis results (calculated)***
k1	0.00	0.0	**1.0**	***1.00***
k2	2.22	-18.8	**0.8**	***0.86***
k3	0.03	-6.2	**1.0**	***0.97***
k4	-0.04	-15.7	**1.0**	***0.86***
k5	0.45	-25.3	**0.4**	***0.32***
k6	0.46	-7.1	**0.8**	***0.73***
k7 (expert)	-0.54	-21.0	**1.0**	***0.86***
k8 (global decision)	**-0.52**	**17.2**	**1.0**	***0.95***

Table 3: Examples of prediction

Machine learning technique was selected and performed by the Weka platform [W1]. For prediction of quality analysis results (ARQ), the quadratic error for Multi Layer Perceptron technique (3 nodes layers) is about 14% with a cross validation. This score should be increased by adding more examples. Table 3 gives values of ARQ predicted with neural network and calculated. These values show that the choice of the learning model is suitable for decision on the quality of the analysis. Comparative studies between configuration k_7 proposed by expert and k_8 predicted by learning model, shows that this last configuration is more accurate (features on inlet and outlet are retained for k_8).

The set of features to delete after decision based on results from different configurations are rounds, chamfers far to boundary conditions and small holes far to boundary conditions. Configuration k_8 in table 3 gives predicted values for the global configuration resulting to this decision.

In all cases tested, it turned out that the defeaturing made possible meshing and analysis for most complex cases and allowed to accelerate processing time for simple cases (from 5 to 35%).

The global configuration is shown in figure 3. 3a) represents the initial CAD model. In 3b) red features are features to retain and green features are features to deleted after global decision.

3c) represents defeatured CAD model. As indicated, the analysis duration is reduced for a little average error on temperature value. The mesh quality is significantly increased.

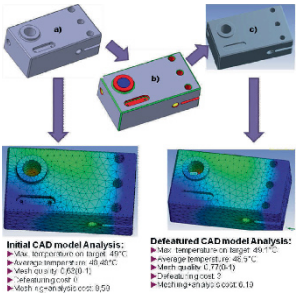

Figure 3: global configuration and comparative analysis results

5.- Conclusion

The results of this study have shown that machine learning techniques can be used to learn how to defeature CAD model for heat transfer analysis. The proposed approach to predict the simulation quality can be easily applied to the prediction of cost and to the global decision making. Machine learning techniques can be a good mean to capitalize the knowledge embedded in empirical processes.

The proposed approach need to have information on post defeaturing (volume and number of mesh elements of CAD model). A first solution consists in defeaturing the new case. The next step is to predict the quality indicator of the analysis without pre defeaturing. This will require to predict unknown attributes or not to use them (which require to have a greater number of attributes and thus a very large number of examples for learning). Future work should take into account other CAD model preparation steps (deleting parts, defeaturing, simplification, merging, idealization). The global configuration proposed at the end of our workflow is not the optimal configuration. Further studies should therefore implement an optimization loop so that using the developed indicator, the best defeaturing configuration can be suggested to the designers. At the end, the proposed approach and tools should reduce significantly the number and duration of design iteration.

REFERENCES

[A1] http://www.ansys.com

[**DM1**] G. Dreyfus, J.M. Martinez, M. Samuelides, M.B. Gordon, F. Badran, S. Thiria, L. Hérault :Réseaux de neurones, Eyrolles, 2ème édition 2004

[**DM2**] L. Ding, J. Matthews : A contemporary study into the application of neural network techniques employed to automate CAD/CAM integration for die manufacture, Computers & Industrial Engineering, Volume 57, Issue 4, November 2009, Pages 1457-1471

[**DP1**] F. Danglade, J.P. Pernot, P. Veron : On the use of Machine Learning to Defeature CAD Models for Simulation, Computer-Aided Design and Applications, Volume 11, Issue 3, 2014, Pages 358-368

[FC1] G. Foucault, J.-C. Cuillière, V. François, J.-C. Léon, R. Maranzana : Adaptation of CAD model topology for finite element analysis, Computer-Aided Design, Volume 40, Issue 2, February 2008, Pages 176-196.

[**GM1**] G.P. Gujarathi, Y.-S. Ma : Parametric CAD/CAE integration using a common data model, Journal of Manufacturing Systems, Volume 30, Issue 3, August 2011, Pages 118-132.

[GS1] S.H. Gopalakrishnan, K. Suresh : A formal theory for estimating defeaturing-induced engineering analysis errors, Computer-Aided Design, Volume 39, Issue 1, January 2007, Pages 60-68.

[I1] http://www.ansys.com/Products/Other+ Products/ ANSYS+ICEM+CFD

[**JK1**] S. Jayanti, Y. Kalyanaraman, K. Ramatni : Shape-based clustering for 3D CAD objects: A compara-tive study of effectiveness, Computer Aided Design, 41 (12), 2009, pp. 999-1007.

[**L1**] S.H. Lee : A CAD-CAE integration approach using feature-based multi-resolution and multi-abstraction modelling techniques, Computer Aided Design, 37 (9), 2005, pp. 941-955.

[M1] T. Mitchell : Machine Learning, McGraw Hill, 1997.

[**SL1**] B.Q. Shi, J. Liang, Q. Liu : Adaptive simplification of point cloud using k-means clustering, CAD Computer Aided Design, 2011, 43 (8), pp. 910-922.

[**SA1**] V.B. Sunil, R. Agarwal, S.S. Pande : An approach to recognize interacting features from B-Rep CAD models of prismatic machined parts using a hybrid (graph and rule based) technique, Computers in Industry, 61(7), pp. 686-701, 2010.

[TB1] A. Thakur, A.G. Banerjee, S.K. Gupta : A survey of CAD model simplification techniques for physics-based simulation applications , CAD Computer Aided Design, 41 (2), pp. 65-80.

[TG1] J. Tang, S. Gao, M. Li : Evaluating defeaturing-induced impact on model analysis, Mathematical and Computer Modelling, Volume 57, Issues 3–4, February 2013, Pages 413-424.

[W1] http://www.cs.waikato.ac.nz/ml/weka/

Article 079-cadcae-77

NURBS patch coupling with Nitsche's method for isogeometric analysis

Stefano Tornincasa [1], Elvio Bonisoli [1], Marco Brino [1]

(1) Politecnico di Torino**:** corso Duca degli Abruzzi, 24 – 10129 Torino (ITALY)
+39 011 0907274
E-mail : { stefano.tornincasa, elvio.bonisoli, marco.brino }@polito.it

Abstract: To model geometrical entities with a certain complexity to be verified with isogeometric analysis (IGA) it is often necessary to use multi-patch. Nitsche's method allows the possibility of coupling the different patches even though the mesh at the interface is not conforming. Examples of three-dimensional models are analysed for linear static and modal analysis to validate the method.

Keywords: NURBS, isogeometric analysis, multi-patch, Nitsche's method, weak coupling.

1- Introduction

Isogeometric analysis (IGA) [HC1, CH1] is a new numerical method with the target of improving the capabilities of Finite Element Method (FEM). Such capabilities are the possibility of integrating design (as Computer-Aided Design, CAD) and analysis using the functions that are used to define the geometry, directly as basis functions for the analysis, calling the isoparametric concept. CAD software use Non-Uniform Rational B-Splines (NURBS) [PT1] to define the geometry and isogeometric analysis confirmed the possibility to use these functions for the formulation of the elemental matrices, while keeping an exact geometry of the discretization even with the coarsest mesh.
Other advantages are the high-order continuity across element boundaries [CH2], a straightforward refinement procedure which does not involve a re-meshing from scratch, a new refinement procedure which is not present in standard FE, accuracy and effectiveness of contact problems [TW1] taking advantage of the exact shape at the interface, with no gap-vs-overlap issue that occurs in standard FE.
In case of dynamics, in particular structural vibrations the possibility of raising the order of the functions at an arbitrary level, shows the property of drastically increasing the accuracy, allowing for better finding a balance between h- and p-refinement.
Some of the disadvantages, which are just considered as directions for future work and development of the research in this field, are the need of using several NURBS patches to model complicated geometry and the possibility of a local refinement step. One of the solutions to this problem is using T-splines [BC1], another geometrical modelling technology which could replace NURBS maintaining its properties and capabilities, plus adding local refinements and single-patch models with complex shape, but tri-variate modelling features are not yet available.
For this reason, NURBS multi-patch modelling is still considered a valuable possibility, but with the limitation of considering matching discretization at the interface.
Nitsche's method [N1] was used to impose boundary conditions in a weak sense, and recently an improved form was developed to couple different domains. This is found to be suitable for NURBS-based isogeometric analysis, defining the coupling at the interface in weak form.

In next section of this paper, the isogeometric analysis basic concept and features are presented, to understand the fey differences, advantages and disadvantages of the method.
In third section the multi-patch version of NURBS isogeometric analysis is described, in particular the coupling of non-conforming meshes with Nitsche's method.
In section 4 some numerical examples are presented to validate the method described.

2- Isogeometric analysis concept and features

From a conceptual point of view, isogeometric analysis can be considered a classical Finite Element Method where the basis functions, instead of being the standard Lagrange polynomials, are replaced by NURBS functions. In the case considered in this paper, tri-variate patches will be considered.
B-Splines must be considered at first. They are defined by a *knot vector* (a set of coordinates in parametric space in ascending order) $\Xi = \left\{ \xi_1 \quad \xi_2 \quad \cdots \quad \xi_{n+p+1} \right\}$, where n is the number of basis functions and p is the polynomial degree. A standard knot vector used in CAD is called *open knot vector*, and its main property is having the first and last knots repeated p+1 times.
B-Spline basis functions are defined with the recursive formula

Article 079-cadcae-77

$$N_{i,0}(\xi) = \begin{cases} 1 & if\ \xi_i \le \xi \le \xi_{i+1} \\ 0 & otherwise \end{cases} \quad (1)$$

$$N_{i,p}(\xi) = \frac{\xi - \xi_i}{\xi_{i+p} - \xi_i} N_{i,p-1}(\xi) + \frac{\xi_{i+p+1} - \xi}{\xi_{i+p+1} - \xi_{i+1}} N_{i+1,p-1}(\xi) \quad (2)$$

As an example, if a knot vector is defined as {0,0,0,1,2,3,4,4,5,5,5}, with quadratic functions, the plot of the eight different functions are shown in Figure 1.

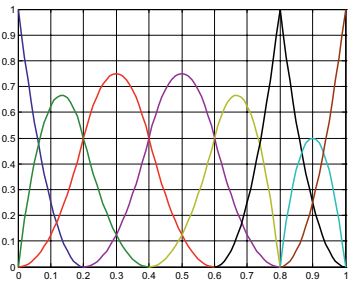

Figure 1: Example of B-spline basis functions.

NURBS are basically an improvement of B-spline, where its rational form allows the exact representation of all conics shapes. The basis functions are defined as follows

$$R_{i,p}(\xi) = \frac{N_{i,p}(\xi) w_i}{W(\xi)} = \frac{N_{i,p}(\xi) w_i}{\sum_{j=1}^{n} N_{j,p}(\xi) w_j} \quad (3)$$

where *w* are called *weights* of the control points.
The volumetric expansion of the basis functions is realized performing tensor product of three parametric coordinates

$$R_{i,j,k}^{p,q,r}(\xi,\eta,\zeta) = \frac{N_i(\xi) M_j(\eta) L_k(\zeta) w_{i,j,k}}{\sum_{i=1}^{n}\sum_{j=1}^{m}\sum_{k=1}^{l} N_i(\xi) M_j(\eta) L_k(\zeta)} \quad (4)$$

$$\mathbf{V}(\xi,\eta,\zeta) = \sum_{i=1}^{n}\sum_{j=1}^{m}\sum_{k=1}^{l} \mathbf{P}_{i,j,k} R_{i,j,k}^{p,q,r}(\xi,\eta,\zeta) \quad (5)$$

where $\mathbf{P}_{i,j,k}$ are the coordinates of control points in physical space.
Thanks to the *isoparametric* property already used in standard Finite Elements, NURBS basis function can be used to discretize the displacement field as well

$$\mathbf{u}^e(\xi,\eta,\zeta) = \sum_{a=1}^{n} \mathbf{d}_a^e R_a^e(\xi,\eta,\zeta) \quad (6)$$

where $\mathbf{d}_a^e$ are the degrees of freedom of the model.
The assembly process of the element matrices is performed in the same way compared to standard Finite Elements.
Considering that Equation 4 calls the concept of trivariate NURBS for volumetric representation (hence, definition of any boundary and internal points of the body) instead of the bivariate representation for boundary representation, a different geometric modelling procedure is considered. In the following examples only extrusion feature is taken into account, where the bivariate representation of one surface is extended with tensor product structure by a third parametric dimension and all the control points are doubled towards a physical dimension.

3- Multi-patch interface coupling

Since a tri-variate NURBS patch could be considered as a deformed six-faced cube, even though very complex geometries are represented by a single patch, the elements inside would not be shaped accordingly to get good results. Jacobian and aspect ratio would be affected a lot.
Multi-patch geometries are able to overcome to this issue, allowing more regular and better shaped elements with the drawback of having separate domains that must be coupled together.
The simplest solution would be to model the patches in such a way that the control mesh at the interface surfaces are conforming (which means that the relative control points are in the same position in physical space and could then be merged), but this sometimes is not possible.
Nitsche's method allows defining the coupling in weak form, so that even non-conforming mesh can be coupled. The starting statement is the continuity of both displacement and normal stress across the patch interface. This can be seen a mixed method between mortar-based and pure penalty.
In Figure 2 a generic domain is represented.

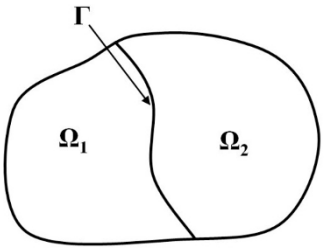

Figure 2: Generic example of two coupled domains with their interface.

Jump and *average stress* are defined

$$[\mathbf{u}] = \mathbf{u}^1 - \mathbf{u}^2 \quad (7)$$

$$\{\boldsymbol{\sigma}\} = \frac{1}{2}\left(\boldsymbol{\sigma}^1 - \boldsymbol{\sigma}^2\right) \quad (8)$$

on [N1, NK1] the complete proof can be found.
The basic concept is to add terms to the weak formulation of the problem, which means more terms in the stiffness matrix

Article 079-cadcae-77

$$\left[\mathbf{K}^b + \mathbf{K}^n + \left(\mathbf{K}^n\right)^T + \mathbf{K}^s\right]\{\mathbf{x}\} = \{\mathbf{f}_{ext}\} \tag{9}$$

where the first terms is the standard assembly before the application of the interface coupling

$$\mathbf{K}^b = \sum_{i=1}^{2}\int_{\Omega^i} (\mathbf{B}^k)^T \mathbf{C}^k \mathbf{B}^k d\Omega \tag{10}$$

while the Nitsche's terms are the following

$$\mathbf{K}^n = \begin{bmatrix} -\int_\Gamma \mathbf{N}^{1T}\mathbf{n}\frac{1}{2}\mathbf{C}^1\mathbf{B}^1 d\Gamma & -\int_\Gamma \mathbf{N}^{1T}\mathbf{n}\frac{1}{2}\mathbf{C}^2\mathbf{B}^2 d\Gamma \\ \int_\Gamma \mathbf{N}^{2T}\mathbf{n}\frac{1}{2}\mathbf{C}^1\mathbf{B}^1 d\Gamma & \int_\Gamma \mathbf{N}^{2T}\mathbf{n}\frac{1}{2}\mathbf{C}^2\mathbf{B}^2 d\Gamma \end{bmatrix} \tag{11}$$

$$\mathbf{K}^s = \begin{bmatrix} \int_\Gamma \alpha\mathbf{N}^{1T}\mathbf{N}^1 d\Gamma & \int_\Gamma \alpha\mathbf{N}^{1T}\mathbf{N}^2 d\Gamma \\ \int_\Gamma \alpha\mathbf{N}^{2T}\mathbf{N}^1 d\Gamma & \int_\Gamma \alpha\mathbf{N}^{2T}\mathbf{N}^2 d\Gamma \end{bmatrix} \tag{12}$$

The penalty-like nature of the method is represented by the *stabilization parameter* α. The need of this parameter is because the terms that are added to the general form could be negative end then the coupled final matrix might not be positive-definite. This parameter, if large enough, can allow the matrix to be again positive definite.
This parameter can be either chosen empirically (as in this work) or estimated considering the studies in [FH1, BH1] where a dependency with respect to material properties and size of elements has been found

$$\alpha = \frac{\lambda + \mu}{2}\frac{\theta(p)}{h_e} \tag{13}$$

4- Numerical examples and results

To validate the method and show the relevant properties some 3D examples were numerically analysed and the results are shown in the following.

4.1 – 3D cantilever beam

The first example is a cantilever beam, where its parameters and boundary conditions are shown in Figure 3, while its geometry and discretization in terms of NURBS is shown in Figure 4. Red dots are the positions of the control points, while blue lines are the knot lines which represent the element boundaries. The two patches can be distinguished by the different discretization along the longitudinal direction.
In this simple case the three parametric coordinates are aligned with the three physical coordinates.
The values of the parameters are: Young modulus $E = 1000$ Pa, Poisson's ratio $\nu = 0.3$, Length $L = 10$ m, Width and Height $W = H = 1$ m, imposed displacement $\bar{u} = 1$ m.
The stabilization parameter α was chosen as 10^6.
The two different patches were discretized in a different way with the purpose of having a non-conforming control mesh across the patch interface: the patch on the left is composed by 16-by-4-by-4 tri-cubic elements, while the right patch is composed by 16-by-1-by-2 tri-cubic elements.

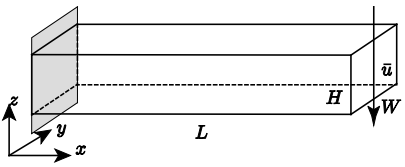

Figure 3: Geometry and boundary conditions of the cantilever beam.

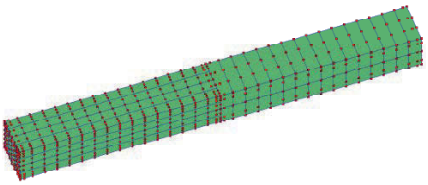

Figure 4: NURBS geometry and discretization of the cantilever beam.

In Figure 5 is presented the comparison of the contour plot of σ_{xx} with the two separate patches described above with the same geometry modelled as a single patch discretized with 32-by-4-by-4 elements. The pattern of the plot is comparable and compatible with the expectations known in theory, and also the maximum and minimum values shown in the legends can be considered equal.

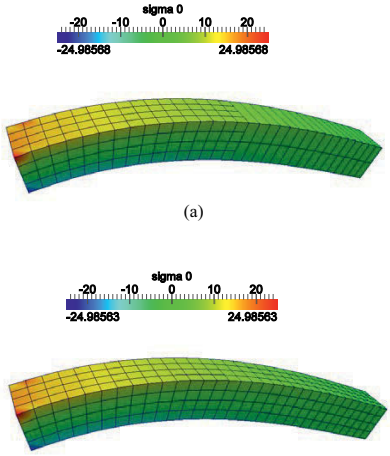

Figure 5: Comparison of results for multi-patch with Nitsche's coupling (a) and single patch (b).

Article 079-cadcae-77

4.2 – 3D connecting-rod

The second example is a more geometrical complex 3-dimentional model, which can feature general issues for the coupling. The model, shown in Figure 6, is a simplified connecting-rod, which is a fundamental component of internal combustion engines and alternative compressors. The different patches and the relative control points can be detected as well as their patch interface. Its functional feature is to convert back and forth a rotating motion to an alternative motion, and vice-versa.

From the point of view of multi-patch isogeometric analysis with Nitsche's coupling, its interesting feature is the complication of the choice of the interface shapes: they are not only non-conforming in discretization, but they also are curved and they have different dimensions, in the sense that one interface surface is bigger than the other.

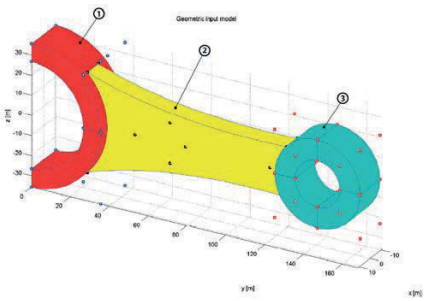

Figure 6: Geometry and boundary conditions of the connecting-rod.

In Figure 7 the model is represented with its dimensions and boundary conditions. The applied force F is 1000 N, while the material properties are the actual standard steel, with Young modulus $E = 2\times10^5$ MPa and Poisson's ratio $\nu = 0.3$. All the dimensions in Figure 7 are in mm. The geometry was modelled defining the surfaces in the yz plane and then extruding them adding the third parametric direction towards negative x.

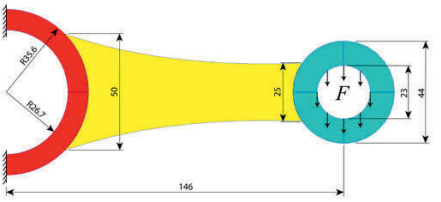

Figure 7: Geometry, dimensions and boundary conditions of the connecting-rod model.

This model, which in the configuration shown is in the so called *coarsest mesh* (that is the minimum number of elements with the minimum function degree to *exactly* represent the geometry), is then refined to better converge to the actual value of stresses. This refinement leads to tri-cubic patches with 32-by-4-by-8 elements for the first patch, 24-by-12-by-4 elements for the second and 64-by-4-by-8 elements for the third, with a total number of 4224 elements with 11305 control points. The stabilization parameter α is empirically chosen as 10^8.

The results of the NURBS model is shown in Figure 8, while the stress plot is compared to the solution of a commercial standard FEM software (NX-NASTRAN) for validation (Figure 9). Also in this case the stress plot pattern of the NURBS solution with Nitsche's method for coupling is comparable to the one obtained with the commercial FEM, and the maximum value of von Mises stress is very close.

The NASTRAN model was composed by 6182 second order tetrahedral elements and 11332 nodes.

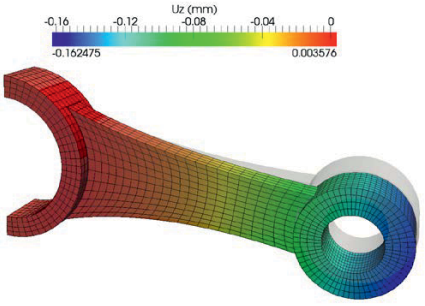

(a)

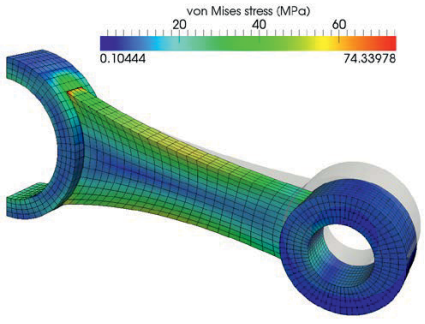

(b)

Figure 8: Results of the connecting-rod model: displacement along z direction (a), von Mises equivalent stress (b).

To check the effect of the stabilization parameter α, different analysis with different values was performed.

Figure 10 shows the result of this test, evaluating the maximum von Mises stress with respect to the parameter value, where a threshold of 10^6 ensures the stiffness matrix to be positive defined and the method reliable.

Article 079-cadcae-77

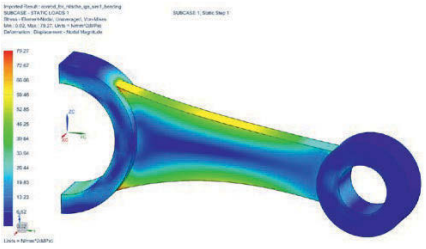

Figure 9: Results of the connecting-rod model using commercial FEM software.

Before the threshold the coupling is not accurate and Figure 11 presents the issues in the coupling zone, where not consistent displacements cause distortions in the deformation, hence high stress concentration, instead in Figure 12 this concentration is not present.

5- Conclusions and future work

The paper presented the reliability and consistency of multi-patch NURBS isogeometric analysis with Nitsche's method to couple the patches which have non-conforming meshes at the interfaces.

Two 3-dimensional examples were presented to prove and validate the method: firstly a simple model of a cantilever beam, then a more geometrical complex model with difficulties on the shape and dimension of the interface surfaces.

The second model was validated comparing the results with the same geometry analysed with commercial FEM code.

Next advances on this topic would be finding a geometrical method to model complex geometries with a single patch in order to maintain the NURBS properties of having smooth element boundaries with high-order stress continuity.

More generally, a tighter integration between the final geometrical CAD model and the first analysis that can be performed without meshing and using directly the geometrical functions would help companies working on this field to solve most of their issues regarding CAD-CAE integration.

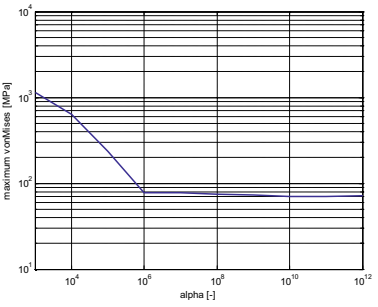

Figure 10: Stress concentration values vs. stabilization parameter value.

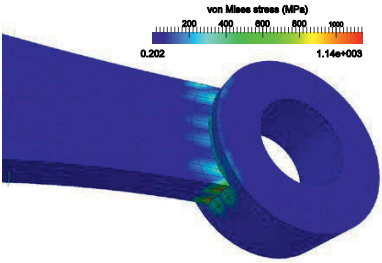

Figure 11: Detail of the coupling zone where the stress concentration occurs, with a stabilization parameter of 10^3.

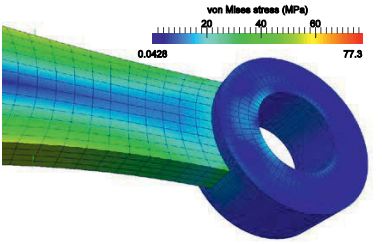

Figure 12: Detail of the coupling zone where the stress concentration occurs, with a stabilization parameter of 10^{12}.

References

[HC1] Hughes T.J.R., Cottrell J.A., Bazilevs Y., "Isogeometric analysis: CAD, finite elements, NURBS, exact geometry and mesh refinement". *Computer Methods in Applied Mechanics and Engineering*, 194(39-41), pp. 4135-4195, 2005.

[CH1] Cottrell J.A., Hughes T.J.R., Bazilevs Y., "Isogeometric analysis: toward integration of CAD and FEA", Wiley, 2009.

[PT1] Piegl L.A., Tiller W., "The NURBS book", Springer, 1996.

[CH2] Cottrell J.A., Hughes T.J.R., Reali A., "Studies of refinement and continuity in isogeometric structural analysis". *Computer Methods in Applied Mechanics and Engineering*, 196(41-44), pp. 4160-4183, 2007.

[TW1] Temizer I., Wriggers P., Hughes T.J.R., "Contact treatment in isogeometric analysis with NURBS". *Computer Methods in Applied Mechanics and Engineering*, 200(9-12), pp. 1100-1112, 2011.

[BC1] Bazilevs Y., Calo V.M., Cottrell J.A., Evans J.A., Hughes T.J.R., Lipton S., Scott M.A., Sederberg T.W., "Isogeometric analysis using T-splines". *Computer Methods*

in Applied Mechanics and Engineering, 199(5-8), pp. 229-263, 2010.

[N1] Nitsche J., "Uber ein variationsprinzip zur losung von dirichlet-problemen bei verwendung von teilraumen, die keinen randbedingungen unterworfen sind", *Abhandlungen aus dem Mathematischen Seminar der Universitat Hamburg*, 36, pp. 9-15, 1971.

[FH1] Fritz A., Hüeber S., Wohlmuth B.I., "A comparison of mortar and Nitsche techniques for linear elasticity". *CALCOLO*, 41(3), pp. 115-137, 2004.

[BH1] Bazilevs Y., Hughes T.J.R., "Weak imposition of Dirichlet boundary conditions in fluid mechanics". *Computers & Fluids*, 36(1), pp. 12-16, 2007.

[NK1] Nguyen V.P., Kerfriden P., Bordas S., "Isogeometric cohesive elements for two and three dimensional composite delamination analysis. *Composites Science and Technology*, 2013. http://arxiv.org/abs/1305.2738

Article 057-cad-55

Reverse Engineering for manufacturing REFM of parts in a routine context: use of graph description and matching algorithm

Salam ALI[1], Pierre Antoine ADRAGNA [1], Alexandre DURUPT [2]

(1) : Université de Technologie de Troyes
ICD-LASMIS
12 rue Marie Curie, 10010 Troyes Cedex, France
+33 325 717 600
E-mail : {salam.ali, pierre_antoine.adragna}@utt.fr

(2) : Université de Technologie de Compiègne
Roberval-UMR7337
15 Rue Roger Couttolenc, 60200 Compiègne, France
+33 44 23 44 23
E-mail : alexandre.durupt @utc.fr

Abstract: This paper meets the needs of industrial companies in defining directly a CAPP (Computer Aided Process Planning) model of an existing part from 3D information. They are confronted to avoid the passage by the CAD model; since existing solutions in the literature are based on CAD models reconstructed from 3D information to define the process planning. This paper is mainly based on routine context and suggests a solution to reuse a generated CAPP model stored in a RE database in order to re-engineer a new part. To apply this concept, a matching method between two adjacency graphs is used to associate the surface precedence graph of a part in the RE database to the query part. The important aspects of this paper are the use of the adjacency graph of a part and the matching algorithm in order to associate existing CAPP model to a new part to be remanufactured.

Key words: reverse engineering, process planning, matching, manufacturing, adjacency graph.

1- Introduction

In mechanical design, Reverse Engineering RE is the process of discovering how to remanufacture an existing part. In this paper, the proposed approach consists in identifying a reversed part in the RE database in order to reuse its CAPP model to reengineer a similar case study. As an assumption, this paper considers the following context: there is no information on the query part (no drawing or scheme); only the physical part is available. To remanufacture this kind of parts, the approach called Reverse Engineering For Manufacturing (REFM) is proposed. REFM allows to define a method of RE of mechanical parts, supported by a software demonstrator. REFM method is divided in two main stages: accumulation stage and re-use stage. In the accumulation stage, the user should be assisted in the RE approach. The result of the accumulation stage is the CAPP model of the reversed part stored in the database. In the reuse stage, the idea is to obtain a CAPP model with a minimum user interaction. For this reason, REFM is considered a recursive approach. Note that REFM system handles only milled or turned parts. Indeed, forged and casted parts are more complex geometrically.

This paper does not deal with the accumulation stage as it has been developed in the previous work [AD1].

Accumulation stage is decomposed in 9 steps as shown in figure 1: (1) segment the 3D point cloud, (2) select the material and the original blank of the part based on the Design For Manufacturing DFM approach, (3) generate the surface precedence graph SPG – the surface precedence graph is based on the part geometrical tolerancing. Geometrical tolerances connect machined surfaces to each other. Thus, To generate the SPG, REFM asks the user to select a machined surface and its reference one, then REFM proposes one or more tolerances and the user can choose the tolerances that he finds the most appropriate as shown in figure 2.-, (4) define machining operations, (5) link each operation to the geometry (3D identification), (6) define the order of machining features and define set-ups – the order of machining features and set-ups of a reengineered part depend on non-geometric information such as geometric dimensions and tolerances. So to reach feature sequencing, REFM system returns to the data mentioned in the SPG step. -, (7) define fixture planning, (8) select machines and (9) select tools.

In order to quickly reverse engineer a part, this paper presents an approach for matching similar parts in a RE database. The matching process is based on the geometric and topological similarity between mechanical parts. This paper is arranged as follows: section 2 presents research literature on reverse engineering methods, and shape matching methods. Section 3 describes the REFM methodology in the case of reuse case. The part considered in this paper is a centring pin used in order to illustrate our approach.

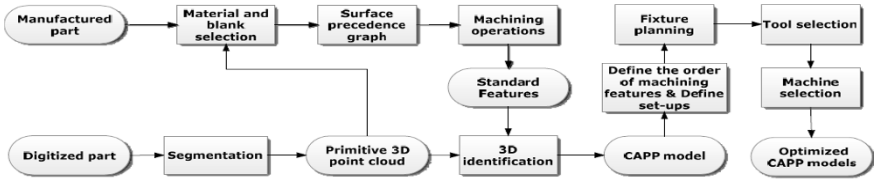

Figure 1: REFM methodology in details [AD1].

2- Related works

2.1 – Reverse Engineering methods

Reverse Engineering methodologies begin with a manufactured part and produce a geometric model. Three main methodologies can be revealed: interactive platform CAD environment, feature extraction and constraints fitting. As an example of CAD environment, the VPERI [VP1] (Virtual Parts Engineering Research Initiative) project was created by the US Army Research Office. Within the VPERI effort there is a strong focus on addressing the need to solve problems of long life cycle product maintenance, and the need to improve re-manufacturing capabilities to provide system-parts. The knowledge of the geometric shape is necessary but not sufficient to reproduce the part. Indeed, reengineering and redesign need functional specifications. Also, a specific design interface is used to allow the additional of knowledge in the form of algebraic equations that represent engineering knowledge such as the functional behavior of the components, the physical laws that govern the behavior, etc. This interface provides mechanisms that guide designers to ascertain that the functional requirements are fulfilled and helps designers to explore alternatives by assisting them as they make changes. Knowledge arises from the analysis and is simply expressed and transcribed in variables that are interpreted by the VPERI tool.

As an example of a feature extraction, we can cite REFAB system [TO1]. It uses a feature based and constraint based methods to reverse engineer mechanical parts. REFAB is a human interactive system where the 3D point cloud is presented to the user, and the user selects predefined feature in a list, specifies the approximate location of the feature in the point cloud. Then the system fits the specified feature to the actual point cloud data using a least square means method iteratively. So, manufacturing knowledge extraction is achieved implicitly by the user. In the same way, Sunil et al. [SP1] suggest extraction of manufacturing feature in a point cloud. Urbanic et al. [UE1] proposed a library of features based on a specific manufacturing process. They explain that features have accurate mathematical definitions for their geometry and tolerances depending on functional requirements.

Other references such as Fisher [F1] and Mills [ML1], present a reverse engineering approach in which a priori knowledge is applied and expressed through constraints. With the additional user's knowledge about the part and using an optimization algorithm, the shape and position parameters are found even with considerable noisy 3D point cloud.

All references do not suggest a structured methodology. The aim of our approach is to bring a methodology to reverse engineer a part. The idea in this paper is based on the matching methods.

2.2 – Shape matching methods

As mentioned above, this paper is based on the matching method to reverse engineer an existing part. Various methods have been developed to perform matching of 3D models. In general, matching methods between two 3D parts can be divided in three categories: feature based methods, graph based methods and geometry based methods. In feature based methods, 3D parts can be differentiated by measuring and comparing their features. For example, IP and Gupta [IG1] described a feature based method to retrieve the CAD model of an artefact using partially scanned point cloud of the artefact. The method allows to segment the point cloud and CAD meshes into surface patches using an identical algorithm, then to identify matching patches in point cloud and CAD meshes by using simple rotationally independent attributes such as surface area and curvature, and finally to align the point cloud with the CAD meshes and evaluate the error associated with the alignment. Zhu et al. [ZW1] describe a method based on 2D images for fast computation and matching of 3D models. The method maps the 3D CAD models to 2D principal images and matches the 3D models to database with their features. Or, feature based methods take into account only the pure geometry of the shape, so connections and dependencies between features are not considered in the matching process. However, graph based methods try to link part components together by extracting a geometric meaning from a 3D part. Cicerello and Regli [CR1] present a graph based method to compare the manufacturing similarity of solid models of machined artefacts based on their machining features. The method consists of constructing a model dependency graph from the set of machining features then finds the nearest neighbours to the query graph using an iterative improvement search across a database of other models. Aouada et al. [AK1] proposed a topological Reeb graph skeleton using an intrinsic global geodesic function defined on the surface of a 3D object. This approach decomposes a shape into primitives, and then detailed geometric information is added by tracking the evolution of Morse's function level curves along each primitive. El-Mehalawi and Miller [EM1] utilize the topological relationship of the faces in a B-Rep model, characterized with a graph data structure. Each graph node represents a face of the model and an edge connects two nodes if the corresponding faces are adjoining. The edges contain information like the curve type to improve the matching process. Including additional attributes in the edges helps the discrimination capability, but it inevitably increases the computational load of the similarity assessment. An

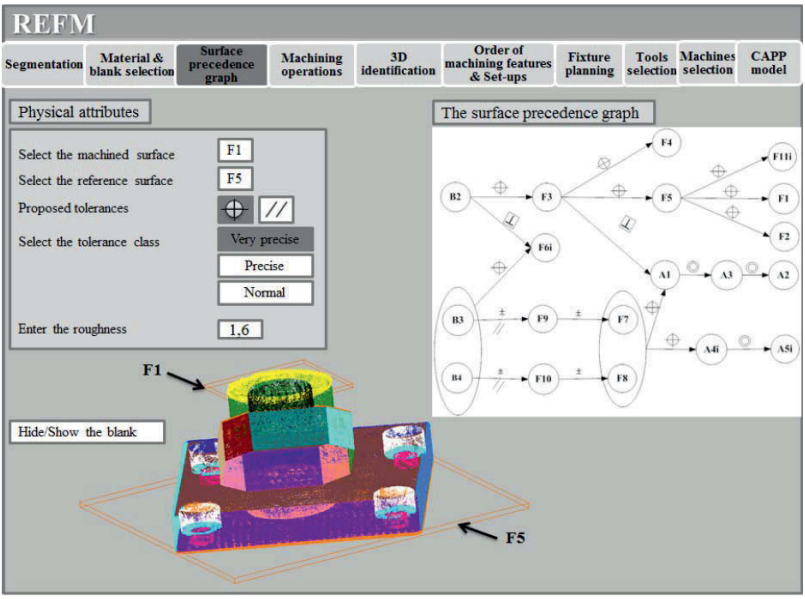

Figure 2: Interface of the surface precedence graph in REFM [AD1]

example of geometry based methods can be given by Cyr and Kimia [2001]. They specified a query by a view of a 3D object. The number of views of each object is kept small by clustering views, and by representing each cluster with one view, which is represented by a shock graph. So shock graph matching is used for the recognition of a 3D shape by comparing a view of the shape with all views of 3D objects.
In the following section of this paper, the REFM method in the case of routine tasks will be explained and illustrated by the centring pin example.

3- REFM methodology: reuse case

REFM in this paper is a new RE process which is based on matching method to reuse the CAPP model of a reverse engineered part in order to reengineer a similar case study. The technical approach is decomposed in six steps: (1) loading the segmented 3D point cloud of the query part, (2) assigning its attribute and using of descriptor, (3) retrieving similar parts from the REFM database, (4) building adjacency graph of the query part, (5) computing the adjacency graphs matching of the query part and the similar parts in the database, (6) fitting the CAPP model of the matched part of the database to the query part.
In this paper, step (1) and step (2) are well known and don't need to be detailed. Step (3) aims to identify possible matching parts in the database. This can be achieved by several means:

- The part attributes: this reduces the number of possible candidates by not selecting camshaft parts to compare to the query part that is a crankshaft for instance.
- The use of descriptor: this allows a second filter on the possible candidate by the use of scalar descriptor such as [BD1] and the use of geometrical comparator [EA1].

Steps (4) and (5) are detailed in this paper and are implemented in Matlab to illustrate results.
Depending on the matching results of step (5), fitting the CAPP model of the candidate part to the query part can be immediate or may need some additional works discussed in step (6). So, step (6) is not detailed here, only cases that can be encountered are discussed.

3.1 – Principle and definition

In the REFM process, the user loads the point cloud of the query part then he assigns attribute to the part (top of a reducer, centring pin, piston…). Using the REFM database, the method allows to reuse existing CAPP model instead of creating a new process planning from scratch. REFM searches in the database based on the information of the attribute, parts that have the same attribute of the query part. Then, it builds the adjacency graph of the query part. Adjacency graph is defined as a representation of machining surfaces of a part and links of those surfaces. The nodes of this graph correspond to surfaces. Each node is represented by the label of the surface (P: planner surface, C: cylindrical surface, and so on). An edge between two nodes exists if the corresponding surfaces have connection between them. To detect the connection between two surfaces, it is sufficient to

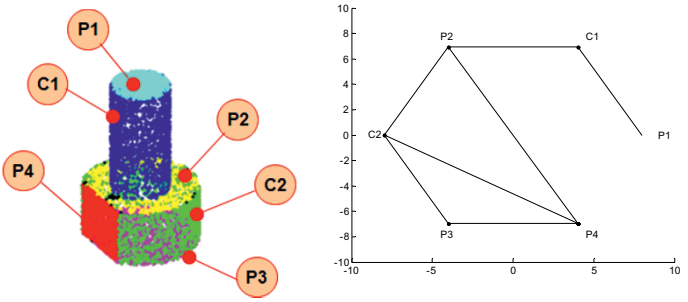

Figure 3: Query part and its adjacency graph.

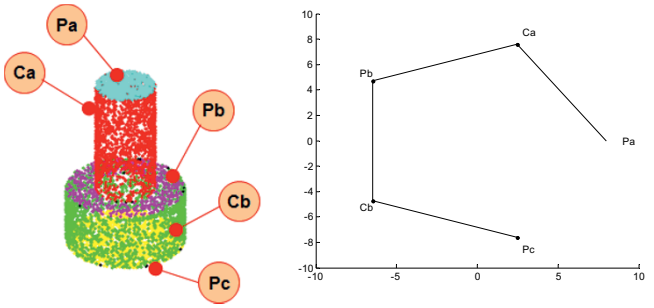

Figure 4: Candidate part from the REFM database and its adjacency graph.

find at least one point cloud having a neighbour point in the other point cloud with a small distance ε. The distance ε depends on the point cloud and the dimensions of the part. Once the adjacency graph of the query part is build, the matching procedure between two graphs must begin. The matching method implemented in Matlab is based on a propagation algorithm. It tests all possible combinations. It begins to match arbitrary two surfaces Xi and Xj that have the same topological surfaces (Xi: a plan or a cylinder in a candidate part, Xj: a plan or a cylinder in the query part) where i=1…n and j=1…m. Using the node connections to define the possible candidate, the graph matching is performed considering here only the nodes nature. Matching is performed until no more nodes are available in one adjacency graph or until nodes nature doesn't match. The result of the graph matching is given by three values: scores of the adjacency graph of the query part and the adjacency graph of the candidate part (SGi) and the total score (TotalScore).

$$SGi = \frac{nb_{Nodes\_SGi}}{nb_{Nodes\_Gi}}$$

$$TotalScore = \frac{SG1 \times SG2}{100}$$

nb_{Nodes_SGi} : Number of matched nodes in the graph Gi.

nb_{Nodes_Gi} : Number of nodes in the graph Gi.

SG1 and SG2 are the scores of the two sub graphs of the query and the candidate part in the same combination.
The best combinations are those with the highest value of TotalScore.

3.2 – Case study

To illustrate the proposed methodology of the reuse case of REFM, a centring pin is used as an example. Figure 3 shows a segmented 3D point cloud of a query part which is to be reengineered. REFM searches in the database a centring pin that has been reengineered. It finds the part in figure 4. It builds the adjacency graph of the query part. Then, the matching algorithm starts. Figure 5 shows the results of the matching method: 42 combinations. To compare these combinations and to choose the bests, REFM compares the score SGi of each graph in each combination and the TotalScore of each combination. Four combinations have the

highest TotalScore: 83.3% as shown in figure 6.
The score SGc of the graph of the candidate part in these four combinations is 100%.
The score SGq of the graph of the query part in these four combinations is 83.3%.

```
Pa - Ca - Pb - Cb - Pc  <---------->  P1 - C1 - P2 - C2 - P3
Pa - Ca - Pb - Cb - Pc  <---------->  P1 - C1 - P2 - C2 - P4
Pa - Ca - Pb - Cb - Pc  <---------->  P3 - C2 - P2 - C1 - P1
Pa - Ca - Pb - Cb - Pc  <---------->  P4 - C2 - P2 - C1 - P1
    Ca - Pb - Cb - Pc   <---------->  C1 - P2 - C2 - P3
    Ca - Pb - Cb - Pc   <---------->  C1 - P2 - C2 - P4
    Ca - Pb - Cb - Pc   <---------->  C2 - P2 - C1 - P1
    Cb - Pb - Ca - Pa   <---------->  C1 - P2 - C2 - P3
    Cb - Pb - Ca - Pa   <---------->  C1 - P2 - C2 - P4
    Cb - Pb - Ca - Pa   <---------->  C2 - P2 - C1 - P1
        Pa - Ca - Pb    <---------->  P2 - C2 - P3
        Pa - Ca - Pb    <---------->  P2 - C2 - P4
        Pa - Ca - Pb    <---------->  P2 - C1 - P1
        Pa - Ca - Pb    <---------->  P3 - C2 - P4
        Pa - Ca - Pb    <---------->  P4 - C2 - P3
        Pb - Cb - Pc    <---------->  P1 - C1 - P2
        Pb - Cb - Pc    <---------->  P2 - C2 - P3
        Pb - Cb - Pc    <---------->  P2 - C2 - P4
        Pb - Cb - Pc    <---------->  P2 - C1 - P1
        Pb - Ca - Pa    <---------->  P2 - C2 - P3
        Pb - Ca - Pa    <---------->  P2 - C2 - P4
        Pb - Ca - Pa    <---------->  P2 - C1 - P1
        Pb - Cb - Pc    <---------->  P3 - C2 - P4
        Pb - Cb - Pc    <---------->  P3 - C2 - P2
        Pb - Cb - Pc    <---------->  P4 - C2 - P3
        Pb - Cb - Pc    <---------->  P4 - C2 - P2
            Ca - Pb     <---------->  C1 - P1
            Ca - Pa     <---------->  C1 - P2
            Ca - Pa     <---------->  C1 - P1
            Ca - Pb     <---------->  C2 - P3
            Ca - Pb     <---------->  C2 - P4
            Ca - Pa     <---------->  C2 - P3
            Ca - Pa     <---------->  C2 - P4
            Ca - Pa     <---------->  C2 - P2
            Cb - Pc     <---------->  C1 - P2
            Cb - Pc     <---------->  C1 - P1
            Cb - Pb     <---------->  C1 - P1
            Cb - Pc     <---------->  C2 - P3
            Cb - Pc     <---------->  C2 - P4
            Cb - Pc     <---------->  C2 - P2
            Cb - Pb     <---------->  C2 - P3
            Cb - Pb     <---------->  C2 - P4
```

Figure 5: All possible combinations.

```
Pa - Ca - Pb - Cb - Pc  <---------->  P1 - C1 - P2 - C2 - P3
Pa - Ca - Pb - Cb - Pc  <---------->  P1 - C1 - P2 - C2 - P4
Pa - Ca - Pb - Cb - Pc  <---------->  P3 - C2 - P2 - C1 - P1
Pa - Ca - Pb - Cb - Pc  <---------->  P4 - C2 - P2 - C1 - P1
```

Figure 6: Best combinations.

Now, surface precedence graph can be used to eliminate the second and the fourth combination by checking the geometrical information similarity. For example, in the second combination if Pa is perpendicular to Ca so P1 should be perpendicular to C1. This condition is not verified for all surfaces in the second and the fourth combinations. Indeed, in the second combination Pc is perpendicular to Cb or P4 which is matched with Pc is parallel to C2 which is matched with Cb.
So finally it remains two possible combinations. Our model does not yet allow to set in evidence the most appropriate.
The user can choose the best according to its needs.
Now, parts are matched thanks to their adjacency graphs. Step (6) of the reuse stage of REFM system is to be reached. In general, four cases can be met.
The first is the simplest one, when the candidate and the query part have the same topology, SGc =SGq = 100%. In this case, the CAPP model in the database can be directly associated to the query part.
The second case is where the query part is fully matched (SGq = 100%) and at least one surface of the candidate part is not matched (SGc < 100%) as shown in figure 7. This case leads to the degradation of the CAPP model of the candidate part in the database; hence REFM will eliminate the additional surface X from the surface precedence graph of the part in the database. If the surface X positions a surface Y, REFM proposes to the user to choose another surface to position Y. Thus, the accumulation stage has to be re-applicable on the surface Y in order to obtain the CAPP model of the query part.
The third case corresponds to the presented case study of figures 3 and 4 where the candidate part is fully matched (SGc = 100%) and at least one surface of the query part is not matched (SGq < 100%). This case leads to the completion of the CAPP model of the candidate part in the database; hence the user should apply the accumulation stage on the additional surface of the query part. Then, REFM will integrate the data of the surface to the CAPP model of the part in the database to obtain the process planning of the query part.
The fourth case is the case that meets the last two cases above; there is at least one surface in the candidate part that is not matched and there is at least one surface in the query part that is not matched as shown in figure 8. In this case, we should apply the last two scenarios above to obtain the CAPP model of the query part: CAPP model of the candidate part is degraded and then completed.

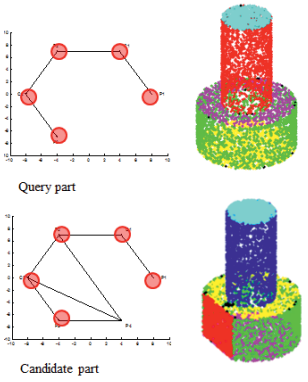

Figure 7: Illustration of the second matching case.

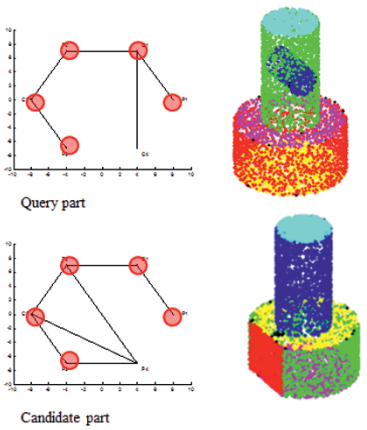

Figure 8: Illustration of the fourth matching case.

4- Discussion

This paper proposed a solution to reuse a generated CAPP model stored in a RE database in order to re-engineer a new part. The proposed method was successfully applied to turning parts which come from a cylindrical blank as shown in this paper.
In the future, the purpose is to try the proposed method on milling parts which come from a parallelepiped blank and on parts which come from the casting process.
In the case of milling parts, the method seems to be similar to the proposed in this paper, while in the case of parts which come from the casting process, the method seems to be more complex.
Indeed, in the case of milling parts, all surfaces are machined. So, the number of surfaces in the part is equal to the number of surfaces in the SPG (a surface precedence graph connects machined surfaces to each other). While in the case of parts which come from the casting process, there is a high chance that the number of surfaces in the part is greater than the number of surfaces in the SPG since not all surfaces are machined (the non-functional surfaces are not machined). So, the adjacency graphs and then the possible combinations between two parts, include surfaces that do not exist in the SPG of the candidate part.

5- Conclusion and future work

This paper meets the needs of industrial companies in defining a new approach to reengineer mechanical parts using 3D point cloud. The Reverse Engineering For Manufacturing REFM approach is divided in two main stages: accumulation stage and re-use stage. The accumulation stage is achieved by the user's assistance to obtain the CAPP model of a part. Once the CAPP model is created, REFM will store it in the database in order to be reused in a similar query part. So, in the reuse stage, RE approach is achieved by REFM system with a minimum user interactive.
The contribution of this research is the introduction of matching adjacency graph in the RE context in order to fit a CAPP model to a part to be reversed. The idea is to reuse the CAPP model of a reengineered part stored in the RE database in order to avoid the design of the process planning from scratch.
In this paper, the two steps (making adjacency graphs of the query part and the retrieving part, matching the two adjacency graphs) are automated in Matlab.
In the future, the final step of the reuse stage should be implemented in order to associate or fit the CAPP model in the database to the query part and the method should be applied on parts that come from a parallelepiped blank and from the casting process.

ACKNOWLEDGEMENTS. The acknowledgment concerns the region Champagne Ardenne through the ESSAIMAGE program. These works are financed by the region.

6- References

[AD1] Ali S., Durupt A. and Adragna P-A. Reverse Engineering For Manufacturing approach: based on the combination of 3D and knowledge information. Proceedings of the 23rd CIRP design conference, 137-146, 2011.
[AK1] Aouda D. and Krim H. Squigraphs for Fine and Compact Modeling of 3-D Shapes, IEEE Transactions on Image Processing, 19: 306-321, 2010.
[BD1] Bruneau M., Durupt A., Roucoules L., Pernot J.P. and Rowson H.: A methodology of reverse engineering for large assemblies products from heterogeneous data, Proceedings of TMCE, 2014
[CK1] Cyr C.M. and Kimia, B.B. 3D Object Recognition Using Shape Similarity-Based Aspect Graph, International Conference on Computer Vision, 254-261, 2001.

[CR1] Cicerello V. and Regli W.C. Machining Feature-based Comparisons of Mechanical Parts, In International Conference on Shape Modelling and Applications, 176-185, 2001.

[EA1] El-Mehalawi M. and Allen Miller R.: A database system of mechanical components based on geometric and topological similarity. Part II: indexing, retrieval, matching, and similarity assessment, Computer-Aided Design, 35: 95-105, 2003.
[F1] Fisher B.: Applying knowledge to reverse engineering problems, Computer Aided Design, 36: 501-510, 2004.

[IG1] IP C.Y. and Gupta S.K. Retrieving Matching CAD Models by Using Partial 3D point clouds, Computer-Aided Design & Applications, 4: 629-638, 2007.
[ML1] Mills B.I., Langbein F.C., Marshall A.D., Martin R.R.: Estimate of frequencies of geometric regularities for use in reverse engineering of simple mechanical components, Technical report, Cardiff University, 2001.
[SP1] Sunil V., Pand S.: Automatic recognition of features from free form surface CAD models, Computer Aided Design, 40: 502-507, 2008.
[TO1] Thompson W., Owen J., De St Germain H., Stark S., Henderson T.: Feature based reverse engineering of mechanicals parts, IEEE Transactions on Robotics and

Automation, 15: 57-67, 1999.

[UE1] Urbanic R., Elmaraghy H., Elmaraghy W.: A reverse engineering methodology for rotary components from point cloud data, International Journal of Advanced Manufacturing Technology, 37: 1146-1167,2008.

[VP1] VPERI, Virtuals Parts Engineering Research Initiative, (http://www.cs.utah.edu/gdc/Viper/Colloborations/VPERI-Final-Report.pdf), the final report, 2003.

[ZW1] Zhu K.P., Wong Y.S., Lu W.F. and Loh H.T. 3D CAD model matching from 2D local invariant features, Computers in Industry, 61: 432-439, 2010.

Article 060-cad-91

New standard of dimensioning adapted to the programs CAD. Creation and unification of symbols dimensioning.

David Arancon [1], Felix Sanz-Adan [1], Jacinto Santamaria [1] Alberto Martínez-Rubio [1]

(1) : University of La Rioja
+34914299537
E-mail : david.arancon@unirioja.es

(1) : University of La Rioja
+34914299533
E-mail : felix.sanz@unirioja.es

Abstract: Vectorl design of objects (CAD3D) indicates its dimensions according to standards previous to existence of the CAD3D systems. In many cases, it does not meet the needs of new Information and Communication Technologies (ICT), causing the repetition of dimensioning tasks in the successive stages of product development. The dimensional standards currently used, take a long product launch time.

This research states a methodology for dimensioning which allows the designer to provide the graphical representation of the product with geometric and dimensional information, complete, accurate and universal; design time is shortened and productivity is increased.

As result of this methodology a new international standard of dimensioning is proposed, which unifies the utilization of signs adapted to 3D design as alternative to those currently in use and allows obtaining clearer technical drawings and with less dimensions.

This proposal for a new standard has been validated by a comparative review of the most widespread dimensioning standards.

Key words: Geometric modelling, Standard dimension, CAD. Technical drawing.

1- Introduction

In an increasingly globalized world, where communication is rapidly changing over the Internet with the important barrier of different written and spoken languages, the correct and productive implementation of any project need, more than ever, rely on the technical drawing as universal, brief and concise language.

A high percentage of technology products and gadgets are designed, manufactured, assembled and distributed in different languages. The communication among them must be instantaneous. Any change in the design, must be known at any point in the manufacturing chain.

A review of state of the art of dimensioning techniques in both product design and process planning, concludes that most of the published work in recent years is in the area of dimensioning techniques with emphasis on tolerance analysis using computer simulation models. However, though research into tolerancing techniques has been fairly extensive, the dimensioning aspect has been neglected. Unfortunately, several organizations have attempted to implement Geometric Dimensioning and Tolerancing without fundamental understanding of the impact in the design process. A perfect design under a wrong application of Geometric Dimensioning and Tolerancing could turn to a bad one. [IS], [KE], [NG].

The purpose of this article is to improve the universality of the symbols used in the Product dimensioning. If that succeed, we will have contributed to reduce errors and improve the technical drawings interpretation between different languages and countries. We propose a new standard of dimensioning adapted to the powerful CAD programs that supplements the various nowadays standards. (AFNOR, UNI, UNE, DIN, ASTM, ISO,...).

The proposed standard of dimensioning is adaptable to CAD3D, regarding the importance of 2D product representation during the sketch development.

2- Dimensioning of simple elements

The draft standard is too large, so in this article it presents only a few study cases that can appear in technical drawings; mainly prismatic pieces with revolution elements, enough to expose the discrepancies of the major global industry standards; the proposed solutions are justified through five study cases.

2.1- Revolution pieces.

2.1.1-Dimension symbols: Diameter and Radius

The Ø symbol:

[ISO 129-4 2011], in Section 4.2.3 indicates that the diameter should always be placed with the symbol.

[ANSI / ASME Y14.5M-1994] Always places the symbol and recommends "*do not use a diagonal diameter inside the circular view, except when clarity is improved"*.

Article 060-cad-91

[UNE 1039 1994] It is possible to skip the symbol when the circle is seen in True Size and Shape (TS). See Figure1.

[DIN 406-07_2004)]: You should always place the symbol, even if the drawing clearly shows that it is a circle or a circular arc. This standard supersedes the DIN406-3_1975-07) indicating that it dispenses with the symbol when the circle is viewed in TS.

[UNI 3975] In paragraph 6 says that it is not forced to place the symbol in the circles seen in TS.

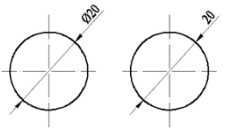

Figure 1: Dimensioning of a circle

[AFNOR]: It always places the symbol, even if the circle is visible in TS.

Besides indicating the Standard, the general recommendation of the authors of books of technical drawing, ([CH], [CT], [FM], [GM]), is to remove the Ø symbol when it is clear that this is a circular element (Fig. 2). This recommendation saves time in the drawings made with traditional tools, but in the CAD3D software the effect is the opposite, because it places the Ø symbol both in space and in orthogonal projection.

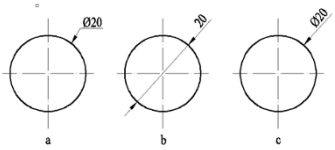

Figure 2: Dimensions of diameters

When the orthogonal projection of the base of a revolution piece is a line segment equal to the diameter in TS (Fig. 3), there is unanimity that you must always place the Ø symbol.

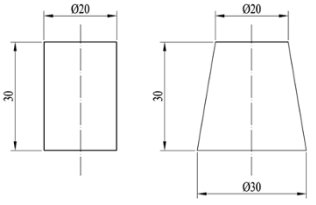

Figure 3: Cylinders and cones

If you remove the Ø symbol from projected plane in 2D, and it is automatically dimensioned by CAD3D programs, it implies an unnecessary waste of time and unlinking this dimension in 3D, preventing future automatic updates. [SB].

If the design has been made directly in 2D (CAD2D), the program can not automatically detect if it is a circle because it is not shown in TS -unless the object attributes in 3D be granted -, so in these cases is preferable to use two views and annotate the diameters where the circle is in TS (Fig.4).

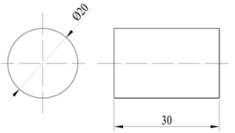

Figure 4: Dimensioning of a cylinder in CAD2D

The R symbol:

When the circular arc is greater than 180, no standard allows you to annotate the symbol of radius R. The reason is very well explained by [GM] "*the radius of cylinder should never be given because measuring tools, such as micrometer caliper, are designed to check diameters".*
The ban is due to an objective criterion of functionality, but CAD programs that have automatic or semi-automatic annotation, place Ø or R in function of the data entered by the designer to do the drawing. This problem has an easy and justifiable solution "the designer will try to design the piece indicating the diameter or radius depending on how the piece should be dimensioned.

2.1.2-Size dimensioning: holes

There are rules to represent holes in simplified form ([UNE-EN ISO 6411_1998], [ASME Y14.5M]

[GM] in chapter 9, uses the ↓ symbol to indicate depth, but it has the disadvantage that this symbol is not widespread on keyboards or CAD programs. Most CAD software have a library of standard symbols [ISO 129-1_2010] paragraph 7.

There are different variants of holes (counterbore, countersink) with specific symbols that facilitate their marking (Fig. 5).

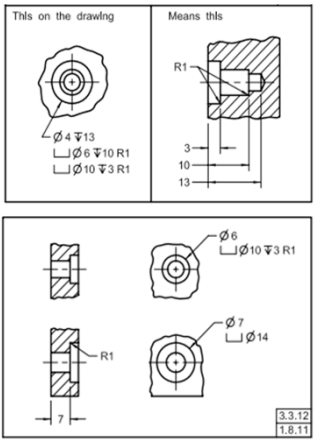

Figure 5: Dimensioning holes [ASME Y14.5M-2009]

Article 060-cad-91

2.1.3-Half sections

In the representation of half-sections of revolution pieces, it is necessary to break the dimension lines. This method does not allow the automatic dimensioning since the program automatically annotates full dimension lines. In some cases de software automatically breaks the dimensions lines but not as it shown in the standard.

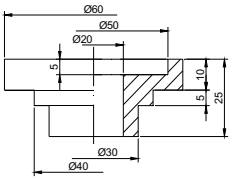

Figure 6: Dimensioning half-section

Figure 7 shows how a half section dimensioning should be in a 3D model. None CAD program offers this representation automatically; however, it would be interesting to incorporate in CAD programs this possibility, in order to avoid having to unlink these dimension lines required when presenting a half-cut work-piece.

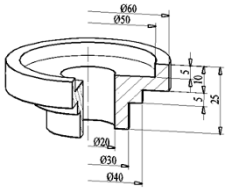

Figure 7: Dimensioning half-section (CAD3D model)

2.1.4- Oblique cylinders and holes

If the work-piece has oblique cylinders or oblique holes to the reference surface, you must annotate: height or depth, axis orientation and inclination. (Fig. 8).

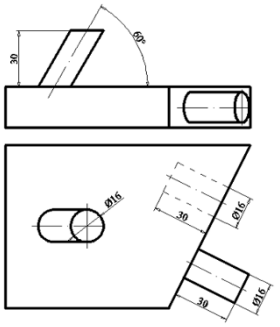

Figure 8: Dimensioning oblique cylinders and holes.

2.2- Prismatic pieces

2.2.1-Dimensioning in 2D: Orthogonal projection

Figure 9 shows the standardized rectangle and square dimensioning.

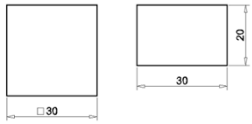

Figure 9: Standard Dimensioning of Rectangles

Figure 10 shows an oblique prism represented in two views, front and top; see an alternative proposal in Figure 23.

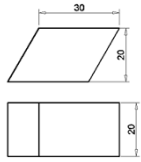

Figure 10 Standard Dimensioning of Oblique Prisms

The proposed for these cases answers the next criteria: less dimension lines and better universal interpretation. (Fig.16)

2.2.2- 3D models

The figures 11 and 12 show the dimensioning of perspective drawings (3D models). No significant differences between the studied standards.

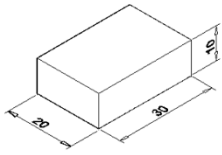

Figure 11: Straight Prism: 3D Standard Dimensioning

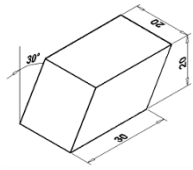

Figure 12: Oblique prism: 3D Standard Dimensioning

When the pieces have holes, the dimensioning of prisms is more complex and datum references should be indicated.

Article 060-cad-91

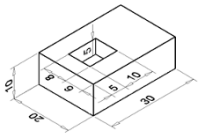

Figure 13: Holes in 3D model. Standard Dimensioning.

3- Dimensioning adapted to software CAD (2D & 3D). Proposals

The project research that supports this paper analyzes all symbols and all cases of the actual standards and, according to the authors, should be amended to improve the interpretation of technical drawings. In this article only six representative proposals are elaborated.

3.1- Revolution pieces

Proposal 1: "R" and "Ø" Symbols.

A circle can be dimensioned with a diameter or radius symbol. We propose to always indicate the symbol (R or Ø), even if it is evident, in order to improve the piece interpretation without increasing the design time.

Some examples:

- In the hole it is recommended to indicate the Ø symbol because it is made by tools defined by diameter.
- In the work-part made on a lathe, it is recommended to annotate the R symbol because the movement of tool is related to radius value.
- Both for drawing (CAD) and to manufacturing (CAM) it is indifferent radius or diameter; but usually the CAD software puts automatically the same dimensioning that the designer has drawn.

Proposal 2: Cylinders Dimensioning: Orthographic views.

In Figure 4 is shown that two dimensions are needed for dimensioning a cylinder. There are three possible alternatives, all with a single dimension line (Figs 14a, b, c).

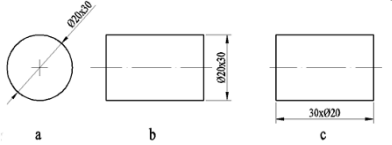

Figure 14: Revolution cylinder: Dimensioning proposal

Proposal 3: Cylinders and cones: 3D models. Dimensioning

Both the cylinder and the truncated cones are well defined by a single dimension line (Fig. 15).

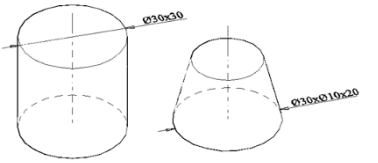

Figure 15: Cylinder and cone: 3D Dimensioning

Proposal 4: Holes.

In the holes design, the depth is indicated by a negative value (-) and the start surface of the hole is assigned as datum reference (see section 4).

3.2- Prismatic pieces

Proposal 5: Rectangles and squares

Reducing two dimensions to only one dimension line, and in the case of a square it is possible to eliminate the □ symbol (Fig. 16).

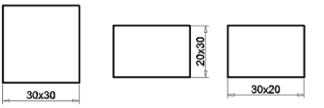

Figure 16: Rectangle and square: Dimensioning in 2D

Proposal 6: Prismatic pieces: 3D models. Dimensioning

The coordinate dimensioning reduces the number of dimensions lines from eight (Fig. 13) to three, (Fig.17). The representation of the object is clean of lines and completely defined.

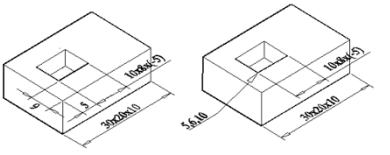

Figure 17: Prismatic parts: Dimensioning 3D

4- Applications

Continued, a few study cases are dimensioned with the new standard adapted to the CAD.

Study case 1: Revolution pieces.

Both in 2D and 3D, the number of dimension lines is reduced from nine (Fig. 6) to six (Fig. 18).

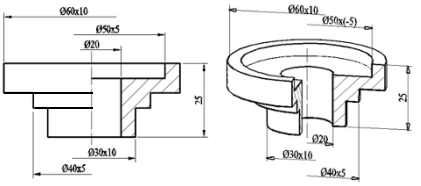

Figure 18: Half section. 2D and 3D dimensioning.

Study case 2: Prismatic piece. Coordinate dimensioning (Fig.19).

The use of coordinate dimensioning is ideal to distribute required data for automatic production machines (CAM, DNC or CNC).

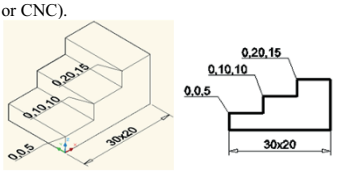

Figure 19: Dimensioning by Cartesian Coordinates

Study case 3: Prismatic piece. Holes and pivots orthogonal to the reference surface (Figs. 20, 21, 22, 23).

The piece is defined with 4 dimension lines in a single view:

- The first circle represents a cylindrical pivot of diameter 16mm and 30mm height.
- The second circle represents a hole of diameter 16mm and 10mm depth.
- The third circle represents a through hole.
- The fourth circle is a hole of diameter 16mm and 30mm depth.

This type of dimensioning allows to design, with CAD3D software, in less time by avoiding unnecessary broken out sections and making easier to understand in other languages.

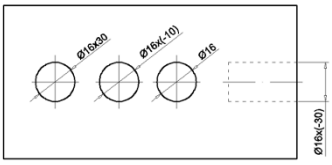

Figure 20: Dimensioning in 2D projection: holes and pivots

Figure 21 shows the dimensioning in a simplified piece view.

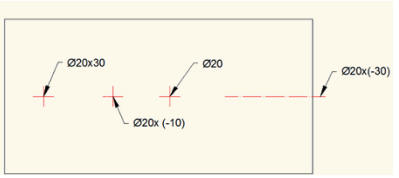

Figure 21: Dimensioning in simplified view

Figure 22 shows the dimensioning of the piece in 3D.

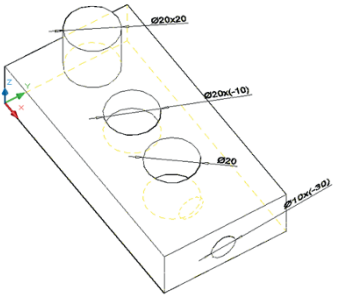

Figure 22: Dimensioning in 3D model: Holes and pivots

Study case 4: Prismatic piece. Holes and pivots oblique to the reference surface (Figs. 23, 24, 25).

The pivot is a no revolution cylinder, its axis measures 60° to upper horizontal plane reference (parallel to plane X-Y), and is parallel to vertical plane X-Z, having circular bases of diameter 16mm and a height of 30mm.

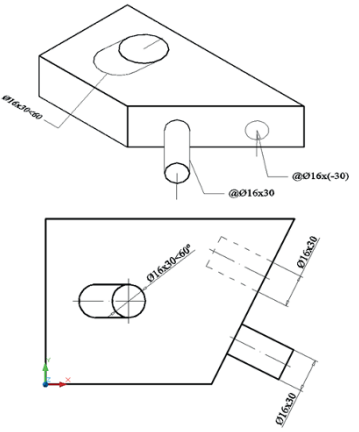

Figure 23: Holes and pivots. Dimensioning

Article 060-cad-91

The traditional 2D representation requires two views and seven dimension lines (Figure 8) while, with the proposed standard, the pivots and the holes are defined by a single view and three dimensions lines (Figure 23), in both 2D and 3D.

You have two options for sizing the pivot:
(Ø16x30, 0º, 60º) = (Ø16x30<60º)
Being:
Height (pivot):+30mm.
Guide angle (horizontal, negative if it is clockwise): 0º.
Elevation angle (vertical, positive for being counter-clockwise): +60º

The figure 24 represents the full dimensioning of the piece (prism dimensions, position and dimensions of the pivot and holes) using only four dimension lines:

1ª. Trapezoidal prism is defined with one dimension line for three dimensions: trapeze bases (100, 50), trapeze height (50) and the orthogonal extrusion (20).

2ª. Oblique non revolution pivot: It is defined with one dimension line for the position of the axis start in Absolute Cartesian Coordinates (10, 10, 20) -referred to piece zero (X=0, Y=0, Z= 0)-, radius Base (Ø16), the angles formed by the axis with the X-Z plane (0°) , and with the X-Y plane (60°) and the pivot height (30) measured along the normal to the reference surface of the pivot start.

3ª. Orthogonal revolution pivot: It is defined with one dimension line by the axis start position in Relative Cartesian Coordinates (@20, 10, 0) where X'-Y' is the reference surface normal to the axis, the diameter of pivot (Ø16) and the height (30) normal to the reference surface.

4ª. Orthogonal drill-hole: As it is a hole, the height is negative (-30) according to the above criteria.
The piece is completely defined with only four dimension lines, however, using the traditional method of dimensioning requires more than fifteen dimension lines.

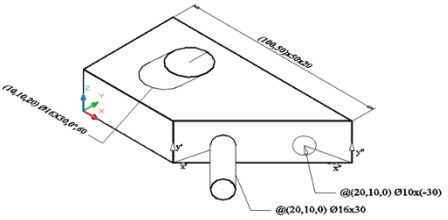

Figure 24: Standard proposal: Dimensioning and position

Study case 5: Assembly dimensioning (Figs. 25, 26).

In order to achieve a correct parts assembly, the datum references of each part are linked and are defined by the type of dimensioning to use. In this case, we believe that the usage of Spherical and Cartesian Coordinates simplifies the dimensioning of both pieces. These pieces are named lower base and upper base.

Lower Base: It is bounded by Cartesian and Spherical Coordinates and it is perfectly defined both in 3D (Fig. 25a) and in a single view:-front view (Fig. 25b) or top view (Fig.25c).

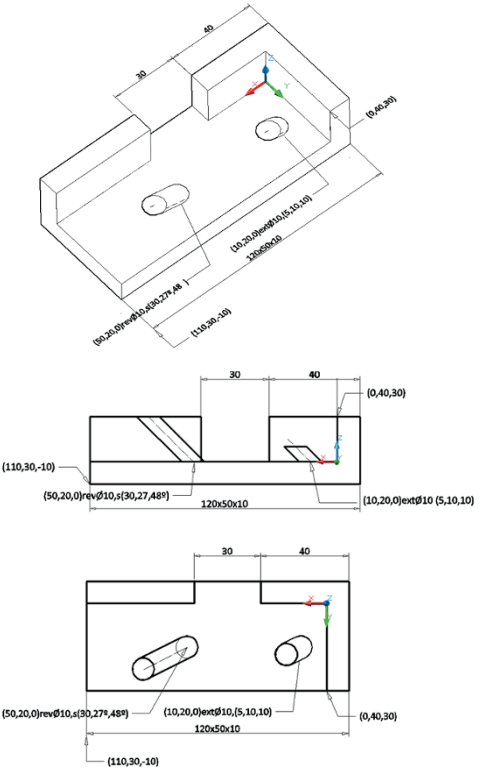

Figure 25: Lower base. Dimensioning

Upper Base: It is fully defined in a single view too.

The first impression may seem to be complex undestarding and dificult to interpretate. However, with a simple, short table giving the symbology to usage, aided by some simple examples and learning the proposed standard is very simple.

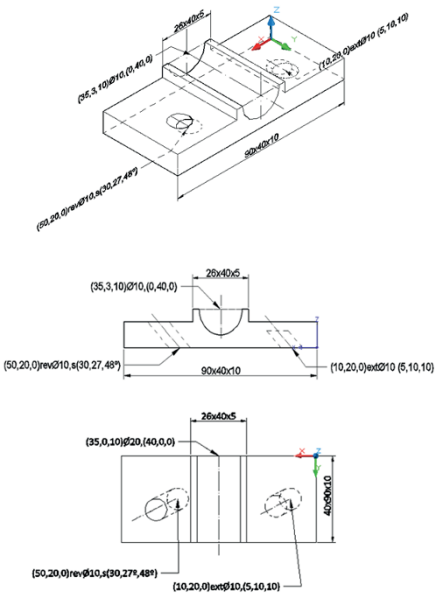

Figure 26: Upper base. Dimensioning

5- Conclusions

The proposed dimensioning standard adapted to CAD3D software, will allow:

- Unifying the symbols utilized by the various national and international standards currently in force.
- Providing guidance to CAD software developers in the same direction, facilitating the exchange of dimensional and geometrical product information.
- Reducing the possibility of mistakes in the design process of a certain product (designing, manufacturing and verification).
- Reducing the number of single dimension lines, using a smaller number of complex dimension lines which indicate: position, orientation and dimension.
- Reducing the number of views, broken out sections and details.
- Possibility of representing the product in a clearer and simpler way.
- Shorten time and less paper waste in drawing.

The main objective of Technical Drawing is to allow a quick, accurate, simple and universal 2D and 3D interpretation using less dimension lines.

6- References

[CH] Chevalier A. Guide du dessinateur industriel. Edit. Hachette libre, 2004.

[CT] Chirone E., Tornincasa S. Disegno técnico industriale. Edit. Il capitello, 2010.

[FM] Félez J., Martínez M. Ingeniería gráfica y diseño. Edit. Síntesis 2008.

[GM] Giesecke F., Mitchell A. et al. Technical Drawing. Edit. Pearson Prentice Hall, 2009.

[IS] Islam M.N. "A dimensioning and tolerancing methodology for concurrent engineering applications I: problem representation". Int J Adv Manuf Technol, pp 910-921, 2009.

[KE] Kevin C., Waleed E."An intelligent system based on concurrent engineering for innovative product design at the conceptual d.". Int J Adv Manuf Technol, pp 421-447, 2012.

[NG] Ngoi B.K.A., Ong C.T. "Product and Process Dimensioning and Tolerancing Techniques. A State of the Art Review". Int J Adv Manuf Technol, pp 910-917, 1998.

[SB] Sanz F., Blanco J. CAD-CAM. Gráficos, animación y simulación por computador. Edit Thomson, 2002.

[ANSI/ASME Y14.5M_2009] Dimensioning and tolerancing [revision on ASME Y14.5M_1994 (R2004)]

[ASME Y14.41_2012] Digital Product. Data Practices.

[BS 308_1972] Engineering Drawing Practice.

[ISO 129-1_2010] Technical drawings. Special Symbols.

[ISO 129-4_2011] Technical drawings. Indication of dimensions and tolerances. Part 1: general principles.

[DIN 406-10_1992-12] Engineering drawing practice; dimensioning; concepts and general principles.

[DIN 406-11_1992-12] Dimensioning in Drawings - Dimensioning by Coordinates

[DIN 406-12_1992-12] Engineering drawing practice; dimensioning. (modified version of ISO 406:1987)

[NF E 04-010_1963] Cotation - Disposition des Cotes.

[NF E 04-550_1983] Cotation et tolerances fonctionnels.

[NF E 04-551_1983] Cotation et tolerancement inscription des tolerances demiensionnelles.

[NF ISO 129-1_2005] Dessins techniques - Indication des cotes et tolérances - partie 1 : principes généraux.

[UNE 1032 1982] Elementos de acotación (a summary version of ISO 128-82, DIN 15 and ANSY Y14.2).

[UNE 1039_1994] Dibujos técnicos. Acotación. (modified version of ISO 129_1985).

[UNE-EN ISO 5456-3_2000] Technical drawings. Projection

[UNE-EN ISO 6411_1998] Technical drawings. Simplified representation of holes.

[UNI 3973] Disegni tecnici. Linee di misura e di riferimento.

[UNI 3974] Disegni tecnici. Quotatura e scelta dei riferimenti

[UNI 3975] Disegni tecnici. Quote e loro disposicion.

[UNI 4820] Disegni tecnici. Definicion e principi.

Article 040-pp-44

Evaluating Current CAD Tools Performances in the Context of Design for Additive Manufacturing

A.H Azman [1], F.Vignat [1], F. Villeneuve [1]

(1) : Grenoble-INP/UJF-Grenoble
1/CNRS,GSCOP UMR 5272
46, avenue Félix Viallet, 38031 Grenoble, France
Tél +33 (0)4 76 57 43 20
Fax +33 (0)4 76 57 46 95
E-mail :{abdul-hadi.azman, frederic.vignat, francois.villeneuve} @g-scop.grenoble-inp.fr

Abstract: Metallic Additive Manufacturing is a technology which opens a new world of opportunities in design and manufacturing. It is mainly based on melting metallic powder layer by layer and turning it into direct end user parts. The creation of complex part forms and lightweight structures have become easier with Additive Manufacturing through large usage of lattice structures. However, current design methods and Computer-Aided-Design (CAD) tools are not tailored for this type of shapes and are not yet optimized to achieve the great potential offered by this new technology. The breakthrough in manufacturing technology is not yet followed by a breakthrough in design and CAD tools. The current study aims at evaluating current CAD software's performances and proposes requirements for CAD tools to be efficient in design for additive manufacturing. The results show that current CAD tools and CAD file formats have insufficient performance in the context of design for Additive Manufacturing and a new file format together with new CAD human interaction needs to be created to overcome these problems.

Key words: Designing Process, Computer-Aided-Design, Designing Methodology, Additive Manufacturing,

1- Introduction

Today, in manufacturing, common processes used to manufacture metallic parts are casting, molding, forging, and machining. Since decades, these have been the general processes used to create parts. Besides their advantages and reliability to manufacture parts, it also comes with its share of disadvantages. For example, the need to create molds, the limits in shape designs of the parts, and wastes generated especially from machining process.

However, since the last 10 years, metallic additive manufacturing (AM), has been a breakthrough in manufacturing process and has succeeded in overcoming some of these disadvantages. It has created a whole new opportunity in metallic parts manufacturing possibilities. These processes create parts by adding metallic powders layer by layer and melting selectively the powder to form a finished part [BA1]. Thus the capability to manufacture direct finished complex parts without the need to use molds allows to create them directly from a 3D file. Parts can be designed without the manufacturing constraints of traditional subtractive manufacturing processes. This gives new opportunities for designers to create products to meet increasing requirements of customers and to manufacture lightweight structures.

Lattice structures or cellular structures are used to obtain lightweight and rigid structures. The realization of lattice structures is no longer limited by conventional manufacturing constraints and is made possible by AM [VV1]. Cellular structures can be used in metallic parts, and no longer limited to plastic components. It can also be used for applicable technical components and no longer just prototype parts. Research must be made to determine how these new requirements in design for additive manufacturing parts changes the demands on Computer-Aided-Design tools.

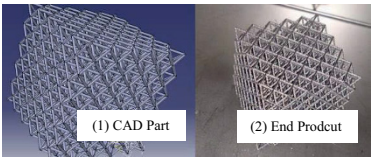

Figure 1: Example of an octet truss lattice structure part created using additive manufacturing. From CAD directly to fabrication of the end product

Computer-Aided-Design (CAD) is an important tool in the numerical chain to design parts. It helps designers to design parts quickly and visualize their designs. Current CAD software are tailored to design parts which are manufactured using current manufacturing processes, namely subtractive manufacturing and molding.

Design for AM brings changes how parts are designed. Additive manufacturing parts have different forms compared to ones manufactured with traditional manufacturing processes. Parts designed for current manufacturing processes consist mainly of volumes bounded by a limited number of surfaces due to the limits of these processes. Whereas parts designed for additive manufacturing consists of solid, hollow, and lattice structures thanks to the capability to create complex forms in obtaining lightweight high strength structures. However, parts containing lattice structures result in larger surface numbers and area than classic ones. Thus, increasing the amount of data that the CAD, CAE and CAM software must process during the various stages of the numerical chain.

This paper focuses on evaluating the performances of current CAD tools in processing and designing lattice structures in terms of human machine interface, CAD file formats, CAE and CAM for additive manufacturing. The results will serve as a basis for future modifications of CAD tools in the context of design for additive manufacturing.

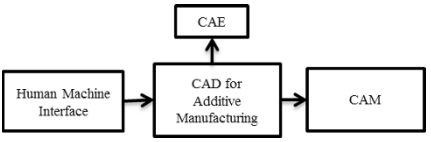

Figure 2: Evaluating CAD tools in the context of design for additive manufacturing

2- Literature Review

2.1 – Additive Manufacturing

Additive manufacturing has many advantages compared to conventional manufacturing processes. For example, the ability to manufacture complex forms and shapes [VV1] [VV2] [R]. This capability gives a whole new freedom for designers when designing the parts. Thus helping engineers to produce lightweight structures [VV1] [VV2] and improve the functionality of components [CS1]. For example, to improve the fluid flow in hydraulic systems. It is also possible to produce graded materials [R1] [RP1]. Additive manufacturing enables the use of titanium alloys and cobalt chromium instead of conventional materials [VV1].

AM is no longer limited to plastic parts and are applicable to produce technical components and not just prototypes [RT1].It is possible to directly manufacture end parts [VV2]. Other advantages of AM are the ability to create hollow parts [RP1] and eradicate the need of molds during the manufacturing process [CS1]. Thus complex designs does not necessarily contribute to an exponentially increase in costs [CS1]. Tests in the most demanding conditions have been done on AM produced parts [CS1]. Parts produced by Direct Metal Laser Sintering (DMLS) show that this technology is reliable in consistently producing accurate dimensions and also in meeting the mechanical criteria's needed [CS1]. Therefore, it provides users the confidence to use this technology to obtain mechanical and geometrical properties that match those of traditional manufacturing processes. AM is beneficial for industries where constant upgrading and improvements of components in small quantities are needed. For example in motorsports such as Formula 1 where redesigns of parts are done repeatedly to enhance performances [CS1].

However, AM does have its constraints and disadvantages. Supports are needed to dissipate heat during the building process and also avoid overhanging surfaces from collapsing [VV1] [VV2]. There is also the need to remove un-molten powder from the build after the process [VV1] and a potential need for post surface-treatment if needed for functional surfaces [CS1].

2.2- Design for Additive Manufacturing

Current design methods are not tailored to optimize AM [VV1]. The advantages of AM will only be reached and optimized to its maximum if the designing methodology is specifically tailored for AM. The challenge is now for designers to be innovative in the design methodology to achieve this objective [CS1]. Some research has been done to improve the designing methodology for AM [R1] and new design methods have been proposed [VV1]. These methods will be a platform for this research and further work will be done to improve this methodology in order to reach further objectives.

As stated in the previous paragraphs, lattice structures are an important element in design for additive manufacturing parts. Lattice structures can be divided into 2 categories: Foams or stochastic structures and periodic structures. The concept of designed cellular materials is aimed to put material only where it is needed for a specific application [R1].

A key advantage offered by cellular materials is high strength [GA1] accompanied by a relatively low mass [R1]. Besides that, the use of cellular structures in parts has other benefits such as heat dissipation [EH1], vibration control [EH1], energy absorption [EH1] [GA1], and good acoustic insulation [GA1]. It is possible to include variable porosity and variable composition (graded materials) in parts with cellular structures [RP1].

Periodic structures have significantly higher strengths than foams and stochastic structures [R1]. Therefore, to maximize the stiffness of parts, this research will only focus on applying periodic structures in the design methodology for additive manufacturing. There are many types of periodic lattice structure patterns such as octet truss, square and rectangular lattice structures. Research has also shown that the strength of the part increases when the bars of the lattice structures are oriented along the flux of force of the part [RT1]. These principals can be found in nature such as cancellous bones [RT1].

2.3 – CAD Tools for Additive Manufacturing

New CAD tools are needed in order to take full advantage of AM capabilities. Many researchers said they see the lack of capable CAD tools as a limit for their research and for the utilization of AM technologies for manufacturing applications in production [R1]. It may require a change in the numerical chain so that AM can be used at its full potential by designers [VV1]. AM requires 3D CAD model of each part, which are then sliced into very thin slices in one direction in CAM software to generate cross section profiles [BA1]. These cross section profiles are exported directly to the additive manufacturing machine to be manufactured layer by layer.

Today, there are no specific CAD tools to design parts for additive manufacturing and especially for parts made of lattice structures. The numerical chain for additive manufacturing parts is still the similar to conventional subtractive manufacturing parts.

3- Evaluating Current CAD Tools in Designing Cellular Structures for AM in CAD

Lattice structure is an important element in designing for additive manufacturing parts. Therefore, there is a need to draw and design parts containing lattice structures quickly and easily in CAD tools. This study case aims at evaluating current CAD tools' performances in the context of design for additive manufacturing, specifically to design lattice structures.

The criteria chosen to evaluate these performances are:

1. Total number of operations needed to design the basic lattice structure pattern.
2. Total time to design a lattice structure
3. Time taken by the CAD software to apply and generate a repetition function.
4. CAD file sizes
5. RAM usage in CAE and CAM software.

These criteria are used to evaluate the performances of current CAD tools in terms of human machine interface, CAD, CAE and CAM for additive manufacturing.

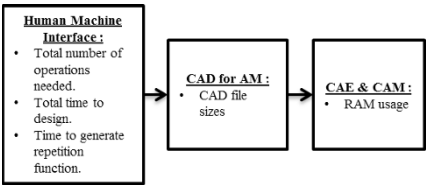

Figure 3 : The roles of each criterion in evaluating CAD tools for additive manufacturing

The computer used to make this experiment has the following specifications:

1. Windows 7 Professional 64 bits
2. Intel® Processor Core i7-3540M CPU @ 3.00 GHz
3. 8 Gb RAM
4. 500GB hard disc

Three variables have been chosen for the experiment:

1. Dimensions and volumes of the parts
2. Lattice structure patterns
3. Section of the bars of the lattice structures

Two lattice structure patterns were chosen to see how the software handles during the design of simple lattice structures and also for more complicated lattice structure patterns such as an octet truss.

1. Octet-truss lattice structures
2. Square lattice structures

Below is an example of a square lattice structure in a CAD software and the end product which was manufactured by an additive manufacturing machine:

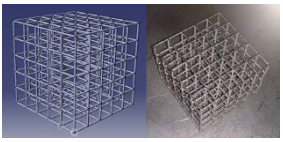

Figure 4: Square Lattice Structures in CAD software and the end product

The bars of the lattice structures were designed with 2 different sections to see if it made any differences in designing the parts and to the performance of the CAD software:

1. Square section
2. Circle section

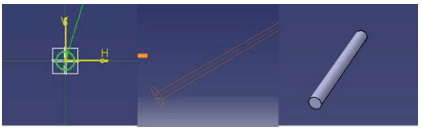

Figure 5: Circle Section Bars of Lattice Structures

Four part dimensions were chosen to see how the software adapts for different size parts. These volumes were chosen to see the gradual effects of volume sizes on the performance of the CAD software. The maximum dimension chosen is 20cm x 20cm x 20cm, which is approximately the maximum dimension that can be built in current additive manufacturing machines. The 4 dimensions and volumes are:

1. 5cm x 5cm x 5cm (volume : 125cm²)
2. 10cm x 10cm x 10cm (volume : 1000cm²)
3. 15cm x 15cm x 15cm (volume : 3375 cm²)
4. 20cm x 20cm x 20cm (volume: 8000cm²)

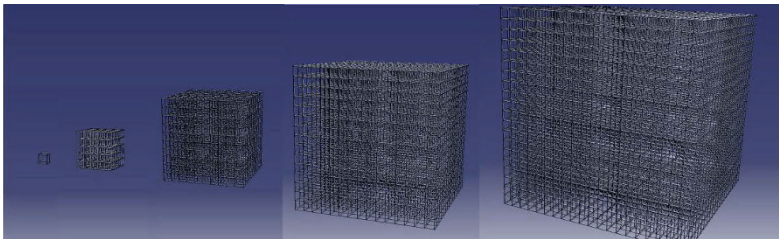

Figure 6: Different Lattice Structure Dimensions

The figure above shows an example of each dimension and volume.

3.1 – Human Machine Interface

The objective of this section is to observe the challenges experienced by the user when designing lattice structures in CAD software. The software used in this experiment is CATIA. A total of 19 different parts with the different variables stated above were designed in CAD software. Each operation and difficulties were observed and noted. Below is an example of some of the steps to design a 10mm x 10mm x 10mm octet truss lattice structure.

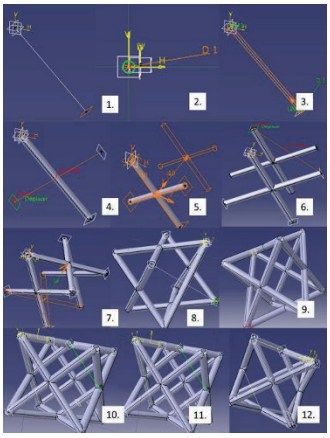

Figure 7: Creating a basic 10mm x10mm x 10mm octet truss lattice structure with circle section bars

Making up this structure elementary feature in a classical CAD environment require not less than 91 operations. Some of these are illustrated in fig. 7:

1. Creating a new plane
2. Drawing a circle in the sketch to form the section of the bar.
3. Extruding the circle to form the bar
4. Creating a new plane to draw the circle section bars
5. Repeating function to generate symmetrical bars.
6. Creating a new plane.
7. Applying the repeat function to generate symmetrical bars.
8. Creating a new plane
9. Applying the extrude function to generate a new bar.
10. Creating a new plane.
11. Applying the extrude function to create a new bar.

These are just some of the operations done to create the elementary feature. Making the 10mm x10mm x 10 mm lattice structure requires 91 operations, consisting of:

1. 35 operations to create a sketch
2. 21 extruding operations
3. 3 rectangular repetition operations
4. 25 operations to define a new plane
5. 7 operations to define a new point

The total time needed to create this 10mm x 10mm x 10mm octet truss lattice structure is 1 hour and 35 minutes. As described in this section, the basic 10mm x 10mm x 10mm lattice structure had to be designed manually step by step and must be represented graphically to obtain the lattice structure pattern in the CAD software. The method is time consuming because the lattice structures have to be represented and designed from scratch. There are no special functions to automatically generate desired lattice structures in current CAD software. Functions which can define and create immediately a lattice structure without having to create it manually step-by-step. This shows that current CAD software are not capable to design lattice structures easily and quickly.

To create a 50mm x 50mm x 50mm lattice structure, the next step is to apply:

1. Rectangular repetition function along the XY plane with a spacing of 1cm and 5 instances to obtain a 5cm x 5cm part dimension.
2. Rectangular repetitions function along XZ plane to obtain a 5cm x5cm x 5cm structure.

The same repetition procedure was done to obtain other dimensions and volumes. For example, 10cm x10cm x10cm, 15cm x 15cm x 15cm, and 20cm x 20cm x 20 cm lattice structures. The figure below shows these two steps of

rectangular repetition to obtain the final desired volume.

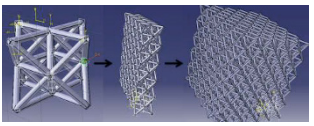

Figure 8: 1st and 2nd repetition from basic 1cm x1cm x 1cm structure to obtain a 5cm x 5cm x 5cm size octet truss lattice structure

The performance of the CAD software when processing certain operations was also examined. The objective is to observe the performance of the software in doing these operations for the 8 cases studied. The time taken to apply the first and second repetitions of the basic lattice structure was used as a criterion to evaluate this performance.

Each of the 1st and 2nd rectangular repetition operation was repeated 3 times during the study to obtain an average time and more reliable results. The table and graph below shows the time taken by the CAD software to accomplish these operations for each part.

Bars Section Forms		Square		Circle	
Repetition		1st	2nd	1st	2nd
Lattice Structure	Dimension (cm)	Average Time (s)	Average Time (s)	Average Time (s)	Average Time (s)
Square	5x5x5	3.8	15.8	24.5	55.0
	10x10x10	19.7	23.7	47.5	137.7
	15x15x15	47.8	90.3	148.7	489.7
	20x20x20	125.9	297.0	261.7	1181.0
Octet Truss	5x5x5	23.9	76.7	34.8	107.1
	10x10x10	103.9	1843.0	88.5	1066.0
	15x15x15	293.3	N/A	401.7	N/A
	20x20x20	770.3	N/A	842.0	N /A

Table 1: Average time to generate 1st and 2nd repetition

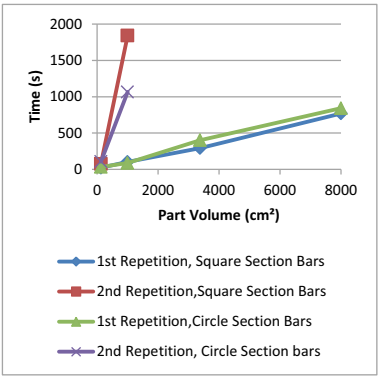

Figure 9: Time taken to apply 1st and 2nd repetition for Square Lattice Structures

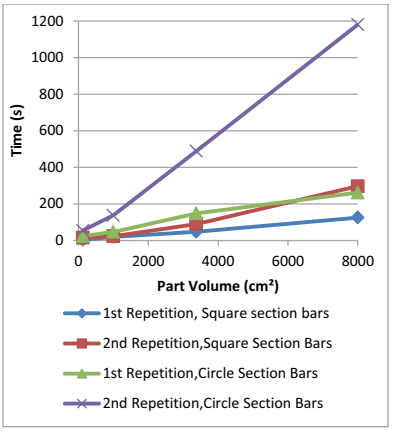

Figure 10: Time taken to apply 1st and 2nd repetition for Octet Truss Lattice Structures

The time that the CAD software needed to generate and execute the repetition function increases linearly when the volume of the parts increases. The CAD software took a long time to generate the repetition function when the volume became big. These operations were time consuming for large volume parts. An octet truss lattice structure took considerably more time than a square lattice structure when applying the repetition function due to the larger surface area and number compared to square lattice structures.

When applying the second repetition function for the parts starting from 15cm x 15cm x 15 cm dimensions, the software could no longer handle the repetition function successfully, even after waiting more than three hours, the RAM used by the CAD software reached 2.292 GB and the software had to be restarted. The software did not respond and had to be restarted. The CAD software and the computer were not capable of generating the 2nd repetition function for these volumes. The 15cm x15cm x 15cm and 20cm x 20cm x 20cm octet truss lattice structures could not be generated by the CAD software.

3.2 – CAD File Sizes

The second result examined is the size of the CAD files for each part when exported to different CAD file formats. The objective is to find out the effects of the type and size of lattice structure on file sizes and whether current file formats are suitable for the requirements of additive manufacturing.

The parts were exported and saved in the CAD software to different file formats such as IGES, STL and STEP. These are common file formats used to import parts in CAM and CEA softwar. Below are the CAD file sizes of the lattice structures for each variable:

Section Forms		Size (cm)	Square Section Bars			Circle Section Bars		
			File Size (mb)					
			IGES	STL	STEP	IGES	STL	STEP
Lattice Structure Type	Square	1x1x1	0.06	0.03	0.04	0.17	0.12	0.08
		5x5x5	3.79	1.89	2.20	6.30	5.51	3.27
		10x10x10	27.94	14.07	17.13	44.12	23.60	38.21
		15x15x15	91.67	46.37	57.57	142.9	122.6	77.14
		20x20x20	214.2	108.6	N/A	N/A	283.4	181.6
	Octet Truss	1x1x1	0.4	0.2	0.2	0.5	0.4	0.3
		5x5x5	29.9	14.9	20.4	42.3	36.4	23.4
		10x10x10	228.1	114.0	161.9	N/A	280.4	67.0
		15x15x15	N/A	N/A	N/A	N/A	N/A	N/A
		20x20x20	N/A	N/A	N/A	N/A	N/A	N/A

Table 2: File Size of Square Lattice Structures

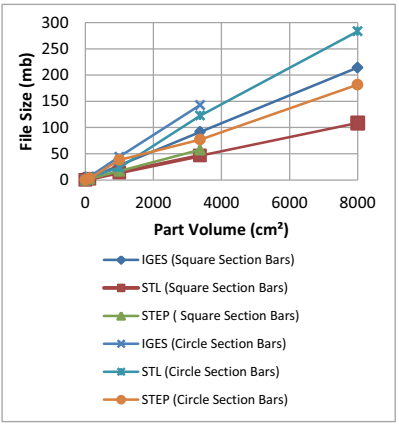

Figure 11: CAD file sizes for Square Lattice Structure

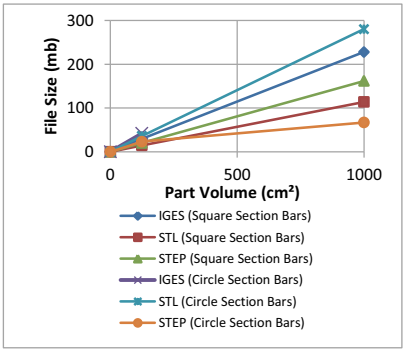

Figure 12: CAD File Size for Octet Truss Lattice Structures

Each file format has different file sizes for the same part. This is because each format is written in a different way. The files sizes depend of how the information of the part is interpreted and written. Each format saves the information differently. The IGES, STL and STEP format generated large file sizes for lattice structures parts. For example, an STL file for 10cm x 10cm x 10cm octet truss reached 280.4mb. This shows that current file formats generate large file sizes and are not suitable to store information of lattice structure parts. For example, STL format generates and stores information on triangular meshes of the surface area of the part. Therefore, when the parts contain large surface areas, the file increases heavily. Currently, there is not yet a file format which can describe lattice structure patterns and dimensions with a minimum set of information. For example, describing the basic elementary structure and repetition should be enough.

3.3 – RAM Usage

The RAM used by the computer to import and load the files in CAD, CAM and FEA software was examined and noted. The objective is to find out whether the files generated could be loaded in CAE and CAM software or if errors occurred. Below are the results:

Section Forms		Size (cm)	Square Section Bars			Circle Section Bars		
			CATIA	MAGICS	ANSYS	CATIA	MAGICS	ANSYS
Lattice Structure Type	Square	1x1x1	260.4	47.9	411.5	260.9	103.6	150.5
		5x5x5	265.7	50.3	430.5	273.5	108.6	196.7
		10x10x10	323.1	70.8	498.4	329.6	132.4	739.5
		15x15x15	498.0	117.2	N/A	513.0	199.8	2347.9
		20x20x20	830.4	209.6	N/A	816.8	389.7	N/A
	Octet Truss	1x1x1	219.4	54.8	148.0	250.8	135.5	147.7
		5x5x5	305.5	78.8	487.4	300.1	162.1	542.4
		10x10x10	882.5	218.3	N/A	712.6	404.4	N/A
		15x15x15	N/A	N/A	N/A	N/A	N/A	N/A
		20x20x20	N/A	N/A	N/A	N/A	N/A	N/A

Table 3: RAM used by software during importing the parts into the software

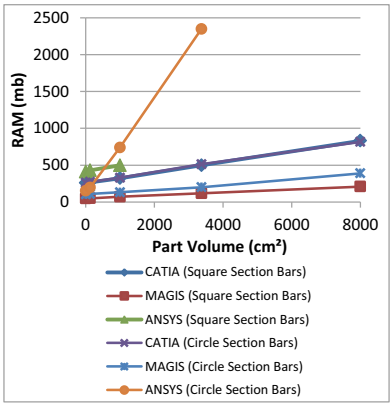

Figure 13: RAM used by software during importing square lattice structure parts in the software

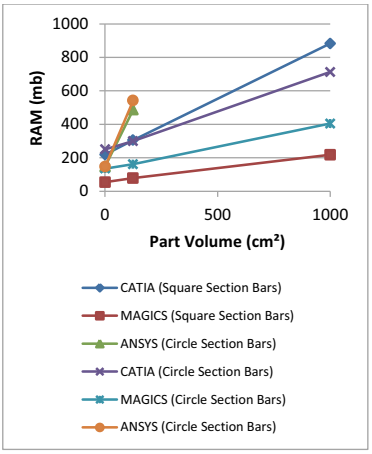

Figure 14: RAM used by software during importing octet truss lattice structure parts in the software

5 STL files of the parts could not be loaded in ANSYS. When loading the part into the software, the computer indicated nearly 4 GB of RAM was used by the software. It eventually failed to load the part into the software. This showed that for large size STL files and lattice structure parts, the CAE software is not capable of processing the information and even loading the part into the software. Large surface areas of the part contributed to high quantity of information to be processed by the software.

From this study case, it was evident that current CAD softwares and files formats are not adapted to design and store lattice structure parts efficiently and was not suited to process the parts in CAD, CAE and CAM softwares. The results showed that it was difficult to design, time consuming, generated large file sizes, high RAM consumption, and very heavy for the software and computer to handle. In certain cases, the softwares were unable to achieve the desired operation.

The patterns of the cellular structures had to be drawn one by one and then the repetition function was used till the desired structure was achieved. For large volumes, the parts became heavy for the computer to manipulate in CAD, CAE and CAM software. This is due to the large surface area and number the lattice structure requires and that the software has to process. These problems made it not practical for users to design usual cellular structures quickly and efficiently. Consequently making the process time consuming.

5- Conclusion on Current Problems and Difficulty of Designing Cellular Structures in CAD softwares

From this research, it can be concluded that current CAD softwares are not practical for users to design usual cellular structures efficiently for additive manufacturing parts. There are two ways to overcome this problem. The first would be to create a CAD application to quickly design a cellular structure in CAD softwares, or the other would be to create a cellular structure part without even representing it graphically in the CAD software. This would be possible by creating a new file format which interprets information of the part as lattice structures. Making it easier to process lattice structures in the CAD software.

New requirements in part designs for additive manufacturing results in new needs for computer-aided design. Current CAD software are not tailored for these new requirements. Actual file formats are insufficient to answer to these new needs for AM and has to be replaced. Product designs, CAD, FEA and CAM requirements are taken into consideration for the creation on a new CAD file format. A new research has to be done to find out how to design quickly and easily lattice structures in CAD software and to create a suitable new CAD file format for data representation for CAD, FEA and CAM for additive manufacturing needs.

7- References

[BA1] Brackett D, Ashcroft A, Hague R. Topology Optimization for Additive Manufacturing. 2011

[CS1] Cooper D.E., Stanford M, Kibble K. A., Gibbons G. J. Additive Manufacturing for Product Improvement at Red Bull Technology. In Journal of Materials and Design 41, 226-230, 2012.

[EH1] Evans A.G, Hutchinson JW, Fleck N. A, Ashby M.F, Wadley H.N.G. The Topological design of multifunctional cellular metals. Progress in Materials Science 46, 309-327, 2001.

[GA1] Gibson L. J., Ashby M. A., Cellular Solids: Structure and Properties: Second Edition, 1999.

[R1] Rosen D.W. Computer-Aided-Design for Additive Manufacturing of Cellular Structures. In Journal of Computer-Aided-Design & Applications. Vol. 4 No. 5,585-594, 2007.

[RP1] Rochus P., Plesseria J.-Y., Van Elsen M. Kruth J.-P., Carrus R. Dormal T. New Applications of Rapid Prototyping and Rapid Manufacturing (RP/RM) technologies for space instrumentation. In Journal of Acta Astronautica 61, 352-359, 2007.

[RT1] Reinhart G, Teufelhart S. Load-Adapted Design of Generative Manufactured Lattice Structures. Physics Procedia 12,385-392, 2011.

[VV1] Vayre B., Vignat F. and Villeneuve F. Designing for Additive Manufacturing. 45th CIRP Conference on Manufacturing Systems 2012.

[VV2] Vayre B., Vignat F. and Villeneuve F. Metallic additive manufacturing: state-of-the-art review and prospects. In Journal of Mechanics & Industry 13,89-96,2012.

Article 047_pp_paper_15

Influence of the tool-material couple on the dental CAD CAM prosthetic roughness

N. LEBON [1], L. TAPIE [2], E. VENNAT [3], B. MAWUSSI [4], JP. ATTAL [5]

(1,2,4,5) Department of Biomaterials, URB2I-EA 4462, Faculty of Dental Surgery, Paris-Descartes University, 1, rue Maurice Arnoux, 92120 Montrouge, France
33 (0)1 58 07 67 25 / 33 (0)1 58 07 67 25
E-mail 1: lebon@iutsd.univ-paris13.fr
E-mail 2: laurent.tapie@univ-paris13.fr
E-mail 4: mawussi@univ-paris13.fr
E-mail 5: jean-pierre.attal@parisdescartes.fr

(3) Laboratoire Mécanique des Sols, Structures et Matériaux-UMR 8579, Ecole Centrale Paris, Grande Voie des Vignes, 92295 Chatenay Malabry Cedex, France
33 (0) 1 41 13 16 58
E-mail : elsa.vennat@ecp.fr

Abstract: This study aims at investigating the tool-material couple in CAD/CAM dental machining. The tool-material couple is studied through the observation of milled surface roughness and tool geometrical properties. The influence of two tool-material couple parameters is also studied: the feedrate and the milling mode (flank, top).
Three diamond burs and three dental biomaterials (ceramic, polymer, hybrid) were tested.
The surface roughness was observed for nine tool-material couples in flank and top milling. Ra, Rt, Rz, Sa, Sq, Sz roughness criteria were measured.
It has been concluded that in flank milling the measured surface roughness is in direct proportion to the diamond tool grain size. In top milling, the roughness is mainly due to the diamond grain size, and the radial depth is not a predominant parameter. The surface roughness was influenced by material hardness in flank milling mode. Moreover, the surface roughness was not affected by the feedrate.

Key words: roughness, dental materials, surface integrity, tool-material couple, milling.

1-Introduction

Computer science has been largely democratized during the last past forty years, and computers are becoming more and more powerful. So, it has become usual to find a full digital Design and Computer Aided Manufacturing (CAD/CAM) process to manufacture dental restorations. Van Noort even says: "the future of dental dentistry is digital" [V1]. On the first hand, CAD/CAM machining is essential at this stage of the dental restoration production process and largely determines the surface integrity properties of dental restoration. These surface integrity properties must be suitable to meet the clinical requirements for the restoration life time. And on the other hand, the economical aspect of the dental restoration production chain is closely linked with the restoration milling time. The main properties for a dental restoration expected by practitioners and patients are: aesthetics [DA1], biocompatibility [BF1], low dental plaque retaining [S1], good adhesion [H1] and restoration lifetime [HP1]. To meet these requirements, several classes of materials are proposed on the marketplace such as ceramics, composites or hybrids [DB1][ZM1]. Unfortunately, few data can be found about their properties after milling. These prosthetic material milling properties can influence the tool-material couple [AF1][VJ1][NL1]. Another important economic model criterion is the restoration machining time. This machining time is closely linked with the tool feedrate and the milling mode used to cover the restoration surface. Thus, the main difficulty is to find the tool-material couple parameters (such as tool feedrate and milling mode, tool and prosthetic materials) which have the greatest influence on the prosthesis surface integrity parameters (such as roughness), without devaluated the economic model parameters, (such as machining time).
Roughness is a major surface integrity parameter in restorative dentistry. Indeed, the dental plaque retaining [BL1], aesthetic [HF1][MS1], and retention [T1][LW1] are linked to the surface roughness. Therefore, all these

interactions will be studied in this article.

2-Context and problematic

When milling a dental restoration, in a CAD/CAM system, several steps are necessary (Fig1). First, a CAD model (geometry and surface integrity) is designed and defined by the practitioner (Fig1). Then, the tool path is automatically generated (Fig1). Actually, in dental CAM software, only parallel plans are usually used to generate the 3-axis tool path. Consequently, the tool-workpiece contact direction is defined by the generated tool path. The occlusal and marginal surfaces are mainly machined by top milling (red areas on Fig1). Top milling uses mainly the half ball area at top of the bur to manufacture the surface (Fig2b). And axial surfaces are mainly machined by flank milling (blue areas on Fig1). At the contrary, flank milling uses mainly the peripheral area of the bur to manufacture the surface (Fig2a). Surface integrity, and more especially roughness, is influenced by this tool-workpiece contact direction. Unfortunately, a difference can be noticed between the expected and the real surface integrity. And the life time restoration can be affected.

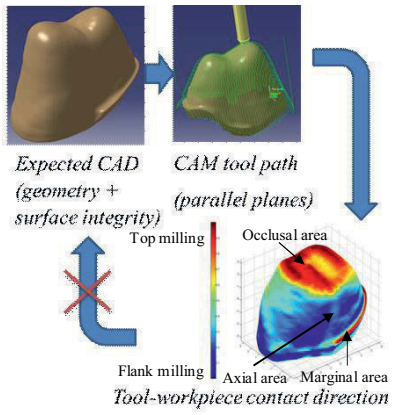

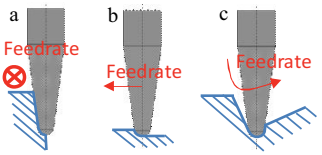

Figure 2: Milling modes.
a. Flank milling mode
b. Top milling mode
c. Mixed (top and flank) milling mode

3-Materials and methods

All the machining tests have been made on a four axis (X, Y, Z, A) milling center. The milling machine is a prototype for dental applications (GACD-LYRA group, Paris, France).
The three machinable biomaterials that were used in this study are presented in table 1.
The three burs that were used in this study are presented in table 2.

Product	Manufacturer	Class of material	Code	Vickers hardness
Mark II	VITA Zahnfabrik Bad Säckingen, Germany	Fine particle feldspar ceramic	MK	640 Hv
Lava Ultimate	3M ESPE St Paul, Minnesota, USA	Resin nano-ceramic composite	LU	107.3 Hv
Enamic	VITA Zahnfabrik Bad Säckingen, Germany	Hybrid (resin infiltrated ceramic)	EN	254.9 Hv

Table 1: Materials used in the study

Then each nine couples were tested with four different feedrates (1000-2000-3000-4800 mm/min). The study was done with the milling parameters shown in Table 3.

Burs	Geometries	SEM observations
Lyra* conical bur Ø1mm (LY1)	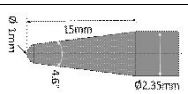	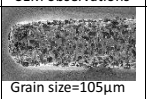 Grain size=105µm
Lyra conical bur Ø1.05mm (LY2)	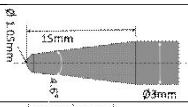	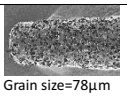 Grain size=78µm
Cerec** Cylinder pointed bur 12S (CER)	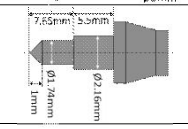	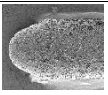 Grain size=43.5µm

Table 2: Tools geometry used in the study
* LYRA (GACD-LYRA group, Paris, France)
**CEREC (Sirona dental Systems GmbH Bensheim, Germany)

Material milled	LU / MK / EN
Bur speed	60000 RPM
Feedrate	1000-2000-3000-4800 mm/min
Coolant	Yes (Water+5%specific lubricant)
Milled surface area	5mm*15mm
FLANK milling mode	
Radial depth	0.5mm
Axial depth	5mm
Milling mode	Climb milling
TOP milling mode	
Radial step	0.03mm and 0.1mm
Axial depth	0.5mm
Milling mode	Climb and up-cut milling (time optimized zig-zag paths milling)

Table 3: Milling parameters

Each surface roughness (Ra, Rt, Rz, Sa, Sq, Sz) were measured, on a focal variation device (Alicona, Infinite Focus, Austria) [IS1] [IS2] [IS3] [IS4] [NF1].
Three profiles (average 1mm length) per sample were recorded in the middle of the milled surface, and then the mean and standard deviation were calculated. To avoid feedrate deceleration and acceleration disturbances, the both end of the milled surface were not used. The 3D roughness criteria were recorded on a 0.8mm*1mm surface. Three surfaces per sample were recorded and then the mean and standard deviation were calculated. According to the NF EN 623-4 standard, aberrant points were removed [NF1].

4-Results and discussion in flank milling mode

The 36 roughness measurements in flank milling are shown on the figures 3 to 5. With the three burs, the 2D and 3D roughness on the LU milled surface is higher than on the two others. (The LU 2D roughness is 18% to 68% higher than the MK; and the LU 3D roughness is 18% to 59% higher than the MK). The MK and EN roughness are similar. The 2D and 3D roughness criteria are in the same order of magnitude. Moreover, the EN and MK material roughness analysis depends on the roughness criteria chosen. In conclusion, the roughness is influenced by the milled dental material.
This is confirming Yin et al. show that roughness depends on manufactured material [YH1]. Yin et al. published that the surface roughness in high speed grinding is found to be material-dependent and that the ground silicon nitride exhibited much smoother than the other ground ceramics.

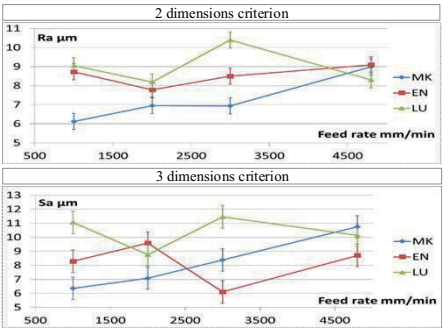

Figure 3: Roughness results when milling in flank with the LY1 bur at different feed rates (vertical bars represent SD)

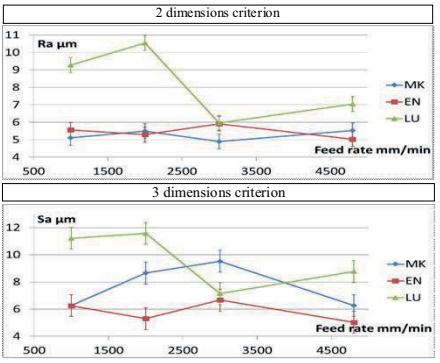

Figure 4: Roughness results when milling in flank with the LY2 bur at different feed rates (vertical bars represent SD)

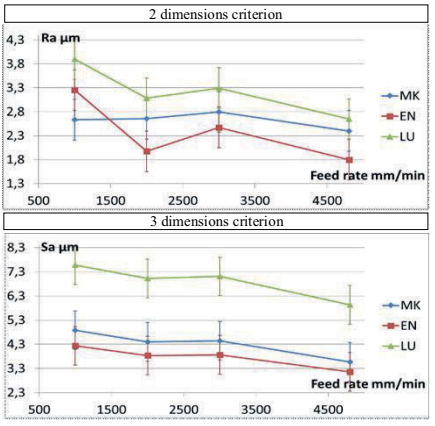

Figure 5: Roughness results when milling in flank with the CER bur at different feed rates (vertical bars represent SD)

It is also observed that material surface roughness (2D and 3D) is not influenced by the feedrate. The 2D roughness profiles overlay confirms this observation (figure 6). Actually, roughness fluctuations can mainly be due to uncertainty of roughness measurements.

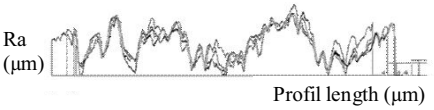

Figure 6: 2D roughness profils overlay EN-LY1 couple. Feedrates F1000-2000-3000-4800mm/min

When the MK material was flank milled by Yin et al. [YS1] and Song et al. [SY1], the roughness was not influenced by the feedrate. In these conditions higher feedrate seems to be a better solution to save manufacturing time, without deteriorating the roughness.

Then, relationship between roughness and Hv hardness was established (figure 7).

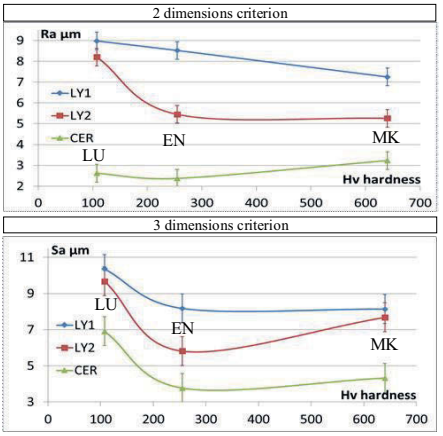

Figure 7: Correlation between roughness and Vickers hardness (vertical bars represent standard deviation)

The 2D and 3D roughness results depend on dental bur used. Higher roughness is obtained with the LY1 bur, and lower roughness with the CER bur on the same material. Nevertheless, the same trend was observed with the three burs. I.e. roughness criteria vary inversely up to a point, with the dental material Vickers hardness. Actually, Ra and Sa decrease while hardness evolve from 107.3Hv (LU) to 254.9Hv (EN). Afterwards, from 254.9Hv to 640Hv the roughness does not clearly depend on Vickers hardness, and a horizontal asymptote can be drawn. Two dental ceramics (feldspathic porcelain (MK, Hv=640) and yttria-stabilized tetragonal zirconia (Hv=1200-1400)) were investigated by Yin et al. [YJ1] using a dental handpiece and diamond burs. The measurement results show that, the roughness does not depend on milled material. This result is in accordance with our results. The materials hardness's tested by Yin et al. are higher than 254.9 Hv.

The milled surface observations (figures 8c and 8d) reveal continuous peaks and valleys parallels to the feedrate direction. This geometry is marked on the machined surface, by the bur diamond grains. On hard material, the roughness is lower, because bur bending is more important due to tool-material interaction/repulsion. It also depends on the dental material hardness, but it is possible up to a point.

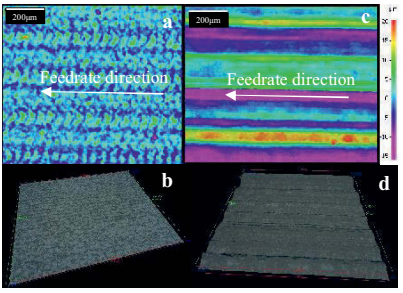

Figure 8: EN-LY2 couple milled surfaces at 1000mm/min
a. 2D view in top milling **b.** 3D view in top milling
c. 2D view in flank milling **d.** 3D view in flank milling

Then, the relationship between roughness and tool-material couple was established (figure 9). The LU milled surface roughness is higher. This result has already been observed previously. It has been shown that a quasi-linear relationship can be established between roughness and diamond tool size with all the tested dental materials. Some authors are agreeing to act, that, roughness is influenced by the diamond grain size [YJ1]. The roughness increases with the diamond grain size, but no evolution law was proposed. Our paper shows that, material roughness is in linear relationship with the diamond grain size.

Mathematical predictive modeling exists to evaluate the surface roughness on metallic material in grinding [HL1]. This modeling is quite difficult to use because a lot of coefficients have to be determined experimentally. Probabilities are used to estimate the diamond grain density on the bur. The results suggests that diamond grain size must be chosen in correlation with the expected surface roughness, and the dental material milled.

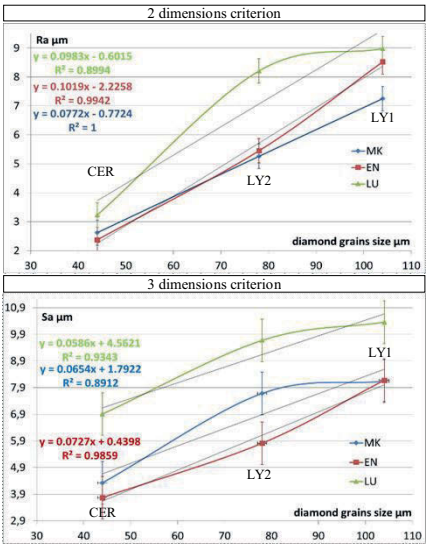

Figure 9: Correlation between roughness criteria and tool-material couple. (vertical bars represent standard deviation)

5-Preliminary results and discussion in top milling mode

Top milling tests with LY2 burs were performed. The top milled surface topology is given in figures 8a and 8b. This surface topology is the same at all feedrates. According to Lin et al. [LK1] and Grzesik [G1] the surface roughness milled with an end ball cutting bur, is given by the equations (1) and (2).

$$R_t = \frac{a_e^2}{8R} \quad (1)$$

$$R_a = \frac{a_e^2}{18\sqrt{3}R} \quad (2)$$

Where:
R_a is the average roughness of profile (mm)
R_t is the maximum peak to valley height of roughness profile (mm)
R is the tool radius (mm)
a_e is the radial step (mm)
In these theorical equations the roughness profile is modelled perpendicular to the feedrate direction.

2D and 3D roughness measurements (a_e=0.1mm) are given figure 10.

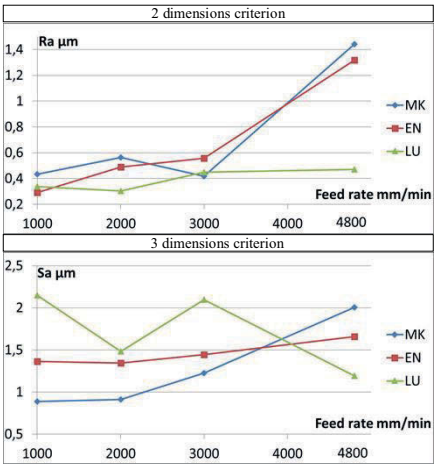

Figure 10: Roughness results when milling in top with the LYR2 bur at different feedrates. a_e=0.1mm

The roughness in top milling mode is also independent from the feedrate, excepted the 2D criteria which increase at 4800mm/min with MK and EN materials (the two hardest materials). 3D criteria are not affected by the feedrate. On the milled surfaces observations (figures 8a and 8b), no peak and valley can be noticed.
No significant roughness difference is observed between the three prosthetic materials. Unlike in flank milling mode, LU material has the same roughness as MK and EN materials in top milling mode.

The top and flank milling mode results are compared together (figure 11).

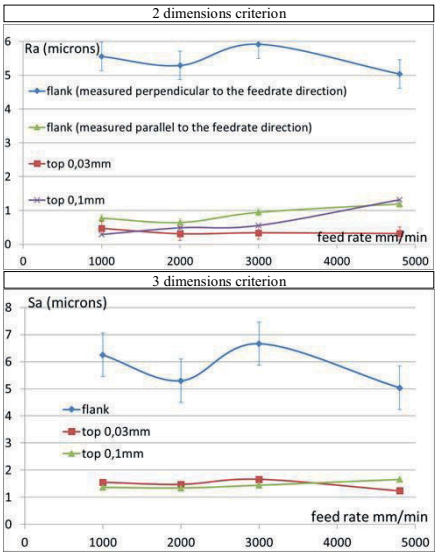

Figure 11: Roughness criteria with EN-LY2 couple in top and flank milling modes. (vertical bars represent standard deviation)

The top milling mode 2D roughness is lower than the flank milling mode 2D roughness when recorded perpendicular to the feedrate direction. But, the top milling mode 2D roughness and the flank milling mode 2D roughness when recorded in the feedrate direction are equal. So, top milling mode might be better for the roughness, but the milling time is higher for the same milled area.

Then the roughness obtained with a_e=0.03mm and a_e=0.1mm are compared together, and with the theoretical values. The 2D and 3D roughness criteria average values are equal for the two tested radial steps. The measured 2D values in top milling mode are higher than the theoretical values when a radial step of 0.03mm is used. The measured roughness agrees with the theoretical equations when a radial step of 0.1mm is used. So it has been concluded that the diamond grain effect on the 2D roughness is more important compared to the geometrical bur effect. Moreover, a higher radial step allows saving milling time, and does not devaluate significantly the CAD/CAM economic model. With the studied milling parameters, the milling time in top milling mode is 50 times higher than in flank milling mode with equal feedrate and with a_e=0.1mm. And milling time is 167 times higher than in flank milling mode with a_e=0.03mm.

6-Conclusion

This paper shows that the tool-material couple must be taken into account when milling dental biomaterial.
In the study conditions, the roughness in flank milling:

- Depends on the dental material milled. The roughness obtained was higher for the smoothest milled dental materials than for the hardest materials.
- Varies inversely with the dental material Vickers hardness, up to a point. After this point, the roughness does not depend on Vickers hardness.
- Depends on the bur used. The measured roughness is in direct proportion with the diamond tool grain size.

In top milling, the roughness is mainly due to the diamond grain size, and the radial depth is not a predominant parameter.

Moreover, in both milling modes the surface roughness was not affected by the feedrate. So, for a defined roughness, a higher feedrate will improve the economic CAD/CAM model.
The criteria (2D and 3D) fluctuate with the same trend.

The diamond bur grain size must be chosen in accordance to the dental material milled to be able to generate the desire roughness. For example, when an Enamic crown restoration is 3-axis machined, the dentist expectations are:

- coarse surface roughness on the intrados shape (better adhesion on axial areas)
- smooth surface roughness on the extrados shape (better aesthetic and customer's feeling of comfort, less dental plaque retaining).

The intrados will be milled in flank with a LY1 bur at 4800mm/min. The extrados occlusal areas will be milled with a LY2 bur in top milling at 3000mm/min. The extrados axial areas will be milled in flank with a CER bur at 4800mm/min.

7-Acknowledgements

This work has benefited from the financial support of the LabeX LaSIPS (ANR-10-LABX-0040-LaSIPS) managed by the French National Research Agency under the "Investissements d'avenir" program (n°ANR-11-IDEX-0003-02).

REFERENCES

[AF1] NF E 66-520 – 1 to 8. Working zones of cutting tools – Couple tool-material, AFNOR, 1997

[BF1] Bertoluzza A., Fagnano C., Monti P., Simoni R., Tinti A., Tosi MR., and Caramazza R. Raman spectroscopy in the study of biocompatibility. In Clinical materials, 9(1): 49-68, 1992

[BL1] Bollen CML., Lambrechts P. and, Quirynen M. Comparison of surface roughness of oral hard materials to the threshold surface roughness for bacterial plaque retention: A review of the literature. In Dental materials, 13(4): 258–269, 1997

[DA1] Davis LG., Ashworth PD., and Spriggs LS. Psychological effects of aesthetic dental treatment. In Journal of dentistry, 26(7): 547-554, 1998

[DB1] Dirxen C., Blunck U., and Preissner S. Clinical Performance of a New Biomimetic Double Network Material. In The Open Dentistry Journal, 7: 118-122, 2013

[G1] Grzesik W. A revised model for predicting surface roughness in turning. In Wear, 194(1): 143-148, 1996

[H1] Heintze SD. Crown pull-off test (crown retention test) to evaluate the bonding effectiveness of luting agents. In Dental Materials, 26(3): 193-206, 2010

[HF1] Heintze S., Forjanic M., and Rousson V. Surface roughness and gloss of dental materials as a function of force and polishing time in vitro. In Dental Materials, 22(2): 146–165, 2005

[HP1] Hickel R., Peschke A., Tyas M., Mjör I., Bayne S., Peters M., Hiller KA., Randall R., Vanherle G., Heintze SD. FDI World Dental Federation: clinical criteria for the evaluation of direct and indirect restorations—update and clinical examples. In Journal of Clinical Oral Investigations, 14(4):349-366, 2010

[IS1] ISO-4287. Geometrical Product Specifications (GPS) - Surface texture: profile method - Terms, definitions and surface texture parameters, 1997

[IS2] ISO-4288. Geometrical product specifications (GPS). Surface texture: profile method. Rules and procedures for the assessment of surface texture, 1998

[IS3] ISO-12085. Geometrical Product Specifications (GPS) - Surface texture: profile method - Motif parameters, 1998

[IS4] ISO-25178. Geometrical product specifications (GPS) - Surface texture: Areal, 2012

[LH1] Luthardt R., Holzhuter M., Rudolph H., Herold V., and Walter M. Cad/Cam-machining effects on Y-TZP zirconia. In Dental Materials, 20(7): 655–662, 2004

[LK1] Lin RS., Koren Y. Efficient Tool-Path Planning for Machining Free-Form Surfaces. In Transactions of the ASME, 118: 20-28, 1996

[LW1] Li YQ., Wang H., Wang YJ., and Chen JH. Effect of different grit sizes of diamond rotary instruments for tooth preparation on the retention and adaptation of complete coverage restorations. In The Journal of Prosthetic Dentistry, 107(2): 86-93, 2012

[MS1] Mormann WH., Stawarczyk B., Ender A., Sener B., Attin T., and Mehl A. Wear characteristics of current aesthetic dental restorative CAD/CAM materials: Two-body wear, gloss retention, roughness and Martens hardness. Journal of the Mechanical Behavior of Biomedical Materials, 20: 113-125, 2013

[NF1] NF-EN-623-4. Advanced technical ceramics - Monolithic ceramics - General and textural properties - Part 4: guidance on the determination of surface roughness. AFNOR, 2005

[NL1] Nouari M., List G., Girot F., and Coupard D. Experimental analysis and optimization of tool wear in dry machining of aluminium alloys. In Wear, 255(7-12): 1359–1368, 2003

[S1] Sorensen JA. A rationale for comparison of plaque retaining properties of crown systems. In The Journal of Prosthetic Dentistry, 62(3): 264–269, 1989

[SY1] Song XF., Yin L., Han YG., Wang H. Micro-fine finishing of a feldspar porcelain for dental prostheses. In Medical Engineering & Physics, 30(7): 856–864, 2008

[T1] Tuntiprawon M. Effect of tooth surface roughness on marginal seating and retention of complete metal crowns. In The Journal of Prosthetic Dentistry, 81(2): 142-147, 1999

[V1] Van Noort R. The future of dental devices is digital. In Dental materials, 28(1): 3–12, 2012

[VJ1] Vleugels J., Jacobs P., Kruth JP., Vanherck P., Du Mong W., and Van Der Biest O. Machining of steel with sialon ceramics: influence of ceramic and workpiece composition on tool wear. In Wear, 189(1-2): 32-44, 1995

[YH1] Yin L., Huang H. Ceramic response to high speed grinding. In Machining Science and Technology, 8: 21–37, 2007

[YJ1] Yin L, Jahanmir S, Ives LK. Abrasive machining of porcelain and zirconia with a dental handpiece. In Wear, 255(7): 975–989, 2003

[YS1] Yin L., Song XF., Qu SF., Han YG., Wang H. Surface integrity and removal mechanism in simulated dental finishing of a feldspathic porcelain. In Journal of Biomedical Materials Research Part B: Applied Biomaterials, 79B(2): 365-378, 2006

[ZM1] Zimmermann M., Mehl A., and Reich S. New CAD/CAM materials and blocks for chairside procedures. In International Journal of Computerized Dentistry, 16: 173-181, 2013

5

Innovation in Product Engineering

Major topics of the full argumentations are the following:

X. Fischer et al. (eds.), *Research in Interactive Design (Vol. 4)*
DOI 10.1007/978-3-319-26121-8_15

Article 034-i-53

AN APPROACH FOR DEFINING A COLLABORATIVE PLATFORM TO SUPPORT THE DEVELOPMENT OF CORPORATE ENGINEERING STANDARDS

Rachad El-Badawi-El-Najjar [1,2], Guy Prudhomme [1], Franck Pourroy [1], Nicolas Maussang-Detaille [2], Eric Blanco [1]

(1) : Grenoble-INP/UJF-Grenoble 1/CNRS, G-SCOP UMR5272, 46, avenue Felix Viallet, Grenoble, F-38031, France
Phone : +33-6-45-07-88-94
E-mail : {guy.prudhomme, franck.pourroy, eric.blanco}@g-scop.inpg.fr

(2) : Alstom Renewable Power – Hydro, 82 Avenue Léon Blum, 38041 Grenoble Cedex 9, France
Phone: +33-6-72-35-17-14
E-mail : {rachad.el-badawi-el-najjar, nicolas.maussang-detaille}@power.alstom.com

Abstract: In a global economy, the conquest of new markets has led many companies to expand their business around the globe. However, new challenges have aroused from this expansion. Our study field context is Alstom Hydro that designs and manufactures hydraulic turbines. Our research aims at studying and supporting the involvement of experts and future users in the co-creation of corporate engineering standards. The paper focuses on the collaborative platform development, more particularly on the approach we propose for specifying such a platform. Formalizing the standardization process stands as a key element of the approach, and we will explain, based on field studies and focus groups, how this was done within the company. Then, we will detail how this standardization process was used to define the collaborative platform, its main features, roles and privileges. Our findings are: a collaborative platform specification method and a collaborative standardization process.

Key words: Standards, standardization, collaborative platform, collaborative platform specification process.

1- Introduction

The globalization of the economy has led many industrial companies to explore new markets by merging or allying with local businesses. If these alliances allow benefiting directly from markets and local production tools, they highlight the necessity to integrate new product development teams, coming with their own rules and design practices, using different design tools (CAD, CAE...) or when they are identical, using them according to different approaches and conventions.

The rationalization of the development activities across a multinational firm is often considered as necessary for maintaining a high level of product performances and the same brand quality in all its operating markets. Nevertheless, this is a complex task and many difficulties arise when the product development teams have different cultures, different engineering methods, and different competencies. To overcome these difficulties, one of the work areas often pointed out is standardization, which tries to unify not only designed products and / or their components, but also the rules and design practices, tools and methods, regulatory frameworks, internal or external documents, such as those dedicated to suppliers for example. To reach this objective, each site has to progressively adopt common (corporate) working methods, similar product architectures, identical control tools, catalog parts, and common selection criteria.

'Standards are described in many businesses as well as in the scientific literature as codified knowledge, a strategic tool, and guides for innovation providing competitive advantage' [S]. As a result this standardization will first allow the simplification and the harmonization of various processes related to the product's design. Second, it will enable designers to integrate different competences and skills from different sites. And finally, it will allow a more comprehensive management of engineering activities, for example a relevant distribution of workloads at different sites.

A first challenge that arises when developing a technical standard is related to the fact that it requires the involvement of many experts and future users. Indeed, collaboration between practitioners is an enabling factor for any standardization process model. All of them are involved in similar engineering activities in the product development life cycle but implementing different reasoning, depending of habits, techniques, and culture of their country site. Engaging the practitioners in the definition and development of standards will facilitate the adoption of the standards and its utilization in future projects.

In the context of globalization, this standardization process has also to take into account the physical distance constraint. This second challenge is to enable dispersed members to work together and to collaborate asynchronously. With the

advent of Internet and communication technologies, new ways of collaboration offer robust opportunities to bring together people and knowledge. Collaborative tools are considered as a possible solution for supporting this collective and distant construction of common standards.

In such a global context, where experts from different sites have to work collaboratively at distance to co-define standards, our research question is to investigate whether or not a collaborative tool is capable of supporting standardization process between remote experts, and under which conditions.

The following section will present a literature review about the concepts of standard and standardization, existing standardization process and collaborative tool specification method. This will lead us to highlight a gap and to refine our research question. A case study in the Alstom Company will support a proposition of new models for these processes in section 3. We concluded in section 4 about the work we have to do to evaluate the functionality of such new models.

2- Literature Review

2.1 – Standards & Standardization

'Standards refer to documents, established by consensus and approved by a recognized body, which provides, for common and repeated use, rules, guidelines, or characteristics for activities or their results, aimed at the achievement of the optimum degree of order in a given context' [I]. Then standardization is the process of developing, implementing and evolving standards.

Standard passes through multiple states during its life span. According to Krechmer [K] 'standard life cycle has five stages: creation, customization, maintenance, availability, and withdrawal'. Another life highlights two key interrelated phases during a standard's life cycle: its development and its adoption [FV].

2.2 – Standardization Process Models

Standardization process models often take into consideration the two main phases of the standard lifecycle presented above. But other authors have different point of views, The 'most common steps in a standardization process are: Identify market need and build consistency, Consensus on requirements, Technical work, Approval process, Testing and implementation, Maintenance' [G]. 'In-company standardization began with essential forms of standardization such as unification, simplification and modularization in product design, processes and manufacturing' [P]. Usually, 'company standardization starts with an initiative to develop a standard and ends with its implementation. In order to describe it, an input-process-output model is proposed' [SD]. For example, see Figure 1.

Different actors participate in the standardization process. 'From both literature and practice it is known that involving

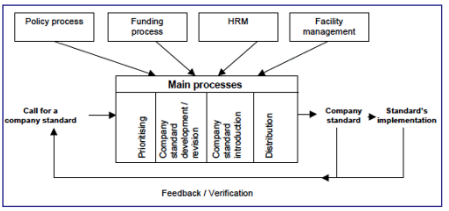

Figure 1: Company Standardization Model [SD]

the users in the standards development process have a positive influence on their actual usage' [SD].

In order to standardize in a distributed environment, collaboration is required in the development phase of the remote standards. 'Collaboration is a process where people work together for a common goal through knowledge sharing, consensus building, and teamwork among group members' [TT]. In this distributed environment, 'E-collaboration formulates a new working relationship in a virtual network space among members to achieve a common goal' [TT]. One possible solution to remotely standardize is to promote the collaboration between the engineers through collaborative tools.

Through this literature review, the presented standardization process models allow to define standards in a co-located environment. These models are generic and they define high level activities which don't give clear insights on how they will be implemented. The collaborative tools that are required to be associated to the execution of these standardization activities are then not clearly specified. In this paper, the approach will rely on collaborative platforms that are one possible type of collaborative tools to be used. Our first question is then to define a collaborative standardization process model that enables the geographically dispersed engineers to co-construct and co-define their standards using these collaborative platforms.

2.3 – Collaborative Platform

Collaborative platforms are classified as knowledge management systems. 'Broadly defined, knowledge management systems (KMS) are a class of information systems aimed at supporting and facilitating the codification, collection, integration, and dissemination of organizational knowledge' [A], [B]. Enterprises continue to invest in the underlying technologies of these information systems. They aim to establish a single entry point to find all product related information. The employees interact with the system on daily basis where they hope to find information related to their work quickly and with minimum guidance.

Such collaborative platforms are developed and configured by non-technical users. This configuration is done through the re-utilization of the components that are available in the development environment. They are supposed to provide intuitive experience and adapted functionalities to its user

requirements. A list of components is used to define the functionalities of a collaborative platform [C]:

- Content: the knowledge repository and articles published on the site.
- Discussion Forum functionality.
- Features: chat, news, e-newsletters, workshops, events, and web-conferencing.
- Tools and learning modules.
- Search functionality.
- Membership: Access to knowledge, tools, and collaboration by members and guests, how open this community was to outsiders, member directory.
- Topic Experts as well as Moderator capabilities for forum and content submissions.

It comes that most of the existing platforms offer a large set of functionalities to the user, but without a clear correlation with specific users' activities. Users are not guided to choose the optimal functionalities to perform their tasks. From our experience [BP] [D], there is a strong interest to associate functionalities to activities to help people to efficiently use the platform. Having a reduced and adapted set of functionalities to perform each standardization activity will help the practitioners to efficiently use the collaborative platform. They will be guided to achieve specific activities and through the different standardization activities to be carried out. Questions that arise are: how to construct this platform? What method should be followed to select this set of functionalities? How they will be organized to support the standardization process?

Specification method that present a collaborative approach to co-define the platform functionalities continues to stay uncultivated. 'As virtual teamwork involves collaboration between virtual groups, whose members work across time and location, their collaborations must be strengthened by communication technology. It is therefore important to incorporate multiple communication media and e-collaboration tools as it has been observed to yield more gratification with the process, more balanced levels of participation, and more desirable results in contrast to single communication means. However, methods of incorporating technology support for e-collaboration still remain a relatively unexplored field' [TT].

Many papers describe collaborative platforms for specific usage. For example, Lecet [L] proposes an implementation of a collaborative platform based on the social web 2.0 technologies. It supports the teacher's community who use a teaching method called MAETIC. Another collaborative platform is developed to support tutor's forum [SB]. 'It plays a vital role in facilitating engagement and professional development for teachers working at a distance'. However, the specification processes are not presented in these papers.

This literature review shows that: on one hand, the existing standardization processes are generic, expressed at a high granularity level, and don't take into consideration the physical distance constraint and the collaborative aspect; and on the other hand, the collaborative platform specification methods are rarely proposed and no paper takes into account the detailed standardization activities.

As a consequence, we refine our research question as follows: 1) which collaborative standardization process could enable the practitioners to collectively define their standards at distance? 2) How to select and organize the collaborative platform functionalities in order to support this distant standardization process? This will lead us to define the collaborative platform specification method. As a first step to answer to these questions, we conduct an empirical study in an industrial company named Alstom. We will present this study hereafter.

3- Research Method

To address the questions of the collaborative standardization process and the collaborative platform functionalities, first we went through a literature review to find out all related work to our problematic. We didn't find standardization models that are collaborative and can be implemented at distance. Second, as researchers, we decided to study the existing engineering practices about standardization. We participated to a face to face engineering workshop: the welded structure workshop. Observations were also gathered from several meetings gathering standardization managers as well as e-mails exchanged through the previous standard working team during distant exchanges. We had a close view to understand the standardization main objectives, identify discussion types, discuss different practices and identify main activities to build a standard. We obtained an informal standardization process model using scenarios, and then we modeled this standardization process using a functional language. The observed process model consisted of two main activities: the co-located development of standards and the remote discussions of standards via e-mail exchange. We made the assumption the new standardization process model should conserve the collaborative aspect due to the face-to-face meetings and overcome difficulties due to the distance factor related to the geographical dispersion of engineers. Third, we proposed a new collaborative standardization process that will enable distant engineer to co-define their standards. The new process will act as a guideline to define the collaborative platform functionalities. Fourth, we went through developing and configuring a collaborative platform to support the implementation of the new standardization activities. In other words, the platform functionalities are shaped to fit these activities and their contextual information. The proposed model and its platform are continuously discussed and updated. In fact, regular discussions are conducted with the standardization managers to get feedback of experience. Although the models worked fine in the context of Alstom Hydro, these models should be tested and validated in other contexts and industries.

4- Empirical Study: Alstom Hydro Context

This study has been realized in Alstom renewable power - hydro company. The distributed hydro business design different operating ranges of turbines/generators on an international market for hydraulic power generation and

provides key-turn power plants. Development at Alstom Hydro is "Design-To-Order" which involves the reuse of existing technologies or product parts. The design process will be tailored to meet the needs of specific customers. Since, globalization has changed the design process of turbine / generator. Entities scattered around the world that previously worked independently found themselves interconnected in complex networks. For these entities, it's now important to adopt common working methods, similar product architectures, identical control tools, catalog parts, and common selection criteria. Top management has identified standardization of practices and engineering techniques as a major performance issue at Alstom Hydro. The standardization process can be particularly cumbersome and time-consuming in the context of physical and cultural differences between the participants in this remote process. At this point, this study aims to improve the remote standardization process. It will allow a more comprehensive management of engineering activities, for example: a relevant distribution of workloads at different sites; a comprehensive integration of different competencies and skills.

The study has been conducted in the Hydro global engineering function. The standardization project's team is composed of members from all the technology centers involved (Latin America, North America, Europe, China and India). In some cases, subject matter experts are invited to participate in the discussions.

4.1 – Standards development activities

The standardization process consists in co-production and sharing of documents with a large team spread around the world. It's important to collect the know-how from all members who will participate in the standard's development. The collaboration between the engineering team members is a big challenge to overcome. The geographical distance and time differences increase the complexity of this process. It requires establishing a collaborative environment and a customized collaborative platform to successfully achieve the team goals in a global context.

In the following sections, we will present the previous standardization process, which was based on a mailing platform. The problems associated with its execution will be discussed. Then, we will discuss the drivers behind a new standardization process and its relationship with the collaborative platform specification process. Finally we will state the expected benefits of the collaborative platform.

4.1.1 –Previous Standards development activities

Mainly a mailing platform and some face-to-face meetings supported the previous remote standardization process. The process followed these steps. For example, see Figure 2.

- Step 1: The team leader created a document that was shared among all team members. He communicated the document (version 1) via e-mail to all team members.
- Step 2: The team members analyzed the document and sent back all their inputs to the leader. They sent by e-mail a new file (versions 1.a, 1.b, 1.c) with their modifications or comments about the document.
- Step 3: The leader analyzed all the recommendations and comments and made a new version of the file (version 2) to consolidate all the inputs. He sent again by e-mail the new version to the team for a new analysis.
- Step 4: The team members approved the new version of the document with all the inputs and sent back new recommendations to the team leader (version 2.a, 2.b, 2.c). The leader consolidated all the recommendations and made a new version of the file (version 3)

Actually, the process was iterated over the multiple steps. A new document version was attached every iteration. The process stopped when an agreement was established on a specific version. The team leader published the final version and made it accessible to all the team members.

The second activity was face-to-face meetings which are organized once a year. They enable participants to make big leap in standards definition but they are time consuming and costly due to trip expenses.

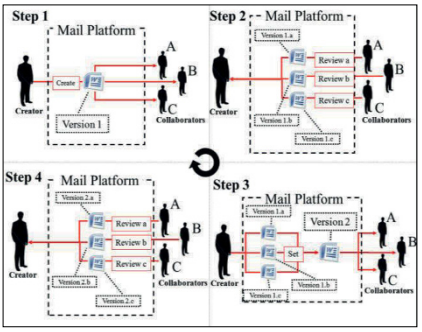

Figure 2: Previous standards development activities

Two major problems occurred during the remote standardization process. The first problem was that valuable comments might be omitted and urgent agreements might be delayed. Since there was a lack of spontaneous discussions, the team members had to wait for the leader to publish a new version. They might lose interests of time sensitive discussions and they might face lack of motivation.

The second problem was related to the data consolidation. As the process iterated, e-mails exchange could grow exponentially and the team members could be confused from the mass mailing. In addition, as the team size went larger, the number of documents received by the leader increased which demanded more integration efforts. Tracking document versions and managing feedbacks could be burdensome tasks. Hence this process was time consuming, demanded a lot of consolidation efforts and was hindering real-time decision-making.

4.1.2 –New scenario for Standards development activities

A new remote standardization process and its collaborative platform have to be designed to overcome these problems. The drivers for this new process were: to have a single entry point for all the standardization documents, which are accessible to the whole standardization team; to reduce the agreement time on decisions and discussions from all regions; and finally to allow asynchronous integration of comments and feedbacks into one shared document.

From these considerations, a new scenario is designed. For example, see Figure 3. The team leader creates a standard working document that is shared among all team members. He uploads the document into a future Hydro collaborative Platform and provides permission access to the document for authorized team members. Team members analyze the document and make all the necessary modifications online. The team members can see others modifications or propositions. After each modification, the leader receives a notification from the system to approve or not the changes. All comments and recommendations can be made in a forum associated with the document. Easy consolidation of discussions and posting comments will be possible with the collaborative platform.

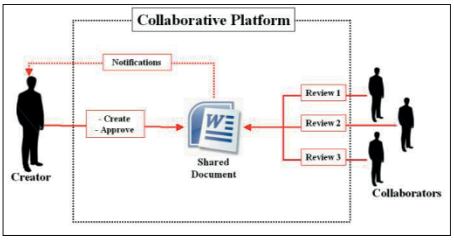

Figure 3: New scenario for standards development activities

As researchers, we expect from the collaborative platform to significantly improve global collaboration and to accelerate solution finding by sharing resolutions to similar problems. It helps the engineering team to understand and to analyze all the standardization related activities.

Not only the standardization team is able to consult the standard documents but also a show room will be designed to give them the visibility to all ongoing standardization projects. Similarly the identification and the proposition of the standardization projects will not be made by e-mail anymore, but through the collaborative platform.

4.2 – Hydro Collaborative Platform Specification Method

4.2.1 –Formalizing the standardization process

The formalization of the standardization process was done first by an informal model. For example, see Table 1. This informal process acted as a base model to develop the formal standardization process model.

Standardization Activity	Scenarios
Collect local practices	Action Owner creates a Library where all members share local standards. If the regions don't have standards, action owner creates a forum for them to share local practices.
Define general concept	Action owner with Library expert analyze the standards objectives and define the key concept
Define the best local standard	Action owner with Library expert analyze the local practices at the Forum and choose the better practice to include in the draft of the global standard.
Conduct a survey	Action Owner shares in a forum with team members the local standard (or practice) chosen and asks if everyone agreed. If necessary, Action Owner can create a survey to choose the best. All remarks in that Forum must be considered for the next activity (write draft standard).
Write the standard's draft	Action Owner writes the draft Standard based on the defined template and all discussion in the forum.

Table 1: informal standardization process model

In order to propose a formal standardization process model, we study the possible modeling tools. The IDEF0, a functional modeling tool, is our candidate to formalize the standardization activities. It is designed to model the decisions, actions, and activities of an organization or a system. As a communication tool, IDEF0 enhances domain expert involvement and consensus decision-making through simplified graphical models. Inputs/outputs are characteristics of the information flow altered by the activities. The resources and the controls are the necessary conditions for each activity to take place. We identify six main activities for the standardization process. For example, see Figure 4. It starts with the planning, development, and follow-up then the release, the re-use in project and finally the feedback of experiences in Hydro global Engineering and manufacturing team. The proposed model is continuously discussed and updated. In fact, regular discussions are conducted with the standardization managers to get feedback of experience for the proposed process model. The evolved process model is communicated to all team members.

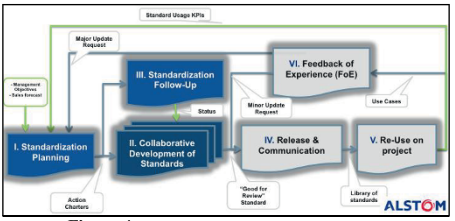

Figure 4: Formal process model using IDEF0

Each of these activities is described by sub-activities at a finer granularity level. We review hereafter the 'collaborative development of standards' activity in details. For example, see Figure 5. The objective of these sub-activities is to collectively create a standard draft version.

All local practices are collected from all regions. General concepts, nomenclatures and common selection criteria are defined. Then the team leader identifies the optimal local standard based on these criteria. This optimal local standard will be the baseline document for the global one. A survey is conducted to collect comments and feedbacks for this baseline document and discussions are made to write the first standard draft version

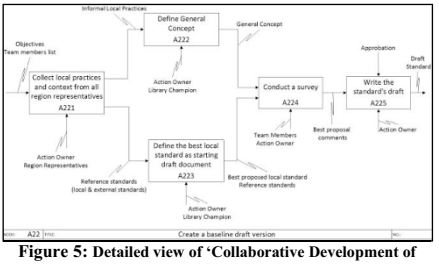

Figure 5: Detailed view of 'Collaborative Development of standards' activity

4.2.2 –Implementing the standardization process

The formalization and the implementation phases are complementary. We loop into these phases to well define the hydro collaborative platform functionalities. These functionalities map the standardization activities and their contextual information into the platform. As starting point, we study the existing IT tools available at Alstom Hydro. MS SharePoint, the collaborative IT tool, is the most adapted to the project requirements. SharePoint presents several features of great importance to our platform, such as site pages, wiki pages, discussion boards, document libraries and item lists. In addition, site permissions can be assigned to the members with different roles (contribute, read, approve…). The features create a solid structure for the standardization process.

The 'collaborative development of standards' sub-activities and their contextual information are mapped to the collaborative platform. For example, see Figure 6. First, the mapping of the 'collect local practices and context from all region representatives' sub-activity with its corresponding inputs/outputs, resources and controls is done through the identification of the following functionalities in SharePoint. A document library is created to collect all the local practices with 'contribute' permission assigned to the region representatives. A custom list is also created to make visible all the agreed objectives. Likewise the 'conduct a survey' sub-activity is mapped into the collaborative platform by creating a survey list to collect the comments of the baseline standard document. A discussion board is also created to elaborate on the feedbacks. The 'write the standard's draft' sub-activity is mapped into an office web app to collaboratively create the document. The team leader approves the baseline standard document and proceeds to the 'release and communication' activity.

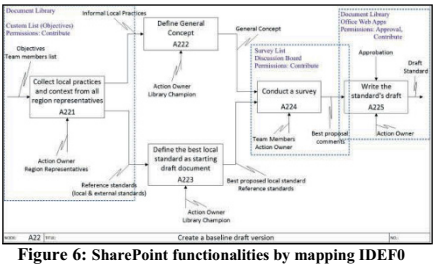

Figure 6: SharePoint functionalities by mapping IDEF0 activities

The functionalities associated with the step-by-step process for the Hydro collaborative platform are performing as expected. The result is an online collaborative platform, based on Share Point, giving only access to functionalities supposed to be necessary for engineers co-defining their standards and following the standardization process previously defined.

5- Conclusion

Standardization of engineering practices is a possible answer to the necessity for multinational firm to rationalize their development activities across their local sites. Stating that a collaborative platform could be valuable for supporting the collective and distant activities for defining corporate engineering standards, this paper more specifically investigates two questions: which collaborative standardization process could enable the practitioners to collectively define their standards at distance? And how to select and to organize the collaborative platform functionalities in order to support this distant standardization process? Based on an empirical study within the Alstom Hydro Company, six main standardization activities were identified and broken down into set of sub-activities. A global standardization process was then formalized using IDEF0. This makes it possible to precisely describe the inputs/output of each activity and to identify the different stakeholders to be involved in every process steps. This

description of the standardization process also proved to be beneficial for the technical specification of the collaborative platform. Indeed, the implemented platform within the company was structured by the process, each activity having its own profile in the platform, with associated functionalities and contributors. Giving this, a user involved in a standardization activity is rapidly aware of the global process stage, of the operational task in which he has to participate, of the relevant platform functionalities to perform his task.

Currently, this standardization process and the associated collaborative platform were only developed and deployed in the context of Alstom Hydro. It's recommended that these models have to be tested and validated in multiple other contexts.

6- Acknowledgements

This research paper was part of a master graduation project hosted by G-SCOP laboratory and Grenoble University. Mr. Vinicius MURARO DA SILVA conducted his internship at Alstom Renewable Power – Hydro Grenoble Site under the industrial supervision of Mr. Charles BORDIER, an industrial engineer in Hydro global engineering and manufacturing team. The authors would like also to acknowledge the editing by Mr. Pierre LAVAYSSIERE, PhD student at Grenoble University, of an earlier draft of this paper.

7- References

[A] M. Alavi, "KNOWLEDGE MANAGEMENT," vol. 1, no. February, pp. 1–37, 1999.

[B] J. Bernard, "A Typology of Knowledge Management System Use by Teams," vol. 00, no. C, pp. 1–10, 2006.

[BP] Beylier, C., Pourroy, F., Villeneuve, F., & Mille, A. (2009). A collaboration-centred approach to manage engineering knowledge: a case study of an engineering SME. *Journal of Engineering Design*, *20*(6), 523-542.

[C] K. Creation, "NRC Publications Archive Archives des publications du CNRC Virtual Communities of Practice : Design for Collaboration and Knowledge Creation Virtual Communities of Practice : Design for Collaboration and Knowledge Creation *."

[D] Dargahi, A., Pourroy, F., & Wurtz, F. (2010). Towards controlling the acceptance factors for a collaborative platform in engineering design. In*Collaborative Networks for a Sustainable World* (pp. 585-592). Springer Berlin Heidelberg.

[FV] E. Folmer, J. Verhoosel, State of the Art on Semantic IS Standardization, Interoperability & Quality. UT, CTIT, TNO en NOiV. ISBN 9789090260303. (2011)

[G] G. Guidelines, "Standardization Guidelines for IST research projects interfacing with ICT standards organizations," no. January, pp. 1–24, 2007.

[I] ISO/IEC Guide 2:2004 Standardization and related activities – General vocabulary definition 3.2

[K] K. Krechmer, "Open Standards Requirements". In K. Jakobs (Ed.), Standardization Research in Information Technology: New Perspectives, Hershey: Information Science Reference, pp. 49-65. (2008)

[L] D. Lecet, "Community Computer Environment supports," pp. 64–68, 2012.

[P] W. Ping, "A Brief History of Standards and Standardization Organizations: A Chinese Perspective," 2011.

[S] W. E. Steinmueller, "The role of technical standards in coordinating the division of labour in complex system industries", in The Business of Complex Systems Industries, Oxford University Press, pp. 133-151 (2003).

[SB] J. Stirling, R. Beaumont, and A. Percy, "Tutors' Forum : Engaging Distributed Communities of Practice Tutors' Forum : Engaging Distributed Communities of Practice," vol. 24, no. 2, pp. 141–153, 2009.

[SD] F. J. C. Slob and H. J. De Vries, "Best Practice In Company Standardisation" ERASMUS RESEARCH INSTITUTE OF MANAGEMENT REPORT SERIES, 2002.

[TT] M. Tan, N. Tripathi, S. J. Zuiker, and S. Hock Soon, "Building an online collaborative platform to advance creativity," 4th IEEE Int. Conf. Digit. Ecosyst. Technol., pp. 421–426, Apr. 2010.

Article 035-i-86

Towards the success of design projects by the alignment of processes in collaborative engineering

Rui XUE [1, 2], Claude BARON [1, 2], Philippe ESTEBAN [1, 3], Daniel ESTEVE [1], Michel MALBERT [4]

(1) : CNRS, LAAS, 7 av. du colonel. Roche, F-31400 Toulouse,
+33 (0)5 61 33 62 00
E-mail : {rui.xue,claude.baron, philippe.esteban daniel.esteve}@laas.fr
(3) : Univ de Toulouse, UPS, LAAS, F-31400 Toulouse, France

(2) : Univ. de Toulouse, INSA, LAAS, F-31400 Toulouse,
+33 (0)5 61 55 98 26
E-mail : {rui.xue,claude.baron}@insa-toulouse.fr
(4) : consultant, 24 rue Cartailhac, 31000 Toulouse,
E-mail : michel.malbert@outlook.fr

Abstract: With increasingly complex systems, relying on systems engineering (SE) as an interdisciplinary method to manage engineering processes is becoming essential for companies. However, too many projects still fail and industrial groups have argued that these failures may be related to the managerial techniques used. Indeed organizational processes are more or less specifically mentioned in SE standards but in practice project managers tend to rely more on their own standards which sometime set forth practices not in line with those of the SE domain, hence the reported discrepancies which very often lead to project failure. Thus to improve the companies' competitiveness when developing new products, cooperation between processes related to system development and project management (PM) is key to getting performance and success. This paper presents arguments which tend to support this theory and introduces an ongoing project with a method and tool aiming to integrate both domains.

Key words: system design, engineering processes, project management, systems engineering standards, decision support.

1- Introduction

Despite heavy investments in the project management sector (about one-fifth of the world's GDP, or more than $12 trillion to be spent on projects each year from 2010 to 2020 [B2]), too many projects still fail [S2]. Only 20% of projects achieve the expected results in terms of quality, costs and deadlines due to a lack of project management [B2]. Half of all project failures could be prevented by more effective systems engineering [I1]. Recent studies have underscored the current partitioning between Systems Engineering processes and Project Management practices, leading to inconsistencies [C1].
Systems Engineering (SE) and Project Management (PM) are two critical aspects in the success of product development projects [B3]. Indeed, SE and PM are two disciplines, two communities, that seem distinct but which however fully complement each other. One defines a design objective; the other determines an optimization objective for the implementation of the engineering project. The obvious path in order to increase competitiveness is to bring closer together both approaches which, separately, rely on their own description of operational processes interacting very little or being fully interdependent. Representation differences set an obstacle to the required establishment of relationships between both communities, and discussions are already underway in an attempt to unify both approaches [P1].
It is in this highly sensitive context at the scientific and industrial level that the research work presented in this paper is positioned. Our research objectives rely on a pragmatic concern, offering methods and support tools to companies to help them improve the rate of success of their design projects.
The paper is organized as follows: Section 2 presents a state of the art on recent initiatives at the normative level aiming at aligning SE and PM; section 3 points out industrial motivations and practices; section 4 describes a proposal of method and tool for SE–PM integration. Section 5 concludes on the benefits of such an approach.

2- Aligning SE and PM at the normative level

This section first introduces important definitions regarding SE and PM; then it gives an overview of the evolution of normative works towards the integration of Systems Engineering and Project Management processes.
Before discussing the need for cooperation between SE and PM, let us first define SE and PM.

1. Systems Engineering: Systems Engineering is an interdisciplinary approach and means to enable the realization of successful systems. It focuses on defining customer needs and required functionality early in the development cycle, documenting

Article 035-i-86

requirements, and then proceeding with design synthesis and system validation while considering the complete problem: operations, cost and schedule, performance, training and support, test, manufacturing, and disposal. SE considers both the business and the technical needs of all customers with the goal of providing a quality product that meets the user needs [I1].

2. Project Management: Project Management is the application of knowledge, skills, tools and technique to project activities to meet project requirements [P2].

Integrating systems engineering and project management has only been considered in the beginning of 21th Century. Sharon stated that system engineering management always uses some subsets of project management methods and tools. The technical activities are related to the product domain and the managerial activities to the project domain. However these constitute two complementary facets of system engineering management [S1].

In January 2011, INCOSE and PMI recognized the importance of integrating SE with PM and formed a strategy to strengthen the integration of the SE and the PM to overcome barriers between systems engineers and project managers, because of their different cultures. Indeed, systems engineers and project managers usually focus on their own tasks, their work being separate from each other in the company.

In October 2012, INCOSE and PMI agreed to conduct a survey to better understand the responsibilities of systems engineers and project managers and thus help organizations reduce program risk and improve ROI (Return On Investment). Another objective was also to better understand how PM and SE are integrated within the organizations. The Consortium for Engineering Program Excellence (CEPE), set up at the Massachusetts Institute of Technology (MIT), provided a method to analyze, review and finalize the results of the joint survey (based on a panel of 680 chief systems engineers and program managers). The results highlighted how critical SE and PM integration is to alleviate unproductive tension between SE and PM. Four methods were put forward to solve this problem, as shown in figure 1.

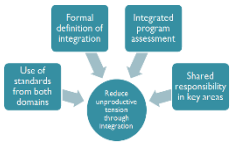

Figure 1: The result of the survey [C1]

The first method is to use standards from both domains; systems engineers use systems engineering standards and program managers opt for project management standards, but none relies on the SE chosen standard in parallel with the PM one. The second method formalizes integration of SE and PM. The survey highlights the fact that the degree of formalization of the integration depends on the size of companies, the larger ones are better at this formalization. The third method develops integrated engineering program assessments. The fourth method integrates the roles of systems engineers and program managers (due to major overlaps between them) and suggests a shared responsibility for risk management, quality, and lifecycle planning and external suppliers.

Based on the joint research of MIT, PMI and INCOSE Community of Practice on Lean in Program Management between January 2011 and March 2012, a guide to help systems engineers and project managers to improve the performance of their programs [O1] was published in May 2012. The third section of this guide is about “integrating project management and systems engineering”. It introduces some important definitions from both domains and indicates some directions to a better integration of PM and SE, and ten challenges/themes for engineering program management and to overcome the barriers between the SE and PM.

3- State of industrial practices and motivations

In the field of the extended enterprise, it becomes increasingly complex to conduct systems engineering projects given the numerous participants and stakeholders, from the design to the retirement stage. Systems development involves many disciplines, i.e. organizational, financial, human decision-making, logistics, environmental…

Thus, in order to manage the projects effectively, many companies rely on standards and PLM tools to guide the industrial processes. However, according to a study by Pierre Audoin consulting PLM tools only help in the collaboration of technical activities [N1]. Likewise they do not offer decision support mechanisms to monitor the project; it will thus be necessary to develop a tool in the near future to implement and coordinate cooperation between the processes of SE and PM and help the project manager in his decisions during the SE project.

Our objective is thus to provide the project manager with a standards-compliant method and tool that support cooperation between systems engineers and managers and their respective processes, to control the project and optimize cooperation between processes. To do this, a first step consists in identifying and modeling SE and PM processes, and then finding the relevant indicators to monitor them. The goal is multiple: 1) to support management by coordinating processes; 2) to offer a method to stakeholders to monitor progress at any time, and at any level, from different points of view, and 3) to provide tools to help them take decisions and explore several directions to guide the project.

4- Proposal of a method and tool towards the integration of SE and PM

The quality of collaboration between organizations (in the increasingly common case of projects within distributed companies) and between project actors (the latter enacting different roles) is a decisive performance factor. Current corporate practices derive from proposals and recommendations particularly those highlighted in the PMBoK guide [P2]. System design project management is a highly multidisciplinary process and as a result a highly difficult one to achieve: corporate experience (usually including an explicit approach with practices feedback) plays an essential part in the progressive definition of a ‘proprietary’ process suitable for the type of product or

service to be developed. This evidence does account for the fact that although the PMBOK guide recommends a number of practices, project management does not benefit from a genuinely standardized approach. Hence in practice, companies have to adapt the general recommendations laid down in PMBOK to suit their operating habits and the engineering processes implemented.

In these corporate approaches, we have already defined the main mechanisms that set an obstacle to the smooth running of the project: insufficiently detailed or even inconsistent set of specifications, *a priori* unjustified not to say hazardous technological choices, clumsy resource allocations, insufficiently shared clear, structured and understandable information… We focus on the problems and deadlocks associated with the fields of detection, analysis, coordination and decision-making: how can an error or insufficient feature be detected at the earliest opportunity? How can the best solution be chosen or at least the best corrective action?

The approach proposed consists in relying on the current dynamic (see section 2) aiming at aligning System Engineering with Project Management to define a generic process for a 'supervised' project management. Its originality lies in the choice of a supervision based on the notion of aggregate indicators coupling information about the system to design with the system for designing (the project); these indicators are recorded in the dashboards and are made available to all the major project leaders for purposes of tracking, assessment of options, diagnosis and decision making aid. In a nutshell we propose a new decision-making and technical coordination tool (decision model, formalization of an integrated project and system evaluation process, indicator dashboard, proactive decision support mechanisms), coupling the system development project and system engineering management. We focus on the evaluation, verification and validation processes which are poorly instrumented using regular project management or engineering tools but which form the backbone of the critical decisions made during project reviews.

The scientific expertise together with an analysis of industrial needs and existing tools led us to design a first prototype, named ATLAS, which progressively evolved towards the definition of a more ambitious one, DECWAYS. Section 4.1 describes the objectives and results of ATLAS and where DECWAYS stands relative to the first prototype; section 4.2 presents two basic pillars of DECWAYS.

4.1 –From ATLAS to DECWAYS: evolution of objectives and results

Research project ANR/ATLAS (2008-2011) dealt with the connection between project management and product design. Formalizing the relationships that necessarily existed between processes of both domains was a novel idea.

Technically speaking, the starting point of the ANR-ATLAS project is the EIA-632 standard for engineering a system. This standard allows the project to be broken down into subprojects leading to a classical tree representation. This also allows the identification of alternative solutions to be memorized for subsequent use when the time comes to opt for a technical solution for the project.

However, the main innovation lies in the implementation of two mechanisms coupling system design tools and project management tools, these mechanisms being used to propagate the managers' operational and managerial decisions:

1. Structural coupling– each subproject is broken down into a design architecture and a project management architecture; these two architectures are logically connected to enable an exchange of information;
2. Information coupling– each subproject is governed by requirements distributed between the two architectures, leading in some cases to the definition of common indicators.

To become operational these two coupling mechanisms necessitate a formal decision-making mechanism to be activated whenever a coupling information or communication network modification justifies it. This mechanism had not been defined by ATLAS.

Beyond this, the main results obtained after completion of this project can be identified at various levels and were essentially used to validate the approach in its principle: the management of options as to the different possible technical solutions, the establishment of an overall supervision shared through dashboards associated with each tree node and displaying the system status, the validation of the specifications, the detection of conflicts.

By focusing on ATLAS limitations (i.e., versions that are not managed, rigid tree structure that must be homomorphic, validation processes not taken into account, …) it became clear that we had to further investigate (i) the methodology used (by conducting a more detailed analysis of the industrial practices and tools), (ii) standards (by implementing highly detailed comparative analyses of SE and PM standards), and (iii) technical features (by integrating in the computing platform project new storage technologies, data access and sharing , new interface generations…).

We thus relied on the results obtained with this first prototype to define a method and to specify a tool for supervision, coordination and control of the evolving stages of a project involving all stakeholders. This proposal really breaks away from current engineering practices by monitoring the whole development cycle of a product or service from its initial design phase to the prototyping of solutions. Regarding ATLAS, DECWAYS adds new proposals:

- Submitting a generic, high-level project management process that can easily be appropriated by companies, handling multidisciplinary features and supplementing PMBOK practices. The goal is to promote an alignment between disciplines and particularly Systems Engineering and Project Management by harmonizing their descriptions of the project notion and processes that make it up, a strategic need as underpinned by the INCOSE/PMBOK alignment [C1].
- Refining the notion of indicators as language elements common to the disciplines concerned. The aim is to highlight those indicators that can be used for checking how the stakeholders handle any mismatch between expectations and results [G1, J1] and showing how to construct «aggregate indicators» and « dashboards » providing an overall process supervision capability.
- Designing a smart system for an integrated management of a development project relying on the generic process model and on indicators and dashboards to master multidisciplinarity and the project progress.

Article 035-i-86

4.2 –DECWAYS basic pillars

To specify the outlines, objectives, functioning and services offered by DECWAYS, a first objective was to work towards the alignment of the Project Management and Systems Engineering process modeling (needs and requirements engineering, architecture design, system analysis, check and validation) applied to a project. Several researches [B1, X1, Z1, Z2] allowed us to analyze the main differences in terms of descriptions, as well as the roles involved in processes. A comparative study of processes identified the main deviations in descriptions [X1] and the roles participating in either process. Ways and means were presented to make these processes more operational by facilitating their cooperation in practice by looking for and defining the links needed between them [X1] This was a prerequisite for successfully arriving at a generic process of project management: coordination, decision making, tracking, analysis, memorizing, follow-up and correction. Standardizing the process descriptions is one of the means used to bring closer together Systems Design and Project Management approaches.

The DECWAYS proposal thus relies on an extended version of ANSI/EIA 632 standard for SE and on the PMBOK for the PM [X1]. As a result the choice made by DECWAYS lies within the scope of the approach identified in the INCOSE-PMI-MIT project (see Section 2). To select a reference standard in SE, DECWAYS introduces four additional analytical criteria relative to the overall comparative study of standards.

1. The standard needs to address the system life cycle broadly, being implemented from design conception to retirement.
2. The level of complexity in simulating the progress depends on the level of abstraction of the standard; therefore the standard should offer a medium level of abstraction.
3. According to the complexity of the project, V&V (validation and verification) becomes increasingly important; the standard should provide a detailed view of the V&V processes.
4. The goal is to simulate progress of the project. As a result, the relationships between processes are keys for standards comparison.

The analysis conducted by DECWAYS leads to the conclusion that no standard fully satisfies all the criteria, and envisions extending the ANSI/EIA-632 standard adding some elements to improve, for example, the maintenance process and the disposal process to the ANSI/EIA-632 to cover the complete system life cycle. The DECWAYS proposal chooses ANSI/EIA-632 as reference, but, given the system life cycle (e.g. maintenance process and disposal process), the integration process, the human process and the tailoring process, it intends to use the ISO/IEC-15288 standard to complete the ANSI/EIA-632 standard.

The resulting architecture of system engineering processes is shown in Figure 2. The underlined processes originate from ISO/IEC-15288, while the others are derived from ANSI/EIA-632 [X1].

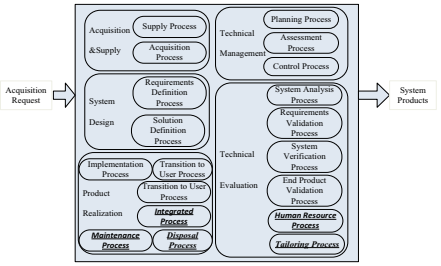

Figure 2: Final systems engineering processes in the extended standard

In this standardization of Systems Engineering and Project Management processes, the second objective is to get greater insights into the notion of indicator and deviation. During task execution, monitoring the evolution of each indicator and checking against the objective will enable an automatic detection of any deviations between the work program initially drawn up and the effective progress in the field.

Operationally, these indicators feature various lifecycles: their definitions, the negotiation between the stakeholders of objective values and related parameters (thresholds, validity ranges, etc.), and their evolution over time as recorded during implementation. They reflect or are computed on the basis of data, tacit information and knowledge recorded by the company in its information system (data originating from the ERP, data about the project progress and follow-up of the planning tool, etc.). In DECWAYS, the objective is therefore to get greater insights into the indicator concept so as to provide it in a multiple indicator approach, with the ability to dialog, to detect danger and drifts, to diagnose and analyze with the ultimate goal of tracing it back to the design and set of specifications if needed, on the technical side and on the organizational side.

To do this, we identified several indicators whose function and nature differ: for example the 'Progress against Requirements' indicator aims to secure the design, since it stands for a requirement laid down in the set of specifications which has to be recorded; another example is the 'Progress against Plans and Schedules' indicator aiming to facilitate project management since it is possible through use of aggregation or weighting procedures to characterize the development of the project in a synthetic manner legible by all. Beyond the pre-definition of these 'classical' indicators associated with the definition of processes in SE standards, the DECWAYS strategy is designed to help decision makers define their own indicators. An example could be the definition of a new indicator, like 'Earned value', showing the amount of budget and time already spent relative to the amount of work done.

As in ATLAS, dashboard definition and operator interfacing are part and parcel of the project: given the necessary hierarchical construct of tasks, indicators will be progressively aggregated, which might lead to a multilevel construct of these indicators. Figure 3 synthetizes the main principles of the method and tool.

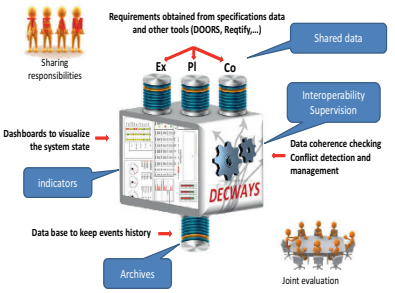

Figure 3: Objectives and principles of the DECWAYS method and tool

5- Conclusion

To develop the system quickly and efficiently, it is not only necessary to implement SE management during systems engineering projects and to use good practices during such projects, but it is crucial to align practices in both domains. Indeed, recent studies have shown that not only the technical processes from SE are essential for the success of the project, but also that managerial process are critical [S1], and overall that there is a real need to integrate both processes. Thus, the issue of SE and PM integration lies at the very heart of current research concerns but as this paper also highlights in its motivations, it is at the core of economic and industrial issues. It is a source of motivation for international standardization organizations, companies or governments alike.

The DECWAYS project and tool also address any inconsistencies that might exist between SE and PM domains, from a pragmatic perspective. It is a follow through on the ATLAS project which has demonstrated the feasibility of concept and served as a prototype to validate the industrial value of these proposals. The latter tackle the issue of collaborative work and project steering aid conducted in a consistent manner in terms of follow-up and decisions. DECWAYS seeks to offer a method and tool capable of bringing closer together SE and PM, detecting practical divergences, making concerted decisions and supervising jointly the proper development of the project and system.

This paper presented a method and tool designed to facilitate greatly SE and PM collaboration. As underscored in the INCOSE-PMI-MIT analysis, a natural means of achieving process cooperation, chosen in DECWAYS, is the use of standards from both domains and processes from these standards. But, beyond the mere issue of choosing between main standards and with the aim of achieving a better match with project management processes, DECWAYS also considers other ways to align processes from both domains such as sharing responsibilities and crossing data towards a collaborative decision process. To do so, it intends to structure collaboration (processes, actors …) and provide project leaders and engineers with information produced to assist with decision making. Such a technical and scientific concern fits in well with the current purpose of reducing the cost of intellectual work (management, engineering, finance …) via « smart » software [M1]

Thus, this proposal should facilitate the management of projects in the company by (i) providing visibility to all as to the progress of tasks, (ii) providing a formal decision-making process and (iii) managing choice traceability.

7- References

[A1] AFIS. Découvrir et comprendre l'ingénierie système. Association Français d'Ingénierie Système, Version 3.1, 2007.

[B3] C. Baron, G. Auriol, M.Zolghadri, A.Wehbe, Ch.Merlo, Ph.Girard, "Livrable L6 : Entités d'organisation et de planification - Version finale des méthodes et principes utilisés", Rapport de Contrat : Projet ANR-RNTL: ATLAS 07TLOG002, Juin 2009, 35p

[B1] M. Beer and N. Nohria. Cracking the code of change. Harvard Business Review, Harvard College, May-June, 2000.

[B2] J.C. Boarder, "The system engineering process," Proceedings of the IEEE Annual International International, 1995, pp. 293-298.

[C1] E. Conforto, M. Rossi, E. Rebentisch, J. Oejmen and M. Pacenza. Improving the Integration of Program Management and System Engineering. White paper presented at the 23th INCOSE Annual International Symsposium Philadelphia, USA, June 2013.

[G1]L. Geneste, Y. Reversat, A. Robert, P. Esteban, D. Esteve, J.C. Pascal, J. Abeille, "Livrable L5: Spécification détaillée complète de l'environnement de conception", Rapport de Contrat : Projet ANR-RNTL: ATLAS 07TLOG002, Juin 2009, 74p.

[I1] INCOSE. 2010. Systems Engineering Handbook: A Guide for System Life Cycle Processes and Activities. Version 3.2. Revised by M. Krueger, D. Walden, and R. D. Hamelin. San Diego, CA (US): INCOSE, 2010.

[J1] A. Jakjoud, M. Zrikem, C. Baron, A. Ayadi " SysPEM: A SysML and SPEM Based Process Modeling Language for Systems Engineering ", International Journal of Services Operations and Informatics (IJSOI), 2012.

[M1] McKinsey Global Institute. McKinsey & Company. Disruptive technologies: Advances that will transform life, business, and the global economy. May 2013.

[N1] C. Nayagam. Enquête sur les usages de solutions PLM en enterprise, Paris 2011.

[O1] J. Oehmen et al. The Guide to Lean Enablers for Managing Engineering Programs, Version 1.0. Cambridge, MA: Joint MIT PMI INCOSE Community of Practice on Lean in Program Management. URI: http://hdl.handle.net/1721.1/70495, 2012.

[P1] A. Pyster and D.Olwell, "The Guide to the Systems Engineering Body of Knowledge (SEBoK), v.1.1. Hoboken,NJ: The Trustees of the Stevens Institute of Technology,. Accessed DATE .www.sebokwiki.org/, 2013

[P2] PMI. A Guide to the Project Management Body of Knowledge: PMBOK® Guide. Project Management Institute, 2008.

[S1] A. Sharon, D. Weck and L. Olivier. Project Management vs. Systems Engineering Management: A Practitioner's View on Integrating the Project and Product Domains. Systems Engineering, 14(4):427–440, 2011.

[S2] Standish Group International, Inc,. report in Computer World, February 17, 2013.

[X1] R. Xue, C. Baron, P. Esteban, "Managing systems engineering processes: a multi-standard approach," processing of the 8th annual IEEE International Systems Conference (SYSCON), Ottawa, Canada, March 31-April 3, 2014.

[Z1] M. Zolghadri, C. Baron, P. Girard, "Modelling the mutual dependencies between product architectures and a network of partners ", International Journal on Product Development, Inderscience Publishers, Vol: 10, pp. 62 – 86, n°1-3, 2010.

[Z2] M. Zolghadri, C. Baron, M. Aldanondo, P. Girard, " A general framework for new product development projects ", International Journal of Technology Management, Indersciences, vol. 55, n°.3/4, pp. 250 - 262, 2011.

Article 038-i-100

UP: A unified paradigm to compare computer-based and paper-based supporting tools for collective co-located preliminary engineering design activities

Thierry Gidel [1], Andrea Luigi Guerra [1,2], Enrico Vezzetti[2]

(1): Université de Technologie de Compiègne
Laboratoire COSTECH - CRI
E-mail:{thierry.gidel,andrea.guerra}@utc.fr

(2): Politecnico di Torino
DIGEP
E-mail:{andrea.guerra,enrico.vezzetti}@polito.it

Abstract: Are Computer Supported Cooperative Work in Design (CSCWD) media worth to be used or do we need to maintain the traditional paper-based ones? Several studies exist, but address heterogeneous functions and criteria, and are not comparable. This contribution introduces an exploratory study toward a Unified Paradigm of evaluation (UP). UP aims to ease the set-up of comparable design studies to evaluate if CSCWD are worth to be used in respect of actual supports. The most adapted paradigm to provide a valuable answer prescribes ethnographic qualitative descriptive studies between a traditional paper-based and a CSCWD media. A scenario centered on a common function is presented (isofunctional comparison). The criterion assessed is effectiveness, expressed as the combination of efficacy and usefulness. Efficacy is measurable through objective factors. Usefulness is measurable through subjective factors. In order to confront studies involving different people, we suggest that individual characteristics should be properly considered.

Key words: Disruptive Innovation, Design methods and tools, Design observations paradigm, Computer Supported Cooperative Work in Design, Design research.

1- Introduction

A disruptive innovation [C1] is an innovation that disrupts an existing market, displacing an earlier technology. For example, with the introduction of engine-propelled cars, the use of horses as mean of transportation was progressively dismissed. The introduction of a new product with a disruptive technology can cause the decline of an existing product.
We define as "**transitional phase**" when one technology emerges, trying to substitute another one in use (Figure 1). During the transitional phase, the two technologies are evaluated for sake of comparison. However, the products incarnating those different technologies are generally extremely dissimilar, making the comparison difficult. As an example, while passing from horses to cars for human transportation, how horses were compared to cars? How is it possible to compare heterogeneous products or services? (From now on in the paper, with product we mean the technology embedded in a product or as well in a service or a process).

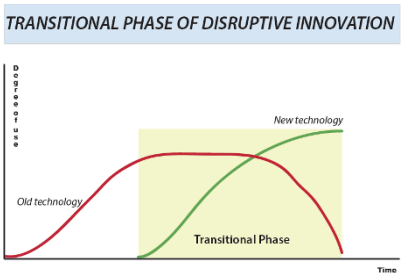

Figure 1: The transitional phase of disruptive innovation (derived from [HT2])

Considering two products, each one has a set of functions. A function can be measured through a criterion. A criterion is a standard to compare and judge individual things. A criterion could have sub-criteria. A possible strategy is to find a relationship between equivalent functions of both products to compare them through common criteria. Watt's horsepower is an immediate and bright example of a criterion used to compare a common function of horses and cars, the production of Power.
Section 2 introduces a Unified Paradigm (UP) of evaluation. Section 3 explains the reasons for applying UP to the transitional phase, from paper-based toward computer-based media, for supporting co-located collective preliminary engineering design activities during the early design phase. Section 4 provides a state of the art for what concern different comparative studies and their associated criteria, proposing a common evaluative procedure. Section 5 shows an example of isofunctional comparison, between paper-based and computer-based supportive media. Section 6 critically reflects on our contribution and highlights its limits. Finally Section 7 summarizes our conclusions and perspectives.

Article 038-i-100

2- UP: a Unified Paradigm for evaluation.

We introduce the notion of Unified Paradigm (UP) of evaluation. UP represents a model for comparing the functions of a product, during its transitional phase. We describe it mathematically, for the sake of comprehension and interoperability, because UP can and should be applied independently from the nature of the products compared.

We have two entities: an *OLD_PRODUCT* that needs to be compared with a *NEW_PRODUCT*. The more similar the two products compared are, the more similar *OLD_PRODUCT* and *NEW_PRODUCT* are, to the point to be equivalent.
If we define:
OLD_PRODUCT = {x: P(x) },
NEW_PRODUCT = {y : P(y) },
with P(t) as {t : t is a function of the product},
we obtain two sets representing the functions of each product; they can have equal or different cardinality.

When a comparable set of functions is identified, we have a subset *COMMON_F ~ COMMON_F_OLD_PRODUCT ~ COMMON_F_NEW_PRODUCT (~ means equivalent).* The subsets have the same cardinality, containing the same functions, and so being equivalent.
COMMON_F_OLD_PRODUCT ⊆ OLD_PRODUCT and COMMON F_NEW_PRODUCT ⊆ NEW_PRODUCT.
A bijection *f: COMMON_F_OLD_PRODUCT → COMMON F_NEW_PRODUCT* exists. This bijection represents an "**iso-functional**" comparison.

We define also
UNCOMMON_F_ OLD_PRODUCT = OLD_PRODUCT — COMMON_F_OLD_PRODUCT
and
UNCOMMON_F_NEW_PRODUCT = NEW_PRODUCT — COMMON F_NEW_PRODUCT (— means subtraction).
They represent the functions for which the only possible comparison is in term of possession, so that one product has that function and the other does not. We define this as a "**heterofunctional**" comparison.
If the subsets of comparable functions contain all the functions of the product, they become improper subsets, and the uncommon functions sets are ∅.

A criterion is associated to one or more common functions (more than one quality can be measured through the same criterion), building a set of common criteria *COMMON_CRITERIA*. Criteria are function-dependent; hence a relevant criterion for one function can become irrelevant for another one. The number of people, a car or a horse can load, may be fundamental as a mean of transport, while loose importance when considering the hectares they could respectively work in one day.
The faster the subsets *COMMON_F_OLD_PRODUCT and COMMON_F_NEW_PRODUCT* are identified, and a common consensus rises around them, the faster a set of common criteria *COMMON_CRITERIA* can be used to compare (or not) a product to a previous one.
Venn diagram in figure 2 represents our model.

3- Co-located collective computer supported tools for engineering preliminary design activities.

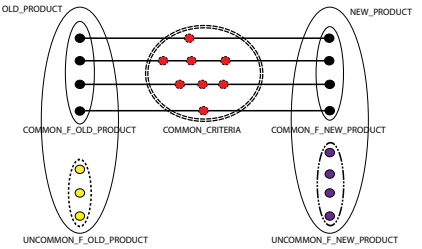

Figure 2: UP: Unified Paradigm of evaluation

We want to apply UP to the transitional phase from paper-based supporting tools toward computer-based supported tools, for co-located collective preliminary engineering design activities during the early design phase. Why this choice?
Engineering preliminary design is a collaborative multidisciplinary process conducted by a design team [G1], allowing it to be more effective and responsive to the challenges of the markets [S2]. This explains our interest for collective design activities.

Design activities, which are identified as design process, are extremely heterogeneous. According to several authors (as resumed by [S1], the design process can be divided into a detailed phase where production, components architecture, and materials are discussed and an early one, or conceptual design phase [S1]. The early stage of the design process is dominated by the generation of ideas, which are subsequently evaluated against general requirements' criteria. [GK1]. As outlined by [PB1], [WS1] and [ML1], among others, early design phase is the most impactful in terms of performances and costs. This explains our attention for the early design phase.

Design activities can also be separated between co-located [OT1] and distal activities, as the CSCW-matrix shows [J1]. According to Olson et al., "*co-located teams are twice as productive as teams that are merely nearby*" [OT1]. This explains our attention for co-located activities.

Wang et al. defend the interest in experiencing a significant paradigm shift, the conceptual design needs to *adopt a more pragmatic and aggressive approach through collaboration, supported by artificial intelligence, and fuelled by information technologies*. [WS1].
This is why we, are interested in computer-based tools and why we developed, among others, a CSCWD tool for conceptual design activities [JK1], [GG1]. CSCWD is the acronym for Computer Supported Cooperative Work in Design. CSCWD systems, such as the one in figure 3, are extremely heterogeneous; no standard configuration has

emerged, even if interactive tabletops and walls are the main component of such systems.

Figure 3: An example of CSCWD media [GG1]

This computer-based technology is disruptive in respect of the actual one, paper-based. Thus, we are in the "transitional phase" from a paper-based product to a computer-based one.
Understanding the benefits of such devices is pivotal to promote their use among designers; what are the benefits if these CSCWD systems are used? Are they "better" than paper-based tools? Are they worth to be employed? Should they substitute paper-based tools?
Without a unified evaluation paradigm, no valiant answers can be proposed for these questions. There is a lack of a set of common criteria for comparing CSCWD and paper-based tools. This is why we want to apply UP to identify a basic set of common functions and associated criteria to enable comparison.

4- A proposal for an evaluation procedure for the UP.

The evaluation paradigm requires a procedure to be followed. The procedure contains the practical aspects describing the set-up of the evaluative studies. According to Buisine's et al. work [BB1], evaluative studies can be grouped in three categories: user needs analyses, interfaces evaluations, and paradigm evaluation. The first two categories aim to improve the quality of the device, erasing system failures and interaction ambiguities. Several studies fall within these two categories (e.g. [SC1], [SC2], [HT1]).
However, their approaches are not based on comparison, and this a key element for our unified paradigm of evaluation. This is why we follow the third category of studies, paradigm evaluation that is a comparative study of the same design activity (the same task), between computer-based condition and a traditional paper-based setting.
A critical analysis of the literature concerning paradigm evaluation (between CSCWD devices and control paper-based settings for co-located collective preliminary engineering design activities) has been conducted. The main studies used in this paper are Buisine's and al. work [BB1] and Gidel's and al. [GK1] works.

Furthermore, Buisine et al.'s article states that to get an "*increasingly detailed picture of user experience in tabletop interface use (e.g. effectiveness, usability, pleasantness of interaction, etc.)*" ethnographic studies should be used [BB1]. The proposed procedure associated to UP can be formally defined with the following attributes:

- **Qualitative**: studying things in their natural settings, attempting to make sense of, or to interpret, phenomena in terms of the meanings people bring to them, according to Denzin and Lincoln's definition [DL1];
- **Descriptive**: cross-sectional study according to Blessing and Chakrabarti [BC1]'s definition of Descriptive Study I;
- **Ethnographic**: realistic context of observation with a minimalist intervention of the experimenter, concurring Buisine et al.'s [BB1] definition.

Figure 4 provides an example of such qualitative, descriptive, and ethnographic evaluative studies [GG1, GG2]. Two design teams are evaluated performing the same design activity, but on different media.

Figure 4: An example of qualitative, descriptive, ethnographic comparative studies [GG2]

Interestingly, this kind of studies is still not very diffused [HR1][RL1][GK1][GG2]. In our opinion, this poor diffusion is mainly due to a lack of a common set of functions to compare those two conditions, confirming the urgencies to find it. After the proposition of a common procedure, it is essential to agree upon common criteria to decide which product (paper or computer based supporting tools) is "better" than the other.
What is the criterion associated to better? Buisine et al. [BB1] propose that be the **usefulness**, transforming the generic "Which product is better?" into "Which product is more useful?" Although we share Buisine et al. [BB1] approach concerning the evaluation paradigm, we would argue against considering usefulness as the main criterion for comparison. In the next section, we detail our proposal for the main criteria to assess.

Article 038-i-100

5- Applying UP to compare computer and paper-based product for co-located collective preliminary engineering design.

In the following section we are going to present only the isofunctional comparison. As we will argument extensively in section 6, this choice is to avoid any possible criticism about the impossibility to heterofunctionally compare two products. Moreover, an isofunctional comparison is a worst-case scenario. Usually, a new product, on top of improving existing function satisfaction, also introduces new function. Therefore, when making an isofunctional comparison, all the new functions that are absent in the old product are put aside, lowering the perceived effectiveness of the new product.
If even in this worst-case scenario the new product (in this case CSCWD) is more effective than the traditional one (in this case paper-based), the heterofunctional comparison cannot but augment the effectiveness gap.
We define
OLD_PRODUCT = {The set of paper-based product for co-located collective preliminary design activities}
and
NEW_PRODUCT = {The set of computer-based product for co-located collective preliminary activities}.

The first step of UP is to find a set of common functions *COMMON_F*. We propose to consider *COMMON_F ={The ability of a product to support co-located collective engineering preliminary design activities}.*
This is, in our opinion, the main function to start with. Other functions can be considered, as we will discuss over in section 6.
In order to find a set of common criteria, *COMMON_CRITERIA*, we need to evaluate the impact of a product that mediate a collective human cognitive activity such as design. Literature on cognitive interaction is extremely wide and out of the scope of this article. We simply report three important school of though: intra-cranial cognition [AA1], extra-cranial cognition ([CC1], [H2]), and enactive cognition [SG1]. We share the latter position, so that a product, with which we are interacting, is a mediator of the perception of the world.
The human perceptive component, subjective to each person, is one of the two aspects to consider for the identification of a set of criteria. This subjective component, for us, is what Buisine et al. call usefulness. We define **usefulness** as the users' perceived quality of having utility and especially practical worth or applicability; it summarizes the set of functions related to **subjective criteria**.
However, we also have to assess an objective point of view that is what we define as efficiency. We define **efficiency** as performing a task with the least waste of resources (time, efforts, money, etc.); it resumes the set of functions related to **objective criteria**.
A product can be useful but not efficient or, on the contrary, efficient but not useful. In both cases there is no benefit in using it. It becomes really interesting for the user only when it is both useful and efficient. Our proposition is to identify **effectiveness** as the main criterion to use. Effectiveness is given by efficiency and usefulness. We define effectiveness as something adequate to accomplish a task. It is adequate to accomplish a task, because it does it with the least waste or resources, and the quality of the result is clearly perceived by the users.
COMMON_CRITERIA contains two subsets of criteria, objective criteria *OBJECTIVE_CRITERIA* and subjective criteria *SUBJECTIVE_CRITERIA*.

COMMON_CRITERIA = OBJECTIVE_CRITERIA ∪ SUBJECTIVE_CRITERIA.

As a consequence, objective criteria and subjective criteria, need to be both assessed but in a different way.

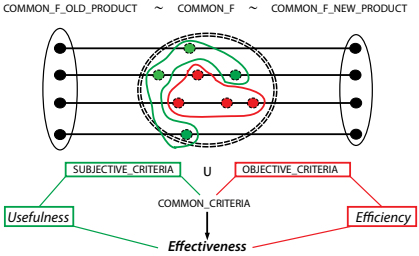

Figure 5: Objective and subjective criteria representation

5.1 – Assessing Efficiency

All the criteria contained into OBJECTIVE_CRITERIA compare the efficiency.
As we said in section 3, CSCWD systems for co-located collective engineering preliminary design activities are still research prototypes, quite far away from industrial ones. Measuring the efficiency of such prototypes can be worthless, because as all research prototypes, they are less efficient compared to industrial prototypes. In literature, specific techniques to assess human-performances using CSCWD are proposed, such as [FA1]. Aiming to assess an eventual transition on markets, our proposal is more adapted for industrial prototypes.
To measure efficiency we should consider that in the actual capitalistic market model, we neither approve nor criticize (we assume it as a standard "de facto"), an activity should generate a profit. Starting with an amount X of resources, we should obtain at the end, an amount X + Y, where Y is the created added value.
From an external point of view, the above-described process looks like Figure 6:

Figure 6: The creation of the added value

The added value Y can so measure efficiency. Using a paper-based tool or a computer-supported one, which condition generates the greatest added value Y compared to the resources used X?

If $\frac{Y_{computer}}{X_{computer}} \geq \frac{Y_{paper}}{X_{paper}}$ then it is possible to say that computer-based supporting tools are more efficacious than paper-based supported tools. This idea is reproduced in Figure 7.

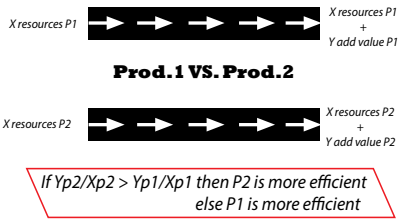

Figure 7: Measuring added value to assess efficiency

Independently from the type of resources considered, they can all be translated into an economic value, such as the cost of the material, the cost of labour, the operating cost, etc. We are aware that an extremely heterogeneous set of costs can be included under the term resources. We propose a list, which should serve as a basis for a discussion. The idea is that it is possible to calculate all the different costs that can pass through our mind, but at least the following costs need to be calculated and compared to assess efficiency.

- Cost of the support tool / hour of work.
- Cost of labour (cost x hours of work).
- Cost of learning (cost x hour of training).

In the actual studies, based on research prototypes, efficiency is very frequently assessed as a matter of time; e.g. which condition is the fastest?

5.2 – Assessing Usefulness

All the criteria contained into *SUBJECTIVE_CRITERIA* compare the usefulness.
Usefulness is measured trough subjective factors. The term subjective apparently clashes with the idea of universal criteria, equal for everyone. Nevertheless, by being able to compare numerous studies, through a unified paradigm of evaluation, we will reach a statistically significant number of people, to assess usefulness.
To statistically process their perceptions, questionnaires based on a Likert's scale of 10 (that guarantee an adequate precision [D1]) should be used.
We propose 7 basic and recurrent subjective factors in the above-cited literature:

- Individual motivation: if users feel engaged or not in their activities.
- Agreement on results: if users agree or not with the results produced by the group.
- Entertainment: if users perceive a recreational aspect or not when using the support.
- Ease of use: if users find supports easy to use or not.
- Communication easiness: if users perceive their communication, when using the supports, easier or more difficult than usual.
- Group cohesion: if users feel or not as a part of greater entity.
- Agreeableness: if users had an agreeable experience or not, concerning the whole activity.

More that for quantitative criteria, there is a plethora of qualitative criteria that can be assessed, and we totally agree about this observation. Nonetheless the proposed set should stay simple for the purpose of being comparable. The authors of each study then can add other criteria, for the sake of their particular research purpose.

6- Reflecting on the limits of the UP

Some authors disagree about the possibility of comparing CSCWD systems and their traditional counterpart [H1] [ND1]. Different technologies may offer different functions, and thus, being not comparable. For them, the existence of *UNCOMMON_F_OLD_PRODUCT* or UNCOMMON_F_NEW_PRODUCT, will bias the comparison. For example, computer-based tools can store ubiquitous data, while paper-based tools cannot. We understand this position, and in fact, we present only an application based on an "isofunctional" comparison, but we disagree with it.
The very essence of disruptive technologies is to propose new ways of carrying out a function.

By comparing cardinalities, if:
$|UNCOMMON\_F\_OLD\_PRODUCT| <$
$|UNCOMMON\_F\_NEW\_PRODUCT|$,
then the new product can offer more than the previous one in term of functionalities, and the criterion of existence is able to provide a mean of comparison.

Otherwise if:
$|UNCOMMON\_F\_OLD\_PRODUCT| >$
$|UNCOMMON\_F\_NEW\_PRODUCT|$,
the new product is offering less functionalities than the previous one.
Heterofunctional comparison follows a binary logic, either the product has the function or it has not. This comparison completes the isofunctional one, giving a holistic evaluation of the two products. To explain this concept, consider as example, the shift from chemical photography to digital one. Isofunctionally, chemical photography was (and in some cases is still) more effective than digital one. However, the new functionalities introduced by the digital (that are missing on chemical photography), such as the ability to instantaneously share a photo, made the digital photography to substitute almost totally the chemical one. Without a model describing the heterogeneous comparison, this phenomenon was inexplicable. We do not deny that a set of common function is needed; otherwise we will derive in comparing products that have no functional affinity. The point is that perception of a missing function can both influence the subjective perception of the user, and so the

usefulness or the objective performance of the product, and so the efficiency. Considering our case study, a function of computer-based technology is to allow the access to ubiquitous data, on the contrary of paper-based one. If the users perceive this disparity, their opinion will be influenced, affecting the criterion of usefulness. Besides, this function may decrease the time needed to complete a preliminary design task, clearly impacting on the criterion of efficiency.

Observing our proposal for a unified paradigm to compare disruptive technologies, an attentive lector may take expectation about the human subjectivity that plays a pivotal role, which cannot be neglected. Our objective to compare several studies (and so a greater number of people than in the actual study in the domain) will statistically ease this problem. Additionally, in order to be able to confront different studies involving different people, individual characteristic can be considered. We share the use of the "Wonderlic Personnel Test", the "NEO Five Factor Inventory" test, and the "Reading the Mind in the Eyes" test to provide an optimal characterization of a person, as in Woolley et al. [WC1].

Moreover, our proposition for comparing CSCWD systems and their traditional paper-based counterpart is itself a subjective proposition. As a consequence, different judgements about the functions and the associated criteria to assess are possible.

Concerning the identification of a set of common functions, we may be accused of being too abstract, only assessing one general function. We can answer by saying that we are afraid that the more we detail, the more we will increase the number of criteria to address, especially for an introductory case study as in this paper. The more the number of criteria grows, the more is going to be difficult to reach a common consensus. On the other hand, we agree that finding the correct level of "functional depth" is crucial. UP is able to describe all the functional levels addressable. It can be used to compare high-level function, such as supporting a preliminary design session, as well as low-level function, such as comparing a virtual keyboard with a physical one. The choice of the functional depth is up to the user; we think that this freedom endorses the interest for our proposal.

Although, we defend our criteria, we strongly point out, that our main goal is to find a common consensus around a basic set of shared criteria to use. We welcome a discussion nourished by other proposals.

7- Conclusion

The current paper proposes an exploratory study toward a Unified Paradigm (UP) of evaluation for the transitional phase between two products (when a disruptive technology tries to substitute another one on the market).

We want to apply it for the study of the transitional phase from paper-based to computer-based products to support co-located collective engineering preliminary design activities.

This simplified vision can be widely applied to other sectors: personal computers substituted the typewriting machines, or postal mail and email.

Our goal is to understand if CSCWD systems are worth to substitute actual paper-based products.

Analyzing the actual studies in the sector, we get the conclusion that they are too heterogeneous in term of functions (and associated criteria) addressed, making a comparison among them worthless.

To overcome this gap, we propose a common protocol of evaluation based on the use of qualitative, descriptive, ethnographic comparative studies to collect the data.

To avoid criticism about the impossibility to use a heterofunctional comparison, we used only an isofunctional comparison. Isofunctional comparison, in our specific case, is not far from the worst-case scenario, because a lot of the advantages deriving from computer-based-technology new functions are not assessed. Our point is that, if computer-based products are isofunctionally more effective than traditional paper-based ones, when we will compare these two products, also heterofunctionally, the effectiveness gap cannot but increase.

We used a high level function as common function to compare: the ability of a product to support co-located collective engineering preliminary design activities.

Due to our quest for a simple set of criteria, we assess effectiveness, which is the combination of efficiency and usefulness, objective and subjective criteria. Those are high-level criteria that constitute the tip of the iceberg as in figure 8.

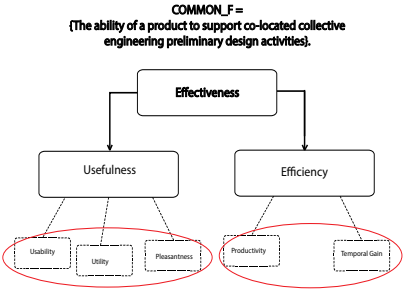

Figure 8: The criteria of effectiveness

The future of the research is to identify other functions to be compared, or to detail the criteria, as done in the red ovals.

We are well aware that the Holy Grail of a common shared standard for comparing computer-based and paper-based computer tools is far from being reached. On the other hand, we defend the necessity to introduce and to discuss over a minimalist set of functions (with their criteria) to assess across the different studies in the domain.

Acknowledgement

The TATIN-PIC project is co-funded by the European Union and the region of Picardy. Europe is committed to the Picardy Region with "Le Fond Européen de Dévelopement Régional" (The European Fund for Regional Development).

Article 038-i-100

7- References

[AA1] Adams F. and Aizawa, K. The bounds of Cognition. Blackwell Publishing, 2008.

[BB1] Buisine S., Besacier, G., Aoussat, A. and Vernier, F.: How do interactive tabletop systems influence collaboration? In Computers in Human Behaviour 28:49-9, 2012.

[BC1] Blessing, L. and Chakrabarthi, A. DRM: a Design Research Methodology, Springer Berlin, 2009.

[C1] Christenses C., The Ongoing Process of Building a Theory of Disruption. In Journal of Product Innovation Management, 23:39-55, 2006.

[CC1] Clark, A. and Chalmers, D.J. The extended mind. In Analysis 58 :7-19, 1998.

[D1] Dawes, J. Do data characteristics change according to the number of scale points used ? In International Journal of Market Research. 51(1), 2008.

[DL1] Denzin, N. K., and Lincon, Y. S. The discipline and practice of qualitative research. In Handbook of qualitative research, 2000(2) :1-28, 1994.

[FA1] Ferreira A. and Antunes P. A Technique for Evaluating Shared Workspaces Efficiency. In: Shen, W., Luo, J., Lin, Z., Barthès, J.-P.A. and Hao, Q. (Eds.), Computer Supported Cooperative Work in Design III, Lecture Notes in Computer Science. 1:82–91.. Springer Berlin Heidelberg,

[G1] Goldschmidt G., The designer as a team o f one. In Design Studies, 6(2) :89–209, 1995.

[GG1] Guerra, A.L., Gidel, T., Vezzetti, E. and Kendira, A. Co-evolution of design methods and CSCWD systems to improve the preliminary design process, Colloque CONFERE, 2012.

[GG2] Guerra, A.L., Gidel, T., Vezzetti, E., Kendira and A., Jones, A. Co-evolution of design tactics and CSCWD systems: Methodological circulation and the TATIN-PIC platform, Proocedings of the 19th International Conference on Engineering Design – ICED13, 9:315-324, 2013.

[GK1] Gidel, T., Kendira, A., Jones, A., Lenne, D., Barthès, J.P. and Moulin, C. Conducting Preliminary Design around an interactive tabletop. ICED - International Conference on Engineering Design, 2011.

[H1] Huber, G.P., A Theory of the Effects of Advanced Information Technology on Organisational Design, Intelligence, and Decision Making. In Academy of Management Review, 15(1):47-71, 1990.

[H2] Hutchins, E., Cognition in the wild. Cambridge, MA, MIT Press, 1995.

[HR1] Hartmann, B., Ringel Morris, M., Benko, H., Wilson, A. D.: Pictionaire: Supporting collaborative design work by integrating physical and digital artefacts. In: CSCW'10 international conference on computer-supported cooperative work, 421–424, ACM Press, 2010.

[HT1] Hilliges, O., Terrenghi, L., Boring, S., Kim, D., Richter, H. and Butz, A. Designing for collaborative creative problem solving. In Proceedings of C&C'07 international conference on creativity and cognition, 1:137–146, ACM Press, 2007.

[HT2] Herrmann A., Tomczak T., Befurt R., Determinants of radical product innovations. In European Journal of Innovation Management, 9(1) :20 – 43, 2006.

[J1] Johansen R., Groupware: Computer Support for Business Teams. The Free Press, Macmillan Inc, New York,1988.

[JK1] Jones A., Kendira, A., Lenne D., Gidel, T. and Moulin C. The TATIN-PIC Project – A Multi-modal Collaborative Work Environment for Preliminary Design. CSCWD – International Conference on CSCWD, 2011.

[ML1] Mac Leamy, P. Collaboration, integrated information and the project lifecycle in building design, construction and operation. The Construction Users Roundtable, WP-1202. 2004.

[ND1] Nunamaker, J.F., Dennis, A.R., Valalich, J.S., Vogel, D.R. and George, J.F. Electronic Meeting Systems to Support Group Work. In communications of the ACM, 34(7):40-61, 1991.

[OT1] Olson J.S., Teasley S., Covi L. and Olson G. The (Currently) Unique Advantages of Collocated Work. In P.J., Kiesler, S.B., Distributed Work. MIT Press, 2002.

[P1] Goldschmidt G., The designer as a team o f one. In Design Studies, 6(2) :89–209, 1995.

[PB1] Paulson Jr., Boyd C., Designing to Reduce Construction Costs. In Journal of the Construction Division, 102(4):587-592, 1976.

[RL1] Rogers, Y., Lim, Y. K., Hazlewood, W. R. and Marshall, P. Equal opportunities: Do shareable interfaces promote more group participation than single user displays? In Human–Computer Interaction 24:79–116, 2009.

[SC1] Scott, S. D. and Carpendale, S.. Interacting with digital tabletops. In: Special issue of IEEE computer graphics and applications, 26, 2006.

[SC2] Scott, S. D., Carpendale, M. S. T. and Inkpen, K. M.: Territoriality in collaborative tabletop workspaces. In Proceedings of CSCW international conference on computer-supported cooperative work, 1:294–303, ACM Press, 2004.

[SG1] Stewart, J., Gapenne, O. and Di Paolo, E. Enaction: Toward a New Paradigm for Cognitive Science, MIT Press, 2010.

[S1] Scaravetti, D., Formulation préalable d'un problème de conception, pour l'aide à la décision en conception préliminaire. Thèse de doctorat, Bordeaux, France: ENSAM, 2004.

[S2] Shiba S., Les outils du management de la qualité: guide pédagogique. Nanterre, Paris: Mouvement français pour la qualité, 1995.

[WC1] Woolley, A. N., Chabris, C. F., Pentland, A., Hashmi, N. and Malone, T. W.: Evidence for a collective intelligence factor in the performance of human groups. In Science, 330:686–688, 2010.

[WS1] Wang L., Shen W., Xie H., Neelamkavil J. and Pardasani A. Collaborative conceptual design – state of the art and future trend. In Computer-Aided Design, 34:981-996, 2002.

Article 037-i-48

Consistency management and PLM interoperability to support collaboration in preliminary design

Diana Penciuc[1], Alexandre Durupt[1], Matthieu Bricogne[1], Benoît Eynard[1]

(1) : Department of Mechanical Systems Engineering,
Université de Technologie de Compiègne (UTC), UMR 7337 Roberval, Compiègne, France
E-mail : {diana.penciuc, alexandre.durupt, benoit.eynard, matthieu.bricogne}@utc.fr

Abstract: During design, several actors contribute with their expertise in specific design tasks and need to collaborate several times in order to validate the decisions taken in order to converge to a common-agreed solution. Although a lot of tools exist to support collaborative activities during design, there still is a lack of tools enabling the integration of all the engineering results and consistency check. To overcome this drawback, a new approach of Product Lifecycle Management (PLM) interoperability is proposed in this paper, taking in account the coherence and collaboration needs specific to early design activities. The proposal is explained trough a case study and PLM connector prototype.

Key words: collaborative engineering, preliminary design, product lifecycle management, PLM interoperability, PLM connector.

1- Introduction

Because of the increasing complexity of systems, their variability, and evolution of customer needs, engineering design has become more and more challenging and requires the collaboration between heterogeneous teams holding expertise in specific design-tasks. Thus, design outcomes of each expert have to be put together without affecting the global design integrity. As the representation of design knowledge varies according to the expertise field, the interoperability between knowledge coming from different experts is necessary in order to correlate the representation of one knowledge domain to another. Typical enterprise application integration solutions propose dedicated tools which allow the coupling between engineering software by mapping data representation from one tool to another. Nevertheless, this has resulted in a considerable mass of one-to-one interlinked software, which cannot provide an overall coherence between data coming from each design engineering tool.

Contrary to the point-to-point architecture, the mediator architecture [Guyot, 2007] suggests the use of a central structure storing a reference model to which all the systems to be integrated are connected. This paper presents an approach for consistency management and PLM interoperability in preliminary design based on the mediator architecture.

The work presented here is closely related to the French ADN project (ADN comes from "Alliance des Données Numériques", meaning digital data alliance: http://www.systematic-paris-region.org/fr/projets/adn). The ADN project proposed a knowledge meta-modelling framework with the purpose of maintaining the coherence of knowledge and data along the engineering activities. For this purpose, the framework enabled to define the Knowledge Configuration Model (KCModel). The KCModel corresponds to the reference model in the mediator architecture approach. The platform implementing the reference KCModel is connected via application connectors to the engineering tools (PLM, CAx etc.) in order to support expert data synchronization. In this paper the interoperability problem is addressed with a PLM tool and an architecture implementation of a connector enabling the communication with other engineering tools via the central ADNCore platform. The aim is to develop a technical framework for interoperability with a PLM system. The proposed framework is implemented for the interconnection with the Windchill10.0 [PT1] system based on the web-services provided by this tool. The approach is illustrated by a case study and several examples demonstrating the interlinking between Windchill10.0 and ADNCore.

First, a literature review of the main PLM interoperability approaches is presented. Next, the ADN project is introduced and the knowledge model (KCModel) is explained. The latter sets the basis for knowledge representation and exchange between the stakeholders contributing to the preliminary design. The third section describes the proposal of a PLM connector based on the mediator architecture approach (the communication model and specifications are detailed). Section 5 gives the actual implementation of the connector: a generic, re-usable architecture is given and the web interfaces. Next sections discuss the results and conclude with future directions.

2- Literature review of PLM interoperability approaches

According to [TB1], PLM can be defined as “a product-centric lifecycle-oriented business model, supported by ICT (Information and Communications Technology), in which product data are shared among actors, processes and organisations in the different phases of the product lifecycle for achieving desired performances and sustainability for the product and related services”. ICT plays a major role in the implementation of the PLM concept in terms of tools, architectural choices, interoperability etc. and is considered one of the three fundamentals of PLM along with methodologies and processes [TB1]. In the extended enterprise, the scope and purpose of PLM evolve [S1], to meet new needs and allow people to work more efficiently [SI1] and interconnect with other information systems like ERP (Enterprise Resource Planning), CRM (Customer Relationship Management) etc. [SR1]. In this paper, the ICT point of view is addressed and more particularly the interoperability aspect, which is crucial with respect to the need of interconnecting several systems to obtain the global enterprise information system [EG1].

The interoperability needs are confirmed in several projects like ATHENA project (Advanced Technologies for Interoperability of Heterogeneous Enterprise Networks and their Applications) [R2], INTEROP (Interoperability research for networked enterprises applications and software), COIN (Collaboration and interoperability for Networked enterprises) etc.

In practice, three major approaches are currently used to support interoperability and data exchange between Computer Aided applications (CAX) (X such as Design, simulation, etc.) and between CAX and other data management systems: 1) ontology and semantic web technologies, 2) standards and 3) web services. In the following, each one of the three approaches is described.

2.1 Ontology and Semantic Web technologies

The first approach uses the ontology and Web Semantic technologies to achieve the data mapping between heterogeneous software at the conceptual level. Several studies implementing different approaches to product design have been conducted on ontology, as standard for data exchange between design and other engineering activities in collaborative tasks [BX1]. In the PLM field, [PD1] have proposed the ONTO-PLM framework, as a common core model to provide an interoperability solution between product data (encapsulated in PLM) and enterprise applications that manage them such as ERP, CAD (Computer Aided Design) and MES (Manufacturing Execution System). The conceptual framework proposed to conceptualize existing standards, particularly the ISO 10303 and IEC 62264 standards related to product technical data modeling. Model-driven and knowledge-based architecture also advocate semantic interoperability between PLM systems and other applications [BG1]. For example, the concept of generic product model is used by [MH1] for the development of a neutral data model used to support the interconnection between a data warehouse and an ERP system.

2.2 Standards

The second category uses a standard-based mechanism to guarantee the semantic translation between heterogeneous models [6]. Several standards exist, and may be classified in product standards, process standards, web standards etc. Some of them were studied in the ATHENA project: process standards (ISO15288, CMII), product standards like STEP - STandard for the Exchange of Product model data (e.g.: AP214, 233, 209, 239) [R2]. In this category, can be included IGES (Initial Graphics Exchange Specifications) and DXF (Drawing Exchange Format) standards used to manage the geometric data of the product [CM1], or XML (eXtensible Markup Language) to support data mapping and communication between heterogeneous data on the web.

In the PLM field, the PLCS (Product LifeCycle Support) corresponds to the STEP AP239 standard created by the International Standard Organization in 2005 [R1] to offer a generic framework for the integration, exchange and management of technical data necessary for the support of a complex product and its evolution along its whole lifecycle. Based on this standard, [PC1] have proposed an interoperability framework to perform data mapping between ERP and PLM.

2.3 Web services

The last category uses dynamic interfaces, based on API Standards (Application Programming Interface) and web services technologies, to guarantee the communication between software [SR2]. In this kind of interoperability mechanism, software integration is fulfilled through the web services to support the distribution of heterogeneous information between the members of a project team. In the PLM field, the "OMG PLM Enablers" based on middleware technologies and the "PLM Services" [GH1] are Web technologies developed to support communication between PLM systems and between PLM and other CAX applications [WG1], [LN1], [CY1]. Another way to support inter-enterprise collaboration throughout the product lifecycle is to focus on the interactions at the workflow level, as in: [JS1], [AM1].

3- Reference knowledge model to maintain the consistency of engineering data (the KCModel)

As explained previously, contrary to the point-to-point architecture, the mediator architecture is based on a central system holding a reference model, to which are linked all the systems to be connected. In the same way, the ADN project proposed a reference model (the KCModel) and a central system (the ADNCore) which are described in this section. The KCModel provides a unique representation of the knowledge produced by the experts working on the preliminary design of a product.

In engineering design, the need of knowledge capitalization appears at several levels: 1) capitalize knowledge during a project-phase to re-use it during the same project-phase, 2)

capitalize knowledge of a project to re-use it for other projects, 3) capitalize knowledge from one project-phase to re-use it in other project phases, 4) cross-processes knowledge capitalization which allows an analysis of production processes and know-how with the purpose of their continuous improvement. The purpose of ADN covers mainly the first two capitalization needs. The third need of knowledge capitalization from one project phase to another, is only partially enclosed, as ADN targets only the early-phases of design and do not consider the entire product lifecycle.

The objective of the ADN project is to answer to the increasing need of design process optimization, which is crucial mainly in early phases of product development, by providing a new knowledge management model. The incentives for this new model are based on the observation of recurring problems in system design:

- Data duplication, data loss, non-coordination between expert data, which causes incoherence,
- Great diversity of expertise fields (mechanical, thermal, etc.),
- Diversity of modelling situations,
- Heterogeneity of tools used and implicitly of data and knowledge representation,
- Constant evolution of models all along the product development process; this is even more critical in early phases like trade-off and pre-sizing;

In this context, the target knowledge consists of expert rules jointly used with design parameters. These are considered as critical knowledge essential for successful design result.

In order to overcome the above-mentioned problems and to ensure the coherence between data of all stakeholders, ADN proposed a unique knowledge representation through the KCM model. Based on the analysis of several product models, [BM1] remarks that the critical knowledge "does not depend on a function or a particular component but needs to be managed at a higher level of abstraction". The critical knowledge must have its own structure and organization, its own life cycle to be exchanged and maintained in coherence during the collaboration process where many disparate expert models are used". In consequence, the KCM (Knowledge Configuration Model) defined the concept of "knowledge configuration" which consists of a set of parameters and constraints on the parameters (expert rules, mathematic relations etc.). The basic knowledge unit defined is the "Information Core Entity" (ICE) which represents a generic multi-domain baseline. The usage of the ICE in a particular context is denoted by a "Configuration Entity". Each expert may then hold several "user configurations" in their working context and the coherence between different expert outcomes is maintained through synchronization of user configurations in "skeleton configurations". The KCM approach is presented with more details in [BM1], [BC1], [FD1].

In the following, a simple example is given (extracted from [BM1]) with the purpose of explaining the use of KCM in a real-world situation.

Consider two expert models that share the same parameters: Ø and λ, as shown in Figure 1. These are represented in the KCM by the ICE1. Each expert model contains a supplementary parameter, which is contained each in a separate ICE (ICE2 and ICE3 respectively). Two user configurations exist in this case, each composed of an instance of the common ICE1 and an instance of the ICEs holding the third parameter of each model (ICE2 and ICE3). Synchronization of the two configurations will allow the ICE1 instances to be coherent and to hold the same parameter values.

As stated earlier, knowledge may come from experts working each on a specific engineering tool. Therefore, the ADN core application implementing the KCModel needs to communicate with each of the engineering tools to federate the whole engineering knowledge. To accomplish this goal, application connectors are needed to allow information exchange between the ADN core and the engineering tools as well as the synchronisation task described earlier in this section. Thus, the ADN project identified four connectors that are crucial for early-design activities:

1- Connector for CAD applications to support integration of knowledge resulting from mechanical design,
2- Connector for knowledge-based engineering applications which enables conflict management,
3- Connector for product-data and lifecycle management applications to support integration of technical product and lifecycle data,
4- Connector for requirements management applications to integrate knowledge resulting from customer need specification.

In this paper, a proposal of a product-data management connector is given from specifications to the description of the first connector prototype.

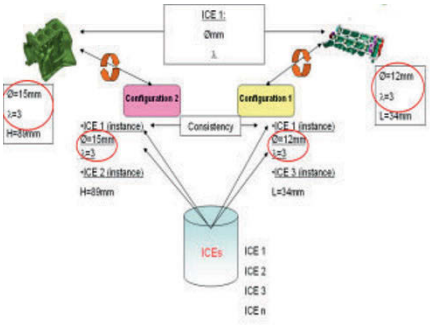

Figure 1: Example of the KCM usage in a real-world application.

4- Connector specifications for PLM interoperability

4.1 – Scenario of information flows between PLM, ADN and CAx systems

Checking the consistency between design ICEs, as described above, is part of a more global collaborative process that

implies several interactions between experts and information systems (CAX, AND, PLM) on one hand, and in-between these systems on another hand.

In industry, PLM systems are considered as the official repository for the management of all technical data of a product. Data considered should take into account product configuration, document versioning and history traceability, etc. To this end, the expert must create a part in the PLM system before creating all associated technical documents, such as the CAD files, as shown in Figure 2. In the next step, the expert creates new user configurations in his ADN workspace, in order to guarantee that his activity results will considered during the "consistency checking" process. For this purpose, a reference link should be created to associate the part created in PLM to the user configuration created in ADN.
In parallel, the expert can check out his CAX model, modify it and "check-in" it to the PLM tool. He updates his user configuration in the ADN workspace to consider new parameters values.

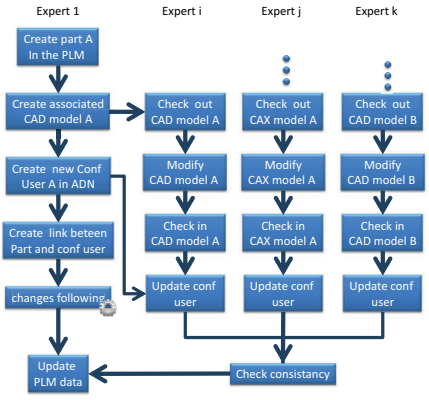

Figure 2: interaction between ADN, CAX and PLM.

However, to guarantee that the last user configuration is the official version shared by all design project experts, the PLM system should be automatically notified in order to update the version of the associated part. This important synchronization action is fulfilled by means of the "changes following" mechanism which exploits the reference links to automatically identify correspondences between ADN modified objects and associated product parts in PLM.

The synchronization process can be envisaged in the opposite way, from PLM to ADN. In this case, the user works directly in PLM and after the "check-in" operation, the PLM notifies all the concerned ADN users that they must update the version of the associated user configurations.

In both cases, the PLM connector has the role to ensure the synchronization between the ADN and PLM objects according to a set of functionalities covering different integration levels. Our proposal is to manage the mapping between the reference links (extracted from heterogeneous information systems) in an independent application (the PLM connector), with the purpose of maintaining data coherence by synchronizing it with the unique ADN reference.

The next section presents the conceptual specifications of the proposed connector as a list of connector functions. The interactions between ADN, PLM and the connector are highlighted.

4.2 – Functional specifications of the PLM connector

The PLM connector was conceived to function independently of the connected information systems. This is an important requirement with respect to the need of generality. The overall connector functions can be classified in two main functional classes:

- connection management,
- objects management.

At the connection level, the connector should verify the user credentials and access rights to the connector application. At object level, the connector should manage application-specific object types. Two main types were identified as relevant for mapping and synchronization, according to the use cases mentioned in section 3.3:

- projects in the PLM system/ workspaces in the ADN system,
- parts in the PLM system/ user configurations in the ADN system.

The synchronization is accomplished following the mechanism of notification subscription and based on the mapping of reference links stored at connector level.
Thus, the user can:

- search for and identify the objects he wants to subscribe to: objects are searched for in the ADN and PLM systems; additionally, filters may be used to refine and contextualize search,
- manage subscription to an object: once subscribed to an object, the user will be notified when the object was modified in the corresponding IS,
- manage reference links: the user can choose the pairs of objects he wants to synchronize; a reference link holds the unique identifiers of the linked objects and all the reference links are stored in the connector mapping table.

5- PLM connector implementation

5.1 – Architecture of the PLM connector

The connector was designed as a web application which is accessible independently of the information systems considered. In our case, the Windchill10.0 and the ADN2.2 environments were chosen to illustrate the implementation of the PLM connector. The connector architecture is flexible enough to allow portability and interoperability with external applications due to the separation between the interface and the application logic and the use of web services.

The implementation follows the MVC software architecture pattern. The view is defined using HTML and for the application logic, the JAX-RS Java API for RESTful web services which are controlled by JavaScript (JQuery). The communication with the external applications (Windchill10.0 and ADN2.2) is handled by the SOAPClient2.4 component, which is a JavaScript library implementing the SOAP1.1 protocol (see Figure 3).

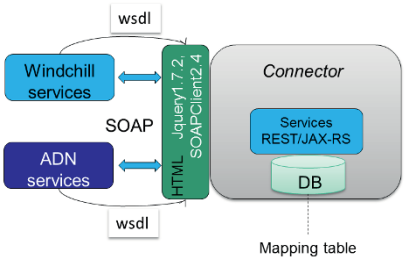

Figure 3: Windchill-ADN connector architecture.

The difference between the web service specifications used by Windchill10.0 and ADN2.2 are also handled at the connector level. As a consequence, the processing of sent and received SOAP messages is adapted according to the format accepted by each of the two environments.

It has to be noted that the Windchill component may be replaced with a different PLM application having published its services and available via SOAP. This would only affect the processing of messages sent/received from the new PLM application, and would have no impact on the other components of the architecture.

5.2 – The PLM connector application

As explained in the scenario from the section 3.1, a user will work in the integrated environment proposed by the ADN project in the following order (see Figure 2): 1) create objects in Windchill, 2) create objects in ADN, 3) use the connector to create references between ADN and PLM objects, to maintain the consistency between engineering results. In the next paragraphs, the connector prototype is illustrated following these three steps. The case study considered in this paper is related to the preliminary design phases for a "mounting bracket". These phases are considered: specification of the need, design and simulation.

5.2.1 Creation of the Windchill objects

First action is to create a project under Windchill. The project owner defines the team, the project planning etc. and the parts corresponding to the "mounting bracket". A view of the project phases and the parts are shown in Figure 4.

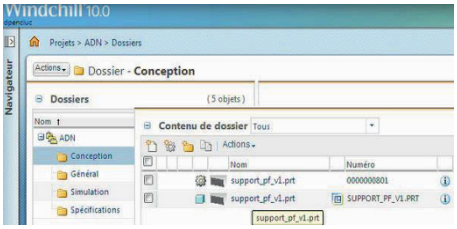

Figure 4: Windchill objects

5.2.2 Creation of the ADN collaborative objects

According to the KCModel presented in section 3, an adequate representation of knowledge is needed in order to maintain consistency across the results from different stakeholders: user configurations, ICEs, workspaces, etc. The ADN2.2 collaborative platform implements the KCModel allowing thus to create objects of the type ICEs, user configurations etc. and to operate on them: create, modify, update, delete objects, consistency check of objects submitted by distinct users, etc.

In Figure 5, a holistic view of the platform interface is given, and a focus on the *user configurations* is shown in figure 6. This view gives an inside of the last created user configurations with their characteristics (name, version, creation date, description etc.). Two of the user configurations were created by the user during the design of the "mounting bracket": "conf user cao" and "conf user fao". Meta-data is displayed along with the name of the configuration: version, creation date, description, parent configuration (which ensures the consistency between several user configurations) and status.

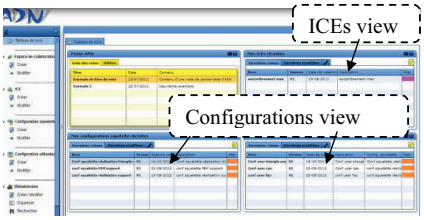

Figure 5: ADN main interface

Figure 6: ADN user configurations view

5.2.3 Creation of reference links in the connector

Three "views" are available from the main connector page, allowing user to visualize ADN and Windchill objects grouped by type, as well as the mapping table containing the synchronized objects. As an example, Figure 8 shows the ADN view from which the user can check the list of ADN workspaces and user configurations. A detailed view is available for each object, displaying its meta-data. In the figure, for the user configuration object named "Conf user cao", the meta-data and associated values are: criticality (Low), description (conf user cao) and version (V1). The "Conf user cao" object is selected for reference link creation with the Windchill object "support_pf_v1.prt", which is a CAO part created during the conception activity (see Figure 8).

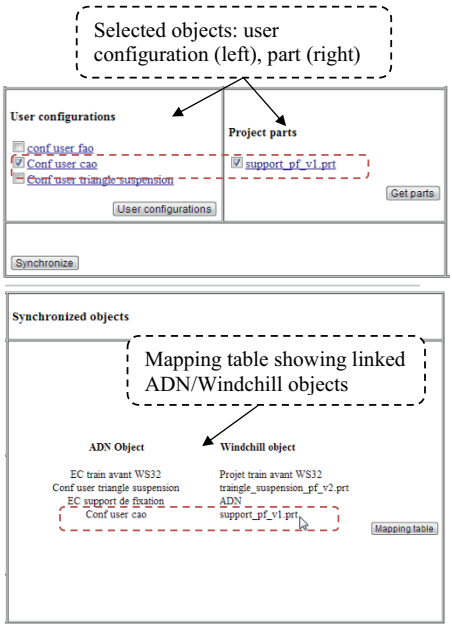

Figure 8: ADN workspace/ Windchill project synchronization.

Once the reference link is created, the linked pair is visible in the updated mapping table: in Figure 8, the last pair appearing in the mapping table is ("Conf user cao", "support_pf_v1.prt"). The pairs stored in the mapping table are all candidates for the trigger of the notification mechanism.

6- Discussion

The first prototype of the connector is a proof-of-concept for the PLM interoperability based on web services and the use of a central reference model. Nevertheless, several limits are to be noted as regard to the prototype and its evaluation. Although the connector was designed with a flexible architecture, it was only tested with a particular PLM solution, which is Windchill10.0. A step forward would be to verify its adaptability in the context of another PLM solution.
The case studies considered for the tests refer to relatively simple products, more complex case studies (by a large number of components and parameters) should be defined.
Moreover, an evaluation framework should be defined with the partner companies, in order to measure the efficiency of the prototype. The metrics to consider should take into account two aspects: the generality of the PLM connector and the performances obtained in a given setting.

7- Conclusion

In this paper, a new approach for PLM interoperability was proposed based on the need of consistency maintenance and interoperability which play a major role in collaborative engineering design. In order to cooperate efficiently, the stakeholders have to share a common understanding of the product they work on and an adequate ICT infrastructure is essential to enable knowledge exchange between heterogeneous expert models. Both issues are addressed by the ADN project proposing a common knowledge model (the KCModel) and application connectors on-purpose created to maintain interoperability between the engineering tools used in design. As an example of application connector, the Windchill-ADN connector was illustrated in this paper starting from the initial specifications to the actual architecture and prototype. Several perspectives of the present research work are envisaged: testing of the connector in an industrial setting and improvement of the HMI. The flexible architecture proposed opens perspectives on its re-use for connection with a different PLM solution, provided that this latter has already published web-services. In the long-term, the connectors proposed by the ADN project will serve as a basis for the development of generic and application-independent connectors.

8- References

[AM1] Alexopoulos K., Makris S., Xanthakis V. and Chryssolouris G. A web-services oriented workflow management system for integrated digital production engineering. CIRP Journal of Manufacturing Science and Technology, 4, p.290–295, 2011.

[BC1] Badin J., Chamoret D., Gomes S. and Monticolo, D. Knowledge configuration management for product design and numerical simulation. In The 18th international conference on engineering design (ICED11), Copenhagen, Denmark, Copenhagen, August, 15–18, p. 161–172, 2011.

[BM1] Badin J., Monticolo D., Chamoret D. and Gomes S. Using the knowledge configuration model to manage knowledge in configuration for upstream phases of the design process. International Journal on Interactive Design and Manufacturing (IJIDeM), 5:3, p. 171–185, 2011.

[BX1] Bellatreche L., Xuan D.N., Pierra G. and Dehainsala H. Contribution of Ontology-based Data Modeling to

Automatic Integration of Electronic Catalogues within Engineering Databases, Computers in Industry Vol. 57, No. 8-9, p. 711—724, 2006.

[BG1] Bermell-Garcia P., Fan I.S. and Murton A. Towards the semantic interoperability between KBE and PLM systems. International conference on engineering design, 28–31 August, Cite des sciences et de l'industrie, Paris, France, 2007.

[CV1] Chen D. and Vernadat F. Standards on enterprise integration and engineering: A state of the art. International Journal of Computer Integrated Manufacturing, Vol. 17, No. 3, pp.235-253, 2004.

[CM1] Choi G.H., Mun D. and Han S. Exchange of CAD Part Models Based on the Macro-Parametric Approach, International Journal of CAD/CAM Vol. 2, No. 1, p. 13-21, 2002.

[CY1] Choi S.S., Yoon T.H. and Noh S.D. XML-based neutral file and PLM integrator for PPR information exchange between heterogeneous PLM systems. International Journal of Computer Integrated Manufacturing, Vol. 23, No. 3, March, p. 216–228, 2010.

[EG1] Eynard B., Gallet T., Nowak P. and Roucoules, L. UML based specifications of PDM product structure and workflow. Computers in Industry, 55:3, 301–316, 2004.

[FD1] Farouk B., Dremont N., Notin A., Troussier N. and Messadia, M. A meta-modelling framework for knowledge consistency in collaborative design. Annual Reviews in Control, Volume 36, Issue 2, December, p. 346-358, 2012.

[GH1] Gunpinar, E. and Han, S. Interfacing heterogeneous PLM systems using the PLM Services. Advanced Engineering Informatics 22, p. 307–316, 2008.

[JS1] Jiang, P., Shao, X., Qiu, H., Gao, L. and Li, P. A Web services and process-view combined approach for process management of collaborative product development. Computers in Industry 60, p. 416–427, 2009.

[KA1] Kleiner S., Anderl R. and Gräb R. A collaborative design system for product data integration. Journal of Engineering Design, 14(4), p. 421–428, 2003.

[K1] Kvan, T. Collaborative design: What is it? Automation in Construction, 9(4), p. 409–415, 2000.

[LN1] Lukas, U. and Nowacki, S. High Level Integration based on the PLM Services Standard. ProSTEP iViP Science Days 2005, 28–29 September 2005, Darmstadt: Cross-Domain Engineering, p. 50–61, 2005.

[MH1] Mun D., Hwang J., Han S., Seki H. and Yang, J. Sharing product data of nuclear power plants across their lifecycles by utilizing a neutral model. Annals of Nuclear Energy 35, p. 175–186, 2008.

[NR1] Noel F., Roucoules L. and Teissandier D. Specification of a product modeling concepts dedicating to information sharing in a collaborative design context. Advances in integrated design and manufacturing in mechanical engineering, Part 1, p. 135–146, 2005.

[PD1] Panetto H., Dassisti M. and Tursi A. ONTO-PLM: Product-driven ONTOlogy for Product Data Management interoperability within manufacturing process environment. Advanced Engineering Informatics 26, p. 334–348, 2012.

[PC1] Paviot T., Cheutet V. and Lamouri S. A PLCS framework for PLM/ERP interoperability. International Journal of Product Lifecycle Management, Vol.5, No.2/3/4, p.295 – 313, 2011.

[PT1] PTC White Paper. PTC Windchill and a Service Oriented Architecture: Strategies for Optimizing New Product Development. PT Ref. Windchill/SOA-WP-1008, 2008.

[R1] Rosen J. Federated through life-cycle support, 1st Nordic conference on PLM, NordPLM 06, Göteborg, Sweden, January, 25-26, 2006.

[R2] Ruggaber R. ATHENA - Advanced Technologies for Interoperability of Heterogeneous Enterprise Networks and their Application. International Conference on Interoperability of Enterprise Software and Applications, Geneva, Switzerland, 23-25 February, 2005.

[SI1] Saaksvuori A. and Immonen A. Product Lifecycle Management, Springer, Berlin, 2004.

[SR1] Schuh G., Rozenfeld H., Assmus D. and Zancul E. Process oriented framework to support PLM implementation. Computers in Industry, Vol. 59, p. 210–218, 2008.

[SR2] Song H., Roucoules L., Eynard B. and Lafon, P. Interoperability between Cooperative Design Modeller and a CAD System: Software Integration versus Data Exchange. International Journal for Manufacturing Science & Production, Vol. 7, No. 2, p. 139-149, 2006.

[S1] Srinivasan V. An integration framework for product lifecycle management. Computer-Aided Design, Volume 43, Issue 5, May 2011, p. 464-478, 2011.

[TB1] Terzi S., Bouras A., Dutta D., Garetti M. and Kiritsis D. Product lifecycle management – from its history to its new role, International Journal of Product Lifecycle Management, Vol 4, No. 4, P. 360-389, 2010.

[WG1] Wang Y., GE J., Shao J. and Han, S. Research on Web Service-based Interoperability of Heterogeneous PLM Systems. International Conference on Measuring Technology and Mechatronic Automation. Hunan, China, April, 11-12, 2009.

Article 037-i-57

Facilitating Integration to face modern Quality Challenges in Automotive

A. Riel [1], S. Tichkiewitch [1], C. Kreiner [2], R. Messnarz [3], D. Theisens [4]

(1) : EMIRAcle,
46 av. Félix Viallet, 38031 Grenobole, France
+33 4 768 25156
E-mail : {andreas.riel,
serge.tichkiewitch}@emiracle.eu

(2) : Graz University of Technology,
Inffeldgasse 16, 8010 Graz, Austria
+43 316 873 6408
E-mail : christian.kreiner@tugraz.at

(3) : ISCN GmbH,
Schieszstattgasse 4, 8010 Graz, Austria
+43 316 811198
E-mail : rmess@iscn.com

(4) : Symbol BV,
Palatijn 14
7521PN Enschede
+31 53 2030240
E-mail : dick.theisens@symbolbv.nl

Abstract: Assuring quality in automotive has grown to a huge challenge and competition factor driven mainly by the permanent cost pressure in a mass market that is increasingly confronted with the safety criticality of various mechatronic systems and subsystems. The most successful companies have realized the necessity of integrating the development and manufacturing processes significantly more than this is done today even in the most innovative industrial organizations. This article introduces a novel vehicular qualification concept facilitating this integration process for quality and risk management in automotive industry. In particular, this concept integrates the various dimensions of the quality, safety and reliability of automotive products and systems as well as their associated processes in a way that allows quality, reliability, and safety experts from development and manufacturing to collaborate in an integrated manner.

Key words: Integration, Quality, Knowledge Management, Integrated Manufacturing, Sector Skill Alliance

1- Introduction

Nowadays electronics and software control more than 70% of a modern car's functions, and several studies predict this share to grow to 90% and more in the future [W1]. This leads to a level of complexity that has never been experienced before – both of the system "car" and the related development processes. There is a strong common agreement in the sector that interdisciplinary expertise is the absolutely indispensable fundamental basis for being able to tackle this complexity under the heavy pressure of shorter development and innovation cycles. Moreover, this demand is reinforced by the necessity of mastering essential horizontal topics such as product and process quality, reliability, and functional safety. International standards and norms about Development Quality (Automotive SPICE® [S1], ISO/IEC 15504), Functional Safety (ISO 26262 [I1], IEC 61508) and Six Sigma (production and process quality) form the backbone of the modern automotive and supplier industry. These standards make the smooth coupling of the different companies along the supply chain possible, and enable the successful integration of all parts and subsystems. In order to be eligible for OEMs, suppliers have to implement and master all these standards. This applies equally well to big companies as to small and middle-sized ones.

The holistic nature of these quality requirements and the ever increasing need for shortening development cycles imply that the topics linked to quality aspects have to be addressed in a totally integrated way. Furthermore, the capability of suppliers to master this integration is increasingly a subject of rigorous assessments demanded by OEMs [MK1]. This strong need, however, is confronted with a lack of qualified specialists and even more so of interdisciplinary "all-rounders" that can act as the links between different expert groups [KM1]. The research presented here addresses this lack by identifying the essence of the concerned specialist topics and integrating it in a compact and modular certified and e-learning enabled training program. The "essence" is considered to be the very share of knowledge in all three topics that is vehicular, i.e., that can drive the integration of related stakeholders within existing organisations. Identifying and explicitly elaborating this vehicular knowledge [TG1] has never been done before, and is therefore considered a real research challenge. The strong need for it is manifested by the fact that this research has been selected for co-funding by the European Commission as a pilot action for the automotive sector in the AQUA project of the H2020 Sector Skill Alliances program.

Section 2 of this paper explains the principal research objectives, while section 3 outlines the applied research methodology applied by the newly created automotive sector skill alliance. Section 4 summarises one of the key results obtained so far, which is essentially the qualification program for integrated quality engineering and management in automotive. Section 6 concludes the paper and gives an outlook on further research and valorisation activities.

2- Objectives

Integrated design and manufacturing form a central research area of the IDMEE community. The work presented here capitalizes on this research in that it investigates the integration of stakeholders who are somehow concerned with quality and risk for the purpose of mastering product-level quality and risk better than organisations do today. Beyond the "why" and "what for", it deals with the essential question of "how" to achieve this integration challenge on an organisational level using the lever of qualification for vehicular knowledge on a broad level.

The three core objectives of our research program are the following:

1- The integration of Automotive SPICE, Functional Safety and Six Sigma in one compact and modular e-learning enabled certified VET training program,
2- a sustainable alliance of key stakeholders for the continuous further development of this program,
3- the dissemination and deployment of the research results in the automotive sector, in particular the European automotive supplier industry.

This article mainly focuses on the achievement of the first two objectives.

3- Methodology

The core idea is to identify vehicular bricks of knowledge about essential quality- and risk-related activities in the product creation process (i.e., design, development, and production), and to explain them in the context of the three target domain experts' points of view. The identification of such bricks was done systematically by the analysis of the following sources:

1- The standards relevant to the respective three areas,
2- published experience reports about best practices in the implementation of these standards,
3- Unpublished results of expert working groups (German and French industry and university representatives) around the topics quality, reliability, and functional safety.

In order to identify these knowledge items, the European Sector Skill Alliance AQUA (Knowledge Alliance for Quality and Excellence in Automotive) was formed according to the architecture shown in Figure 1. The key issue in this alliance is that it brings together key representatives of the automotive supplier industry (via the automotive clusters in Austria and Slovenia) with renowned assessment, consulting, coaching and training service providers (ISCN in Austria and Ireland, Symbol in The Netherlands), as well as innovation and research authorities (via EMIRAcle and Graz University of Technology). This alliance will launch further research and research valorisation initiatives that address specific challenges related to quality and excellent performance of the automotive industry. It represents a particular instantiation of a knowledge triangle linking industry with research and education.

The key criteria for a specific term to be considered vehicular

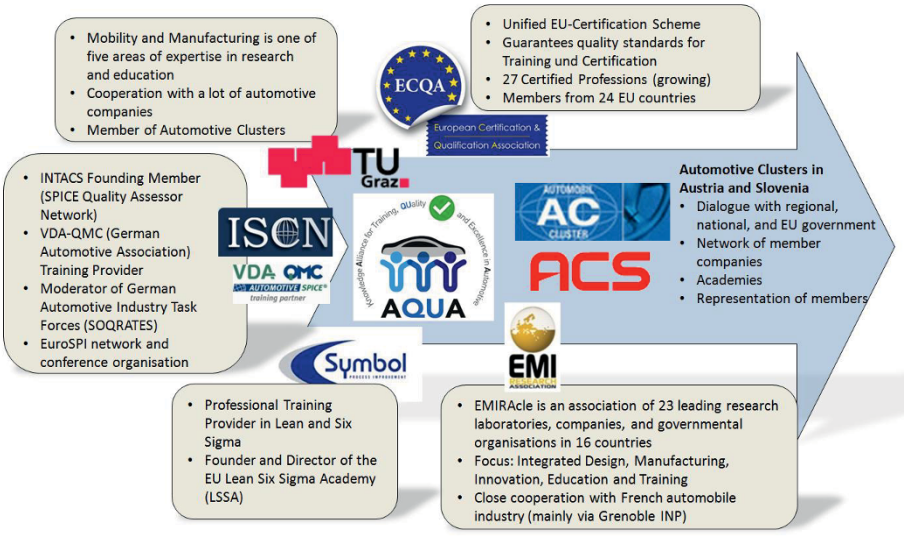

Figure 1: The AQUA Automotive Sector Skill Alliance.

are that

- it represents a notion that has an essential meaning in all three expert areas,
- it is used with same or different wordings in at least two of the three areas,
- It contributes essentially to the systemic quality and risk and/or reliability aspect of the product, service, and related processes.

The results have been compiled into an EQF-compliant [E1] skill card which describes the competency requirements to a quality integration expert in a hierarchical manner: on the top level there are the skill units which contain skill elements characterised by performance criteria. This initial skill card has been reviewed systematically by several experts from various automotive clusters with respect to specific qualification needs, in particular those of tier-1 and tier-2 suppliers. It provides the basis for the definition of the training program, the elaboration of the training material, as well as the certification process. The strong need for such an interdisciplinary certified training program has also been confirmed by several automotive clusters [KM1]. Furthermore, the positive impact of targeted qualification on company's quality management maturity has been shown in scientific research [RW1].

Another key methodological step was to come up with an architectural concept that allows both trainers and trainees to capitalise on existing training programs in the three expert areas while providing them convenient and understandable access to the core vehicular knowledge that links them together. Figure 2 indicates the concept that the project team has implemented: based on existing established programs in the areas Automotive SPICE, Functional Safety, and Six Sigma, some specific "linking elements" have been defined. For each of these elements (e.g. life cycle, requirements, etc. in Figure 2), new training modules have been developed ("AQUA Integrated View" in Figure 2), explaining the relevance of key terms related to the respective element, and how they relate to the specific (vernacular) terms used in the three expert areas. Thanks to this modular architecture, companies can compose trainings that correspond to their specific needs in terms of building up capacities fostering the integrated treatment of quality and risk aspects in their specific organisations. This is a very important success factor of the training program, as automotive OEMs and suppliers will have to have a large number of employees trained in order for the integration to be able to happen effectively and sustainably. Even for large enterprises it is financially unviable to train a significant number of employees in Automotive SPICE, Functional Safety,, and Six Sigma using the existing specialised training programs (indicated by the large horizontal bars in Figure 2). The presented training program and approach, however, enables them to pick concise and practice-oriented training modules on essential vehicular quality and risk aspects, as well as on how to integrate them in engineering and production processes.

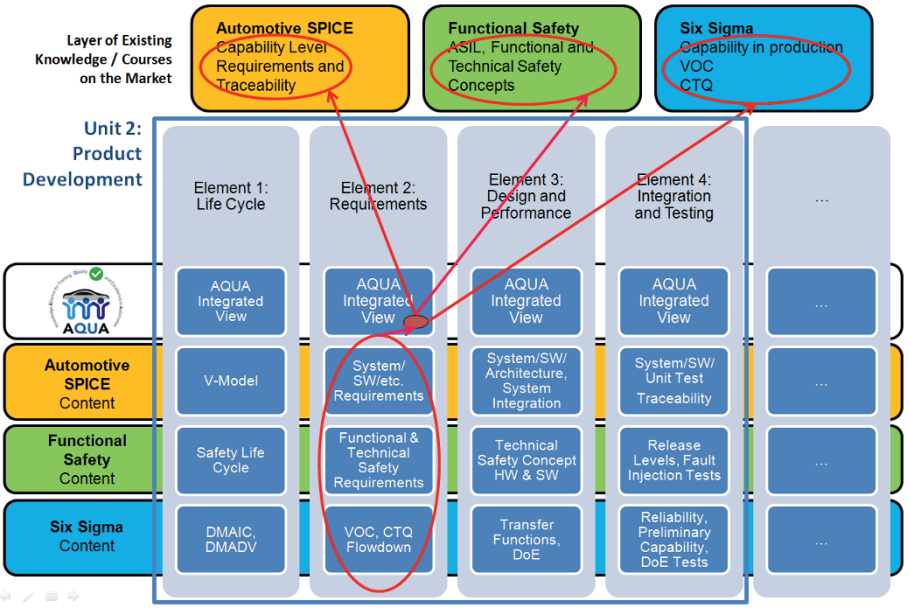

Figure 2: Modular Architecture of the AQUA Training Program for Integrated Quality and Risk Engineering in Automotive

4- Results

In our research project so far, we have identified and agreed on a skill structure that clearly identifies the vertical (vernacular) and horizontal (vehicular) competencies that serve as keys to integrating stakeholders of the three expert domains in order to achieve the required quality levels in a holistic manner. This holistic approach has been identified by automotive stakeholders in our sector skill alliance as one of the most crucial levers of increasing the competitive edge.

Training material covering the performance criteria related to Automotive SPICE, Functional Safety and Six Sigma can be developed based on existing training programs (cf. Figure 2). Our current key research challenge, however, is to establish the integrated views on the identified vehicular subjects relating to each competency element. This is completely new, we do not know of any related published works. While there are publications about how to integrate Automotive SPICE with Functional Safety [MK1], there are no materials available so far about how to integrate all three methods in an integrated engineering life cycle.

The following sections will give an outline of the complete program in the form of training units that are composed of training elements. Each element is characterised by four performance criteria (in this order):

- Performance criterion related to the integrated view on Automotive SPICE, Functional Safety, and Six Sigma.
- Performance criterion related to Automotive SPICE.
- Performance criterion related to Functional Safety.
- Performance criterion related to Six Sigma.

For each of these skill elements, training material in the form of slides with notes has been developed. To facilitate e-learning, recorded versions of these presentations have been made available in the integrated e-learning environment of the ECQA [E2]. Furthermore, for each performance criterion, a set of multiple-choice test questions has been created. These questions are the basis for the certification of candidates within the ECQA exam portal.

4.1 – U1 Introduction

This unit gives an overview about the purpose and necessity of each expert domain with respect to quality and safety, as well as the need of an integrated approach. Both technical and organisational viewpoints are elaborated.

4.1.1 – U1.E1 Standards, Norms, and Guidelines

This element introduces the essentials technical challenges of each AQUA expert domain, and provides an integrated view on them.

- Understand how the Six Sigma, Automotive SPICE, and Functional Safety can be combined in the overall engineering process.
- Describe the motivation and the architecture of Automotive SPICE.
- Describe the motivation and the architecture of ISO 26262.
- Understand the DMAIC methodology and tools & techniques according ISO 13053. Understand the skills sets needed by Lean Six Sigma Belts.

4.1.2 – U1.E2 Organisational Readiness

This element introduces the essentials organisational challenges of each AQUA expert domain, and provides an integrated view on them.

- Understand the essential role of interdisciplinary teams to facilitate integration in the specific context of holistic quality engineering and management.
- Describe the organisational requirements to development teams and their competencies according to Automotive SPICE.
- Describe the organisational requirements for a good safety culture and successful safety management.
- Describe Six Sigma level of expertise: Master Black Belt, Black Belt, Green Belt, Orange Belt and Yellow Belt.

4.2 – U2 Product Development

This unit investigates the domain expert and integrated views on the subject of product development. Based on the life cycle view, the principal subjects are requirements management, design, as well as integration and testing.

4.2.1 – U2.E1 Life cycle

This element deals with the life cycle view and understanding according to the three expert domains, as well as their integration.

- Understand how the Six Sigma, Automotive SPICE, and Functional Safety can be combined in an integrated life cycle approach.
- Describe the life cycle concepts underlying Automotive SPICE.
- Describe the safety life cycle according to ISO 26262.
- Understand and follow the Six Sigma DMADV and DMAIC roadmap. Identify and select the proper tools to use during the Process Improvement project and the design (DFSS) phase.

4.2.2 – U2.E2 Requirements

This element explains how requirements are managed in the three expert domains, as well as how an integrated approach looks like.

- Understand the complementary key roles of requirements management in the three expert domains.
- Describe the requirements related processes and traceability concept in Automotive SPICE.
- Describe the derivation of the safety requirements from the hazard analysis and risk assessment, as well as the integration of the safety requirements into the system requirements and the technical safety concept.
- Show how the project will impact customers. Identify internal and external customers. Define and describe CTQ requirements (critical to quality) and the importance of aligning projects with those requirements. Translate Voice of the customer (VOC) requirements into project goals and objectives. Translate objectives into CTQ targets and specifications.

4.2.3 – U2.E3 Design and Performance

This element deals with the view on the design approach of the three expert domains, as well as their integration.

- Understand the complementary views on design in the three expert domains.

- Describe the different levels of design and the traceability concept in Automotive SPICE.
- Describe the different levels of the functional safety related design process.
- Describe and apply DOE principles and terms: Responses, Variables, Factors, Levels, Interactions, transfer function. Understand the difference between full factorial experiments and fractional factorial experiments.

4.2.4 – U2.E4 Integration and Testing

This element explains how integration and testing are managed in the three expert domains, as well as how an integrated approach looks like.

- Understand the complementary views on integration and testing in the three expert domains.
- Describe the different levels of testing and the traceability concept in Automotive SPICE.
- Describe the verification and validation concepts according to ISO 26262.
- Understand which different types of tests can be used during product development.

4.3 – U3 Quality and Safety Management

This unit puts a focus on the program's essential aspects quality and safety management in terms of the transversal subjects Capability, Hazard and Risk Management, as well as Assessment and Audit. It explains the particular significance of these subjects in each expert domain, and why and how an integrated view can and should be adopted.

4.3.1 – U2.E1 Capability

This element explains how the term Capability is understood in each of the three expert domains, and shows an integrated view allowing understanding capability holistically.

- Understand how the Six Sigma, Automotive SPICE, and Functional Safety can lead to a more complete concept of capability of the development process, product, and production (P3 concept).
- Describe the capability dimension in Automotive SPICE.
- Describe the concept of automotive safety integrity levels (ASILs) as a principal requirement and measure of capability in automotive functional safety.
- Understand the relationship between long-term and short-term capability. Define, select and calculate Cp and Cpk to assess process capability. Define, select and calculate Pp and Ppk to assess process performance.

4.3.2 – U2.E2 Hazard & Risk Management

This element deals with the management of hazards and risks from the three expert areas' points of view, and explains an integrated approach.

- Understand the complementary views on hazard and risk management in the three expert domains.
- Describe how Risk Management is implemented in Automotive SPICE.
- Describe the Hazard Analysis and Risk Assessment and Management concept according to ISO 26262.
- Define and document the key functions of a design, the primary potential failure modes relative to each function and the potential causes of each failure mode.

4.3.3 – U2.E3 Assessment and Audit

This element explains the essential role of assessments and audits in all the expert areas, as well as an integrated approach to these activities.

- Understand how the Automotive SPICE, Functional Safety, and Six Sigma assessment and audits methods form an integrated concept.
- Describe the assessment method of Automotive SPICE.
- Describe safety audit and assessment requirements according to ISO 26262.
- Understand how to prepare for internal audits. Understand the audit process and different roles.

4.4 – U4 Measure

This unit deals with measurements and reliability in the context of the three expert domains and their integration.

4.4.1 – U4.E1 Measurements

This element investigates the role of measurements in the three experts, as well as the integrated view on it.

- Understand how the Six Sigma, Automotive SPICE, and Functional Safety can be combined in the overall measurement system.
- Describe the typical metrics and measurements expected by Automotive SPICE.
- Describe key metrics used to measure risk in automotive functional safety.
- Calculate process performance metrics such parts per million (PPM), defects per million opportunities (DPMO), defects per unit (DPU), process yield and First Time Right (FTR) yield. Understand the various factors that influence Measurement System Variation (accuracy (bias), precision (repeatability and reproducibility) and stability.

4.4.2 – U4.E2 Reliability

This element explains the significance of reliability in the three expert domains, as well as in an integrated view.

- Understand the role of the reliability notion in an integrated development approach linking Six Sigma, Automotive SPICE, and Functional Safety.
- Describe the connection of Automotive SPICE with reliability.
- Describe the key role of reliability measures, in particular FIT rates, for the achievement of the overall functional safety integrity level achievement,
- Define reliability specifications and design tests to demonstrate these reliability specifications. Analyze failure data of life time tests.

5- Conclusion and Outlook

The need for organisations, methods and tools for the integration of different expert groups and departments has been widely documented in the research community over several years. Our research addresses this challenge for the topic of quality and risk in automotive essentially via the terminology lever in that it has developed a sophisticated and worldwide unique training architecture around the principal

vehicular terms and subjects in the area of quality in development and production of mechatronic systems and subsystems. The idea and approach are completely new, and first dissemination actions targeting automotive suppliers in Austria, Czech Republic, Germany, France, Slovenia, and The Netherlands have confirmed their high relevance to their needs. Given the huge challenges that organisations have been facing with the realisation of integrated product creation concepts, we believe that our research results can be considered a significant contribution to the research question of how such integration concepts can actually be driven, leveraged, and deployed in existing industrial environments without changing the complete organisation and central processes (as changing these takes a long time and huge investments). Many organisations have learned the lesson that integration of stakeholders does not happen, but can only be the result of much targeted specific actions and strategies aiming at enabling stakeholder communication and collaboration on all organisational levels. In the presented approach, the main lever is a very specific targeted interdisciplinary training program based on a sophisticated modular architecture allowing the focussed investment of companies in the acquisition of vehicular knowledge by a large number of concerned stakeholders. In order to help them maintain these investments at a reasonable level while at the same time making the training accessible to as many concerned employees as possible, the training is supported by fully-blown e-learning facilities. Moreover, a Europe-wide certification by the ISO 17024 [I2] compliant ECQA [E1] assures the high level of both the recognition of the program and its quality and continuous improvement und update. As such, this program neatly integrates into the series of certified e-learning enabled training programs for industry and academia that have been created under strong involvement of the EMIRAcle association, and which are also available to IDMME members [TR1].

Future research activities include the assessment of several indicators obtained by the actual deployment of the training program in several companies in terms of efficiency, effectiveness, influence of the training lever on the organisations' integration capabilities, etc. These figures, in combination with further experiences and feedback collected during the trainings will enable progress in judging the relative importance of the explicit presence and support of vehicular knowledge in an organisation in order to leverage stakeholder integration for a very specific objective.

6- Acknowledgements

This research is financially supported by the European Commission in the AQUA (Knowledge Alliance for Training, Quality and Excellence in Automotive) project as a pilot in the new Horizon 2020 (H2020) Erasmus+ Sector Skill Alliances Programme under the project number EAC-2012-0635. This publication reflects the views only of the authors, and the Commission cannot be held responsible for any use which may be made of the information contained therein.

7- References

[E1] The European Qualifications Framework (EQF), http://ec.europa.eu/education/lifelong-learning-policy/eqf_en.htm, last accessed on 06/01/2013.

[E2] ECQA - European Certification and Qualification Association, http://www.ecqa.org, last accessed on 19/04/2014.

[I1] International Organization for Standardization (ISO): ISO 26262. Road vehicles – Functional safety – Parts 1–9 (2011).

[I2] ISO (2012): ISO 17024. General Requirements for Bodies operating Certification of Per-sons. http://www.iso.org, last accessed on 20/02/2014.

[KM1] Kreiner C., Messnarz R., Riel A., Ekert D., Langgner M., Theisens D., Reiner M.: Automotive Knowledge Alliance AQUA – Integrating Automotive SPICE, Six Sigma, and Functional Safety. Mc Caffery, F., O'Connor, R.V., Messnarz, R. (eds.): Systems, Software and Service Process Improvement. Springer Communications in Computer and Information Science, Vol. 364 (2013), pp. 333–344.

[MK1] Messnarz R., König F., Bachmann O.: Experiences with Trial Assessments Combining Automotive SPICE and Functional Safety Standards. Winkler D., O'Connor R.V., Messnarz R. (eds): Systems, Software and Services Process Improvement, Springer Communications in Computer and Information Science, Vol. 301, (2012), pp. 266-275.

[MR1] McDermid J., Ripken K. : Life cycle support in the ADA environment. University Press, 1984.

[RT1] Riel A., Tichkiewitch S., Messnarz R.: Qualification and Certification for the Competitive Edge in Integrated Design. CIRP Journal of Manufacturing Science and Technology. Special Issue on Competitive Design, 2(4), 2010, pp. 279-289.

[RW1] Rosnah M.Y., Wan Nurul Karismah W.A., Zulkifli N.: Quality Management Maturity and Its Relationship with Human Resource Development Strategies in Manufacturing Industry. AIJSTPME (2010) 3(3): 53-63.

[S1] Automotive SPICE, www.automotive-spice.com, an international standard used in automotive industry, last accessed on 07/03/2014.

[SK1] Shimomura Y., Kimita K., Tateyama T., Akasaka F., Nemoto Y.: A method for human resource evaluation to realize high-quality PSSs. CIRP Annals - Manufacturing Technology 62 (2013), pp. 471–474.

[TG1] Tichkiewitch S., Gaucheron Th.: A recycling view for integrated design in car manufacture, 2000 International CIRP Design Seminar-Design with manufacturing: Intelligent Design Concepts Methods and Algorithms, Haifa, Israel, May 16-18, 2000, pp. 313-318.

[TR1] Tichkiewitch S., Riel A.: European Qualification and Certification for the Lifelong Learning. Keynote Paper. Fischer X., Nadeau J-P. (eds.): Research in Interactive Design: Virtual, Interactive and Integrated Product Design and Manufacturing for Industrial Innovation, 2010, Springer, ISBN 978-2817801681, pp. 135-146.

[W1] Oliver Wyman Automotive: 2015 Car Innovation. A comprehensive study on innovation in the automotive industry. Retrieved from: http://www.car-innovation .com on 11/12/2013.

Article 033-i-23

Toward a descriptive model of knowledge transfer within organisations

J. Mougin [1,2], J-F Boujut [1], F. Pourroy [1], G. Poussier [2]

(1) : Univ. Grenoble Alpes, G-SCOP, F-38000 Grenoble, France
CNRS, G-SCOP, F-38000 Grenoble, France
E-mail : {jonathan.mougin, jean-francois.boujut, franck.pourroy}@g-scop.grenoble-inp.fr

(2) : Bassetti
91Bis, Rue Général Mangin
38100 Grenoble, France
E-mail : { jonathan.mougin, gregory.poussier}@bassetti.fr

Abstract: Design activities are becoming more and more complex. This leads designers to work in highly collaborative and distributed teams. The Purpose of this study is to investigate on improving the use of KMS by defining a descriptive model of the knowledge transfer within engineering teams. We started by a literature review and we adopted a participant observation methodology in order to propose this model. Then we tested our model through case studies. This investigation enables us to observe, define and model more finely the dynamics of the exchanges between knowledge workers.

Key words: Knowledge transformation, Descriptive model, Participant observation, Knowledge management.

1- Introduction

Design is a highly cognitive process. Design involves logical reasoning and creativity activities in which knowledge has a key role. This knowledge can be of different nature, including technical or organizational, declarative or procedural, theoretical or resulting from experience, and so forth. While some part of this knowledge preexists to the design and is used as a support for the related activities, some new knowledge is also created by the design activities themselves. Both make it possible for the design process to take place.

The importance of this knowledge is particularly noticeable in the engineering design domain. Manufactured products tend to become more and more complex, which is making further demands on the skills and experience of designers. Combined with high competitive pressure and globalization of the economy, this often leads to highly collaborative and distributed design activities, making knowledge flows between the design stakeholders as vital as disrupted.

Knowledge management is hence considered "as one of the key enabling technologies for distributed engineering enterprises in the 21st century" [ML1], and companies have started to adopt different technical and managerial initiatives in order to foster the sharing of knowledge within their design teams. Among these initiatives, the adoption of a KMS (Knowledge Management Systems) is one of the more popular one. A KMS can be defined as an information technology (IT)-based system developed to support and enhance the three processes of knowledge creation, knowledge codification, and knowledge application [AT1]. This kind of system has been the focus of many research works in engineering design over the past decade. Examples are the engineering design reuse methodology from [B1], the CPD-based engineering knowledge management methodology from [CC1], the KALIS approach [B3], and so forth.

Nevertheless, beyond the promising idea of supporting knowledge flows though those KMS, only few organizations have implemented successful KMS [A2] and some studies even depict major failures (i.e. [AJ1] or [M1]). Much attention has been given to the possible reasons of these failures which are often discussed in terms psychological, social, technical and organizational factors that influence the use and acceptance of KMS [B2], [DP1]. Beyond these factors, Bernard suggests that "what is important is not to focus on what is captured by the KMS, but on what is not captured by the KMS: the 'near-misses' that are hard to identify and disclose" [B2]. Moreover, Grant argues that significant failures in KMS could result from the overly simplistic view of the tacit/explicit dimension of knowledge adopted by some knowledge transformation theories [G1].

The aim of our research is to investigate on improving the use of KMS by engineering teams. Paying attention to the above issues, in this paper we focus on defining a descriptive model of knowledge flows within such a context.

Starting from essential considerations about knowledge and information, the following section briefly reviews some key knowledge transformation models from the literature. Then, section 3 describes both our research methodology and the context of this research. The proposed model for knowledge transfer is then presented in section 4, and tested in a real-life situation in section 5.

2- Related work

2.1 – Knowledge and Information

Our initial point aims at reminding the different use made of the concept of knowledge. Indeed there is not today any consensus on the term “knowledge” and no uniform definition of this concept can be provided as Wilson [W1] explained. He points out the “problems in the distinction between 'knowledge' and 'information"' as being crucial when we consider the dynamic aspects of knowledge (i.e., creation, transfer, acquisition). Moreover, Nonaka and Takeuchi [NT1], whose work inspired many other researchers, make the distinction between tacit and explicit knowledge. Citing Polanyi [P1], they define tacit knowledge as personal and hard to transfer from a person to another, and which is consequently not easy to externalise. On the other hand, explicit knowledge is considered to be easily formalised, transmitted and stored. Following these definitions, many research works take a shortcut and consider explicit knowledge as something potentially easily stored in documents and databases, and therefore many of these works claim that computers store knowledge. According to their definition, they assumed that even tacit knowledge can be made explicit. When this conversion occurs, they consider that knowledge is “crystallised”. This confusion between knowledge and information as underlined by Wilson [W1] explains lots of failures and disappointments in knowledge management projects.

For many authors, knowledge cannot be directly transmitted from a person to another [PP1], [E1]. Knowledge transfer requires complex learning process that implies information elicitation, transformation and sharing [NW1]. Bannon and Kuutti [BK1] also stress this point from the perspective of collaborative work and corporate memory. They point out the underlying representation of memory used in many computer tools as being storage bins where one can store and retrieve items regardless the evolution of the context of use of the given item. These authors follow some recent advances in psychology and propose that memory and particularly the process of “recalling” is a process of construction and reconstruction. This approach to knowledge and memory puts the human being at the center of the loop and considers the tool as an assistant in a very complex process. This may explain partially why many so called knowledge management projects failed because the stakeholders only considered the instrumental aspects of the problem and neglected the dynamic aspect of knowledge.

The contribution of this paper is in the analysis and modelling of knowledge transfer and more precisely in the way people explains their knowledge through more or less structured information, share, transform information, and provide eventually a consensual shared object that can be stored and reused afterwards. Our aim is to provide a tool for analysing knowledge transfer dynamics in a corporate context.

2.2 – Implications for Knowledge reuse

In this section we focus on the stakeholders that are involved in the transformation of knowledge into information from the perspective of knowledge reuse. In her paper, Markus [M2] describes the knowledge reuse process in which she identifies three major roles:

- Knowledge producers are people who own knowledge. They are involved in the process of externalising knowledge into information.
- Knowledge intermediaries are the one that help the knowledge producers to elicitate their knowledge. They also transform externalised information for purpose of reuse by summarising it and packaging information. Then they spread what they formalised to the knowledge reusers as well.
- Knowledge reusers retrieve the content prepared by the knowledge intermediaries and use it for their own purpose.

These roles will help us to clarify our own model of the knowledge transfer process. We will now address the question of how these knowledge producers (or brokers [M3]) do to externalise their knowledge.

2.3 – Knowledge transfer model

Many researchers worked on modelling the knowledge transfer process. We briefly present here five of these models. After analysing them, we have been able to classify them into two different categories. On the one hand, models which deal with knowledge *transformation*, and on the other hand, models which deal with the process of knowledge *transfer*.

Knowledge transformation models:

- Historically, The SECI model from Nonaka [NT1] focuses on knowledge creation and knowledge transformation. These transformations describe how knowledge is converted through four different modes, passing successively from tacit to explicit (externalisation), from explicit to explicit (combination), from explicit to tacit (internalisation) and from tacit to tacit (socialisation). Unfortunately, this model focuses on the mechanism of the transformation of knowledge and does not capture the process itself and the related objects.
- The I-Space model from Max Boisot [BC1] is represented within a cube with three axes: abstraction, codification and diffusion. Within this cube and its dimensions, he draws a social learning cycle which is composed of six phases, scanning, codification, abstraction, diffusion, absorption and impacting. These six phases describe the flow of information within a knowledge transformation cycle. More work is required to explicitly define the process that allows to pass from one phase to the other and the requirements of these phases.
- The knowledge-based theory of the firm from Sveiby [S1] illustrates the knowledge conversion between three structures. It starts from the individual competence family which represents the competences of people from an organisation. Then he introduces the external and internal structure families. The first one represents the relationship between the organisation and its customers and suppliers and the second one is represents the internal processes and the structure of the

organisation. Then he explains that conversions are occurring from one structure to another and within a structure itself. Moreover, he points out that talking about "transfer" and "conversion" suggests a directional movement. This idea of movement is important because it implies that knowledge is subjected to different transformations, which is close to our understanding of knowledge. This model illustrates the complexity of knowledge exchange within and across firms. Again some work is required in order to model the different states of transformation within the process.

Knowledge transfer models:

- Generic Knowledge Management (KM) Processes from Grundstein [G2] allow to answer to answer the following question: "How to capitalise on company's knowledge", which is called here "corporate knowledge". Grunstein identifies four Generic KM Processes. *Locating* process allows to identify where crucial knowledge is located (e.g. is it close to the problem statement phase in design?). For him crucial knowledge means both explicit and tacit knowledge. Then *preserving* process stands for the *formalisation* of knowledge into words. Thus enhancing process deals with *combining* and sharing formalised knowledge. Finally *actualising* process is a necessary step to keep it up to date. Grundstein shows the process steps of the knowledge transfer but does not model the knowledge transformation itself.
- Theory of Knowledge Reuse [M2]: The knowledge reuse process can be described in terms of the following stages: capturing or documenting knowledge, packaging knowledge for reuse, distributing or disseminating knowledge (providing people with access to it), and reusing knowledge.

Through these two different categories of models, we identified some key points to approach our research question. First, we consider that knowledge can be subjected to transformation and we now have more insights to qualify these transformations. Second, we observed that the notion of process is important and allows to implement actions in order to foster knowledge transfer. Nevertheless it would be interesting to define a model which deals with both sides to explain this knowledge transfer process and which would enable us to model this process.

3- Research methodology and context definition

In order to address the issue introduced in the previous sections, we adopted a bottom up approach by starting with observations of industrial practice. As shown in Figure 1, we started by reviewing the literature which has been presented in section 2 and we adopted a participant observation methodology. Then we proposed a model to answer the research question. Finally we tested our model through other case studies.

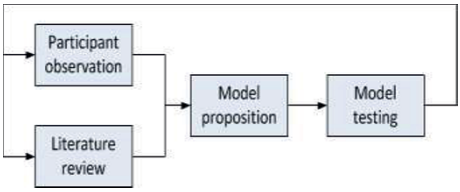

Figure 1. Research methodology

3.1 – Participant observation

First we adopted participant observation method within a company. This approach is based on a long immersion which allows the participant observer to perform interviews, to take notes or to make audio or video recordings. Our main objective is to observe the knowledge transfer process, so we integrate an IT company that we will name BAS. This company is an SME that is specialised in knowledge management. It provides consulting services such as setting up communities of practice or supporting engineering experts departure. It also develops and implements its own knowledge management system.
Within BAS, we participated to the company's activities e.g. we implemented its knowledge management system and trained customers to use it. We also conducted direct observations and performed 10 semi-structured interviews with two knowledge management experts of the company. Each interview lasted about 2h. During these interviews experts were invited to describe cases that they experienced in the past when they were implementing communities of experts. This method allowed to investigate and to get insights about the knowledge transfer process and our model is mainly inspired by these data.

3.2 – Observation

In a second time, we wanted to test our knowledge transfer model in real situations. So we took the opportunity offered by BAS to directly observe one of their customers. This customer is also an SME which we call here A2D. It helps companies to set up communities of practice and provides trainings and organises inter-company communities of practice for project managers, CEOs, community managers and human resources managers. The participants who sign up to one of these communities can take part in the four sessions organized by the company each year. Their subscription also allows them to participate to others trainings provided. Between each session, participants can exchange through an enterprise social network and share contents through BAS's knowledge based system.

4- Proposition for modelling knowledge transfer process

4.1 – Knowledge transfer process

The experience we got from the participant observation at BAS has been encouraging and fruitful. This method was appropriated to answer our research question since we were

able to participate to BAS activities including the monthly workshops of the community of practice project managers. These workshops aim at sharing and improving project management practices between all the project managers.
As we saw in the previous section the literature review is not sufficient to explain the co-construction of "common knowledge" [AL1] and the transition of knowledge into a formalised object, as it provides no sufficiently refined model. Taking inspiration from these models we then proposed our own descriptive model.
We will use one of the workshops that we observed to present and illustrate our descriptive model. The workshop we are talking about dealt with the topic "*How to manage the end of a project*?" and lasted about 3h. This topic has been chosen by the technical director who centralised the issues of the project managers. The aim was not just to exchange on the topic but to formalise a template of a presentation document which can be used by the future new project managers. So we (project managers and I) started to talk about what is necessary to close a project. The following sentences illustrate a part of these exchanges:

1: Person A: We should start the document by reminding the objectives of the project and then continue with the presentation of the initial perimeter.
2: Person B: yes,
3: Person B: and we should also present the use cases
4: Person C: Why do you want to present that?
5: Person B: because the use cases illustrate what we have done in the project.
6: Person C: OK, it can be interesting,
7: Person C: especially for the large project.
8: Person D: All right, if I summarise, we have 1- the project objectives, 2- initial perimeter
and 3- the use cases (for large project only)
9: Person D records it on the paperboard)

About 30 minutes before the end of the session, the technical director asks the project managers to sort all the ideas. Then he recorded the main ideas in order to formalise them later. After few days, we received a notification from the knowledge based system to warn us about the publication of the presentation document.

4.2 – Model definition: tracking knowledge footprints

Now, let's take a closer look at what happened in this situation. We noticed there are the three major roles mentioned by Markus [M2]. First the technical director acted as *knowledge intermediary*. He organised workshops and chose the topics with the project managers' issues. This latter activity is also similar to the locating phase described by Grundstein [G2]. Then we have the projects managers who attended to the sessions and who are in position of *knowledge producers*. They externalised their knowledge (transformation step from Nonaka) into ***knowledge footprints***. We introduce this concept of Knowledge Footprint as an oral or written element which is externalised by a person and which contributes to answer the issue. An utterance is considered as a footprint if it brings "a new quantum of novelty" [AB1] to the discussion. For example, when the persons A, B and C externalised their knowledge at the line 1, 3 and 7, they produced knowledge footprints. However, the peripheral interactions are not considered as footprints because they refer to a previous utterance. Typically argumentation, questions, opinion are considered as peripheral interactions. So, we consider the exchanges 2, 4, 5 and 6 as peripheral interactions. These kinds of exchanges make evolve the knowledge footprint into a ***shared knowledge footprint***. In our case, the Shared Knowledge Footprint is represented by the line 8. We define a shared knowledge footprint as follows: it is a knowledge footprint on which people agree and recognise as relevant in their own domain of expertise. This element has been constructed by at least 2 persons. Nevertheless, this shared knowledge footprint is represented in an ad-hoc format and therefore may not have the format required by the context of the meeting and it can be recognised only by the originators of the discussion. We can notice that all these elements describe the *preserving* phase of Grundstein.

At the end of the workshop, the technical director recorded the shared knowledge footprints (as at line 9) in order to formalise them into a ***Knowledge Object***. This kind of object is supposed to be interpretable by the people who did not participate to its construction. This was not the case of our previous shared knowledge footprints that has been elaborated locally in an ad hoc format. To build this element, the knowledge intermediary had to transform (synthesising, combining and filtering) the previous shared knowledge footprints.
After the validation, the object of knowledge has been stored in the information system. As presented by Markus, the knowledge intermediary indexes and classifies the object of knowledge into a knowledge management system, here, in BAS knowledge management system. According to the knowledge management system, the knowledge intermediary can provide elements of context to the object of knowledge e.g. adding metadata. In this step, we can find again the main activities of the knowledge intermediary which are gathering, formalising and packaging the elicited knowledge into an object of knowledge.

Element Name	Element representation
Issue	
Knowledge Footprint	
Shared Knowledge Footprint	
Knowledge Object	
Packaged Knowledge Object	

Table 1. Graphical representation of our elements

Table 1 summarises the graphical representation of the above presented elements. We will use these graphic signs for tracing the various session profiles.

5- Case study and discussion

5.1 – Modelling the case study

We have been investigating both literature and situations in practice to build our knowledge transfer model. We now illustrate this model through a case study. We first performed 5 semi-structured interviews with one of the community managers. These interviews allowed us to understand how their communities are organised. After these interviews, we observed one session (8 hours) of the human resources community. In that case, our knowledge intermediary is the community manager who prepared the session. To do so, the community manager asked the participants (who are the knowledge producers) what their current projects and needs are. This step aimed at planning the next session by choosing the issues to work on. During the morning session, the community manager first explained to the participants the topics which will be dealt by the community in the sessions. To deal with a maximum of issues, the community split in small groups (about 5 persons per group). We joined one of these groups to record their exchanges. Before the group began, the community manager also precised that they have to find 5 topics on the issue "The role of human resources manager towards managers". Here, we can observe that the community manager expressed the issue and the expected format. We gathered 1h audio recording that we transcribed in a spreadsheet (Table 2 shows an excerpt of the transcript).

We wanted to track the expressions of the different states of knowledge within the discussion. So we constructed this spreadsheet as follow: first we numbered the exchanges, then we gave to each participant a letter, thus we wrote the exchanges (which are translated here in English in Table 2). Finally, we matched each exchange with the graphical representation of our elements. We started with double-coding (20% of the exchanges) and then we finished with simple-coding. We needed additional information for consolidating our analysis, so we performed one structured interview afterwards. We identified a knowledge footprint at the line 50 when the person E proposed to work on the evaluation of the manager's needs. Then the person A reformulated the knowledge footprint but misunderstood it. So person B precised that the evaluation concerns the manager's needs. This precision brought additional information, so we consider it as a knowledge footprint, as the next exchange, when person C proposed to add the means of communication. Afterwards, person B reformulated all the knowledge footprints to constitute the shared knowledge footprint which has been tracked by A on the paperboard.

After tracking all the exchanges, we represented them on a chart (Figure 2). The lines correspond to the participants. Each line carries the graphical elements which has been externalised by the participants. To identify the exchanges more easily, we signed the graphical elements with the exchange number.

On Figure 2 we can observe that the participants produced knowledge footprints and then shared knowledge footprints (8, 24, 42, 48, 55, 66, 75, 88, 90, 98). However, they produced too many shared knowledge footprints, so they had to negotiate, classify and gather the shared knowledge footprints into new shared knowledge footprints (red dotted arrows) in order to reach the initial requirement of 5.

At the end of the workshop, the organiser asked person A to formalise the five shared knowledge footprints in a minutes (providing an object of knowledge). A couple of days later, person A sent the minutes to the community manager who indexed it in the knowledge management system with some information on the context (session where it has been created, the contributors, etc).

5.2 – Analysing the case study

We have observed a community of practice and tracked their exchanges. So what can we retain from that case study? As we were expecting, we identified the knowledge transformations described by Nonaka. The participants externalised their knowledge, they combined what they codified and internalised the codified object to create new knowledge. Moreover, the generic KM processes from Grundstein are almost all identified, *the community manager locate the crucial knowledge before the workshop*, then participants exchange to preserve the knowledge and then the community manager enhance the object of knowledge in the information system but we did not observe the actualisation. We also distinguished the different roles cited by Markus. For instance, the person A combined the role of knowledge producer during the workshop and the role of knowledge intermediary when she formalised the shared knowledge footprints. It leads to Markus' words which point out that someone can play several roles. Then the different representations allow us to observe what happened in the discussion. With the transcript spreadsheet, we have been able to perceive the participant's knowledge changing. For instance, the following utterances show that transformation:

Person A: So we were saying, what are the evolutions of the manager's roles?

Person B: No, the role of HR, this topic would aim at dealing with the added value of the HR to the managers

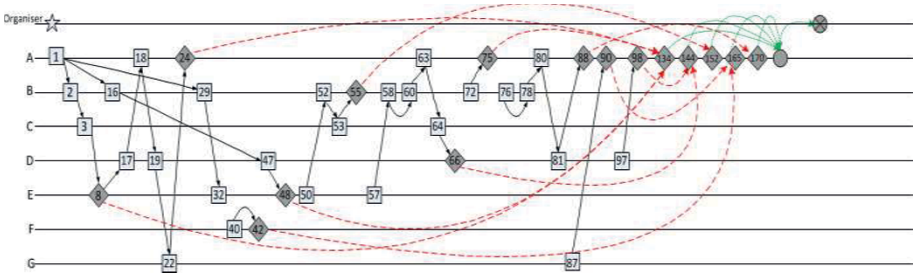

Figure 2. Graphical representation chart

N°	Participant	Exchanges	Representation
50	E	Now, we could work on how to evaluate their needs?	Knowledge Footprint
51	A	Yes, how do we evaluate them?	Agreement
52	B	Not really them, but their needs as managers	Knowledge Footprint
53	C	And we should add "What are the means of communication (phone, meeting, mail)?"	Knowledge Footprint
54	E	It now looks like an interesting topic	Agreement
55	B	OK, so it would be "How to evaluate the manager needs? How do we communicate with them (phone, mail, meeting)?"	Shared Knowledge Footprint
56	A	<elle écrit au tableau>	

Table 2. Extract of the audio transcription in our spreadsheet template

Person A: OK, I understand, so it would be "What are the evolution of the HR roles?"

In a further work, it would be interesting to track and model more precisely this kind of moments. We will also need to perform interviews with the participants after the session in order to get more accurate data. Thus, the chart shows that a knowledge footprint can give birth to several other knowledge footprints by association, e.g. the exchanges 1, 2, 3, 8, 17, 18, 19, 22 and 24. At the end we have cross checked by an interview the validity of this interpretation. The shared knowledge footprints 134, 144, 152, 165, 170 have been transformed in object of knowledge. Knowledge object have been formalised by the knowledge intermediary and packaged in a knowledge repository

5- Conclusion

This paper presents a model that is consistent with the state-of-the art of knowledge management models. As our focus is on knowledge dynamics we adopted a point of view that fits to the latest development of the cognitive psychology by considering knowledge as a process. This position led us to observe and model more finely the dynamics of the exchanges between knowledge workers. Starting from that, we proposed a descriptive model of the knowledge transfer process. In this paper we modelled the first dimension of knowledge transfer, the elicitation process where knowledge is externalised, shared and transformed into an object of knowledge. Traditionally the research works do not pay attention to this phase as it is mainly an oral phase that occurs before the storing phase. In further work, we will implement a process of double-coding as means of checking reliability for all the coprus. Additional developments are being carried out in order to cover the entire process including reuse of objects of knowledge. Our project is then to provide an entire model for describing knowledge transformation in a context of corporate knowledge creation and management. This model should include links between roles (personas) and objects of knowledge.

8- Acknowledgments

We warmly thank Bassetti company (http://www.bassetti.fr/en/) for its entire support of this research.

8- References

[A1] Aalst, J. Distinguishing knowledge-sharing, knowledge-construction, and knowledge-creation discourses. Int. J. Comput. Collab. Learn. 4: 259–287, 2009.

[AJ1] Akhavan, P., Jafari, M. & Fathian, M., Exploring Failure-Factors Of Implementing Knowledge Management Systems In Organizations. Journal of Knowledge Management Practice: 1–10, 2005.

[AT1] Alavi, M. & Tiwana, A., Knowledge integration in virtual teams: The potential role of KMS. Journal of the American Society for Information Science and Technology, 53(12): 1029–1037, 2002.

[AL1] Alterman, R. & Larusson, J. A. Participation and common knowledge in a case study of student blogging. Int. J. Comput. Collab. Learn. 8: 149–187, 2013.

[AB1] Ancori, B, Bureth, A. and Cohendet, P. 2000. The Economics of Knowledge: The Debate about Codification and Tacit Knowledge. Industrial and Corporate Change 9: 255-287, 2000.

[A2] Atwood, M.E., Organizational Memory Systems: Challenges For Information Technology. 35th Hawaii International Conference on System Sciences. 2002.

[BK1] Bannon, Liam J. and Kari Kuuti, Shifting Perspectives on Organizational Memory: From Storage to Active Remembering. Proceedings of Hawaii International Conference on System Sciences (HICSS-29). Los Alamitos, CA: IEEE Computer Society Press: 156–167, 1996.

[B1] Baxter, D. et al., An Engineering Design Knowledge Reuse Methodology Using Process Modelling 1 Introduction: 37–48, 2007.

[B2] Bernard, J., A typology of knowledge management system use by teams. In System Sciences, HICSS'06. Proceedings of the 39th Hawaii International Conference on System Sciences: 1–10, 2006.

[B3] Beylier, C. et al, A collaboration-centred approach to manage engineering knowledge: a case study of an engineering SME. Journal of Engineering Design, 20(6): 523–542, 2009.

[BC1] Boisot, M. & Canals, A. Data, information and knowledge: have we got it right? J. Evol. Econ. 14: 43–67, 2004.

[CC1] Chen, Y.-J., Chen, Y.-M. & Chu, H.-C., Enabling collaborative product design through distributed engineering knowledge management. Computers in Industry, 59(4): 395–409, 2008.

[DP1] Dargahi, A., Pourroy, F. & Wurtz, F., Towards controlling the acceptance factors for a collaborative platform in engineering design. In 11th IFIP Working Conference on VIRTUAL ENTERPRISES. Saint-Etienne, France, 2010.

[E1] Eberhagen, N., On the Design of Support Systems for Knowledge Sharing within a Social Learning and Sharing Context. Proceedings of the First International Conference on Information and Management Science: 380-389, 2002.

[G1] Grant, K.A., Tacit Knowledge Revisited – We Can Still Learn from Polanyi. Electronic Journal of Knowledge Management, 5(2), 173–180, 2007.

[G2] Grundstein M., "Repérer et mettre en valeur les connaissances cruciales pour l'entreprise." Actes de 10ème Congrès International de l'AFAV, Paris, France, 2000.

[M1] Malhotra, Y., Why Knowledge Management Systems Fail ? Enablers and Constraints of Knowledge Management in Human Enterprises. In M. E. D. Koenig & T. K. Srikantaiah, eds. Knowledge Management Lessons Learned: What Works and What Doesn't:87–112, 2004.

[M2] Markus, L. M. Toward a Theory of Knowledge Reuse: Types of Knowledge Reuse Situations and Factors in Reuse Success. J. Manag. Inf. Syst. 18: 57–93, 2001.

[M3] Meyer, M., 'The rise of the knowledge broker', Science Communication, 32: 118–27, 2010.

[ML1] Mcmahon, C., Lowe, A. & Culley, S., Knowledge management in engineering design : personalization and codification. Journal of Engineering Design, 15(4): 307–325, 2004.

[N1] Nonaka, I., Toyama, R. & Konno, N. SECI, Ba and Leadership: a Unified Model of Dynamic Knowledge Creation. Long Range Plann: 33, 5–34, 2000.

[NW1] Novak, J. and Wurst, M., Supporting Knowledge Creation and Sharing in Communities Based on Mapping Implicit Knowledge. In j-jucs, Vol. 10, No. 3, 235-251, 2004.

[P1] Polanyi M., The tacit dimension, Routledge & Kegan Paul:London. 1966.

[PP1] Prudhomme, G., Pourroy, F., & Lund, K.., An empirical study of engineering knowledge dynamics in a design situation. Journal of Design Research. 6(3): 333-358, 2007.

[S1] Sveiby, K. A knowledge-based theory of the firm to guide in strategy formulation. J. Intellect. Cap. 2: 1–14, 2001.

[W1] Wilson, T.D., "The nonsense of 'knowledge management'" Information Research, 8(1), paper no. 144, 2002.

Article 036-i-99

Innovative field exploration and associated patent portfolio design models

Olga Kokshagina [1], Pascal Le Masson [1], Benoit Weil [1], Yacine Felk [2]

(1) : Mines ParisTech 60 Boulevard Saint-Michel

E-mail: {olga.kokshagina, pascal.le_masson, benoit.weil}@mines-paristech.fr.

(2) : STMicroelectronics

Chemin du Champ-des-Filles 39, 21 Geneva

E-mail: {yacine.felk}@st.com

Abstract: Patents play an ever-increasing role in the modern economies and are often used as a measure of technology innovativeness. This paper deals with the innovative field exploration where companies are constantly under pressure to generate high quality patents that will ensure future firms growth, their survival and protect their inventions at the early stages of technological exploration. This work builds on the methods of patent modeling that appear to be adapted for disruptive innovation. By drawing on the patentability criteria, their interpretation in the patent model driven by the design theory frameworks like Concept-Knowledge theory, the paper examines the means of applicability of these methods within the high-velocity industries like semiconductors or nanotechnologies. As a result, two processes of patent design are proposed: 1) technology design that brings to define patent proposals or 2) patent proposals design that add new innovative attributes prior to technology creation. The insights are given on which approach companies have to pursue regarding their problematic.

Key words: industrial property, innovation, patent design, C-K Theory, patentability criteria

1- Introduction

Companies aim to cover the inventions that they will use in the future. In that matter, one of the commonly adopted strategies is a creation of broad patent portfolio that will protect future business, secure exploration area and provide a possibility to discuss with competitors and partners. Various researchers have showed the positive relations between the issued patents and innovative capacities of R&D centers over time [G3, M9]. Patents are largely used as economic indicators [S12] and various researchers employ them as a measure of innovation.

Patents are commonly defined as a result of research on inventive activity; they are filled normally at the latter stages of technological development in order to protect the invention. Patent portfolios can offer important advantages for companies' business by shaping its future strategy, by strengthening its position against competitors and offering a possibility to freely operate in a protected domain. Thee factors drive the companies to launch patent exploration at the earlier phases when technology is immature [JK7] and even unknown. Each year a number of patents filled before the technology is even commercialized increases. In this case patents appear as an objective that a group of designers and scientists have to achieve before the technology is commercialized or its exploration started. The latter brought companies, research centers to actually seek for methods that allow maximizing the number of potential patents, pursuing creativity in patent design, possibility of strategic inventing [N10].

While dealing with incremental innovations, problem-solving techniques are suited to generate patents. These methods are based on the description of contradictions and potential solutions (see Theory of Inventive Problem Solving - TRIZ and the derived from it techniques like Advanced System Inventive Thinking - ASIT [RS4]). Yet, TRIZ is often criticized for its limited inventive novelty due to the departure from the already issued patents – existing physical system. [RS4] demonstrated that ASIT is suitable for 'in- and near- box' designs.

These methods appear to be limited when the problem is not given *a priori* and the design is a subject of disruptive innovative exploration. Dealing with highly innovative fields, there is a clear need to protect the expected value proposed by promising emerging technologies. Companies

Article 036-i-99

have to define their patent strategies well in advance the validated technological design is developed, which require methods to support reasoning.

Design analogy methods [JK7] attempted to be used for patents creation by assuming that similar problems can appear in technologies that have similar functions and properties. For instance, [JK7] aim to generate patents by creating an analogy between mature wireless router and emerging wireless charger. Engineers or designers can use this method systematically to create patents. Yet this method is limited once applied to novel properties or functions in case of disruptive technology where the analogy cannot be pursued.

By pursuing innovative field exploration, a patenting can be modeled as design activity. In this matter, the literature proposes to use of the recent design formalism like Concept-Knowledge design theory to account for patent design (see [CD1, FL2, S13]). In [CD1] a model for determine patents using action, effects and knowledge is proposed. In [FL2] this way of patents description is used to design patents portfolio in case of innovative design field. At STMicroelectronics a conducted exploration using these tools enabled to generate a high number of inventions for the emerging technology. While this approach appeared to be particularly relevant for patent portfolio design, the means of their applicability, their properties, the expected outcomes and the ways to control the high quality of the issued patent proposals remain unclear.

For instance, to increase reliability and originality of the solution [K8] indicated the importance of patent infringement checks before and during the design of solutions. Though, author admits that these controls might influence the resulted creativity. The maturity of technology under exploration and the level of expertise would certainly influence the capacity to design a robust patent portfolio [NZ11]. Moreover, while dealing with the patent design before technology is designed, the relevance and value of the proposals need to be carefully evaluated and tested. These aspects lead to the following research questions: **How to control future patent proposal's quality, ensure their patentability while dealing with highly disruptive exploration fields? How to successfully deploy the patent design methods and what are the means and conditions of their applicability?**

In order to do that, this paper gives first of all the definition of patent and the patentability criteria that the invention has to meet to obtain the patent grant (Section 2). Section 3 presents the model of patent design where 1) an (Action, Effect, Knowledge) model for patent definition based on the work of [CD1] is presented; 2) Built on the C-K invent method for patent design introduced in [FL2], the exploration process to design patent proposals is defined; the patentability criteria are interpreted using the model. In section 4 based on the experimental work conducted at STMicroelectronics, two processes of patent design are determined: 1) **technology design** that brings to define patent proposals or 2) **patent proposals design** that add new innovative attributes prior to technology creation. The importance and applicability of these two processes are discussed.

2 - Industrial property

2.1 – On the definition of patent

According to the World Intellectual Property Organization (WIPO), Intellectual Property (IP) refers to « creation of the mind such as inventions, literature and artistes works, designs and symbols, names and images using in commerce». It is protected by law through patents, copyright and trademarks. Our focus in this article is on patents which represent a document, issued, upon application, by a government office (such as the European Patent Office (EPO) or United States Patent and Trademark office), which describes an invention and creates a legal situation in which the patented invention can normally only be exploited with the authorization of the owner of the patent. Patents offer a legal right title for the owner to prevent others from using, making or selling the protected invention in a country where patent has been granted for an allowed period of time (limited by 20 years).

"Invention" is defined as a solution to a specific (mostly technical) problem. An invention may relate to a product or a process. To be protected by a patent, invention has to meet several criteria: 1) the invention must consist of patentable subject matter, 2) the invention must be industrially applicable (useful) 3) it must be novel, 4) it must exhibit a sufficient "inventive step" (be non-obvious for a person skilled in the field), and 5) the disclosure of the invention in the patent application must meet certain standards.

2.2 – Patentability criteria

Patentable subject matter is open to all fields of technology. The non-patentability is often due to specific methods of treatment for living organism schemes and models that perform purely mental activities; methods that exist in nature (for further details see Article 27.1 of the TRIPS agreement). The patentability of the invention can be questioned using morality principles as well.

Usefulness of the invention, its applicability defines the practical purpose of the proposed invention, the possibility to actually manufacture the proposed product and implement a part of the process to serve its purpose. It is the utility of the proposed invention.

Novelty and "inventive step" are appreciated with respect to the state of the art at the date of patent application. Novelty is a critical criteria and the invention appears to be

Article 036-i-99

novel when it is not anticipated by the prior art. *"State of the art shall be held to comprise everything made available to the public by means of a written or oral description, by use, or in any other way, before the date of filing of the European patent application*" according to Article 54(2) EPC.

The inventive step of a proposition questions the nature of the invention on its obviousness for a person having ordinary skill in the art. The question "is there inventive step?" only arises if there is novelty. WIPO suggests analyzing inventive step in relation to the problem to be solved, the solution to that problem and the advantageous that the invention offers to the state of the art. Generally, if a person skilled in the art (PSA) is capable to pose that problem, solve it similarly to a propose invention and predict the results – the inventive step is missing.

The last criterion is a disclosure of the invention that defines whether the proposed invention is sufficiently disclosed in the application and PSA can carry out the invention claimed. These are the criteria that inventor has to fulfill to be granted patent rights.

3 – Model of patent design: use of C-K design theory

3.1 – (Action, Effect, Knowledge) model for patent definition

A patent can be represented as: a solution to a technical problem that differs from the prior art. The actions can characterize the solution and comprise the object description and the interventions performed by an agent (human, fluid ...) on an object. The effects represent a problem and can be external and internal. Knowledge defines the prior art and the results obtained during the invention preparation. The knowledge basis comprises 1) public knowledge: patents, research, commercial papers, all the available documentation and all the knowledge generally available and evident for the person skilled in the art; 2) knowledge developed by an inventor during his research or design process. In this regard patent is a combination of actions, effects and knowledge [CD1]. Patent is a proposition where *Action* represents the intervention made on objects and their interrelations. *Effects* are actions' consequences and *Knowledge* is the set of technical information used by the invention.

Using the famous Nespresso capsules patent example (EP 2643241 A1), let's analyze Claim 1:

"*1) Nespresso ™ compatible capsule for making coffee and/or brews with a body in the shape of a truncated cone (2), characterized by the fact that on the side where the water and/or steam goes in there is a concavity or a depression (6) that stretches out and penetrates the interior of the body (2) of the capsule, in which depression (6) there is a series of radial holes (9) through which the inflow of water and/or steam that comes into said depression (6), with an axis parallel to the main axis of said capsule (1), is deviated to pass through the inside body (2) of the capsule (1) itself*".

In this text "*for making coffee and/or brews with a body in the shape of a truncated cone*" is an effect that the new invention offers. The knowledge is embedded in the principles of concavity or a depression and action is the process 1 – 6 described using knowledge elements to achieve the desired effects. (A, E, K) model defines the patent proposal.

In case of radical innovation, (A, E, K) are unknown in advance. Dealing with this problematic, [FL2] mobilized Concept-Knowledge design theory to propose a patent generation model based on (A, E, K) triples creation. This method derived from C-K design theory is called CK Invent. In the following section we present the method defined in [FL2] and verify that is corresponds to the patentability criteria in section 2.2.

3.2 – C-K based method for patent design

Concept-Knowledge (C-K) design theory [HW5,6] defines the design process as a continuous refinement of a concept described by various properties that need to be met based on the existing knowledge and producing new one. The process of design is defined as a double expansion of the concept and knowledge spaces through the application of four types of operators (for further details see [HW5,6]). Design theory is useful for patent modeling since it separates a knowledge model and design reasoning.

In that matter knowledge space includes public knowledge (K_0), which comprises patent, publications, customer references, internal company expertise – "state of the art". Person skilled in the art (PSA) presumed to be a skilled practitioner in the relevant field, who is possessed of average knowledge and ability and have had at his disposal the normal means and capacity for routine work and experimentation. K_0 should be evident for PSA.

In case of intellectual property design the concept is defined as a combination of actions and effects meaning that a concept in C-K is defined as (A-E) using Zwicky matrixes [Z14]. According to the C-K formalism concept is "undecidable" in knowledge basis meaning that its logical status is neither true nor false (Figure 1). The patent can be achieved through (A-E) concepts exploration and can be defined as new (A, E, K) that fulfills patent criteria [CD1].

All reasoning that a PSA is capable to conduct is based on the initial knowledge base K_0. It is not inventive but can be novel. Invention is considered novel only when Action (interventions made on objects) and Effects (consequences brought by actions) don't make part of a common knowledge and as a result new knowledge is created. PSA is capable to be novel, though his partitions are restrictive.

Article 036-i-99

So he is capable to propose novel actions and effects based on the existing state of the art.

While dealing with radical innovation action, effects and associated knowledge are missing. According to C-K theory, creative design requires an expansive partition, which expands the concept space. These expansive partitions significantly modify or propose new actions and effects that generate new "sentences" – new ideas for patent proposals (Figure 1). They add new knowledge to the K space that can have A or E nature and not evident for person skilled in the art.

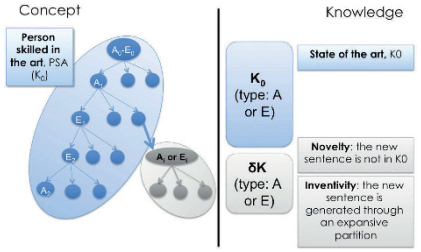

Figure 1 : C-K Models based on A, K, E (built based on [FL2])

These expansive partitions fulfill the criteria of novelty and inventive step. Novelty implies the absence of A-E relations in the knowledge basis; inventive step means that A-E is not evident for PSA (Table 1). Moreover, disclosure of the invention is achieved once the (A, E, K) can be understandable and repeatable by technical experts.

Table 1 : Patentability criteria

Patentability Criteria	**Interpretation in patent model (related to PSA)**
Patentable subject matter	Ei and Ai under investigation are not subject of non-patentability (see Article 27.1 of the TRIPS Agreement)
Usefulness of the invention	Ei useful and Ai feasible
Novelty	$(A,E) \not\subset K_0$
Inventive step	$(A,E) \not\subset PSA(K_0)$
Disclosure of the invention	$(A,E) \subset (K_0 \cup \delta K)$

Patent design appears as **design a new** (A, K, E) proposition that is not **already in K_0 and PSA** (K_0) does not consider the patent proposal as obvious.

If the dominant technological proposition already exists, the reference solution in the form (A*, E*, K*) can be determined and the patent exploration is often consisted on extracting potentially subsets (A, E, K) from the properties of that technology and checking its patentability (see table 1). As [FL2] underlined, with (A, E, K) model, TRIZ combination of contradiction and solution principle can be defined as combination of (E_ixE_j ; Actions that enable to get E_ixE_j), where E_i and E_j are the effects in contradiction.

But what happens when the reference solution is absent and the level of uncertainty is high to be predict the relevant action and effects? In the work of [FL2] the design methodology was successfully used to organize exploration of innovative design space by actually defining the exploration space and proposing robust patent portfolio when reference solution did not initially exist. By conducting an empirical study at ST, the authors showed how to enlarge design space and identify a wide range of opportunities for specific problems. The resulted method contains two principal phases: 1) Knowledge structure and organization in order to define high-level (A-E) concepts that identify a wide range of opportunities using C-K design tools. This phase results in a list of ideas that might result in potential patents. 2) Ideas evaluation using criteria in Table 1.

CK Invent offers an attractive way of designing a wide-scope portfolio of patents that are linked to the central problematic. The discussed in this paper patentability criteria applied with CK Invent ensure the quality of inventions. Yet the conditions, context and means of the CK Invent applicability have to be examined. By drawing on the defined interpretation of patent criteria and innovative design methodology, this paper aims to investigate the means of applying design reasoning for patent proposals creation. The chosen method is an experimental approach conducted at STMicroelectronics. In section 4 the paper extends the single experiment presented in [FL2] to different technological areas and contexts of exploration. The first author conducted the experiments within different groups; the fourth author participated as a moderator in several of experiments. The second and the third author helped to control the quality and variety of the results and observation issued from CK Invent.

4 - Experiment conducted at STMicroelectronics

At STMicroelectronics (ST), one of the leading European Semiconductor companies, the process of patent design was initially tested in 2008. The first experiment was conducted and documented by [FL2] in disruptive 3D Integration technology field. In 2008, when the 3D integration technology was still immature and the unknowns were high, the authors demonstrated that by working on the generative concepts like "*definition of a Trough-X-Via (TXV) as interconnect between devices rather than Through-Silicon-Via (TSV)*" allowed considering any type of substrate and ways of interconnecting devices trough this substrate. The high rate of issued ideas form this and relevant concepts lead to high

Article 036-i-99

number of inventions which in turn enabled ST to obtain patents and launch new exploration projects.

While pursuing the goal of exploring different patent strategies, we attempted to reuse the proposed by [FL2] model of patent design in case of disruptive innovation and apply it to the following contexts: 1) emerging technological field with lack of internal expertise – prior art is mostly unknown, high probability of disruption; 2) patent portfolio creation for actual predefined problematic – prior art is available and exploration does not start from the "green field"; 3) markets related innovative technology exploration – the later phases of technology maturation where the market interest is identified but the technology is still emerging. It is important to underline that in all conducted experiments the dominant technological solution was absent and the situations were quantified as "innovative design". The variety of contexts was examined to understand the issue of patent design across the number of rather distinct cases.

Overall, 4 empirical tests were conducted in various technological areas: 1) 3D Integration technological area for a problematic of thermal management, 2) Energy harvesting, 3) Multi-touch haptic solutions, 4) Silicon photonics. These four explorations were launched with the aim to design strategic patent portfolios with high number of valuable inventions. Each experiment was conducted during 3 – 6 months period with teams in charge of developing relevant technological blocks. Teams comprised engineers, researchers, doctoral students who participated in ideas generation. Coordinator and facilitators were in charge of deploying the method and control the quality of the corresponding proposals. The issued propositions were later discussed and presented to the service in charge of the intellectual property deposition and valorization. All four experiments have resulted in a number of inventions and patent proposals were filled.

The results of the conducted experiment have shown the existence of two rather different approaches: 1) technology-first design that brings to define patent proposals with new innovative attributes or 2) patent proposals-first design that add new innovative attributes prior to technology creation.

4.1 – Technology-first approach

Technology-first approach consists in pursuing first of all the exploration of a reference technology – technological concepts. This exploration was conducted in the field of 3D Integration and the goal was to explore alternative architectures to connect previously planar devices. The team that participated in the sessions identified various number of interesting for «3D Integration » architectures that varied depending on active face positioning and embodiment of interconnections through substrates (Figure 2).

This approach proved to maximally reuse the existing technological design rules and related knowledge and expertise (K_0). The participants attempted to combine the existing technological building blocks (PSA(K_0)) to actually find new patent proposition. This process resulted in screening large number of technologies and developing an extensive state-of-the-art cartography.

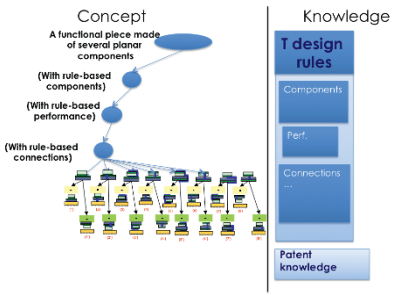

Figure 2: Technological design initially

This process is mostly driven by PSA(K_0) reasoning based on the existing knowledge and expertise. The knowledge expansion is deeply routed to the existing expertise and thus harder to provoke. This process resulted in a high number of incremental innovations that are useful for the emerging field but not all of them appear to be patentable. T-first approach often creates in a fewer number of patent proposals but help to structure knowledge, to identify new issues and challenges. It enriches the patent family by contributing to the exploration of the initially defined concept.

This approach is limited in case of radical innovations when the field is new and company aim to protect and valorize their exploration zone ahead of the competitors. It appears relevant when the state of the art is rather solid or analogy can be made with rather similar field (i.e., wireless router and wireless charger). T-first approach inventions often produce the improvement patents that protect the differences between new products and already existing ones by adding new properties or substituting the old ones.

4.2 – Patent proposals-first approach

The second approach consists in exploring an emerging field by defining patent propositions in (A, E, K) forms and then producing the reference solutions, engage in the technology development.

Let's take the example of the design team that worked on multi-touch haptic solutions where touch was considered as a way of interactive communications. The team did not

Article 036-i-99

pursue the axis to improve and find alternatives to the already emerging solutions that consider haptic feedback. Instead they aim to enrich the exploration spaces by adding new Effects and ensuring new Actions that haptic touch can propose in the future.

Two outcomes of the process – two types of expansions were observed. First, the team added new Action – flexible electronics using Organic Light-Emitting Diode (OLED) or graphene sheet (Figure 3). The haptic multitouch domain did not previously consider these actions (object type of action). The team aimed to explore potentially disruptive solutions that account for capacitive multitouch flexible transparent display solutions. The desired effect was to achieve rich and precise multitouch feedback despite the screen flexibility. As a result the design team proposed inventions that deal with the innovative fabrication processes. They created new, disruptive (A, E, K) combinations and their starting point included an Action that was completely new and not evident for PSA. The team explored radical concepts in this case.

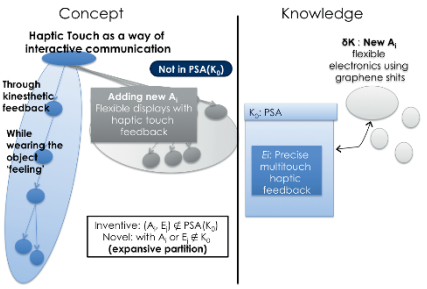

Figure 3: Patent design initially: expansive partition

Second the team actually brought the knowledge on electroactive polymers (Action) that exhibit shape or size change in response to electrical stimulation and allow independent volume rendering (Effect) (Figure 4). While starting from this partially known (A, E) set they were able to propose a range of expansive partitions and define new patent proposals. The second logic proposes limited breakthrough by extending the effects or actions.

As these examples demonstrate, the initial concept should prompt new innovative ideas where new actions and/or effects can de generated and explored. It should be sufficiently generic (as "haptic touch as a way of interactive communication") to cover the existence of several knowledge gaps. The emerging (A, E, K) combinations are then controlled using criteria in Table 1.

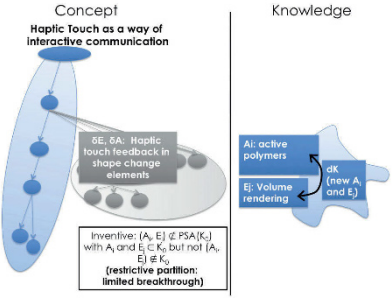

Figure 4: Patent design initially: limited breakthrough

The presented here and other conducted at ST explorations demonstrated that patent-first method result not in single patent proposals but in a range of inventions that might result in high quality patent portfolios. The defined previously patentability criteria actually help to reduce risks of non-relevance of the issued from the exploration sessions' ideas. Patent proposals-first reasoning is relevant when the level of uncertainty is high and the goal is not a problem solving but knowledge expansion. In this case the state of the art is still immature and the research is still in its initial phase.

5- Results and discussion

The proposed technology-first and patent-first approaches derived from CK Invent model (which is defined in [FL2]) offer rule-breaking ways to account for the design of patents (by adding new actions and effects) or by starting from the technological design references to account for patent propositions in stable design spaces. The paper reveals that there is a clear difference on whether we start by defining propositions (expansive partitions in C-space) or by exploring the existing design rules.

The technology-first approach is suitable in case of dominant design where the goal is to propose better action and effects to actually solve predefined problem by designing patent portfolio. In this case patent portfolio analyzed with (A, E, K) model helps to identify knowledge gaps and actually determine "patent-free" zones where engineers and designers can systematically create patents.

The patent proposal-first approach leads to design new patent portfolio. It expands both actions and effects offering strong inventiveness. Yet in the second approach there is a risk of non-relevance and thus, the process is controlled by patentability criteria and by company managers that can estimate the interest of the issued solutions internally. The ideas positioning according to the extended action and effects allows determining the design

Article 036-i-99

space and list the concepts that remain to be explored.

Design reasoning that considers patentability criteria actually increases the quality of patent propositions. It shows the necessity to have various processes of ideas exploration regarding the available knowledge, the level of maturity, competition and offers the relevant patent exploration models.

Regarding the applicability of the C-K design theory in case of innovative portfolio exploration, the experience shows that participants do not have to be the experts of neither C-K theory, nor intellectual property. They have to have prior knowledge in the technical field. Though the animator of the session should be able to mobilize both the design reasoning tools and be able to evaluate ideas using the patentability criteria.

Further research should examine the role of animator and expertise in the applicability of the design driven tools like C-K. Moreover, the applicability of CK Invent might be examined in case of SMEs and start-ups whose IP strategy is much more limited in terms of resources.

Finally, this work allows companies to think their patent strategies according to the area of exploration, to their innovative strategies and available resources.

6- References

[CD1] Couble, Y. and D. Devillers, Une approche innovante du processus de rédaction de brevet, Technical Report, Ecole des Mines de Paris, 2006.

[FL2] Felk, Y., Le Masson, P., Weil, B., Cogez, P. & Hatchuel, A. Published. Designing patent portfolio for disruptive innovation - a new methodology based on CK theory Proceedings of the 18th International Conference on Engineering Design (ICED11), Vol. 2: 214-225, 2011.

[G3] Granstrand, O. The economics and management of intellectual property: Towards intellectual capitalism, Edward Elgar Cheltenham, UK, 1999.

[RS4] Reich, Y., et al., A theoretical analysis of creativity methods in engineering design: casting and improving ASIT within C-K theory Journal of Engineering Design pp. 1466-1837, 2010.

[HW5] Hatchuel, A. and B. Weil. A new approach of innovative design: An introduction to C-K Theory. in International Conference on Engineering Design (ICED). Stockholm, 2003.

[HW6] Hatchuel, A. and B. Weil, C-K design theory: an advanced formulation. Research in Engineering Design, 19: 181-192, 2009.

[JK7] Jeong C., Kim K. Creating patents on the new technology using analogy-based patent mining. Expert Systems with Applications, 41: 3605 – 3614, 2014.

[K8] Koh, E. C. Engineering design and intellectual property: where do they meet? Research in Engineering Design, 1-5, 2013.

[M9] Mansfield, E. Patents and innovation: an empirical study. Management science, 32: 173-181, 1986.

[N10] Nissing, N., Strategic Inventing. In a war of patents, choose your own battleground. Research Technology Management, Vol. 48(No. 3): 17-22, 2013.

[NZ11] Nguyen A, Zeng Y A theoretical model of design creativity: nonlinear design dynamics and mental stress-creativity relation. Journal of Integrated Design & Process Science, 16(3), pp. 65-88, 2012

[S12] Schmookler, J. Invention and economic growth, Harvard University Press Cambridge, MA, 1966.

[S13] Sincholle, V., « De la gestion des brevets d'inventions au pilotage de l'innovation : Le cas d'un centre de recherche de haute technologie », in Economie et Sciences Sociales. Ecole Polytechnique: Paris. p. 265, 2009.

[Z14] Zwicky, F. New Methods of Thought and Procedure. in Contributions to the Symposium on Methodologies. Pasadena, 1967.

Article 031-itm-42

PRELIMINARY CONTRIBUTIONS OF INDUSTRIAL MANAGEMENT METHODS TO MICROFACTORY CONTEXT: CASE OF MICRO-CONVEYORS INTEGRATION

Magali BOSCH-MAUCHAND [1], Christine PRELLE [1], Joanna DAABOUL [1], The Anh Tuan DANG [1], Sandy BRADBURY LOBATO [1]

(1) : Université de Technologie de Compiègne
Centre Pierre Guillaumat
CS60319
60203 Compiègne Cedex FRANCE
+33 (0) 3 44 23 73 57
E-mail : {magali.bosch, christine.prelle, joanna.daaboul, the-anh-tuan.dang, sandy.bradbury}@ utc.fr

Abstract: The increased interest in manufacturing smaller products leads to develop automatic, flexible, reconfigurable and upgradable microfactory systems. To achieve this, a specific information system is required to have access to the small scale of the micro-world and to control it. The conveying systems used to transport the micro-components within the microfactory have specific characteristics adapted to the small scale requirements. The proposed approach consists in defining the technical information system needed to control and manage specific micro-conveyors using the Unified Modeling Language (UML). At the Université de Technologie de Compiègne, some researchers of the Roberval Laboratory have been working on the mechatronic devices used in the micro scale. These include actuators, sensors, three-dimensional optical inspection and conveyance systems. An initial database for managing the technical information of these systems is created. Conventional industrial management methods are analysed for their adaptation and application on microfactories.

Key words: microfactory, micro-conveyor, control, information system.

1- Introduction

A microfactory can be defined as a small manufacturing system for achieving higher throughput with less space and reduced consumption of both resources and energy via downsizing of production processes. The term microfactory represents an approach to design and manufacture that minimizes production systems to match the size of the parts they produce [O1].
The microfactories equipment's and accessories required are as traditional as in the classical scale factory, just that there is the difference in size, mass and in accuracy [Q1]. As a matter of fact, microfactory needs extremely precise machining, gripping, and handling units with user friendly interfaces [AC1].
The main characteristics of microfactories are:

- To work with precisions in the scale of micro-meters,
- To face difficult interventions of an operator, especially when troubleshooting.
- To take into account the scale effects like adhesion forces.
- To assure flexibility, modularity [GG1], and reconfigurability of assembly systems and system components [BL1].
- To adapt the transfer system or conveying system so it's the same for all product variants [DL1].

There are several drawbacks when working in the mini and micro scale. The main disadvantage of a microfactory is to overcome the overlying technical challenges ahead of it. It can be a very difficult work for engineers and researchers to find a suitable product platform for micro-manufacturing. The standardization, which would make these things easier, in the micro-world, seems like it is still far away.
Finally, assuming that the microfactory concept could be accepted in a wide range around the world, it would also have an impact on a more general economic point of view. Firstly, a small scale factory needs fewer personnel; hence many people would lose their jobs, which affects the job market. Currently, many manufacturers relocate their production plant to another country, due to low labour cost. This enhances the technology transfer; poor and underdeveloped countries find themselves in the area of modern technology, working in the multinational companies. The microfactory concept will prevent this type of manufacturing shipment making huge technological and economical gap between the industrial and non-industrial world [I1]. Nowadays, much of the work in the field of microfactory is focalised on developing miniaturized machining units, miniaturized robotic and assembly cells, sets of small-size production equipment and modular microfactory platforms [TH1; AC1; RQ1; [GH1]]. Few

works focus on the management of such a factory and on the optimisation of its workflow. This article is a first step towards managing a microfactory and analysing the differences with managing a conventional factory. Its first part is dedicated to the drawing of the characterisation of microfactory systems. The second part presents the UML Class Diagram of the proposed Information System (IS) structure aiming to manage the microfactory system.

2- Characterisation of microfactory systems

2.1 – Disadvantages

The main disadvantages are due to the non-maturity of the microfactory systems.
Some of these disadvantages are:

- Subsystems availability and price.
- Low productivity compared with conventional plants.
- The interface between micro and macro: it needs extensive R&D: Highly technology based advanced society.
- Difficult system integration: difficult wiring and mounting, and difficult components integration.
- Physical restrictions of small equipment size: smaller lever arms and pneumatic lines; relative mass of sensors and actuators; sensitivity to vibration and temperature; difficult to work around in case of troubleshooting.
- Restrictions of micro environment: Gravity becomes insignificant, adhesion and other surface forces dominate instead.

2.2 – Advantages

Based on the literature, multiple advantages are linked to miniature production systems. The advantages can be categorized in four groups: ecological, economic, technical and engineering aspects and human aspect [O1; Q1].

- Ecological advantages: energy and resource saving; reduced heat, vibration, noise and waste; local environmental control: easier control of pollution and waste.
- Economic advantages: reduced required investment; reduced running costs; efficient use of space; high portability; reconfigurability and scalability: easiness in changing or removing production modules allowing easy reoptimization when production changes; agile ramp up; enchained cell manufacturing.
- Technical and engineering aspects: higher speed of reconfiguration; precision due to small size manipulators; productivity via parallel layout; piece-by-piece processing; process integration; small and fast production series.
- Human aspect: less stress and physical effort for the operator; educational and non-expertise applications; human machine harmonization; human can see in a look most of the factory and process chain and therefore it is easier to manage and understand.

2.2 – Microfactory system characterisation

To achieve an automated micro-production, the microfactory should have the following requirements, attached to the recent technological advances and recent fundamental knowledge [D1]:

- Reconfigurability, to allow the ongoing evolution of production of a micro-product series.
- Rearrangeable, to allow a micro-product change inside a same microfactory.
- Evolvement, to accommodate new technologies (that implies certain modularity as well as a sustainability concept).
- Acquisition of new knowledge, to enrich databases and ensure the increase of efficiency.
- Generation of new knowledge, to meet new technical needs.
- Productivity, to optimise time and cost.
- Quality, to ensure traceability of the micro-products and the undertaken operations.
- Flexibility, to produce small to medium quantities.

The microfactory has to manage physical flows (of micro-components, micro-assemblies and micro-products), flows of information and the critical flow of energy (nowadays it is a major concern [ZP1]).

3- Proposal for microfactory structure and Information System

Often replaced by the acronym IS, the Information System comprises the organization of a set of resources for the acquisition, structuring, storage, communication, exchange and control of data inside a business. This objective is usually achieved through various hardware, software and human resources. If the IS provides the data communication globally inside an organization of the business, in the industry there are two categories of information systems: the IS for the management support, and the IS for the operations production support. Obviously, it is this second category which really concerns the microfactory. This information system dedicated to the support of operations of the microfactory is the only possible access to the micro-world for the operator; either to be able to act or to make measurements [D1].

3.1 – Microfactory Information Structure

A microfactory system is basically formed by four groups of elements that have to interact with each other to fulfil the microfactory's goal (the assembly and/or operation of micro-components to obtain micro-products) [DG1]:

- A MicroFactory Layout (MFL);
- An Organization System (OS);
- An environment;
- A Human-Machine Interface (HMI).

This work focuses on the MFL structure and on the IS needed to interact with the OS to analyse, control and manage the elements and production process of the microfactory.
The MFL defines the working platform which consists of a combination of micro-modules. A micro-module is defined as a (micro)-sub-system formed by a group of basic components that when linked together can perform a specific task. Examples of modules are machining or assembly module, transport or handling module and stocking module. It will contain the information about its name, its task, its

type (if it is an assembly module, or a transport module, etc.), the number of degrees of freedom it has depending if it is a conveyor, a robot or a machine, the environment required to fulfil its task; and finally its size.
The MFL performs multiple tasks. Firstly, it allows the relative positioning of modules. These positions can be changed and adapted to the current production plan and are likely to evolve to better adjust to a production configuration. As opposed to the traditional linear representation of a production line, the MFL is able to accommodate various layouts. Secondly, it allows the establishment of three types of links between the various parts involved in a microfactory. First, it manages the flow of micro-products: the inter-module transfers, the material supply and the shipment of the produced micro-products. Second, it takes into consideration constraints related to energy supply of the micro-modules. All handling or assembly interventions require energy due to non-human intervention. Third, the MFL exchanges information with all modules via the OS.

3.2 – A focus on Organization System

A production system adapted for micro-products has to be concentrated on improving productivity, requiring high availability, defining a production volume according to the demand and providing a great reliability. To achieve this, it is necessary to have a centralized Organization System (OS) to manage the data and information in an appropriate way [DD1]. This manufacturing control commonly denotes the task performed by a Manufacturing Execution System (MES) [VV1].
MES are information technology systems that manage manufacturing operations in factories. It is basically a computer system which has as a main goal to collect in real-time all or one part of the production data of a factory. The collection of these data is a prerequisite for the execution of multiple analysis activities [JH1].
The analysis of the remaining activities will define the specific needs of the micro-world and the information to manage:

- The resource allocation and status is needed to manage the supply of energy, a key feature in the microfactory due to its low consumption and specific supply, and the supply of raw material. It is named **Resource Management**.
- The operations/detail scheduling activity has the same function as in a conventional factory but with the added factor that an evolutionary knowledge generation will be important to enable the criterion of reconfigurability during the production and rearrangeability for each new production. It is named **Task Scheduling**.
- The dispatching production unit's activity has also the same function as in a conventional factory. It has to manage transfers between modules and within the modules. It is named **Parts and Products State**.
- The data collection/acquisition keeps track of all the data containing the necessary information needed to interact with the microfactory. It is the only possibility of information for the operator from the micro-world. The data will also be useful for the capitalization of know-how, taking into account that the concepts of microfactories are still under development. It is named **Data Acquisition**.
- The process management activity has the same function but more focused on the remote-controlled manipulation and the precisions required during the production process. It is named **Analysis and Control of Processes**.

To the five activities previously mentioned two extra activities or control functions are added. The first one is **Communication Control**. The communication within a microfactory is a very important aspect for a good and smooth running of it. The communication control will deal with the communication between modules, between conveyors, between the modules and the MFL, etc., making sure the connections are working correctly and alerting if there is any troubleshooting.
The second one is **Configuration**. Due to the importance of reconfigurability and modularity, managing the configuration of the modules in the microfactory will be vital. Therefore, a dedicated function seems reasonable.
Table 1 summarizes these activities and highlights the differences with the management of a conventional factory.

	Difference with conventional factory
Resource Management	Allocation of resource in conventional factory concerns the allocation of human resources/tools/materials handling resources to tasks. While in a microfactory it is mainly about allocating energy. The problem changes for it is not about optimizing the utilisation of a resource with a defined capacity but to optimize the utilisation of resources while minimizing the maximal used of capacity.
Task scheduling	In a conventional factory the scheduling optimisation considers a fix layout. In a microfactory the layout may change at any time.
Parts and Products State	No significant difference.
Data Acquisition	This task is much crucial for the managing of a microfactory than for a conventional one. A real time data acquisition with high accuracy is crucial to successfully manage a microfactory.
Analysis and Control of Processes	No significant difference. High precision required for all processes.
Communication control	Specific to microfactory
Configuration	Specific to microfactory.

Table 1: Synthesis of a microfactory OS structure and difference with a conventional factory.

3.3 – Information System for the micro-module

The MFL can be formed by one or more micro-modules. A micro-module (or micro-cell or micro-station) can perform one task independently of other micro-modules. Each micro-module contains control, communication and supply systems. It has an input and output of data that is accessible by other micro-modules and by the MFL – *µFactoryModule* (Figure 1).
The control system is in charge of managing and controlling the different elements for the correct execution of the micro-module process. The communication system takes care of transferring the information to the right place to coordinate all the different elements. Finally the supply system is in charge of supplying the necessary energy to the elements that need it at a specific time. It can also refer to the supply of raw material or micro-products into the micro-module.

Finally, one of the most important elements in the microfactory is the micro-product, the one that has to be operated on and depending on its characteristics the microfactory will use one configuration or another. Thus at least there will be one micro-component which will be carried around the micro-module in a pallet or directly with micro-conveying system. During the production process, it is possible that the micro-component is assembled with another to become a micro-subset.
Furthermore, if it's the end of the assembly process, then it will be a micro-product. As mentioned before, these micro-components will have certain characteristics that will be primordial for the organization of the microfactory; hence it will be necessary to have access to the information containing its geometry, material and other characteristics.

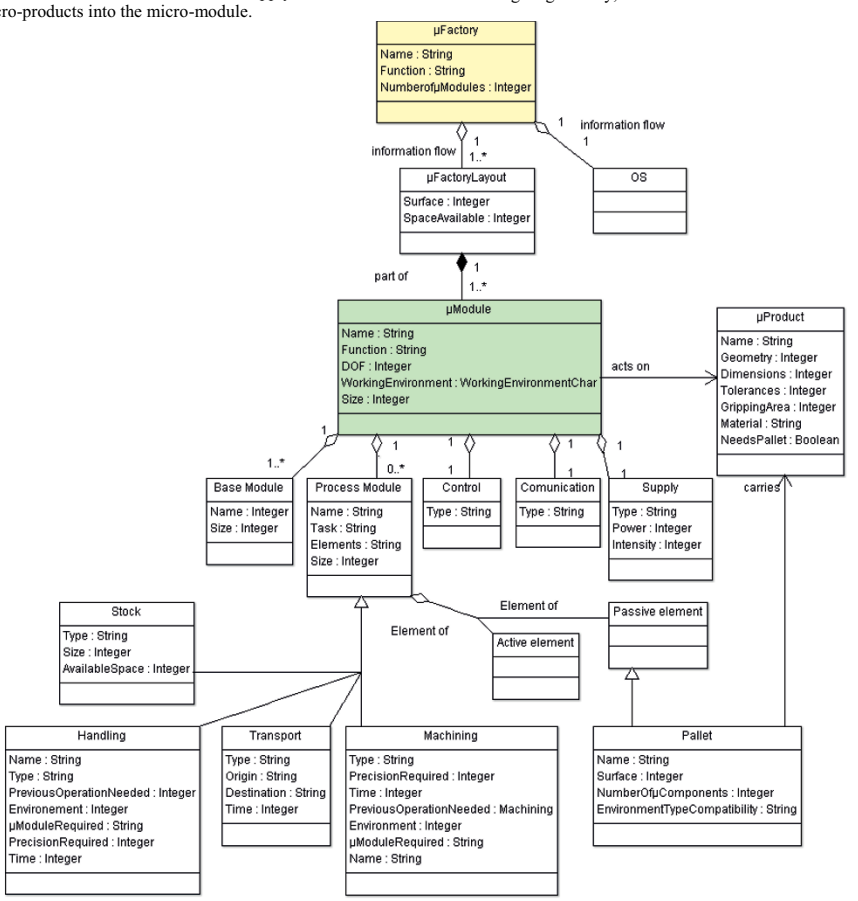

Figure 1: Class Diagram of the micro-module information structure – *µModule*.

A micro-module is formed of at least one base module and process modules. A base module is defined as a support module connecting the control and supply. Thus it assures the interaction at all levels with other micro-modules and with the microfactory as a whole. A process module interacts directly with the micro-product by transforming (machining/assembly), handling and moving it.

A micro-module has to be autonomous and designed on the principle of modularity. This principle means that the structure approach of the microfactory has to permit to divide or split the production system into these subsystems called modules [P1]. These basic elements will be contained in what is called the process module. As an example, for the assembly of two micro-products, a transport system is needed to move and orient the micro-products to the operating machine, where the assembly will take place, and then again the transport system may carry and deposit the assembled micro-product into a stock area within the module.

Examples of micro-modules at the laboratory are of two types: micro-conveyors and micro-Coordinate Measuring Machine (µCMM) (Figure 2). The displacement of micro-product can be executed by continuous or discrete devices.

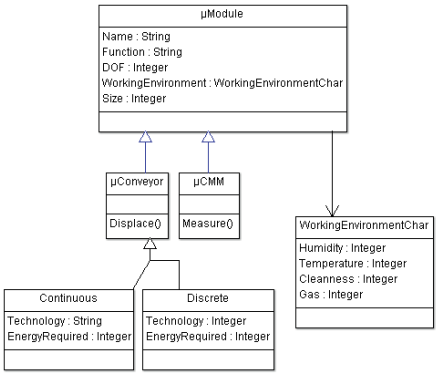

Figure 2: Class Diagram of the micro-module physical structure.

3.4 – Information System for the micro-conveyors

At UTC, there are two options for conveying the micro-objects, one formed by a digital meso-actuators network, and the other one by micro-actuators moving on a smart surface.

A micro-conveyor is a micro-module for transportation. Its main function is to transfer the micro-products around a micro-module (station) or the microfactory itself. The Class Diagram in Figure 3 shows the structure of the elements of a micro-conveyor.

The micro-conveyor needs a source to generate the movement; this is accomplished by a motor, which is formed basically by actuators. The coordinated actuation of these generates the required displacement.

Depending on the technology used to convey, the micro-conveyor will have a specific working surface. This concerns the shape of the micro-conveyor and the structure of the path on which it moves or it is guided through (in the case that the route is fixed).

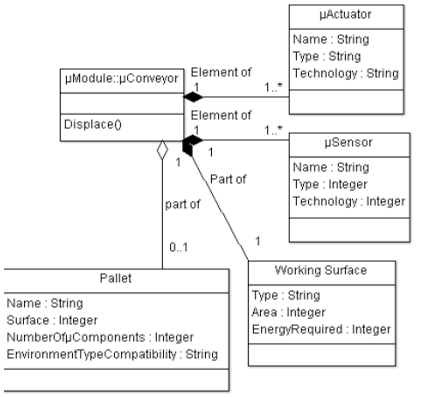

Figure 3: Class Diagram of the UTC conveyor.

It will also have a set of micro-sensors to constantly keep track of its position, to insure it moves into the right places as accurately as possible and to send the information containing the exact position at each time to the organization system hence it can manage it in the appropriate way. Depending on the technology used there might be no need for micro-sensor feedback.

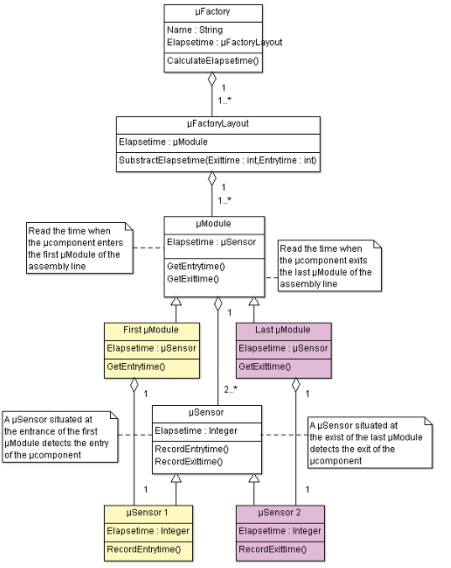

Figure 4: Class Diagram of the elapse time of a micro-conveyor in a microfactory.

Finally, the micro-conveyor can also contain a pallet to carry the micro-components. This pallet can be flexible or not, in the sense that it can have a fixed shape, so the micro-components will all have to be adapted to it. The advantage is that they will be fixed and won't move during conveying.The pallet can just be a plane surface where different kinds of micro-component shapes can be carried, though, in this case, it is limited by the fact that the micro-component must have at least one side that is planar.
Elapse time of micro-conveyor is one of the main important data for the organization system, a performance driver. The knowledge of the required time to execute the operations is essential for managing and optimizing the microfactory's performance (Figure 4).
The communication system must not be specific to one type of technology used for conveying. To adapt to the micro-scale, compact and efficient basic electronics will be needed (for instance, RFID or optical fiber). The information shared will depend on the technology used. But the main limitation will be to develop a positioning system (geolocation) adapted to the micro-scale.

4-Discussion

The presented work in the previous section leads to the following conclusions:

- Managing a microfactory is not totally similar to managing a conventional factory.
- The adaptability of existing algorithms or the development of new ones is necessary to properly manage a microfactory, especially for resource management and facility layout.
- Data acquisition is a crucial factor for the good performance of a microfactory.
- An organisation system for conventional factory is not sufficient for managing a microfactory. Two new modules should be added to the OS: communication control and configuration.
- Research is required to optimise the configuration/reconfiguration of a microfactory.
- Research is required to develop and optimise a communication system dedicated to microfactories. Also an analysis on the advantages/disadvantages of certain communication systems for microfactories is necessary.

5- Conclusion

The research work described in this paper is a first step in the field of microfactory management. Its aim is to define differences between required information system and technology for managing a microfactory compared to a conventional one. This is realised by a first specification of the data meta-model of an information system for micro-factory. The research activity on the subject of micro-factory management is a combined activity between different researchers at UTC. Currently it is the subject of a starting PhD thesis. The future activities will be to design the organisation system and the MFL dedicated to microfactory including the two new modules: Communication Control and Configuration.

6- References

[AC1] J. Agnus, N. Chaillet, C. Clévy, S. Dembélé, M. Gauthier, Y. Haddab, G.J. Laurent, P. Lutz, N. Piat, K. Rabenorosoa, M. Rakotondrabe & B. Tamadazte, Robotic microassembly and micromanipulation at FEMTO-ST, Journal of Micro-Bio Robotics, Springer-Verlag, 8, 91-106, 2013.

[BL1] A. A. Bruzzone, P. M. Lonardo & A. A. Traverso, A non-contact control architecture for micro-components assembly, CIRP Journal of Manufacturing Science and Technology, 4, 44 – 50, 2011.

[D1] E. Descourvières, "Contribution à l'évaluation de la reconfigurabilité et réorganisabilité d'un micro système de production: application à une micro-usine d'assemblage », Thèse présentée à L'UFR des Sciences et Techniques de l'Université de Franche-Comté, France, 2010.

[DD1] E. Descourvières, S. Debricon, D. Gendreau, P. Lutz, L. Philippe, and F. Bouquet. Towards automatic control for microfactories. In 5th Int. Conf. on Industrial Automation, Montréal, Québec, Canada, June 2007.

[DG1] E. Descourvières, D. Gendreau, P. Lutz, "Data representation for the control of full-automated microfactories", published in "Proceedings of the 5th International Workshop on MicroFactories", IWMF'06, Besançon, France, 2006.

[DL1] A. Delettre, G.J. Laurent, Y. Haddab & N. Le Fort-Piat, Robust control of a planar manipulator for flexible and contactless handling, Mechatronics, 22, 852 – 861, 2012.

[GG1] D. Gendreau, M. Gauthier, D. Hériban, P., Modular architecture of the microfactories for automatic micro-assembly, Robotics and Computer-Integrated Manufacturing, Vol. 26, pp. 354–360, 2010.

[GH1] A. Giorgetti, A. Hammad, and B. Tatibouët, Using SysML for Smart Surface Modeling, in Proc of the IEEE First Workshop on Hardware and Software Implementation and Control of Distributed MEMS, pp. 100-107, 2010.

[I1] A. Islam, "Literature Survey Report on Microfactory", IPL, DTU, 2005.

[JH1] E. Järvenpää, R. Heikkilä, R. Tuokko, "Factory Level Logistics and Control Aspects for Flexible and Reactive Microfactory Concept", Frontiers of Assembly and Manufacturing, Springer Berlin Heidelberg, 2010, pp. 127-139.

[O1] Y. Okazaki, "Microfactories – A New Methodology for Sustainable Manufacturing", International Journal of Automation Technology, Vol.4, No.2, 2010.

[P1] M. Paris, "Conception et commande de systèmes d'alimentation en composants de petites tailles pour micro-usine d'assemblage de haute précision", Thèse présentée à L'UFR des Sciences et Techniques de l'Université de Franche-Comté, 2008.

[Q1]Y. Qin, "Micromanufacturing Engineering and Technology", 1st Edition, Elsevier, ISBN9780815515456.

[RQ1] A. R. Razali & Y. Qin, A Review on Micro-manufacturing, Micro-forming and their Key Issues, Procedia Engineering, 53, 665 - 672, 2013.

[TH1] R. Tuokko, R. Heikkilä, E. Järvenpää, A. Nurmi, T. Prusi, N. Siltala, A. Vuola, "Micro and Desktop Factory Roadmap", 2011. http://URN.fi/URN:ISBN:978-952-15-2984-9.

[VV1] P. Valckenaers, H. Van Brussel, "Holonic Manufacturing Execution Systems", CIRP Annals - Manufacturing Technology, Vol. 54, N° 1, pp. 427–432, 2005. Source: MESA (Manufacturing Execution Solutions Association) International.

[ZP1] E. Zampou, S. Plitsos, A. Karagiannaki & I. Mourtos, Towards a framework for energy-aware information systems in manufacturing, Computers in Industry, 65, 419-433, 2014.

6

Sustainability

Major topics of the full argumentations are the following:

X. Fischer et al. (eds.), *Research in Interactive Design (Vol. 4)*
DOI 10.1007/978-3-319-26121-8_16

Article 019-sd-18

LIFE CYCLE ANALYSIS IN PRELIMINARY DESIGN STAGES

Lina-María Agudelo[1,2], Ricardo Mejía-Gutiérrez[2], Jean-Pierre Nadeau[1], Jérôme Pailhes[1]

(1) : Arts et Metiers ParisTech, I2M, UMR 5295
F-33400 Talence, France.
{jean-pierre.nadeau, jerome.pailhes}@ensam.eu

(2) : Universidad EAFIT, GRID
050034 Medellín, Colombia
{lagudel8, rmejiag}@eafit.edu.co

Abstract: In a design process the product is decomposed into systems along the disciplinary lines. Each stage has its own goals and constraints that must be satisfied and has control over a subset of design variables that describe the overall system. When using different tools to initiate a product life cycle, including the environment and impacts, its noticeable that there is a gap in tools that linked the stages of preliminary design and the stages of materialization. Different eco-design methodologies under the common denominator of the use of a life cycle analysis have been compared in time efficiency of use and in which stages of the life cycle they can be used. A case study was developed by the application of these methodologies to obtain first-hand information and interpretable results to define advantages and disadvantages of the selected methodologies.

Key words: Sustainability, Life Cycle Analysis, Eco-Design, Design Process.

1- Introduction

The product´s life cycle varies dramatically, from processors embedded in disposable consumer goods to applications requiring maintenance and support for decades. Taking into account the complete product life cycle is a design requirement. It covers from the initial product concept, through its operational period, finishing with the replacement with advanced equipment [K2]. The specific concern areas in a life cycle perspective are: an accurate life cycle economic model to guide engineering tradeoffs, taking into account requirements for logistics and support during the product operational period, and other issues regarding to refurbishing/retiring/discarding the system at the end-of-life. Despite the fact that the "life cycle" term has different meanings for various technical communities, the main idea is to expand the traditional engineering emphasis on the "design cycle" to include optimizing utility, profits, and tradeoffs across the entire lifetime of the product being designed. [K1]

2- Design process

Design is an iterative process; since the solution is not found on the first attempt (technical parameters, ergonomics, aesthetics, economics, logistics, legal, etc.). The more is explored about a problem domain (different alternatives being explored), there is a need to start from scratch more than once. This is a core issue when designing in diverse fields such as building, product design and computer system design. Even though design activities within those fields are apparently not related, all of them aim to solve an often ill-specified problem with a solution that suits conflicting goals.

In a typical sequential design process [PB1] (Figure 2), the product is decomposed into systems, each system has its own goals and constraints that must be satisfied, [HG1] [B1] and has control over a subset of the design variables that describe the overall system. [H1] Clearly, a new approach is needed in order to take into account the complex interactions that exist among the disciplinary lines.

Many functions or design constraints are associated with the life cycle and should be considered for a deep understanding of the product, including design stages, inputs and outputs of the system.

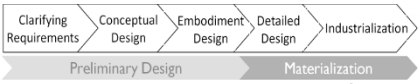

Figure 2: Overview of development of a product´s cycle

It is during the design process when an estimated 60-85% of the product's cost is determined [Z1]. This has led to the increased interest in the activities incorporated in the design process [AB1]. Rapid product development cycles require design methodologies to explore efficiently design spaces to build world wide competent products by reducing costs and environmental impacts, also, improving functionality and quality.

One of the design steps that is least supported, is the transition from early design phases to the final design stages, which is considered a major activity within the design process. [AB1]. This is the transition from vague and imprecise parameters to precise and exact values. In contrast, many design methods only attempt to provide design support

in the domain of well defined variables and parameters in which all values used during design must be known with certainty. This certainty restriction limits the utility of these systems to the later stages in the design process.

Imprecision is most noticeable in the early phases of the design process (Figure 3) and has been defined as the choice between alternatives [AO1]. Uncertainty can be described as the cloud of alternatives the designer must consider [LA1]. The concept of this "cloud" is related to the presence of facts that haven't been concretized and will be critical for the product performance. Moreover, is during this stage in where designers might be judgmental because there are no certain variables thus giving their own meaning to them, enhancing the randomness and indeterminacy within the stage [WE1].

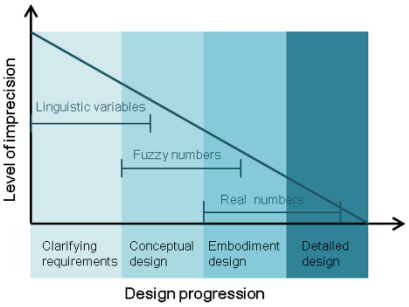

Figure 3: Design stages versus imprecision level [AO1].

3- Life cycle Analysis

The life cycle analysis emerges from the term "sustainable development", that was first introduced in the report of the World Commission on Environment and Development that appeared as Our Common Future in 1987 [HG1]. Since then, sustainable development is steadily defined as "development that meets the needs of the present generation without compromising the ability of future generations to meet their own needs" [B1] sustainable development has been adopted as a policy principle by the UN, the EU, many countries, but it has also become a central notion for many designers, engineers, companies, business councils, political parties, etc.

The term sustainability has directed policy makers, environmentalists and industrial decision-makers to a broadened focus in various directions regarding the life cycle of a product**:**

3.1 – Life cycle thinking

Successful and sustainable innovation relies on having a clear understanding of product's impacts and benefits or service throughout the entire life cycle, starting from the sourcing of raw materials and ending up by ultimate disposal at the end of life. It is imperative to consider all stages in the life cycle, not just the ones that go until the company's factory gate [LS1].

Life cycle thinking is sometimes referred to a "cradle to grave" approach, as it follows a product or a service from sourcing of primary materials ("cradle") to ultimate disposal of waste ("grave"). A related term "cradle to cradle" refers to the design of products that can be easily reused or recycled at the end of their useful life. This helps to use resources in a more sustainable way. Moreover, it avoids waste when the use life is over. Therefore, a sustainable approach to design of products is essential, as the product life cycle and its subsequent impacts are determined at this stage, then, it is crucial for the conceptual and architectural stages that all future impacts must be taken into consideration.

"Life cycle thinking" can be translated into sustainability quantitative measurement. Considering the sustainability basis (environmental, social and economic dimensions), examples of such measures are illustrated in Figure 4. In order to life-cycle-thinking be an effective early stage approach tool for the industry, by speeding up the decision making process, designers must completely understand which parameters are meaningful and meaningless for a product's environmental impact. This parameter relevance is found in materials to be used, manufacturing process, measurement shipping, logistics and maintenance. However, evaluation of the environmental performance of these parameters for generating alternatives that improve upon the performance of designs are typically not performed until the design development stage [BF1] and they evolve along the product´s life cycle.

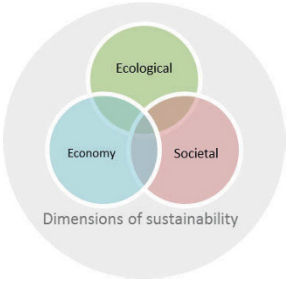

Figure 4: Pillars of sustainability

3.2 – Life Cycle Assessment (LCA)

Life Cycle Assessment (LCA) is a compilation and evaluation of inputs, outputs and potential environmental impacts of a product or service throughout its life cycle. LCA as outlined by International Standards Organization –ISO- [HG1] has been widely applied as a decision support tool to identify the important environmental factors in product systems. Moreover, it is able to compare the full range of environmental effects assignable to products and services in order to improve processes, support policy and provide a sound basis for informed decisions [G1**].** LCA enables the identification of the most significant impacts and stages within the life cycle which maximum improvements are required to be targeted (Figure 5). This helps to avoid the shift from environmental burdens from one stage to another, as would be the case if the production process was

considered in itself.

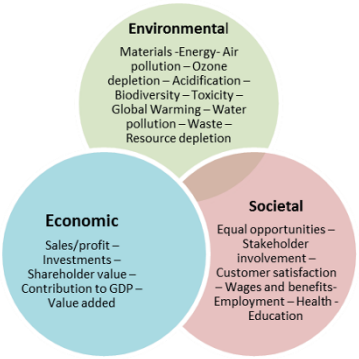

Figure 5: Sustainability issues in the life cycle of a product [AS1].

Such developments have produced an overabundance of concepts, approaches, strategies, policies, models, tools, and indicators. To mention a few, sustainability analysis, technology assessment, life cycle costing, life cycle assessment, green chemistry, and eco-efficiency attempt to provide an answer to questions regarding the sustainability of overall industry, and of the production-consumption system in an even more general sense. [HH1] However, this area has matured to the point that there are international standards to approach towards the problem, including the ISO 14000 series, and in particular ISO 14040 "Life Cycle Assessment"(LCA) [K1]. The main phases of an LCA Methodology [P1] [HG1] are:

• Goal & Scope definition: The goal & scope definition is a guide that ensures the consistent performance of the LCA. In this section, the most important (often subjective) choices of the study are described in detail i.e. methodological choices, assumptions and limitations, particularly with regards to the following topics.

• Inventory analysis: A Life Cycle Inventory (LCI) includes information on all of the environmental inputs and outputs associated with a product or service i.e. material and energy requirements, as well as emissions and waste. The inventory process seems simple enough in principle, in practice however, it is subject to a number of practical issues.

• Impact assessment: The inventory list is the result of all input and output environmental flows in a product system. Nonetheless, a long list of substances is difficult to understand and that is the reason of why a further step is needed, this step is known as life cycle impact assessment.

3.2.1 –LCA principle

There are diverse LCA methodologies that can be applied. They differ according to categories (Energy consumption, toxicity, raw materials, emissions), and they have an impact on their indicator selection and the geographical focus. There are also some “Eco-design” tools and software that use LCA principle to reduce the environmental impact, but LCA has some limitations, which are related to the insufficient transparency of the results, which can hinder the utilization of existing studies as an information source and comparisons. Moreover, LCA does not consider the social and economic impact during the product life cycle (even though the life cycle approach and methodologies can also be applied to these aspects) [P1] and requires the design parameters and extensive knowledge to be developed (dimensional parameters, types of materials, mechanical and thermal parameters, obtaining and manufacturing processes) which are known at each stage of the life cycle and evolve along the cycle.

Even in complete design processes, the use of different policy tools to begin with a product life cycle, including the environment and the possible impacts, there is a gap between tools that link the preliminary and materialization stages. (See Figure7).

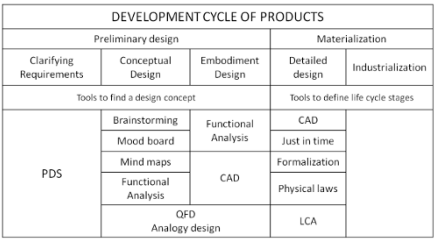

Figure 7: Development cycle of products with tools

4- Methodological approach

Several eco-design methodologies were chosen from a set of methodologies using LCA as a common denominator. These methodologies have been compared (quantitative and qualitative) and analyzed in order to know which stages during the entire life cycle can they be used in.

A case study was made for the implementation of methodologies, in order to get firsthand experience and have interpretable results throughout the design process to find the advantages and disadvantages of the selected methodologies.

It’s important to take into account the previous knowledge a designer must have in order to develop a specific product, such as a full understanding of the main components, material and available technologies in the context where the product will be developed. Hence, the design practice will be an approximation to a feasible concept.

The methodologies used LCA as a basis for analysing and creating an improved design solution. Nonetheless, it was found that existing tools could be used only after the concept development and product’s architectural design, which means that environmental impacts cannot be measured at the

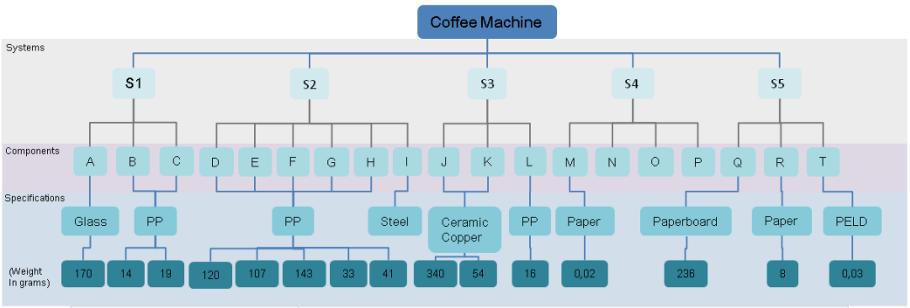

Systems				Components															
S1	Coffee container	S4	Packaging	A	Glass bowl	D	Filter shell	G	Cover top	J	Heating	M	Paper filter	P	Coffe waste	T	Plastic bag		
S2	Body	S5	External Environment	B	Glass top	E	Heating shell	H	Lower top	K	Cable	N	Water	Q	Paperboard				
S3	Heating			C	Handle	F	Body shell	I	Screws	L	Filter	O	Coffee	R	Manual				

Figure 8: Coffee Machine organization chart

early stages of the product's life cycle (Clarifying requirements, conceptual design, and embodiment design).

The analysis was applied to a SAMURAI 6 cups coffee maker (Figure 8) since the chosen methodologies where found to have a void regarding the initial phases of the design process, which grounds the understanding of the LCA being a method that doesn't cover the preliminary design process.

The methodologies used are:

• Eco-indicator 99: Is a quantitative methodological tool that has evolved over time, is one of the most characteristic tools within the LCA. There are numbers that express the total environmental load of a product or process, analysing the product over the life cycle, if the indicator is higher, the environmental impact will be higher. Next to this different design alternatives can be compared [I1]. It is a tool to be used in the search for more environmentally-friendly design alternatives and is intended for the internal use [M1].

• MET matrix: Is a qualitative method that is used to obtain a global view of the inputs and outputs in each stage of the product life-cycle. It also provides a first indicator of aspects for which additional information is required. In developing the MET matrix it is important to consider first all parts that the product has, as its weight in kg, and which processes are used to manufacture the product, also the processes of transport and disposal. This method helps to know if additional information is needed to further establish a prioritization of the elements that the study shows [I1].

• SIMAPRO: It is a software tool often used in LCA to obtain many of the CO2 impacts [S1]. These factors are critical for converting product component material quantities into embodied impacts. SimaPro is chosen because the software contains impact measurements for many different products materials [BF1]. A limitation of the program is that the software cannot be integrated when going through the preliminary stages of design.

• LiDS Wheel: is a visual tool that allows to contemplate the differences in environmental impacts when two products are being analysed, for that, the tool presents eight major areas of interest to be consider in the design and optimization of a product: Selection of low-impact materials, Reduced use of materials, Techniques to optimize production, Optimizing the distribution system, Reduction of impact during use, Lifetime optimization, System optimization end of life and Development of a new concept [I1].

• Okala Wheel: Is one of the newest qualitative methodological tools. It also has a comprehensive database where the designers base an environmental product improvement in quantitative data. The wheel serves as a powerful brainstorming tool to explore areas of product development or improvement that have not yet been considered [O1].

5- Case study and comparison

In order to apply and compare the different eco design methodologies, a product composed by several systems was chosen. Therefore, it was possible to compare their applicability, time efficiency and usability. In addition, design parameters for each of the methodologies were determined in order to decrease environmental impacts. The study case was made in the following two stages:

5.1 – LCA comparison

The Pugh matrix below (Figure 9) shows which methodologies could be used or not during the different stages of the product life cycle.

Measurement:
(-) The tool provides no solution or decision-making aid at this stage.
(+) The tool provides a solution or decision-making aid at this stage.

				Qualitative			Quantitative		
				Okala Wheel	LiDS Wheel	MET Matrix	Ecoindicators 99	SimaPro	Analysis
Development cycle	Preliminary Design	Clarifying requirements		-	-	-	-	-	A1
		Conceptual design		+	-	-	-	-	A2
		Embodiment design		+	-	-	-	-	
	Life cycle stages	Detailed design	Raw material extraction	+	Δ	Δ	+	+	A3
			Manufacture	+	Δ	Δ	+	+	
		Industrialization	Transport	Δ	Δ	Δ	Δ	+	A4
			Use and Maintenance	+	Δ	Δ	Δ	Δ	A5
			End of Life	+	Δ	-	+	+	A6

Figure 9: Evaluation of eco-design methodologies

(Δ) The tool provides partial solutions or help decision-making at this stage.

Analysis 1 (A1): in "clarifying requirements" stage, from the preliminary design, none of the LCA methodologies provide any tool to obtain a solution or decision-making aids. In addition, it's noticeable that the LCA has no intervention during the need-searching phase.

Analysis 2 (A2): During the conceptual design stage, Okala gives the designer a number of examples in each stage of the life cycle, which can be taken as a basis to develop a full concept design. In the stage of embodiment design, "Okala" presents a quantitative way to help decision making, easy to use and understand, fast and affordable

Analysis 3 (A3): In both stages: raw materials extraction and manufacturing processes, the Okala, Eco-indicators and Simapro, provides a database that allows to make decisions related to materials and processes selection with lower environmental impact. Also, it allows a comparison over other substitute products. Instead LiDS and MET matrix are tools that don't even give the designer an aid for making design decisions during these stages; the designer can measure their impact comparing them with old or competitive products.

Analysis 4 (A4): In the transportation stage, the quantitative tools give the designer a numerical data that can guide the decision regarding which transport mode, shipping and logistics is better to use.

Analysis 5 (A5): Okala, is the tool that gives the designer a number of improvement examples for the use and maintenance stages, making it more attractive if a new design concept will be developed and not just a comparison with the competition

Analysis 6 (A6): At the end of life stage; Okala, Ecoindicators and Simapro, offers to the designer a database and examples of appropriate final disposition parameters, also a metric comparison. Instead, MET gives a series of data that can only be used when the product is developed, which makes this tool, purely qualitative and only useful to compare existing designs.

5.2 – LCA Parameters analysis

Then, in order to define the parameters required by each method, a component (S1-A) from the assembly was chosen.

It started from the need to design the glass bowl for the coffee machine, in order to follow a complete design process. Also, the studied methodologies were applied to detect the parameters required to implement them, and which parameters are known or not.

Most parameters (weight, volume, materials, processes, etc.) are obtained in the detailed design stage (to avoid assumptions and imprecision of design parameters and rework); limiting the methodology application to the early stages of design development.

The following matrix (Figure 10) shows which parameters are required for the application of different methodologies.

Measurement:

(-) The parameter is not required for the application

(+) The parameter is required for the application

After defining the parameters needed to implement the methodologies, it can be seen that in the early stages of product development, these parameters are vague and diffuse [AO1] even some of these parameters are not known yet, (Weight, volume, dimensions, materials) even when based on redesign process.

In a complete new design process the imprecision and ambiguity of the parameters make the design process slower, less time-efficient and more costly, usually forcing the reprocessing.

	Materials	Weight	Volume	Manufacturing Process	Energetic consumption processes	Toxic emissions	Packaging	Transport system	Energy consumption in use	Disposal
Ecoind 99	+	+	-	+	+	-	+	+	+	+
LiDS Wheel	+	+	+	+	-	-	+	+	+	+
Okala Wheel	+	-	-	+	+	-	+	+	+	+
MET Matrix	+	+	-	+	+	+	+	+	+	+
SimaPro	+	+	-	+	+	-	+	+	+	+

Figure 10: Parameters required for the application

6- Further work

Currently, in order to measure the environmental impact according to material selection, the designer might choose between several ways to proceed, to give an example, an existing product data base or a tool that facilitates to carry on with uncertain variables, such as a fuzzy logic tool [AM1]. The importance of this process it's the level of uncertainty that will be found in early stages of the design process, grounding the results according to design variables. Therefore, tackling uncertainty in early stages is not only imperative in order to address user requirements accurately; it also opens a possibility to cover sustainable requirements since the design process begins.

A review of the different methods that aim to solve uncertainty issues, may give a clue of how sustainability can be defined since the task clarification phase within a product design process.

At the beginning of a design process, it is evident that ideas are vague and might vary easily, what makes difficult to find an environmental impact measure of a concept. In contrast, it might be different if the process it's already in the detailed design phase, in where variables such as measures, materials and manufacture processes are already defined. (See figure 11)

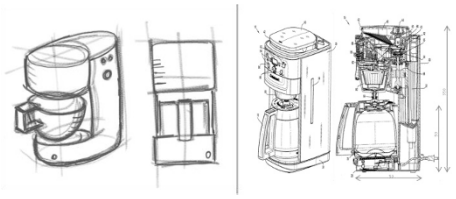

Figure 11: Coffee Machine sketch Vs Coffee Machine technical drawing.

7- Conclusions

A case study analysis was presented in order to show which LCA methodology has the highest contribution to a product's embodied impact by aiding consistently the design process. They should have participation during early design stages as well, leading to an embodied impact reduction and leave not so important decisions to the design development stage.

The scope of the evaluated methodologies is limited to the constraints and parameters, requiring the knowledge of the previous existing products in the preliminary design and the indicators adaptation. The imprecision of the specific parameters, estimates the value range (materials, dimensioning), among others.

A significant portion of the environmental impacts of the product is determined by the decisions made in the early stages of design. An early stages, there is evidence of an absence of indicators to guide designers on their decision-making.

It has been noticed that during stages where needs are identified, there are not enough general rules that supply adequate information that could reduce the environmental impacts and cost of the final product. In addition, the preliminary design stage should seek to reduce uncertainty by suiting the indicators to easily known general parameters, estimates of intervals and parametric models (a guideline is defined by variables) or grouping linguistic variables.

8- Acknowledgment

Thanks to EAFIT University and Arts et Métiers ParisTech for funding and give academicals support to this study in their research groups.

9- References

[AB1] Abeln, O. 1990, "CAD-Systeme der 90er Jahre - Vision und Realität", VDI-Berichte Nr. 861.1, Dilsseldorf 1990.

[AO1] Antonsson, E.K., and Otto, K.N. 1995, "Imprecision in engineering design", ASME Journal of Mechanical Design 17, 25-32. 1995.

[AM1] Agudelo, L.M.; Mejía-Gutiérrez, R.; Nadeau, J.P and Pailhes, J. "*Environmental uncertainty fuzzy analysis in early stages of the design process*. In Proceedings of the Virtual Concept International workshop (VC-IW'14) in Innovation

in Product Design and Manufacture. Mars 26-27, 2014. ISBN: 978-2-9548927-0-2

[AS1] Azapagic, A and Stichnothe, H. 2009. A Life Cycle Approach to Measuring Sustainability. Chemistry Today. 2009. Vol. 27.

[BF1] Basbagill, J, et al. 2013. Building and Environment. Application of life cycle assessment to early stage building design for reduced embodied environmental impacts. Elsevier, 2013. Vol. 60, pp. 81-92. ISSN: 0360-1323.

[B1] BSI, British Standards Institutions. 2006. BS EN ISO 14040 Environmental Management - Life cycle assessment. Principles and framework. London: BSI, 2006.

[G1] "GHG Product Life Cycle Assessments". Ecométrica. Retrieved on: April 25, 2013

[H1] Hacker, Kurt. 1999. Comparison of design methodologies in the preliminary design of a passenger aircraft. Buffalo : AIAA Student Journal, 1999. Vol. 37.

[HH1] Heijungs, Reinout, Huppes, Gjalt and Guinée, Jeroen. 2010. Polymer degradation and stability. Leiden : Elsevier, 2010.

[HG1] Horne, Ralph, Grant, Tim and Verghese, Karli. 2009. Life Cycle Assessment . Principles, practice and prospects. Collingwood: CSIRO, 2009.

[I1] IHOBE. 2000. Manual práctico de ecodiseño. Operativa de implantación en 7 pasos. País Vasco: IHOBE, 2000.

[K1] Koopman, Philip. 1999. Life Cycle considerations. Dependable Embedded Systems. Pittsburgh: Springer, 1999.

[K2] Koopman, Philip. 1998. Obstacles to using CAD tools for embeddeb System Design. Pittsburgh: Springer, 1998.

[LA1] Law, William S, and Antonsson Erik K. 1995. “Optimization Methods for Calculating Design.” (September 1995): 17–21.

[LS1] Lehtinen, Hannele, Saarentaus, Anna and Rouhiainen, Juulia. 2011. A Review of LCA Methods and Tools and their Suitability for SMEs. Manchester: Biochem, 2011.

[M1] Ministry of Housing, Spatial Planning and the Environment. “Eco-Indicator 99 Manual for Designers.” 2000.

[O1] Okala, team. 2013. Okala practitioner. Phoenix : 2013.

[PB1] Pahl, G, et al. 2007. Engineering design - a systematic approach. London: Springer, 2007.

[P1] PRé. Putting the metrics behind sustainability. [Online] [Cited: Agosto 30, 2013.] http://www.pre-sustainability.com/content/databases/.

[S1] Simapro. Simapro. [Online] Lavola Sostenibilidad. [Cited: 01 10, 2013.] http://www.simapro.es/versions.html.

[WE1] Weck, Olivier De, Eckert Claudia, and Clarkson John. 2007. “A CLASSIFICATION OF UNCERTAINTY FOR EARLY.” (480): 1–12.

[Z1] Zangwill, W.I. 1992, "Concurrent engineering: Concepts and implementation", IEEE Management Review 20/4, 40-52. 1992.

Article 020-sd-20

Integration of end-of-life options as a design criterion in methods and tools for ecodesign

Yoann Le Diagon [1], Nicolas Perry [1], Stéphane Pompidou [2], Reidson Pereira Gouvinhas [3]

(1) Arts et Metiers ParisTech, I2M
UMR 5295
F-33400 Talence
France

Phone: +33 (0)5 56 84 53 27
E-mail: yoann.le-diagon@ensam.eu
n.perry@i2m.u-bordeaux1.fr

(2) Univ. Bordeaux, I2M
UMR 5295
F-33400 Talence
France

Phone: +33 (0)5 56 84 79 80
E-mail: s.pompidou@i2m.u-bordeaux1.fr

(3) Dep. de Engenharia de Produção
Univ. Federal do Rio Grande do Norte
Av. Senador Salgado Filho
3000 Campus Universitário Lagoa Nova
Br-59078 Natal
Brazil

E-mail: reidson@ct.ufrn.br

Abstract Ecodesigning a product consists (amongst other things) in assessing what its environmental impacts will be throughout its life (that is to say from its design phase to its end of life), in order to limit them.
Some tools and methods exist to (eco)design a product, just like methods that assess its environmental impacts (more often, *a posteriori*). But it is now well accepted that these are the early design decisions that will initiate the greatest consequences on the product's end-of-life options and their impacts. Thus, the present work aims at analysing traditional design tools, so as to integrate end-of-life possibilities in the form of recommendations for the design step.
This proposal will be illustrated by means of a wind turbine design.

Keywords Ecodesign, design for X, life cycle assessment, end-of-life, wind turbine

1- Purpose of the work

Ecodesign is an alternative approach to design a product with at least the same functional level, but (amongst other things) using less materials or fewer energy in the manufacturing process, favouring the use of higher renewable resources, optimising design for limiting maintenance operations, and improving product end-of-life treatments.
The goal of this paper is to show how traditional design tools can be used for *eco*designing a product. More specifically, it aims at integrating end-of-life options from the early stages of the product's design, to limit the environmental impacts due to this life phase.
A product's environmental impacts can quite easily be estimated *a posteriori* by a lifecycle assessment (LCA), even if some materials, constituents, processes or life stages are less known than others. On the contrary, it is more difficult to assess its impacts *a priori* in the early design phase, when the product definition is low-detailed. However, it is well known that the early to preliminary design decisions will initiate the greatest consequences in terms of impacts due to its end-of-life options, both environmentally and economically [FB1]. Indeed, some raw materials become strategic because of their decreasing availability: more and more constituents must be easily recycled. Lastly in a legislative point of view, regulations get stricter about the environmental impacts of a product. As a consequence, integrating ecodesign approaches becomes a strategic action for companies. Besides, they improve their image for consumers who seek more and more ecofriendly products.
In this framework, the present analysis aims at integrating end-of-life into previous studies that were rather focused on the implementation of the ecodesign approach, and its benefits on the development of tools for ecodesign.
This paper will start with a quick state-of-the-art of ecodesign approaches. The next section presents the product development cycle. Then, end of life and recycling criteria are introduced as key characteristics to evaluate. The fifth section describes the proposal linking end-of-life options into the product development cycle. Finally, the last section applies the proposal to a wind turbine design case study, before concluding.

2- Ecodesign framework

2.1- Overview

Ecodesign approaches can be applied to any product, that is to say a good or a service. However in the present analysis, we will mainly focus on the design of mechanical systems.
First of all, let us claim that assessing a product life cycle does not mean following an ecodesign approach. Even if LCA gives the most realistic environmental impacts' assessment for the designed product, this method is only practicable on a fully designed product. Indeed, the product definition (structure, material and manufacturing process) and its envis-

aged life scenarios (logistic, use phase and end-of-life option) must be as complete as possible in order to get the best assessment. So, how can this tool be used at the early design stages? To fill the gap between environmental assessment and analyses led by classical design tools, we propose to enrich design methods with criteria and systematic questions.
In spite of the potential benefits of the implementation of ecodesign, the method is not used yet in all design cases. On the one hand, collecting data is particularly difficult because the product lifecycle steps should be precisely known, including all stakeholders involved (*i.e.* raw materials suppliers, manufacturing stakeholders, transporters, consumers and recycling companies). On the other hand, some existing tools (see below) can be difficult to use and to implement for designing the product. Actually, the main barrier is the lack of know-how in the product design steps.

2.2- Ecodesign tools

Ecodesign tools have been developed to ease and guide societies, team project and designers to implement associated approaches and processes. They especially help companies in assessing the environmental impacts of their products, and in defining the main improvement axes to (re)design them. More than 150 ecodesign and communication tools already exist for the design process; strategic tools can also be added to the list [BB1]. But they often turned out not suitable for SME companies [GC1], as they are too complicated to be useful for their daily work [GC2].
Among ecodesign tools [VM1], two types stand out: *assessment* and *recommendation* tools.

2.2.1- Assessment tools

Both *qualitative* and *quantitative* assessment tools can be taken in consideration [BJ1]:

- *Qualitative assessment tools* include streamlined life cycle assessment and complete monocriteria-LCA, matrix approaches as MET (material cycle, energy use and toxic emissions) [BH1], MECO (materials, energy, chemicals, others), ERPA (environmentally responsible product assessment).
- *Quantitative assessment tools* include all mono-criteria analyses (*e.g.* water footprint or carbon footprint) and multi-criteria LCA; they lead to an accurate evaluation of the product's environmental weak points.

2.2.2- Recommendation tools

In order to help design teams make decision [G1,GB1], all checklists, standards, guidelines and substances lists (*e.g.* REACH regulation and RoHS directive) can be used [L1]. Moreover, design for X [T1] (where *X* is for recycling, disassembly, environment [AZ1], reuse, remanufacturing or sustainability) are suitable in this case [RR1].

3- Formalisation of the product development cycle

In order to introduce end-of-life options from the design phase (cf. figure 1), that is to say either in classical design or ecodesign tools (depending on the available data at each step), the product development cycle has to be detailed.
As defined by Pahl *et al.* [PB1], it can be divided into the following main steps.

3.1- The early design

The early design phase is mainly based on the customer's needs. In this way, the product's major function is translated by designers in a technical requirements list that also takes into account the constraints related to the market, a business strategy, technology, legislation, etc. (see also figure 1.a)

3.2- The preliminary design

The preliminary design usually involves the two following steps:

- *conceptual design* that aims at defining the functional structure. Many concepts are developed to answer the needs previously listed, then compared to assess issues that could stem from every choice. A *solution principle* is thus selected;
- *architectural design* that consists in assessing the previous proposal. The most suitable structure from technical and economic points of view is chosen, including components (shapes and materials), pre-sized or nonstandard constituents, etc.

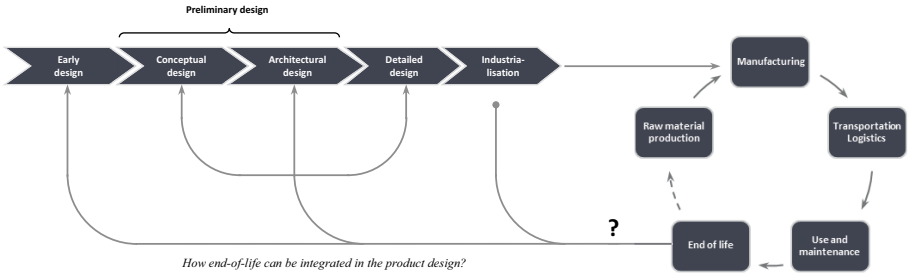

a. Product development process **b.** Product lifecycle

Figure 1: Integration of the end-of-life options as a design criterion in the product development process

3.3- The detail design

In the detail design step, the selected architecture is mocked up by CAD, optimised and finally approved. A definition file containing all sized parts and assembly drawings is provided (the *definitive layout*).

3.4- The industrialisation

Lastly, the industrialisation phase aims at choosing the best manufacturing process, optimising the supply chain, drafting a quality plan, and eventually implementing a prototype to be tested.

4- Formalisation of the product's lifecycle and focus on its end-of-life

The product lifecycle is usually divided into the following main consecutive steps, as sketched in figure 1.b.

4.1- Raw materials production

This first phase mainly consists in the raw materials production; they can either be first extraction or recycled ones (usually called *secondary-raw materials*).

4.2- Manufacturing

The second step includes all manufacturing operations; that is to say, amongst others, raw materials transformation, production operations previously chosen for the industrial process, thermal and mechanical treatments, and packaging.

4.3- Transportation and logistics

This step includes all transport and logistics issues in relation with the product throughout its lifecycle. Consequently, these operations do not only concern the distribution phase (*i.e.* between the manufacturing and the purchasing sites) as suggested by figure 1.b, but can actually be found between all the other phases.

4.1- Use and maintenance

This phase of the lifecycle focuses on the period during which the product is used, *i.e.* between its purchase and its end-of-life (*e.g.* when it becomes a cause of failure). This step also includes all the maintenance operations needed for increasing its lifespan.

4.2- The end-of-life

When the product becomes unused, it is generally more suitable to talk about its *end-of-life* phase, rather than to consider it as a *waste*. Indeed, this last expression would imply an absolute loss of value, while several ways exist to extend the life of either the whole product (and thus, preserve part of the worth) or only some parts (components, constituents or constitutive materials).

4.2.1- Ways of treatment of an end-of-life product

The five main options to treat a life-ending (sub-)product are listed below, from the most valuable to the less profitable solution.

- First of all, the *reuse* option mainly consists in the recovery of the whole product. It can be reused for the function it was designed, or another one. This end-of-life treatment is clearly the best in terms of maximisation of the product value.
- The second way is the *remanufacturing* process. It more often consists in recovering parts that will be reinserted in a new product, during a later manufacturing process. However, this option is possible if previous design choices assure an easy disassembly. Only then, parts may be modified, adapted, or simply reassembled in a second generation product; their value is preserved.
- The *recycling* is the third possible way of treatment. It mainly consists in extracting strategic materials from the waste flow, and regenerating them in new ones, usually called *secondary raw materials.* They are more eco-friendly, and theoretically have the potential of other recycling loops. However, this reprocessing path requires firstly the preparation of the waste; it includes collect, depollution, cleaning, dismantling, part and/or material identification, sorting, etc. Early design options would obviously ease the product disassembly, the accessibility to the (sub-)parts and then, the materials separation.
  With respect to the recycling process (specific for each nature of material), performance indicators will be varied as a function of the dismantling quality. Again, early design choices thus impact the recycling ratio (*e.g.* ease/difficulty to reach target materials), the efficiency of the recycling process (*e.g.* downcycling likelihood due to a bad separability), and then, the availability of good secondary-raw materials for new manufacturing processes.
- The fourth end-of-life option mainly comes down to an *energy recovery* by burning the product (manifestly likened to a waste).
- Lastly, the worst end-of-life option consists in *landfilling* and *burying* the inert waste that couldn't be treated by one of the previous ways.

4.2.2- Environmental impacts of the end-of-life

A product inevitably impacts the environment almost continuously, from the extraction of the raw materials, and all along its use phase (energy used for its working, associated substances rejected in water or in the air, etc.). But even after, environment remains impacted by the landfilled parts (*e.g.* land occupation or constituent toxicity), or by the reprocessing or recycling treatments (*e.g.* energy consumption, supplies needed for the process, etc.). However, as previously mentioned, design choices may assure an easier disassembly of the product, a better materials separability, or a greater reintegration of the secondary-raw materials in a next manufacturing process.
As a consequence, we propose to assess how the end-of-life step could be integrated as a design criterion, while controlling potential transfers of pollution.

5- The proposal

The goal of this part is to display, for each design step, (i) the tools that can be used and (ii) the questions to ask for integrating end-of-life options as design criteria, in order to provide indicators which could help the design phase. Both aim at improving the performance of the end-of-life product. But before that, it is important to differentiate, in terms of scale of treatment, the management of the production waste (*e.g.* unused constituents, off-cuts, rejected parts, etc.), and the end-of-life products. Moreover, there is no added value for a production waste. Thus, efforts have to be kept to minimize production wastes in an ecodesign context.
Our analysis will be linked to the three main steps of the design phase.

5.1- Early design

It has been previously seen that the earlier the end-of-life is taken into account in the design process, the better the economic and environmental impacts of the associated valorisations are. However at the early design step, the product is still an idea, or at best a customer's requirement (cf. § 3.1-); in all cases, available data are extremely limited.
Despite that, questions about the strategic position of the manufacturer (*i.e.* a company) must be taken into consideration. A first level of thought must be led about existing regulations, and legislation to come. Some regulations already limit the use of materials and chemicals, or will require a minimum recycling rate at the end-of-life. As an example, this first analysis of legal texts will force designers and manufacturers to limit the use of hazardous substances that will be difficult to treat at a later stage.
The second focus for reflection is related to the company's management strategy. Usually, the company favours some end-of-life options (*e.g.* recycling or thermal recovery) for internal processes (*i.e.* production waste) and external ones (*i.e.* when user feels/reckons the product reaches its end-of-life). This will enable to choose the most suitable materials and constituents to fit in the more easily treatment sectors.
Both questions directly influence the design possibilities. For example, if the company gives priority to recycling (and so to recycling rates), then mass and volume will be key design criteria. Giving priority to reuse, the design will have to be modular, and each sub-system will only fulfil one function. In this case, number and nature of functions, and then number of sub-parts to disassemble will be the key parameter.
In order to integrate end of life criteria at this step, the work focuses on functional analysis tools: tools called (in a mundane way) *octopus diagram* (or *functional interactor diagram*) and *bull chart*, technical specifications, SADT (structured analysis and design technique), FAST (functional analysis system technique) and FBD (function block diagram), etc.
The *functional interactor diagram* enables to find all external interactors to the product for all its living phases. Analysing end-of-life emphasis the functions linked with this step. Then, technical specifications allow matching functions with criteria (*e.g.* a recycling rate required by regulations). In the context of an eco-*re*design, FAST diagram allows putting emphasis on the materials choice regarding the end-of-life (*e.g.* recycled or recyclable material, strategic material, chemicals and assembly methods). The BFD, which depicts flows and links between components, enable to determinate subsystems and their imbrication.
Lastly, only two end-of-life indicators can guide designers: a composition indicator (if design is monitored by legislation) and a separability/disassembility indicator which can fix objectives in terms of accessibility and ease for the associated end-of-life options.

5.2- Preliminary design

In the present part and the next one, we will only focus on the *recycling* option because of the lack of knowledge and available data, as already mentioned.
Let us remind that the preliminary design step firstly consists in translating technical specifications in a concept, then in an architecture with pre-sized components (cf. § 3.2-). Taking into account end-of-life options from this step, requires looking at two main parameters: the assembly (in order to anticipate the components separation) and the nature of materials (that will have to be recycled). Thus, the present analysis focuses on several tools: CAD, simulation and materials choice tools, decision matrix, physical rules, etc.
Firstly, design must be managed to take into consideration an easy disassembly, of parts or components, but also, with a view to recycling, of materials.
Disassembling difficulty is tested by assessing means and time needed; degree of linkage standardisation and accessibility to the joint (which is important for both end-of-life and maintenance operations) are deduced. Indeed, a FMECA (failure mode, effects and criticality analysis) can highlight critical components which can easily be repairable or replaceable. The second reflexion axis relates to the assembly process because welding or riveting for example, can introduce filler material which can be a pollutant for the recycling process. Then, CAD tools and kinematic drawings enable to give a first evaluation of the separability performance.
Otherwise, analysing the used materials is a requirement to improve the end-of-life treatment. Obviously, they are mainly chosen in accordance with their mechanical properties; however, it is important to evaluate the recycled ones, depending on the treatment industry. Another key point is the identification of constituents. Indeed, in order to choose the better way of treatment, materials have to be easily identifiable, particularly for high-value materials. Lastly, materials can have an incidence for technical intervention (*i.e.* maintenance or lubrication), so these choice criteria must be taken into consideration at the same level. A decision matrix is suitable to compare them.
Previous indicators also guide designers and become more and more accurate, especially thanks to the increase of available data due to the knowledge of the product. Another indicator assesses the pollution due to the recycling process, that is to say chemicals or materials which will have a negative or hazardous impact on the process. Quantification of this indicator will depend on the recycling option.

5.3- Detailed design

One of the goals of the detailed design is to optimize shapes and materials, for example with CAD tools (cf. § 3.3-). At this stage, the involved tools are overall the same as in the previous one.
A new way to optimise end-of-life lays in searching alternative materials with (at less) the same mechanical properties that would balance environmental performances (*e.g.* with CES software).
Another reflexion must be led about the choice between different grades of material. Indeed, some can be more or less desirable depending on the recycling process and the quality of the recycled material. In this sense, one must take a close look on surface treatments; as an example, tinplating or copper plating reduce the mechanical performances of a recycled steel [CR1]. Coatings have to be taken into consideration for the same reason.
Moreover, it is essential to compare all the possible alternatives of assembly. With an eye to recycling, joints easier to disassemble are more desirable. On the contrary, if a rigid linkage is required, the main problem remains the polluting effect of one constituent on the other in the recycling process, and the degradation of the material (*i.e.* downcycling); a less efficient recycling way could be chosen.
Lastly, other constituents' properties can be taken into account. As examples, ferromagnetic materials can be easily sorted in a waste flow, just like materials of different density floating in a fluid. Use of such materials will ease their separation and orientation in the recycling process.
In an economic point of view, it is essential to know if the ratio (by mass or volume) recyclable constituent/total waste is likely to be profitable to recycling industries [RS1].

6- Case study: wind system

This part aims at showing how end-of-life option can be integrated in the design of a wind turbine.

6.1- Legislative framework

The present work matches with two improvement points identified by the French Ministry of Ecology, Sustainable Development and Energy in June 2012. The first one gives priority on ecodesign approaches and the research on alternative materials in place of rare or strategic ones. The second point forces designer to use ecodesign approaches not only throughout the main mechanical system lifecycle, but also to all annex components and structural parts (*e.g.* foundations, etc.).

6.2- Material composition and treatment performances

6.2.1- Material composition study

This part aims at studying the arrangement of a horizontal-axis wind turbine (HAWT), with a 85m high tower and a 90m in diameter rotor. Mass of components are classified in table 1.

Figure 2 details the contribution of these components to its overall cost. These data are also classified in table 2 to highlight the economic impacts of the two possible end-of-life scenarios we propose for the wind system. The first one is an assumption of what could be considered as end-of-life options; the second one is an alternative version that favours the reuse of some parts instead of their only recycling. This leads us to ask three questions.
First, blades are made of glass reinforced plastic. But to date, there is no industrial solution to recycle such composites. Consequently, the end-of-life option currently led is the thermal recovery, although blades are high added value components (about 20% of overall cost of the HAWT).
Secondly, the electrical components remain difficult to recycle. Indeed, generator includes a copper-steel mix difficult to treat. As previously explained, copper is a pollutant for steel in terms of quality of the secondary raw material.
Lastly, foundation is a huge buried structure. Consequently, it also has to be dismantled when the HAWT reaches its end-of-life. Otherwise, a repowering could be planned with the same foundation. Thus, designer have to wonder if it is better profitable to extract it (if it is not required), or if it is well enough sized for fixing a new wind system.

Components	Concrete	Steel	Alu.	Copper	Glass reinf. plastic
Hub		18 t			
Blades		1 t			19 t
Gearbox		25 t			
Generator		13 t		7 t	
Frame, machinery and shell		21 t	2 t	1 t	1 t
Tower	3 t	145 t			
Foundation	480 t	2 t			

Table 1: Material composition of the studied HAWT [AV1]

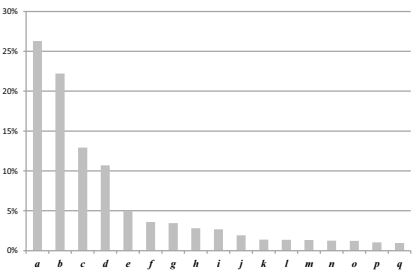

Caption: ***a***: tower; ***b***: rotor blades; ***c***: gearbox; ***d***: others (foundations; grid connections); ***e***: power converter; ***f***: transformer; ***g***: generator; ***h***: main frame; ***i***: pitch system; ***j***: main shaft; ***k***: rotor hub; ***l***: nacelle housing; ***m***: brake system; ***n***: yaw system; ***o***: rotor bearings; ***p***: screws; ***q***: cables

Figure 2: Contribution of wind turbine components to the system overall cost [E1]

.

These three points have so to be taken into account from the design stage in order to (i) anticipate the components' end of life, and (ii) avoid a loss of the added value with a treatment which wouldn't be effective enough.

6.2.1- Treatment performances

Designers now have to focus on the loss of added value due to the choices of end-of-life treatments. Indeed, components of a wind system represent about 90% of the overall cost.
In order to highlight the loss of value in the end-of-life phase, two scenarios are proposed:

Scenario 1: Only electrical components are reused;
Scenario 2: Electrical components, gearbox and main shaft are reused.

In both approaches, rotor blades and nacelle housing are burned; non-quoted materials are supposed to be recycled.

The table 2 compares these scenarios in terms of allocation of value. In this economic-only point of view, we have already mentioned that recycling is more attractive: it leads to a new material, when burning option is just elimination, admittedly with an energy gain, but leading to wastes difficult to make more attractive.
Firstly as already mentioned, the treatment of composite parts lead to a 24% loss of the overall value (even if energy can be recovered). Secondly, since gearbox and main shaft can be reused, 20% of the system value could be preserved.
As a conclusion, to enhance end-of-life performances, two points have to be studied: (i) develop recycling methods for composites, or substitute composite parts in the blades design, and (ii) better control mechanical fatigue of some components in order to reuse them.

	Scenario 1			Scenario 2		
	Reuse	**Recycling**	**Burning + ER**	**Reuse**	**Recycling**	**Burning + ER**
Tower		26.30%			26.30%	
Rotor blades			22.20%			22.20%
Gearbox		12.90%		12.90%*		
Power converter	5.00%			5.00%		
Transformer	3.60%			3.60%		
Generator	3.40%			3.40%		
Main frame		2.80%			2.80%	
Pitch system	2.70%			2.70%		
Main shaft		1.90%		1.90%*		
Rotor hub		1.40%			1.40%	
Nacelle housing			1.40%			1.40%
Brake system		1.30%		1.30%*		
Yaw system		1.30%		1.30%*		
Rotor bearings		1.20%		1.20%*		
Screws		1.00%		1.00%*		
Cables	1.00%			1.00%		
Total	**15.70%**	**50.10%**	**23.60%**	**35.30%**	**30.50%**	**23.60%**

Table 2: Economic-based analysis of two possible end-of-life scenarios for a wind turbine (ER: energy recovery) [E1]. Data are the contribution of the wind turbine components to the system overall cost [E1]. The second scenario (optimisation of the first one) favours the reuse of some parts instead of their recycling (data marked with an asterisk)

Structural choices	**Consequences for recycling**	**Involved indicators**	**Decision tools**		
			Early design	***Preliminary design***	***Detailed design***
Nacelle rotation	Yaw drives reuse/recycling Yaw gears disassembly Yaw system constituents Maintainability	Disassembly Composition Separability	Characterisation of functions	FMECA Simulation	
Blades orientation	Hub size Hub complexity Maintainability and reuse of pitch cylinders Blades disassembly	Disassembly Composition Economic viability		FMECA Simulation	
Number of blades and constituents	Quantity of material to treat Disassembly Hub complexity	Disassembly Composition Separability Pollutant Economic viability	Client demand (personal choices) Characterisation of functions	FMECA Simulation	Optimisation (production gain)
Driving system	Quantity of material to treat Number of components Maintainability	Disassembly Separability Composition	Strategic positioning of the company	FMECA Simulation	
Rotor size	Quantity and nature of materials to treat Size of the main frame (dimensioning) Size of the tower (dimensioning)	Composition Disassembly Economic viability	Legislation Characterisation of functions	Simulation	Optimisation (production gain)
Tower size	Type of material	Composition Disassembly Economic viability Pollutant	Legislation Characterisation of functions	Simulation	Optimisation (production gain)

Table 3: Impacts of structual choices on the only recycling

6.3- Integration of the recycling option as design criteria

Since we assume to favour recycling option, consequences of the preliminary structural choices must now be studied, and connections between choices, end-of-life indicators and tools must be underlined.
Our analysis deals with six main structural choices for a HAWT: nacelle rotation, blades rotation, number and material of blades, drive system (with or without gearbox), rotor size and tower size. The table 3 displays a first proposition to show how end-of-life indicators can be linked with a design step. Thus, it is important to note that preliminary design is the step where end of life criteria are the more likely to be taken into account. Before, it is difficult to constraint some functions by end-of-life options, even if a wide range of hypothesises can be adopted regarding recycling rates, material composition and facility for disassembly, which will all be affined in preliminary design and optimized in detailed design, in order to balance production gain and end-of-life performances.

7- Conclusions. Application and limits

The purpose of this paper is to analyse how end-of-life options can be integrated as a criterion in the design process. For that, we propose to integrate questions about end of life or indicators in each design steps. It enables to see what step is the more suitable to consider end-of-life issues and to also highlight the role that tools can play to improve the end-of-life performances of a product. These examples of very simple reflexions can be led in all design cases. Currently, the main limit is the case per case quantification of indicators, and the study of how they can be precisely be integrated into tools (*e.g.* how can designers link a recycling rate to FMECA? To what extent can indicators influence the use of tools?)
These questions deserve to be solved because, as shown in the wind system example, the improvement of the design by the consideration of end-of-life issue, may preserve a lot of the invested value. Indeed, taking into account the analysis of the end-of-life scenarios, 20% of invested value could be reused in order to save the investment, rather than recycling parts.

8- References

[AV1] D. Ancona and J. McVeigh, “Wind Turbine - Materials and Manufacturing Fact Sheet.” Princeton Energy Resources International, 29-Aug-2001.

[AZ1] H. Alhomsi and P. Zwolinski, “The use of DfE rules during the conceptual design phase of a product to give a quantitative environmental evaluation to designers,” in *Proceedings of the 19th CIRP Design Conference*, Cranfield (United Kingdom), 2009.

[BB1] H. Baumann, F. Boons, and A. Bragd, “Mapping the green product development field: engineering, policy and business perspectives,” *J. Clean. Prod.*, vol. 10, no. 5, pp. 409–425, Oct. 2002.

[BH1] H. Brezet, C. van Hemel, UNEP IE Cleaner Production Network, Rathenau Instituut, and Technische Universiteit Delft, *Ecodesign: a promising approach to sustainable production and consumption*. Paris : UNEP : United Nations Environment Programme, Industry and Environment, 1997.

[BJ1] B. Bellini and M. Janin, “Écoconception : état de l’art des outils disponibles,” *Tech. Ing.*, vol. Systèmes de management environnemental, no. G 6010v2, pp. 1–35; doc. 1–10, Oct. 2011.

[CR1] M. B. G. Castro, J. A. M. Remmerswaal, M. A. Reuter, and U. J. M. Boin, “A thermodynamic approach to the compatibility of materials combinations for recycling,” *Resour. Conserv. Recycl.*, vol. 43, no. 1, pp. 1–19, décembre 2004.

[E1] European Wind Energy Association, “Supply chain: the race to meet demand.,” *Wind Dir.*, pp. 27–34, Feb. 2007.

[FB1] W. J. Fabrycky and B. S. Blanchard, *Life-cycle cost and economic analysis*. Prentice Hall, 1991.

[G1] R.-A. Gheorghe, “A new fuzzy multicriteria decision aid method for conceptual design,” 2005.

[GB1] R. A. Gheorghe, A. Bufardi, and P. Xirouchakis, “Fuzzy Multicriteria Decision Aid Method for Conceptual Design,” *CIRP Ann. - Manuf. Technol.*, vol. 54, no. 1, pp. 151–154, 2005.

[GC1] R. P. Gouvinhas and G. J. Costa, “The Utilization of Ecodesign Practices within Brazilian SME Companies,” in *7th International “Towards Sustainable Product Design Conference” Proceedings*, London (UK), 2002.

[GC2] R. P. Gouvinhas and J. Corbett, “The use of design methods within production machinery companies,” *Proc. Inst. Mech. Eng. Part B J. Eng. Manuf.*, vol. 213, no. 3, pp. 285–293, Mar. 1999.

[L1] M. Lemagnen, “Intégration du risque chimique dans la conception de produits industriels. Application au secteur de l’aéronautique,” Thèse de Doctorat, Université de Grenoble, Grenoble, 2011.

[PB1] G. Pahl and W. Beitz, *Engineering design: a systematic approach*. London; New York: Springer, 1996.

[RR1] M. Rio, T. Reyes, and L. Roucoules, “Toward proactive (eco)design process: modeling information transformations among designers activities,” *J. Clean. Prod.*, vol. 39, pp. 105–116, Jan. 2013.

[RS1] M. Reuter and A. van Schaik, “Opportunities and limits of recycling: A dynamic-model-based analysis,” *MRS Bull.*, vol. 37, no. 04, pp. 339–347, 2012.

[T1] N. Tchertchian, “Mise en place d’une méthodologie d’évaluation environnementale et économique à priori sur le cycle de vie complet de systèmes mécaniques complexes,Application industrielle: conception d’une navette maritime hybride à performances environnementales maîtrisiées,” Ecole Centrale de Paris, 2013.

[VM1] F. Vallet, D. Millet, and B. Eynard, “How ecodesign tools are really used. Requirements list for a context-related ecodesign tool,” in *Proceedings of the 20th CIRP Design Conference*, Nantes (France), 2010.

Article 022-sd-82

Increase Sustainability of Decentralized Electricity with Remotely Monitored Product-Service Systems

Kevin Wrasse [1], Haygazun Hayka [1], Anne Pförtner [2], Rainer Stark [1,2]

(1) : Division Virtual Product Creation, Fraunhofer IPK, Berlin, Germany
+49 30 39006-218
E-mail : {kevin.robert.wrasse, haygazun.hayka, rainer.stark}@ipk.fraunhofer.de

(2) : Chair of Industrial Information Technology, Technische Universität Berlin, Germany
+49 30 39006-358
E-mail : {anne.pfoertner}@tu-berlin.de

Abstract: Solar home systems (SHS) are a potential sustainable solution for rural areas of developing countries in order to supply human beings with electricity. However, those SHS face many challenges in those particular areas e.g. minimal traffic infrastructure, inadequate education or declining confidence in handling this technology. Therefore, SHS give much of its potential away to improve all dimensions of sustainability. A new approach is described which is applied within the MESUS (micro-energy supply system) project where SHS as a single product are shifted to a product-service system in combination with an information system based on remote monitoring. Sustainability can be increased by focusing on customer needs with respect to the whole product lifecycle. Efficiency of service processes is increased by gathering and analysing operational data. In conclusion, the new approach is capable of granting incentives for providers of SHS and their end-users to create long-term satisfactory relationships and to support the socio-economic development.

Key words: product service system, solar home system, decentralized electricity, lifecycle-engineering, remote monitoring

1- Introduction

In many developing countries, solar home systems have been established as a successful option for electrification of households in rural areas without access to electrical infrastructure. In Figure 1, a micro-energy system (MES) is shown schematically, which is a generalization of a SHS and provides a basic electricity supply for people especially in rural areas. The source of electric power can be a solar panel, a wind turbine or a diesel generator set. This definition shows the variety and scalability of systems for decentralized electricity generation. All solutions that were developed within this project should be ready to adapt various power sources. Prototypical implementation and evaluation of MESUS (translation of the German project name "MEVIS") were carried out by a SHS, so these systems were further

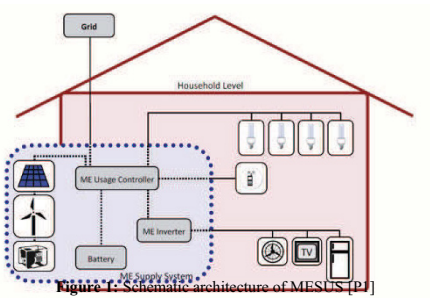

Figure 1: Schematic architecture of MESUS [F1]

mentioned hereinafter. To finance the systems, there has been taken advantage of a widespread network of microfinance institutions which enable people with low incomes to divide the high acquisition costs with a micro loan into small fractions for a longer period.

1.1 Solar home systems in rural areas – a sustainable solution?

Solar home systems offer a high potential of sustainability to regions in the world with the highest growth rates. To tap the full potential it is necessary to analyse the state of existing solar home systems in detail. Energy is a crucial resource to generate prosperity. The installation of solar home systems improves the living situation of individual people but also of entire communities if access to electricity is used to install businesses. The entire economy of a region can be improved by broadening the access to energy. Solar home systems address primarily the social dimension of sustainability, including socio- economic effects. The social dimension considers the evolution of quality of life and living conditions [F1]. Access to electricity is a basis to increase quality of life

and fulfil several needs such as healthy and ergonomic working procedures. For instance, wood working can be assisted by electric saws. Solar home systems further substitute health risking substances such as kerosene for lamps and increase light quality. The social dimension further includes the fairness of distribution of goods. Solar home systems can reduce the gap between poor and wealthy people regarding access to reliable electric power. The need for installation and maintenance of these systems creates new jobs such as technician, loan officer, distributor and subcontractor.

Solar home systems rely on renewable energy produced by a solar panel but partly still perform a little worse in the environmental perspective. Fuel-based lighting is replaced reducing the primary source of greenhouse gas emissions [RG1]. Solar home systems further replace dry-cell batteries applied in conventional torches which involve a high risk of contaminating local water and soil resources with toxic heavy metals [RG1]. On the other hand the availability of energy will likely drive additional resource consumption such as additionally used electric devices. Assuming that providing energy supply to less developed countries is a goal to be pursued in order to foster prosperity and a fair distribution of goods, solar home systems are a rather sustainable solution. If components are reused or remanufactured and material is recycled the negative impact on the environmental perspective can be reduced.

1.2 Project goals

So far, the systems are passed into the possession of customers and after installation the only responsibility of the manufacturer is in terms of the guarantee agreement. Due to poor infrastructure of the regions and the lack of qualified personnel no appropriate service is offered to date and there is no responsibility of the manufacturer for disposal or recycling of the systems after the end of its service life. To solve the problems, the development of new solar home systems should be carried out according to a methodology for development of product-service systems (PSS). This means that from the outset, both development of the technical components and development of supporting services throughout the product life cycle are taken into account equally. The requirements for PSS are defined primarily from the perspective of the end user taking into account basic needs. Ensuring service quality is performed by analysing the provider networks and their capabilities in early stages of development. To control the service during operation, and to prevent improper operation, the operating data of the system is recorded and sent to a central database. The data is analysed in the backend in order to generate events or alerts that will control the service processes. The aim of this paper is to provide an overview of the applied methods and technologies and how they can influence sustainability of electric power generation.

2- Potential of improvement towards sustainability for solar home systems

The use of solar home systems in rural areas of developing countries makes it more difficult in many ways to exploit the potential for sustainability. One aspect is poor transport infrastructure with long and poorly developed routes to individual customers that increase the time required, and thus the cost, for the provision of services in maintenance and repair. In addition, supply of high quality system components and spare parts is not guaranteed [JM1]. Furthermore, inadequate education causes a lack of trained service personnel. This results in a low density of specialized companies that ensure maintenance of the systems [JM1]. Due to these circumstances, it is often more economical for suppliers of solar home systems, to replace a system in case of malfunction, rather than to repair it. This leads to an excessive consumption of resources, which reduces the economic and environmental sustainability. Besides, local people are deprived of the opportunity to be qualified and to set up their own service network.

In after sales the product and all related responsibilities are transferred completely to the customer. A relationship with the manufacturer, besides credit agreement and warranty, does not exist. As soon as individual components reach their end of life, they stay with the end user who needs to decide how to dispose them. This circumstance causes inappropriate disposal decisions particularly with environmental harmful substances such as lead and acid of a battery.

The components of a solar home system are very sensitive to wrong installation and false operation. For example, their performance is strongly reliant on surface temperature and its ideal orientation to the sun, which may be affected during the installation. Batteries have a limited lifetime, which depends on maintenance and care. In the field of maintenance, the user is responsible to periodically check the state of the acid and lubricated contacts. This task requires a certain training of the user that is not yet ensured. The battery's life is largely based on the utilization of the maximum and minimum charging levels during loading and unloading. For example, a battery may become unusable due to a single deep discharge. Through intentional or unwitting misuse of the systems, they can be easily damaged. In such cases it is still difficult to prove the inherent fault of the customer, if they make claims under warranty. Manufacturers and distributors of SHS are in charge of a proper installation and to educate the customer adequately on use and maintenance of the system. The income of solar salesmen depends on their sales figures; consequently, they do not point out the limitations of the SHS sufficiently [LS1]. As end users miss training and the manufacturer often lacks expertise on needs-based design of systems, SHS are overused and especially, it shortens the life span of batteries. At this point, the confidence of the end user in this technology decreases permanently, which is opposed to the sustainable distribution of those systems. Instead of integrating the needs and local knowledge of users into the process of developing and implementing this technology, the SHS implementation strategy has been focusing on a marketing and sales policy for a standardized and existing product [LS1]. Regardless of the causes, the misconfigured, unmonitored or poorly controlled solar home systems are in terms of loss of reputation a problem for technology suppliers in Europe or Germany. Even if all system components are flawless and the defect of a system was brought about by misinterpretation or misuse, the company's reputation will suffer.

Article 022-sd-82

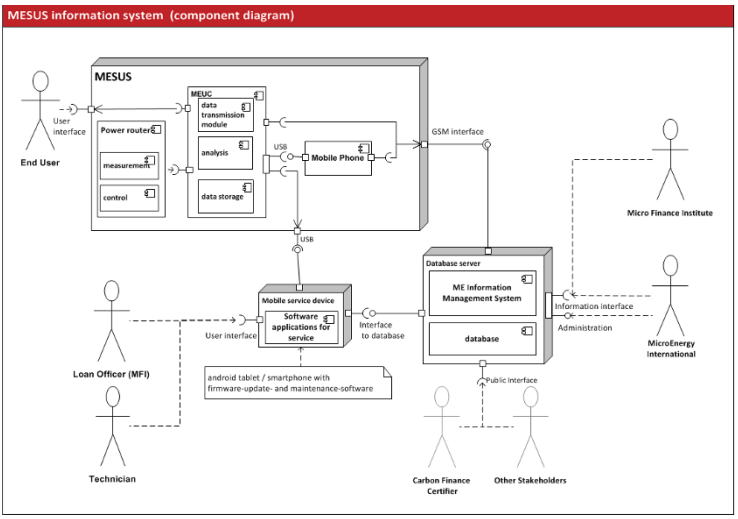

Figure 2: Architecture of micro-energy information system

From the sum of problems enumerated above three consequences can be derived. Firstly, the systems are run uneconomical because inefficient maintenance occurs. Secondly, it may lead to environmental pollution due to improperly disposal of components. And finally, the confidence of potential and existing end users in SHS diminishes because the reliability and performance of the systems are not consistent with their expectations [JM1].

3- Enhancements by usage data logging

The difficulties of rural areas, mentioned before, make it complicated to provide a micro-energy system as a PSS satisfactorily. For present sellers of SHS it is hard to make those investments to enhance their services. Therefore, it is necessary to develop solutions that support future PSS-providers. These solutions will be examined throughout this project. The key idea is to monitor system parameters and process them for relevant tasks, such as:

- control maintenance, repair and overhaul (MRO) processes
- transparent warranty cases
- detect improper use
- statistics for future development
- carbon emission certification

The control of service processes is based on predefined critical events, such as the overload of the system, insufficient energy sources or an insufficient battery. Events are processed by the information system from transmitted system parameters and were communicated to the target user. One reaction could be an alert to the end user to shut down some of the connected devices. Secondly, time-recurring events, e.g. the status check of the battery, can be triggered to remind the end user of its maintenance activities. Additionally, these features enable continuous product improvements to meet changing customer requirements. Remote controlling facilitates risk management in difficult market environments. For example, the system can be programmed to deactivate automatically at the end of a payment period until payment is received. To perform these functions the system consists of two main components. The micro-energy information system (MEIS) integrates micro-energy systems and a central database. In figure 2 the technical implementation of the information system is shown schematically. The system parameters (performance of power source, battery voltage and load) are measured and stored temporarily by the micro-energy usage controller (MEUC). The transmission of data is carried out via a GSM interface, through which the data is passed to the central database. Another interface to the system is a mobile device, which is operated by a service technician. This ensures data transmission without an existing GSM network coverage. With this system, all stakeholders can get the relevant information, so that the processes for servicing and maintenance can proceed efficiently. The data of all supervised SHS is stored and processed in a central database. This is the backbone of the information system where incoming data is analysed and managed as well as necessary tasks and signals were distributed automatically to the responsible actors in the whole system. This ensures that the single SHS is in an ideal operation mode, and thus has a maximum lifetime. Thus, a tool is given to increase the lifetime of SHS, which has positive effects on sustainability.

The micro-energy usage controller (MEUC) is designed to be an intelligent electricity router for households and small

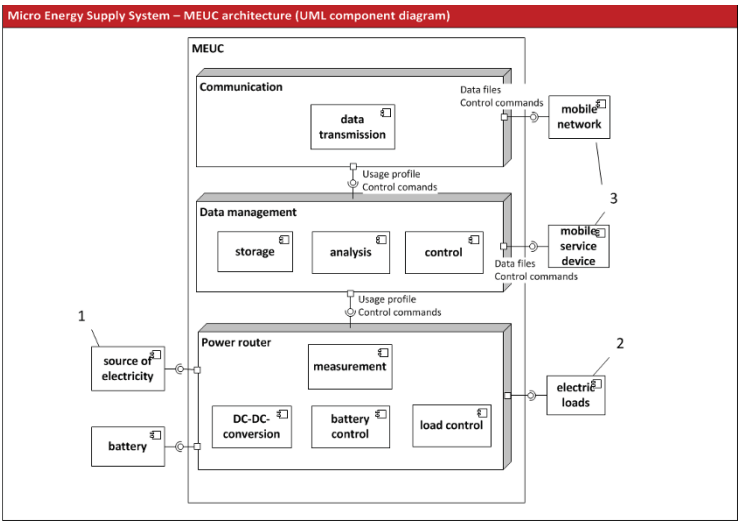

Figure 3 : Architecture of micro energy usage controller (MEUC)

businesses. Figure 3 shows a more detailed architecture of this device. It will provide compatibility with multiple incoming sources of power by its intelligent source management (1). The connection unit provides simple plug-in extensions to distribute electricity around the building and includes a power distribution management that assigns hierarchies to different electric loads (2). The MEUC supports loads from 12 to 24 V. Higher Voltages can be realized by an external inverter that is controlled by the MEUC. To ensure stable and continuous power supply, the system balances any mixture of power sources automatically and can even enable connection to the central electricity grid if expansion is planned to reach the application area. In that case, the MEUC maintains its advantages by providing electrical surge protection and continuous backup power supply to bridge grid outages. The MEUC contains a data logger for creating usage profiles, which can be transmitted conveniently via cellular network or USB interface (3). A low level analysis of the system parameters is already executed within the MEUC that alerts end-user and provider in the case of a critical system failure.

The core function of the information system is to collect and process operational data of solar home systems. By continuous recording of the system parameters, a user profile can be generated. Thus, different conclusions can be drawn from that. It can be evaluated whether the system is designed according to the needs of the user. It is also possible to make more precise assumptions about the development and commercialization of future systems by means of a broad analysis of all user profiles from the customer base. Emission savings through SHS can be proven transparently on the emission certificate market. This creates an additional value for the provider.

The sensors inside the power router of the MEUC are measuring voltage and current of source, battery and load, as well as the temperature of the controller. With this data record and a number of specific analysis algorithms it is possible to detect frequent faults of solar home systems [JM1]:

- dead battery
- overload
- corroded connectors
- bad wiring
- undersized or damaged PV-panel

If this information is distributed and displayed intuitively to available service technicians, taking into account their skill level, service quality and efficiency can be raised even under bad infrastructural conditions.

4- A product service system approach for micro-energy systems

With the idea of the information system a conceptual basis was build up for the application of a PSS methodology. Many difficulties of providing reliable maintenance services in rural areas can be covered with remote data logging. The tasks are to be approached by the use of methods for development of product-service systems.

4.1- Motivation for PSS-methodology

Although PSS development methods do not necessarily offer solutions to increase sustainability, they can be a tool for assessment. In addition, those methods provide the ability to

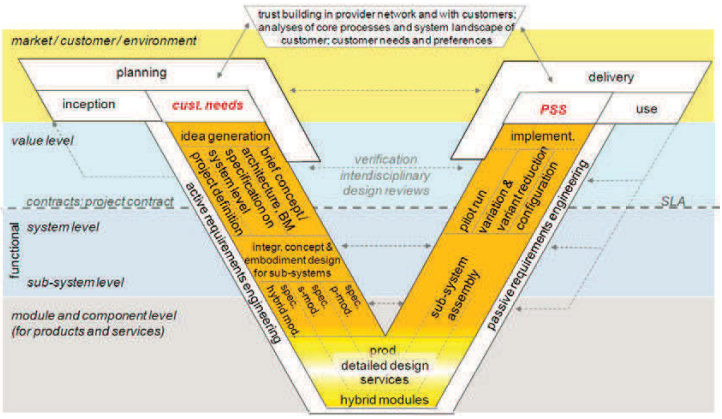

Figure 4: Generic PSS development process model

influence aspects of PSS that are responsible for sustainability [MK1]. From an economic perspective the provider accepts major responsibilities for product-oriented services. Therefore, those services gain quality by which provider as well as end user profit. The confidence of both business partners in the technology increases and is the basis for a long-term relationship. The success of the business model also encourages other competitors who start to offer similar systems and support the continuous distribution of SHS [MK1]. Sustainable PSS were understood as the "opportunity to decoupling material consumption from generating profit through integrating services and by this means reducing the environmental impact in production systems" [SG1]. It is assumed that environmental sustainability is achieved by shifting the property right of products from the customer to the provider and deliver incentives for the provider to invest more money in energy and material savings. The provider's know-how entails a more efficient use of material and energy during the use phase, resulting in less emissions and waste. The needs of the customers and their fulfilment are central to the development of PSS. The role of the customer is upgraded to a business partner at eye level. Electricity becomes a reliable good to him and a stable basis for the social and economic development. The provision of services generates an increased number of skilled workers in the area of SHS, which affects the development of social structures in the region positively [SG1]

4.2- Application of PSS methods

The methods chosen for the development are based on the generic development methodology for PSS, which were developed at Fraunhofer IPK and Technische Universität Berlin. They arise from a v-model, which maps the entire development process in a generalized representation. The customer needs are defined as one basis of development [MS1], which is shown in Figure 4. In the beginning planning of prerequisites for the realization of PSS is very important. This is supported by a methodology on an operational level that transfers the generic process model into a detailed project plan. Within this plan several tasks were described, how to set up the PSS development [NM1]. These were, for example, provider networks, the provider's capabilities and environmental conditions. Once these have been analyzed and evaluated, the identification of customer needs is performed by using case studies, referred to in chapter 2. Experiences of the project partner Micro Energy International through their close contact with the micro-finance institutions also helps to find customer needs. After that ideas have to be generated how values can be created to fulfil the needs. This task is supported by the PSS-layer-method that is shown in Figure 5.

Needs	•Lighting/ health/ productivity
Values	•Electricity
Deliverables	•Availability of reliable Solar Home Systems
Life-Cycle-Activities	•Installation -> usage -> maintenance -> disposal
Actors	•End-User/ provider/ MFI/ supplier/ technician
Core products	•Charge controller/ data logger/ PV panel/ battery
Periphery	•Mobile phone network/ internet
Contracts	•Loan agreement/ Service Level Agreements
Finance	•Micro loan/ pay-per-use

Figure 5: PSS layer model for solar home systems

In order to obtain a better overview the concept has to be arranged in a model where all relevant aspects of the PSS are included. The method that is suitable in this context is the PSS-layer-method. Its purpose is to support the clarification of design tasks and conceptual design. This is a method to analyze and synthesize PSS ideas and concepts and enables a structured documentation of an existing or a future PSS. It defines a model of nine main element classes for a PSS. As a result the user gets a structured outline and the "big picture" of his PSS concept. This helps to highlight requirements and

tasks for the PSS design [MK1]. The figure shows an example of a PSS-layer model with specific descriptions for each layer. Going through iterative loops, the level of detail is raised. Finally, the requirements can be derived from the model with the help of a checklist. With this checklist specific topics, concerning PSS, are helping to identify and arrange require-ments that were developed by elaborating the PSS layer method. This helps to allocate responsibilities and links in subsystems and design models. Secondly, the model helps to develop a specific business model. It defines customer value, ownership, risk diversification and organizational activities. In the case of MESUS, the solution idea is described as an availability-oriented PSS.

Further development is performed by different teams for each discipline. Detailed description of the business model and service processes for finance, installation and maintenance is one part. Implementation of the information system with different views for all relevant actors and the analysis algorithms is the second part, and finally the development and manufacturing of the MEUC is performed by the third team. The previously created models help to consider dependencies between the disciplines. This simplifies merging all partial solutions to a valuable PSS in the end.

5- Conclusion

With the application of PSS development methodology and the remote monitoring methods were found to improve the sustainability of solar home systems. The knowledge about the aspects of sustainability that can be influenced helps to identify them at an early stage of development. These are taken into account for the development of requirements and the business model for the PSS. The goals to be attained can be summarized in three points:

- Environmental responsibility
- Socio-economic development of the regions
- Long-term customer relationships

The information system creates a basis for the future application of PSS methods for SHS by collecting. These methods need very detailed information about the conditions under which the PSS will be implemented. The collected data and experiences from the field trial will help to close these gaps.

The project is currently in the conceptual phase, so the methods previously mentioned could not be verified yet. The first stage of the verification is executed subsequently to the system design and is carried out by using a simulation. Within this simulation all system properties and service activities were modeled in an agent-based simulation system that will evaluate the interaction of the information system, components and processes. After successfully simulating the entire system and identifying improvement potentials regarding interaction between solar home systems, different stakeholders and the information system, the project can be transferred to a prototype implementation. A field trial is planned in the model region India, and is intended to secure the suitability of the system for use in practice.

The elaboration of early concepts has also shown some weaknesses of the approaches that must be taken into account within the further development. Firstly, the remote monitoring depends on an existing communication infrastructure. That is not self-evident in developing countries and alternative transmission options, such as removable data storages, must be evaluated for its usability. Secondly, the PSS approach is in some cases too static for the heterogeneous structure of potential regions. Networks of local service technicians and sellers and their behavior must be analyzed with much effort for each market. Consequently, technical solutions within this system must be adaptable to various business models and to various skill-levels of users.

6- Acknowledgement

We like to thank the funder Federal Ministry of Education and Research of Germany and the supervisor DLR project promoters. The MEVIS project is funded under the topic “KMU innovativ” and aims on support of German SMEs with regard to renewable energies. It is operated jointly with the project partners MicroEnergy International and iPLON, we also like to thank for the collaboration.

7- References

[A1] AGECC: Energy for a sustainable future: the secretary-general's. advisory group on energy and climate. change (AGECC). summary report and. recommendations. 28 April 2010. New York

[F1] Finkbeiner M. (2007) Nachhaltigkeitsbewertung von Produkten und Prozessen – vom Leitbild zur Umsetzung, Produktionstechnisches Kolloquium, Berlin.

[JM1] John P. John, Moses Mkumbwa: Opportunities and challenges for solar home systems in tanzania for rural electrification. In: Technische Universität Berlin (Hg.) (2011): Micro perspectives for decentralized energy supply. Pp. 124 – 132.

[LS1] Dino Laufer, Martina Schäfer: The Contribution of Microenergy Systems towards Poverty Reduction: Case Study of an Implementation Strategy for Solar Home Systems in Sri Lanka. In: Technische Universität Berlin (Hg.) (2011): Micro perspectives for decentralized energy supply. pp. 133–139.

[LZ1] Liu, Xing; Qian, Xiaobo; Zhou, Xiaojiang (2010): A new approach to realize sustainability - Integrated design under the product and service system framework. In: Institute of Electrical and Electronics Engineers (ed.): Computer-Aided Industrial Design & Conceptual Design (CAIDCD).

[MK1] Müller, Patrick; Kebir, Noara; Stark, Rainer; Blessing, Luciënne: PSS Layer Method – Application to Microenergy Systems. In: Sakao, Lindahl (ed.) 2009 – Introduction to Product/Service-System Design, pp. 3–30.

[MS1] Patrick Müller; Rainer Stark (2010): A generic PSS development process model based on theory and an empirical study. In: International design conference - DESIGN 2010. Dubrovnik, Croatia.

[NM1] Hoai Nam Nguyen, Patrick Müller, Rainer Stark (2013): Transformation towards an IPS2 business: A deploy-

ment approach for process-based PSS development projects. In: Yoshiki Shimomura und Koji Kimita (Hg.): The philosopher's stone for sustainability. Proceedings of the 4th CIRP International Conference on Industrial Product-Service Systems, Tokyo, Japan, November 8th - 9th, 2012. International Conference on Industrial Product Service Systems. Berlin, Heidelberg: Springer, S. 251–256.

[P1] Philip, Daniel (2011): Re-Thinking Electrification. Berlin. Available online at www.microenergy-project.de, last checked on 30.04.2014.

[RG1] Reiche, K., Grüner, R., Attigah, B. Hellpap, C. & Brüderle, A. (2010). What difference can a PicoPV system make? Early findings on small Photovoltaic systems - an emerging low-cost energy technology for developing countries. Eschborn: Deutsche Gesellschaft für Technische Zusammenarbeit GmbH (GTZ).

[SG1] Schröter, Marcus; Gandenberger, Carsten; Biege, Sabine; Buschak, Daniela (2010): Assessment of the sustainability effects of product-service systems. In: Tomohiko (Ed.) Sakao, Tobias (Ed.) Larsson und Mattias (Ed.) Lindahl (Hg.): Industrial Product-Service Systems (IPS²). Proceedings of the 2nd CIRP IPS² Conference. Linköping, Sweden, 14-15 April 2010. Linköping University, S. 67–73.

[T1] Tukker, Arnold (2004): Eight types of product–service system: eight ways to sustainability? Experiences from SusProNet. In: Business Strategy and the Environment 13, July/August 2004 (4), S. 246–260.

Article 021-sd-46

DFD EVALUATION FOR NOT AUTOMATED PRODUCTS

Daniela Francia [1], Gianni Caligiana , Alfredo Liverani

(1) : V.le Risorgimento 2,
40136 Bologna (Italy)
0039.051.2093352
E-mail :
{d.francia,gianni.caligiana,alfredo.liverani@unibo.it}

Abstract: The design process is subjected to economical and environmental restrictions since the early phases of preliminary design. Recycling or reusing of parts have to be optimized in order to enhance the ecological impact of a product. This impact can be evaluated through the disassembly capability of joints assembling the product, even when the production process is subject to an important contribute of workmanship. In this paper a useful method is proposed to analyze the disassembly capability of products, also of handcrafted products, in order to optimize the design process in the early preliminary phase. The aim is to define some parameters that describes the attitude of a product to be disassembled by means of the evaluation of an index. The Disassembly Index is influenced by three parameters: the number of different materials of each joint, the time necessary to disassemble each joint, the recoverability of parts after the disassembly is completed.

Key words: Design for Disassembly, Handcrafted product, Assembly time, Disassembly time, Reusing of parts.

1- Introduction

The last trends in the Simultaneous Engineering are addressed to support all phases of product's life cycle through the evaluation of the impact they produce on the environment. Since 90' it was evident that the manufacturing processes, and the consequent manufacturing wastes, strongly affect the environment and the consequent disposal of products at their End of Life (EoL) **[**KZ1**].**

Gungor and Gupta [GG1] defined the Environmentally Conscious Manufacturing (ECM) as:

1. understanding the life cycle of the product and its impact on the environment at each of its life stages;
2. making better decisions during product design and manufacturing so that the environmental attributes of the product and manufacturing process are kept at a desired level.

These issues can be translated in some rules that pay particular attention to cunning solutions such as long product life with the minimized use of raw materials, the selection and use of materials of a product, the selection and use of joints and connectors in an engineered system.

These criteria have been discussed and some strategy have been proposed [B1]: the use of plastics or of metals, with the consequent discussion on their advantages or limits, or the use of smart materials, such as memory form materials.

The importance of the environmental aspects, in addition to considerations on cost benefits and material scarcity, has been translated in various environmental legislations all around the Europe and the USA. So, manufacturers have to develop EoL strategies, integrating constraints from EoL into the early phases of design. The 3R strategy (Reuse, Remanufacture and Recycle) for EoL solutions has been proposed in [GZ1] to develop design aids which permits designers to compare their products to ''Remanufacturable Product Profiles''. Starting from the functional definition of the product and the definition of its architecture, they suggested a tool able to evaluate the environmental impact of the product during its total life cycle while it is being designed.

Manny studies presented in literature are focused on evaluations of the disassembly capability that, even when quantitative, is all referred to fasteners and tools. The aim was to minimize the number of parts, increasing the use of common materials and choosing fastener and joint types easy to remove, in order to evaluate the recovery and recyclability convenience.

For conventional products that have to be produced in large numbers or that are addressed to mass production, assembly and disassembly operations are optimized and, in the most part of cases, they are mechanized [AZ2].

However, when the production is limited to few samples and when the assembly operations are mostly due to hand workmanship, all these tasks become an hard issue.

In order to meet the sustainable product design, production strategies have been proposed to reduce the use of raw materials and save energy: in [ZB1] remanufacturing and reuse approaches are proposed to help designers to integrate the environmental criteria in the decision making process.

This paper introduces a Disassembly Index, indicated in the text as DI, that can be applied also to handcrafted products and that gives quantitative information about the amount of

Article 021-sd-46

parts of the product that can be recovered after disassembly, faced to the total parts of the assembly.

2-The objective description

For conventional products, whose manufacturing process can be automatized, good principles are: to minimize number of union elements, to use detachable or elements of union easy to destroy, to prevent change of direction for dismount, to standardize and to simplify union techniques, to make possible simultaneous separation and dismount, to provide access for tools with dismount [AR1, AZ1, DM1, KT1].
These general principles are not immediate to be pursued when products are subject to handcrafted assembly operations that can't be standardized or generalized. For these categories of products a different and more specific analysis is necessary to schedule the disassembly operations and to make them quantifiable. Some significant parameters have to be identified and defined in order to describe the disassembly work. Moreover, these parameters have to be easily quantifiable for a large variety of products.
In this paper three parameters, that influence the easiness in disassembling a non conventional product, have been proposed and defined: they have been evaluated from considerations on the use of materials that constitute each joint of the product, on the disassembly time necessary to complete the disassembly operation and on the reusability of parts at their EoL.
Data are collected in a table, where an ID number is assigned to each kind of joint (in general the joint assembles two parts) and, corresponding to it, structural elements of parts to be joined are specified, how many times the same kind of joint is repeated in the same product, how many connections are necessary in the specific junction and how the junction is realized.
A case study is proposed in this paper to detail the way of quantifying the Disassembly Index of a single, not standardizable product, made of a considerable number of parts, through a sharable quantitative analysis.

3-The model

The disassembly capability has been first evaluated by the number of materials that constitute each joint of the product (or of a product significant subassembly). A second parameter takes into account the time necessary to disassemble each specific joint. A final parameter describes the reusability of a part, after the disassembly has been completed.

ID	Structural elements to be joined	n_i	n. of connecting elements	Kind of junction
1	Hull-basement	1		manual layered VTR reinforcement
2	Basement-undercarriage	2	4	fasteners
3	Hull-principal bulkheads	7		manual layered VTR reinforcement

Table 1 : The ID number assignment for each junction.

Data are collected in a table, arranged as shown in Table 1, where an ID number is assigned to each kind of joint (in general the joint assembles two parts) and, corresponding to it, are specified:

- the structural elements of parts to be joined;
- how many times the same kind of joint is repeated in the same product, column n_i;
- how many connections are necessary in the specific junction;
- how the junction is realized.

No number of connecting elements is specified when the manufacturing process can be obtained in a unique operation (manual layered reinforcement, gluying, just positioning).
The three parameters that influence the Disassembly Index are indicated as **z**, **k** and **h**. All the three can vary from near 0 to 1 and a variation scale is defined to assign a specific value to each parameter depending on work conditions.
Parameter **z** depends on the number of materials employed in the junction; parameter **k** varies in function of time and it describes the time necessary to disassemble a joint; parameter **h** depends on the reusability of parts after they have been disassembled and it is evaluated depending whether the reuse is complete or partial and whether it is immediate or it needs refurbishing.
Parameter **z** varies from 0,05 to 1 and it assumes a specific value depending on how many different materials have been employed in a joint. In terms of dismantling, the use of different materials has to be minimized [L1]. For this reason parameter **z** assumes value 1 when the connectors of the joint are made all of the same material, it assumes values from 0,75 to the minimum 0,05 when materials employed go from 2 to a maximum of 5 different types, as defined in Table 2 that follows.

z	Nr. of materials
1	1
0,75	2
0,5	3
0,25	4
0,05	5

Table 2 : Values for **z** in function of the number of materials.

Parameter **k** varies from 0,1 to 1 and it is defined as an exponential function whose argument is given by the ratio of the disassembly time to the assembly time, through a normalizing factor. The trend of the function has been defined and tested with the software Mathemathica, by Wolfram. In Table 3, as example, data are collected for **k**.

Article 021-sd-46

k	Disassembly time
1	1 to 10 min
0,8	11 to 20 min
0,6	21 to 30 min
0,4	31 to 40 min
0,3	41 to 50 min
0,2	51 to 60 min
0,1	Beyond 60 min

Table 3 : Values for **k**, in function of the disassembly time.

Parameter **h** varies from 0,05 to 1 and it gives information about the behavior of the disassembly.
In particular, it assumes value 1 when the disassembly gives back parts that are all intact and reusable, it values 0,75 when the disassembly gives back parts that are all reusable, but they need refurbishing, it values 0,5 when the disassembly gives back parts that are not all intact and reusable, it values 0,25 when the disassembly gives back parts that are not all reusable and they need refurbishing in any case, it values 0,05 when no part can be reused after the disassembly. This is shown in Table 4 as follows.

h	Reuse
1	Complete
0,75	Complete whit refurbishing
0,5	Partial
0,25	Partial with refurbishing
0,05	Null

Table 4 : Values for **h**, in function of the reusability of parts.

All parameters above described contribute to the formula (1) that computes the Disassembly Index as the ability of a non conventional product to be easily disassembled with particular attention to the capacity of recovering parts after the disassembly have been completed. The formula has been arranged for the calculation of the DI by the authors and can be defined as follows:

$$DI = \frac{\sum_{i=1}^{N_u} k_i(t) * h_i(r) * z_i(m) * n_i}{N} \qquad (1)$$

In (1) n_i is a number relative to how many times the same kind of junction is considered, N_u is the number of the different kind of joints employed to assemble the whole product, N is the number of total junctions considered.
The formula gives as output a value that can vary from a minimum near to 0 to a maximum of 1. The final value gives a quantitative information about the ability of a product to be disassembled in order to recover parts, to dismantle materials, to gain time. It can be also intended as the percentage of recovered parts faced to the whole product.

4- Case study: the DI application

To test the model proposed, this paper presents the evaluation of the DI to a sailboat, object of studies in the project 'Econaut', in which the scientific partner is the 'Tecnopolo della Nautica' (http://www.tecnopolonautico.it) for simulation and optimization of the geometries and materials and the other partners are two important companies: the Riba Composites for rigging and the Sly Marine for its recent creation 'The Sly '38'.
The realization of the project and the product is led by a new way of thinking, dedicated both to enjoy sailing and lowest environmental impact, keeping the same comfort, improving safety and giving the superior performances in the tradition of Sly yachts.
The goal is to get, through the gradual implementation of new methodologies, at the version '38 of the Sly, shown in Fig. 1, that can be defined as the forerunner of a new generation of Green-Boats.
In this context a DfD analysis have been carried on, starting from considerations on the main blocks assembling the whole Sly 38.

Figure 1 : The sailboat Sly '38.

The macro-blocks that can be considered for the Sly '38 are listed as follows and are illustrated in Fig.2:

- hull and deck;
- fiberglass structural supports;
- bulkheads and flat;
- furniture;
- on-board instrumentations;
- propulsion and power transmission;
- deck instrumentations;
- mast and rigging;
- sail propulsion;
- appendices.

Article 021-sd-46

Figure 2 : The hull and deck and fiberglass structural supports.

In the following study only the first 4 blocks of the list above have been analyzed, the remaining blocks being separate entities which are mounted on board in a second time and for which only a possible disassembly for ordinary or extraordinary maintenance has been considered.

4.1 - The main blocks description

The hull and deck block is the most relevant, in terms of weight of material, of the whole product. It can be considered as a box in which the walls represents the hull and the deck its top cover. They can be realized in different materials requiring different manufacturing processes, such as metal, glass-vinyl ester resin, glass-epoxy or carbon-epoxy. Furthermore, the process can be realized in hand lay up, vacuum, or vacuum infusion. For the boat here considered, the hull and deck are made of glass-vinyl ester resin in hand lay up of skins.
The hull and the deck are made of single blocks. So they are single bodies without chemical or mechanical connections of any kind. Even where the product is made from multiple parts, these are joined together again with the help of fiberglass, then the final product will be an homogeneous single block.
The structural strength of the hull of the boat is ensured by reinforcing structures, suitably dimensioned, positioned on the bottom of the hull. These structures can be the floor frame which together with the spar form a reinforcing structure. In some cases, the reinforcement structures have already been realized in a unique block. These structures can be joined to the hull by a manual layered VTR(fiberglass) reinforcement, i.e. with the lamination of a glass resin piece throughout their edge, or by gluing them with structural adhesive. The Sly 38 has a central basement where floor frames and spars are merged into a single structure, as shown in Fig. 3. The basement also has the function of guide for the transverse bulkheads, which together with the basement have the task of supporting the hull and deck in the load holding.
The inner spaces of the boat is divided by means of the bulkheads that can have a structural function or not, depending on they help to support the loads between the hull and deck, or they have only to separate the living space and to support plans and the furniture. The bulkheads are joined to the hull and deck by the manual layered VTR reinforcement, as shown in Fig.4, 5.

Figure 3 : The basement of the Sly 38 and the guides for transverse bulkheads.

Figure 4 : The bulkheads is joined to the hull and deck by manual layered VTR reinforcement.

Article 021-sd-46

Figure 5 : A junction made by manual layered VTR reinforcement.

The furniture of sailing boats significantly varies, depending on they are addressed to cruise boats or racing boats. While the first design criterion is the on-board comfort, aesthetics and ease of rigging, for the latter it is focused on the sailing speed, the lightness and the thinness, neglecting factors such as the internal volume and the simplicity of operation. For the same sailboat model usually several layouts for the interior of the boat are available, increasing or decreasing the cabins and / or bathrooms on the boat.
Common materials used in the furniture are wood of different types such as okumé, albasia, oak, teak, or metals such as steel and aluminum employed for the profiles or also special plexiglass and glass in the bathrooms decor.
All the furniture such as dinette table, kitchen furniture, chart table is generally preassembled outside the boat and it is transported in blocks to be assembled inside the boat. However, they will be placed inside the boat and stowed on board before the deck has been placed, when the boat is easily accessible from the top. The furniture is then fixed on bulkheads, by gluing and screwing further.

4.2 - Parameters definition and the Disassembly Index computation

In this case study assembly operations are mainly handmade and this entail an approximation in the attribution of values to each operation. In particular for factor **k** we have supposed time for assembly and disassembly for each junction that are strongly influenced by the operator.
The manufacturing operations employed in the sail blocks considered are listed in Table 5, where specific values are assigned to parameters **k**, **z** and **h** .
As described before, all the data considered for the DI computation are collected in a table: Table 6, that follows, lists 32 identification numbers, IDs, that correspond to all the structural elements of the blocks considered for the Sly ’38. More in particular, in the first column the **ID** number is listed: it identifies two structural elements that have to be joined, that are reported in the second column; in the third column to $\mathbf{n_i}$ corresponds the number of junctions of the same kind that are repeated in the assembly/disassembly; in the fourth column, **n. of connecting elements,** the number of connections used in the junction are specified, where connecting elements are used (no number of connecting elements is specified when the manufacturing process can be obtained in a unique operation as manual layered reinforcement, gluying, just positioning); the last column, **Kind of junction,** describes the manufacturing process adopted for the structural elements joining.
The computation of the formula (1) for the Disassembly Index of the sail boat analyzed, whose assembly/disassembly operations can be defined through the parameters **k**, **z**, and **h** as detailed in Table 5, gives back a value of 0,417.

Kind of junction	k	z	h
Manual layered VTR reinforcement	0,1	0,5	0,25
Fasteners	1	1	1
Structural gluing	0,4	1	0,05
Silicone gluing	0,6	1	0,5
Plastic clips	0,6	0,5	0,75
Just posed	1	1	1

Table 5 : The values considered for parameters k, z and h.

Article 021-sd-46

ID	Structural elements	n_i	n. of connecting elements	Kind of junction
1	Hull-basement	1		manual layered VTR reinforcement
2	Basement-fixed undercarriage	2	4	fasteners
3	Basement- just posed undercarriage	5		Just posed
4	Hull-principal bulkheads	7		manual layered VTR reinforcement
5	Hull-secondary bulkheads	6		manual layered VTR reinforcement
6	Hull-separation bulkheads	13		manual layered VTR reinforcement
7	Principal bulkheads - cabin top coat	7		manual layered VTR reinforcement
8	Secondary bulkheads -cabin top coat	6		manual layered VTR reinforcement
9	Fiberglass cabin top coat -deck	1		structural gluing
10	Cabin top coat -deck	5	20	plastic clips
11	Cabin top coat -deck	2		Silicone gluing
12	cabin ceiling -deck	3	7	plastic clips
13	Lateral panels	7	30	plastic clips
14	Dinette lateral panels	1	6	Silicone gluing
15	Skylight	12	20	bolt
16	Anchor compartemnt	1	2 +6	hinge+ fasteners
17	Fixed table	1	4	fasteners
18	Mobile table	1	4	fasteners
19	Dinette cabinet	4	2	fasteners
20	Dinette cabinet	3	2	fasteners + Silicone gluing
21	Fixed refrigerator	1	2	fasteners + Silicone gluing
22	Mobile refrigerator	1	6	fasteners
23	Chart table and side	1	6	fasteners + Silicone gluing
24	Kitchen cabinet	1	4	fasteners + Silicone gluing
25	Cabin and bathroom closet	3+1		Silicone gluing
26	Seatback bench	2		Silicone gluing
27	Footing	2		Just posed
28	Bathroom washbasin	1		Silicone gluing
29	Long bench panel	2	6	plastic clips
30	Short Bench panel	1	4	plastic clips
31	Door	4	2 + 6	hinge + fasteners
32	Boarding ladder	1	2 + 4	hinge + fasteners

Table 6 : The elements for each junction of the Sly'38.

5- Discussion

The value obtained for the DI of the sail boat proposed as case study evidences that little less than an half of the total assembled elements of the main blocks of the Sly '38 can be efficiently disassembled. This result can be also read as the percentage of junctions used in the assembly that provides for the reusing parts: it is a good result, especially if considered the preponderant workmanship in the manufacturing processes.
In fact, the manual layered VTR reinforcement, that is a traditional process not yet optimized in terms of recyclability of products, is mostly used in the assembly of structural parts.
The optimization of this process could enhance the DI and could be of great interest, in line with the attention paid on the ecological impact of products.
In order to check the model validity and to quantify the improvement of the DI depending on the assembly manufacturing process adopted, a second simulation has been performed, that considered a different kind of junction instead of the manual layered VTR reinforcement. The manual layered VTR reinforcement has been replaced with fastener connections and the DI has been recalculated with the relative parameters: it assumed the value of 0,8.

6- Conclusion

Generally, for handcrafted products, the classification of assembly/disassembly operations is an hard issue because they strictly depend on the ability of the operator and, in general, on human factors. The innovative approach we proposed entails the evaluation of only three parameters, that can be quantified through simple considerations about the number of materials, the time necessary to the operations and the integrity of parts after their disassembly, and calculates a value that gives a quantitative and immediate idea of the ability of products to be disassembled efficiently.
The robustness of the model has been tested on a second simulation of the process, that differed in a manufacturing process thus influencing the global parameters. A significant variation of the DI validated the model sensitiveness and highlighted how immediate and meaningful is the response of the index in function of the parameters variation, influenced by the choice of the manufacturing process in the assembly of parts.
However, this model does not yet take into account important factors that actually influence the easiness of a product to be disassembled efficiently, as the cost of operations to disassemble parts, the hierarchic level number and the sequence of operations.

7- References

[AR1] Abdullah A. B., Ripin Z.M., Mokhtar M. A methodology to evaluate design efficiency based on assembly criteria in support of design for modularity. In The Institution of Engineers journal, 66: 34-40, 2005.

[AZ1] Afrinaldi F., Zakuan N., Blount G., Goodyer J., Jones R., Jawaid A. Strategic Guidance Model for Product Development in Relation with Recycling Aspects for Automotive Products. In Journal of Sustainable Development, 3: 142-158, 2010.

[AZ2] Afrinaldi F., Zakuan N., Blount G., Goodyer J., Jones R., Jawaid A. Strategic Guidance Model for Product Development in Relation with Recycling Aspects for Automotive Products. In Journal of Sustainable Development 3 :142-158, 2010.

[B1] Bogue R. Design for disassembly: a critical twenty-first century discipline. In Assembly Automation, 27/4: 285–289, 2007.

[DM1] Desai A., Mital A. Evaluation of disassemblability to enable design for disassembly in mass production. In International Journal of Industrial Ergonomics, 32: 265-281, 2003.

[GG1] Gungor A., Gupta S.M. Issues in environmentally conscious manufacturing and product recovery: a survey. In Computers & Industrial Engineering, 36: 811- 853, 1999.

[KT1] Kroll E., Thomas A. Hanft Quantitative Evaluation of Product Disassembly for Recycling. In Research in Engineering Design, 10: 1-14, 1998.

[KZ1] Kriwet A., Zussman E., Seliger, G. Systematic integration of design-for-recycling into product design. In International Journal of Production Economics, 38: 15-22, 1995.

[L1] Ljungberg L. Materials selection and design for development of sustainable products. In Materials & Design, 28: 466–479, 2007.

[GZ1] Gehin A., Zwolinski P., Brissaud D. A tool to implement sustainable end-of-life strategies in the product development phase. In Journal of Cleaner Production, 16 : 566-576, 2008.

[ZB1] Zwolinski P., Brissaud D. Remanufacturing strategies to support product design and redesign. In Journal of Engineering Design, 19 : 321-335, 2008.

Article 023-sd-109

Disassembly sequencing for end-of-life products

H. Said [1], P. Mitrouchev [1], M. Tollenaere [1]

(1) : Univ. Grenoble Alpes, G-SCOP, F-38000, Grenoble, France
CNRS, G-SCOP, F-38000 Grenoble, France
Phone: 04 76 57 47 00 /Fax: 04 76 57 46 95
E-mail : Hibo.Said-Chekh-Waiss@grenoble-inp.fr

Abstract: When a product reaches its end of lifecycle, its components can be reused, recycled or disposed depending on their conditions and recovery value. All these strategies involve the disassembly of products. A method for generation of disassembly sequences is proposed in this paper. It is based on hierarchical analysis of the modules constituting the product. The method uses informations such as: list of subsets (modules), liaison-component graph, part geometry, functional contacts between components and modules, component properties (density, surface treatment,) all contained in a database. It has been tested on several products disassembly. The application of the method is explained with an example.

Key words: Disassembly, disassembly sequences, modules, products, hierarchical analysis.

1- Introduction

Disassembly plays a key role when it comes to choosing the product's end of life cycle scenario. On one hand, it is essential to ensure the required purity of recycled materials so they can be accepted by secondary manufacturers. On the other hand, it is necessary to leave the components and sub-assemblies sensitive to the repair, reuse, remanufacturing or reconditioning. Note, that there is an absence of eco-design tools for products in the early stages of the design process especially in the domain of complex systems, as mentioned in [TY1].

Various studies have been conducted in the field of Disassembly Planning (DP), offering exact methods, approximate methods or methods based on learning. Note that DP is often dealing with determining the optimal disassembly sequence: optimal should be heard as lower resource involvement for maximized benefit. Some of these works draw their foundations from previous methods developed for assembly. Bourjault [B1] was amongst the first who suggested a set of rules for generating all the possible assembly sequences based on the so called *liaison graph*. This concept was modified later by De Fazio *et al*. [DW1] to simplify the approach for more complex products and has been after then used for disassembly sequence planning by Dong et *al.* [DZ1]. Mascle and *al.* [MJ1] proposed a method that considers the different states of the product during its assembly for the determination of assembly plan. The state graph proposed by the authors is used for the determination of disassembly plan. In 2003, Lambert [L1] presented a review of the literature research on generation of Disassembly sequencing (DS). All of these methods start by modelling the product's structure. Currently there are four common graphical methods to generate disassembly sequences [TZ1], namely: *connection graph*, *direct graph*, *and/or graph* and *disassembly Petri nets*.

The exact methods, such as: *graph search* [KZ], *the mathematical programming technical* [L2], *branch and bound method* [ZZ1] and *wave propagation* [SG1] are used for determining the optimal disassembly sequence when the product components are limited.

Note that, the problem of Disassembly Sequence Planning (DSP) is *NP-hard* combinatorial optimization problem. Generally, with increasing the number of the components in a product, the computational complexity of the search for optimal disassembly sequence in a large solution space increases more rapidly.

Therefore, the exact methods cannot solve this problem effectively. Thus, heuristics and meta-heuristics methods such as: *Genetic algorithm* [TK1], *ant colony* [SS1] and *Simulated Annealing* [HH1] are often used to find a solution close to the optimal. However, the results of the heuristics are often far from the optimal ones. For example, the heuristics proposed by Kuo *et al*. [KZ1] and Gungor *et al*. [GS1] are only applied for electromechanical products disassembly sequencing. Note that heuristics can be combined with other optimization methods as presented in Lambert et *al*. [L3].

Most of the works on the generation of disassembly sequences were not considering the modular aspect of the product design. The present work provides a new way to generate disassembly sequences. This method formulates the disassembly problem in terms of module that should be disassembled. The analysis of the interaction between the components is a decision making aid for designers to

Article 023-sd-109

generate disassembly sequences. Thus, the results of this study may be useful for designers allowing them to evaluate A/D operations sequencing at the initial phase of a product design.
This paper is organized as following: Section 2 presents the method based on the hierarchical analysis of the product which leads to a disassembly tree. Section 3 describes an example of application illustrating the proposed method.

2- Method proposed

The method for the generation of disassembly sequences is based on hierarchical analysis modules forming a product.

2.1 – Assumptions

Disassembly of a product is carried out by a non-destructive disassembly approach. We assume that the graph connection $G=\{C, R\}$ is given. Let $C= \{c1, c2..., c_n\}$ be the set of all product components of cardinality n. Let $R= \{r1, r2..., r_m\}$ be the set of all relations between the components of the product, of cardinality m.

2.2 –Matrix of connections' intensity

For each connection between two components of the graph, we assign the value obtained by the calculation of an indicator called *"Easy to separate fixation*".
These values are presented in the form of a matrix of connections which element a_{ij} is defined as:

$$a_{ij} = \begin{cases} IF_{es}, \text{ if there is an arc} \\ 0, \text{else} \end{cases} \quad (1)$$

The formulation of the proposed indicator "*easy to remove fixation*" is:

$$IF_{es} = \frac{\sum_{n}^{n} \left(A_{TF} CTF_i + A_{TT} CTT_i + A_{AD} CAD_i \right)}{n} \quad (2)$$

with:
CTF - coefficient type fastening,
CTT - coefficient type of tool,
CAD - coefficient access direction,
n - number of fixations.

A_{TF}, A_{TT} and A_{AD} are respectively the weight factors of the indicator IF_{es}.

Those factors are calculated as follows:

$$A_i = \frac{2(m+1-k)}{m(m+1)} \quad (3)$$

with: *m* - number of coefficients of the attachment indicator,
k - number corresponding to priority order of the factors.
The proposed values of *k* are:

- for the access direction *k*=1, (the most important, as the bigger is *k* the lower is A_i)
- for the type of connection $k = 2$,
- for the tool type $k = 3$

with $m = 3$, then:

$$A_{AD} = \frac{2(3+1-1)}{3(3+1)} = 0.5, \quad A_{TF} = \frac{2(3+1-2)}{3(3+1)} = 0.34$$

and $A_{TO} = \frac{2(3+1-3)}{3(3+1)} = 0.16$

The connection type can be qualified according to a predetermined scale. To describe the type of fixation, a weighting is proposed which increases with the difficulty to break the considered fixation (see Table 1).

Attachment type	Coefficients
Put	*1/5*
Insertion, riveting	*1/4*
Turn	*1/3*
Combine	*1/2*
Gluing, welding	*1*

Table 1: Degree of difficulty of separation used for some types of fasteners.

As for the types of fasteners, the factors: *tool type* and a*ccess direction* are weighted by coefficients that represent their difficulty level (see Tables 2 and 3).

Tool Type	Coefficients
Manual	*1/5*
Screwdriver	*1/4*
Small tool	*1/3*
Special tool	*1/2*
Great tool	*1*

Table 2: Coefficients associated with some types of tools

Number of access directions	Coefficients
5 angles	*1/5*
4 angles	*1/4*
3 angles	*1/3*
2 angles	*1/2*
1 angle	*1*

Table 3: Coefficients associated with some numbers access directions types of fasteners.

2.3 – Product modularisation method

To estimate the possible number of modules in a product (assembly), the formula proposed by Ericsson and Erixon [EE1] is used:

$$NMP \leq \sqrt{NCP} \quad (4)$$

with:
NCP: number of the product components

Article 023-sd-109

From the connection graph and matrix of connections' intensity (see § 2.2), we can regroup product components into modules by analyzing the interactions between them. This grouping is done by the following steps:

1. Total the entries in each column of the matrix of connections' intensity.
2. Choose the components with the highest intensities connections and assign them to a module. Remove the components assigned to the module from the matrix of connections' intensity.
3. Select the column which has the highest sum of the entries of the matrix of connections' intensity and draw a vertical line.
4. For each entry (value) different from 0 (zero) intersected by a vertical line, draw a horizontal line.
5. Assign components to the module which contains the component of the selected column so as to maximize the intensity connection of the components of the same module and to minimize the interactions between components of different modules.
6. Transform the matrix by removing its components assigned to the module.
7. Repeat steps 4-6 until each component is assigned to a module.

2.4 – Generating the sequence of disassembly

For disassembly sequence generation, two steps are required:

1. Choice of a disassembly direction.
2. Analysis of the interaction between the components: the aim is to determine, according to the chosen direction, the matrix of precedence between components. This matrix itself is defined from the connection graph and the product structure. An element P_{ij} of the matrix is such that:

$$P_{ij} = \begin{cases} 1, \text{if the component } i \text{ is disassembled before the component } j \\ 0, \text{if the component } i \text{ can not be disassembled prior to the component } j \\ x, \text{if no precedence constrant exists between the components } i \text{ and } j \end{cases} \quad (5)$$

Note, that resulting sequence(s) of disassembly may be represented in different ways. We propose to represent them as a disassembly tree, associated with an undirected graph. The proposed sequence generation disassembly algorithm is shown in Fig. 1.

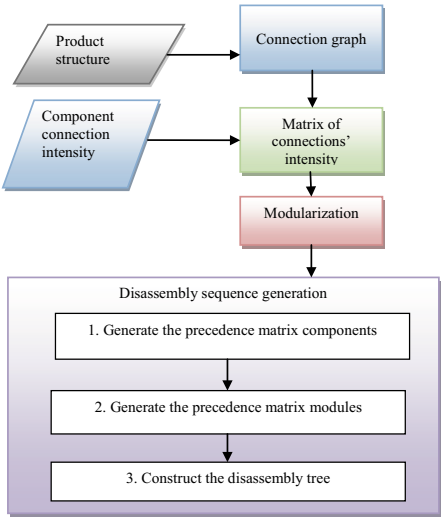

Figure 1: Sequence generation disassembly algorithm.

3- Case study

3.1 – Modelling the structure of the product

In this section, we propose to apply the algorithm for disassembly sequence generation to a stapler. Figure 2 shows an illustration of the product describing an exploded solution. The stapler consists of *18* components as listed in Table 4.

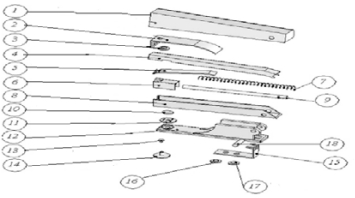

Figure 2: Exploded view of the alternative solution and associated nomenclature.

No	Components	Material	Weight (kg)
1	Steel cover	iron	0.015
2	Bracket spring	Fer	0.005
3	Rivet 1	Fer	0.003
4	Steel top	steel	0.008
5	Pivot spring	Acier	0.0025
6	Slide foot	Aluminum	0.003
7	Staple spring	Fer	0.00125
8	Bottom track	Acier	0.006
9	Guid rod	Fer	0.002
10	Rivet 2	Fer	0.003
11	Impact plate	Aluminum	0.002
12	Base	Acier	0.012
13	Spring	Fer	0.0009
14	Rivet Buttom	Acier	0.0021
15	Fastener piece	Acier	0.025
16	Rivet 3	Fer	0.003
17	Rivet 4	Fer	0.003
18	Pivot rod	Acier	0.004

Table 4: Components, materials and weight of the stapler

Article 023-sd-109

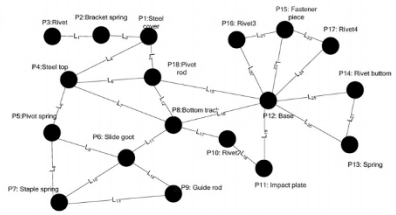

Figure 3: Connection Graph

3.2 – Matrix of connections' intensity

As mentioned in section *2.2* the value obtained by the calculation of "*Easy to separate fixation*" indicator for each type of fixation, is allocated for each connection between two components of the graph. The result is shown in the form of an matrix of connections intensity between the components (see Table 5 in Appendix A).

3.3 – Grouping components in module

As previously said, the number of possible modules is calculated by eq. *(4)* [EE1]. As the stapler is formed of *18* components, the number of possible modules is *4*.

From the connection graph (see Fig. 3) and the matrix of connections (Appendix A), the components can be regrouped into modules, according to the methodology of grouping components presented in section *2.3*. The addition of entries in each column of the matrix of connections showed that components *7*, *12*, *15* and *18* (highlighted in yellow values in the matrix of connections) have higher intensities of the bonds. We assign components *7*, *12*, *15* and *18* to each module. Then we assign to the other components of such a module so as to maximize the interaction between the components of a module and by minimizing interactions between components of different modules. The obtained modular decomposition of the stapler is shown in Fig. 4.

Thus, module *M1* is composed of components *1*, *2*, *3*, *4* and *18*. Module *M2* of components *5*, *6*, *7*, *8* and *9*; module *M3* of components *10*, *11*, *12*, *13* and *14* and finally module *M4* of components *15*, *16* and *17*.

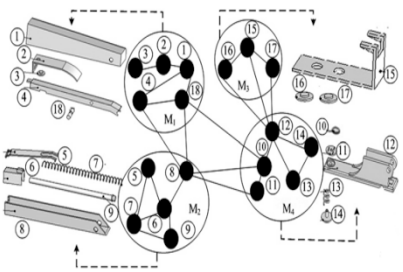

Figure 4: Grouping result of stapler.

3.4 –Precedence matrix for stapler

We illustrate via equation *(6)*, the matrix of precedence for the case study. To construct this matrix, we determine for each component of the stapler, all the components to be disassembled before it. The set of components is determined from connection graph.

$P_{18} =$

	18	1	2	3	4	5	6	7	8	9	10	11	12	13	14	15	16	17	
18	0	1	1	X	1	0	0	0	0	0	0	0	0	0	0	0	0	0	
1	0	0	0	0	0	X	X	X	X	X	X	X	X	X	X	X	X	X	M1
2	0	1	0	0	0	0	0	0	X	X	X	X	X	X	X	X	X	X	
3	X	1	1	0	0	X	X	X	X	X	X	X	X	X	X	X	X	X	
4	0	1	1	1	0	0	0	0	X	X	X	X	X	X	X	X	X	X	
5	1	X	1	X	0	0	1	1	1	1	X	X	X	X	X	X	X	X	
6	1	X	1	X	0	0	0	1	1	1	X	X	X	X	X	X	X	X	M2
7	1	X	1	X	0	0	0	0	1	1	X	X	X	X	X	X	X	X	
8	1	X	X	X	X	0	0	0	0	1	X	X	X	X	X	X	X	X	
9	1	X	X	X	X	0	0	0	0	X	X	X	X	X	X	X	X	X	
10	1	X	X	X	X	X	X	X	X	X	0	1	1	1	X	X	X	X	
11	1	X	X	X	X	X	X	X	X	X	0	0	1	0	0	X	X	X	M3
12	1	X	X	X	X	X	X	X	X	X	0	0	0	0	0	0	0	0	
13	1	X	X	X	X	X	X	X	X	X	0	1	1	0	0	X	X	X	
14	1	X	X	X	X	X	X	X	X	X	X	1	1	1	0	X	X	X	
15	1	X	X	X	X	X	X	X	X	X	X	X	1	X	X	0	0	0	
16	1	X	X	X	X	X	X	X	X	X	X	X	1	X	X	1	0	X	M4
17	1	X	X	X	X	X	X	X	X	X	X	1	X	X	1	X	X	0	

(6)

3.5 – Generating disassembly tree

To the value *1* of the components belonging to the same module of equation *(6)*, the value *0* is assigned. Thus the precedence matrix, equation *(6)* becomes:

$P_{18} =$

	18	1	2	3	4	5	6	7	8	9	10	11	12	13	14	15	16	17	
18	0	0	0	X	0	0	0	0	0	0	0	0	0	0	0	0	0	0	
1	0	0	0	0	0	X	X	X	X	X	X	X	X	X	X	X	X	X	M1
2	0	0	0	0	0	0	0	0	X	X	X	X	X	X	X	X	X	X	
3	X	0	0	0	0	X	X	X	X	X	X	X	X	X	X	X	X	X	
4	0	0	0	0	0	0	0	0	X	X	X	X	X	X	X	X	X	X	
5	1	X	1	X	0	0	0	0	0	0	X	X	X	X	X	X	X	X	
6	1	X	1	X	0	0	0	0	0	0	X	X	X	X	X	X	X	X	M2
7	1	X	1	X	0	0	0	0	0	0	X	X	X	X	X	X	X	X	
8	1	X	X	X	X	0	0	0	0	0	X	X	X	X	X	X	X	X	
9	1	X	X	X	X	0	0	0	0	0	X	X	X	X	X	X	X	X	
10	1	X	X	X	X	X	X	X	X	X	0	0	0	0	X	X	X	X	
11	1	X	X	X	X	X	X	X	X	X	0	0	0	0	0	X	X	X	M3
12	1	X	X	X	X	X	X	X	X	X	0	0	0	0	0	0	0	0	
13	1	X	X	X	X	X	X	X	X	X	0	0	0	0	0	X	X	X	
14	1	X	X	X	X	X	X	X	X	X	X	0	0	0	0	X	X	X	
15	1	X	X	X	X	X	X	X	X	X	X	X	1	X	X	0	0	0	
16	1	X	X	X	X	X	X	X	X	X	X	X	1	X	X	0	0	X	M4
17	1	X	X	X	X	X	X	X	X	X	X	1	X	X	0	X	0	0	

(7)

Considering the sub-modules and the relationships existing amongst them, we get the simplified matrix issued from eq. (7):

Article 023-sd-109

$$M_{ij} = \begin{array}{c} \\ M_1 \\ M_2 \\ M_3 \\ M_4 \end{array} \begin{array}{c} \begin{array}{cccc} M_1 & M_2 & M_3 & M_4 \end{array} \\ \begin{bmatrix} 0 & 0 & 0 & 0 \\ 1 & 0 & X & X \\ 1 & X & 0 & X \\ 1 & X & 1 & 0 \end{bmatrix} \end{array} \begin{array}{c} Level \\ 0 \\ 1 \\ 1 \\ 2 \end{array} \quad (8)$$

Thus, combining the results of the hierarchical analysis of modules constituting the stapler and the precedence matrix components that constitute the modules allows us to generate the associate disassembly tree (see Fig. 5) which represent itself the disassembly sequencing.

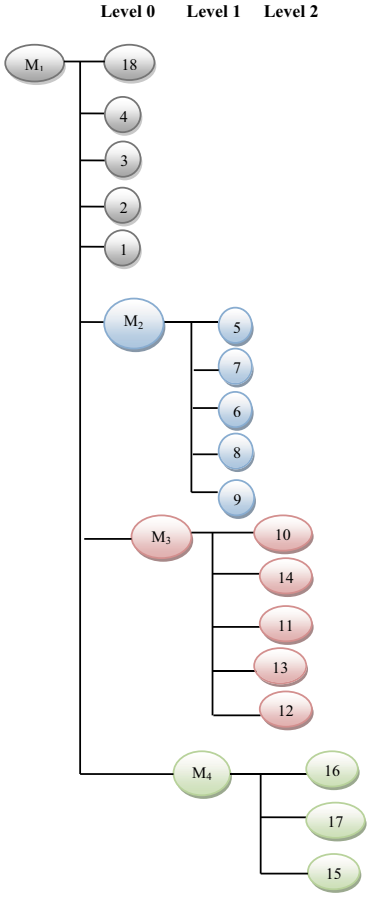

Figure 5: Disassembly tree

4- Conclusion

A clustering algorithm of the product components in the module and a generation disassembly sequences algorithm have been proposed here. Thus, the product may be optimally designed by modules on disassembly viewpoint in order to reduce environmental impacts when it reaches the end of its life cycle. The algorithm allows reaching a disassembly tree based on a hierarchical analysis of the modules constituting the product. Consequently, the tree generates the disassembly plans. Note, that the disassembly sequences are often not unique and here a *NP complex* problem might appear that will oblige to use artificial intelligence search heuristics such as: *genetic algorithm* (GA), *Dynamic Differential Evolution* (DDE) etc. The algorithms for modularization and disassembly tree generation proposed in this paper address the problems of limited size. In the future we plan to use GA to handle larger problems and to consider the evaluation of the disassembly sequences upon different criteria thus allowing finding the optimal one.

5- References

[B1] Bourjault A. Contribution to a methodological approach of automated assembly: automatic generation of assembly sequence. Thèse de doctorat, Faculté Des Sciences et Des Techniques de l'université de Franche-Comté, Besançon, France, 1984.

[DW1] De Fazio T.L and Whitney D.E. Simplified generation of all mechanical assembly sequences. In IEEE Journal of Robotics and Automation, RA-3(6): 640-658, 1987.

[DZ1] Dong T., Zhang L., Tong R. and Dong J. A hierarchical approach to disassembly sequence planning for mechanical product. In International Journal Advanced Manufacturing Technology, 30(5-6): 507-520, 2006.

[GS1] Gungor A. and Surendra G. An evaluation methodology for disassembly process. In Computers and Industrial Engineering, 33(1–2): 329–332, 1997.

[EE1] Ericsson A. and Erixon G. Controlling design variants: modular product platforms. New York: ASME Press, 1999.

[HH1] Hao W. and Hongfu Z. Using genetic annealing simulated annealing algorithm to solve disassembly sequence planning. In Journal of Systems Engineering and Electronics, 20(4): 906-912, 2009.

[KZ1] Kuo T., Zhang H. C. and Huang S.H. Disassembly analysis for electromechanical products: a graph-based heuristic approach. In International Journal of Production Research, 38(5): 993-1007, 2000.

[L1] Lambert A. J. D. Disassembly sequencing: a survey. In International Journal of Production Research, 41(16): 3721-3759, 2003.

[L2] Lambert A. J. D. Linear programming in disassembly/clustering sequence generation. In Computer & Industrial Engineering, (36): 723-738, 1999.

Article 023-sd-109

[L3] Lambert A. J. D. Exact methods in optimum disassembly sequence search for problems subject to sequence dependent costs. In Omega, 34(6): 538-549, 2006.

[MJ1] Mascle A. and Jabbour T. A database for the representation of assembly features mechanical products. In International Journal of Computional Geometry & Apllications, (8): 5-6, 1998.

[SG1] Srinivasan H. and Gadh R. A geometric algorithm for single selective disassembly using wave propagation abstraction. In Computer-Aided Design, 30(8): 603-613, 1998.

[SS1] Seamus M. and Surendra M.G. Ant colony optimization for disassembly sequencing with multiple objectives. In International Advanced Manufacturing Technology, 20: 481-496, 2006.

[TK1] Tseng Y., Kaoa H. and Huang F. Integrated assembly and disassembly sequence planning using a GA approach. In International Journal of Production Research: 1-23, 2009.

[TY1] Tchertchian N., Yvars P.-A., Millet D., Benefits and limits of a Constraint Satisfaction Problem/Life Cycle Assessment approach for the ecodesign of complex systems: a case applied to a hybrid passenger ferry. In Journal of Cleaner Production, (42): 1-18, 2013.

[TZ1] Tang Y., Zhou M. C., Zussman E. and Caudill R. Disassembly modelling, planning, and application. In Journal Manufacturing System, 21(3): 200-217, 2002.

[ZZ1] Zhang X. and Zhang S. Y. Product cooperative disassembly sequence planning based on branch-and-bound algorithm. In International Journal Advanced Manufacturing Technology, 51(9-12): 1139-1147, 2010.

Appendix A

	1	2	3	4	5	6	7	8	9	10	11	12	13	14	15	16	17	18
1	0	0,6		0,35														0,617
2	0,6	0	0,345															
3		0,345	0															
4	0,35			0	0,46			0,35										0,617
5				0,46	0	0,2667	0,35											
6					0,26665	0	0,367	0,26665	0,358									
7					0,35	0,367	0		0,617									
8				0,35		0,2667		0		0,29165		0,26665						0,367
9						0,358	0,617		0									
10								0,29165		0	0,62133							
11										0,621328	0	0,375						
12								0,26665			0,375	0	0,375	0,638328	0,375	0,6383	0,6383	0,617
13												0,375	0	0,367				
14												0,638328	0,367	0				
15												0,375			0	0,6383	0,6383	
16												0,638328			0,63833	0		
17												0,638328			0,63833		0	
18	0,617			0,617				0,367				0,617						0
	0,95	0,945	0,345	1,16	1,0767	1,258	1,334	1,175	0,975	0,912978	0,9963	3,92363	0,742	1,00533	1,6517	1,277	1,277	2,218

Table 5: Matrix of connections' intensity

Article 024-sd-17

TOWARD SUSTAINABLE MANUFACTURING: EVALUATION OF THE ECONOMIC AND ECOLOGICAL IMPACTS OF PRODUCTION LINES

Michele Germani [1], Marco Mandolini [1], Marco Marconi [1], Eugenia Marilungo [1]

(1) : via Brecce Bianche 12, 60131 Ancona, Italy
+39 071 220 4797
E-mail : { m.germani, m.mandolini, marco.marconi, e.marilungo }@univpm.it

Abstract: The **s**ustainable manufacturing is becoming an ever more important research topic since the industry is the main responsible of the environmental problem. This paper presents a method to estimate the economic and ecological impact of production lines, to the aim of favouring the adoption of sustainable processes within a manufacturing company. It considers the whole lifecycle, from manufacturing to use and maintenance, till dismantling at the end-of-life. The method considers costs and environmental impacts of the initial deployment (i.e. initial investment and set-up), use (i.e. workload or maintenance required by each machine) and end of life (i.e. retirement) of the analysed system. The method has been validated by a company producing extruded plastic pipes, during the re-design of one of its production lines.

Key words: Environmental and economic sustainability, sustainable manufacturing, energy consumption.

1 - Introduction

Sustainable manufacturing is recognized as the only possible way for industries to promote products and processes which minimize the environmental impact whilst maintaining economic profits. This is an important goal, necessary to face one of the most critical problems of the modern society: the environmental pollution and the related global warming. In fact, as it is well known, manufacturing industry is the main responsible of the environmental problem, since it uses about 31% of primary energy, and emits more than 36% of the total carbon dioxide [BV1]. In the long period, this situation will cause important changes in the climate and will certainly lead to heavy consequences for the humanity, as well as, for the global Earth ecosystem.

In this context, there has been an increasing pressure on manufacturing companies to think not only to the economic benefits, but to consider also the environmental and social effects of their activities [PK1]. Furthermore, International governments have issued set of legislations about this aspect, such as the "European climate and energy package" which aims to reduce the greenhouse gas emissions and to increase energy efficiency and production of energy from renewable resources [E1].

For the reasons described above, this paper presents a method to estimate the economic and ecological impact of production lines, to the aim of favouring the adoption of sustainable processes within a manufacturing company. In general, the sustainability and energy efficiency is measured through the use of expensive sensors and monitoring systems within existing production lines. The proposed method, instead, aims to provide a pre-emptive sustainability estimation, in order to help companies in the selection of the most appropriate solution. It considers the whole lifecycle, from manufacturing to use and maintenance, till dismantling at the end-of-life. The concurrent estimation of the lifecycle cost and environmental impacts, caused by the production line during the whole life time, allows to verify if the investment is economically sustainable and, at the same time, if the production line is compliant with the long term environmental objectives. This is an essential aspect toward the implementation of a sustainable manufacturing approach within a factory.

After the Introduction, the paper presents the most important works about sustainable manufacturing, which is possible to find in the State of the Art. Then, in Section 3 the proposed method for the estimation of the environmental and economic sustainability is deeply described considering the necessary input, output and formulas, with a focus on the use phase, which represents the most critical one in a life cycle perspective. Section 4 presents a first application of the method in a practical case study regarding a plastic extrusion line. Finally, some conclusions and proposal for future works are provided in the last section.

2 - State of the art

In the last years, the growing interest by industries on the environmental and economic issues has involved not only the eco-design and re-design of the industrial products but also the related processes, promoting the development and the advancement of the Sustainable Manufacturing theme. It involves, for example, issues such as the environmental impacts reduction on the industrial process, the employees safety during the manufacturing and the industrial costs

decrease in order to enhance the company profits. Instead, the current industrial trend is focusing on the transition from the traditional strategy based on the product sustainability, to a new industrial strategy according to the processes sustainability. This new philosophy has been supported also by the U.S. Department of Commerce that promotes the production of manufactured products using industrial processes able to minimize negative environmental impacts, conserve energy and natural resources, be safe for involved employees, communities and consumers and be economically sound. [U1].
Lots of studies and researches are conducted following these Sustainable Manufacturing concepts, Like consequence, the main affected fields in the research activities are the green value chain definition, assessment and management; the metrics and analytical tools for assessing the processes, systems and enterprises impacts; the manufacturing processes modelling according to environmental and economic resources reduction; . and finally the research of manufacturing technologies able to both reduce production impacts and to advance energy sources exploitation [B1]. Applying Sustainable Manufacturing principles allows the process monitoring and control, the evaluation of energy consumption both for the factory and its single processes, the environmental impacts assessment, the identification of all factory costs involved and the decrease of the main impacts calculated.

According to such themes, several authors deal with different facets of the question. Marilungo et al. [ML1] presented a method focused on the monitoring and control of a generic industrial process in order to optimize the energy consumption costs in a context where the process environmental and economic impacts should be decreased. Herrmann et al. [HZ1] proposed a framework which use the virtual reality to visualize the environmental impact of the manufacturing processes. Lofgren and Tillman [LT1] proposed a method able to combine discrete-event simulation (DES) with the life-cycle assessment (LCA) analysis in order to configure the manufacturing process changes, capturing the dynamic interrelationships among the process itself.

Moreover, numerous researches report examples on how evaluate the product sustainability, analysing the industrial process involved. There are several studies on agriculture, livestock production and biofuel systems; these heterogeneous studies demonstrate the growing interest and care on the sustainability theme in the industrial field like new strength to create innovation. For example, Dantsis et al. [DD1] proposed an approach to assess and compare the sustainability of different agricultural plant through questionnaires and surveys. Castellini et al. [CB1] analysed the sustainability of different poultry production systems in order to select the most relevant economic, ecological, social, and quality issue. Mengoyana et al. [MS1] presented a method to assess the sustainability of biofuel systems in order to learn a better management and organization of the system itself. In order to achieve the industrial needs to have a sustainable factory, customized algorithms to obtain the industrial processes optimization and efficiency should be created, developed and implemented in the factory. Their aims could be different, according to each main scope. For instance, they should be implemented only to monitoring and control the current process exploitation in order to understand its environmental and economic impacts, trying to optimize the results through the process parameters setting. Examples of this work are several. Heilala et al. [HV1] show in their research a tool which simulates the maximum production efficiency and helps to balance environmental constraints; the context is the linkage between the lean manufacturing principles and the assessment of the environmental impacts. Thiede et al. [TS1] propose the manufacturing system simulation like a means to implement efficient and effective usage of energy and resources. Instead, other authors focus their research on the energy efficiency modelling and related algorithms [HL1][BF1][NN1][SR1][WO1]. However in all these studies the focus is the optimization of the existed processes through the usage of methods and tools able to help companies in increasing the efficiency of their manufacturing or production processes. A purpose less investigated in researches and in the industry field, starting from the environmental and economic impacts assessment by the point of view of process components' engineers and designers. According to this aim, having a method able to preventively estimate the environmental and economic impacts of an industrial process and each its components represents a strategic means by companies to differ from their main competitors, in terms of which process components they should sale or reengineer.

3 - Method for sustainability estimation

The method described in this section is oriented to process design managers who want to reduce the environmental impact of their manufacturing processes, yet during the design phase of new production lines. The proposed methodology for an objective evaluation of alternative solutions is an essential support to reach a sustainable factory.

So far, the most used selection drivers for new production lines are based on the initial economic investment, overall dimensions, production capacity and degree of automation, without any evaluation of the environmental impact. In the proposed methodology, two indicators, one related to the environment and another related to costs, are considered. The next sections describe how to estimate the environmental impact and costs, actualized to a specific moment, for a new production line, during its life span.

3.1 – The sustainability calculation model

The environmental and economic indicators selected for the method have been classified into three groups which reflect the relative life cycle phases (manufacturing, use and End of Life). The economic indicator (LCC), equation (1), is given by the sum of the cost of each phase (the cost sources will be detailed in the next paragraph), discounted back using the discount rate, estimated by the manufacturing processes manager, considering several factors, such as the investment risk of the production line.

$$LCC = C_{man} + \sum_{n=1}^{N} \frac{C_{ene,n} + C_{mai,n}}{(1+r)^n} + \frac{C_{EoL}}{(1+r)^N} \quad (1)$$

where C_{man}, C_{ene}, C_{mai}, C_{EoL} are respectively the costs related of the initial investment, energy used during the use phase, maintenance and dismantling (End of Life), N is the life cycle time (in years), r is the discount rate (dimensionless). The subscript "n" used for C_{ene} and C_{mai} means that values are referred to the n-th year.

From the environmental point of view, the literature presents a lot of indicators , such as the Carbon Footprint, Energy Consumption, Global Warming Potential, etc. Since the aim of this methodology is to suggest the manufacturing process manager, the authors has chosen one indicator, in order to avoid any kind of interpretation of the results provided as output. The selected indicator, the Equivalent Carbon Dioxide (CO2e), is defined as a metric measure used to compare the emissions from various greenhouse gases on the basis of their global-warming potential (GWP), by converting amounts of other gases to the equivalent amount of carbon dioxide with the same global warming potential [European Commission]. This particular choice is due by the possibility to compare the effect of the gas emissions of different energy sources, required during the use phase (this is generally the most critical life cycle phase for a production line). The environmental impact (LCA indicator) is then assessed summing the contributions of each life cycle phase, as shown in equation (2).

$$LCA = EI_{man} + EI_{use} = EI_{man} + EI_{ene} + EI_{mai} \quad (2)$$

where EI_{man}, EI_{ene}, EI_{mai} are respectively the Environmental Impacts related to the initial manufacturing of the line, energy consumed during the life span and maintenance.

The manufacturing phase is related to all the activities required to make the manufacturing line with the relative machines (work carried out by the supplier of the system), to set-up the system within the production plant and to configure it for the manufacturing of a specific product. The cost assessment (C_{man}) is carried out according to the quotation provided by the supplier: this cost is the cost of investment for a new production line. The environmental assessment (EI_{man}) is determined summing the impact of each machine within the line. This indicator, as the cost, should be provided by the supplier.

The use phase of a production line is related to its normal running plus the accessory operations such as the maintenance. During this phase, the environmental and economic indicators are calculated considering the energy used and the maintenance required by each machine of the line. Since this approach is energy oriented, the flow of material though the line is not considered (the related environmental and economic indicators are not calculated). The next chapter explains in detail how it is possible to calculate the energy consumption and related indicators, taking into account the nameplate data (power, efficiency, working points) and driving cycle of each machine within the line. The proposed method considers only those energy sources which are transportable (i.e. electricity, compressed air, steam, hot water, gasoline, etc.). Ordinary and extraordinary maintenance activities (predictive ones have been neglected) provide the contributions to the economic and environmental indicators: the next chapter describes them in more detail.

For the End of Life Phase, only the cost indicator has been considered (C_{EoL}). For its calculation, two scenarios for the production lines have been thought: re-manufacturing or dismantling. For the first scenario, the cost is calculated as a percentage of the initial investment, which mainly depends by the years of use. For the second one, the cost is calculated as a sum of the effort spent to disassemble the line and treat hazardous substances, and the revenue got from the material recycling. The calculation of the environmental impact has been postponed in a further research.

3.2 – Use phase and maintenance sustainability evaluation

Considering production lines, which is the topic of this research work, the most important phase of the entire life cycle is certainly the use. As for the other Energy related Products (ErP), the energy consumed during this phase is considerably much higher than the contributions of all the other phases. This is essentially due to the fact that production lines have a very long duration of life, even more than 20-25 years. It is possible to estimate that about 85% of the total lifecycle cost is determined during the use phase. This consideration can be also extended to the environmental impact which is strictly correlated to the consumption of the various energy typologies. As a direct consequence, a fundamental prerequisite for a careful environmental impact and cost assessment is certainly the accurate modelling of the use scenario.

The proposed approach is based on a classification of the most common energy typologies which can be used to power the different equipment within a production line (Table 1). Each energy has been characterized by a unitary cost, to consider during the LCC calculation, and by a unitary emission, to consider for the environmental impact estimation. Regarding the availability of data for the analysis, the costs can be retrieved by the market or directly from the company which will use the production line, while the unitary emissions, can derive from a common LCA database, which certainly stores these necessary values.

Class	**Typology**	**Cost**	**Environmental Impact**
Chemical	Gasoline	€/l	Unitary CO2e (from LCA DB)
	Diesel oil	€/l	
	Coal	€/kg	
	Methane	€/m3	
	Liquid Petroleum Gas	€/l	
Electrical	Electricity Mix	€/kWh	
Thermal	Heat water	€/m3	
	Steam	€/m3	
Potential	Compressed air	€/m3	

Table 1: Energy typologies.

A very common way to model the use phase of energy using components is to consider their working time and their consumption in a single working point during their life time (or for each year). This simplified approach can allow to perform quick analysis of the energy consumption, but unfortunately can lead to significant errors in the consumption estimation, because very often energy using components can work in different working points (i.e. different speeds). Variable speed electric motors, controlled by electronic drives, are generally designed to be used at several speeds with an established driving cycle. These equipment are very common within production lines where, for example, electric spindles can operate at different speed and power on the basis of the process to perform. This underlines the need of a very accurate modelling of the use scenario for each component and for each energy typology, to the aim of obtaining an estimation with an acceptable accuracy.

In the proposed approach, the estimation of the energy consumption is performed considering different distributions of working points for each energy using component and for each energy typology [CG1]. In particular, each driving cycle (e.g. 1 second or 1 hour) is modelled by a list of couples of working points (e.g. different speeds for motors) and consumptions (e.g. different powers). This model is general and valid for all the considered energy typologies. However, it is essential only in some cases and for some energy typologies, such the electrical energy, while for others, such as the compressed air or the thermal energy, the simplified model can be used without losing accuracy, because the equipment can work in only one working point. Therefore, the yearly energy consumption for each energy typology, can be calculated using the following equation (3):

$$E_{k,n} = \sum_{i=1}^{I} DC_i \cdot \sum_{j=1}^{J} (EC_{i,j} \cdot WT_{i,j}) \tag{3}$$

where $E_{k,n}$ is the yearly energy consumption of the n-th year relative to the k-th energy typology (e.g. electrical, heat water, compressed air, etc.), I is the number of components in the production line, DC_i is the number of driving cycle in an year for the i-th component, J is the number of working points considered, $EC_{i,j}$ and $WT_{i,j}$ are respectively the consumption (e.g. power consumption for electricity, litres per time unit for gasoline or diesel oil, cubic meters per time unit for methane, etc.) and the working time of the i-th component at the j-th working point.

Regarding the use stage of the lifecycle, not only the energy consumption has to be considered for the estimation of the production line sustainability. Another important aspect needs to be managed: the maintenance, which is relevant in particular in terms of costs. The indicators related to the ordinary maintenance are calculated considering the plan, reported in the maintenance manual of every machine, from which it is possible to extract the replacement interval of each component. The contribution relative to the extraordinary maintenance, instead, is calculated considering the same data used for the ordinary one, but with a replacement interval of component estimated on statistical basis. The maintenance cost (C_{mai}) is calculated briefly considering the disassembly ad reassembly time, the unitary cost of the maintainer and the unitary cost of the replaced parts, available from the repository of the maintenance department. The environmental indicator is estimated using the same data used for the manufacturing phase for those components which is necessary to substitute, as well as data coming from an LCA DB for other materials (i.e. used oil).

Therefore, the total environmental impact (in terms of CO2e emissions) can be calculated considering the unitary impacts of the different energy typology (coming from an LCA DB), as well as the contribution relative to maintenance (equation (4)):

$$EI_{use} = EI_{ene} + EI_{mai} = \sum_{n=1}^{N} (\sum_{k=1}^{K} (E_{k,n} \cdot UEI_k) + \sum_{i=1}^{I} EI_i) \tag{4}$$

where EI_{use} is the total environmental impact for the use and maintenance phase, N is the number of year of the life time, K is the number of energy typology considered, $E_{k,n}$ is the yearly energy consumption of the n-th year relative to the k-th energy typology, UEI_k is the unitary environmental impact of the k-th energy typology, I is the number of components in the production line and finally $EI_{i,k}$ is the environmental impact relative to components which is necessary to substitute.

Regarding use phase costs, instead, it is necessary to consider the yearly costs, because they have to be discounted back as reported in the equation (1). On the basis of the energy consumptions (calculated by equation (3)), unitary costs of each energy typology and maintenance costs, the total costs relative to the use phase can be calculated by the following equation (5):

$$C_{use,n} = C_{ene,n} + C_{mai,n}$$
$$C_{use,n} = \sum_{k=1}^{K} (E_{k,n} \cdot UC_k) + \sum_{i=1}^{I} (C_{ord,i,n} + C_{ext,i,n}) \tag{5}$$

where the first summation represents the yearly cost of energy, while the second represents the yearly cost of maintenance. In the formulas, $C_{use,n}$ is the yearly cost of the use phase at the n-th year, K is the number of energy typology considered, $E_{k,n}$ is the yearly energy consumption of the n-th year relative to the k-th energy typology, UC_k is the unitary cost of the k-th energy typology, I is the number of components in the production line, $C_{ord,i,n}$ and $C_{ext,i,n}$ are respectively the costs for the ordinary and extraordinary maintenance relative to the i-th component at the n-th year.

4 - Test case and results discussion

According to the methodology proposed and fully detailed in the previous paragraph, a case study on an high energy using industrial company has been carried out in order to assess and validate the method and to demonstrate its advantages for the process design manager.

Such test case is a good example in order to identify the

components of an industrial process that are most energy consumption and high cost impact. In fact, in order to support the process design manger to re-engineer the company production phase it is necessary to understand how the process works, what are the main process components and how each of them consumes the needed resources.

4.1 – Test case

The study has been performed on a plastic pipes manufacturing industry made of three plants, one for each product family (PE pipes, PVC pipes and corrugate pipes). The plant involved in this study is related to the production of polyethylene (PE) pipes, because it has the new generation production lines. Their assessment allows to estimate the environmental and economic impacts caused by the exploitation of young technologies in order to design a new plant with the latest technologies lines.

The plastic extrusion process is a semi-continuous method used to realize products such as pipes, profiles or and cable sheaths. Although the design of the mould and some extrusion components are specific for each product, all the pipes have the same production method; this means that the manufacturing process efficiency, in economic and environmental terms, is the result of a set of rules and of the operators' experience and not on explicit knowledge. In this context, it is necessary to have a method able to address the process design manager to achieve an object solution, to respect the company business strategy in terms of process sustainability.

The test case conducted involves several machines (i.e. all the extrusion lines belonging to the PE plant) which consume a lot of resources, such as direct energy, water and raw materials. The main macro-areas in the PE plant are the raw materials storehouse, the extrusion lines, the refrigeration unit and the finished product storage area.

The test case was conducted on the entire plant and the sustainability of each line has been assessed calculating the environmental and economic impacts through the respectively application of LCA and LCC techniques. In both analyses the lifetime considered is 25 years and the main lifecycle phases involved are the manufacturing, use and EoL; for each one, the related environmental and economic impacts, in terms of Global Warming Potential (quantity of CO2e delivered) and amount of money spent (€), have been accurately estimated. Moreover, only the electrical energy resource has been considered in this test case, because this is the most impacting for the extrusion line, during its lifetime. Concerning the LCC analysis, the economic values have been calculated discounting back the cost spent each year, throughout the lifespan. The result has been achieved using the Equivalent Annual Cash Flow technique, with 3% as discount rate (value estimated by the company), as the final results will demonstrate, the use phase will impact more than the other phases.

The figure 1 shows a schematic representation of an extrusion line in the PE plant and its components: the feeder system dedicated to the raw materials storage and distribution, the head and body extruder to mould the plastic granules, the co-extruder to mark with a different colour the pipe in order to identify the final product usage, the vacuum tank to stabilize the white-out extruder pipe, the cooling tanks to cool the white-out pipe, and finally the downstream stage composed by the seal press, the drag system and the cutting system.

Using the proposed method, the process design manager has a baseline which could be compared with the other potential process solutions. In fact, he can define for each extender line components the LCA and LCC impacts, and he can use such assessment to design a new production line in order to substituting an existing one or to realize a new production plant.

4.2 – Results discussion

The test case results are gathered in the table 2 below, which shows in detail the environmental and economic impacts resulted by the LCA and LCC analysis on a sample line (i.e. the latest generation line). These impacts have been collected according to the lifecycle phases, paying attention especially to the use phase due to the process in object is high energy consumption especially during the process exploitation (i.e. the process use phase). Indeed, this is justified by the fact that there is a difference of three orders of magnitude between the LCA impacts of the manufacturing and use phases. For this reason, the impacts related to the use phase are divided both per each functional group and per contribution, in terms of energy and maintenance.

Concerning the EoL phase, instead, it has been estimated that the extrusion company balances the costs for the production line regeneration through the economic benefit due to the technology innovation of each production line components.

The table of results highlights that the impacts (environmental and economic) for the maintenance activities, are a very low percentage of the energy related impacts, even if the overall monetary during the considered lifetime cannot be neglected.

In conclusion, through the application of this method, it is possible to deduce that the extruder (functional group of the production line) is the most impacting element within the line, throughout its lifespan. In this way, the process design manager has immediately clear which is the strategic factor where he should pay more attention, either to optimize an existing production line or to design a new one. Moreover, the information in table 2 give to process manager an idea of which are the most affected process components (e.g. head and body extruder, vacuum tank and cooling tanks) to consider in particular way when a new production line should be sold by new.

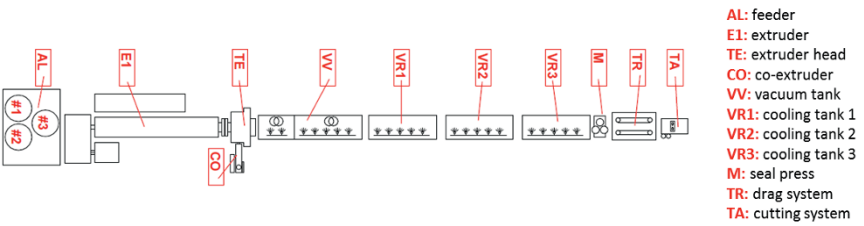

Figure 1: Schematic representation of an extrusion line in the PE plant.

FUNCTIONAL GROUPS	LIFECYCLE PHASES	LCA impacts [kg CO_2e]		LCC impacts [€]	
		ENERGY	MAINTENANCE	ENERGY	MAINTENANCE
Extrusion line	MANUFACTURING	2,08E+04		300.000,00	
AL	USE	8,97E+05	8,95E+01	301.653,18	41.191,52
E1 and TE		1,36E+07	1,70E+03	4.570.502,70	51.489,40
CO		3,06E+05	7,65E+00	102.836,3	10.297,88
VV		1,90E+06	9,50E+01	639.870,38	20.595,76
VR1, VR2 and VR3		1,53E+06	7,65E+01	514.181,55	€ 20.595,76
TR		6,12E+05	maintenance free	205.672,62	maintenance free
M		1,02E+05	maintenance free	34.278,77	maintenance free
TA		5,44E+05	maintenance free	182.820,11	maintenance free
Extrusion line	EoL	X		0,00	
	TOTAL	**1,95E+07**	**1,97E+03**	**6.551.815,61**	**144.170,32**

Table 2. Results of the LCA/LCC analysis.

5 - Conclusions

Sustainable manufacturing is recognized as the only possible way for industries to promote products and processes which minimize the environmental impact whilst maintaining economic profits. In this context, the methodology presented in this paper represents an important step toward the increase of process energy efficiency and environmental/economic sustainability.

The formulas proposed in this method allows production engineers to accurately estimate the overall energy consumption, as well as the CO2e emissions and costs for the entire production line life span. The indicators calculated by the method are necessary to evaluate which is the status quo of the manufacturing processes and to understand the most important criticalities, and to simulate different scenarios for the improvement of a line, by the substitution of the crucial functional groups/components or the entire line.

Future works will be focused on the development of a software tool for the implementation of the proposed approach in order to provide a concrete tool for the manufacturing companies that helps them in the process sustainability estimation. Furthermore, the methodology will be improved to include new and advanced algorithms to model the maintenance and EoL phases, and to expand the boundaries to the entire factory sustainability, considering, for example, the building or the ventilation and heating systems.

7- References

[BF1] Bahmani-Firouzi B., Farjah E. and Seifi A. A new algorithm for combined heat and power dynamic economic dispatch considering valve-point effects. In Energy, 52: 320–332, 2013.

[B1] Bi Z. Revisiting System Paradigms from the Viewpoint of Manufacturing Sustainability. In Sustainability, 3(9): 1323–1340, 2011.

[BV1] Bunse K., Vodicka M., Schönsleben P., Brülhart M. and Ernst F.O. Integrating energy efficiency performance in production management – gap analysis between industrial needs and scientific literature. In Journal of Cleaner Production, 19(6–7): 667–679, 2011.

[CB1] Castellini C., Boggia A., Cortina C., Dal Bosco A., Paolotti L., Novelli E. and Mugnai C. A multi-criteria approach for measuring the sustainability of different poultry production systems. In Journal of Cleaner Production, 37: 192–201, 2012.

[CG1] Cicconi P., Germani M., Mandolini M., and Marconi M. Tool for Life Cycle Costing of Electric Motors during the early Design Phases. In Proceedings of the 5th International Conference on Changeable, Agile, Reconfigurable and Virtual Production (CARV), Munich – Germany, 2008.

[DD1] Dantsis T., Douma C., Giourga C., Loumou A. and Polychronaki E.A. A methodological approach to assess and compare the sustainability level of agricultural plant

production systems. In Ecological indicators, 10(2): 256–263, 2010.

[E1] European Commission. The EU Climate and Energy Package. http://ec.europa.eu/clima/policies/package/, accessed on October 2013.

[HL1] He Y., Liu B., Zhang X., Gao H. and Liu X. A modelling method of task-oriented energy consumption for machining manufacturing system. In Journal of Cleaner Production, 23(1): 167–174, 2012.

[HV1] Heilala J., Vatanen S., Tonteri H., Montonen J., Lind S., Johansson B. and Stahre J. Simulation-based sustainable manufacturing system design. In Proceedings of the 2008 IEEE Winter Simulation Conference, Miami – Florida, 2008.

[HZ1] Herrmann C., Zein A., Wits W. and Van Houten F. Visualization of Environmental Impacts for Manufacturing Processes using Virtual Reality. In Proceedings of the 2011 CIRP Conference on Manufacturing Systems, Madison – Wisconsin, 2011.

[LT1] Löfgren B. and Tillman A.M. Relating manufacturing system configuration to life-cycle environmental performance: discrete-event simulation supplemented with LCA. In Journal of Cleaner Production, 19(17–18): 2015–2024, 2011.

[ML1] Marilungo E., Luzi A. and Germani M, Energy monitoring for investigating the sustainability of extrusion process. In proceedings of CARV Conference, Munich, 2013.

[MS1] Mangoyana R.B., Smith T.F. and Simpson R. A systems approach to evaluating sustainability of biofuel systems. In Renewable and Sustainable Energy Reviews, 25: 371–380, 2013.

[NN1] Niknam T., Narimani M.R. and Azizipanah-Abarghooee R. A new hybrid algorithm for optimal power flow considering prohibited zones and valve point effect. In Energy Conversion and Management, 58: 197–206, 2012.

[PK1] Pusavec F., Krajnik P. and Kopac J. Transitioning to sustainable production – Part I: application on machining technologies. In Journal of Cleaner Production, 18(2): 174–184, 2010.

[SR1] Seow Y. and Rahimifard S. A framework for modelling energy consumption within manufacturing systems. In CIRP Journal of Manufacturing Science and Technology, 4(3): 258–264, 2011.

[TS1] Thiede S., Seow Y., Andersson J. and Johansson B. Environmental aspects in manufacturing system modelling and simulation – State of the art and research perspectives. In CIRP Journal of Manufacturing Science and Technology, 6(1): 78–87, 2013.

[U1] U.S. Department of Commerce – International Trade Administration. Sustainable Manufacturing Initiative (SMI) and Public Private Dialogue. Washington, 2010. trade.gov/competitiveness/sustainablemanufacturing/docs/2010_Next_Steps.pdf, accessed on October 2013.

[WO1] Wright A.J., Oates M.R. and Greenough R. Concepts for dynamic modelling of energy-related flows in manufacturing. In Applied Energy, 112: 1342–1348, 2013.

Article 026-sd-108

IT framework for Sustainable Manufacturing

Kiyan Vadoudi[1], Nadege Troussier[1], Toney Wh Zhu[2]

[1]University of Technology of TroyesTroyes,
France *+33- 351 59 12 66*
[2]Shanghai University

{kiyan.vadoudi, nadege.troussier}@utt.fr
Toney_wh_zhu@shu.edu.cn

Abstract: With today's global awareness of environmental issue as well as social and economic aspects, manufacturing industry is seeking a comprehensive strategic approach to be more sustainable. By continuous sharing of information among the different product lifecycle phases product lifecycle management acts as an information strategy, which builds a coherent data structure by consolidating systems. Moreover, when the manufacturing is happening, there is location base information available within manufacturing process, which can be used into tools to assess manufacturing process in context of sustainability. This paper presents a new information strategy framework for the green manufacturing paradigm based on integration between current PLM structure and geographical information systems. The proposed IT framework is a comprehensive qualitative answer to the question of how to design and/or improve green manufacturing systems as well as a roadmap for future quantitative research to better evaluate this new paradigm.

Key words: Sustainability Manufacturing, Eco design, Product Lifecycle Management, Geographical Information System, Lifecycle Assessment

1- Introduction

In the recent decade rising consumption in natural resources, increase of world-population, environmental impacts, limited natural resources (energy, materials), global communication networks based on standards and an unstoppable worldwide globalization, are increased pressure on companies to think beyond the economic benefits of their processes and products and consider the environmental and social effects. In this context manufacturing industries play important role on environmental dimension of sustainability and it has become the goal for manufacturers to promote manufacturing processes and manufactured products to minimize environmental impacts while maintaining social and economic benefits. Green Manufacturing is presented as an advanced manufacturing mode and a sustainable development strategy, to integrate all the issues of manufacturing through reducing the use of natural resources and the waste and emission, while retaining quality of products and services.

Furthermore, product related processes are strongly based on the use of information and Product Life-cycle Management (PLM), as a business strategy, represents a very important approach for achieving a more sustainable way of work and life by managing the entire lifecycle of a product, from ideation, design and manufacture, through service and disposal. PLM, as an information technology platform is able to response this need and drives faster time-to-market, enhances collaboration for global engineering teams, reduces development costs, improves customer satisfaction, and increases the value of product portfolios.

On the other side, when the manufacturing is happening there is location-based information available within manufacturing process, which can be used into tools to characterize manufacturing process. In fact manufacturing operations occur in both space and time and by tying these together managers can quickly the action to reduce environmental effects, wastes and bottlenecks through the whole manufacturing process. In this regard Geographical Information System (GIS) is the most efficient location-based technologies, which can be used for businesses to achieve their manufacturing and logistics goals.

What is needed now is a new version of IT platform that makes manufactures able to comply better with sustainability requirements. Therefore, the main objective of this paper is to assist manufactures to be more sustainable by using new IT structure, which is based on using geographical information through the structure of PLM to lead, develop and implement the strategic change from conventional design and manufacturing to eco-innovative product design and sustainable manufacturing.

This research purpose is to link GIS and PLM to have a global and systematic approach to improve company sustainable performance and potential improvement of sustainability at territorial scale. It argues on the necessity to take into account local information concerning where the business takes place. Then, from an information system point of view, it argues the necessity to integrate geographical information in the definition of products and processes, and

Article 026-sd-108

in the whole PLM. It will lead to an integrated data model including geographic and industrial system data.

2- Green Manufacturing and Sustainable Manufacturing

Manufacturing as one of the most important stages of production [1] is in the heart of ongoing environmental debates, the most serious since the early 1970s when air and toxic pollutions became significant industrial issues. Moreover, the rapid consumption of natural resources and the growing interest in global warming have increased tendency for manufacturing companies to develop innovative manufacturing systems to shift from traditional manufacturing to green manufacturing.

Green manufacturing employs various green objectives, principles, technologies and innovations in all phases of lifecycle to become more eco-efficient. This includes creating products that consumes less material and energy, substituting non-toxic and renewable input materials, reducing unwanted outputs and converting outputs to inputs as recycled materials and products. Thus the word "green" is used to reflect environmental friendly situation, when it is added to manufacturing it is used to describe manufacturing approach that is aware of its processes and products impact on the environment and resources [2]. Furthermore, green manufacturing has a positive effect on other aspects by increasing product quality, improve production lead time and decrease costs. Therefore, green manufacturing could be a comparative advantage for companies who can efficiently use financial resources, technological knowledge and operations to implement green manufacturing principles [27].

Hence, efforts to make manufacturing green must consider at all levels of product, process, and system and not just one or more. In product level there is a need to have green technologies (reduce, reuse, recycle) [19], at the process level need to achieve optimized technological improvements and process planning for reducing energy and resource consumptions, toxic wastes, occupational hazards, etc., and for improving product life by manipulating process-induced surface integrity [3]. Finally at the system level there is a need to consider all aspects of the entire supply chain, taking into account all the major lifecycle stages from beginning of life until the end of life [20].

By considering the complexities involved for implementation of green manufacturing, it is necessary to distinct "Green" and "Sustainable" terms [21], which are still not well interpreted in many contexts and the scenario is complicated when involving many types of product returns and recovery. There are many definitions of sustainability, including this landmark one which first appeared in 1987: "Meeting the needs of the present without compromising the ability of future generations to meet their own needs" [22], which indicates on different implementation and interpretation in different fields for sustainability paradigm.

Since manufacturing is the core operation in a product's supply chain, when considering physical products, designing the system and promoting sustainability in its operations must center on a sustainable manufacturing approach by focusing on a broader, innovation-based 6R (reduce, reuse, recover, redesign, remanufacture, recycle) methodology (Figure 1) [2]. US department of commerce [26] defines sustainable manufacturing as; the creation of manufactured products that use processes that minimize negative environmental impacts, conserve energy and natural resources, are safe for employees, communities, and consumers and are economically sound.'' More specifically, in the green supply chain approach emphasis is only on the environmentally friendly product lifecycle within its use whereas a sustainable supply chain approach examines multiple product lifecycle within its use and post-use stages to balance environmental, economic, and social dimensions [4].

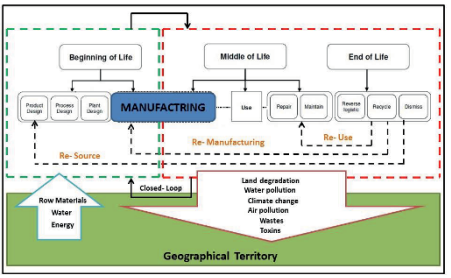

Figure1: Closed-loop product life-cycle system

In order to achieve the best practices of green and sustainability for manufacturing phase, comparison and selection between different alternative designs or production scenarios [20], PLM is introduced as information driven approach to achieve efficiency by using a shared information core system that helps a business to efficiently manage whole product's life cycle from design to disposal [12]. PLM can be a key component in helping business to reduce the costs and to increase the efficiency of resources (Material, Machines, Energy, Water and human resources) by taking into account the reduction of the consumption of the natural resources and impacts on the environment [26].

3- Lifecycle thinking and product lifecycle management

The Product lifecycle thinking is an attempt to recognize whole stages of a product within the expected life cycle and through production engineering perspective, it is related with the development, production and distribution of the product, which is defined as three main phases; Beginning-of-life (BOL), Middle-of-life (MOL) and End-of-life (EOL) [24]. BOL stage includes the initial design of a product, its development, testing and initial marketing. Design contains design of plant, product and process, manufacturing and end of life until despoil. It includes production of the artifacts and

relevant internal plant logistic and in some cases parts of external logistic. During design phase by using many tools, techniques and methodologies, designers, planners and engineers initial design of a product is defined and sent to manufacturing phase, which includes production process, plans, production facilities and manufacturing. MOL is including external logistic, use and support (in terms of repair and maintenance). In this phase, the product is in the hands of the final product user/consumer and/or some service providers, maintenance and logistic actors [23]. Finally, in EOL, retired products are re-collected and remanufactured for recovery. The product recovery processes consist in collecting, inspection, disassembly, reuse, remanufacturing, recycling, redistribution, and disposal. During BOL, the information flow is quite complete because it is supported by several information systems like CAD/CAM, product data management (PDM), knowledge management (KM). However, the information flow becomes vague or unrecognized after BOL which prevents the feedback of product-related information such as product usage data, and disposal conditions, from MOL and EOL back to BOL. Hence, lifecycle activities of MOL and EOL phases have limited visibility of the product-related information [18] considering the fact that sustainability in product development is tied with closed-loop flow of information.

Product Lifecycle Management integrates information-driven approach comprised of people, processes/practices and technology to all aspects of a product's life and provides a central system to centralize product data, standardize business processes and streamline communication of information across distributed product development teams to shorten development cycles, improve quality and speed time-to-market [21]. All these aspects are needed in order to develop and manufacture products which fulfill customer requirements and regulations set by authorities as well as comply with environmental requirements. Therefore, to be able to plan the implementation of PLM effectively into an organization, it needs to be understood also the strategic aspect of PLM far more than just an IT system, in order to develop the company as a whole to integrate all organizational aspects and levels. In this regard, Anneli Silventoinen [7] presented a holistic PLM model that includes five elements of strategies defining main approaches; operational processes of the value chain; structures of product, knowledge and organization; people and culture, and information technology means [7].

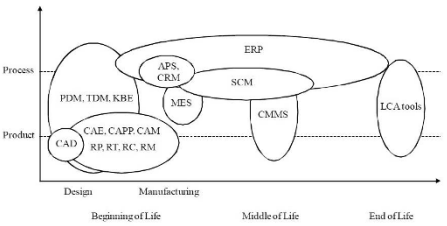

Figure.2: Mapping of ICT tools along the product lifecycle [6]

Since ICT plays an important role in PLM, the ICT architecture of a company and its dynamic adaptation to new technological developments is necessary for realizing the full PLM potential. ICT is used in running the PLM processes and in up-dating of data and information structures, mainly for creation, acquisition, storing, sharing and application of documented knowledge, but also for collaboration. In this regards different IT tools, platform and systems that are spread through complete lifecycle of product (Figure 2) are dividing in two categories of "ICT tools and systems" and "ICT interoperability and architectures"[6].

Despite progresses in traditional tools; computer aided design (CAD), computer aided manufacturing (CAM), computer aided process planning (CAPP), which helped to make decision in the design process, there are still shortcomings in this stage because they were usually separate from a manufacturing company's mainstream operations. During past years modern manufacturing application systems such as product data management (PDM), supply chain management (SCM), enterprise resource management (ERP), manufacturing execution system (MES), customer relationship management (CRM), demand chain management (DCM), Lifecycle Assessment (LCA) have been developed to overcome certain aspects of those difficulties in product design, but they cannot adequately address the need for collaborative capabilities throughout the whole product lifecycle, because they focus on special activities in an enterprise and are not adequately designed to meet new business requirements. Especially, Lifecycle Assessments (LCA) can feed PLM to improve global performance in a sustainable framework, but to have a represent-ability of the model, it may be necessary to have the input data as specific as possible including geographic specificities [2].

4- Lifecycle assessment

The most significant challenge for implementing sustainable manufacturing at the product level is to develop rapid/convenient sustainability evaluation procedures without significantly compromising the aims of LCA [3].

Life Cycle Assessment (LCA) methodology has been developed to enable the generation of more Eco-efficient design alternatives [8]. Specifically it is a method to assess the environmental impact of a product during its lifecycle, from the extraction of raw materials to the production and distribution of energy through the use, reuse, recycling and final disposal. LCA is a tool for relative comparison and not for absolute evaluation, thereby it can be used as decision makers to compare all major environmental impacts in the choice of alternative courses of action [9]. LCA is carried out in four distinct phases as; Goal and scope, Life Cycle Inventory, Life Cycle Impact Assessment (LCIA) and Interpretation. The core phase of an LCA analysis is the Life Cycle Inventory compilation that regards the identification of all input and output flows concurring in the product lifecycle. This phase is both time and resource consuming and for this reason complete LCA can be carried out mainly to assess the environmental impact of an existing product, where manufacturing, use and dismantling can be estimated with accuracy [10].

Article 026-sd-108

Regionalization, in the context of LCA, is the recognition that industrial production characteristics and the environmental impact of environmental flows vary among site-generic, site-dependent, and site-specific assessments, where site-generic is globally valid, site-dependent operates on the regional scale, and site-specific is only locally applicable [11]. During the LCA modeling each subsystem of the life cycle is linked together into a chain of processes, in one end extracting resources and in the other giving various types of emissions or waste. This chain of linked processes is referred to as the technical system. In reality a technical system is under some sort of human control and designed for a certain purpose, to deliver a certain benefit or good, which in the LCA is expressed through the functional unit of the system. The processes are also located somewhere, which implies that they can be geographically referenced. Environmental impact caused by a technical system, or its LCA equivalent, the functional unit, is estimated in terms of the negative change implied by the technical system upon the environmental system, as evaluated by the social system. These systems may also be geographically referenced, which is an important starting point for a consideration of the relations between LCA and localized environmental impacts [12].

5- Geographical information systems

Geography seeks to understand the Earth with all of its human and natural complexities that puts understanding of social and physical processes within the context of places and regions, recognizing the great differences in cultures, political systems, economies, landscapes and environments across the world, and the links between them [13]. Progress within geography as spatial science and integrate it with technical advances leads to develop Geographical Information System (GIS), which integrates hardware, software, and data for capturing, managing, analyzing and displaying all forms of geographically referenced information. Globally, there are more than 2 million users of GIS and most companies are still unaware of how this technologies influences upon their daily activities [9]. A GIS is essentially a tool for decision-making and its powerful analytical and visualization capabilities provide the answers to important questions that must be answered in order to make sound and to inform for decisions. A GIS allows us to develop models, create scenarios and ultimately provide solutions for various environmental and socio-economic problems that exist [14].

Although GIS have been used for several years in the natural resources, forestry, and environmental industries, only recently have they begun to be used for a broader array of business and management functions such as logistics, site and facilities management, marketing, decision making and planning. GIS can help a retail business in locating the best site for its next store and helps marketers in finding new prospects [15].

6- Sustainable manufacturing and eco-innovation

Manufacturing industries are one of the significant sectors of resources consumption and waste generation, which are responsible for 36% of global CO2 emissions [42] that nevertheless have the potential to become a driving force for the creation of a sustainable society. They can design and implement integrated sustainable practices and develop products and services that contribute to better environmental performance, which requires a shift in the perception and understanding of industrial production and the adoption of a more holistic approach to conducting business [31]. More recently, industries are trying to disperse pollution in less harmful or less apparent ways by moving towards thinking in terms of lifecycle and integrated environmental strategies and management systems, which can potentially lead to significant environmental benefits. Creating closed-loop production systems which have specifically focuses on revitalizing disposed products into new resources for production. In this context eco-industrial parks is established, where economic and environmental synergies between traditionally unrelated industrial producers can be harnessed (Figure 3).

In response to growing global environmental concern, climate change, energy and raw material uses and other environmental issues, what is needed now is a new vision and policies that will enable the creation of business and job opportunities that go hand in hand with a reduction in negative environmental impacts. Today's short-term relief packages should help stimulate investments in environmental technologies and infrastructures that support innovative solutions and address long-term societal challenges, and thus help to realize such a vision. In this context, sustainable manufacturing and eco-innovation are very much at the heart of this century's policy and industry practices. These concepts have become popular with policy makers and business leaders in recent years, and they encourage business solutions and entrepreneurial ideas for tackling environmental challenges.

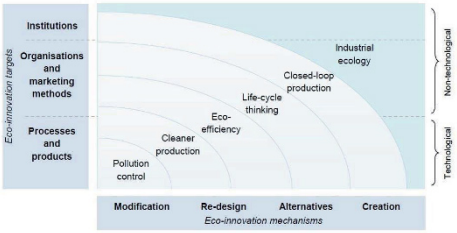

Figure.3: Conceptual relationship between sustainable manufacturing and eco innovation [29]

Many companies have started to use eco-innovation or similar terms to describe their contributions to sustainable development as a way to achieve more radical, systemic improvements in corporate environmental practices and performances. A few governments are also promoting the concept as a way to meet sustainable development targets while keeping industry and the economy competitive. However, while the promotion of eco-innovation by industry and government involves the pursuit of both economic and environmental sustainability, the scope and application of the concept tend to differ. The concept is promoted primarily

Article 026-sd-108

through the Environmental Technology Action Plan (ETAP), which defines eco-innovation as "the production, assimilation or exploitation of a novelty in products, production processes, services or in management and business methods, which aims, throughout its lifecycle, to prevent or substantially reduce environmental risk, pollution and other negative impacts of resource and energy use". There are two significant characteristics about eco-innovation; It reflects the concepts of explicit emphasis about reduction of environmental impacts and it is not limited to innovation in products, processes, marketing methods and organizational methods, but also includes innovation in social and institutional structures [32]. Charter and Clark believe that co-innovation can be understood and analyzed in terms of an innovation's in target, mechanism, and impact.

Innovation plays a key role for both industry and government to better understand and determine how to move towards a sustainable manufacturing. Evolving sustainable manufacturing initiatives from traditional pollution control through cleaner production initiatives, to a lifecycle view, to the establishment of closed-loop production – can be viewed as facilitated by eco-innovation.

While more integrated sustainable manufacturing initiatives such as closed-loop production can potentially yield higher environmental improvements in the medium to long term, they can only be realized through a combination of a wider range of innovation targets and mechanisms. For instance, an eco-industrial park cannot be successfully established simply by locating manufacturing plants in the same space in the absence of technologies or procedures for exchanging resources.

7- New IT framework for Sustainable Manufacturing

Models such as Manufacturing Requirement Planning (MRP), Enterprise Recourse Planning (ERP), Customer Relationship Management (CRM) and Manufacturing Execution System (MES) are adapted with manufacturing management, which separate the logical needs of manufacturing, material control, resource planning and scheduling from the locations aspects. While manufacturing activities clearly must happen at a specific location, MRP operates by cascading assemblies to their sub-assemblies to their component to the raw materials by assigning the demand to logical "buckets". There is no regard for location in any explicit sense although elements of lead time, up-time, or move time may include adjustments for location. [16]. Furthermore, there are some materials such as clear air, clear water that are necessary for manufacturing process which must be available at a given location at but don't appear in bill of materials. In parallel, increasing consumption in natural resources (energy and material) and environmental impacts emphasize on management of resources and pollutions. Therefore GIS-based environmental modeling, which is combined with manufacturing scenario, could be an opportunity for decision makers to reach sustainable manufacturing and as a noted by Kolli, which manufacturing could benefit from the application of GIS to a large class of logistics and operations management functions [28].

The fact that manufacture industries can start to use GIS within their PLM structure to reach sustainability is not surprising, particularly given the fact that much of the data that organizations typically use include significant spatial components (estimates range between 50% and 85%) [14]. Researchers and professionals have seen the potential of using GIS in the planning for a sustainable manufacturing; by mapping the same factor in different time spans and spatial areas an overview of changes is created and hence make it easier and more correct to predict future changes and make well founded planning decisions in urban areas [23]. By implementing GIS, "Territory" in macro level adds to the structure of PLM and makes it able to provide a proper catalog of the surroundings, including; environmental impact on natural ecosystems, transportation, community demographics, public safety, utilities, services and accessibility (Figure 4).

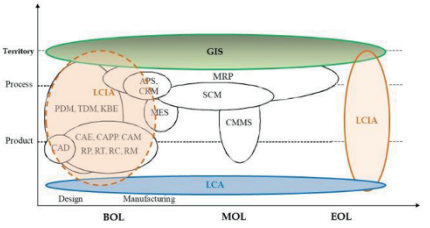

Figure 4: Improved ICT structure in product lifecycle

The nature of each geographical aspect is presented in the structure of LCA as the three subsections of technical, environmental and social systems, which make link between "production" and "process" scales with "territory" through the results of LCIA. A technical system generally includes processes which might be geographically referenced, and which are connected via different types of transport systems, such as goods (road, sea, air) or energy ware (pipelines, electricity grid) distribution systems. The geographic location and extension of such a technical system gives relevant information for the modeling and assessment of its environmental impact [24]. By giving the geographical location of the different parts of the technical system, it will be possible to model the dispersion of various agents, so that the varying sensitivity of ecosystems, regions, etc., can be taken into account where this is relevant. A geographically large technical system and the environmental impacts of such a system may cross national, regional and even continental boundaries, and therefore also affects different cultures or groups of people, holding different attitudes towards changes in the environment.

The amassing of these tangible elements of a community goes a long way toward informing the design process, and should always be considered to look at efficiency and sustainability". For instance, by using this new structure it would be possible to develop companies' energy consumption, water usage, CO2 emissions and wastes generation to build scenarios, assess them and make decision.

Article 026-sd-108

When it comes to model, it will able companies to locate points of water usage, transportation of water from its source to its consumption point, distance of water transportation, climate change, air pollutions, soil-map, location of landfill, customers distribution and other information related with lifecycle that can be useful in BOL to design product, process and plant (Figure 5). It will enable to enhance circular economy and industrial ecology.

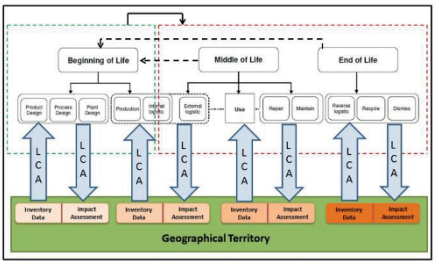

Figure 5: Interaction between Product lifecycle, GIS, LCA and LCIA

By using sustainability monitoring, it will be possible to analysis the result of this new PLM structure. Several solutions for the monitoring of sustainability of manufacturing processes have been developed but the one that is much more related with PLM, is proposed by Che B. Jounga, based on Categorization of indicators [25] by selecting specific indicators for different aspects of sustainability. Each indicator is a group of indicators that comprise a holistic view of sustainability. Combining indicators from the more common environmental, economic, and social dimensions and evaluating those indicators together is a practice to measure the sustainability on a much larger scale than individual indicators. Results from the measurement help companies create focus areas for improvement in regards to sustainability[25].

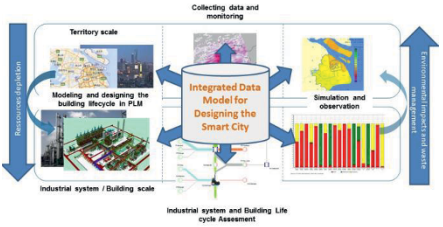

Figure 6: Integrated data model for designing the Smart City

The proposed IT framework can act as a platform to use in closed-loop manufacturing systems same as Eco-Industrial parks. This platform acts as a base to introduce a model (Figure 6), which will be very useful for industries that have high percentage of relation with geographical information. Modeling and designing of smart city is doing through two types of information which is collecting from territory, product lifecycle and presenting in new PLM structure. Then, the impacts of new design is assessing by LCA tool. New result of LCA is guidance for new design and improvement through system that will present as simulations in territorial scale. Biorefinery is one of the main industries, which is possible to implement this model.

8- Conclusion

There is no doubt that there is a lot of complexity in the sustainability concept. A possible reduction of this complexity is a proper management, planning and design actions. Therefore, it can be concluded that a holistic management of resources is presented in both consumption and production activities. The goal is to reach from a micro scale of design to macro scale to expand boundary beyond the factory wall to optimize the resources utilization. In macro level businesses measure the sustainability level of same industry or territory to make decision for their design stages and this means they don't think about themselves alone, but there exist a higher level entity who is managing the sustainability as a whole. Vertical integration of industries, cross industry mix and community involvement could be subjects for further studies, in order to bring them into PLM structure by using geographical information as driven cross industries.

In summary, the paper shows that GIS should be included in PLM framework to localize environmental, economic and social, related to specific locations when designing green manufacturing systems. It will lead to the definition of an integrated framework (integration of geographic and industrial data) in order to support decision making, especially in BOL. It will enable both:

- Industrial ecology principles to be applied in BOL reasoning;
- Environmental impact assessment with respect to the local context.

9- References

[1] E. Westkämper, F. Breu, S. Guggenbichler, and J. Wollmann, "Life cycle management and assessment: approaches and visions towards sustainable manufacturing (keynote paper)," CIRP Ann. Technol., vol. 49, no. 2, pp. 501–526, 2000.

[2] A. M. Deif, "A system model for green manufacturing," J. Clean. Prod., vol. 19, no. 14, pp. 1553–1559, Sep. 2011.

[3] a. D. Jayal, F. Badurdeen, O. W. Dillon, and I. S. Jawahir, "Sustainable manufacturing: Modeling and optimization challenges at the product, process and system levels," CIRP J. Manuf. Sci. Technol., vol. 2, no. 3, pp. 144–152, Jan. 2010.

[4] S. Kuik, S. Nagalingam, and Y. Amer, "A Framework of Product Recovery to Improve Sustainability in Manufacturing," vol. 2, no. 1, pp. 40–46, 2011.

[5] L. V. Barreto, H. C. Anderson, A. Anglin, and C. L. Tomovic, "Product lifecycle management in support of green manufacturing: addressing the challenges of global climate change," Int. J. Manuf. Technol. Manag., vol. 19, no. 3, pp. 294–305, 2010.

[6] S. Terzi, A. Bouras, D. Dutta, and M. Garetti, "Product lifecycle management–from its history to its new role," Int. J. Prod. Lifecycle Manag., vol. 4, no. 4, pp. 360–389, 2010.

[7] A. Silventoinen, H. Pels, H. Kärkkäinen, and H. Lampela, "Towards future PLM maturity assessment dimensions," 2011.

[8] a. Hart, R. Clift, S. Riddlestone, and J. Buntin, "Use of Life Cycle Assessment to Develop Industrial Ecologies—A Case Study," Process Saf. Environ. Prot., vol. 83, no. 4, pp. 359–363, Jul. 2005.

[9] G. Finnveden, M. Z. Hauschild, T. Ekvall, J. Guinée, R. Heijungs, S. Hellweg, A. Koehler, D. Pennington, and S. Suh, "Recent developments in Life Cycle Assessment.," J. Environ. Manage., vol. 91, no. 1, pp. 1–21, Oct. 2009.

[10] A. Morbidoni, C. Favi, F. Mandorli, M. Germani, O. Delle, and A. Of, "Environmental evaluation from cradle to grave with CAD-integrated LCA tools.," Acta Tech. Corvininesis-Bulletin Eng., vol. 5, no. 1, pp. 109–115, 2012.

[11] C. L. Mutel, S. Pfister, and S. Hellweg, "GIS-based regionalized life cycle assessment: how big is small enough? Methodology and case study of electricity generation.," Environ. Sci. Technol., vol. 46, no. 2, pp. 1096–103, Jan. 2012.

[12] M. Bengtsson, R. Carlson, S. Molander, and B. Steen, "An approach for handling geographical information in life cycle assessment using a relational database," J. Hazard. Mater., vol. 61, no. 1–3, pp. 67–75, Aug. 1998.

[13] R. Johnston, "Geography and GIS," Geogr. Inf. Syst. Princ. …, pp. 39–48, 1999.

[14] L. Azaz, "The use of Geographic Information Systems (GIS) in Business," Int. Conf. Humanit., pp. 299–303, 2011.

[15] J. Pick, Geographic information systems in business. IGI Global, 2004.

[16] L. D. Murphy, "GIS-based environmental modelling manufacturing and GIS : A proposal for integrating

[17] T. Dyllick and K. Hockerts, "Beyond the business case for corporate sustainability," Bus. Strateg. Environ., vol. 11, no. 2, pp. 130–141, 2002.

[18] C. B. Joung, J. Carrell, P. Sarkar, and S. C. Feng, "Categorization of indicators for sustainable manufacturing," Ecol. Indic., vol. 24, pp. 148–157, Jan. 2013.

[19] Joshi, K., Venkatachalam, A., Jawahir, I.S., 2006, A New Methodology for Transforming 3R Concept into 6R Concept for Improved Product Sustainability, in: Proceedings of the IV Global Conference on Sustainable Product Development and Life Cycle Engineering (Sa˜o Carlos, Brazil),

[20] Jawahir, I.S., Dillon Jr O.W.. 2007, Sustainable Manufacturing Processes: New Challenges for Developing Predictive Models and Optimization Techniques, in: Proceedings of the 1st International Conference on Sustainable Manufacturing (SM1) (Montreal, Canada),

[21] S. Byggeth and E. Hochschorner, Handling trade-offs in Ecodesign tools for sustainable product development and procurement, Journal of Cleaner Production, vol. 14, pp. 1420-1430, 2006.

[22] World Commission on Environment and Development's (the Brundtland Commission) report Our Common Future (Oxford: Oxford University Press, 1987).

[23] S. Terzi, A. Bouras, D. Dutta, and M. Garetti, "Product lifecycle management–from its history to its new role," Int. J. Prod. Lifecycle Management, vol. 4, pp. 360–389, 2010.

[24] D. Kiritsis, A. Bufardi, and P. Xirouchakis, "Research issues on product lifecycle management and information tracking using smart embedded systems," Adv. Eng. Informatics, vol. 17, no. 3–4, pp. 189–202, Jul. 2003.

[25] J. Niemann, S. Tichkiewitch, and E. Westkämper, Design of sustainable product life cycles. Springer, 2008.

[26] International Trade Administration. 2007, How Does Commerce Define Sustainable Manufacturing? U.S. Department of Commerce.

[27] Jaafar, I.H., Venkatachalam, A., Joshi, K., Ungureanu, A.C., De Silva, N., Dillon Jr O.W., Rouch, K.E., Jawahir, I.S., 2007, Product Design for Sustainability: A New Assessment Methodology and Case Studies, in Kutz M, (Ed.) Handbook of Environmentally Conscious Mechanical Design. John Wiley & Sons, pp. pp.25– 65.

[28] Kolli, S.S., Damodara, P.S., and Evans, G.W. (1993) Geographic Information System Based Decision Support Systems for Facility Location, Routing, and Scheduling. Computers and Industrial Engineering. 24 (1-4), pp. 369-372.

[29] OECD and Statistical Office of the European Communities (Eurostat) (2005), Oslo Manual: Guidelines for Collecting and Interpreting Innovation Data (3rd ed.), OECD, Paris.

[30] International Energy Agency (IEA) (2007), Tracking Industrial Energy Efficiency and CO2 Emissions, OECD/IEA, Paris.

[31] Maxwell, D., W. Sheate and R. van der Volst (2006), "Functional and systems aspects of the sustainable product and service development approach for industry", Journal of Cleaner Production, Vol. 14, No. 17, pp. 1466-1479.

[32] Rennings, K. (2000), "Redefining Innovation: Eco-innovation Research and the Contribution from Ecological Economics", Journal of Ecological Economics, Vol. 32, pp. 319-332.

[33] Gaurav, A., Rachuri, S., Fiorentini, X., Mani, M., Fenves, S., Lyons, K., Sriram, R., 2008. Extending the Notion of Quality from Physical Metrology to Information and Sustainability, NISTIR 7517. The National Institute of Standards and Technology, Gaithersburg, Maryland.

[34] Mihelcic, J., Crittenden, J., Small, M., Shonnard, D., Hokanson, D., Zhang, Q., Hui, C., Sorby, S., James, V., Sutherland, J., Schnoor, J., 2003. Sustainability science and engineering: the emergence of a new metadiscipline. Environ. Sci. Technol. 37, 5234–5314.

Article 025-sd-47

Design methodology for energy efficiency of production system

T.A.L. Nguyen [1], M. Museau [1], H. Paris [1]

(1) : Grenoble University, Sciences Laboratory for Design, Optimization and Production of Grenoble,
Phone/Fax : 04 76 50 82
E-mail : {thi-ai-lanh.nguyen, matthieu.museau, Henri.Paris} @grenoble-inp.fr

Abstract: Nowadays, it is important to reduce the energy consumption of production system because of the deficit of energy resource, the growing concern of the carbon emission and environment impact in industrial production. Therefore, to achieve the long term goal "sustainable manufacturing", energy efficiency has to be considered as the central priority in the design process of the production system. In this paper, the principal objective is to present the issues of the integration of "energy efficiency" in the design process and then to propose a design methodology to redesign the production system with a high "energy efficiency", while maintaining the initial manufacturing process. First of all, an analysis of existing production system is realized in order to identify the opportunities of saving energy in production system. From that, the strategies to reduce energy consumption of production system will be identified and proposed. Then, these scenarios of redesign will be tested to obtain the information of the best scenario of redesign.
Key words: Energy efficiency, production system, energy consumption, design for energy efficiency, methodology.

1- Introduction

Today, because of the growing concern of environmental impact in industrial production and because the limited energy resources and global energy demand continues to grow, the energy saving in an industrial site has became an important target to reduce the environmental footprint products. This allows us to meet the long-term goal of "sustainable development"- an approach that takes into account the ecology as an important pillar.
Until now, a lot of researches focus on different strategies to reduce energy consumption of production system. These studies focus on:
- Optimization of process parameter: In different studies [KL, DR], the author justifies that the more productivity capacity of production system is high, the more energy efficiency is better. As showed in figure 1, the relation between energy consumption of production system and the value of Material Removal Rate (MRR) of a milling operation:

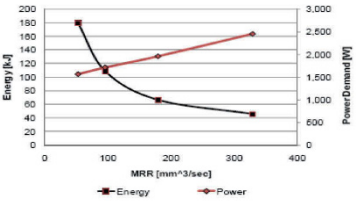

Figure1: Power demand and energy consumption of a milling operation [KL]

- Using innovative production technique [ST, VV]: In the research of B.Vayre et al [VV], a review and prospect of metallic additive manufacturing technologies is presented. But until now, the environmental impact of these manufacturing technologies is still a question unanswered.
In summary, there are a lot of researches focus on energy consumption optimisation of production system but little research concentrate on design for energy efficiency of production system that allow to reduce its energy consumption. So, it is important to propose a design methodology that takes into account "energy efficiency" at the earliest stage of process design to reduce energy consumption of production system.

2- The integration of "energy efficiency" in design process

Theories of design process is become one of the most focus of scientific work. Design for "X" (with "X" may be: manufacturing, assembly...) that allows to optimize a specific aspect of design (manufacturing, assembly...) became one of a good approach in engineering design. So, design for "energy efficiency" can be considered as a design approach that takes "energy efficiency" like one of the most important constraints of product at the earliest stage of product design process in order to optimize energy consumption of production system.

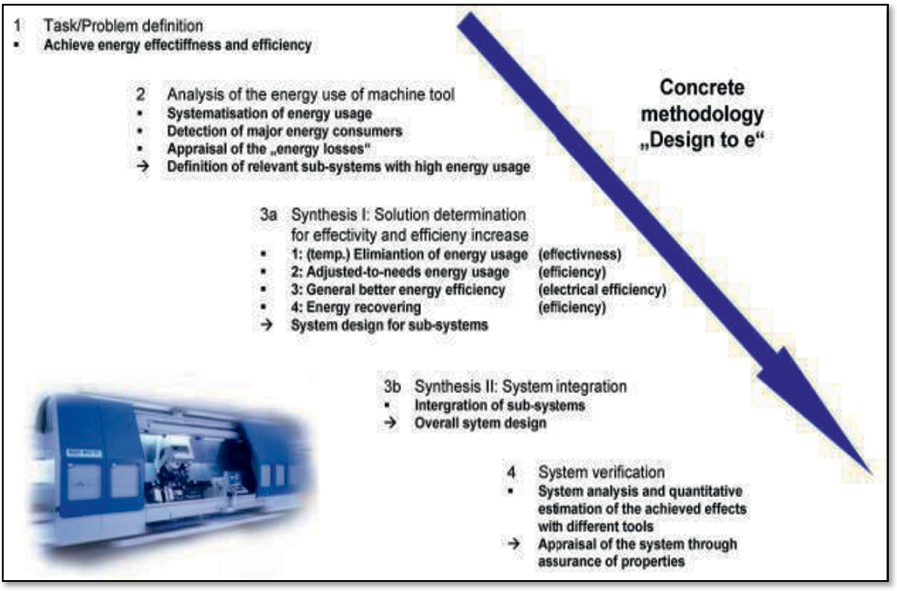

Figure 2: Methodology for energy efficiency [DR]

Until now, there is little research on the development of a design methodology that takes into account the energy impact of the resources and integrates energy efficiency as one of the essentials constraints in the design process proposed in the field of design theories and methodologies.

Neugebauer et al. [NF] proposed an approach for energy efficiency design of production system. This approach is based on the "property- driven design methodology" proposed by Weber [W] that defines the design process as a compromise between the requirements (eg: productivity, quality of final product ...) and the characteristics defined (eg: geometry, material ...) to achieve these proposed requirements. In this approach, a detailed knowledge about the energy consumption of each sub-system is necessary. This methodology for energy efficiency is illustrated in figure 2.

Zein et al. [ZL] present an axiomatic approach for the design process in order to optimize its "energy efficiency". The principle of this approach is based on the mapping of "functional requirement" and "design parameter". A functional requirement can be defined as a set of functional needs of a system. A related "design parameter" fulfils the functional requirement, hence leading to a structured design process. This connection can be mathematical described in form of a matrix.

In these researches, the key energy consumers (the major energy consumers) are considered like the "energy saving opportunities" of design for "energy efficiency" by measurement phase.

However, in the context of redesign of a production system, it is important at the first time to have a systematic approach that allows designer to identify the "energy saving opportunities". So, having an energy consumption assessment and identifying the potential energy savings of production system and their sub-systems are become one of the most important parts of our work.

3- Proposition of design methodology for energy efficiency

In this section, a proposition of methodology for design production system that takes into account energy efficiency as an essential requirement in the design process is proposed. This methodology is a composition of three main phases: analysis of energy flow, scenarios proposition for improvement of energy consumption and system validation phase.

First of all, an "analysis of energy flow" step is important to have knowledge of energy consumption and opportunities of saving energy in existing production system. After that, the "Scenarios of redesign for improvement of energy efficiency" to reduce energy consumption of production system will be proposed. Then, these scenarios of redesign will be tested to obtain the information of the best scenario of redesign.

We note that, this methodology is under development in our work. So, in this paper, we focus on the information of the first part –"analysis of the energy flow" of our methodology, the two others phases will be developed in the future.

3.1 – Analysis of the energy flow

As we know, manufacturing processes include a wide variety of operations from raw materials to products, generating wastes. Similarly, the inputs energy in these processes are also devised into "useful work"- energy used that is directly related to product and a portion of "wasteful work"- use of energy that do not add value to product (e.g. waste heat) as shown in the following figure :

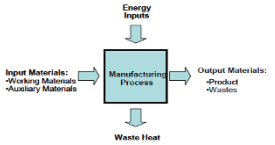

Figure 3: Energy and Material Inputs and Outputs for Manufacturing Processes [GD]

At the first time of our design methodology for energy efficiency of production system, the energy consumption of production system and their sub-system must be identified. These energy consumption knowledge could be determined by measurement (in case of redesign of an existing production system) or by forecasting energy tool (in case of design of a new production system). In case of using forecasting energy tool, the forecasting energy tool can be a generic model that composes various modules customized for a specific production system. This model allows us to get information about the energy consumption of production system and its various components.

In order to reduce energy consumption of production system, first of all, the potential energy saving of production system and their sub-systems must be identified. The potential energy gain will help designer determine the energy efficiency of each component (production system and their sub-systems) and thus identify the energy saving opportunities of production system. Therefore, at the first time of our work, we propose an indicator that will allow designer to determine the potential energy gain of each component. This indicator is calculated by using the theoretical value of energy needed to add value to final product in manufacturing process and its real value. It can be introduced by the following equation:

$$I = \frac{E_{Theory}}{E_{Expected}} \quad (1)$$

E_{theory}: This is the value of energy directly related to add value to product in manufacturing process. For the identification of this theoretical energy value, it is important to have information about the knowledge process of production system. So, information of knowledge process like: cutting force F_c, cutting speed V_c, cutting time... is important to calculate the theoretical energy value. For example, in case of a machine tool, this value is the energy value required just to: remove the material, ensure the good process operation of machine tool and change the cutting tool (in case there are cutting tool changes). It can be calculated by using material removal power ($F_c V_c + F_a V_a$ with F_a is feed force, V_a is feed rate), cutting time, tool change puissance (*e.g:* puissance necessary to release/clamp the cutting tool), tool change time...
As we noted at the first part of this paper, in our methodology, the initial manufacturing process is maintained during the context of redesign. Thus, the knowledge of manufacturing process allows the designer to have all the parameters to calculate the value of E_{theory} .

$E_{Expected}$: This is the real energy consumption of production system. This value can be measured on the production system or its sub-system in case of reconception of an existing production system or it can be simulated by using a forecasting energy tool in case of conception of a new production system.

The calculation and using of this indicator value is illustrated in the figure 4. In this figure, we noted that the production system is composed of different sub-system i. As we can see, at the first time of energy flow analysis phase of production system, by using the total value of the real energy consumption and the theoretical value of energy consumption that is calculated using the knowledge of the process, the "indicator" can be calculated. If the value of indicator is close to 1 (i.e. $E_{expected} \approx E_{theory}$), we can declare that our existing production system is efficient in term of energy consumption. If not, we conclude that our production system is not efficient, the designer must decompose the production system into various sub-systems and calculate the indicator for each sub-system to obtain its potential energy gain. In fact, the indicator value is between 0 and 1:

- The value of I is close to 1 ($E_{Expected} \approx E_{theory}$): in this case, we conclude that our sub-system is efficient.
- The value of I is not close to 1: In this case, we conclude that our sub-system is not efficient and there are two choices:
  - The value of E_{theory} is close to 0($E_{theory} \approx 0$): In this case, we can consider that this sub-system is not theoretically necessary to realize the manufacturing process of existing production system in term of adding energy to final product. So that, it is not necessary to decompose this sub-system into components to calculate their indicator value.
  - The value of $E_{Expected}$ is much greater than the value of E_{theory} : designer must decompose this sub-system into various components and calculate the indicator value for each component.

In order to illustrate the proposed design methodology, the design context of a machining centre, in term of energy efficiency, is presented as an example. This machining centre is used to produce a product with two different operations: roughing operation and finishing operation; there is a cutting tool change between these two operations. As we known, a machining centre is composed of various organs that can be devised into different energy consumption groups like: spindle sub-system, working table sub-system...

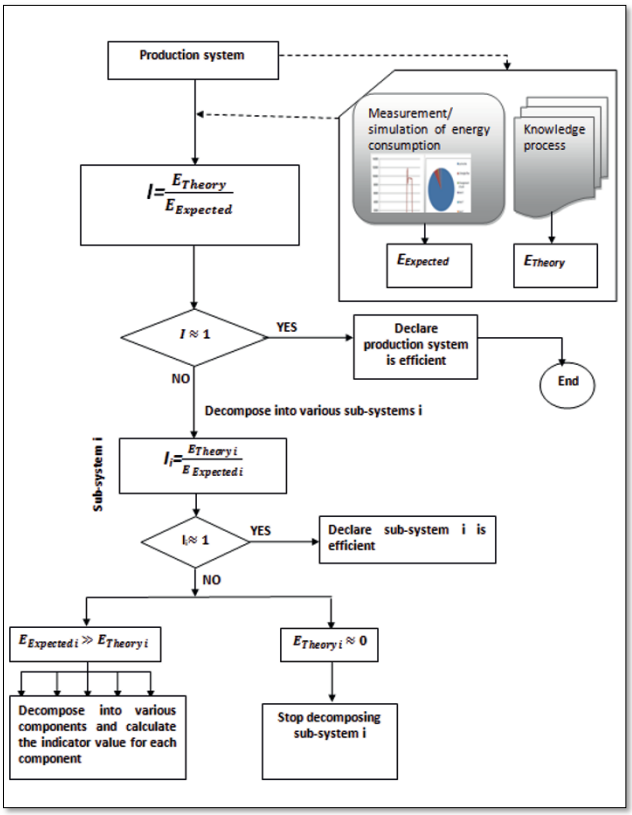

Figure 4: Energy flow analysis of production system

As illustrated in figure 4, the first step in our design process is to calculate the "indicator" of our existing machining centre by using the formula:

$$I_{\Pr oduction-system} = \frac{E_{Theory}}{E_{Expected}} \quad (2)$$

With:

- E_{theory} is the energy consumption value required to realize the transformation of machining process. It is the sum of energy value necessary for removing the material, ensuring the good process operation of machine tool and for changing tool.
- $E_{Expected}$ is the real value of the total energy consumption of the machining centre.

Obviously, the value of $I_{production\_system}$ must be much smaller than 1 because there are many actions that do not add value to final production like: the working table movement without cutting, the hydraulic unit sub-system is always active even if it is not necessary… From that we can conclude that our existing machining centre is not good in term of energy consumption. So, a system decomposition phase is necessary. Designer can calculate the "indicator" value for each sub-system to determine its potential energy saving. From this step, designer will propose various solutions for energy consumption reduction of existing machining centre. In these following paragraphs, we will apply this step for some sub-systems of machining centre like: spindle sub-system, refrigeration system and hydraulic system. Then, we propose some possible solutions for redesign, in order to reduce the energy consumption of the machining centre.

First of all, we use some assumptions like:

- In the existing machining centre used, the spindle sub-system is equipped by a refrigeration system to evacuate heat generated during the machining operation.
- The hydraulic system is needed just during each change of tools.

Now, we calculate the value of the "indicator" for some sub-systems of the machining centre:

- For the refrigeration sub-system:

$$I_{refrigeration} = \frac{E_{Theory}}{E_{Expected}} = 0 \quad (3)$$

In fact, in theory, the refrigeration sub-system is not related to add value to the final product (*e.g:* remove material). It means that this sub-system is not theoretically necessary so that E_{theory}=0. But in reality, because of the spindle technology used, the existing refrigeration system will contribute to the real energy consumption value of machining centre. Therefore, $I_{refrigeration}$ =0. From that, in an optimisation point of view, designer must think of an alternatives technology to overcome this sub-system. For example: choosing a spindle technology that can be used without refrigeration system, or optimizing refrigeration system in term of energy consumption.

- For the spindle sub-system, this value is calculated by using formula:

$$I_{spindle} = \frac{E_{Theory}}{E_{Expected}} = \frac{F_c.v_c.t_c}{E_{Expected}} \quad (4)$$

We observe that the real energy used by spindle directly adds value to the final product (it means that allow to remove material) and the cutting parameters are usually optimized so the value of $E_{Expected}$ is close to the value of E_{theory}. It derives that $I_{spindle}\approx 1$. So, we can conclude that, the spindle sub-system is good in term of energy consumption. Therefore, it is not necessary to optimize this sub-system to obtain an optimal production system in term of energy efficiency.

- For the hydraulic unit sub-system, the indicator value is calculated:

$$I_{hydraulic\_system} = \frac{E_{Theory}}{E_{Expected}} \quad (5)$$

With E_{theory} is the energy required to release/clamp the cutting tool in tool change phase. $E_{Expected}$ is the real energy measured, it composes energy consumed during all time when hydraulic system active.

We can observe that $I_{hydraulic\ system}$ can be much smaller than 1 (for example a tool change times/ 10 minute) because of the hydraulic sub-system that is always active even if it is not necessary. So that, in redesign context for energy efficiency, designer can propose various solutions that allow to reduce energy consumption of hydraulic system like: activate the hydraulic system just when it is necessary (just during the tool change) or accumulate energy in order to have enough energy for each change of tools...

3.2 Scenarios of redesign for "energy efficiency" of production system

By using the "indicator" in the energy assessment phase of the production system, the information of potential energy saving for each component of the production system can be identified. From that, designer can propose various scenario of redesign to reduce the total energy consumption of existing production system. In our work, this step is under development, but until now, there are different strategies that can be considered, for example:

- Technology solution optimization: Applying various best available technologies to reduce energy consumption of production sub-system. For example, in the case of machine tool, using the more efficient compressor can reduce energy consumption of refrigerant system...
- Operational solution for energy efficiency: Sometime a good control of each sub-system or between sub-systems of production system can reduce energy consumption of production system.
- Change of production system structure: At the early time of our work, we used this idea to reduce energy consumption by making a case study on a machining centre and the result from this case study shows that the "change of production system structure" can become one of the major propositions to reduce its energy consumption [NM].
- Energy recuperation: Reutilise secondary energy

At the end of our methodology, these scenarios of redesign must be tested and evaluated by taking into account different design constraints in design process (for example: economical aspect) in order to identify the best scenario of redesign for production system.

4- Conclusions:

In this paper, the problem of integration of energy efficiency constraint in design process is presented. Moreover, an indicator used in the energy analysis phase to determine the potential energy gain of each energy consumer is also presented in order to determine the energy saving opportunities of existing production system. It is one of the important phases of our redesign methodology for energy efficiency. In the future, we will provide information about the two other phases of our redesign methodology.

Acknowledgements: The authors would like to thank to Region Rhône Alpes for its support in this project.

5- References

[DR] Diaz N., Redelsheimer E., Dornfeld D. Energy Consumption Characterization and Reduction Strategies for Milling Machine Tool Use, Glocalized Solutions for Sustainability in Manufacturing, 2011, pp 263–267

[GD] Gutowski T., Dahmus J., Thiriez A. .Electrical Energy Requirements for Manufacturing Processes. 13th CIRP International Conference on Life Cycle Engineering, 2006

[KL] Kara S., Li W., Unit process energy consumption models for material removal processes, CIRP Annals - Manufacturing Technology, 60(1), 2011, pp 37–40

[NF] Neugebauer R., Frieß U., Paetzold J., Wabner M., Richter M., Approach for the development of energy

efficiency machine tools. Conference on Supervising and Diagnostics of Machining Systems, 2010

[NM] Nguyen T.A.L., Museau M., Paris H. Méthodologie de (re)conception de l'outil de production pour minimiser sa consommation d'énergie, 21eme Congrès Français de Mécanique, 2013

[ST] Serres N., Tid D., Sankare S., Hlawka F. : Environmental comparison of MESO-CLAD_ process and conventional machining implementing life cycle assessment, Journal of Cleaner Production 19 (2011) , pp 1117- 1124

[VV] Vayre B., Vignat F., Villeneuve F. Metallic additive manufacturing: state-of-the art review and prospects, Mechanics & Industry Mechanics & Industry, 2012, pp 89–96

[W] Weber C, Locking at "DFX" and "Product Maturity" from the Prospective of a new Approach to Modeling Product and Product Development Processes. The Future of Product Development. Vol. 3, 2007, pp. 85-104

[ZL] Zein A., Li W., Herrmann C., Kara. S., Energy Efficiency Measures for the Design and Operation of Machine Tools: An Axiomatic Approach. Glocalized Solutions for Sustainability in Manufacturing, 2011 pp.274-279

7

Manufacturing Process

Major topics of the full argumentations are the following:

X. Fischer et al. (eds.), *Research in Interactive Design (Vol. 4)*
DOI 10.1007/978-3-319-26121-8_17

Article 039-pp-9

Profile incision modeling in Abrasive Waterjet Milling of Titanium alloys Ti6Al4V

Tarek SULTAN[1], Patrick GILLES[2], Guillaume COHEN[3], François CENAC[4], Walter RUBIO[5]

(1) (2) : Institut Clément Ader/INSA Toulouse 135 Avenue de Rangueil 31077 TOULOUSE CEDEX 4
Tél : 05 61 55 95 13 - Fax : 05 61 55 95 00
E-mail : {tarek.sultan,patrick.gilles}@insa-toulouse.fr

(3) (5) : Institut Clément Ader/Université Toulouse III - Paul Sabatier - 118 route de Narbonne 31062 TOULOUSE CEDEX 9
E-mail : {guillaume.cohen,walter.rubio}@univ-tlse3.fr

(4) : JEDO Technologies, Rue du Chêne Vert - BP 78204 - 31682 Labège
E-mail : {fcenac}@jedotechnologies.net

Abstract: Abrasive water jet milling (AWJM) is a new way to perform controlled depth milling especially for hard materials, but it's not yet enough reliable because of large variety of process parameters and complex footprint geometries that are not well mastered. In order to master the milling device in AWJM, a deep study on the footprint of a single path of the cutting head should first be considered. The flow of the AWJ and the distribution of abrasive particles coming out of the jet are related to the profile measured on the footprint. In this study, experiments were made on titanium alloys specimen to compare several theoretical models to the measured profile of the footprint. This study establishes new models to fit the incision profile taking in consideration the behavior of the abrasive particles impacting the workpiece.

Key words: Abrasive waterjet milling, incision, titanium alloy, process parameters, Gaussian model.

Nomenclature:

a	maximum depth parameter (mm)
b	width parameter (mm)
b0.5	width at half of maximum depth (mm)
b1	width parameter of first Gaussian part (mm)
b2	width parameter of second Gaussian part (mm)
Da	abrasive flow rate (L/min)
Dc	focusing tube diameter (mm)
f	traverse speed (mm/min)
h	incision's depth (mm)
K	width parameter of Pearson equation (mm)
M	width parameter of Pearson equation (mm)
P	pressure (bar)
SOD	standoff distance (mm)
SSE	sum square error (mm^2)

1- Introduction

Abrasive water jet (AWJ) acquired a great technological progress in the last decades. Its popularity has changed considerably thanks to its high pressure joined to the flow of abrasive particles allowing the cut of any type of material. AWJ is a non-conventional machining process in which a mixture of abrasive particles and water at very high pressure is converted into a high velocity jet to cut various materials that can range from brittle to ductile materials. The water jet cutting is considered as a very efficient manufacturing process involving small amounts of heat transferred to the workpiece. Thereby, metal parts made by AWJ process does not change the crystal structure usually caused by the heat generated with other methods of material removal such as laser cutting, EDM (Electrical Discharge Machining), milling machining... The AWJ has become an emerging technology with versatile features.

Controlled depth milling appeared in the early 1990s and is intended for the production of pockets. Until now this process has not yet been mastered, especially for hard materials. In order to comprehend the milling of pockets in AWJ, milling incisions (representing a single path of the cutting head on the workpiece) should firstly be studied. Several works were established to investigate this technology, F. CENAC studied controlled depth milling on Composites and aluminum alloys [C1] [CC1], and G. FLOWER worked on Titanium alloys [Fo1]. In their studies masks were used to avoid irregularities in the bottom of the milled pocket. In the case of maskless pocket milling in AWJ, a precise study on the impinging water jet is required to understand the mechanisms of abrasive and water flow machining and their impact on the workpiece.

Article 039-pp-9

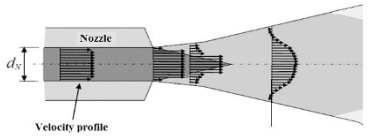

Figure 1: Water particles velocity profile according to F. Cenac [C1]**.**

F. CENAC showed in his studies [C1] that the velocity profile of water particles going out of the cutting head (Fig. 1) brings to mind a Gaussian profile as described in the literature [SA2]. D. S. Srinivasu and D. Axinte [SA1] also associated the bell's profile obtained on the material to be milled after one path of the jet to the fluid behavior of water particles outgoing the cutting head (Fig. 2). It is to be noted that the Gaussian shape is found on any kind of material.

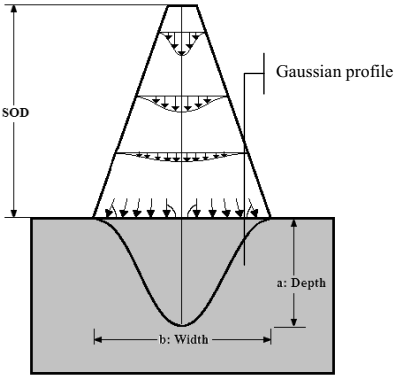

Figure 2: Velocity jet profile according to D. S. Srinivasu [SA1]**.**

This assumption is not justified in all cases since the fluidic behavior of these particles can differ by varying the parameters of the machine. N. ZUCKERMAN and N. LIOR analyzed the behavior of the jet at high velocity [ZL1] (Fig. 3). They showed that the abrasive particles coming out through the jet and gaining kinetic energy due to waterjet won't have a regular influence on the workpiece. Initially, with high pressure, the material to be milled is ploughed by the fine abrasives outgoing along the jet axis which come in contact with the workpiece as the rub over of the surface [KA1][KA2][W1]. It is to be noted that there is another mechanism of abrasive flow during AWJ milling. In addition of ploughing mechanism, some particles on the sideways of the water flow erode the surface of the workpiece with micro cutting action [Fi1][ZH1][MK1]. Thus, during this mechanism, the abrasive particles physically remove the material by eroding the surface producing micro incisions. This mechanism is seen in the material removal processes such as grinding.

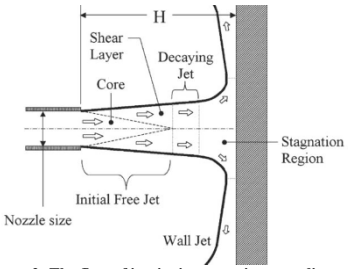

Figure 3: The flow of impinging waterjet according to N. Zuckerman and N. Lior [ZL1]**.**

1.1 – Incision profile analysis

While milling an incision in AWJ, abrasive particles in the lateral direction of the jet tend to erode the surface. The aim of this work is to analyze the shape of the kerf resulting from a single straight passage of the cutting head performing what is called an incision in AWJM. Any technological machining method used for the generation of surfaces leaves some technical irregularities which have fundamental influence on functional surfaces. In fact, the first step is to understand the shape of incisions before being concerned about milling pockets in AWJ. Therefore, a study of the correlation between the experimental incisions milled by AWJ machining and a consistent theoretical model is required. The theoretical models are based on mathematical equations defining the profile generated by a single path of the jet on the material (Fig. 4) here titanium alloys Ti6AlV is expressed.

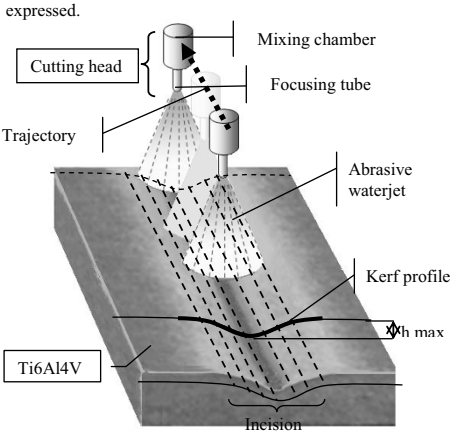

Figure 4: Single path of the cutting head creating an incision on titanium alloys workpiece.

Once the theoretical model is built, it can be used to predict the corresponding surface geometry each time the operating conditions are known. Following a study on ceramics in 2009, Srinivasu [SA1] shows experimentally the

influence of the angle of the cutting head on the depth and the width of the incision. He presented an analysis of the geometry of an incision by taking into account the kinematic parameters (impact angle and the feed rate of the jet) in AWJ machining of SiC ceramics, and added that the velocity of water and abrasive particles were assumed to follow the shape of Gaussian distribution.

Once the geometrical modeling is found, a prediction of the jet footprint can be made even in the case of changing process parameters. D. Axinte [AA1] used a finite element model also based on Gaussian model explaining that abrasive particles follow a Gaussian distribution. In the same way, Alberdi [AR1][CA1][AR2] associated the kerf profile obtained after a rectilinear passage of the jet on the workpiece, to a Gaussian shape. These studies showed that the energy distribution of the jet follows a Gaussian distribution due to the good implementation of the Gaussian bell with incision's form found using experimental tests. In addition the Gaussian distribution results from the random distribution of abrasive particles during mixing with water particles and air. According to his study, the other advantage of using the Gaussian function (Eq. 1) is to describe the profile of an incision with only two coefficients to be modeled using at first the maximum cutting depth factor and secondly the width factor:

$$h = hmax * e^{\frac{-b^2}{2c^2}} \text{ where } c = \frac{b0.5}{2*\sqrt{(2)*(ln2)}} \quad (1)$$

In this expression, *hmax* is the incision's maximum depth and $b_{0.5}$ is the width at half of the maximum depth.

On the other hand, F. Cénac [C1] presented an erosion model separating micro-cutting (abrasion mechanism) and fragile fracture (ploughing mechanism) based on a calculation of the kinetic energy of the abrasive particles made by I. Finnie [Fi1] and affecting the workpiece. Erosion models for predicting depth of cut in AWJ require determining the velocity of the particles that involves measures in order to be calculated. The methods used to determine these velocities are difficult to implement and require a significant numerical processing. Thus, F. Cénac expressed the depth of the incision as a function of the pressure *P*, the traverse speed *f*, the flow of abrasive *Da*, the standoff distance *SOD* and the diameter of the focusing tube *Dc*. Cenac's model (Eq. 2) is based only on the depth and do not consider the width of the incision.

$$h = A0 * P^{A1} * Da^{A2} * f^{A3} * Dc^{A4} * SOD^{A5} \quad (2)$$

1.2 – Abrasive water jet phenomenology

The present work, besides modeling the kerf profile of incisions, studies the physical phenomena when milling incisions in three-axis AWJM. It also focuses on the analysis of the phenomenology of the abrasive water jet flow and its precise influence on the result found on the workpiece. Several works explained the waterjet flowing and the dragging of abrasive particles in the jet [Co1] [F1]. Furthermore M. Zaki explained [Z1] that abrasive particles are accumulated on the borders of the mixing chamber (Fig. 4) while inflowing the focusing tube. He also showed that particles amassed in the conical area at the entrance of the focusing tube have a very low velocity while in the heart of the jet the velocity is very high and with very few abrasive particles (Fig. 5).

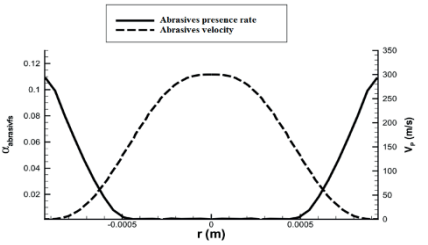

Figure 5: Distribution of abrasive particles in the jet [Z1].

Kulekci [K1] showed the path of abrasive particles flowing on the side of the focusing tube. Each particle enters the jet with a very low velocity. It is then accelerated by the jet on its way into the focusing tube. By hitting the tube sides this particle reaches a parallel trajectory to the jet axis.

2- Modelling analysis of incision's profile

The most used equation in AWJM [1,5,16] to fit incision profile is the Gaussian model Eq. 3:

$$z(x) = ae^{-\left(\frac{x-x0}{b}\right)^2} \quad (3)$$

Where: a = amplitude (maximum depth), x_0 = adjusting stance on x axis and b = width parameters.

The Gaussian model (Eq. 3) and experimental incision profile are shown in Figure 6. A good correlation is seen in the higher part of the profile unlike the lower part where the Gaussian model does not well correlate with the experimental profile.

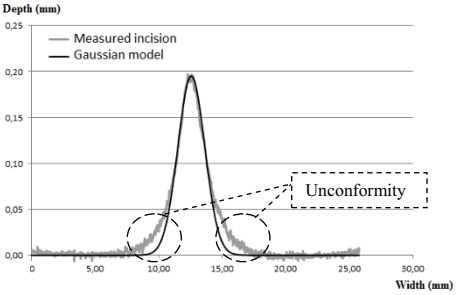

Figure 6: Incision profile fitted with Gaussian model.

Some incisions, especially when machining with high SOD, showed some unconformity between Gaussian curves and experimental incision form particularly in the border zone of the kerf profile (Fig. 6). This observation leads to a deep study on the phenomenology of the jet and on the theoretical models in order to find the most suitable model for incision's profile obtained in AWJM of Ti6AlV.

Figure 6 shows that Gaussian model is not taking into account a distribution taking place especially in the border zone of the kerf profile. This remark leads to a belief

that there are two main zones in the abrasive waterjet not flowing similarly [Co1]. Zone "A" is the central zone of the jet where the least quantity of abrasive particles is going at very high velocity (Fig. 7). And secondly the zone "B" where the biggest amount of abrasive particles is going at low velocity [Z1]. This theory leads to a deduction that each zone is having its proper Gaussian distribution.

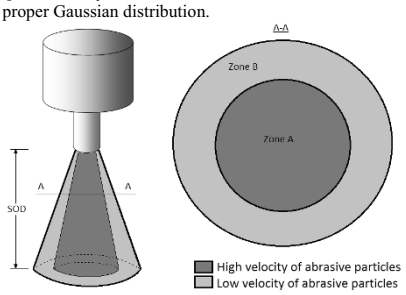

Figure 7: Characterization of abrasive velocity in the jet.

The larger SOD is, the bigger the zone B will become comparing to the zone A. Therefore incision's profile obtained in that case will diverge from the normal Gaussian distribution and it will be more consistent to be represented by an extended Gaussian model. This means that a first normal Gaussian distribution characterizes the distribution of the first zone and a second Gaussian model characterizes the second one. This leads to a sum of the two Gaussian models that represents the entire distribution taking place in the abrasive water jet. Moreover, the smaller SOD is, the minor the zone B will become. Thereby the distribution of abrasive particles will tend to a Gaussian model. So the second Gaussian model representing the zone B will be negligible comparing to the entire jet and won't have a significant influence on the profile obtained on the workpiece. For small SODs the model fitting the measured profile of incision emerges to a normal Gaussian profile which joins the hypothesis of the consistence of the Gauss distribution found in literature [ZL1][AR1][AS1].

To improve Gaussian modeling, other mathematical functions exist to correlate with the bell's shape. Thereby, many were interesting to scoop out Fig. (9):

- Lorentz model:

The Lorentz distribution is often used in statistics and has a bell's shape. By adding the depth parameter « a » and the parameter « x0 » adjusting the stance on the x axis, the Lorentz equation becomes Eq. 4:

$$z(x) = a * \frac{b^2}{2} * \frac{1}{\frac{1}{2} * b^2 + (x - x0)^2} \quad (4)$$

- a = amplitude (maximum depth)
- x_0 = adjusting stance on x axis
- b = width parameter

- Pearson model :

The Pearson model is usually used for peak detection in X-ray diffraction measurement. A simplified Pearson equation is:

$$z(x) = a * \left(1 + \frac{K^2}{M} * (x - x0)^2\right)^{-M} \quad (5)$$

Where a is the maximum depth, K and M are parameters that define width.

- Gauss decomposed (GD) model:

Gaussian distribution characterizes the best random distribution of particles in the jet, and is the finest model representing the physics of abrasive water jet. For this reason it was selected and improved using two parts corresponding to the two different distributions subsisting in the same jet (Fig. 8). Assuming that two similar phenomena exist but not flowing identically in the jet, the corresponding model to fit incision's form will be written as follows:

$$z(x) = \frac{a}{2} * e^{-\left(\frac{x - x0}{b1}\right)^2} + \frac{a}{2} * e^{-\left(\frac{x - x0}{b2}\right)^2} \quad (6)$$

- a = amplitude (maximum depth)
- x_0= adjusting stance on x axis
- $b1$ and $b2$ = width parameters relative to each distribution

The amplitude coefficients multiplying Gaussian parts in this model were a_1 and a_2 respectively. Nevertheless several testing were used to define the most appropriate amplitude coefficient multiplying each Gaussian part of the GD model. The difference, using the comparison with the minimum SSE (Sum Square Error), between amplitude coefficients was negligible. And the most suitable amplitude coefficient fitting the measured profiles in all trials of incisions was a_1=a_2=Z_{max}/2 which explains the use of a/2 in the GD equation.

All models presented before are computed in figure 8.

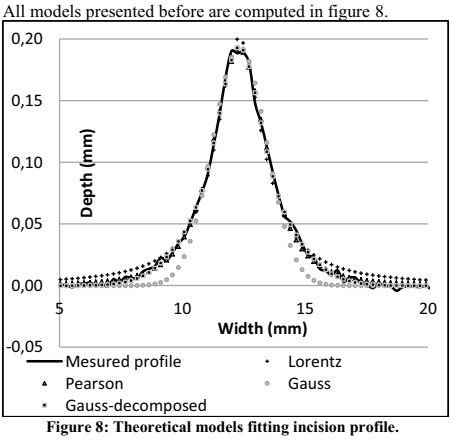

Figure 8: Theoretical models fitting incision profile.

Least square method for nonlinear equations:

The goal is to find the parameters value for the model which "best" fits the measured profile. It is used in this paper for the four nonlinear equations (3), (4), (5) and (6).

A residual is defined as the difference between the actual value of the dependent variable and the value predicted by the model (Fig. 9):

$$ri = z_{measured} - z_{model} \quad (7)$$

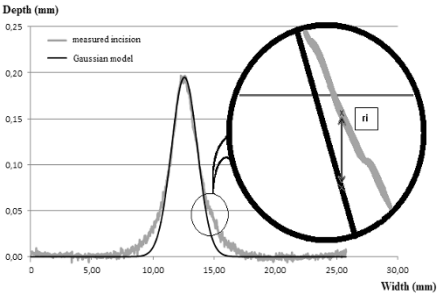

Figure 9: Difference between measured value and theoretical value = ri.

The least square method is an iterative method which finds its optimum when the sum square error (SSE) is minimal.

$$S = \sum_{i=1}^{n} ri^2 \quad (8)$$

	Gauss	Lorentz	Pearson	Gauss Decomposed
SSE (mm²)	0.3	0.16	0.06	0.04

Table 1: Sum Square Error (SSE) between measured and theoretical profiles for arbitrary incision.

3- Experimental procedure

To be sure that GD model has the best consistence with the measured incision profile; an extensive set of trials took place on a Flow Mach 3 AWJ machine. The experience presented in this sheet includes 27 incisions made on titanium alloys specimens with a constant pressure (1000 bars), abrasive flow rate (2L/min) involving various ranges of process parameters:
Traverse speed f (mm/min) (66 - 2182)
Standoff distance s (mm) (30; 80; 140)
Once incisions were made on titanium samples, several measures were done on Alicona optical 3D profilometer for high resolution measurement (Fig. 10).

Figure 10: Measuring tool: Alicona 3D optical profilometer for high resolution measurement.

Each measurement is an acquisition on a surface of 16 mm*2 mm (Fig. 11).

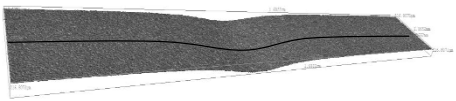

Figure 11: Acquisition of the measured surface

Then a line is drawn on the measured surface giving the coordinates of 6000 points which is accurately enough to draw the measured incision's profile (Fig. 12).

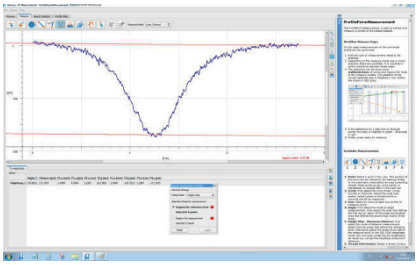

Figure 12: The result of incision profile measured on Alicona

The four theoretical models were applied to fit on each incision. The least square method for nonlinear equations was used and a comparison of the minimum of SSE was set.

Operating parameters		SSE (mm²)				
SOD (mm)	*Traverse speed (mm/min)*	Gauss	Lorentz	Pearson (P)	Gauss Decomposed (GD)	Best model
30	263	0,067	0,504	0,045	0,043	GD
30	383	0,059	0,328	0,028	0,027	GD
30	406	0,048	0,284	0,048	0,048	P
30	581	0,055	0,081	0,055	0,034	GD
30	724	0,032	0,100	0,029	0,029	P
30	811	0,019	0,096	0,019	0,019	P
30	1085	0,016	0,049	0,015	0,016	P
30	1162	0,019	0,034	0,016	0,015	GD
30	2182	0,015	0,022	0,015	0,014	GD
80	110	0,351	1,337	0,190	0,187	GD
80	164	0,196	0,361	0,038	0,027	GD
80	175	0,111	0,352	0,093	0,095	P
80	252	0,358	0,214	0,062	0,064	P
80	307	0,065	0,155	0,037	0,037	GD
80	351	0,052	0,125	0,042	0,04	GD
80	460	0,100	0,210	0,088	0,085	GD
80	504	0,039	0,062	0,023	0,02	GD
80	932	0,025	0,055	0,025	0,024	GD
140	66	0,952	0,416	0,410	0,338	GD
140	98	0,244	0,389	0,128	0,12	GD
140	104	0,317	0,350	0,051	0,037	GD
140	153	0,137	0,210	0,045	0,03	GD
140	186	0,141	0,146	0,064	0,06	GD
140	209	0,068	0,096	0,068	0,058	GD
140	285	0,056	0,093	0,041	0,041	GD
140	307	0,061	0,065	0,032	0,031	GD
140	581	0,036	0,059	0,036	0,035	GD

Table 2: Milling process parameters and models comparison.

4- Results and discussions

In order to study the best model fitting the incision profile, models presented earlier were used and compared. The results show that 21 incisions were best fitted with Gauss decomposed (GD) model, 6 incisions with Pearson model and none with Gaussian or Lorentz model using SSE minimum as a comparison criteria. For 6 incisions, Pearson outweighs the GD model. The difference, between SSE values for Pearson and Gauss decomposed model, is insignificant (around 10^{-3} mm). Thereby GD model shows the best correlation with the measured profiles for any value of SOD and traverse speed which makes it a new accurate model to fit kerf shapes in AWJM.

These outcomes are in harmony with the theory raised in the §2 according to M. Zaki [Z1]. The profile obtained by a single jet path in AWJ machine is not only a Gaussian profile but a sum of two Gaussian profiles which are the two parts of the Gauss decomposed model corresponding to the two physical phenomena occurring in AWJ:

- The first part is the central one where are the highest velocity and the lowest quantity of abrasive particles.
- The second sub-jet is the lateral one where are the biggest amount of abrasive particles and the lowest velocity of the jet.

These results give clear evidence that the Gauss decomposed model is the most suitable theoretical model in AWJM.

The proposed model integrates three variables (*a* for the depth, *b1* and *b2* for the width) instead of two parameters for the Gaussian model (*a* for the depth and *b* for the width). The coefficient *b* representing the width of the Gaussian model is the mean of the two coefficients *b1* and *b2*. Figure 10 shows calculated width values *b*, *b1* and *b2* for the 27 incisions made on titanium alloys.

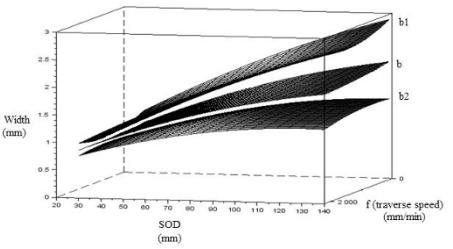

Figure 13: Relation between width parameter for Gaussian and Gauss decomposed models.

4.1 – Comments on figure 13:

- When SOD is small, calculated values *b1* and *b2* tend to the calculated value *b*. This means that the Gauss decomposed model converges to a simple Gaussian model.
- Traverse speed seems to have a negligible effect on incision's width unlike SOD which has a remarkable influence.

5- Conclusion and further work

This paper presents a study based on theoretical models fitting the footprint done by a single path of the jet on titanium workpiece. On the first hand, most of works describe this footprint resulting of a single toolpath in AWJ as a Gaussian profile. On the other hand, some works show that abrasive particles are accumulated on the borders of the mixing chamber. Consequently incisions obtained while milling in AWJ can't be fitted with a simple Gaussian model. This hypothesis drives the analytical study on theoretical models to search other formulas of bell shapes. The theoretical study used in this sheet gives clear evidence that the Gaussian profile is not the most suitable theoretical model in AWJ milling. Results show that the Gauss decomposed model is the most efficient when using a big interval of traverse speed and SOD. This new model takes into account the particularity of the jet. In small SOD the second part of the Gauss decomposed model characterizing the zone of low velocity will be negligible and the final Gauss decomposed model will tend to a normal Gaussian model. And in the other hand, with big SOD the second part will have a greater effect and the model fitting the footprint of incision is the two Gaussian models characterizing the two zones of the jet.

Once the most accurate theoretical model for incisions is found, the predictive equation of depth and width of cut for titanium alloys can be set. Further studies will include this predictive equation to define predictive models for incisions and pockets in abrasive waterjet milling of titanium alloys.

6- References

[AR1] Alberdi A., Rivero A., López de Lacalle, L.N., Etxeberria I., and Suárez A. Effect of process parameter on the kerf geometry in abrasive water jet milling. *The International Journal of Advanced Manufacturing Technology 51*, 5-8, 467-480, 2010.

[AR2] Alberdi A., Rivero A., and López de Lacalle, L.N. Experimental study of the slot overlapping and tool path variation effect in Abrasive Waterjet Milling. *Journal of Manufacturing Science and Engineering 133*, 3, 2011.

[AA1] Anwar S., Axinte D., and Becker A. A finite element modelling of overlapping abrasive waterjet milled footprints. *Wear*, 2013.

[AS1] Axinte D., Srinivasu D.S., Billingham J., and Cooper M. Geometrical modelling of abrasive waterjet footprints: A study for 90° jet impact angle. *CIRP Annals - Manufacturing Technology 59*, 1, 341-346, 2010.

[CA1] Carrascal A., Alberdi A., Fatronik-tecnalia F., Mikeletegi P., and Tecnológico P. Evolutionary Industrial Physical Model Generation. Fundación Fatronik-Tecnalia, Paseo Mikeletegi 7, Parque Tecnológico, 327-334, 2010.

[C1] CENAC F. Etude de l'usinage non débouchant par jet d'eau abrasif des composites. Thèse de doctorat, Université Paul Sabatier, 2011.

[Co1] CORNIER A. Developement d'un modèle d'enlèvement de matière par granulation utilisant le jet d'eau haute pression : application au démentelement de pneumatiques. Thèse de doctorat, Ecole Nationale Supérieure des Arts et Métiers, 2004.

[CC1] Crouzeix L., Collombet F., and Grunevald Y. Comportement d' une réparation en escalier obtenue par Jet d'Eau Abrasif Step repaired coupons involving Abrasive Water Jet machining. Comptes Rendus des JNC 17 - Poitiers, 2011

[F1] FERRENDIER, S. Influence de l'Evolution Granulométrique des Abrasifs sur l'Enlèvement de Matière lors de la découpe par JEA. Thèse de doctorat, Ecole Nationale Supérieure des Arts et Métiers, 2001.

[Fi1] FINNIE, I. Erosion of surface by solid particles. *Shell Development Company*, 1960.

[Fo1] Fowler, G. Abrasive Water-jet - Controlled Depth Milling Titanium Alloys, Thèse de doctorat, University of Nottingham, 2003.

[KA1] Kong M.C., Axinte D., and Voice W. Aspects of material removal mechanism in plain waterjet milling on gamma titanium aluminide. *Journal of Materials Processing Technology 210*(3): 573-584, 2010.

[KA2] Kong M.C., Axinte D., and Voice W. Challenges in using waterjet machining of NiTi shape memory alloys: An analysis of controlled-depth milling. *Journal of Materials Processing* Technology 211(6): 959-971, 2011.

[K1] Kulekci M.K. Processes and apparatus developments in industrial waterjet applications. International Journal of Machine Tools & Manufacture *42*: 1297–1306, 2002.

[MK1] Maniadaki K., Kestis T., Bilalis N., and Antoniadis A. A finite element-based model for pure waterjet process simulation. *The International Journal of Advanced Manufacturing Technology 31*, 9-10: 933–940, 2006.

[SA1] Srinivasu D.S., Axinte D. a., Shipway P.H. and Folkes J. Influence of kinematic operating parameters on kerf geometry in abrasive waterjet machining of silicon carbide ceramics. *International Journal of Machine Tools and Manufacture 49*, 14, 1077–1088, 2009.

[SA2] Srinivasu D.S. and Axinte D. An analytical model for top width of jet footprint in abrasive waterjet milling : a case study on SiC ceramics. Proceedings of the Institution of Mechanical Engineers 2011. Journal of Engineering Manufacture, 2011.

[W1] Wang J. Abrasive Waterjet Machining of Polymer Matrix Composites - Cutting Performance, Erosive Process and Predictive Models. *The International Journal of Advanced Manufacturing Technology 15*, 10, 757–768, 1999.

[Z1] Zaki M. Modélisation et simulation numérique du procédé de perçage non débouchant par jet d'eau abrasif. Thèse de doctorat, Ecole Nationale Supérieure des Arts et Métiers, 2009.

[ZH1] Zhu H.T., Huang C.Z., Wang J., Li Q.L., and Che C.L. Experimental study on abrasive waterjet polishing for hard–brittle materials. *International Journal of Machine Tools and Manufacture 49*, 7-8, 569–578, 2009.

[ZL1] Zuckerman N. and Lior N. Jet Impingement Heat Transfer : Physics , Correlations , and Numerical Modeling. Advances in heat transfer *39*, 06, 565–631, 2006.

Article 041-pp-60

Evolution of chip morphology during high strength stainless steel turning

V. Wagner [1], G. Dessein [1], J.Y. Gendron [2]

(1) : Laboratoire Génie de Production
Ecole Nationale d'Ingénieurs de Tarbes
47 Avenue d'Azereix - BP 1629
65016 Tarbes Cedex, France
Phone/Fax : 0562442700
E-mail : vincent.wagner@enit.fr
gilles.dessein@enit.fr

(2) : Messier-Bugatti-Dowty
Etablissement de Bidos - BP 39
64401 Oloron Sainte Marie Cedex, FRANCE
E-mail : jean-yves.gendron@safranmbd.com

Abstract: During machining operation, the control of the chip morphology is essential in order to ensure the surface quality and to improve the chip convoying. However, the development of new materials with low thermal properties and high mechanical properties limits the chip fragmentation. In order to improve the knowledge of chip formation during turning of high strength stainless steel an experimental campaign has been done. The chip morphology and the cutting process have also been analysed. Concerning the cutting process, based on cutting power, the tests show a high influence of cutting speed and a poor influence of feed. The chip morphology and the chip formation show the difficult to get some fragmented and small chips. The chip fragmentation occurs generally with the chip curling which increases the strength inside the workpiece material.

Key words: chip formation, stainless steel, cutting process, chip morphology.

1- Introduction

During turning operation, to control the chip formation seems essential in order to improve chip evacuation and to avoid interaction during cutting between chips and the machined surface. Indeed, some chips may alter the surface finish and part quality if some long and snarled chips are produced.
Moreover, some new alloys have been developed often with detrimental mechanical and thermal properties for their machining.
During machining, different types of chips of various shape, size, colour are produced depending upon :

- type of operations, i.e., continuous (turning, boring etc.) or intermittent cut (milling),
- work material (brittle, ductile…),
- cutting tool geometry (rake angle, honed edge radius…),
- cutting conditions (cutting speed, feed, radial depth),
- cutting assistance (type of lubrication, pressure…).

The type of chip is variable in shape and size. In order to define all type of chip, the [NF1] standard classifies the different shape of chips (Figure 1). This first analysis allows characterizing the chip in macroscopic scale.

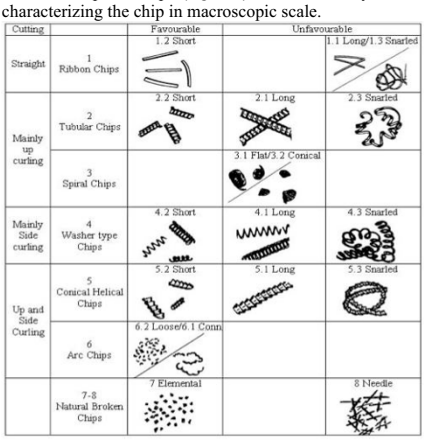

Figure 1 : Chips form classification

In order to understand the chip formation, the analysis of the chip microstructure is required. Based on experimental campaign, [KB1] have classified the type of chip as :

- the segmental chip,
- the wavy chip,
- the shear-localized chip,
- the discontinuous chip.

The segmental chip is a continuous chip with a periodic and asymmetric variation in chip thickness. Its formation is due to instabilities in the primary and the secondary shear zones and to dynamical response of machine tool structure. Contrary to the continuous chip, cutting process is characterized by large strains; low and oscillating shear angles and cyclic variations of thrust forces. The wavy chip is characterized by cyclic variation in undeformed chip thickness, shear and rake angle. It forms generally by

regenerative chatter under self-excited vibrations.
The shear-localised chip is generally observed with the difficult-to-cut materials such as titanium alloys and nickel alloys with poor thermal properties and high mechanical properties. This sort of chip has been observed during AISI 304 steel machining by [K1] with high-speed cutting. These serrations are mainly due to plastic instability and intense localized deformation localized in the primary shear plane. The formation of concentrated shear bands was due to concentration of thermal energy in primary shear plane. The last type of chip is the discontinuous chip, which occurs generally during machining of ductile materials.
The machining of high strength stainless steel is still unknown because of their rapidly evolving. Moreover, some initial tests show some high cutting forces and above all some long, which can induce some rapid wear and surface damaging. Some work concern the chip formation during steel machining but the mechanical properties of these alloys are different in hardness ([PM1], [DE1]) and often for high cutting speeds, which generate for stainless steel machining a rapid tool wear.
Based on experimental tests, the motive of this work is the study between cutting conditions, cutting process, chip formation and chip morphology in order to define the best couple of cutting conditions to obtain some fragmented chips.

2- Experimental set-up

For this work, the material studied is a very high strength stainless steel with high fracture toughness (1200 MPa), elongation ≈14% and hardness ≈48 HRC. This steel alloy is composed of C, Si, Mn, Cr, Mo, Ni, Al and Ti.
The lubricant used an emulsion with a 6% concentration. The distance between the tube (diameter = 3 mm) and the insert is 60 mm and the angle between the rake angle is 4°.
Two tools have been used with two types of cutting tool geometries measured with the Alicona® system (Figure 2).

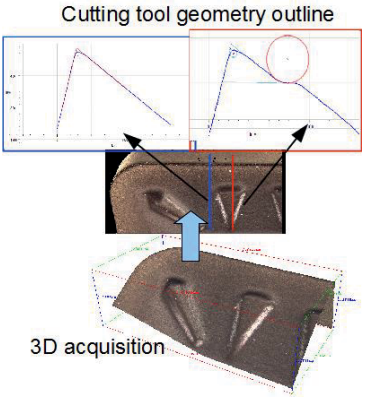

Figure 2 : Cutting tool geometry acquisition method

This technic allows measuring the cutting tool geometry based on 3D acquisitions. For each tool, the outline of cutting tool geometry is extracted and treated. Concerning the first tool, the rake angle is 3°, the edge radius is equal to 40 µm and the second rake angle is 24°. The rake angle of the second tool is -3°, the second rake angle is 15° and the edge radius is equal to 45 µm. Both tools are composed of tungsten carbide substrate and TiAlN PVD coating. A lubricant concentrate to 7% has been used at low pressure during these tests.

The cutting process is controlled with the cutting power measured with the Siemens Simucon NC with a sampling rate equal to 500 Hz.

The cutting pressure is defined according to cutting power. For each test, the cutting power is defined as :

$$P_{cutting} = P_{total} - P_{noload}$$

where $P_{cutting}$ is the cutting power, P_{total} is the power measured by the Siemens Sinucom NC, P_{noload} is the no-load power before the machining.

The cutting pressure is defined according to :

$$K_{cc} = \frac{60 P_{cutting} a_p t_u}{V_c}$$

where K_{cc} is the cutting pressure, t_u is the uncut chip section, a_p is the radial depth and V_c is the cutting speed.

The chip analysis will be performed on two scales. The chip is considered in its totality in the macroscopic scale. The second named microscopic scale allows the study of the chip formation based on the grain deformations.

3- Cutting speed influence

3.1 – Cutting process

The cutting speed has major influence on the cutting process and the material removal rate. The motive of this section is to define the cutting speed effect on cutting process and the chip morphology.
For these tests, f=0.2 mm/rev, ap=3 mm and $\kappa_r = 90°$ and each test has been performed on a length of 50 mm.
Figure 3 shows the evolution of specific pressure according to the cutting speeds and for both tools. Two levels of specific pressure appear clearly on figure 3. When the cutting speed is below than 115 m/min, the specific pressure is the same for the two tools and at its highest level ($K_{cc} \approx 2050\ MPa$).
When the cutting speed exceeds 135 m/min, the specific pressure decreases to its lowest level. Once this limit exceeds, the specific pressure is stable ($K_{cc} \approx 1800\ MPa$) for both tools and whatever the cutting speed.
The cutting speed effect on the cutting process is mainly due to the thermal softening. Indeed when the cutting speed increases, the temperature inside the work-piece material and at the tool-chip interface rises. Consequently, the mechanical properties of the materials decrease and generate some lowest specific pressures.

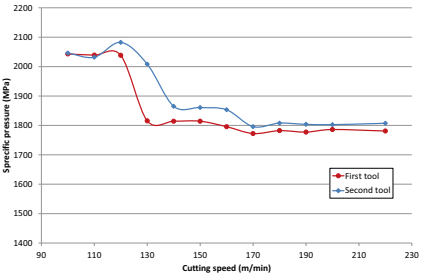

Figure 3 : Evolution of specific pressure according to cutting speeds

3.2 – Chip morphology

Erreur ! Source du renvoi introuvable. presents the evolution of chip morphology for both tools and for several cutting speeds. Concerning the macroscopic scale, the chip morphology and consequently the chip formation seems not affected by the increasing of cutting speed. Indeed, all chips are similar and can be assimilated to a non-segmented chip (type 2.3 figure 1). According to figure 1, these types of chip are so unfavourable. The strains generated by the cutting process are lower than mechanical properties of steel. [L1] observes, in his work, an oxidation of steel, which is revealed by a chip's coloration (blue) when the cutting speed exceeds 120 m/min. During these tests, oxidation was not observed. The chip colour is unchanged and is grey. However, compared to Lee the chemical composition of stainless steel where some chromium is added can induce some difference of coloration [L1]. The cutting speed effect and moreover the thermal energy generated with highest cutting speeds do not generate some fragmented the chip.

In order to understand the cutting speed effect on chip formation, two chips have been collected. These chips were embedded to a resin and polished. A Kalling solution has been applied in order to reveal the alloy microstructure. The chips have been generated with the first tool and for Vc=110 m/min and Vc=190 m/min respectively when the specific pressure is the highest and when the specific pressure is the lowest.

As observed on figure 6, the chip microstructure is affected by the cutting speeds. The chip is always assimilated to a shear localized where primary shear bands are always observable. The deformation of the chip was found to be inhomogeneous in two wide regions, one where deformation was very high (i.e., between the segments) and the other where deformation was relatively low (i.e., within the segments). According to [K1], this type of chip is a shear-localized chip, which also observed on AISI 304. Its formation is mainly due to plastic instability, intense localized deformation in the primary zone leading to intense shear between the segments. The concentration of thermal energy in narrow bands can be due to insufficient time for dissipation of heat from these bands. This phenomenon is amplified by the low thermal conductivity and the low specific heat of the stainless steel.

As seen on Figure 4, the thickness of the shear bands rises with a highest cutting speed. The increasing of cutting speed generates some highest cutting temperature.

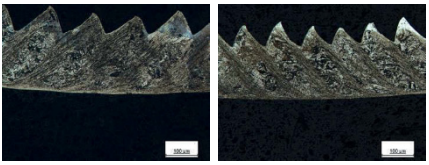

Figure 4 : Chip microstructure evolution when Vc=110 m/min and when Vc=220 m/min

Based on the chip formation described by [K1], (1) represents the undeformed surface of chip (Figure 5). As seen on Figure 4, some deformations occur the microstructure where the grains are deformed along the slip line. (2) is the section of the primary shear plane as can be observed on Figure 6. This zone is the part of the catastrophic shear-failed zone, which is separated to the previous segment. (3) is the zone where the intense shear band is formed by catastrophic shear during upsetting stage of the segment being formed. (4) is the zone in contact with the rake face where some intense shear occur. (5) is the primary shear plane where some intense localized deformations appear. As described by [K1], the primary shear plane is curved and (6) is the machined surface (Figure 4).

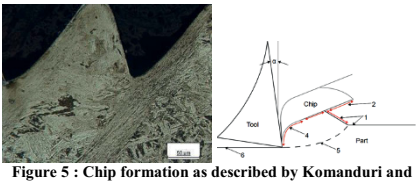

Figure 5 : Chip formation as described by Komanduri and observed after machining

Concerning the chip geometry (Figure 6) a highest cutting speed generates a chip thickness and a shear angle stable (Figure 5). This stability is due to the uncut chip thickness and rake angle invariant during the test. Moreover, the lowest chip thickness or the segment height is also slightly affected by the cutting speed. Therefore the sliding phenomena between the segments are amplified by the cutting speed or the temperature generated.

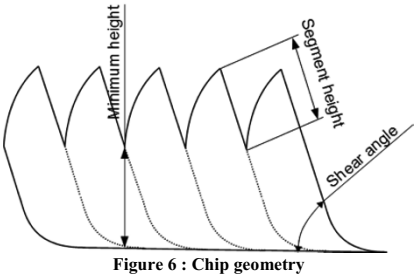

Figure 6 : Chip geometry

Article 041-pp-60

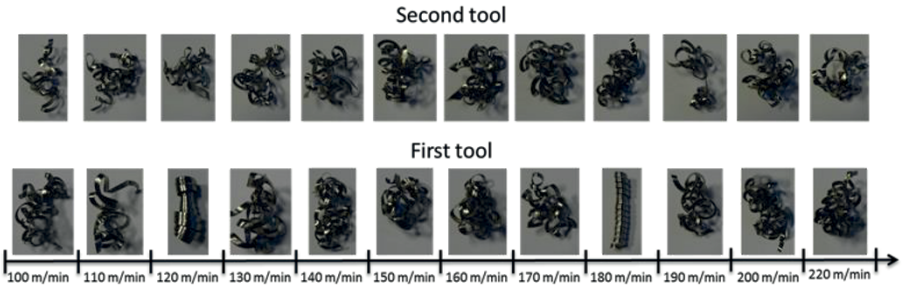

Figure 7 : Evolution of chip morphology according to cutting speed

As shown on Figure 4, the lamellae frequency is affected. It is due to a highest chip velocity, which increases the chip formation phenomena.

4- Feed and radial depth effects

The second conditions tested are the radial depth and the uncut chip thickness. In order to limit the specific pressure and to control the tool wear, according to the previous tests made, the cutting speed used is Vc=150 m/min.

4.1 – Cutting process

As on the previous section, the cutting process is controlled with the specific pressure (Kcc).
Contrary to the previous tests, the specific pressure is stable. Figure 8 shows a slight evolution of specific pressure with the rise of feed. When the feed is above 0.45 mm/rev, the specific pressure decreases. As soon as the feed exceeds 0.45 mm/rev, the specific pressure increases slightly. The relation between the cutting forces and the cross section area is always the same. However, the cutting power and consequently the cutting forces are three times higher among the lowest and the highest feed. This difference can induce some tool wear phenomena.

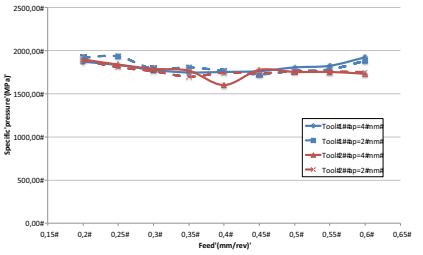

Figure 8 : Evolution of specific pressure according to feed

4.2 – Chip morphology

Contrary to the cutting speed effect, there is a relationship between the increasing of uncut chip thickness and the chip morphology (Figure 9 and Figure 10).

Concerning the first tool and when ap=4mm, the chips is fragmented only above tu=0.45 mm/rev. Before, the chips are non-fragmented and they are similar to long and snarled chips (type 2.3) according to figure 1. When ap=2 mm, the chip fragmentation occurs above tu=0.4 mm/rev. When the chips are smaller, they become some arc chips (type 6.2 in Figure 1).
The chips are never fragmented with the second tool whatever the radial depth and the uncut chip thickness. However, there is a great evolution of the chip morphology. When ap=2 mm, the chips are snarled when the uncut chip thickness is above 0.25 mm/rev. As soon as the feed increases, the chips become long and helical (type 4.1 and type 5.1 in Figure 1). For ap=4 mm, this transitions (chips snarled/chips helical) occur when the feed is beyond 0.45 mm/rev.
Concerning the chip evacuation, the optimal chip is the smallest chip because they allow a better convoying. Concerning the tool wear, a lowest length of contact on the rake face can induce a smallest chip curl radius and decreases the temperature and consequently the tool wear. Moreover during machining operations, the smallest chips are directly evacuated and cannot touch and damage the machined surface.

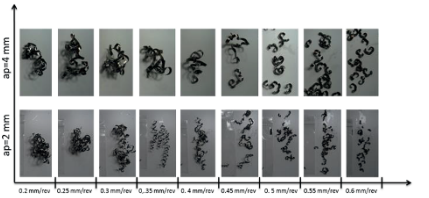

Figure 9 : Evolution of chip morphology according to the uncut chip thickness and radial depth for the first tool

Article 041-pp-60

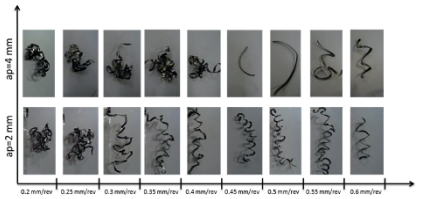

Figure 10 : Evolution of chip morphology according to the uncut chip thickness and radial depth for the first tool

As described on Figure 9, the increasing of feed allow getting smallest chips only with the first tool. Consequently, the cutting tool geometry affects the chip formation and consequently the chip morphology.

Indeed, the chip up-curl radius is affected by the cutting tool geometry. With the first tool, the curl radius of chip is the lowest due to the effect of the chip breaker (Figure 11). According to the cutting tool geometry measurements, the radius of chip groove is 2.5 mm. Concerning the second tool, the chip groove radius is the lowest (0.5 mm) and the chip breaker geometry is like some studs distributed along the cutting edge (Figure 10).

The effect of chip breaker is then different. With the first tool, the chip is curled according to the tool groove radius (Figure 11). The deformations increase in the chip and induce its fragmentation. With the second tool, the tests show the low effect of the chip breaker. Indeed, as shown Figure 9, the chip-curled radius is always higher compared to the chips generated with the first tool.

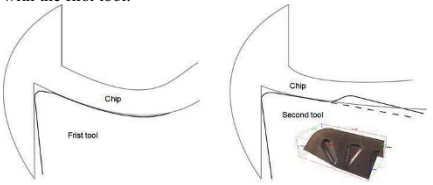

Figure 11 : Chip formation for the both tools

The difference of the chip breaker distribution limits its effect on the chip formation. Indeed as seen on Figure 12, with the second tool some marks occur on the surface in contact with the rake face and the chip breaker. These marks are due to the difference between the tow materials (stainless steel and tungsten carbide) hardness. Consequently, the tool groove radius is very high and generates a high chip-curled radius.

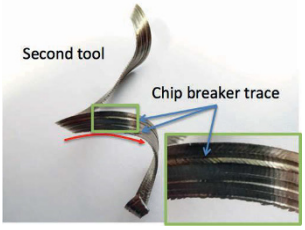

Figure 12 : Chip breaker traces

As observed on Figure 9 and Figure 10, the tool nose radius also modifies the chip flow. Indeed, the chip flow is not collinear to cutting speed.

Two ways are possible to get the chip fragmentation. The first is to generate some high strains and temperatures in the primary shear plane in order to generate some stresses, which are higher than the ultimate tensile stress of the alloy. The second is fragmented the chip with the chip breaker.

To understand the chip morphology, the chip microstructure has been analysed with the method presented previously. Based on the previous tests and the chips morphology gotten with the first tool, two cutting conditions are analysed. When f=0.4 m/rev and ap=4 mm, the chips are never fragmented while f=0.6 mm/rev and ap=4 mm, the chip are fragmented. This choice allows understanding the difference in chip formation between the feed where the fragmentation occur and the feed where the chips are long.

Whatever the feed, the deformation in the chip was found to be inhomogeneous with two wide regions (Figure 13 and Figure 14). A region where the deformation was very high and localized between the segments and the other where deformation was relatively low (inside the segments). According to [K1], the type of chip is an always shear-localized chip.

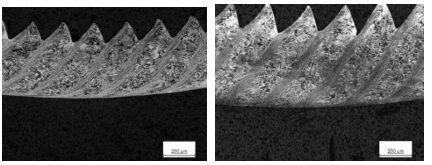

Figure 13 : Chip microstructure when tu=0,4 mm and when tu=0,6 mm with the first tool (Vc=150 m/min – ap=4 mm)

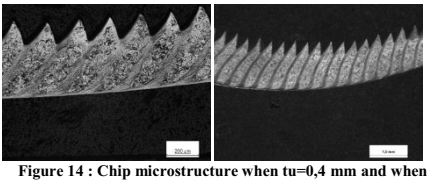

Figure 14 : Chip microstructure when tu=0,4 mm and when tu=0,6 mm with the second tool (Vc=150 m/min – ap=4 mm)

Concerning the second shear zone (contact area between chip and rake face), in despite of [K1] conclusions some high deformations occur in this zone. As seen Figure 15, the microstructure is deformed according to the chip velocity.

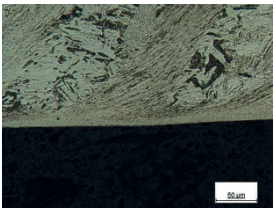

Figure 15 : Second shear zone

Concerning the chip geometry and for the first tool, the evolution is very slight (Figure 16). Indeed, the shear angle (ϕ) is constant. The distance between two segments increase with a highest feed. Concerning the chip thickness, the ration between feed and chip thickness is 0.8 when the f=0.4 mm/rev and 0.9 when f=0.6 mm/rev.

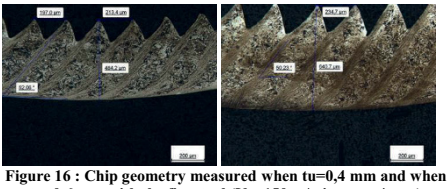

Figure 16 : Chip geometry measured when tu=0,4 mm and when tu=0,6 mm with the first tool (Vc=150 m/min – ap=4 mm)

The chip formation is unchanged by the feed but some chips are fragmented. This fragmentation can be due to the chip curling. When the tool advances, the chip is formed. According to [J1], the chips curl according to the tool groove radius. During machining, the stress in the workpiece material is too low, the cutting process does not fragment the chip and a long chip is developed on the rake face. Due to the tool groove radius, the chips curl and when the length of chip is sufficient, the end of chip meets the chip's root. The tool continues to advance but the chip is blocked which generates some high stresses. When the stress in the chip exceeds the ultimate tensile stress the chip is fragmented (Figure 17). When the chip thickness is too low, the chip strength is too poor to get the chip fragmentation. When the end of chip meets the chip roots, the chip is deformed but the stress inside the material is always too low.

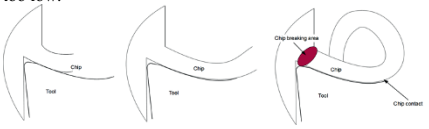

Figure 17 : Evolution of chip morphology

As shown Figure 18, the chip is curled and its fragmentation seems occur when the end of chip presses the chip root. Moreover, the SEM analysis shows also the friction contact between the chip and the tool. Two areas are observed. The first is the contact length close to the cutting edge. The second area is situated on the chip breaker where some stainless steel deposit is observed.

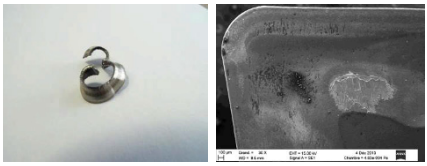

Figure 18 : Fragmented chip collected and friction area on chip breaker

7- Conclusion

The presents document deals about the relation between cutting conditions and chip formation during machining of high strength stainless steel. This first study is the preamble of a study on the effect of high-pressure lubrication chip breaking.

Some tests have been conducted where the cutting power has been measured and where the chips have been analysed. The chip analysis has been made in two scales: the macroscopic scale and the microscopic scale.

Concerning the cutting process, the increasing of cutting speed generates lowest specific cutting pressure due to the thermal softening. Whatever the cutting tool geometry, the decreasing of specific pressure occur after Vc=150 m/min. By contrast, the feed does not influence the specific cutting pressure.

Concerning the chip formation and the chip morphology, the chips are always classified as shear localized chip. Its fragmentation is very difficult. Some small chips are generated only with the first tool and when the cutting conditions are the higher. This chip morphology is the result between chip thickness and cutting tool geometry. Based on the chip formation, the chip can be segmented only by the cutting process. The chip curling increases strength inside material when the end of chip meets the chip root explains the segmentation process.

8- Acknowledgment

The authors would like to express their thanks to Mr Jean Yves Gendron from Messier Dowty Bidos (France) for his support during this experimental work.

9- Reference

[DE1] Dolinsek S., Ekinovic S. and Kopac J. A contribution to the understanding of chip formation mechanism in high-speed cutting of hardened steel, In Journal of materials processing technology 157-158: 485-490 (2004)

[J1] Jawahir I.S. On the controllability of chip breaking cycles and modes of chip breaking in metal machining, In Annals of CIRP 39:47-51 (1990)

[KB1] Komanduri R. and Brown R.H. On the mechanics of chip segmentation in machining, In Journal of Engineering for Industry 103: 33-51 (1981)

[KS1] Komanduri R., Schroeder T., Hazra J. von Turkovich B.F. and Flom D.G. On the catastrophic shear instability in high speed machining of an AISI 4340 Steel, In Journal of Engineering for Industry 103: 121-131 (1982)

[L1] Lee D. The effect of cutting speed on chip formation under orthogonal machining, In Journal of Engineering for Industry 107: 55-63 (1985)

[NF1] NFE 66-520-4 Domaine de fonctionnement des outils coupants – Couple outil matière – Partie 4 : Mode d'obtention du coupe outil-matière en tournage (1997)

[PM1] Poulachon G., Moisan A. and Jawahir I.S. On modelling the influence of thermo-mechanical behavior in chip formation during hard turning of 100Cr6 bearing steel, In CIRP Annals - Manufacturing Technology 50(1): 31-36 (2001)

Article 049-pp-38

HIGH SPEED INTERACTION BETWEEN AN ABRADABLE COATING AND A LABYRINTH SEAL IN TURBO-ENGINE APPLICATION

C. Delebarre [1,2], V. Wagner [2], J.Y. Paris [2], G. Dessein [2], J. Denape [2], J. Gurt-Santanach [1]

(1) : TURBOMECA, Avenue Joseph Szydlowski, 64510 Bordes, France

E-mail : corentin.delebarre@turbomeca.fr

(2) : Université de Toulouse, Laboratoire Génie de Production, Ecole Nationale d'Ingénieurs de Tarbes, 47 Avenue d'Azereix, BP 1629, 65016 Tarbes Cedex, France
Phone/Fax : 0562442700

E-mail : corentin.delebarre@enit.fr
vincent.wagner@enit.fr

Abstract: The design of gas turbine aims to enhance the engine efficiency by developing new materials able to work at higher temperatures, or to promote new technologies, fuel management and airflow direction. One solution is the reduction of clearance between rotary parts in turbomachinery air systems. This clearance reduction causes direct interactions in the secondary air system of a turbo-engine when a rotary seal, called labyrinth seal, rubs on the turbo-engine as a result of successive starts and stops, thermal expansions and vibrations. The purpose of the present paper is to study interaction phenomena between an abradable material (Al-Si 6%) and a nickel alloy (718 alloy) during high speed contacts. A high speed test rig has been designed to simulate interactions between labyrinth seals and abradable coatings in similar operating conditions of turbo-engine in terms of geometries, rotational and linear velocities. A series of experiments has been carried out in order to get a first assessment under different turbo-engine operating conditions. Experimental results are presented using visual observations of test samples, quantitative approaches of interacting forces and micrographic observations. This work provides new basic data for a preliminary study of the interaction between a labyrinth seal teeth tips and its casing for turbo-engine applications.

Key words: Labyrinth seal, abradable material, high speed interaction

1- Introduction

During decades, turbomachinery manufacturers try to find how to save energy by increasing engine efficiency. One way to improve engine efficiency is to control the airflow direction by reducing the clearance between rotary parts in air systems [DE1]. In the secondary air and sealing systems, the control pressure differences and the levels of cooling between modules of the engines are crucial in order to operate the turbine. As a part of dynamic sealing systems, labyrinth seals are used to reduce the loss of high pressure gas within the engine cycle. This special type of rotary seal controls cooling air flow through the hot section of the engine and maintains pressure balance on the rotor shaft system. They are located on the rotating shafts between the compression stages and are composed of several teeth [DW1].

Nevertheless, reducing the clearance might cause undesirable interactions between labyrinth teeth tips and housing [SG1]. This is also true for successive start and stop cycles, thermal expansions, vibrations and mechanical loadings occurring during engine operation [JT1]. In this case, labyrinth teeth rub into the housing surface and form rub-grooves on it. To avoid undesirable wear due to incursions of labyrinth teeth in the bare metal housing, the insert of a few millimeters abradable material layer was widely recognized as a robust solution. The turbo-engine housing is coated with a sacrificial abradable material (rub tolerant material) sprayed by thermal spraying [R1]. This coating can be composed of metal phase and self-lubricating non-metal phase, which provides a high porosity rate and offers a good balance between abradability and erosion resistance [MB1]. This method is widespread in other turbine-engine applications such as blade tip and compressor housing where extensive researches are conducted to characterise blade-abradable interaction [CT1]. The use of abradable seal to prevent rub interactions encourages aeronautical engineers to characterize the abradable behavior during labyrinth seal interactions and to validate the design choices in the various stages of the engine.

Today, research activities are mainly concentrated on the labyrinth seal behavior in their sealing performance before and after interaction. Many experimental studies (with development of specific test rig) and numerical studies help characterize the effect of interactions on the aerodynamic seal performance, leakage levels generated by the grooves left by labyrinth teeth and the effect on tooth profiles [DP1, CT1, GV1].

Concerning interactions between labyrinth seal and abradable

coating, very few studies are devoted to understanding the contact. Dowson *et al* [DR1] and Whalen *et al* [WA1] developed a full-scale facility based on a grinding machine, to study the behavior of abradable materials (mica filled tetrafluoroethylene (TFE), silicone rubber, aluminium polyester and nickel graphite) in contact with labyrinth seal at relative speed up to 25 $m{\cdot}s^{-1}$ and 130 $m{\cdot}s^{-1}$ respectively. They performed contact with incursion speeds varying from 2.54 $m{\cdot}s^{-1}$ to 25.4 $m{\cdot}s^{-}1$ which are defined as representative conditions of labyrinth thermal expansions and vibrations. They established a "good abradability" condition for tested materials by defining a special ratio. Mutazim *et al* [MH1] introduce an additional condition describing interaction by characterizing the rub-groove geometry of seven abradable materials (aluminium, Al-bronze, Al-Si-polyester, Al-bronze-polyester, Al-Si-polyimide, Cu-Sn-Bi, Cu-Sn-Pb) subjected to labyrinth seal interaction. A specific full-scale test rig was developed and performed under unlubricated conditions.

Later, Sulzer Innotec and Sulzer Metco companies [W1] worked closely on the development of abradable materials, by using special test rig adapted to the application of labyrinth/abradable interactions. It consists of an alloy disc that accommodates four continuous seal trips on the outer circumference, a movable specimen controlled by a programmable controller coated with abradable (step length of 0.15 µm), and a heating device (from 25°C to 700°C). The wear behavior is evaluated using the seal strip cutting-edge velocity, the temperature of the shroud segment, the wear track depth and the incursion depth and the video of test.

The present paper describes the results of an experimental investigation carried out to undertake a first assessment of high speed mechanical interactions between a labyrinth seal of 718 alloy and an abradable Al-Si 6% coating. An original test rig is specially designed to simulate these interactions in realistic operating conditions.

2- Experimental protocol

2-1 Test rig description

The experimental device presented in Fig. 1 has been specially designed and developed to simulate and to study operational wear interactions between labyrinth seals and abradable coatings in similar operating conditions as turbo-engine. For that, a 5-axis milling machine UCP600 VARIO from Mikron is used as a test rig and receives a specific experimental device. The 5-axis milling machine has the particularity to be fitted with a special magnetic bearings spindle which allows a maximum rotation speed of 40 000 rpm and maintains the spindle vertically without any mechanical contact.

A labyrinth seal, representative of an actual part of a motor shaft section is shrinking on a HSK-50 tool holder instead of a cutting tool (Fig. 2a). The contact is performed inside a special tube sample coated with abradable materials in this inner periphery. This specimen is representative of the housing facing labyrinth seals in the secondary airflow turbo-engine section (Fig. 2b). A diffuser and a base piece precisely fasten the tube sample coated with abradable on the machine tool table. The diffuser is specially designed to simulate the sealing of the labyrinth seal during operation by pressurizing the entire system. It will allow, for future tests, the measurement of their leakage level and their sealing performance after interactions. In case of sample break during the test, a protective shielding has been designed.

The rotation speed of labyrinth seal varies from 0 to 40 000 rpm, representative of typical speed reached by free turbines in turbo-engines, and corresponding to a labyrinth tip speed varying from 0 to 130 $m{\cdot}s^{-1}$. Contact between labyrinth seal and abradable is controlled by using capabilities of the high speed milling machine, which gives rise to a radial incursion speed ranged from 0.001 $mm{\cdot}s^{-1}$ to 25 $mm{\cdot}s^{-1}$. Geometric tolerances of samples and theirs assemblies require a precise control of a clearance of 150 µm between labyrinth teeth tips and abradable coating, according to real engine conditions.

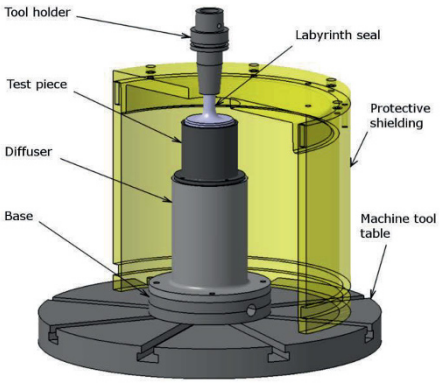

Figure 1: Labyrinth-abradable interaction test rig.

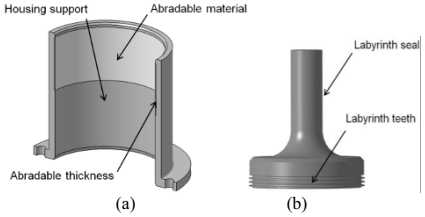

Figure 2: (a) Labyrinth seal specimen, (b) Abradable coating on housing support.

2-2 Contact geometry

Interactions between labyrinth tips teeth and abradable coating are characterized by a complex contact geometry induced by the incursion of a circular tooth of trapezoidal

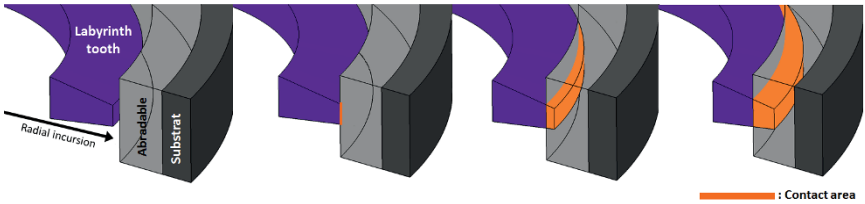

Figure 3: Sectional view of the evolution of the contact geometry.

section in a tube coated with abradable. This contact geometry evolves during the test according to the incursion depth, as shown in Fig. 3. Nevertheless, the machining precision of labyrinth seal teeth (geometric tolerances, unbalance…), the positioning precision of test pieces and the spindle stiffness (supposed infinite during contact), have an important impact on the nature of the interaction. Once the labyrinth seal precisely positioned in the abradable test piece, the concentricity error is stated to ±30 µm. In addition, for the reasons given above, the use of three teeth labyrinth seal leads to get three different contact behaviors, one for each tooth, with the same test condition. The geometric confinement of the central tooth probably leads to thermal phenomenon during the interaction.

2-3 Contact forces measurement

A special instrumentation has been developed on the rig test to record forces during interactions thought the continuous control current of the spindle magnetic bearings. This continuous control current is performed to maintain the rotation shaft axis in the centre responsive to any change of load (external force, disturbance of a solid rotor imbalance). In our case, interacting forces induced by the labyrinth seal incursion are directly transmitted in the magnetic bearings and compensated through control current signals. These compensated signals are then recorded by a special Matlab toolbox, and processed as contact force signals (Fig. 4). The force measurements are then represented using the norm defined in the following equation:

$$\left\|\vec{F}\right\| = \sqrt{(fx)^2 + (fy)^2 + (fz)^2} \qquad (1)$$

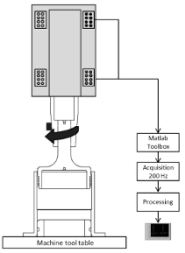

Figure 4: Schematic diagram of forces acquisition.

2-4 Test parameters

As mentioned earlier, the labyrinth seal specimens analyzed in this study was made of 718 alloy whose chemical composition is presented in Table 1. It was designed with three circular teeth of 65.8 mm in external diameter. The Al-Si 6% coating was sprayed inside the housing support on a stainless steel substrate. Spraying is realized with a thermal wire flame spray process onto a bond coat approximately ranged from 20 to 150 µm (Fig. 5). The high roughness of the bond coat promotes good cohesion of the deposit. Once coated, the housing support is machined by milling to control the abradable thickness (about 1 mm) which defined the mechanical clearance between abradable coating and labyrinth seal teeth.

	Elements (% by mass)						
	Ni	Cr	Fe	Mo	Nb	Co	Mn
Min	50	15		2.8	4.75		
Max	55	21	Base	3.3	5.50	1.0	0.35
Material properties :							
	Tensile strength (MPa)						1310
	Yield Strength (MPa)						1110
	Elastic modulus (GPa)						206
	Hardness (HV_{150})						370
	Density ($g \cdot cm^3$)						8.19
	Melting point (°C)						1300
	Thermal conductivity ($W \cdot m \cdot K^{-1}$)						11.2

Table 1 : Chemical composition and properties of 718 alloy.

The main studied test parameters are labyrinth tip speed, rotation speed, incursion speed and incursion depth. A test matrix has been selected to cover various conditions encountered in turbo-engine such as engine vibrations, excessive mechanical loading or thermal expansion. Table 2 shows the test parameters studied in this work. It is important to mention that all the tests were carried out with only one labyrinth seal sample.

Test n°	Rotation Speed (V_r) (rpm)	Labyrinth tip speed (V_t) ($m \cdot s^{-1}$)	Incursion speed (V_{inc}) ($mm \cdot s^{-1}$)	Incursion depth (D_p) (mm)
1	37500	130	0.005	0.2
2	37500	130	25	0.2
3	12500	43	0.005	0.2
4	12500	43	25	0.2
5	5000	17	0.005	0.2
6	5000	17	25	0.2

Table 2: Test parameters.

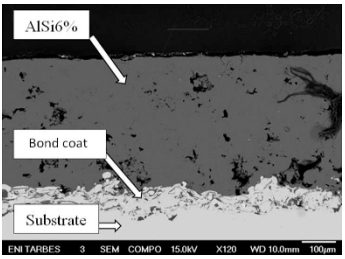

Figure 5: Microstructure in section view of Al-Si 6% coating on stainless steel substrate.

3- Data analysis and discussion

3-1 Analysis of test samples

A first *post mortem* analysis is performed by a visual observation of labyrinth seal teeth and abradable coating after test. Fig. 6 presents all the rub-grooves left by labyrinth seal teeth on Al-Si 6% abradable for each test parameter.

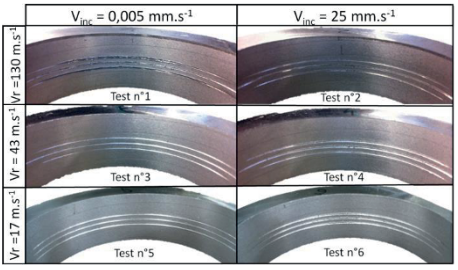

Figure 6: Images of abradable rub-grooves after testing.

As seen in Fig. 6, different morphologies of rub-grooves are observed according to test parameters. Some rub-grooves present a significant amount of plastically deformed material on both sides of the groove. This is the case for tests at high incursion speed (tests n°2, 4, 6) and for test n°1 at low incursion speed and labyrinth tip speed of 130 m·s^{-1}. Unlike others, rub-grooves from tests n°3 and 5 (low incursion speed and low rotational speed) display geometries that may be qualified as "clear-cut" appearance without positive amount of material. Visual observations of labyrinth seal teeth after test did not show any noticeable changes or severe wear except for labyrinth seal teeth from tests n°3 and 4. Al-Si 6% coating transfer was observed on the top of labyrinth seal teeth, as shown in Fig. 7.

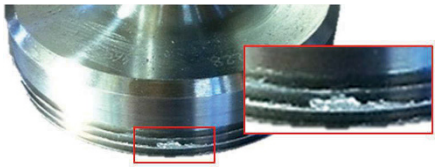

Figure 7: Al-Si 6% transfer on labyrinth seal teeth after test n°3 (V_r = 12 500 rpm, V_{inc} = 0.005 m·s^{-1}).

Such results suggest that incursion speed V_{inc} is a significant parameter for rub-grooves morphology. However, results of test n°1 demonstrate the additional influence of the labyrinth rotation speed. To confirm rub-grooves visual observations, accurate profile measurements were carried out with a SOMICRONIC 2C profilometer at the maximum incursion depth area (Fig. 8). Positive heights and negative depths are identified and quantified respectively by Z_1 and Z_2 values.

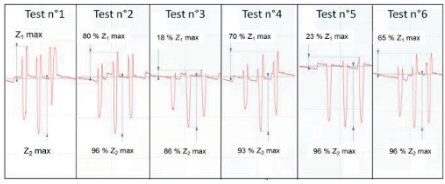

Figure 8: Rub-grooves measurement depth, corresponding to the six test conditions.

In most cases, rub-grooves formed on Al-Si 6% were widely deeper than the 200 µm fixed by the maximum labyrinth seal radial incursion. In addition, on each test, the deeper rub-groove corresponds to the tooth which is confined between the others two. This is consistent with the hypothesis of the presence of an additional wear phenomenon within the affected area because of thermal confinement.

Fig. 9 presents the maximum heights of the deformed coating according to the rotation and the incursion speed. As the heights bars show, the labyrinth tip speed has a significant effect on the heights of deformed coating at low incursion speed (V_{inc} = 0.005 mm·s^{-1}). In fact, at 43 m·s^{-1} and 17 m·s^{-1}, deformed coating is lower whereas rub-grooves depths are identical. This examination indicates the presence of material deformation phenomena at high rotation speed, in contrast to material removal for lower rotation speed. This difference of wear mechanism may be explained by different dissipation level of the contact temperature in the Al-Si 6% coating. This difference is affected by the rotation speed of the labyrinth seal, which impacts the ductile behavior of the coating. It is therefore interesting to observe the interaction forces during the contact.

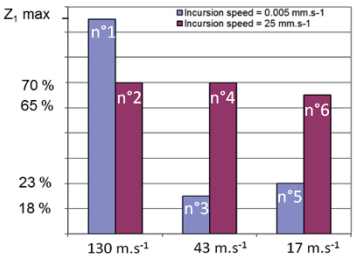

Figure 9: Maximum heights of deformed coating according to rotational and incursion speed.

3-2 Analysis of interaction forces

The use of interaction force norm provides a global vision of the changing forces during tests. Firstly, two different sets of signals are observed and are associated to different incursion speed (25 mm·s^{-1} and 0.005 mm·s^{-1}). Fig. 10 shows a typical signal recorded at low incursion speed. It reveals cyclic variations characterized by non-contact periods where forces are close to zero. This phenomenon may probably be associated to a sudden Al-Si 6% pick-up and non-contact time because mechanical clearance adjustment. The increase in maximum forces at each cycle can be in part explained by the increasing of the contact surfaces. Fig. 11 shows a typical signal recorded at high incursion speed. It is composed of a very fast rise time (≈ 0.005 ms), of a maximum which corresponds to the halt of the labyrinth seal incursion and of a fall of forces.

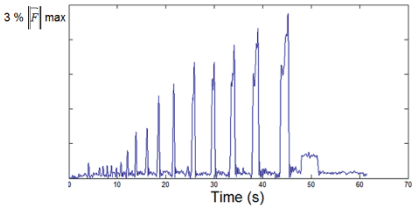

Figure 10: Typical forces signal at low incursion speed (V_{inc} = 0.005 mm·s^{-1}, Vr = 12 500 rpm).

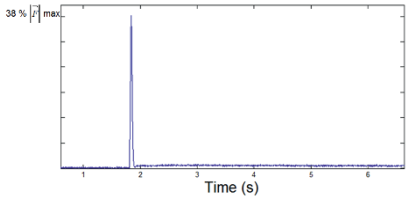

Figure 11: Typical forces signal at high incursion speed (V_{inc} = 25 mm·s^{-1}, Vr = 37 500 rpm).

Secondly, the norm is used as a quantitative approach and allows the establishment of a maximum force value induced by the contact. Fig. 12 presents maximal forces recorded versus rotation and incursion speed. Maximum forces generated by tests at high incursion speed are significantly higher than those at low incursion speed. At low incursion speed, maximum forces are included in a range from 1 % to 9 % of the maximum forces compared to a range from 38 % to 100 % of the maximum forces for high incursion speed. Moreover, rub-grooves characterized by a low amount of deformed coating are obtained with forces lower to 9 % of the maximum forces.

Another trend is observed by comparing the maximum forces evolution for different incursion speeds. At low incursion speed, the increase of rotation speed induces a gradual increasing of the maximum interaction forces. Conversely for high incursion speed, when the rotation speed decreases, interaction forces increases.

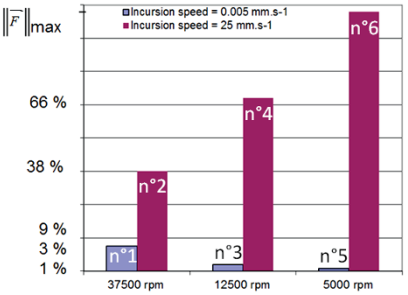

Figure 12: Maximum interaction forces versus rotation speed (Vr) and incursion speed (V_{inc}).

3-3 Micrographic rub-grooves observations

Micrographic rub-grooves observations were performed on the Al-Si 6% abradable surface from test n°1. Fig. 13 shows a section view of three rub-grooves from test n°1 (V_{inc} = 0.005 mm·s^{-1}, V_r = 37 500 rpm, D_p = 0.2 mm). This view is the place where the incursion depth of the labyrinth teeth is the greatest. Rub-grooves formed in Al-Si 6% are slightly wider than the initial tooth dimension. Considering the coiled shape of coating deformed outside the rub-groove, the SEM image demonstrates the existence of a material expulsion mechanism by plastic deformation on the both side of the rub-groove (fig.13). Moreover, a slight Al-Si 6% densification is identified around the rub-groove.

Nevertheless, EDX analysis of the rub-grooves on the Al-Si 6% coating identified the presence of nickel and chrome, which are basic elements of 718 alloy, coming from the labyrinth seal teeth (Fig. 14a). This mater transfer from the labyrinth seal to the abradable coating is made of an accumulation of layers in the rub-groove (Fig. 14b).

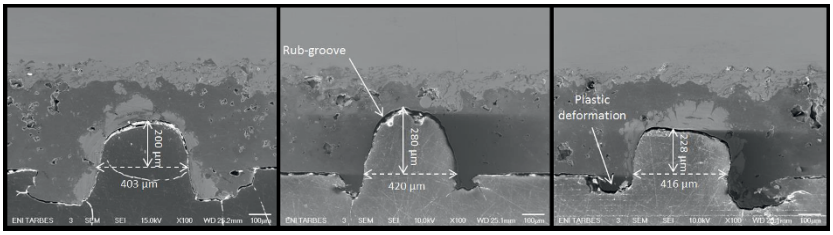

Figure 13: SEM image in section view of the three rub-grooves from test n° 1 at maximum incursion depth.

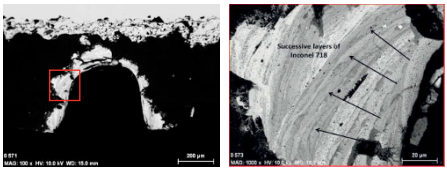

(a) (b)

Figure 14: (a) SEM image in backscattered electron mode of the first rub-groove from test n°1, (b) SEM image of accumulated layers of 718 alloy.

4- Conclusion

To optimize turbo-engines performances by reducing the mechanical clearance between rotary parts, contact between labyrinth seals and abradable coatings must be understood. This requirement needs to study and characterize a material couple (where one material undergoes while the other imposes) by simulating interactions in operating conditions. Interactions between an Al-Si 6% abradable coating and a 718 alloy labyrinth seal were performed using a high speed test rig specially developed to achieve a maximum interaction speed of 130 $m \cdot s^{-1}$.

A first assessment of high speed interactions has been carried out by an analysis of test samples. Visual rub-grooves observations, accurate profile measurements, maximum interaction forces analysis and micrographic examinations reveal different material deformation and wear phenomena and significant interaction parameters:

- Observation of damages by a phenomenon of deformation on the Al-Si 6% coating at high incursion speed and high rotation speed.
- Observation of a material removal wear phenomenon at low incursion speed and low rotation speed considering transfer on Al-Si 6% coating from labyrinth seal teeth, characterized by an accumulation of layers in the rub-groove.
- Influence of the labyrinth rotation speed on the rub-groove morphology and on interaction forces.

However, it is necessary to complement this study by evaluating the abradable behavior about radial incursion. A test campaign should be achieved by fixing test parameters to perform successive incursions.

5- Acknowledgment

These investigations were supported by the European Commission within the FP7 E-BREAK project under Grant agreement no: 314366 and by SAFRAN-TURBOMECA, and received the financial support of the Agence Nationale de la Recherche et de la Technologie (ANRT) which are both gratefully acknowledged.

7- References

[CT1] D. Collins, J. Teixeira, and P. Crudgington. The degradation of abradable honeycomb labyrinth seal performance due to wear. Sealing Technology, pages 7 – 10, 2008.

[C1] M. Cuny. Contribution to the local characterization of pairs of materials involved during rotor / stator contact in a turbomachine. PhD thesis, Université de Lorraine, 2012.

[DP1] I.R. Delgado and M.P. Proctor. Continued investigation of leakage and power loss test results for competing turbine engine seals. Technical report, NASA/TM-2006-214420, 2006.

[DE1] M. Dorfman, U. Erning, and J. Mallon. Gas turbines use abradable coatings for clearance-control seals. Sealing Technology, 97(1):7- 8, 2002.

[DR1] P. Dowson, S.L. Ross, and C. Schuster. The investigation of suitability of abradable seal materials for application in centrifugal compressors and steam turbines. In Proceedings of the twentieth turbomachinery symposium, 1991.

[DW1] P. Dowson, M.S. Walker, and A.P. Watson. Development of abradable and rub-tolerant seal materials for application in centrifugal compressors and steam turbines. Sealing Technology, (12):5 – 10, 2004.

[GV1] A.J.M Gamal and J.M. Vance. Labyrinth seal leakage test: tooth profile, tooth thickness, and eccentricity effects. ASME Journal of Engineering for Gas Turbines and Power, page 130:012510, 2008.

[JT1] G. Jacquet-Richardet, M. Torkhani, P. Cartraud, F. Thouverez, T. Nouri Baranger, M. Herran, C. Gibert, S. Baguet, P. Almeida, and L. Peletan. Rotor to stator contacts in turbomachines. review and application. Mechanical Systems and Signal Processing, 40(2):401 – 420, 2013.

[MB1] Y. Maozhong, H. Baiyun, and H. Jiawen. Erosion wear behaviour and model of abradable seal coating. Wear, 252:9 – 15, 2002.

[MH1] Z. Mutasim, L. Hsu, and E. Wong. Evaluation of plasma sprayed abradable coatings. Surface and Coatings Technology, 54-55:39 – 44, 1992.

[R1] R. Rajendran. Gas turbine coatings: An overview. Engineering Failure Analysis, 26(0):355 – 369, 2012.

[SG1] R.K Schmid, F. Ghasripoor, M. Dorfman, and X. Wie. An overview of compressor abradable thermal sprays. In Surface Engineering International Thermal Spray Conference ITSC, page 406, 2000.

[WA1] J.K. Whalen, E. Alvarez, and L.P. Palliser. Thermoplastic labyrinth seals for centrifugal compressors. In Proceeding of the thirty third Turbo Symposium, 2004.

[W1] S. Wilson. Ensuring tight seals. Technical report, Sulzer Technical Review 2, 2007.

Article 027-itm-89

Conversion of G-code programs for milling into STEP-NC

Shixin XÚ [1,2], Nabil ANWER [1], Sylvain LAVERNHE [1]

(1) Laboratoire Universitaire de Recherche en Production Automatisée, ENS de Cachan, 94235 Cachan, France
{anwer; lavernhe; sxu}@ens-cachan.fr

(2) School of Mechanical Engineering and Automation, Beihang University, Beijing 100191,China
xushixin@buaa.edu.cn

Abstract: STEP-NC (ISO 14649) is becoming a promising standard to replace or supplement the conventional G-code programs based on ISO 6983 due to its feature based machine independent characteristics and its centric role to enable efficient CAD/CAM/CNC interoperability. The re-use of G-code programs is important for both manufacturing and capitalization of machining knowledge, nevertheless the conversion is a tedious task when carried out manually and machining knowledge is almost hidden in the low level G-code. Mapping G-code into STEP-NC should benefit from more expressiveness of the manufacturing feature-based characteristics of this new standard.

The work presented here proposes an overall method for G-code to STEP-NC conversion. First, G-code is converted into canonical machining functions, this can make the method more applicable and make subsequent processes easier to implement; then these functions are parsed to generate the neutral format of STEP-NC Part21 toolpath file, this turns G-code into object instances, and can facilitate company's usage of legacy programs; and finally, also optionally, machining features are extracted to generate Part21 CC2 (conformance class) file. The proposed extraction method employs geometric information of cutting area inferred from toolpaths and machining strategies, in addition to cutting tools' data and workpiece's dimension data. This comprehensive use of available data makes the extraction more accurate and reliable. The conversion method is holistic, and can be extended to process a wide range of G-code programs (e.g. turning or mill-turn codes) with as few user interventions as possible.

Key words: G-code; STEP-NC; manufacturing features; canonical machining functions; process plan.

1- Introduction

Most CNC machines are programmed in the ISO 6983 G-code language, which limits program portability because the language focuses on coding the tool center path with respect to machine axes, rather than the machining process with regard to the part. Moreover CNC vendors usually extend the language beyond the limited scope of ISO 6983 creating their own macro-languages implying that they can only be executed on specific machine-tools. STEP-NC (STEP Data Model for Computerized Numerical Controllers) is a model of data transfer between CAD/CAM systems and CNC machines. It aims at standardizing the data formats used at the machine level, one key link in the entire process chain in a manufacturing enterprise. STEP-NC specifies machining processes rather than machine tool motion, using the object-oriented paradigm and the concept of "workingsteps", which correspond to high-level manufacturing features and associated process parameters. Thus STEP-NC creates an exchangeable, workpiece-oriented data model for CNC machine tools, supports the direct use of computer-generated product data from ISO 10303, and ensures compatibility of CNC input data. CNCs are responsible for translating workingsteps to axis motion and tool operation [**I1**].

In the course of STEP-NC adoption, there are many needs to convert legacy G-codes into STEP-NC programs. With the impending prevalence of this new standard, manual conversion of G-codes will be a huge, tedious task. Therefore, automatic and effective conversion will be highly adopted by manufacturing enterprises. On the other hand, legacy programs are important resources for enterprises. They contain optimal cutting conditions and machining strategies for making products, and embody implicitly the machining know-how from various experts. So converting legacy G-codes to get corresponding STEP-NC files, instead of designing from scratch, would save much costs and resources for enterprises. Also this practice would facilitate the accumulation of machining know-how due to information storage in object-oriented structures.

The essential of the conversion is reconstruction of a manufacturing feature oriented NC program from a G-code program. NC programming by feature approach can streamline the manufacturing cycle and make CAM/CNC integration easier since manufacturing feature data and the associated process data originate from CAM. Also the feature approach makes NC-to-CAM feedback link realizable. The core of STEP-NC data model is manufacturing features and machining operations, which are encapsulated in a workingstep. Figure 1 shows STEP-NC data model structure [**I1**]. A workingstep represents the machining process for a specified area of the workpiece. It specifies the association

between "machining_feature" and "machining_operation" to be performed on the feature. The "machining_workingstep" is characterized by the use of a single tool and a set of technological parameters. A machining operation contains technological data for a workingstep. A workplan is a collection of workingsteps with an execution sequence. The "project" serves as a starting point for the program execution. The division of information means that changing the sequence of workingsteps or optimizing tool paths can be done with minimal impact on the rest of the data.

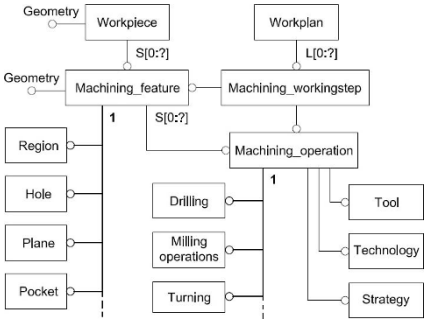

Figure 1: STEP-NC data model.

Only few researches addressed G-code to STEP-NC conversion. Shin et al. developed a system, called G2STEP, to convert G-codes into STEP-NC for turning applications [SS1]. The system is based on two main functions: the pre-processor function and the turning feature recognition function. In the pre-processor, each block of a G-code program is interpreted and stored in a pre-defined data structure. These blocks are divided using some hints and these blocks are grouped into workingsteps. At the turning feature recognition level, the feature profile remaining after a workingstep is generated, and the manufacturing feature, defined in STEP-NC, is recognized by a profile and pre-determined machining operation. However, this work did not handle milling applications and not fit well for roughing operations in G-code programs.

Zhang et al. proposed a method to re-use the process knowledge embedded in G-code part programs with different manufacturing resources [ZN1]. The authors emphasized the "process comprehension", which is "essentially restructuring the combined manufacturing information in an NC program into a high-level process plan and the associated resource information." They proposed an abstract meta-model for different CNC controllers. The method briefly involves how to get a STEP-NC file from a G-code. They recognized features from a G-code mainly by tool types, toolpath boundary and the rawpiece geometry. STEP-NC entities are then created. However details of feature types and feature parameters, are not mentioned in the paper. Their method tries to decode a G-code to get a STEP-NC file directly. Thus increasing the implementation difficulty and limiting the applicable scopes.

This paper aims to present a systematic method for automatically converting G-code part programs into STEP-NC formats. The method is applicable to both milling and turning G-codes. In Section 2, we first make clear what should be given as inputs to the conversion process, followed by the overall strategy of the conversion. In Section 3, detailed descriptions of the conversion of G-codes into canonical machining functions are described. In Sections 4 and 5, detailed descriptions for obtaining STEP-NC Part21 files, implemented in explicit tool path level, and in manufacturing feature level are presented. The system development and a testing example are given in Section 6, followed by concluding remarks in Section 7.

2- Method overview

Since there is no information about tools, rawpiece and its setup in a G-code, we should supplement them for ensuring successful conversion. And the G-code should be an error-free part program, hopefully, with high-quality, to make the conversion significant.

For example, one simple G-code with different shape of rawpieces will produce different final workpieces (Figure 2). With the following G-code, if a small rawpiece is used, it will make a profile feature; if a large rawpiece, it will make a slot feature. Similarly, the rawpiece's setup location, or its offsets with regard to the programming frame also affects the workpiece's geometry. Therefore the rawpiece's geometry, location, etc. are necessary supplements for the conversion. In fact, these supplements for the conversion roughly correspond to the phase of machining definition for carrying out a CNC machining.

```
G90 G54 G0 X0 Y0 Z100
Y-50
G1 Z-50 F200 S300 M3
X100
Y50
X-100
Y-50
X0
Z100
G0 Y0 M5
M30
```

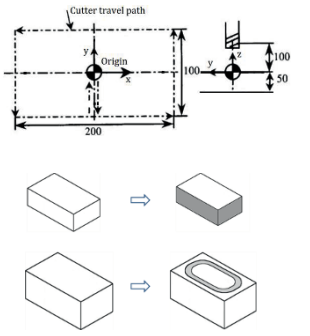

Figure 2: From rawpiece to final workpiece.

In this work, we consider G-code program, information of cutting tools used in the G-code, rawpiece's shape and location. Besides, we should know whether the given G-code is a milling program, or a turning one, as well as the number of axis involved in the program as far as current realization.

Two types of conversion outcomes are proposed: STEP-NC Part21 file in explicit toolpaths (conformance class 1, or CC1) and STEP-NC Part21 file in manufacturing features (CC2). The first type mainly use toolpath features, and can deal with 3 to 5-axis part programs. The second type performs manufacturing feature extraction from the given G-code part program, and it can deal with G-code programs for 2½D machining at present realization. The information flow is illustrated in Figure 3.

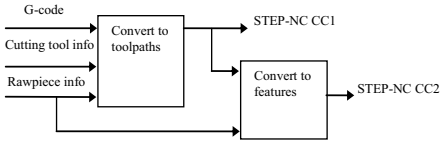

Figure 3: The information flow.

In order to illustrate the method, we use a very simple example as shown in Figure 4a. The case study is a finish milling in one layer to remove a 5mm-depth material on the planar top face of the stock. In this case the only machining feature is the planar face. The toolpath for one layer cutting is shown in Figure 4b, followed by the G-code in Table 1.

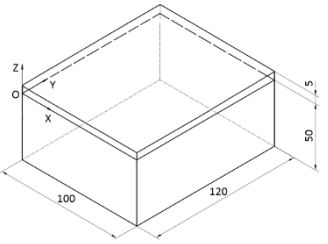

a) The rawpiece

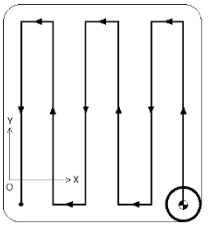

b) The toolpath

Figure 4: Illustration example.

Table 1: G-code for milling the planar face

G54 G90 G21 G40 G49 M5 M9	Y133.50
T1 M6 (Use an endmill, Ø18mm)	X40.60
G43 H1 (Cutter length compensation by 50mm)	Y-13.50
M8 S720 M3	X23.50
G0 X91.90 Y-13.50 Z100.00	Y133.50
Z15.00	X6.40
G1 Z0.00 F240.00	Y-13.50
Y133.50	G0 Z15.00
X74.80	G49 M9 M5
Y-13.50	M30
X57.70	

The functions of any CNC machine can be viewed as a set of canonical machining functions defined by NIST based on ISO 6983 [K1]. If a machine has new functions beyond this standard, one can add new canonical functions. The G-code program is firstly mapped into canonical functions that the machine should execute. Secondly, by analyzing hints (such as tool changes, speed changes) in the canonical functions, workingsteps can be generated. In these workingsteps all operations are treated as freeform operations and features as toolpath features, except those that can be easily attached to operations, like canned cycles. Then toolpath data is converted into the data structure "toolpath" of freeform operations. Thus we can generate STEP-NC Part21 file in explicit toolpaths.

The "toolpath_feature" is introduced in STEP-NC to enable the definition of tool movements not covered by regular machining features (such as pockets, holes, slots, steps). It is a placeholder for explicit toolpaths assigned to the operations associated with it. 3 to 5-axis milling of freeform surfaces typically requires explicit specification of toolpaths. This kind of Part21 file (CC1) still has advantage over G-code. By connecting this information with the high-level operation and feature data, the toolpaths can always be interpreted within their semantic context. They are also provided in a structure which allows to identify the individual toolpath rather than to search through thousands of lines of unstructured code for axis movements.

Finally, we can extract manufacturing features from the toolpath data of the Part21 file by analyzing the machining regions, machining strategies, etc. In this process we need to merge some workingsteps and reorganize them. When achieved, the STEP-NC Part21 file in features and operations can be generated. The final step can be optional according to the needs of each company.

The overall procedures can be summarized as follows. A G-code program is firstly translated into canonical functions, which are then interpreted into a STEP-NC Part21 file (CC1). The CC1 file is further converted into the higher level STEP-NC Part21 file (CC2) after manufacturing feature extraction [**I2**] [**I3**] [**I4**]. If we want to share a G-code program in a higher level, or want to establish a bidirectional information flow between CNC and CAM, we can choose CC2 conversion. Figure 5 shows the overall strategy.

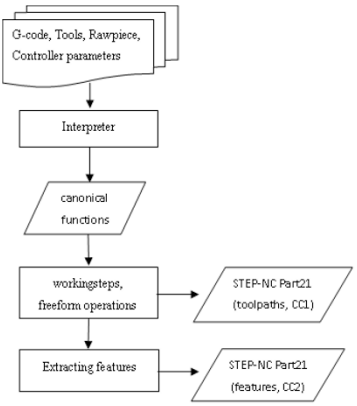

Figure 5: The overall strategy.

3- G-code to canonical functions

3.1 – Canonical functions

Canonical machining functions were defined by NIST with two objectives. First, all the functionality of common 3 to 5-axis machining centers had to be covered by them; for any function a machining center can perform, there has to be a way to tell it to do that function. Second, it should be possible to interpret an ISO 6983/RS274 compatible NC program into canonical function calls.

Canonical functions are atomic commands. Each function produces a single tool motion or a single logical action. NC commands include two types: those for which a single NC command corresponds exactly to a canonical function call, and those for which a single one will be decomposed into several canonical function calls. For instance, G1 (move in a straight line), M8 (turn flood coolant on) are of the first type; G83 (peck drilling) is of the second type.

Some main canonical functions are listed below:

1) Representation: SET_ORIGIN_OFFSETS(); USE_LENGTH_UNITS()
2) Free Space Motion: STRAIGHT_TRAVERSE()
3) Machining Attributes: SELECT_PLANE(); SET_FEED_RATE()
4) Machining Functions: STRAIGHT_FEED(); ARC_FEED()
5) Spindle Functions: SET_SPINDLE_SPEED();
START_SPINDLE_CLOCKWISE();
START_SPINDLE_COUNTERCLOCKWISE();
6) Tool Functions: CHANGE_TOOL(); SELECT_TOOL();
USE_TOOL_LENGTH_OFFSET()
7) Miscellaneous Functions: FLOOD_OFF(); FLOOD_ON()
8) Program Functions: PROGRAM_STOP()

In G-code, canned cycles (G81-G89) are for hole machining operations. A canned cycle is decomposed into its basic moves expressed by the above canonical functions. For example, (G81 X…Y…Z…R…L…) is intended for drilling. Its motions are: preliminary motion(s); move Z-axis at current feedrate to the Z position; Retract Z-axis at traverse rate to clear Z. This work does not handle G-codes programs that have macro-commands. Non-linear G-code program structure, like parallel, selective, non-sequential, are not handled, either.

3.2 – The role of the conversion

In a G-code program, the working coordinate system may change frequently, and the coordinate data may be absolute or relative, and the radius/length compensation may be used. All these are up to the user's choice according to programming convenience. In addition, as in all dialects of G-codes, a line of code may specify several different things to do, such as moving from one place to another along a line/arc, changing the feed rate, starting the spindle turning, etc. The Interpreter reads lines of a G-code one at a time, emulates the execution, and keeps track of the current state of the controller. We use the Interpreter: to check the correctness of the inputting G-code; to unify the coordinates and parameters for a line/arc move with respect to a chosen coordinate system; to determine the correct execution order of the G-code. The Interpreter outputs the following canonical functions as shown in Table 2, for the example G-code. This conversion facilitates greatly the subsequent processes.

Table 2: Canonical functions for milling the planar face

1USE_LENGTH_UNITS(UNITS_MM)	17 STRAIGHT_FEED(91.9, 133.5, 0)
2 SET_ORIGIN_OFFSETS(0, 0, 0)	18 STRAIGHT_FEED(74.8, 133.5, 0)
3 SET_FEED_REFERENCE(CANON_XYZ)	19 STRAIGHT_FEED(74.8, -13.5, 0)
4 STOP_SPINDLE_TURNING()	20 STRAIGHT_FEED(57.7, -13.5, 0)
5 FLOOD_OFF()	21 STRAIGHT_FEED(57.7, 133.5, 0)
6 SPINDLE_RETRACT()	22 STRAIGHT_FEED(40.6, 133.5, 0)
7 USE_TOOL_LENGTH_OFFSET(0)	23 STRAIGHT_FEED(40.6, -13.5, 0)
8 CHANGE_TOOL(ENDMILL_18MM)	24 STRAIGHT_FEED(23.5, -13.5, 0)
9 USE_TOOL_LENGTH_OFFSET(50)	25 STRAIGHT_FEED(23.5,133.5,0)
10 FLOOD_ON()	26 STRAIGHT_FEED(6.4, 133.5, 0)
11 SET_SPINDLE_SPEED(720)	27 STRAIGHT_FEED(6.4, -13.5, 0)
12 START_SPINDLE_CLOCKWISE()	28 STRAIGHT_TRAVERSE(6.4,-13.5,15)
13 STRAIGHT_TRAVERSE(91.9,-13.5,100)	29 STOP_SPINDLE_TURNING()
14 STRAIGHT_TRAVERSE(91.9,-13.5,15)	30 FLOOD_OFF()
15 SET_FEED_RATE(240)	31 SPINDLE_RETRACT()
16 STRAIGHT_FEED(91.9, -13.5, 0)	32 PROGRAM_END()

4- Canonical functions to STEP-NC Part21

A STEP Part 21 file contains two sections: the header section and the data section. Since the conversion is only relevant to the data section, the following will only consider the data section of a Part21 file. The data section has the following main types of entities: cutting tools; definitions and their setups of rawpieces (usually only one); one project, workplans and workingsteps; manufacturing features; machining operations; technology, functions and machining strategies; and placements, planes, dimensions, etc. The entities for tools and rawpieces can be written in the Part21 file directly as per the inputting information since they have less connection involved with other entities.

We devised a canonical function interpreter for the generation of other entities. In the beginning a "struct" buffer is defined to keep track of the controller status, such as the units, the security plane, the coolant switch, feed rate, spindle speed, the current tool and its position. The interpreter maintains this buffer when it runs. The interpreter emulates the execution of the canonical functions one by one: if it meets a "STRAIGHT_TRAVERSE", a "rapid movement" entity is created; if it meets one or several consecutive "STRAIGHT_FEED"s or "ARC_FEED"s, a "machining workingstep" which includes a freeform operation is created. The parameters of these functions are used as cutter location data stored in the toolpath list of the freeform operation. Of course sometimes computation is needed for obtaining the toolpaths. Other data, such as technology and machining functions can be inferred from the buffer. The entities of "toolpath features" here are used for information only. For cycle operations, hole features, not toolpath features are used. Thus when the emulation comes to an end, we can get a STEP-NC Part21 CC1 file in explicit toolpaths (cf. Appendix A.1, here only the data section is shown).

5- STEP-NC Part21 file to manufacturing features

This phase deals with mainly the extraction of manufacturing/machining features from toolpaths based on the previous Part21 CC1 file. Yan [YY1] adopts a Z-map based method; Other type of method is: first build a CAD model from a simulated or cut model usually in a STL file, then using conventional methods do the recognition [**AY1**, SP1]. Here we carry out the work based on toolpaths and tool's geometry. In this phase, one freeform operation

corresponds to one machining workingstep. Many freeform operations might correspond to one manufacturing feature because often there are several layers of a rough machining and finish machining, which are needed to make a final feature. So one major procedure is to merge those freeform operations that machine the same feature, as well as the relevant workingsteps and rapid movements.

The feature types we are coping with are the machining features defined in ISO 14649 Part 10[**12**]. The procedure for processing phase 1 is detailed as follows.
Step 1: From a freeform operation, get the tool and the toolpath list. If no freeform operations left, end phase 1.
Step 2: Analyse the feature type by tool type first. If the tool type is for drilling, the feature is a round hole, and note down the diameter and the axis. They can be used to identify the same hole in other operations; if the tool is a facemill, the feature is a planar_face; if the tool is a T-slot_mill or dovetail_mill or woodruff_keyseat_mill, the feature is obviously a slot. Go to Step 1.
Step 3: If the tool is an endmill (including tapered_endmill, ball_endmill, bullnose_endmill), then analyse the x, y, z-values of the CL (cutter location) data in the toolpath list.
If z-value varies and x, y-values keep constant, it is milling a hole feature. Note down the diameter and axis. Go to Step 1.
Step 4: If x, y, z-values are all varying, it is a freeform milling operation to make a region (surface). Go to Step 6.
Step 5: If z-value keeps constant and x, y-values vary, it is a 2½D milling operation.
Step 6: Compare the toolpath list with the one of the next freeform operation, for each CL-data, if the corresponding x, y-values are the same and the z-value is decreased, the two operations are cutting different layers of the same feature, then they can be merged. For a region feature, go to Step 1.

After the above processing, extracted features are easily found; processing phase 2 deals with the remaining toolpaths to find planar_faces, general_outside_profiles, closed_pockets and open_pockets. A step feature is a special type of open_pocket that has only one wall face (the open boundary is a line segment). A slot feature is also a special type of pocket, whose profile shape has a constant width. The main grounds to find features in phase 2 are the cutting area (the tool's covering region for cutting movements, Figure 3b) and the milling strategy, which are computed based on toolpath CL data.

Common 2½D milling strategies are shown in Figure 6. Unidirectional milling is going from one side to the other, then lifting the tool and going back to the starting point. Bidirectional milling is in a zigzag fashion, i.e. going from one side to the other and back. Center milling is along the center of the feature. It is often used for milling along the center of a slot. Contour milling, which is a typical strategy for pocket milling, is in several paths following the contour of the feature. Contour spiral milling is similar to contour parallel milling, with the exception, that in this case the milling path is a truly spiral path rather than concentric paths which are connected by an orthogonal movement. In general practices, the relationship between features and milling strategies is as follows.

"closed_pocket", "round_hole" ——contour parallel milling, contour spiral milling.
"open_pocket" —— bidirectional/unidirectional milling.
"planar_face" —— bidirectional/unidirectional milling, contour parallel milling (outside-in).
"step" —— bidirectional/unidirectional milling.
"slot" —— center milling.
"general_outside_profile" —— contour parallel milling.

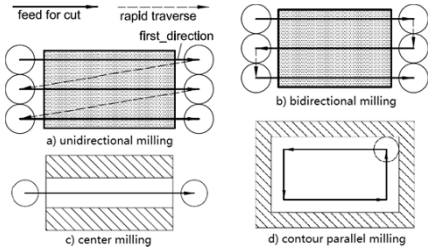

Figure 6: Common milling strategies.

In phase 2 the method is illustrated as in Figure 7. In 2½D manufacturing, the computation of the cutting area and milling strategy from toolpath CL data is not difficult since they are 2D geometries. The milling strategy can also be used for checking the correctness of the extracted features. After characterizing the feature types, the profiles of features are obtained from the boundaries of the cutting areas, which are determined by toolpaths and cutters' geometry.

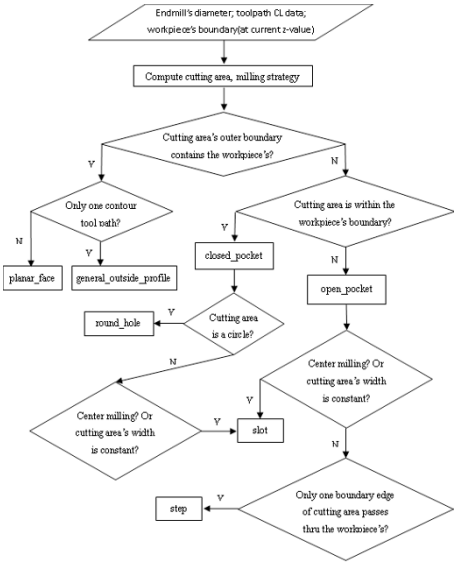

Figure 7: Milled feature extraction.

Sometimes the feature profiles thus obtained need to be fixed a bit if there is finish cutting or supplementary cutting to make the feature. For open features, such as planar_faces, steps, open_pockets, their profiles need not to be exact, as

long as the open parts of their profiles are outside the workpiece's boundary. This requirement can simplify the computation. Some cutting parameters, as required by the machining technology in STEP-NC, such as radial/axial depths, can also be inferred from the milling strategy.

The converted STEP-NC Part21 CC2 file in manufacturing features is shown in appendix A.2 (only the data section shown). In this file the only feature is "PLANAR_FACE".

6- Implementation and examples

The entities of STEP-NC Parts 10, 11, 111 [**I2**] [**I3**] [**I4**] are mapped to C++ classes. The syntax of G-code and Part21 files is checked during the generation. The conversion of G-codes into canonical functions, and canonical functions into STEP-NC Part21 (CC1) can cope with 3 to 5-axis milling programs. The method for generating STEP-NC Part21 (CC2) is applied for 2½D G-code programs. In a future work, entities of STEP-NC Parts 12,121 (turning) will be mapped to C++ classes, so that turning programs can be also processed.

A test example is given in Figure 8. It has 3 machining features: a planar face, a round hole and a closed pocket. A section of the resulting Part 21 CC2 file is shown as follows, and part of the initial G-code program is shown in appendix A.3.

```
.....
#10= MACHINING_WORKINGSTEP('WS FINISH PLANAR FACE1',#60,#20,#31,$);
#11= MACHINING_WORKINGSTEP('WS DRILL HOLE1',#60,#21,#32,$);
#12= MACHINING_WORKINGSTEP('WS REAM HOLE1',#60,#21,#33,$);
#13= MACHINING_WORKINGSTEP('WS ROUGH POCKET1',#60,#22,#34,$);
#14= MACHINING_WORKINGSTEP('WS FINISH POCKET1',#60,#22,#35,$);

#20= PLANAR_FACE('PLANAR FACE',#2,(#31),#64,#65,#23,#24,$,());
#21= ROUND_HOLE('HOLE1 D=22MM',#2,(#32,#33),#67,#70,#111,$,#25);
#22= CLOSED_POCKET('POCKET1',#2,(#34,#35),#69,#71,(),$,#26,$,#112,#27);
#23= LINEAR_PATH($,#110,#83);
#24= LINEAR_PROFILE($,#101);
#25= THROUGH_BOTTOM_CONDITION();
#26= PLANAR_POCKET_BOTTOM_CONDITION();
#27= RECTANGULAR_CLOSED_PROFILE($,#113,#114);

#31= PLANE_FINISH_MILLING($,$,'FINISH PLANAR FACE1',15.00,$,#40,#50,#51,$,
    #52,#52,#53,2.50,$);
#32= DRILLING($,$,'DRILL HOLE1',15.00,$,#44,#54,#51,$,$,$,$,$,#55);
#33= REAMING($,$,'REAM HOLE1',15.00,$,#47,#54,#51,$,$,$,$,$,#56,.T.,$,$);
#34= BOTTOM_AND_SIDE_ROUGH_MILLING($,$,'ROUGH POCKET1',15.00,$,#40,
    #57,#51,$,$,$,#58,6.50,5.00,1.00,0.50);
#35= BOTTOM_AND_SIDE_FINISH_MILLING($,$,'FINISH POCKET1',15.00,$,#40,#57,
    #51,$,$,$,#59,2.00,10.00,$,$);
.....
```

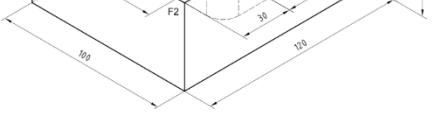

Figure 8: A test example.

7- Conclusions

While STEP-NC is gaining popularity in the manufacturing industry, the issue of legacy G-code program conversion is arising. This paper proposes an overall approach for the conversion of a G-code program into STEP-NC. The conditions for a valid conversion are detailed. This approach includes three main phases: first, G-code program is converted into canonical functions; then, canonical functions are analyzed to create a Part21 file in explicit toolpaths (CC1); and finally, by applying machining feature recognition techniques, the Part21 file is rewritten into a higher level Part21 file in manufacturing features (CC2). Although, 2½D machining features can be recognized, and the machining feature recognition approach developed here have no feature interaction issues, the problem of merging freeform operations that make the same feature has to be solved. Future work will include: (a) detecting turning or milling machining type should be automatic, as well as the number of axis involved in the program, (b) the extension of the approach to handle turning/mill-turn G-code programs, (c) to increase the capacity of manufacturing feature recognition, especially for the case of region features.

Acknowledgements

This work is a part of the ANGEL FUI project recently funded by the French Inter-ministerial Fund and endorsed by top French competiveness clusters (SYSTEMATIC PARIS REGION "Systems & ICT", VIAMECA "Advanced Manufacturing" and ASTECH "Aeronautics & Space").

8- References

[AY1] Anwer N., Yang Y., Zhao H., Coma O. and Paul J. Reverse engineering for NC machining simulation. In IDMME'2010-Virtual Concept 2010, Bordeaux, France, 2010.

[I1] ISO 14649 Part 1: Overview and fundamental principles, 2002.

[I2] ISO 14649 Part 10: Process general data, 2002.

[I3] ISO 14649 Part 11: Process data for milling, 2002.

[I4] ISO 14649 Part 111: Tools for milling, 2002.

[K1] Kramer T. R. The NIST RS274/NGC Interpreter—Version 3. In ISD of NIST, Gaithersburg, 2000.

[SP1] V.B. Sunil and S.S. Pande. Automatic recognition of features from freeform surface CAD models. In Computer-Aided Design 40:502–517, 2008.

[SS1] Shin S. J., Suh S. H. and Stroud I. Reincarnation of G-code based part programs into STEP-NC for turning applications. In *Computer-Aided Design* 39 (1): 1–16, 2007.

[YY1] X. Yan, K. Yamazaki and J. Liu. Recognition of machining features and feature topologies from NC programs. In *Computer-Aided Design*, 32: 605-616, 2000.

[ZN1] X. Zhang, A. Nassehi, M. Safaieh and S.T. Newman. Process comprehension for shopfloor manufacturing knowledge reuse. In *Int. J. of Prod. Research*, 51:1-15, 2013

Appendix

A.1 – Part21 file (CC1)

```
DATA;
#0= PROJECT('EXECUTE EXAMPLE1',#1,(#2),$,$,$);
#1= WORKPLAN('MAIN WORKPLAN',(#10, ,#13),$,#3,$);
#2= WORKPIECE('CUBOID WORKPIECE',$,0.01,$,$,$,(#91,#92,#93,#94));
#3= SETUP('SETUP1',#62,#60,(#4));
#4= WORKPIECE_SETUP(#2,#63,$,$,());
#10= MACHINING_WORKINGSTEP('WS FINISH PLANAR FACE1',#60,#20,#30,$);
#13= RAPID_MOVEMENT('rapid after milling plane', #60,#401,$);
#20= TOOLPATH_FEATURE('FACE1:LAYER1',#2,(#30),#63,#64);
#30= FREEFORM_OPERATION(#101,$,'FINISH FACE1 L1',15.00,$,#40,#50,#51,$,$,$,$);

#40= MILLING_CUTTING_TOOL('ENDMILL_18MM',#41,(#43),80.00,$,$);
#41= TAPERED_ENDMILL(#42,4,.RIGHT.,.F.,$,$);
#42= MILLING_TOOL_DIMENSION(18.00, $,$, 29.0, 0.0, $,$);
#43= CUTTING_COMPONENT(80.00,$,$,$,$);
#50= MILLING_TECHNOLOGY(0.04,.TCP.,$,-12.00,$,.F.,.F.,.F.,$);
#51= MILLING_MACHINE_FUNCTIONS(.T.,$,$..F.,$,(),.T.,$,$,());

#60= PLANE('SECURITY PLANE',#61);
#61= AXIS2_PLACEMENT_3D('PLANE1',#90,#81,#82);
#62= AXIS2_PLACEMENT_3D('SETUP1',#80,#81,#82);
#63= AXIS2_PLACEMENT_3D('CUBOID WORKPIECE',#80,#81,#82);
#64= PLANE('PLANAR FACE1:DEPTH PLANE',#65);
#65= AXIS2_PLACEMENT_3D('PLANAR FACE1',#95,#81,#82);
#80= CARTESIAN_POINT('ORIGIN',(0.00,0.00,0.00));
#81= DIRECTION('K-VECTOR',(0.00,0.00,1.00));
#82= DIRECTION('I-VECTOR',(1.00,0.00,0.00));
#90= CARTESIAN_POINT('SECURITY PLANE:LOCATION',(0.00,0.00,100.00));
#91= CARTESIAN_POINT('CLAMPING_P1',(0.00,20.00,25.00));
#92= CARTESIAN_POINT('CLAMPING_P2',(100.00,20.00,25.00));
#93= CARTESIAN_POINT('CLAMPING_P3',(0.00,100.00,25.00));
#94= CARTESIAN_POINT('CLAMPING_P4',(100.00,100.00,25.00));
#95= CARTESIAN_POINT('PLANAR FACE1:DEPTH ',(0.00,0.00,0.00));

#101= TOOLPATH_LIST((#102));
#102= CUTTER_LOCATION_TRAJECTORY(.T.,.TRAJECTORY_PATH.,$,#50,$,$,#103,$,$);
#103= POLYLINE('1st cut of planar FACE1',(#110,#111,#112,#113,#114,#115,#116,
    #117,#118,#119,#120,#121,#122));
#110= CARTESIAN_POINT('',(91.90, -13.50, 15.00));
#111= CARTESIAN_POINT('',(91.90, -13.50, 0.00));
#112= CARTESIAN_POINT('',(91.90, 133.50, 0.00));
#113= CARTESIAN_POINT('',(74.80, 133.50, 0.00));
#114= CARTESIAN_POINT('',(74.80, -13.50, 0.00));
#115= CARTESIAN_POINT('',(57.70, -13.50, 0.00));
#116= CARTESIAN_POINT('',(57.70, 133.50, 0.00));
#117= CARTESIAN_POINT('',(40.60, 133.50, 0.00));
#118= CARTESIAN_POINT('',(40.60, -13.50, 0.00));
#119= CARTESIAN_POINT('',(23.50, -13.50, 0.00));
#120= CARTESIAN_POINT('',(23.50, 133.50, 0.00));
#121= CARTESIAN_POINT('',(6.40, 133.50, 0.00));
#122= CARTESIAN_POINT('',(6.40, -13.50, 0.00));

#401=TOOLPATH_LIST((#402));
#402= CUTTER_LOCATION_TRAJECTORY(.T.,.TRAJECTORY_PATH.,$,$,$,$,#403,$,$);
#403= POLYLINE('rapid after milling plane',(#410,#411));
#410= CARTESIAN_POINT('',(6.40, -13.50, 0.00));
#411= CARTESIAN_POINT('',(6.40, -13.50, 15.00));
ENDSEC ;
```

A.2 –Part21 file (CC2)

```
DATA;
#0= PROJECT('EXECUTE EXAMPLE1',#1,(#2),$,$,$);
#1= WORKPLAN('MAIN WORKPLAN',(#10),$,#3,$);
#2= WORKPIECE('CUBOID WORKPIECE',$,0.01,$,$,$,(#91,#92,#93,#94));
#3= SETUP('SETUP1',#62,#60,(#4));
#4= WORKPIECE_SETUP(#2,#63,$,$,());
#10= MACHINING_WORKINGSTEP('WS FINISH PLANAR FACE',#60,#20,#30,$);

#20= PLANAR_FACE('PLANAR FACE1',#2,(#30),#64,#65,#21,#22,$,());
#21= LINEAR_PATH($,#23,#83);
#22= LINEAR_PROFILE($,#25);
#23= TOLERANCED_LENGTH_MEASURE(120.00,#24);
#24= PLUS_MINUS_VALUE(0.30,0.30,3);
#25= NUMERIC_PARAMETER('PROFILE LENGTH',100.00,'MM');

#30= PLANE_FINISH_MILLING($, $, 'FINISH PLANAR FACE1', 15.00, $, #40, #50, #51, $,
#52, #52, #53, 2.50, $);

#40= MILLING_CUTTING_TOOL('ENDMILL_18MM',#41,(#43),80.00,$,$);
#41= TAPERED_ENDMILL(#42,4,.RIGHT.,.F.,$,$);
#42= MILLING_TOOL_DIMENSION(18.00, $,$, 29.0, 0.0, $,$);
#43= CUTTING_COMPONENT(80.00,$,$,$,$);

#50= MILLING_TECHNOLOGY(0.04,.TCP.,$,-12.00,$,.F.,.F.,.F.,$);
#51= MILLING_MACHINE_FUNCTIONS(.T.,$,$..F.,$,(),.T.,$,$,());
#52= PLUNGE_TOOLAXIS($);
#53= BIDIRECTIONAL_MILLING(0.05,.T.,#83,.LEFT.,$);

#60= PLANE('SECURITY PLANE',#61);
#61= AXIS2_PLACEMENT_3D('PLANE1',#90,#81,#82);
#62= AXIS2_PLACEMENT_3D('SETUP1',#80,#81,#82);
#63= AXIS2_PLACEMENT_3D('CUBOID WORKPIECE',#80,#81,#82);
#64= AXIS2_PLACEMENT_3D('PLANAR FACE1',#95,#81,#82);
#65= PLANE('PLANAR FACE1-DEPTH PLANE',#66);
#66= AXIS2_PLACEMENT_3D('PLANAR FACE1',#96,#81,#82);
#80= CARTESIAN_POINT('ORIGIN',(0.00,0.00,0.00));
#81= DIRECTION('K-VECTOR',(0.00,0.00,1.00));
#82= DIRECTION('I-VECTOR',(1.00,0.00,0.00));
#83= DIRECTION('J-VECTOR',(0.00,1.00,0.00));
#90= CARTESIAN_POINT('SECURITY PLANE:LOCATION',(0.00,0.00,100.00));
#91= CARTESIAN_POINT('CLAMPING_P1',(0.00,20.00,25.00));
#92= CARTESIAN_POINT('CLAMPING_P2',(100.00,20.00,25.00));
#93= CARTESIAN_POINT('CLAMPING_P3',(0.00,100.00,25.00));
#94= CARTESIAN_POINT('CLAMPING_P4',(100.00,100.00,25.00));
#95= CARTESIAN_POINT('PLANAR FACE1:LOCATION ',(0.00,0.00,5.00));
#96= CARTESIAN_POINT('PLANAR FACE1:DEPTH ',(0.00,0.00,-5.00));
ENDSEC;
```

A.3 –Part of the initial G-code for the test

G54 G90 G21 G40 G49 M5 M9	(To rough pocket in 5 layers, 5.9/layer)
T1 M6 (Use an endmill, diameter 18mm)	(First 2 blocks: to run helical approach)
G43 H1 (Length compensation by 50mm)	G2 X77.2 Y55. Z-5.9 I5.246 J4.932
M8 S720 M3	G2 X70. Y55. I-3.60 J0.
G0 X91.9 Y-13.5 Z100.	G1 Y90.
	X75.
(To finish top face of rawpiece in 2 layers)	Y50.
Z15.	X65.
G1 Z2.5 F240. (1st layer, depth 2.5mm)	Y90.
Y133.5	X70.
X74.8	Y95.
Y-13.5	X80.
X57.7	Y45.
Y133.5	X60.
X40.6	Y95.
Y-13.5	X70.
X23.5	Y100.
Y133.5	X85.
X6.4	Y40.
Y-13.5	X55.
G0 Z15.	Y100.
X91.9	X70.
G1 Z0. (2nd layer, depth 2.5mm)	Z0.
Y133.5	G0 X69.532 Y47.815 (End of 1st layer)
X74.8	…… (Code of next 4 layers omitted)
Y-13.5	
X57.7	(To finish pocket in 6 layers. 5mm/layer)
Y133.5	(Bottom allowance 0.5, side allowance 1)
X40.6	G0 Z30.
Y-13.5	X74.890 Y60.285
X23.5	Z15.
Y133.5	(First 2 blocks: to run helical approach)
X6.4	G2 X77.2 Y55. Z-2. I-4.891 J-5.285
Y-13.5	G2 X70. Y55. I-3.60 J0.
	G1 Y93.
(To drill and ream a thru hole)	X78.
G0 Z15.	Y47.
G49 M9 M5	X62.
T2 M6 (Use a spiral drill, diameter 20mm)	Y93.
G43 H2 (Length compensation by 70mm)	X70.
M8 M3 F900. S720	Y101.
G0 Z30.	X85.
G90 G99 G81 X20. Y60. Z-18. R10.	G2 X86. Y100. I0. J-1.
G99 G81 X20. Y60. Z-36. R10. F1800.	G1 Y40.
G99 G81 X20. Y60. Z-60. R10. F1350.	G2 X85. Y39. I-1. J0.
G1 Z10. F1800.	G1 X55.
G80 G49 M5 M9 (end of drilling cycle)	G2 X54. Y40. I0. J1.
T3 M6 (Use a reamer, diameter 22mm)	G1 Y100.
G43 H3 (Length compensation by 50mm)	G2 X55. Y101. I1. J0.
M8 M3 S1080	G1 X70.
G90 G99 G85 X20. Y60. Z-60. R10.	Z0. (End of 1st layer)
G80 G49 M5 M9 (End of reaming cycle)	.....(Code of rest of layers omitted)
	G2 X55. Y101. I1. J0. (now Z-30.00)
(To cut a pocket, rough & finish)	G1 X70.
T1 M6 (Use an endmill, diameter 18mm)	Z15. (End of finishing)
G43 H1 (Length compensation by 50mm)	M30
M8 S1200 M3 F2400.	
G0 Z30.	
X64.754 Y50.069	
Z15.	

Article 042-p-67

Modeling of the chip geometry in orbital drilling

Rey.P.A, Moussaoui.K, Senatore.J, Landon.Y

Institut Clément Ader (ICA) Université de Toulouse ; INSA, UPS, Mines Albi, ISAE
Bât 3R1, 118 route de Narbonne, F-31062 Toulouse Cedex 9, France.
Phone: 05 61 55 84 26
pierre-andre.rey@univ-tlse3.fr

Abstract: The orbital drilling is a complex operation. Due to the tool trajectory, which is helical, chip thickness is highly variable. This is why the cutting forces are very difficult to estimate.
The aim of this study is to develop a model to predict cutting forces depending on the tool geometry and cutting conditions in order to control the final quality of the machined hole. At first, the geometry of the chip is modeled taking into account the parameters defining the trajectory and the tool. A cutting force model based on the instantaneous chip thickness is then set up. An experimental part validates the cutting force model through measures of cutting force made during orbital drilling tests.

Keywords: Orbital drilling, TiAl6V4, tool geometry, cutting forces,

1. Introduction

The orbital drilling, also called helical milling, is a process notably used in the aeronautical industry. It is very different from the axial drilling. It consists in machining a hole with a tool which has a smaller diameter, driven on a helical trajectory (Figure 1).

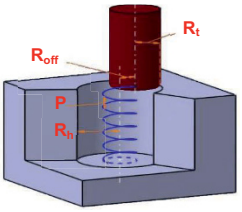

Figure 1 Orbital drilling's trajectory

This process is used especially because it generates low cutting forces **[Lutze, 2008]**. As a consequence, the burr formation at the entry and at the exit of the hole is largely reduced, and also the risk of delamination when drilling composite materials is highly reduced. **[Denkena and al., 2008] [Brinksmeier et al., 2008]**. Operations such as cleaning or deburring are then considerably reduced.

For the cutting force model in orbital drilling, three approaches are possible: the numerical approach, the analytical and the semi analytical approach. The numerical approach used in the work of Lorong **[Lorong et al, 2002]** aims to simulate chip formation by a finite element study. Analytics approaches as Merchant's model **Merchant, 1945]** or Oxley's model **[Oxley, 1989]** consist to describe the most physically possible the cutting phenomenon in order to calculate the cutting forces. The semi-analytics approaches, also called mechanistic approaches, are the most used one to calculate machining cutting forces and particularly when the process is complex **[Fontaine, 2004],** like helical milling. This approach is based on analytics approaches by simplifying all the parameters of the tool geometry or of the tool/workpiece couple by a constant experimentally defined with calibration test.

2. Modeling of orbital drilling

2.1. Geometrics settings of the orbital drilling

In order to be able to develop a model of the chip geometry, the input data of the model and the references that are necessary to form the equation, need to be previously defined.

1.1.1 The defining data of the tool's geometry:

The global tool geometry (Figure 2) is generically defined using the following parameters:

- Tool outside radius: R_t
- Number of tooth: Z
- Number of tooth with center cut: Z_{cc}
- Corner radius: R_b
- Radius without center cut: R_{cc}
- Tool cutting edge angle: κ_r

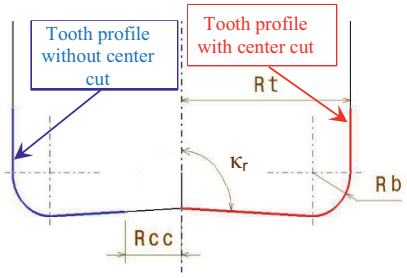

Figure 2 : Tool geometry

1.1.2 Cutting's parameters:

In order to determine the chip thickness, it is necessary to define the cutting parameters. The tool feed, along helical trajectory, can be decomposed in an axial feed f_a and a tangential feed f_t.
Drilling radius: R_h
Interpolation radius, called offset: $R_{off} = R_h - R_t$
Pitch (mm): P
Cutting speed (m/min): Vc
Axial feed (mm/rev): f_a
Tangential feed (mm/rev): f_t
Axial feed per tooth: $f_{za} = \frac{f_a}{z}$
Tangential feed per tooth: $f_{zt} = \frac{f_t}{z}$

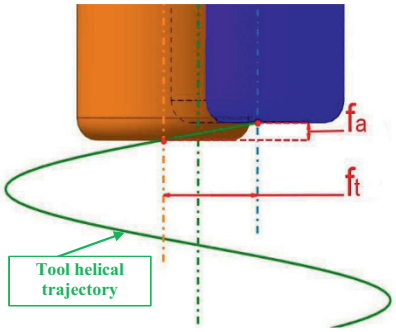

Figure 3 : Feed definition.

1.1.3 References definition:

Hole center to drill: HL
Machine's reference: this reference is fixed.

$$\boldsymbol{R_m} = (\boldsymbol{HL}, \boldsymbol{X}, \boldsymbol{Y}, \boldsymbol{Z})$$

Orbital reference: this reference permit to define the tool's positions « i » on the helical trajectory.

$$\boldsymbol{R_{oi}} = (\boldsymbol{HL}, \boldsymbol{X_{oi}}, \boldsymbol{Y_{oi}}, \boldsymbol{Z})$$

With: $\begin{vmatrix} \boldsymbol{X_{oi}} = cos\,\theta_i.\boldsymbol{X} + sin\,\theta_i.\boldsymbol{Y} \\ \boldsymbol{Y_{oi}} = -sin\,\theta_i.\boldsymbol{X} + cos\,\theta_i.\boldsymbol{Y} \end{vmatrix}$

The angle θ_i defines the tool angular position considered in the machine reference. The tool center position in position « i » is called CL_i, at a distance R_{off} to HL.

Tool reference: This reference can get the location of every points of the tool « i » in the orbital reference.

$$\boldsymbol{R_t} = (\boldsymbol{CL_i}, \boldsymbol{X_{ci}}, \boldsymbol{Y_{ci}}, \boldsymbol{Z})$$

With: $\begin{vmatrix} \boldsymbol{X_{ci}} = cos\,\varphi_i.\boldsymbol{X_{oi}} + sin\,\varphi_i.\boldsymbol{Y_{oi}} \\ \boldsymbol{Y_{ci}} = -sin\,\varphi_i.\boldsymbol{X_{oi}} + cos\,\varphi_i.\boldsymbol{Y_{oi}} \end{vmatrix}$

The angle φ_i defines the angular position of considerate point of the tool in the orbital reference

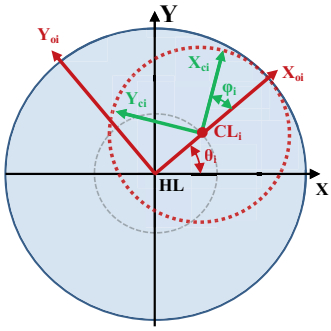

Figure 4 References definition

2.2. Representative function of cutting edge profile

In order to calculate the chips section, it's necessary to define the cutting edge profile. The function $H_k(r)$ is established, to give the elevation of each cutting edge point versus radius r. The lowest tool point « k » is defined at the elevation Z = 0. This function is decomposed into several successive functions, to take into consideration the different tool geometries.

Examples, the evolution of the function $H_k(r)$ for a tooth without center cut, is represented Figure 5.

- If $0 < r < R_{cc}$:

$$H_k(r) = d$$

d is a value arbitrarily set to ensure the non-participation of the area during the machining.

- If $R_{cc} < r < R_t - R_b$:

$$H_k(r) = [r - (R_t - R_b)].tan\left(\frac{\pi}{2} - \kappa_r\right)$$

- If $R_t - R_b < r < R_t$:

$$H_k(r) = R_b - \sqrt{{R_b}^2 - [r - (R_t - R_b)]^2}$$

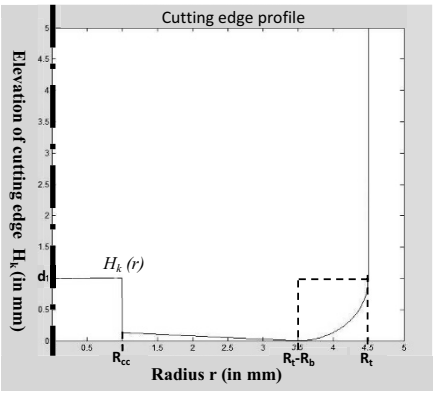

Figure 5 : Representation of the cutting edge profile « k » without cutting tool center

2.3. Calculation of the machined chip section by a tooth

Hypothesis:

As the cutting speed is largely higher than the tool feed speed, two simplifying hypothesis are made:

- The tooth trajectory is considered circular (cycloid neglected) **[Seconds et al., 2006]**
- The calculation of volume machined by the tool at the present moment is the result of a Boolean subtraction operation between the volume of the machined work piece at the previous moment and the volume envelope of the tool, the tool being positioned on its trajectory.

Therefore, to calculate the chip section machined by a tool tooth « i » at the present time (the tool identified by its tool center's point $\mathbf{CL_i}$) two calculation steps are made:

First, each point A_i belonging to the envelope surface of the tool « i » is detected in $\boldsymbol{R_{oi}}$ from its coordinates (X_{Ai}, Y_{Ai}, Z_{Ai}) in function of r_{Ai} et φ_i ($r_{Ai} \epsilon [0, R_t]$, $\varphi_i \epsilon [0, 2\pi]$), and the function H_k applied at the tool « i » :

$$\boldsymbol{A_i} \begin{cases} X_{Ai}(r_{Ai}, \varphi_i) = r_{Ai}.cos\ \varphi_i \\ Y_{Ai}(r_{Ai}, \varphi_i) = r_{Ai}.sin\ \varphi_i \\ Z_{Ai}(r_{Ai}, \varphi_i) = H_i(r_{Ai}) \end{cases}$$

The set of the points A_i for a constant φ_i , represent the tooth where the chip section is assessed on.

Then, to identify the surface location previously machined on each point A_i, all the locations of the tool that interve before the location « i » on a complete orbit revolution are considered. It will then be possible to estimate the height of the machined material at the point A_i. Each considered previous location is identified by its tool center point $\mathbf{CL_k}$.

The difference of altitude following $\boldsymbol{Z}$ between two tool locations $\mathbf{CL_i}$ and $\mathbf{CL_k}$ is called H_{ki}. Knowing that the tool describes a helical trajectory characterized by its pitch P (Figure 3), the height H_{ki} is defined according to the relative angular position of $\mathbf{CL_i}$ and $\mathbf{CL_k}$ on the trajectory characterized by θ_{ki} (Figure 6):

$$H_{ki}(\theta_{ki}) = P - \frac{P \times \theta_{ki}}{2 \times \pi}$$

Then, for each tool point A_i considered, the set of the point s A_k of which the coordinates in the locator $\boldsymbol{R_{oi}}$ are such that $(X_{Ak} = X_{Ai}, Y_{Ak} = Y_{Ai})$ are identified. The coordinate Z_{Ak} of the point A_k can be calculated through the function H_k :

$$\boldsymbol{A_k} \begin{cases} X_{Ak}(r_{Ai}, \varphi_i) = X_{Ai} \\ Y_{Ak}(r_{Ai}, \varphi_i) = Y_{Ai} \\ Z_{Ak}(r_{Ak}, \theta_{ki}) = H_k(r_{Ak}) + H_{ki}(\theta_{ki}) \end{cases}$$

For this the radius r_{Ak} has to be previously determined. From Figure 6, by considering the triangle(CL_k, A_k, HL) :

$$r_{Ak}(r_{Ai}, \varphi_i, \theta_{ki}) = \sqrt{\left| {r_{ki}}^2 + {R_{off}}^2 - 2 \times R_{off} \times r_{ki} \times cos(\theta_{ki} - \alpha) \right|}$$

With: $\alpha(r_{Ai}, \varphi_i) = cos^{-1}\left(\frac{{r_{ki}}^2 + {R_{off}}^2 - {r_{Ai}}^2}{2 \times r_{ki} \times R_{off}}\right)$

And by considering the triangle(A_i, HL, CL_i) :

$$r_{ki}(r_{Ai}, \varphi_i) = \sqrt{\left| {r_{Ai}}^2 + {R_{off}}^2 - 2 \times R_{off} \times r_{Ai} \times cos(\pi - \varphi_i) \right|}$$

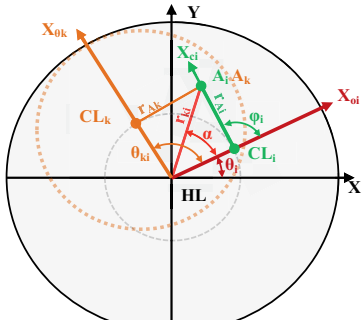

Figure 6 Locating a tool "k" relative to the tool "i"

For each point A_i considered, points A_k for every tool location « k » of the previous orbit revolution are calculated. To determinate the location of the machined surface, the point A_k with the weakest altitude is kept and called S_k.

$$\boldsymbol{S_k} \begin{cases} X_{Sk}(r_{Ai}, \varphi_i) = X_{Ak} \\ Y_{Sk}(r_{Ai}, \varphi_i) = Y_{Ak} \\ Z_{Sk}(r_{Ai}, \varphi_i) = \min\limits_{0 \le \theta_{ki} \le 2\pi} (Z_{Ak}) \end{cases}$$

The chip section on a tooth is then obtained by plotting the set of points A_i and the associated points S_k, for a fixed angle φ_i (representing a tooth of the tool) and for $r_{Ai} \epsilon [0, R_t]$ (Figure 7).
This section is then split into trapezoids of thickness h_k and width b_k.
The thickness h_k is the normal distance to the tool profile between the profile A_i and the previously machined surface S_k, it represents the chip thickness.
The width b_k is the distance between points A_i, it is set arbitrarily.

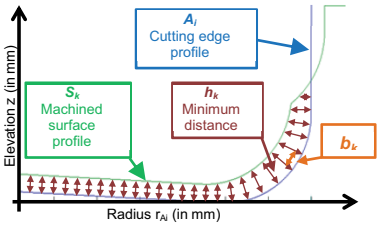

Figure 7 : Decomposition of the chip section

If the decomposition is sufficiently thin (small width b_k compared to the radius of the tool), each trapezoid can be approximated and simplified by a rectangle. The chip section S_c can then be written:

$$S_c(\varphi_i) = \sum_{r_{Ai}=0}^{Rt} b_k(r_{Ai}, \varphi_i).h_k(r_{Ai}, \varphi_i)$$

2.4. Calculation of the cutting force

The chip section in each moment being determined, the forces applied on the tool during drilling can be modeled.
In this article, only the modeling of the cutting force normal to the chip section is presented and discussed. This effort is the most important and is the main cause of tool bending.
The other two components can be modeled in the same way.
The modeling approach is semi-analytical [Merchant, 1945], which gives for the same tool/work piece couple:

$$F_{cut} = K_c \times b \times h$$

Where K_c is a specific cutting coefficient that will remain constant for the first part of the study and will be identified with calibration tests.

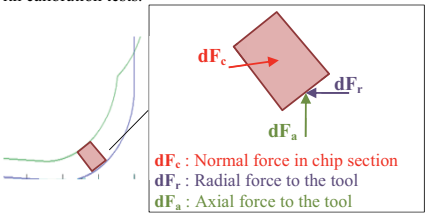

Figure 8 : Forces applied on the tool for a chip section

This model is applied to each trapezoid of the chip section and then summed to obtain the total cutting force when the tooth is in position φ_i.

$$dF_{c\,zi}(r_{Ai}, \varphi_i) = K_c \times b_k(r_{Ai}, \varphi_i) \times h_k(r_{Ai}, \varphi_i)$$

$$F_{c\,zi}(\varphi_i) = \sum_{r_{Ai}=0}^{Rt} dF_c(r_{Ai}, \varphi_i)$$

The evolution of the cutting force of a tooth on a tool revolution is calculated by varying φ_i from 0 to 2π (Figure 9).

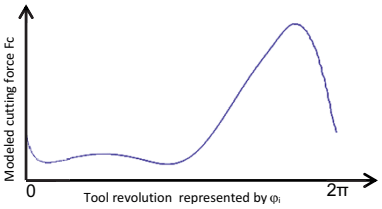

Figure 9 : Evolution of the cutting force for a tooth without the center cut on a tool revolution

This cutting force $F_{c\,zi}(\varphi_i)$ must be calculated for each tooth of the tool, taking into account the differences in the tooth profile which may exist (ex: with or without center cut).

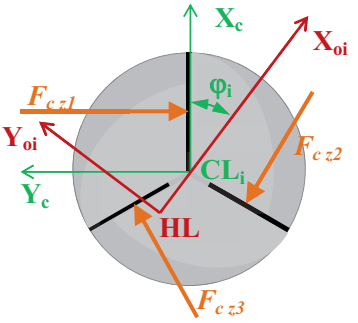

Figure 10 : Representation of cutting forces on a tool with three teeth and with a single tooth with center cut.

To calculate the resulting force, every effort is expressed in the orbital reference R_{oi}, so (Figure 10):

$$\boldsymbol{F}_{c\,z1}\left\{\begin{matrix} F_{cut\,z1}(\varphi_i).\sin(\varphi_i) \\ -F_{cut\,z2}(\varphi_i).\cos(\varphi_i). \\ 0 \end{matrix}\right\}_{R_{oi}}$$

$$\boldsymbol{F}_{c\,z2}\left\{\begin{matrix} F_{cut\,z2}\left(\varphi_i + \frac{2\pi}{Z}\right).\sin(\varphi_i + \frac{2\pi}{Z}) \\ -F_{cut\,z2}\left(\varphi_i + \frac{2\pi}{Z}\right).\cos(\varphi_i + \frac{2\pi}{Z}) \\ 0 \end{matrix}\right\}_{R_{oi}}$$

$$\boldsymbol{F_{c\,z3}} \begin{Bmatrix} F_{cut\ z3}\left(\varphi_i + \frac{4\pi}{Z}\right).\sin\left(\varphi_i + \frac{4\pi}{Z}\right) \\ -F_{cut\ z3}\left(\varphi_i + \frac{4\pi}{Z}\right).\cos\left(\varphi_i + \frac{4\pi}{Z}\right) \\ 0 \end{Bmatrix}_{R_{oi}}$$

The resulting force $\boldsymbol{F_c}$ is then:

$$\boldsymbol{F_c = F_{c\,z1} + F_{c\,z2} + F_{c\,z3}}$$

3. Experimental procedures

All tests were performed in a test piece in TiAl6V4 of 19mm thick. The cutting conditions are as follows:
Vc= 30mm/min;
Fza=0.005mm/tooth;
Fzt= 0.04mm/tooth.
The tool used is a tool with three teeth (Z=3) ,with a single tooth with center cut and of diameter D_t = 9mm.

3.1. Identification of specific cutting coefficient

To identify the specific cutting coefficient Kc, tests of slot machining were carried out on a machining center. The force measurement is performed using a Kistler dynamometer. The cutting coefficient, assumed to be constant, can be identified from the measurement of the maximum cutting force. The chip thickness is 0.04mm per tooth, the depth of cut is 0.75mm, and so the maximum chip section is 0.03mm ².
It can be deduced: $Kc = \frac{Fc_{max}}{Sc_{max}}$
Maximum force Fxy observed during the test is 105N. This gives a specific cutting coefficient for our tool/work piece couple of: Kc = 3500N/mm ².
This Kc value is a first approximation for model validation. It doesn't take into account influence of chip thickness or possible influence of speeds. And thereafter, two coefficient will be identified, one for the axial part and one for radial part, because the radial and axial parts present different cutting angles.

3.2. Force measurement in orbital drilling

Tests are also conducted in orbital drilling, in order to have a database to validate the modeling. These tests are performed on a drill bench equipped with an orbital spindle. On all tests, cutting forces are recorded using the dynamometer Kistler and sampled at 10 kHz. On the signals obtained when measuring just a taring is performed.
The hole diameter is 11.1mm and it is made with the same tool which has diameter of 9mm.

4. Results and discussions

The Kistler 9257B dynamometer allows measuring the resultant force in the plane normal to the axis of the tool *Fxy*
With $Fxy = \sqrt{Fx^2 + Fy^2}$ (Figure 11)
The force F_{cT} obtained by modeling differs from the real effort measured Fxy (Figure 11)

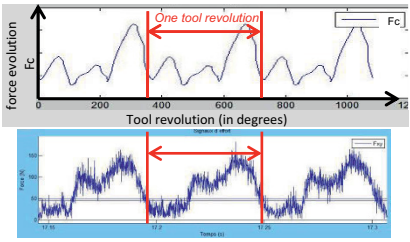

Figure 11: Comparison of the evolution of the cutting force over three revolution of tools (modeling at top; measure down)

The evolution of the modeled force on a tool revolution shows the successive passage of three teeth. This is explained by the fact that the radial chip is not constant on the tool revolution. In addition there is a single tooth with center cut, therefore causing disruption on the tool revolution.
The force measurement Fxy shows only two peaks of effort. Either the force is compensated perfectly on the third revolution, or either the chip is not constant for all three teeth. This difference between the two graphs is the lack of taking into consideration of cutting phenomena. To improve the model, the tool will be divided into two different parts, in order to better understand how each part works. The axial and radial part of the tool is defined as (Figure 12).

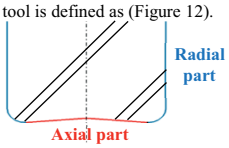

Figure 12: Tool division in two parts

The tool performance and the cutting phenomena caused by the radial part of the tool are known and already considerably studied in the literature. Modeling the cutting force of the axial part is more complex because the tool profile of the tip (Figure 12) combined with the tool trajectory is not classical.
In order to better understand the mechanisms during drilling, the evolution of the tangential force F_t at the contact point tool / work piece (according to $\mathbf{Y_{oi}}$) and of the radial force F_r (Figure 13) are modeled.
These two efforts strongly oscillate on a tool revolution, causing a variable bending force of the latter.
So a dynamic phenomenon is established and must be taken into account in the model to adjust the chip thickness of the radial cut. The Figure 13 shows that when the tooth with center cut is located in the "A" area ($0 < \varphi < \frac{\pi}{2}$), the radial force and tangential force are positive but quite low, not causing a significant modification in radial section.
When the tooth with center cut (z_1) is located in the "B" area ($\frac{3\pi}{2} < \varphi < 2\pi$), the radial force and tangential force are positive. Therefore this resultant force tends to push the tooth being machined towards the surface.
When the tooth with center cut is located in the area "C", the radial force is positive and tangential force is negative. Therefore this resultant force tends to push the tooth (z_2)

towards hole surface and in reverse tends to withdraw the tooth (z3) of hole surface.
And when the tooth with center cut is located in the area "D", the radial and tangential force are negatives. Therefore this resultant force tends to withdraw the tooth (z3) of hole surface.

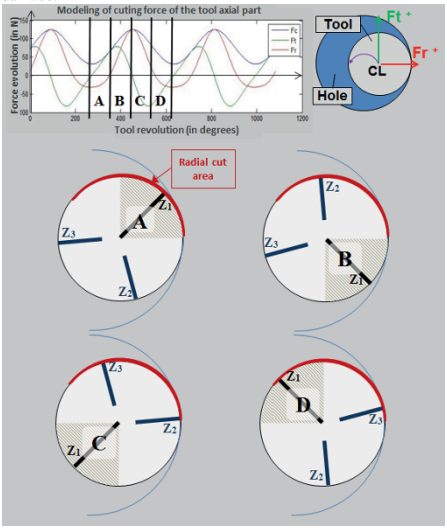

Figure 13 Modeling of the radial and tangential force of the tool axial part, taking into account the three teeth.

The hypothesis is that the radial section isn't homogeneous for the three teeth, because bending forces are different to each passage of various teeth on the radial cut area. The radial chip thickness machined by the tooth z_2 is greater than that machined by the tooth z_3.
After integration of this dynamic phenomenon in the model, the force profile is similar to the force measure by its evolution and maximum values (Figure 14).

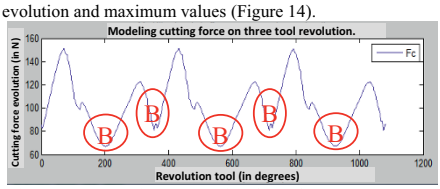

Figure 14: Modeling the cutting force from the corrected model.

A further difference is found between the model and the measure (denoted "B" in Figure 14).
In these areas, modeling tends to decrease cutting force versus measured force. This difference is explained by the hypothesis made on the "Kc" at baseline: the cutting coefficient is not constant and tends to increase in areas where the chip thickness is very low. This evolution of cutting coefficient will be therefore taken into account in order to improve the model.

5. Conclusions

This model, with the integration of the tool geometry, allowed knowing the exact geometry of the chip. With this knowledge, the modeling of the cutting force is possible which allows a better understanding of the cut phenomena when orbital drilling with a specific tool. It is therefore possible to vary the tool geometry or the cutting conditions in the model to predict the cutting forces, and thus be able to optimize these parameters. If the link between effort and drilling defects are known (ex: bending force → decrease in diameter), it is possible to optimize these parameters to improve the quality of the hole.

6. Acknowledgements

This work was carried out within the context of the working group Manufacturing'21 which gathers 18 French research laboratories. We would also like to thank the project called OPOSAP (Optimisiation du Perçage orbital avec Surveillance Active du Process) and above all the partners who helped us to make this research.

7. References

[Brinksmeier et al., 2008] Brinksmeier, B; Sascha Fangmann.; Meyer, I; *"Helical milling of CFRP-Titanium layer compounds"*; In: *Prod. Eng. Res. Devel* , pp. 2:277–283; Germany 2008

[Denkena et al., 2008] Denkena, B; Boehnke, D; Dege, J.H.; "Helical milling of CFRP-Titanium layer compounds"; In: *CIRP Journal of Manufacturing Science and Technology*, pp. 64-69; Germany 2008

[Fontaine, 2004] Fontaine, M ; "Modélisation thermomécanique du fraisage de forme et validation expérimentale" Thesis at Metz University ; France ; 2004

[Lorong et al., 2008] Lorong, P; Ali,; "Logiciel explicite en thermomécanique pour la simulation et la formation d'un copeau en usinage"; In: *Mécanique et industrie*, pp. 343-349; Vol3 ; 2002

[Lutze, 2008] S. Lutze. State of the art and expectations for the future of orbital drilling. Thesis at Leuphana University Lüneburg School III 2008

[Merchant, 1945] M.E.Merchant. Mechanics of the metal cutting process, I.Orthogonal cutting, In :*Journal of Applied physics*, vol 16 p318-324 . 1945

[Oxley, 1989] Oxley, P.L.B. Mechanics of metal cutting, Ellis horwood, Chichester, UK, 1989

[Segonds et al, 2006] S.Segonds, Y.Landon, F.Monies, P.Lagarrigue, Method for rapid characterisation of cutting forces in end milling considering runout, in: *International Journal of Machining and Machinability of Materials*, vol. 1 (1), pp. 45-61, 2006.

Article 048-pp-32

Thrust force and torque model applied to the vibratory drilling process

John LE DREF [1], Yann LANDON [2], Gilles DESSEIN [1], Florent BLANCHET [2]

(1) : Laboratoire Génie de Production, École Nationale d'Ingénieurs de Tarbes, 47 Avenue d'Azereix, BP 1629, 65016 Tarbes Cedex, France
05 61 55 84 26
E-mail : ledref@lgmt.ups-tlse.fr
Gilles.Dessein@enit.fr

(2) : Institut Clément Ader (ICA) Université de Toulouse ; INSA, UPS, Mines Albi, ISAE Bât 3R1, 118 route de Narbonne, F-31062 Toulouse cedex 9, France
05 61 55 77 01
E-mail : yann.landon@univ-tlse3.fr
florent.blanchet@isae.fr

Abstract: Drilling process is highly complex however necessary to assemble parts. It gets even more complex with the assembly of metallic parts with carbon-based composites in the aircraft industry. Vibratory drilling has been developed to meet industrial needs in terms of productivity and quality. This process is quite young and optimal cutting conditions with vibrations have yet to be determined. To assess the quality, and to understand the cutting mechanisms, vibratory drilling has been studied and a thrust force model and a torque model have been carried out. These models present the interaction of several zones of the tool with the material and explain the particular shape of the thrust force observed. The work presented in this paper is a part of a complete study of the impact of vibratory drilling on hole quality. The models are identified and validated through an application on aluminium 7010.

Key words: Vibratory drilling, thrust force, torque, indentation.

1- Introduction

The increasing use of Carbon Fibres Reinforced Plastics (CFRP) in aircraft industry and its association with metallic parts create needs for new processes to improve productivity and hole quality. Among the processes suggested, vibratory drilling offers a good compromise. The use of vibrations along the axis of the tool ensures chip fragmentation in metals and easy chip removal from the cutting area while reducing the defects generated **[J1, A1]**. However, its impact on hole quality is undetermined as well as the changes that tool vibrations provoke to the cutting mechanisms.
As far as stacks of multi-materials are concerned, hole quality is assessed by observing and measuring several types of defect, specific to the materials concerned. While it is desired to have an active monitoring of those defects, it is necessary to first understand their apparition and to identify the most influencing parameters. Burrs on metals **[C1, P1]**, delamination and surface quality on composites **[B1, TH1, P2]** are considered the most important defects.
Future parts of this project will study precisely the generation of surfaces and delamination of composite stacks. Concerning delamination, a study of the process is needed.. As previous works on delamination explained **[HT1, S1, R1]**, its presence and size is highly correlated to the thrust force. A critical thrust force can be identified, i.e. if the thrust force at the exit of the hole is higher than this critical force Fc, then the last plies will delaminate. To study delamination of CFRP, it is necessary to first understand the specific cutting processes in vibratory drilling and to model the thrust force precisely.
Previous studies determined the chip height from the sinusoidal trajectories [J1]. However, several clues, as the chip geometry, or the underestimated conditions to create discontinuous chip, points out a decrease of the amplitude of vibrations during the drilling. Therefore, as the real trajectories of the tool are unknown, chip height is also unknown and it is difficult to identify a model of the thrust force generated.
This paper present a thorough study of the thrust force and the torque generated in vibratory drilling applied to an aluminium alloy. A first part studied several models issued from traditional drilling. Those models were identified through experiments on traditional drilling then applied to vibratory drilling. In a second part, the reduction of amplitude of the vibrations will be assessed and taken into account.

2- Thrust force model and torque model

2.1 – Thrust force model

The model presented in this paper is based on the model established by **[G1]**, slightly modified to take into account

the vibrations and its consequences. The identification follows the edge-material pair method: for the entry of the tip of the tool, the thrust force versus time/penetrated radius is plotted, considering perfect tool geometry. Change of slope of the thrust force signal point out a few zones with different cutting mechanisms (fig.1).

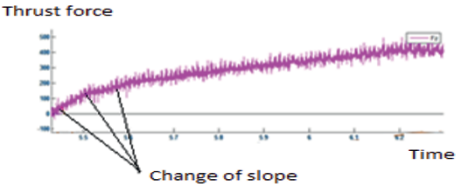

Figure 1: Thrust force measured and observation of the changes of slope

Those three zones are explained by the combination of the local geometry of the tool and the local kinematics (fig.2). They are determined by the study of the force signal and its derivative.

- At the centre of the tool, there is close to no cutting speed. This part of the tool works as an indenter, pushing out the material, generating a large amount of thrust force in comparison to its size.
- Farther from the centre, the cutting speed is sufficient to create a chip, but not enough for the cutting phenomenon to be efficient. The comparison of the feed rate with the cutting speed shows a presence of ploughing effect in this area. The thrust force generated increases rapidly with the feed rate, up to 40% of the thrust force for feed rates of 0.2mm/rev.
- On the cutting edges, the cutting speed still increase with the radius and it is several times the value of the feed rate.

As far as traditional drilling is concerned, chip height and feed rate are constant: therefore cutting mechanism and their associated area are also constant.

When considering vibration drilling, chip height and feed rate are varying with time. Moreover, the correlation between those two through the rotational speed is irrelevant. Interferences between the chip height and the instantaneous feed rate V_{fi} are expected, in regards to the size of area and the thrust force generated for each cutting mechanism encountered.

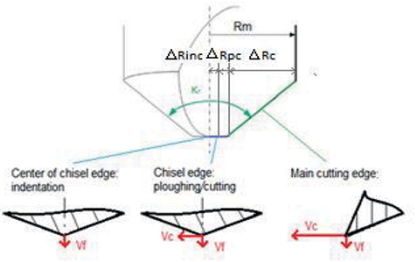

Figure 2: The main cutting phenomena in drilling operation

In contrary to the cutting edges where the cutting speed is high, the indentation zone and the ploughing zone are highly related to the feed rate. The extents of their areas as well as the thrust force generated are both increasing with the feed rate in vibratory drilling. It calls for changes on the thrust force models of those two zones.

Because the feed rate varies, and bear both positive and negative values, a few assumptions were made:

- When the instantaneous feed rate is negative (the tool goes up) there is no indentation. It becomes part of the ploughing zone which presents bad cutting conditions (fig. 3).
- The indentation zone as its area related to the feed rate. The chip height regulates the size of the others since the higher cutting speed implies cutting mechanisms and chipping.

The model presented in this paper is compared to a power regression model, eq.1, also identified with traditional drilling data:

$$F_z = K * \Delta R * h_c^{qind} \quad (1)$$

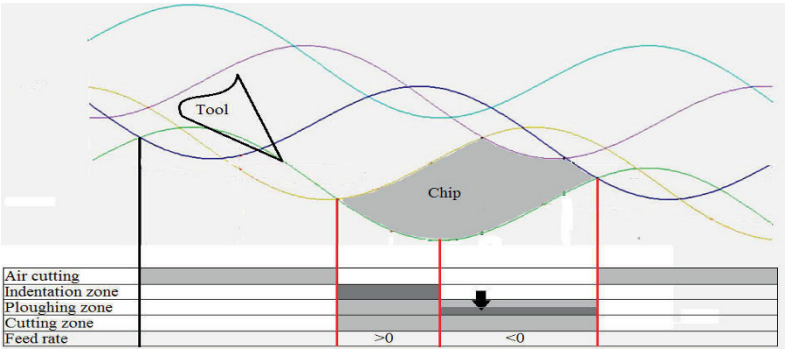

Figure 3: Trajectories in vibratory drilling and presence of cutting mechanisms

2.1.1 –Indentation zone

In [W1], a theoretical radius is calculated as the indentation zone is represented by a disc (fig.4). The radius corresponds to the point for which the cutting speed is five times the feed rate. It accounts for a few tenth of mm. However precise it can be, this model is arbitrary.

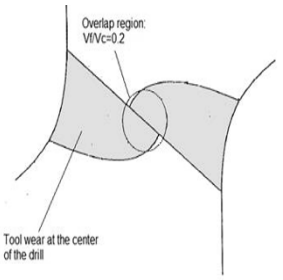

Figure 4: Tool wear and approximate indentation radius.

[G1] suggested an experimental definition of the indentation radius in function of the feed: by deriving the thrust force, it is possible to point out precisely the first change of slope corresponding to the indentation phenomenon (fig.5). In this paper, the indentation radius is chosen to be represented as a function of the feed rate instead of the feed. (eq.3)

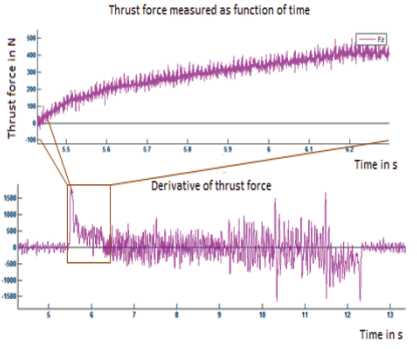

Figure 5: Identification of the indentation radius.

A fractional model [B2] is used to model the indentation force $\boldsymbol{F_{ind}}$. The indentation radius $\boldsymbol{\Delta R_{ind}}$ and the indentation force are identified though experimental data from traditional drilling with eq.2 and eq.3, where h_c is the chip height and h_c^* and K_{ind} parameters:

$$F_{ind} = K_{ind} * h_c^* * \Delta R_{ind} * \frac{(\frac{h_c}{h_c^*}) + r_c(\frac{h_c}{h_c^*})^2}{1+(\frac{h_c}{h_c^*})} \quad (2)$$

$$\Delta R_{ind} = K_{rind} * V_f^{qind} \quad (3)$$

It is hypothesized that, when the feed rate is negative and the tool goes upward, the extent of the indentation zone is zero: there is no indentation when the tool goes up. However, the tool is still locally in contact with the material, meaning that the area induces another cutting mechanism: it is swept into the ploughing area ΔR_{pe}.

2.1.2 –Ploughing zone

In the second zone, ploughing effect is present, while a chip is formed. It can be explained by an addition of cutting phenomenon and ploughing phenomenon where the clearance face is in contact with the material (fig. 6)

The contribution of cutting speed, feed rate and tool geometry to the ploughing phenomenon is quite unclear. Based on the model presented in [G1], a term was added to show the contribution of those three variables though the dynamic cutting angle γ_{fe}. It is usually used to determine the presence of ploughing.

While the indentation force nullifies when the tool goes upward, the formulation of the ploughing force defines an increased or decreased thrust force depending on the sign of the feed rate. Ploughing force is increased when the feed rate is positive i.e. the tool goes downward.

The ploughing force is calculated with (eq.4), where the parameters to identify are K_{pe}, q_{pe}, d_{pe}:

$$F_{pe} = K_{pe} * (1 - \sin \gamma_{fe})^{q_{pe}} * \Delta R_{pe} * h_c^{d_{pe}} \quad (4)$$

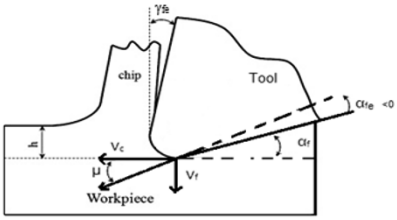

Figure 6: The case of ploughing effect.

2.1.3 –Main cutting zone

The cutting speed ranges approximately from 10% to 100% at the diameter of the tool. Because the cutting speed V_c at any given radius of the cutting zone is high, the influence of the feed rate is reduced but still considered. The variation of the instantaneous feed rate in vibratory drilling implies a feeble variation of the dynamic cutting angle. The important variation of V_c has a greater influence on the thrust force. As the cutting speed increases with the radius, it is expected that the mean cutting pressure lowers and the thrust force is reduced. The model, presented in [G1] for the cutting zone, is unaltered. It calculates the thrust force locally for each element with a length ΔR_c and sums them up to get the total contribution of the cutting edges. It makes it possible to define the influence of the variation of both cutting speed and feed rate in vibratory drilling as they appear in the calculation

of the dynamic cutting angle. The thrust force of an element of the cutting edge is (eq.5), where K_c, q_c, b and d_c are identified with traditional drilling data:

$$\Delta F_c = K_c * (1 - \sin \gamma_{fe})^{q_c} * V_c{}^{b} * \Delta R_c * h_c{}^{d_c} \quad (5)$$

2.2 – Torque

Figure 7 shows a measure of the thrust force and the torque in vibratory drilling with the condition f=0.2mm/rev and A=0.5mm. It was observed that the torque had a quasi-linear relation with the chip height while the thrust force did not.

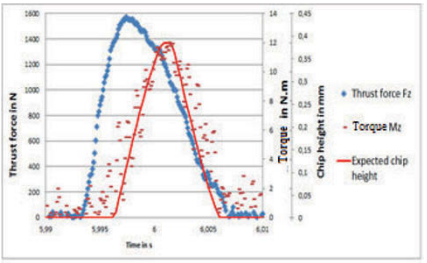

Figure 7: Comparison of experimental and theoretical thrust forces for f=0.1 and A=0.05.

A linear model is established from vibratory drilling data, eq.6:

$$M_z = K_{mz} * h_c \quad (6)$$

3- Experimental procedures

The drilling tests were carried out on a five-axis CNC machine with two twisted drills: drill 1 Ø12.7mm and drill 2 Ø15.9mm, with two lips and a drill point thinning. Internal minimal quantity lubrication was used. Cutting forces were measured using a Kistler 9257B dynamometer, while drilling Aluminium 7010 at several feed from 0.025mm/rev to 1mm/rev (feed rates from 47 to 1880mm/min) and with a cutting speed of 75m/min in traditional drilling. For feed rates higher than 564mm/min, only the tip of the tool penetrated the material to avoid unnecessary tool wear or tool breakage. Model obtained through traditional drilling data is verified with vibratory drilling for two feed rates f (0.1mm/rev;0.2mm/rev) and several amplitudes of vibrations A from 0.05mm to 0.5mm.

4- Results and discussions

Several comparisons of the model and the power regression model identified though traditional data, and compared to experimental data are represented.
At low amplitude of vibrations (fig. 8), it can be seen that the thrust force measured is close to a sinusoid as the theoretical chip is. However, when the amplitude is increased, a particular shape of the thrust force can be seen (fig.9 and 10). The first part, in regards to the tool going down, shows a fast increase of the thrust force. On the second part, it can be thought of the shape of the thrust force as successive interactions of the different cutting mechanisms, as the tool goes upward.
From the various tests, it was observed that the maximal thrust force appeared ahead of time (fig. 8). While the maximal chip height appears on B (cf. power model), the maximal thrust force appears in advance on A. This maximal thrust force does not correspond to the maximal chip height. The model studied points out this behaviour in vibratory drilling which is a direct consequence of the instantaneous feed rate V_{fi}.
Following the oscillations of the tool, it is expected to increase or decrease the thrust force when the tool goes down or up respectively. The higher the amplitude of vibrations is, the higher the influence of the instantaneous feed rate and the amplification of the thrust force is.

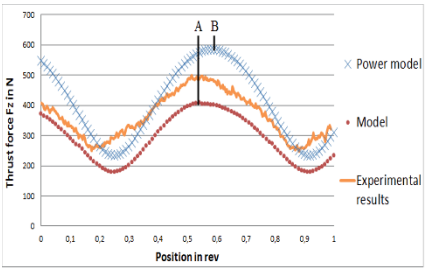

Figure 8: Comparison of experimental and theoretical thrust forces for f=0.1mm/rev and A=0.05mm.

Observations can be made about the relevance of the model over a power regression model to represent the thrust force in vibratory drilling (fig.9 and 10). The main point of the portioned model is its ability to define the evolution of the thrust force, which is completely different from the evolution of the chip height. Furthermore, the model presented shows an earlier maximal thrust force than expected.
Despite its ability to represent and to explain the shape of the experimental thrust force, the model still underestimates the contribution of vibrations, therefore also underestimating the thrust force.

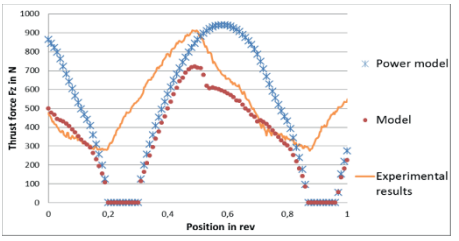

Figure 9: Comparison of experimental and theoretical thrust forces for f=0.2 mm/rev and A=0.4 mm.

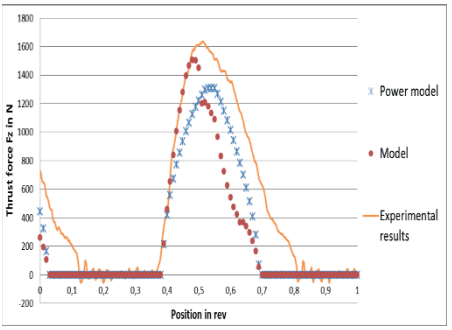

Figure 10: Comparison of experimental and theoretical thrust forces for f=0.2mm/rev and A=0.5 mm.

The weak point of the model remains in the determination of the chip height through the study of the kinematics of vibratory drilling. As it can be seen, cutting time is underestimated, fig.9-10, where the amplitude is theoretically enough to have a chip fragmentation i.e. chip height and thrust force equal to zero when air cutting. Particularly, for the cutting conditions for fig.9, the chip is continuous and the thrust force never equals zero when the chip was expected to fragment. The main hypothesis is a reduction of the amplitude while cutting.

Figure 11 represents the expected limit for chip fragmentation. From the formulation of the sinusoidal trajectories in vibratory drilling [J1], it is possible to deduce the amplitude needed to obtain fragmentation for a specific feed rate, eq.7:

$$h_c = 0 \Rightarrow f = \left|2 * Z * A * \sin\left(\frac{-\pi * osc}{z}\right)\right| \qquad (7)$$

In a feed versus amplitude plot, this limit is the theoretical straight line. From experimental tests, observation of the shape of the chip in relation to the cutting conditions, allows to define the experimental limit of fragmentation at about twice the amplitude expected, regardless of the tool (fig. 11: dotted line).

A thorough dynamic study in the same cutting conditions should be carried out to highlight this reduction of amplitude but will not be part of this work.

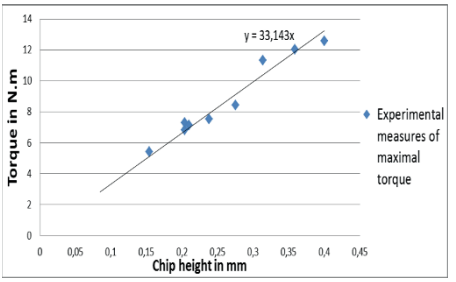

Figure 12: Results of the torque measured in relation to the chip height.

Because of its linear relation to chip height (fig. 6), the torque model can be determined from the maximal torque. When plotting the maximal torque and the theoretical maximal chip height for each test in vibratory drilling (fig.12), the model for the torque in vibratory drilling can be identified from vibratory drilling data. The study of the torque along with the thrust force pointed out the differences of their generation. The conclusion is that, in contrary to the thrust force, the torque is not influenced by the varying feed rate. A global model of the torque in vibratory drilling is precise enough and simpler.

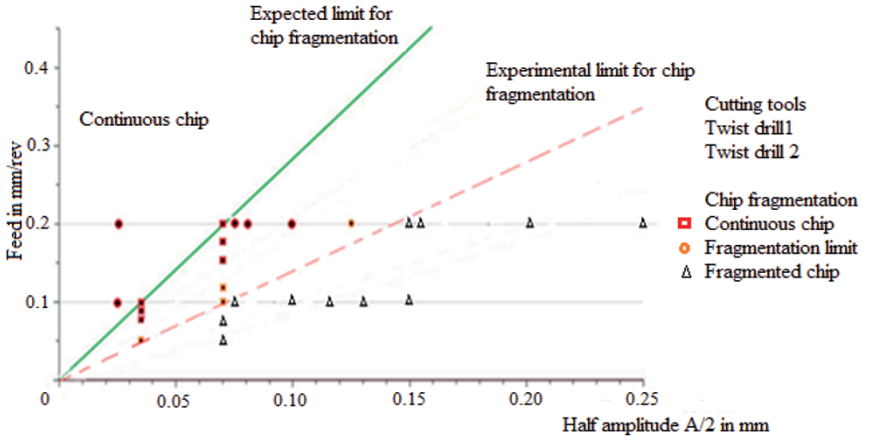

Figure 11: Underestimated amplitude for chip fragmentation.

5- Conclusions

This paper presented a partitioned model of the thrust force and a torque model applied to vibratory drilling in aluminium:

- The relevance of the study of several part of the tool with different cutting mechanisms is pointed out, for traditional and vibratory drilling.
- As far as vibratory drilling is concerned, the representation of the thrust force in relation to the chip height needs to take into account the evolution of cutting speed and feed rate over the cutting edges and over time.
- However, it is necessary to control the dynamic process, and specifically to precisely determine the reduction of the amplitude, expected to be around 40-50%.
- Torque can be expressed by a global model of the tool. In contrary to the thrust force, it varies in a linear fashion with the chip height.

Because the model is underestimating the thrust force, while the dynamic process is not precisely determined, future investigations will be carried out to assess the reduction of amplitude. To avoid underestimation of the thrust force, a new methodology will be studied to identify the partitioned model presented in this paper with vibratory drilling data.

6- Acknowledgements

This work was funded by the region Midi-Pyrenees and carried out within the context of the working group Manufacturing'21. It gathers 21 French research laboratories. The topics approached are the modelling of the manufacturing process, virtual machining and emerging manufacturing methods. We would also like to thank Airbus (Toulouse) and MITIS for providing the materials needed to carry out the study.

7- References

[A1] S. Arul. *The effect of vibratory drilling on hole quality in polymeric composites*. In International Journal of machine tools & Manufacture 46, 252-259, 2006.

[B1] S. Basavarajappa. *Drilling of hybrid metal matrix composites—Workpiece surface integrity*. In International Journal of Machine Tools & Manufacture 47 92–96, 2007.

[B2] D. Bondarenko, *Etude mésoscopique de l'interaction mécanique outil/pièce et contribution sur le comportement dynamique du système usinant*, mémoire de thèse à l'université de Bordeaux, 2011

[C1] S. Chang. *Burr height model for vibration assisted drilling of aluminum 6061-T6*. In Precision engineering 34, 369-375, 2010.

[G1] N. Guibert. *Identification of thrust force models for vibratory drilling*. International Journal of Machine Tools and Manufacture 49, 730-738, 2009.

[HT1] H. Hocheng, C.C. Tsao. *The path towards delamination-free drilling of composite materials*. In Journal of Materials Processing Technology 167 251-264, 2005.

[J1] J. Jallageas. *Optimisation du perçage de multi-matériaux sur unite de perçage automatique (UPA)*. mémoire de thèse à l'université de Bordeaux, 2013.

[P1] B. Pena. *Monitoring of drilling for burr detection using spindle torque*. In International Journal of Machine Tools & Manufacture 45, 1614–1621, 2005.

[P2] K. Palanikumar. *Modeling and analysis for surface roughness in machining glass fibre reinforced plastics using response surface methodology*. In Materials and Design 28 2611–2618, 2007.

[R1] P. Rahmé. *Contribution à l'étude de l'effet des procédés Perçage-Alésage sur l'apparition du délaminage dans les structures composites épaisses*. mémoire de thèse à l'université de Toulouse, 2008.

[S1] L. Surcin. *Contribution à l'étude théorique et expérimentale du perçage de plaques composites minces*. mémoire de thèse à l'université Paul Sabatier de Toulouse, 2005.

[TH1] C.C. Tsao, H. Hocheng. *Evaluation of thrust force and surface roughness in drilling composite material using Taguchi analysis and neural network*. In Journal of Materials Processing Technology 203 342–348, 2008.

[W1] R. A. Williams. *A study of the basic mechanics of the chisel edge of a twist drill*. In International Journal of production research, volume 8, 1969

Article 050-pp-41

Analysis of a turning process strongly coupled to a vibro-impact nonlinear energy sink

Li TAO [1], Etienne GOURC [1], Sébastien SEGUY [1], Alain BERLIOZ [2]

(1): Université de Toulouse; INSA; ICA (Institut Clément Ader); F-31077 Toulouse, France
E-mail : {tli, seguy}@insa-toulouse.fr
etienne.gourc@gmail.com

(2): Université de Toulouse; UPS; ICA (Institut Clément Ader); F-31062 Toulouse, France
E-mail : alain.berlioz@univ-tls3.fr

Abstract: Recently, it has been demonstrated that a vibro-impact nonlinear energy sink (VI-NES) can be used to efficiently mitigate vibration of a Linear Oscillator (LO) under transient loading by irreversible energy transfer from LO to VI-NES. In this paper, the possibility of application of VI-NES to control the instability of chatter in turning as a passive control method is studied as a typical delay system. The dynamic responses of machine tool strongly coupled to VI-NES in turning are investigated theoretically by supposing that the tool just vibrates in the predominant direction and numerically with the help of Matlab dde23 algorithm. Three typical response regimes are obtained through numerical simulation under different parameters, that is, stable oscillation and complete suppression of regeneration chatter, relaxation oscillation and partial suppression, and unstable oscillation. Finally, a developed experimental setup is presented and the first test to acquire the stability lobe without VI-NES is accomplished.

Key words: Dynamics, Turning, Chatter, Nonlinear Energy Sink, Vibro-Impact

1- Introduction

The surface quality of parts produced by machining operation is strongly affected by the well know regenerative chatter. The chatter instability is induced by the time delay between two consecutive cutting teeth, linked to spindle speed. By the effect of some external disturbance, the tool start damped oscillation relative to the workpiece, and the surface roughness is undulated. For the consecutive cutting teeth, the chip thickness is modulated. This regenerative mechanism is well known and presented first by Tobias [TF1]. Since this work, many researcher have improved the knowledge by the well know stability lobe representation, see e.g. [AB1] [MI1] [ML1].

Various techniques for chatter suppression have been studied. The idea behind various techniques is to disturb the time delay by variable pitch tool or spindle speed variation [SI1]. The use of magnetic bearing spindle is also a promising way for chatter reduction [GS1].

Another approach to reduce chatter is the use of linear tuned vibration absorbers, presented first by Ormondroyd and Hartog in 1928 [OH1]. More recently, an analytical optimized method was presented for linear absorbers in the context of chatter [S1]. These linear absorbers are successfully applied on boring process [MB1]. Active absorbers have been also proposed with piezoelectric tool [HD1]. However all this linear absorbers are limited by the small frequency bandwidth, and in practice the efficiency is not interesting for the machinist.

The idea of attaching a nonlinear oscillator to a turning machine is relatively recent [W1] [GS2] [NS1]. It has been showed that various systems consisting of a primary structure and of a strong nonlinear oscillator (SNO) are able to transfer irreversibly the energy from the primary structure to SNO with almost any mode of the primary system and therefore over broad frequency bands through resonance capture [GG1] [VR1] [GM2]. Such a feature has revealed interesting behavior for vibration mitigation. In recent studies, it has been demonstrated that systems comprising with a Nonlinear Energy Sink (NES) can exhibit regimes which are not related to fixed points, and cannot be explained using local analysis. These regimes are related to relaxation oscillation of the slow flow and can be efficiently analyzed by applying the multiple scale method. A VI-NES coupled to linear systems and convenient for engineering application is analytically treated using multiple scale method in [G1] and further studied experimentally in [GM1].

The dynamics of the turning machine have been studied by applying different and efficient methods. A systematic approach comprised of a path-following scheme, the method of multiple scales, the method of harmonic balance, Floquet theory, and numerical simulations to investigate its local and global dynamics and stability has been proposed in [NN1]. Specially, a method mixed with the method of multiple scales and that of harmonic balance is proposed in [LZ1] to

analyze the delay system like the turning system. Moreover, the analytic approach to obtain the complete solutions for systems of delay differential equations like turning is presented in [AU1].

In this paper, the possibility of regenerative chatter suppression using a Vibro-Impact Nonlinear Energy Sink (VI-NES) is analyzed for turning process. The paper is organized as follow. In the next section, the model considered in this study is described. Then, different response regimes accompanied with numerical simulation are presented. Finally, the experimental setup is presented.

2- Mechanical Model with Vibro Impact NES

The model developed herein consists of a cutting tool on a lathe with an embedded VI-NES. The cutting tool is assumed to vibrate only on its first flexible mode and the workpiece is considered to be rigid. A schematic of the model is given in Fig. 1.

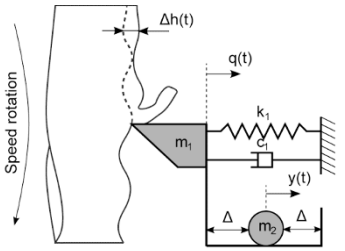

Figure 1: Mechanical model.

The governing equation of motion, between impact, are expressed as:

$$\begin{cases} m_1 \dfrac{d^2q}{dt^2} + c_1 \dfrac{dq}{dt} + k_1 q = F_c \\ m_2 \dfrac{d^2y}{dt^2} = 0 \quad \forall \left| q - y \right| \langle \Delta \end{cases} \tag{1}$$

where q and y represent the tool tip and VI-NES displacement respectively. m_1, c_1 and k_1 are the mass, damping and stiffness of the tool and m_2 is the mass of the VI-NES.

F_c is the cutting force taking into account the regenerative effect. The cubic polynomial form due to Shi and Tobias [ST2] is expressed as follow:

$$F(\Delta h(t)) = p(\rho_1 h(t) + \rho_2 h(t)^2 + \rho_3 h(t)^3) \tag{2}$$

where p is the chip width (depth of cut), $h(t)$ is the chip thickness and ρ_i (i=1…3) are specific cutting coefficients obtained by fitting the experimental cutting force measurement with a third order polynomial [DB1]. The chip thickness $h(t)$ is expressed as follow:

$$h(t) = h_0 + \Delta h(t) \tag{3}$$

h_0 represent the nominal chip thickness in the absence of vibration and $\Delta h(t)$ is the chip thickness variation gives by:

$$\Delta h(t) = q(t-\tau) - q(t) \tag{4}$$

where $q(t\text{-}\tau)$ is the delayed position of the tool and τ is the time delay between two workpiece revolutions $\tau = 2\pi/\Omega$, with Ω the spindle speed. In the steady state, $q(t) = q_0$. Substituting Eq. 3 and Eq. 2 into Eq. 1 gives:

$$k_1 q_0 = p(\rho_1 h_0 + \rho_2 h_0^2 + \rho_3 h_0^3) \tag{5}$$

In the unsteady state, the displacement would be the sum of the steady state component q_0 and an unsteady component $u(t)$

$$q(t) = q_0 + u(t) \tag{6}$$

Substituting Eq. 3, Eq. 5, Eq. 6 into Eq. 1 gives:

$$\begin{cases} m_1 \dfrac{d^2u}{dt^2} + c_1 \dfrac{du}{dt} + k_1 u = p(\alpha_1 \Delta\tilde{h} + \alpha_2 \Delta\tilde{h}^2 + \alpha_3 \Delta\tilde{h}_0^3) \\ m_2 \dfrac{d^2y}{dt^2} = 0 \quad \forall \left| q - y \right| < \Delta \end{cases} \tag{7}$$

where $\Delta\tilde{h} = u(t-\tau)$, $\alpha_1 = 2\rho_1 h_0 + 3\rho_3 h_0^2 + \rho_1$, $\alpha_2 = 3\rho_3 h_0 + \rho_2$, $\alpha_3 = \rho_3$. Changes of variables are introduced as follow:

$$\begin{aligned} &T = \omega_1 t, \quad \omega_1^2 = \frac{k_1}{m_1}, \quad 2\mu_1 = \frac{c_1}{m_1 \omega_1}, \quad \varepsilon^2 = \frac{m_2}{m_1} \\ &\psi = \frac{p\alpha 1}{m_1 \omega_1^2}, \quad \eta_1 = \frac{p\alpha_2}{\psi m_1 \omega_1^2}, \quad \eta_2 = \frac{p\alpha_3}{\psi m_1 \omega_1^2} \end{aligned} \tag{8}$$

Substituting Eq. (8) into Eq. (7), the compact form of equations of motion is as follow:

$$\begin{cases} \ddot{u} + 2\mu_1 \dot{u} + u = \psi(\Delta\tilde{h} + \eta_1 \Delta\tilde{h}^2 + \eta_2 \Delta\tilde{h}_0^3) \\ \varepsilon^2 \ddot{y} = 0, \quad \forall \left| ru - y \right| < \Delta \end{cases} \tag{9}$$

where $\varepsilon^2 \ll 1$ represents the mass ratio between the VI-NES and the modal mass of the first bending mode of the tool, r is the influence coefficient, depending on the position of the VI-NES on the tool and the dots denotes differentiation with respect to the non-dimensional time T.

A detuning parameter σ representing the nearness of ψ to the critical value ψ_c is introduced as $\psi = \psi_c + \varepsilon^2 \sigma$.

When $|ru - y| = \Delta$, a collision occurs. The state of the system after impact is obtained using the simplified shock theory and the condition of total momentum conservation:

$$\begin{aligned} u_+ &= u_-, \quad y_+ = y_- \\ r\dot{u}_+ - \dot{y}_+ &= R(r\dot{u}_- - \dot{y}_-) \\ \dot{u}_+ + \varepsilon^2 \dot{y}_+ &= \dot{u}_- + \varepsilon^2 \dot{y}_- \end{aligned} \tag{10}$$

where R is the restitution coefficient of impact and the superscripts + and − denotes time immediately after and before impact.

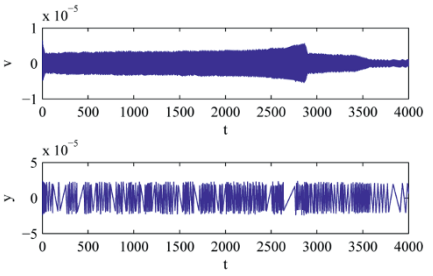

Figure 2: Numerical integration for σ=0.15, stabilization of chatter.

3- Numerical simulation

In this section, different scenarios of passive control of chatter are presented. The equations of motion Eq. 9 were numerically integrated using Matlab dde23 algorithm [ST1] together with the event function to detect impacts. The dynamic parameters of the system used for the numerical simulations are:

$$\begin{aligned} &\mu_1 = 0.03; \quad \varepsilon^2 = 0.01; \quad r = 0.8 \\ &R = 0.65; \quad \Delta = 2 \times 10^{-5} \end{aligned} \tag{11}$$

3.1 – Stabilization of chatter

For σ=0.15, various numerical simulations were performed. In this case, the amplitude growth of the main system is limited by the random impact of the ball on the walls. An example of a numerical integration is shown in Fig. 2.

It is observed that the oscillation amplitude of the main system increases, which reflects the fact that the system is unstable, but the growth of these is hampered by the chaotic impacts of the free mass of the VI-NES on the walls. Furthermore, it is observed that the system has other sub-harmonic attractors with type responses z=2/3 according to the classification of Peterka [P1]. This phenomenon is not detailed here.

3.2 – Passive control of chatter

If we increase the depth of cut to σ=1, the system is unstable and the amplitude of the oscillations of the main system increases sufficiently, to activate the movement of the ball. In this case, the VI-NES is synchronized with the main system, the energy in the system is dissipated by the successive impacts and the oscillation amplitude decreases to a lower level. The numerical integration shown in Fig. 3 illustrates this behavior.

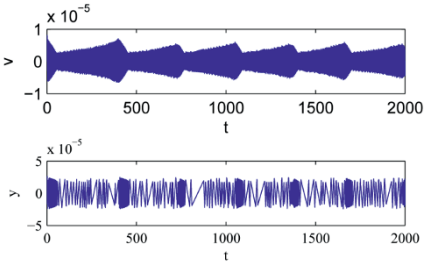

Figure 3: Numerical integration of motion equation for σ=1, passive control of chatter.

3.3 – Limit of passive control of chatter

When the value of σ further increases, the system is very unstable and the amplitude is very important. During cycles of relaxation the system is no longer controlled. The result of the numerical integration in this case is shown in Fig.4, for σ=4.16. It confirm predicted scenario.

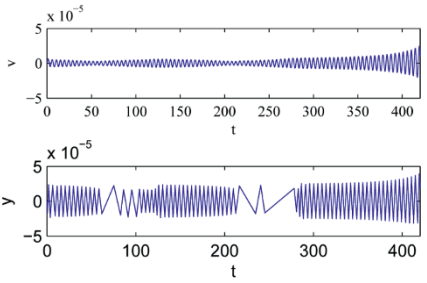

Figure 4: Numerical integration of motion equation for σ=4.16, chatter not controlled.

4- Experimental tests

In this section, the experimental setup developed is presented. After the first test for stability identification are presented.

3.1 – Experimental setup

The cutting tests are performed on a lathe Cazeneuve three axes (CT210). The experimental setup is show in Fig. 5. It's composed by steel bar 40mm diameter in XC38. The part is considered as infinitely rigid compared to the tool. Cutting tool, modeled as a single degree of freedom, is a boring bar to insert, with a length of 250mm. It has been deliberately modified by embedding (in the tool holder), in order to activate the bending mode in the feed direction. In addition, a mass was added on the tool to reduce the natural frequency of this mode. The operation of straight turning is conducted with a feed per revolution set to $h_0 = 0.1$ mm/rev.

Figure 5: Experimental setup.

The VI-NES is mounted on the mass tool tip. Machining operations consist of turning operations with different cutting parameters (speed and depth of cut).

The vibrations of the tool are measured using a laser velocimeter. The cutting coefficients are derived from the literature [Do]. The dynamic characteristics of the tool are obtained by acter. The data are summarized in Table 1.

Table 1 : Dynamic parameter of the experimental setup.

m_1	3.1 kg	μ_1	3 %
f_1	95 Hz	m_2	0.032 kg
R	0.8		

3.2 – Stability lobe without VI NES

Preliminary tests without the ball of the VI-NES have been made in order to find the behavior of the dynamical system. Determining stability or instability of a test can be difficult. In fact, the tool is subjected to forced vibration, as they may be due to a lack of concentricity for example. The direct or indirect measurement of the vibration does not allow itself to detect the presence of regenerative vibrations. However, there are simple methods in the time domain to detect. A first step is to resample the measured frequency of rotation of the workpiece signal [MI1]. In this case, a stable machining is in the form of a line, since the relative position between the tool part is always the same. On the other side, unstable machining present a mess. A second possibility is to plot the Poincare section of the measured signal. Stable machining then present an attractor point type, then an unstable machining present an attractor type circle [MI1]. Finally, the comparison between the stability lobes obtained theoretically and those obtained experimentally is shown in Fig. 6.

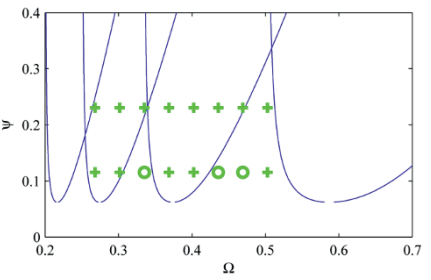

Figure 6: Experimental stability lobe Circles and crosses correspond respectively to stable and unstable machining.

5- Conclusion

The purpose of this paper is to analyze the dynamic response regimes of the machine tool strongly coupled to VI-NES in turning theoretically and numerically and to acquire the clues for further research in the future. Three different response regimes, that is, stable oscillation and complete suppression of regeneration chatter, relaxation oscillation and partial suppression, and unstable oscillation are identified through numerical simulation. The experimental setup is established for tests of different conditions and goals. A preliminary test to get stability lobe is accomplished and the result between theory and experiment is consistent.

6- References

[AB1] Y. Altintas, E. Budak, Analytical prediction of stability lobes in milling, Ann CIRP 44, (1995), p. 357–362

[AU1] F.M. Als and A.G. Ulsoy: Analysis of a system of linear delay differential equations, ASME J. Dyn. Syst., Meas., Control Vol. 125, (2003), p. 215–223

[DB1] Z. Dombovari, D.A.W. Barton, R.E. Wilson, and G. Stepan: On the global dynamics of chatter in the orthogonal cuttingmodel. Int. J. Non-Linear Mech. Vol. 46, (2011), p. 330–338

[G1] OV Gendelman: Analytic treatment of a system with a vibroimpact nonlinear energy sink. J. Sound Vib. Vol. 331, (2012), p 4599–4608

[GG1] O.V. Gendelman, E. Gourdon, and C.H. Lamarque: Quasiperiodic energy pumping in coupled oscillators under periodic forcing. J. Sound Vib. Vol. 294, (2006), p. 651–662

[**GM1**] E. Gourc, G. Michon, S. Seguy and A. Berlioz: Theoretical and experimental study of an harmonically forced vibro-impact nonlinear energy sink. Proceedings of the ASME-IDETC, Oregon, USA, 2013

[GM2] E. Gourc, G. Michon, S. Seguy, A. Berlioz: Experimental investigation and design optimization of targeted energy transfer under periodic forcing, J. Vib. Acoust. Vol. 136, (2014), p. 021021

[GS1] E. Gourc, S. Seguy, and L. Arnaud: Chatter milling modeling of active magnetic bearing spindle in high-speed domain. Int. J. Mach. Tools Manuf. Vol. 51, (2011), p. 928–936

[GS2] E. Gourc, S. Seguy, G. Michon, and A. Berlioz: Chatter control in turning process with a nonlinear energy sink, Adv. Mater. Res. Vol. 698, (2013), p. 89–98

[HD1] A. Harms, B. Denkena, and N. Lhermet: Tool adaptator for active vibration control in turning operations. In 9th International Conference on New Actuators, Brême, Germany, 2004

[LZ1] A. Luongo, and D. Zulli: Dynamic analysis of externally excited NES-controlled systems via a mixed Multiple Scale/Harmonic Balance algorithm, Nonlinear Dyn. Vol. 70, (2012), p. 2049–2061

[MB1] H. Moradi, F. Bakhtiari-Nejad, and M.R. Movahhedy: Tuneable vibration absorber design to suppress vibrations: an application in boring manufacturing process. J. Sound Vib. Vol. 318, (2008), p. 93–108

[MI1] B.P. Mann, T. Insperger, G. Stepan, and P.V. Bayly: Stability of up-milling and down-milling, part 2: experimental verification. Int. J. Mach. Tools Manuf. Vol. 43, (2003), p. 35–40

[ML1] M. Mousseigne, Y. Landon, S. Seguy, G. Dessein and J.M. Redonnet: Predicting the dynamic behaviour of torus milling tools when climb milling using the stability lobes theory, Int. J. Mach. Tools Manuf. Vol. 65, (2013), p. 47–57

[NN1] A.H. Nayfeh and N.A. Nayfeh: Analysis of the cutting tool on a lathe. Nonlinear Dyn. Vol. 63, (2010), p. 395–416

[NS1] A. Nankali, H. Surampalli, Y.S. Lee, and T. Kalmar-Nagy: Suppression of machine tool chatter using non- linear energy sink. Proceedings of ASME-IDETC, Washington DC, USA, 2011

[OH1] J. Ormondroyd, D. Hartog: The theory of the dynamic vibration absorber. J. Appl. Mech. Vol. 49–50, (1928), p. A9–A22.

[P1] F. Peterka; Bifurcations and transition phenomena in an impact oscillator. Ch. Sol. Fract. Vol. 7, (1996), p. 1635–1647

[S1] N.D. Sims: Vibration absorbers for chatter suppression: a new analytical tuning methodology. J. Sound Vib. Vol. 301, (2007), p. 592–607

[SI1] S. Seguy, T. Insperger, L. Arnaud, G. Dessein, and G. Peigne: Suppression of period doubling chatter in high-speed milling by spindle speed variation. Mach. Sci. Technol. Vol. 15, (2011), p. 153–171

[ST1] L.F. Shampine, S. Thompson: Solving ddes in matlab. Appl. Num. Math. Vol. 37, (2001), p. 441–458

[ST2] H. Shi, and S. Tobias: Theory of finite amplitude machine tool instability, Int. J. Mach. Tools Manuf. Vol. 24, (1984), p. 45–69

[TF2] S.A. Tobias and W. Fishwick: Theory of regenerative machine tool chatter. Eng. Vol. 205, (1958), p. 199–203 238–239

[VR1] A.F. Vakakis and R.H. Rand: Non-linear dynamics of a system of coupled oscillators with essential stiffness non-linearities. Int. J. Non-linear Mech. Vol. 39, (2004), p. 1079–1091

[W1] M. Wang: Feasibility study of nonlinear tuned mass damper for machining chatter suppression. J. Sound Vib. Vol. 330, (2011), p. 1917–1930

Article 044-pp-19

Analytical model for pre-drilled thick composite plates

Pierre Rahme[1], Yann Landon[2], Robert Piquet[2], Frederic Lachaud[2], Pierre Lagarrigue[2]

(1) : Notre Dame University, Mechanical Engineering Department; Faculty of Engineering P.O. Box : 72, Zouk Mikael, Zouk Mosbeh, Lebanon
Phone: +961 9 218950
Fax: +961 9 225164
E-mail : prahme@ndu.edu.lb

(2) : Université de Toulouse; INSA, UPS, Mines Albi, ISAE; ICA (Institut Clément Ader); UPS, Bât 3R1, 118 Route de Narbonne, F-31062 Toulouse cedex 9, France
Phone: +33 5 61 55 77 01
E-mail : yann.landon@univ-tlse3.fr
{robert.piquet,Frederic.lachaud}@isae.fr
pierre.lagarrigue@univ-jfc.fr

Abstract:

In aeronautical, the machining of composite materials is more and more used. Drilling is in particular the most used process in the assembly of aeronautical structures. When drilling composite materials, delamination occurs at the exit of the hole. These defects diminish the strength of the structure to failure. To minimize delamination, drilling process with pilot hole is used. In this paper, analytical model for drilling thick composite structures with pilot hole using a twist drill is proposed. This model predicts the critical thrust force at delamination. Different hypothesis of boundary conditions and external loading are proposed. Punching tests with twist drill are realized in order to select the corresponding hypothesis of boundary conditions and external loading. These results may be used to optimize the cutting conditions when drilling thick composite plates with pilot hole.

Key words: Drilling – Reaming – Composite materials – Analytical models – Twist drill – Delamination.

1- Introduction

Modern aeronautical structures require typically the use of composite materials. The assembly of composite parts requires knowledge in drilling of composite materials. Indeed, drilling of thick composite structures using the conventional twist drill provokes defects at the entry, on the wall and at the exit of the hole [HT1]. These defects diminish the strength of the structure to failure. Delamination at the exit of the hole is among the serious concerns in drilling composite-based components in practice [TH1]. It is considered to be the major drilling defect ([PF1], [RL1]). A solution to minimize delamination is to drill a pilot hole [WD1]. Drilling process with pilot hole minimizes the delamination at exit. This paper focuses on the drilling with pilot hole of thick composite structures using a twist drill in order to minimize the defects at the exit of the hole.

The mechanisms involved in initiation and propagation of delamination at the hole exit were identified by Rahme et al. [RL1]. Matrix cracks are initiated under the chisel edge of the twist drill and interlaminar delamination is then propagated by the main cutting edges. Tsao et al. [TC1] developed an analytical approach for the determination of the position of the onset of delamination during the drilling of composite laminates. Rahme et al. [RL2] developed an analytical and numerical model to predict the critical thrust force at delamination when drilling thick composite structures.

According to Rahme et al. [RL3], delamination is directly related to the axial cutting force which in turn depends on the tool geometry and the feed rate per tooth. The optimal drilling thrust force is defined as the minimum force for which delamination is initiated [HD1]. Delamination at exit can be controlled by taking into account the relationships between machining parameters and forces and torque [VD1]. The size of the delamination zone has been showed to be related to the thrust force developed during drilling [KW1]. The critical thrust force at delamanition was found by several authors. Lachaud et al. [LP1] proposed a model which links the axial penetration of the drill bit to the conditions of delamination (crack opening mode I) of the last few plies. Rahme et al. [RL2] showed the effect of the chisel edge on the critical thrust force at delamination when drilling thick composite material with a twist drill. Rahme et al. [RL4] showed the effect of various parameters on the critical thrust force at delamination. Hocheng et al. [HT1] presented the expression of the critical thrust force at delamination when drilling with a twist drill and other special drills as saw drill, core drill and candle stick drill. However, the critical thrust force at delamination when drilling with pilot hole thick composite structures was not found before.

When drilling composite materials, the contribution of chisel edge to the thrust force is often up to 40-60% [JY1]. Delamination can be reduced significantly when drilling with a pilot hole, since the chisel edge no more interacts with material [JY1]. Moreover, the chisel edge width has been identified as an important factor contributing to the thrust force and hence delamination [JY2]. Tsao et al. [TH2]

determined the optimal range of chisel edge length with respect to drill diameter in order to minimize delamination.
In this paper, drilling with pilot hole of thick composite plates using a conventional twist drill is studied. An analytical model for predicting the critical thrust force at delamination is developed when drilling with pilot hole composite structures using a twist drill. This model is based on fracture mechanics. Different hypotheses for boundary conditions and external loading are proposed. To select the corresponding hypothesis, experimental punching tests are realized. These tests allow finding experimentally the critical thrust force in function of the remaining non-drilled plies under the drill.

2- Analytical model

According to Rahme et al. [RL1], the crack opening mode at the exit of the hole is considered to be due to normal perpendicular to the ply surface. The circular defect is considered to be initiated by the drill in contact with the material during the drilling process [LP1]. The cracks at the exit of the hole are initiated under the chisel edge and propagated under the action of the two main cutting edges of the twist drill [RL1]. Drilling with pilot hole process reduces the defects at the exit produced by the chisel edge. The diameter of the pilot hole is taken equal to the diameter of the chisel edge of the drill. A smaller diameter will not completely cover the length of the chisel edge and a greater diameter will also produce delamination that passes the boundary of the hole.
In the present paper, the part of the plate located under the main cutting edges is modelled by a thin circular orthotropic plate with a pilot hole as shown in Figure 1. The thickness of this plate is assumed small with respect to the hole diameter and the shear effect is then neglected. The outer diameter of this plate equals the diameter of the drill (2a). The inner diameter (diameter of the pilot hole) is also similar to the length of the chisel edge (2b).
Three hypotheses of boundary conditions and external loading are proposed for this model. A first hypothesis of fixed end plate at the circumferential boundary subjected to a uniformly distributed load is taken (Figure 1-a). This hypothesis takes into account the resistance of the plate to the moment. The fixed end develops a moment reaction. The action of the main cutting edges of the twist drill is modelled by a uniformly distributed load. In the second hypothesis, only action of the edges between the chisel edge and the main cutting edges of the twist drill is taken into account. This action is modelled by a circular distributed load along the circumferential of the pilot hole (Figure 1-b). A third hypothesis, that takes into account the action of the drill main cutting edges but does not develop a moment reaction, is proposed. In this hypothesis, the plate is modelled by a simply supported thin circular plate subjected to a uniformly distributed loading (Figure 1-c).

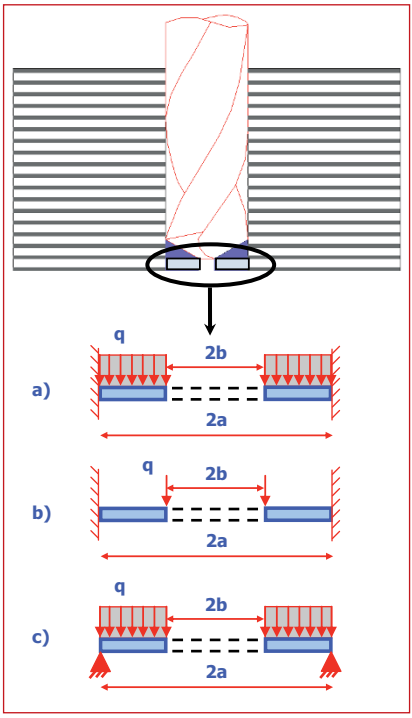

Figure 1 : Different hypotheses for drilling with pilot hole of thick composite plates

To calculate the critical thrust force at delamination corresponding to the previous hypotheses, an energetic approach based on the virtual work principle is used. Indeed, at the exit of the plate, the motion of the drill can be associated to a small displacement dx. The thrust force produces an external work on the plate which is a function of the distance dx. This external work tends to produce bending of the plate and to propagate the cracks later. The conservation of energy is written as :

$$\delta W = \delta U + \delta U_d \qquad (1)$$

The radius of the drill (a) is the parameter which varies virtually. Consider δa the fictitious length of the cracks. To find the work and the potential energy, the deflection w(r) of the simply supported circular plate of diameter (2a) must be calculated as a function of the thrust force. Using the plate theory developed by Timoshenko [TW1] applied to axisymetrical circular plates, the equilibrium equation of the plate is given in polar coordinates for small deformations as :

$$\frac{d}{dr}\left[\frac{1}{r}\frac{d}{dr}\left(r\,\frac{d\,w(r)}{dr}\right)\right] = \frac{Q}{D} \qquad (2)$$

Q is the shear per unit of length at any point of the plate as function of the load q for any hypothesis. For an orthotropic material, D is given by:

$$D = \frac{1}{8}(3D_{11} + 3D_{22} + 2D_{12} + 4D_{66}) \quad (3)$$

With :

$$|D_{ij}| = \sum_{k=1}^{n}(\overline{Q_{ij}})_k \left(\frac{z_k^3 - z_{k-1}^3}{3}\right) \quad (4)$$

And Q_{ij} are the terms of the rigidity matrix of the plate.
The elementary virtual work δW of the external forces is then :

$$\delta W = \frac{\partial W}{\partial a}\delta a = \frac{\partial\left(\iint_S F\, dS\right)}{\partial a}\delta a \quad (5)$$

Where S is the surface of the plate. The virtual variation δU of the potential energy U is given by :

$$2U = \int_S \left[M_{xx}\frac{\partial^2 w}{\partial x^2} + M_{yy}\frac{\partial^2 w}{\partial y^2} + 2M_{xy}\frac{\partial^2 w}{\partial x\,\partial y}\right] dS \quad (6)$$

Furthermore, the variation of the energy absorbed by the propagation of cracks is given by δU_d. This energy U_d is the product of the critical restitution energy corresponding to mode I (G_{IC}) and the circular surface :

$$U_d = G_{IC}\,.S = G_{IC}\pi\, a^2 \quad (7)$$

The equation of energy conservation is then solved for the critical thrust force at delamination for the three proposed hypotheses. The results corresponding to these hypotheses are shown in
Table 1.

Case	Critical Thrust Force at Delamination
a)	$F_{CA} = 8\pi D\sqrt{\frac{3\,G_{IC}\left((-1-\vartheta)b^2 + a^2(\vartheta-1)\right)^3(a^2-b^2)^3}{(a-b)K_A}}$
b)	$F_{CB} = 8\pi D\sqrt{\frac{G_{IC}b\left((-1-\vartheta)b^2 + a^2(\vartheta-1)\right)^3}{3\,K_B}}$
c)	$F_{CC} = 16\pi D(a^2-b^2)^2(\vartheta-1)^2\sqrt{\frac{128\,G_{IC}}{b^4(\vartheta+1)K_C}}$

Table 1 : Critical thrust force at delamination corresponding to three hypotheses.

When ϑ is the Poisson's ratio of the non-drilled plate remaining under the drill. In this paper, the value of this ratio is taken 0.3 based on material characterisation tests.
The expressions of K_A, K_B and K_C are given in appendix.

3 - Experimental part

In this part, the critical thrust force at delamination is found experimentally. Punching tests are realized using tension/compression machine (Instron 8862). Carbon fiber reinforced epoxy polymer plates (CFRP) T800/M21 of thickness 20 mm are used. Quasi-isotropic plates of sequence $[90°,+45°,0°,-45°]_{S10}$ are made in the laboratory. The thickness of one ply is 0.25 mm. For the used material, the critical restitution energy G_{IC} corresponding to propagation of cracks is taken equal to 800 J/m^2. This value is found experimentally using standard ISO 15024. To punch the remaining non-drilled plies under the drill, standard sharpened twist drill (DIN 1897) tapered without thinning of the chisel edge of diameter 15.8 mm is used. This twist drill was also used to drill a blind hole with pilot hole. The number of plies remaining non-drilled varies from 1 to 6 plies. The diameter of the pilot hole is taken equal to the length of the chisel edge 3.9 mm. Figure 2 shows a punching test on the composite plate using a twist drill and the corresponding setup. The same setup was also used to drill the pilot hole and the blind hole. An example of the applied force curve by the machine during the punching test is shown as function of the displacement in Figure 3. The maximum force on the curve corresponds to the critical thrust force at delamination. The punching test is repeated by varying the number of non-drilled plies remaining under the drill. The critical thrust force is then plotted in function of the number of delaminated non-drilled plies.

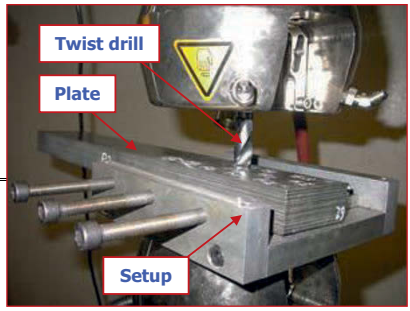

Figure 2 : Experimental punching tests using Instron tension/compression machine

Figure 3 shows the curve of the thrust force during the punching test of one non-drilled ply remaining under the drill. The thrust force increases in function of the drill displacement and reaches in this case a maximum value of 260 N. This value corresponds to critical thrust force at delamination for one non-drilled ply.

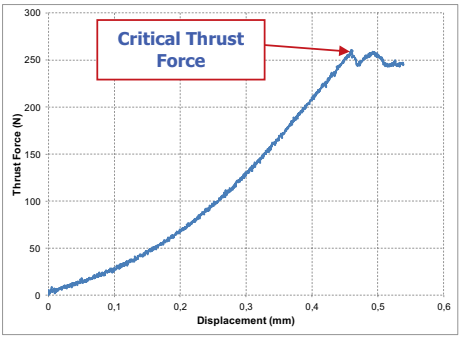

Figure 3 : Punching test, curve of the thrust force for one ply remaining under the drill in function of the displacement

4 - Results and discussion

The critical thrust forces at delamination found in the previous sections are presented in this paragraph. The results of the three hypotheses are compared with the experimental results of punching test. The critical thrust force is plotted in function of the number of delaminated plies remaining under the drill. Figure 4 presents the comparison for critical thrust forces at delamination of composite structures when drilling with pilot hole of the three analytical hypotheses with experimentation.

On Figure 4, a large critical thrust force corresponding to hypothesis a) (fixed end plate with uniformly distributed load) is presented by the analytical model. The results of this hypothesis are relatively outsized with respect to experimental results. The critical thrust force of hypothesis b) with circular distributed load is also bigger than experimental results. The third hypothesis c) for the simply supported plate subjected to a uniformly distributed load is the nearest to experimentation. This shows that the fixed end hypothesis does not meet with the experimental results. This hypothesis can be used to model drilling with exit back-up support. The simply supported plate is in this case the suitable hypothesis to model drilling without exit back-up support. The results of the third hypothesis of analytical model validate the choice of the boundary conditions and the external loading. Indeed, the results of experimentation and modelling are close. For six plies under the drill, the results are very close with an error of 8%. On the other hand, for two delaminated plies, a maximum error of 28% is found. However, the proposed analytical model is always conservative since it presents critical thrust force at delamination less than the results found in experimentation. These results correlate with the results found by Rahme et al. [RL1]. The hypothesis of the inexistence of the moment reaction at the exit of the hole is proved. When the critical thrust force corresponding for a couple tool/material is found for drilling with pilot hole, it can be used to determine the critical cutting conditions at delamination.

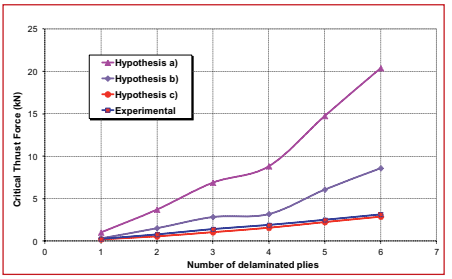

Figure 4 : Comparison between different hypotheses of analytical model and experimentation results

5 - Conclusion

Drilling process with pilot hole is used to minimize delamination at exit of the hole for thick composite structure. The pre-drilled pilot hole eliminates the effect of chisel edge which is important on delamination. In this paper, an analytical model is developed for drilling with pilot hole thick composite plates using a twist drill. This analytical model predicts the critical thrust force at delamination corresponding to propagation of the cracks for the last plies at the exit. Three hypotheses of boundary conditions and external loading are proposed for drilling with pilot hole process using a twist drill. Punching experimental tests have been realized in order to choose the corresponding boundary conditions and external loading. The simply supported plate subjected to a uniformly distributed load corresponds to the closest results between analytical model and experimentation. These results can be used to optimize the cutting conditions when drilling with pilot hole composite structures.

6 - Acknowledgements

We are grateful for the materials resources provided by AIRBUS Toulouse France. We thank Cédric Leroy, Benoît Marguet and Jacques Bourriquet for helping and supporting us in this work.

This work was carried out within the context of the working group Manufacturing 21 which gathers 16 French research laboratories. The topics approached are:

- The modeling of the manufacturing process,
- The virtual machining,
- The ermerging of new manufacturing methods.

7 - References

[HD1] Hocheng, H. and Dharan, C.K.H. Delamination during drilling in composite laminates. ASME Journal of Eng. Ind. 112 236-239, 1990.

[HT1] Hocheng, H. and Tsao, C.C. The path towards delamination-free drilling of composite materials. Journal of Materials Processing Technology, 167, 251-264, 2005.

[JY1] Jain S. and Yang D.C.H. Delamination-Free drilling of composite laminates. ASME Mater. Div. Publ., MD, Anaheim, CA, USA, pp. 45–59, 1992.

[JY2] Jain S. and Yang D. C. H. Effects of feed rate and chisel edge on delamination in composites drilling. J. Eng. Ind. 115(4), 398-405, 1993.

[KW1] Koenig W., Wulf C., Grass P. and Willerscheid H. Machining of fiber reinforced plastics. Ann. CIRP, 34, 537-548, 1985.

[LP1] Lachaud F., Piquet R., Collombet F. and Surcin L. Drilling of composite structures. Composite Structures, vol. 52, issues 3–4, pages 511–516, 2001.

[PF1] Piquet R., Ferret B., Lachaud F. and Swider P. Experimental analysis of drilling damage in thin carbon/epoxy plate using special drills. Composites: Part A, 31, 1107-1115, 2000.

[RL1] Rahmé P., Landon Y., Lagarrigue P., Piquet R. and Lachaud F. Study into causes of damage to carbon epoxy composite material during the drilling process. International Journal of Machining and Machinability of Materials, vol. 3, no. ¾, pp. 309 – 325, 2008.

[RL2] Rahmé P., Landon Y., Lagarrigue P., Piquet R., Lachaud F., Marguet B., Bourriquet J. and Le Roy C. Chisel edge effect on delamination when drilling thick composite materials with a twist drill. SAE International Journal of Aerospace, 1 : 776-781, 2009.

[RL3] Rahmé P., Landon Y., Lagarrigue P., Lachaud F. and Piquet R. Drilling thick composite materials using large diameter drills. Int. J. of Machining and Machinability of Materials, vol. 10, no. 3, pp. 202-221, 2011.

[RL4] Rahmé P., Landon Y., Lagarrigue P., Piquet R., Lachaud F., Marguet B., Bourriquet J. and Le Roy C. Drilling of think composite structures – State of the art. SAE International, Toulouse, France, 2006.

[TC1] Tsao C.C., Chen W.C. Prediction of the location of delamination in the drilling of composite laminates, International Journal of Materials Processing Technology, 70, 185-189, 1997.

[TH1] Tsao C.C., Hocheng H. and Chen Y.C. Delamination reduction in drilling composite materials by active backup force. CIRP Annals – Manufacturing Technology, volume 61, issue 1, pages 91-94, 2012.

[TH2] Tsao C.C., Hocheng H. The effect of chisel length and associated pilot hole on delamination when drilling composite materials. International Journal of Machine Tools and Manufacture, volume 43, issue 11, pages 1087-1092, 2003.

[TW1] Timoshenko S., Woinowsky-Krieger S., Theory of plates and shells. Mcgraw-Hill, ISBN 13: 9780070647794, June 1959.

[VD1] Veniali F., Di Ilio A. and Tagliaferri V. An Experimental Study of the Drilling of Aramid Composites. J. Energy Resour. Technol. 117(4), 271-278, 1995.

[WD1] Won M.S. and Dharan C. K. H. Chisel edge and pilot hole effects in drilling composite laminates. Jounal of Manufacturing Science and Engineering, Volume 124, Issue 2, 242-247, 2002.

8 - Appendix

For a given composite material, coefficient D' is taken as :

$$D' = \frac{(D_{11}+D_{22})}{2} + \frac{(D_{12}+2D_{66})}{3} \tag{8}$$

The coefficients K_A, K_B and K_C used in the formulas of the critical thrust force are :

$$K_A = 96\,b^6\left[\frac{1}{2}\left(D-\frac{3D'}{8}\right)(1+\vartheta)^3b^6+\left(\left(D-\frac{9D'}{8}\right)\vartheta+\frac{2D_{12}}{3}+D-\frac{2D_{66}}{3}-\frac{D'}{8}\right)a^2(1+\vartheta)b^4-\frac{3}{2}(\vartheta-1)\left(D-\frac{3D'}{D}\right)(1+\vartheta)^2a^4b^2+(\vartheta+1)\left(\left(D-\frac{3D'}{D}\right)\vartheta^2+\frac{3\vartheta D'}{4}+\frac{D'}{8}-\frac{2D_{12}}{3}-D+\frac{2D_{66}}{3}\right)a^6\right]\ln\left(\frac{b}{a}\right)^2++24b^4\left[-3\left(\left(D-\frac{3D'}{D}\right)\vartheta^2+\left(\frac{4D}{3}-\frac{3D'}{4}\right)\vartheta-\frac{2D_{66}}{9}-\frac{D'}{24}+\frac{2D_{12}}{9}+\frac{D}{3}\right)(1+\vartheta)b^8+8a^2b^6\left(\left(D-\frac{3D'}{8}\right)\vartheta^3+\left(-\frac{9D'}{32}+\frac{7D}{4}\right)\vartheta^2+\left(\frac{D_{66}}{3}+D-\frac{D_{12}}{3}-\frac{5D'}{16}\right)\vartheta+\frac{D}{4}-\frac{D_{12}}{6}+\frac{D_{66}}{6}-\frac{5D'}{32}\right)-6a^4b^4\left(\left(D-\frac{3D'}{8}\right)\vartheta^3+\left(\frac{3D'}{4}+\frac{4D}{3}\right)\vartheta^2+\left(\frac{10D_{66}}{9}-D-\frac{10D_{12}}{9}-\frac{D'}{24}\right)\vartheta-\frac{4D}{3}+\frac{D'}{2}\right)+2a^6b^2\left(\left(D+\frac{9D'}{8}\right)\vartheta^2+\left(\frac{4D_{66}}{3}-\frac{4D_{12}}{3}+\frac{D'}{4}-4D\right)\vartheta-\frac{2D_{66}}{3}-\frac{7D'}{8}+\frac{2D_{12}}{3}+3D\right)a^8(\vartheta-1)\left(\left(D-\frac{3D'}{8}\right)\vartheta^2+\frac{3D'\vartheta}{4}+\frac{D'}{8}-D+\frac{2D_{66}}{3}-\frac{2D_{12}}{3}\right)\Big]\ln\frac{b}{a}+(a+b)\left[b^{10}\left(\left(-13D+\frac{39D'}{8}\right)\vartheta^3+\left(\frac{117D'}{8}+9D\right)\vartheta^2+\left(45D-\frac{111D'}{8}+16D_{66}-16D_{12}\right)\vartheta+23D-\frac{93D'}{8}-8D_{12}+8D_{66}\right)+41a^2b^8\left(\left(D-\frac{3D'}{8}\right)\vartheta^3+\left(-\frac{135D'}{328}-\frac{3D}{41}\right)\vartheta^2+\left(\frac{51D}{41}-\frac{33D'}{328}-\frac{16D_{66}}{41}+\frac{16D_{12}}{41}\right)\vartheta+\frac{71D}{41}-\frac{237D'}{328}-\frac{8D_{12}}{41}+\frac{8D_{66}}{41}\right)-46\,a^4b^6\left(\left(D-\frac{3D'}{8}\right)\vartheta^3+\left(\frac{45D'}{184}+\frac{9D}{23}\right)\vartheta^2+\left(\frac{21D}{23}-\frac{51D'}{184}+\frac{8D_{66}}{23}-\frac{8D_{12}}{23}\right)\vartheta-\frac{37D}{23}+\frac{99D'}{184}-\frac{4D_{12}}{23}+\frac{4D_{66}}{23}\right)+22a^6b^4\left(\left(D-\frac{3D'}{8}\right)\vartheta^3+\left(\frac{63D'}{88}+\frac{3D}{11}\right)\vartheta^2+\left(-\frac{27D}{11}+\frac{21D'}{88}+\frac{8D_{66}}{11}-\frac{8D_{12}}{11}\right)\vartheta+\frac{13D}{11}-\frac{27D'}{88}+\frac{4D_{12}}{11}-\frac{4D_{66}}{11}\right)-5\,a^8b^2\left(D-\frac{3D'}{8}\right)\left(\vartheta+\frac{1}{5}\right)(\vartheta-1)^2+a^{10}(\vartheta-1)^3\left(D-\frac{3D'}{8}\right)\Big] \tag{9}$$

$$K_B = \left(b^2(1+\vartheta)\ln\frac{b}{a}+\frac{1}{2}(a^2-b^2)(\vartheta-1)\right)\Big[-2D'(1+\vartheta)^2b^3+\frac{16D}{3}(1+\vartheta)^2b^2-\frac{16a^2b^2D}{3}\left(\vartheta^2-1\right)\ln\frac{b}{a}+a^2b(2D'\vartheta^2-8D'\vartheta+\frac{D_{11}}{3}+\frac{D_{22}}{3}+\frac{22D_{12}}{3}-\frac{20D_{66}}{3}+\frac{a^2-b^2}{2}\left(\left(-2D'\vartheta^2-8D'\vartheta+\frac{7D_{11}}{3}+\frac{7D_{22}}{3}+\frac{26D_{12}}{3}-4D_{66}\right)b^3+\frac{16Db^2}{3}\left(\vartheta^2-1\right)+2D'a^2b(\vartheta-1)^2-16D\frac{a^2}{3}(\vartheta-1)^2\right)\Big] \tag{10}$$

$$K_C = \Big[\left((-9D'+24D)\vartheta^3+(9D'+24D)\vartheta^2+(48D_{66}-24D+21D'-16D_{12})\vartheta-16D_{12}+3D'+16D_{66}\right)\frac{a^4}{48}+\frac{\left((24D-9D')\vartheta_{7\vartheta}^2+18D'\vartheta_{7\vartheta}-16D_{12}+16D_{66}-24D+3D'\right)(\vartheta_{7\vartheta}+1)a^2b^2}{24}+\frac{Da^4}{2}(\vartheta-1)\Big]\ln\left(\frac{b}{a}\right)^2+\frac{b^4(a^2-b^2)(\vartheta+1)}{4}\Big[-4D(a^2+b^2)(\vartheta-1)\ln b+\left(\left(3D-\frac{9D'}{8}\right)\vartheta^3+\left(5D-\frac{9D'}{8}\right)\vartheta^2+\left(-5D+\frac{25D'}{8}-\frac{8D_{12}}{3}+\frac{8D_{66}}{3}\right)\vartheta+\frac{8D_{66}}{3}-\frac{8D_{12}}{3}+\frac{7D'}{8}-3D\right)b^2+\left(\left(D-\frac{3D'}{8}\right)\vartheta^3+\left(3D+\frac{3D'}{8}\right)\vartheta^2+\left(D+\frac{11D'}{8}+\frac{4D_{66}}{3}-\frac{4D_{12}}{3}\right)\vartheta-5D+\frac{5D'}{8}+\frac{4D_{66}}{3}-\frac{4D_{12}}{3}\right)a^2\Big]\ln\frac{b}{a}+\frac{(a^2-b^2)}{96}\Big[48Db^4(a^2+b^2)\left(\vartheta^2-1\right)\ln\left(\frac{b}{a}\right)^2-48Db^4(a^2-b^2)\left(\vartheta^2-1\right)\ln b+\left(\left(\left(13D-\frac{39D'}{8}\right)\vartheta^4+78D\vartheta^3+\left(88D+\frac{99D'}{4}-26D_{12}+26D_{66}\right)\vartheta^2+(-78D+42D'-44D_{12}+44D_{66})\vartheta-101D+\frac{81D'}{8}-26D_{12}+26D_{66}\right)b^4-2\left(\left(D-\frac{3D'}{8}\right)\vartheta^2+\left(8D-\frac{3D'}{4}\right)\vartheta+7D-\frac{27D'}{8}-2D_{12}+2D_{66}\right)(\vartheta-1)^2a^2(a^2+2b^2)\right)(a^2-b^2)\Big] \tag{11}$$

Article 052-pp-105

BURR HEIGHT STUDY FOR DRILLING CARBON EPOXY COMPOSITE/TITANIUM/ALUMINUM STACKS

Xavier Rimpault [1], Jean-François Chatelain [2], Jolanta E. Klemberg-Sapieha [3], Marek Balazinski [1]

(1) : Aluminium Research Centre-REGAL, École Polytechnique de Montréal, Montréal, Canada
+1 (514) 340-4711
E-mail : {xavier.rimpault, marek.balazinski}@polymtl.ca

(2) : École de technologie supérieure, Montréal, Canada
+1 (514) 396-8800
E-mail : jean-francois.chatelain@etsmtl.ca

(3) : École Polytechnique de Montréal, Montréal, Canada
+1 (514) 340-4711
E-mail : jolanta-ewa.sapieha@polymtl.ca

Abstract: In this study, a stack of carbon fibre reinforced polymer (CFRP), titanium and aluminium alloys was drilled using a different set of cutting parameters for each layer. This paper focuses on the analysis of the burr heights at the outlet of the titanium and aluminium alloys. The burr heights are observed in terms of the thrust force, the torque, the hole diameter and circularity, and the clearance tool wear. The selected input parameters were the feeds and speeds of each layer of the studied stack, with three feeds and three speeds for each material of the stack selected. The impact of these parameters on the burr heights of aluminium and titanium parts is presented, as well as correlations between the burr heights with the thrust force, the torque and the clearance tool wear. Three twist drills, with a common geometry and coating, were used in this study.

Keywords: Drilling, Burr heights, Titanium alloy, Aluminium alloy, Carbon fibre reinforced polymer.

1- Introduction

Thanks to their high strength/weight ratios, carbon fibre reinforced polymers (CFRP), also called carbon epoxy composites, are used more and more in the aerospace industry. In commercial airplanes, CFRP panels are stacked with other metallic parts such as aluminium and titanium alloys for assemblies. Generally, in the aeronautical industry, traditional drilling and mechanical bolting operations are used to fasten these parts together. With this fastening process, assembly and dismantling operations which take place during maintenance or repairs, are easier to conduct. However, one-shot drilling is required to machine all the layers of the stack **[SS1]**.
The efficiency of the bolted joints highly depends on the quality of the holes. However, due to the differences in the machining characteristics of CFRP and metallic materials, it becomes more difficult to control the drilling operation **[MR1]**. In addition to specific problems resulting from drilling each material separately, diverse problems, such as delamination, erosion, dissimilar diameter, intense tool wear, heat damage, etc., may occur when drilling sandwiched materials **[TF1]**.
One of the difficulties encountered when drilling metallic parts is burr formation control. Although deburring costs can account for as much as 30% of total components cost in the aerospace industry **[DK1]**, deburring is currently not selected for multimaterial stacks, as is the case with titanium for instance, in CFRP/Titanium/Aluminium stacks. Secondly, the use of shim between the layers in stacks does not allow the isolation of a part and the measurement of the burr height **[BJ1]**.

2– Selection of materials and workpiece

2.1 – Carbon epoxy composite

Numerous problems appear following the drilling operation, including inlet and outlet delamination, pulled fibres and burnt composite **[GL1] [KW1] [PE1]**.
Although Tsao and Hocheng found that the feed rate and the drill diameter influence the delamination factor, they also noticed that more delamination is caused by increased tool wear **[TH1]**. Because of the hardness and abrasiveness of the carbon fibres, the main wear mechanism affecting the tool is abrasion **[SA1]**. Dry drilling generates higher temperatures than what is seen with the use of a coolant thanks to the low heat conductivity of the matrix resin.

2.2 – Titanium alloy

Titanium alloys are widely used in the aerospace industry, and are known to be difficult to machine, mostly due to burr formation during the drilling process. Tool wear is severe due to high temperatures seen during cutting as a result of low thermal conductivity **[MM1]**. The rapid wear is caused mainly by the high temperature generated in the primary

cutting zone **[P1]**.
In addition to the intensive tool wear, the quality and the surface integrity of drilled holes are affected as well, mostly due to the temperature generated in the cutting zone This impact can be observed through the surface roughness parameters, the burr height, the diameter, as well as the changes in microstructure near the surface of the walls of the holes **[CT1]**.

2.3 – Aluminium alloy

Most aluminium alloys are known to have excellent machinability properties. However, the main problem encountered when drilling such alloys is the adhesion of the cut material on the tool, which increases tool wear and leads to low surface quality. While this impact may be reduced by increasing the cutting speed, doing so however raises the temperature in the cutting area **[LN1] [NL1]**.
The 7000 series family of aluminium alloys is characterized by high strength, good machinability and heat treatment capacity. The series however also does present one weakness, namely, low resistance to corrosion **[C1] [C2]**. It is in the light of the latter that one alloy from this series was selected in this study.

2- Experimental set-up

The components of the workpiece used for the experiments presented are shown in Figure 1. Drilling tests were performed on a 3-axis computerised numerical control (CNC) machine, the Huron K2X10.

Figure 1: Stack specifications

The CFRP layer was manufactured with an autoclave-cured 24-ply CFRP laminate using the pre-impregnated ply technology. The CFRP laminate was prepared with continuous unidirectional fibre layers with 0°, 90° and ±45° orientations. The fraction of volume fibre was 64%, and the thickness, 3.3 mm. The titanium layer was a Ti-6Al-4V, with a thickness of 2.0 mm. The aluminium layer was comprised of one 3.5 mm thick 7000 series aluminium alloy.
A Thermex® thermoreactive paper was placed between each two layers of the stack. Its reactive side was oriented in the direction of the titanium layer, which allowed a verification of the temperature at the interface of two materials to see if it was not high enough to affect the materials of the stack. The paper used was 0.05 mm thick, and colour-reacted at temperatures ranging between 90 °C and 150 °C. Above 150 °C, the paper became darker and darker until combustion.
Figure 2 shows the experimental set-up. A sponge filled with coolant was placed on the junction frame part between the Kistler® table and the fixture of the workpiece.
This mounting, shown in Figure 3, allowed the drilling of 120 holes, with a maximum diameter of 6 mm in an 80 mm x 300 mm workpiece. Two series of 120 holes were drilled for this study.
The torque and thrust force were measured for each drilling using a 9255B Kistler® piezoelectric dynamometer table. The signals were transmitted to an amplifier, and then acquired through an analog/digital converter and a data acquisition system.

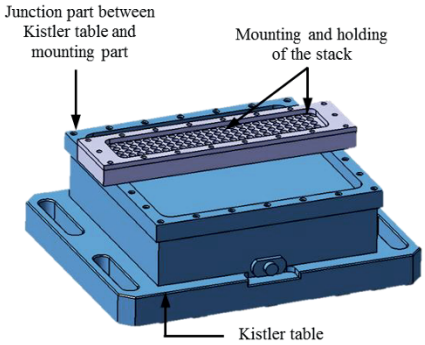

Figure 2: Experimental set-up of the positioning and holding of the workpiece, mounted over the Kistler force measurement table and a junction part

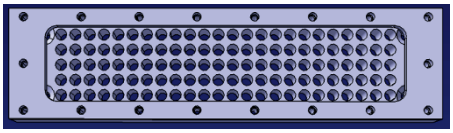

Figure 3: Top view of the holding table and frame of the stack

3- Methodology

3.1 - Design of experiments

This study, which covers the drilling of a stack of multimaterials composed of CFRP, titanium and aluminium alloys was carried out to improve the stability of the process as well as the hole quality. Burr heights were investigated for the outlets of metallic parts of the stack for different cutting parameters and different cutting strategies, with the parameters being the heights of pecks during peck drilling, feed variations while cutting, and cutting height parameter changes. However, because the selected strategies have only a minor impact on the burr heights, we saw no need to present the strategy variations versus the burr height.
For each type of material in the stack, three feed and three speed levels were selected. The design of experiments, which was divided into two parts, included an $L_{27}(3^6)$ Taguchi plan of experiment and a full plan of the couple feed-speed for each of the three materials.
For these two plans of experiments, only the cutting parameters of the different layers of the stack were used for the selection of the experiment factors.
Each design of experiments was repeated three times, and although each was repeated separately from the others, the order of the drillings was randomized for each repetition.
The values of the cutting parameters will be presented as

normalised using the middle selected level as a cutting parameter reference.
Three twist drills with a common geometry and coating were used for the experiments described. The use of diamond-coated tools is listed in Table I.

Tool #	Number of holes drilled	Experiments
1	118	2 Taguchi + 1 Full
2	64	1 Taguchi + 1 Strategy
3	56	1 Full + 1 Strategy

Table I: Plans of experiments conducted for the twist drills

Before each change of cutting parameters, the drill was put in contact with a sponge filled with coolant. No coolant thru or other external coolant or pressurized air was present in the cutting area.

3.2 - Measurements

Although on-line measurements (forces, torque and vibrations) were performed, they are not presented in detail in this article, but they will be compared to the burr height ratio. The burr height ratio corresponds to the measured burr height over the maximum burr height obtained. The results of these burr height ratios will be presented in percentages. Other features, such as hole dimension and burr measurements, were performed. They will be presented in relation to the burr height ratio.
Burr heights were measured at the outlet of the titanium and aluminium layers of the stack.
Each burr height was estimated as an average of three measurements, and the burr height measurements were performed using a digital probe indicator.

The tool wear VB_Bmax was measured on the clearance faces of the twist drill with every five drillings. A picture of each clearance face was taken using the digital optical microscope Keyence VHX-500F. Then, the tool wear VB_Bmax on both clearance faces was estimated using the digital images obtained. In this article, the tool wear VB_Bmax corresponds to the means of the tool wear VB_Bmax measured on both clearance faces of the drill. Tool wear evolution is compared to the burr height ratios.

The hole dimensions were measured using the Mitutoyo Bright Strato coordinate measuring machine (CMM). The diameter and circularity were measured for each hole, and at the same depths from their references, given in Figure 4.

Moreover, the thrust force and torque are the averages of the signal obtained during one peck when the drill edges are fully engaged in a same material. The final thrust force and torque values are calculated with the average of all the pecks.

3.3 - Analyses performed

Separate analyses of variance (ANOVA) were performed for the thrust force, the torque burr height, the hole diameter and the circularity, allowing an identification of their impact and the quantification of the different cutting parameters. The results of the analyses of the burr heights are presented in this paper.

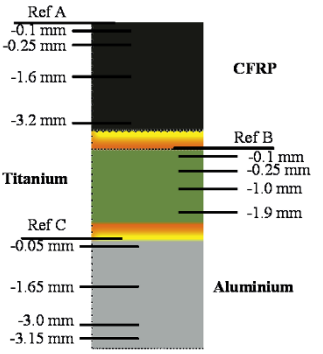

Figure 4: Depths for the measurements of hole diameter and circularity for the three parts of the stack (the references are at the top of each layer in the stack)

4- Results and discussion

4.1 - Titanium burr height analysis

The burr height ratio versus the tool wear is preferred to the same burr height ratio versus the number of drilled holes performed with the tool. Indeed, the tool wear of identical tools can differ from the same cutting conditions after a certain number of drilled holes. Figure 5 shows the evolution of the measured burr heights versus the measured tool wear VB_Bmax.
The dependency between the burr height ratio and the tool wear is shown in Figure 5. A regression was calculated using a third-order polynomial function. The tests were performed on the stack of materials where there was no clearance at the outlet of the titanium layer. Indeed, the burr height versus the tool wear should become steady, and thus tend to be limited under a maximal value due to the presence of the aluminium layer at the outlet side of the titanium plate. Nevertheless, it has not been observed in our results, as shown in Figure 5. Two possible explanations are considered in this situation. The first one is that this maximal limit was not reached in our tests. Perhaps, the same experiments conducted with a higher tool wear could show this limit or at least a reduction of the increase. The second explanation is that the titanium burr is pushing onto the aluminium layer which is locally deformed, due to the lower hardness of the aluminium comparatively to the titanium.

No significant correlation was observed between the burr height and the diameter nor the correlation between the burr height and the circularity of the hole. The correlation coefficient between circularity and burr height or diameter and burr height is very close to zero for results obtained with the same cutting conditions. Both, hole circularity and diameter have a normal distribution and are independent to the burr produced at the outlet of the metallic parts.
Figure 6 and Figure 7 depict the burr height ratio versus the

thrust force and the torque for the same cutting conditions selected as cutting parameters at the centre point of the variation factors, speed and feed, for the titanium cutting parameters. In presented graphs, a linear regression was calculated. The *R*-squared coefficient is lower for the torque due to a higher dispersion, 0.77 for Figure 6 and 0.5 for Figure 7.

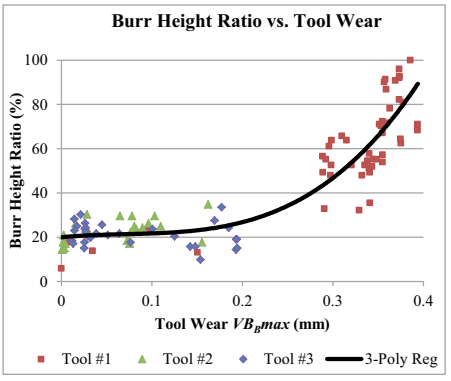

Figure 5: Titanium burr height ratio versus the clearance tool wear VB_Bmax

Table II shows the means of the obtained burr height ratios for each set of cutting parameters. According to the results, the burrs are mainly impacted by the feed. The higher the feed is, the lower the burr heights are. The speed influence does not significantly affect the burr height.

Additionally, the standard deviation of burr height ratio was calculated using the measurement results of the holes drilled with the same cutting conditions with a tool wear inferior to 0.20 mm, giving the result of 5.5 %.

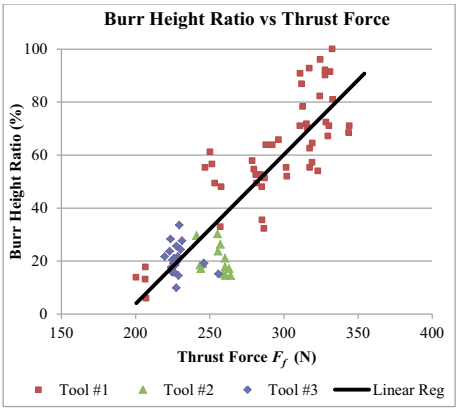

Figure 6: Titanium burr height ratio versus the thrust force under same cutting parameters corresponding to the centre point of the variation parameters for titanium

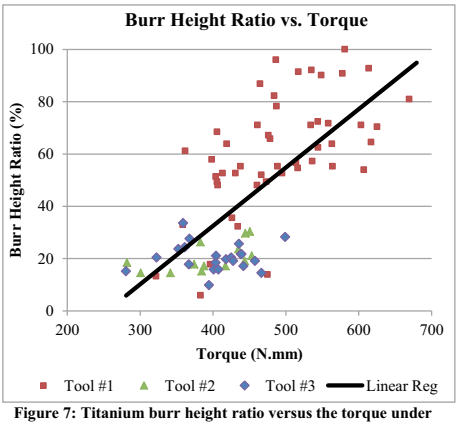

Figure 7: Titanium burr height ratio versus the torque under same cutting parameters corresponding to the centre point of the variation parameters for titanium

Feed/Speed Levels	Titanium Speed 70%	Titanium Speed 100%	Titanium Speed 130%
Titanium Feed 60%	51.3	48.5	50.6
Titanium Feed 100%	42.9	43.9	42.2
Titanium Feed 140%	36.6	40.4	26.8

Table II: Means of the titanium burr height ratios for each couple of feed and speed corresponding to the titanium layer

For each drilling of the thermoreactive paper, a dark halo surrounding the hole made was observed. The radial halo measurement of the thermoreactive paper placed at the interface between the titanium and the aluminium layers gave results of between 0.02 and 0.05 mm. Around this dark halo, no other colour was present, meaning that the temperature gradient was high at the outer limits of the halo.

4.2 - Aluminium burr height analysis

In all the feed, speed and cutting strategy configurations, the aluminium burrs at the outlet of the hole were without attachment on the exit surface. In all the drillings performed, no burr was formed with a ring or with a drill cap.
Figure 8 depicts the evolution of the measured burr height ratio versus the tool wear VB_Bmax. A third-order polynomial regression function was calculated, and is shown in Figure 8.

For the titanium layer, no correlation was found as well either between the burr height and the diameter or between the hole circularity and the burr height. The correlation coefficients for both cases at different depths in the aluminium layer were very close to zero. These correlation coefficients were calculated for the holes drilled with the same cutting conditions.

Article 052-pp-105

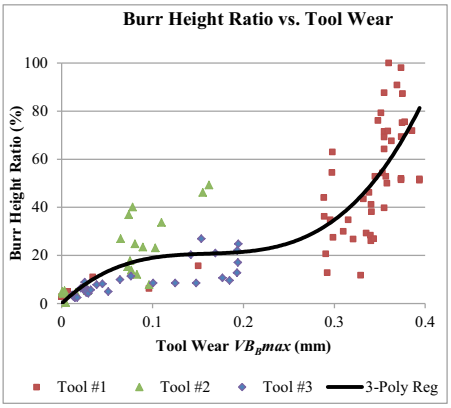

Figure 8: Aluminium burr height ratio versus the clearance tool wear VB_Bmax

The burr height ratio versus the thrust force is shown in Figure 9. An exponential regression function was calculated and drawn in Figure 9, and the *R*-squared coefficient of the exponential regression equals 0.54.

No significant correlation can be observed between the torque and the aluminium burr heights, while the correlation coefficient calculated was close to zero.

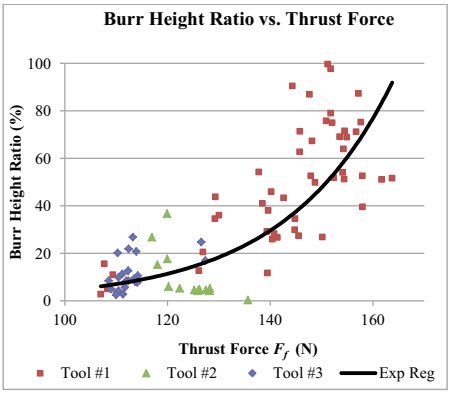

Figure 9: Aluminium burr height ratio versus the thrust force under same cutting parameters corresponding to the centre point of the variation parameters for titanium

The averages of the burr height ratios obtained for each set of cutting parameters are presented in Table III. According to the results, for low and middle cutting speeds, the feed affects the burr height, while for high cutting, the burr height becomes more stable whatever the feed is.

Feed/Speed Levels	Aluminium Speed 60%	Aluminium Speed 100%	Aluminium Speed 140%
Aluminium Feed 75%	29.2	31.0	33.7
Aluminium Feed 100%	34.6	35.7	32.2
Aluminium Feed 125%	40.5	42.0	32.9

Table III: Means of the aluminium burr height ratios for each couple of feed and speed corresponding to the aluminium layer

Additionally, the standard deviation of the aluminium burr height ratio was calculated using the measurements of the holes drilled with the same cutting conditions with a tool wear lower than 0.20 mm. This standard deviation is approximately 10%.

5- Conclusion

Multimaterial stack drilling experiments were conducted using diamond-coated twist drills. The burr heights versus factors such as speed and feed levels, tool wear, thrust force, torque, diameter and circularity were studied.

Because a deburring process may not be used following the drilling of a multimaterial stack, the burr heights need to be controlled. For titanium burrs, the process can be controlled on-line thanks to the torque and, for more accuracy, with the thrust force. The tool wear is also an effective way to control the burr height.

The results show that the titanium burr height can be reduced using a higher feed.

The aluminium burrs can be monitored on-line as well with the thrust force, and also with the tool wear.

The aluminium burrs can be reduced by increasing the cutting speed or by decreasing the feed.

6- Acknowledgement

The authors wish to thank the Consortium for Research and Innovation in Aerospace in Québec (CRIAQ) and its partners, the Natural Sciences and Engineering Research Council of Canada (NSERC), Mitacs, Bombardier Aerospace, Avior Integrated Products, Delastek and AVR&R Aerospatiale, for their financial support. A part of the research presented in this paper was financed by the Fonds de recherche du Québec - Nature et technologies by the intermediary of the Aluminium Research Centre – REGAL

7- References

[BJ1] Brinksmeier, E., & Janssen, R. (2002). Drilling of Multi-Layer Composite Materials consisting of Carbon Fiber Reinforced Plastics (CFRP), Titanium and Aluminum Alloys. *CIRP Annals - Manufacturing Technology, 51*(1), 87-90. doi: http://dx.doi.org/10.1016/S0007-8506(07)61472-3.

[CT1] Cantero, J. L., Tardio, M. M., Canteli, J. A., Marcos, M., & Miguelez, M. H. (2005). Dry drilling of alloy Ti-6Al-

4V. *International Journal of Machine Tools & Manufacture, 45*(11), 1246-1255. doi: 10.1016/j.ijmachtools.2005.01.010.

[C1] Committee, A. I. H. (1992a). Machining. In A. International (Ed.), *ASM Handbook* (Vol. 16, p. 929): ASM International.

[C2] Committee, A. I. H. (1992b). Properties and Selection: Nonferrrous Alloys and Special-Purpose Materials. In A. International (Ed.), *ASM Handbook* (Vol. 2, p. 3470): ASM International.

[DK1] Dornfeld, D. A., Kim, J. S., Dechow, H., Hewson, J., & Chen, L. J. (1999). Drilling Burr Formation in Titanium Alloy, Ti-6AI-4V. *CIRP Annals - Manufacturing Technology, 48*(1), 73-76. doi: http://dx.doi.org/10.1016/S0007-8506(07)63134-5.

[GL1] Guegan, P., Lemaitre, F., & Hamann, J. (1992). Contribution a l'usinage des materiaux composites.

[KW1] König, W., Wulf, C., Graß, P., & Willerscheid, H. (1985). Machining of Fibre Reinforced Plastics. *CIRP Annals - Manufacturing Technology, 34*(2), 537-548. doi: http://dx.doi.org/10.1016/S0007-8506(07)60186-3.

[LN1] List, G., Nouari, M., Géhin, D., Gomez, S., Manaud, J. P., Le Petitcorps, Y., & Girot, F. (2005). Wear behaviour of cemented carbide tools in dry machining of aluminium alloy. *Wear, 259*(7–12), 1177-1189. doi: 10.1016/j.wear.2005.02.056.

[MR1] Mathew, J., Ramakrishnan, N., & Naik, N. K. (1999). Investigations into the effect of geometry of a trepanning tool on thrust and torque during drilling of GFRP composites. *Journal of Materials Processing Technology, 91*(1–3), 1-11. doi: http://dx.doi.org/10.1016/S0924-0136(98)00416-6.

[MM1] Molinari, A., Musquar, C., & Sutter, G. (2002). Adiabatic shear banding in high speed machining of Ti-6Al-4V: experiments and modeling. *International Journal of Plasticity, 18*(4), 443-459. doi: http://dx.doi.org/10.1016/S0749-6419(01)00003-1.

[NL1] Nouari, M., List, G., Girot, F., & Géhin, D. (2005). Effect of machining parameters and coating on wear mechanisms in dry drilling of aluminium alloys. *International Journal of Machine Tools and Manufacture, 45*(12-13), 1436-1442. doi: 10.1016/j.ijmachtools.2005.01.026.

[PE1] Persson, E., Eriksson, I., & Zackrisson, L. (1997). Effects of hole machining defects on strength and fatigue life of composite laminates. *Composites Part A: Applied Science and Manufacturing, 28*(2), 141-151. doi: 10.1016/s1359-835x(96)00106-6.

[P1] Polmear, I. J. (1996). *Light Alloys - Metallurgy of the Light Metals*: Halsted Press.

[SS1] Shyha, I. S., Soo, S. L., Aspinwall, D. K., Bradley, S., Perry, R., Harden, P., & Dawson, S. (2011). Hole quality assessment following drilling of metallic-composite stacks. *International Journal of Machine Tools and Manufacture, 51*(7-8), 569-578. doi: http://dx.doi.org/10.1016/j.ijmachtools.2011.04.007.

[SA1] Stephenson, D. A., & Agapiou, J. S. (2005). *Metal cutting theory and practice* (Vol. 68): CRC press.

[TF1] Tönsheff, H. K., Friemuth, T., & Groppe, M. (2001, June 27-28). *A solution for an economical machining of bore holes in composite materials (CFK, aluminum).* Paper presented at the Proceedings of 3rd International Conference on Metal Cutting and High Speed Machining, Metz (France).

[TH1] Tsao, C. C., & Hocheng, H. (2007). Effect of tool wear on delamination in drilling composite materials. *International Journal of Mechanical Sciences, 49*(8), 983-988. doi: http://dx.doi.org/10.1016/j.ijmecsci.2007.01.001.

Article 065-ap-49

Arezzo: an emulator for the bench4star initiative

Thierry Berger[1,2], Dominique Deneux[1,2], Thérèse Bonte[1,2], Etienne Cocquebert[1,2], Damien Trentesaux[1,2]

(1) : University Lille Nord de France, F-59000 Lille, France
(2) : UVHC, TEMPO Research Center, F-59313 Valenciennes, France
Phone: +33 (0)3 2751 1463
E-mail : { firstname.lastname }@univ-valenciennes.fr

Abstract: In the manufacturing and production shop floor control context, benchmarking is a popular means to test and compare several strategies, so as to make high level design decisions, to fix the main control choices and to adjust the control parameters. A benchmarking process involves experimentation. Several kinds of experiments can be performed, either in simulation or based on the real manufacturing system. An advantageous intermediary approach can be adopted, based on emulation. For this purpose, an emulator of the shop floor of the targeted manufacturing system is required. After defining the general benchmark context, the Bench4star initiative is introduced in this paper. Thereafter, the Arezzo emulator we have developed in Bench4star is described. Arezzo emulates the shop floor of the real AIP-Primeca Flexible Assembly Cell, located in the University of Valenciennes. It is implemented in NetLogo.

Key words: Benchmarking, Flexible manufacturing systems, Manufacturing control, Component-based, Emulation.

1- Introduction

A manufacturing system is composed of a shop floor (real machines and low level PLC-based control) and a high level control system (shop floor control for real-time allocation and routing) [TP1]. Research in manufacturing and production control is constantly growing, leading to an increasing number of innovative scheduling and control solutions, each of them characterized by specific assumptions and potential advantages [T1]. But a very small number reaches the stage of industrial implementation and tests in real condition are seldom for several reasons [ML1], in particular the difficulty to obtain an affordable performance evaluation that is robust and reliable enough to convince industrials to take the risk to actually implement it. This situation is appealing for a rigorous benchmarking process. The Bench4star initiative is an answer to this issue [TP2].

Benchmarking means comparing the outputs of different controlled systems for a given set of input data, with a view to seek for improved performance. The Bench4star initiative has been conjointly developed by the TEMPO Research Center of the University of Valenciennes (UVHC-TEMPO, France) and the Polytechnic Institute of Bragança (IPB, Portugal) [B1, TP2]. Bench4star is fully consistent with the recent IFAC TC 5.1 resolution [I1], which suggests designing, using and disseminating manufacturing control benchmarks. It has been designed to fit the benchmarking requirements of both the control research (CR) and the operation research (OR) communities [TP2]. The CR community specifically requires an accurate, stable and reproducible behavior of the physical production system and the possibility to monitor all its components, including perturbations characterized by both predictable (e.g.: planned maintenance) and unpredictable events (e.g.: unplanned failures, machine breakdown). The OR community requires a formal static model of the production system but does not need a precise and realistic modeling of the production system and its behavior facing perturbations.

To limit the appropriation risk for the CR community, an open and easy-to-use emulator of a real production system is needed, in which events can be modeled on demand. Thus, researchers from the CR community can put their effort on testing their own control laws just as if they were plugged on a real system. They can speed up their developments and be assured, when these latter are validated on the emulator, to be able to plug the same design control system on the real manufacturing system. Moreover, when researchers aim at using the real system for validation purpose, they must deal with many issues such as manufacturing system setup, installation and programming of hardware/software tools, scenarios description, sequencing and management of experiments, data collection, analysis, and generation of reports… [RT1]. All these tasks can be facilitated by ensuring that the proposed emulator is designed “as if” control laws were plugged on the real system.

The core subject of this paper is to describe such an emulator and to illustrate its benefits. Our emulator, called Arezzo, is associated to the Bench4star benchmarking initiative. It is accessible for free to anybody interested in using Bench4star as a benchmarking environment. Section 2 introduces the Bench4star initiative and the positioning of emulation.

Section 3 presents the design principle of the Arezzo emulator. Section 4 exposes the real system to be emulated and presents some implementation elements of Arezzo in NetLogo. Section 5 gives some illustrations of Arezzo. Section 6 draws the conclusions and introduces future works.

2- Bench4star initiative

2.1 - Bench4star benchmark

Bench4star has been constructed based upon a real full-size physical system, to stimulate benchmarking activities to be grounded in reality: the AIP-Primeca cell. This benchmark allows the evaluation of static optimization performances using traditional operation research tools and the evaluation of control system's robustness faced with unexpected events. The process associated to Bench4star is constituted of data preparation, experimentation, and reporting steps, as illustrated in Figure 1. For more details on this Bench4star process, please refer to the original communication of Trentesaux et al. [TP2] and the Bench4star web site [B1].

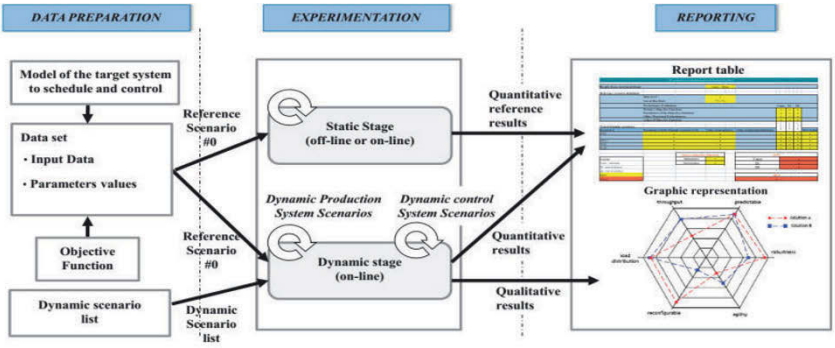

Figure 1: Bench4star process [TP2].

2.2 - Positioning of emulation in Bench4star

According to Auinger et al. [AV1], there are four situations characterizing the testing and debugging of PLC-based control software. Extended to our context, Figure 2 exposes the corresponding four possible combinations between “reality” and “simulation”.

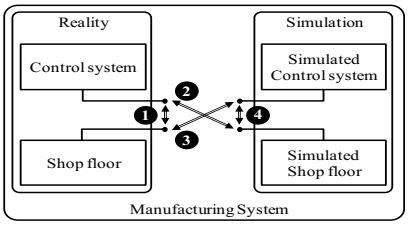

Figure 2: Four possible connections [AV1].

The double arrows represent the possible connections:

1- Traditional way to test control systems, where control and shop floor are real,
2- Soft-Commissioning, where control is real and shop floor is simulated,
3- Reality-in-the-loop, where control is simulated and shop floor is real,
4- Off-line simulation, where both control and shop floor are simulated.

Situation #2 (Soft-Commissioning) corresponds to the emulation situation for which a realistic simulation that mimics the real shop floor has to be done. The Arezzo emulator corresponds to this situation #2. It aims at easing the switch to situation #1 with the less possible effort, enabling the evaluation “on the lab/office not on the plant floor” [M1, S1], thus reducing time, cost and effort [JC1]. In other words, our will is that any Bench4star-based designed control system can be indifferently connected to the AIP-Primeca cell or to Arezzo. The next section introduces the design approach adopted to develop the Arezzo emulator for the shop floor of the AIP-Primeca cell associated to the Bench4star benchmark.

3- Specifying the Arezzo approach

Arezzo is an emulator of the AIP-Primeca cell usable with Bench4star. But it has been designed in a generic way to be applicable on different target systems, not only the AIP-Primeca cell. This paper sums up all the specifications for that purpose.

First, the design approach of Arezzo integrates the usual requirements [AV1, HF1] for “soft-commissioning” (a detailed list of ten requirements is suggested by Auinger et al. [AV1]) to which the following ones were added:

- For ensuring the independence from any tool, the emulated and the real shop floor both communicate with the control layer using the same communication interface,

- For managing scalability issues, the emulator is made of bricks (Lego™ principle).

Second, it has been assumed that in the context of manufacturing system, three major control levels are defined, which is usual [C1, TP1]:

- Level 0 (L0) encompasses the physical manufacturing process, composed of equipments (e.g., mechanical parts of robots, conveyors, shuttles…), sensors and basic actuators.
- Level 1 (L1) has an informational nature. It is supported by controllers (PLC, robot controllers, and communication networks) in charge of the low level control (e.g.: simple product transfer, robot trajectory control).
- Level 2 (L2) also has an informational nature. It is supported by computers and networks in charge of the high level control (e.g.: allocating tasks, routing products).

This organization enables us to specify that Arezzo emulates levels 0 and 1. Level 2 is independent from Arezzo and is designed by the final user (the researcher). It is assumed that L2 will be modeled by any researcher using decisional and autonomous entities (e.g., agents, actors, holons...).

Third, so as to capture the requirement of scalability and the possibility to indifferently plug, without noticeable change, any L2 control either to the real shop floor or to its emulated version, the real shop floor is modeled by means of components [LW1] and services. The next part presents this approach in details.

3.1 - Component-based approach

In Arezzo, a component is identified (Comp-ID) and implements a set of specific services actually realized at levels L1 and L0 (See Figure 3). So as to trigger a Si service, an agent at L2 sends a request (denoted “Req. Si”) to a component that can implement it. The triggered component sends back a state/response (denoted “Resp. Si”) to this agent. The component approach helps reduce the informational (L1) and physical (L0) device to a pure informational piece of software. A component can be implemented with any programming paradigm (e.g., imperative, object, agent…).

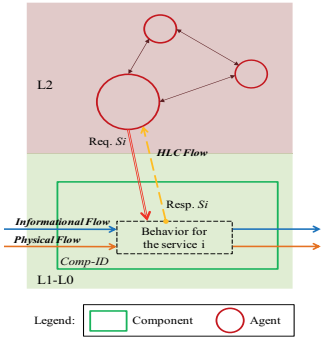

Figure 3: Towards component as a service container.

3.2 - Interfacing L2 and L1-L0

As previously introduced, the interface layer (denoted “ILy”) indifferently supports the interfacing of the control layer L2 with either the real or emulated shop floor (L1 and L0). The ILy in Arezzo uses data tables [ML1] for service request (table Req. Si) and feedback (table Resp. Si) (See Figure 4).

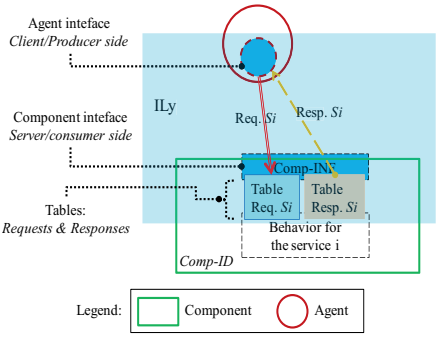

Figure 4: Interface layer table-oriented.

3.3 - Component identification

Basically, a component has an interface to trigger services (e.g.: via writing in the write-table Req. Si) and to collect state/response of services (e.g.: via reading in the read-table Resp. Si). A component also contains services that can be obtained by level L2. The identification of the component interface is in direct link with the data access (e.g.: PLC network adapters and protocols) used in the real shop floor to be emulated.

In production control the two major components are products and resources. A product requires services from resources and a resource offers services to products. These services can usually be split into three categories [FC1], which is the case in Arezzo: space services (e.g.: product transported by a shuttle within a conveying system), time services (e.g.: temporary storage of the product) and transformation services (e.g.: product properties modification like machining, assembly, inspection or measurement).

So as to define a component in Arezzo, it is required to determine:

- The set of services belonging to space, time and transformation categories, which act on physical flows,
- The interface to and from Req. Si and Resp. Si tables,
- The write-table allowing services to be triggered (Req. Table),
- The other read-table (Resp. Table) to store the state/response of the services providers (e.g., ready, running, waiting, dead, in defect…),
- The physical flows on which services apply,
- Optionally, the informational flow exchanged between all components (e.g., data shared from sensors).

Figure 5 shows an illustration of a transfer gate allowing a shuttle (carrying a product, for example) to be transferred on a conveying system from PF1 to PF2 or PF3.

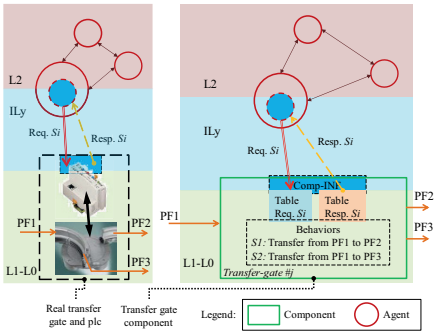

Figure 5: Transfer gate component (left in reality, right in Arezzo)

The next section presents the application of the Arezzo approach to design the emulator usable with the Bench4star.

4- Arezzo Implementation of the AIP-Primeca cell for the Bench4star initiative

4.1 - Presentation of the AIP-Primeca cell

The AIP-Primeca cell of the University of Valenciennes is built with industrial components and comprises a monorail conveying system exposing 11 transfer blocks (TB, association of 2 transfer gates) permitting the flexible routing of up to 15 identified shuttles (RFID tagged) across 7 workstations (W) in charge of performing specific operations (e.g.: robotic assembly, inspection…) upon products being manufactured.
Each product is associated to a dedicated shuttle during its manufacturing cycle. It has to be conveyed on this shuttle from a workstation to the next one according to a process plan. Figure 6 gives a view on the workstations and their localizations.

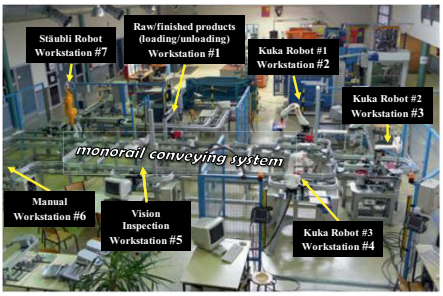

Figure 6: General view of the real AIP-Primeca Cell.

The architecture of the cell is shown Figure 7. It is mainly composed of the following levels:

- Levels 0 and 1 (shop floor) are implemented by electro-mechanical systems (Stäubli and Kuka robots; Cognex cameras; Montratec monorails, transfer gates and positioning units), PLCs (750-841 Wago controllers), stop & go shuttle devices, RFID R/W equipment (Schneider OsiSense XG) and Ethernet switched automation network. Modbus is the standard communication protocol used between all equipments. 26 Modbus/TCP servers exist on the cell (one on each of the 18 Wago PLCs, and one on each of the 8 gateways for the 22 RFID R/W).
- Level 2 is the high level control layer. The major problem to solve at this level 2, taking into account perturbations, is the use of workstations over the time (allocating problem) and the routing of the work in progress by means of shuttles (routing problem), so that the process plans can be executed on the available resources.

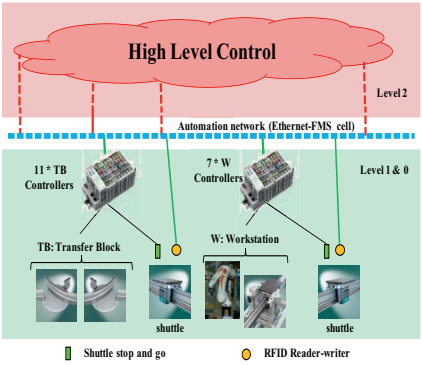

Figure 7: AIP-Primeca cell physical architecture.

Figure 8 shows a schematic view of the cell with its 7 workstations (from W1 to W7).

4.2 - Component model of Arezzo

The Arezzo modular model creation consists in defining the components permitting to model the shop floor of the AIP-Primeca cell and the component architecture defining the connections between some instances of these components.

4.2.1 -Identified components

Considering the actual network access points (PLCs and RFID gateway) and the existing resources of the AIP-Primeca cell, six basic components (one product **P**-component and five resources **Sh**/**W**/**S**/**T**/**R**-components) have been defined, characterized by the following attributes:

- **P** (product) attributes: product-id, an ordered list of services to be requested and obtained,
- **Sh** (shuttle) attributes: shuttle-id, product-id of the conveyed product, component-id of the component (e.g.: W, S, T) on which it is and its approximate position on the

conveyor section, state (stopped, moving)…,
- **W** (workstation) attributes: workstation-id, list of services that can be obtained, state of the services, duration of each service, IP address, modbus access to its two data tables…,
- **S** (switch) attributes: switch-id, a list defining the connections with other components, the services provided (switch from an input physical flow to an output physical flow, restart (go) a stopped shuttle), IP address, modbus access to its two data tables…,
- **T** (track) attributes: track-id, the connection with others components, shuttle regular moving speed on it…,
- **R** (RFID Reader/Writer) attributes: RFID-id, IP address, modbus access to its two data tables…

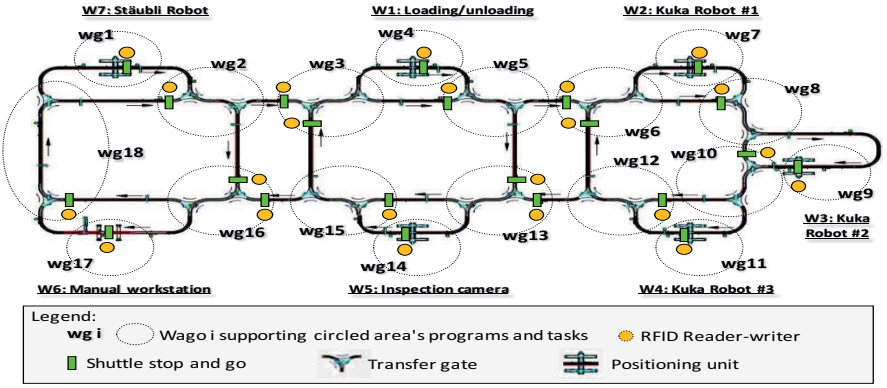

Figure 8: Schematic view of the Aip-Primeca cell.

4.2.2 -Component architecture

The component architecture models the components needed and their connections (by physical and/or informational flows). For clarification purpose, Figure 9 shows the detail of some connected components of the AIP-Primeca cell (at workstation W1). The double arrows represent T-components, which permit to connect others components by means of physical links. The W#1 component encapsulates workstation W1, in charge of two loading and unloading services of a P-component on a Sh-component. The R#1 component represents a RFID Reader/Writer and the bidirectional thin arrow represents the informational flow by which R#1 can access to its associated "RFID Reading/Writing pad" (circle) inside W#1. The S#5 component is a switch. Figure 9 shows the 2 physical input flows and the 2 physical output flows. The services provided by an S-component are the dynamic creation, when requested via data-tables, of a physical flow between one of the two inputs and one of the two outputs. This allows a Sh-component to cross the S-component like in the reality, when a shuttle crosses a switch.

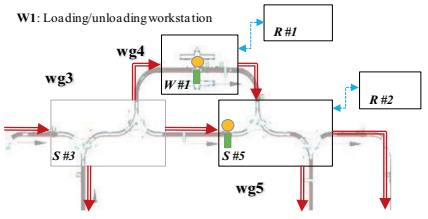

Figure 9: Arezzo Component architecture - workstation W1 area.

4.3 – Arezzo implementation

The implementation of the emulator model consists in instantiating each component, the physical and/or informational links between them, executing the behavior components when needed, realizing the interface with the high level control (L2) and maintaining the state of the emulated plant up-to-date. This is done through a software platform developed in NetLogo.

4.3.1 -NetLogo choice

Several commercial platforms (e.g.: Visual Component [V1], Rockwell Automation [R1]...), free tools (e.g.: Emulica [E1], NetLogo [N1]...) and paradigms (e.g.: object, multi-agent) exist [AA1]. The very popular and widely used NetLogo multi-agent simulation platform was chosen for its openness, ease of implementation, large community, comprehensive documentation and gratuity [TW1]. Comparisons with other agent platforms [RL1] confirm this choice. NetLogo is a high-level platform providing a simple yet powerful programming language and a built-in graphical interface. It was primarily designed for agent-based modeling of physically mobile individuals with local interactions in a grid space. NetLogo is also recommended for prototyping complex models [TW1].

4.3.2 -Emulator architecture

Arezzo runs on a usual computer. Its connection with the high level control is shown Figure 10. The main module is the NetLogo "emulation engine". This module implements, via the "Interaction" module, the bidirectional

communication with level L2 and the state update of each component. Its graphical display is taken in charge by a "Visualization" module. The communication is implemented by the interface layer constituted by several "Virtual network" adapters and a "Modbus/TCP server".

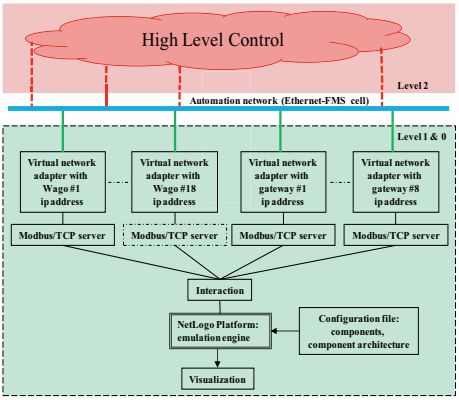

Figure 10: General architecture of Arezzo - AIP cell application.

A "Virtual network adapter" corresponds to a real access point from level L2 to L1-L0, as for example a Wago PLC or a RFID gateway. Each "Modbus/TCP server" contains the required data-tables (Req. Si and Resp. Si). These tables, in the reality, correspond to specific memory areas in a Wago PLC or RFID gateway. The interface layer between the level L2 and L1-L0 is the same in the real cell and in its emulation.

4.3.3 –Switch component illustration

The NetLogo emulator model deals with five kinds of agents, one for each type of component. Shuttles are mobile agents. The four other kinds of agents are stationary. Several types of node agents exist: nodes defining the topology, nodes associated with sensors and workstations... Link agents are defined among node agents, to define the transportation network. An S-component becomes a switch-breed in NetLogo. It is a combination of node agents and links between these nodes. A switch-breed has the specificity to include mobile parts. This was modeled by dynamically creating or deleting link agents between the corresponding nodes. Figure 11 highlights the correspondence between the graphical view of a switch and its NetLogo agent model.

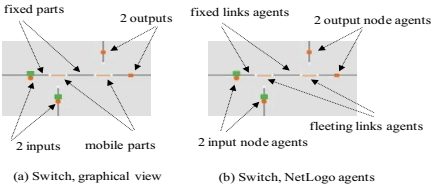

Figure 11: model of a switch.

5- Illustration

Figure 12 shows a global view of the display in Arezzo. Shuttles are symbolized by vehicles (green if the shuttle is free of any product, purple otherwise), workstations are marked with W# (e.g.: W1 for workstation #1). As it can be seen, this view is very similar to the one in Figure 8.

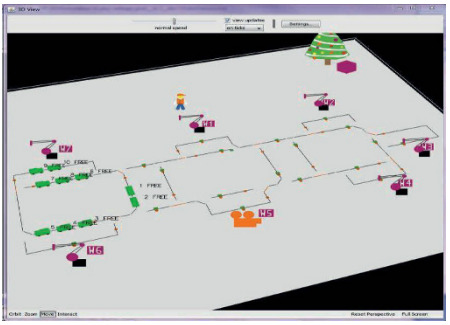

Figure 12: global view of the Arezzo display.

Figure 13 shows the same situation, in the reality (Figure 13-a) and in Arezzo (Figure 13-b). At the entry gate of switch S#3 (already seen Figure 9) two shuttles are waiting for transfer.

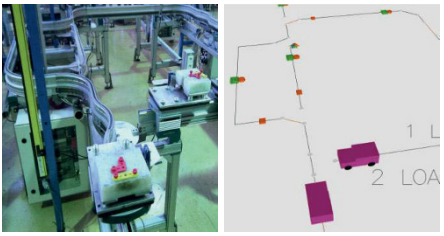

(a) **(b)**

Figure 13: local view of the cell, a: reality, b: Arezzo.

We consider, as an example (Figure 13), that the leftmost shuttle has to be unlocked to cross over the switch S#3. This "shuttle unlocking" service is obtained when the high level control (L2), sending a "write data" modbus request, sets the Word#300 to value "1" in the write-table accessed by the modbus/TCP server top of switch #3. For example, in the Java object language (with Jamod: Java Modbus library[J1]) the code, used at level L2 to set the Word#300, which can be seen as an action variable, to the value 1 (to unlock left shuttle, Figure 13) would be:

```
// comment: in Java, Write to the register 300 the value 1
   //Prepare the request
SimpleRegister data = new SimpleRegister(1);
write_reg = new WriteSingleRegisterRequest(300, data);
   //Equipment_S3 represents the socket for the switch S#3
trans = new ModbusTCPTransaction(Equipment_S3);
```

```
trans.setRequest(write_reg);
trans.execute();   //execute the write (1 in register 300)
// .....
```

Doing this indifferently produces the same effect on the AIP-Primeca cell or on Arezzo. So as to control the AIP-Primeca cell shop floor (real or emulated) the programmer of level L2 uses a list. It describes the components/equipments with their IP addresses, state-services (read-tables with inside "state variables") and request-services (write-tables with inside "action variables"). So the high level control (L2) is unable to determine whether it controls the reality (e.g.: AIP cell) or its emulated version (e.g., Arezzo). This was actually the goal!

6- Conclusion

This paper described Arezzo, an easy-to-use and accurate emulator and illustrated the application of this emulator to the AIP-Primeca cell in the context of the Bench4star initiative. Its component-based modular organization and standardized interface makes it possible to test the performance of several high-level control strategies, implementing the allocation of product, time and transformation operations as well as spatial routing, so as to compare them and improve the performance of the designed control layer, without being burdened by the efforts dedicated to model the low-level control and the physical layer components. Arezzo provides the ability to objectively compare various high level control research contributions, whatever the models or tools implement them. Arezzo is currently being deployed to our network of research partners. The future developments concern the possibility to generate defects on emulated components and to record emulation runs, for example to analyze a specific run a posteriori. It would be equally interesting to compare Arezzo to concurrent initiatives (e.g. [LS1]).

7- References

[AA1] Azab, A., & AlGeddawy, T. (2012). Simulation Methods for Changeable Manufacturing. CIRP, 3, 179-184.

[AV1] Auinger, F., Vorderwinkler, M., & Buchtela, G. (1999, December). Interface driven domain-independent modeling architecture for "soft-commissioning" and "reality in the loop". In Proceedings of the 31st conference on Winter simulation: a bridge to the future-Volume 1 (pp. 798-805). ACM.

[B1] BENCH4STAR (2013): Bench4star benchmark, http://www.univ-valenciennes.fr/bench4star/ (accessed 2013/12/29).

[BS1] Bratukhin, A., & Sauter, T. (2010, September). Bridging the gap between centralized and distributed manufacturing execution planning. In Emerging Technologies and Factory Automation (ETFA), 2010 IEEE Conference on (pp. 1-8).

[C1] Christensen, J. H. (2003). HMS/FB architecture and its implementation. In Agent-based manufacturing (pp. 53-87). Springer Berlin Heidelberg.

[E1] EMULICA (2013): Emulica, http://emulica.sourceforge.net/ (accessed 2013/12/29).

[FC1] Féliot, C., Cassar, J. Ph., & Staroswiecki, M., (1996). Towards a Language of Physical Systems, IEEE SMC Conference, Beijing, Oct. 4-10, 1996.

[HF1] Hibino, H., & Fukuda, Y. (2008). Emulation in manufacturing engineering processes. In Simulation Conference, 2008. WSC 2008 (pp. 1785-1793). IEEE.

[I1] IFAC-TC 5.1. Manufacturing Plant Control (2013): Benchmarking Platform, http://tc.ifac-control.org/5/1 (accessed 2013/12/29).

[J1] JAMOD (2013): Java Modbus library, http://sourceforge.net/projects/jamod/ (accessed 2013/12/29).

[JC1] Johnstone, M., Creighton, D., & Nahavandi, S. (2007, December). Enabling industrial scale simulation/emulation models. In Proceedings of the 39th conference on Winter simulation: 40 years! The best is yet to come (pp. 1028-1034). IEEE Press.

[LS1] Lind, M., & Skavhaug, A. (2012). Using the blender game engine for real-time emulation of production devices. Int. Journal of Production Research, 50(22), 6219-6235.

[LW1] Lau, K. K., & Wang, Z. (2007). Software component models. Software Engineering, IEEE Transactions on, 33(10), 709-724.

[M1] McGregor, I. (2002, December). The relationship between simulation and emulation. In Simulation Conference, 2002. Proceedings of the Winter (Vol. 2, pp. 1683-1688). IEEE.

[ML1] Mařík, V., & Lažanský, J. (2007). Industrial applications of agent technologies. Control Engineering Practice, 15(11), 1364-1380.

[N1] NETLOGO (2013): NetLogo, *http://ccl.northwestern.edu/netlogo/index.shtml* (accessed 2013/12/29).

[R1] ROCKWELL AUTOMATION (2013): Siman, http://www.arenasimulation.com/Arena_Home.aspx (accessed 2013/12/29).

[RL1] Railsback, S. F., Lytinen, S. L., & Jackson, S. K. (2006). Agent-based simulation platforms: Review and development recommendations. Simulation, 82(9), 609-623.

[RT1] Rehman, S., Turletti, T., & Dabbous, W. (2011). A Roadmap for Benchmarking in Wireless Networks, ISRN INRIA/RR--7707.

[S1] Schiess, C. (2001). Emulation: debug it in the lab-not on the floor. In Simulation Conference, 2001. Proceedings of the Winter (Vol. 2, pp. 1463-1465). IEEE.

[T1] Trentesaux, D. (2009). Distributed control of production systems. Engineering Applications of Artificial Intelligence, 22(7), 971-978.

[TP1] Trentesaux, D., & Prabhu, V. V. (2013). Introduction to shop-floor control. In Wiley Encyclopedia of Operations Research and Management Science, edited by James J. Cochran, John Wiley & Sons, Inc.

[TP2] Trentesaux, D., Pach, C., Bekrar, A., Sallez, Y., Berger, T., Bonte, T., Leitão, P. & Barbosa, J. (2013). Benchmarking flexible job-shop scheduling and control systems. Control Engineering Practice, 21(9), 1204-1225.

[TW1] Tisue, S., & Wilensky, U. (2004, October). NetLogo: Design and implementation of a multi-agent modeling environment. In Proceedings of Agent (Vol. 2004).

[V1] VISUALCOMPONENTS (2013): Visual Components, http://www.visualcomponents.com/ (accessed 2013/12/29).

Article 068-m-94

Influence of part geometrical tolerancing in the REFM methodology

Pierre-Antoine ADRAGNA [1], Salam ALI[1], Alexandre DURUPT [2], Von Dim NGUYEN[1], Pascal LAFON[1]

(1) : Université de Technologie de Troyes
ICD-LASMIS
12 rue Marie Curie, 10010 Troyes Cedex, France
+33 3 25 51 76 00
E-mail : {pierre_antoine.adragna, salam.ali , von_dim.nguyen1, pascal.lafon}@utt.fr

(2) : Université de Technologie de Compiègne
Roberval-UMR7337
15 Rue Roger Couttolenc, 60200 Compiègne, France
+33 44 23 44 23
E-mail : alexandre.durupt @utc.fr

Abstract: This paper deals with the remanufacturing of existing part in a context of Reverse Engineering (RE). The proposed methodology called Reverse Engineering for Manufacturing (REFM) consists in generating a Computer Aided Process Planning (CAPP) of a part from 3D information, point cloud, and user knowledge. The idea of this methodology is to avoid the passage by the CAD model. Steps of this methodology are based on a Surface Precedence Graph (SPG) build on a suggested geometrical tolerancing of the part. This graph leads to machining operation precedence graph (MOPG) that leads to the CAPP model. A problem of this approach is that different tolerancing of the same part lead to different process planning. To solve this problem, rules are presented to facilitate the user work. This paper presents the REFM methodology illustrated on a study case.

Key words: reverse engineering, CAPP, set-ups, directed graph, tolerancing.

1- Introduction

In mechanical design, Reverse Engineering RE is the process of discovering how to remanufacture an existing part. In this paper, RE is an activity which consists in creating a CAPP model from a suggested tolerancing of the part to remanufacture. As an assumption, this paper considers the following context: there is no information on the query part (no drawing or scheme); only the physical part is available. To remanufacture this kind of parts, an approach called Reverse Engineering For Manufacturing (REFM) is proposed. REFM method is divided in two main stages: accumulation stage and re-use stage. In the accumulation stage, the user is assisted in the RE approach. Once the CAPP model of a part is created, it is stored in the REFM database for a future reuse on a similar part. So, in the reuse stage, the aim is to minimize the user work. For this reason, REFM is considered a recursive approach. Note that REFM system handles only milling and turning machining operations for now.
This paper details some steps of the accumulation stage developed in [AD1] that are automated in Matlab. The accumulation stage is composed of 9 steps as shown in figure 1: (1) segment the 3D point cloud, (2) define the material and the original blank of the part, (3) generate the surface precedence graph SPG based on the part tolerancing, (4) define machining operations, (5) link operations to the geometry (3D identification), (6) define the order of machining features and define set-ups, (7) define fixture planning, (8) select machines and (9) select tools.
This paper details the methodology used for steps 3 to 6 in the accumulation stage of the REFM methodology. This paper is arranged as follows: section 2 presents research literature on reverse engineering methods and process planning; section 3 describes the REFM methodology that generates the CAPP from the part tolerancing; section 4 presents a robust interpretation of the part tolerancing. The existing part considered in this paper is a centering pin, presented in figure 2.

2- Related works

Reverse Engineering methodologies begin with a manufactured part and produce a geometric model. Three main methodologies can be revealed: interactive platform CAD environment, feature extraction and constraints fitting. As an example of CAD environment, the VPERI [VP1] (Virtual Parts Engineering Research Initiative) project was created by the US Army Research Office. Within the VPERI effort there is a strong focus on addressing the need to solve problems of long life cycle product maintenance, and the need to improve re-manufacturing capabilities to provide system-parts. The knowledge of the geometric shape is necessary but not sufficient to reproduce the part. Indeed, reengineering and redesign need functional specifications. Also, a specific design interface is used to allow the additional of knowledge in the form of algebraic equations that represent engineering knowledge such as the functional behavior of the components, the physical laws that govern the behavior, etc. This interface provides mechanisms that guide designers to ascertain that the functional requirements are fulfilled and helps designers to explore alternatives by assisting them as they make changes. Knowledge arises from

the analysis and is simply expressed and transcribed in variables that are interpreted by the VPERI tool.
As an example of a feature extraction, we can cite REFAB system [TO1]. It uses a feature based and constraint based methods to reverse engineer mechanical parts. REFAB is a human interactive system where the 3D point cloud is presented to the user, and the user selects predefined feature in a list, specifies the approximate location of the feature in the point cloud. Then the system fits the specified feature to the actual point cloud data using a least square means method iteratively. So, manufacturing knowledge extraction is achieved implicitly by the user. In the same way, Sunil et al. [SP1] suggest extraction of manufacturing feature in a point cloud. Urbanic et al. [UE1] proposed a library of features based on a specific manufacturing process. They explain that features have accurate mathematical definitions for their geometry and tolerances depending on functional requirements.
Other references such as Fisher [F1] and Mills [ML1], present a reverse engineering approach in which a priori knowledge is applied and expressed through constraints. With the additional user's knowledge about the part and using an optimization algorithm, the shape and position parameters are found even with considerable noisy 3D point cloud.
All references of part remanufacturing do not suggest a structured methodology. The aim of our approach is to bring a methodology to remanufacture a part. The idea in this paper is based on the generation of CAPP.
Several methods can be cited concerning CAPP. [MG1] presents a state of art of CAPP based on literature available between 1989 and 1996 providing details on existing systems, their approach and programming languages. Several manufacturing process are presented such as machining processes (for rotating or prismatic parts), stamping etc. [SY1] proposes a generative approach for process planning of prismatic part. Other solutions of process planning are based on graphs. [ZH1] proposes a solution based on tolerance graph that is decomposed on set-ups. [ZL1] also proposes a graph based approach based on part tolerancing translated in directed graph.

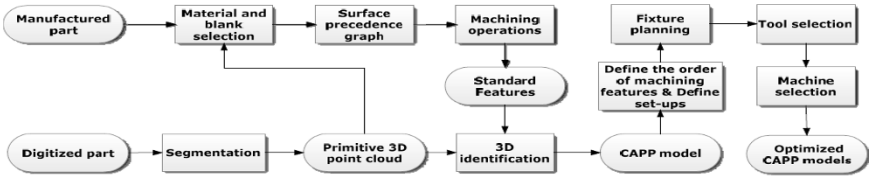

Figure 1: Entire accumulation stage of the REFM methodology [AD1].

3- REFM methodology: from the geometrical part tolerancing to the CAPP model

This section presents in detail the generation of the CAPP model starting from a segmented 3D point cloud and the supposed geometrical part tolerancing. In this section, the part geometrical tolerancing is considered as an input. Several steps are necessary such as:

- Getting the surface precedence graph,
- Defining the machining operations,
- Getting the machining operation precedence graph,
- Defining set-ups,
- Defining part fixture for set-ups, tools and machine for machining operation (not detailed in this paper).

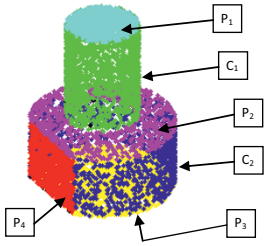

Figure 2: segmented 3D point cloud of the study case (centring pin) to be reversed

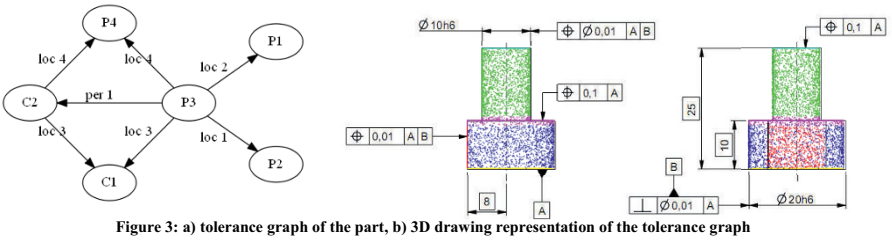

Figure 3: a) tolerance graph of the part, b) 3D drawing representation of the tolerance graph

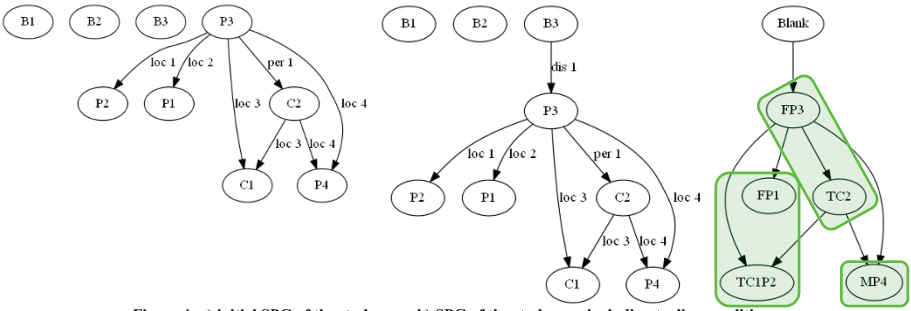

Figure 4: a) initial SPG of the study case, b) SPG of the study case including tooling conditions to create a link from the blank material to the part, c) MOPG and its three identified set-ups

To illustrate the proposed solution, a centring pin is considered. The following figure 2 shows the segmented 3D point cloud of this centring pin and its surfaces label.

The part tolerancing is defined by the user. Tolerances define directed constraints from the reference surfaces to the toleranced surfaces. As no CAD model exists, the part tolerancing cannot be drawn but can be represented as a directed graph. An arbitrary part tolerancing is proposed in figure 3 a) with a graph representation. The CAD drawing presented in figure 3 b) is not proposed by REFM but is manually drawn to facilitate the reading and understanding of the tolerance graph.

3.1 – CAPP: from the part tolerancing to the set-ups

For this section, the part tolerancing is considered as already defined (by the user or another way). Part tolerancing is composed of:

- Dimensional tolerance of surfaces (cylinder, sphere, ...)
- Dimensional tolerance between two surfaces (plane to plane, …),
- Geometrical tolerance of form of surfaces (flatness, roundness, …),
- Geometrical tolerance of orientation of surfaces from others (parallelism, perpendicular, …),
- Geometrical tolerance of position of surfaces from others (location, coaxiality, …),

To simplify the tolerance graph that interprets the part tolerancing, 2 cases are considered:

- Tolerance of a group of entity from another entity or group of entity: the tolerance is interpreted as several tolerances (one entity is toleranced),
- Tolerance using a group of entity as a reference: the tolerance is interpreted as several tolerances using each entity as reference.

The part tolerancing is viewed as a directed graph where reference surfaces leads to toleranced surfaces. In that point of view, tolerances linking two surfaces are considered (dimension between two surfaces, tolerance of orientation or location) and other tolerances applied on only one surface (dimension of one entity, tolerance of form) are not considered. The question is how to consider dimension between two surfaces; as none is reference of the other one which one should lead to the other in the directed graph. This point will be clarified in the next section, let consider this problem solved for now.

Additionally to the part tolerancing, links to the blank material is defined by tolerances. These tolerances can be considered as tolerances defined by tooling department and can be defined by dimensional tolerance (surface to surface to define the minimum chip thickness …) or geometrical tolerance (coaxiality …). However, if no link to the blank is defined by the user, this can easily be detected by the REFM methodology and necessary tolerances are asked to the user. Figure 4 a) shows the initial tolerance graph where no link to the blank material exists, and figure 4 b) shows the minimum tolerance (dis 1 is a dimensional tolerance between plane P3 of the part and plane B3 of the blank material) that can be interpreted as a minimum chip thickness condition.

Now, the tolerance graph is defined, it is possible to define the Surface Precedence Graph (SPG) which is a sorted tolerance graph where surfaces have appearing order. This order is found by a releasing constraints algorithm:

- Surfaces that have no constraint (i.e. surfaces that lead to others but are not leaded from others) are at the i^{th} order. Surfaces of the blank material are at the first order because they are leading and not leaded surfaces.
- Release the constraint of surfaces that are ordered. Hence new surfaces have no constraint and are consider at the $i+1^{th}$ order.
- …

The next step concerns the definition of the machining operation. This step is for now entirely defined by the user that indicates which surfaces are machined in the same operation depending on the part geometry. Defining the machining operations consists in grouping surfaces that are made within the same machining operation (turning, contours …). Hence, surfaces of the SPG can be regrouped in machining operations in order to create a new directed graph based on the machining operations and direction constraints inherited from the SPG. As for the tolerance graph, this new graph is directed and its nodes, machining operation here, can be ordered to define the Machining Operation Precedence Graph (MOPG). The machining operation order proposed by this method (the MOPG) respects a logical order defined by the part tolerancing. Concerning the case study, faces P1 and P3 are machined in independent facing

operation named FP1 and FP3 respectively, faces C1 and P2 are machined in the same turning operation named TC1P2, face C2 is machined in a turning operation named TC2, and finally face P4 is machined in a milling operation MP4. Figure 4 c) illustrates the machining operation precedence graph (MOPG) composed of the machining operation and the inherited precedence constraints from the tolerance graph.

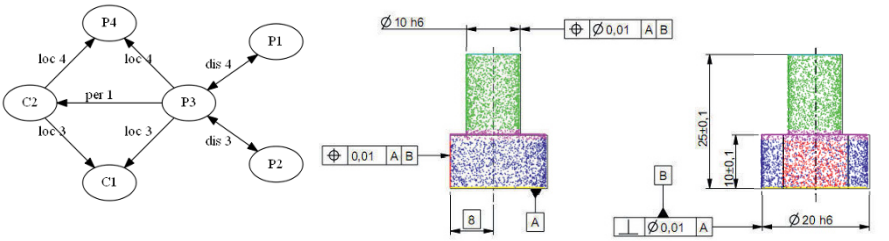

Figure 5: part tolerancing with two dimensional tolerances to interpret in the SPG

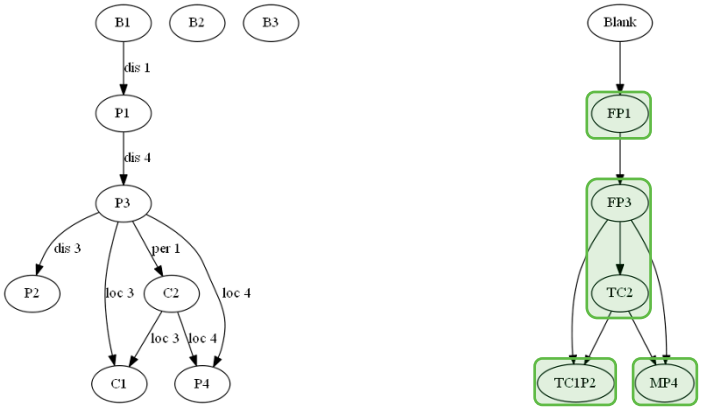

Figure 6: first interpretation of the tolerance part, its SPG, its associated MOPG and its four identified set-ups

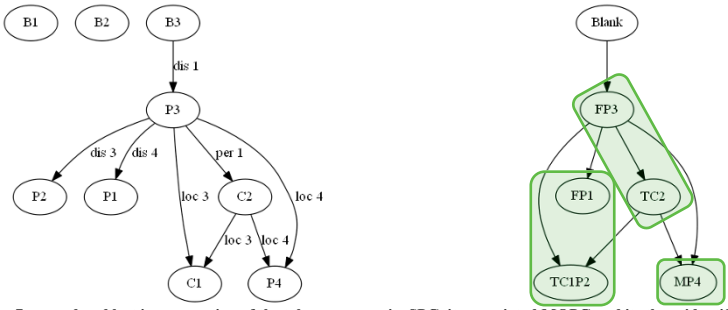

Figure 7: second and last interpretation of the tolerance part, its SPG, its associated MOPG and its three identified set-ups

At this step, set-ups can be defined by grouping the ordered machining operations. Machining operation grouping is defined by the user who knows which following machining operations can be machined in the same set-up due to the part and tools orientation. Concerning the case study, 5 machining operations have been defined and 3 set-ups are found. Figure 4 c) shows MOPG of the study case and the three identified set-ups that are the following machining operation groups: FP3 and TC2, FP1 and TC1P2, and the last set-up that is MP4.

The next steps are not detailed in this paper; they concern the fixture planning definition based on the identified set-ups and the tool and machine selection.

3.2 – Influence of the part tolerancing on the CAPP result

According to the presented REFM methodology, the CAPP result depends on the part tolerancing. A possible cause of variation of the CAPP model is the possible miss-understanding of a dimensional tolerance between two surfaces; as none is considered as reference to the other one, the interpreted constraint in the directed tolerance graph is not directed. Considering this constraint as bidirectional constraint would give no result by the releasing constraint algorithm. Hence, this constraint has to be oriented; both directions may give different CAPP results. Let consider a new tolerancing of the study case presented in figure 5. Two location geometrical tolerances are simplified with dimensional tolerances between planes. This part tolerancing can be interpreted as the two directed tolerance graphs presented in figure 6 a) and figure 7 a). Considering the same machining operation, the obtained CAPP's are presented in figure 6 b) and figure 7 b).

It can be seen that the first interpretation presented in figure 6 lead to feasible CAPP where four set-ups are found. Hence it can be concluded that this CAPP result is degraded compared to the CAPP result of the part tolerancing using location tolerances.

On the other hand, it can be seen that the second interpretation presented in figure 7 lead to the same CAPP as the part tolerancing using location tolerances.

Two other part tolerancing interpretations are not presented here. They lead to unsolvable solutions because two machining operations have inherited constraints from one to the other that create a loop and make impossible the identification of orders.

Hence, this simple case using two dimensional tolerances shows that out of four interpretation cases, only one is optimal, another is feasible and the last two are not possible.

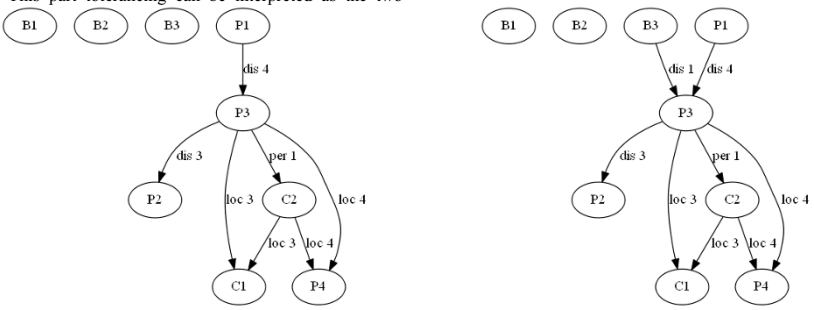

Figure 8: a) one machined entity at the first order of the SPG having dimensional directed constraint, b) one machined entity and one raw entity of the blank material at the first order of the SPG having dimensional directed constraint.

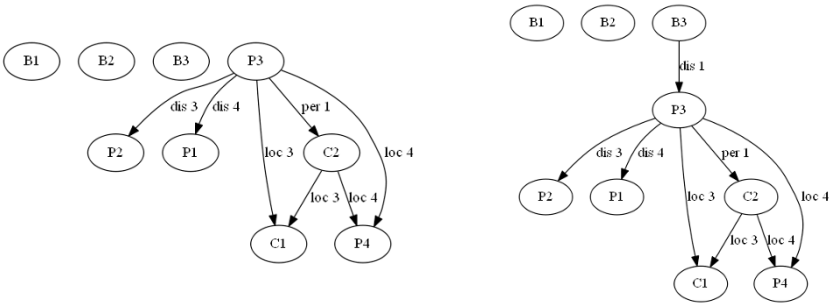

Figure 9: a) one machined entity at the first order of the SPG having geometrical directed constraints, b) acceptable SPG, no machined entity at the first order of the SPG.

4 – Robust interpretation of the part tolerancing

The previous section has presented the REFM methodology for generating the CAPP model based on the SPG. Although the proposed approach seems to be automated (except for the face grouping and the machining operation grouping), the wrong interpretation of the input (SPG) leads to bad or unsolvable solutions. To solve these problems, this section proposes solutions to correctly orientate the direction of dimensional tolerance constraint.

4.1 – Linking the blank material to the part

This subsection discusses the necessary link between the blank material and the part. The first set-up of the CAPP should be the blank material, hence at the first level of the SPG only surfaces of the blank material should appear. If machined surfaces are present at the first order, two situations can be distinguished:

- Situation 1: the machined entity at the first order only imposes dimensional constraints to other surfaces; hence a constraint reorientation strategy consists in reorienting dimensional directed constraints in order to remove this entity from the first order of the SPG. This situation is illustrated by figure 8 a) and b) where the P1 machined plane is present at the first order. In case of figure 8 a), the reorientation of the "dis 4" constraint leads to the configuration of figure 9 a) that will be treated in the situation 2. In case of figure 8 b), the reorientation of the "dis 4" constraint leads to the configuration of figure 9 b) that is an acceptable SPG.
- Situation 2: the machined entity at the first order imposes at least one geometrical constraint to other surfaces; hence one dimensional constraint is necessary between a raw entity of the blank material and this identified machined entity in order to remove it from the first order of the SPG. This situation is illustrated in figure 9 a) where the creation of a new dimensional constraint "dis 1" from the raw entity B3 to the P3 machined entity leads to the configuration of figure 9 b) that is an acceptable SPG.

One case not treaded here may cause some trouble. This case would be a part toleranced with dimensional tolerances only. Although ISO 14405 limits the use of dimensional tolerances, this particular case can exists and won't give stable SPG because the constraints reorientation strategy will loop to the initial interpretation of the part tolerancing. In that particular case, a solution could be to ask the user to define at least one constraint with non-ambiguous interpretation.

4.2 – Reorienting dimensional tolerances directed constraints

This case of reorienting constraints is mainly used when the tolerance graph is defined by the user where dimensional tolerances may be present. The figure 5 a) presents a tolerancing of the part using two dimensional tolerances between machined surfaces. This tolerancing can be interpreted in four cases where two of them are unsolvable. The two feasible CAPP results are very different, one is optimal with only 3 set-ups and the other one is not with nearly as many set-ups as manufacturing operations.
A solution to optimize the CAPP and the number of set-ups could be the use of iterative changes in the orientation interpretation of the dimensional tolerance constraints in order to exploit all possible configurations and find optimal ones. Of course this solution is not realistic due to two reasons:

- The growing complexity of changes: 2^n where n is the number of dimensional tolerances. Hence, the number of changes can be large with complex part and non-influent changes can be made and waist time,
- The machining operation grouping is done manually, hence for each change in dimensional tolerance orientation the user needs to group machining operations. This second reason is more blocking than the previous one.

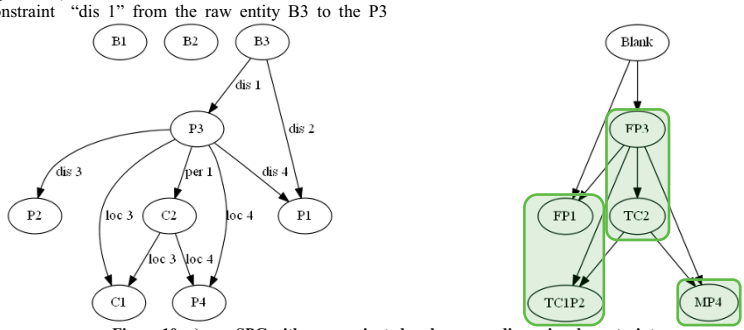

Figure 10: a) new SPG with one reoriented and one new dimensional constraint, b) SPG leading to machining operation groups respecting the user will.

A smarter solution to optimize the CAPP and the number of set-ups is to identify which are the dimensional tolerances to reorient. This can be achieved thanks to the user who defines machining operations that can be regrouped in the same set-up. Machining operations can be regrouped if they are order neighbored in the MOPG as illustrated in figure 7 b) for machining operation FP3 and TC2 and for machining operation FP1 and TC1P2. On the other hand, in case of

figure 6 b), machining operation FP1 and TC1P2 can't be regrouped with the given methodology but the user may want to machine these operations in the same set-up. Hence, the will of the user may be respected; as directed constraints on the MOPG are inherited from directed constraints of the SPG, identifying the directed constraints on the MOPG that blocks the user will leads to identify the directed constraints of the SPG. If at least one of these directed constraints is only based on dimensional constraints, these one may be wrongly interpreted and their direction inversion may lead to satisfy the user will.

To illustrate this solution, a scenario is based on the first interpretation of the dimensional tolerance presented in figure 6. If the user wants to regroup in the same set-up the machining operation FP1 and TC1P2, the directed constraints of the MOPG to change are the directed constraint FP1 -> FP3 (inherited from dis 4), FP3 -> TC2 (inherited from per 1), TC2 -> TC1P2 (inherited from loc 3) and FP3 -> TC1P2 (inherited from dis 3 and loc 3). Out of this four directed constraints, the one here that is only based on a dimensional tolerance constraint and can be reoriented is the directed constraint FP1 -> FP3. Hence, reorienting the dis 1 dimensional constraint leads to a new SPG, presented in figure 10 a), where entity P3 needs a dimensional tolerance to the blank material (to respect the non-presence of machined entity at the first order). This SPG leads to a new MOPG, presented in figure 10 b), where machining operations can be regrouped following the user will.

5 - Conclusion and future work

This paper presents the accumulation stage of the Reverse Engineering For Manufacturing (REFM) which aims to generate the CAPP model of a part based on its 3D points cloud, geometrical tolerancing and the user knowledge. The proposed methodology is based on directed graphs; the Surface Precedence Graph (SPG) created from the part tolerancing and the Machining operation Precedence Graph (MOPG) derived from the SPG. Based on this MOPG, the user defines set-ups of the CAPP. In order to optimize the CAPP, rules are defined to correct possible wrong interpretation of dimensional tolerances.

ACKNOWLEDGEMENTS. The acknowledgment concerns the region Champagne-Ardenne through the ESSAIMAGE program. These works are financed by the region.

5- References

[AD1] Ali S., Durupt A. and Adragna P-A. Reverse Engineering For Manufacturing approach: based on the combination of 3D and knowledge information. Proceedings of the 23rd CIRP design conference, 137-146, 2011.

[F1] Fisher B.: Applying knowledge to reverse engineering problems, Computer Aided Design, 36: 501-510, 2004.

[MG1] Marri H. B.., Gunasekaran A., Grieve R. J.: Computer-Aided Process Planning: A State of Art, International Journal of Advanced Manufacturing Technology, 14: 261-268, 1998.

[ML1] Mills B.I., Langbein F.C., Marshall A.D., Martin R.R.: Estimate of frequencies of geometric regularities for use in reverse engineering of simple mechanical components, Technical report, Cardiff University, 2001.

[SP1] Sunil V., Pand S.: Automatic recognition of features from free form surface CAD models, Computer Aided Design, 40: 502-507, 2008.

[SY1] Sadaiah M., Yadav D. R., Mohanram P. V., Radhakrishnan P.: A Generative Computer-Aided Process Planning System for Prismatic Components, International Journal of Advanced Manufacturing Technology, 20: 709-719,2002.

[TO1] Thompson W., Owen J., De St Germain H., Stark S., Henderson T.: Feature based reverse engineering of mechanicals parts, IEEE Transactions on Robotics and Automation, 15: 57-67, 1999.

[UE1] Urbanic R., Elmaraghy H., Elmaraghy W.: A reverse engineering methodology for rotary components from point cloud data, International Journal of Advanced Manufacturing Technology, 37: 1146-1167,2008.

[VP1] VPERI, Virtuals Parts Engineering Research Initiative, (http://www.cs.utah.edu/gdc/Viper/Colloborations/VPERI-Final-Report.pdf), the final report, 2003.

[ZH1] Zhang Y., Hu W., Rong Y, Yen D. W.: Graph-Based set-up planning and tolerance decomposition for computer-aided fixture design, International Journal of Production Research, 39: 3109-3126, 2001.

[ZL1] Zhang H.-C., Lin E.: A hybrid-graph approach for automated setyp planning in CAPP, Robotic and Computer-Integrated Manufacturing, 15: 89-100, 1999.

Article 032-itm-58

Multi-sensor approach for multi-scale machining defect detection

Lorène Dubreuil [1], Yann Quinsat [1], Claire Lartigue[1,2]

(1) : LURPA
ENS de Cachan - Université Paris Sud 11
61 avenue du Président Wilson, 94235 Cachan cedex, France
(2) : IUT Cachan
Université Paris Sud
9 avenue de la division Leclerc, 94230 Cachan, France
+33 1 47 40 29 86/+33 1 47 40 22 20

E-mail : {lorene.dubreuil, yann.quinsat, claire.lartigue}@lurpa.ens-cachan.fr

Abstract: Several measuring systems used in industries are most often used in a separated way and not efficiently. Multi-scale multi-sensor measurements are nowadays challenging to improve quality and decrease measuring time. However, this requires that each class of defects can be link with the appropriate measuring system. This paper deals with a comparative study of several measuring techniques for the measurement of multi-scale machining defects. In particular, an attention is paid to a new measuring method based on stereo-correlation along with classical measuring technique such as laser scanner, touch probe and confocal interferometry. Considering some well-known defects, the comparative study assesses the ability of each system to measure a class of defects. This study constitutes the first stage towards the definition of a multi-sensor multi-scale measuring system.

Key words: multi-sensor, digitalization, stereoscopic system, machining defect, sculptured surface

1- Introduction

Multi-scale multi-sensor measurement becomes an essential issue to improve productivity of industries. Indeed, the use of multiple systems allows simultaneous measurements, and thus a decrease in measuring time. Moreover, the use of multi-scale multi-sensors permits to linked the characteristic to be measured with the appropriate measuring system in accordance with the scale.
Many families of sensors are used in industry. Several authors offer a classification of existing measuring systems [SN1], [ST1], [CV1], [LG1]. Savio et al. [SD1] suggest a state of the art in metrology of freeform surfaces regarding the most measuring techniques used. To classify measuring systems, some authors propose comparative studies of the most common techniques used [BU1]-[ZM1]. Audfray et al. [AM1] put forward an approach of optical sensor qualification aiming at the choice of the most appropriate measuring system according to the feature to be measured. The application is limited to standardized dimensional specifications.
Several studies focus on multi-sensor measurement. Weckenmann et al. [WJ1] classifies multi-sensor measurement in three classes depending on how the sensor works (complementary, competitive or cooperative). The association of an optical sensor and a touch probe is especially explored. Chan et al. [CB1] associate a CCD camera to a touch probe in a complementary way to improve the accuracy and rapidity of the measurement, as well as Zexia et al. [ZJ1] which employ a structured-light sensor. Martinez et al. [MC1] used competitively a laser scanning and a touch probe.

Few researches address the issue of multi-scale multi-sensor measurements. Actually, manufacturing parts that have to be measured generally present deviations relative to the nominal model induced by the process. These deviations are multi-scales. Therefore, it seems necessary to adapt the measuring system with regard to its ability to locate or/and quantify deviations. However, it is not simple to directly associate the deviation to be evaluated with the appropriate measuring system. This issue is challenging.
In this context, the present paper focuses on a study of feasibility of different measuring systems to measure specific deviations induced by machining. More particularly, the addressed deviations are those obtained during a 3-axis milling operation using a ball-end cutter tool (mismatches, scallop heights, overcut).
Two different measuring systems are tested corresponding to two different measuring technologies. The first system consists of CMM equipped with a laser scanner (laser Kréon) mounted on an orientation head to increase the sensor accessibilities. The second measuring technique is the 3D-

Article 032-itm-58

DIC system based on stereo-vision by image correlation. This technique is relatively new in the domain of dimensional metrology.
The feasibility study is carried out thanks to a part which is defined in figure 1. The part is simple on purpose. On the one hand, classical deviations encountered during milling can be controlled, and on the other hand, the shapes are simple to measure. The part includes three different types of deviations: mismatches, scallop heights and overcuts.

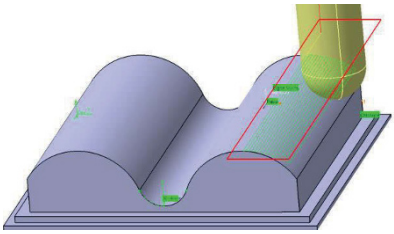

Figure 1: CAD model and example of tool path of the study part.

The test part is milled on a HSM (High Speed Machining) 3-axis milling center according a back and forth parallel plane strategy. The finishing tool used is a 5 mm ball-end cutter. With such a strategy it is possible to simply control the height of the 3D topography (scallop heights) by controlling the distance between passes. Hence, 2 different topographies are defined for the tests (Rt_1 and Rt_2). The radius of the fillet that links the two cylinders of the part is equal to 4 mm. As the tool radius is equal to 5mm, a form error is generated on the fillet corresponding to an overcut during machining (ΔZ_1). Finally, to perform the mismatch, an offset by 0.1 mm following the Z axis (tool axis) is achieved during the milling (ΔZ_2). All the deviations aforementioned are summarized in figure 2.

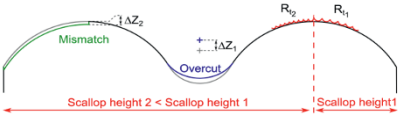

Figure 2: Diagram of the deviations applied to the test part

Whatever the technology used, the deviations are obtained by measuring a collection of 3D points on the part surfaces. It is thus necessary to present the stage of point measurement for the three measuring systems considered.
As the 3D-DIC system is new in dimensional metrology, the next section is dedicated to the description of this specific measuring method. The third section shortly details the measurement principle associated with the laser plane sensor (Kréon system). Measurement results and the feasibility study are addressed in section 4. Finally, conclusions and future works complete this study.

2- 3D-DIC system with a mesh based approach

3D-DIC system is a stereoscopic measuring technique. The difference compared to photogrammetry or stereovision relies in the way of picture pairing. Indeed, picture correlation on speckled parts is the core of the method [HR1]. Nevertheless, as for any vision system, it requires a calibration procedure to identify the parameters of the model (which is classically a model). Several calibration methods may be considered as in [LV1], [B1], [BD1].

2.1 – Stereoscopic system model and calibration

A stereoscopic system permits to build 3D points from two 2D pictures. Figure 3 puts forward this principle. As it can be seen, 2 pictures are required in order to remove the ambiguity associated with a unique picture. Due to the projective transformation, a 2D point belonging to a picture corresponds to infinity of 3D points. For instance, in figure 3, the 2D point *m* in picture 1 could be anywhere on the 3D line ΔM. With a second camera, the intersection of the two lines of a same point will give the corresponding 3D point.

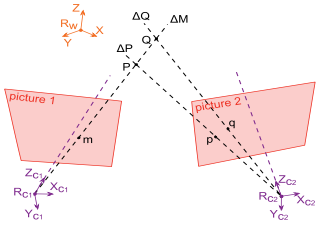

Figure 3: Stereoscopic principle with 3D point construction from two pictures.

However, a pairing technique has to be chosen to determine the same 2D points of the two pictures (*m* and *p* in the proposed example). The pairing technique used in the 3D-DIC measurement is the picture correlation.
Let us detail in the following of this section, the pinhole model, the stereoscopic model and the calibration developed to perform 3D point measurements.

2.1.1 – Pinhole model

The pinhole model is a projection perspective model which allows us to express the 3D point coordinates defined in a reference frame in the picture frame. This consists of three geometric transformations [FT1], [T1] as defined in figure 4. The transformation T between the world frame R_w and the camera frame R_c, consists of a rotation and a translation defined thanks to a homogeneous matrix (see Equation 1). The parameters associated with this transformation are called the extrinsic parameters.

$$\begin{bmatrix} X_c \\ Y_c \\ Z_c \\ 1 \end{bmatrix}_{R_c} = [T].\begin{bmatrix} X \\ Y \\ Z \\ 1 \end{bmatrix}_{R_w} = \begin{bmatrix} R_{3*3} & t \\ 0 & 1 \end{bmatrix}.\begin{bmatrix} X \\ Y \\ Z \\ 1 \end{bmatrix}_{R_w} \quad (1)$$

The second transformation P is a perspective projection of R_C in the retinal plane R_r. The last one A is an affine transformation from the picture center R_r to the picture

Article 032-itm-58

corner R_p.

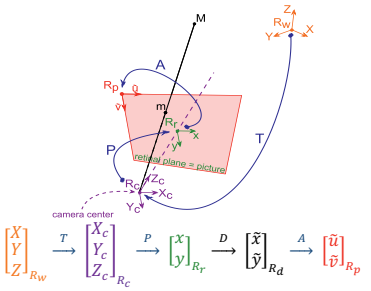

Figure 4: Pinhole model of a camera.

The parameters associated with the matrix transformations P and A are called the intrinsic parameters as for the internal parameters (focal, pixel size and number, picture center). An additional transformation D could be taken into account which corresponds to distortions of the camera. In this study, distortions are not considered. Both intrinsic and extrinsic parameters need to be identified. This is performed thanks to the calibration process.

2.1.2 – Calibration of the measuring system

The purpose of the calibration is to identify all the parameters of the pinhole model. Thus, the relationships between 3D points and picture points are assumed to be known (equation 2).

$$\begin{bmatrix}\tilde{u}\\ \tilde{v}\\ 1\end{bmatrix}_{R_p} = [APT].\begin{bmatrix}X\\ Y\\ Z\\ 1\end{bmatrix}_{R_w} \tag{2}$$

Lavest et al. [LV1] summarize all the mathematical procedure leading to camera calibration. Technically, a minimum number of points has to be known in the two frames (R_w and R_p) to achieve calibration. Several methods could be considered for this purpose. Bouguet [B1] achieves the calibration of the measuring system by shooting a well-known pattern, commonly a checkerboard pattern, in several positions. As the geometry of the pattern is supposed to be completely defined the intrinsic and extrinsic parameters can be calculated from equation 2. As this method requires numerous views of the checkerboard pattern according to different locations, acquisition time could be important.
Another method puts forward by Beaubier et al. [BD1], offers a new technique of calibration based on stereo-correlation. The particularity of this method is that the object leading to the calibration will no longer be a calibration pattern but directly the test part and its CAD model. The CAD model is more specifically a NURBS model of the test part. Hence, links between picture frames and 3D frame is virtual because the 3D frame is the CAD frame. The pairing technique is the picture correlation. The pictures shot by the left and right cameras are respectively denoted by $f(x^l)$ and $g(x^r)$, where $x^l = (\tilde{u}^l, \tilde{v}^l)$ and $x^r = (\tilde{u}^r, \tilde{v}^r)$. Conservation of the gray scale for both pictures yields equation 3.

$$f(x^l) = g(x^r) \tag{3}$$

This conservation is carried out only if the exact calibration parameters are known. As it is seldom the case, a global formulation of the sum of squared differences over the region of interest (ROI) is expressed in equation 4.

$$\tau = \int_{ROI} [f(x^l) - g(x^r)]^2 d\tilde{u}d\tilde{v} \tag{4}$$

By minimizing the correlation residual τ, calibration parameters are obtained. Contrary to the method proposed by Bouguet, this one only uses two pictures; acquisition time is thus reduced.
Another technique for extrinsic parameters identification relies on feature recognition such as lines or circles. Knowing the CAD model of a part with specified features, it is possible to associate a feature in a picture to the same feature in the CAD model. As this technique does not lead to intrinsic parameters, it only can be complementary to the previous one [B1]. The use of the two calibration methods in a complementary way permits to maximize the benefit of each one.

2.2 – 3D shape reconstruction

This section addresses the measuring method with the 3D-DIC system based on picture correlation once calibration has been performed. It is considered that the stereoscopic system is beforehand calibrated with the method proposed by Beaubier et al. [BD1].
The method proposed in the paper has drawn on the prior work developed in [BD1] but uses mesh-based approach to represent the part shapes instead of the NURBS representation previously adopted. This enlarges the possibility of shape representation in particular non-continuous in tangency surfaces can be easily described. Therefore, the parts are defined as mesh models which can be calculated from a CAD model. The minimization problem written previously in equation 4 becomes the problem linearized in equations 5 and 6 for which the unknowns correspond to the displacements of nodes of the mesh model dX.

$$\tau_{lin}(dX) = \int_{ROI} [f(x^l) - g(x^r) + (\nabla f.\delta x^l)(x^l) - (\nabla g.\delta x^r)(x^r)]^2 d\tilde{u}d\tilde{v} \tag{5}$$

$$\delta x^{l,r} = \frac{\partial x^{l,r}}{\partial X} dX \tag{6}$$

In order to respect the mesh consistency, to avoid unexpected displacements and to reduce the number of unknowns, displacements are enforced along the normal vectors of the node. In figure 5, a mesh before and after displacement is

Article 032-itm-58

presented. The initial mesh is pictured by nodes X_i, the final mesh is represented by nodes X_i' and the normal vectors are $\overrightarrow{n_{X_i}}$. This method also involves displacement to be evaluated only in one direction and therefore computational time is reduced.

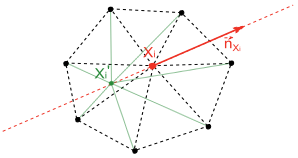

Figure 5: Principle of displacement of nodes along their normal vectors.

Considering these displacement directions, equation 6 becomes equation 7 with X_N the coordinate of nodes following its vector normal in the CAD frame.

$$\delta x^{l,r} = \frac{\partial x^{l,r}}{\partial X} \frac{\partial X}{\partial X_N} dX_N \tag{7}$$

The vector normal to a node is evaluated as the mean value of the facets surrounding the node.
As deviations are small, the assumption of small displacements of nodes is adopted. This supposes that all the normal vectors at nodes are invariant whilst the reconstruction. To improve the resolution of the equation system, integration points are added on each facet as described in figure 6.

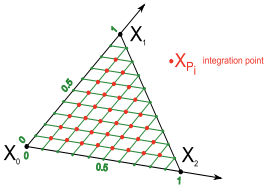

Figure 6: Discretization of a facet in integration points.

Taking into account the addition of integration points in the algorithm, equation 7 becomes equation 8 with X_P coordinates of integration points in the CAD frame.

$$\delta x^{l,r} = \frac{\partial x^{l,r}}{\partial X_p} \frac{\partial X_p}{\partial X} \frac{\partial X}{\partial X_N} dX_N \tag{8}$$

3- Laser scanning Kréon

This section introduces the measuring system also used to qualify the machined part. Laser scanners acquire a high density of point data with an acquisition time reduced. The principle of measurement is based on triangulation. Indeed, a laser plane is projected on the surface to be measured and its intersection (the profile stripe) with the surface is observed by a camera (figure 7). The coordinates of the profile stripe are determined thanks to triangulation (equation 9). The association of the laser scanner with a displacement system permits to measure the whole surface.

$$d = b * \frac{\sin\alpha . \sin\beta}{\sin(\alpha + \beta)} \tag{9}$$

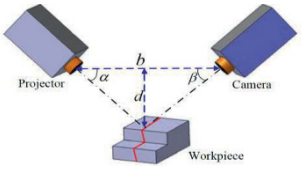

Figure 7: Triangulation principle of the laser scanner.

Nevertheless the laser scanner has several disadvantages, such as a limited viewpoint, sensitiveness to the optical conditions, digitizing noise and overlaps due to the necessity of several sensor orientations. The accuracy of the sensor is related to many factors: relative position between the sensor and the measured surface, view angle, surface conditions, etc. [AM1]. Studies have enhanced that the best conditions of scanning is obtained with a unique orientation of the laser scanner. Under these conditions, the measuring system accuracy can be assessed thanks to quality indicators: a noise of 9 µm and a trueness of 2 µm/mm [AM1].

4- Measurement of the test part and results

This section deals with the results of the comparative study conducted to evaluate the ability of each measuring system to measure the deviations previously defined (see figure 2). To define a reference, the test part has been measured with a touch probe mounted on a CMM and the sensor Stil. These measurements are chosen as references and are compared to the measurements carried out with the laser scanner Kréon and the 3D DIC system (second part of this section). Finally, the feasibility study is performed.

4.1 – First measurements of the test part

A first measurement of the part is performed to stand for the reference. Macro-defects are measured with a touch probe (Renishaw TP2 stylus), mounted on a CMM while the micro-defects are measured thanks to the Stil sensor.
Touch probe measurement is commonly used in dimensional metrology due to its high accuracy. However, its use is limited to inspection of known surfaces (prisms, cylinders, etc.) which requires lower data density. Other limitations are the accessibility of the touch probe which is impossible in areas smaller than the diameter of the tip ball.
Based on the chromatic confocal sensing technology, the sensor Stil evaluates the surface topography at micro-scale. A study conducted by Quinsat and Tournier [QT1] put forward that this sensor, used in a machine tool, is able to discriminate the surface topography evolution during machining and polishing.

Article 032-itm-58

The measured features acquired with the touch probe are the different cylindrical surfaces (convex and concave) presented in figure 9. The measurement of the three planes (YZ), (XZ) and (XY), allows the determination of a reference frame. This frame permits to analyze the coordinate Z of the measured data and to evaluate ΔZ_1 and ΔZ_2 in figure 2.

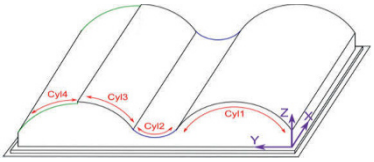

Figure 9: Features identification on the study part.

The points collected are treated thanks to the workspace "Quick Surface Reconstruction" of Catia V5. To each point cloud corresponding to a feature, a cylinder is associated via the module "Basic Surface Recognition" considering that for each one the radius and the axis are imposed. Indeed, it leads to evaluate the deviation following the Z axis corresponding to the displacement of the tool axis (see figure2). Results are displayed in table 1.

Micro-scale geometries are acquired with the STIL sensor. In particular, this sensor is well-adapted to measure the mismatch as well as the 3D topographies induced by ball-end milling. The mismatch is presented in figure 10; figure 11 illustrates an example of scallop height.

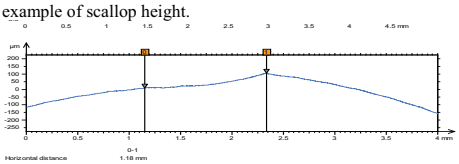

Figure 10: Mismatch (ΔZ_2) measurement with the chromatic confocal sensor Stil.

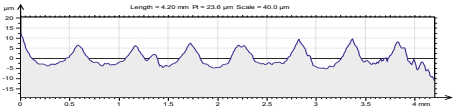

Figure 11: Scallop height (Rt_1) measurement with the chromatic confocal sensor Stil.

Mismatch (ΔZ_2) is evaluated thanks to the analysis software Mountains Map on a measured profile as in figure 10 as well as Rt_1 and Rt_2 which are evaluated directly on the extracted profile as for instance in figure 11. Results are summarized in table 1.

4.2 – Comparative study

Measurements proposed in the previous section give a reference for the errors to be evaluated. These results are compared to those obtained with the two measuring systems (Kréon and 3D-DIC). Measurements are analyzed in the same way and are displayed in table 1.

With regards to the Kréon system, it has been chosen to scan the surface with only one orientation of the laser in order to avoid overlapping errors generally appearing when using multiple sensor orientations. Based on the ICP Algorithm (Iterative Closest Point) a registration of the digitized point cloud is performed. Results from are given in figure 12 by the mapping of the deviations between the CAD model and the measured point cloud. By analyzing this mapping, overcut and mismatch are easily identified; contrary to scallop heights which are not observed.

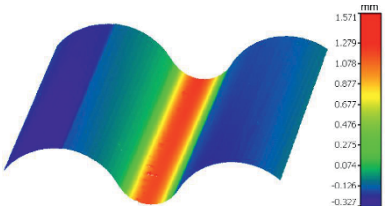

Figure 12: Mapping of deviations between the CAD model and the point cloud acquired by the Kréon after ICP registration.

Following this measurement, only the mismatch and the overcut can be thus quantified with this measuring system. With such a system, it is not possible to quantify the value of the scallop height. In table 1, the value of the deviations following Z axis obtained with the Kréon system are compared to those obtained previously with the touch probe TP2 and the sensor Stil.

To achieve 3D DIC, a black and white random pattern is projected onto the test part, and two pictures are recorded. The calibration of the stereoscopic system is achieved thanks to the CAD meshed model. In figure 14 the residual following the calibration is observed. Locations of deviations are putted forward to the places for which the residual increases. For instance, the overcut in the center of the study part is easily identifiable in figure 14.

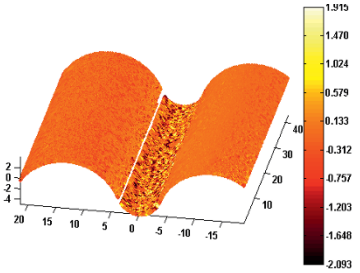

Figure 14: Residual (%) on the test part after calibration of the stereoscopic system.

Therefore, the study only concerns the overcut on the fillet (Cyl2 in figure 9). The objective is here to reconstruct the 3D-shape using the method detailed in §2.2 by node displacements. Figure 15 displayed the values of the residual on the fillet before and after node displacements with 3D-DIC. A global decrease can be observed. It is thus possible to evaluate the value of the overcut. Results relative to values of the defects obtained with 3D-DIC are summarized in table 1.
.

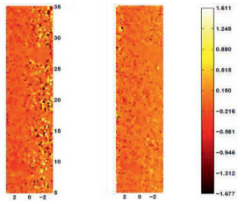

Figure 15: Residual (%) on the fillet before and after node displacements.

4.3 – Feasibility study

Table 1 summarizes all the results: those obtained with the two measuring systems (Kréon, 3D-DIC) we want to assess and the reference measurements (TP2 and Stil). After surface association to each point cloud corresponding to a feature via the module "Basic Surface Recognition" of Catia V5, ΔZ_1 and ΔZ_2 are evaluated and displayed in table 1.

Deviations	TP2	Stil	Kréon	3D-DIC
Overcut ΔZ_1 (mm)	2.077		2.059	1.934
Mismatch ΔZ_2 (mm)	0.111	0.097	0.118	
Scallop height 1 Rt_1 (µm)		11.9		
Scallop height 2 Rt_2 (µm)		5.32		

Table 1: Measurement results.

Table 1 enhances the capability of a measuring system to evaluate a class of defect. Crossed boxes put forward incompatible couples (defect/measuring system). Concerning the crossed boxes of the Kréon ant the 3D-DIC, the amplitude of the defects is of the same order as the measurement noise. The touch probe is not able to acquire surface topography. Finally, the measuring range of the sensor Stil is smaller than the size of the overcut ΔZ_1.

As might be expected, only the sensor Stil is able to detect micro-defects. Therefore, it remains the measuring system the most adapted to evaluate 3D topographies.
The system Kréon turns out to be a good solution to measure macro-defects within a large range. Indeed, results obtained with such a system a comparable to those obtained with the TP2 reference system for the overcut (of 2 mm) as well as for the mismatch (of 0.1 mm). This makes the choice of this sensor particularly relevant for this class of defects considering acquisition time and the high density of the acquired points.
The 3D-DIC measuring system only provides a result for the overcut defect, but the value remains distant from the reference value. This method needs to be improved in future works to be usable to quantify defects with a better accuracy. However, this method provides a very smart, simple and fast method to locate macro-defects by an analysis of the residual as shown in figure 14. Therefore, once the defect is located, another system (such as TP2 or Kréon) more accurate can be used in a complementary way to quantify the value of the defect.

6- Conclusions and future works

The aim of the paper was to study the feasibility of measuring systems to measure specific defects. The study is carried out on a test part including classical defects encountered during milling (mismatch, form error, scallop height), with the objective of linking the characteristic to be measured with the appropriate measuring system. The study addressed to particular system: a commonly used laser-plane scanner Kréon, and a new system, 3D-DIC, based on stereo-correlation,
Results have highlighted that the system Kréon is the most efficient measuring system for the majority of the macro-defects. On the other hand, 3D-DIC seems to be useful to locate deviations on a part. Indeed, this study shows that deviations lower than 0.1 mm cannot be identifiable due to high noise measurement, contrary to larger deviations which are easily locate but not yet quantifiable. As expected, micro-defects are only measurable thanks to appropriate system to micro-geometry measurements such as the Stil sensor. This study enhanced the need of complementary multi-system measurements within a multi-scale multi-sensor context.
In the aftermath of this study, a multi-scale multi-sensor measuring system could be imagined. A choice on the way of how the sensor works [WJ1], will have to be established, to carry out an efficient multi-scale multi-sensor measuring system.

7- References

[AM1] Audfray, N., Mehdi-Souzani, C., and Lartigue, C. (2012). Qualification et performances des systèmes de mesure optiques : Qualipso.

[B1] Bouguet, J.-Y. (2010). Camera calibration toolbox for matlab.http://www.vision.caltech.edu/bouguetj/calib_doc/index.html

[BD1] B. Beaubier, J.-E. Dufour, F. Hild, S. Roux, S. Lavernhe and K. Lavernhe-Taillard. (2013). CAD-based calibration and shape measurement with StereoDIC. Experimental Mechanics

[BU1] Basilio Ramos Barbero and Elena Santos Ureta. Comparative study of different digitization techniques and their accuracy. Computer-Aided Design, 43(2):188 – 206, 2011.

[CB1] Chan, V., Bradley, C., and Vickers, G. (2001). A multi-sensor approach to automating coordinate measuring

machine-based reverse engineering. Computers in Industry, 44(2):105 – 115.

[CV1] Cuypers, W., Gestel, N. V., Voet, A., Kruth, J.-P., Mingneau, J., and Bleys, P. (2009). Optical measurement techniques for mobile and large-scale dimensional metrology. Optics and Lasers in Engineering, 47(34):292 – 300.

[HR1] F. Hild and S. Roux. Digital image correlation. In P. Rastogi and E. (eds) Hack, editors, Optical Methods for Solid Mechanics. A full-Fild Approach. Wiley-VCH, Weinheim (Germany), 2012.

[FT1] Faugeras O, Toscani G (1987), Camera calibration for 3D computer Vision. International Workshop on Machine Vision and Machine Intelligence 240-247.

[LG1] Yadong Li and Peihua Gu. Free-form surface inspection techniques state of the art review. Computer-Aided Design, 36(13):1395 – 1417, 2004.

[LV1] Lavest, J.-M., Viala, M., and Dhome, M. (1999). Quelle précision pour une mire d'étalonnage ?

[MC1] Martinez, S., Cuesta, E., Barreiro, J., and Alvarez, B. (2010). Analysis of laser scanning and strategies for dimensional and geometrical control. The International Journal of Advanced Manufacturing Technology, 46(5-8):621–629.

[QT1] Quinsat, Y. and Tournier, C. (2012). In situ non-contact measurements of surface roughness. Precision Engineering, 36(1):97 – 103.

[SD1] Savio, E., Chiffre, L. D., and Schmitt, R. (2007). Metrology of freeform shaped parts. {CIRP} Annals - Manufacturing Technology, 56(2):810 – 835.

[SN1] Schwenke, H., Neuschaefer-Rube, U., Pfeifer, T., and Kunzmann, H. (2002). Optical methods for dimensional metrology in production engineering. {CIRP} Annals - Manufacturing Technology, 51(2):685 – 699.

[ST1] Sansoni, G., Trebeschi, M., and Docchio, F. (2009). State-of-the-art and applications of 3d imaging sensors in industry, cultural heritage, medicine, and criminal investigation. Sensors, 9(1):568–601.

[T1] Tsai, R.Y. (1986). An Efficient and Accurate Camera Calibration Technique for 3D Machine Vision. Proceedings of IEEE Conference on Computer Vision and Pattern Recognition, Miami Beach, FL, pp. 364-374.

[WJ1] Weckenmann, A., Jiang, X., Sommer, K.-D., Neuschaefer-Rube, U., Seewig, J., Shaw, L., and Estler, T. (2009). Multisensor data fusion in dimensional metrology. {CIRP} Annals - Manufacturing Technology, 58(2):701 – 721.

[ZJ1] Zexiao, X., Jianguo, W., and Qiumei, Z. (2005). Complete 3d measurement in reverse engineering using a multi-probe system. International Journal of Machine Tools and Manufacture, 45(1213):1474 – 1486.

8

Robotics, Mechatronics and Product Engineering

Major topics of the full argumentations are the following:

X. Fischer et al. (eds.), *Research in Interactive Design (Vol. 4)*
DOI 10.1007/978-3-319-26121-8_18

Article 046-pp-39

Definition of a robotic polishing process for aeronautics parts in high strength steel

Bastien GUICHARD [1], Hélène CHANAL [1], Laurent SABOURIN [1]

(1) : Clermont Université, IFMA, UMR 6602, Institut Pascal, BP 10448, F-63000 Clermont-Ferrand
04 73 28 80 75
E-mail : { bastien.guichard ,helene.chanal ,laurent.sabourin}@ifma.fr

Abstract: This article presents the first step of the robotic polishing process for aircraft large parts on the choice of tools and adjustment of process parameters. The parts have a finish state obtained by 5 axis machining with ball end tool. The objective of the polishing operation is to erase the tool marks, ensuring the imposed profile surface defect and surface state. This requires the choice of polishing tools and the setting of strategy parameters, particularly the polishing force. It must be controlled according to the contact surface between the tool and the part and the attempted polishing pressure. This polishing pressure is defined from a desired removal rate and surface quality. Then, polishing condition parameters are studied in order to propose a first setting for flat parts and cylinders polishing.

Key words: polishing, robot, force control, aeronautic

1- Introduction

In aeronautical industry, improvement of productivity and working conditions implies an automation of manual operations such as polishing. In this paper, we focus on the polishing operation of landing gear component made of high-strength steel (Rm=1000MPa, 300HB) (Figure 1).

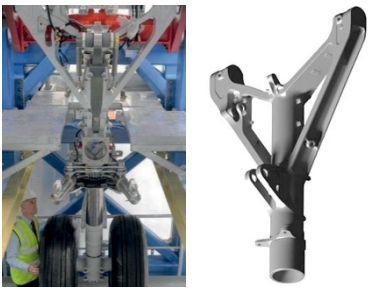

Figure 1 : A350 front landing gear and polished landing gear component

Moreover, a landing gear component weighs more than 250kg and its length can overstep 1m50. Requirement of such part impose to erase the surface profile due to machining while respecting a profile surface defect less than 0.1mm.

This article presents a study of polishing tools and associated operating conditions in order to robotize the polishing operations of a landing gear component in hard material. The challenge is to develop a polishing process for complex parts in hard material with high machining roughness defect. Indeed, for polish this kind of material, rigid polishing tools should be employed which penalize the control of the contact between tool and polished surface.

Anthropomorphic robot associated with a force control is generally used for polishing operation [M1] [R1]. Two types of polishing tools are studied: wheels and disks. These two kinds of tool shapes ensure to polish plans and cylinder surfaces. The test is performed on high-strength steel with a serial robot with a force control system. The choice of the abrasive grain size is made with first experimentation with regard to the attempted surface quality and polished material.

This article presents a first study of the influent polishing parameters. Polishing parameters are separated in two classes: first one linked to force control system and second one to polishing conditions. In a first time, the polishing robot used and the test parts are presented. Then, robotic polishing parameters are studied and we conclude on the shape of generated surface profile. The final section deals with the determination of the polishing force as a function of the polished geometry.

2- Definition of the polishing tests

2.1 – Test parts description

The polishing tests have been made with a serial robot on the same material (40NiSiCrMo7) than the landing gear component.

The test parts are a flat part and a cylinder of 210mm diameter, corresponding to the diameter of the landing gear's leg (Figure 2). The initial profile is realized by a machining operation with a ball end tool of 20mm diameter, in the same cutting conditions than the work piece.

Figure 2 : Test parts

The initial arithmetic average roughness *Ra* measured in the transverse direction is equal to 3.32µm and the transverse pitch is equal to 1.5mm. The initial crest level is equal to 30 µm.

2.2 – Polishing cell

The robotic cell used for the tests is made up of an anthropomorphic 6 axis robot ABB IRB 6660 (Figure 3). The specified absolute accuracy is equal to 0.1mm and the repeatability is equal to 0.07mm. This robot is equipped with a HSM spindle Fisher MFW 1412 (36000rpm – 15.6kW) and a force control system from ABB.

Figure 3: Polishing cell

2.3 – Polishing tools

Tested tools are nonwoven abrasive. Nonwoven abrasive tools are constituted by abrasives incorporated into three-dimensional layer of synthetic fibers (Figure 4). Advantages of this type of tool are to present a constant abrasion rate during the tool wear and to reduce the loading.

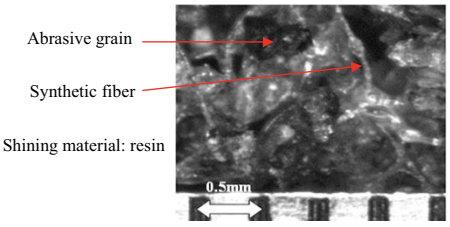

Figure 4 : Microscopy of a nonwoven abrasive tool P120

The two types of tested tools are Scotch-Brite tools 6AM from 3M (Figure 5). The abrasive grains are aluminium oxyde size P150 or P120. The disk is assembled on a flexible plate.

Figure 5: Abrasive wheel (Ø150mm, width=25mm) and disk P150 or P120 (Ø75mm)

3- Process control

Several parameters have to be defined in order to control a robotized polishing operation. Polishing parameters can be separated into two classes: parameters linked to force control system and parameters linked to polishing condition (geometrical and kinematic).

3.1 –Force control presentation

Force control implemented in the controller of the used polishing cell ensures to guarantee a contact force between tool and surface part [NH1]. The robot adapts the tool position in order to respect a programmed constant contact force. Thus, this kind of force control system can support some deviation of the real polished surface with regard to the nominal surface (Figure 6).

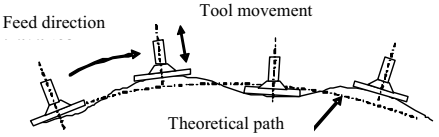

Figure 6 : Force control principle

However, in case of polishing operation, the programmed force has to be computed with regard to the desired polishing contact pressure and the tool/part contact surface. The force control is based on a 6 components force sensor ATI 160.

3.1.1 –Tools inertial and spindle weight influence

Tool holder and tool must be balanced to not disturb the measure of the polishing contact force. Thus, the noise of the force sensor is less than 2N for disks at 11000 rpm, and 10N for wheels at 3000 rpm. For the wheel, the noise generated of the measured force is higher due to a higher inertial moment.

The influence of the spindle/tool system weight on the force measured by the sensor has to be identified. An automatic procedure is defined by ABB; consisting in a force measurement for different positions and orientations of the spindle/tool system. This procedure allows identifying gravity center and mass. The aim is to offset the force value measured by the sensor with the static weight effect.

In this test, we consider that the polished force is directly deduced by the force sensor with regard to the offset generated by the spindle/tool weight.

3.1.2 –Setting of force control

A damping parameter is used in the force control loop. It allows controlling the settling time when variations of the contact surface appear. The damping has been experimentally set to 5000N/m/s in order to avoid oscillations.

Deactivation threshold of the force control is set to 10N in our case. Indeed, experimentally, we observe that if it is higher, force control can be canceled during a polishing operation. Lower, the force control deactivation is not realized due to noise force measurement induced by the tool rotation.

The measured force for a plan polished with a straight line tool path and with a disk is presented on Figure 7. After force control activation, the tool moves in the direction of the programmed polishing force in order to be in contact with the part (here normal to the surface). Finally, the tool begins to follow programmed tool path when the programmed force is reached. It moves away from the surface when the end point of the tool polishing surface is reached and the force control is deactivated with a program instruction.

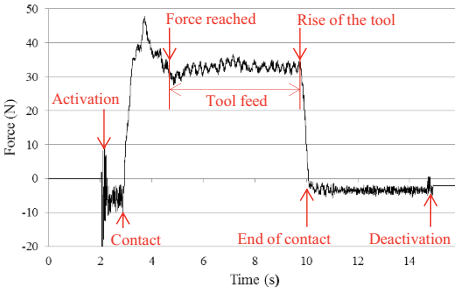

Figure 7: Polishing force for a disk 6AM Ø75 F=30N, N=5000rpm, V=10mm/s

After the setting of force control system, polishing conditions have to be studied.

3.2 – Setting of polishing parameters

Macroscopic modelling of material removal with the law of Preston [P1] gives an idea of the influence of polishing condition parameters (1).

$$Z = K.p.V \quad (1)$$

Z: removed debit (mm^3/s)

K: Preston constant ($mm^3/N.m$)

p: normal force (N)

V: slipping speed (m/s)

To compute the global material removal rate, Preston law must be integrated with regard to the contact surface between polishing tool and part. Thus, in our case, a more relevant form for our application is given by eq. (2).

$$\Delta h = \frac{K.F.Vc.L}{S.Vf} \quad (2)$$

Δh: Height of removed material (mm)

F: Normal force between tool and part (N)

Vc: Cutting speed (m/min)

L: Length of the contact surface (mm)

S: Contact surface (mm^2)

Vf: Feed rate (mm/min)

Note that the cutting speed is directly a function of the spindle speed and the tool diameter.

In the following, the polishing operation of plan is studied with abrasive wheel and disk in order to define the more relevant tool. The associated setting of polishing parameters is then determined.

4- Study of abrasive wheels

In a first time, the polishing operation with wheels is studied. Wheels have to be rectified before polishing in order to control tool/part surface and to avoid inhomogeneous polishing trace (Figure 8a). A surface polished with a wheel of 25mm width is presented in Figure 8b and Figure 9.

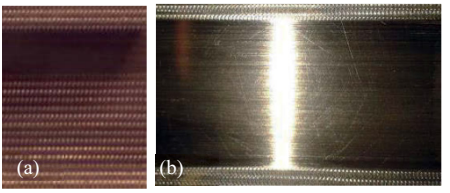

Figure 8 : (a) Polishing trace with no rectified wheel, (b) Polished surface with wheel 6AM turning rectified Vf = 5mm/s, N = 3000rpm, F = 30N

The machined profile is not visible anymore and the arithmetic average roughness is equal to 1.5µm.

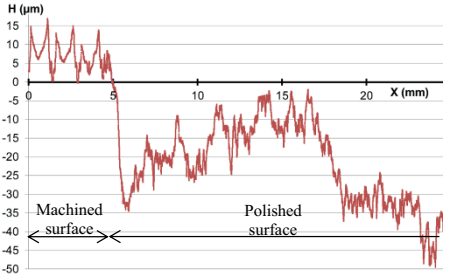

Figure 9 : Profile of the surface polished with a wheel compared with machined surface

Article 046-pp-39

The shape defect is about 0.05 mm because the height of removed material oscillates between 5 µm and 50 µm. The specifications are respected, but the profile of the polished surface is not homogeneous. This comes from scratches generated by grains removing material in a unique direction. However, due to the high diameter of this tool, the realized balancing is not sufficient accurate in order to propose a robust behaviour of the force control. Smaller wheels have to be tested in the future. In following, we study only disks.

5- Study of abrasive disks

Studied disks have a diameter of 75mm and are assembled on a flexible plate. In the following, the influence of polishing parameters on polished surface is analysed.

5.1 – Influence of the spindle speed

The Preston law shows that material removal rate increases with the spindle speed. Thus, the polished width increases due to the increase of material removed by the tool edge. However, we observe that from a certain value, the polished width decreases (Figure 10). We call "polished width" the width where the work trace of the milling tool cannot be visible to the naked eye.

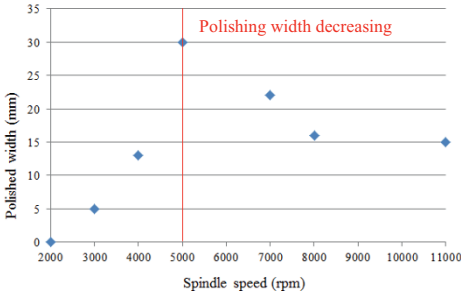

Figure 10: Influence of the spindle speed on the polished width Disk 6AM Ø75, V_f = 5mm/s, F = 30N, angle inclination = 5°

It seems to result from the inertial effect which tends to flat the disk with an increase of the rotation speed. Indeed, the surface contact decreases with the stiffness of the disk.

5.2 –Influence of the polishing force

The material removal rate increases with the force applied, what improve the arithmetic average roughness of one path polished surface. Moreover, the contact surface increases with the force, what increase the polished width (Table 1).

If the force is too low, the machining marks are visible. However we observe that a too large force deteriorates the tool. Experimentally, we observe that a programmed polishing force less than 15 N does not ensure a good behaviour of the force control. However, according to eq. (2), we can think the feed rate and polishing forces have a combine influence on removed debit.

Force (N)	Polished width (mm)	Ra (µm)
20	10	0.15
30	30	0.1

Table 1: Influence of polishing force on polished width and Ra Disk 6AM Ø75, Vf = 5mm/s, N = 5000rpm, angle inclination = 5°

5.3 – Influence of the angle inclination

For disk tool, the contact surface increases when the tool inclination angle with regard to polishing surface decreases [G1]. Thus, a material removal rate is higher for an inclination angle of 5° than for one of 3°. In our experimentation, an inclination angle of 5° is used, this value is recommended by the tool manufacturer.

5.4 –Influence of the feed rate

There is a maximum feed rate value which does not have to be overstepped. In our case, a feed rate of 10mm/s is too high to polish the part in good conditions (Table 2).

Feed rate (mm/s)	Polished width (mm)
5	30
10	0

Table 2: Influence of the feed rate on the polished width with disk 6AM Ø75, N = 5000 rpm, F = 30N, inclination angle=5°

Thus, we used a feed rate of 5mm/s. Then, results of these observations have been applied on test parts polishing.

5.5 – Study of tool behavior during polishing

The polished surface with disk tool is presented in Figure 11; the polished width is 30mm for a disk tool of Ø 75 mm with a roughness *Ra* in the cross directions equal to 0.1µm.

Figure 11 : Surface polished with disk 6AM Ø75, V_f = 5mm/s, N=5000rpm, F = 30N, inclination angle = 5°

However, a decrease of the material removal rate is observed after a while. After 100mm length of polishing, the polished width decreases by 10mm. This can be explained by the fouling of the tool (Figure 12).

Article 046-pp-39

Figure 12 : New tool and fouling tool

A solution is to use a disk 8ACRS (more abrasive and more rigid), its structure is less dense and the size of the particle is taller (P120).

5.6 – Results on a flat part

The polishing strategy is a zig sweeping. Several overlap tests have been performed. The greater transverse pitch which allows erasing machining profile is retained. In our case, a transverse pitch of 13mm is obtained corresponding to an overlap of 2mm.

Polishing results with disk 8ACRS are presented in Table 3 and in Figure 13.

Tool	Disk 8ACRS (P120)
Polishing parameters	V=5mm/s, F=30N, N=5000 rpm, D=5°
Polishing strategy	Overlap: 2mm Transverse pitch: 13mm
Surface roughness	**Ra (cross direction) = 0.17 µm** **Ra (machining direction) = 0.3 µm** **Shape defect = 0.03mm**

Table 3 : Results on a flat part

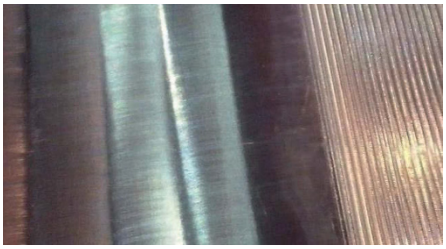

Figure 13 : Polished flat part

With this last tool, no significant tool wear or fouling has been observed. Figure 14 presents the machined surface roughness with regard to the polished surface roughness. The arithmetic average roughness after polishing is better, but we can observe a waviness defect due to the non homogeneous distribution of polishing pressure on the contact surface (Tableau 3).

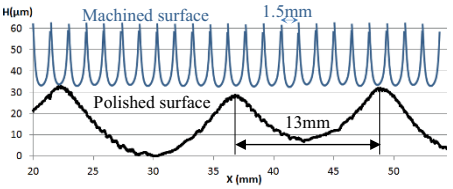

Figure 14 : Machined and polished surface roughness

Form and roughness specifications are respected, but the generated waviness defect is not esthetically acceptable. However, the hardness of the polished material does not allow using a less rigid tool. Thus, we have to define a finishing operation. In a second time, we study polishing of a convex surface.

5.7 – Results on a cylinder

For this type of convex parts, the contact surface is two times smaller. So, in order to obtain the same material removal rate a feed rate two times greater is used. Indeed the equation (2) shows that it should have the same effect on the material removal rate.

Disks 6AM are used for this part, more flexible than the 8ACRS. The results on the cylinder diameter 210mm are presented in Figure 15 and Table 4.

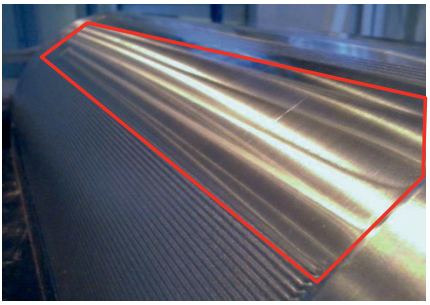

Figure 15 : Polished cylinder

Tool	Disk 6AM (P150)
Polishing parameters	V=10mm/s, F=30N, N=5000 rpm, D=5°
Polishing strategy	Overlap: 1mm Transverse pitch: 8mm
Surface roughness	**Ra (machining direction) = 0.26µm** **Shape defect = 0.05mm**

Table 4 : Results on a cylinder

We observe that the facet effect is amplified due to the fact that the polished surface is a convex surface. However, the surface roughness specifications are respected but the generated waviness defect is not aesthetically acceptable.

A first perspective of this work is then to control the polishing surface shape by controlling polishing force. Thus, we have to compute the polishing pressure with regard to the polishing force, polished shape and tool behaviour.

6- Conclusion

In this article, we present a first study of polishing parameters. A setting of the control force system is proposed with a setting of polishing condition for wheel and disk. Results for plan and convex parts are then presented.

Experimentation presented in this work show that to polish hard material with a high machining surface roughness, tools with a high stiffness should be used. Thus, we can note two particular behaviours. First one, the polished width decreases after a certain spindle speed. Second one, a non neglected waviness defect is generated by the polishing operation. This behaviour imposes to define a finishing polishing operation.

Moreover, landing gear polished component is composed of complex surfaces as cylinder, thus the polishing surface contact have to be determined in order to define polishing radial depth according to polished length. Values of Young modulus and Poisson's ratio of polishing tools have to be identified in order to model the contact surface and pressure distribution.

7- Acknowledgements

This work was supported by Aubert & Duval.

This work was carried out within the Manufacturing 21 working group, which comprises 17 French research laboratories. The topics approached are: modeling of the manufacturing process, virtual machining and emergence of new manufacturing methods.

8- References

[G1] Guiot A. Modélisation et simulation du procédé de prépolissage automatique sur centre d'usinage 5 axes. Thèse de doctorat, Ecole Normale Supérieure de Cachan, 2012.

[M1] Márquez, J.J. et al. Process modeling for robotic polishing. Journal of Materials Processing Technology, 159(1), pp.69–82, 2005.

[NH1] Nagata, F., Hase, T., et al. CAD/CAM-based position/force controller for a mold polishing robot. Mechatronics, 17(4-5), pp.207–216, 2007.

[P1] Preston F. The Theory and Design of Plate Glass Polishing Machines. J. Soc. Glass Tech., 11, p.214, 1927.

[R1] Robin, V. Contribution à la mise en œuvre et l'optimisation d'une cellule robotisée : application au parachèvement de pièces de fonderie. Thèse de Doctorat, Université Blaise Pascal, 2007.

Article 051-pp-103

MATERIAL REMOVAL DISTRIBUTION IN ROBOTIZED RANDOM ORBITAL SANDING

Raphaël POIRÉE[1], Sébastien GARNIER[1], Benoît FURET[1]

(1) : Université de Nantes – Institut de Recherche en Communication et Cybernétique de Nantes (IRCCyN) – UMR CNRS 6597
IRCCyN, 1 rue de la Noë, BP 92101 44321 Nantes Cedex 3, France
E-mail : {raphael.poiree,sebastien.garnier,benoit.furet}@univ-nantes.fr

Abstract: In random orbital sanding, in order to automate the process, the Material Removal (MR) has to be controlled at each point of the sanded part. Being a two body abrasive process, the pressure and the velocity are two mains parameters which have to be controlled. The pressure depends on the normal force, the lead angle and the curvature of the surface. It is shown that a particularity of random orbital sanding is that the velocity depends on the motor speed but also of the normal force, the lead angle and the curvature. In this study, the MR on a random orbital sander is simulated and validated on a point trajectory. The validation is used to simulate and validate the MR on a whole fractal trajectory on a flat surface. The influence of pressure distribution is shown by the sanding of a free-form surface with the same fractal trajectory. A comparison of the MR on the flat and on the free-form surface with the same trajectory permits to discuss about the influence of the curvature of the surface.

Key words: random orbital sanding, material removal, Preston law, free-form surface

1- Introduction

The automation of finalization of composites parts benefits of an important industrial demand, especially in fields like boating, aeronautic, building or green energies. The automation of sanding which is as drilling or trimming part of finalization presents technological and scientific problems. This is due to the manual aspect of sanding, which requires a high know-how of the sander where the control is done through intuitive perception without scientific established criteria. In order to automate the process, the control on sanding appears essential and depends on the control of the MR which can take various forms depending of the application. In the case of polishing, the goal is to reduce the surface roughness by removing some microns. In sanding, the goal is to increase the surface roughness in order to increase gripping and wettability of the surface before painting or collage. The difficulty here is to suppress enough material to increase the surface roughness while not suppressing too much material in order to not attack fibers of material composites or making flat sections.

Sanding being a two-body abrasion process this study is based on the abrasion/wear-based Preston's equation $\dot{h} = k_p p \Delta v$ [P1] at the contact element scale assumed large in front of the size of micro contacts (Figure 2), where $\dot{h}$ is the normal MR rate, p the pressure, Δv the relative velocity and k_p a constant representing the effect of other remaining parameters like abrasive paper, material sanded, wear of abrasives, temperature. Several authors studied the MR profile on a line [G1] [GT1] [R1][PG1]. The trajectory has a high influence on the MR distribution [PT1] [HC1].To obtain an homogeneous covering of the abrasion of the surface, several authors studied the influence of a carrier tool path (scanning, bi-scanning, [TC1] Hilbert [PT1], Peano [MS1], ziz-zag, zig-zig, parallel planes [TH1]) with adding eventually elementary patterns (Trochoid [PT1], Spade [CL1], Triangular).

Free-form surfaces sanding requires robotic systems giving a constant sanding force [NK1]. Studies which deal with the MR simulation are essentially on flat surfaces. This is mainly due to the difficulty to measure the difference on free-form surface before and after the process when the MR is of few microns. In order to validate a MR model on a free-form surface, it is necessary to be able to measure the MR. The pressure distribution depending of the surface curvature has been studied by [G1].

The goal of this paper is to simulate the MR in robotized random orbital sanding. Based on the Preston law, a comparison is done for a point trajectory between the simulation of the MR (given by the product of the pressure and the velocity) and the real MR (obtained by measure of the surface before and after sanding). Once the MR model is obtained on a point trajectory, it is validated on a whole fractal trajectory. Then, we compare the MR with a fractal trajectory on a flat surface to the MR obtained on a free-form surface.

With a measure of the MR on a free-form surface, it is then possible to compare it with simulations taking into account the curvature of the free-form surface

2- Robotized random orbital sanding

A random orbital sander is mounted on an anthropomorphic robot (Figure 1). Like several abrasive processes, sanding has to be controlled in effort. To maintain a constant normal force on a free-form surface, an active contact flange is mounted between the robot and the sander. Between the abrasive paper and the backing pad, a foam of 10mm height reduces the effects of the surface curvature (Figure 21)

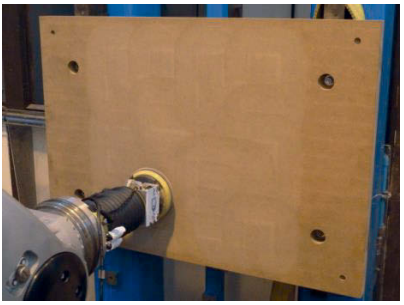

Figure 1: Sanding a Medium Density Fiberboard flat surface with a MIRKA CEROS 650 Random Orbital Sander, an ACF FERROBOTICS contact flange on KUKA KR270 anthropomorphic robot

The random orbital sander (represented Figure 2) is composed of a motorized pivoting link and a free pivoting link. Consequently, the rotation speed of the backing pad depends of the motor rotation speed but also of other parameters like the normal force, the abrasive paper, the lead angle (Figure 18), the sanded part, etc.

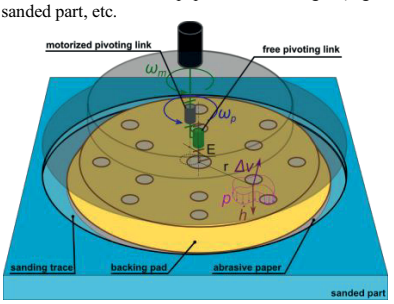

Figure 2: Scheme of a random orbital sander

3- MR distribution on the sanding trace

The first step of this study is to determine the MR distribution on the sanding trace. It is important to distinguish the backing pad (on which the abrasive paper is scratched) of the sanding trace (the MR for a sanding with a point trajectory of the sander) (Figure 2). For example, with an eccentricity $E = 5mm$ and a backing pad diameter of $150mm$, the sanding trace has a $160mm$ diameter. So, in order to compare the MR to the product of the velocity and the pressure, it is necessary to study the sanding trace because we can't isolate the MR on the backing pad due to the random orbital movement.

3.1 – Study of the velocity distribution

In circular sanding, the velocity of a point is $\Delta v = \omega r$. In random orbital sanding, the velocity is given by (1):

$$\Delta v(r,t) = \sqrt{r^2{\omega_p}^2 + E^2{\omega_m}^2 + 2rE\omega_p\omega_m \cos(\omega_p - \omega_m)t} \quad (1)$$

With $r\ (mm)$ the distance between the point and the center of the backing pad, $E\ (mm)$ the eccentricity between the two pivoting links, ω_p the rotation speed of the backing pad in relation of the sander (rad/s) and ω_m the motor rotation speed (rad/s). With a normal force $P = 40N$ and $N_m = 5946\ rpm$ the backing pad rotation speed is measured at $N_p = 211\ rpm$. For further explanation about the random orbital movement, the movement of a point is plotted Figure 3. A combination of a circular movement and an orbital movement is noticed.

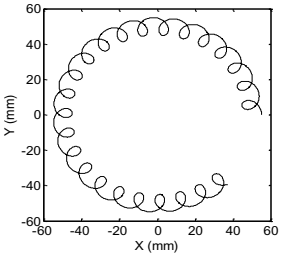

Figure 3: Random orbital movement of a point (r=50mm)

On Figure 4 is represented the evolution of the velocity in function of the radius and time based on equation (1). The velocity varies depending whether the orbital movement goes in the same way than the circular movement whether in the other way. With a time long enough (100s) the average velocity is taken for each radius of the backing pad (Figure 4).

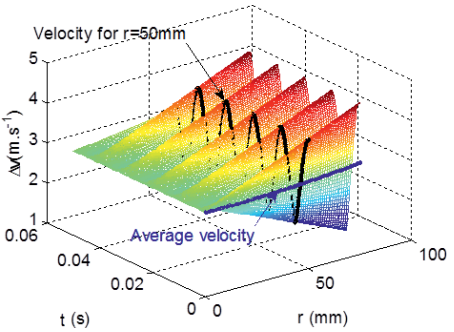

Figure 4: Evolution of the velocity for Nm=5946rpm and Np=211rpm

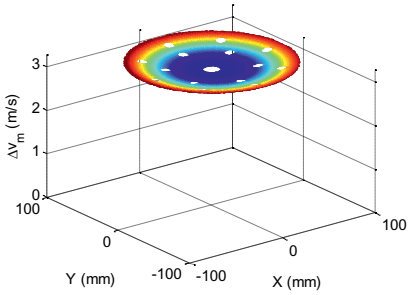

Figure 5: Average speed for each point on the backing pad

The average velocity is quite constant (between 3,12m/s and 3,4m/s when the velocity for a circular movement would be between 0 and 46m/s). From the average velocity, the average speed Δv_m is determined for each point of the backing pad (with a zero-speed in the aspiration holes of the backing pad) (Figure 5). The integral of the average speed during 1 s on the sanding trace is calculated by summing matrix at each point of the movement of the backing pad (which is a circle of 5mm radius) (Figure 6). This does not represent the MR which is determined in section 3.3.

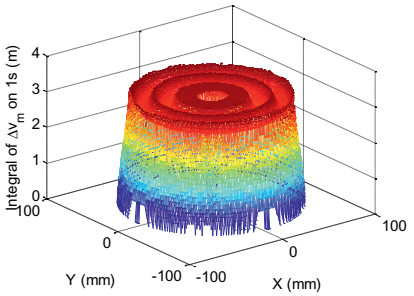

Figure 6: Integral of the average speed during 1s on the sanding trace

3.2 – Study of the pressure distribution

With the Finite Element Method (revolution elastic case with small deformations) the distribution of pressure on the backing pad is determined and with the same methodology as for the velocity the integral of the pressure during 1s on the sanding trace is obtained. A study taking into account dynamical effects, interface between the backing pad and the abrasive paper, friction between the abrasive paper and the part and side effects due to aspiration holes would be more accurate but requires a finer modelling not desired in this study.

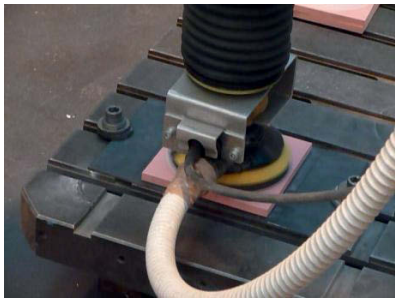

Figure 7: Random orbital sanding in a polyurethane part with a point trajectory

3.3 – Measure of the MR

The MR is obtained with sanding tests on polyurethane part with a point trajectory (Figure 7). Then it is measured with a continuous sensor mounted on a coordinate measuring machine (Figure 8).

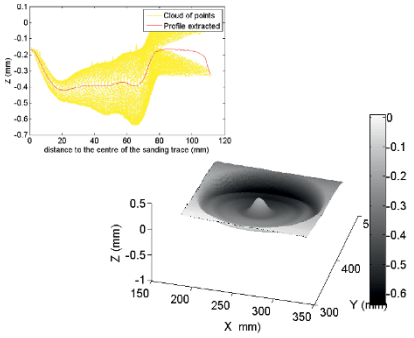

Figure 8: Measure of the MR on a sanding trace with a point trajectory – Extraction of the mean profile (top left corner)

As we can see on Figure 8, the lead angle of the tool was not null here and causes non axisymmetric sanding trace. To obtain the MR profile, we determine the center of the MR and for each point of the measure we calculate the distance to the center [PG1]. We obtain the mean profile of MR (top left corner on Figure 8).

By repeating those experiments with different times, the mean profile for 1s is determined (Figure 9). Actually, it represents the integral of the normal MR rate $\dot{h}$ during 1s.

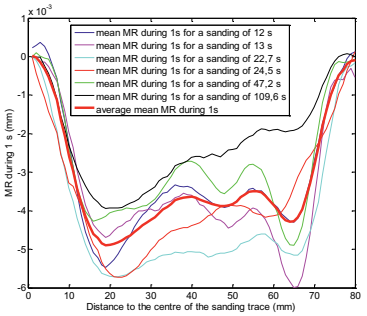

Figure 9: Determination of the mean profile of MR for 1s

3.3 – Comparison

The Preston law is verified by comparing the integral of the normal MR rate $\int_0^{1s} \dot{h}dt$ to the product of the integral of the pressure with the integral of the velocity $\int_0^{1s} pdt \,.\, \int_0^{1s} \Delta vdt$ (Figure 10). The recalibration is computed using the least square method. The Preston law is validated with a difference of 15% for random orbital sanding. Then, it can be used to simulate the MR on a full trajectory. The differences between the two curves are discussed in the discussion section.

4- MR distribution on a whole trajectory

Once the MR is validated on a point trajectory, the experimental results are used to simulate the MR on a whole trajectory. A fractal trajectory is generated on a MDF part (Figures 11, 12 and 15). This fractal trajectory is generated on a flat surface and on a free-form surface in order to study the influence of the curvature. The aim of this trajectory is not to optimize the MR distribution but to isolate the MR of sanding without recovery. In order to optimize the MR distribution, elementary patterns could be added.

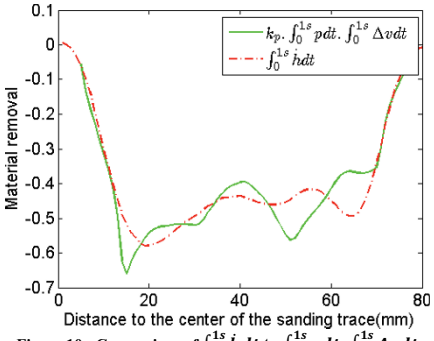

Figure 10: Comparison of $\int_0^{1s} \dot{h}dt$ to $\int_0^{1s} pdt \,.\, \int_0^{1s} \Delta vdt$

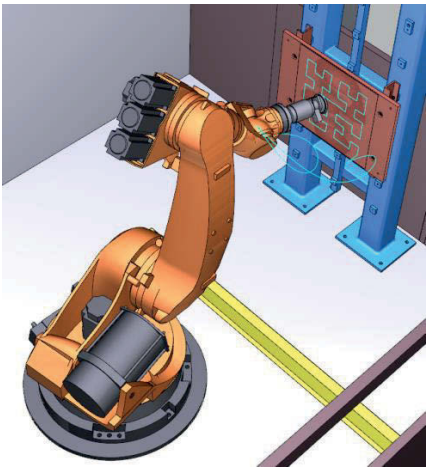

Figure 11: Fractal sanding trajectory generated with RobotMaster

4.1 – Experiments

The flat surface and free-form surfaces are generated with MATLAB. The free-form surface was generated with MATLAB "peaks" function. Each side is 680mm long and the amplitude on Z is 2. The equation is given Figure 12 and the free-form surface is visible Figure 15. Consequently, Z-max is 16.2123mm and Z-min is -13.1021mm. Then, a fractal trajectory Hilbert Curve H_2 is projected on the surface at 80mm of the borders of the surface. The normal of the surface is calculated at each point of the trajectory.

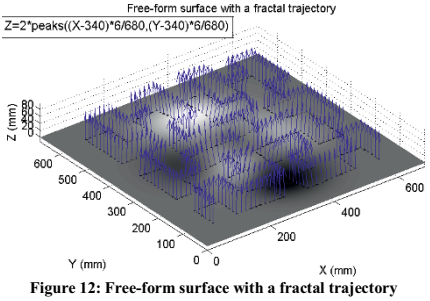

Figure 12: Free-form surface with a fractal trajectory

The surface is exported to CATIA V5 in order to generate the CAD and CAM in order to mill the surface with a 5-axis CNC (BELOTTI). The trajectory is exported to RobotMaster in order to generate the sanding trajectory with a 6-axis Robot (KUKA KR270) (Figure 11). Before sanding, the part is measured on a Coordinate Measuring Machine CCM (Hexagon) in order determine the geometry before sanding.

Once the part is sanded, the surface is measured with a CMM (Figure 15). By difference, the MR is determined.

4.2 – Simulation

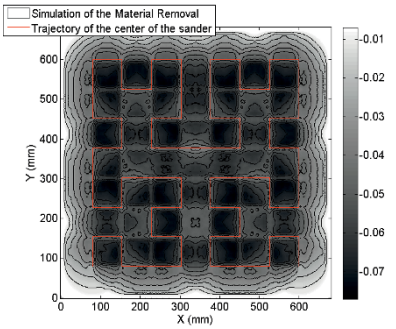

Figure 13: Simulation of MR in Random Orbital Sanding on the fractal trajectory on a flat surface

For the flat surface, results of experiments on the point trajectory are used. For each point of the trajectory, the MR is simulated and MR simulation on the whole surface is obtained (Figure 13).

For the free-form surface, the simulation requires finer modelling not investigated in this study. [G1] established an abacus of the pressure distribution for polishing but couldn't validate it due to the difficulty to measure a free-form surface with a precision of few microns.

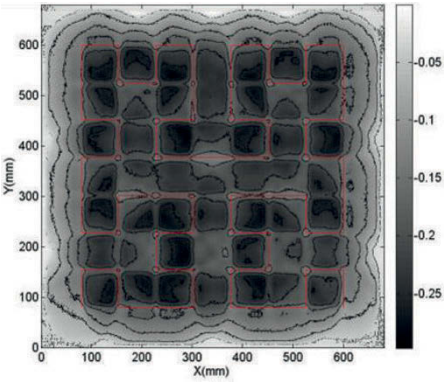

Figure 14: MR of Random Orbital Sanding on the fractal trajectory on a flat surface (Difference of the measure after milling and after sanding)

4.3 – Results

By difference of the measure before sanding and after sanding, the MR is obtained on the whole surface for the flat surface (Figure 14) and the free-form surface (Figure 16). To make the comparison between the MR measured and the MR simulated, the percentage of difference between the measured recalibrated on the simulation is studied. The recalibration is based on the sum of the MR on the whole surface. The percentage of error between the MR measured (experiment) and the MR simulated on the flat surface is represented Figure 19. For the free-form surface, the experiment is recalibrated to the simulation with the same ratio used on the flat surface (Figure 20).

Figure 15: Measure of a Medium Density Fiberboard (MDF) free-form surface after milling with a CCM Hexagon and a continuous probe Renishaw SP25

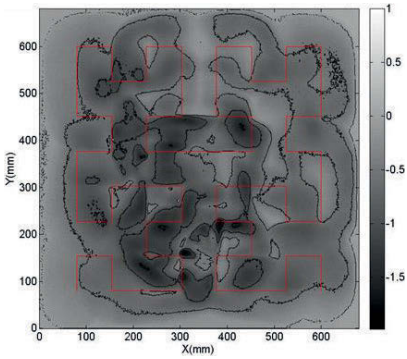

Figure 16: MR of Random Orbital Sanding on the fractal trajectory on the free-form surface (Difference of the measure after milling and after sanding)

Moreover, considering that the backing pad rotation speed ω_p evolves with the normal force and the lead angle (Figure 17), it is measured during the fractal trajectory on the flat and on the free-form surface (Figure 18). With the curvature of the surface the "apparent lead angle" evolves and so the backing pad rotation speed (Figure 18). The "apparent lead angle" is defined on Figure 21 as the angle between the

normal direction to surface at the centre of the ROS and the normal direction to surface at the contact point (which is the centre of the surface contact).

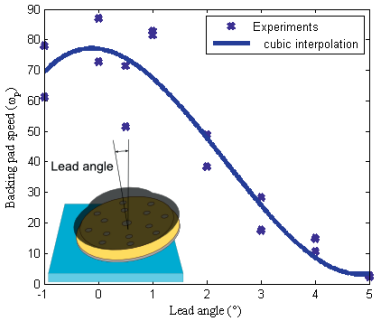

Figure 17: Influence of the lead angle on the backing pad speed

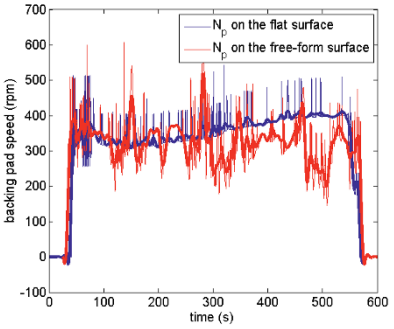

Figure 18: Backing pad rotation speed Np during sanding

5 – Discussion

- The Preston law validation a point trajectory permits to predict the MR on a point trajectory through the pressure and the velocity. Several authors chose to determine the MR on a line trajectory. This reflects better the real process but it is then harder to take into account the pressure distribution. As it can be seen on Figure 10, the simulation is not exactly the same than the experiment (difference of 15%). This could be due to the pressure distribution and to the natural inclination of abrasive processes to smooth the surface. Indeed, when a peak appears, the pressure increases and so the MR. Furthermore, other abrasives models could be used like [K1] based on Preston's law $\dot{\boldsymbol{h}} = \boldsymbol{k_p p^{\alpha} \Delta v^{\beta}}$.

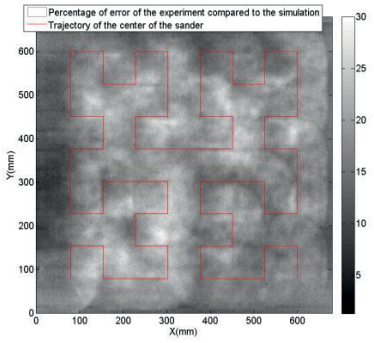

Figure 19: Percentage of error between the MR measured and the MR simulated on the flat surface

- For a flat surface, the simulation of the MR is quite acceptable compared to the experiments (difference up to 30% or 0.09mm). This difference could be due to the natural inclination of random orbital sanding to smooth the surface. But, for a free-form surface, the simulation is quite different of experiments and especially heterogeneous at some locations (difference up to 700% or 1.6mm). This could be due to a bigger pressure at some locations when the "apparent" lead angle is important. The surface sanded is smaller, so the pressure is higher (because the normal force is constant) and so the MR. On the sanded surface, light flats can be seen on the surface (for example at coordinates X=400m and Y=200mm on Figures 16 and 20). This will mean a not acceptable sanding.

- In order to simulate the MR on a free-form surface, it is necessary to simulate the pressure distribution at each point of the trajectory and to simulate the backing pad speed. As

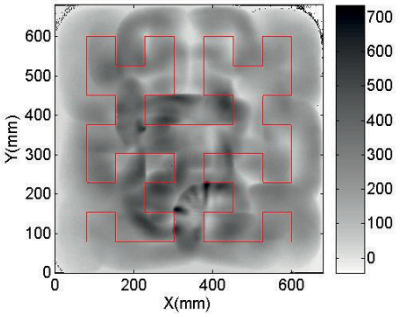

Figure 20: Percentage of error between the MR measured and the MR simulated on the free-form surface

it can be seen on Figure 18, the backing pad rotation speed varies with the curvature of the free-form surface. However, this does not explain the difference of 700% at some locations between the MR on the flat surface and on the free-form surface. In order to correlate the MR on a free-form surface, experiments are in progress on surfaces more elementary like singles curvatures.

- Backing pad rotation speed variations can't be controlled in random orbital sanding. Nevertheless, they are negligible in front of the difference of 700% between the flat and the free-form surface. In order to take into account backing pad rotation speed variations, a dynamic study of random orbital sanding should be achieved in order to predict the backing pad rotation speed in function of the normal force and of the "apparent lead angle". On the free-form surface, the "apparent lead angle" should be reduced by taking into account the curvature of the surface in the tool path generation.

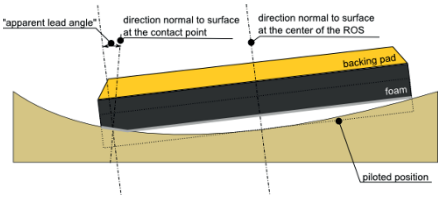

Figure 21: Percentage of error between the MR measured and the MR simulated on the free-form surface

6 – Conclusion

In this paper, robotized random orbital sanding developed in IRCCyN/University of Nantes is presented. The Preston law widely used for abrasive processes is validated on a point trajectory. Thanks to this validation, a simulation and validation of the MR on a flat surface with a whole fractal trajectory is achieved. Experiment with the same trajectory on a free-form surface is realized in order to show the influence of the curvature of the surface on the MR distribution. Difference up to 700% is measured between the MR on the flat surface and on the free-form surface. In order to reduce this difference, the modelling of the MR on the free-form surface should be achieved.

Acknowledgement

The authors would like to thank Samuel Bonnet (Capacités SAS), Joachim Marais, Fabien Truchet and Guillaume Gallot, research engineers at the Université de Nantes for the help during the robotized sanding tests and the metrology.

References

[CL1] J. Chaves-Jacob, J.-M. Linares, J.-M. Sprauel, Improving tool wear and surface covering in polishing via tool path optimization, Journal of Materials Processing Technology 213, 2013, 1661-1668

[G1] A. Guiot, Modélisation et simulation du procédé de prépolissage automatique sur centre d'usinage 5 axes, Thèse de doctorat, École Normale Supérieure de Cachan, 2012

[GT1] A. Guiot, C. Tournier, L. Mathieu, Simulation of the material removal rate and tool wear to improve 5-axis automatic polishing operations, IDMME – Virtual Concept 2010

[K1] F. Klocke, A. Chandra, R. Zunke, P. Karra, Modeling of material removal in polishing of advanced ceramics, Other Abrasive Machining Processes, p597-604, 2010

[MS1] Y. Mizugaki, M. Sakamoto. Development of a Metal-Mold Polishing Robot System with Contact Pressure Control, Annals of the CIRP, 39(1), 1990, 523-526

[NK] F. Nagata, Y. Kusumoto, Y. Fujimotok, K. Watanabe, Robotic sanding system for a new designed furniture with free-formed surface, Robotics and Computer-Integrated Manufacturing 23, 2007, 371-379

[P1] P. W. Preston, The theory and design of plate glass polishing machines, Journal of the society of glass technology, 1927, 214-256

[PT1] X. Pessoles, C. Tournier, Automatic polishing process of plastic injection molds on a 5-axis milling center, Journal of materials processing technology, 2009, 3665-3673

[PG1] R. Poirée, S. Garnier, B. Furet, S. Bonnet, Étude de la répartition d'enlèvement de matière en ponçage roto-orbital, 7ème assise MUGV 2012 ENISE-CETIM, Saint-Etienne, 2012

[R1] V. Robin, Contribution à la mise en œuvre d'une cellule robotisée: application au parachèvement des pièces de fonderie. Thèse de doctorat, Université Blaise Pascal-Clermont II, 2008

[TC1] H-Y. Tam, H. Cheng, An investigation of the effects of the tool path on the removal of material in polishing, Journal of material processing technology, 2010, 807-818

[TH1] H-Y. Tam, C. Hang Lui, A.C.K. Mok, Robotic polishing of free-form surfaces using scanning paths, Journals of Materials Processing Technology, 95 1999, 191-200

Article 053-r-10

Harmonic Functions-based Type-2 fuzzy logic controller for autonomous navigation of mobile robots

Achille MELINGUI [1, 2], Rochdi MERZOUKI[1], Jean Bosco MBEDE [2]

(1): University of Lille1, 59655 Villeneuve d'Ascq, France
+3352477360
E-mail: achille.melingui@etudiant.univ-lille1.fr, rochdi.merzouki@polytech-lille.fr

(2): University of Yaoundé I, P. O. Box: 8390 Yaoundé, Cameroon
Phone/Fax
E-mail: mbede@neuf.fr

Abstract: One of the requirements for navigation algorithms is to cope with the large amount of uncertainties that are inherent in real environments. Traditional type-1 Fuzzy Logic Systems (FLSs) using precise type-1 fuzzy sets cannot fully handle such uncertainties. Higher order FLSs, such as an interval type-2 FLSs have been proven to be able to model and handle such uncertainties. The performances of the latter are strongly related to the fuzzy rule base, usually given by experts. However, the linguistic rules obtained from experts are usually not enough for designing a successful control system, because some information is lost when the experts express their experience by linguistic rules. Thus, the sampled input-output data pairs obtained from a navigation system based on harmonic potential functions are combined with the linguistic rules to build the Interval Type-2 Fuzzy Logic (IT2FL) Controller rule base. One of the most important properties of harmonic functions is that they are free from local minima; they completely eliminate the local minima even in cluttered environments. The proposed controller is implemented in real-time on an omnidirectional mobile robot navigating in unstructured dynamic environments. Through comprehensive experiments, the effectiveness of the proposed IT2FL controller is demonstrated.

Key words: Type-2 Fuzzy Logic Control, Artificial Potential Field, Autonomous Navigation, Hybrid Control, Intelligent Control.

1- Introduction

Artificial Potential Field (APF) approach, thanks to its elegant mathematical analysis and simplicity implementation has been widely used for navigation of mobile robots [K1], [MC1], [MH1], [TV1]. In contrast to other approaches (learning-based, fuzzy logic...), the robot navigation problem through APF considers simultaneously the path planning, the trajectory planning, and the control problems [RK1]. The APF approach is conceptually simple; it can be easily implemented in the feedback form and also extended to moving obstacles. The concept of APF approach is a creation of artificial potential fields in the robot workspace in which the robot is repulsed by obstacles and attracted to its goal position [K1]. The robot follows the gradient of this APF towards its minimum. However, the potential field introduced exhibits local minima other than at the goal position of the robot, which may stop the goal from being achieved.

To overcome this problem, Kim et al. [KK1] have used harmonic functions to build an artificial potential field that eliminates local minima and the panel method to derive the potential field for obstacle avoidance. Connolly et al. [CB1] have proposed a global method which generates smooth collision-free paths. Their approach computes solutions to Laplace's equation, and results in weak form of what Rimon et al. [RK1] defined as navigation functions. The solutions of Laplace's equation are called harmonic functions or potential functions. These solutions equation can be obtained numerically [CB1] or analytically [KK1]. Whatever the method used, for navigation in dynamic and unstructured environments, the computational time becomes prohibitive for an autonomous system, because the solution need to be recomputed whenever the configuration of the environment changes. In this paper, the APF controller based on harmonic functions runs offline; it is developed for generating fuzzy rules.

Fuzzy logic controller is credited with being an adequate methodology for designing robust controllers that are able to deliver a satisfactory performance face of large amounts of uncertainty and imprecision [S1]. Inspired by the human being, it has an important characteristic in the way it deals with various situations without a model of the environment; such that it has become a popular approach to reactive mobile robot control in recent years [S1], [H1], [MC1] [MM1], [MH1]. However, it has been shown that, the traditional type-1 fuzzy logic controller using precise type-1 fuzzy sets cannot fully handle the uncertainties present in changing and dynamic unstructured environments [M1]. They face many sources of uncertainties and imprecision (inputs Fuzzy Logic Controller uncertainties, control action uncertainties, linguistic uncertainties [H1]).

Higher order FLSs, such as the interval type-2 FLSs, have

been shown to be suitable to deal with these uncertainties [M1]. This ability is justified by the fact that an interval type-2 fuzzy set can be seen to possess an uncountable number of type-1 sets. The third type-2 fuzzy logic sets dimension and its footprint of uncertainty gives them more degrees of freedom sufficient for better modeling uncertainty in comparison to type-1 fuzzy sets [M1], [MJ1]. The performance of the latter is strongly related to the size of the fuzzy rule base, which is usually given by experts. However, some information is usually lost when the experts express their experience by linguistic rules [WM1]. Hence, linguistic rules are usually not enough for designing a successful control system. On the other hand, the information from sampled input-output data pairs is also not enough for a successful design (difficult to cover all the situation the control system will face). Thus, in this work, the sampled input-output data pairs obtained from a navigation system based on harmonic potential functions are combined with the linguistic rules into a common framework to build the IT2FL rule base. The problem addressed in this paper is the autonomous navigation of mobile robots in dynamic unstructured environments. This problem is formulated and solved in the configuration space of the mobile robot. In this particular application, the proposed IT2FL controller is used to approximate an APF controller based on harmonic functions, and simulate the experience of the human controller.

The remainder of this paper is organized as follows: Section 2 examines the navigation problem through the artificial potential functions and introduces the harmonic functions. Section 3 proposes an IT2FL control strategy involving artificial potential functions. Section 4 presents some experimental results obtained from an omnidirectional mobile robot. Finally, Section 5 gives conclusions and some remarks.

2- Motion planning through the artificial potential fields

In this section, we first recall the concepts of APF, followed by the notions of harmonic functions. The section ends with a summary on type-2 fuzzy logic.

2.1 – Artificial Potential Field General Concepts

The idea of using an artificial potential field for robot planning and obstacle avoidance has been pioneered by Khatib [K1]. The mobile robot moves into a field of forces. The goal position is attractive pole for the mobile robot and the obstacles are repulsive surfaces. The introduced potential field $U_{art}(x)$ consists of the attractive potential field $U_{att}(x)$ and repulsive potential field $U_{rep}(x)$. The total artificial potential acting on the robot is the sum of these two potential fields:

$$U_{art}(x) = U_{att}(x) + U_{rep}(x) \qquad (1)$$

The negative of the gradient of the total potential field $U_{art}(x)$ consists of two terms, the attractive force $F_{att}(x) = -\nabla U_{att}(x)$ driving the mobile robot to reach the goal position, and the repulsive force $F_{rep}(x) = -\nabla U_{rep}(x)$ which keeps the mobile robot away from obstacles; hence the name "Force inducing and artificial repulsion from the surface of obstacles (FIRAS from the French)".

2.2 – Harmonic functions

A function on a domain $\Omega \subset \mathbb{R}^n$ which satisfies Laplace's equation (2) is called harmonic function.

$$\nabla^2 \phi = \sum_{i=1}^{n} \frac{\partial^2 \phi}{\partial x_i^2} = 0 \qquad (2)$$

The most important properties of harmonic functions are that they are free of local minima, and any linear combination of two harmonic functions is also a harmonic function. These properties have been exploited by several researchers to guide a robot in the C-space [Rk1], [KK1]. The harmonic functions with spherical symmetry are introduced from [C1]. These functions depend only on r (distance from the origin). The general n-dimensional expression of the Laplace equation (2) in a polar coordinate can be written as [kK1]:

$$\nabla^2 \phi = \frac{\partial^2 \phi}{\partial r^2} + \frac{n-1}{r}\frac{\partial \phi}{\partial r} + \text{angular terms} \qquad (3)$$

Depending on the dimension n, the solutions of equation (3) are:

$$\phi = c_1 \log r + c_2 \text{, } if\ n = 2 \quad (4)$$

$$\phi = \frac{c_3}{r^{n-2}} + c_4, if\ n > 2 \qquad (5)$$

Where c_i's are constants. In hydrodynamics, the above harmonic functions with spherical symmetry is called source or sink, depending on the sign of c_1 in (4) and c_3 in (5). A source can be used to represent a point obstacle and a sink can be used to represent the goal position. The total potential due to the obstacles, goal, and uniform flow at any point (x, y) in C-space can be expressed following [KK1] as:

$$\phi(x,y) = -U(x\cos\alpha + y\sin\alpha) + \frac{\lambda_g}{2\pi}\log R_g + \sum_{i=1}^{m}\frac{\lambda_i}{2\pi}\int_i \log R_i dl_i \qquad (6)$$

Where $R_g = \left((x-x_g)^2 + (y-y_g)^2\right)^{1/2}$ is the distance between the point (x, y) and the goal point $G(x_g, y_g)$. U is the strength of the uniform flow, and λ_g is the strength of the goal sink. $R_g = \left((x-x_i)^2 + (y-y_i)^2\right)^{1/2}$ is the distance from point (x, y) to center of panel (x_i, y_i). $\lambda_{i=1,\ldots m}$ represent the source/sink strengths per unit length of the panels. We referred the reader to [KK1] for more details.

2.3 – Type-2 Fuzzy Logic Concepts

The concept of type-2 fuzzy was introduced by Zadeh

[Z1] as an extension of type-1 fuzzy sets. While a type-1 fuzzy set noted A is characterized by a type-1 MF $\mu_A(x)$ (i.e the membership grade is a crisp number in $[0,1]$), where $x \in X$ and $\mu_A(x) \in [0,1]$, a general type-2 set noted $\tilde{A}$ is characterized by a type-2 MF $\mu_{\tilde{A}}(x,u)$, where $x \in X$ and $u \in J_x \subseteq [0,1]$, i.e.,

$$\tilde{A} = \left\{ \begin{array}{l} \left((x,u), \mu_{\tilde{A}}(x,u) \right) \middle| \forall x \in X \\ \forall u \in J_x \subseteq [0,1] \end{array} \right\} \quad (7)$$

In which $\mu_{\tilde{A}}(x,u) \in [0,1]$. $\tilde{A}$ can also be expressed as follows [M1]:

$$\tilde{A} = \int_{x \in X} \int_{u \in J_x} \mu_{\tilde{A}}(x,u) / (x,u), \quad J_x \subseteq [0,1] \quad (8)$$

Where $\int\int$ denotes union over all admissible x and u. For discrete universes discourse, $\int$ is replaced by $\sum$. J_x is called the primary membership of x in $\tilde{A}$. At each value of x say $x = x'$, the 2-D plane, whose axes are u and $\mu_{\tilde{A}}(x',u)$ is called a vertical slice of $\mu_{\tilde{A}}(x,u)$ [KM1]. $\mu_{\tilde{A}}(x = x',u)$ can be represented for each $x \in X$ and $\forall u \in J_{x'} \subseteq [0,1]$ as:

$$\mu_{\tilde{A}}(x = x',u) = \int_{u \in J_{x'}} f_{x'}(u)/u, J_{x'} \subseteq [0,1] \quad (9)$$

In which $0 \le f_{x'}(u) \le 1$. $\mu_{\tilde{A}}(x)$ is referred as a secondary MF; it is a type-1 fuzzy set. When the secondary MF's are type-1 interval sets, where $f_x(u) = 1$, we call the type-2 set an interval type-2 set. Figure 1 shows the schematic diagram of an interval type-2 FLS; it is similar to Type-1 FL, the major difference being that at least one of the fuzzy set in the rule base is an interval type-2 FLS. Hence, the outputs of the inference engine are interval type-2 fuzzy set, and a type-reducer [M1] is needed to convert them into a Type-1 fuzzy set before defuzzification can be carried out. In this work, the Karnik Mendel (KM) algorithm [KM1] is used for type-reduction process.

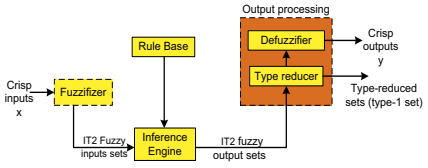

Figure 1: Structure of an interval type-2 fuzzy logic system

3- Mobile robot control

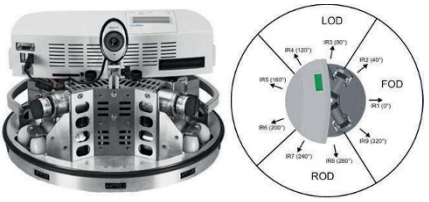

Figure 2: Robotino mobile robot

Robotino mobile robot is endowed with 9 infrared sensors as shown in Figure 2. These sensors are used to detect static and mobile obstacles. They are clustered into 3 groups for surrounding obstacles detections: Left Obstacle Detection (LOD), Front Obstacle Detection (FOD) and Right Obstacle Detection (ROD). The longitudinal $\Delta X = x - x_G$ and lateral $\Delta Y = y - y_G$ variations, and the distances (LOD, FOD and ROD) are considered as inputs to the IT2FL controller. Note that, (x,y) is the current robot position, and (x_G, y_G) is the goal position. The IT2FL controller generates the longitudinal (v_x) and lateral (v_y) velocities as outputs. The linguistic variable ΔX is modelled by three interval type-2 Gaussian MFs (Figure 3-a) representing the linguistic labels: Zero ($\tilde{Z}$), Middle ($\tilde{M}$) and Large ($\tilde{L}$). The linguistic variable ΔY is modelled by five interval type-2 Gaussian MFs (Figure 3-b) representing the linguistic labels: Negative ($\tilde{N}$), Small Negative ($\tilde{SN}$), Zero ($\tilde{Z}$), Small Positive ($\tilde{SP}$), and Positive ($\tilde{P}$). The linguistic variables (LOD, FOD and ROD) are modelled by two interval type-2 Gaussian MFs (Figure 3-c) representing the linguistic labels: Near ($\tilde{N}$) and Far ($\tilde{F}$). Finally, the linguistic variables (v_x and v_y) are modeled by five interval type-2 Gaussian MFs (Figure 3-d) representing the linguistic labels: Fast Backward ($\tilde{FB}$), Backward ($\tilde{B}$), Stop ($\tilde{S}$), Forward ($\tilde{F}$), Fast forward ($\tilde{FF}$).

In this work, the sampled input-output data pairs obtained from a navigation system based on harmonic potential function are combined with the linguistic rules into a common framework to build the IT2FL fuzzy rule base. The APF based on harmonic controller function runs offline.

The sampled input-output data pairs over eight simple navigation cases [MC1] are recorded, and constitute our learning base. By using the Wu and Mendel algorithm [WM1], we get respectively 24 and 40 fuzzy rules for the longitudinal and lateral velocities. Due to the limitation of the number of pages, the numerical fuzzy rules are not presented; only their linguistic counterparts are given (Table I and Table II).

The first rule of the Table I can be expressed as follows:

$$R^i: \text{If LOD is } \tilde{N} \text{ and FOD is } \tilde{N} \text{ and ROD is } \tilde{N} \text{ and } \Delta X \text{ is } \tilde{Z} \text{ THEN } V_x \text{ is FB} \quad (10)$$

TABLE I
LONGITUDINAL VELOCITY RULES BASE

LOD	FOD	ROD	Δx	Vx	LOD	FOD	ROD	Δx	Vx
Ñ	Ñ	Ñ	Ž	FB	F̃	F̃	Ñ	Ž	F
Ñ	Ñ	Ñ	M̃	FB	F̃	F̃	Ñ	M̃	F
Ñ	Ñ	Ñ	L̃	FB	F̃	F̃	Ñ	L̃	FF
F̃	Ñ	F̃	Ž	S̃	Ñ	Ñ	F̃	Ž	S̃
F̃	Ñ	F̃	M̃	S̃	Ñ	Ñ	F̃	M̃	S̃
F̃	Ñ	F̃	L̃	S̃	Ñ	Ñ	F̃	L̃	S̃
Ñ	F̃	Ñ	Ž	F	F̃	Ñ	Ñ	Ž	S̃
Ñ	F̃	Ñ	M̃	F	F̃	Ñ	Ñ	M̃	S̃
Ñ	F̃	Ñ	L̃	FF	F̃	Ñ	Ñ	L̃	S̃
Ñ	F̃	F̃	Ž	F	F̃	F̃	F̃	Ž	S̃
Ñ	F̃	F̃	M̃	F	F̃	F̃	F̃	M̃	F
Ñ	F̃	F̃	L̃	FF	F̃	F̃	F̃	L̃	FF

TABLE II
LATERAL VELOCITY RULES BASE

LOD	FOD	ROD	Δy	Vy	LOD	FOD	ROD	Δy	Vy
Ñ	Ñ	Ñ	Ñ	S̃	F̃	F̃	Ñ	Ñ	F
Ñ	Ñ	Ñ	SN	S̃	F̃	F̃	Ñ	SN	F
Ñ	Ñ	Ñ	Ž	S̃	F̃	F̃	Ñ	Ž	S̃
Ñ	Ñ	Ñ	SP	S̃	F̃	F̃	Ñ	SP	S̃
Ñ	Ñ	Ñ	P̃	S̃	F̃	F̃	Ñ	P̃	S̃
F̃	Ñ	F̃	Ñ	FF	Ñ	Ñ	F̃	Ñ	FB
F̃	Ñ	F̃	SN	FF	Ñ	Ñ	F̃	SN	FB
F̃	Ñ	F̃	Ž	FF	Ñ	Ñ	F̃	Ž	FB
F̃	Ñ	F̃	SP	FB	Ñ	Ñ	F̃	SP	FB
F̃	Ñ	F̃	P̃	FB	Ñ	Ñ	F̃	P̃	FB
Ñ	F̃	Ñ	Ñ	S̃	F̃	Ñ	Ñ	Ñ	FF
Ñ	F̃	Ñ	SN	S̃	F̃	Ñ	Ñ	SN	FF
Ñ	F̃	Ñ	Ž	S̃	F̃	Ñ	Ñ	Ž	FF
Ñ	F̃	Ñ	SP	S̃	F̃	Ñ	Ñ	SP	FF
Ñ	F̃	Ñ	P̃	S̃	F̃	Ñ	Ñ	P̃	FF
Ñ	F̃	F̃	Ñ	S̃	F̃	F̃	F̃	Ñ	FF
Ñ	F̃	F̃	SN	S̃	F̃	F̃	F̃	SN	F
Ñ	F̃	F̃	Ž	S̃	F̃	F̃	F̃	Ž	S̃
Ñ	F̃	F̃	SP	B	F̃	F̃	F̃	SP	B
Ñ	F̃	F̃	P̃	B	F̃	F̃	F̃	P̃	FB

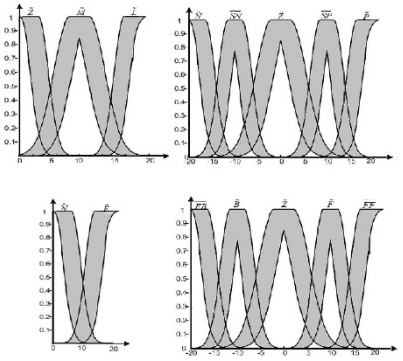

Figure 3: Membership functions.

4- Results and experiments

In this subsection, we first present experimental devices, followed by the results obtained. A discussion is presented at the end of the section.

4.1 – Experimental environment and navigation strategy

The experimental environment is like FESTO Hokey Challenge League area, with small pebbles, dust, which affect the performance of the robot, and introduce additional sources of uncertainty (Figure 4). It consists of three computers running on Windows OS and three Robotinos. Two Robotinos are used as mobiles obstacles, while the last one is the controlled robot. Nine infrared distance sensors are mounted in the chassis at an angle of 40° to one another. They are capable to detect the objects from 4 to 30cm (by expressing the length as a linear function of voltage). But, in our experiments, to deal with mobile obstacles, a neural network has been used to measure distances up to 70 cm (by expressing the length as a nonlinear function of voltage). With this distance, the mobile robot can avoid the mobile obstacles with a certain velocity by dealing them like static obstacles. The mobile obstacles move randomly in navigation environment; their shapes are circular with a diameter of 36cm. Hence, at least two infrared sensors detect its presence when it surroundings of the robot. Our navigation system is capable to avoid mobile obstacles with the velocities up to 15cm/s. In this paper a same rule base is used both for static and mobile obstacles. Video and image processing subsystem allows cracking the blue target object coordinates in order to estimate the distance from robot to target. The system starts with an image acquisition from video flow provided by Robotino webcam. Afterwards, the image passes through pre-processing such as filtering and smoothing. The Hough Transform algorithm is applied to detect colored object before the process of distance estimation [WS1]. The optical shaft encoders (dead reckoning method and neural network for the error correction) are used for mobile robot localization. The correction odometry system compensates for the difference between the real coordinates and those given by the navigation system.

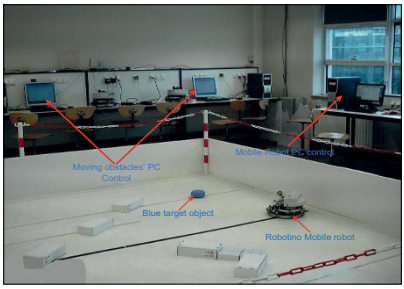

Figure 4: Experimental environment devices

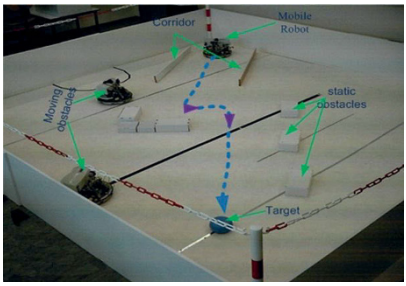

Figure 5: Navigation environment

4.2 – Experimental results

The main goal in these experiments is to reach the mobile robot to the blue colored object whatever the initial and final positions. The first step is to track the colored target using the embedded webcam, the video and image processing. The robot rotates on itself (by using the yaw speed) to track the colored target (blue object). The second step is to evaluate the distance between the robot and the target object. Finally, in the last step, the robot uses the IT2FL controller to reach the goal in a straight line if there is no obstacles or plan instantly another trajectory according to the clutter of the environment and the unpredicted events. The robot does not track a predetermined trajectory; it plans its trajectory in real-time. Several experiments have been carried out using the Robotino mobile robot to validate the theory and evaluate the performance of IT2FL controller. To better evaluate the performance of the proposed controller, two controllers have been designed and implemented in real-time: A type-1 FL controller, and an interval type-2 FL controller. The same fuzzy rule base has been used for the implementation of two controllers. The navigation environment is depicted in Figure 5; it comprises a corridor, a right corner, and two mobile obstacles. The two controllers achieve their specific task (reach blue object) in a different way. Trajectories achieved by each controller are represented in Figure 6. They depict the displacement of the center of gravity of the robot. We

notice that, the trajectory achieved by the IT2FL controller is smoother than that achieved by the type-1 FL controller. The velocities generated by the IT2FL controller are represented in Figure 7, while those generated by type-1 FL controller are depicted in Figure 8. They depict the evolution of the longitudinal and lateral velocities at each sample time. The velocities range between -0.4 and +0.3m/s. The IT2FL controller generates stable velocities, while the velocities generated by the type-1 FL controller present some oscillations. Moreover, the type-1 FL controller remains faster than IT2FL controller.

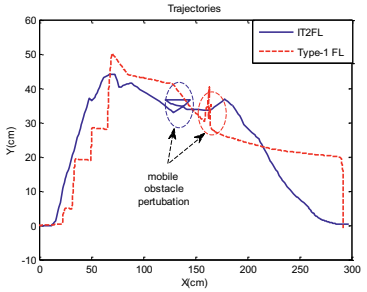

Figure 6: Trajectories achieved by the mobile robot

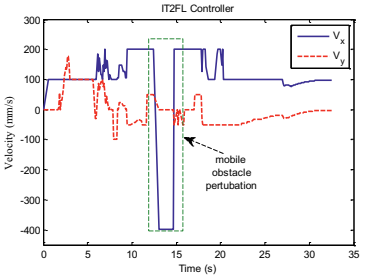

Figure 7: Velocities generated by the IT2FL controller

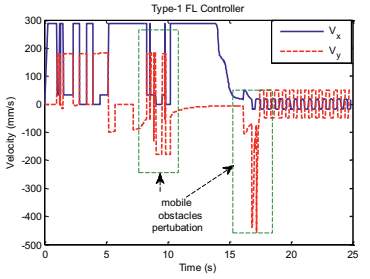

Figure 8: Velocities generated by the type-1 FL controller

4.3 – Discussions

On the whole, the results obtained are satisfactory, each controller achieves its task without hitting obstacles, and takes a reasonable time to perform the task. About ten tests have been conducted in the present environment (Figure 5), and the performances achieved by each controller have been satisfying. By observing Figure 6, Figure 7 and Figure 8, it is obvious that the IT2FL controller outperforms the performances of the type-1 FL controller. It generates smooth paths and stable velocities. However, it remains slower than the type-1 FL controller. This can be justified by type-reduction process. In fact, the KM algorithm involves many iterative loops which add a small computation overhead. In addition, the latter increases with the number of fuzzy rules (24 and 40 fuzzy rules in this work). In the view of the trajectories obtained, and the velocities generated by each controller, we can conclude that the IT2FL controller handles better uncertainties and impressions.

5- Conclusions

In this paper, we have presented an intelligent navigation system based on type-2 fuzzy logic, namely IT2FL for autonomous navigation of mobile robots in dynamic and unstructured indoor environments. Several experiments have been carried out to validate the performances of the proposed intelligent system. In this work, an APF controller has been used to generate suitable fuzzy rules. Using the generated fuzzy rules, we have shown that the IT2FL controller can handle the uncertainties present in real environments, and achieve performance that outperform their type-1 counterparts (in terms of the smooth paths, and the stability of the generated velocities). However, we have noticed that it remains slower than the type-1 FL controller.

In the future, we plan to divide the navigation problem into simple navigation cases in order to improve the controller performance.

7- References

[C1] C. R. Chester. Techniques in Partial Differential Equation. New York: McGraw-Hill, 1971.

[CB1] Connolly, C. I., Burns, J. B. and Weiss, R.. Path planning using Laplace's equation. In Robotics and Automation, 1990. Proceedings of IEEE International Conference on, 2102-2106, 1990.

[H1] H. Hagras. A hierarchical type-2 fuzzy logic control architecture for autonomous mobile robots. In IEEE T. Fuzzy Systems, 12(4): 524-539, 2004.

[K1] O. Khatib. Real-time obstacle avoidance for manipulators and mobile robots. Int. J. Robotics Res., 5(1): 90-98, 1986.

[KK1] Kim J. O. and Khosla P. K. Real-time obstacle avoidance using harmonic potential functions, IEEE Transactions on Robotics and Automation 8 (3) (1992) 338–349.

[KM1] Karnik N. N., Mendel J. M., and Liang Q. Type-2 fuzzy logic systems. Fuzzy Systems, IEEE Transactions on, 7(6): 643-658, 2002.

[M1] J. Mendel. Uncertain Rule-Based Fuzzy Logic Systems: Introduction and New Directions. Upper Saddle River, NJ: Prentice-Hall. 2001.

[MC1] Melingui A., Chettibi T., Merzouki R., and Mbede J. B. Adaptive navigation of an omni-drive autonomous mobile robot in unstructured dynamic environments. In Robotics and Biomimetics (ROBIO), 2013 IEEE International Conference on (pp. 1924-1929). IEEE.

[MH1] Mbede J. B., Huang X., and Wang M. Fuzzy motion planning among dynamic obstacles using artificial potential fields for robot manipulators. Robotics and Autonomous Systems, 2000; 32(1): 61-72.

[MJ1] Mendel J., and John R. Type-2 fuzzy sets made simple. In IEEE Trans. Fuzzy Syst., 10(2): 117-127, 2002.

[MM1] Mbede J. B., Melingui A., Zobo B. E., Merzouki R. and Bouamama B. O. zSlices based type-2 fuzzy motion control for autonomous robotino mobile robot. In Mechatronics and Embedded Systems and Applications (MESA), 2012 IEEE/ASME International Conference on, 63-68, 2012.

[RK1] Rimon E. and Koditschek D.E. Exact robot navigation using artificial potential functions. In IEEE Transactions on Robotics and Automation, 8 (5): 501–518, 1992.

[S1] A. Saffiotti. The uses of fuzzy logic in autonomous robot navigation. In J. Soft Comput., 1(4): 180-197, 1997.

[TV1] Tsourveloudis N. C., Valavanis K. P. and Hebert T. Autonomous vehicle navigation utilizing electrostatic potential fields and fuzzy logic. IEEE Transactions on Robotics and Automation. 2001; 17(4): 490–497.

[WM1] Wang L. X. and Mendel J. M. Generating fuzzy rules by learning from examples. Systems, Man and Cybernetics, IEEE Transactions on, 22(6): 1414-1427, 1992.

[WS1] Wahab M. N. A., Sivadev N. and Sundaraj K. Target Distance Estimation Using Monocular Vision System for Mobile Robot. In Proc. IEEE Int. Conf. Open Systems, 11-15 Langkawi 2011.

[Z1] L. A. Zadeh. The concept of a linguistic variable and its application to approximate reasoning. Information sciences, 8(3): 199-249, 1975.

Article 055-r-50

A hybrid force/position control for a 6 DOF parallel testing machine

Julien Le Flohic[1], Flavien Paccot[2], Nicolas Bouton[1], Hélène Chanal[1]

(1) : Institut Pascal UMR 6602 UBP/CNRS/IFMA,
Campus des Cézeaux BP 265 - 63175 Aubière Cedex, France
(+33) 04.73.28.80.00
E-mail : { Julien.Le-Flohic, Nicolas.Bouton, Helene.Chanal}@ifma.fr
(2) : Institut Pascal UMR 6602 UBP/CNRS/IFMA,
Campus des Cézeaux BP 265 - 63175 Aubière Cedex, FRANCE
E-mail : flavien.paccot@udamail.fr

Abstract: For the first time, a Nooru-Mohammed test was realized using a new kind of loading machine based on Gough-Stewart platform. However, it has been shown that boundary conditions on the concrete specimen are not respected. As a consequence, a new control strategy needs to be developed. This paper aims at applying a well-known control loop based on hybrid force/position law to a loading application. This new control algorithm has been developed according to the task and the structure specificities. Indeed, it permits to realize multi-axial test where the boundary conditions are controlled and respected by using the extra degrees of freedom of the platform.

Key words: Parallel machine, Hybrid control, Testing machine, Multiaxial test, Model.

1- Introduction

Compared to serial structure machines, parallel ones can propose greater dynamic ability, stiffness and accuracy [M1]. Therefore, according to the task load and constraints, parallel structure machines can bring benefit in term of task quality (cost, time, accuracy, ...) [PA1] [CD1]. However, the complexity of associated models and control laws, in addition to a reduced workspace, are their main drawbacks [M2].

In the context of mechanical test, very few parallel loading machines are developed [SG1] [MH1] [GK1]. Indeed, extra degrees of freedom (DOF) are often considerate as disruptive for the specimen load. In case of rigid specimen like concrete or steel, they might reduce the load direction stiffness. Multi-axial tests are therefore mainly realized with different synchronized structures. However, such testing machines are not versatile and are designed for one specific specimen load (bi-tension/compression or tension/torsion for example). On the contrary, parallel kinematic machines allow mixing different kind of specimen load configuration. Thus, we can state that the use of parallel kinematic machines is relevant for multi-axial mechanical test. Moreover, the possibility to control the specimen load in the 6-space components can improve the identification accuracy of the model material parameters.
However, only very few mechanical testing applications have been performed with parallel kinematic machines, and are mainly developed for biomechanical context with large displacements [SG1] [MH1] [GK1]. Nevertheless, it has been demonstrated that hexapod architecture are suitable for multi-axial testing of materials through a specific case study, the Nooru-Mohamed (NM) test [NP1] (see fig. 1). Its principle is to subject a double edge notched specimen to a combination of shear and tension (or compression) using numerous loading paths [N1] and requiring position and/or force controlled. According to Nooru-Mohamed himself, boundary conditions of the tests are difficult to control and since 1992, nobody has been able to perfectly reproduce it with conventional machine. This observation has motivated the use of extra degrees of freedom.

Due to very small displacement at failure in comparison to the specimen dimension with very low speed, the NM test is considered as a quasi-static test. First experimentation of using a parallel structure for NM test has proven that the instrumentation set up allow a relevant measurement of the displacement field, even for complex load trajectory and very stiff and quasi-brittle specimen [NP1]. But this experiment also revealed the influence of the compliance of the machine. Indeed, during NM test, an important rigid body motion of the specimen is observed with unwanted force acting on it. Due to the sensitivity to boundary conditions of the NM test, these disturbances may extremely degrade identification accuracy results.

Therefore, the aim of this paper is to design an advanced control law for the hexapod, considering the specificities of the machine and the NM test, in order to control boundary conditions. The control algorithm must allow controlling the position of two axis in order to generate the shear and tension load and null forces on the other directions. Due to

Article 055-r-50

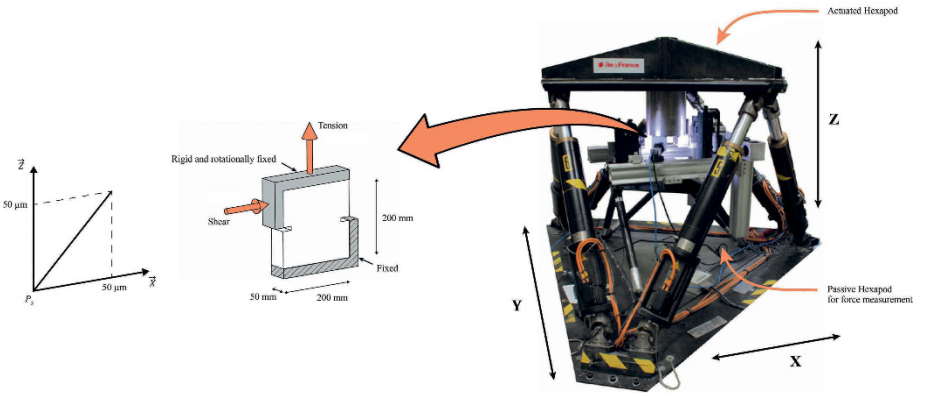

Figure 1: Principle of Nooru-Mohamed test [N1] and associate trajectory

the specificities of the task, the control of the applied force is required. To reach this aim, a lot of methods have been developed for force control and can be classified in two categories: impedance control and hybrid control [DB1].
Impedance control consists in regulating the mechanical impedance, which is defined as the ratio of force to motion [H1]. Therefore in this kind of strategy, the effort exerted by the end-effector on the environment is not explicitly specified [KD1]. It is mainly used for assembling [LA1] or manipulation [PC1], or more generally for any tasks requiring a position control of a robot which may come into contact with the environment.
The hybrid force control is chosen in particular when the environment is highly deformable, as in a medical context, using flexible environment and tool [MM1], or when the task requires accurate tracking coupled with high loads, as in a machining context [ZP1] [SF1]. This method is based on the decomposition of the task space into purely motion controlled directions and purely force controlled directions [RC1]. That is to say that any interaction with the environment is idealized as a geometric constraint [DB1]. For a 6-DOF parallel manipulator, the *n* force controlled directions and the *6-n* position controlled directions are independently regulated. However, in case of parallel kinematic machine, each joint has an influence on the position and the force applied by the mobile platform.

Then, considering the specificities of the machine (compliant parallel structure) and the specificities of the task (quasi-static test with complex load trajectory), hybrid force/position control is therefore naturally proposed. Thus, test requirements can easily be described in the Cartesian space in term of position controlled axis (if the trajectory is a position path) and force controlled axis (if the trajectory is a load path).

However, the main limitation of this kind of force control is due to the sensitivity to errors in the dynamic model [DB1]. In our case, this limitation is overcome assuming that:

- Static model can be used instead of dynamic model
- The jacobian matrix linking the actuated joint torques/forces with the force applied by the end effector can be consider as constant during the test part distortion

Impact of these assumptions is discussed further. Therefore, the paper is organized as follows. Section 2 presents the experimental setup considered and the static model associated to the hexapod. Based on this formalism, section 3 describes the control scheme developed. Section 4 illustrates the method with simulations realized on a Simulink®/Adams™ environment. Finally, concluding remarks and expectation on further works are given in section 5.

2- Experimental setup and model

A first experimentation has been performed in [NP1] using the hexapod presented below in the case study of the Nooru-Mohamed test. It revealed that an advanced control law is needed to use extra DOF to control boundary conditions.

2.1 – The Nooru-Mohamed test

The principle of the Nooru-Mohamed test (described in fig. 1) is to submit a double notched concrete test part to a position slope, inducing a combination of shear and tension loading. As predicted in the introduction, previous test shown that displacement at failure are negligible in comparison to the specimen dimension (0.01%). During this test, position of the upper limit of the specimen and the load on the specimen are measured.

2.2 – Sensors

2.2.1 – Position

During a Nooru-Mohamed test (and by extension, for all tests including highly rigid specimen), the structure is extensively solicited: the concrete test part needs 10 to 20 kN to break. Thus, due to the flexibility of the structure, proprioceptive measurements are not relevant. This is why a set of cameras coupled with an Integrated Digital Image Correlation technique [LP1] is used. In practice, cameras are fixed to the bottom of the specimen and measure the displacement of the top of the specimen. Then, displacements due to the flexibility of the structure are not taking into account in the measurement of the specimen deformation. This instrumentation enables a resolution of 0.2 µm with a 20 Hz frame rate.

2.2.2 – Force/Torque

The force/torque sensor consists in a passive hexapod placed under the specimen. The wrench at the top of this hexapod is computed by measuring the load in each leg. It allows a measurement of the forces with an uncertainty of 80 N and the torques with an uncertainty of 20 N.m [VN1]. These two sensors instrument the loading machine presented below.

2.3 – Loading Machine

The loading machine is a 6-DOF Bosch-Rexroth hexapod with ballscrew electrically actuated cylinder presented on fig. 1. Mechanical features are listed in Table 1 and show that it is adapted to mechanical tests purpose. $\mathbf{X} = [x, y, z, \psi, \theta, \phi]^T$ is a 6-components vector. x, y and z are the components of the origin P_S of the frame $\mathbf{R}_{Ps}$ linked to the end effector with regard to the frame $\mathbf{R}_{P_0}$ linked to the base (see fig. 2). ψ, θ and ϕ are the Euler angles which represents the orientation of frame $\mathbf{R}_{Ps}$ with regard to $\mathbf{R}_{P_0}$. $q = [q_1, q_2, q_3, q_4, q_5, q_6]^T$ represents the length of each actuated joint. Further details can be found in [NP1]. This machine is then used for the NM test, *i.e.* for generating a quasi-static load.

	Axis X	Axis Y	Axis Z
Forces	58 kN	54 kN	126 kN
Torques	46 kNm	41 kNm	71 kNm
Translation resolution	3.95 µm	0.54 µm	0.19 µm

Table 1: Loads capacity of the hexapod in neutral position

2.4 – Static Model

The NM test requires very low speed (15 µm/min), dynamic effects have thus no influence on the motion generation. Therefore, the development of a complex dynamic model is not relevant. To link the force applied by the end effector to the actuated joint torques/forces, the static model is then used.

2.4.1 – Generality

The static model of a machine is the mathematical relation which links the actuated joint torques/forces with the force applied by the end effector [M1]. Principle of virtual works implies [SS1] :

$$\mathbf{f} = \mathbf{J}^T \boldsymbol{\Gamma} \tag{1}$$

where $\boldsymbol{\Gamma}$ is the torque/force vector applied by the end effector. The vector $\mathbf{f}$ represents the actuated joint torque/force. $\mathbf{J}^T$ is the geometric transposed jacobian matrix. This matrix links the actuated joint velocity $\dot{\mathbf{q}}$ with the cartesian velocity $\dot{\mathbf{X}}$ of the end effector as [KD1] :

$$\dot{\mathbf{q}} = \mathbf{J}^{-1} \dot{\mathbf{X}} \tag{2}$$

Based on our test bed, all the angular components are null, then the geometric and the analytical jacobians are the same [SS1]. $\mathbf{J}^{-1}$ is then computed from the inverse kinematic model (IKM) as it can be expressed analytically for a parallel machine:

$$\mathbf{J}^{-1} = \frac{\partial \mathrm{IKM}(\mathbf{X})}{\partial \mathbf{X}} \tag{3}$$

with

$$\mathbf{q} = \mathrm{IKM}(\mathbf{X}) \tag{4}$$

IKM of the hexapod is computed using six geometric closing relations (one for each leg) [M1]. Fig. 2 shows the geometric closing relation for the leg 1. Using same reasoning for the five other legs, IKM of the hexapod can be found and the jacobian matrix $\mathbf{J}$ can be computed.

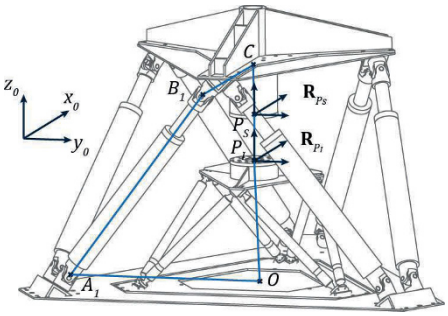

Figure 2: Geometric closing relation on leg 1

However, since the NM test is a quasi-static test (which means that very small displacement of the end-effector is needed), then we can assume that this jacobian matrix is constant during the test. This assumption is discussed in the next paragraph.

2.4.2 – Sensibility Analysis

$\mathbf{J}$ is a 6x6 matrix and depends on the position $\mathbf{X}$ of the end effector. In order to simplify the hybrid Force/Position

control and to be robust to numerical errors during the test, we suggest assuming that $\mathbf{J}$ can be constant during a Nooru-Mohamed test. The error made on $\mathbf{\Gamma}$ due to this assumption can be expressed as

$$\begin{aligned} e_{\mathbf{X}} &= \mathbf{\Gamma}_{Updated} + \mathbf{\Gamma}_{Fixed} \\ &= \mathbf{J}_{\mathbf{X}}^{-T}\mathbf{f}_{Updated} - \mathbf{J}_{\mathbf{X}}^{-T}\mathbf{f}_{Fixed} \\ &= \mathbf{J}_{\mathbf{X}}^{-T}\mathbf{J}_{\mathbf{X}}^{T}\mathbf{\Gamma}^{d} - \mathbf{J}_{\mathbf{X}}^{-T}\mathbf{J}_{In}^{T}\mathbf{\Gamma}^{d} \\ &= [\mathbf{I} - \mathbf{J}_{\mathbf{X}}^{-T}\mathbf{J}_{In}^{T}]\mathbf{\Gamma}^{d} \end{aligned} \quad (5)$$

with:

- $\mathbf{X}_{In}$ the initial position of the end effector at the beginning of the mechanical test
- $\mathbf{\Gamma}_{Updated}$ and $\mathbf{f}_{Updated}$ the torque/force vector applied by the end effector and the torque/force actuated joint vector, computed with an expression of the jacobian $\mathbf{J}$ depending on the position $\mathbf{X}$
- $\mathbf{\Gamma}_{Fixed}$ and $\mathbf{f}_{Fixed}$ the torque/force vector applied by the end effector and the torque/force actuated joint vector computed with $\mathbf{X} = \mathbf{X}_{In}$
- $\mathbf{\Gamma}^{d}$ the desired force/torque vector applied by the end effector
- $\mathbf{I}$ the identity matrix

This equation can be used to determine the workspace where we can assume that $\mathbf{J}$ is constant and does not induced critical error. It can also help to determine optimized size of the test part, initial position or stress direction.

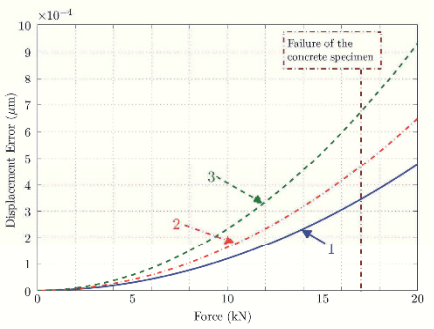

Figure 3: Displacement error made in function of the force applied on the Nooru-Mohamed specimen about:
- axis X if tractive direction is *X-Z* (curve 1)
- axis Y if tractive direction is *Y-Z* (curve 2)
- axis Z (curve 3)

For example, fig. 3 shows the displacement error made in function of the force applied on the specimen. Curve 1 represents the displacement error on axis $\mathbf{X}$ when the specimen is loaded in direction $\mathbf{X}$-$\mathbf{Z}$ (like in fig. 1). Curve 2 represents the displacement error on axis $\mathbf{Y}$ when the specimen is loaded in direction $\mathbf{Y}$-$\mathbf{Z}$. Finally, curve 3 represents the displacement error on axis $\mathbf{Z}$ for the two kinds of precedent loads. Based on fig. 3, it can be deduced that the error made on axis $\mathbf{Z}$ is negligible (less than 0.002% of the total displacement at the failure, at about 17000 N) and that axis $\mathbf{X}$ is preferable for a Nooru-Mohamed test. The error made in force is less than 0.001% of the force applied at failure.

As a consequence, we can assume that using a constant jacobian matrix for NM test of a concrete specimen is relevant.

3- Control Scheme

Based on the constant Jacobian and the static model of the hexapod, control scheme (fig. 4) is then developed.

3.1 – Hybrid Force/Position Control Scheme

Hybrid Force/Position control consists in controlling simultaneously some axis on position, and some axis on force, depending on the task to realize. The selection is made by a matrix $\mathbf{S}$ which indicate how the axis is controlled [KD1]:

$$\mathbf{S} = \mathrm{Diag}(s_1, s_2, s_3, s_4, s_5, s_6) \quad (6)$$

with

- $s_i = 1$ if axis i is position controlled
- $s_i = 0$ if axis i is force controlled

As sensors used allow a direct measurement of the pose and the specimen load, feedback is directly applied without any estimation. Controls from position and force loop are then mixed together to form a global control vector $\mathbf{G}$. Fig. 4 presents the control scheme with:

- $\mathbf{X}^{d}$ and $\mathbf{\Gamma}^{d}$ the desired position and force/torque
- $e_{\mathbf{X}} = \mathbf{X}^{d} - \mathbf{X}$ and $e_{\mathbf{\Gamma}} = \mathbf{\Gamma}^{d} - \mathbf{\Gamma}$ the position and force error
- PCL the Position Control Law (output: $\mathbf{\Gamma}_{\mathrm{PCL}}$) and FCL the Force Control Law (output: $\mathbf{\Gamma}_{\mathrm{FCL}}$)

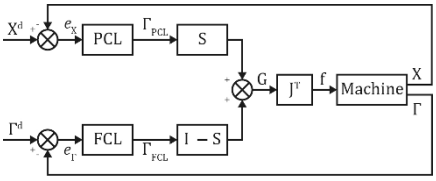

Figure 4: Hybrid Force/Position control scheme

In order to develop the two control laws, a mechanical model of the test part is used. This model is obtained by considering the Young's modulus and Poisson's ratio of the material [BP1]. Thus, the mathematical model of the specimen behaviour during NM test is:

$$\mathbf{\Gamma}_{Mod} = \mathbf{R}\mathbf{X} + \mathbf{C}\dot{\mathbf{X}} \quad (7)$$

with $\mathbf{R}$ the stiffness vector and $\mathbf{C}$ the damping vector.

3.1.1 – Position control Law (PCL)

The position error $e_{\mathbf{X}}$ gives the first control law ($\mathbf{\Gamma}_{\text{PCL}}$) by:

$$\dot{e}_{\mathbf{X}} = \dot{\mathbf{X}}^{\text{d}} - \dot{\mathbf{X}} = -\mathbf{K}_P e_{\mathbf{X}} - \mathbf{K}_{Ip} \int e_{\mathbf{X}} \tag{8}$$

Thereby, $\mathbf{K}_P$, the proportional gain vector, and $\mathbf{K}_{Ip}$, the integral gain vector, allows to impose the error speed decrease to 0 with

$$\mathbf{K}_P = 2\xi\omega_0 \tag{9}$$

$$\mathbf{K}_{Ip} = {\omega_0}^2 \tag{10}$$

The damping ξ is used to regulate the transitional regime and avoid oscillation. It should be greater than or equal to 1, in order to obtain a soft behaviour during shocks. ω_0 is tuned considering the desired five percent settling time $tr_{5\%i}$, but should be small enough not to cause shock. From (7) and (8):

$$\dot{\mathbf{X}}^{\text{d}} - \mathbf{C}^{-1}(\mathbf{\Gamma}_{Mod} - \mathbf{R}\mathbf{X}) = -\mathbf{K}_P e_{\mathbf{X}} - \mathbf{K}_{Ip} \int e_{\mathbf{X}} \tag{11}$$

In the case of position control, we assume that $\mathbf{\Gamma}$ is the control vector, thus $\mathbf{\Gamma}_{Mod} = \mathbf{\Gamma}_{\text{PCL}}$. Finally, $\mathbf{\Gamma}_{\text{PCL}}$ can be computed from:

$$\mathbf{\Gamma}_{\text{PCL}} = \mathbf{K}_P \mathbf{C} e_{\mathbf{X}} + \mathbf{R}\mathbf{X} + \mathbf{C}\dot{\mathbf{X}}^{\text{d}} + \mathbf{K}_{Ip}\mathbf{C} \int e_{\mathbf{X}} \tag{12}$$

3.1.2 – Force control Law (FCL)

The force error $e_{\mathbf{\Gamma}}$ gives the first control law ($\mathbf{\Gamma}_{\text{FCL}}$) by:

$$e_{\mathbf{\Gamma}} = \mathbf{\Gamma}^{\text{d}} - \mathbf{\Gamma} = -\mathbf{K}_{If} \int e_{\mathbf{\Gamma}} \tag{13}$$

Thereby $\mathbf{K}_{If}$, the integral gain vector, allows to impose the error speed decrease to 0 with

$$\frac{3}{\mathbf{K}_{If}} = tr_{5\%i} \tag{14}$$

Each $\mathbf{K}_{Ii}$ is thus tunable for each axis i, with $tr_{5\%i}$ the five percent settling time. From (13):

$$\mathbf{\Gamma} = \mathbf{\Gamma}^{\text{d}} - \mathbf{K}_{If} \int e_{\mathbf{\Gamma}} \tag{15}$$

In the case of force control, we assume that $\mathbf{\Gamma}$ is the control vector, thus $\mathbf{\Gamma}_{Mod} = \mathbf{\Gamma}_{\text{FCL}}$. Finally, $\mathbf{\Gamma}_{\text{FCL}}$ can be computed from:

$$\mathbf{\Gamma}_{\text{FCL}} = \mathbf{\Gamma}^{\text{d}} + \mathbf{K}_{If} \int e_{\mathbf{\Gamma}} \tag{16}$$

Due to the shape of the matrix $\mathbf{S}$ (see (6)), $\mathbf{\Gamma}_{\text{PCL}}\mathbf{S}$ and $\mathbf{\Gamma}_{\text{FCL}}(\mathbf{I}\text{-}\mathbf{S})$ are orthogonal and are then added to form vector $\mathbf{G} = \mathbf{\Gamma}_{\text{PCL}} + \mathbf{\Gamma}_{\text{FCL}}$: there is no force composition and no axis which are not controlled. Finally,

$$\mathbf{f} = \mathbf{J}^T\mathbf{G} \tag{17}$$

3.2 – Control Law Interpretation

The control scheme is designed from the task specificities and testing material characteristics. Then, we note that $\mathbf{\Gamma}_{\text{PCL}}$ consists in a proportional and integral term to the error coherent with the viscosity of the material, a stiffness compensation term and a viscosity anticipation term. $\mathbf{\Gamma}_{\text{FCL}}$ is characterized by a force anticipation term and an integral term. Position slope are regulated by a second order while fixed load are regulated by a first order. This strategy is thus consistent with the material behaviour and with the desired trajectory as long as the specimen is not broken. When the worpiece fails (detected both by the cameras and the passive hexapod), the test is over and the actuators are immediately stopped [NP1]. Note that the parallel robot gravity is directly compensated in the Bosch controller. Control scheme inevitably suffered from perturbations. In order to clarify their origins, error behavior is presented in next section.

3.3 – Error Analysis

Generally, real behavior of the specimen is [PA1]:

$$\mathbf{\Gamma}_{Mod} = \left(\hat{\mathbf{R}} + \tilde{\mathbf{R}}\right)\mathbf{X} + \left(\hat{\mathbf{C}} + \tilde{\mathbf{C}}\right)\dot{\mathbf{X}} \tag{18}$$

where $\hat{\cdot}$ is the estimation and $\tilde{\cdot}$ the error estimation. For control, only estimation is used, thus equation (12) becomes

$$\mathbf{\Gamma}_{\text{PCL}} = \mathbf{K}_P \hat{\mathbf{C}} e_{\mathbf{X}} + \hat{\mathbf{R}}\mathbf{X} + \hat{\mathbf{C}}\dot{\mathbf{X}}^{\text{d}} + \mathbf{K}_{Ip}\hat{\mathbf{C}} \int e_{\mathbf{X}} \tag{19}$$

which leads at the following error behavior

$$e_{\dot{\mathbf{X}}} + \mathbf{K}_P e_{\mathbf{X}} + \mathbf{K}_{Ip} \int e_{\mathbf{X}} = \hat{\mathbf{C}}^{+}\left(\tilde{\mathbf{R}}\mathbf{X} + \tilde{\mathbf{C}}\dot{\mathbf{X}}\right) \tag{20}$$

Therefore, perturbations mainly result from modeling errors. Identification step is thus necessary.
Results from simulation environment are then presented in the next section.

4- Results

4.1 – Environment

A NM test is simulated using the multi-body dynamic software Adams™ to model the structure and specimen behaviour. In addition, Simulink® is used to realize the control law. The global scheme is presented on fig. 5. Two schemes are considerate. The first controller consists in regulated each axis with a Proportional-Integral (PI) regulation and corresponds to the one used in the first realized NM test [NP1]. The second control law is based on the hybrid force/position (HFP) controller proposed in the paper.

The simulated sensors are sampled and noised so as to match the true resolution and frame rate. In order to take into account the model uncertainties, an error of 10% is applied to the matrix $\mathbf{R}$ and $\mathbf{C}$. Then, to take into account the displacement induced by the release of the breaks at the beginning of the experiment, an offset of 1 µm is applied to the position trajectory. In order to take into account the uncertainties concerning the specimen behaviour and causing partial sudden breaks (due to the heterogeneity of

the material, as grit in the concrete or knot in the wood), a step effort is applied to the hexapod at t=2sec (F_X=300N, F_Y =200N and F_Z =400N). Finally, in order to take into account the load induced by the drying of the glue and to show that HFP is capable of controlling the boundary conditions, an interfering preload is applied to the specimen on axis **Y**.

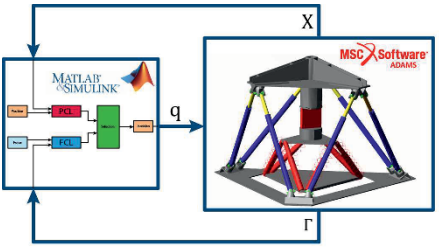

Figure 5: Simulation environment

4.2 – Nooru-Mohamed Simulation

A **X-Z** slope trajectory is imposed with a 15 µm/min velocity. Fig. 6 shows that both controllers allow to correctly follow the trajectory with almost identical error behaviour. $tr_{5\%i}$ is tuned in order to obtain a behaviour consistent with the quasi-static hypothesis, and soft enough to avoid shocks.

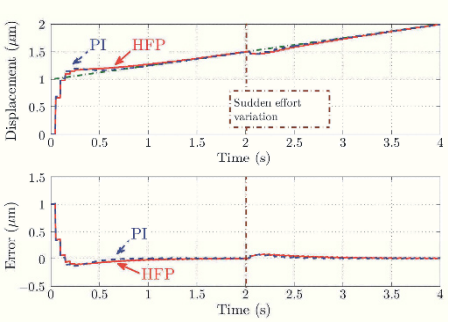

Figure 6: Trajectory on axis X (Top) and error ex (Bottom) for position loop. (Graphs for Z direction are about the same)

Fig. 7 shows the added value of the hybrid force/position controller. PI strategy is not able to compensate the **Y** direction preload, and generate a high uncontrolled load in axis **Y**. The hybrid strategy uses extra DOF to regulate the load on the unsolicited axis. A rigid body motion is generated, but this is not prejudicial as boundary conditions are perfectly controlled. Finally, the concrete specimen is solicited on **X** and **Z** directions, as desired. At failure (about 200 sec. of simulations), after the transitional regime, a maximal error of 0.34 µm is detected, and all preload effects and unpredictable effort variations are dissipated.

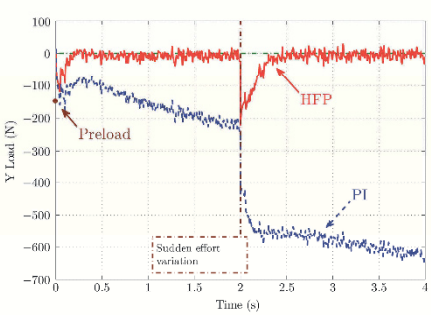

Figure 7: Force on the unsolicited axis *Y*

5- Conclusions

This paper presents the design of a hybrid force/position controller adapted to a novel loading machine (hexapod) and to the task specificities (Nooru-Mohammed test). Simulations show that this strategy is more relevant than the previous controller (PI axis by axis), indeed, unwanted load are avoid and boundary conditions (which are crucial for the success of the test) are controlled.

Contribution of this paper is to proposed, in a context of mechanical test, a complete strategy which allows to perfectly control the test course. The hexapod is a new loading machine and thus, control strategy needs to be optimized. Introducing mechanical notions in the control process allows to have a behaviour directly linked to the structure and the specimen. Second point is that assumptions in relation with the task specificities are made to make technically feasible the realization of this advanced controller.

The strategy developed is adaptable and it is easily possible to achieve other kind of loading tests. However, it is necessary to check the viability of the assumptions made, particularly with highly deformable specimen as elastomer. Our future work will focus on using more advanced model for materials and, if needed, improvement of the control strategy through external control for example. Initial experimentations considering one axe are in progress and we will then realize a second practical test on the hexapod in order to compare with the first PI control strategy.

6- Acknowledgment

This work has been sponsored by the French government research through a ministerial doctoral grant. Authors thank Laboratoire de Mécanique et Technologie (LMT) Cachan for their technical contribution.

7- References

[BP1] C. Bacon, J. Pouyet. Mécanique des solides déformables, HERMES, Paris, 2000.

[CD1] H. Chanal, E. Duc, P. Ray. A study of the impact of machine tool structure on machining processes, International Journal of Robotics Research, vol. 46, pp. 98-106, 2006.

[DB1] J. De Schutter, H. Bruyninckx, W.-H. Zhu, M.W. Spong Force control : a bird's eye view, IEE CSS/RAS International Workshop on Control Problems in Robotics and Automation : Future Directions, San Diego, CA, 1997.

[GK1] J. Goertzen, N. Kawchuk. A Novel Application of Velocity-Based Force Control for Use in Robotic Biomechanical Testing, Journal of Biomechanics, vol. 42, pp. 366-369, 2009.

[H1] N. Hogan. Impedance control : an approach to manipulation, Trans. of ASME, Journal of Dynamic Systems, Measurement, and Control, vol. 107, pp. 1-24, 1985.

[KD1] W. Khalil, E. Dombre. Modeling, Identification & Control of Robots, HERMES Penton Science, 2002.

[LA1] A. Lopes, F. Almeida. A force-impedance controlled industrial robot using an active robotic auxiliary device, Robotics and Computer-Integrated Manufacturing, vol. 24, pp. 299-309, 2008.

[LP1] H. Leclerc, J.-N. Périé, S. Roux, F. Hild. Integrated Digital Image Correlation for the Identification of Mechanical Properties, Lecture Notes in Computer Science, vol. 5496, pp. 161-171, 2009.

[M1] J. P Merlet. Les robots parallèles, 2nd Edition, HERMES, Paris, 1997.

[M2] J.P. Merlet. Still a long way to go on the road for parallel mechanisms, ASME 27th Biennial Mechanisms and Robotics Conf., vol. 29, 2002.

[MH1] J.G. Michopoulos, J.C. Hermanson, T. Furukawa. Towards the robotic characterization of the constitutive response of composite materials, Composite Structure, vol. 86, pp. 154-164, 2008.

[MM1] M. Madani, M. Moallem. Hybrid position/force control of a flexible parallel manipulator, Journal of the Franklin Institute, vol. 348, pp. 999-1012, 2011.

[N1] M.B. Nooru-Mohamed. Mixed mode fracture of concrete : An experimental approach, Doctoral thesis, Delft University, 1992.

[NP1] M. Nierenberger, M. Poncelet, S. Pattofatto, A. Hamouche, B. Raka, J.M. Virely. Multiaxial Testing of Materials Using a Stewart Platform : Case Study of the Nooru-Mohamed Test, Exp. Tech, in press, 2012.

[PA1] F. Paccot and N. Andreff and P. Martinet. A review on dynamic control of parallel kinematic machine : theory and experiments, International Journal of Robotics Research, vol. 28, no. 3, pp. 395-416, 2009.

[PC1] J.H. Park, H.C. Cho. Impedance Control with Varying Stiffness for Parallel-Link Manipulators, Proceedings of the American Control Conference, 1998.

[RC1] M.H. Raibert, J.J. Craig. Hybrid positon/force control of manipulators, Trans. of ASME, Journal of Dynamic Systems, Measurement, and Control, vol. 103, pp. 126-133, 1981.

[SF1] S.M. Satya, P.M. Ferreira, M.W. Spong. Hybrid Control of a Planar 3 DOF Parallel Manipulator for Machining Operations, Transactions of the NAMRI/SME 23, pp. 273-280, 1995.

[SB1] J. De Schutter, H. Bruyninckx, W.-H. Zhu, M.W. Spong. Force control : a bird's eye view, IEE CSS/RAS International Workshop on Control Problems in Robotics and Automation : Future Directions, San Diego, CA, 1997.

[SG1] I.A. Stokes, M. Gardner-Morse, D. Churchill, J.P. Laible. Measurement of a spinal motion segment stiffness matrix, Journal of Biomechanics, vol. 35, pp. 517-521, 2002.

[SS1] L. Sciavicco, B. Siciliano. Modelling and control of robot manipulators, 2nd Edition, SPRINGER, London, 2001.

[VN1] J.M. Virely, M. Nierenberger. (ENS Cachan, CNRS) Dispositif de mesure de torseur d'efforts, de structure du type multipode, French Pat. Appl. 2013. Priority number : FR13 50658 - Patent pending.

[ZP1] X. Zhao, Y. Pan. Draft : Force-Position Hybrid Control of a New Parallel Hexapod Robot for Drilling Holes on Fuselage Surface, Proceedings of the ASME 2013 International Design Engineering Technical Conferences & Computers and informations in Engineering Conference, 2013.

Article 056-r-56

Identification of material and joint properties based on the 3D mapping of the Quattro static stiffness

Adel Mekaouche [1], Frédéric Chapelle [1], Xavier Balandraud [1]

(1) : Institut Pascal UMR CNRS/UBP/IFMA 6602
Campus des Cézeaux, 24 Avenue des Landais, BP 80026, 63171 Aubière Cedex, France
Phone/Fax : +33 4 7328 8006/8027
E-mail : {amekaouche,chapelle,balandraud}@ifma.fr

Abstract: In this paper, we present an identification procedure of mechanical parameters of a parallel robotic structure, the Adept Quattro robot. Two parameters are identified: the torsional stiffness of the actuated revolute joints, and the Young's modulus of the composite material used for the arms of the robot. The experimental static stiffness map is obtained using static loads and a tracker laser. A wire-frame finite element model is used to simulate static stiffness maps. The identification is based on the comparison between the numerical and the experimental 3D maps. The Quattro robot is mainly studied in the literature for its dynamic performances. The present analysis of its static stiffness is however interesting for the determination of its polyvalence in operational tasks.

Key words: Identification, Robotic structure, Static stiffness, Mapping, Adept Quattro.

1- Introduction

For robotic structures, static stiffness maps can be used to assess the level of positioning error for a given production task, i.e. for a given type of loading condition [CD1] [XZ1] [BC1]. They can be used also to compare different architectures or use configurations between them [XZ1] [BC1] [DH1]. Different type of modeling can be found in the literature (see Table 1):

- Using the Virtual Joint Method (VJM), Gosselin [G1] provided and analyzed stiffness maps by taking into account the joints compliances, with the aim to set a tool for computer-aided kinematic design of a planar 3 degrees of freedom (DOF) parallel manipulator and a spatial 6-DOF parallel manipulator. Majou *et al.* [MG1], considering the compliance of the joints (modeled by virtual springs) and using a parametric analysis, studied the stiffness map of the Orthoglide parallel manipulator, and determined the stiffest zone for a specific task. The number of virtual springs was increased, in the sense that the stiffness of a joint was modeled in several spatial directions. Klimchik *et al.* [KP1] used three axial springs and three torsional springs.

- Using the Matrix Structural Analysis (MSA), Chanal *et al.* [CD1] studied the Tricept manipulator. By considering small displacements and taking into account the compliance of the arms, the authors identified the zone in the workspace where the stiffness is optimal for a machining task. Abele *et al.* [AW1] studied a 5-DOF serial industrial robot. They considered only the compliance of joint gears and analyzed the system stiffness and its behavior during the milling process. Ruggiu [R1] mapped the stiffness of a translational parallel mechanism using a general formulation based on the development of the principle of virtual work. Pinto *et al.* [PC1] used MSA, FEM and experimental measurement for mapping the stiffness of a low mobility DEADALUS I parallel manipulator, and compared the three approaches. Briot and Khalil [BK1] have built the elasto-dynamic model of a planar parallel manipulator with distributed compliances, taking into account both link and joint compliance, and have then compared the results with those obtained with commercial softwares RDM6 and ADAMS/Flex.

- Using the Finite Element Method (FEM), Bouzgarrou *et al.* [BF1] reproduced the real geometrical shape and material data of a T3R1 uncoupled kinematic robot, and identified static and dynamic stiffness maps with a FEM-based model. Rizk *et al.* [RF1], using the same method, studied and compared the stiffness maps of a reconfigurable parallel machines with 3 (ISOGLIDE3-T3) and 4 (ISOGLIDE4-T3R1) degrees of freedom. Shabana [S1], Bauchau [B1], and Rognant [RC1] have developed an elasto-dynamic FEM model for structures including open and closed chains.

Reference	Method	Compliance	
		Joints	Links
Gosselin 90 [G1]	VJM	Yes	No
Majou 07 [MG1]	VJM	Yes	No
Chanal 06 [CD1]	MSA	No	Yes
Abele 07 [AW1]	MSA	Yes	No
Ruggiu 12 [R1]	MSA	Yes	No
Pinto 09 [PC1]	MSA	Yes	Yes
Bouzgarrou 04 [BF1]	FEM	Yes	Yes
Rizk 06 [RF1]	FEM	Yes	Yes

Table 1: static stiffness maps presented in the literature.

In a complementary work [MC1], we have developed a software based on the FEM method for the generation of 3D static stiffness maps with a good compromise between available functionalities and CPU time. This software is intended more specifically for the design and optimization of robotic structures with particular distributions of the stiffness. The parameters taken into account in the modeling are of geometry and material natures. This model proved to be also useful for the issue of identification of parameters based on stiffness maps.
Several identifications of stiffness models are available in the literature. Alici and Shirinzadeh [AS1] used an enhanced stiffness formulation based on the conservative congruence transformation (CCT) given by Chen and Kao [CK1]. This latter reported the limits of the conventional stiffness formulation derived by Mason and Salisbury [MS1]. Alici and Shirinzadeh estimated the joints stiffness of the hybrid Motoman SK120 robot for three configurations. A laser-based dynamic measurement system was calibrated to measure the manipulator end. Abele *et al.* [AW1] identified the compliance of the gears in the joints of a 5-DOF serial robot. One axis was loaded whereas the others were clamped, in order to decouple the five axes. As a result, five experiments were necessary to evaluate the stiffnesses along the five axes. Dumas *et al.* [DC1] used a method based on the CCT. This method was used to evaluate the joint stiffness of the 6-DOF Kuka KR240-2 serial robot.

The purpose of this paper is to present an identification of some parameters of the fully parallel Adept Quattro robot from stiffness maps obtained with the help of a commercial FEM software. This manipulator is characterized by a parallel architecture with four DOFs for the effector: three translations and one rotation. Corbel *et al.* [CC1] presented a geometrical calibration of the Par4, from which the Quattro is derived. The method was based on the measurement of distances, and the evaluation of the quadratic error between the nominal and real distances. However, the values of the joint stiffness were not assessed, which is an issue of this paper. The objective of the study is to advance in:
- the possibility to identify parameters which differ in nature from stiffness maps,
- the knowledge of the Quattro stiffness for quasi-static tasks.

The paper is organized as follows: first the model used for plotting the 3D static stiffness map of the Quattro robot is presented; then, the experimental setup for measuring stiffness is described; the experimental results are presented; finally, the identification of a structural parameter (torsional stiffness of actuated revolute joints) and a material parameter (Young's modulus of the arms made of composite materials) is presented.

2- Construction of stiffness maps by simulation

This section presents the numerical method employed for the generation of stiffness maps of the Adept Quattro robot. The Quattro robot is devoted to pick-and-place tasks. It is composed of a fixed platform and four kinematic chains which enable the movement of an articulated mobile platform. The effector is attached to the mobile platform. Its architecture is parallel with four DOF for the effector: three translations and one rotation (around vertical **z** axis in the present modelling). In the present study, the rotation of the effector is not used. However, the deformation of the structure leads to small translations and also rotations of the end effector. The present identification procedure is based on the value of the vertical stiffness K_{zz}, which is defined as the ratio of the vertical force F_z over the vertical displacement U_z of the end effector.

The calculation of the displacement is based on a finite element model. Figure 1 presents the joint and loop graph (Fig. 1-a) and the wire-frame model (Fig. 1-b) of the Quattro robot. Beam elements and spring elements are used for the arms and the joints, respectively. Geometric parameters are the dimensions of the arms (lengths and cross sections). Materials are supposed to be linear elastic for the levels of applied loading. Three different materials are considered: aluminum alloy for the mobile platform, carbon-epoxy composite for the arms, and steel for other components. The composite has a symmetrical stratified twill 2×2 structure, leading to a quasi-isotropic elasticity. The material parameters are the Young's moduli and the Poisson's ratios. Each kinematic chain is similar in terms of architecture. Each one is composed of two parallel rods, with passive spherical joints at their ends (noted S in Fig. 1-a). Each chain is connected to the fixed platform by an actuated revolute joint (noted R). It is connected to the mobile platform with passive revolute joints (noted R).

Ansys finite element package is used. Employing a commercial FE package is interesting as it is easily available for users and general in terms of functionality (possibility to consider large displacements, plasticity...). Element BEAM188 is employed for the arms. Axial and torsional spring elements are used for the joints (COMBIN14). A connection between two components is represented by two coincident nodes, each of them belonging to a component. A spring element couples a DOF of two nodes according to a given stiffness. For the actuated revolute joints (R), a torsional spring is employed for coupling the rotations of the nodes along the joint axis. In the case of the passive joints (S and R), the DOFs along the joint axes are not constrained. For instance for the passive spherical joint R, the three rotational DOFs are not constrained. For the other DOFs in the joints, we have here used large stiffness values compared to the others.

A unitary force F_z is applied to the end effector along the vertical direction. Calculations are performed in static configuration, as dynamic stiffness is not discussed in the present paper. Static stiffness maps are expected to provide a first-order indicator of the rigidity of the robot in service. Moreover, it can be assumed that the static stiffness is related to the definition of a manufacturing task (independently of the velocity), to be distinguished with the dynamic stiffness which would be related to the achievement of the task. The displacements resulting from elastic strains are assumed to be small. In other words, no change in the application point of the external loading as a function of the structure deformation is considered for solving the equations.

The operational space is browsed using the inverse geometrical model of the Quattro robot. The articular coordinates of the end effector are determined as a function of the Cartesian coordinates. The stiffness K_{zz} is then calculated for each location of the end effector in the operational space according to a given discretization. Two programs are coupled: Matlab and Ansys. The former is used to browse the operational space, to build the finite element code lines for each location in the discretized space, and to finally calculate and plot the stiffness maps.

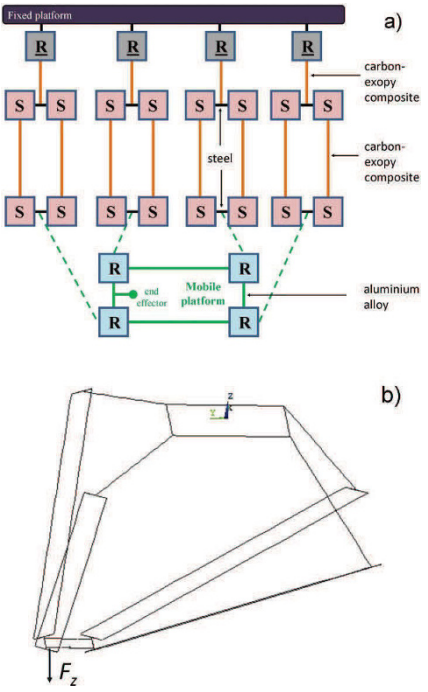

Figure 1: a) joint and loop graph. b) wire-frame model.

3- Experimental measurement of stiffness map

Figure 2 presents the experimental setup used to map the stiffness map of the Quattro robot. The objective is to measure the vertical displacement U_z of the end effector due to a vertical load F_z applied to the end effector. Two force levels were used in order to verify the linearity of the mechanical response: -35 N and -70 N. Vertical displacements U_z were measured using a laser tracker ATD-901 (Leica). Laser tracker is an instrument used to accurately measure positions of optical targets. This fast tree-dimensional coordinate measuring sends a laser beam to the measured point, which is materialized by a spherical mounted reflector (SMA). The resolution of the displacement measurement, i.e. the standard-deviation σ of the noise, was calculated equal to 0.017 µm by performing several times the same measurement, meaning that the error amplitude ±3σ is estimated to ±0.050 µm. We focus on two horizontal cross sections of the 3D stiffness map (see Figure 3). They are located at z = -0.727 m (plane A) and z = -0.950 m (plane B), which corresponded respectively to the maximum and minimum altitudes available to map a whole plane. Measurements were done over to a regular grid along x- and y-directions with a pitch of 50 mm.

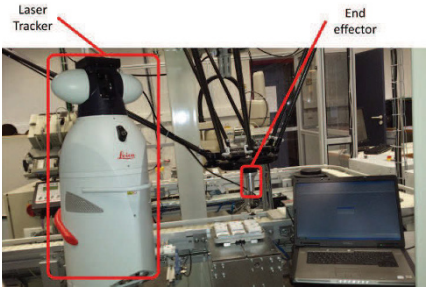

Figure 2: experimental set-up.

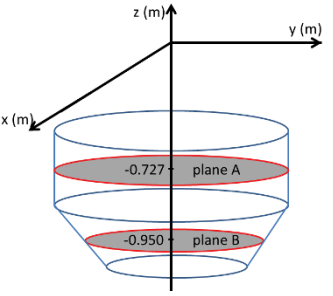

Figure 3: planes A and B in the Quattro workspace.

For symmetrical reasons, the measurements were performed in a quarter of the workspace. To illustrate the obtained results, Figure 4 shows the experimental stiffness map in plane A. Logically, the highest value of stiffness is located along the symmetry axis of the workspace.

4- Structural and material parameter identification

In the model presented in Section 2, two parameters need to be identified: the torsional stiffness (K_{joint}) of the four actuated revolute joints, and the Young's modulus (E_{comp}) of the upper and lower arms, which are made of the same composite material. This choice was done because no information about these structural and material data is available. Contrary to the Young's modulus of the composite, the moduli for steels and aluminum alloys are well known

and do not strongly depend on chemical composition, heat treatment, mechanical hardening, etc. The stiffnesses of the joints are not known a priori. The choice of identifying only the torsional stiffness along the axis of the actuated revolute joints was done because this quantity strongly influences the global stiffness measured at the end effector. Indeed, the rotation of the upper arms (as well as their bending) strongly influences the position of the end effector under load. Note that the objective was not to perform a complete identification of the actuated joint stiffness. Indeed, it is well known that the global stiffness of actuated joints depends on many parameters, in particular the command.

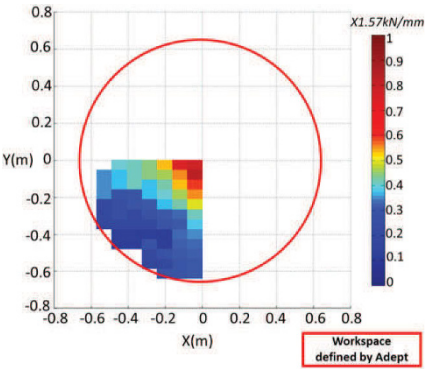

Figure 4: experimental stiffness map K_{zz} in plane A.

As indicated above, upper and lower arms are made of carbon-epoxy, with symmetrical stratified twill 2×2 structure. The Young modulus value of this composite can be limited in an interval using the fraction of the percentage of fiber and matrix of the composite material. In the case of the present composite, the percentages of fiber extend from 35% to 70%, and the percentage of matrix from 30% to 65%. Using a rule of mixture (Voigt bounds), the variation range of the longitudinal Young's modulus can be determined:

$$E_{comp} = \nu_f \cdot E_f + \nu_m \cdot E_m \qquad (1)$$

with:

E_{comp} is Young's modulus of the composite,
E_f is Young's modulus of the carbon fibers,
E_m is Young's modulus of the matrix,
ν_f is the volume fraction of carbon fibers,
ν_m is the volume fraction of matrix.

Using the percentages indicated above and the values of Young's moduli for the fibers and the matrix (E_f = 250 GPa and E_m = 5 GPa), the interval for E_{comp} can be calculated: $E_{comp}(min)$ = 90 GPa and $E_{comp}(max)$ = 176 GPa. This limits the range of identification of the arms Young's modulus to the interval [90; 176] GPa. It can be noted that no interval can be a priori assessed for the torsional stiffness (K_{joint}) of the actuated revolute joints. The bounds of this interval was defined after some preliminary tests (not reported here): [1; 70] kN.m/rad. The plane (E_{comp}, K_{joint}) is browsed in these intervals using thirty values for each quantity.

Figure 5 presents the identification procedure. To identify the two parameters, the absolute error (ΔK) of the stiffness in some points of the workspace is evaluated. It corresponds to the difference between the experimental stiffness ($K_{zz\ exp}$) and the numerical one ($K_{zz\ num}$):

$$\Delta K = abs\ (K_{zz\ num} - K_{zz\ exp}) \qquad (2)$$

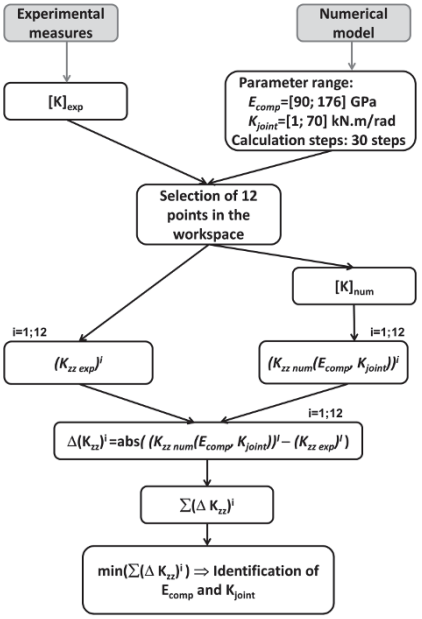

Figure 5: identification procedure.

Two simplifying hypotheses were considered. First, as for the modeling, identification was performed in static configuration. Note however that the servo regulation was active in order to be closer to in-service configurations. Second, it was assumed that the four actuated revolute joints have the same stiffness.

Two evaluations have been done. For the first one, 12 locations have been randomly chosen inside the workspace. For the second one, 12 points have been chosen along a radial direction in plane A. The aim of these two evaluations is to analyze the influence of the distribution and the location of the points used for the identification. Figure 6 presents the sum of absolute error for the first evaluation (12 locations randomly chosen), whereas Figure 7 shows the same plot for the second evaluation (12 locations chosen in a radial direction in plane A).

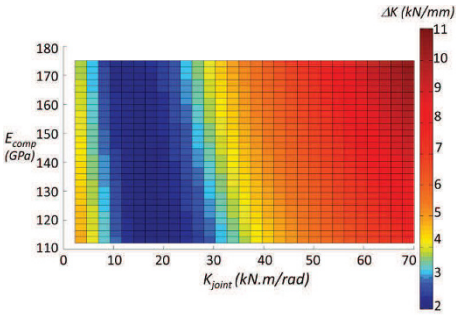

Figure 6: sum of absolute errors using 12 points randomly chosen in the workspace.

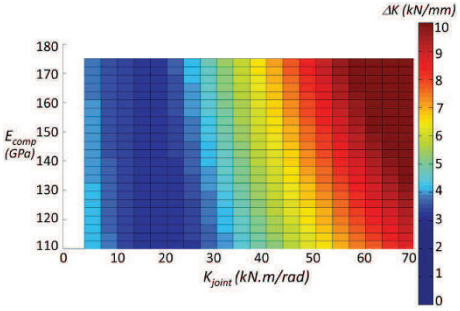

Figure 7: sum of absolute errors using 12 points along a radial direction.

Figures 6 and 7 show that the minimum error corresponds to a curve in the plane (E_{comp}, K_{joint}): a "valley" is visible in both figures. By comparing these figures, it can be noted that the distribution and the location of the 12 points selected for the identification do not affect the result. The valley enables us to define a convergence zone of K_{joint}, reducing the initial variation range for this parameter. There is no similar restriction for E_{comp}. However, the inclination of the valley reveals an influence of E_{comp} on the choice of K_{joint}, which *a priori* implies a second-order impact of E_{comp} on the global stiffness of the structure. As a consequence, we have identified the two quantities to be used in the model at the middle of the valley: E_{comp} = 140 GPa and K_{joint} = 16 kN.m/rad.

To validate this experimental identification, Figures 8 and 9 enable us to compare the experimental stiffness map and the simulated one using the identified parameters, for plane A and plane B. These figures present the maps of the normalized value of K_{zz}, which corresponds to the value divided by the maximum value:

$$K_{zz\,norm} = \frac{K_{zz}}{\max(K_{zz})} \quad (3)$$

From these figures, it can be noted that the numerical stiffness map is in correct agreement with the experimental one. Some differences are however observed. For instance, the blue zone cover a larger area in the simulation. However, it can be seen that the stiffness gradients over the planes are quite correctly assessed, although the number of points in the experiment is smaller than in the simulation. As a general comment, the numerical stiffness is overestimated compared with the experimental one. This can be explained by the choice done to model the other joint stiffnesses (unilateral spherical joints, other stiffnesses in the actuated revolute joints...).

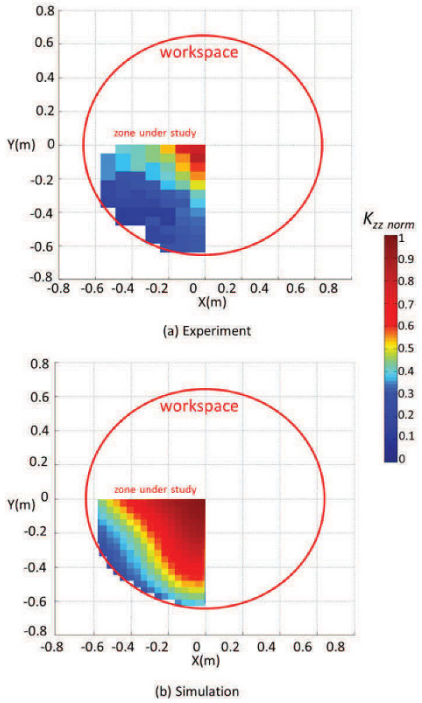

Figure 8: stiffness map in the plane A. (a) experiment, (b) simulation.

5- Conclusion

A method of identification of structural and material parameters of the Quattro robot has been detailed in this study. It is based on the assessment of the experimental static stiffness. Measurements were carried out using a laser tracker to plot the experimental stiffness map. The Young's modulus of the arms and the torsional stiffness of actuated revolute joints were then identified using a model based on FEM approach. This study enables us to update the numerical model for more accuracy in further complex design tasks. It can also be used to evaluate the static performances of this high speed parallel manipulator (which is basically devoted to high dynamic performances) and provide comparisons with other manipulators in static

conditions.

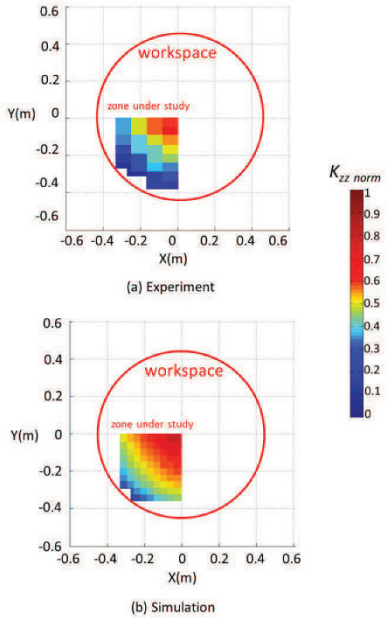

Figure 9: stiffness map in the plane B. (a) experiment, (b) simulation.

6- References

[AS1] Alici G. and Shirinzadeh B. Enhanced stiffness modeling, identification and characterization for robot manipulators. In IEEE Transactions on Robotics 21 (4): 554-564, 2005.

[AW1] Abele E., Weigold M. and Rothenbücher S. Modeling and Identification of an Industrial Robot for Machining Applications. In Annals of the CIRP, STC M, 56: 387-390, 2007.

[B1] Bauchau O.A. Flexible Multibody Dynamics, Springer, 2011.

[BC1] Bonnemains T., Chanal H., Bouzgarrou B.C. and Ray P. Stiffness computation and identification of parallel kinematic machine tools. In Journal of Manufacturing Science and Engineering, 131(4): 1-7, 2009.

[BF1] Bouzgarrou B.C., Fauroux J.C., Gogu G. and Heerah Y. Rigidity analysis of T3R1 parallel robot with uncoupled kinematics. In Proceedings of the 35th International Symposium on Robotics, Paris, France, 2004.

[BK1] Briot S. and Khalil W. Recursive Symbolic Calculation of the Dynamic Model of Flexible Parallel Robots. In IEEE international Conference of Robotics and Automation (ICRA'2013). Karlsruhe, Germany, 2013.

[CC1] Corbel D., Company O., Nabat V. and Maurine P. Geometrical calibration of the high speed robot Par4 using a Laser Tracker. In Proceeding of the 12th IEEE International Conference on Method and Models in Automation and Robotics (MMAR'06), Miedzyzdroje, Poland, 2006.

[CD1] Chanal, H., Duc E. and Ray P. A study of the impact of machine tool structure on machining processes. In International Journal of Machine Tools & Manufacture, 46(2): 98-106, 2006.

[CK1] Chen S.F. and Kao I. Conservative congruence transformation for joint and Cartesian stiffness matrices of robotic hands and fingers. In International Journal of Robotics Research. 19(9): 835-847, 2000.

[DC1] Dumas C., Caro S., Mehdi Ch., Garnier S. and Furet B. Joint Stiffness Identification of Industrial Serial Robots. In Robotica. 30(4): 649-659, 2012.

[DH1] Deblaise D., Hernot X. and Maurine P. A systematic analytical method for PKM stiffness matrix calculation. In Proceedings of the IEEE International Conference on Robotics and Automation (ICRA), Orlando, FL. (4213–4219), 2006.

[G1] Gosselin C. Stiffness Mapping for Parallel Manipulators. In IEEE Transactions on Robotics and Automation, 6(3): 377-382, 1990.

[KP1] Klimchik A, Pashkevich A., Caro S. and Chablat D. Stiffness matrix of manipulators with passive joints: computational aspects. In IEEE Transaction on Robotics, 28(4): 955-958, 2012.

[MC1] Mekaouche A., Chapelle F. and Balandraud X. Study of a method of stiffness map generation intended to be used in optimal design algorithms for robotic structures. [submitted].

[MG1] Majou F., Gosselin C., Wenger P. and Chablat D. Parametric stiffness analysis of the Orthoglide. In Mechanism and Machine Theory, 42(3): 296-311, 2007.

[MS1] Mason M. T. and Salisbury J. K., Robot Hands and the Mechanics of Manipulation. Cambridge, MA: MIT Press, 1985.

[PC1] Pinto C., Corral J., Altuzarra O. and Hernández A. A methodology for static stiffness mapping in lower mobility parallel manipulators with decoupled motions. In Robotica, 28(5): 719-735, 2010.

[R1] Ruggiu M. Cartesian Stiffness Matrix Mapping of a Translational Parallel Mechanism with Elastic Joints. In International Journal of Advanced Robotic Systems, 9: 1-8, 2012.

[RC1] Rognant M., Courteille E. and Maurine P. A systematic procedure for the elasto-dynamic modeling and identification of robot manipulators. In IEEE Transaction on Robotics, 26(6): 1085–1093, 2010.

[S1] Shabana A.A. Dynamics of Multibody systems, 2nd Ed, Cambridge University Press, 1998.

Article 054-r-36

Design graphs for sizing procedures and optimization problems definition of mechatronic systems

Marc Budinger[1], Aurélien Reysset[1], Jean-Charles Maré[1]

(3) : Université de Toulouse, INSA/UPS, Institut Clément Ader, Toulouse, 31077, France
E-mail : {marc.budinger, aurelien.reysset, jean-charles.mare}@insa-toulouse.fr

Abstract: This paper is dedicated to the generation of sizing procedures used during the preliminary optimal sizing of physical parts of mechatronic systems. The inputs are the objectives and design constraints coming from the specifications document or the chosen architecture. As output, components (rod end, roller or ball screw, gear reducer, brushless motor ...) specifications are generated in order to obtain an assembled actuation system which fully meets upper requirements. Graphs are used to represent the constraints and links between models. This graphical representation, here called "Design Graph", can be used with advantage as a teaching tool with students or as an analysis tool for an engineer in the case of new design scenarios or new technology.

Key words: mechatronics, sizing procedure, graph theory, matching.

1. From models to optimal preliminary design of mechatronics systems

1.1 - Preliminary design of mechatronic systems

A mechatronic system [V1][A1] expands the capabilities of conventional mechanical systems through the integration of different technological areas around a power transmission part and an information processing part. The references [VA1], [H1] highlight the fact that the design of such multi-domain systems requires different modelling layers:

- A mechatronic layer, to take into account the functional and physical coupling between components. This level of modeling is usually done using 0D-1D models [VA1] also called lumped parameter models represented by algebraic equations, ordinary differential equations (ODE) or differential algebraic equations (DAE) [CG1]. During preliminary design, meta-modelling techniques often enable to represent those models by algebraic equations for a quicker optimization [BH1].
- A specific domain layer, to describe the performance limits and parameters necessary in the previous layer, based on a geometric representation. The specific domain phenomena are generally represented through partial differential equations (PDE). This level of modeling can be achieved, for simplified geometries by using analytical models or, for complex 2D and 3D geometries, by using numerical approximations like the finite element method (FEM) for instance. During preliminary design and optimization, this layer can be represented by analytical models, meta-models or scaling laws [BJ1] [BP1].

1.2 - Sizing procedure vs. optimization

Generally the engineering models enable to determine the opposite relationship to what is desired during sizing, i.e. calculate the performance of the system (which is required by the specification) from the characteristics of components (which sizing activities we want to get). All representative models have to be manipulated in order to solve this inverse problem. There are essentially two types of solutions to this problem:

- Selection or sizing procedures, judicious succession of calculations and tests which determine the main characteristics of components to select.
- Optimization algorithms that minimize the difference between the desired and achieved performances by changing the main characteristics of components.

In this paper, we seek to make joint use of these two approaches (procedures, optimization). Part 2 of this chapter will present a state of the art of the different ways for representing a design procedure. Part 3 of this chapter will then show the typical problems encountered in the implementation of a design procedure. We will then focus on their resolution using the proposed design graphs which are simple graphical means. We will illustrate the different approaches and issues with examples.

2. State of the art on Sizing procedure representations

The sizing procedure can be considered as a major part of the whole preliminary sizing process. When the problem is complex with a lot of interactions between components of various fields (mechanical, electrical, etc.), methods enabling representation and analysis of such interactions become valuable. We will focus here on such representation methods.

2.1 - Causal diagram

The causal diagram is a graphical tool representing the causal relationships between variables. It is in fact an oriented graph representing a calculation scheme. Examples of causal diagrams can be found in [S1] or [LH1]. With a causal diagram, the couplings between the different entities can be difficult to visualize. An important problem is that of algebraic loops which is well known in industrial process where Excel spread-sheets gather components sizing procedures which must not present circular reference errors (i.e. loops) as y=f(x) and x=g(y).

2.2 - N2 diagrams

The N2D formalism was introduced in the 70s by the system engineer Robert J. Lano [N1]. N gives the number of entities considered. This diagram is a causal diagram where the graphical entities (blocks) and interactions (arrows) are dictated by an organization convention as shown in Figure 1. The inputs of the blocks are represented by vertical arrows while the outputs must be horizontal arrows. This display provides a quick visual summary of the organization of the system studied. In particular, the couplings and algebraic loops between blocks are easily identifiable: for example, Figure 1, when a block "2" provides an input to block "3" and the block "3" provides an input to block "2".

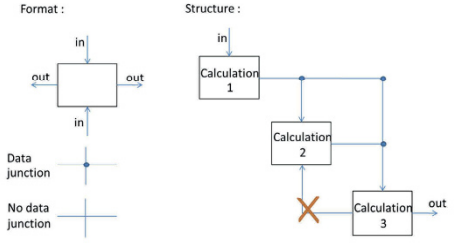

Figure 1 – N² diagram principle

2.3 - DSM matrix

A Design Structure Matrix or Dependency Structure Matrix (DSM) is the adjacency matrix of a N2D. The DSM, as its name shows is a matrix representing links or information exchanges which can be used at various levels: working group, system level, component level [B1]. In this representation, a perfect sequence is represented by a lower triangular matrix, while upper non-empty box represents a feedback loop.

2.4 - Graphs

Finally, a sizing procedure is quite similar to a constraint network [GF1], since sizing parameters represent variables, equalities and inequalities are viewed as constraints. Therefore, all the tools applied to the representation of constraints network and therefore graph theory can be applied. That is why, various algorithm applied to graph theory can be integrated to a global calculation ordering method.
In the following sub-parts, different graphical representations will be used. Some of them represent how equations will match parameters; in this case both equations (square node) and non-determined parameters (circular node) are represented in a non-oriented graph. Let us take the equation (declarative equation, not imperative assignment), Figure 2a, to show this representation. A matching is generally represented in what is called a bi-partite graph, Figure 2b, with on one side all the equations nodes and on the other side all the non-determined parameters nodes. A matching parameter/equation is then represented by a double-column. Once equations are oriented (one parameter is matched to the equation, i.e. is calculated by the equation), Figure 2c, a simplified graph can be drawn with no more equation nodes.

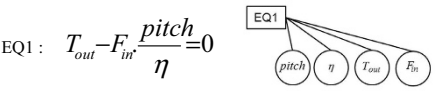

a) No-oriented graph and equation

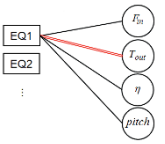

b) Bi-partite graph

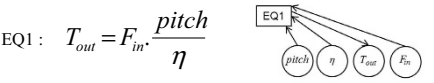

c) Oriented graph and equation

Figure 2 – Graph representations of equation

A set of equations can be represented by a graph or also by a dependency matrix as illustrated by a non-oriented graph (Figure 3a). Once treated, the simple problem presented below will look like (Figure 3b) where the sizing sequence is represented once again by a lower triangular matrix.

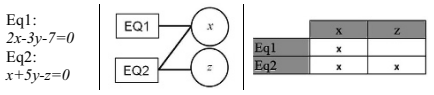

a) representation of a 2x2 problem before matching

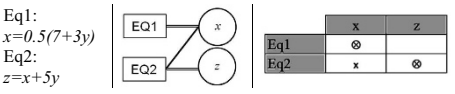

b) representation of a 2x2 problem after matching

Figure 3 – Matching of a 2x2 problem

3. Sizing procedure definition and design graph

3.1 - Objectives

This section will develop on how to represent a set of design calculations and how to order flows of information into a sizing procedure. In order to have a sizing procedure well posed and easy to use in any computing environment, this procedure must be explicit without internal numerical solver. Section 3.2 presents the typical inputs and outputs of such procedure which will be used in an optimization problem. Section 3.3 describes the proposed methodology and process. Section 3.4 illustrates how to set up manually a sizing procedure using graphical tools. Section 4 identifies the main typical possible problems on elementary examples.

3.1.1 - Inputs and outputs of an optimization problem

An optimization problem can be formulated mathematically as follows:
Minimize the objective function: f(x)
Subject to equality/inequality constraints: h(x) = 0, g(x) < 0
Acting on the parameters vector in the range: $x_{low}<x<x_{up}$

Where:

- The goal is the objective function f;
- Design alternatives are expressed by a set of values assigned to the design variables x within a design domain;
- Constraints (h & g) limit the number of alternatives to those satisfying physical principles and design specifications.

The functions (f, g, h) can be explicit or implicit, algebraic or achieved by subroutines that solve systems of differential equations iteratively. The goal here is to define those functions within a sizing procedure. This sizing procedure should be preferably explicit and quick to evaluate.

3.1.2 - Ordering methodology and process

The equation ordering methodology is organized into 3 main steps summed-up in Table 1. This global method helps to reveal additional design parameters and to structure the sizing procedure which can be used by an optimization algorithm.
This process of block lower triangulation may be applied to any type of knowledge represented by models. However, in the case of a mechatronic system, it is possible to distinguish two levels of knowledge:

- A component layer that represents the specific domains knowledge for each component. This knowledge is represented by parameters (definition, integration, simulation, evaluation) and equations (estimation models) linking the parameters of only one component. Each set of equations and parameters is independent component by component and can be thus stored and reused in the form of library.
- A system layer that represents the system-level interactions between components and specifications declined on all sizing scenarios. These models can link characteristics of multiple components from component layer freely.

3.2 - "Design Graph": Sizing procedure synthesis thanks to graphical manipulations

For design problems characterized by a reduced set of equations, a skill designer will be able to order quickly and intuitively design constraints of his area of knowledge. However, it is also possible to graphically represent and order these equations. This graphical representation, here called "Design Graph", can be used with advantage as a teaching tool with students or as an analysis tool for an engineer in the case of new design scenarios or new technology.

Table 1 - Synthesis of the proposed methodology

	Process (« WHATs »)		Methods (« HOWs »)	Tools (implement the «HOWs ») : Design Graphs
1	Problem definition	1.1	Gather all the equations/inequalities describing the problem.	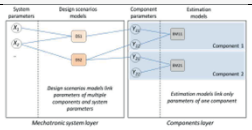
2	Orientate the problem	2.1	Match equations/parameters	
		2.2	Identify and highlight over-constrained and under-constrained singularities	
		2.3	Errors are fixed by the designer manually modifying parameters status (to determined/input) or moving inequalities to constraint while introducing safety factors.	
3	Break problem calculation loops.	3.1	Identify and highlight algebraic loops	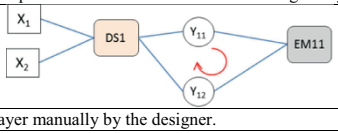
		3.2	Identify and highlight the minimum set of parameters to be fixed to suppress loop.	
		3.3	Loops are displaced to upper layer manually by the designer.	

The problem definition, Task 1 of Table 1, is achieved with a bipartite graph for each design layer, mechatronic system layer and components layer, as represented in Figure 4 where :

- The parameters are set at mechatronic system layer from requirements specifications (performances, constraints) and at components layer by listing the components of the architecture and their main characteristics.
- The equations are then introduced to link the different parameters: at mechatronic system layer level with equations representing design scenarios, at components layer level with estimation models.

At this point the relationships between the parameters and equations are represented as non-oriented edges. It is not necessary to express in detail the equations.

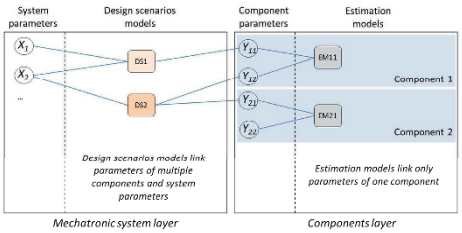

Figure 4 – Component layer and Mechatronic system layer

The orientation of the equations is the next step and corresponds to Task 2 of Table 1. Select as inputs for the sizing procedure the parameters set by the specifications. Some parameters in the specification may take the form of outputs if the wording of the requirement defines them as an objective to minimize or maximize or as a maximum or minimum limit constraint to respect. Figure 5a summarizes the graphical notation that can be chosen to represent these parameters in a form approaching an influence diagram [MT1] in order to prepare the implementation of the optimization problem.

As an equation can generate only one output, the edges have to be oriented in order to have only one output per calculation node (Figure 5b). If a same equation remains undetermined for several parameters (Figure 5c), some design assumptions have to be done by stating that some parameters are known. These new design parameters can be included in the optimization problem and their optimal value can be determined via the optimization algorithm. A preferred choice for these new design parameters is parameters participating in a large number of equations (such as reduction ratio) and values defined into a known range (min, max). These assumptions allow to balance the number of equations available and the number of parameters to be determined by the calculation procedure. Example 1 from section 0 illustrates this case of over-constrained problem.

If several equations of design scenarios have the same output, Figure 5d, the problem may be over-constrained. Two solutions can be applied: by adding a safety factor and managing one of the equations as a constraint in the optimization problem, by giving the assignment to the most restrictive equation when direct comparison is possible. Example 2 from section 0 illustrates this case of over-constrained problem.

The treatment of possible algebraic loop is the last step and corresponds to Task 3 in Table 1. We typically find an algebraic loop in the selection of a component involving the use of characteristics of this same component. This case is represented graphically by a loop involving a design scenario equation and an estimation model equation as shown in Figure 5e. Adding once again a new design parameter, such as an oversizing coefficient, and a constraint to be checked by the optimization algorithm makes the sizing procedure explicit. Example 3 from section 0 illustrates this case.

At the end of this graphical treatment, the final sequence of equations can be represented as an upper triangular N^2 diagram (Figure 1) or as a lower triangular matrix (Figure 3) in order to check that the sequence of equations is explicit.

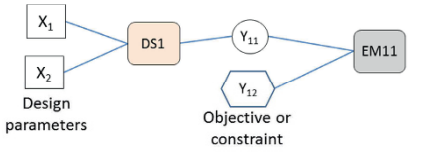

Inputs (design parameters) and outputs (objectives or constraint) representation

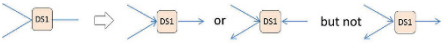

Equation orientation

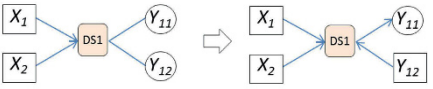

Under-constraint equation

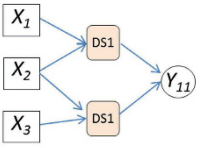

Over-constraint equations

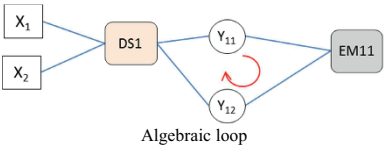

Algebraic loop

Figure 5 – Graphical orientation of equations

This sequence of tasks can be implemented using computer algorithms from graph theory [HE1] or constraints theory [GE1]. Problems of large dimensions can thus be addressed.

4. Typical problems

Global concepts were presented in previous parts; the idea is now to present a few examples to highlight the interest of such methods. The examples discussed here are deliberately simple to facilitate the demonstration but deal with each typical issue encountered in the implementation of sizing procedure.

4.1 - Under-constrained singularity: hydraulic jack

The aim is to implement the selection procedure of a hydraulic servo-actuator (jack and servo-valve) to ensure a nominal load F_0 and a nominal speed V_0 for a useful stroke dx. The anchorage structure has a stiffness K and does not tolerate effort higher than F_{max}. The maximum flow rate Q_{max} required by the actuator should be minimized to reduce the mass of the hydraulic supply system.

The physical equations for such a system are the given in Table **2** and can be represented using a Design Graph, as shown in Figure 6.

Table 2 – Hydraulic jack equations

Eq1: $F_{max} \geq S.P_{net}$	F_{max}: stall load S: piston section P_{net}: network pressure
Eq2: $C=dx+K.F_0$	C: total stroke dx: wished stroke K: structure stiffness
Eq3: $F_0=S.P_0$	$F0$: maximal load P_0: maximal pressure
Eq4: $V_0=Q_0/S$	V_0: maximal speed Q_0: maximal flow
Eq5: $Q_0 = Q_{nom}\sqrt{\frac{Pnet-P_0}{dP_{nom}}}$	Q_{nom}: nominal valve flow dP_{nom}: nominal valve pressure drop
Eq6: $Q_{max} = Q_{nom}\sqrt{\frac{P_{net}}{dP_{nom}}}$	Q_{max}: no load flow

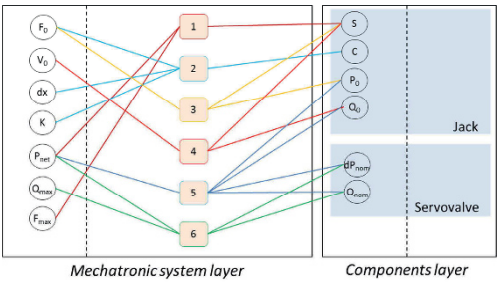

Figure 6 – Servo-actuator design graph (un-oriented)

From the listed parameters, some will be determined as input by the customer's specification document: F_0, V_0, d_x, P_{net} and K; while others are objective: Q_{max} (which must be minimized) or constraint: F_{max} (limited by maximum allowable load of the structure). But even if some parameters are defined as outputs they are still undetermined and therefore the problem is reduced to 6 equations and 8 parameters.

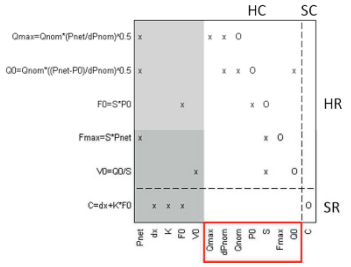

Figure 7 – Dependency matrix for the hydraulic jack with Ah sub-matrix

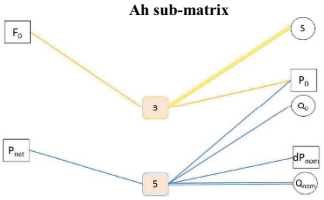

Under-constraint equations

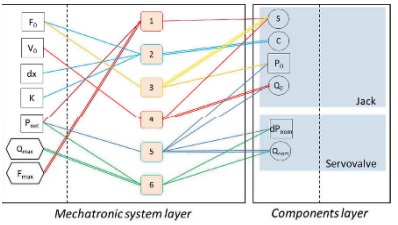

Oriented equations

Figure 8 – Servo-actuator design graph (oriented)

The design graph allows to highlight the sub-constraints: calculation nodes 3 and 5 (Figure 8a) indeed require to assume that 2 parameters are known to allow the sequencing of computations. As d_{Pnom} may be given by the valve technology, it may be taken as input and P_0 is easy to limit to a range equal to $[0, P_{net}]$, so it will be taken as second input (variable). A new set of equations, given **Figure 9**, fixes and solves under-constrained singularity.

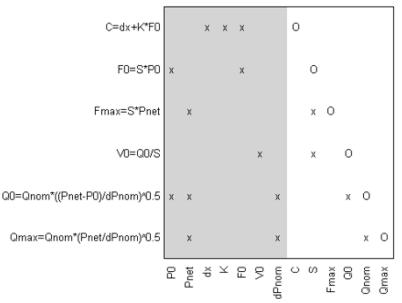

Figure 9 – Perfectly matched hydraulic jack problem

An optimization problem with P_0 as design parameter, Q_{max} as objective and F_{max} as constraint is thus obtained. The optimization enables to find a classical hydraulic design rule: the pressure P_0 must be equal to *2/3* of P_{net} in order to minimize Q_{max}.

4.2 - Over-constrained singularity: rollers-screw

Here will be presented an over-constrained problem which is quite simple but which will allow to present the way to solve this kind of singularity. The objective is to select a roller screw subjected to two constraints: a static load and a dynamic load. Let us consider the equations of Table 3 where some scaling laws (3, 4, 6) are explained in [BL1].

Table 3 – Roller-screw equations (initial set)

Eq1: $F_0 \geq F_{max}$	F_0: rollers-screw static load F_{max}: maximum applied load F_d: rollers-screw dynamic load
Eq2: $F_d \geq F_{rmc}$	F_{rmc}: rolling fatigue applied load F_{dref}: rollers-screw dynamic load (reference component)
Eq3: $F_d=F_{dref}(F_0/F_{0ref})^{0.9}$	F_{0ref}: rollers-screw static load (reference component) L_n: rollers-screw nut length
Eq4: $L_n=L_{nref}(F_0/F_{0ref})^{0.5}$	L_{nref}: rollers-screw nut length (reference component) L_s: screw length
Eq5: $L_s=C+L_n+L_b$	C: actuator stroke L_b: thrust bearing width m_s: screw linear mass
Eq6: $m_s=m_{sref}(F_0/F_{0ref})$	m_{sref}: screw linear mass (reference component)
Eq7: $M_s=m_sL_s$	M_s: screw total mass

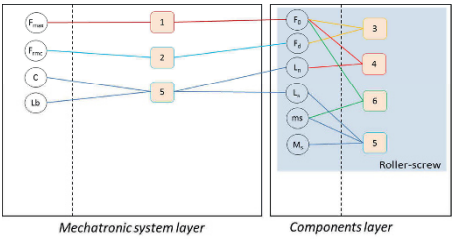

Full non-oriented graph

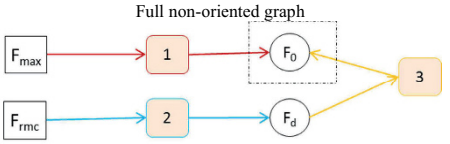

Over-constraint part

Figure 10 – Roller-screw design graph

As reference component data are available for sizing just like F_{max} and F_{rmc} specifications, and as thrust bearing will be considered to be sized first, then the problem is in fact 7 equations with 6 undetermined parameters.

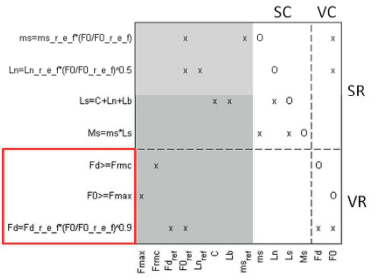

Figure 11 – Dependency matrix for the rollers-screw with Av sub-matrix

The obtained matrix clearly highlights that one of the last 3 equations must be removed to obtain non-singular problem. To do so, one of the inequalities must be displaced to constraints ($F_d>=F_{rmc}$ for example). Yet, without modifying the other equation (considered as: $F_0=F_{max}$), if fatigue is the sizing criteria, the constraint will never be met. That is why a degree of freedom 'k_c' must be introduced to the equation: k_c $F_0=F_{max}$, with k_c a variable input here within the range [1;Inf]. Then the final result is the one presented in the figure below, where k_c will represent an over-sizing coefficient to validate dynamic sizing.

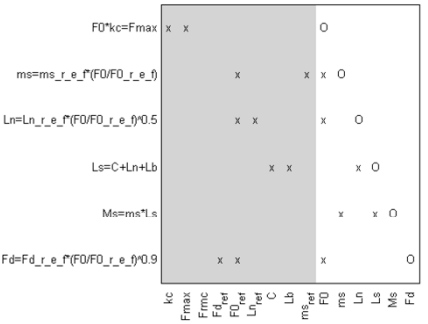

Figure 12 – Perfectly matched rollers-screw problem

4.3 - Algebraic loop: brushless electric motor

The purpose of the last example is to highlight algebraic loop within a sizing procedure. To do so, a brushless electric motor will be sized considering only the maximum transient torque it has to deliver. In that case and one more time by applying [BL1], we have the equations of Table 4.

Table 4 – Brushless electric motor equations (initial set)

Eq1: $T_0=T_{load}+J.d_w$	T_0: motor maximum torque T_{load}: torque demanded J: motor inertia dw: acceleration demand
Eq2: $J=J_{ref}(T_0/T_{0ref})^{(5/3.5)}$	$Jref$: motor inertia (reference component) T_{0ref}: motor maximum torque (reference component)
Eq3: $M=M_{ref}(T_0/T_{0ref})^{(3/3.5)}$	M: motor mass M_{ref}: motor mass (reference

component)

As reference components such as torque and acceleration demand are determined, the problem is composed of 3 equations and 3 unknowns.

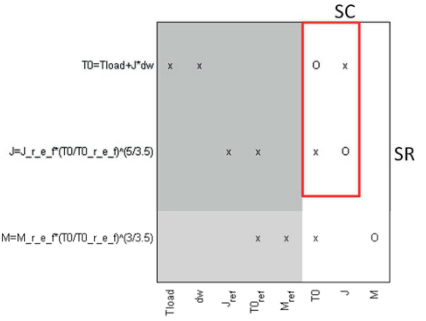

Figure 13 – Brushless electric motor sizing procedure highlighting SCC

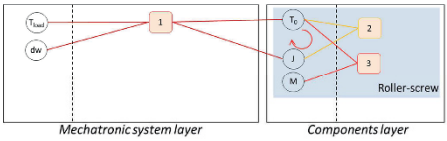

Figure 14 – Brushless motor design graph

In Figure 13, an algebraic loop appears since T_0 and J computation are linked. To break the loop, an oversizing coefficient can be introduced within Eq1 and reuse the initial equation as a constraint:
Eq1 : $T0=k_m T_{load}$ and
Cst1 : $T_0>T_{load}+J.dw$.
This new sizing procedure has no algebraic loop thanks to the introduction of a new design parameter and a new constraint for the optimization problem.

5. Conclusion

Mechatronic systems are characterized by strong interactions between fields. We showed in this paper that ordering the calculation steps of a whole highly constrained sizing procedure is not always an easy task. We proposed here graphical representation that can be applied to highlight the different problems the designer has to face (singularity, calculation loop) and may help him solve those errors by proposing alternatives. Finally the problem is formulated in a generic way which can be implemented in as many solvers/optimization tools as possible. These design graphs can be used pedagogically to introduce students to the design. They can also be implemented by algorithms to help the designer for the cases of more complex devices. A matlab toolbox has been realized and a Java graphical user interface is planned.

6. Bibliography

[A1] Auslander, DM 1996, 'What is mechatronics?', Mechatronics, IEEE/ASME Transactions on, vol 1, no. 1, pp. 5-9.

[BF1] Black, TA, Fine, CH & Sachs, EM Massachusetts Institute of Technology, 1990., 'A method for systems design using precedence relationships: an application to automotive brake systems'.

[B1] Browning, TR, 'Applying the design structure matrix to system decomposition and integration problems: a review and new directions', IEEE transactions on engineering management, vol. 48, no.3, pp. 292-306, 2001.

[BH1] Budinger, M, Halabi, TE & Maré, J-C 2011, 'Optimal preliminary design of electromechanical actuation systems', « More electrical » aircraft technologies, Symposium SPEC, Lyon, France.

[BL1] Budinger, M, Liscouet, J, Mare, J & others 2012, 'Estimation models for the preliminary design of electromechanical actuators', Proceedings of the Institution of Mechanical Engineers, Part G: Journal of Aerospace Engineering, vol 226, no. 3, pp. 243-259.

[BP1] Budinger, M, Passieux, J-C, Gogu, C & Fraj, A, 'Scaling-law-based metamodels for the sizing of mechatronic systems', Mechatronics, no. doi: 10.1016/j.mechatronics.2013.11.012.

[CG1] Cellier, F & Greifeneder, J 1991, Continuous System Modeling.

[DW1] Delinchant, B, Wurtz, F, Magot, D & Gerbaud, L 2004, 'A Component-Based Framework for the Composition of Simulation Software Modeling Electrical Systems', SIMULATION, vol Vol. 80, no. Issue 8.

[GF1] Gelle, E & Faltings, B, 'Solving mixed and conditional constraint satisfication problems', Kluwer academic publishers, no. 8, pp. 107-141, 2003.

[HE1] J. M. Helary, Algorithmique des graphes. Rennes university publication, 2004.

[HP1] Hehenberger, P, Poltschak, F, Zeman, K & Amrhein, W 2010, 'Hierarchical design models in the mechatronic product development process of synchronous machines', Mechatronics, vol 20, pp. pp. 864-875.

[LH1] Liscouet-Hanke, S & Huynh, K, 'A Methodology for Systems Integration in Aircraft Conceptual Design – Estimation of Required Space', SAE Technical Paper 2013-01-2235, 2013, doi:10.4271/2013-01-2235.

[MT1] Malak, RJ, Tucker, L & Paredis, CJJ, 'Compositional modelling of fluid power systems using predictive tradeoff models', International of fluid power, vol. 10 number 2, pp. 45-56, 2009.

[N1] NASA 1995, Techniques of Functional Analysis, NASA Systems Engineering Handbook.

[S1] Salome, www.salome-platform.org/about/yacs

[VA1] Van der Auweraer, H, Anthonis, J, De Bruyne, S & Leurdian, J 2013, 'Virtual engineering at work: the challenges for designing mechatronic products', Engineering with Computers, vol 29, pp. pp. 389-408.

[V1] VDI-Richtlinien, Design methodology for mechatronic systems, VDI, Düsseldorf.

9

Education in Product Engineering

Major topics of the full argumentations are the following:

X. Fischer et al. (eds.), *Research in Interactive Design (Vol. 4)*
DOI 10.1007/978-3-319-26121-8_19

Article 014-e-97

Knowledge discovery from traceability of design projects

Xinghang DAI [1], Nada MATTA [2], Guillaume DUCELLIER [3]

(1) : Université de technologie de Troyes, Troyes
10000 France
0033 0686150452
E-mail : {Xinghang.dai, nada.matta,
guillaume.ducellier}@utt.fr

Abstract: Nowadays, design projects tend to be undertaken concurrently by a project team with a diversity of competences and backgrounds (culture, organization etc.). Knowledge management is supposed to enhance experience reuse by transforming tacit knowledge that is produced in projects into reusable explicit one. However, due to the characteristics of modern design projects, knowledge management has to pay attention not only to decision-making activities, but also the influence of project context.

Key words: knowledge representation, engineering design, project management, classification, project memory.

1- Introduction

Design is a collaborative activity that requires project team members with different skills and background to work together. Design project organization has two particular characteristics: firstly, it is a short-lived organization; project team members will be engaged in another project with a different work environment; secondly, project team can consist people with different skills, from different companies, different countries etc. Given these types of organizations, the goal for knowledge management is how to learn from past design project experience to help to solve new design problems. Knowledge is commonly defined by data and information used by an actor in a specific context [MR1]. Knowledge is produced in project activities for a given goal. Knowledge management aims at enhancing organizational learning in a company based on knowledge produced. It is defined as a cycle of transformation from tacit to explicit knowledge in a company [NT1]. This type of organizational learning will be based on "knowing how" and "knowing when" [EL1].

In this paper, we try to face the problem of learning from design project experience. We believe that deep knowledge can be discovered through classification of design project experiences. Project memory is defined in the first place in order to represent the knowledge structure of design projects, and then a knowledge discovery method by classification according to different views of project memory is introduced to extract knowledge rules.

2- The nature of knowledge and project memory

There are different definitions for knowledge. The common one, used in knowledge engineering, is information and data used for an activity and in a given context [B1]. Contextual information can be encoded into more abstract and more organized concept networks in long-term memory [CK1], and knowledge resides in the concepts as well as associations in-between. Based on that, several Knowledge engineering approaches develop techniques [S1], [SW1], in order to extract and tackle this type of knowledge as semantic networks.

The famous semiotic triangle has shown three dimensions of knowledge: "sense", "reference" and "sign". Sign stands for the object that human refers to, and sense is the concept or idea associated with sign and object [P1]. For the same object, people with different background can give different signs; concept alters according to different context. To represent the meaning triangle, approaches based on semantic network, ontology, logic etc. has been developed. In this type of representation, knowledge used in problem solving is showed into networks that emphasize the "Why", "What" and "How" of a reasoning [SW1].

As we noted above, a design project is a cooperative activity. Team members with different skills and different backgrounds form project organization. During the whole project, decision-making activities play an important role on balancing different project elements in search for the optimal solution. To show the "Why", "What" and "How" in this type of cooperative reasoning, we should represent specially:

1- The organization of the project (actors, skills, roles, tasks, etc.)
2- The design rationale (negotiation, argumentation and cooperative decision making)
3- The consequences of problem solving (evolution of the artefact)
4- The context of the project (rules, techniques, resource, etc.)

We called the structure representing this type of knowledge

Article 014-e-97

project memory [MD1].

3- Knowledge discovery by classification for project memory

In the section above, the concept project memory is introduced. The goal of project memory is to enhance learning from expertise and past project experience [MR1]. Current representation approaches emphasize on organizing and structuring the experience and let human to interpret concepts. The problem is that human can only learn from others by matching to one's own experience, and the knowledge level between expert and learner are always not the same. The traditional knowledge engineering methods ignore completely or partially the mutual influence between context and solution [MD1]. Instead of a single, best classification system that suits everyone, everywhere [M21], we have to come up with classification models suited within specific contexts [M1]. Therefore, to enhance learning in an organization, the knowledge modelling has to emphasize the "know what" and "know how" [NT1] [EL1], and the context in which the knowledge is produced has to be represented as knowledge "know why".

More effort has been done recently to represent project memory, we note especially DyPKM [BM1]. DyPKM is an approach that trace and structure project information. However it is not sufficient to extract knowledge rules. In order to discover knowledge in design project memory, information has to be structured, and more importantly mapping low-level data into other forms that might be more compact, more abstract, or more useful [FP1]. Therefore, a knowledge discovery method to extract knowledge from design project memory is proposed. In the section below, we are going to introduce the concept knowledge classification and semantic networks of project memory.

3.1. Knowledge discovery by classification

A knowledge engineer can interpret expert experiences to conceptualize them then formalize them into explicit representation, where knowledge can be recognized and learned. Logic, ontology and semantic network are frequently referred to for knowledge representation. A semantic network graph enable knowledge engineers to communicate with domain experts in language and notations that avoid the jargon of AI and computer science [S1]. Ontology is a description of shared concepts. It consists of term, definitions, axioms, and taxonomy [G1]. Our representation of project memory is based on a general semantic network of four modules, and then four modules are represented in sub-networks. Ontological hierarchy of concepts may be necessary for generalization. Classification can be defined as the process in which ideas and objects are recognized, differentiated, and understood [CL1], while knowledge classification is the process in which knowledge is recognized and reasoned. Classification algorithms are used in biology, documentation, etc. [CL1]. They help to recognize an object with characteristics, related to a predefined hierarchy. Machine learning methods are frequently used to classify a concept automatically in a quantitative manner. However, design project information is usually not voluminous and quite distinctive. Therefore it is not necessary to use powerful machine learning algorithms for concept classification; in our work, we will focus on how to classify interaction of concepts to extract knowledge rules.

3.2. Knowledge discovery framework for design project memory

Previous work on traceability of project memory makes effort on structuring project information, but little on concept interaction or knowledge extraction. Our knowledge discovery model is supposed to not only represent information structure of project memory, but also propose useful knowledge-oriented classification views for learning purpose.

Firstly, in order to discover knowledge in different context, the general semantic network of project memory (figure 1.) is decomposed into 4 sub-networks:

1- Decision-making process: this part represents the core activity of design project, which helps designers to learn from negotiation and decision-making experience.
2- Project organization makes decision: this part represents interaction between organization and decision, which provides an organizational view of decision-making.
3- Project organization realizes project: this part represents arrangement of task and project team organization, which focuses learning on project management.
4- Decision-making and project realization: this part represents the mutual influence between decision and project realization, which reveals part of work environment and background.

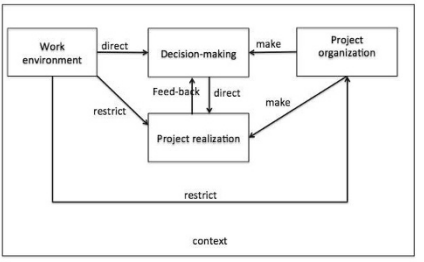

Figure 1. General semantic network of project memory

Secondly, in each sub-network, important concepts and relations that are involved in potential knowledge extraction are highlighted, and ontological class hierarchy may be required for conceptualization. Thirdly, according to each project memory component, knowledge rules are generated (figure 2).

Article 014-e-97

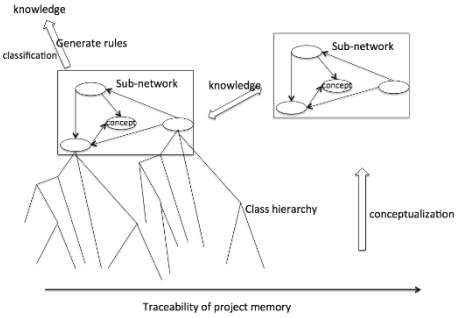

Figure 2: Knowledge discovery framework

3.2.1 –semantic network of different project views

We consider the decision-making process sub-network the most important one for the reason that it represents the most important activity of design projects. Concepts that are identified in a decision-making process are: issue, proposition, argument and decision. Issue is the major question or problem that we need to address, it can be about product design, organization or project realization; proposition is the solution proposed to the issue; argument evaluates the proposition by supporting or objecting it, which can push proposal to evolve into another version [CB1], [MC1], [B21]; argument can also aims at issue which can possibly modify the specification of the issue. Decision is made by selecting the best proposition for the issue and setting up a goal for next step of project realization. Fig.3 shows the decision-making process sub-network. One of the most important and useful knowledge that we want to represent is the context behind design rationale [MC1]. We have to not only represent the concept structure of proposition, decision and argument, but also the interaction between them. Propositions are considered to be possible solutions for issue, and arguments are supposed to explain the reason why. Therefore, we want to attribute criteria to argument in order to generalize the category of arguments.

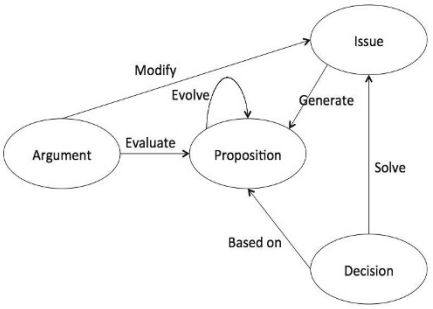

Figure 3: Decision-making process

We give an example of argument criteria tree, which is based on evaluation criteria of design rational in the field of engineering design [MD2]. The ontological hierarchy of issue and should be constructed according to a specific context, it is important to show different categories of issue as a specification of project context.

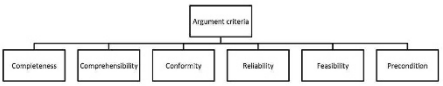

Figure 4: an example of argument criteria tree

In this sub-network (Fig.5), we want to find a concept that serves as a bridge to connect project organization and decision- making process. So the concept "member" is added into the decision-making sub-network to represent the organizational dimension of decision-making process. Member is an important concept of project organization that links to competence, role and task.

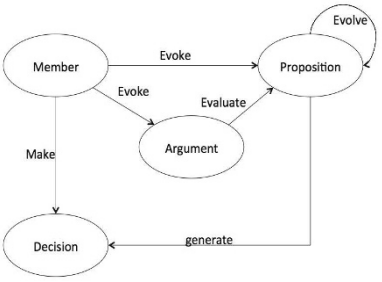

Figure 5: Project organization making decision

This sub-network (Fig.6) offers a learning perspective on project realization with an organizational dimension. Il allows us to study the interaction between task and project organization. Task is linked to two important attributes of project member: competence and role.

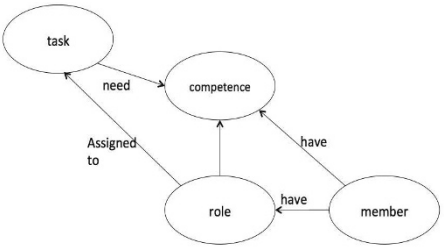

Figure 6: Project organization realizing a project

We believe that class hierarchy is needed for conceptualization of "role", "task" and "competence".

At last, we want to represent the triangle between task, decision and issue in order to show a mutual influence of task arrangement and decision-making process (Fig.6). A decision sets up a goal for a task; another issue can be evoked during a task, which initiate another decision-making process. The triangle ends by achieving the final result of a

Article 014-e-97

task. During a product design, the result of a task can be a new version of a product, and the version of product evolves between decision-making meeting and tasks.

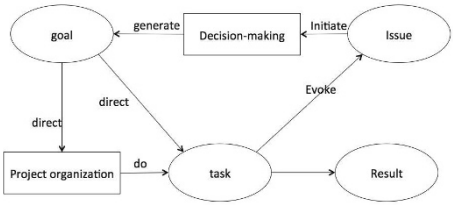

Figure 7: Decision-making and project realization

3.2.2 – knowledge discovery algorithms

The ability to extract general information from example sets is a fundamental characteristic of knowledge acquisition. Machine learning technique is now a hot topic at present, it can figure out how to perform important tasks by generalizing from examples. One of the most mature and widely used algorithms is classification [D21]. However, as we mentioned above, due to the particular characteristics of design project information, present machine learning techniques are not suitable for design project memory classification. We studied four major categories of machine learning algorithms: statistical methods, decision tree, rule based methods and artificial neural network [D1] [KC1] [SG1] [MS1]. These methods are not considered for two reasons: 1). Classification process is not transparent to human interpretation. 2). A large recursive training set is needed for classification. The advantage of our classification model in project memory is that it is guided by meaningful project views with well-defined semantic networks. Therefore, according to these semantic networks, we generate rules by simple comparison. Additionally, the learning process will not ignore non-recursive instances; on the contrary, they will be put aside as explorative attempts with a condition.

First of all, project information will be structured according to teach semantic network as follow:

- Project organization: Member (name, role, competence);
- Decision making process: Issue (issue, proposition, decision); Proposition (proposition, member, argument); Argument (argument, member, criteria, position value);
- Project realization: Task (task, member, issue or result);
- Decision making process and project realization: Decision (decision, task); Task (task, member, issue or result);

Then project information will be classified to extract knowledge rules. Here we propose three algorithms that extract rules in three different aspects:

1- Problem-solving rules: at a specific project phase, we can classify decision-making process for one particular issue. Solutions that are repetitive will be classified as essential solutions, the solutions that are distinctive will be considered as explorative attempt with its precondition.
2- Cooperation rules: an important subject that we tried to study in our model is cooperative knowledge. Therefore another algorithm on project realization is proposed to verify whether there are tasks that involves cooperative design or regular meetings involves whole project team. Projects that are not undertaken concurrently can lead to unsatisfactory results, for example, solution duplication or excess of project constraint. This rule will reveal the influence of concurrent design on project result.
3- Management rules: this algorithm will focus on the interaction between project organization and project realization. We will classify project realization with an organizational dimension to examine how project organization can influence project realization.

The three aspects that are proposed above are the most interesting classification views that we find so far, however we do not exclude possibility that more useful classification views exist. In the next section, these algorithms will be applied to two example projects to demonstrate the knowledge discovery model.

4- Example and result

In this section, we are going to demonstrate our knowledge discovery model on two projects that are undertaken by two groups of students in the year 2012 and 2013. The group members are students majored in computer science or mechanic design. They are supposed to work together on a tablet application design project. The goal of the project is to design a tablet application, which proposes solutions for product maintenance; it should allow a technician to access and modify PLM and ERP information in order to facilitate information flow in supply chain. MMreport and MMrecord were employed to keep track of meetings from the beginning to the end of the project. XML documents were generated by these two applications. We analyzed these XML documents as well as other documents (email, forum discussion and result). Then they were structured and classified by our knowledge discovery model.

Problem solving rule on the issue function definition can be extracted by comparing decision-making process of both projects.

Tablet application for product maintenance				
Year	2012		2013	
Issue	Function definition		Function definition	
Negotiation	Proposition	Argument	Proposition	Argument
	Automatic object reconnaissance	• More efficient • Help operator without enough mechanic skills • More expensive • Technology obstacles	Manuel object search engine	• Easy to design • Require certain mechanic skills for operator
	ERP and PLM connection	• Reduce data redundancy • Technology obstacles	Tablet connection with PLM and ERP	
	Tablet connection with PLM and ERP			
Decision	Automatic object reconnaissance, Tablet connection with PLM and ERP.		Manuel object search engine, Tablet connection with PLM and ERP	

Figure 8: project information on the issue "function definition"

We classify repetitive solutions as essential solutions for the issue function definition, and distinctive solutions as

explorative cases with a precondition.

Tablet application for product maintenance		
Issue	Function definition	
Essential solutions	Tablet connection with PLM and ERP, object search with tablet applications	
Conditional solutions	Solution	Condition
	Automatic object reconnaissance	Enough budget
	PLM and ERP connection	Feasible technology

Figure 9: Result of classification on the issue "function definition"

Cooperation rules on this project can be extracted by classifying project planning. If there are tasks concern module integration and regular meetings of whole project team, then this project is undertaken concurrently.

Tablet application for product maintenance		
Year	2012	2013
Phase	Project realization	Project realization
Project organization	Three sub-groups for each application module (ERP,PLM, Object reconnaissance)	Three sub-groups for each application module (ERP, PLM, object search engine)
Project planning	• 4 working meetings inside each sub-group to validate project specification • A final meeting to simply collect each sub-group's work	• 12 work meetings of whole project team • Sub-group meetings are organized freely
Result	• Each module has its own database, the application has 3 databases in total • Automatic image recognition increase the cost drastically	• Client-server architecture that requires only one database • Centralized data management

Figure 10: Project information on project realization and task planning

Apparently for the project 2012 design activities were not organized concurrently. In fact, they organized only one final meeting with the whole group to assemble sub-groups' work, but there is no negotiation on integration design, which leads to the result "database duplication" and "expensive project cost".

Linear project planning leads to bad communication between different sub-group designers, which result in poor integration design. From the management point of view, we can further this classification by adding an organizational dimension to project planning.

Tablet application for product maintenance				
Year	2012		2013	
Phase	Project realization		Project realization	
Project organization	Three sub-groups for each application module (ERP,PLM, Object reconnaissance)	Competence distribution: ERP(computer science) PLM (mechanical design) Object reconnaissance (computer science)	Three sub-groups for each application module (ERP, PLM, object search engine)	ERP(computer science) PLM (computer science, mechanical design) Object search engine (computer science, mechanical design)
Project planning	• 4 working meetings inside each sub-group to validate project specification • A final meeting to simply collect each sub-group's work		• 12 work meetings of whole project team • Sub-group meetings are organized freely	
Result	• Each module has its own database, the application has 3 databases in total • Automatic image recognition increase the cost drastically		• Client-server architecture that requires only one database • Centralized data management	

Figure 11: Project planning with an organizational dimension

2012 project group are divided into sub-groups with unique competence, while 2013 project sub-groups contain at least two different competences. We may say that design decisions in project 2013 were made based on opinions from both software designers and mechanical designers, which was not the case in 2012. From this classification view, we can find that if designers with different skills are assigned to the same task, there are more constructive cooperation and communication.

Extraction of these rules are all guided by comparison of structured information according to different project views, rules may change as more project information will be captured. It is possible that a weight factor that indicates the importance of rule may be introduced according to different recursive frequencies.

5- Conclusion and discussion

In this paper, we presented a knowledge discovery method based on project memory in order to enhance learning in organizations. At the beginning, we demonstrated the concept "project memory" in order to introduce a representation structure that is adapted to the new trend of collaborative concurrent design. Then, a knowledge-oriented classification method is proposed. At last, we showed the sub-networks based on different views of project. An example of application of knowledge discovery model is given in the end. We showed a technique to extract deep knowledge in project experience by classification according to different project views. The classification focuses on the interaction between different concepts. We try to enrich simple conceptualization by revealing the context of concept. Therefore, learning from the past is guided not only concept structures but also concept relation rules. Three classification views are proposed in this pater, they are problem solving, cooperation and management. Detailed project information will also be attached to knowledge rules to illustrate real examples.

The semantic networks that we gave are based on the traditional knowledge management methods, but we make a connection between different elements in order to give design activities a context with an organizational collaborative dimension. No classification can be argued to be a representation of the true structure of knowledge [19], our knowledge discovery model aims at enhancing organizational learning of design project, class conceptualization and knowledge extraction is strictly linked to project context.

5- References

[B1] Bachimont B., "Pourquoi n'y a-t-il pas d'experience en ingenierie des connaissances?.", in Ingénierie des Connaissances, pp. 53-64. 2004.

[B21] Buckingham Shum S., "Representing Hard-to-Formalise, Contextualised, Multidisciplinary, Organisational Knowledge ", in AAI Spring Symposium on Artificial Intelligence in Knowledge Management, 1997, pp. 9–16.

[BM1] Bekhti S. and Matta N., "Project memory: An approach of modelling and reusing the context and the design rationale", Proc. of IJCAI, Vol. 3, 2003.

[CB1] Conklin J. and Begeman M. L., "gIBIS: a hypertext tool for exploratory policy discussion," ACM Transactions on Information Systems, vol. 6., 1988, pp. 303–331.

[CL1] Cohen H. and Lefebvre C. eds, "Handbook of categorization in cognitive science", Vol.4, No.9.1, Elsevier, Amsterdam, 2005.

[D1] Dietterich T.G., "Machine-learning research", AI magazine, Vol.18, No.4, 1997, pp 97.

[D21] Domingos P., "A few useful things to know about machine learning," Commun. ACM, vol. 55, no. 10, Oct. 2012, p. 78.

[CK1] Claire D. and Kolmayer E., Éléments de psychologie cognitive pour les sciences de l'information: avec exercices corrigés. Presses de l'enssib, École nationale supérieure des sciences de l'information et des bibliothèques, 2006.

[MS1] Michie E. D., Spiegelhalter D. J., and Taylor C.C., "Machine Learning , Neural and Statistical Classification," 1994.

[EL1] Easterby-Smith M. P. V and Lyles M., "The Blackwell Handbook of Organizational Learning and Knowledge Management.," Adm. Sci. Q., vol. 48, 2003, p. 676.

[FP1] Fayyad U., Piatetsky-shapiro G., and Smyth P., "From Data Mining to Knowledge Discovery in," vol. 17, no. 3, 1996, pp. 37–54.

[G1] Gruber T.R., "Toward principles for the design of ontologies used for knowledge sharing?", International journal of human-computer studies, Vol.43, No.5, 1995, pp 907-928.

[K1] Klein M., "Capturing design rationale in concurrent engineering teams," Computer , Calif., vol. 26, no. 1, pp. 39–47, Jan. 1993.

[KC1] King R.D., Cao F., Sutherland A., "Statlog: comparison of classification algorithms on large real-world problems", Applied Artificial Intelligence an International Journal, Vol.9, No.3, 1995, pp289-333.

[M1] Mai J., "Classification in context: relativity, reality, and representation", Knowledge organization, Vol.31, No.1, 2004, pp 39-48.

[M21] Miksa F., "The DDC, the universe of knowledge, and the post-modern library", NY: Forest Press, Albany, 1998.

[MC1] Moran T.P. and Carroll J.M. eds, Design rationale: concepts, techniques, and use, Routledge, US,1996.

[MD1] Matta N. and Ducellier G., "An approach to keep track of project knowledge in design," Proc. IC3K/KMIS, 5th International Conference on Knowledge Management and Information Sharing, Vilamoura Algarve, Portugal, 2013.

[MR1] Matta N., Ribière M., Corby O., Lewkowicz M., Zacklad M., "Project Memory in Design", Industrial Knowledge Management - A Micro Level Approach, SPRINGER-VERLAG : RAJKUMAR ROY, 2000

[NT1] Nonaka I., Takeuchi H., "The knowledge-Creating Company: How Japanese Companies Create the Dynamics of Innovation", Oxford University Press, 1995

[P1] Peirce C.S., "Collected papers of charles sanders peirce", Vol. 3, Harvard University Press, USA, 1974.

[PB1] Pahl G., and Beitz W., "Engineering Design: a Systematic Approach", Springer-Verlag London, UK, 1996.

[SG1] Smyth P. and Goodman R.M., "An information theoretic approach to rule induction from databases," Knowledge and Data Engineering, IEEE transactions, Vol.4, No. 4 ,1992, pp 301-316.

[R1] Richard J.F., "Les activités mentales, Comprendre, raisonner, trouver des solutions", Armand Colin, Paris,1990.

[S1] Sowa, John F, "Knowledge representation: logical, philosophical, and computational foundations", Brooks/Cole, Pacific Grove, 2000.

[SW1] Schreiber G., Wielinga B., Van de Velde W., Anjewierden A., "CML: The CommonKADS Conceptual Modelling Language", Proceedings of EKAW'94, Lecture Notes in AI N.867, L.Steels, G. Schreiber, W.Van de Velde (Eds), Bonn: SpringerVerlag, September 1994,pp 1-25.

Article 015-e-14

MULTIDISCIPLINAR APPROACH IN TEACHING INTERFACES DESIGN: A PILOT PROJECT

Aranzazu Fernández Vázquez [1], Anna Maria Biedermann [2]

(1) : University of Zaragoza.
Department of Design and Manufacturing Engineering.
876555098
aranfer@unizar.es

(2) : University of Zaragoza.
Department of Design and Manufacturing Engineering.
876555098
anna@unizar.es

Abstract: This paper presents the multidisciplinary approach in interface design performed as a pilot project on the University of Zaragoza in collaboration between the Industrial Design and Product Development Engineering Degree and the Informatics Engineering Degree. It presents the complementary development of the interfaces' aspects of usability, the differences along its evaluation, the conclusions from the pilot project seen from the perspective of graphic design and improvement proposals for implementing future experiences. The aim of the project is to prepare students for fulfilling their future professional works in the complex field of interfaces design, enabling them to work in collaborative environments.

Key words: Multidisciplinary work, interfaces design, graphic design and informatics teaching.

1- Introduction

The task of designing interfaces is complex and involves many disciplines and knowledge areas, such as ergonomics, graphic design, perception theory or computer sciences [M2]. For that reason, teachers of the subject of Graphic Design and Communication (DGyC) of the 2nd year of Industrial Design and Product Development Engineering Degree, and teachers of the subject Person-Computer Interaction (IPO) of the 2nd year of the Informatics Engineering Degree raised a collaboration project during the 2012-2013 course, as a mean of supplementing the expertise provided by the educational program in Degrees involved [D1] [I1].

Teaching methods based on experimental versus traditional lecture, as processes that develop interdisciplinary workgroups and focus in specific training, are considered a substantial and necessary improvement over the traditional generalist approach to the subjects within the field of Engineering Education [Z1][H1][M1]. Therefore, teachers should try to encourage students to participate in experiences like this in the earliest stage of their university course, although the subjects in their first year of a university degree are too broad for dealing with this practice. The active methods of learning like the one proposed here have some problems when dealing with too general subjects, such as the ones that comprises the first year of both Degrees, but could be very effective when the professional objectives are clear [R1], which is the case of both subjects involved in this practice.

For students of the subject of IPO, the goal was to enhance their knowledge of the communicative role that the graphical elements of the interface must have, and to learn how they ought to design and develop those elements. And for the DGyC students the aim was to increase their knowledge on interaction between person and computer, in order to qualify them to design a proper graphic interface.

Collaboration materialized in a pilot project that consisted of a common practice for students of both disciplines, taking into account the learning objectives of the two subjects involved.

1.1 – Approach to the assessment

The exercise title was the "Design of the prototype of an interactive support system for patients with polypharmacy." In the design process it had to be considered that the application should be used both by patients and by doctors or the person who coded the medication to be taken by the patient. Since two types of users with different levels of knowledge, diverse needs, expectations or abilities to interact were entailed, students had to ponder about the appropriate code to be applied depending on the user.

The assessment was considered suitable for both subjects due to the kind of knowledge needed to arise a project in the field of Human Computer Interaction (HCI), a domain in which graphic design and computing might work together for an optimal outcome [M2].

Specifying the requirements of each course:

- Students of IPO should make an application for patient assistance, consisting in the development of a simulator of two subsystems (subsystem for the

prescriber and subsystem for the patient) by using Axure and showing the results on the PC screen.

- Students of the subject of DGyC should develop the graphic image of the brand for use on mobile devices, as well as the layout of the two basic screens for users of each subsystem (doctor and patient).

Students had to work in groups of two or three people in both disciplines, being one of the five practices under the subject of DGyC but the only mandatory one for IPO pupils.

1.2 – Structure and development of the assessment

Given its nature of pilot project, and the impossibility of establishing for this first experience a common calendar within programs of studies completely independent, it was decided that the work of each subject was going to be developed in parallel, with specific moments in common for sharing experiences and evaluation of results (Figure 1). This initial approach would serve to evaluate how the drill was worked out in each subject to find common ground for developing and organizing the assessment in the future, with a view to further improvement of the initial proposal and to reinforce the basis for guiding collaboration between students of different degrees.
The assignment started, after the presentation of the exercise made by teachers of each Degree to their own students, with crossed technical talks by teachers of the other grade, in which the basic parameters to consider for the execution of the practice from the perspective of their subject were explained. This was meant for students to have a wider view of the work and to come up with additional information in comparison to the one provided under their specific course syllabus.
The labour was developed, from this point, depending on the specific program established by each subject, although it is pertinent to note that part of the work required in each subject was coincidental, especially at the stage of analysis of both market and users.
In the course of IPO, the assessment was structured in three phases, with two partial deliveries that were corrected and returned to students for improvement, so that each of these already checked partial papers were part of the final work that was handed for the final evaluation.
In the course of DGyC, several partial corrections were made during the practice sessions and tutorial hours. All work results ought to be collected in a dossier, with the phases of analysis and study required, and delivered to the teachers at the deadline.
In concluding the assessment, students of IPO evaluated the work submitted by students of DGyC, choosing those which in their opinion had a better development and fit better the goals of the assessment.

2- Educational framework and objectives

2.1 – Educational framework

As a pilot project, the acquisition of transversal competences was constituted not as mandatory but desirable, given the accomplishment complexity these types of skills have. When speaking of competencies, it was referred to the ability to integrate the knowledge, skills and attitudes for performing complex professional tasks [V1]. The transversal competencies are part of the new demands that arise in university education in the new framework resulting from the establishment of the European Higher Education Area (EHEA) after the beginning of the convergence process that started from the Sorbonne Declaration of 1998 [C1] and the Bologna Declaration of 1999 [E1].
It was intended, among other objectives, to improve the competitiveness of European higher education, and to establish a process of cumulative learning that could continue throughout life and go beyond the mere transmission of knowledge, focusing on the promotion and encouragement of learning. It is pretended not only to teach, but to teach how to learn, by a comprehensive education in the context of learning throughout life [M3].
Some transversal skills that were considered necessary to accomplish these objectives were directly related to the ones of the proposed exercise, such as getting familiar with new technologies and the most common associated tools; to acquire analysis and synthesis capacities, accompanied by the development of critical and self-critical spirit; to achieve the abilities to work individually and in groups; to work being part of multidisciplinary teams; and to promote the concern for quality.

2.2 – Relationship between objectives and competencies to be acquired

Practices of this kind could be framed within project-based learning (PBL), which is one of the methods of teaching and learning that has become established over the current educational framework [I2][R1]. This method makes students acquire the information precised therefore skills for training for learning are enhanced ,in the research and analysis processes. These abilities could fit into a comprehensive training, common aim to all the EHEA. These were objectives shared by both subjects, and were therefore jointly raised.

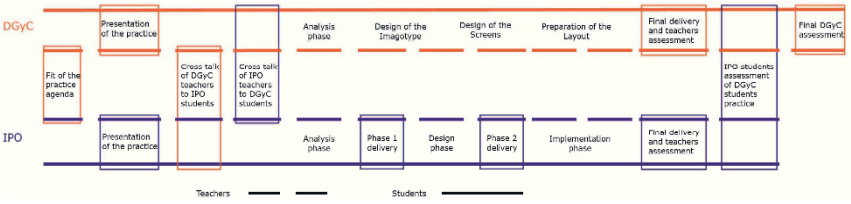

Figure 1: Scheme of practice development

2.2.1 –Skills for multidisciplinary work

The practice required from the student to manage the resolution of a drill, but being aware that in parallel the same problem was being addressed from another area of knowledge.
This approach was intended to make the student conscious of the need of performing a reflection exceeding the strict bounds of their educational program when confronting a new project, making them aware that new perspectives, angles of analysis or factors to consider were possible. That was one of the reasons why we thought that this experience could be enriching: although not in an entirely practical way yet, like the one they would probably have to face in their future professional experiences.

2.2.2 – Getting familiar with new technologies and the most common associated tools

In an environment with increasing types of devices, the complementary analysis of the HCI made by people from other areas or fields of knowledge was considered essential. It could allow a better study of the user and the ways in which any system must get adapted to each individual.
The Interest in achieving this objective was evident in the subject of DGyC, because the environment of new technologies and its tools are an important area for students´ future employment possibilities. Improving the students´ understanding of the technical development of systems and applications for all types of devices, would allow the graphic design to meet with the specific needs of both designers and computer programmers as well as end users.

2.2.3 –Students motivation and development of critical spirit

The first stage of the exercise required the student to make a critical analysis of the collected information, in order to obtain useful conclusions for further development.
Besides, since all students were working in an application on polypharmacy, an extra effort was necessary for each group to achieve product differentiation from the one developed by others.
This first level of competitiveness among students of DGyC was strengthened by further evaluation by students of IPO. To motivate with an incentive beyond the mere rating of the practice made by teachers was always promoted as a project aim, and has proven to be very satisfying for students when their work has been positively valued by fellows of another degree.

2.2.4 – Team work and project management

The proposal involved the need of working in groups, and it was mandatory to accomplish several stages to solve the practice completely. The definition of the project phases was intended to work as a model or script that would help students during the conception and management of both the labor itself as for their future professional growth.
This was perhaps most clearly shown in the case of IPO, because as the practice was the only one for the students, it was structured in three consecutive deliveries, being the last delivery a compilation of all stages of previous work plus the last one. This structure, in addition to serving students as a dash to organize and gather all necessary job execution phases, allowed them to correct minor faults.
In DGyC no intermediate deliveries to teachers were conducted, due to the less time committed to the project, but the statement of the exercise suggested different phases that had to be accomplished in order to complete it. Thereby, despite of the corrections made by teachers during the sessions and tutorials, the responsibility for meeting the objectives within the deadline set belonged to the students. Thereby, part of learning consisted of time management, which implied the need to properly plan the time demanded for each stage within the project.

3- Evaluation criteria

The assessment of practice was conducted independently by teachers of both subjects as the evaluation criteria were specific for each of them.
Students of IPO rated the work of students of DGyC. Each work of students groups of DGyC chosen by IPO students scored an additional 0.5 over the evaluation of DGyC teachers, executed independently and prior to the assessment of students of IPO.
The comparison between the criteria adopted by the teachers of DGyC and those used by students of IPO highlighted and detected interesting differences.

3.1 – Evaluation criteria of IPO subject over the DGyC assessments

When assessing the work of DGyC students by the IPO students, five criteria were provided by the subject teachers.
The five criteria were selected from those exposed by Jakob Nielsen in ”Usability Heuristics for User Interface Design” [N1], and are as follows:
“- Visibility of system status: The system should always keep users informed about what is going on, through appropriate feedback within reasonable time.
- Match between system and the real world: The system should speak the users´ language, with words, phrases and concepts familiar to the user, rather than system oriented terms. Follow real world conventions, making information appear in a natural and logical order.
- User control and freedom: Users often choose system functions by mistake and will need a clearly marked “emergency exit” to leave the unwanted state without having to go through an extended dialogue. Support undo and redo.
- Flexibility and efficiency of use: Accelerators - unseen by the novice user- may often speed up the interaction for the expert user such that the system can cater to both inexperienced and experienced users. Allow users to tailor frequent actions.
- Aesthetic and minimalist design: Dialogues should not contain information which is irrelevant or rarely needed. Every extra unit of information in a dialogue competes with the relevant units of information and diminishes their relative visibility.”
Each of the criterion was assessed with a value form 1 to 5, with 1 being the worst and 5 the best, and since five criteria were used, the maximum possible score was 25
At the evaluation criteria considered by the students of IPO there were mainly overseen aspects related to the operational features of the application usability, rather than its

appearance.
Usability, as it was stated, relied mostly in the architecture of the application, in the definition of its subroutines, in the manner in which the user could log in, and in respecting logical sequences in the interaction between user and application.
It is the aesthetic appearance the criterion that presented bigger differences in its definition, as IPO criteria were not including any of the aspects taken into consideration in DGyC assessment.

3.2 – Evaluation criteria of DGyC subject

The brief of the practice of DGyC included the definition of the topics that were going to be evaluated and the weight of each one in the final mark obtained. These criteria were:
"1. The depth of forethought and research made that will define the concept to further develop and the adequacy of the message to be transmitted (5%).
2. The innovation and creativity of the different concepts raised (5%).
3. The application of the main idea, the graphic quality and the formal development of the imagotype, symbol or logo (40%).
4. The usability of the warning screen for the patient (25%).
5. The usability of the screen to the medical professional or family member, to load the data into the system (25%)."
It was as well explained in the brief that the project chosen by a group of IPO students would upload half point over the overall rating.
Communicating the particular issues that were going to be evaluated was meant to help maximizing the outcomes of students´ endeavours.
The value assigned to each criterion in the final assessment relied on experience with other work carried out on the subject. It was also pretending, through the different relevance allocated, clarify the domains which were intended to centralize the biggest amount of work on the course.
The development of the brand image, embodied in the imagotype, symbol or logo, is the highest score. The design of the two screens of the application was, on the whole, the part of exercise with greater importance in the evaluation, as usability was the characteristic in which was pretended to act more specifically in this drill.
When speaking about usability, to measure the following items was undertaken:
- The proper symbology, good readability and efficiency in conveying a message.
- The graphical coherence with the trademark.
- The adequacy of composition, considering the balance, proper hierarchy and easy interpretation of every element.
- The integration of the study of graphics perception by the user into the proposed solution.
These factors were measured and valued by the appearance the interface had.

3.3 – Comparison of the evaluation criteria

The set of criteria used by students of IPO in their assessment considered especially the usability aspects that have been previously exhibited.
Analyzing in detail each of them, it could be discovered however that "Visibility" and "Match With the Real World" comprise aspects shared with the specific usability issues considered in assessing DGyC, like the readability or the use of a proper symbology.
It was "Aesthetic" the one showing more differences between evaluations, as an outcome of the comprehensive approach developed both in the subject of DGyC and in the Degree of which it belongs to. Thereby, the application of the term "minimalist" in the way used by students of IPO is a bit puzzling in this context, since its connotations for DGyC students are broader than those outlined in the evaluation criterion of IPO.
What could be seen by confronting the evaluation criteria was that this practice provided the teachers a new and interesting focal point on the work approach. The spotlights of the IPO students evaluation took into consideration aspects overflowing the interface appearance, like the possibility of using accelerators. Thus, it was provided information to DGyC Teachers about elements that could be heeded on their own assessment as way of improving the design of the screens, and making the performance of the application more clear for users.
On the other side, the assessment made by DGyC teachers gave more relevance to aspects related to graphic composition of the visual appearance of the interface, which provided a view that could enrich the perception of the IPO students.

4- Benchmarking

To make the comparison between the assessments reached by the students of IPO and the evaluation of teachers of DGyC, two representative examples of the detected different criteria used were chosen.
Firstly, it should be highlighted that the maximum number of times a DGyC practice held as the best by IPO students was up to three times, then the mark of the work of students of DGyC was increased, in the best case, by 1.5 points. This circumstance appears to indicate that there was a homogeneous level in the practices developed.
Secondly, the works of DGyC which were elected by the students of IPO were generally well rated by the teachers, but there were differences between the marks assigned by each of the parties. Those cases in which the differences were bigger were the ones that brought more information, and two of them are explained below.

4.1 – Example of a work better rated by DGyC teachers than by IPO students.

This first exercise consisted of an application for young women that proposed, as main objective, to control the administration of contraceptive pills. The application was called "Pillina", wordplay between the word "Pill" and the significance of the word in Spanish language, which stands for a kind of female scamp or rascal, but in a loving sense.
The imagotype design for the application (Figure 2) comprises the silhouette of a woman standing near the first letter of the logo, capital P, all in pink. And the logotype is the name of the application, "Pillina", with the first four letters in pink and the last three ones in light gray.

Figure 2: "Pillina" Imagotype

The application was designed for a market niche, and for a specific group of customers. The colors, symbology, typography, message and composition of the imagotype was considered by the DGyC teachers quite appropriate for the customers that was planned for, and for that reason it reached a 7 out of ten in the corresponding section.

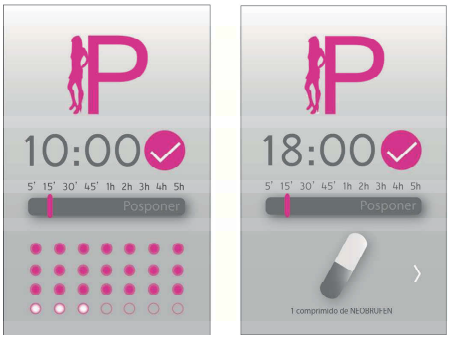

Figure 3: Pillina Warning Screen.

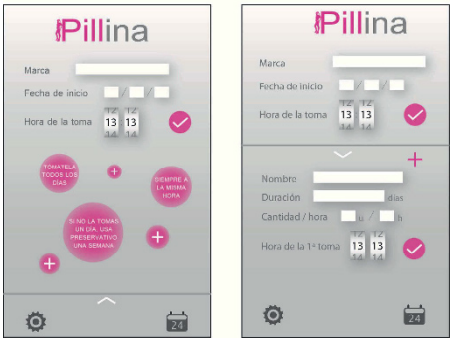

Figure 4: "Pillina" screen for charge of data.

In designing the requested screens, main design aspects well used in the imagotype remained. The warning screen (Figure 3) changed depending on the kind of pill that had to be administrated, offering either a calendar of the contraceptive pill or a picture of a medication and its name.
These screens were considered very well designed as a whole, and a 9 out of ten was assigned to this section.

The designed screen for charge of data (Figure 4) had more information, but kept the same graphic and design references used both for the imagotype and for the warning screen. However, it presented some composition problems, such as lack of order in the way the pink bubbles that contain information were disposed, the different place in which the Imagotype appeared in the screen depending on the information shown or the position of the "tick" symbol.
For all those reasons, this part of the labour was rated by the teachers of DGyC with a mark of 7 in this section.
In the evaluation made by students of IPO - twenty one groups evaluated the papers - no one of them considered this as the best one. And only two of the twenty one, i.e. only 9,5% of the groups, considered it as one of the top five.
If we examine in detail the assessment made by IPO students regarding the five criteria considered (Table 1), it could be found that the grades given by every group were not fairly uniform, with an average of each section ranging from 2,86 to 3,14. And the best rated criteria were "Visibility" and "Aesthetic", which matched to those indicated as more related to the ones used by teachers of DGyC in their assessment.

nº	Visibility	Match	User control	Flexibility	Aesthetic	TOTAL
1	1	1	1	1	1	5
2	3	3	3	3	3	15
3	4	5	4	4	4	21
4	3	2	3	3	2	13
5	4	4	3	4	5	20
6	4	3	4	3	4	18
7	3	3	2	3	3	14
8	2	2	3	2	3	12
9	4	2	1	2	4	13
10	4	3	2	2	4	15
11	4	4	4	3	3	18
12	2	1	2	4	4	13
13	3	4	3	4	4	18
14	3	4	3	3	3	16
15	1	1	1	1	1	5
16	4	2	5	4	4	19
17	2	2	2	2	2	10
18	4	4	4	4	4	20
19	4	4	4	4	4	20
20	4	3	4	3	1	15
21	3	3	4	3	3	16
TOTAL	3,14	2,86	2,95	2,95	3,14	15,05

Table 1: Evaluation table of "Pillina" by IPO pupils

4.2 – Example of a work better rated by IPO students than by DGyC teachers.

Among the projects better rated by students of "IPO" than by teachers of DGyC perhaps the most significant was the one that developed an application called "mymed", because it was in general highly regarded by the students of IPO, even being chosen as the best three times. Moreover, in 12 of the 21 cases, i.e. 57% of the IPO groups, considered this work as one of the top five.
The proposed Imagotype (Figure 5) comprised the symbol, a tablet with a clockwise over its surface within a box, and the logotype located beneath. The primary color was light green similar to the one of the medical gowns, used both in the symbol and in the logotype, written in black and green.
As a whole, the developed Imagotype was considered less interesting, worse graphically and formally developed, and less innovative, so that its valuation was lower, obtaining a score of 6.5 in Imagotype rating.

Figure 5 "mymed" Imagotype

The warning screen of this project (Figure 6) presented a graphical solution similar to the "Pillina" work, using analogous elements, but was rated with a lower grade because it presented certain problems in proportion and hierarchy of information, besides establishing a more simple composition with less provision of data. Nevertheless, since the screen had all the necessary information, and there were no serious errors of approach and usability, earned a score of 7 on this part of the project.

Figure 6: "mymed" alert screen.

The screen for data charge (Figure 7), with more details than the warning one, displayed information in a more orderly manner, the choice of graphic language is more appropriate and the elements were better proportioned, although there were still some mistakes with the hierarchy of the information. This screen was evaluated by the teachers of DGyC with 8.

Figure 7: "mymed" screen for charge of data.

The evaluation by the students of IPO, as already indicated, was significantly better than that of the teachers of DGyC, as can be noted in Table 2.

nº	Visibility	Match	User control	Flexibility	Aesthetic	TOTAL
1	2	3	2	2	2	11
2	4	4	4	4	4	20
3	5	5	4	5	5	24
4	3	2	3	3	4	15
5	3	4	5	5	3	20
6	4	4	5	4	5	22
7	4	5	4	4	4	21
8	3	3	4	3	3	16
9	4	4	2	3	4	17
10	2	2	3	3	2	12
11	3	3	3	3	3	15
12	4	4	4	5	4	21
13	5	4	3	3	4	19
14	4	4	4	4	3	19
15	4	3	4	4	4	19
16	4	5	4	4	4	21
17	5	5	5	5	5	25
18	4	4	5	5	4	22
19	4	4	4	4	5	21
20	3	2	2	1	5	13
21	3	3	4	3	4	17
TOTAL	3,67	3,67	3,71	3,67	3,86	18,57

Table 2: Evaluation table of "mymed" by IPO pupils

The highest rated section was "Aesthetic", and the very positive score earned by this application was quite striking for DGyC teachers, since their evaluation considered that there were facets of composition not properly resolved. Yet this section got the highest overall rating in the assessment made by IPO students.

The explanation probably is connected to the manner that students of IPO understand the "aesthetic" criterion, in the way that conciseness and the absence of unnecessary elements should prevail over aspects of balance, composition and order, characteristics that have been considered by the DGyC teachers.

5- Conclusions drawn from the experience

The initial approach was to develop a drill as a pilot project,

so that the results could be analyzed and applied in future collaborations of multidisciplinary works. Therefore, the work was executed in each subject most of the time in parallel, with few points of contact except for the initial proposal and the final assessment.

Based on the experience gained, and considering the outcomes, the exercise has been quite enriching since it has offered very valuable information to help to close the gap in the way each discipline confronts design of interfaces. Likewise, various aspects of work that can be perfectly performed with a larger level of cooperation between the parties have been detected, such as market analysis or user research. Part of the information that was produced by IPO students in the early phases of their work, like navigation maps, could function as a base for further work of DGyC students, who could focus on improving specific issues taking these maps as a guidance on the operation of the application.

Another consideration for future practices would be the possibility of establishing common criteria assessment over certain issues, such as Aesthetic. It would be desirable that the Aesthetic evaluation performed by the students of IPO took into account more elaborated design criteria, further than the conciseness or the inclusion of irrelevant information. The assessment of DGyC might also incorporate some of the values considered by students of IPO, as "Flexibility" and "User Control".

With a more general perspective, it became clear for teachers that many of the transversal competencies that were intended to be developed were actually strengthened. The contact with teachers and students with different backgrounds for doing the same project, and the competitive factor related to the evaluation made by IPO students, reinforced the working structures of the DGyC pupils approach to the practice, making their work in this practice more deep, thoughtful and adjusted to the final purpose.

Due to the possibilities glimpsed, the experience raised should only be considered as a starting point for future development of authentic experiences of collaborative work, in order to serve students an experience as close as possible to professional world. Thereby we could surpass the bare training syllabus of one specific degree, and allow students to achieve skills that they will need in future, such as being able to understand what is going to be valued or what they are expected to perform when working within a multidisciplinary team.

By participating in this experience, students could face the task of working in the complex domain of interfaces design, being aware that implies many disciplines and subjects and providing them with the necessary skills to be able to contribute productively in the context of collaborative work.

6- References

[C1] Conference of four European Ministers in charge of Education. Sorbonne Joint Declaration, 1998. http://www.eees.es/pdf/Sorbona_EN.pdf

[D1] Diseño gráfico y comunicación-Guía docente. http://titulaciones.unizar.es/asignaturas/25814/contexto13.html

[E1] European Ministers of Education. The Bologna Declaration of 19 June 1999, 1999. http://www.bologna-berlin2003.de/pdf/bologna_declaration.pdf

[H1] Herrero, I., García Berdonés, C., González Parada, E., Molina Tanco, L., Pérez Rodríguez, E., Urdiales García, C. Aprendizaje cooperativo en el ámbito de la ingeniería : una experiencia de iniciación al Trabajo en Grupo, Revista de la Red Estatal de Docencia Universitaria, 2013, Volumen 11, Número especial, Pages : 221-251

[I1] Interacción persona ordenador – Guía docente. http://titulaciones.unizar.es/asignaturas/30217/contexto13.html

[I2] Instituto de Ciencias de la Educación de la Universidad de Zaragoza. Competencias genéricas y transversales de los titulados universitarios. Publicaciones ICE, 2008.

[**M1**] Manchado Pérez, E., Berges Muro, L. Una experiencia de PBL en Grado de Ingeniería de Diseño Industrial, adaptando el método de sistemas de retículas de Diseño Gráfico, Revista de la Red Estatal de Docencia Universitaria, 2013, Volumen 11, Número especial, Pag: 19-46

[M2] Mercovich, E. Ponencia sobre diseño de interfaces y usabilidad: como hacer productos más útiles, eficientes y seductores, 1.999. http://www.gaiasur.com.ar/infoteca/siggraph99/diseno-de-interfaces-y-usabilidad.html

[M3] Ministerio de Educación Cultura y Deporte. La integración del sistema universitario español en el Espacio Europeo de Enseñanza Superior. Documento marco, 2.003.

[N1] Nielsen, J. Usability heuristics for users interface design. Nielssen Norman Group 1995. Disponible en: http://www.nngroup.com/articles/ten-usability-heuristics/

[R1] Romainville, M., Esquisse d'une didactique universitaire, Revue francophone de gestion, 2004, numéro spécial consacré au Deuxième prix de l'innovation pédagogique en sciences de gestion, La Sorbonne, CIDEGEF, Pag: 5-24

[V1] Vanderweerd, J-M., Cambier, C., Romainville, M., Perrenoud, P., Desbrosse, F., Dugdale, A., Gustin, P., Competency Frameworks: Wich Format for Which Target ?, Journal of Veterinnary Medical Education, 2014, Volumen 41, Number 1, Pag: 27-36

[Z1] Zabalza, M.A., Editorial: Formar Ingenieros para el siglo XXI, Revista de la Red Estatal de Docencia Universitaria, 2013, Volumen 11, Número especial, Pages : 9-12

Article 016-e-80

A multidisciplinary PBL-based learning environment for training non-technical skills in the CAD subject

Nerea Toledo [1], Jaime Lopez [1], Pello Jimbert [1] , Isabel Herrero[1]

(1) : EUITI – University of The Basque Country (UPV/EHU)
Rafael Moreno Pitxitxi, nº3, 48013 Bilbao
+34 946014320/+34 946014199
E-mail : {nerea.toledo,jaime.lopez, pello.jimbert, isabel.herrero}@ehu.es

Abstract: Future engineers need to foster technical and non-technical skills to confront global societies' competitiveness in terms of innovative products and solutions. To this end, a multidisciplinary learning environment provides a perfect framework to train the required transversal competences as well as gain expertise in their knowledge area. Following our previous work in teaching innovation for the Graphic Expression subject and more precisely for the CAD part, we have opened the scope of the assemblies students have to address by defining a multidisciplinary project where students from different knowledge areas solve corresponding issues using PBL methodology while they work on a collaborative environment. With this initiative we expect that students train non-technical skills and get acquainted with coordination, teamwork and meeting methodologies, and therefore, get accustomed to labour reality dynamics.

Key words: PBL, CAD, multidisciplinary projects, teaching innovation, skills

1- Introduction

The main goal of the Bologna Process which begun in 1999, was to put in place by 2010 the European Higher Education Area (EHEA) strengthening the competitiveness and attractiveness of European higher education by means of fostering social dimension education, employability, mobility and student-centred learning [B1]. These priorities have raised the suitability of traditional teaching methodologies to accomplish the demands not only of the EHEA but also of the current tough labour market. In this regard, The University of The Basque Country (UPV/EHU) has developed a student-centred dynamic and cooperative learning-teaching model named IKD (Irakaskuntza Dinamiko eta Kooperatiboa) [I1] that promotes active learning methodologies such as PBL.

PBL is an active student-centred learning-teaching methodology where students go through an extended process of inquiry in response to a question, problem or challenge [M1]. In the PBL methodology, students follow the "learning by doing" concept working on a collaborative environment in order to gain not only specific knowledge but also the 21st century skills, which are also known as the 4Cs: critical thinking and problem solving, collaboration, communication, and creativity and innovation [P1].

Since engineering is an applied science, where basic scientific knowledge is put at the disposal of a specific technological application, products and solutions to address the needs of the global competitiveness are expected to be designed under a versatile environment that encompasses different knowledge areas or disciplines. Owning to this issue, future engineers are expected to improve their knowledge and train their technical and non-technical skills in interdisciplinary environments.

In this paper, we present the approach of our action, which has the aim of defining a multidisciplinary learning environment to bring closer the real labour reality to the students in the Graphic Expression subject using the PBL methodology that has been specially promoted in engineering education [L1], and specifically in teaching computer-aided design (CAD), in order to cover industrial design competences, software skills and the 4Cs.

The rest of the paper is organized as follows. Section 2 describes the motivations that have triggered our work and the goals we seek with it. In Section 3, we describe the multidisciplinary learning environment we have created, and we introduce the specific project that our students are developing. Section 4 presents the followed methodology and the evaluation system that accommodates the new learning framework, and in Section 5, we present the future work we are planning to accomplish and last section describes the concluding remarks of this work.

2- Motivation and goals

With the global society and the current trends in competitiveness, engineers are expected to master a

combination of skills embracing not only technical and technological skills concerning efficient problem-solving and innovation of technology, but also transversal skills like communication, cooperation and creativity competences that have to put in practice especially in interdisciplinary environments. This issue puts the responsibility in the court of education, where new teaching methodologies that cover the demanding skills have to be implemented.

In engineering education, the Graphic Expression subject constitutes a pillar for providing graduates with the basic knowledge of graphical representation, dimensioning and standards. Hand-drawing and paper blueprints have been replaced with CAD tools which have revolutionized engineering and industrial design and so, these have been introduced in the Graphic Expression subject. Owing to this fact, knowledge on CAD has turned into an essential part of the Graphic Expression subject.

Up to now, in our Engineering School, the goal of the CAD subject has been to teach students to gain software skills. First the potential of CAD and of a specific software (Solid Edge in our case) is presented to the students, to afterwards conduct exercises where the presented functionalities are applied. Complex mechanical assemblies are also represented by the students to learn advanced operations of the tool. Due to the complexity of the assemblies these are solved in team, which helps the students to gain teamwork competence.

Teachers provide a number of assemblies to solve, from which students select one. Recently, we have included the option to select an assembly out of the ones specified by the teacher in order to motivate the students with their projects. Next, some of the projects selected by the students are shown:

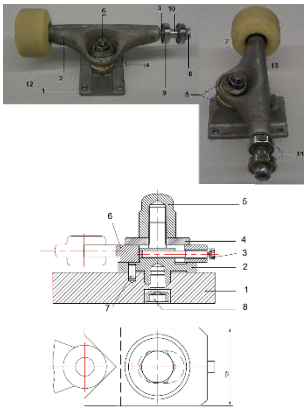

Figure 1: Selected assembly projects

Since the assemblies like those shown in Figure 1 are completely defined and the students are requested to represent them in the CAD tool, students do not train creativity not problem solving, which are critical skills that a competitive engineer should master. Moreover, no relation with other knowledge areas is established when solving this kind of assemblies which is envisioned as a disadvantage of this methodology.

The introduction of PBL in the CAD subject may aid in providing students with the demanded skills and a suitable context for defining a challenge that requires the work of different knowledge areas. In this regard, there are different experiences that have demonstrated that PBL outperforms traditional teaching methodology [G1-M2] when teaching CAD. In fact, PBL is a long tested methodology that has been particularly promoted in engineering teaching [P1], since it is expected that it will provide graduates with the required skills for confronting the challenges that current and future society presents.

Considering previous actions introducing PBL in the CAD subject or in related ones, and as a result of a work that we begun with the SimABP project [T1] (a project funded by the University of The Basque Country), we have opened the scope of the projects that students have to address by defining a multidisciplinary environment across the different degrees taught in our Engineering School [E1]. This way, we intend to introduce the students to real work that an engineer is expected to perform in its career, and foster non-technical skills that these environments demand. That is, our aim is to bring closer the work experience to students based on PBL in the CAD subject in order to provide students a context to train also non-technical skills.

To this aim, we are currently collaborating with teachers from other knowledge areas to define an integral, interdisciplinary learning context. Therefore, our action has the following goal:

Provide first year students an environment that builds a framework where different knowledge areas are present to simulate a working experience in order to train technical knowledge together with the transversal skills. Specifically, students will gain software skills, problem solving by addressing the challenge proposed and creativity and innovation thanks to the openness of the solution. Moreover, collaboration and communication skills will also be covered by teamwork and meetings among the involved parties, creating an enriched learning scenario.

3- A multidisciplinary PBL-based learning environment for the CAD subject

Following the satisfactory results we obtained in the SimABP project, which is the precursor of the approach presented in this paper, and has triggered this ongoing work, Graphic Expression teachers have decided to create a multidisciplinary collaborative environment together with teachers from the Electronics discipline.

The goal of this environment is to have multidisciplinary student teams working together on a single project, where each team addresses the aspects related to their specific knowledge area. This way, students can envision all the

aspects that the design of a specific technological product concerns as well as deal with the technical problems raised related to their expertise.

In the current teaching year, teachers from both disciplines have agreed on formulating a project that has the goal of designing and implementing a lantern or a lamp. Students from electronics should address the concerns related to the led switching circuit, while students from graphic expression should design a skeleton to protect the circuit. This way, the entire product will be designed in the project, and hence, a more ambitious work and with a major scope can be accomplished jointly.

To that end, students from electronics address the project proposed in their subject, named *Tecnología Electrónica* and taught in the third teaching year, to design and implement a circuit that turns on a led when the switch is in on position. Figure 2 shows a circuit designed by the students.

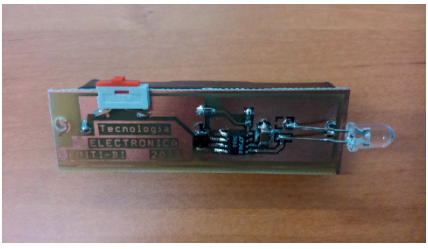

Figure 2: A circuit designed by students from electronics

In the same way, students from the Graphic Expression subject, which is taught in the first teaching year, have to complete the project by designing a skeleton beginning with the circuit developed by the students from electronics. It is necessary to underline that the design that first year students can work out does not imply manufacturing process selection or material selection but the scope of the design is limited to form and dimensioning. This is because subjects where manufacturing processes are taught are later seen in the degree, so the work we present here can be considered as students' first approximation to industrial design.

The designed skeleton has to protect the circuit while resulting in a simple, easy to manipulate and ergonomic design. At the same time, it has to fulfil the product specifications. In order to do so, Graphic Expression students have to consider the dimensions of the different elements (led, battery, microprocessor, etc.) to work out their design, which are defined as design requirements by the students from electronics. Students will follow the design methodology described in [L2], which has been developed for this aim. Hence, they should begin sketching their conceptual design in paper to afterwards detail it.

Once the conceptual design is detailed students have to properly draw the design they worked out in the CAD tool using drawing standards and regulation. The blueprints created by the students will be used to prototype the skeletons and further joint with the electronic programmable badge where circuit is implemented.

In conclusion, what we propose to the Graphic Expression subject students is creativity, innovation and problem solving by accomplishing the specifications for completing the design and software skills in the use of the CAD tools, together with drawing regulation correctness.

With this collaborative environment we expect that students will gain expertise in their specific field while they learn to work on a multidisciplinary environment to train the different technical and social aspects that have to be addressed in the overall process of a specific product definition. It is worth pointing out that we expect that students from the Graphic Expression subject from the first teaching year will gain expertise from the students from Electronics that are in third year. We envision that learning between students from different years will be more productive because they are in a more relaxed environment than in that where the teacher is present.

Moreover, since meetings are required between the students from the different disciplines to develop the project in order to describe the requirements and control the progress, we expect that students get acquainted with work meetings and coordination issues beginning from their first university year. In fact, this work dynamic can be further encompassed in project management methodologies, which opens the door to the introduction of the Project Management subject to the playground, which is taught in the last teaching year. Consequently, we envision a large number of working groups among all the disciplines, different teaching years, and even different degrees that can be established to define enriched collaborative environments for engineering students of our school.

One of the most critical issues foreseen in this initiative is the coordinated work that these kind of multidisciplinary projects require. Although this environment could result appealing not only for the students but also for the teachers, we are fearful due to its coordination complexity. Nevertheless, we have defined a constraint planning with specific milestones for the work that teachers and students have to complete to control the development of the projects and detect possible problems or deviations.

4- Methodology

In order to gain the essential skills to develop the project, the potential and the features of the CAD subject are first introduced in class. Then, students work out individual exercises to train the introduced software operations. This way, we guarantee that students gain the required basic knowledge to be able to address the challenge proposed. Individual exercises represent the 50% of the classroom hours, but they are intended to be the 30% of the working hours of each student of the CAD subject, while project hours are expected to be 70%. It is worth mentioning that the CAD subject is part of the Graphic Expression subject taught

throughout the entire first teaching year. Specifically, the CAD part is taught in the laboratory in the second semester while students still attend master classes to learn drawing standards and representation issues.

During the development of the project, students work in teams of three in order to ensure positive interdependence and collaboration among them. With the goal of guaranteeing proper communication between students from electronics and from Graphic Expression and teachers from the different disciplines, a forum is being developed in the Moodle platform to post queries, comments and exchange information. Additionally, meetings are established to coordinate the work between students from the different knowledge areas and control the progress of the work. This way, discussion as well as collaboration and communication skills will be promoted.

As part of their work, students are requested to store all the work they are developing, from preliminary ideas to the detailed sketches of the solution adopted. In the same way, the working groups have to collect the minutes of the meetings, the action points and the people in charge of them. These working documents will also be used to evaluate the students.

In order to monitor continuously students work, a planning has been defined with specific milestones that allow teachers to supervise the development of the project. That is, the teacher interviews each team in class to know the level of fulfilment of their scheduling and to be aware of the problems they might be facing. Apart from active monitoring in class by the teacher, students are requested to store all the drafts, notes, etc. they develop during the project to analyse not only the work in class, but also the work outside the classroom of each team.

4.1- Trained competences

The CAD subject has learning competences that are classified in two different groups: specific competences and traversal competences. Specific competences are mainly related to CAD software learning. In addition, students will train spatial ability to solve graphical problems and train creativity, and will also learn graphical representation standards to interpret and draw normalized blueprints. Regarding traversal competences, students will train the teamwork competence.

4.2– Evaluation system

Having modified the approach of the subject, the evaluation system has also been modified accordingly. Specifically, the goal of the evaluation system is to assess software skills, along with the non-technical skills our initiative seeks. The evaluation system then, consists on the following aspects:

- *Software skills:* We evaluate this aspect by the individual work performed by each student through the exercises and with the team work conducted to produce the assembly in the project.
- *Critical thinking and problem solving:* We evaluate this aspect by assessing the design of the assembly produced and evaluating the fulfilment of the specifications.
- *Creativity and innovation:* Thanks to the openness of the challenge, each team will work out different ideas. We evaluate the creativity and innovation of the students by evaluating the ideas and solutions students conceive in the development of the project.
- *Collaboration and communication skills:* We assess this skill by supervising classroom teamwork, along with the presentation and defense of the solution in the end of the teaching year. In addition, the client is also queried about the communication skills of the students in the meetings.

Regarding software skill evaluation, it should be noted that since the aforementioned individual exercises are part of the evaluation system, each student is given an individual mark, which makes certain that the overall score will be weighted with the mentioned individual work, and not shaded with the overall work of the team. By doing so, we guarantee that the evaluation of each student is directly related to his/her work, as well as assure that the required knowledge is gained by each student.

4.3- Expected learning results

With this multidisciplinary learning environment we expect that the students not only gain the competences presented in section 4.1. but will also develop additional non-technical competences like critical thinking, creativity and innovation and collaboration and communication skills.

Furthermore, we expect that students from both Graphic Expression and Electronics disciplines will find the need to define clearly technical specifications to work out the design. On the other hand, since cooperative work is required we expect that students will also learn project management dynamics. At this point, it is important to underline that this multidisciplinary learning environment is developed in the first degree year, which is not common due to the difficulties this issue implies. Consequently, with this innovative experience we provide to the students a means to interrelate different subjects from the degree which we consider is an important concern to gain the required maturity and understanding.

5- Future Works

The results of the performed SimABP project [T1] have leaded us to define an advanced learning environment that comprises different knowledge areas in the development of a single project. More specifically, the SimABP project has resulted in an excellent initiative to present our innovative approach to other teachers in the entire curricula of the different degrees our Engineering School offers. In fact, the work done up to now, has triggered the establishment of relationships among different disciplines and departments to generate innovative project that let students train technical and non-technical skills.

Currently, we have defined a multidisciplinary learning environment with teachers from the Electronics area, but it is expected that we will establish extensive ties with teachers from Mechanics, Electricity, Chemistry and even Project Management since they have already expressed their interest in doing so. Owing to this success, students from the Graphic Expression subject of the first teaching year are expected to work as a cornerstone of the development of the wide variety of the projects that are developed in our school. In other words, our students will act as design and drawing producers for different consumers or even as partners in a specific project. Therefore, Graphic Expression students and teachers will aid in rounding the outcome of the overall project.

Note that although the project is confined in the university arena, companies interested in this work could also be potential clients. With the goal of promoting this aspect of the university, we are also planning a visiting day for the companies.

6- Conclusions

Having observed the needs that future engineers have to address when developing their careers, and aligned with the student-centred dynamic and cooperative learning-teaching model our University is promoting, we observe that enriched learning environments are required for our students. Hence, methodologies similar to PBL are requested to be introduced in class to encourage active learning-teaching methodologies.

The proposal this paper presents, has been triggered as a result of the satisfactory results we obtained in our previous innovative project, named SimABP [T1]. The goal of the SimABP project was to bring closer labour reality proposing to the students a real challenge which they solved designing and modelling a mechanical assembly. This time, we decided to define a multidisciplinary environment with teachers from the Electronics discipline to define an integral project that encompasses third year students from electronics, and first year students from the Graphic Expression subject. This way, each student group solve their own challenge, while they work on a collaborative environment to address the issues of their own knowledge areas. More specifically, the goal of the Graphic Expression students is to work out a simple skeleton design (forms and dimensions) for a lantern or a lamp that students from Electronics have designed and implemented. Once the skeleton is designed, they have to put in practice and use drawing standards and regulation to properly create the blueprints of their solution in the CAD software tool. The entire process is completed following PBL methodology.

It is worth pointing out the learning environment presented in this paper generates the perfect framework to train technical skills related to the different knowledge areas while it presents a suitable scenario for training non-technical skills as well as an appropriate context to gain labour reality dynamics. With this collaborative environment we expect that students will gain expertise in their specific field while they learn to work on a multidisciplinary environment. Moreover, we envision that students will get acquainted with work meetings and coordination issues beginning from their first university year, which will help in their careers.

We are planning to open our proposal to other subjects from different knowledge areas that have already expressed their interest and also to companies that could be interested in CAD modelling. This way, we will enrich the presented multidisciplinary PBL-based learning environment and have qualified engineers.

7- Acknowledgements

This work has been funded by the Vicerectorate of Quality and Teaching Innovation of The University of The Basque Country (UPV/EHU) through the PIE project initiative [P2], and it has been produced within the Training and Research Unit UFI11/16 [U1] supported by the UPV/EHU.

8- References

[B1] Bologna-process – European Higher Education Area. *http://www.ehea.info/*

[E1] Escuela Universitaria de Ingeniería Técnica Industrial de Bilbao – EUITI (UPV/EHU). http://www.industria-ingeniaritza-tekniko-bilbao.ehu.es/p229-home/es/

[G1] Garikano. X., Osinaga, M., Garmendia Mujika, M., Perez Manso, A., "Problem-based learning, implementation and qualitative study in computer aided design subject", INTED2011 Proceedings, pp. 1305-1314

[I1] IKD-Irakaskuntza Kooperatibo eta Dinamikoa *http://www.ikasketa-berrikuntza.ehu.es/p272-shikdct/es/contenidos/informacion/ikd_educacion_activa/es_educ/educacion_activa.html*

[L1] Lehmann, M., Christensen, P., Du X., Thrane M. "Problem-oriented and project-based learning (POPBL) as an innovative learning strategy for sustainable development in engineering education", *European Journal of Engineering Education*, 33:3, 283-29, 2008

[L2] Lopez, J., Toledo, N., Jimbert, P., Herrero, I., Caro, J.L. "CAD con Solid Edge. Resolución de conjuntos basada en PBL", OCW, ISSN: 2255-2316

[M1] Markham, T., Larner, J., Ravitz J., "Project Based Learning Handbook: A Guide to Standards-Focused Project Based Learning for Middle and High School Teachers" *Buck Institute for Education*, ISBN-13: 978-0974034300, 2003

[M2] Marquez, J.J., Martinez, M.L., Romero, G., Perez, M., "New Methodology for Integrating Teams into Multidisciplinary Project Based Learning", *The International Journal of Engineering Education,* vol. 27, nº 4, pp. 746-756, 2011

[P1] The Partnership for 21st Century Skills. P21 Mission: *http://www.p21.org/*

[P2] Convocatoria de Proyectos de Innovación Educativa PIE 2012-2014. Vicerrectorado de Calidad e Innovación Docente (UPV/EHU).

http://www.ehu.es/ehusfera/helaz/2012/10/15/hpb-2012-14-ardirako-deialdia-convocatoria-pie-2012-14/

[T1] Toledo N.; Lopez J.; Herrero I.; Caro J.L.; "Simulating a work experience in the Graphic Expression subject. Project-based learning as the enabler", *International Conference on Education IADAT e-2013*, July 2013

[U1] Convocatoria de Concesión de Ayudas a las Unidades de Formación e Investigación en la UPV/EHU. Vicerrectorado de Investigación (UPV/EHU).

http://www.ikerkuntza.ehu.es/p273-content/es/contenidos/ayuda_subvencion/vri_ufis/es_vri_ufi/vri_ufi.html

Article 017-e-92

DESCRIPTIVE GEOMETRY 2.0

Javier García Mateo[1], Fernando Lara Ortega[2], Lara García Calvo[3]

(1) : Superior Polytechnic School Burgos (Spain)
Phone 34947258020/Fax 34947259478
E-mail: jgmateo@ubu.es

(2) : Faculty of Humanities and Education
Phone 34947258072Phone/Fax34901706977
E-mail: flara@ubu.es

(3) : E.T.S.A.Madrid
34685469492
E-mail: laragc9@gmail.com

Abstract: Both plane and spatial graphic geometry are allotted fewer teaching hours in Spanish study plans. This reduction in hours applies equally to traditional methods and to the incorporation of technology, in the form of CAD programmes, which facilitate operations and precision in the study of this discipline. We shall present the example of the Civil Engineering qualification at Burgos University and will moreover show the way we have adapted to these changes, trying not to weaken the capabilities of our future professionals. We shall demonstrate how spatial vision capabilities are developed in similar ways using classic procedures from descriptive geometry and the spatial constructions that 3D CAD offers us.

Keywords: Descriptive geometry, spatial visualization, education

1- INTRODUCTION

With the adaptation of qualifications to the Bologna process, a new reduction in teaching hours has taken place in the "Descriptive Geometry" subject module, which incorporates knowledge of CAD in addition to the traditional topics.
It is a subject module that requires a great deal of effort and dedication from students, as it requires structured spatial thought. Graphic language has hardly been studied in previous educational courses, where much greater emphasis is placed on written and numerical thought processes.
We have had to adapt the subject module to continue exacting the knowledge and skills related to problem-solving and spatial visualization skills that are expected of a professional engineer trained at university. To do so, we have maintained the classic exercises in spatial geometry, but these are now solved in a virtual three-dimensional space provided by a specific CAD programme that will not automatically solve every problem.

2- BACKGROUND

Recently, a new change has taken place in the study plans of Spanish Universities, in order to adapt the qualifications to the Bologna process and to structure them into degrees, masters and doctorates (RD 1393/2007). The requirements have subsequently been established for the validation of official academic awards that qualify students to work in certain professions, which in our case are: *Ingeniero Técnico de Obras Públicas* [Technical Engineer of Public Works] and *Ingeniero de Caminos, Canales y Puertos* [Engineer of Roads, Canals and Ports] (Official Bulletin of State 42/2009). The specific competence of the qualification (CE5) for Graphic Expression is as follows:
"Spatial vision skills and knowledge of the techniques of graphic representation, by traditional methods of metric geometry and descriptive geometry, as well as through CAD applications."
The same competence applies to all Spanish engineers and architects and is acquired along with other general degree-related competences specific to the qualification, as well as instrumental, personal, systematic, transversal and academic competences.
In concrete, the evolution of graphic expression at the University of Burgos, within the scope of civil engineering has been as follows:

Subject Module	Year	Term	Cred.	hr/wk
Technical Drawing	1st	1+2	15	5
Systems of Representation	2nd	1+2	15	5

Tab. 1: 1972 Plan

Subject Module	Year	Term	Cred.	hr/wk
Techniques of Representation	1st	1	6	5
Applied Geometry	2nd	1	7.5	5
2D CAD (optional)	1st	2	4.5	3
3D CAD (optional)	3rd	1	4.5	3

Tab. 2: 1998 Plan

Subject Module	Year	Term	Cred.	hr/wk
Techniques of Representation	1st	1	6	4
Descriptive Geometry	1st	2	6	4

Tab. 3: 2010 Plan

Article 017-e-92

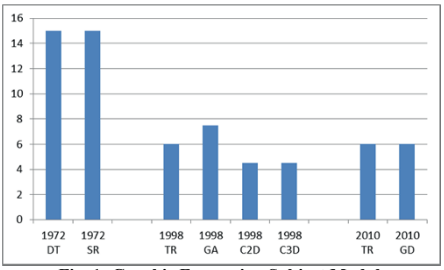

Fig. 1: Graphic Expression Subject Modules

The reduction in teaching hours is equal to 60%, in comparison with the 1972 plan, and to 50% in comparison with the 1998 plan.

3- DESCRIPTIVE GEOMETRY AND 3D CAD

As shown above, the teaching load dedicated to graphic expression has been drastically reduced over a few years. In addition, the need to incorporate CAD into their teaching has been evident to teachers over a number of years. We decided not to reduce the time given to ordinary classes and, in 1992, started to give extra classes, offered freely on a voluntary basis to teach students 2D CAD, in addition to the timetabled classes.

Subsequently, in accordance with the 1998 plan, the students chose the 2D CAD optional subject module and to a lesser extent the 3D CAD module.

Traditional Descriptive Geometry classes along with a few CAD classes, but with no links between their respective contents, was taught in the current plan, which took effect in the 2010/11 academic year. As the time available for the subject module meant these separate modules were no longer feasible, it was decided to integrate 3D CAD and Descriptive Geometry and to conduct an experiment with two groups: an experimental group and a control group. The experimental group followed the new learning module.

We selected the AutoCAD programme, because our students had already worked with it over the first term (on the "Techniques of Representation" module), and because it is one of the most widely used programmes at a professional level, it is precise and because the 3D work is yet to become highly automated, making it ideal for academic use.

The conventional curricula content was similar to courses at other universities and was structured into 12 topics, to each of which we dedicate about one week.

In the first topic, we look at the fundamentals of systems of representation, the concepts of slope and modulus, membership, intersection, parallelism, perpendicularity and distance between simple elements (point, straight line and plane). In the second, we look at three dihedral operations and their operations and applications. Topic 3 concerns itself with the angles between straight lines, planes and straight lines to the plane. Topic 4 is taken up with the study of prismatic and pyramidal surfaces, their projections, transformations, the intersection of plane sections with straight lines etc. In Topic 5, we go over regular polyhedra of similar forms. Topics 6, 7 and 8 are dedicated to cylinders, cones and other surfaces. In Topic 9, we study surface intersections. In Topic 10, roofs with curved surfaces, as flat surfaces are also studied as part of the intersection of planes in the first week. In Topic 11, we study soil levelling, longitudinal and transversal profiles and material assessment. Finally, we finish with Topic 12 on cylindrical and conic shadows.

To do so, around 25 hours of theoretical classes and a further 25 hours of practical classes are used and students are given some basic 3D CAD instruction on the virtual platform and 107 exercises with answers and explanations, three of which are presented here as examples. These are classic exercises of descriptive geometry.

Example 1.- *Topic 5. Problem 6.* Point **A** is the vertex of a cube contained in the first dihedron with a 6 cm. edge, which the student is asked to represent. The three concurrent edges at point **A** are horizontally projected along **A'M'**, **A'N'** and **A'L'**. A(90.70.0), M(130.10.-), N(100.130.-), L(30.50.-).

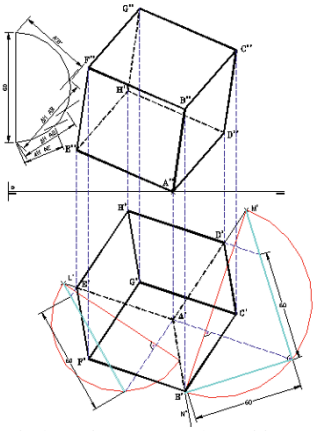

Fig. 2: Topic 5. Problem 6. Traditional

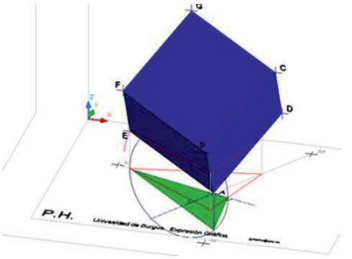

Fig. 3: Topic 5. Problem 6. Virtual 3D model

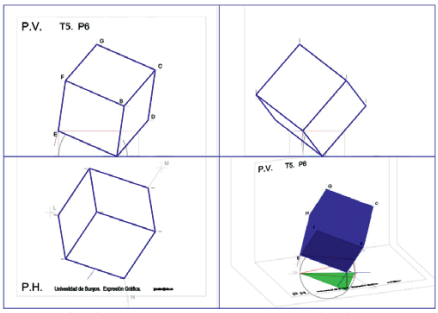

Fig. 4: Topic 5. Problem 6. 3D projections

In this exercise, manipulation is slightly simpler when working directly in the virtual 3D space, but the exercise is a clear example of the need for traditional geometric knowledge to be able to understand it and solve it.

Example 2.- *Topic 8. Problem 7.* **M** is the mid-way point on edge **AB** of a regular tetrahedron, while edge **CD** is found on the straight line defined by points **X** and **Y.** The student is asked to represent the polyhedron along its projections, as well as the four spheres inscribed within it and tangent to each other. The spheres must be visibly represented as if the tetrahedron were transparent. M(40.30.50); X(40.120.70); Y(130.30.70).

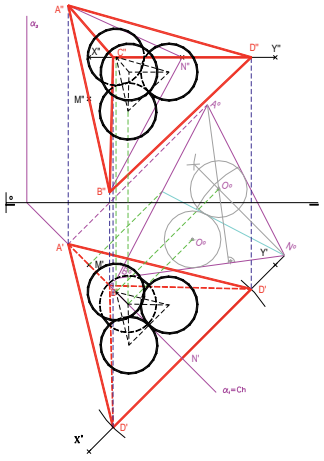

Fig. 5: Topic 8. Problem 7. Traditional

In this exercise, the solution with a software programme that works directly in the virtual space does not have too many advantages, because the position is very favourable in the traditional system. However, a good arrangement of the elements is of less importance in the computer model when facilitating the task. It could also have been solved in another way in both systems. The displacements, rotations and the scaling are undoubtedly of lesser difficulty in the virtual space.

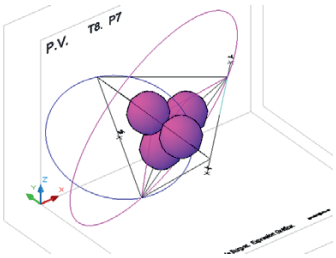

Fig. 6: Topic 8. Problem 7. Virtual 3D model

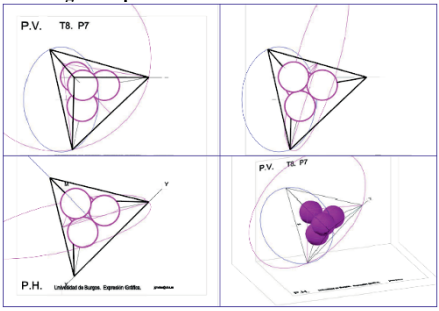

Fig. 7: Topic 8. Problem 7. 3D projections

Example 3.- *Topic 10. Problem 10.* Define the roof of the figure, knowing that all the roofs are sloped at 45º. The lines of the eaves are at 10, 11 and 12 metres, and the circular curve is the equator of a hemisphere. The side elevation of the roof is also represented. The scale of the drawing is 1:250

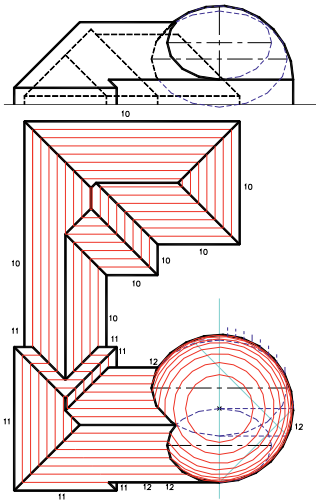

Fig. 8: Topic 10. Problem 10. Traditional

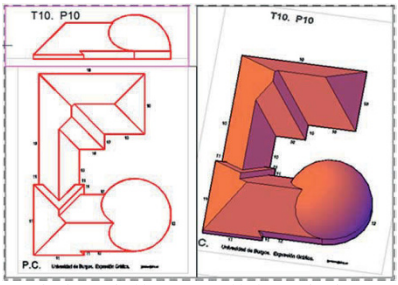

Fig. 9: Topic 10. Problem 10. 3D projections

In the topic on the definition of the roofs, the traditional method based on horizontal planes may possibly be simpler, if it involves sloping roofs or contour lines if there are other surfaces to consider. Nevertheless, to define a roof using solids, with sweep profiles, Boolean operations, etc. demands, in our opinion, considerable effort and is therefore an excellent task to broaden spatial vision.

4.- EXPERIMENTAL PROJECT, SPATIAL VISION

The group that participated in the experimental project was limited to the Escuela Politécnica Superior [Superior Polytechnic School] of the University of Burgos. The experimental project was completed with students from the "descriptive geometry" subject module in the first year of an Engineering Degree in Road Technologies during the 2011/12 academic year.

The methodology consisted of giving the theory classes jointly to all of the students (from the two practical groups: both the experimental and the control groups). By doing so, the basic competence of the subject module was taught to students in the experimental group. In the practical classes, students were separated into two subgroups, one of which answered the problems in the traditional way (the control group using the traditional methods), and another group solved those same exercises with the 3D CAD programme (experimental or CAD group).

At the start of the course, a pre-test was given, followed by a post-test consisting of the MCT Mental Cutting Test [C1], DAT Differential Aptitude Test [BS1] and MRT Mental Rotation Test [VK1], to test for improvements in spatial vision. The equivalence between both groups was tested with four variables, the three pre-tests mentioned above and the grades from their academic records. The Kolmogorov-Smirnov test was used, with the Lilliefors test and the Shapiro-Wilk correction factor, showing normality for both groups, with a significance of over 0.05 in all cases. This result indicates that the groups were equivalent.

The evaluation consisted of four tests (20% of the grade for each one) of two exercise of equal difficulty, similar to those completed in the practical sessions. The same exams were given simultaneously to both groups. 20% of the mark was given for participation in the classroom or, in some cases, for an assignment consisting in a model, discussion of the plans of a technical project or study and the solution of a social geometric problem.

The results of the experimental project were as follows:

- All the students improved their spatial vision in a significant way.

The average improvement was 9.11 points (14%) in the MCT test, 22.99 points (37.5%) in the DAT test, and 11.35 points (16.8%) in the MRT test. Overall (average of three) improvement was 14.47 points (22.4%).

	Related differences							
				95% Confidence interval for the difference				
	Average	Standard Deviation	Standard Error of the Mean	Lower	Upper	t	gl	Sig. (bilateral)
MCT post-test – MCT pre-test	9.114	13.219	1.487	6.153	12.075	6.128	78	.000
DAT post-test – DAT pre-test	22.991	8.127	.920	21.159	24.823	24.984	77	.000
MRT post-test – MRT pre-test	11.348	13.792	1.562	8.237	14.456	7.266	77	.000
Post-test– Pre-test	14.472	7.457	.839	12.802	16.142	17.250	78	.000

Tab. 4: Paired samples t-test on pairs of scores

The improvement in spatial vision was similar in both groups, although slightly greater in the control group, if we average out the three test results, but the gain is heterogeneous.

Group			Mean	N	Standard Deviation	Standard Error of the Mean
Control Group	Pair 1	MCT post-test	72.64	44	16.457	2.481
		MCT pre-test	65.27	44	18.132	2.733
	Pair 2	DAT post-test	84.43	44	12.294	1.853
		DAT pre-test	60.83	44	11.017	1.661
	Pair 3	MRT post-test	78.58	44	17.307	2.609
		MRT pre-test	64.94	44	22.318	3.365
	Pair 4	Post-test	78.55	44	13.073	1.971
		Pre-test	63.68	44	14.000	2.111
Gr. Experimental	Pair 1	MCT post-test	75.89	35	16.705	2.824
		MCT pre-test	64.57	35	18.990	3.210
	Pair 2	DAT post-test	84.02	34	13.891	2.382
		DAT pre-test	61.81	34	13.801	2.367
	Pair 3	MRT post-test	79.04	34	18.007	3.088
		MRT pre-test	70.66	34	20.582	3.530
	Pair 4	Post-test	79.77	35	13.890	2.348
		Pre-test	65.79	35	14.250	2.409

Tab. 5: Paired samples t-test

- The students from the experimental (CAD) group achieved better qualifications in the exams.

It was observed that the students, in general, worked on the constructions of the dihedral operations to complete the constructions needed to solve an exercise with greater ease in the 3D virtual space than on a blank sheet of paper. The CAD group was also at an advantage for the intersection of surfaces, as the software programme helps the user when unable to arrive at a solution with traditional methods.

Group		Cont. Eval.	Exam result
Control Group	Mean	7,529	4,896
	N	51	50
	Std.Desv.	1,9797	1,7287
Experimental Group	Mean	7,874	5,856
	N	38	38
	Std. Desv.	1,7620	1,9297
Both	Mean	7,676	5,311
	N	89	88
	Std. Desv.	1,8872	1,8696

Article 017-e-92

Tab. 6: Qualifications

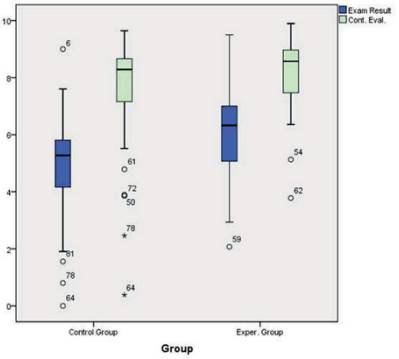

Fig. 10: Graph box scores

5.- CONCLUSIONS

Geometry is and will continue to be present in our lives; when we are driving, practicing sport, do-it-yourself, home improvements or just playing with building bricks we are using and developing our spatial thought processes. All the objects which help us to move around have required geometric design. Gaspard Monge, using the resources at the time, bequeathed a process that was able to solve spatial problems. He represented three dimensions in two bi-dimensional projections that are related through the repeated dimension.

Spatial intelligence tests, the simplest part of descriptive geometry, are based on rotations of objects, or changes in perspective, plane sections and projections. Clearly, the complexity of graphic thought is far greater in the representation of a hexahedron, for example, on the basis of a single section, as an isosceles trapezium, or a triangle.

Descriptive geometry understood in the traditional sense has without a doubt been outmoded, by the possibility of working directly with modern three-dimensional models, this discipline still has, as Migliari [M1] said, a long life ahead of it. Its two fundamental objectives remain valid: to learn to solve problems (seeking the most suitable point of view), and to improve our spatial capability.

In the study, we have demonstrated that solving classic problems of descriptive geometry with a virtual three-dimensional model helps to increase spatial capability in a significant way.

It has also been shown that students generally, in the 21st c., use the methods that technology offers us and that these methods suppose quicker learning and greater accuracy.

The experimental study has demonstrated that it is highly recommendable to teach descriptive geometry using the CAD tool, because it practices the two skills (or competences) simultaneously (descriptive geometry and CAD applications).

6.- REFERENCES AND BIBLIOGRAPHY

[BS1] Bennett G.K., Seashore H.G., Wesman A.G.: Deferential Aptitude Tests, Forms S and T. The Psychological Corporation, New York (1973)

[C1] CEEB Special Aptitude Test in Spatial Relations (MCT). Developed by the College Entrance Examination Board, USA (1939)

[M1] Migliari R., Descriptive Geometry: From its Past to its Future. Nexus Netw J 14 555–571 Kim Williams Books, Turin (2012)

[VK1] Vandenberg S.G., Kuse A.R.: Mental Rotations, a Group Test of Three-dimensional Spatial Visualization. Perceptual and Motor Skils 47, 599-604(1978)

[BS1] Bokan N.., Sykilovic T., Vukmirovic Srdjan., On Modeling of competencies in a descriptive geometry course. Pollack periodica. International Journal for Engineering and Information Sciences. 7 173-183 (2012).

[L1] Leopold C., Geometry education for developing spatial visualization abilities of engineering students. The Journal of Polish Society for Geometry and Engineering Graphics, 15 39-45. (2005)

[M1] Meagy-Kondor R., Spatial ability, descriptive geometry and dynamic geometry systems. Annales Mathematicae et Informaticae, 37(1), 199-210. (2010)

[MR1] Melgosa C., Ramos B., Baños E., Designing an interactive web manager applied to the development of spatial abilities. International Conference on Innovative Methods in Product Design. Italy (2011)

[S1] Sorby S. A., Educational Research in Developing 3-D Spatial Skills for Engineering Students. International Journal of Science Education 31(3), 459-480.Michigan (2009).

[S1] Stachel, H. Descriptive geometry in today's engineering curriculum. Transactions of Famena, 29(2), 35-44. (2005).

[S1] Suzuki K., Activities of the Japan society for graphic science-research and education. J. Geometry Graphics 6, no. 2, 221–229. (2003).

Article 012-e-13

LEARNING BY DOING- A COOPERATIVE PROJECT BETWEEN THE UNIVERSITY OF ZARAGOZA AND THE SEMILLERO DE IDEAS (THE IDEAS HUB)

Anna MariaBiedermann[1], Aránzazu Fernández Vázquez, [2]

(1): University of Zaragoza.
Department of Design and Manufacturing Engineering.
876555098
anna@unizar.es

(2): University of Zaragoza.
Department of Design and Manufacturing Engineering.
876555098
aranfer@unizar.es

Abstract: This article describes a pilot project developed between the subject of "Graphic Design and Communication" (DGyC) of the 2nd year of Industrial Design and Product Development Engineering Degree at the University of Zaragoza and the program "Semillero de Ideas" (Ideas Hub) - a 1st stage business incubator. It presents the objectives and the project development by which the students create a graphic image for the business projects raised by the entrepreneurs while they learn to use graphic creation tools and the principles of corporate design. The results reached and the satisfaction level of the students as well as the entrepreneurs ones, together with the subject academic goals fulfillment allow to positively evaluate this experience, where the learning process is done by doing and not only simulating a real work.

Key words: graphic design teaching, corporate design, knowledge transfer, entrepreneurship, University - Business collaboration.

1- Introduction

The study came up as a collaboration between the subject of "Graphic Design and Communication" (DGyC) of the 2nd year of Industrial Design and Product Development Engineering Degree at the University of Zaragoza and the program "Semillero de Ideas" (Ideas Hub) - a 1st stage business incubator, included in the training-residential service of Zaragoza's City Council -Zaragoza Activa [ZA1]. This initiative provides support, training and workspace during six months to twenty enterprise projects selected by public competition. During that period the business plan and marketing strategy is getting completed, next to other issues that start-up companies are facing to.
The collaboration between Ideas Hub and the University consisted on making one of the exercises within the subject's framework to be the creation of the graphic image for business projects developed by the entrepreneurs of the Ideas' Hub. This experience began in the academic year 2011-2012 and has returned to be performed in the 2012-2013 one. In both cases, a win-win philosophy that benefits both parties involved was pursued.

During the exercise students developed creative thinking [ZJ 1] and the ability to synthesize in the representation of the ideas, doing what graphic designers were doing since the beginning of the profession "Making Ideas Visible" [M1]. The binding of technical skills needed for industrial engineers with the competence to formulate clear graphic releases acquired in the subject of DGyC aimed to educate versatile professionals capable of facing varied tasks, as well as the profession pioneers did [E1], using professional design tools. This is reflected in the curriculum, where new Degree of the DGyC subject is compulsory unlike the old plan [D1]. This change and the importance of graphic design in shaping the future career in Industrial Design and Product Development, is also recognized in other Spanish Universities [AG1] and has already been pointed out by Richard Buchanan in 1992 [B1]. The methodology applied to structure the exercise was the one of collaborative projects [A1], [NS1], and learning by doing [TW1], [G1], [PM1].

2- Objectives of the work:

The experience joined academic and practical goals, developing the specific competencies for DGyC as well as transversal skills that are being trained in different subjects along the Degree. The objectives of the collaboration were as follows:

1- To provide students with "real work experience", with a client presenting precise needs to be done within a certain period of time.
2- To promote the culture of entrepreneurship, by facilitating the students' exposure to new

entrepreneurs that could make them consider the possibility of undertaking themselves a business.

3- To create networks among designers, students and potential future customers.
4- To enable the visualization of the "starting line" out of the University, not only through the physical location of the meeting between the students and new entrepreneurs outside of it, but with the accomplishment of a work that surpasses the very solely goals of a purely academic work, that can also result into conforming a part of the student's professional CV.
5- To equip entrepreneurs starting their business with a graphic image of their company that provides them professionalism, viability and visibility to their project.
6- To motivate students to complete their projects to be used by the customer.
7- To motivate through competition among several groups.
8- To make a transfer between the University and businesses at a very basic level, reinforcing the image of the University as a place of practical and applicable knowledge [RY1].

This purposes were the guidelines for the creation of the practice agenda, the development of the exercise and the establishment of the evaluation criteria.

3- Development of the collaborative project

The exercise realized by the students of the DGyC subject consisted in the development of a graphic image (imagotype, symbol or an appropriate logo, basic brand manual and a professional card-business card) for the new business projects presented by the entrepreneurs.

The student had to reflect on the message the company wanted to transmit and, based on that analysis, design the appropriate symbol accompanied by a consistent typography and composition. Students started with a basic knowledge of graphic and artistic expression, and throughout the exercise enhanced their knowledge of both tools and communication in graphic design and branding.

Picture 1: Work Meeting. Academic Year 2012-2013

The exercise begun with a meeting at the Plaza de Zaragoza Activa, in which all business projects first performed the Elevator Pitch, and in the next phase meetings between entrepreneurs and designers previously randomly assigned were developed. (See Picture 1). Entrepreneurs in advance had facilitated to the students a presentation of their business activity and a definition of the Mission, Vision and Values, i.e., aspects that are immutable through time [S1], as well as the contact details and information for the card. The meeting served to begin a more personal contact and to fix possible doubts that might have arisen from the documentation presented by entrepreneurs. Throughout the performance of the exercise period (one and half months-5 practice units of 3 hours each) the students were in contact with entrepreneurs, being able to get a feedback of their work every time.

In 2011-2012 the work was done individually, that is, each of the 89 registered students was required to perform one of the 10 images for the young companies. The following year, in order to obtain better developed results, it was decided to conduct the exercise in pairs. Among the 68 students, 34 groups that submitted proposals for 14 business ventures were formed.

4- Evaluation criteria

The assessments had to accomplish the requirements of the subject, as they were assessed by the teachers with the following criteria:

- The depth of the forethought and the research that defines the concept to further develop and the adequacy the message to be transmitted. (5%)
- Innovation and creativity of the different concepts raised. (5%)
- The application of the main idea, the graphic quality and the formal development of the imagotype, symbol or logo. (40%)
- Basic brand handbook, the main identifiers. (25%)
- The professional card, its balanced composition and application of the rules presented at the brand's basic handbook. (20%)
- The quality of the presentation. (5%)

The main evaluation instrument was the basic manual of corporate image which included all the parts and the dummy of the visit card.

In parallel, entrepreneurs independently reviewed the assessments. They could have decided to use the graphic image for their company, if it met their expectations, or to assign a recognition of the best work, even if they would have decided not to use it. In the first case the students got an added mark to the teachers' evaluation, in the second they got half mark.

5- Experience results

After carrying out the experience over two courses, the following final results can be observed (to compare with Table 1).

Results from the year 2011-2012.

- 10 projects of entrepreneurs involving 89 students, participated in the experience. 4 students did not submit the work.
- 5 companies got finally the corporate design, 5 projects were acknowledged by the entrepreneurs even though the image was not used.
- The average mark was 6.4. The results were announced via Poster (Figure 1).

Results from the year 2012-2013

- 14 projects of entrepreneurs involving 34 groups of 68 students participated in the experience.
- 9 companies kept the corporate design, 4 projects were acknowledged , 1 company dropped the project.
- Average score was 7.1. The results were announced with poster (Figure 2).

When analyzing the results of the different sections of the exercise (presented in the section 4) it was noted that:

- In the section of forethought and research the results were quite homogeneous, they hover a mark around 6.8. The task in this part of the exercise gathered both research of the competitors of the sector and the analysis of symbolic language of companies of other sectors which transmitted related values. Similar projects were made by students in previous semesters analyzing products, thus methodology posed no difficulty for them, either when creating different concepts in which students used techniques freely chosen and simultaneously studied in the subject of creativity [C1].
- In the case of the section of the basic handbook of the brand, the best results were observed during 2012-2013 after the incorporation of a mandatory index in the statement of the exercise, which gave a more complete and better structured assessments (in 2011-2012-6.4; in 2012-2013-7.1 as an average).
- In both courses the greatest difficulty has meant the correct layout of the professional card (2011-2012-5.8, in 2012-2013 -6.2 on average), but even though it appears a slight improvement in the second year, after setting more emphasis on this part of the project.

The evaluation by the teachers was conducted independently and not always agreed with the decisions of entrepreneurs. In fact, out of 10 projects chosen or recognized by the entrepreneurs in the first year, 8 were the best rated by the teacher, and in the second year out of 13 elected or recognized, 9 were the best rated by teachers. The difference between the teachers' evaluation and the entrepreneur's decision about which design will be used for its company was based on the following asserts:

- Entrepreneurs evaluations were usually focused only on the imagotype, symbol or logo and its representation of the values their business wants to transmit, meanwhile for professors this section represented only a 40% of the evaluation.
- In the entrepreneurs' decisions the subjective and personal tastes were reflected; on the contrary to the professors for whom the objectives and the appropriation of the message to be transmitted was crucial.

This gave the students different perspectives. The score reflected their academic progress and the feedback of the client gave a clear sample of the client's identification with the design and his/her satisfaction with the task done.

Table 1: Results Ex. 2011-2012 and 2012-2013

	2011-2012	**2012-2013**
Number of participating entrepreneurs projects	10	14
Number of participating students	89 (individual work)	68 (in pairs -34 groups)
Companies that applied the corporate design	5 (50%)	9 (64,3%)
Companies that acknowledged the corporate design although did not use it	5	4
Companies that dropped the project	-	1
Students that dropped the project	4	-
Average final score	6.4	7.1
- Average research score	6.8	6.8
- Average basic handbook of the brand score	6.4	7.1
- Average professional card score	5.8	6.2

Overall we see a positive evolution of the satisfaction of entrepreneurs that in the first experience reached 50% and raised in the following year to 64.2%. Also the average score of students went up from 6.4 in the first year to 7.08 in the second year. In the survey covering students' satisfaction with the DGyC subject, performed in the course 2012-2013, this exercise, which was one of five different ones developed throughout the semester, had been evaluated positively by the 85% of students. As inconveniences mentioned by them, they highlighted the luck factor in allocating business projects and the differences when involving different entrepreneurs. Students also pointed out the need to learn specific layout software apart from the vector graphic design tools taught in class. Nevertheless this has been the best exercise valued throughout the semester. In the evaluation students recorded that they were aware of the importance of working with real companies and of being able to place their labor in the market.

The modification of the exercise, from the individual one to executed in pairs, has proved improvements in both quality of work and the practical sessions' dynamics of the projects.

6- Advantages and disadvantages of the exercise

The two years of experience with this exercise gave us the chance to detect the following benefits:

1- The course enabled students to develop a complete professional work for a real client and this was perceived as very positive by the students. This exercise showed students that one of the multiple

career paths the Degree allows them is the one as a graphic designer.

2- The publication of the results of the assessment was a recognition and publicity for the student, as well as an item in their professional CV.
3- An appropriated level of competitiveness was provided by the fact that there were a small number of groups working for the same client. This number of groups was not too large, because it would make a group to get demotivated when facing the possibility of not being the chosen one, neither too small, because it would allow groups to relax too much in a competition absence.
4- The allocation of fixed groups who had to work for a client, who was randomly assigned, required students to confront a project that initially may not had too much affinity with, so that they were obliged to perform an activity of documentation, research and analysis greater than the usual, to get to work effectively as a group.
5- Establishment of a link between the University and the City. Students related to other infrastructures that the city offers to them, through contact with entrepreneurs that intend to carry out a business project there.
6- A knowledge transfer was made from a very basic level, so it was created a practical case and conviction that all knowledge acquired during the studies have a practical and direct application.

Figure 1: Poster with the results Ex. 2011-2012

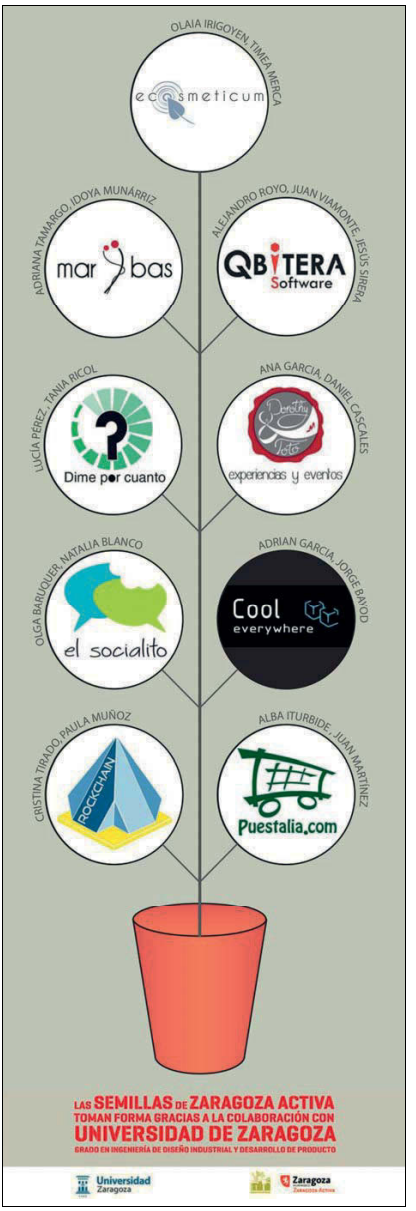

Figure 2: Poster with the results Ex. 2012-2013

We have been able to observe the following drawbacks:

1- From the educational point of view the exercise required a bigger effort because simultaneously we had to continue with the development of multiple projects with very different themes and sectors.
2- The exercise both required an additional work both for the meeting organization as well as the transmission projects coordination to entrepreneurs and the evaluation of them.
3- The clarity of the business idea by the entrepreneurs affected the creation process, thus indecision of promoters is a factor to consider as it may hinder the development of some projects creating unequal conditions when evaluating.

As presented above the exercise showed to offer much more advantages than its drawbacks and the additional effort is worth it. The relation between entrepreneurs and students is the objective of improvements proposed for the next edition of the exercise.

7- Conclusions and future improvements

The exercise aroused students' interest in the subject, got to motivate them and awaken in them a healthy competitiveness. It had also been proved to be very useful in the learning of software design tools, since students learned starting with some very basic knowledge of Adobe Illustrator, which was explained in a practical class in parallel when working on the image. At the same time, students were provided with an opportunity to present their work to the non-university public and the experience of dealing with a client for whom they were not students but designers who offered the graphic image for a real business project.

However several ways have been identified to improve the project that will be implemented during the year 2013-2014.

1- The need to establish a contract between the parties to link both sides in a more formal way, which forces to make commitments to improve the temporal development of the works: deadlines for responding to proposals, minimum number of contacts or meetings between promoter and student, maximum number of proposals to raise the customer not to overwhelm them, etc..
2- The ability to incorporate a multidisciplinary factor to the project, through collaboration with other degrees that could improve some phases of work, such as marketing or ADE (Administration and management) [FP1], to complement the business plan, market research, etc..
3- To establish evaluation rubrics for the exercise as well as satisfaction surveys by both students and the entrepreneurs, in order to make the evaluation even more transparent and objective, and to get more feedback from the students and the entrepreneurs.
4- To increase the significance of the section "The innovation and creativity of the different concepts raised" in the assessment to encourage further exploration of different concepts before developing one.
5- To extend the time dedicated for learning design tools in order to introduce, apart from vector design software, another specific layout tools for better results in this field.

The will of the University as well as of Zaragoza Activa is to continue with this collaboration, providing quality graphic design for start-up companies while training market-oriented design professionals.

8- References

[A1] Augustin S, The Burnout Phenomenon: A Comparative Study of Student Attitudes Toward Collaborative Learning and Sustainability, Journal of Interior Design, Volume 39 Number: 1 Pages: IX-XVIII, 2014

[AG1] Ampuero-Canellas O., Gonzalez-del-Rio J., Jorda-Albiñana B., Brusola F., Graphic design in bachelor's degree in industrial design engineering and product development, Procedia - Social and Behavioral Sciences 51 (2012) 4 – 9

[B1]Buchanan, R. (1992). Wicked Problems in Design Thinking. Design Issues, 8, 2, 5-21

[C1] Creatividad- Guia docente http://titulaciones.unizar.es/asignaturas/25815/actividades13.html

[D1] Diseño gráfico y comunicación- Guía docentehttp://titulaciones.unizar.es/asignaturas/25814/contexto13.html

[E1] Eskilson S., Graphic Design: A New History, Yale University Press, 2007 p. 102-106

[FP1] Fernandez Pascual, R.; Navarro Ruiz, M. A.; Gonzalez Aguilera, S.; et al., A comparative study of the subjects, statistics and financial management, of Degree in Business Administration and Management and Degree in Finance and Accounting in Spain, Conference: 6th International Conference of Technology, Education and Development, INTED Proceedings, 2012, Pages: 6022-6029

[G1] Garcia Belmar A, Learning by Doing. Experiments and Instruments in the History of Science Teaching, AMBIX, 2013, Volume: 60, Number:3, Pages: 301-302

[M1]Mazur Thomson E, The Origins of Graphic Design in America, 1870-1920, Yale University Press, 1997, p.1-5

[NS1] Nimnual R, Suksakulchai S, Work in Progress - Collaborative Learning for Packaging Design Using KM and VR, IEEE Frontiers in Education Conference, 2008, Volume 1-3, Pages: 1431-1432

[PM1] Penzenstadler B, Mahaux M, Heymans P, University Meets Industry: Calling in Real Stakeholders, 2013, IEEE Conference on Software Engineering Education and Training, Pages: 1-10

[RY1] Rong F., Yan X., An Exploration About Practical Teaching of Design Courses of Colleges, 2013, 2nd International Conference on Science and Social Research

(ICSSR), Book Series: Advances in Intelligent Systems Research, WangHS, Volume: 64 Pages: 225-228

[S1] Suso J., La nueva gestión estratégica de marcas: comunicar para vender en la era del consumidor, chapter 8 in Cuesta U., Planificación estratégica y creatividad. ESIC Editorial- Madrid, 2012. p. 135

[TW1] Temmen K, Walther T, 'Learning by doing' Improving academic skills, IEEE Global Engineering Education Conference, 2013, Pages 118-122.

[ZA1] Zaragoza Activa, Semillero de Ideas, 2013, http://www.zaragoza.es/ciudad/sectores/activa/semillero.htm

[ZJ 1] Zhang, Junhua, Research on Creative Thinking of Teaching in Universities' Art Designing, 2012, International Conference on Education Reform and Management Innovation (ERMI 2012), VOL 1 (2013-01-01) p. 34-37.

Article 018-e-96

3D IMMERSIVE ENVIRONMENTS IN HIGHER EDUCATION B-LEARNING IMPLEMENTATIONS. PRELIMINARY RESULTS

Fernando J. Aguilar[1], Manuel Lucas [2], Manuel A. Aguilar[1]Juan Reca[1], Antonio Luque[3], Antonio Cardona[4], María S. Cruz[5], José J. Carrión[3],

(1): Department of Engineering. University of Almeria. Ctra. de Sacramento s/n La Cañada de San Urbano, 04120 Almería (Spain)
Phone +34950015339/Fax +34950015491
E-mail : {faguilar,maguilar, jreca}@ual.es

(2): Health Ministry of Andalusia Government. Head of Service, Almería (Spain)
Phone/Fax
E-mail : lucasmatheu@ono.com

(3): Department of Education. University of Almeria. Ctra. de Sacramento s/n La Cañada de San Urbano, 04120 Almería (Spain)
Phone +34950015492
E-mail : { aluque,jcarrion}@ual.es

(4): Department of Law. University of Almeria. Ctra. de Sacramento s/n La Cañada de San Urbano, 04120 Almería (Spain)
Phone +34950015470
E-mail : cardona@ual.es

(5): Department of Philology. University of Almeria. Ctra. de Sacramento s/n La Cañada de San Urbano, 04120 Almería (Spain)
Phone +34950014285
E-mail : mcruz@ual.es

Abstract: The emergence of a fourth dimension (time) and the development of photorealism, by including materials, textures, lights and special effects, allow the configuration of more and more realistic 3D virtual worlds. These are true 3D immersive spaces where the user can interact with virtual objects and other users. These emergent technologies are being applied, we believe in a definitive way, for improving the teaching-learning process in b-Learning environments. The preliminary results of our teaching innovation group are presented in this paper, briefly consisting of creating a WWW 3D virtual meeting point between students and teachers by using the semi open source WWW platform called "Second Life". The first stage of experimentation has proved the potential of 3D immersive environments to develop a formative offer wherein the universities can provide an alternative to the traditional face-to-face learning regarding the presential component. In this sense it is boosted a distance learning approach but mainly using almost a presential method where the meeting point turns out to be a virtual classroom rather than a physical one.

Key words: b-Learning, e-Learning, 3D Immersive Environments, Second Life, Higher Education.

1- Blended Learning model

Terms such as "on-line learning", "blended-learning", "personalized learning", "customized learning" and "competency-based learning" have become very common in our educational dialogue and they are often used interchangeably [BE1]. The fundamentals are related, but they are not the same. Therefore it would be welcome to firstly establish the most important differences by introducing what exactly means the term of blended-learning. In this sense blended-learning, henceforth b-Learning, can be defined as "a formal education program in which student learns at least in part through the online delivery of content and instruction, with certain element of student control over time, place, path, and/or pace, and, maybe the most important, at least in part at a supervised brick-and-mortar location away from home" [SH1].

Nowadays, more and more students around the world choose one of the different kinds of e-Learning models. For example, and if current trends continue in EEUU, by 2018 there will be more full-time online post-secondary students than students who take all their classes in a physical location [A1]. In the same way, challenges are rising as well, partially overcome with the arrival of new set of tools related to which is known as Virtual Learning, that is, any learning that occurs where either the teacher or students are present for an educational event in virtual rather than physical form. This is the main issue to be faced along this communication.

The technological development of the last years has encouraged, together with the significant restructuring of our European Space of Higher Education, the progressive incorporation of educative tools designed, at least initially, to make easier the learning process by means of increasing the

communication and cooperation between teachers (maybe called instructors in some contexts) and students thanks to the rising of Information Technology (IT). For example, in [J1] an in-depth survey of medical applications that make use of Web3D technologies, covering the period from 1995 to 2005 is provided.

The application of IT in Higher Education is mainly headed up to allow students the access to the campus and its educational resources from wherever and whenever, thus facilitating the development of their learning activities in a personal and self-sufficient way. Therefore these technologies have been principally evolved in the context of the eLearning models, later deriving into a myriad of variations which have been previously mentioned, currently emerging the b-Learning as one of the most relevant among them.

As it was said before, the eLearning could be considered an integration of common elements belonging to both traditional face-to-face teaching and internet distance learning [A2]. In this way, it embraces the positive characteristics of presential teaching (focuses on skills and attitudes) and the best features from eLearning (interaction, economy, efficiency, promptness, etc.). This mix of learning channels enriches the teaching method, allowing its individualization for each student and covering more learning objectives.

Both e-Learning and b-Learning use internet as the place where teachers and student meet and interact. In fact, it is widely known that interactivity has been referred to as the most important element for successful e-learning in the context of a web-based learning environment [VV1]. It constitutes a learning approach pretty adapted to carry out and drive, for example, long-life learning programmes, allowing working professionals to continue their training along their free time. To do that, it is necessary to use a software and hardware designed to automate and manage the flow of learning activities, what is usually called *Learning Management System* (LMS).

Currently there are several LMS platforms, either commercial or open source. Regarding Higher Education, Blackboard (proprietary platform) and Moodle (open source) are likely some of the most used. Those LMS can only be used as a teaching support (i.e., just to complement face-to-face teaching), online learning (where does not exist any physical contact between teacher and student) and, finally, semi-presential teaching (b-Learning where the presential component is maintained together with a variable grade of virtual learning). All these LMS make possible providing learning materials to students as well as facilitating an efficient tutoring process.

From here on, we will focus on the teaching methodology based on b-Learning model and, above all, how to replace part of the physical contact between teacher and student without giving up the widely known advantages bounded to the traditional face-to-face teaching in classrooms such as a permanent contact and so a more in-depth human relationship, the feeling of belonging to an educative community or learning group, and the higher grade of motivation needed to follow an e-Learning course [P1]. In this regard, the introduction of 3D immersive environments described in the next section is proposed in this paper as an innovative tool to maintain, as much as possible, the contact and interaction between teaching and learning agents.

2- 3D immersive environments

The future, maybe the present, is perceived like a virtual 3D world, very similar to our real wold, where the creation of 3D interactive web sites stands out. The addition of the fourth dimension (time) and the development of photorealism by including materials, textures, lights and special effects, have fostered the configuration of 3D virtual worlds, nowadays considered as true immersive environments where the user, represented as an avatar or virtual character, can interact with that 3Ddigital world and other users. These emergent technologies are being applied, in our opinion, to improve the process of teaching-learning in b-Learning environments.

The development of Computer Graphics technology and Virtual Reality (VR) can be qualified as astonishing if we take into account the first basic ideas forged in the 60s and 70s. The last decade has finally seen the mass accommodation of 3D graphics when every modern PC is capable of producing high-quality computer-generated images, mostly in the form of video games and virtual-life environments [G1]. Nobody is today flinched when watching the amazing digital special effects which appear in movies (e.g. Pixar movies). It is simply expected.

At the same time, the current wide spread of WWW technology and 3D Computer Graphics let us create and also access to 3D immersive environments from home. These 3D immersive environments consist of synthetic scenarios, trying to simulate real life, which, when well-designed, perform as learning leverage elements allowing a certain kind of groupal work (WWW distance communication) where all the involved students participate in an active way by using their role in the virtual classroom group as the key to achieve an almost physical social interaction [LB1]. These systems are especially appropriate to facilitate the interaction among all the people who take part in the teaching-learning process through using synchronous tools (3D avatars who interact with each other) which overtake the traditional distance synchronous tool usually based on video conference. Therefore, it is an integrated environment, called technological platform, for making easier the learning process. It comes up like a response to the evidence that students present very different needs, requirements and experiences, so it impels the creation of a flexible and adaptable learning environment to foster the distance/self-sufficient learning through WWW tools and 3D immersive and interactive environments.

3- Objectives

Focusing on the aforementioned premises, a new teaching innovation group has been recently created in the University of Almeria, Spain, in order to study the application of 3D immersive environments in a b-Learning framework. This is a pioneering experience of trans-disciplinary collaboration launched by 8 researchers mainly keen on developing innovative methods for improving the teaching-learning process in higher education. They come from very different fields such as engineering, education, philology, medicine and law.

The main goals of the first stage of this teaching innovation experience would be the following:

1- Testing and applying the emergent 3D immersive

technologies on improving the teaching-learning process in the University of Almeria under b-Learning schemes. This implies choosing the technological platform, creating the virtual environment and training the people who constitute the teaching innovation group in using the implemented tools.

2- Practical training of the 3D immersive tools on subjects belonging to different knowledge disciplines such as engineering, social and law sciences, engineering and arts and humanities.

4- Methodology

The basic tool employed to create our 3D immersive environment, still remaining in an experimental stage, is being *Second Life* (www.secondlife.com). It is a WWW platform based on computer technology called Metaverse (i.e., meta = "beyond" the universe). It could be very shortly defined as a set of 3D virtual spaces linked into a perceived virtual universe [I1]. This platform was developed by *Linden Lab*© and it has free access through internet. Their users, also called residents, can go into the virtual world by using an interface which let them interact with each other by means of avatars. The residents, in this case teachers and students, can explore and move around the virtual world, establishing social relationships and interacting and participating in several activities, either conducted in group or individually. In our particular case, the meeting point would be a hypothetical virtual classroom, called "Eei3D seminar" (see Figures 1 and 2), located at the Virtual University of Almeria or "UAL Island".

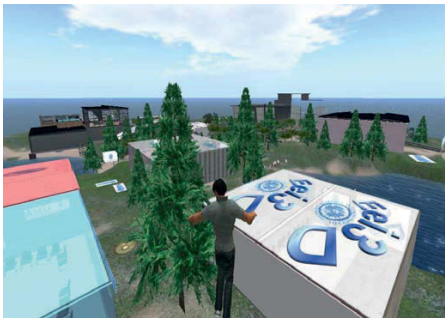

Figure 1: Avatar flying over the virtual UAL Island, just in front of the Eei3D seminar.

Actually, this technology is very similar to what is known as Building Information Modelling (BIM) in the sense that it is understood like an organized process to generate and manage the data corresponding to a certain building during its whole life cycle from using a dynamic and object oriented software for modelling a 3D building [H1].

In this context, The BIM technology indexes, in an organized and easy to retrieve way, the geometry and shape of the objects constituting the scene, the spatial and neighbourhood relationships, the geographical information and the objects properties (landscapes, browsers, slides projectors, furniture, buildings, etc.). They are true smart objects which show the growing trend in Computer Graphics and Virtual Reality towards the creation of 3D models based on objects (i.e. replicable and configurable from parametric features) rather than on the traditional representation of vectorial models (solids or surfaces).

During the first phase of this teaching innovation project, it has been undertaken a theoretical-practical methodology supported by periodical working sessions including reflexion about practice, a rigorous analysis about the experiences and contexts and a final formulation of proposals of innovation and intervention headed up to improve the tool. At this point it is important to highlight that only presenting course contents on the web, without using appropriate pedagogical models and principles, without appropriate means of communication between participants and instructors and without the use of modern information technologies is not enough to fulfil educational goals [VV2]. During the second stage of the project, the mentioned proposals should lead to the adaptation of the presential methodology applied in the subjects taught by the team members towards a new methodology supported by distance learning through WWW environments.

Figure 2: Outside view of the Eei3D seminar where the teaching innovation group is working with different strategies.

5- Preliminary results

During the first phase of this teaching innovation project it has been built up an attractive 3D virtual space ("UAL Island") where all the members of the teaching group have learnt to move around easily. In this sense, it has been achieved the integration of several technologies into the same virtual classroom, counting on a WWW browser screen, a device to show slides (e.g. PowerPoint presentations), interaction between avatars by means of chat, synchronous voice, gestural communication, webminar sessions from remote classroom (Adobe Connect® or TeamViewer®), etc. (Figures 3, 4 and 5).

This learning scheme has been proved to be very interesting for postgraduate students (e.g. Official Masters courses). In fact, they are usually mature enough and present a high potential of self-learning, showing very different formative profiles (sometimes they come from different degrees).

Furthermore, the class size uses to be very small (less than 20-25 students) as compared with the one observed in degree titles. Consequently, we could state that postgraduate students turn out to be ideal for applying a teaching-learning process based on what is named Personal Learning Environments. The fact that each student is unique and presents different needs and motivations promotes the development of personalized learning environments run by the own student [FK1].

Summing up, it has been successfully tested the potential of the WWW Second-Life-based 3D immersive environments for the development of a formative offer based on the possibilities provided by the alternative presential teaching derived from navigating and interacting in 3D virtual worlds as a substitute of the traditional face-to-face teaching and learning. It is not about removing the support of interactive WWW platforms such as Moodle or Blackboard, but complementing them by using a b-Learning methodology and achieving that students and teachers interact with each other like they would do it in a physical classroom. In this respect, it has been widely checked that our students usually tend to replicate their own real social interactions, actually like a carbon copy, when they are immersed in a virtual classroom.

Figure 3: Example of teaching where it is shown the integration of Webminar and BlackBoard resources within the same virtual session in the Eei3D seminar.

6- Conclusions

Throughout this work, still on going, it has been proved how the WWW 3D immersive environments by using Second-Life interface allow an astonishing synthetic simulation of real life. These scenarios, when well designed, perform as learning leverage elements facilitating the work in group where all the students participate in an active way by using the role as the key to attain a real social interaction within the virtual classroom context. As a result, higher education institutions can encourage the ability to work in group-based environments which is often approached as a skill to be learnt.

On the other hand, and from a basically institutional point of view, the joint use of 3D immersive environments and WWW technological platforms would make possible to increase the potential market of students to be enrolled in the University of Almeria, boosting and facilitating the development of, for instance, official masters with a clear international character. This strategy can be considered vital for the survival of our postgraduate titles related to the knowledge fields which show a low local demand such as Engineering or Sciences. Actually, the number of students doing Engineering and Science degrees turns out to be insufficient to maintain official masters with an appropriate economic viability.

Figure 4: Example of teaching where it is shown the use of the slides projector screen and a browser object to facilitate the navigation on internet.

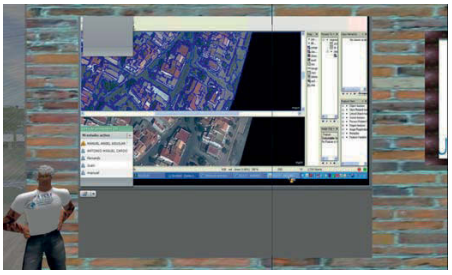

Figure 5: Webminar session by means of Remote Classroom (Adobe Connect®) in the case of a postgraduate subject called Geomatics Engineering.

7- Further works

Along the next year the team who make up this teaching innovation project has planned to refine the tested tool including new tailor made teaching objects and improving the realism of the buildings and landscapes conforming the "UAL Island". The main idea is to expand the initial buildings to house more and more official masters, especially those showing a marked international character. Furthermore, it has been scheduled to deploy different experiments designed to check whether the proposed innovative method is accepted by our students as compared to the traditional one. The synchronization of face-to-face classes, practices in labs and virtual meetings by means of second life environment has to be studied in depth to optimize the efficiency of our teaching-learning process depending on the group of students to whom it is addressed.

8- Acknowledgments

Thanks are due to the Faculty Staff and Academic Organization Vice-Rectorate of University of Almeria for partially supporting this teaching innovation project through promoting annual calls to bring up new teaching innovation groups. The authors are also very grateful to the Centre for Production of Digital Content (University of Almeria) and the Programme Red.es (Spanish Ministry of Industry) for facilitating the use of their infrastructures and their contribution to this work through a joint collaboration.

7- References

[A1] Adkins S.S. Ambient Insight. The U.S. Market for Self-paced eLearning product and services. 2010-2015 forecast and analysis. January 2011.

[A2] Andrade A. eLearning Papers.In Open Education Europe, 3, 2007.

[BE1] Bailey J., Ellis S., Schneider C., Ark T.V. Blended Learning Implementation Guide. Last access February 2014:http://net.educause.edu/ir/library/pdf/CSD6190.pdf.

[FK1] Fournier H., Kop R. Factors affecting the design and development of a Personal Learning Environment: research on super-users. In International Journal of Virtual and Personal Learning Environments, 2(4):12-22, 2011.

[G1]Gortler S.J. Foundations of 3D Computer Graphics.The MIT Press, Cambridge, MA, 2012.

[H1] Holness G.V.R. Building information modeling gaining momentum. In ASHRAE Journal, 50(6):28-40, 2008.

[I1] IEEE VW Standard Working Group. Last access February 2014:http://www.metaversestandards.org/index.php?title=Main_Page

[J1] John N.W. The impact of Web3D technologies on medical education and training.In Computers&Education, 49(1):19– 31, 2007.

[LB1] Lacruz M., Bravo C., Redondo M.A. Educación y nuevas tecnologías ante el siglo XXI.In Comunicación y Pedagogía, 164:25-40, 2000.

[P1] Pascual M.P. (2003). El Blendedlearning reduce el ahorro de la formación on-line pero gana en calidad. Educaweb, 69, 2003.

[SH1] Staker H., Horn M.B. Classifying k-12 Blended Learning. Innosight Institute White Paper, May 2012.

[VV1] Violante M.G., Vezzetti E. Virtual interactive e-learning application: An evaluation of the student satisfaction.In Computer Applications in Engineering Education.doi: 10.1002/cae.21580, 2013.

[VV2] Violante M.G., Vezzetti E. Implementing a new approach for the design of an e-learning platform in engineering education. In Computer Applications in Engineering Education.doi: 10.1002/cae.21564, 2012.

Article 013-e-88

Learning dimensional metrology in practice: Students controlling a coordinate measuring machine (CMM) from their computers

César García-Hernández [1], José-Luis Huertas-Talón [2], Rafael-María Gella-Marín [3], José-María Falcó-Boudet [4], Panagiotis Kyratsis [5], Jean-Noël Felices [6]

(1) : Departamento de Ingeniería de Diseño y Fabricación, Universidad de Zaragoza, María de Luna 3, Edificio Torres Quevedo, 50018 Zaragoza, Spain
Phone: (+34) 876 555 182
E-mail : garcia-hernandez.cesar@unizar.es

(2) : Departamento de Ingeniería de Diseño y Fabricación, Universidad de Zaragoza, María de Luna 3, Edificio Torres Quevedo, 50018 Zaragoza, Spain
Phone: (+34) 976 761 891
E-mail : jhuertas@unizar.es

(3) : Departamento de Ingeniería de Diseño y Fabricación, Universidad de Zaragoza, María de Luna 3, Edificio Torres Quevedo, 50018 Zaragoza, Spain
Phone: (+34) 976 761 000
E-mail : rgella@unizar.es

(4) : Departamento de Informática e Ingeniería de Sistemas, Universidad de Zaragoza, 50018 Zaragoza, Spain
Phone: (+34) 976 761 000
E-mail : chema.falco@unizar.es

(5) : Technological Educational Institution of West Macedonia, Kila Kozani GR50100, Greece
Phone: (+30) 24610 68294
E-mail : pkyratsis@teikoz.gr

(6) : Institut Clement Ader (EA 814) IUT, 1 rue Lautréamont 65016 Tarbes, France
Phone: (+33) 562 444 211
E-mail : jean.noel.felices@iut-tarbes.fr

Abstract: This paper presents a pilot study in which a coordinate measuring machine (CMM) is handled by students, using remote control software. This is part of a metrology practical session, during a professional training course. They, instead of just paying attention to what their teacher is doing and his explanations, have to practice with a real machine, giving instructions, from their laptops, to the computer that is controlling that CMM. This research article describes the preparation process, the experience, how it was assessed and, finally, results are assessed. These results confirm an improvement, both in students' skills and in other important aspects, like participation, interest and friendliness. Although further studies are needed, this teaching methodology can be applied to remote and in-person classes, especially in professional training, where different educational centres and even industries can share their different machines, helping to optimize resources.

Key words: Interactive learning; collaborative learning; metrology; remote control; educational-resources optimization.

1- Introduction

Explaining how to use metrology equipment is not always easy, especially if student interaction is required. In this sense, we considered that the learning process of manufacturing metrology, in our practical sessions, could be improved. Coordinate measuring machines (CMM) are usually controlled using an external computer, so we asked ourselves why not let students do it from their laptops during those sessions, being able to directly visualize the results in the classroom screen. Furthermore, we were unable to find published articles covering the ideas we wanted to apply in the classroom. Just a few previous experiences could be found covering the computer-assisted training concepts for education in metrology **[WW1]** or the development of an interactive simulator for teaching dimensional metrology **[GM1]**.

The intention of this study was not to let students simulate the measurement process or to use an interactive tool; the real purpose was to let students take control of a real device from their computers in the classroom, being able to observe the results immediately. To reach this purpose, students could practice with a real tool (CMM), controlling it from their laptops. The use of laptops in classes is not new, as described in previous studies **[KS1]**, and it made possible to observe the results of their interaction with the machine, directly projected on screen. There are, of course, previous experiences in which student interaction have been applied with positive results in fields like electronics **[ES1]**. The main difference in this case is that interaction was totally integrated with the teacher explanations to maintain student attention, being participation a key factor, and mixing basic concepts with advanced results.

A lot of previous research studies were consulted, particularly along the preparation of this study, as described in this section. Interesting initiatives were found, like the Practical Experimentation by Accessible Remote Learning (PEARL), which was an EU funded project, to develop a remote experimentation system by university sites **[CS1]**. Previous experiences included the development of systems to interact with remote laboratories with different approaches (**[BP1]**; **[CV1]**; **[CC1]**; **[CT1]**; **[FF1]**; **[HY1]**; **[JC1]**; **[KY1]**; **[L1]**; **[MA2]**; **[NC1]**; **[SF1]**; **[TA1]**; **[VR1]**; among others), that were used in different disciplines and with a variety of study levels. In a similar way, Bourne, Harres & Mayadas **[BH1]** stated the importance of establishing connections between the teaching subject and the real world, particularly in distance engineering education. According to these authors, there are three key attributes (quality, scale and breadth) necessary in order to make online engineering education accepted and utilized.

Although there are a lot of previous studies based on the use of software or modules specifically developed, like several of the previously cited, and many others (e.g., **[CH1]**; **[LL1]**; **[SS1]**; **[WA1]**) or web-based tools/contents (e.g., **[NA1]**; **[HF1]**; **[MA1]**; **[P1]**); it is not uncommon to use previously existing tools, not developed by the researchers. This is our case: we tried to take advantage of existent software, like in other previous researches (e.g., **[BT1]**; **[GM2]**; **[LZ1]**; **[R1]**). In fact, one of the programs used in this study was developed by the manufacturer (Mitutoyo) to control the CMM machine (MCOSMOS 1 V3.0) and one of the goals of this kind of courses was that students were able to learn how to use it.

Previous researches have confirmed the positive aspects that the use of the web can provide to learning processes, e.g., Tsai **[T1]** indicated that "the college students' conceptions of web-based learning were often more sophisticated than those of learning in general". A number of engineering education web-based projects have been developed, not only for university levels, but also for previous studies, e.g., P-12 learning **[BK1]**. Web-based applications have also been used to offer simulations of basic concepts, e.g., simple concepts of physics **[CP1]**.

Taking into account the professional requirements that our students typically have to face in their real employments, the adaptation ability to quickly solve technical problems can be considered a key aspect, being necessary to have skills with different software tools, including CMM. For this reason a pilot experiment to teach the students how to use the CMM was developed and put into practice, also including the mathematical required concepts. Finally, after this experience, students were able to perform a measurement in a workpiece, as final assessment confirmed.

2- Material and methods

2.1 – Participants

A group of 12 students, with ages from 17 to 23 years old, with an average age of 19.27, participated in this pilot study. They were students of a professional training course at the Centre of Professional Training "Corona de Aragón" at Zaragoza, Spain, and this experience was carried out during the Spring Semester of course 2012-2013.

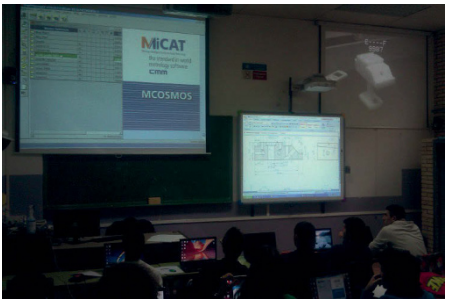

Fig. 1. Students starting their laptops and classroom layout: CMM software (top-left), technical concepts (centre) and real-time video showing the measured workpiece (top-right).

2.2 – Technical equipment

A laptop was used by each student. The 12 computers were property of the CFP Corona de Aragón and had identical features: ASUS brand, with Intel Core I7 processor, 2.2.GHz, 4GB RAM and 500 GB hard drives. The operating system was Windows 7. TeamViewer 8 was previously installed in each laptop. Students used the available Wi-Fi to connect to the Internet (managed by the technical staff and without needing a local area network) in order to control the computer connected to the CMM, using TeamViewer.

Fig. 2. CMM (Mitutoyo EURO-C544) and sample workpiece for training purposes.

The computer connected to the CMM was a generic PC with Intel Core 2 6400, 2.13 GHz and 1GB RAM and 128 GB hard drive. The operating system was Windows XP. TeamViewer 8 was also installed in this computer, which was connected to the Internet (again, without a local area network) using the Ethernet protocol. The software in this computer to control the CMM was MCOSMOS 1 V3.0.

The video projector used to project the images of the CMM computer was an Epson EMP-83.

Article 013-e-88

A conventional video camera was used to show in real time the CMM probe performing the measurement process of the workpiece. The video captured with this camera was also shown using another projector (Acer PDS27W).

The CMM used was a Mitutoyo EURO-C544 and the sample workpiece measured in these classes was specifically manufactured, according to pedagogical criteria and recommended by this machine manufacturer for training courses (Fig. 2).

Finally, an interactive whiteboard (a combination of a projector, EPSON EB-440W, and an electronic blackboard, Interwrite Dualboard) was also used to explain the layout of the workpiece and other concepts similarly to a conventional class.

2.3 – Questionnaires about previous and acquired knowledge

In order to check the feasibility of this new teaching method, it was crucial that the students had no previous knowledge related to CMM. To do it, students were previously evaluated with an initial test, or pre-test. After the class, students were evaluated again, using the same questionnaire (called post-test) in order to check the acquired knowledge.

The contents of these tests included the required mathematical concepts and aspects related to numeric control, computer-aided manufacturing and machining technology. They were divided into three blocks, as follows:

- MTM block: six questions evaluated the mathematical concepts, including geometrical aspects related to measuring processes.

- TCM block: five questions were used to assess the general knowledge, related to milling and materials, of the participants.

- CMM block: five questions tested the knowledge related to measuring process using CMM.

2.4 – Class description

During the class, the teacher explained how to use the CMM to measure generic workpieces. He connected his laptop (identical features to the previously described laptops) to the CMM computer using TeamViewer 8. He performed a workpiece partial measurement, so the students could follow his explanations watching the previously described screens (Fig. 1). The top-left projection showed the CMM software, so the students could follow the commands and actions used to perform the measurement, in real-time, while the CMM probe measuring the workpiece could be observed on the top-right screen.

After a first measurement, performed by the teacher, he briefly explained how to connect their laptops to the CMM computer (again, using TeamViewer 8). After these previous explanations, each student (one by one) connected the laptop to the CMM computer, solving short exercises that were proposed by the teacher. This is how each student had participated in a real measurement process of a workpiece at the end of the class, while all the students could follow the entire practice.

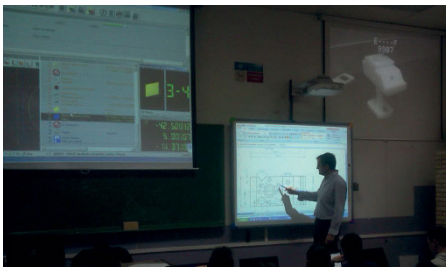

Fig. 3. Explanation of metrology concepts combined with their practical application during the class.

2.5 – Experience assessment

After the classes, the teacher assessed the level of acquired concepts, as explained before, and also the students' affinity to this teaching method. This assessment was based on a questionnaire to be answered with a Likert scale, from 1 to 5 (1 = "Strongly disagree", 2 = "Disagree", 3 = "Neither agree nor disagree", 4 = "Agree", 5 = "Strongly agree").

The questions that participants answered, in order to evaluate their perception to this teaching method, were:

Q1. Learning how to use the CMM with this method is better than watching the teacher doing it in the cabin

Q2. After this class I feel able to measure a hole's diameter and the distance between two holes.

Q3. This method allows students to take a more participant role in the class.

Q4. I think I will be able to use these tools (TeamViewer and remote desktop connection) to other jobs in the future, whether they are studying or professional jobs.

Q5. I consider that this is a friendly method to learn how to use the CMM.

Q6. I have paid attention and I have understood what has been explained during the class.

Q7. I think that, using this method, more operating details are learnt, compared to just watching another student measuring a workpiece in the cabin.

Q8. I think that this is a good method to learn how to use this kind of machines.

Q9. This method has enhanced my learning process.

Q10. The class has been pleasant.

3- Results

This section is divided according to the two different assessed aspects: previous vs. acquired knowledge and perception of this learning process. Stata/IC was used to analyse the obtained data and to generate the graphs that makes easier to interpret these results, as shown below.

3.1 – Previous knowledge vs. acquired knowledge

With the intention to evaluate participants' acquired knowledge, according to the three different fields explained in the previous section, questionnaires with three different blocks were used, in the beginning and after the class, with the following results.

3.1.1 – MTM block results

The obtained results in the pre-test about mathematical concepts were good, as reflected on Fig. 4 (left histogram) and, after the class, the post-test marks were quite better (Fig. 4, right histogram). These are not the main aspects to be learnt in this kind of classes, but they are put into practice by students, so their assimilation is clearly benefitted, as results reflected.

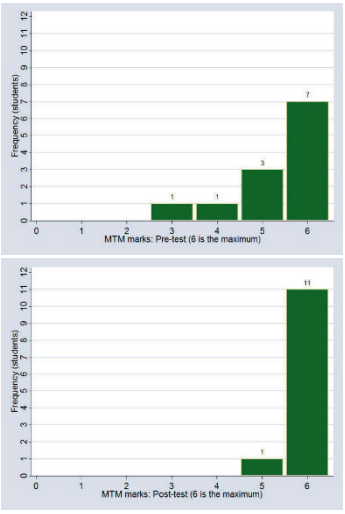

Fig. 4. Results of MTM pre-test vs. post-test.

3.1.2 – TCM block results

Although the concepts related to milling and materials were not directly treated, they were also tangentially covered and applied, so results in the post-test were also significantly improved, as shown in Fig. 5.

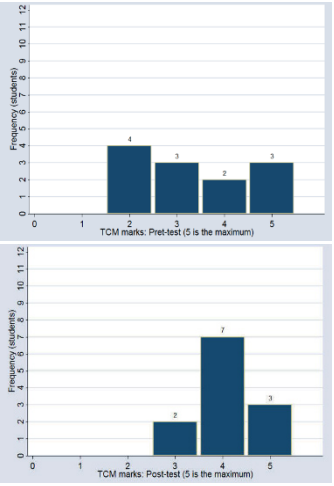

Fig. 5. Results of TCM pre-test vs. post-test.

3.1.3 – CMM block results

As these contents were totally new for participants, they could only answer correctly one or two questions in the best cases, having not even one correct answer in a 50% of the questionnaires. After one class, results became better, as Fig. 6 reveals, but no student reached the maximum and results could clearly be improved, what gave valuable information about concepts to be reinforced in subsequent classes.

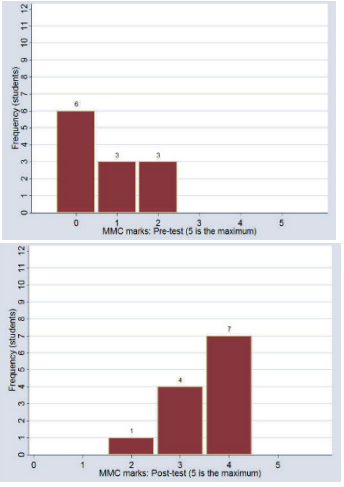

Fig. 6. Results of CMM pre-test vs. post-test.

3.2 – Experience perception

This learning experience was assessed at the end, by students, obtaining the results summarized in this boxplot (Fig. 7).

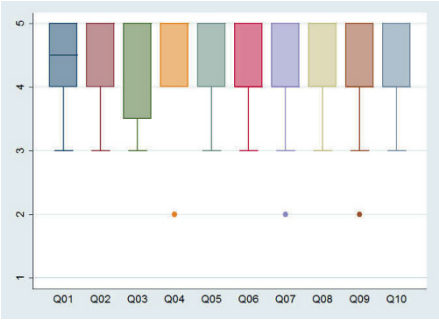

Fig. 7. Boxplot with the results of the experience perception questionnaire.

Most of the students (91.7%) considered that learning how to use the CMM with this method was better than just watching the teacher performing the measurement process in the cabin (Q01), which was the method previously applied (50.0% strongly agreed, 41.7% agreed and just 8.3% neither agreed nor disagreed).

When students were asked if, after the class, they felt able to measure a hole's diameter and the distance between two holes (Q02), 66.7% strongly agreed, 16.7% agreed and 16.7% neither agreed nor disagreed, meaning that they probably needed to perform more measurements under the teacher's guidance.

Results were similar regarding the the idea that this method allows students to take a more participant role in the class (Q03): 58.3% strongly agreed, 16.7% agreed and 25.0% neither agreed nor disagreed.

Students considering themselves able to use these tools (TeamViewer and remote desktop connection) in the future (Q04) were a 91.7%. In fact, 58.3% strongly agreed, 33.3% agreed and just one of them (8.3%) disagreed.

When participants were asked if they considered that this was a friendly method to learn how to use the CMM (Q05), only one of them (8.3%) neither agreed nor disagreed, while the rest agreed (25.0%) or strongly agreed (66.7%).

According to the results obtained in Q06, almost all students (91.7%) considered that they paid attention and understood what was explained during the class (41.7% strongly agreed, 50.0% agreed and 8.3% neither agreed nor disagreed). In fact, the atmosphere during the class was distended. They could ask the teacher during the class and they could also ask their partners for advice, while the teacher could confirm or correct the suggestions.

A clear majority of the class (41.7% strongly agreed and 41.7% agreed) also considered that, using this method, more operating details were learnt, compared to just watching another student measuring a workpiece in the cabin (Q07). Only one student (8.3%) neither agreed nor disagreed and another one disagreed.

Again, most of the participants (66.7% strongly agreed, 25.0% agreed and 8.3% neither agreed nor disagreed) thought that this was a good method to learn how to use this kind of machines (Q08).

This method was considered to be enhancing the learning process (Q09) of 83.3% of the participants (41.7% strongly agreed and 41.7% agreed), while one student (8.3%) neither agreed nor disagreed and another one disagreed.

Finally, the class was pleasant (Q10) for 91.7% of the students (41.7% strongly agreed and 50.0% agreed) and one student (8.3%) neither agreed nor disagreed.

4- Discussion and conclusions

The main goal of this research is to continue developing an educational network, to multiply the number of benefited students that will be able to practice with real machines that can be in other professional training centres. Although this paper describes an experience in which all the equipment was in the centre, the CMM was controlled by students using Internet, so proximity was not required at all. This means that the expensive CMM equipment (hardware and software license) could be virtually shared to other training centres (just needing remote control software and the commonly available computers), while those centres would also be able to share other machines, following the described process. It is easy to preview the positive consequences and the value of applying this procedure, particularly to professional training classes.

While other approaches are based on remote laboratories (several references can be found in the introduction of this paper), this project is based on the use of professional tools (real machines and their control software) that students need to learn how to use.

Using a camera (commonly available) to visualize the path of the measuring probe of the CMM, which is projected in real time, while the CMM software is also displayed as previously described, made possible to understand all the software commands and their effects.

Results reflected that applying this method to the conventional classes is very positive. The economic costs should not be a problem because, apart from the CMM (that could be shared), the used equipment (or similar) is commonly available in this kind of training centres.

The obtained results made us decide to keep on using this teaching methodology, at least in the metrology classroom, in which the required equipment, as described before, has been already installed. One of the main reasons to continue adopting this method was the clear improvements in aspects like participation, interest, friendliness and even professional applicability of the introduced tools, according to the students assessed.

It is considered important that the time required to adapt classes to use this method and prepare teachers to put it into

practice was not significant, especially if it is compared with the helpful results. As an important percentage of students bring laptops to classes, according to previously published research, e.g. **[F1]**, they could even use them for controlling the CMM. Although, in this pilot experience, students used laptops previously prepared by the research team, they could even use their own computers to do the same, just installing the necessary remote control software (e.g., TeamViewer, like previously described). This would make the described methodology even more affordable for the education centres, and students could become familiar with that tool (some participants recognised to be users previously) in their own computers and apply it to other interesting uses.

Screen resolution in the remote laptops can be considered a relevant issue to make possible to visualize the complete screen of the control computer that is connected to the CMM. The resolution of the control computer can be adapted to make this possible and, in fact, common screen resolutions in nowadays laptops are big enough for this purpose.

In this pilot study, distractions of participants caused by the use of laptops were not observed. Whereas, authors like Sana, Weston, & Cepeda **[SW1]** have recently confirmed significant distractions due to laptop multitasking, their suggestion to "explicitly discourage laptop use in courses" is referred to those cases where there is no need of technology for learning, which is the opposite of our classes. In our case, computers are required to control the machine (CMM) that students will learn to use, so the time that students spent getting the necessary skills and learning the required concepts related to metrology was reduced (compared with previous courses). So, in these classes, the use of laptops (only for the described purposes) means no additional distraction and helps to reinforce concepts of metrology, mathematics and geometry.

It can be observed that this method benefits from both, remote and in-person classes. A teacher can explain concepts in practice, increasing interaction with students, maintaining the regular coordination and support of the teacher and using equipment that can be remotely controlled thanks to network connection tools, making possible to optimize important resources.

This experience can be considered a starting point for further innovative educational projects. The fast development of tablet PCs, which are not new in education (e.g., **[SP1]**; **[FB1]**) makes possible to plan their integration as controlling devices for this kind of classes. Although new problems should be considered in the future, e.g. safety issues, the number of expected advantages could be a good reason to continue applying and improving this methodology. The next stage in this research project will be the implementation of this methodology in other educational centres to remotely control the previously described machine. This will make possible to check aspects related to, e.g., connection speeds or to detect issues that could appear with the distance increments.

Finally, the obtained results were considered very positive, especially for being a pilot experiment in which a number of aspects could be improved for future implementations. We consider that this method forces each student to pay attention because they will apply the acquired knowledge during the class, being part of the learning-teaching process.

5- Acknowledgements

This research has been possible thanks to a group of people and institutions. The authors would like to thank the Direction Team of the Centre of Professional Training "Corona de Aragón", the Centre of Teachers and Resources num. 1, especially to the professional training coordinator, José Ramón Insa, for believing in this project and promoting the required research team.

The researchers' appreciation is also extended to Jesús Gálvez, for helping in the testing process among his group of students, and to Francisco Valdivia, for collaborating with the initial installation and testing protocols, as well as the preparation of the learning materials for the students.

Finally, the students of the Master's Degree in Education for Secondary Teachers of the University of Zaragoza that conducted practices in the Centre of Professional Training "Corona de Aragón": Armando Díez, Eva Felipe and María Vidal, for their suggestions and for assuming this project for further validation.

6- References

[BP1] Barrios, A., Panche, S., Duque, M., Grisales, V. H., Prieto, F., Villa, J. L., Chevrel, P., & Canu, M. (2013). A multi-user remote academic laboratory system. Computers & Education, 62, 111–122.

[BT1] Bhatt, R. M., Tang, C.-P., Lee, L.-F., & Krovi, V. (2008). A Case for Scaffolded Virtual Prototyping Tutorial Case-Studies in Engineering Education. International Journal of Engineering Education, 00, 1-10.

[BH1] Bourne, J., Harres, D., & Mayadas, F. (2005). Online Engineering Education: Learning Anywhere, Anytime. Journal of Engineering Education, 94, 131-146.

[BK1] Brophy, S., Klein, S., Portsmore, M., & Rogers, C. (2008). Advancing Engineering Education in P-12 Classrooms. Journal of Engineering Education, 97, 369-387.

[CP1] Cantrell, P., Pekcan, G., Itani, A., & Velasquez-Bryant, N. (2006). The Effects of Engineering Modules on Student Learning in Middle School Science Classrooms. Journal of Engineering Education, 95, 301-309.

[CV1] Chandra, A. P. J., & Venugopal, C. R. (2012). Novel Design Solutions for Remote Access, Acquire and Control of Laboratory Experiments on DC Machines. IEEE Transactions on Instrumentation and Measurement, 61, 349-357.

[CC1] Chaos, D., Chacon, J., Lopez-Orozco, J. A., & Dormido, S. (2013). Virtual and Remote Robotic Laboratory Using EJS, MATLAB and LabVIEW. Sensors, 13, 2595-2612.

[CS1] Colwell, C., Scanlon, E., & Cooper, M. (2002). Using remote laboratories to extend access to science and engineering. Computers & Education, 38, 65–76.

[CH1] Cordray, D. S., Harris, T. R., & Klein, S. (2009). A Research Synthesis of the Effectiveness, Replicability, and Generality of the VaNTH Challenge-based Instructional Modules in Bioengineering. Journal of Engineering Education, 98, 335-348.

[CT1] Cui, L., Tso, F. P., Yao, D., Jia, W. J. (2012).

WeFiLab: A Web-Based WiFi Laboratory Platform for Wireless Networking Education. IEEE Transactions on Learning Technologies, 5, 291-303.

[ES1] Eddings, M. A., Stephenson, J. C., & Harvey, I. R. (2009). A Hands-On Freshman Survey Course to Steer Undergraduates Into Microsystems Coursework and Research. IEEE Transactions on Education, 52, 312-317.

[FF1] Fabregas, E., Farias, G., Dormido-Canto, S., Dormido, S., & Esquembre, F. (2011). Developing a remote laboratory for engineering education. Computers & Education, 57, 1686–1697.

[FB1] Ferrer, F., Belvís, E., & Pàmies, J. (2011). Tablet PCs, academic results and educational inequalities. Computers & Education, 56, 280–288.

[F1] Fried, C. B. (2008). In-class laptop use and its eVects on student learning. Computers & Education, 50, 906–914.

[GM1] Gómez, E., Maresca, P., Caja, J., Barajas, C., & Berzal. M. (2011). Developing a new interactive simulation environment with Macromedia Director for teaching applied dimensional metrology. Measurement, 44, 1730–1746.

[GM2] Graesser, A. C., McNamara, D., & VanLehn, K. (2005). Scaffolding deep comprehension strategies through Point&Query, AutoTutor, and iSTART. Educational Psychologist, 40, 225-234.

[HF1] Henson, A. B., Fridley, K. J., Pollock, D. G., & Brahler C. J. (2002). Efficacy of Interactive Internet-Based Education in Structural Timber Design. Journal of Engineering Education, 91, 371–378.

[HY1] Hwang, G.-J., Yang, T.-C., Tsai, C.-C., & Yang, S. J. H. (2009). A context-aware ubiquitous learning environment for conducting complex science experiments. Computers & Education, 53, 402–413.

[JC1] Jara, C. A., Candelas, F. A., Puente, S. T., & Torres, F. (2011). Hands-on experiences of undergraduate students in Automatics and Robotics using a virtual and remote laboratory. Computers & Education, 57, 2451–2461.

[KS1] Kolar, R. L., Sabatini, D. A., & Fink L. D. (2002). Laptops in the Classroom: Do They Make a Difference?. Journal of Engineering Education, 91, 397- 401.

[KY1] Kong, S. C., Yeung, Y. Y., & Wu, X. Q. (2009). An experience of teaching for learning by observation: Remote-controlled experiments on electrical circuits. Computers & Education, 52, 702–717.

[LZ1] Land, S. M., & Zembal-Saul, C. (2003). Scaffolding reflection and articulation of scientific explanations in a data-rich, project-based learning environment: An investigation of progress portfolio. ETR&D-Educational Technology Research and Development, 51, 65-84.

[LL1] Lee, H. S., Linn, M. C., Varma, K., & Liu, O. L. (2010). How Do Technology-Enhanced Inquiry Science Units Impact Classroom Learning?. Journal of Research in Science Teaching, 47, 71-90.

[L1] Lowe, D. (2013). Integrating Reservations and Queuing in Remote Laboratory Scheduling. IEEE Transactions on Learning Technologies, 6, 73-84.

[MA1] McKenna, A., & Agogino, A. (1997) Engineering for middle school: a web-based module for learning and designing with simple machines. Published in: Frontiers in Education Conference, 1997. 27th Annual Conference. Teaching and Learning in an Era of Change. Proceedings (Pages: 1496 – 1501 - Volume 3). Pittsburgh, PA. DOI: 10.1109/FIE.1997.632726.

[MA2] Mejias Borrero, A., & Andujar Marquez, J. M. (2012). A Pilot Study of the Effectiveness of Augmented Reality to Enhance the Use of Remote Labs in Electrical Engineering Education. Journal of Science Education and Technology, 21, 540-557.

[NA1] Newman, D., & Amir, A. (2001). Innovative First Year Aerospace Design Course at MIT. Journal of Engineering Education, 90, 375-381.

[NC1] Nickerson, J. V., Corter, J. E., Esche, S. K., & Chassapis, C. (2007). A model for evaluating the effectiveness of remote engineering laboratories and simulations in education. Computers & Education, 49, 708–725.

[P1] Paterson, K. (1999). Student Perceptions of Internet-Based Learning Tools in Environmental Engineering Education. Journal of Engineering Education, 88, 295-304.

[R1] Rojas, E. (2002). Use of Web-Based Tools to Enhance Collaborative Learning. Journal of Engineering Education, 91, 89-95.

[SW1] Sana, F., Weston, T., & Cepeda, N. J. (2013). Laptop multitasking hinders classroom learning for both users and nearby peers. Computers & Education, 62, 24–31.

[SF1] Santana, I., Ferre, M., Izaguirre, E., Aracil, R., & Hernandez, L. (2013). Remote Laboratories for Education and Research Purposes in Automatic Control Systems. IEEE Transactions on Industrial Informatics, 9, 547-556.

[SS1] Silk, E., Schunn, C., & Strand Cary, M. (2009). The Impact of an Engineering Design Curriculum on Science Reasoning in an Urban Setting. Journal of Science Education and Technology, 18, 209–223.

[SP1] Siozos, P., Palaigeorgiou, G., Triantafyllakos, G., & Despotakis, T. (2009). Computer based testing using "digital ink": Participatory design of a Tablet PC based assessment application for secondary education. Computers & Education, 52, 811–819.

[TA1] Tekin, A., Ata, F., & Gokbulut, M. (2012). Remote control laboratory for DSP-controlled induction motor drives. Computer Applications in Engineering Education, 20, 702-712.

[T1] Tsai, C.-C. (2009). Conceptions of learning versus conceptions of web-based learning: The differences revealed by college students. Computers & Education, 53, 1092–1103.

[VR1] Velasco, F. J., Revestido, E., Moyano, E., & Lopez, E. (2012). Remote laboratory for marine vehicles experimentation. Computer Applications in Engineering Education, 20, 728-740.

[WW1] Werner, T., & Weckenmann, A. (2010). Computer-assisted generation of individual training concepts for advanced education in manufacturing metrology. Measurement Science and Technology, 21, article id. 054018, 1-6.

[WA1] Wieman, C., Adams, W., Loeblein, P., Perkins, K. (2010). Teaching Physics Using PhET Simulations. The Physics Teacher, 48, 225.

Index